Het Pand, Ghent, Belgium
15-16 October 2019

40th AIVC Conference
8th TightVent Conference
6th venticool Conference

From energy crisis to sustainable indoor climate – 40 years of AIVC

PROCEEDINGS

In cooperation with:

In the past 40 years, since the first oil crisis in the seventies, energy and climate goals have been shaping many countries´ policy and legislative agendas. The building sector plays a crucial role in achieving these goals, considering the energy use attributed to buildings and its huge potential for improved energy performance.

Whereas in the past most of the focus was on reducing the energy consumption, it is now clear that better performing buildings must ensure an acceptable Indoor Environmental Quality (IEQ), by providing higher Indoor Air Quality (IAQ) and comfort levels for their occupants. Building ventilation entails both challenges and opportunities to achieve this goal.

In 2019 the AIVC completes its 40th year of existence and the conference organisers thought that it would be good to pay a particular interest to the evolution during these 40 years.

This is the context defining the core theme of the joint 40th AIVC, 8th TightVent and 6th venticool Conference as: "**From Energy crisis to sustainable indoor climate – 40 years of AIVC".**

Within its 40th year of operation and annual Conference, the AIVC board decided to offer authors the opportunity for a peer review of their paper.The procedure was twofold including 2 separate calls for abstracts & papers depending on whether the authors were interested in the peer review of their papers or not.

The papers which have been peer reviewed are indicated in the table of contents.

Acknowledgments

The conference organisers gratefully acknowledge the support from:

AIVC with its member countries : Australia, Belgium, China, Denmark, France, Greece, Ireland, Italy, Japan, the Netherlands, New Zealand, Norway, Republic of Korea, Spain, Sweden, UK and USA.

Since 1980, the annual AIVC conferences have been the meeting point for presenting and discussing major developments and results regarding infiltration and ventilation in buildings. AIVC contributes to the programme development, selection of speakers and dissemination of the results. pdf files of the papers of older conferences can be found in AIRBASE. See www.aivc.org.

Ghent University

Ghent University was founded in 1817 and is a top 100 university and one of the major Belgian universities counting over 41,000 students and 9,000 employees.Located in Flanders, the Dutch-speaking part of Belgium and the cultural and economical heart of Europe, Ghent University is an active partner in national and international educational, scientific and industrial cooperation. Our 11 faculties offer a wide range of courses and conduct in-depth research within a wide range of scientific domains.

TightVent Europe

The TightVent Europe 'Building and Ductwork Airtightness Platform' was launched in January 2011.
It aims at facilitating exchanges and progress on building and ductwork airtightness issues, including the production and dissemination of policy oriented reference documents and the organization of conferences, workshops, webinars, etc.
TightVent Europe has been initiated by INIVE EEIG (International Network for Information on Ventilation and Energy Performance) with at present the financial and/or technical support of the following partners: Lindab, MEZ-TECHNIK, Retrotec, BlowerDoor GmbH, Eurima, Soudal, Gonal, SIGA, Buildings Performance Institute Europe and the Covenant of Mayors for Climate & Energy.

venticool

The international ventilative cooling platform, venticool (venticool.eu) was launched in October 2012 to accelerate the uptake of ventilative cooling by raising awareness, sharing experience and steering research and development efforts in the field of ventilative cooling. The platform supports better guidance for the appropriate implementation of ventilative cooling strategies as well as adequate credit for such strategies in building regulations. The platform philosophy is pull resources together and to avoid duplicating efforts to maximize the impact of existing and new initiatives. venticool collaborates with organizations with significant experience and/or well identified in the field of ventilation and thermal comfort like AIVC (www.aivc.org) and REHVA (www.rehva.eu). venticool has been initiated by INIVE EEIG (International Network for Information on Ventilation and Energy Performance) with the financial and/or technical support of the following partners: Agoria-NAVENTA, Velux, WindowMaster, CIBSE nvg, the Covenant of Mayors for Climate & Energy and REHVA.

INIVE EEIG (International Network for Information on Ventilation and Energy performance)

INIVE was founded in 2001. INIVE is a registered European Economic Interest Grouping (EEIG), whereby from a legal viewpoint its full members act together as a single organisation and bring together the best available knowledge from its member organisations. The present full members are all leading organisations in the building sector, with expertise in building technology, human sciences and dissemination/publishing of information. They also actively conduct research in this field - the development of new knowledge will always be important for INIVE members.

INIVE has multiple aims, including the collection and efficient storage of relevant information, providing guidance and identifying major trends, developing intelligent systems to provide the world of construction with useful knowledge in the area of energy efficiency, indoor climate and ventilation. Building energy-performance regulations are another major area of interest for the INIVE members, especially the implementation of the European Energy Performance of Buildings Directive.

With respect to the dissemination of information, INIVE EEIG aims for the widest possible distribution of information.

The following organisations are members of INIVE EEIG (www.inive.org):

BBRI - Belgian Building Research Institute - Belgium
CETIAT - Centre Technique des Industries Aérauliques et Thermiques - France
CSTB - Centre Scientifique et Technique du Bâtiment - France
IBP - Fraunhofer Institute for Building Physics - Germany
SINTEF - SINTEF Building and Infrastructure - Norway
NKUA - National & Kapodistrian University of Athens - Greece

TNO - TNO Built Environment and Geosciences, business unit Building and Construction - Netherlands

The following organisations are associated members.

eERG - End-use Efficiency Research Group, Politecnico di Milano, Italy

IEQ-GA (Indoor Environmental Quality – Global Alliance)

The Indoor Environmental Quality – Global Alliance (IEQ-GA) was started by six (6) member organizations in 2014 with the signing of a Memorandum of Understanding (MOU). The member organizations include: AIHA; AIVC; ASHRAE; AWMA; IAQA; REHVA. In 2018, IISHRAE joined as the seventh member organization. The mission of IEQ-GA is to provide a scientific and technical basis for an acceptable indoor environmental quality (thermal environment; indoor air quality; lighting; acoustic; etc.) to occupants in buildings and places of work around the world, and to make sure the knowledge from research on IEQ is implemented in practice by engineers and practitioners.

The objective of the IEQ-GA is to get the member organizations to think together, work together and speak with the same voice. Our emphasis is on communications, coordination, cooperation and collaboration between the member organizations on indoor environmental quality issues. The alliance is formed as an interdisciplinary, international working group of member organizations interested in indoor air quality, thermal comfort, lighting and acoustic science, technology, and applications to stimulate activities that will help in a significant way to improve the actual delivered indoor environmental quality in buildings.

REHVA (The Federation of European Heating, Ventilation and Air Conditioning associations)

REHVA, The Federation of European Heating, Ventilation and Air Conditioning associations founded in 1963, is an umbrella organization that represents over 120,000 HVAC designers, building services engineers, technicians and experts across 27 European Countries. REHVA is dedicated to the improvement of the health, comfort and energy efficiency in all buildings and communities. The association provides its members with a strong platform for international professional networking, and knowledge exchange pursuing the vision of

improving health, comfort, safety and energy efficiency in all buildings and communities. It follows EU policy developments and represents the interests of its members in Europe and worldwide. This is achieved through the exchange of technical information, practical experience and research results by REHVA's working groups, seminars, publications and journal.

Event sponsors

The conference organizers are grateful to the following companies for their support to this event

Table of Contents

Facing the global overheating through mitigation and adaptation technologies - the role of ventilation 19
Mattheos Santamouris

CurieuzeNeuzen: monitoring air quality together with 20.000 citizens 20
Sam De Craemer, Jordy Vercauteren, Frans Fierens, Wouter Lefebvre, Hans Hooyberghs, Filip Meysman

Industry views on the future of ventilation 23
Yves Lambert

Introduction: Why performance-based assessment methods? Overview of the needs and the possibilities 24
Gaëlle Guyot

Performance-based assessment methods for ventilation systems: Overview of on-going work in France and in Europe 30
François Parsy, Gaëlle Guyot

Performance-based Spanish regulations relating to indoor air quality 33
Pilar Linares, Sonia García

Challenges and limitations of performance based approaches: the Belgian experience 35
Samuel Caillou, Sébastien Pecceu

Demand controlled ventilation: Sensitivity and robustness of the performances 38
Xavier Faure

Applicability of a simple and new airtightness measuring method and further comparisons with blower door measurements 40
Timothy Lanooy, Niek-Jan Bink, Wim Kornaat, Wouter Borsboom

Refined assessment and comparison of airtightness measurement of indoor chambers using the blower door and Pulse methods 49
Xiaofeng Zheng, Luke Smith, Adam Moring, Christopher J. Wood

Evaluation of indoor pressure distributions in a detached house using the Pulse airtightness measurement technique 60
Yun-Sheng Hsu, Xiaofeng Zheng, Edward Cooper, Mark Gillott, Shin-Ku Lee, Christopher J. Wood

Insights into the impact of wind on the Pulse airtightness test in a UK dwelling 70
Yun-Sheng Hsu, Xiaofeng Zheng, Dimitrios Kraniotis, Mark Gillott, Shin-Ku Lee, Christopher J. Wood

Estimation of air leakage sizes in building envelope using high-frequency acoustic impulse response technique 80
Benedikt Kölsch, Björn Schiricke, Jacob Estevam Schmiedt, Bernhard Hoffschmidt

Deviation of blower-door fans over years through the analysis of fan calibration certificates 90
Valérie Leprince, Christophe Delmotte, Isabelle Caré

The AIVC of the 20th Century 104
Martin Liddament

40 years of modeling airflows 114
Iain Walker

The role of carbon dioxide in ventilation and IAQ evaluation: 40 years of AIVC 118
Andrew Persily

HVAC and VOCs: interaction between building systems and indoor VOC concentrations 122
Klaas De Jonge, Jelle Laverge

Alternative ducting options for balanced mechanical ventilation systems in multifamily housing 124
Gabriel Rojas, Rainer Pfluger

Lessons learned from a ten-year monitoring in residential buildings equipped with humidity based demand controlled ventilation in France 127
Gaëlle Guyot

Practical use of the Annex68 IAQ Dashboard 130
Marc Abadie

Lessons learned from design and operation of ventilation systems in low-energy dwellings in the UK 133
Esfand Burman

Moisture in indoor air: findings of 40 years 136
Paula Wahlgren

Issues on humidity environment and health problem 138
Hiroshi Yoshino, Kenichi Hasegawa

Fungal growth on timber frame houses 148
Michiel Vanpachtenbeke, Liselotte De Ligne, Jan Van den Bulcke, Jelle Langmans, Joris Van Acker, Staf Roles

Big humidity data from smart ventilation systems 150
Loes Lokere, Arnold Janssens, Steven Vandekerckhove, Ivan Pollet, Marc Delghust, Klaas De Jonge, Jelle Laverge

ByggaF - a method to include moisture safety in the construction process 152
Kristina Mjörnell, Thorbjörn Gustavsson

Analysis of the effects of ventilation method on indoor humidity distribution and condensation by CFD method 160
Fangyuan Zhang, Yuji Ryu

Performance of a heat recovery ventilation system in the Canadian arctic 168
Justin Berquist, Carsen Banister, Dennis Krys

Long-term performance and resiliency testing of a dual core energy recovery ventilation system for the Arctic 179
Boualem Ouazia, Chantal Arsenault, Yunyi Li, Michael Brown, Gerald Kolsteren, Christopher Chisholm

Experimental investigation of frost formation on air to air counter flow heat exchanger in air handling unit and climatic influence on dry, wet, frost operation condition 189
Michal Pomianowski, Rasmus Lund Jensen, Dzhanan Osman Metin, Nils Kristian Kure Rasmussen, Diana State

Efficiency of heat recovery ventilation in real conditions: feedback from several measurement campaigns 198
Sébastien Pecceu, Samuel Caillou

Impact of ductwork leakage on the fan energy use and sound production of central mechanical ventilation units in houses 211
Valérie Leprince, Marcus Lightfoot, Jelmer de Jong

The contribution of a solar air heater collector to the cooling load in a Building 220
Pavlos Toumpoulidis, Argiro Dimoudi, Panos Kosmopoulos, Stamatis Zoras

Evolution of ventilation strategies in air-conditioned buildings in Singapore - IAQ and energy perspectives 231
Chandra Sekhar

Dynamic performance of displacement ventilation in a lecture hall 234
Natalia Lastovets, Kai Sirén, Risto Kosonen, Juha Jokisalo, Simo Kilpeläinen

Numerical modelling of large air-conditioned space: comparison of two ventilation systems 245
Ali Alzaid, Maria Kolokotroni, Hazim Awbi

Proposal of optimal control method in order to reduce mutual interference of air conditioning indoor units 255
Yuga Urata, Yasuyuki Shiraishi

Minimising the influence of the stack effect and wind on the operation of mechanical exhaust ventilation systems 263
Romy Van Gaever, Samuel Caillou, Sébastien Pecceu

Multi-objective optimization of energy saving and thermal comfort in thermo active building system based on model predictive control 272
Ogawa Yohei, Shiraishi Yasuyuki

Two case studies on ventilation for indoor radon control 280
Justin Berquist, Liang Grace Zhou, Jeffrey Whyte, Yunyi Ethan Li, Mark Vuotari, Gang Nong

Influence of ventilation on radon concentration in a study case in Spain 290
Pilar Linares-Alemparte, Sonia García-Ortega

Energy and indoor air quality analysis of mixed air and displacement ventilation systems 297
Walid Chakroun, Sorour Alotaibi, Kamel Ghali, Nesreen Ghaddar

Investigation of the combined effect of indoor air stability and displacement ventilation on pollutant transport in human breathing microenvironment 305
Xiaorui Deng, Guangcai Gong

Indoor environment and adverse health symptoms among children under home damp conditions 314
Kenichi Hasegawa, Naoki Kagi, Nobuhiro Kanazawa, Jun Sakaguchi, Naohide Shinohara, Yasuyuki Shiraishi, Teruaki Mitamura, Jun Fukushima

Relationship between indoor allergen and occupants' allergic symptoms before and after moving in the house with the countermeasure against allergy 322
Teruaki Mitamura, Kunio Dobashi, Hiroki Harasawa

Learning performance in odor environment with aroma oils: influence of odor of essential oils on learning performance in classroom 328
Aya Eto, Narae Choi, Toshio Yamanaka, Akihisa Takemura, Tomohiro Kobayashi

A large-scale longitudinal indoor air quality study: is low-cost sensor deployment a viable approach? 338
James A. McGrath, Alison Connolly, Miriam A. Byrne

An argument for a reality check in the ventilation industry: We still have an energy crisis, in practice, and are not generally, in practice, achieving better indoor climate 347
Sergio George Fox

Status of air filter energy performance and product characteristics 358
Kiyan Vadoudi, Gregory Kelijian

Influence of building envelope's solar reflectivity, wind speed and building coverage ratio on urban heat environment 365
Haruto Kitakaze, Jihui Yuan, Toshio Yamanaka, Tomohiro Kobayashi

The influence of external environment characteristics on the heating and cooling load of super-tall residential building 375
Hyoeng-Tae Kim, Hee-Gang Kim, Chang-Ho Jeong, Myoung-Souk Yeo

Improvement method of thermal environmental near windows during heating period-thermal and air flow characteristics of two-dimensional jet from breeze line diffuser in free field 382
Shaoyu Sheng, Toshio Yamanaka, Tomohiro Kobayashi, Jihui Yuan, Masahiro Katou, Saori Yumino

Airtightness and energy impact of air infiltration in residential buildings in Spain 394
Irene Poza-Casado, Alberto Meiss, Miguel Ángel Padilla-Marcos, Jesús Feijó-Muñoz

Exist'air: airtightness measurement campaign and ventilation evaluation in 117 pre-2005 French dwellings 402
Sylvain Berthault, Lucille Labat, Cédric Delahais, Elodie Héberlé, Sabrina Talon

New findings on measurements of very airtight buildings and apartments 412
Stefanie Rolfsmeier

Comparison between infiltration rate predictions using the divide-by-20 rule of thumb and real measurements 420
Alan Vega Pasos, Xiaofeng Zheng, Mark Gillott, Christopher J. Wood

On the experimental validation of the infiltration model DOMVENT3D 430
Alan Vega Pasos, Xiaofeng Zheng, Benjamin Jones, Mark Gillott, Christopher J. Wood

How accurate is our leakage extrapolation? Modeling building leakage using the Darcy-Weisbach equation 440
Steven Rogers

Vertical distribution of temperature and contaminant concentration in a room with impinging jet ventilation system 453
Mako Matsuzaki, Tomohiro Kobayashi, Toshio Yamanaka, Narae Choi, Haruna Yamasawa

Analysis of convective heat transfer coefficient correlations for ventilative cooling based on reduced-scale measurements 463
Katarina Kosutova, Christina Vanderwel, Twan van Hooff, Bert Blocken, Jan Hensen

Overheating reduction in a house with balanced ventilation and postcooling 471
Bart Cremers

Modelling thermal comfort and energy consumption of a typical mixed-cooling apartment in Guilin, China 476
Jie Han, Wenheng Zheng, Guoqiang Zhang

Comfort at hospital reception desks 483
R. M. J. Bokel, P. J. W. van den Engel, A. M. Eijkelenboom, M. A. Ortiz Sanchez

Prediction of the influence of solar radiation on adaptive thermal comfort using CFD simulation 493
Juti Hu, Ge Song, Guoqiang Zhang

Developing a new passive tracer gas test for air change rate measurement 507
Sarah L. Paralovo, Maarten Spruyt, Joris Lauwers, Borislav Lazarov, Marianne Stranger, Jelle Laverge

Measuring the ventilation rate in occupied buildings and adapting the CO2 tracer gas technique 517
Jessica Few, Clifford Elwell

Airtightness and non-uniformity of ventilation rates in a naturally ventilated building with trickle vents 527
Jessica Few, David Allinson, Clifford Elwell

Effects of outdoor environment on air exchange rate 537
Maria Marrero, Manuel Gameiro da Silva, Leslie Norford

Successive indoor air pressure calculation method for natural ventilation rate prediction 545
Haruna Yamasawa, Toshio Yamanaka, Tomohiro Kobayashi, Jihui Yuan

Using CFD simulation to improve estimation of wind pressure coefficient for naturally-ventilated buildings in tropical climate 555
Matthieu Zubialde-Elzaurdia, Franck Lucas, Alain Bastide

Experimental study of the combination of a positive input ventilation and active air vents on the air change rates of a house 564
Antoine Leconte, Clément Lafféter, Thomas Fritsch, Nicolas Giordano, Julien Escaich, Ophélie Ouvrier Bonnaz

An investigation of ventilation control strategies for louver windows in different climate zones 574
Leonie Scheuring, Bernhard Weller

Cooling performance of air-conditioning system with ceiling suspended packaged air conditioning unit over divided-type membrane ceilings in large classroom 585
Shogo Ito, Toshio Yamanaka, Tomohiro Kobayashi, Jihui Yuan, Narae Choi

Modelling of supply air jet from diffusers of four-way packaged air-conditioner for CFD analysis on unsteady airflow in room 595
Norikazu Yasuda, Toshio Yamanaka, Tomohiro Kobayashi, Jihui Yuan, Choi Narae

Multi-objective design of single room ventilation units with heat and water recovery 605
Antoine Parthoens, Luc Prieels, Jean-Jacques Embrechts, Yves Detandt, Sébastien Pecceu, Samuel Gendebien, Vincent Lemort

Review of building services solution fitted for a low emission building stock in urban areas 615
Matthias Haase, Øystein Rønneseth, Kari Thunshelle, Laurent Georges, Sverre Holøs, Judith Thomsen

Comparative life-cycle assessment of constant air volume, variable air volume and active climate beam systems for a Swedish office building 627
Nadeen Hassan, Saqib Javed

Enhancing thermal comfort and indoor air quality in Australian school classrooms 637
Shamila Haddad, Afroditi Synnefa, Miguel Ángel Padilla Marcos, Riccardo Paolini, Deo Prasad, Mattheos Santamouris

Indoor air and environmental quality in social housing dwellings in Australia 645
Shamila Haddad, Afroditi Synnefa, Riccardo Paolini, Mattheos Santamouris

Radiant heating and cooling systems combined with displacement ventilation in schools; strategies to improve IAQ 653
Michel Tardif, Sébastien Brideau

The evaluation of real-time indoor environment parameters measured in 297 Chilean dwellings (*Peer reviewed paper*) 662
Constanza Molina, Amy Jackson, Benjamin Jones

Ventilation and measured IAQ in new US homes (*Peer reviewed paper*) 672
Iain Walker, Brett Singer, Rengie Chan

Overview of model based control strategies for ventilation systems 679
Bart Merema, Maarten Sourbron, Hilde Breesch

Predictive control for an all-air ventilation system in an educational nZEB building 683
Bart Merema, Dirk Saelens, Hilde Breesch

Model based design of intelligent ventilation concepts 693
Koen Maertens

A case study on residential mixed-mode ventilation using the ventilation controls virtual test bed 694
Bert Belmans, Dorien Aerts, Stijn Verbeke, Amaryllis Audenaert, Filip Descamps

Influence of the external pressure tap position on the airtightness test result 704
Jiří Novák

Airtightness of buildings - considerations regarding place and nature of pressure taps 706
Christophe Delmotte

Quantification of uncertainty in zero-flow pressure approximation due to short term wind fluctuations 713
Martin Prignon, Arnaud Dawans, Geoffrey van Moeseke

Designing a model-scale experiment to evaluate the impact of steady wind on building air leakage measurements 723
Adeline Bailly Mélois, Anh Dung Tran, Mohamed El Mankibi, François Rémi Carrié, Bassam Moujalled, Gaëlle Guyot

CFD modelling of fan pressurization method in buildings - The impact of dynamic wind on airtightness tests 729
Dimitrios Kraniotis, Arnab Chaudhuri

Using co-simulation between EnergyPlus and CONTAM to develop IAQ and energy-centric demand-controlled ventilation systems 730
Maria Justo Alonso, W. Stuart Dols, Hans Martin Mathisen

Performances of a demand-controlled mechanical supply ventilation system under real conditions: indoor air quality and power distribution for thermal comfort 741
Clement Laffeter, Xavier Faure, Michele Potard, Claude Bardoul, Julien Escaich, Ophelie Ouvrier Bonnaz, Etienne Wurtz

Large-scale performance analysis of a smart residential MEV system based on cloud data 751
Bavo De Maré, Stijn Germonpré, Jelle Laverge, Frederik Losfeld, Ivan Pollet, Steven Vandekerckhove

Individualised dynamic model-based monitoring of occupant's thermal comfort for adaptive HVAC controlling 766
Ali Youssef, Nicolás Caballero, Jean-Marie Aerts

Assessment of long-term and mid-term building airtightness durability: field study of 61 French low energy single-family dwellings 776
Bassam Moujalled, Sylvain Berthault, Andrés Litvak, Valérie Leprince, Gilles Frances

Assessment of the durability of airtightness products in laboratory controlled conditions: development and presentation of the experimental protocol 788
Andrés Litvak, Fabien Allègre, Bassam Moujalled, Valérie Leprince

Moisture impact on dimensional changes and air leakage in wooden buildings 801
Paula Wahlgren, Fredrik Domhagen

Association between indoor air quality and sleep quality 811
Chenxi Liao, Marc Delghust, Jelle Laverge

Measurements of sleep quality with low-cost sleep monitors: Effect of bedroom air quality and sleep quality 821
Pawel Wargocki

CO_2-concentration of the surrounding air near sleeping infants inside a crib 822
Gert-Jan Braun, Wim Zeiler

Quality framework for residential ventilation systems in Flemish region in Belgium - feedback after three years' experience 832
Maarten De Strycker, Liesje Van Gelder, Martyna Andrzejewicz, Valérie Leprince

Commission and performance contracting of ventilation systems in practice. Determination, analyses and consequences for practitioners and contractors 843
Wouter Borsboom, Wim Kornaat, Pieter van Beek, Niek-Jan Bink, Timothy Lanooy

Test of new analysis methodologies to assess dynamic airflow rate with the tracer gas decay method 852
Gabriel Remion, Bassam Moujalled, Mohamed El Mankibi

Reliability of ductwork airtightness measurement: impact of pressure drop and leakage repartition on the test result 860
Sylvain Berthault, Valérie Leprince

Techniques to estimate commercial building infiltration rates 874
Andrew Persily, Lisa Ng, W. Stuart Dols, Steven Emmerich

Wind pressure coefficient and wind velocity around buildings in high density block of metropolis for natural ventilation design 883
Toshio Yamanaka, Eunsu Lim, Tomohiro Kobayashi, Toshihiko Sajima, Kanji Fukuyama

Alternative solution proposal to improve the air change in light shafts based on flaps 893
Ángel Padilla-Marcos Miguel, Alberto Meiss, Raquel Gil-Valverde, Irene Poza-Casado, Jesús Feijó-Muñoz

Probabilistic modelling of wind induced air exchange in buildings 903
Krystyna Pietrzyk

Impact of an occupancy and activity based window use model on the prediction of the residential energy use and thermal comfort 912
Silke Verbruggen, Marc Delghust, Jelle Laverge, Arnold Janssens

Ambient air filter efficiency in airtight, highly energy efficient dwellings - A simulation study to evaluate benefits and associated energy costs 920
Gabriel Rojas

Out2In: impact of filtration and air purification on the penetration of outdoor air pollutants into the indoor environment by ventilation 932
Joris Van Herreweghe, Samuel Caillou, Tom Haerinck, Johan Van Dessel

Future trends in laboratory methods to predict HVAC in service filter performance 941
Jesús Marval, Luis Medina, Emanuele Norata, Paolo Tronville

A study of the influence of the position of a chimney terminal on the vertical walls of a building on the air quality of the ventilation air supply 951
Xavier Kuborn, Sébastien Pecceu

When the EPR hits the fan, or…the killing of the fan energy 962
Ad van der Aa, Per Heiselberg, Willem de Gids

Existing standards for testing gas phase air cleaners 973
Paolo Tronville

Methods to evaluate gas phase air-cleaning technologies 974
Pawel Wargocki

Development of subjective evaluation tool of work environment for office workers' work performance and health promotion 975
Yuko Abe, Yasuyuki Shiraishi, Toshiharu Ikaga, Yoshihisa Fujino

Evaluation potential of indoor environments' ecological valency 985
Ardeshir Mahdavi, Helene Teufl, Christiane Berger

Residential application of an indoor carbon dioxide metric 995
Andrew Persily, Brian J. Polidoro

Trade-offs between ventilation rates and formaldehyde concentrations in new-build dwellings in the UK 1008
Esfand Burman, Samuel Stamp

Modeling dynamic behavior of volatile organic compounds in a zero energy building 1019
Klaas De Jonge, Jelle Laverge

Indoor air quality in nearly zero energy buildings, reduction of exposure 1029
Piet Jacobs, Wouter Borsboom, Willem de Gids

Better implementation of ventilative cooling (cooling of buildings using outside air as main source) in national building standards, legislation and compliance tools 1038
Christoffer Plesner, Jannick K. Roth, Per Heiselberg

Ventilative cooling - time for large scale implementation? 1041
Per Heiselberg

Facing the global overheating through mitigation and adaptation technologies - the role of ventilation

Mattheos Santamouris

Anita Lawrence Chair on High Performance Architecture
Faculty of Built Environment
University of New South Wales, Sydney, Australia
m.santamouris@unsw.edu.au

SUMMARY

Regional climate change in cities is the most documented phenomenon of climate change . Higher urban temperatures are documented experimentally for more than 450 major cities in the world. Numerous investigations demonstrate that the mean magnitude of the temperature increase may exceed 4-6 C, while at the peak it may exceed 10 C. The serious increase of the frequency and the strength of heat waves creates strong synergies between the global and regional climate change and intensify the magnitude of the overheating

Urban overheating causes a serious impact both on the energy demand and generation sectors. It increases the cooling energy consumption of buildings, rises the peak electricity demand and obliges utilities to built additional power plants, it affects seriously health issues and in particular heat related mortality and morbidity, impacts the concentration of pollutants and damages the urban environmental quality, and finally deteriorates the levels of local vulnerability and thermal comfort.

To counterbalance the problem of urban overheating, numerous heat mitigation systems and technologies are proposed, and implemented in more thyan 250 large scale urban projects. Mitigation policies and technologies aim to strength the cooling potential of heat sinks and weaken the intensity of the heat sources. Among the developed mitigation technologies, the use of advanced, materials like the recently developed photonic components and the reflective, cool materials, the implementation of additional greenery in buildings and open spaces, the use of passive evaporative systems involving additional irrigation of urban zones and finally the dissipation of the excess heat into the ground seems to provide the higher mitigation potential

Although mitigation seems to seriously counterbalance the impacts of urban overheating, there is a need to adapt the built environment to face the present and future climate challenges. Adaptation technologies involving advanced energy and environmental systems for buildings, may minimize the energy needs of buildings and provide indoor comfortable conditions with the minimum energy use. Advanced ventilation technologies assisted by hybrid dissipation technologies like sub-ambient radiative systems, seems to provide a very high adaptation potential.

The present paper reviews and reports the recent progress and knowledge on the specific impact of current and projected urban overheating in energy, peak electricity demand, air quality, mortality and morbidity and urban vulnerability. In parallel, it discusses new findings related to the characteristics and the magnitude of urban overheating, .and reports and analyse the recent knowledge on the synergies between urban heat island and heat waves. Finally, it presents the recent developments in the field of mitigation and adaptation technologies for buildings and cities and provides inside information on the current and future potential

CurieuzeNeuzen: monitoring air quality together with 20.000 citizens

Sam De Craemer[1*], Jordy Vercauteren[2], Frans Fierens[2], Wouter Lefebvre[3], Hans Hooyberghs[3], Filip Meysman[1]

1 Universiteit Antwerpen
Universiteitsplein 1
2610 Wilrijk, Belgium
**Corresponding author:*
sam.decraemer@uantwerpen.be

2 Vlaamse Milieumaatschappij
Kronenburgstraat 45
2000 Antwerpen, Belgium

3 VITO
Boeretang 200
2400 Mol, Belgium

KEYWORDS
CurieuzeNeuzen, nitrogen dioxide, citizen science, air quality, policy

1 INTRODUCTION

Traffic sources contribute a large portion of the ambient nitrogen dioxide, particulate matter and ozone concentrations, the three ambient air pollutants with the largest impact on human health in Europe (EEA, 2018). High spatial resolution air quality data capturing the high spatial variability of this traffic related pollution are necessary in order to inform policy. The approach of environmental protection agencies around the world to measure using expensive monitoring stations allows monitoring in high temporal, but not spatial, resolution (Snyder et al., 2013). Air quality models are used to achieve the necessary spatial resolution, but their full validation still requires a dense measurement set.

To obtain such a set for the traffic dense region of Flanders, Belgium, an unusual consortium, uniting the University of Antwerp, the Flanders Environment Agency, and the newspaper De Standaard as main partners, collaborated with citizens in the CurieuzeNeuzen project (CurieuzeNeuzen Vlaanderen, 2019). The involvement of citizens allowed to raise community awareness regarding air quality, and support for related research and measures.

2 METHOD

The aim was to recruit at least 20.000 participants using a multimedia campaign centred around a positive and motivating message. Despite requiring a contribution of €10 per participant due to budget restraints, many more people wanted to participate. A selection from the registrations was performed taking into consideration the spatial distribution and the different situations in which the model needs to be evaluated. In order to obtain high quality measurements, the straightforward principle of Palmes samplers (Palmes, Gunnison, Dimattio, & Tomczyk, 1976) was combined with an easy-to-use but reproducible measurement setup so citizens could measure nitrogen dioxide, a good marker of traffic pollution, at their façade window.

Measurements were carried out during the month of May. First, these results were calibrated using reference measurements of the Flanders Environment Agency. Next, a temporal extrapolation to yearly values that can be compared with health guidelines was performed, based on monitoring data of the Flanders Environment Agency. The dataset was submitted to several analyses to provide policy recommendations, and to test the ATMO-Street model (VITO, 2019) used for air quality monitoring and evaluating policy scenarios in Flanders.

3 RESULTS

In the end more than 52.000 people registered to participate. After measurement at 20.000 locations and data quality check more than 17.800 measurements were retained for analyses. The resulting map (Figure 1) reveals some intense local variations in air quality, visually highlighting traffic intense roads and street canyons, especially in urban areas.

2.3% of the measurement locations exceed EU/WGO yearly limit value of 40 µg/m³, and a modelling exercise confirmed that this is representative for the concentrations at all facades of the Flemish population. While these exceedances were more concentrated in cities and suburbs, also a quarter of the villages and small cities (inhabitants < 50.000) have at least one sampling location in exceedance. In all cases, a combination of traffic intensity, traffic flow, and street geometry seem to play a role, which is confirmed by statistical analysis.

Comparison of the calibrated concentrations for the month of May to ATMO-Street model results of the same period showed that the model is performing quite well (bias= -4µg/m³; root-mean-square-error= 6.13 µg/m³). Based on the measurement dataset, some further improvements to the model have been made. Some remaining problems, such as a remaining underestimation in traffic dense street canyons, are likely related to incorrect and outdated traffic data used as input for the model.

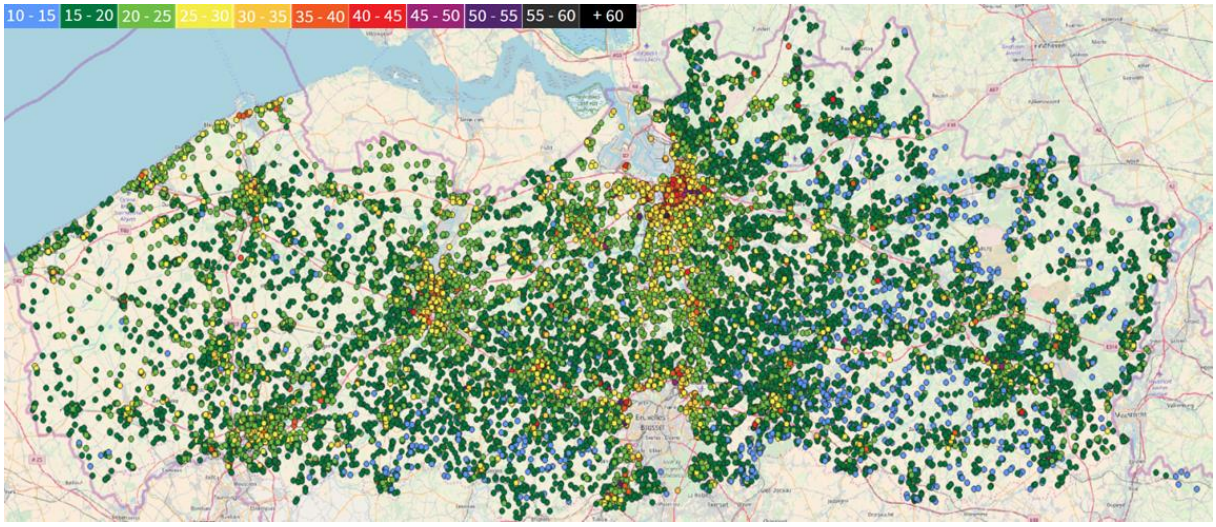

Figure 1: Map (background © OpenStreetMap contributors) of NO2 concentrations (µg/m³) measured in CurieuzeNeuzen Flanders

4 CONCLUSIONS

The recruitment strategy was a big success, and the motivation of the citizen scientists led to a high proportion of high-quality measurements, demonstrating that involving citizens in measurement can result in reliable data. The visual representation of the high variability in air quality linked to traffic intensity is useful to inform the public of ways to reduce their contribution to the problem and to reduce their exposure, including how to approach ventilation.

Exceedances of annual limit values in villages and smaller cities show that air quality is not only a problem of large city centres. Policy should take this into account, and the dataset indicates that smoother traffic flow and especially lower intensity should be priorities in this regard. A strengthening of urban centres will be important for the latter but achieving air quality standards in cities will always be harder than in less populated areas.

The good performance of the ATMO-Street model, even before any optimizations, demonstrates its reliability as a tool to inform policy and research, but underestimation of traffic dense street canyons should be considered. The largest potential for model improvement is likely to be better traffic data, possibly including traffic flow, should such data become affordable in the future.

5 ACKNOWLEDGEMENTS

We thank all citizens scientists involved for their enthusiasm and efforts, and all team members of University of Antwerp, De Standaard, the Flanders Environment Agency, VITO, HIVA KUleuven and Kariboo! for their contribution to planning, logistics and communication. We also acknowledge the citizen movement Ringland and Stad Antwerpen for their contribution the CurieuzeNeuzen Antwerpen project, which acted as a pilot for the present project.

6 REFERENCES

CurieuzeNeuzen Vlaanderen. (2019). Website CurieuzeNeuzen Vlaanderen. curieuzeneuzen.be

EEA. (2018). *Air quality in Europe - 2018 report*. Luxembourg.

Palmes, E. D., Gunnison, A. F., Dimattio, J., & Tomczyk, C. (1976). Personal sampler for nitrogen dioxide. *American Industrial Hygiene Association Journal*.

Snyder, E. G., Watkins, T. H., Solomon, P. A., Thoma, E. D., Williams, R. W., Hagler, G. S. W., … Preuss, P. W. (2013). The changing paradigm of air pollution monitoring. *Environmental Science and Technology*, *47*(20), 11369–11377.

VITO. (2019). Webpage ATMO-Street. https://vito.be/en/atmo-street

Industry views on the future of ventilation

Yves Lambert

EVIA European Ventilation Industry Association
Avenue des Arts 46 Kunstlaan
1000 Brussels
Belgium

SUMMARY

Smartness is all around us. The HVAC industry is developing more and more products that have sensors, are intelligent, are connected to the Internet and are being controlled via apps. According to a recent European survey among installers, the request and demand from clients for installing home automation and smart products is the highest for HVAC installations.
In what way can we use smart ventilation systems to help to convince the general public of the importance of ventilation in their daily life ? If most marketing efforts from the industry fail due to the non-interest of consumers, maybe it is time to present them with factual proof. Providing understandable monitoring data has already proven its worth in other sectors to make a technology trustworthy.
If the industry decides to move further down this path, both the industry and scientists have a great challenge ahead of them and are faced with an opportunity to work more closely together.
When, in a near future, the industry is willing to share more and more actual data on IAQ and energy performance of ventilation systems in use, this will generate an enormous source of information for future research into the actual performance of different ventilation approaches, occupational patterns, actual airflows etc. Moreover, this could be the basis for optimising current validation models.

However, this approach also opens the door to a whole range of new questions:

How do we deal with this data when it conflicts with existing models or simulations ?
How much deviation can an existing model/simulation have from the actual data ?
How much data is needed before it is considered sufficient proof to review the assumptions used in a model ?

All of this and more is food for thought.

KEYWORDS

Smartness, monitoring, data, assumptions, modelling, validation

Introduction: Why performance-based assessment methods? Overview of the needs and the possibilities.

Gaëlle Guyot*[1,2]

1 Cerema Cerema Direction Centre-Est, 46 rue St Théobald, F-38080, L'Isle d'Abeau, France

2 Univ. Grenoble-Alpes, Univ. Savoie Mont Blanc, CNRS, LOCIE, 73 000 Chambéry, France

**Corresponding author: gaelle.guyot@cerema.fr*

SUMMARY

In future building regulations 2020, building performance is going to be extended to global performance, including indoor air quality (IAQ). In the energy performance (EP) field, successive regulations pushed for a "performance-based" approach, based on an energy consumption requirement at the design stage. Nevertheless, ventilation regulations throughout the world are still mostly based on prescriptive approaches, setting airflows requirements. A performance-based approach for ventilation would insure that ventilation is designed to avoid risks for occupant's health.

Given the European context with the generalization of nearly zero energy buildings, envelope airtightness is often included in EP-calculations, frequently through single-zone models with uniform air leakage. Because more consideration is often given to EP than to IAQ, impact of several zones interconnected by unevenly distributed leaks, on the envelope and on internal partition walls, is a rarely investigated issue, which is investigated in this work.

Faced with this issue, we conducted an experimental study on multizone air leakages of 23 detached houses and developed an innovative database. The analysis of this database reveals that internal air leakage can become significant at door undercuts and that the type of building structure has a great influence. We propose airleakage values and dispersion input data for multizone IAQ models. Then, through a multizone modelling of a low energy house case study, we quantify impacts of these airleakage distribution data on IAQ. We model CO_2, humidity and formaldehyde with two type of ventilation (exhaust-only or balanced). We highlight strong impacts and conclude that detailed airleakage distributions should be used in IAQ performance assessment methods.

An extensive review work combined with complementary analysis allows us to come up with the development of a performance-based approach for house ventilation to be used at the design stage in a regulatory calculation. We select the use of five relevant IAQ performance indicators, based on CO_2, formaldehyde and $PM_{2.5}$ exposures, and RH-based indicators assessing both condensation and health risks. We propose also pollutant emission data and occupancy schedules to be used. Lastly, we describe the multizone modelling laws, the physical models and associated assumptions, and the boundary conditions.

Importantly, we demonstrate that our proposed performance-based method was applicable, applying it to a low-energy house case study. We assume being at the design stage of a house which should comply with a hypothetical regulation, requiring IAQ performance indicators and associated thresholds. We also demonstrate how such an approach could help at the design stage in key choices as the type of structure (regarding its impact on airleakage distributions), the type of ventilation system, the level of pollutant emissions. Indeed, in the case study, only the balanced ventilation combined with low or medium-emission class of formaldehyde emissions allow to fulfil the IAQ requirements. We show also that such an approach could help in the ventilation design, notably the distribution of the air inlets and/or outlets, or even the airflows, in order to secure the fulfilment of IAQ requirements.

At the end of this work, we highlight the needs for such performance-based approaches, from the robustness of performance indicators which should also be based on acute exposures, to the lack of data to be used to assess the pollutants emissions at the dwelling scale.

KEYWORDS

Ventilation, performance, design, indoor air quality

1 INTRODUCTION

In new labels and future building regulations, building performance should be extended to indoor environment quality, beyond energy performance. In the energy performance field, successive regulations pushed to a ***"performance-based" approach***, based at least on an energy consumption requirement for heating and/or cooling at the design stage (Spekkink 2005).

Nevertheless, in the building ventilation field, regulations throughout the world are mainly still based on ***"prescriptive" approaches***, such as airflows or air change rates requirements (Dimitroulopoulou 2012). As the list of identified indoor pollutants is long and may still increase, it has been impossible to create definitive IAQ indicators for standards and regulations governing residential buildings (Borsboom et al. 2016). As a result, standards and regulations generally set ventilation rates based on comfort considerations and not on health criteria as suggested in the Healthvent project (Seppanen and et. al. 2012; Wargocki 2012). The trouble with this approach is that it assumes that in addition to displacing human bio-effluents including odors, ventilation is a sufficient mean of controlling other contaminants (Matson and Sherman, 2004 and Persily, 2006). Against such prescriptive approaches, it is possible to develop **performance-based approaches** for residential building ventilation. Regarding the fact that prescribed ventilation rates are only an (unperfected) way to achieve a given IAQ, it could be imagined to require IAQ performance indicators instead of ventilation rates. The performance-based approach concept is illustrated on Figure 1.

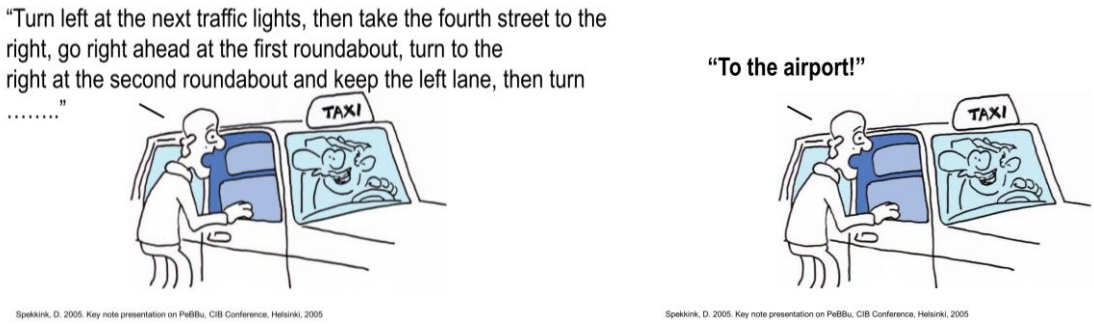

Figure 1. Illustration of (a) a prescriptive approach; (b) a performance-based approach. Source : (Spekkink 2005)

"Performance-based" approaches for ventilation would insure that it is designed to avoid risks for occupant's health and building damages. Such an approach could be required at different scales:

1. At the ventilation system scale: for allowing the use of an innovative ventilation system instead of "reference" systems. "Reference" ventilation systems are usually defined as the widely used ventilation systems, or the ventilation systems directly providing the constant airflows required by the regulation. In this case, standardized input data and scenarii should be used,
2. **At the building scale: at the design stage of a building, input data from the given building should also be used.**

Such approaches could also be used at different stages of the building's construction:

1. At the design stage, as a design method;
2. **Later at the end of design stage, during the regulatory compliance stage, to assess the design. It could be called a design assessment method;**
3. At initial commissioning, or later once the building is occupied, as an in-situ performance assessment method.

If we compare to the energy performance field, the design method is the detailed energy simulation performed to optimize the energy consumption of the building, the design assessment method is the regulatory energy performance calculation based on simplified assumptions and a limited number of performance indicators, complete in-situ performance assessment methods are rare but could be based on several measurements (airleakage test, wall thermal conductivity, energy consumption, …).

Facing a lack of data about the relevant method for ventilation, we propose in this work to develop a performance-based approach for assessing ventilation performance at the building

scale and at the end of the design stage, as does an energy performance regulatory calculation. We propose also to be at the regulatory compliance stage (number 2) as developed just above.

2 A PERFORMANCE-BASED APPROACH IN THREE STEPS

In order to develop such a performance-based approach, we need to address the following topics:

1. What are the relevant pollutants and/or parameters to use for calculating performance indicators and what indicators should be used?
2. What are the relevant input data to use regarding the occupancy and pollutant emission scenarii?
3. Lastly, what level of detail should we use for modelling airflows and pollutants throughout the house, concerning general modelling assumptions (multizone, weather data, …), the airleakage distributions, the moisture buffering effect?

It is important to divide the inputs in two categories:

1. The ones which correspond to "standard" data, called "Standard conditions and scenarii",
2. The ones which are data from a given building due to design choices on this building, called "Building design data".

Each of these three steps constitutes a scientific barrier that we propose to come down in this work.

2.1 Review of existing performance-based approaches and ventilation performance indicators in residential smart ventilation strategies

Because this specific field has been shown as worthwhile for identifying both existing performance-based approaches for ventilation and performance indicators, the "smart ventilation" concept has been investigated. Smart ventilation has been defined as "*a process to continually adjust the ventilation system in time, and optionally by location, to provide the desired IAQ benefits while minimizing energy consumption, utility bills and other non-IAQ costs (such as thermal discomfort or noise)"*(Durier, Carrié, and Sherman 2018). The demand-controlled ventilation (DCV) concept is a specific subset of smart ventilation.
Analysis of performance-based approaches that both enable and reward smart ventilation used in five countries (France, Belgium, The Netherlands, USA, Spain) revels emission scenarii, often multizone modelling levels and indicators taken into account (Guyot et al., 2018b).
Through our meta-analysis on the performance reported in 38 studies of various residential smart ventilation systems since 1983 (Guyot et al., 2017), we very clearly identified a scientific problem due to the lack of ventilation performance indicators, most of them being only CO_2 and humidity based indicators.

From these both reviews, we showed the need of robust performance-based approaches for ventilation, using notably better IAQ performance assessment calculation and better IAQ indicators. Moreover, their applicability to all types of ventilation, and not only to smart ventilation is an issue of concern. Indeed, with CO_2-based DCV ventilation for instance, it is easy to obtain a good IAQ performance indicator based on CO_2 cumulative exposure over a threshold, if the switching value of the ventilation system is set just below this threshold. Consequently, the proposed method should allow to obtain a more robust IAQ assessment, based on several IAQ performance indicators using several indoor pollutants, to avoid such pitfalls.

2.2 First proposition of an applicable method

We described and proposed the method with three steps (Figure 2).

In the first step, we identified from a literature review five relevant IAQ performance indicators to be used as output data of such an approach:

- the maximum cumulative exceeding CO_2 exposure over 1000 ppm in the bedrooms,
- the maximum cumulative occupant formaldehyde exposure,
- the maximum cumulative occupant $PM_{2.5}$ exposure,
- the maximum of the percentage of time with RH higher than 70% in all rooms (condensation risk),
- the maximum of the percentage of time with RH outside of the range [30%–70%] in the bedrooms (health risk).

In the second step, we proposed pollutant emission data and occupancy schedules to be used, from an extensive review. Face to the lack of data, we focus on chronic exposure and gave up at the moment $PM_{2.5}$. We proposed a method to calculate average constant formaldehyde emission rates and applied it on a sample of ten low-energy houses. As a result, we proposed to use three levels of formaldehyde emissions: the low-emission class: 4.5 $\mu g.h^{-1}.m^{-2}$, the medium-emission class: 12.0 $\mu g.h^{-1}.m^{-2}$, the high-emission class: 23.6 $\mu g.h^{-1}.m^{-2}$. We also proposed emission data and associated schedules for relative humidity and CO_2.
In the third step, we described the modelling laws and assumptions to be used. We showed notably that it was essential to use multizone modelling, with detailed airleakage distributions on internal partition and external walls (Guyot et al. 2019). Then, we describe the physical model and its resolution, the building modelling, and the boundary conditions to be used in such an approach.
Then, we showed that this method was applicable. Indeed, we applied the proposed performance-based approach on a case study, a low-energy house. We assumed being at the design stage of this house which must comply with a hypothetical regulation, code or label, requiring to calculate the proposed IAQ ventilation performance indicators according to the proposed method. We showed that the method allows to assess the IAQ performance through a radar scheme. We also demonstrated how such an approach could help at the design stage in key choices as the type of structure (regarding its impact on airleakage distributions), the type of ventilation system, the level of pollutant emissions. Indeed, in the studied case, only the balanced ventilation combined with low or medium-emission class of formaldehyde emissions allow to fulfil the IAQ requirements.
We showed also that such an approach could help in the ventilation design, notably the distribution of the air inlets and/or outlets. We showed that with the same total exhaust airflow it was possible to adjust these distributions to fulfil the IAQ requirements.

Lastly, we proposed also a complementary discussion about the non-equivalence of "reference" ventilation systems. "Reference" ventilation systems being usually defined as the widely used ventilation systems, or the ventilation systems directly providing the constant airflows required by the regulation. We showed also that both studied reference ventilation systems: balanced and exhaust-only ventilation system, were not IAQ equivalent with relative gaps between 26 and 70% depending the indicators.

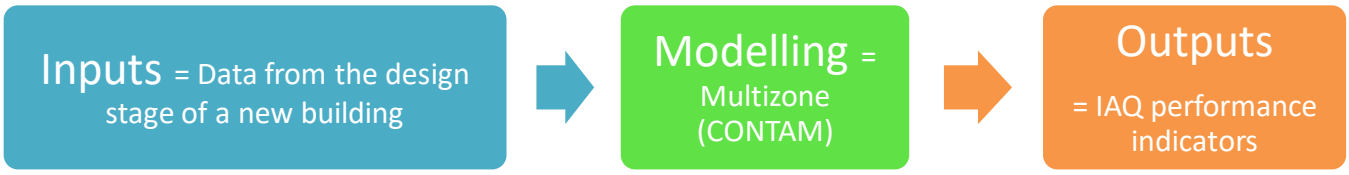

Building design data

- Geometry data for each of the room (multizone approach)
- Envelope airleakage value
- Type of structure: heavy/wooden (regarding the impact of envelope and internal partitions wall airleakage distributions)
- Ventilation system (exhaust-only, balanced, ...) and associated airflows at each of the air inlets and outlets
- Doors (location, size and undercut)
- IAQ labelling of material and products => level of emission (high/middle/low)

Standard conditions and scenarios

1-Standard boundary conditions (as representative as possible):

- Weather : wind speed and direction, temperature, atmospheric pressure, relative humidity,
- Pollutants concentration profiles

2-Standard occupancy scenario

- Number of occupants = f(number of bedrooms), only adults
- At each time-step, how many occupants in each room + activities, for France (see):
- A unique schedule,
- Time spent for each occupant: 9h20 in its bedroom, 2h50 in the living room, 2h40 in the kitchen in 3 periods for breakfast, lunch and dinner, 40 minutes in the bathroom.
- A ventilation high-speed in the kitchen switched-on for 1 hour twice a day.

3-Standard pollutant emissions scenario

- At least: CO_2, humidity, formaldehyde, $PM_{2.5}$
- See Table 14.

Physical model

- Need of multizone (CONTAM, COMIS, ...)
- stack effect model and assumptions,
- wind model and pressure coefficients c_p distribution,
- moisture buffering effect model and assumptions,
- calculation period adapted to the climate and habits of the country,
- time-step > 10 minutes,

Buildings model

- Closed doors,
- Uneven distributions of envelope and internal partition walls airleakage with data proposed in Part 3,
- Models used for airflow calculation at each of the ventilation components,
- Ducts and ventilators could also be modelled in a more detailed approach.

IAQ performance indicators

- At least 5 indicators: see Table 6 with associated thresholds

1.Maximum cumulative exceeding CO_2 exposure (for instance: over 1000 ppm) in the bedrooms,

2.Maximum cumulative occupant formaldehyde exposure,

3.Maximum cumulative occupant $PM_{2.5}$ exposure,

4.Maximum of the percentage of time with RH higher than 70% in all rooms (condensation risk),

5.Maximum of the percentage of time with RH outside of the range [30%–70%] in the bedrooms (health risk).

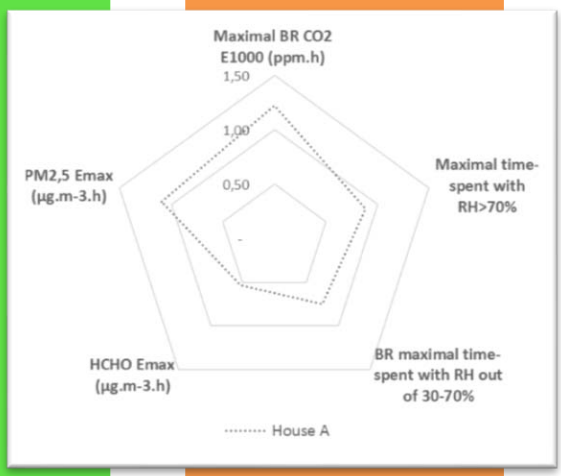

- Rooms ACR also usefull as intermediate metrics

Figure 2. Overview scheme illustrating the proposed performance-based approach for ventilation.

3 CONCLUSIONS AND PERSPECTIVES ABOUT THE REMAINING SCIENTIFIC BARRIERS

At the end of this work, several limitations and perspectives could be highlighted.
Facing a lack of data on pollutant emissions rates at the building scale, it was not possible to include peak exposure and $PM_{2.5}$ in our approach, but it should definitively be completed later as soon as additional data are published.
We showed that the proposed performance-based approach for ventilation was already applicable on houses equipped with constant-airflow reference ventilation systems. We should now check the applicability of our method when applied to smart ventilation systems, as the humidity-based one being also a reference system for France.
From a general perspective, this would be now suitable to study how such a performance-based method at the design stage of a building, could be combined with IAQ or airflows in-situ measurements, to secure the performance at initial commissioning and its sustainably for the whole residential building life.
Lastly, ventilation performance has been restricted to IAQ performance in this work. It is absolutely necessary to extend our method to the global performance of a building, including the energy performance issue, the indoor environment quality (not only IAQ but also comfort …), life-cycle and environmental performance…

4 REFERENCES

Borsboom, W., W. De Gids, J. Logue, M. Sherman, and P. Wargocki. 2016. *TN 68: Residential Ventilation and Health*. AIVC Technical Note 68. http://www.aivc.org/sites/default/files/TN68_Heath%26Ventilation.pdf.

Dimitroulopoulou, C. 2012. "Ventilation in European Dwellings: A Review." *Building and Environment* 47 (January): 109–125. doi:10.1016/j.buildenv.2011.07.016.

Durier, François, F. Rémi Carrié, and Max Sherman. 2018. "VIP 38: What Is Smart Ventilation?" *AIVC*, March. http://aivc.org/sites/default/files/VIP38.pdf.

Guyot, Gaëlle, Hugo Geoffroy, Michel Ondarts, Léna Migne, Mallory Bobee, Evelyne Gonze, and Monika Woloszyn. 2019. "Modelling the Impact of Multizone Airleakage on Ventilation Performance and Indoor Air Quality in Low-Energy Homes." *Building Simulation*, June. doi:10.1007/s12273-019-0557-x.

Guyot, Gaëlle, Max H. Sherman, and Iain S. Walker. 2017. "Smart Ventilation Energy and Indoor Air Quality Performance in Residential Buildings: A Review." *Energy and Buildings*, December. doi:10.1016/j.enbuild.2017.12.051.

Guyot, Gaëlle, Iain S. Walker, and M. H. Sherman. 2018. "Performance Based Approaches in Standards and Regulations for Smart Ventilation in Residential Buildings: A Summary Review." *International Journal of Ventilation*, In-Press.

Matson, Nance E., and Max H. Sherman. 2004. "Why We Ventilate Our Houses-An Historical Look." *Lawrence Berkeley National Laboratory*. http://escholarship.org/uc/item/581331nw.pdf.

Persily, Andrew. 2006. "What We Think We Know about Ventilation." *International Journal of Ventilation* 5 (3): 275–290. doi:10.1080/14733315.2006.11683745.

Seppanen, Olli, and et. al. 2012. *HealthVent Project Report WP5 – Existing Buildings, Buildings Codes, Ventilation Standards and Ventilation in Europe*.

Spekkink, D. 2005. "Key Note Presentation on Performance-Based Building (PeBBu)." In *CIB Conference*. Helsinki, Finland.

Wargocki, Pawel. 2012. "The Effects of Ventilation in Homes on Health." In *Ventilation 2012*, 21 p. Paris, France: INRS.

Performance-based assessment methods for ventilation systems: Overview of on-going work in France and in Europe

François Parsy*[1], Gaëlle Guyot[2]

1 AERECO S.A., 62 rue de Lamirault - Collégien 77615 Marne la Vallée cedex 3 – France

2 Cerema, BPE Research team, 46 rue St Théobald, F-38080, L'Isle d'Abeau, France

**Corresponding author: francois.parsy@aereco.com*

1 KEYWORDS

Ventilation, normalization, regulation, performance, design, indoor air quality

2 SUMMARY

In the field of energy performance, successive regulations pushed a "performance-based" approach, based at least on an energy consumption requirement at the design stage for heating and/or cooling systems (Spekkink 2005). Nevertheless, in the field of building ventilation, regulations throughout the world are mainly still based on "prescriptive" approaches, using airflows or air change rates requirements (Dimitroulopoulou 2012).

This paper introduces the evolution of the French context towards performance-based approaches in the frame of the national building code revision, and on-going work at the European level with the revision of EN 15665 and TR 14788.

2.1 The context in France towards performance-based approaches

Over the past few years, the French context of building performance codes – and especially ventilation – has been changing at an unprecedented pace.

The French dwellings airing regulation (J.O. 1982) consists in a prescriptive approach requiring a general and continuous airing system, a compulsory general layout of ventilation installations, and minimal exhaust airflows in each humid room depending on the total number of rooms in the dwelling.
This regulation has been modified in 1983 to allow a reduction of these minimal airflows for demand-controlled ventilation (DCV) systems. In this case, the manufacturer must follow a performance-based compliance procedure to ensure adequate ventilation. The procedure (CCFAT 2015) describes the common hypotheses (dwellings, occupancy scenarios, weather files, …) used to evaluate the DCV systems using the multizone software MATHIS (Demouge, Le Roux, and Faure 2011). Two IAQ performance indicators are calculated: a condensation risk (number of hours with relative humidity higher than 75%) and a cumulative CO2 exposure exceeding 2000 ppm, further described in (Guyot, Walker, and Sherman 2018). Each room of the dwelling is modelled as single zone, with a time-step of 15 minutes. Once a system receives certification of compliance via this procedure called "Technical Agreement", it can be installed in new dwellings according to its specifications. For each type and size of dwelling, the agreement gives the references of inlets and outlets to be installed, as well as the input data for energy calculations.

This procedure is based on the evaluation of widely used humidity-based DCV systems and thus must be adapted for other types of DCV systems.
In 2018, a working group of the national consultative body described in (Jobert et al. 2018) has been put in charge of developing a methodology to extend this performance-based approach to any new DCV system. This method is based on the procedure used in the Technical Agreements and proposes more relevant performance indicators:

- The cumulative CO2 exposure as a function of CO2 threshold (ppm.h): for concentrations higher than 400 ppm above the outdoor concentration, in every living room and bedroom, the calculated value for a new ventilation system must be lower than the one obtained with a reference system.
- Percentage of cumulative hours with relative humidity higher than the threshold (%): for every threshold higher than 60%, in every room of the dwelling, the calculated value for a new ventilation system must be lower than the one obtained with a reference system.

In addition, the building code is currently being revisited with the aim to allow innovative systems (J.O. 2018). Several working groups (called GT ESSOC) are translating all the prescriptive approaches in the building regulation into performance-based approaches. For ventilation, the on-going work finds its roots in the approaches described above and aims to generalize them at the building stage of every new building.

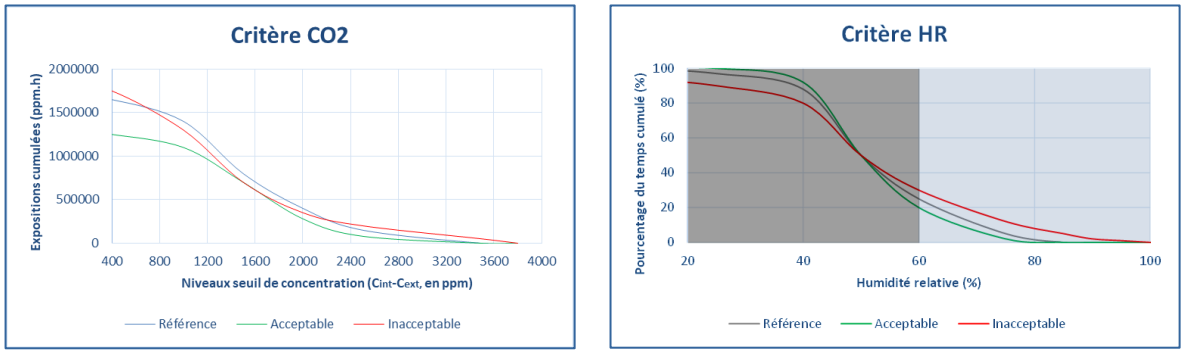

Figure 1: New performance indicators.

2.2 On-going work for the revision of EN 15665 and TR 14788

The performance-based approach has been formally introduced in European standards in 2009 via EN 15665. It was a methodology for regulators to determine minimal airflows to impose in local standards. Today, the revision of this standard, along with the revision of TR 14788, a technical report on design of ventilation systems, is an opportunity to introduce performance-based approaches at a design stage.

EN 15665 is a normative document which purpose is to give a method and to define criteria for evaluating the performance of residential ventilation systems. The target group of this document is the people involved in the redaction of standards and regulations.
A comprehensive method for determining the airflows to require in regulations is described. The procedure includes the selection of key pollutants in each room, of emission scenarios, of criteria to calculate for each pollutant and of requirements to apply to the selected criteria. Three levels of calculation details are proposed to evaluate the performances, ranging from simply specifying a flowrate (prescriptive approach, only evaluated performance is energy, no IAQ) to a full year-long multizone calculation (performance-based approach).
The criteria are a central element in performance-based approach. The standard includes a list of possible criteria to quantify IAQ, as well as recommendations on their use sorted by type of pollutants (humidity, specific pollutants or background pollutants).

TR 14788 is an informative document issued by CEN complementing EN 15665. It gives guidelines for designing and dimensioning residential ventilation systems. The target group for this document is architects, designers, builders and regulators.
First, the document lists parameters to consider when designing and dimensioning a ventilation system: mainly weather, building geometry and airtightness, occupancy and external noise and pollution levels. Second, it describes the end goals of the design: good IAQ, but also thermal comfort, acoustics, and ease of use and maintenance. Third, it gives an overview of common residential ventilation systems. Finally, it sets general and specific design rules concerning

noise, energy and modulation. Information about emission rates of pollutants and calculation methods are given in annexes.

Revision of these documents has begun in 2018. An objective has been set by the working group to merge the two documents in order to create a clear link between the design and the performance of the system.
The two main objectives of this on-going work are: 1) Better describing the performance-based approach in EN 15665 to promote a broader use and expend its normative existence to the design stage, thus backing the existing national regulations of several countries in Europe and opening the way to innovative systems, and 2) Further including hybrid and natural ventilation systems in the text.
The work done so far in this working group tackled the scope and writing rules, system definitions and the structure of the document. The main redactional difficulty ahead will be the articulation of prescriptive and performance-based approaches in the future text.
Registration as a CEN Work Item will be done before the end of 2019, publication can be expected in year 2023.

3 REFERENCES

CCFAT. 2015. “VMC Simple Flux Hygroréglable - Règles de Calculs Pour l’instruction d’une Demande d’avis Techniques - GS14.5 - Equipements / Ventilation et Systèmes Par Vecteur Air.” http://www.ccfat.fr/groupe-specialise/14-5/.

Demouge, François, Nicolas Le Roux, and Xavier Faure. 2011. “Numerical Validation Fo Natural Ventilation Design.” In *32nd AIVC Conference “ Towards Optimal Airtightness Performance.”* Brussels, Belgium. https://www.researchgate.net/profile/Francois_Demouge/publication/232621659_Numerical_validation_for_natural_ventilation_design/links/542123d50cf241a65a1e606b.pdf.

Dimitroulopoulou, C. 2012. “Ventilation in European Dwellings: A Review.” *Building and Environment* 47 (January): 109–125. doi:10.1016/j.buildenv.2011.07.016.

Guyot, Gaëlle, Iain S. Walker, and Max H. Sherman. 2018. “Performance Based Approaches in Standards and Regulations for Smart Ventilation in Residential Buildings: A Summary Review.” *International Journal of Ventilation* 0 (0): 1–17. doi:10.1080/14733315.2018.1435025.

J.O. 1983. *Arrêté Du 24 Mars 1982 Relatif à l’aération Des Logements*.

J.O. 2018. *LOI n° 2018-727 du 10 août 2018 pour un Etat au service d'une société de confiance. (ESSOC law)*

Jobert, Romuald, Andrès Litvak, Gaelle Guyot, and Laurent Deleersnyder. 2018. “Presentation of a National Consultative Body on Ventilation Issues: Actors, Working Groups and Projects Overview.” In *Smart Ventilation for Buildings*. Juan les Pins, France.

Spekkink, D. 2005. “Key Note Presentation on Performance-Based Building (PeBBu).” In *CIB Conference*. Helsinki, Finland.

Performance-based Spanish regulations relating to indoor air quality

Pilar Linares[*1], Sonia García[1]

1 Eduardo Torroja Institute for construction sciences-CSIC
4, Serrano Galvache St.
Madrid, Spain

**Corresponding author: plinares@ietcc.csic.es*

ABSTRACT

As a consequence of the sustainable politics demanding regulations that allow the use of more efficient ventilation systems, the IAQ Spanish regulations were modified and enforced in 2017. The new regulations became performance-based in order to accommodate the use of systems which are capable of adapting required ventilation rates to real needs. The new requirement is based on both CO_2 concentration and a minimum ventilation rate.

The new IAQ requirement is able to keep acceptable IAQ values and to reduce energy demand in relation to the previous IAQ requirement.

KEYWORDS

Ventilation, IAQ, regulations

1 IAQ REQUIREMENT

IAQ level is usually characterized by a maximum level of pollutants that may affect people´s health and comfort and which could be achieved by different ventilation systems.

However, common pollutants are not easy to assess, so an indicator is commonly taken to represent the state of the rest of the pollutants. Among the possible pollutants that are commonly produced indoors, CO_2 is the most commonplace and closest related to human activity. Despite the fact that CO_2 does not entail any health risk in the commonly encountered concentrations, CO_2 is nevertheless a reliable indicator of ventilation rate, for which reason it is the most common indicator used in regulations and guides.

The chosen indicator in the Spanish IAQ regulations is CO_2 concentration, which is limited in two ways:

- 900 ppm maximum yearly average;

- 500000 ppm per hour maximum yearly accumulated above 1600 ppm. This parameter shows the relationship between the CO_2 concentrations reached above a limit value and their duration over a year. It can be calculated as the sum of the areas (ppm·h) within the representation of the CO_2 concentration as a time function and the limit value.

These required concentration levels shall be achieved under certain design conditions (such as occupancy scenarios, CO_2 production rate, yearly average outdoor CO_2 concentration, etc.), that should be set in the regulation. That is, it is a "design performance" because it can only be measurable *in situ* under these conditions.

In addition to this performance-based indicator, a minimum ventilation flow has been established in order to control the concentration of pollutants not related to human activity, but to furniture, paint, etc. such as formaldehydes.

2 VERIFICATION METHOD

Fulfilment of the requirement can be achieved through expert methods (such as specialized software), as well as a simplified verification method. This simplified method is easy to use by non-expert practitioners and consists of a table with different ventilation rates (continuous) (See table 1) that provide fulfilment of the requirement for different dwelling types.

Table 1. Continuous ventilation rates values

Dwelling case study	Continuous ventilation rate (1) (l/s)	Total whole dwelling continuous ventilation rate (l/s)	Yearly average CO_2 concentration (2) (ppm)	Yearly accumulated over 1.600 ppm (2) (ppm·h)
1	6	12	816	0
2	8	24	812	145860
3	11	33	789	150020
4	11	33	848	247000
5	8	24	826	105560

(1) In kitchen and each bathroom.
(2) The highest value per room in each dwelling.

The dwelling types are classified taking into account their bedroom and bathroom counts (See Table 2).

Table 2. Dwellings types

Kind and composition of dwelling	Types
Flat: Living/Kitchen+1 Bedroom+1 Bathroom	1
Flat: Living+Kitchen+2 Bedrooms+2 Bathrooms	2
Flat: Living+Kitchen+3 Bedrooms+2 Bathrooms	3
Flat: Living+Kitchen+4 Bedrooms+2 Bathrooms	4
Terraced house: Living+Kitchen+4 Bedrooms+2 Bathrooms	5

3 REFERENCES

Linares, P., García, S. et al (2014). Proposed change in Spanish regulations relating to indoor air quality with the aim of reducing energy consumption of ventilation systems. PROCEEDINGS of 35th AIVC Conference, 4th TightVent Conference and 2nd venticool Conference: Ventilation and airtightness in transforming the building stock to high performance. Poznań (Poland).

*Código Técnico de la Edificación (*Building Code*). Ministerio de Fomento*. On line. http://www.codigotecnico.org/web/recursos/documentos/ [Consulted 18/06/2015]

Challenges and limitations of performance based approaches: the Belgian experience

Samuel Caillou[1], Sébastien Pecceu[*1]

1 Belgian Building Research Institute (BBRI)
Brussel, Belgium
* sebastien.pecceu@bbri.be

KEYWORDS

Demand controlled ventilation, IAQ criteria, performance based approach.

INTRODUCTION

Performance based approached for ventilation started to be used in Belgium in 2008 in the context of EP regulation. Until 2015, demand controlled ventilation (DCV) systems were considered as "innovative" products and were not directly taken into account in the EP calculation method. Their energy performance was then considered through a principle of equivalency. A first performance based approach was developed in this frame.

As DCV systems became more and more common, it became considered as a "mature" technology and then was included in the basis EP calculation method in 2015. The reduction factors of the method were determined using an updated method based on the existing equivalency approach.

This experience has been then used in many research projects. Among these projects, the recent PREVENT project aimed at the elaboration of new performance criteria and design rules (simplified rules) for ventilation systems in dwellings. This project emphasized also the need, in complement to simplified rules easily applied for simple systems, to have performance based approaches to be able to evaluate the performances (IAQ and Energy) of some more complex systems, such as natural ventilation systems, some DCV systems, etc. Performance criteria were used to compare different ventilation systems, whether they were using DCV or not.

The challenges are however still big and experience acquired through these various steps are of great value. The aim of this paper is to illustrate some challenges and limitations of such performance based approaches for ventilation system.

SIMULATION METHODOLOGY

The simulation methodology used in the equivalency principle in Belgium has evolved with time and the complexity of the systems which have been tested. The last evolvements of this method has already be described (Caillou, Laverge, Van Gaever, & Janssens, 2014) (Pecceu, Caillou, & Van Gaever, 2018) and the main common principles can be summarized as follows.

- The simulations are carried out on model dwelling using the simulation software CONTAM.
- The used IAQ metrics are cumulated CO_2 exposure of occupants and risks of condensation based on RH in service spaces

The IAQ criteria and energy references have evolved with time, from an absolute, but weak, IAQ criteria and a fixed flow rate in the first methodology to a trade-off approach combining IAQ and energy evaluation together in the last evolution steps of the methodology.

However, one of the challenges of this methodology was that the ventilation systems prescribed in the current ventilation standard in Belgium (NBN D 50-001) were not necessarily equivalent regarding IAQ and flow rate performances.

CHALLENGES AND LIMITATIONS: ILLUSTRATION FROM EXAMPLES

We choose to illustrate the challenges and limitation by several examples encountered at various steps in the above-mentioned history.

- Natural ventilation system with DCV

A first example concerns a natural system (natural exhaust and supply – A system in the Belgian Standard). In this example, a natural exhaust opening controlled by humidity in the service lead to a lower CO_2 exposure (better IAQ) for the occupants in the living spaces, while average flow rate at building scale was lower than for the system at full capacity.

Analysis showed that the controlled exhaust in closed position indirectly redirects the flow rate to the living spaces at the first floor, where the air is leaving the building rather than entering but resulting in a higher air change rate in these rooms. The improvement is in fact mainly due to the poor performance of the not controlled system used as reference.

- Mechanical exhaust ventilation (MEV) with DCV based on RH in service spaces

With an absolute and weak IAQ criteria in the first versions of the methodology, using a RH detection in service spaces lead to a significant flow rate reduction compared to a constant flow system. This translated into a significant advantage in the EP calculation, but with a decrease in IAQ (while still respecting the absolute criteria).

In a latter version, using the reference curve approach (considering both flow rate reduction and IAQ, see “Methodology), one showed that this type of regulation presents no advantage compared to a constant flow rate ventilation.

- Mechanical exhaust ventilation (MEV) with CO_2 controllable supply grid in the day zone

In the studied case, this system with a CO_2 controllable grid in the day zone allowed to better control the fresh air supply in the bedrooms in the night zone. This system was particularly effective, compared to the reference MEV, in an airtight model dwelling with the day and the night zones opened on each other via a common hallway (as considered in the basis methodology).

However, more detailed analysis showed that this advantage decreased when the day and night zones were closed on each other, and was completely loosed, compared to the reference MEV, when theses zones are separated by an airtight partition.

- MEV system with supply grid on roof pane

Supply grid should normally be on walls but are sometimes placed on roof panes in specific configurations (e.g. attic transformed in bedroom). For non-airtight building, simulations showed that the CO_2 exposure in these conditions is quite low (good IAQ), but it is mainly

because the flow is going out through the inlet grid (due to wind under pressure). This is not the expected working of the system, and it is well possible that air from the service spaces or the living room is transferred to this bedroom. This is not covered by the used criteria.

CONCLUSIONS

All these examples illustrate the main challenges to solve in order set-up a relevant performance based approach for ventilation systems

- The difficulty to consider both energy and IAQ at the same time
- The risks and difficulties inherent to the use of an absolute criteria (definition and threshold) or a relative criterion (strongly dependent of the reference(s))
- The possibility that the criteria miss some aspects, or inversely the possible multiplication of criteria to cover all aspects.

REFERENCES

Caillou, S., Laverge, J., Van Gaever, R., & Janssens, A. (2014). Méthode de calcul PER - Facteurs de réduction pour la ventilation à la demande.

Pecceu, S., Caillou, S., & Van Gaever, R. (2018). Demand Controlled Ventilation: relevance of Humidity Based Detection Systems for the Control of Ventilation in the Spaces Occupied by Persons. *AIVC*.

Demand controlled ventilation: Sensitivity and robustness of the performances

Xavier Faure

Univ Paris Saclay, CEA, CTReg
PdlL, F-44340 Bouguenais, France

SUMMARY

Demand controlled ventilation (DCV) seems to be the main way to comply with both energy and internal air quality (IAQ) concerns. Largely spread in non-residential building since more than 2 decades (Fisk, 1998) because of large potential energy savings, its application for the residential sector is nowadays becoming the basis of ventilation systems for dwellings. Indeed, thermal regulations for residential buildings in several countries give targets that are difficult to reach with constant air changes rates. In France, the successive higher thermal regulation requirements have led to the development of humidity based DCV systems. Since a decade, it is considered as the reference system of ventilation.
DCV strategy are developed under performance targets in order to reach threshold values for IAQ evaluation while minimising the energy impact. The performance based approach in France consist in making multizone simulation for each type of dwelling with fixed parameters. These lasts are the envelope leakage in each zone, the weather conditions (pressure coefficient, wind velocity and direction, temperature, external humidity), the domestic activities and occupant presence in the different zones.
These fixed parameters enable to make objective evaluation between two systems and thus quantify the performance of each system. The inconvenient of such approach, and mainly the deterministic parameters used, is that DCV strategies are optimized for these specific cases and thus the DCV strategy might be less effective in real situation than the numerical ones.
The present study aim to identify the global sensitivity of the DCV performance on these deterministic parameters. RBD FAST global sensitivity analysis is realized on a specific building configuration with a specific DCV system that comply with today French thresholds targets. Analyses are realized dynamically and thus integrates weather conditions variability on the sensitivity indexes. The most important parameters are highlighted as well as the influence of external conditions on the main indexes. Even though DCV strategy enable to comply with both IAQ and energy targets, their performances might be not guarantee for any cases for both, occupancy and building characteristics. Thus, the next issues migth be, how DCV could be more resilient in the future.

KEYWORDS

Demand controlled ventilation, sensitivity analyses, RDB FAST

1 METHODS

1.1 Studied case

This study is realized on a F4 type dwelling with two levels. It consist in a kitchen and living room in the first floor. Three bedrooms, bath room ad toilet are in the second floor. A common hall enable the link between the two floors. The building characteristics, occupancy, domestic activities follow the recommendation of the French evaluation [CCFAT, 2017].

1.2 Methods

Global sensitivity analyse is used to identify the first order indexes of the studied parameters on a specific outputs. Several outputs are considered in this study as well as the global value that should comply with the evaluation thresholds in the French protocol.
Fourier Amplitude Sensitivity Test (FAST) is realized on the studied case presented above. FAST consist in analysing the impact of several parameters in the frequency domain. A pool of simulation runs is realized modifying, for each, the different parameter's value. Analyses are then realized at each time step along the number of runs axis.
In order to limit the number of simulation, the RBD FAST methods is used. It enable to considerably reduce the number of simulation needed to evaluate the first order indexes. More information on this specific methods can be found in [Sobol (1993), Mara (2009)].

2 RESULTS

The figure below presents, on the same studied case the impact of the zone leakage on the threshold value for several runs with randomly distributed leakage, keeping identical the global building leakage. The French threshold value is highlighted by the black horizontal line. The influence of the leakage is highlight but is not the only important element that influences this computed IAQ Index as shown by the several uncorrelated points in the figure: even for high leakage value, IAQ isn't satisfied.

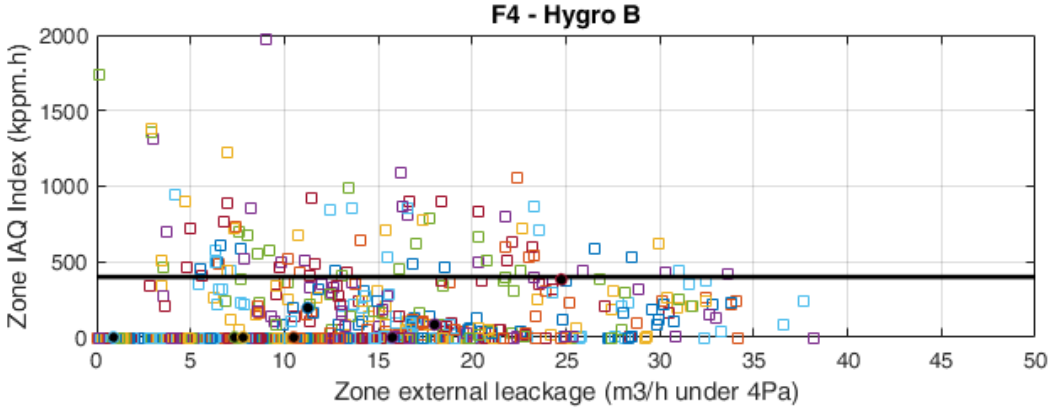

These present study aim into identifying, in a first part, for which external conditions the leakage can be the most important parameter. In a second part, between other parameters as wind pressure coefficient assumptions, occupancy, internal leakage, who is the most important and for which conditions on several time dependent outputs as well as global outputs such as the one that should comply with the threshold in the French evaluation protocol. Analyses and discussion are proposed around these methods and results.

3 REFERENCES

CCFAT (2017), *VMC simple flux hygroréglable : règles de calculs pour l'instruction d'une demande d'avis technique (rev. 01, 2017)*, http://www.ccfat.fr/groupe-specialise/14-5/

T. Mara (2009) *Extension of the RBD-FAST method to the computation of global sensitivity indices* Reliab. Eng. Syst. Saf., 94 (8) (2009), pp. 1274-1281

Sobol, I. M. (1993) *,Sensitivity estimates for nonlinear mathematical models,.* Mathematical Modelling and Computational Experiment 1 :407-414

Applicability of a simple and new airtightness measuring method and further comparisons with blowerdoor measurements

Timothy Lanooy[*1], Niek-Jan Bink[1], Wim Kornaat[2], and Wouter Borsboom[2]

1 ACIN instrumenten B.V
Handelskade 76
Rijswijk,the Netherlands
**Corresponding author: t.lanooy@acin.nl*

2 TNO
Leeghwaterstraat 44
Delft, the Netherlands

ABSTRACT

The building airtightness is essential to achieve a high energy performance. In most countries however, it is not mandatory to measure the airtightness. In the Netherlands it is common practice to just take a couple samples in a housing project. These samples do not give a good indication for all the buildings in a project. It is therefore important to measure the airtightness of all the buildings.

Current methods for airtightness measuring are too expensive and time consuming to make this feasible. A method with a new device , the AirTightnessTester (ATT), is tested. By using the buildings ventilation system, a reduction in price and time can be achieved. The ATT measures in compliance with RESNET-380-2016.

The ATT makes use of the ventilation system of the building. It will be explained when and how the ATT actually can cooperate with a ventilation system. We have looked at the different brands of ventilation systems in somewhat more detail to analyze the feasibility of our method in practice. It is concluded that several systems can be used as they are now. The systems that can't be used directly or easily could be modified by the manufacturer to accommodate our method, which is also to their advantage. Some ventilation systems cannot be turned on and off easily. For these ventilation systems a setting switching method has been developed. The theory behind this method, and some preliminary results using this method will be presented.

To validate measurements with the ATT, comparisons have been done to the blowerdoor. Preliminary results were already presented during the 2018 AIVC conference (Lanooy et al, 2018) but further validation was still necessary. The measurements with the blowerdoor are multi-point measurements and are all done in compliance with ISO9972. The measurements done with the ATT are all single-point The comparisons are done to the blowerdoor, because it is the most used method for airtightness measuring. To get a fair comparison, the uncertainty of both methods are taken into account.

Overall the blowerdoor and the ATT give similar results for the airtigthness. However, it has been observed that in most cases the ATT will measure a higher leakage in comparison to the blowerdoor.

KEYWORDS

Airtightness, Single-point, blowerdoor, RESNET

1 INTRODUCTION

The building airtightness is essential to achieve a high energy performance. In most countries however, it is not mandatory to measure the airtightness. In the Netherlands it is common practice to just take a couple samples in a housing project. These samples do not give a good indication for all the buildings in a project. It is therefore important to measure the airtightness of all the buildings.

Current methods for airtightness measuring are too expensive and time consuming to make this feasible. A method with a new device , the AirTightnessTester (ATT), is tested. By using the buildings ventilation system, a reduction in cost and time can be achieved.

The ATT makes use of the ventilation system of the building. Measuring the airtightness with the ventilation system of the building is not a new method, and has been described in the RESNET-380-2016[3]. What the ATT does different is the use of an indoor reference vessel. Instead of measuring the pressure differential inside and outside of the building, it is measured between the reference vessel and inside the building.

The use of an indoor reference vessel has some technical advantages. No opening in the building envelope is necessary, meaning the whole building envelope, including the exterior door, is measured. Another advantage is that the reference is an average of the pressure over the whole building, instead of a reference at one point, which is the case with a blowerdoor. The fact that the reference is an average of the whole building, and is measured indoors also makes the measurement with the ATT less susceptible to wind.

To validate measurements with the ATT, comparisons have been done to the blowerdoor. Preliminary results were already presented during the 2018 AIVC conference (Lanooy et al, 2018[1]). Some ventilation systems cannot be turned on and off easily. For these ventilation systems a setting switching method has been developed. The theory behind this method, and some preliminary results using this method will be presented. All measurements with the blowerdoor are done in compliance with the ISO9972 standard[2].

2 METHOD

2.1 General workings of the ATT

At the start of the measurement, the reference vessel is closed when the ventilation system is turned off and will remain closed for the duration of the measurement. The pressure inside the vessel is now equal to the pressure of the building with the ventilation system turned off.

When the ventilation system is turned on, a pressure difference will occur between the reference vessel and the building itself. This pressure difference, together with the flow rate of the ventilation system, is a measure for the airtightness (equation 1).

$$q_{v,P_r} = q_{v,sys} \cdot \left(\frac{P_r}{\Delta P} \right)^n \tag{1}$$

where:

$q_{v,Pr}$:	airtightness at the reference pressure P_r	[l/s]
$q_{v,sys}$:	flow of the ventilation system	[l/s]
P_r:	reference pressure	[Pa]
ΔP:	pressure differential between the reference vessel and building	[Pa]
n:	air flow exponent.	[-]

Because the airtightness is measured at only one pressure difference and flow rate, it is not possible to determine the flow exponent. This means that an assumption must be made on the flow exponent. The flow exponent in houses typically ranges between 0,55 and 0,75. The average flow exponent is determined to be 0,66.

Multiple cycles of turning the ventilation system on and off are done. This way an uncertainty can be calculated and errors caused by pressure variations reduced. The total uncertainty of a measurement done with the ATT is calculated through propagation of error. All uncertainties involved in this calculation are independent.

$$\sigma_{q_{v,P_r}} = \sqrt{\left(\frac{\delta q_{v,P_r}}{\delta q_{v,sys}}\right)^2 \cdot {\sigma_{q_{v,sys}}}^2 + \left(\frac{\delta q_{v,P_r}}{\delta \Delta P}\right)^2 \cdot {\sigma_{\Delta P}}^2 + \left(\frac{\delta q_{v,P_r}}{\delta n}\right)^2 \cdot {\sigma_n}^2} \quad (2)$$

The uncertainty of the flow of the ventilation system is dependent on the device that is used to measure this flow. The uncertainty of the air flow exponent is an assumed value of ±0,10[1]. The uncertainty is of the pressure differential is the deviation of the average block signals. This uncertainty contains the most information in terms of the measured signal itself. The deviation between block signals can be caused by various sources.

One of the factors that can cause a variation in the signal is a change in the bias pressure. A constant bias cannot be observed by the ATT, as the pressure difference between the vessel and the building at the start of a measurement is 0 Pa. However, when measuring the block signal, a change in the pressure difference whilst the ventilation system is turned, could be caused by a change in bias.

Another factor that could be the cause of a variation in the pressure signal is a variation in the flow of the ventilation system. It cannot be determined which of the factors is the cause for a variation in the block signal, and the most likely scenario is that it is a combination of the factors, but for the calculation of the total uncertainty it is not necessary to know which of the factors is the cause for this variation, as long as the variation is taken into account in equation 2.

2.2 Equations for the adjusted ATT measurement method

In practice it has been noticed that it is not always possible to turn the ventilation system on and off without causing a long start up sequence. This sequence can negatively impact the measured signal, making it impossible to get a proper pressure signal for the calculation. For systems where this is the case, an alternative method has been theorized.

Instead of measuring between the ventilation system turned on and off, a measurement can be done by switching the settings of the system between a high and a low flow. This way a long start up sequence can be avoided. The equation to calculate the airtightness will need to be altered to accommodate an extra flow.

$$q_{v,P_r} = \left(q_{v,high}^{\frac{1}{n}} - q_{v,low}^{\frac{1}{n}}\right)^n \cdot \left(\frac{P_r}{\Delta P}\right)^n \quad (3)$$

It can be observed that when $q_{v,low} = 0$ is filled into this equation, the original ATT equation (equation 1) is regained. The extra flow also brings an extra uncertainty, making the total uncertainty, calculated through propagation of error:

$$\sigma_{q_{v,P_r}} = \sqrt{\left(\frac{\delta q_{v,P_r}}{\delta q_{v,high}}\right)^2 \cdot \sigma_{q_{v,high}}{}^2 + \left(\frac{\delta q_{v,P_r}}{\delta q_{v,low}}\right)^2 \cdot \sigma_{q_{v,low}}{}^2 + \left(\frac{\delta q_{v,P_r}}{\delta \Delta P}\right)^2 \cdot \sigma_{\Delta P}{}^2 + \left(\frac{\delta q_{v,P_r}}{\delta n}\right)^2 \cdot \sigma_n{}^2} \quad (4)$$

Because of an extra flow uncertainty and multiple occurrences of the flow exponent in equation 1 (in general the largest uncertainty of measurement done with the ATT), it is expected that the total uncertainty with this method will be higher in comparison to a measurement done where the ventilation system is turned on and off.

2.3 Uncertainty of a measurement with the blowerdoor

All measurements with the blowerdoor are done in compliance with the ISO9972 standard. With regards to the uncertainty, this standard only gives a recommended procedure for estimating the uncertainty in the air leakage coefficient and air flow exponent. This procedure does not take into account the uncertainty in the flow and the pressure measurement.

A method to calculate the total uncertainty of a blowerdoor measurement, taking into account all variables, has been described before (Delmotte, 2013[4]). These variables include the bias pressure, external temperature and internal temperature. It also correlates the errors in the air leakage coefficient and air flow exponent. Two equations are derived, one for depressurization (equation 5) and one for pressurization (equation 6).

$$\sigma_{q_{v,P_r}} = \sqrt{\left(\frac{\delta q_{v,P_r}}{\delta a}\right)^2 \cdot \sigma_a{}^2 + \left(\frac{\delta q_{v,P_r}}{\delta b}\right)^2 \cdot \sigma_b{}^2 + \left(\frac{\delta q_{v,P_r}}{\delta T_e}\right)^2 \cdot \sigma_{T_e}{}^2 + 2\left(\frac{\delta q_{v,P_r}}{\delta a}\right)\left(\frac{\delta q_{v,P_r}}{\delta b}\right)\sigma_a \sigma_b r(a,b)} \quad (5)$$

$$\sigma_{q_{v,P_r}} = \sqrt{\left(\frac{\delta q_{v,P_r}}{\delta a}\right)^2 \cdot \sigma_a{}^2 + \left(\frac{\delta q_{v,P_r}}{\delta b}\right)^2 \cdot \sigma_b{}^2 + \left(\frac{\delta q_{v,P_r}}{\delta T_i}\right)^2 \cdot \sigma_{T_i}{}^2 + 2\left(\frac{\delta q_{v,P_r}}{\delta a}\right)\left(\frac{\delta q_{v,P_r}}{\delta b}\right)\sigma_a \sigma_b r(a,b)} \quad (6)$$

where:

a:	air flow exponent	[-]
b:	natural log of the air leakage coefficient	[l/s/Pa^n]
T_i:	internal temperature at the time of measurement	[K]
T_e:	external temperature at the time of measurement.	[K]

All blowerdoor uncertainties in this paper are calculated according to these equations. To determine the uncertainty in a and b, a weighted least-square calculation is used. This calculation takes into consideration the uncertainties in the flow and pressure measurement in the regression calculation for a and b (Cantrell, 2008[5]). This method requires an iterative calculation, which is done via Excel.

3 RESULTS

All measurements were done in the same order. First a blowerdoor measurement is done in compliance with ISO9972, including closing off the buildings own ventilation system. After the blowerdoor measurement is done, the blowerdoor remains setup, with the blowerdoor fan closed off. This is done to get the situation as comparable as possible and because the new buildings measured did not always have a front door yet. The buildings own ventilation system was then connected back up and a measurement ATT was done, either by switching the ventilation system on and off or by switching between a high or a low setting.

3.1 ATT measurements done by switching the ventilation system on and off

Most of the collected data was done via the original ATT measurement method, switching between a flow and zero. The results of the collected dataset of comparison are split into two figures for readability, figures 1 and 2.

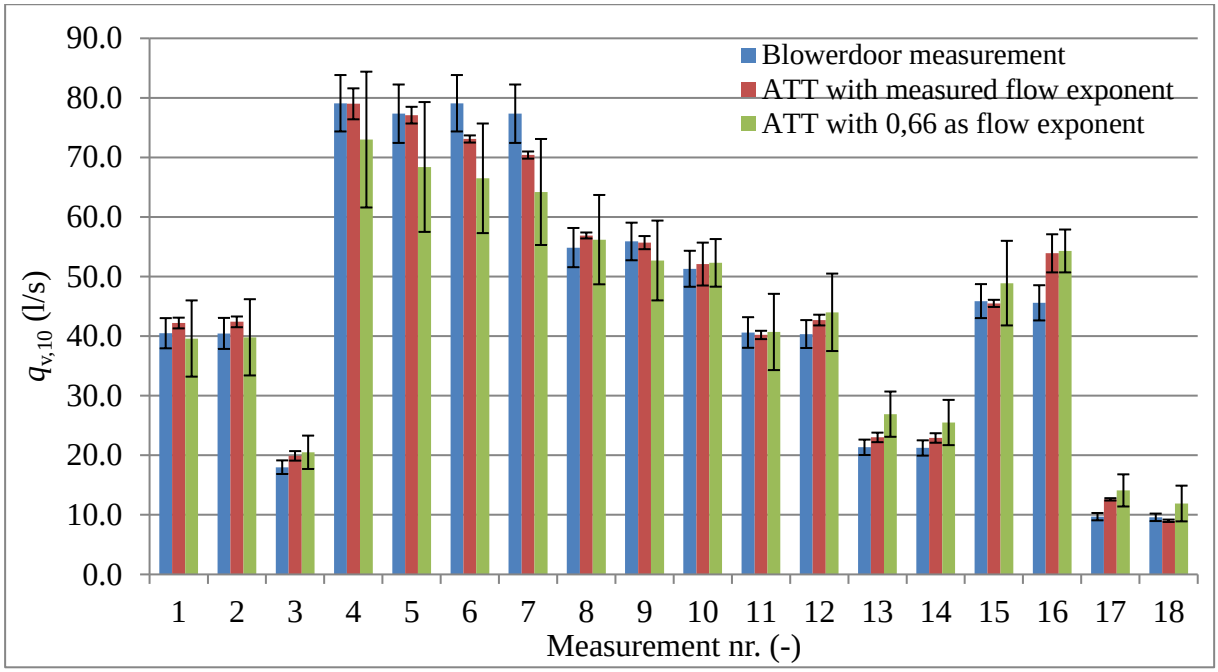

Figure 1: ATT measurement with a measured and fixed flow exponent compared to the blowerdoor.

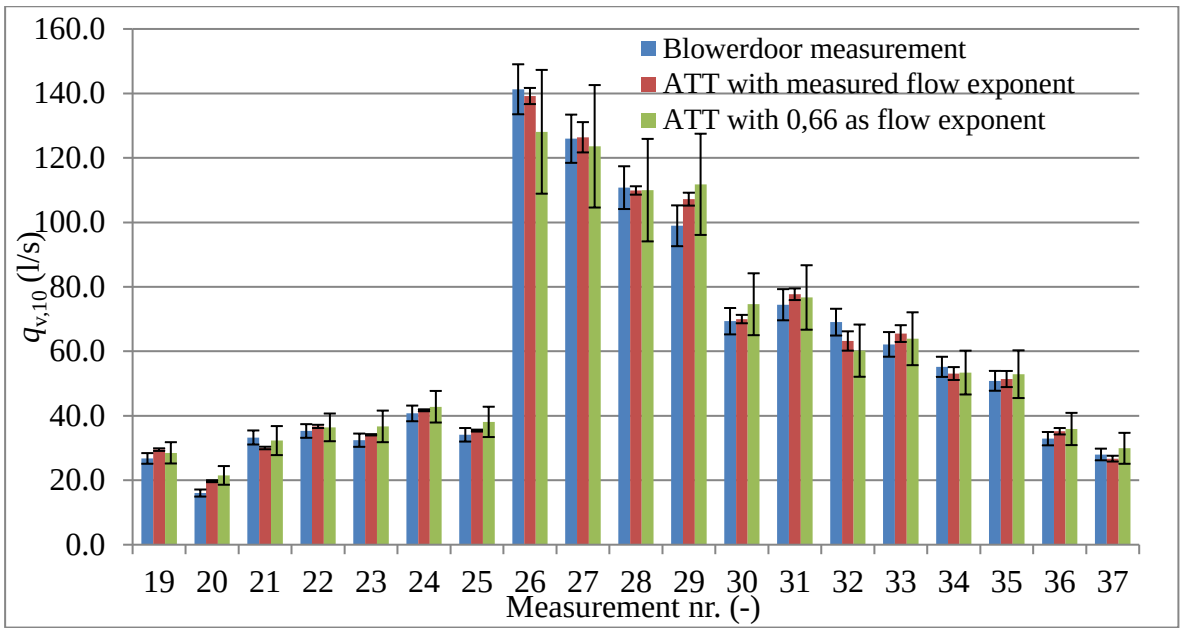

Figure 2: ATT measurement with a measured and fixed flow exponent compared to the blowerdoor.

In 23 of the 37 measurements it was found that the measured airtightness with the ATT was slightly higher than the measurement with the blowerdoor. Together with the data collected and presented in the first paper regarding the ATT[1], it can be concluded that this increase appears to be systemic needs to be researched further.

3.2 ATT measurements done by switching the ventilation system high and low

In figure 3 the results of measurements done with the ATT using a high and a low ventilation system flow are plotted, together with the blowerdoor measurement. To give an indication of the impact of using a fixed air flow exponent of 0,66, the calculation with the ATT has been done with both the flow exponent as measured with the blowerdoor and a flow exponent of 0,66. The uncertainty has also been plotted as error bars.

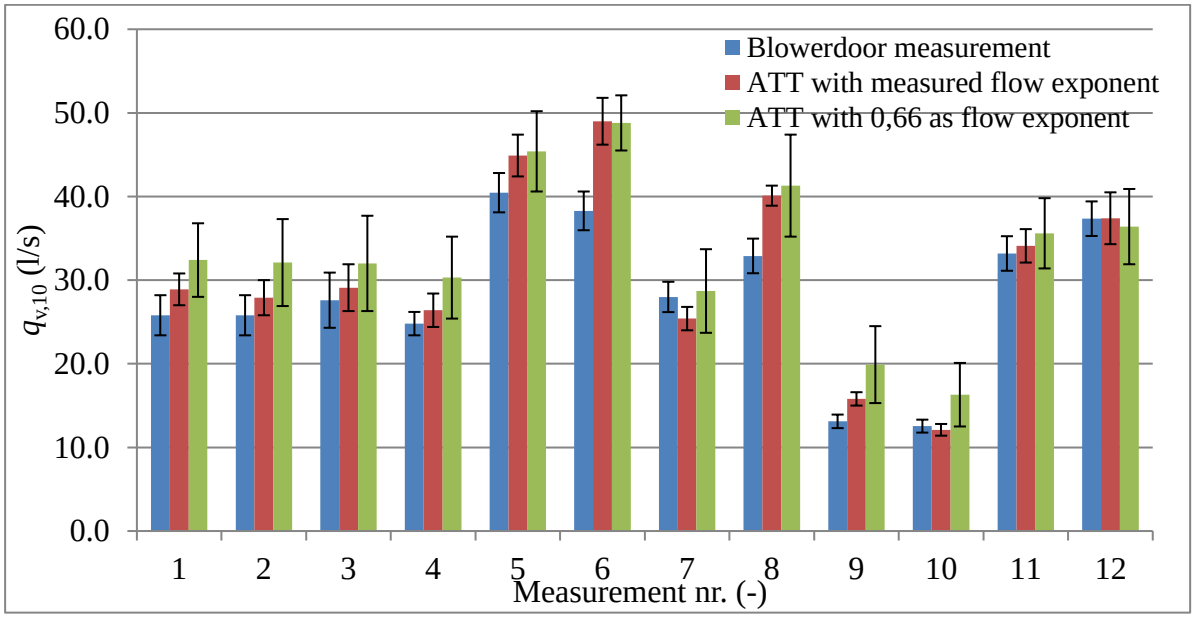

Figure 3: ATT new calculation with a measured and fixed flow exponent compared to the blowerdoor.

The airtightness value as measured with ATT with a measured flow exponent is higher in 10 of the 12 cases. The airtightness when using a fixed flow exponent is higher or lower depending on whether the measured flow exponent is higher or lower than 0,66.

It can be observed that when using a measured flow exponent, the ATT and the blowerdoor have similar uncertainties. The uncertainty when using a fixed flow exponent is always higher, which was expected.

From this dataset is can be concluded that measuring by changing the flow between high and low does not give any big differences with the blowerdoor measurement and could be used as an alternative in case of a situation where the ventilation system cannot be turned on and off without causing disturbances in the measured signal.

3.3 ATT measurement with on/off compared to measurement with high/low

Six measurements have been done where a building was measured twice with the ATT, once by switching the ventilation system between on and off and once by switching between high and a lower setting. The results from these measurements are in table 1.

Table 1: Measurements done with the ATT with both methods.

Measurement	$q_{v,10}$ on/off (l/s)	$\Delta P_{on\text{-}off}$ (Pa)	$q_{v,10}$ high/low (l/s)	$\Delta P_{high\text{-}low}$ (Pa)
1	30,9±3,2	27,5	32,4±4,4	22,4
2	28,2±3,5	34,6	32,0±5,7	20,2
3	27,4±2,9	28,7	30,3±4,9	15,9
4	29,9±4,8	48,6	28,7±5,0	25,1
5	30,9±3,2	27,5	32,1±5,2	17,8
6	35,9±5,0	39,5	41,3±6,1	27,5

As expected, the uncertainty is higher when using switching between a high and a low setting in comparison to switching the system on and off. This is caused by the second flow and the lower pressure signal. In measurement 4 the difference in uncertainty is small. This is caused by the reference pressure. Since the airtightness is calculated to a reference pressure of 10 Pa, the uncertainty caused by the flow exponent will be bigger when the measured pressure signal is further away from 10 Pa. When switching between a high and low setting, the generated pressure signal will be lower than when the ventilation system is switched between on and off.

4 CONCLUSIONS

In this paper a methodology for airtightness measurements through fan pressurization is described. This methodology measures the airtightness through the ventilation system of the building itself. Instead of measuring the pressure between inside and outside the building, the ATT measures the pressure differential between inside the building and an indoor reference vessel. This makes it possible to measure the entire building envelope, including an exterior door.

Measurements with the ATT were further validated by comparing measurements done with the ATT with a blowerdoor measurement. In general it can be concluded that a measurement with the ATT gives a slightly higher airtightness value then a blowerdoor measurement. More research is still being done to determine the cause of the difference. The current theory is that this is caused by the difference in reference pressure, as the blowerdoor takes the reference in one place and the ATT takes its reference as an average over the whole building.

In this paper an adjusted method for measuring was also presented. Instead of switching the ventilation system on and off, it is possible to switch between a high and low flow. Switching between high and low is not the preferred method of testing, because of the increase in the uncertainty, caused by the extra flow in the calculation and the low pressure signal. The increase in uncertainty is however not that large that the measurement becomes unusable to judge whether a building passes its airtightness requirement. It can therefore be used when it is not possible to do a measurement by switching between on and off.

5 REFERENCES

[1] Lanooy, T., Kornaat, W., Bink, N.J., Borsboom, W., (2018). *A new method to measure building airtightness.* Juan-les-Pins, France, Proceedings of the 39th AIVC Conference, 18-19 September 2018.

[2] International Organization for Standardization (ISO). *ISO 9972:2006*: *Thermal performance of buildings – Determination of air permeability of buildings -- Fan pressurization method*. Geneva, Switzerland.

[3] Residential Energy Services Network (RESNET). *RESNET 380-2016: Standard for Testing Airtightness of Building Enclosures, Airtightness of Heating and Cooling Air Distribution Systems, and Airflow of Mechanical Ventilation Systems.* Washington, USA.

[4] Delmotte, C., (2013). *Airtightness of buildings - Calculation of combined standard uncertainty*. Athens, Greece, Proceedings of the 34th AIVC Conference, 25-26 September 2013.

[5] Cantrell, C. A., (2008). *Technical Note: Review of methods for linear least-squares fitting of data and application to atmospheric chemistry problems*. Atmos. Chem. Phys., 8, 5477-5487.

Refined assessment and comparison of airtightness measurement of indoor chambers using the blower door and Pulse methods

Xiaofeng Zheng[*1], Luke Smith[2], Adam Moring [2], and Christopher J Wood[*1]

1 Building, Energy and Environment Research Group,
Faculty of Engineering, University of Nottingham
University Park, Nottingham NG7 2RD, UK

***2** Build Test Solutions Ltd., 16 St Johns Business Park, Lutterworth LE17 4HB, United Kingdom K*
**Corresponding author:*
xiaofeng.zheng@nottingham.ac.uk
christopher.wood@nottingham.ac.uk

ABSTRACT

Previous studies have compared the airtightness measurement of test enclosures utilising both the novel Pulse technique and the conventional blower door method. Discrepancies between results of the two test methods were observed and it was concluded that differences either caused by wind or blower door installation integrity would have had an impact upon the results. This study, as a continued investigation as well as validation process for product development, reports on an experimental investigation that assesses the airtightness of an indoor chamber using both the blower door and Pulse methods with the envelope difference and wind impact being minimized. This was achieved by utilising two door-sized rigid panels to replace the existing door of an indoor chamber in the setup of the blower door and Pulse units. The blower door fan was located within one of these solid panels, which then negated any impact of leakage that would have otherwise been incurred around the frame of the blower door. A wooden plate with multiple openings was utilised and mounted in the chamber envelope to provide various leakage levels and characteristics for testing by taping up different number of openings, in which airtightness tests were performed using both methods in an overlapped pressure range. This allowed both methods to be compared directly with minimum difference in testing conditions. Tests were also carried out in a house-sized indoor chamber to assess the repeatability of the Pulse unit and its agreement with the blower door test. The initial results showed that in most of the testing scenarios a good agreement (up to 7.4%) was observed between the leakage results given by both methods; however a larger discrepancy was seen in the case where the largest opening was present. Strong repeatability was observed in the Pulse testing with an overall measurement uncertainty of ±5%; with a similar spread also presented by the blower door test method as part of the chamber testing.

KEYWORDS

Building airtightness, Blower door, Pulse, Sheltered environment

1 INTRODUCTION

A fundamental challenge for the Pulse technique is that its primary function, the ability to measure air leakage reliably at low pressures and report air permeability at a pressure rise of 4Pa, is difficult to directly validate. Citing air leakage at 4Pa is also at odds with established industry practices and building regulations which conform only to the established blower door method of testing at high pressure (typically reporting leakage at a 50Pa pressure difference).
Pulse has been specifically developed to measure leakage at 4Pa because this value is citied within a range of ASHRAE (Sherman 2004, Sherman 2009) and CIBSE standards (CIBSE TM23) as being a representative ambient background pressure level within occupied buildings i.e. the pressure level at which background exfiltration/infiltration occurs. Under normal real world test conditions, the blower door cannot directly measure at this low-pressure level and its results must therefore be extrapolated down which in itself causes large uncertainty errors,

whilst similarly, the Pulse 4Pa results cannot be reliably extrapolated up to 50Pa. One of the primary objectives of the lab-based chamber testing therefore has been to evaluate 4Pa Pulse vs 50Pa Blower Door further through a range of constructed lab based tests where blower door test pressures and Pulse test pressures are made to overlap.

Studies on the comparison of the blower door and Pulse methods in natural (Zheng 2018) and sheltered conditions (Zheng 2017) were previously reported. It was found that under sheltered conditions where the external weather condition has reduced impact on the testing, both methods showed a close agreement (0-5.3%) with each other on the measurement of air permeability at 4 Pa under most testing scenarios. Larger discrepancies, shown in the highly airtight scenarios, were attributed to the fact that insufficient time was captured in the 'quasi-steady period' of the Pulse test due to the combination of the fixed pulse test timing and delayed pressure pulse. In the natural conditions, the comparison study gave discrepancies ranging from 7.9% to 16.2%, it was suggested that this greater discrepancy compared to that in the sheltered environment might be caused by various factors such as environmental conditions, extrapolation and blower door installation.

This paper reports a refined comparison study of the two methods in a sheltered condition accounting for some of the factors that were not considered in the previous investigations. The testing arrangement achieved herein provided better testing conditions by minimizing the impact of equipment setup on the enclosure airtightness and eliminating the site interference. A door-sized wooden panel was cut out to install the blower door fan into and airtight tapes were applied to the edges around the perimeter of the fan to aim for a near-identical condition in the envelope of a small chamber (13-feet sized cargo container). Tests were also carried out in a house-sized chamber to assess the repeatability of the Pulse unit and see how it compares with the blower door test method. Known openings were also used in the small chamber to compare how accurately each method measured these, further building on previous similar tests (Zheng 2017, Zheng 2019: Building and Environment). Both chambers were sheltered in a large detached building, which was solely used for testing, and therefore this eliminates any possible interferences of other building users during testing, such as operation of windows and doors.

2 METHODOLOGY

2.1 Equipment

The equipment used for blower door and Pulse testing includes a Minneapolis blower door Duct Blaster series B and a Pulse unit with a 60 litre, a 40-litre and a 20-litre aluminium tank. Table 1 lists the photos of the test equipment. PULSE-60 was used for testing in the large chamber while prototype PULSE-20 and PULSE-40 devices were mainly used for testing in the small chamber where smaller flow was required.

Table 1 Equipment and setup for the three testing methods

PULSE-60/40 (cased)	PULSE-20 (without casing)	Duct Blaster B
	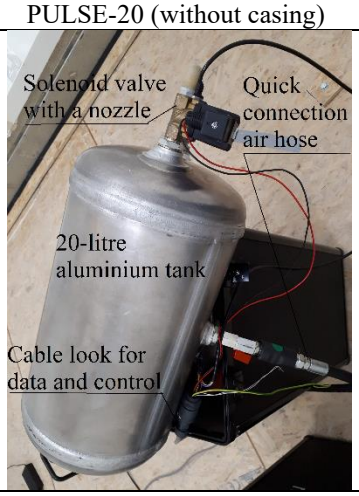	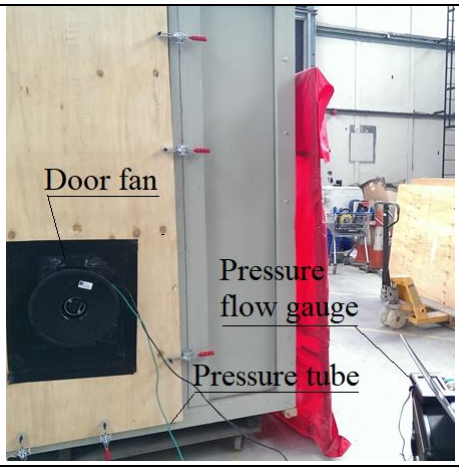
The Pulse units		Minneapolis blower door

2.2 Chambers

Two test chambers sheltered in a large detached building were utilised to provide testing spaces with two very different volumes. This allowed for an easy setup of multiple testing scenarios in the small chamber, and in the larger chamber a test space of sufficient size to represent a typical dwelling. The small test chamber (Figure 1) has dimensions of 4.0m (length) ×2.0m (width) ×2.0m (height), giving a volume of 16 m^3 and an envelope area of 40 m^2. This chamber shares a similar size with the one reported by Zheng (Zheng 2017, Zheng 2019: Building and Environment), which was improvised from half a standard 20-feet long cargo container with dimensions of 2.84m×2.23m×2.03m. There are two major differences between the chamber used in the investigation of the previous paper and the small chamber in this study. Firstly, the chamber used here is in a sheltered environment while the other one was exposed to an outdoor condition and secondly, the chamber here is detached, whilst the other one was semi-detached. The larger test chamber in this study (Figure 2) has an L-shaped structure, with dimensions similar to that of a typical dwelling. The volume and envelope area of the large chamber are 310 m^2 and 269 m^3, sharing a similar but slightly larger size than the one reported in a previous sheltered condition investigation by Zheng (Zheng 2018). The small chamber was used to carry out testing with different known openings, which provided various leakage levels while the large chamber on the other hand was used in its standard form i.e. without modification for leakage levels and would therefore have typical penetrations as found in a dwelling i.e. Door frame, service penetrations etc. This large chamber was primarily used for the Pulse repeatability test, with a simple comparison between the two testing methods being made to see how the two test methods compare in a large sheltered test space. The impact of the Pulse location was also experimentally investigated in various chamber conditions in the large chamber; the findings are not reported here but will be presented in later publications.

Figure 1 Small test chamber

Figure 2 Large test chamber

Two test plates were used for testing in the small chamber, herein named as test plate A and test plate B, which are shown in Figure 3 and Figure 4, respectively. The test plate A has four square (150mm×150mm) openings and four circular (diameter: 50mm) openings in the middle of the plate, all the openings are short sharp-edged, similar to holes that might be found in construction material layers or in window frames. Test plate B has three circular openings with tubular pipes connected to the top two openings. Panel B seeks to represent those openings found in service penetrations such as ventilation ducts or cable casing running through the wall. More details about the various testing scenarios are given in section 2.3. During testing, these plates were installed on the opposite side of the fenestration where the blower door was mounted. Wing screws were utilised to fix the plate onto the external surface of the chamber wall, as shown in Figure 5.

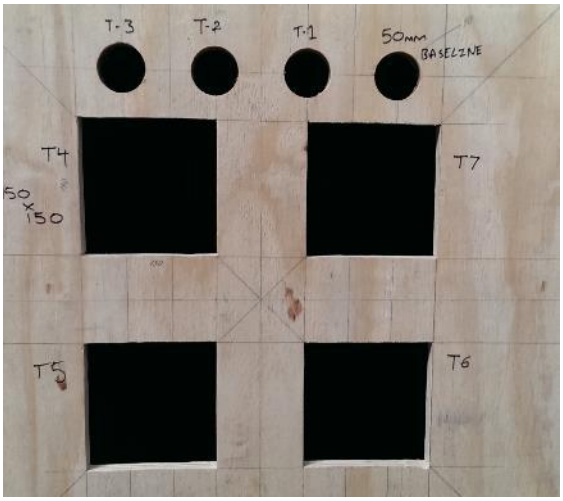

Figure 3 Testing plate A with a number of well-defined openings

Figure 4 Testing plate B with three circular holes (two extended by pipes)

Figure 5 The mounted test plate on the chamber wall

2.3 Setup

To prepare the small chamber with minimized leakage difference between the blower door testing and the Pulse testing, two identical rigid wooden panels were prepared, one with an opening for the installation of the door fan during the blower door testing and the other one without any opening for the Pulse testing, as shown in Figure 6. Both panels were installed in an existing doorway using a number of lateral press type clamps, which were distributed around the perimeter of the door frame in both testing, as shown in Figure 7. Figure 7 also shows the installation of the blower door fan with the edges being sealed up by tapes to avoid air leaks around the boundary between the fan case and the opening in the panel during the testing.

Figure 6 Doorplates used for setting up both tests

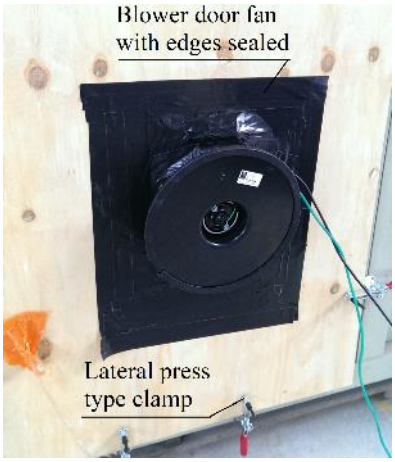

Figure 7 Installation of blower door fan

Figure 8 shows the setup of the PULSE-60 in the large chamber, where it was placed in the centre of the internal space. The blower door was installed in the existing doorway and the installation is shown in Figure 2.

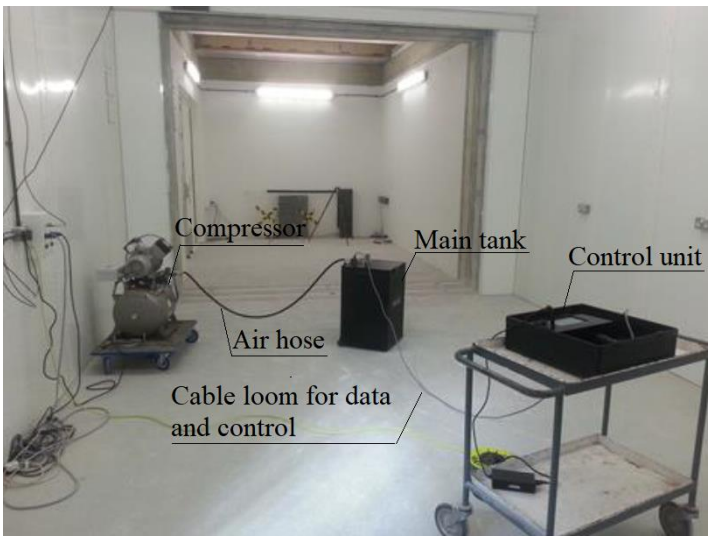

Figure 8 Setup of the Pulse unit in the large chamber

3 TESTING ARRANGEMENT

Compared to the Pulse unit used in the previous study (Zheng 2017, Zheng 2019: Building and Environment), the Pulse unit used in this study has gone through a product development phase. Modifications were made to the unit on a few aspects (Zheng 2019: Future Cities and Environment) to address issues related to the safe handling weight, exposed pressure reference tube and being vulnerable to rough site condition. Changes were also made to the system construction and design such as the operating system and differential pressure transducer to improve the user friendliness and cost effectiveness. One of the main objectives of this experimental study was to assess the precision and accuracy of the Pulse unit after it went through product developments.

In the small chamber, eight different testing scenarios were achieved by sealing up various combinations of openings using the two testing plates (A+B). Figure 9 shows the details of how the eight testing scenarios were prepared using sealing tapes. Each testing scenario was named according to the testing order, i.e. starting from scenario T0 and ending with scenario T7. For instance, the blower door tests were carried out first in scenario T0. After the scenario T0 was completed, a piece of sealing tape was removed to introduce one more opening to the scenario T1, and this testing procedure was repeated until the scenario T7 was completed. The same testing process was repeated for the Pulse unit after the blower door testing was done. One pressurisation test was run in each scenario while the Pulse test was repeated three or four times in each scenario, along with scenarios T6 and T7, which could only be performed twice due to the time constraint at the end of testing. This testing arrangement allowed both testing methods to be subjected to various leakage characteristics and levels.

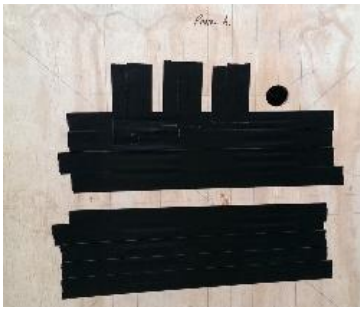
T0: Panel A – 1×circular opening

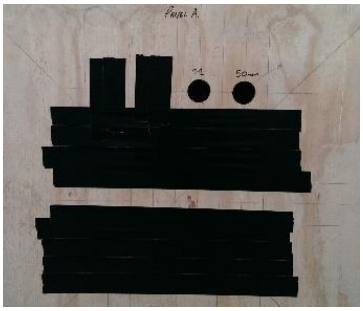
T1: Panel A – 2 circular openings

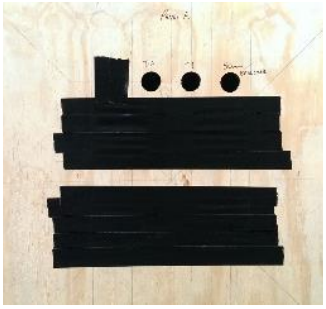
T2: Panel A – 3 circular openings

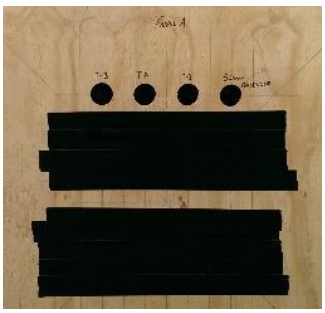

T3: Panel A – 4 circular openings

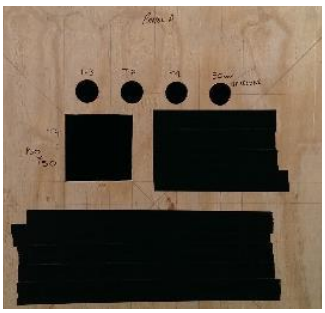

T4: Panel A – 4 circular openings plus 1 square opening

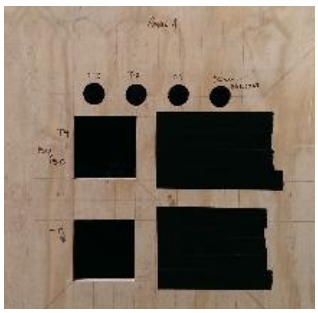

T5: Panel A – 4 circular openings plus 2 square openings

T6: Panel B (White blocked grey open)

T7: Panel B (both pipes open)

Figure 9 Testing scenarios in the small chamber

In the second test using the large chamber, the objective of the investigation was to assess the repeatability of the Pulse test in a 'house' sized sheltered condition and to compare with the blower door test. Ten repeated Pulse tests were carried out alongside the blower door.

4 RESULTS AND ANALYSIS

Figure 10 shows the test results of both blower door and Pulse tests taken in the small chamber in eight scenarios. Crossover in data in most of the scenarios were achieved to make direct comparison. For instance, in scenario T0, the lowest point in the overlapped pressure range was at 10Pa where the difference in test result between the blower door and the Pulse test was 8.8% and the highest was at 18Pa with 4.8% difference. The percentage difference of the test results in all testing scenarios given by blower door and Pulse is summarised in Table 2.

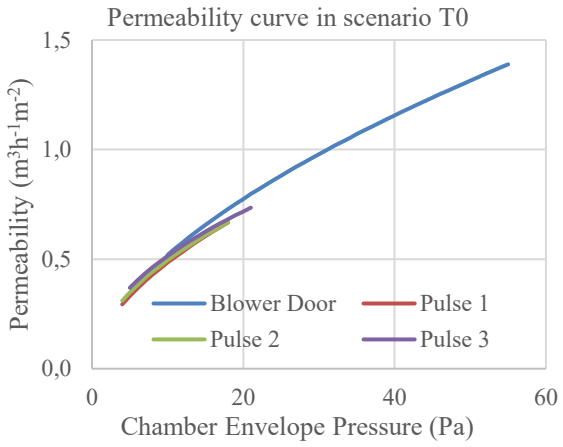

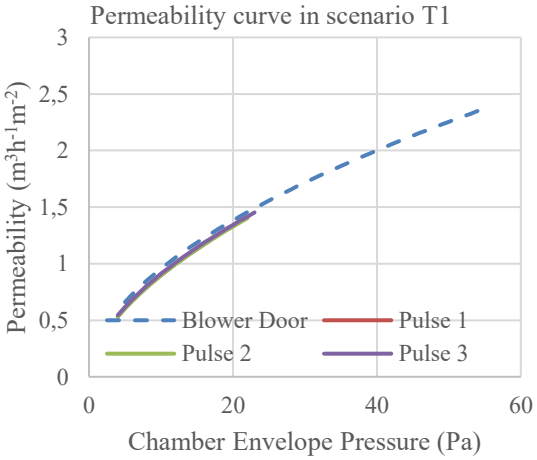

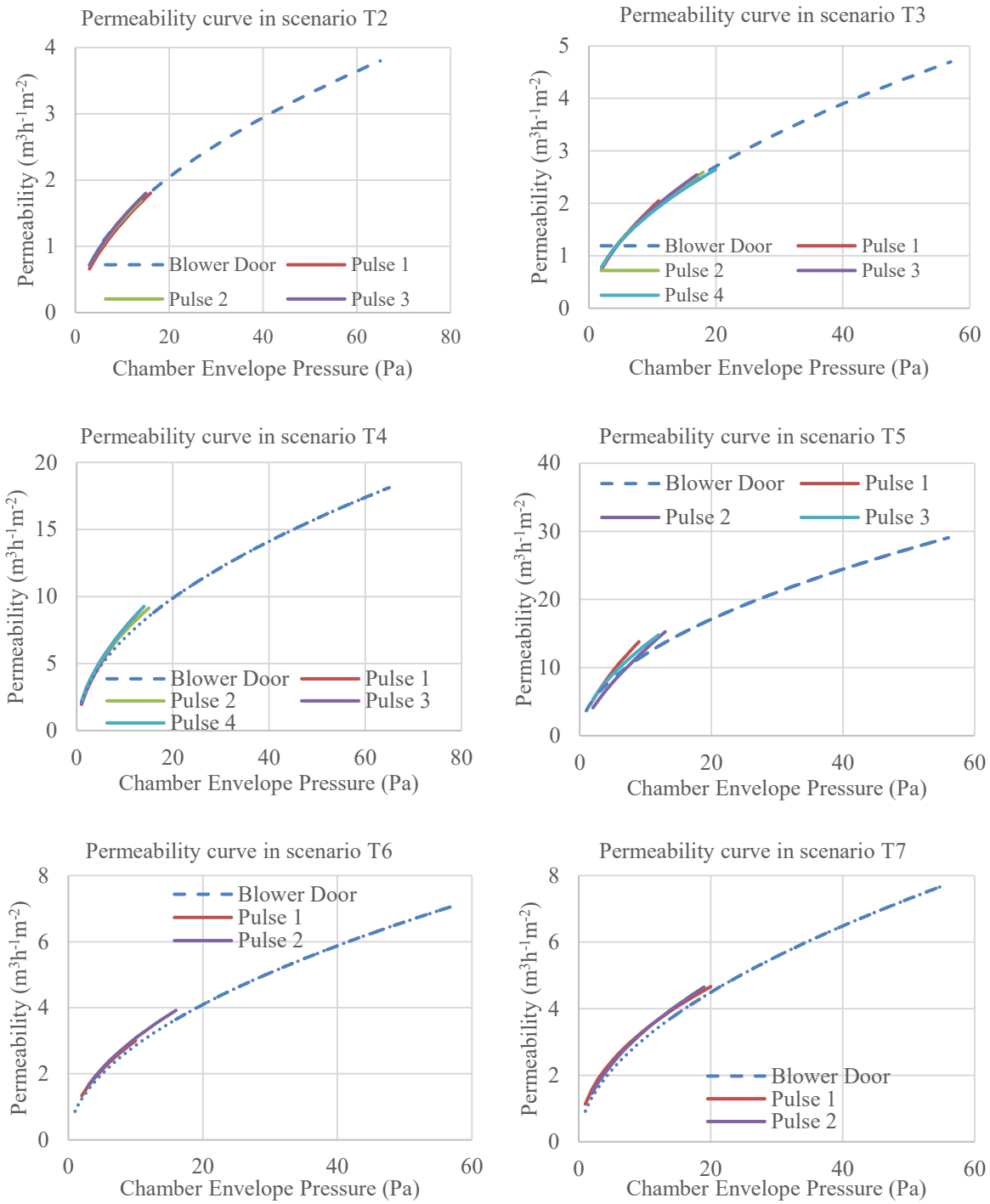

Figure 10 Testing results of all the scenarios in the small chamber

Table 2 Summary of test results given by the blower door and Pulse tests in all scenarios (the small chamber)

Scenario	Range of crossover (Pa)	Minimum (%)	Maximum (%)	Average (%)
T0	10-18	4.1%	7.8%	6.4%
T1	5-23	2.5%	7.8%	4.9%
T2	6-16	0.8%	4.1%	1.6%
T3	7-20	0%	2.2%	0.6%
T4	N/A	N/A	N/A	N/A
T5	9-13	6.0%	12.8%	9.6%
T6	16	7.4%	7.4%	7.4%
T7	14-20	3.8%	6.4%	5.5%

Note: N/A means no pressure overlap was achieved.

The results show the difference between the two testing methods varies from scenario to scenario with the average difference ranging from 0.6% to 9.6%. Scenario T3 gave the best agreement followed by the scenario T2, both of which showed an average percentage difference less than 2%. The largest difference was seen in the scenario T5 where four circular openings and two square openings were present in the test plate. The openings were lying closely in the centre of the test plate and hence large net fluid flow was generated through the test plate likely creating a 'pressure sink' near openings, i.e. non-uniform pressure distribution. This might consequently lead to errors in the pressure measurement, especially so in a small test space and therefore produce larger percentage difference between the two. The average difference in overlap between the blower door and Pulse data is 6.0%. Although this testing does not yield a consistent offset that may easily be accounted for, all testing comes with an inherent level of measurement uncertainty with ISO 9972:2015 (BS ISO 9972) citing an overall uncertainty of lower than ±10% in calm conditions for the blower door fan and the manufacturer citing ±5% uncertainty for Pulse measurements. In this context, the level of agreement is generally encouraging, especially for test scenario T2, T3 and T7.

In the large chamber without introducing external openings, repeated tests were carried out to assess the repeatability of the Pulse test and its agreement with the blower door test. The Pulse test was repeated 10 times and one blower door test was performed in both pressurisation and depressurisation modes. The permeability curves obtained in the Pulse tests as shown in Figure 11, are lying closely with each other, which is an indicator of a good repeatability. Figure 12 illustrates the repeatability of the Pulse test in the achieved pressure range (1-10 Pa) in the form of measurement uncertainty. The uncertainty of measuring the permeability at a pressure level lower than 4 Pa is greater than 5% and the uncertainty increases when the measured pressure decreases. However, it lies within ±5% when the measured level is no smaller than 4 Pa. In relation to the comparison of the blower door and Pulse measurements, the achieved pressure overlap includes 9 Pa and 10 Pa, where a 6.7% and 7.5% difference were observed respectively. Figure 11 shows the permeability curves obtained in the Pulse and blower door tests, which follow the same trend. It is worth to mention that it was observed that the sealing tape around the blower door fan had loosened slightly after the scenario T0 was completed. Therefore, sealing tapes were checked and reinforced prior to the testing in other scenarios. This might explain why the blower door test gave slightly leakier measurement than the Pulse test in the scenario T0.

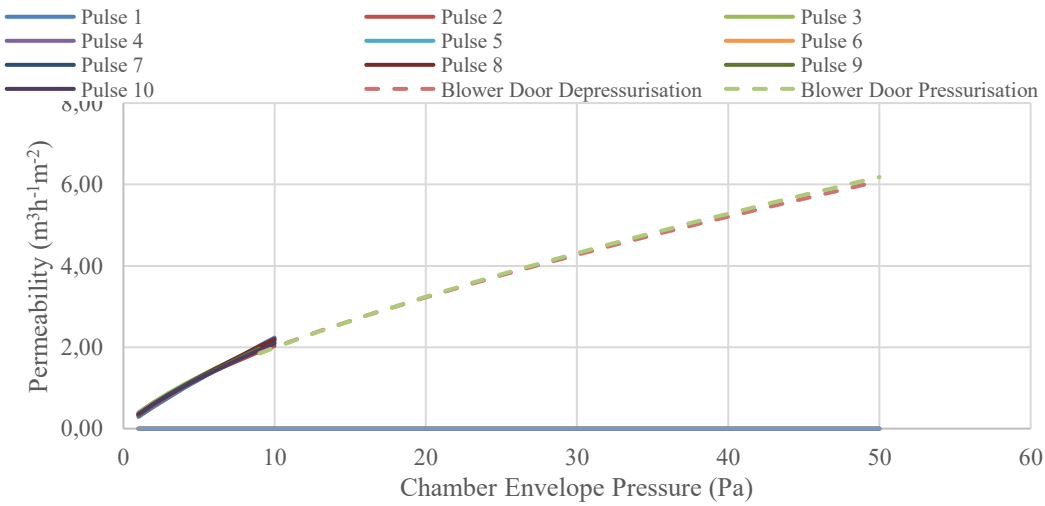

Figure 11 Permeability curves obtained in 10 repeated Pulse tests and one set of blower door tests

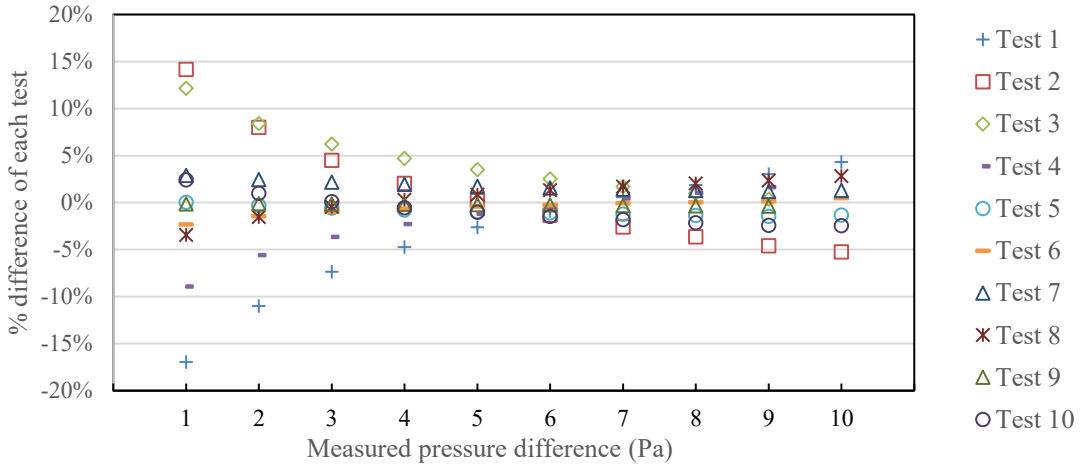

Figure 12 Measurement uncertainty (1-10Pa) of 10 repeated tests

5 CONCLUSIONS

Following on from previous studies concerning the repeatability of the Pulse test in determining air permeability and comparison to blower door results in a sheltered condition, this study has sought to perform similar tests but with improvements to the test arrangement. In the test setup, greater attention has been given to the preparation of the both testing methods in order to gain a 'clean' comparison by minimizing the difference in the testing and envelope conditions that both testing methods were subjected to. Such improvements have included the use of a bespoke solid panel installed in the external doorway for mounting the blower door in order to negate any potential movement of air through the blower door/ doorframe interface. Another improvement was to use a test building inside an outer building, which contained no other potential influences i.e. other windows and people movement etc. Since previous tests developments have also been made to the Pulse unit itself, in terms of its overall system design, instruments and control. In this experimental study, testing was performed in two chambers with very different sizes to verify the accuracy and repeatability of the Pulse unit in a sheltered environment alongside a calibrated blower door unit.

In most of the testing scenarios in the small chamber, where various leakage characteristic and levels were achieved, the Pulse tests provided a good agreement with the blower door tests in reporting the permeability in an overlapped pressure range measured by both testing methods, with a maximum difference of 7.4%. A similar difference was observed in the large chamber. Although this difference is slightly greater than that reported by Zheng (Zheng 2017, Zheng 2019: Building and Environment), an agreement was achieved to a similar extent. A slightly larger discrepancy was shown in the test scenario where the openings with the largest opening area were present when the small chamber was tested. The authors think this might be attributable to uneven pressure distribution around the large openings in the test plate and this could introduce errors in measuring the chamber pressure especially when the test space has a small volume. A good repeatability was demonstrated in the repeated tests carried out in the large chamber and the results showed the measurement uncertainty was within ±5% when the measured pressure level is no smaller than 4 Pa. Below 4 Pa, the measurement uncertainty increased up to ±17% when the measurement pressure level decreased to 1 Pa. This suggests measuring building airtightness at a pressure level below 4 Pa is subjected to a greater background noise.

ACKNOWLEDGEMENTS

The authors gratefully acknowledge funding received from: Department for Business, Energy and Industrial Strategy Energy Entrepreneurs Fund Scheme, Phase 5 (EEF5029).

REFERENCE

BS EN ISO 9972. Thermal performance of buildings-Determination of air permeability of buildings-Fan pressurisation method. BSI Standards Publication (2015)

CIBSE standard TM23: Testing Buildings for Air Leakage. CIBSE (2000), ISBN 9781903287101

M.H. Sherman, R. Chan. Building Airtightness: Research and Practice. Lawrence Berkeley National Laboratory Report (2004), Report No. LBNL-53356

M.H. Sherman. Infiltration in ASHRAE's residential ventilation standards. Lawrence Berkeley National Laboratory, LBNL-1220E (2009)

Zheng X.F., Mazzon J., Wallis I., Wood, C.J. Experimental study of of enclosure airtightness of an outdoor chamber using the pulse technique and blower door method under various leakage and wind conditions In: 39th AIVC - 7th TightVent & 5th venticool Conference, 18-19 September 2018, Antibes Juan-Les-Pins. 352-362.

Zheng X.F., Cooper E.W., Mazzon J., Wallis I., Wood, C.J. A comparison study of the blower door and novel pulse technique on measuring enclosure airtightness in a controlled environment In: 38th AIVC conference, Nottingham, United Kingdom, 13-14 September 2017.

Zheng X.F., Cooper E.W., Mazzon J., Wallis I., Wood, C.J. Experimental insights into the airtightness measurement of a house-sized chamber in a sheltered environment using blower door and pulse methods. Building and Environment. https://doi.org/10.1016/j.buildenv.2019.106269.

Zheng, X. F., Cooper, E., Zu, Y. Q., Gillott, M., Tetlow D., Riffat S., WOOD C. J., 2019. Experimental Studies of a Pulse Pressurisation Technique for Measuring Building Airtightness. Future Cities and Environment, 5(1), 10.

Evaluation of indoor pressure distributions in a detached house using the Pulse airtightness measurement technique

Yun-Sheng Hsu*[1], Xiaofeng Zheng[1], Edward Cooper[2], Mark Gillott[1], Shin-Ku Lee[3] and Christopher J Wood[1]

1 Buildings, Energy and Environment Research Group, Faculty of Engineering, University of Nottingham
University Park, Nottingham NG7 2RD, UK
** Yun-Sheng Hsu: yunsheng.hsu@nottingham.ac.uk*

2 Department of Architecture and Built Environment, Faculty of Science and Engineering, University of Nottingham
199 Taikang East Road,
Ningbo, 315100, China

3 Research Centre for Energy Technology and Strategy, National Cheng Kung University
No.1, University Road,
Tainan, 701, Taiwan

ABSTRACT

Building airtightness is a critical aspect for energy-efficient buildings as energy performance of a building can be reduced significantly by poor airtightness. The Pulse technique has been regarded as a promising technology, which measures the building airtightness at a low pressure of 4Pa by rapidly releasing a 1.5-second pulse of air from a pressurised vessel into the test building and thereby creating an instant pressure rise that quickly reaches a "quasi-steady" condition. However, questions have often been asked on the test viability due to the nature of the test. One of the frequently raised questions concerns uniformity of the pressure distribution across the internal space of the test building during the air pulse release. To provide insight into this, experimental work was conducted to measure the indoor pressure distribution during the pulse pressurisation process. The effect of the specific pulse release location on the building airtightness measurement has also been assessed by performing tests at various locations within the building. The test building, which is a five-bedroom house located in the University of Nottingham, was chosen for the testing. Five differential pressure transducers were used to obtain the pressure distribution within the dwelling. In addition, an ultrasonic anemometer was employed to measure the outdoor wind condition to eliminate the impact of wind on the indoor pressure. All the tests were conducted in December 2018 at wind speeds less than 0.5m/s (at a height of 2.2 metres above ground). The results show that a maximum relative percentage difference of 1.4% was obtained by comparing the pressure distribution between living room (Pulse test location) and the other rooms. This indicates that a pressure difference within the building during the Pulse test does exist but considering the accuracy of pressure transducers (0.15%), the deviation is not significant. Comparatively, smaller differences of the pressure level in the five rooms were observed in the fan pressurisation (Duct Blaster B, abbreviated as DBB) test at 10Pa and 15Pa, which are 0.5% and 0.2% respectively. In terms of building airtightness measurement, a subtle variation (i.e. 1.05%) is noted when the Pulse test was conducted at different locations on the ground floor, which may also be caused by variations in the environmental condition (e.g. temperature and wind condition).

KEYWORDS

Building airtightness, Pulse technique, Blower door, Pressure distribution, Anemometer

1 INTRODUCTION

In recent years, energy saving has attracted increased attention, especially in the domestic sector as this sector alone accounted for 28% of UK energy consumption in 2017 (Department for

Business, 2018). Research shows that domestic energy consumption is dominated by several factors, such as household characteristics, building energy performance and electrical appliances. Building energy performance plays an important role in energy conservation and can be significantly affected by ventilation, which is influenced by uncontrolled air leakage (i.e. air infiltration) across the building exterior (Wang et al., 2018). Researchers have confirmed that thermal losses from the building envelope are mainly attributed to heat transfer and ventilation, including infiltration (Lerma et al., 2018). Airtightness is regarded as the fundamental building property that impacts infiltration and exfiltration (Han et al., 2015). Due to the fact that building airtightness is a crucial factor for energy-efficient buildings, the influence of poor airtightness on the built environment has aroused wide concern since the 1970s, for example, the impacts on building energy consumption, building damage, indoor air quality and noise transmission (Carrié and Rosenthal, 2008).

The blower door method is a well-known and widely accepted steady pressurisation method, which can be implemented by fan pressurisation in a range of pressure differences, usually in steps of 10–60Pa (British Standards Institute, 2015) . For the blower door test, a range of steady pressure differences across the building envelope is created by a blower door fan, and the corresponding airflow rate through the fan is measured simultaneously to establish the pressure-leakage relationship of the test building. An alternative method for measuring airtightness, is the Pulse technique, which measures building airtightness at lower pressures compared to the blower door. Typically the test is performed at much less than 10Pa and reported at 4Pa, which has been regarded as a more precise indicator of the pressure level experienced by buildings under natural conditions than the conventional steady-state measurement at 50Pa (Sherman and Matson, 2002). It measures the building air leakage by rapidly releasing a known volume of air from a pressurised vessel into the test building and thereby creating an instantaneous pressure rise that quickly reaches “quasi-steady” condition (Zheng et al., 2019a, Zheng et al., 2019b). Theoretically, the underlying principle of Pulse technique is a quasi-steady flow, which can be shown to exist via the temporal inertial model as given in studies by Cooper and Etheridge (2007), Cooper et al. (2007), Cooper et al. (2014). The Pulse technique is capable of measuring the building airtightness dynamically within a short period, typically 11-15s. The quick measurements of the corresponding change in the indoor pressure and the pressure change in the air tank can be measured to obtain the air leakage through the building envelope at 4Pa. The Pulse technique has proven to be of great practical value (Zheng et al., 2017). However, questions have often been asked by professionals in the industry and researchers in academia on the test viability due to the nature of the test. One of the frequently raised questions considers the uniformity of the pressure distribution across the internal spaces of the test building during the air pulse release. In this study, experimental work was conducted in a five-bedroom detached house to verify whether a uniform indoor pressure distribution can be achieved during the pulse pressurisation process. This distribution is also compared with that of a steady pressurisation test. In addition, the effect of the pulse release location on the building airtightness measurement is also investigated. The tests in this study were routinely done as part of the ongoing development of Pulse technique and the investigation presents results of testing using the latest Pulse equipment as an answer to the aforementioned questions.

2 EQUIPMENT

Different devices were used for experimental work in this study, as listed in Table 1. A PULSE-60 unit (Figure 1), which consists of a 58.5-litre lightweight aluminium tank and oil-free compact air compressor, was used for the Pulse test. A ¾ inch (BSP) solenoid valve was installed at the outlet to release compressed air from the air tank into the test building. In addition, the Pulse test data, such as chamber and tank pressures were recorded and analysed

by the on-board PULSE-60 control box, with results displayed on the LCD screen as seen in Figure 1. In this study, a complete three-step Pulse tests consists of three consecutive pulses, namely Pulse 1, Pulse 2 and Pulse 3.

For the blower door test, Duct blaster series B (DBB), which is manufactured by The Energy Conservatory (US), was employed. The photo of the DBB unit is presented in Figure 2. The unit is mainly composed of an adjustable doorframe, a flexible canvas panel, a variable-speed fan and a DG-1000 digital pressure and flow gauge. In order to obtain the weather condition during testing, an ultrasonic anemometer was used to measure the outdoor wind speed (Figure 3), and thermocouples were used to measure ambient temperature. A sensitive FCO44 differential pressure transducers (diaphragm-type), which are manufactured by Furness Controls Ltd, were adopted to measure the pressure level of the internal spaces (Figure 4). Experimental data acquisition was accomplished by Datataker DT85.

Table 1: List of test equipment

Airtightness	**Others**
PULSE-60 Duct blaster series B (DBB)	Ultrasonic anemometer, FCO44 Differential pressure transducers (Accuracy < 0.25%), Temperature sensors, Datataker DT85

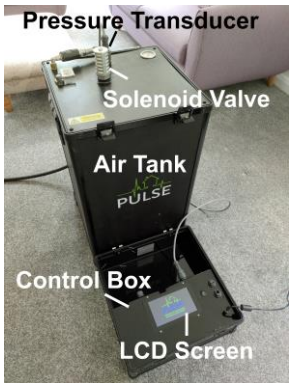

Figure 1: PULSE-60 unit with control box

Figure 2: Energy Conservatory duct blaster series B

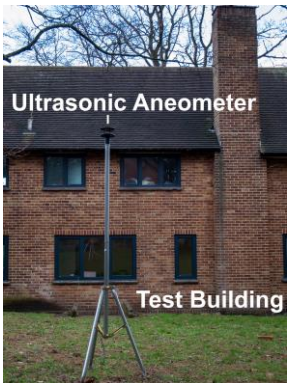

Figure 3: Ultrasonic anemometer

Figure 4: Differential pressure transducers and Datataker DT85

3 DWELLING, SETUP AND TEST ARRANGEMENT

A five-bedroom detached house located on the University Park campus in Nottingham University was chosen as the test building. Figure 5 and Figure 6 show the front and back views of the house and the floor plans are presented in Figure 7 and Figure 8, respectively. The house has one bedroom, one living room, one kitchen on the ground floor and four bedrooms on the first floor. The building parameters are listed in Table 2 and the measurement and calculation of envelope area and volume of the test dwelling complied with ISO 9972.

In this study, all experimental tests were conducted under wind speeds less than 0.5m/s, which was measured at height of 2.2 metre above ground in the backyard and a distance of 12-meter away from the perimeter of the test building, without any obstructions within a radius of 12 meters. The purpose of this arrangement is to minimise the wind impact on the indoor pressure distribution so insights on the pressure distribution produced solely by the Pulse test can be gained. Due to the fact that the sampling rate of data loggers reduces when more differential pressure transducers are connected to them, five differential pressure transducers were utilised

to measure the indoor pressure distribution in order to make a balance between the sampling rate and the number of monitored rooms. The sampling rate was 4hz. The accuracy of the differential pressure transducer is 0.15% and all five differential pressure transducers were calibrated by connecting to the same tapping point.

Figure 5: Front view of test building

Figure 6: Back view of test building

Figure 7: Ground floor plan of test building

Figure 8: First floor plan of test building

Table 2: Envelope area and volume of the test dwelling

Dwelling	Wortley 5 - University of Nottingham, University Park, Nottingham
Volume (m^3)	447
Envelope area (m^2)	416
Approximate ACH @50Pa	3.71 (DBB tested on December 2018)
Approximate ACH @4Pa	0.73 (PULSE-60 tested on December 2018)

4 RESULTS AND ANALYSIS

4.1 Indoor Pressure Distribution During the Pulse Test

A series of Pulse tests have been conducted in the house to verify whether a uniform pressure distribution across the internal spaces of the test building can be achieved during the air pulse release, so that the viability of the Pulse test for accomplishing building airtightness

measurement at 4Pa in a very short period (i.e. typically 11-15s) can also be evaluated. The Pulse unit was placed in the centre of the living room on the ground floor for testing, and the indoor pressure distributions for five rooms on both floor levels (i.e. living room, kitchen and three bedrooms) have been measured respectively during the pulse pressurisation process. This research is part of a wider study to investigate various aspects of the Pulse technology and therefore in total 682 Pulse tests were conducted. However, in this analysis concerning pressure distribution a typical test result is shown which represents the operation in a calm condition i.e. at the lowest external wind speed (<0.5m/s) to avoid any effects which may be caused by wind loading on the building. Figure 8 displays the pressure variation in each room during the complete three-step of the Pulse test (i.e. Pulse 1, Pulse 2 and Pulse 3). A three-step Pulse test consists of three consecutive pulses, and therefore the 1.5-second pressure rise in the third pulse is much lower than that of the first one due to the declining tank air pressure. It can be noted that the curves representing the pressure responses of five rooms are nearly identical, which indicates good uniformity of the pressure distribution across the five rooms during the pulse release. More discussions for each step of the Pulse tests are given in the following sections.

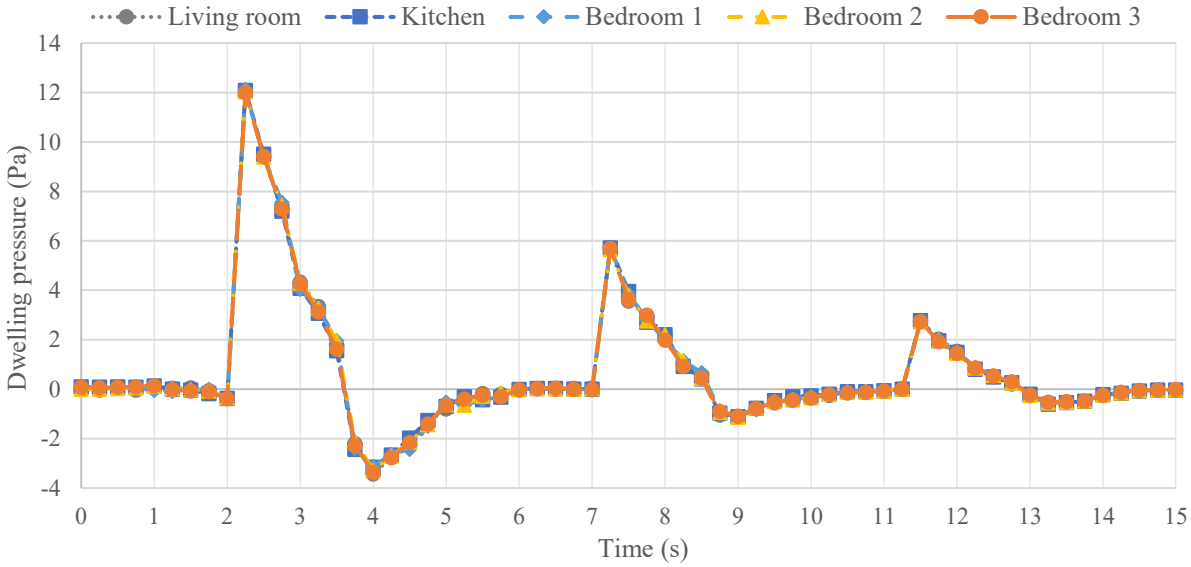

Figure 8: Pressure profiles of five rooms during the complete pulse test

Figure 9 shows the measured pressure distribution of each room during Pulse 1. Similar trends were observed in the five rooms and the indoor pressure of every room reached around 12Pa at 2.25s, i.e. 0.25 second after the valve opened to release compressed air from the tank into the internal spaces. Slight differences of the maximum pressure in each room were obtained. For evaluation, the relative percentage difference between the maximum pressure levels of five rooms is calculated. For Pulse 1, the maximum relative percentage difference between living room and the other rooms is approximately 0.8%, as the maximum pressure measured in the living room is 12.09Pa and 11.99Pa in Bedroom 3.

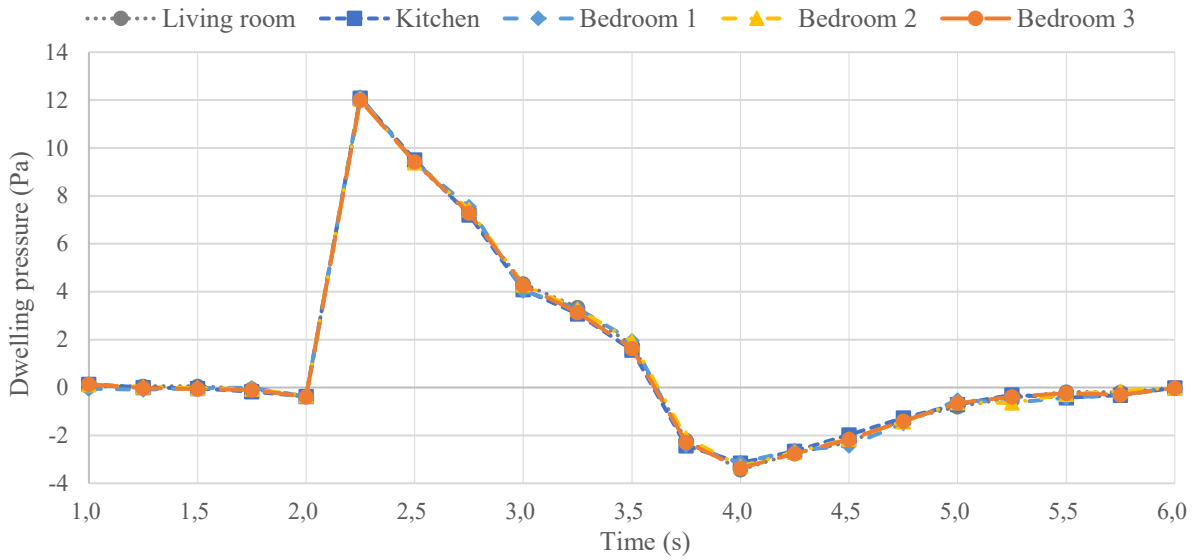

Figure 9: Pressure profiles of five rooms during Pulse 1 testing

The results of pressure distribution in the five rooms for Pulse 2 testing are presented in Figure 10. At 7.25s, 0.25 second after the pulse air was released into the internal rooms, the maximum pressure level was obtained for each room, which ranged from 5.65 to 5.73 Pa. Compared to the curves of the Pulse 1 test in Figure 9, some differences were seen among the five pressure curves of Pulse 2. As the Pulse test unit was located in the living room, the maximum pressure level of 5.73 Pa was achieved in the living room, while 5.65Pa was measured in Bedroom 2. The relative percentage difference is 1.4%, which is slightly higher than that of Pulse 1.

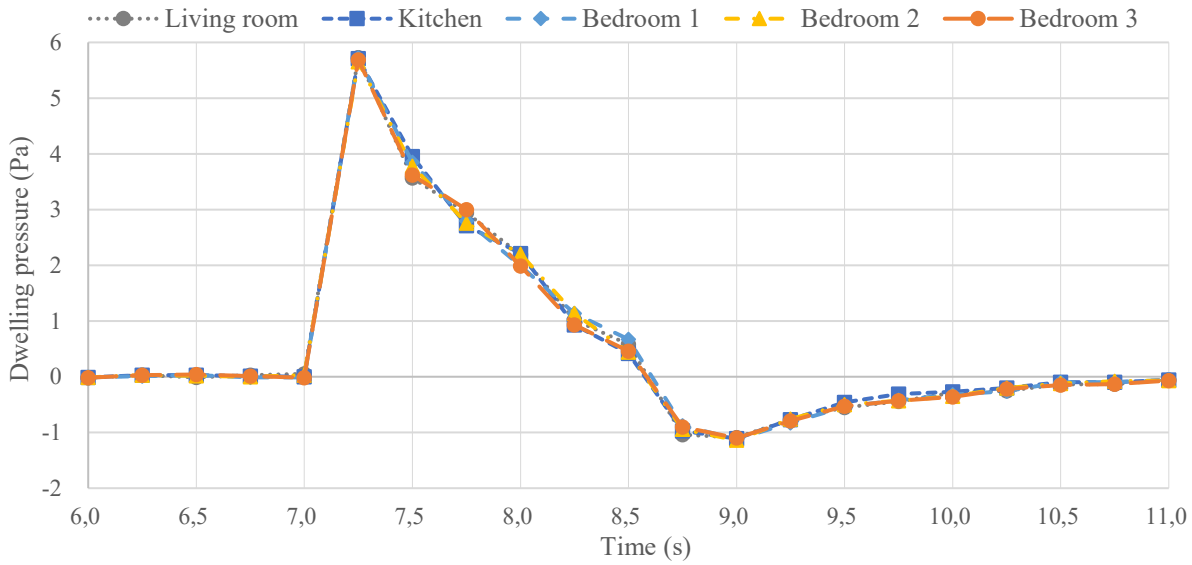

Figure 10: Pressure profiles of five rooms during Pulse 2 testing

Figure 11 demonstrates the pressure distributions of the five rooms during Pulse 3. Similar to Pulse 2 test, the pressure in each room peaked around 2.7 Pa at 11.25s, 0.25 second after the release of air pulse. The relative percentage differences between living room and Bedroom 1, between living room and Bedroom 2 are both 1.4%. Table 3 lists the measured maximum pressure level in each room for Pulse 1, Pulse 2 and Pulse 3 tests.

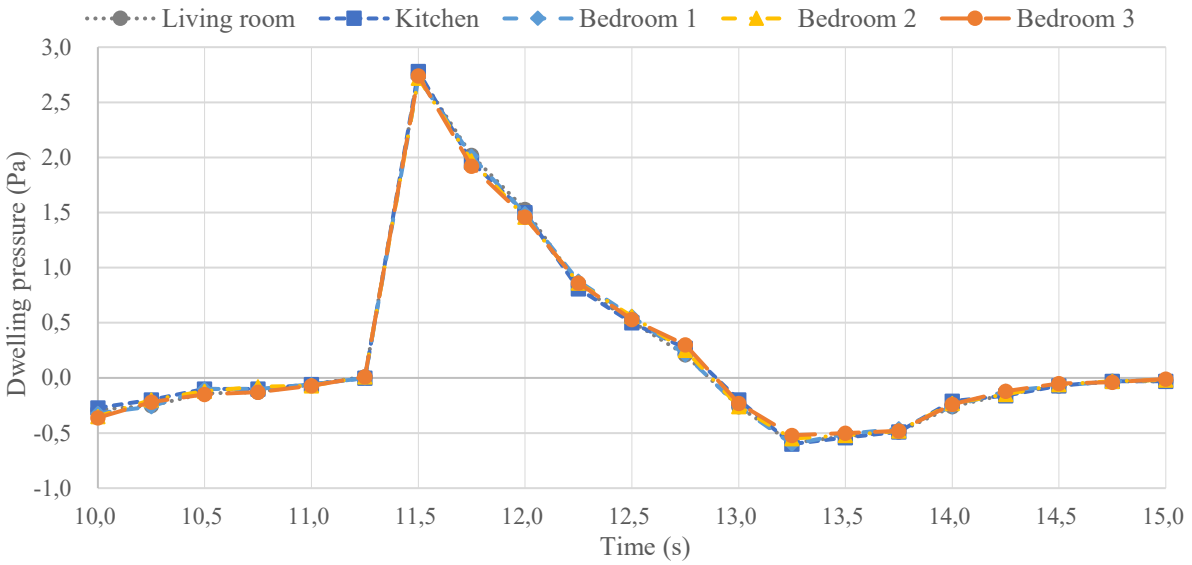

Figure 11: Pressure profiles of five rooms during Pulse 3

Table 3: Maximum pressure level in each room for Pulse 1, Pulse 2 and Pulse 3 tests

	Living room	Kitchen	Bedroom 1	Bedroom 2	Bedroom 3	%*
Pulse 1	12.09 Pa	12.09 Pa	12.13 Pa	12.04 Pa	11.99 Pa	0.8%
Pulse 2	5.73 Pa	5.71 Pa	5.72 Pa	5.65 Pa	5.69 Pa	1.4%
Pulse 3	2.76 Pa	2.78 Pa	2.72 Pa	2.72 Pa	2.74 Pa	1.4%

*The maximum relative percentage difference between living room and the other rooms

4.2 Indoor Pressure Distribution During the DBB Test

Experimental work was also undertaken to investigate the uniformity of pressure distribution within the house during the blower door test. The DBB was installed at the main entrance door of the dwelling and tests were carried out under similar weather conditions as the Pulse test. Due to the limited measurement range (±20 Pa) of the differential pressure transducers, the uniformity of pressure distribution was only investigated at 10Pa and 15Pa. The results are presented in Table 4, Figure 12 and Figure 13 respectively. The overall measurement lasted about 15 seconds after the building pressure became steady. As seen from both figures, the overall trends of the pressure variation in each room are similar. For a test at 10Pa, the maximum pressure difference is about 0.05Pa, with a relative percentage difference of 0.5% and only 0.03Pa of the maximum pressure difference is observed for a test at 15Pa, with a relative percentage difference of 0.2%. Considering the accuracy of pressure transducers (0.15%), uniform pressure distribution across the internal spaces has been demonstrated for the fan pressurisation test. In this study, tests were conducted under calm conditions (i.e. wind speed lower than 0.5m/s) with less notable wind impact on measurement. It is worth noting that for fan pressurisation test, wind speed is usually measured only when the testing starts and after completion, while the variation in wind speed during testing is ignored. Due to the dynamic characteristics of wind, wind condition may vary during testing period, which could affect measurement of building airtightness.

Table 4: Maximum pressure level in each room for DBB tests at 10 Pa and 15Pa

	Living room	Kitchen	Bedroom 1	Bedroom 2	Bedroom 3	%*
DDB 10 Pa	14.93 Pa	14.94 Pa	14.95 Pa	14.92 Pa	14.93 Pa	0.2 %
DDB 15 Pa	10.03 Pa	10.04 Pa	10.03 Pa	10.05 Pa	10.08 Pa	0.5 %

*Relative percentage difference between maximum and minimum

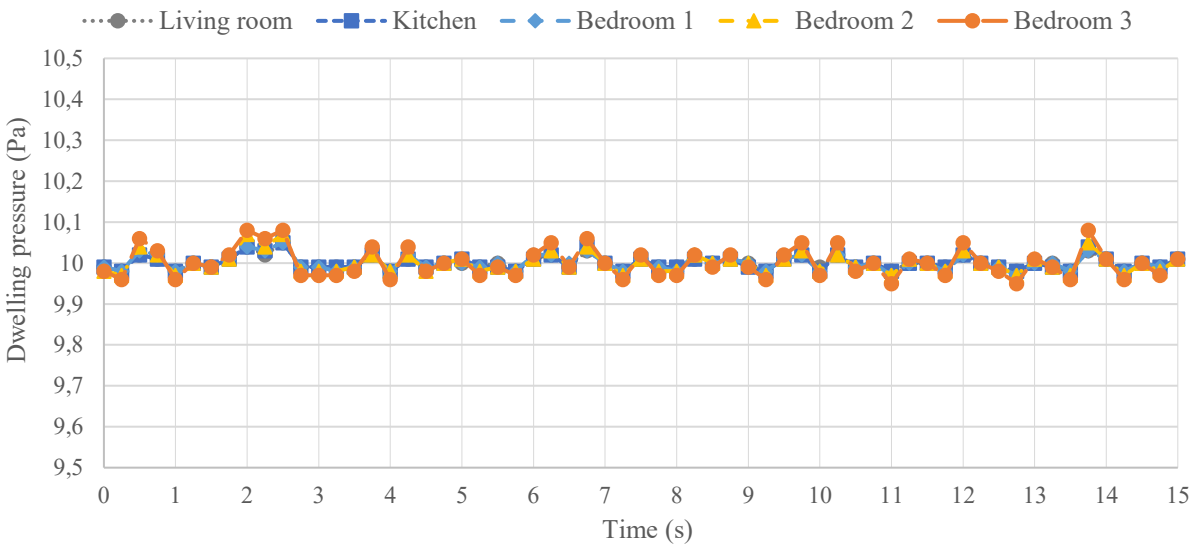

Figure 12: Pressure profiles of five rooms during the DBB test at 10Pa

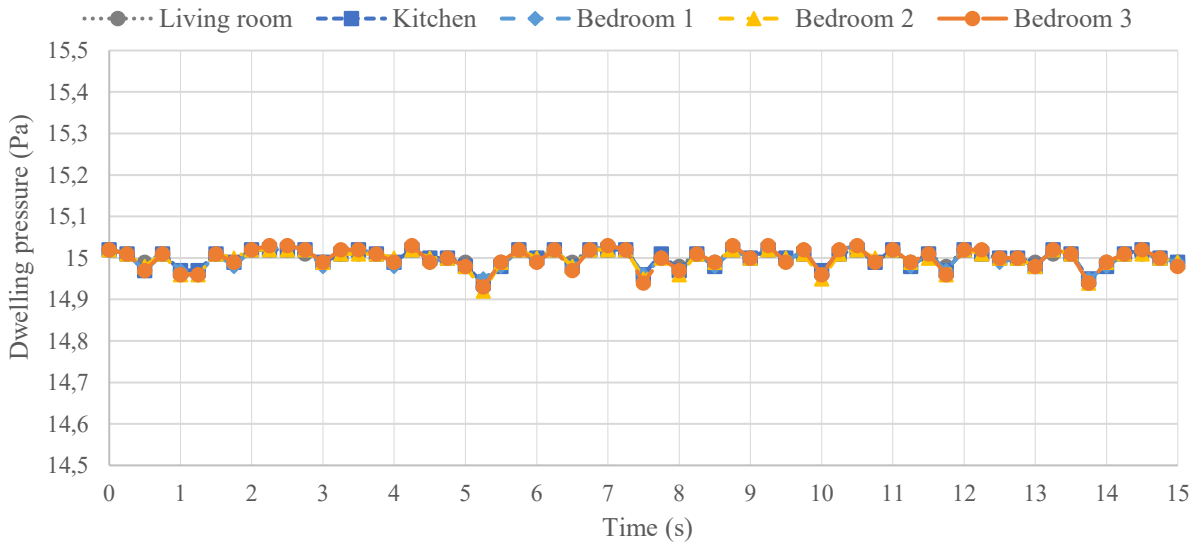

Figure 13: Pressure profiles of five rooms during the DBB test at 15Pa

4.3 Effect of Pulse Release Location

Investigations were made to the effect of the specific pulse release location on the building airtightness measurement by performing tests in various locations within the building. Figure 14 illustrates the floor plan of the dwelling with marked test points. In total, six locations on the ground floor were selected, including living room, living room corner, Bedroom 1, Bedroom 1 corner, kitchen and kitchen corner. At each test location, five repeated tests were implemented under calm weather conditions. Table 5 shows the building airtightness measurement results for the 30 tests at different pulse release locations. The average building permeability value is calculated based on the five tests for each location. As listed in Table 5, the average permeability for pulse release in living room, living room corner, Bedroom 1, Bedroom 1 corner, kitchen and kitchen corner are 0.725, 0.721, 0.721, 0.728, 0.731 and 0.716 m^3/m^2h respectively. A subtle difference in the average building permeability is noted with variability of 1.05%, which is possibly caused by other factors, for instance variation in the environmental condition (temperature and wind condition). Therefore, the results indicate that the Pulse test location in this study has little effect on building airtightness measurement.

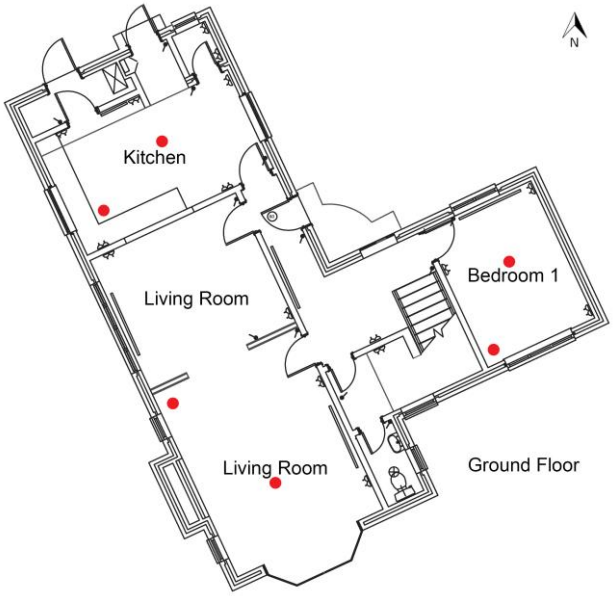

Figure 14: Pulse Test locations

Table 5: Measurement results of building permeability (m^3/m^2h) for the pulse tests at different locations

	Living room	Living room Corner	Bedroom 1	Bedroom 1 Corner	Kitchen	Kitchen Corner
Test 1	0.721	0.715	0.719	0.718	0.721	0.718
Test 2	0.730	0.719	0.726	0.723	0.726	0.722
Test 3	0.725	0.714	0.702	0.730	0.763	0.725
Test 4	0.732	0.722	0.733	0.764	0.732	0.709
Test 5	0.715	0.733	0.723	0.706	0.713	0.706
Average	0.725 (±1.38%) *	0.721 (±1.66%)	0.721 (±2.64%)	0.728 (±4.95%)	0.731 (±4.38%)	0.716 (±1.40%)
Overall Average	0.724					
%**	0.15%	0.40%	0.40%	0.65%	1.03%	1.05%

* Highest relative percentage difference between each test and average
** Relative percentage difference between location average and an overall average

5 CONCLUSIONS

In this study, experimental investigations were made in a five-bedroom detached house using the PULSE-60 unit and the fan pressurisation (Duct Blaster B, abbreviated as DBB) to measure building airtightness under calm weather conditions that wind speeds less than 0.5m/s. For assessment, pressure distributions among five different rooms within the building were monitored together with the building permeability. Based on the experimental results, it can be noted that the pressure distributions among the rooms were identical during the three-step Pulse test. A minor pressure difference within the building during Pulse test was observed, but the deviation is not significant, with the highest relative percentage difference of 1.4% in Pulse 2 and Pulse 3 test when comparing thee pressure in each room with living room pressure. In terms of the DBB tests, the relative percentage difference of the maximum pressure level in each room is 0.5% at 10Pa and 0.2% at 15Pa, which is lower than that of the Pulse tests. It is also worth noting that with longer testing period, a noticeable wind impact is more likely to occur on building indoor pressure variation. Furthermore, an insignificant impact of Pulse test location on building airtightness measurement was observed with a subtle variation (i.e. 1.05%) in building air permeability when Pulse tests were conducted at different locations inside the

building. There is a possibility that the subtle variation is caused by changes in the environmental condition, for example temperature or wind condition.
The adopted data acquisition device in this study has a limited measurement frequency, which led to limitations of the experimental work. Firstly, due to the fact that the rapid 1.5-second pulse of air is released from the pressurised vessel, and the "quasi-steady" condition is achieved only in 0.8s, limited pressure data were gathered by the acquisition device with the maximum measurement frequency of 4Hz, which may not be adequate to entirely describe the pressure variation throughout the Pulse test. In addition, to ensure data is collected at the maximum frequency, only five pressure transducers could be used for testing, which is not enough to measure the pressure distribution in every room of the test building. For future work, CFD-based numerical studies are recommended to identify in detail how the pressure wave propagates within the internal spaces of the test building and how the building pressure distributes across different zones within the building during the Pulse test.

6 REFERENCES

BRITISH STANDARDS INSTITUTE 2015. *BS EN ISO 9972: Thermal performance of buildings - Determination of air permeability of buildings - Fan pressurization method*, British Standards Institute.

CARRIÉ, F. R. & ROSENTHAL, B. 2008. An overview of national trends in envelope and ductwork airtightness. *Ventilation Information Paper,* 29.

COOPER, E. & ETHERIDGE, D. 2007. Determining the adventitious leakage of buildings at low pressure. Part 1: uncertainties. *Building Services Engineering Research and Technology,* 28**,** 71-80.

COOPER, E., ETHERIDGE, D. & SMITH, S. 2007. Determining the adventitious leakage of buildings at low pressure. Part 2: pulse technique. *Building Services Engineering Research and Technology,* 28**,** 81-96.

COOPER, E., ZHENG, X., GILLOT, M., RIFFAT, S. & ZU, Y. A nozzle pulse pressurisation technique for measurement of building leakage at low pressure. 35th AIVC conference, Poznan, September 2014, 2014.

DEPARTMENT FOR BUSINESS, E. I. S. 2018. ENERGY CONSUMPTION IN THE UK. *In:* DEPARTMENT FOR BUSINESS, E. I. S. (ed.).

HAN, G., SREBRIC, J. & ENACHE-POMMER, E. 2015. Different modeling strategies of infiltration rates for an office building to improve accuracy of building energy simulations. *Energy and Buildings,* 86**,** 288-295.

LERMA, C., BARREIRA, E. & ALMEIDA, R. M. S. F. 2018. A discussion concerning active infrared thermography in the evaluation of buildings air infiltration. *Energy and Buildings,* 168**,** 56-66.

SHERMAN, M. H. & MATSON, N. E. 2002. Air tightness of new US houses: A preliminary report. *Lawrence Berkeley National Laboratory, LBNL-48671*.

WANG, Z., XUE, Q., JI, Y. & YU, Z. 2018. Indoor environment quality in a low-energy residential building in winter in Harbin. *Building and Environment,* 135**,** 194-201.

ZHENG, X., COOPER, E., MAZZON, J., WALLIS, I. & WOOD, C. J. 2017. A comparison study of the blower door and novel pulse technique on measuring enclosure airtightness in a controlled environment.

ZHENG, X., COOPER, E., MAZZON, J., WALLIS, I. & WOOD, C. J. 2019a. Experimental insights into the airtightness measurement of a house-sized chamber in a sheltered environment using blower door and pulse methods. *Building and Environment*.

ZHENG, X. F., COOPER, E., ZU, Y. Q., GILLOTT, M., TETLOW, D., RIFFAT, S. & WOOD, C. J. 2019b. Experimental Studies of a Pulse Pressurisation Technique for Measuring Building Airtightness. *Future Cities and Environment,* 5(1)**,** 10.

Insights into the impact of wind on the Pulse airtightness test in a UK dwelling

Yun-Sheng Hsu*[1], Xiaofeng Zheng[1], Dimitrios Kraniotis[2], Mark Gillott[1], Shin-Ku Lee[3] and Christopher J Wood[1]

1 Buildings, Energy and Environment Research Group, Faculty of Engineering, University of Nottingham
University Park, Nottingham NG7 2RD, UK
** Yun-Sheng Hsu: yunsheng.hsu@nottingham.ac.uk*

2 Department of Civil Engineering and Energy Technology, Faculty of Technology, Art and Design, Oslo Metropolitan University
PO box 4 St. Olavs plass
Oslo, NO-0130, Norway

3 Research Centre for Energy Technology and Strategy, National Cheng Kung University
No.1, University Road,
Tainan, 701, Taiwan

ABSTRACT

Requirements for measuring the building airtightness have been proposed and included by many countries for national regulations or energy-efficient programs to address the negative effect of poor airtightness on building energy performance, durability and indoor environment. The methods for measuring building airtightness have continuously improved and evolved over a number of years. At present, the well-established and widely accepted method for quantifying the building airtightness is the fan pressurisation method (blower door being the most well-known), which can be implemented by pressurising the test building to a range of high pressures (usually in steps across 10–60 Pa range) and measuring the corresponding fan flow rate. As an alternative method, the Pulse technique can be utilised to measure building airtightness at low pressures (typically at 4Pa) by rapidly releasing a 1.5-second pulse of air from a pressurised vessel. It is known that the outdoor weather condition and in particular wind velocity can significantly influence building airtightness measurement. For example, ISO 9972 suggests a meteorological wind speed limit of 6m/s and 3m/s at ground level for the fan pressurisation test. However, limited studies have been conducted to evaluate the performance of the Pulse technique under windy conditions. In this study, a series of tests were carried out to measure the building airtightness of a five-bedroom house located at the University of Nottingham, UK using the Pulse technique under various wind conditions. A Pulse unit with a 58.5-litre air tank was employed to measure the building airtightness while an ultrasonic anemometer, located 12 metres away from the building perimeter, was used to obtain the outdoor wind speed at the height of 2.2 metres above ground level. Tests were conducted in March 2019 in a range of wind speed up to 10m/s. Experimental results demonstrate the viability of the Pulse technique for delivering airtightness measurements under certain wind conditions, although analysis has also identified conditions where the test result becomes invalid. This study provides insight into those conditions, which adversely affect the result produced by the Pulse technique and discusses possible areas of improvement to the measurement and calculation process to mitigate such effects. Based on the 423 Pulse tests undertaken, it is recommended that the Pulse tests should be performed when the wind speed is lower than 5m/s (with relative percentage difference of ±10%) in calm conditions and 7.4m/s (with relative percentage difference of ±20%) in windy conditions at the height of 2.2 metres above ground level to minimise the wind impact. If tests are to be carried out when the wind speed is above this limit, multiple Pulse tests should be carried out in order to reduce the wind impact on building airtightness measurement.

KEYWORDS

Building airtightness, Pulse technique, Wind speed, Ultrasonic anemometer, Wind impact

1 INTRODUCTION

Building airtightness is defined as the resistance to inward or outward air leakage through unintentional leakage cracks or gaps in the building envelope, which indicates how well the building envelope is sealed (Guyot et al., 2010). Airtightness of the building envelope needs to be measured because visual observations are difficult to detect gaps and cracks that already exist in building envelope. In addition, leakage paths into the building envelope may be tortuous, and gaps are commonly obscured by internal architectural facings or external cladding (Vinha et al., 2015). Generally, the building airtightness is measured by a pressurization test using a large calibrated fan to create a pressure difference between the inside of the building and the outside; *alias* fan pressurisation test. The most common reference pressure used in this test is 50Pa, though other reference pressures such as 1Pa, 10Pa, 25Pa and 75Pa (Sherman and Chan, 2006), are also used in a number of territories. An alternative to the fan pressurisation test is the novel Pulse technique, which measures the airtightness of a building at a low pressure differential; typically 4Pa. The Pulse method measures the building air leakage by rapidly releasing a 1.5 second pulse of air from a pressurised vessel. This known volume of air release creates an instantaneous pressure rise in the building that quickly reaches a "quasi-steady" condition (Cooper et al., 2007); whereby, with the appropriate analysis the air leakage rate of the building can be deduced.

In recent years, the uncertainty of building airtightness measurement has become an important concern (Cooper and Etheridge, 2007). Based on the review of the literature (Sherman and Palmiter, 1995, Andrews, 1997, Geissler, 1999, Kraniotis et al., 2013, Kraniotis et al., 2014, Leprince et al., 2017, Leprince and Carrié, 2018, Zheng et al., 2019b, Zheng et al., 2019a), the main sources of uncertainty for the airtightness testing include: building preparation for testing, tester behaviour, uncertainties of repeatability and reproducibility, measurement error, uncertainties of measurement instrument, weather effect, thermal draft impact, seasonal variation of building airtightness, leaks with different flow exponents and linear regression. For example, the pressure difference between the building indoor and the outdoor environment could be influenced by the indefinite nature of the wind and buoyancy effect, which would lead to an imprecise measurement of the building airtightness. The impact of outdoor weather condition on building airtightness measurement has been noted from both numerical and experimental work. To address it, requirements on the testing weather condition have been set in the standards for the fan pressurisation method. Table 1 lists the meteorological requirements for performing the fan pressurisation test set out in for the standards of EN13829, ASTM 779-03 and ISO 9972 (EN, 2000, ASTM, 2004, ISO, 2015).

Table 1: EN13829, ASTM 779-03 and ISO 9972 requirements regarding the testing weather condition

	Wind speed	Temperature	Zero-flow pressure
ISO 9972	Wind speed near the ground ≤ 3m/s; meteorological wind speed ≤ 6m/s or ≤ 3 on the Beaufort scale	Large indoor-outdoor temperature difference shall be avoided. The product of the indoor/outdoor air temperature difference by the height of the building ≤ 250m.K	30-second averages, before and after a test. The test is not valid if one zero low-pressure average (in absolute) ≥ 5Pa

EN13829	The wind speed must be Beaufort scale 3 or less. If measured, should be 6m/s or less	The product of the absolute value of the indoor/outdoor air temperature difference (ΔT) multiplied by the building height must be lower than 500m.K (226.85m°C)	30-second averages, before and after a test must be less than 5Pa
ASTM E779-03	Wind speed of 0 to 2 m/s (0 to 4 mph)	Outside temperature: 5-35°C or 41-95°F. The product of the absolute value of the indoor/outdoor air temperature difference (ΔT) by the height of the building shall be ≤ 200m°C	10-second averages, before and after flow measurements to within ±10% of the measured inside/outside pressure difference

The wind pressures are dependent on the wind characteristics, such as the velocity and direction, the shape of the building envelope and the topography of building location and surrounding environment (Kraniotis, 2014). Consequently, measurements are commonly recommended to be performed in low and steady wind speed. Based on ISO 9972 standard, the overall uncertainty of a blower door test can be estimated using error propagation calculation, which is lower than 10% in calm conditions and ±20% in windy conditions (ISO, 2015). The influence of the weather condition leads to specific recommendations for the wind velocity. For instance, Nevander (1978) established static wind loads and simplified load distribution models and suggested a lower outdoor wind speed limit of 5m/s for building airtightness measurement. It has also been noted that a proper definition of wind speed is hard to find in the existing literature. Typically, there are two different definitions of wind speed, namely the meteorological wind speed, which represents wind speed at 10m above the ground and the local wind speed representing the wind speed at the height of the building. Besides, ISO 9972 provides another wind speed reference, which is the wind speed near the ground. Owing to the different wind speed references, confusion may occur, and significant differences can be noticed for measuring or calculating wind speed as researchers employed different definitions of wind speed for investigating the wind effects on building airtightness measurement. For instance, in the numerical study conducted by Bailly et al. (2012), the wind speed at the height of the wall was defined depending on the wind speed at 10m. Based on their simulation results, they claimed that the measurement of building airtightness could be valid when wind speed is lower than 8m/s, which has not been well stated in ISO 9972 standard. On the other hand, Walker et al. (2013) directly adopted wind speed and direction taken from meteorological towers at the test site. Another concern is that the wind speed is usually measured only when the testing starts and after completion, while the variation in wind speed during testing is ignored. Due to the dynamic characteristics of wind, wind condition may vary during the testing period, which could affect the measurement of building airtightness.

Most of the investigations addressing wind impact on building airtightness measurement have been conducted for fan pressurisation testing, while limited studies related to the test performance of the Pulse technique under different wind conditions have been found in the literature. It was reported by Cooper et al. (2016) that seasonal changes in the environmental conditions produced testing repeatability of ±8% in repeated tests to a detached house over a year time. On the other hand, Zheng et al. (2018) conducted a repeatability assessment to the Pulse testing by using a multi-gear portable trailer fan to provide various artificially imposed

steady wind conditions. They found that a small uncertainty (within ±3%) was obtained when the wind speed was below 3.5m/s. However, the uncertainty increased up to ±25.6% as the wind speed was in the range of 4.5-9m/s. Furthermore, currently, no relevant standards or regulations concerning wind condition for the Pulse test are in place. In this study, a large number of the Pulse tests were implemented for measuring building airtightness of a five-bedroom detached house located at the University of Nottingham, UK under wind speeds up to 8.5m/s. Experimental work was conducted in 7 days for 423 Pulse tests in March 2019. Tests were accomplished in a short period in order to minimise the impact of variable ambient conditions. The viability of the Pulse technique for delivering airtightness measurements under different wind conditions was evaluated.

2 EQUIPMENT

In order to conduct experimental work in this study, several devices were used. The main device for building airtightness measurement is a PULSE-60 unit, which includes a 58.5-litre lightweight aluminium tank and oil-free compact air compressor. A ¾ inch (BSP) solenoid valve is installed at the outlet for releasing the compressed air from the air tank into the test building, which is capable of delivering a 1.5-second pressure rise. A photo of the Pulse unit is shown in Figure 1. The Pulse test data are recorded and analysed by the control box, including test room temperature, chamber and tank pressures, with the results displayed on a LCD screen. An ultrasonic anemometer was used to measure the outdoor wind speed (Figure 2), which adopts the time of flight method of air velocity measurement. The anemomter includes four ultrasonic transducers that are arranged as two pairs at right angles to each other, and each pair measures the component of the wind in the direction between the transducers. The accuracy of the anemometer is ±2% at 12m/s for speed and ±3° at 12m/s for direction. Besides, Datataker DT85 was employed for data acquisition.

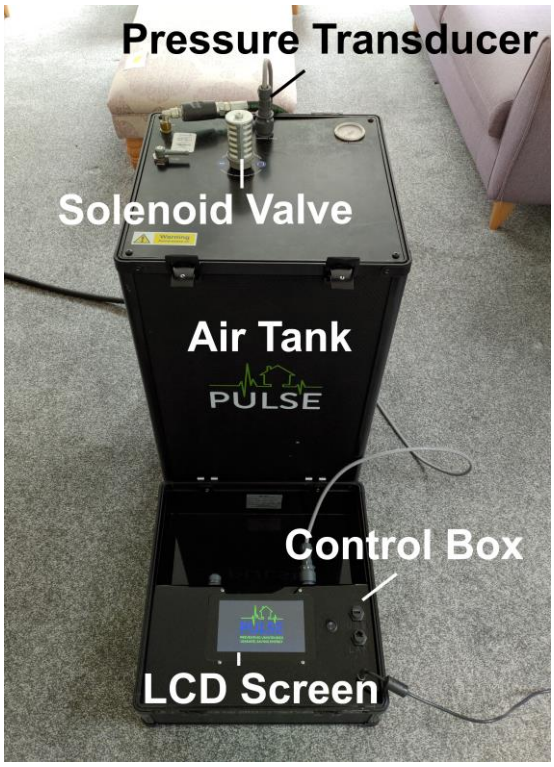

Figure 1: PULSE-60 unit

Figure 2: Ultrasonic anemometer

3 DWELLING AND SETUP

The test building is a five-bedroom detached house located in the Department of Architecture and Built Environment, University Park, Nottingham, UK. The front and back views of the dwelling are presented in Figure 3 and Figure 4. As seen from the floor plans in Figure 5 and Figure 6, the house has one bedroom, one living room, one kitchen on the ground floor and four bedrooms on the first floor. The building parameters are listed in Table 2 and the measurement and calculation of envelope area and volume of the test dwelling complied with ISO 9972.

Figure 3: Front view of test building

Figure 4: Back view of test building

Figure 5: Ground floor plan of test building

Figure 6: First floor plan of test building

Table 2: Envelope area and volume of the test dwelling

Dwelling	Wortley 5 - University of Nottingham, University Park, Nottingham
Volume (m^3)	447
Envelope area (m^2)	416
Approximate ACH @50Pa	3.71 (Blower door tested on December 2018)
Approximate ACH @4Pa	0.73 (PULSE-60 tested on December 2018)

4 RESULTS AND ANALYSIS

The evaluation was conducted based on 423 Pulse tests under different wind conditions; simultaneously, the outdoor wind condition was measured by an anemometer. The anemometer was installed at the height of 2.2m above the ground in the backyard and a distance of 12m away from the perimeter of the test building, without any obstructions within a radius of 12m. In total, 423 Pulse tests were implemented under a variety of wind speed. Figure 7 shows the test results of building air leakage rate (ALR) in the wind speed range of 0-3.5m/s, which includes a total of 133 Pulse tests. Based on the three Pulse tests at low wind speed condition which within 0.5m/s, the average ALR is 288.02m³/h. Therefore, the relative percentage difference is used to indicate the wind impact on building airtightness measurement, which is calculated by comparing the ALR of each single test with the average ALR of 3 Pulse tests at low wind speed condition. Also, Figure 7 presents the relative percentage difference of the 133 tests under the wind speed ranging from 0 to 3.5m/s. Compared to the average of low wind speed ALR, similar results of ALR were obtained when wind speeds were below 2.08m/s, with the highest relative percentage difference within ±3%. Also, it can be noted the relative percentage difference rises above ±5% when the outdoor wind speed higher than 3.14m/s, which indicate that more accurate building airtightness measurement could be achieved for the Pulse test under wind speed around 3m/s with less significant wind impact. Comparatively, a higher relative percentage difference was observed for tests under 3.5 m/s, which is 7.7%.

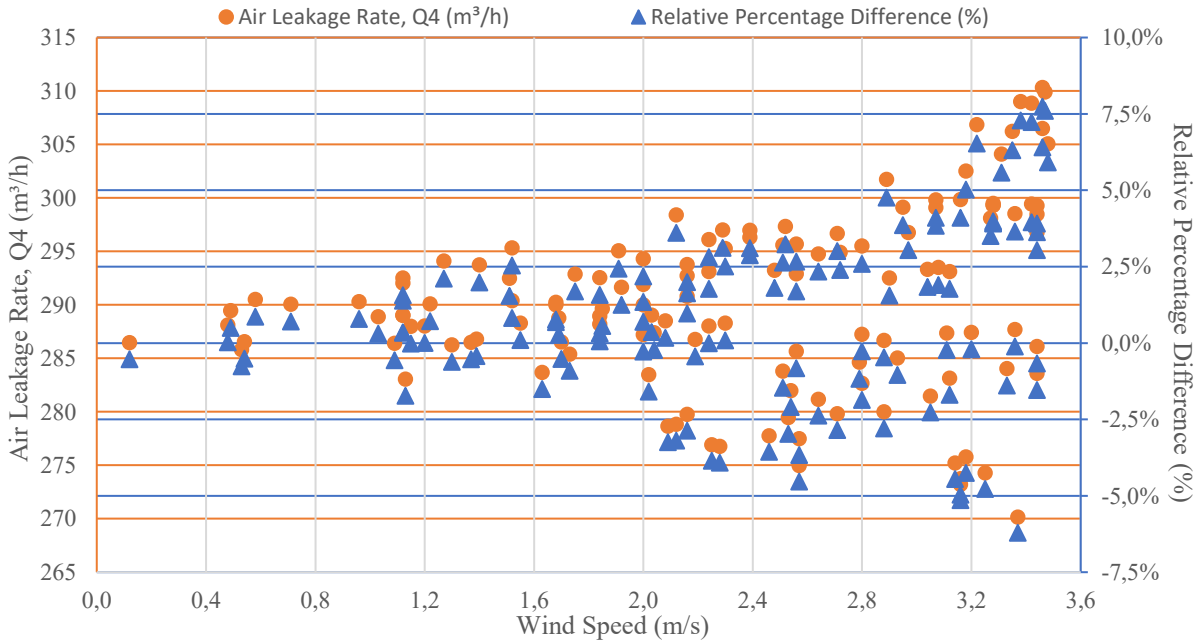

Figure 7: Tests results in the wind speed range of 0- 3.5m/s

The measurement results of ALR for the Pulse tests in the wind speed range of 3.5- 6m/s and the relative percentage difference of each test are presented in Figure 8. As shown in the figure, when wind speed exceeds 5.03m/s, the relative percentage difference is higher than ±10%. Based on the results for wind speed in the range of 3.5- 6m/s, the highest relative percentage difference of -12.19% at wind speeds 5.82m/s is noticed. Compared to the wind speed limit stated in the available standards for blower door testing, for example, ASTM E779-03, the suggested ground wind speed limit is 2m/s and in the ISO 9972, a wind speed limit of 3m/s at ground level is also regulated. Based on the obtained results in this study, building airtightness measurement using Pulse technique is not suggested at wind speed higher than around 5m/s (i.e. at the ground level of 2.2m) as more significant deviation (i.e. >±10%) could be associated.

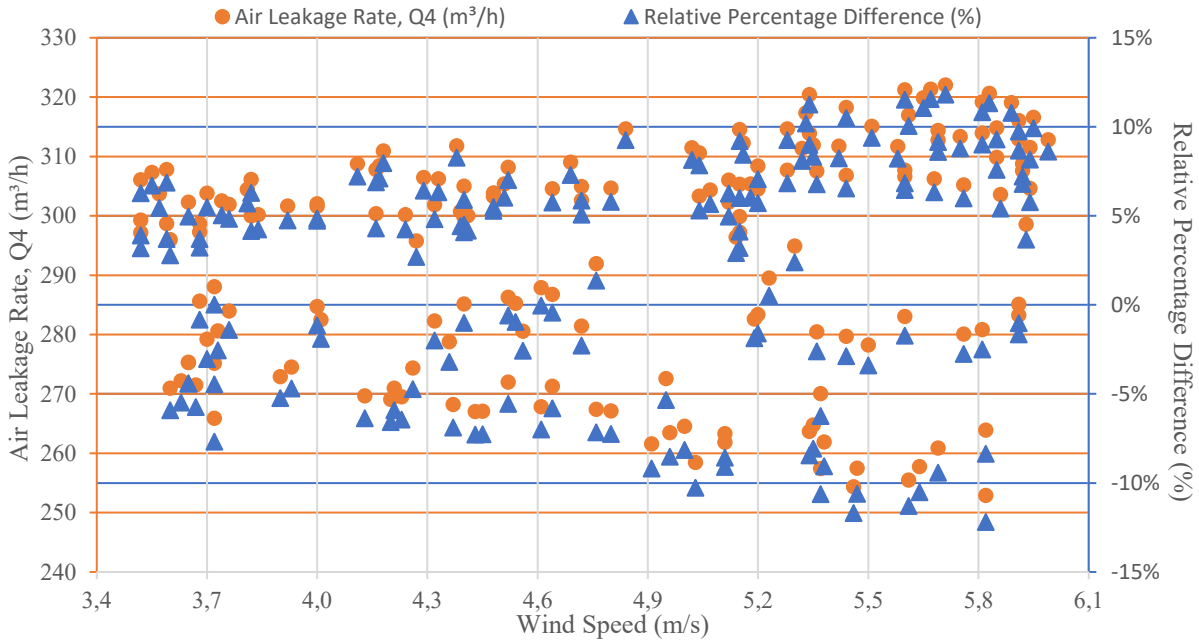

Figure 8: Tests results in the wind speed range of 3.5- 6m/s

Figure 9 shows the ALR and the relative percentage difference results of tests when the wind speed ranged from 6 to 10m/s. A larger difference against the average of low wind speed ALR (288.02m³/h) was observed under the wind condition of 6 to 10m/s. At a wind speed of 9.35m/s, the ALR was reached 348.95m³/h, while 183.67m³/h was obtained at a wind speed of 9.66m/s, with a great relative percentage difference of -36.23%. Even the lowest wind speed in this wind condition (i.e. 6.03m/s) has a relative percentage difference of 13.30%. It can be noted that the relative percentage difference rises above ±20% when the outdoor wind speed higher than 7.37m/s. Therefore, the results imply that for the Pulse test, wind impact should be taken into account under high wind speed condition as the measured building airtightness could vary significantly with the testing wind condition.

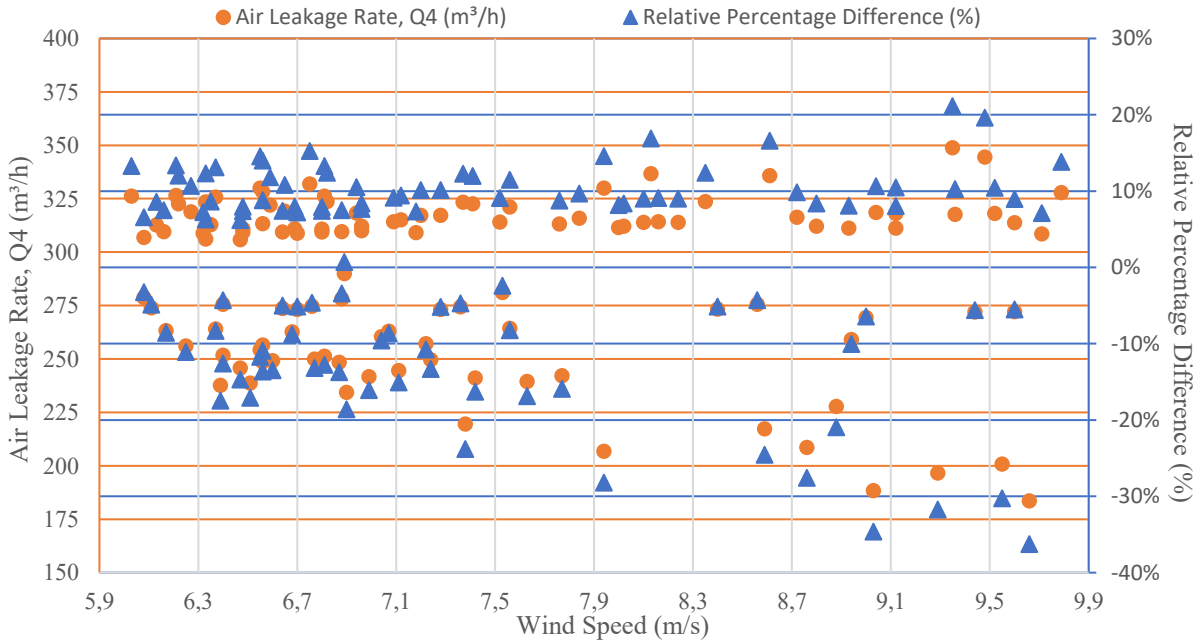

Figure 9: Tests results in the wind speed range of 6- 10m/s

Table 3 lists the measured building ALR of all 423 tests. With a wind speed interval of 0.5m/s, the total 423 tests can be divided into 20 groups for more detailed discussions. The relative percentage difference of each single test and each group are calculated by comparing with the average of low wind speed ALR. As seen in the table, an increased number of the Pulse tests could contribute to a more accurate building airtightness measurement. For instance, the relative percentage difference of each test in Group K (i.e. wind speed 5.0-5.5m/s) is around -11.69%. By considering all 43 Pulse tests in Group K, the overall relative percentage difference is only around 1.84%. As shown in the table, the measurement relative percentage difference of each group fell within ±5% when the wind speed was below 8m/s. That suggests the wind impact reduced significantly when multiple Pulse tests were carried out. However, in order to achieve accurate and rapid testing for multiple Pulse tests, the research also included group average ALR for the first three tests. As shown in the table, the measurement relative percentage difference of the first three tests fell within ±5% when the wind speed was less than 6m/s.

Table 3: Analysis of test ALR, Q4 (m³/h) results for 423 Pulse tests

Test Group	Wind Speed (Ground level)[1]	Number of Tests	Group Average ALR	Group Average ALR (First three tests)	Relative percentage difference		
					Each Test[2]	Each Group[3]	First Three Tests[4]
A	**0 – 0.5 m/s**	3	288.02	288.02	-0.53%	0.00%	0.00%
B	**0.5 – 1.0 m/s**	5	288.66	287.64	-0.76%	0.22%	-0.13%
C	**1.0 – 1.5 m/s**	15	288.97	288.12	-1.72%	0.33%	0.03%
D	**1.5 – 2.0 m/s**	17	290.01	292.74	2.54%	0.69%	1.64%
E	**2.0 – 2.5 m/s**	28	288.84	289.72	-3.91%	0.28%	0.59%
F	**2.5 – 3.0 m/s**	26	288.63	292.25	-4.53%	0.21%	1.47%
G	**3.0 – 3.5 m/s**	39	293.85	291.30	7.74%	2.02%	1.14%
H	**3.5 – 4.0 m/s**	33	291.13	300.87	-7.68%	1.08%	4.46%
I	**4.0 – 4.5 m/s**	33	292.31	296.14	-7.28%	1.49%	2.82%
J	**4.5 – 5.0 m/s**	23	286.88	287.92	-9.18%	-0.40%	-0.03%
K	**5.0 – 5.5 m/s**	43	293.33	278.19	-11.69%	1.84%	-3.42%
L	**5.5 – 6.0 m/s**	41	301.65	301.69	-12.19%	4.73%	4.74%
M	**6.0 – 6.5 m/s**	24	294.78	304.01	-17.47%	2.35%	5.55%
N	**6.5 – 7.0 m/s**	33	288.54	274.40	-18.60%	0.18%	-4.73%
O	**7.0 – 7.5 m/s**	16	281.42	279.31	-23.77%	-2.29%	-3.03%
P	**7.5 – 8.0 m/s**	10	282.87	286.57	-28.18%	-1.79%	-0.50%
Q	**8.0 – 8.5 m/s**	8	312.50	312.63	16.93%	8.50%	8.54%
R	**8.5 – 9.0 m/s**	9	273.82	276.31	-27.56%	-4.93%	-4.07%
S	**9.0 – 9.5 m/s**	10	288.59	258.85	-34.59%	0.20%	-10.13%
T	**9.5 – 10 m/s**	7	275.05	263.75	-36.23%	-4.50%	-8.43%

Based on low wind speed condition 0 – 0.5 m/s (3 Tests)	**Average ALR, Q4 (m³/h)**
	288.02

1. Wind Speed measured at the height of the 2.2m above ground
2. The maximum relative percentage difference of ALR of each single test to the average of low wind speed ALR
3. The relative percentage difference of average ALR of each group to the average of low wind speed ALR
4. The relative percentage difference of average ALR of first three tests to the average of low wind speed ALR

5 CONCLUSIONS

In this study, 423 Pulse tests were carried out to measure the building airtightness of a five-bedroom house under various wind conditions with wind speed up to 10m/s. A Pulse unit with a 58.5-litre air tank was employed to measure the building airtightness whilst an ultrasonic anemometer located 12 metres away from the building perimeter was used to obtain the outdoor wind speed at the height of 2.2 metres above ground level. A relative percentage difference of

each test was defined by comparing with the average building air leakage rate at low wind speed condition within 0.5m/s and used to evaluate the wind impact on the measurement of building airtightness. Based on the experimental data, a more precise building measurement can be achieved for testing under wind speed lower than 5m/s as a relative percentage difference less than ±10% was obtained. When wind speed above 7.3m/s, the relative percentage difference of a single Pulse test can exceed ±20%, which indicates that the measurement may be imprecise owing to the wind impact. Therefore, the Pulse test is suggested to be implemented under wind speed lower than 5m/s at 2.2m above ground level (with relative percentage difference ±10%) in calm conditions and 7.4m/s (with relative percentage difference ±20%) in windy conditions for less wind impact on building airtightness measurement. On the other hand, the results also imply that multiple Pulse tests under a similar wind condition could greatly minimise the wind impact. For instance, the relative percentage difference of a single Pulse test under wind speed of 5.0-5.5m/s is approximate -11.69%, while by implementing 43 repeated Pulse tests, the relative percentage difference decreases to 1.84%. However, in order to achieve accurate and rapid testing for multiple Pulse tests, the measurement relative percentage difference of the first three tests in each group fell within ±5% when the wind speed was less than 6m/s. In addition, future work is recommended for the investigation of quicker air tank charging methods to allow more tests within a short period under similar wind conditions. Furthermore, improving the algorithm of the Pulse technique is also necessary in order to address the wind impact on measurement for wide applicability, especially under high wind speed conditions.

Different from Zheng et al. (2018) using a multi-gear portable trailer fan to provide various artificially imposed steady wind conditions, this study was conducted under natural wind conditions with unpredictable wind characteristics. Both studies investigated the wind speed limit that allowed the Pulse technique to give repeatable and accurate measurements. For the relative percentage difference within ±3%, Zheng et al. (2018) found the test conditions are under steady wind speed below 3.5m/s with fixed wind direction, while wind speed below 2.08m/s under natural wind condition (i.e. ±3%) is noted in this study. A different pattern in airtightness variation was shown between the two studies when the wind level was beyond the limit. This might be attributed to the different wind conditions experienced in the studies, i.e. artificially imposed steady wind in a fixed direction vs. random wind direction under natural conditions. This suggests the wind direction affects the measured airtightness when it is above a certain level. Future studies of the impact of wind direction and leakage distribution on the measurement of airtightness are recommended to obtain further insights into those factors.

6 REFERENCES

ANDREWS, J. 1997. Error analysis for duct leakage tests in ASHRAE Standard 152P. Brookhaven National Lab., Upton, NY (United States).

ASTM, A. 2004. E779-03" Standard Test Method for Determining Air Leakage Rate by Fan Pressurization. *American Society for Testing and Materials, USA*.

BAILLY, A., LEPRINCE, V., GUYOT, G., CARRIÉ, F. & EL MANKIBI, M. Numerical evaluation of airtightness measurement protocols. 33rd AIVC Conference" Optimising Ventilative Cooling and Airtightness for [Nearly] Zero-Energy Buildings, IAQ and Comfort", Copenhagen, Denmark, 2012. 252-255.

COOPER, E. & ETHERIDGE, D. 2007. Determining the adventitious leakage of buildings at low pressure. Part 1: uncertainties. *Building Services Engineering Research and Technology,* 28**,** 71-80.

COOPER, E., ETHERIDGE, D. & SMITH, S. 2007. Determining the adventitious leakage of buildings at low pressure. Part 2: pulse technique. *Building Services Engineering Research and Technology,* 28**,** 81-96.

COOPER, E., ZHENG, X., WOOD, C., GILLOT, M., TETLOW, D., RIFFAT, S. & DE SIMON, L. 2016. Field trialling of a pulse airtightness tester in a range of UK homes. *International Journal of Ventilation*, 1-18.

EN, B. 2000. 13829 Thermal performance of buildings–Determination of air permeability of buildings–Fan pressurization method. *BSI, UK*.

GEISSLER, A. Error Estimation of blower door measurements by computer simulation. The 8th International Conference on Indoor Air Quality and Climate, 1999.

GUYOT, G., CARRIÉ, R., SCHILD, P., THOMSEN, K. E., ROSE, J. & AGGERHOLM, S. 2010. Stimulation of good building and ductwork airtightness through EPBD.

ISO 2015. Thermal performance of buildings–determination of air permeability of buildings–fan pressurization method. International Organization for Standardization (ISO) Geneva.

KRANIOTIS, D. 2014. *Dynamic characteristics of wind-driven air infiltration in buildings The impact of wind gusts under unsteady wind conditions.* Norwegian University of Life Sciences.

KRANIOTIS, D., THIIS, T. K. & AURLIEN, T. Wind direction and leakage distribution in buildings. A CFD transient analysis of their impact on air exchange rates under unsteady wind conditions. 6th European-African conference on wind engineering(EACWE 2013), 2013.

KRANIOTIS, D., THIIS, T. K. & AURLIEN, T. 2014. A numerical study on the impact of wind gust frequency on air exchanges in buildings with variable external and internal leakages. *Buildings,* 4**,** 27-42.

LEPRINCE, V. & CARRIÉ, F. R. 2018. Uncertainties due to steady wind in building pressurisation tests. *REHVA Journal,* 03**,** 53-57.

LEPRINCE, V., MOUJALLED, B. & LITVAK, A. 2017. *Durability of building airtightness, review and analysis of existing studies*.

NEVANDER, L. E. K., J. 1978. Airtightness of buildings - Research in Sweden. *IEA Seminar on R&D projects in the area of infiltration in buildings.* Paris, France.

SHERMAN, M. & PALMITER, L. 1995. Uncertainties in fan pressurization measurements. *Airflow performance of building envelopes, components, and systems.* ASTM International.

SHERMAN, M. H. & CHAN, W. R. 2006. Building air tightness: research and practice. *Building Ventilation.* Routledge.

VINHA, J., MANELIUS, E., KORPI, M., SALMINEN, K., KURNITSKI, J., KIVISTE, M. & LAUKKARINEN, A. 2015. Airtightness of residential buildings in Finland. *Building and Environment,* 93**,** 128-140.

WALKER, I., SHERMAN, M. H., JOH, J. & CHAN, W. 2013. Applying Large Datasets to Developing a Better Understanding of Air Leakage Measurement in Homes. *International Journal of Ventilation,* 11**,** 323-338.

ZHENG, X., COOPER, E., MAZZON, J., WALLIS, I. & WOOD, C. J. 2019a. Experimental insights into the airtightness measurement of a house-sized chamber in a sheltered environment using blower door and pulse methods. *Building and Environment*.

ZHENG, X., MAZZON, J., WALLIS, I. & WOOD, C. J. Experimental study of enclosure airtightness of an outdoor chamber using the pulse technique and blower door method under various leakage and wind conditions. 39th AIVC - 7th TightVent & 5th venticool Conference, 18-19 September 2018 2018 Antibes Juan-Les-Pins. 352-362.

ZHENG, X. F., COOPER, E., ZU, Y. Q., GILLOTT, M., TETLOW, D., RIFFAT, S. & WOOD, C. J. 2019b. Experimental Studies of a Pulse Pressurisation Technique for Measuring Building Airtightness. *Future Cities and Environment,* 5(1)**,** 10.

Estimation of Air Leakage Sizes in Building Envelope using High-Frequency Acoustic Impulse Response Technique

Benedikt Kölsch*[1], Björn Schiricke[2], Jacob Estevam Schmiedt[3], and Bernhard Hoffschmidt[3]

1 German Aerospace Center (DLR)
Institute of Solar Research
Karl-Heinz-Beckurts-Str. 13
52428 Jülich, Germany
**Corresponding author: benedikt.koelsch@dlr.de*

2 German Aerospace Center (DLR)
Institute of Solar Research
Linder Höhe
51147 Cologne, Germany

3 German Aerospace Center (DLR)
Institute for the Protection of Terrestrial Infrastructures
Linder Höhe
51147 Cologne, Germany

ABSTRACT

Heating energy in buildings represents a significant proportion of the total global energy consumption. Uncontrolled airflow through the building envelope contributes significantly to its energy losses.
Existing methods, like the fan pressurisation technique, which measure the air infiltration rate and quantify individual leakage sizes in buildings, are expensive and time-consuming. Additionally, the accurate detection of the leak location with these methods depends strongly on the experience of the respective building inspector. Moreover, it is hardly possible to identify the size of each leakage accurately and quantify their contributions to the entire building air change rate. Thus, the development of a new measurement method is a vital step.
In this paper, a high-frequency acoustic method is proposed to identify leakage sizes. Using an impulse response technique with multiple microphones and a high-frequency broad-band excitation signal enables the identification of frequency components which are predominantly attenuated inside walls. In a laboratory test chamber, different interchangeable walls have been used. Therefore, it was possible to investigate different leakage sizes and compare them directly in a controlled environment. As an excitation signal, an exponential sine sweep is used, which is able to cover a broad frequency range and simultaneously only excites the desired frequencies. By analysing the spectra, it is possible to differentiate between different cracks and leak sizes. Therefore, this technique has the potential to concentrate only on significant leaks during a building renovation and save building owners time and costs.

KEYWORDS

Air leakage, acoustics, high frequency, impulse response, leakage size

1 INTRODUCTION

Climate protection and environmental degradation have arisen as salient topics nowadays. The building sector is responsible for more than one-third of the global energy consumption and is, therefore, the largest end-use sector (International Energy Agency, 2013). Besides thermal conduction, uncontrolled air infiltration is the main source of increased energy consumption in residential and commercial buildings and, thus, of higher costs for the owners. Emmerich et al. predicted in their research, that airtight houses in the U.S. can potentially save heating and

cooling energy cost in the range from 4 % to 36 % per year (Emmerich et al., 2005). Additionally, unwanted airflow through the building envelope may lead to an impairment of indoor air quality and condensation of moisture inside walls, in particular during winter (TenWolde, 1994).

In order to quantify the airtightness of buildings, typically the fan pressurization method ("blower door test") is applied in buildings (Norm DIN EN ISO 9972). Although this test is applicable to quantify the airflow rate mostly at a pressure difference of 50 Pa between indoor and outdoor, it does not serve the purpose to determine airflow under natural condition. The pressure difference of 50 Pa is often used because it is low enough for most blower door configurations to achieve and high enough to be independent of weather influences outside (Sherman and Chan, 2004).
A less frequently consulted method is the tracer gas dilution method (Norm DIN EN ISO 12569). A non-reactive tracer gas will be released inside a room, and the distribution of the gas throughout the room will be monitored. This method is complex and requires a high standard of measurement equipment. Both methods are expensive and time-consuming. Additionally, it is demanding to find the location of the leaks correctly using these methods. One can use smoke sticks to visualize the airflow or consider the additional usage of infrared cameras to identify different air temperature layers. However, the use of infrared cameras requires a significant temperature difference between indoor and outdoor. Moreover, both methods do not provide information about leakage shape and size.

In this paper, we propose a new method using a high-frequency impulse response technique to identify leakage sizes. Acoustic waves take the same paths as air does, and therefore, it is possible to monitor the way the wave takes. The presented work is part of an ongoing research project to make remote-sensing techniques applicable for energy analysis of existing buildings (Estevam Schmiedt et al., 2017). The goal of this project is to develop a toolbox of measurement and analysis methods to determine the thermal properties of buildings and collect crucial information about the building structure.

2 METHODS

The objective of this work is to identify different leak sizes in different materials of the wall. In order to achieve this, the frequency-dependent sound insulation of different walls is determined. The sound insulation between two rooms can be measured using the sound reduction index R (Norm DIN EN ISO 12354-1):

$$R = \Delta L_P + C = \Delta L_P + 10\lg\left(\frac{S}{A}\right) = \Delta L_P + 10\lg\left(\frac{S}{0.163\frac{V}{T}}\right) \quad (1)$$

Here, ΔL_P is the measured sound pressure level difference in dB between two rooms. The sound reduction index can usually not be directly determined by measuring only the sound pressure level difference. In the receiving room, the measured sound pressure is superimposed by reflected sound waves of the surrounding surfaces (Lerch et al., 2009). This fact is considered by the term C of the equation. Here, S is the area of the common partition in m², and A is the equivalent absorption area of the receiving room in m². The equivalent absorption area can be approximated using Sabine's formula, where V is the volume of the receiving room in m³ and T is the reverberation time in seconds which has to be measured in the receiving room. The reverberation time is the time it takes to reduce the energy density to the one-millionth of the

original sound or respectively the time it takes for the sound pressure level to drop 60 dB after the abrupt ending of a generated test signal (Müller and Möser, 2004).
In practice, this formula is usually acceptable and a sufficient approximation of the sound reduction index if rooms are small and the considered frequencies low. However, in this work, higher frequencies are considered as well. Hence, this formula should be adapted, and the air absorption has to be taken into account using the intensity attenuation coefficient *m* in 1/m:

$$R_A = \Delta L_P + C_A = \Delta L_P + 10\lg\left(\frac{S}{V\left(\frac{0.163}{T} - 4m\right)}\right) \tag{2}$$

The attenuation coefficient depends on the frequency, the ambient atmospheric temperature, and the relative humidity and is calculated according to ISO 9613-1 (Norm ISO 9613-1) and Wenmaekers (Wenmaekers et al., 2014). This coefficient increases with increasing ambient temperature and frequency.

2.1 Experimental Setup

In order to be able to compare different materials and leakage sizes under laboratory conditions, a test chamber has been constructed. This chamber consists of two equal sized cells with the following dimensions for each cell: 30.0 cm x 43.5 cm x 31.0 cm. As test specimen replaceable acrylic glass, as well as plywood walls, are used. Each barrier contains an orifice with a diameter of 4, 6, 8 or 10 mm. These orifices simulate potential air leakages inside a wall. Except for these intentional openings, the walls are sealed so that they are airtight.

An ultrasonic omnidirectional dynamic speaker with a frequency range of 1 – 120 kHz is placed in one cell. Two ultrasonic microphones are sited in the test chamber as well, one in each cell. The microphones are 1/4" condenser microphones with an even frequency response and a recommended frequency range of 0.004 – 100 kHz. The signal is generated and evaluated using a python script, and the data acquisition is performed by a USB wide dynamic range signal analyser with a sampling frequency of 216 kHz per channel.

2.2 Measurement Procedure

The calculation of the sound reduction index R_A requires a measurement of the sound pressure level difference ΔL_P and C_A. According to DIN EN ISO 18233 (Norm DIN EN ISO 18233), the sound pressure level difference between two rooms can be calculated using the ratio of the integrated and squared impulse response *h* of the sending (index 1) and receiving room (index 2):

$$\Delta L_P = 10\lg\left(\frac{\int_0^\infty h_1^2(t)\,dt}{\int_0^\infty h_2^2(t)\,dt}\right) \tag{3}$$

Assuming, the acoustics of a room is a linear and time-invariant system, the entire information of the room transfer function is contained in the room impulse response. Unfortunately, in reality, the system is not perfectly linear, because a measured impulse response contains

artefacts caused by noise and the non-linear behaviour of, e.g. amplifiers or transducers. To overcome this problem, a method based on Farina (Farina, 2000) is applied in this paper. Here, an exponential sine sweep with constant amplitude is used as an excitation signal. The excitation signal was generated using a python script and is then recorded in the sending, as well as in the receiving room (see Figure 1). To obtain the desired impulse response, the recorded signal *y(t)* has to be convolved with an inverse filter signal:

$$h(t) = y(t) * ESS^{-1} \tag{4}$$

In practice, the inverse filter signal ESS^{-1} is the reversed time signal of the exponential sine sweep with modulated amplitude in order to compensate the exponentially changing sweep energy. In contrast to other methods employed for measurement of the impulse response (e.g., the maximum length sequence method or the linear sweep method), the accumulation of nonlinearities in the measured signal can be entirely separated from the actual linear room impulse response using this method. Moreover, the signal-to-noise ratio and the repeatability of the measurements (also with the presence of air and temperature fluctuations) are better than for the other methods. Additionally, the use of an exponential sweep enables the user to consider only relevant frequency bands. In this case, the frequency range is 1–100 kHz. All frequency dependent parameters are finally band filtered and evaluated within a 1/3 octave band (Third-octave filter: TF).

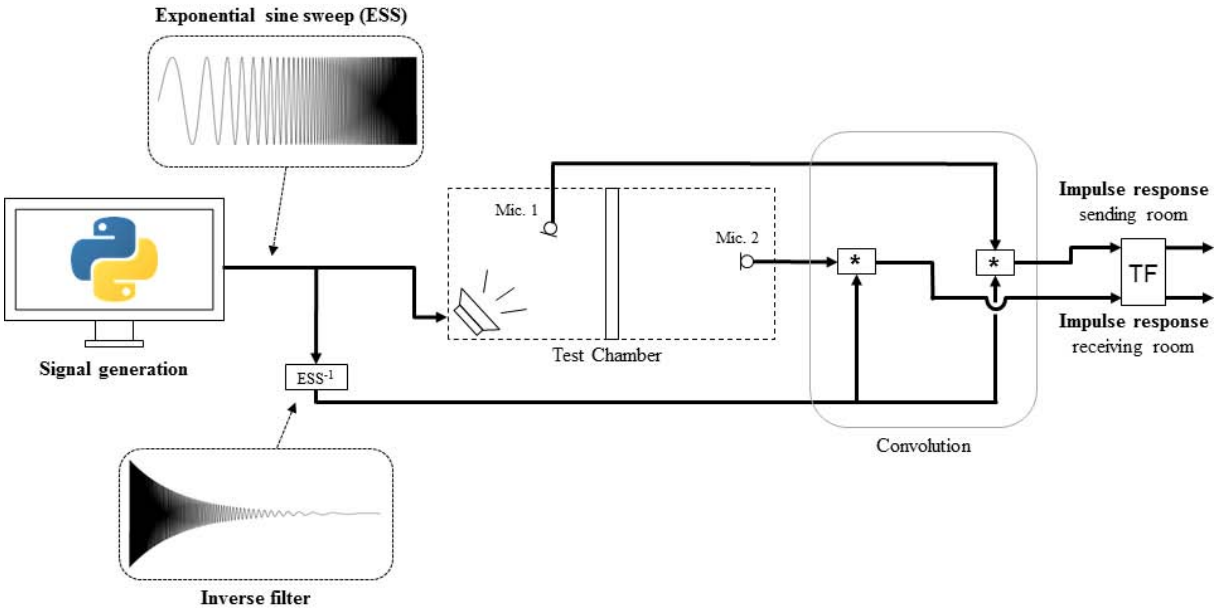

Figure 1: Measurement procedure

Next, the missing parameters for the second part of equation (2) have to be identified. The area of the common partition *S* and the room volume of the receiving room *V* are only geometrical parameters and constants. The reverberation time *t* is frequency dependent and has been measured in the receiving room according to DIN EN ISO 3382-2 (Norm DIN EN ISO 3382-2). In this procedure, the impulse response is measured similar to the method illustrated in Figure 1 in the receiving room for an acrylic glass and a plywood wall in order to calculate the reverberation time. After the impulse responses are 1/3 octave filtered, decay curves are determined for each frequency band by calculating the backwards integration of the squared impulse responses. Subsequently, the sound level can be calculated from the integrated squared impulse responses, and it is possible to determine the time the sound pressure level takes to drop by 60 dB, which is the reverberation time t_{60}. This process is shown in Figure 2.

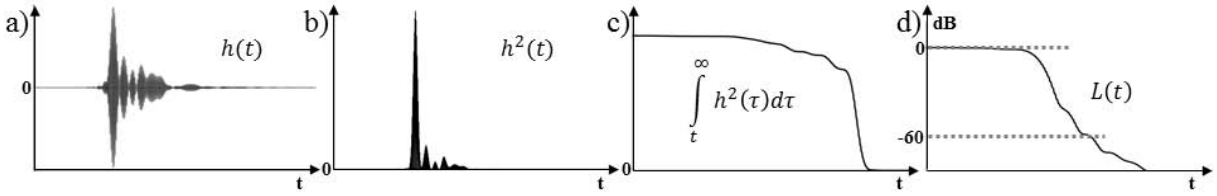

Figure 2: Measurement process of reverberation time: a) Measured impulse response in the receiving room, b) Squared impulse response, c) Backwards integration of the squared impulse response, d) Estimation of reverberation time from sound level *L(t)* drop

3 RESULTS

In this paper, the sound reduction indexes between the two rooms, as well as the required reverberation times in the receiving room have been measured, which are presented in the following section.

3.1 Reverberation Time Measurements

The measured values of the reverberation time t_{60} in the receiving room for a separation wall of acrylic glass and plywood are shown in Figure 3. As stated above, t_{60} is the time span it takes until the sound pressure level in a room decreases by 60 dB. In practice, the t_{60} is often not measured directly because background noise would distort the measurement. Here, the measurements of the t_{30} and t_{20} have been taken and subsequently extrapolated to the required t_{60} value.
It can be seen that the reverberation time using the acrylic glass wall is higher than the reverberation time using the plywood wall for every frequency. The difference is mainly significant for lower frequencies. For high frequencies, the differences are marginal. The lower reverberation times for a plywood wall indicate that a wooden wall absorbs more sound energy which is reflected from the walls compared to a stiff acrylic glass wall.

Figure 4 shows the calculated factors C and C_A, which are the second part of the sound reduction index equations (1) and (2). In contrast to C, C_A considers the damping of the sound waves in air. The black lines are the values for acrylic glass and the grey ones for plywood. For lower frequency values (< 4 Hz), the damping factor does practically not affect C. At higher frequencies, it becomes increasingly important. However, since higher frequencies are considered in this study as well, it is not sufficient to neglect the damping factor. For all following calculations of R, C_A has therefore been used.

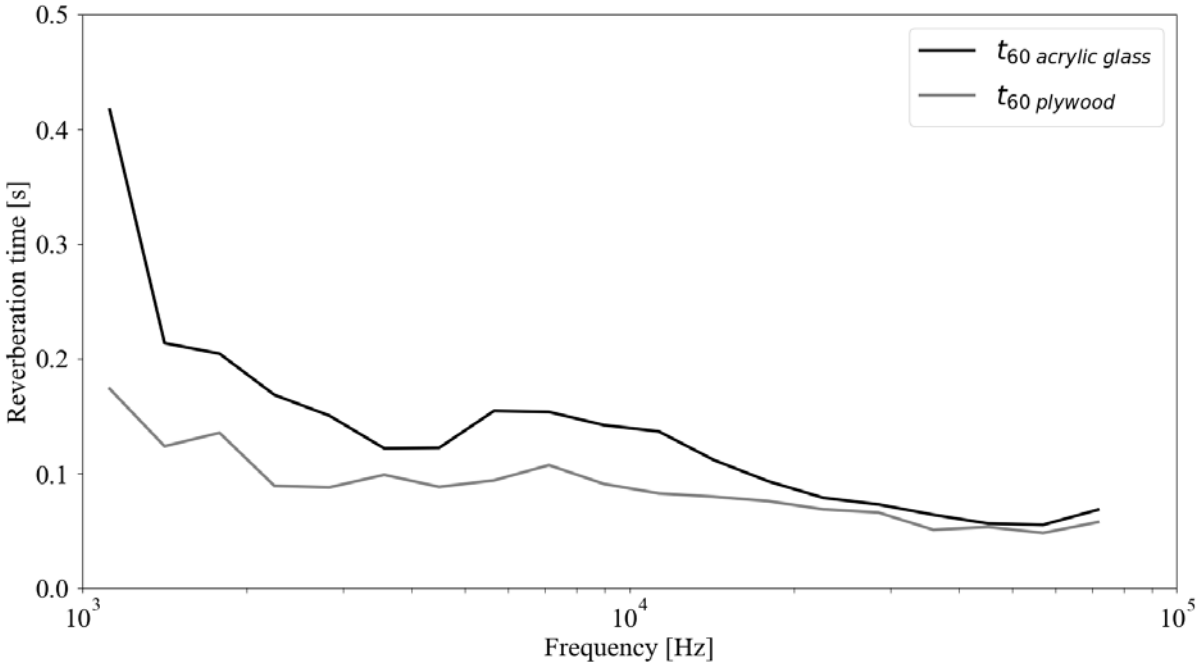

Figure 3: Reverberation times t_{60} in receiving room for acrylic glass and plywood

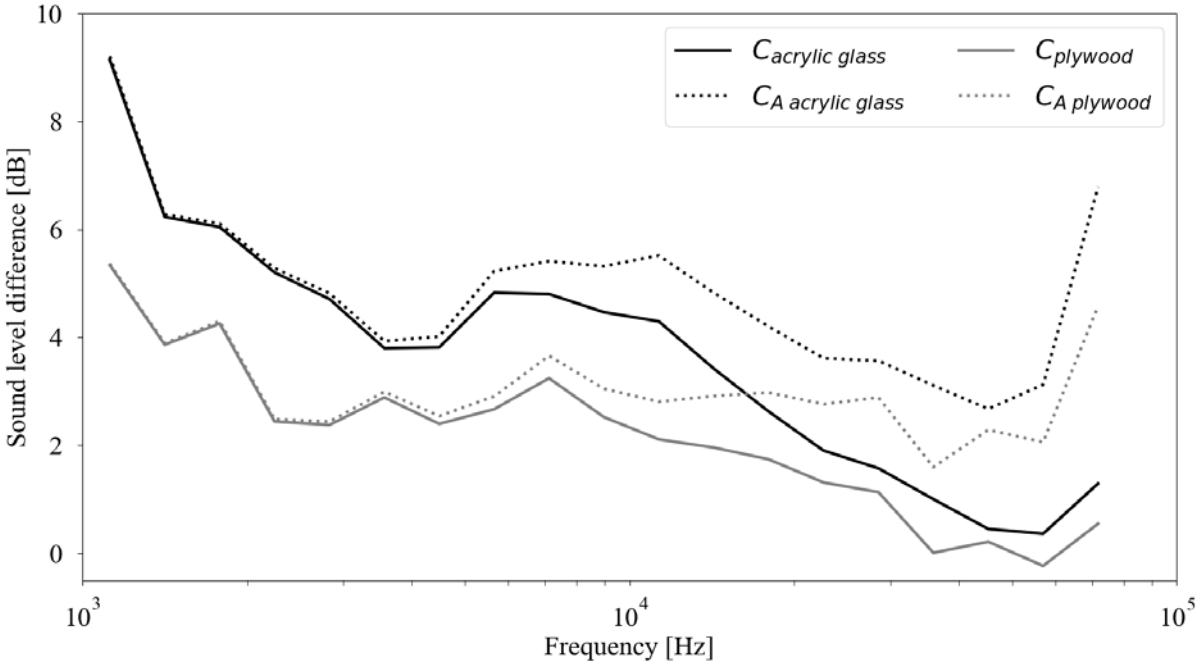

Figure 4: Factors C and C_A of the acrylic glass and the plywood wall at an ambient temperature of 24.3 °C and relative humidity of 23.0 %

3.2 Sound Reduction Index Measurements

In Figure 5 - 8, the sound reduction indexes *R* for acrylic glass and plywood walls are shown. The index indicates the sound transmission and absorption characteristics for these different wall materials at each frequency. In the upper part of each figure, four measured R-values as a function of frequency are illustrated. The solid lines are the measurements, which were taken

with a hole in the wall (4, 6, 8 or 10 mm). To be able to compare the reduction of *R* to a reference value, the same measurements were additionally performed with both wall materials under leak-proof conditions (dotted lines). These reference measurements are identical in all following figures.
In the same figures, the frequency dependence of the difference in *R* between the reference measurement and the measurement for each hole size is shown. This enables the identification of frequencies, where the output signal is predominantly affected by the hole size. If ΔR is negative, the sound reduction index of the measurement of a wall with a hole is lower compared to the same leak-proof wall. A lower sound reduction index indicates that more sound energy is transmitted at these frequencies.

The sound reduction index for plywood walls with no holes and for frequencies which are below 7.5 kHz is significantly lower compared to the same measurement with acrylic glass. For higher frequencies, the R-values for none of these two materials are dominant over a broad frequency band. Moreover, all following measurements show a sudden drop of the sound reduction index at a frequency of around 1.7 kHz, which is probably caused by a resonance.

The difference in sound reduction between measurements on walls with a hole and those with no hole grows with increasing hole diameter. This fact is presented in Table 1, where the mean differences of the sound reduction index are presented.

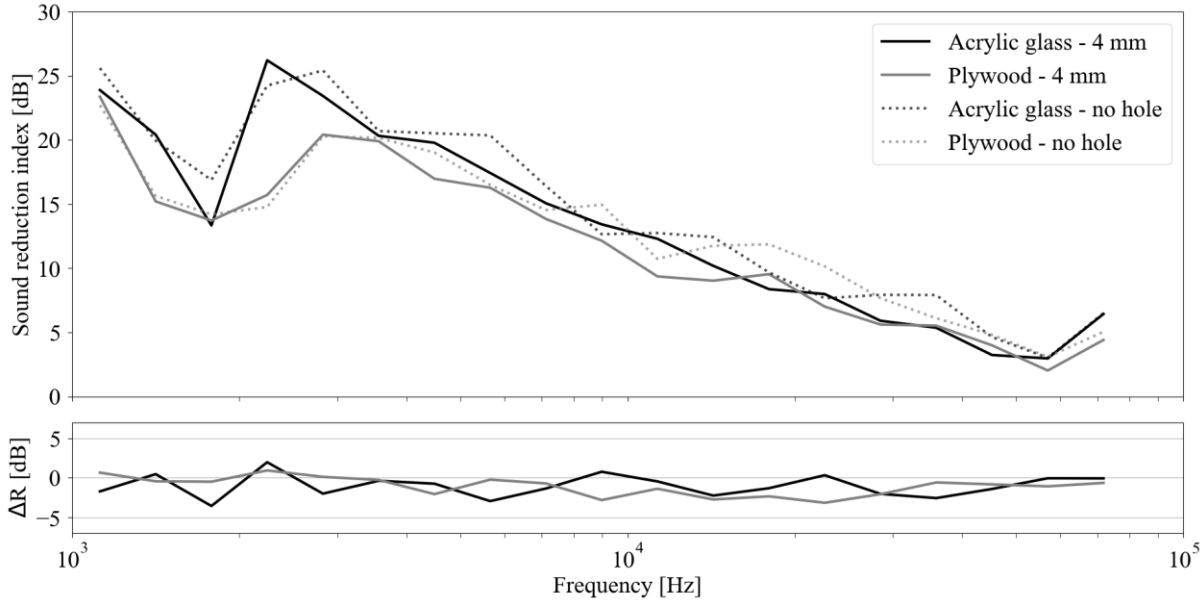

Figure 5: Sound reduction index *R* for measurements at walls with no holes (dotted lines) and walls with a 4 mm hole (solid lines in the upper graph) and differences of *R* from these two measurements (lower graph)

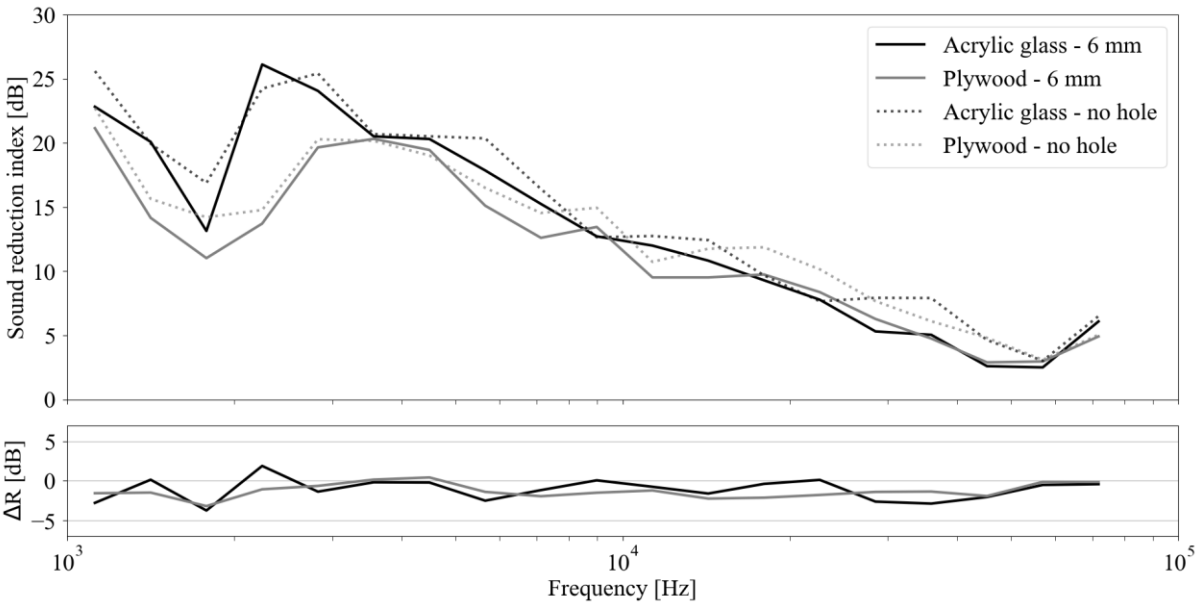

Figure 6: Sound reduction index R for measurements at walls with no holes (dotted lines) and walls with a 6 mm hole (solid lines in the upper graph) and differences of R from these two measurements (lower graph)

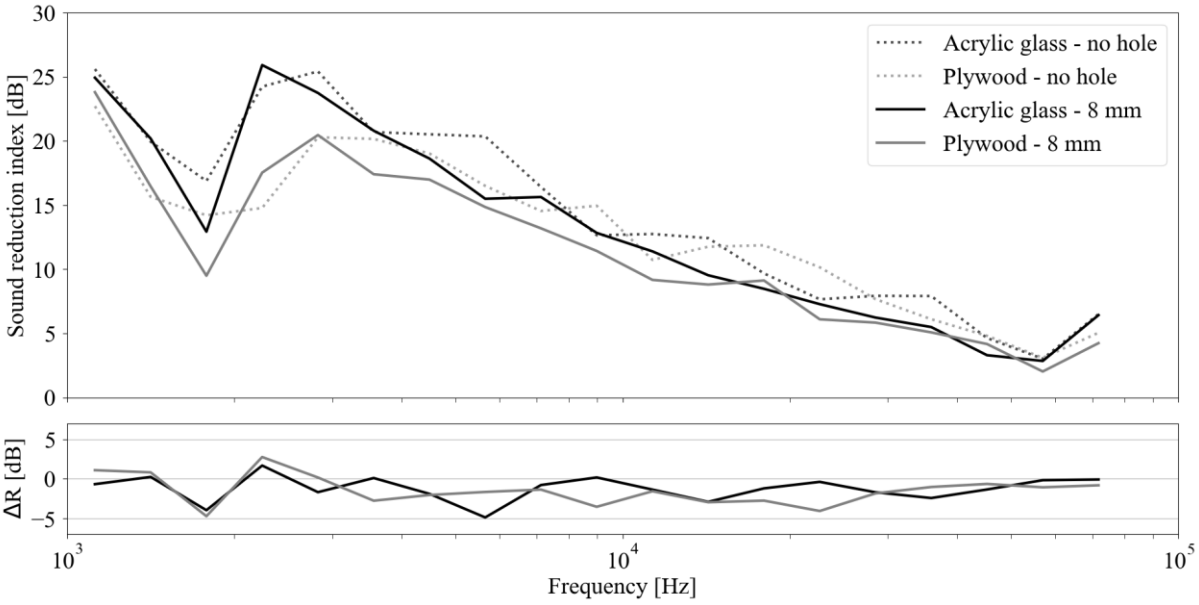

Figure 7: Sound reduction index R for measurements at walls with no holes (dotted lines) and walls with a 8 mm hole (solid lines in the upper graph) and differences of R from these two measurements (lower graph)

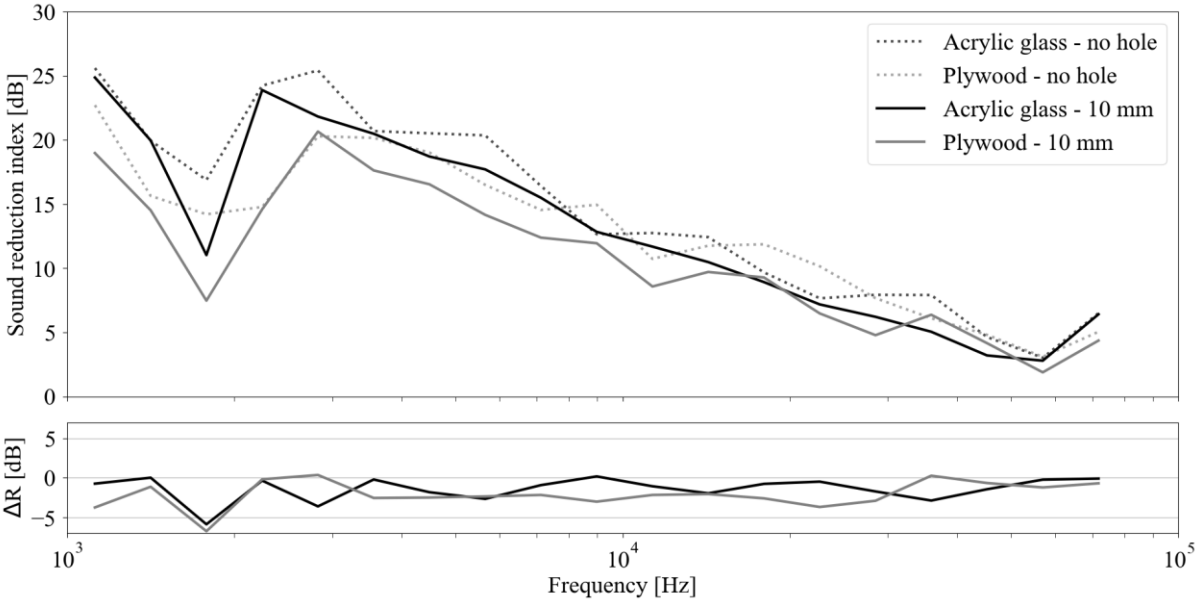

Figure 8: Sound reduction index R for measurements at walls with no holes (dotted lines) and walls with a 10 mm hole (solid lines in the upper graph) and differences of R from these two measurements (lower graph)

Table 1: The mean sound reduction index differences

	4 mm	**6 mm**	**8 mm**	**10 mm**
Acrylic Glass	-1.01	-1.10	-1.22	-1.39
Plywood	-1.05	-1.29	-1.48	-2.08

4 DISCUSSION

On average, over all frequencies, the sound reduction index decreases with increasing hole size. The differences are larger for the plywood walls compared to acrylic glass walls. This indicates that sound reduction and hole size may be correlated. A direct link between a specific frequency and the hole size could not be observed in these measurements.

5 CONCLUSIONS

In this paper, impulse responses over a wide frequency range have been used to determine the sound reduction indexes for an acrylic glass and a plywood wall with various hole sizes. It was possible to differentiate between leak-proof walls and walls with a hole. Furthermore, a distinction between different leakage sizes is possible. This technique may have the potential to locally determine leak sizes in walls, particularly if measurements are compared with nearby leak-proof wall parts as a reference.

In future work, similar measurements will be performed in a larger test bench, where simultaneous air infiltration measurements are possible. This will enable a better test of correlations between acoustic parameters and actual air infiltration. Additionally, more complex slit geometries and replicas of real building parts can be tested. Finally, the measurement procedure has to be validated with measurements at real building parts.

6 ACKNOWLEDGEMENTS

The presented work was embedded in a joint research project of the German Aerospace Center (DLR) and the Solar-Insitut Jülich at FH Aachen which is funded by the German Ministry for Economic Affairs and Energy.

7 REFERENCES

Emmerich, S. J., McDowell, T. P., & Anis, W. (2005). *Investigation of the Impact of Commercial Building Envelope Airtightness on HVAC Energy Use* (US Department of Commerce, Technology Administration, National Institute of Standards and Technology, Ed.).

Estevam Schmiedt, J., Cerra, D., Dahlke, D., Dill, S., Ge, N., Göttsche, J., et al. (Eds.). (2017). *Remote sensing techniques for building models and energy performance studies of buildings*.

Farina, A. (Ed.). (2000). *Simultaneous measurement of impulse response and distortion with a swept-sine technique*.

International Energy Agency. (2013). *Technology Roadmap: Energy-efficient Buildings: Heating and Cooling Equipment,* OECD/IEA.

Lerch, R., Sessler, G., & Wolf, D. (2009). *Technische Akustik. Grundlagen und Anwendungen*. Berlin: Springer-Verlag.

Müller, G., & Möser, M. (2004). *Taschenbuch der Technischen Akustik* (3rd ed.). Berlin: Springer-Verlag.

Norm, DIN EN ISO 12354-1 (2017). *Building acoustics - Estimation of acoustic performance of buildings from the performance of elements - Part 1: Airborne sound insulation between rooms*. Berlin: Beuth Verlag.

Norm, DIN EN ISO 12569 (2018). *Thermal performance of buildings and materials - Determination of specific airflow rate in buildings - Tracer gas dilution method*. Berlin: Beuth Verlag.

Norm, DIN EN ISO 18233 (2006). *Acoustics - Application of new measurement methods in building and room acoustics*. Berlin: Beuth Verlag.

Norm, DIN EN ISO 9972 (2018). *Thermal performance of buildings – Determination of air permeability of buildings – Fan pressurization method*. Berlin: Beuth Verlag.

Norm, DIN EN ISO 3382-2 (2008). *Acoustics - Measurement of room acoustic parameters - Part2: Reverberation time in ordinary rooms*. Berlin: Beuth Verlag.

Norm, ISO 9613-1 (1993). *Acoustics - Attenuation of sound during propagation outdoors - Part 1: Calculation of the absorption of sound by the atmosphere*. Berlin: Beuth Verlag.

Sherman, M. H., & Chan, R. (2004). *Building Airtightness: Research and Practice,* Lawrence Berkeley National Laboratory.

TenWolde, A. (1994). Ventilation, humidity, and condensation in manufactured houses during winter. *ASHRAE Transactions, 100*(*1*), 103–115.

Wenmaekers, R. H. C., Hak, C. C. J. M., & Hornikx, M. C. J. (2014). The effective air absorption coefficient for predicting reverberation time in full octave bands. *The Journal of the Acoustical Society of America, 136*(*6*), 3063–3071. doi:10.1121/1.4901710

Deviation of blower-door fans over years through the analysis of fan calibration certificates

Valérie Leprince[1*], Christophe Delmotte[2], Isabelle Caré[3]

1 PLEIAQ
84 C Av de la Libération
69330 Meyzieu, France
**Corresponding author: valerie.leprince@pleiaq.net*

2 Belgian Building Research Institute
Rue du Lombard 42
1000 Bruxelles, Belgium

3 CETIAT
Domaine scientifique de la Doua, 25 avenue des Arts
69100 Villeurbanne, France

ABSTRACT

Mandatory building airtightness testing has come gradually into force in European countries, mostly because of the increasing impact of building leakage on the overall energy performance of low-energy buildings.
Therefore, because of related legal and financial issues, the reliability of the airtightness test has become a crucial issue and has raised the question of the fan calibration process.
Stake-holders need to find the right balance between cost for testers and test reliability. While some manufacturers recommend a 4 years frequency for calibration, fan calibration is required every year in UK and every 2 years in France. In these 2 countries building airtightness testing are mandatory.
The objective of this paper is to evaluate fan deviation over years. This evaluation has been done through the analysis of calibration certificates issued by certified bodies.
According to these certificates the fan deviation is low but not negligible with 5% of the fan varying of more than 8.5% compared to manufacturer coefficients. It has also been observed that:

- Low-used and well-stored fans deviate less than daily used ones.
- Configurations measuring large flowrate deviate less than configurations that measure small flowrates.
- A significant difference of deviation is observed according to the background test pressure during calibration (30 or 50 Pa);

Besides, conclusions cannot be drawn without taking into account the calibration uncertainty mentioned in the certificates. Therefore this paper is completed by a discussion about the uncertainties stated by the calibration laboratories and the need for an appropriate level in regard with the maximum permissible error when a verification report is required.

KEYWORDS

Airtightness measurement, fan calibration, uncertainty

1 INTRODUCTION

Mandatory building airtightness testing has come gradually into force in European countries, mostly because of the increasing impact of building leakage on the overall energy performance of low-energy buildings.
Therefore, because of related legal and financial issues, the reliability of the airtightness test has become a crucial issue and has raised the question of the fan calibration process.
Stake-holders need to find the right balance between cost for testers and test reliability.

In France and UK the fan calibration is mandatory. However, the 2 countries have 2 different approaches regarding calibration. In UK, the calibration is done every year and fan coefficients are systematically adjusted, while in France the verification is required every 2 years and coefficients are recalculated only if the error exceeds the Maximum Permissible Error. Therefore we have gathered calibration data coming mainly from UK and France.
The objective of this paper is to evaluate fan deviation over years. This evaluation has been done through the analysis of calibration certificates issued by certified bodies.
In the first part of the study we have studied the deviation of fan with the British approach, that is to say by recalculating fan coefficients from the calibration points (systematic adjustment of fan coefficients).
In the second part of the study we have studied the deviation compared to the manufacturer coefficients.
At the end, we have also discussed the impact of the calibration uncertainty and sources of deviations.

2 METHODOLOGY

For the first part of the study, we have recalculated fan coefficients for each configuration with each certificate and calculate the deviation of associated flowrate.
Each fan has up to 10 configurations and may have been calibrated more than twice. Therefore the number of data from each body used in the statistic study is given in Table 1. In UK fans are calibrated every year, therefore Stromatech has provided C and n coefficients calculated every year for 12 fans, some fans have been calibrated 5 years in a row.

Table 1: Number of data per provider according to the time between calibrations

	1 year	**2 years**	**3 years**	**4 years**	**5 years**
Stromatech	67	55	43	32	21
Cerema	0	22	0	6	0
Syneole	11	76	10	6	0
BCCA	0	0	0	0	6
Total	78	153	53	44	27

Data provided by the four bodies are quite different. Stromatech (12 fans) is a calibration laboratory in UK. They have provided new calibration coefficients (C and n) but without giving more details (reference flow, pressure difference, uncertainty).

Syneole (13 fans), BCCA (1 fan) and Cerema (5 fans) have provided fan calibration certificates. However, it has to be noticed that Cerema fans are rarely used, well maintained and well stored. While Syneole (trade union of French airtightness testers) has a "classical" use of their fans so their data may be the most representative of the market.
The 2 years results are probably the most representative, as we have data from the three bodies and more than 100 data.

For Syneole, BCCA, and Cerema, verification data (reference flowrate) of the certificate were used to recalculate the coefficients C and n for each configuration: a regression was done from tests points (at least 3) provided in the calibration certificate.
The flowrate at 150 Pa has been calculated and was used to calculate the deviation. The flowrate (Q) through the device according to the pressure difference and the coefficients is

$$Q = C * \Delta P^{n} \quad (1)$$

The deviation is

$$Deviation = ABS\left(\frac{Q_{new} - Q_{prev}}{Q_{new}}\right) \quad (2)$$

Q_{new}	m^3/h	Flowrate calculated with new coefficients
Q_{prev}	m^3/h	Flowrate calculated with coefficients of the previous calibration

For the second part of the study, as far as the deviation was compared to manufacturer data we no longer needed to have 2 calibration certificates, nevertheless new information on calibration were now needed. Therefore, it is another set of data that has been used in this part of the study:

- part of the previous data has been used, when the following information were available:
  - calibration uncertainty
  - reference and device flowrates.
- New fans, for which only one certificate was available, have been added.

As far as the coefficients were not recalculated, every measurement data has been used (3 to 5 checking points per configuration) which means that 1007 data of 325 fan configurations from 62 calibration certificates have been used.
We have included in the analysis the calibration uncertainty, the difference has been made between "reliable" calibration data and all data.
Reliable data are those for which the given calibration uncertainty is maximum a third of the French Maximum Permissible Error (2 m^3/h or 5% the largest) or a third of the observed deviation:

$$U < \max\left(\frac{q_{vd}-q_{vr}}{3}; \frac{0.05\ q_{vr}}{3}; 2\right) \qquad (3)$$

U	m^3/h	Calibration uncertainty
q_{vr}	m^3/h	Reference flowrate
q_{vd}	m^3/h	Device flowrate

In the calibration certificates, the mentioned expanded measurement uncertainty (of the laboratory) is equal to the standard uncertainty multiplied by a coverage factor equal to 2, so as the level of confidence is about 95%.

3 RESULTS

3.1 Part 1: Deviation from calculated coefficient

This part provides the results of the deviation calculated with the British approach, that is to say with the recalculation of fan coefficients at each calibration. The existing deviation (with coefficients of the previous adjustment) and the new deviation (with coefficients of the new adjustement) are cumulated. Therefore, it is important to keep in mind that the observed deviation not only include the deviation of fan but also:

- calibration uncertainty
- the error due to the linear regression for the calculation of coefficients.

There is also no guarantee that these last points are not significant compared to the accuracy of the fan.

Also, we have noticed that the value of the pressure for which the flowrate through fan is calculated (here 150 Pa) has an important impact on the observed deviation: the smaller the fan pressure the larger the deviation. 150 Pa is the average fan pressure in studied calibration certificates.

Observed deviation according to the time between calibrations

These results use the absolute value of the relative deviation.

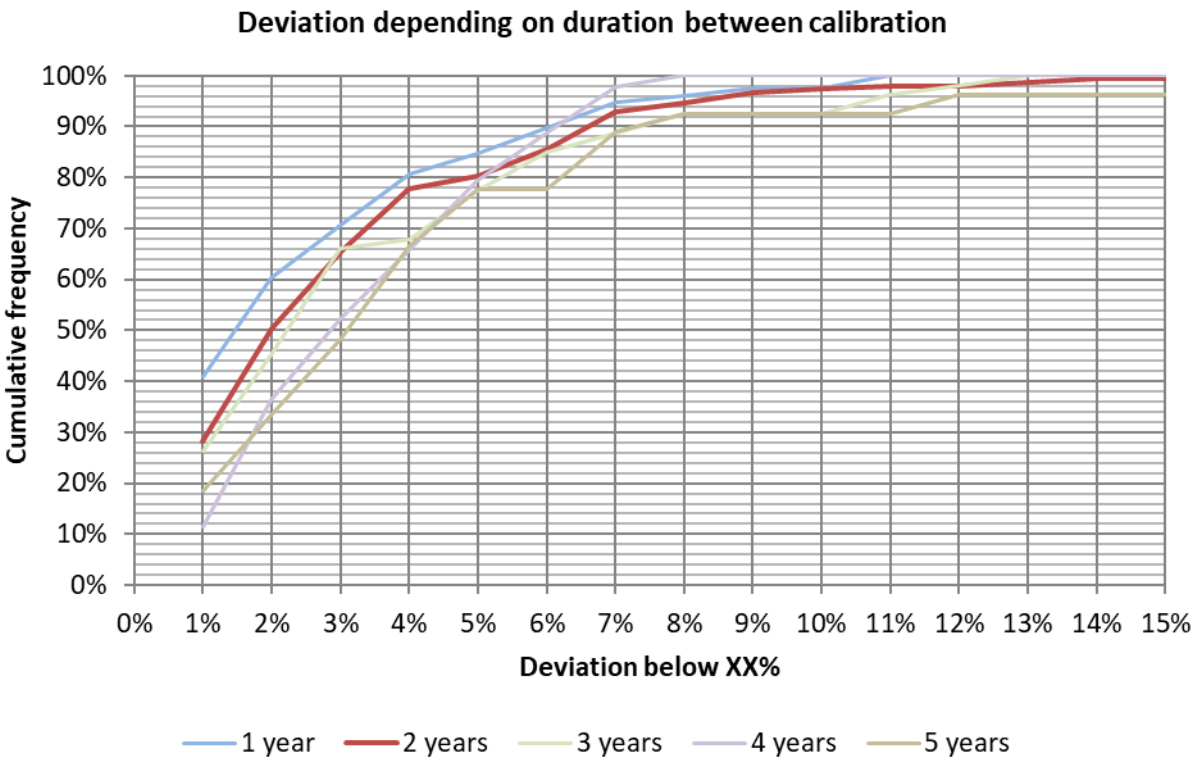

Figure 1: Deviation depending on time between calibrations

The graph presents the deviation of fan over 1 to 5 years. The 2 years line is drawn thicker as it is the one with the largest amount of fans and gathers data from three different bodies.
It shows that **10% of fans deviate of more than 6.5% after 2 years, and 5% of more than 8%.** Table 2 gives the median, average, minimum and maximum deviation according to the time between calibration.
If the calculation of the flowrate is done at 50 Pa instead of 150 Pa, the results are that 10% of fans deviate of more than 10% and 5% more than 14%.

Table 2: Statistics on the deviation

	Time between calibrations				
	1 year	**2 years**	3 years	4 years	5 years
Median	1.5%	**1.9%**	2.2%	2.5%	3.1%
Average	2.4%	**2.9%**	3.3%	3.1%	3.8%
Minimum	0.0%	**0.0%**	0.0%	0.1%	0.1%
Maximum	10.9%	**22.4%**	12.9%	7.9%	15.5%

Positive and negative deviation
The following graph gives the value of the deviation when taking into account the sign.

$$Deviation = \left(\frac{Q_{new} - Q_{prev}}{Q_{new}}\right) \quad (4)$$

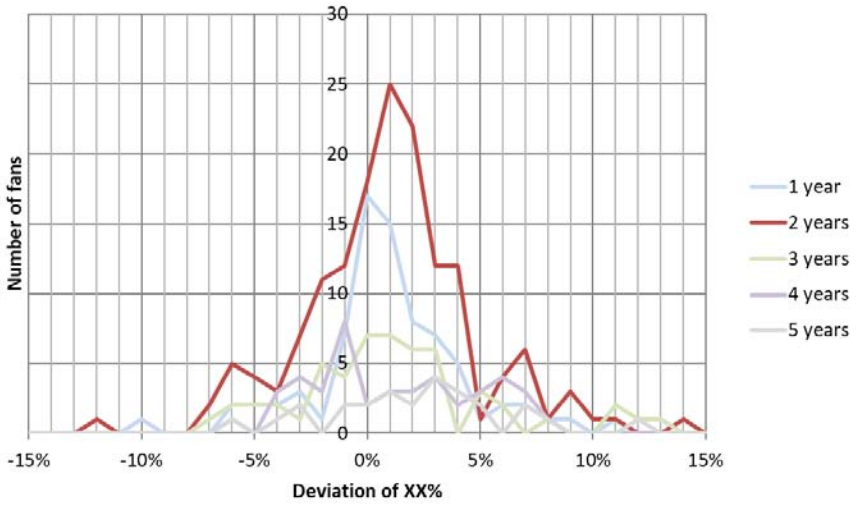

Figure 2: Value of the deviation

The following table gives average, median, minimum and maximum when the sign is considered.

Table 3: Statistics on the deviation when the sign is considered

	Duration between calibration				
	1 year	**2 years**	3 years	4 years	5 years
Median	0.4%	0.5%	0.6%	0.2%	2.3%
Average	0.5%	0.6%	0.7%	0.7%	2.1%
Minimum	-10.1%	-12.5%	-7.7%	-6.3%	-6.3%
Maximum	10.9%	22.4%	12.9%	7.9%	15.5%

Observed deviation according to various parameters

The observed deviation according to the data provider is given in Figure 3. It shows a smaller deviation of fan coming from CEREMA (well stored little used) than others.

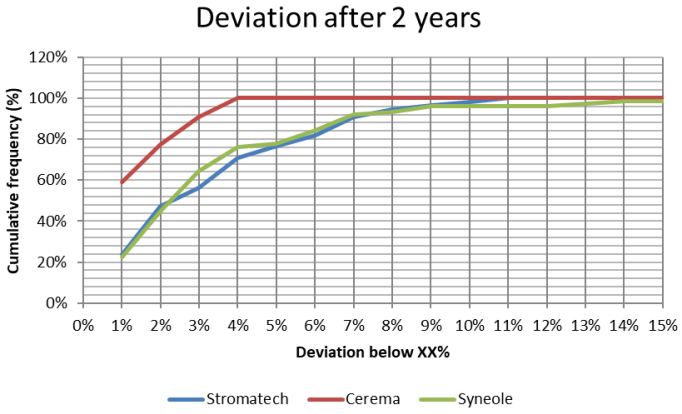

Figure 3: Deviation after 2 years according to the data provider

In the following graph we have studied the variation according to the flowrate of the configuration.

We have considered as "large flowrate" :

- Minneapolis model 4 configurations Open and A
- Retrotec model 3000 configurations Open, A and B

- Retrotec model 6000 configurations Open, A and B8

as "Medium flowrate":

- Minneapolis model 4 configurations B and C
- Retrotec model 3000 configurations C8, C6, C4, C2
- Retrotec model 6000 configurations B4 and B2

as "Small flowrate":

- Minneapolis model 4 configurations D and E
- Retrotec model 3000 configurations C1, L4 and L2
- Retrotec model 6000 configurations B1, B74, B47 and B29

Minneapolis Ductblaster and Retrotec Model 300 have not been taken into account in this part of the study has they only cover small and very small flowrate.
The following table gives the number of data per year and per flowrate:

	1 year	2 years	3 years	4 years	5 years
Large	2	30	3	4	2
Medium	69	86	47	36	23
Small	2	27	3	4	2
Total	73	143	53	44	27

Table 4: Number of data according to the flowrate of the configuration

To have enough significant data only 2 years variations have been considered for this part of the study.
The following graph gives the deviations after 2 years according to the flowrate of the configuration.

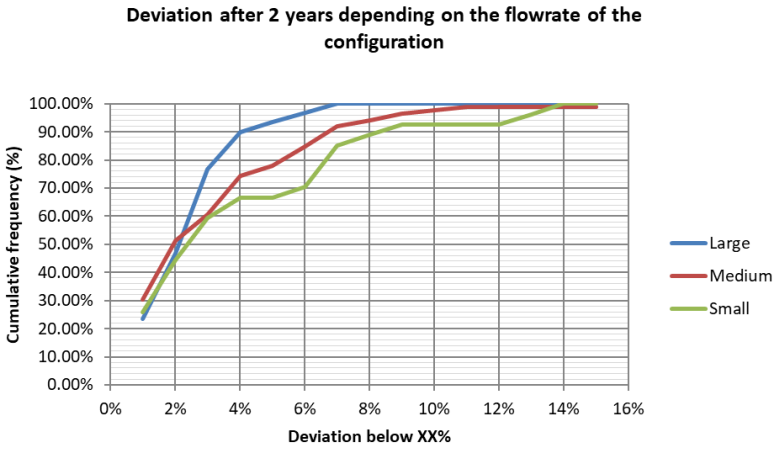

Figure 4: Deviations depending on the flowrate of the configuration

3.2 2nd part of the study, deviation compared to manufacturer coefficients

For the 2nd part of the study we have studied the deviation compared to manufacturers coefficients according the following parameters:

- The measurement capability index
- The flowrate
- The background test pressure
- The fan pressure

On the 1007 data only 235 have a measurement capability index above 3 and are named “reliable” in the following graph.

Observed deviation compared to manufacturer default coefficient

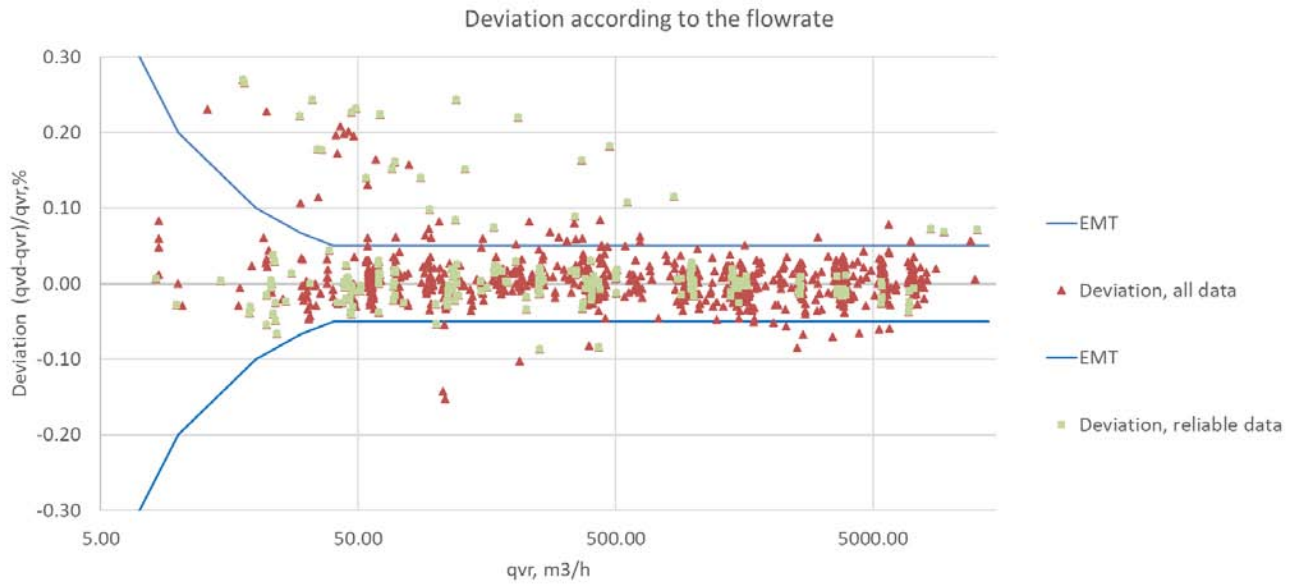

Figure 5: Observed deviation compared to manufacturer default coefficients according to the flowrate, “reliable data” are in green

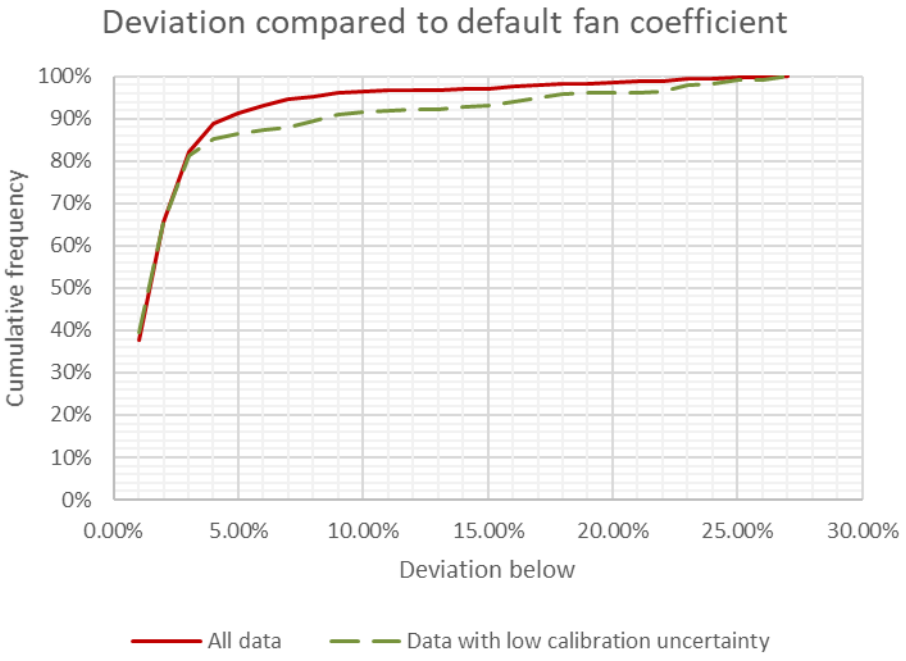

Figure 6: Cumulative frequency of observed deviation compared to manufacturer coefficients

If we look at all data 10% deviate of more than 4.5% compare to manufacture coefficients and 5% of more than 8.5%.

If we only look at calibration with small uncertainty (1/4 of the data) 10% deviate of more than 8.5% and 5% of more than 13.5%.
However, as the French standard requires a maximum of 5% of deviation or 2 m^3/h, only 65 data out of the 1007 are non-compliant (6.5%)

Deviation according to the flowrate
For this part of the study the following assumptions have been made:

- Small flowrate is below 500 m^3/h
- Medium flowrate is between 500 and 2000 m^3/h
- Large flowrate is above 2000 m^3/h

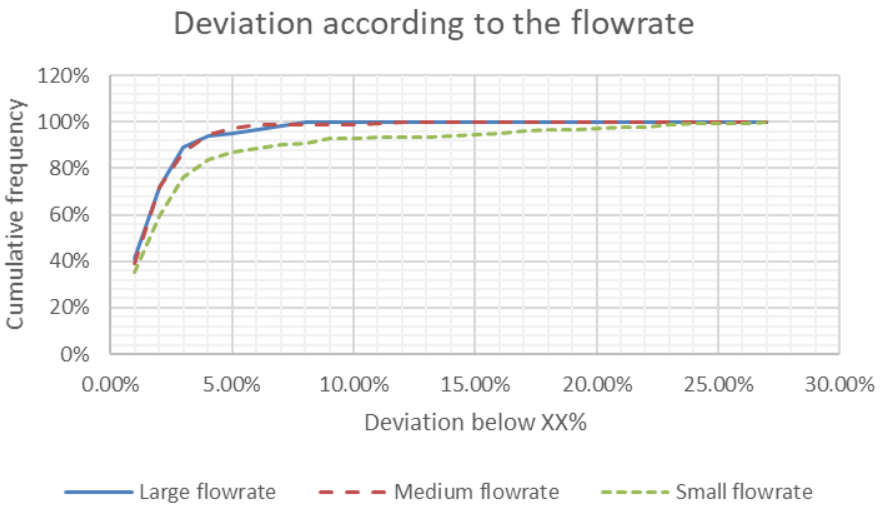

Figure 7: Cumulative frequency of observed deviation compared to manufacturer coefficients according to the flowrate

As in section one the deviation is larger for small flowrates, which is expected as the relative Maximum Permissible Error is higher (2 m^3/h or 5% the biggest). In this case, the large and medium flowrate deviation is similar and quite low: only 4% deviate of more than 6%.

Deviation according to the data provider

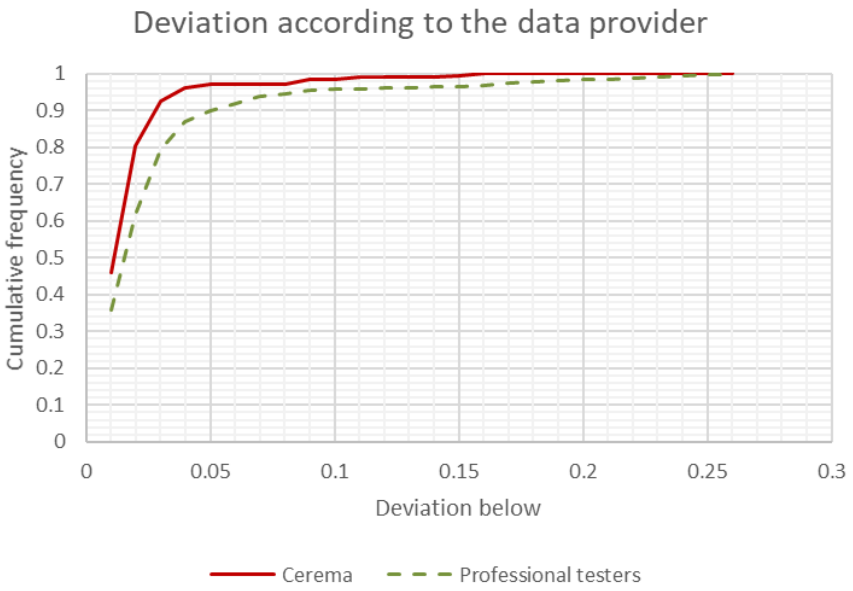

Figure 8: Cumulative frequency of observed deviation compared to manufacturer coefficients according to the data provider

Cerema has provided 204 data out of the 1007. Low used and well-stored fans deviate less than daily used ones. However, this statistic is slightly biased by the fact that Cerema is only using one type of device and has not calibrated its instruments in all the seven laboratories.

Deviation according to the background test pressure

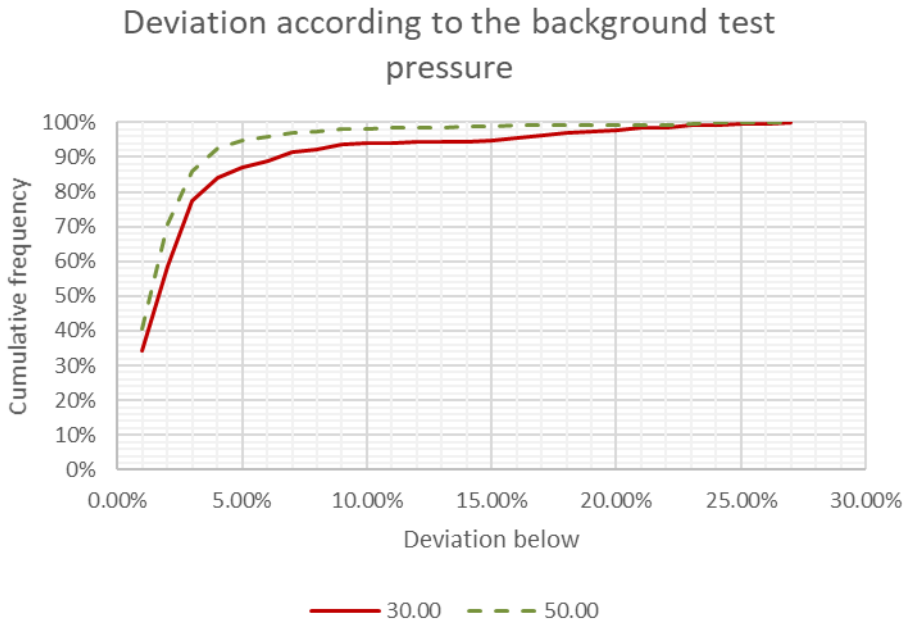

Figure 9: Cumulative frequency of observed deviation compared to manufacturer coefficients according to the background pressure (30 and 50 Pa)

Significant difference of deviation according to the background test pressure is observed.

- With a 50 Pa background pressure 10% deviate of more than 3.5% and 5% of more than 5% which is very low

- With a 30 Pa background pressure 10% deviate of more than 5.5% and 5% of more than 15%.

Deviation according to the fan pressure

Figure 10 shows the deviation of calibration points according to the pressure at fan. Calibration points have been split in three categories:

- Small fan pressure : less than 100 Pa,
- Medium fan pressure: between 100 and 300 Pa,
- Large fan pressure: over 300 Pa.

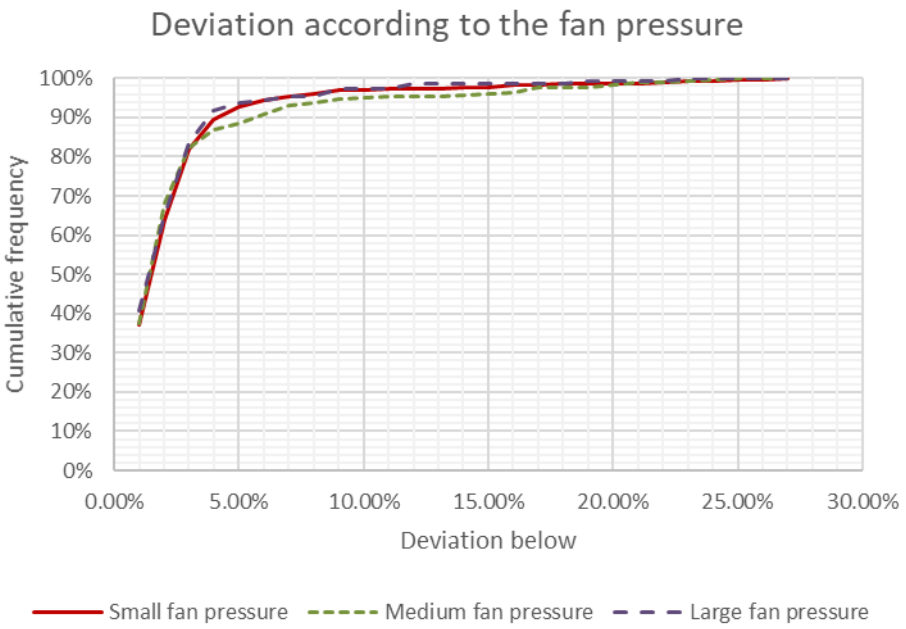

Figure 10: Cumulative frequency of observed deviation compared to manufacturer coefficients according to the fan pressure

Contrary to the first part of the study there is almost no impact of the fan pressure on the deviation.

3.3 Uncertainty of calibration

The following figures provide the calibration uncertainty according to the flowrate and the measurement capability index (Cm) which is the ratio between the Maximal Permissible Error and the calibration uncertainty (JCGM 106:2012).

If the measurement capability index is high, the probability of conformity of the verification is low. It is commonly accepted that a measurement capability index of at least 3 provides good probability of conformity, 2 is low and 1 is not acceptable. If the Cm is below 1 it means that the reference device is less accurate than what the measuring device under calibration is supposed to be.

Most laboratories have a probability of conformity between 1 and 3. Some laboratories get value above 6. In this case it is unclear whether the uncertainty is correctly estimated in the certificates, and whether or not it includes both uncertainties (pressure and flowrate).

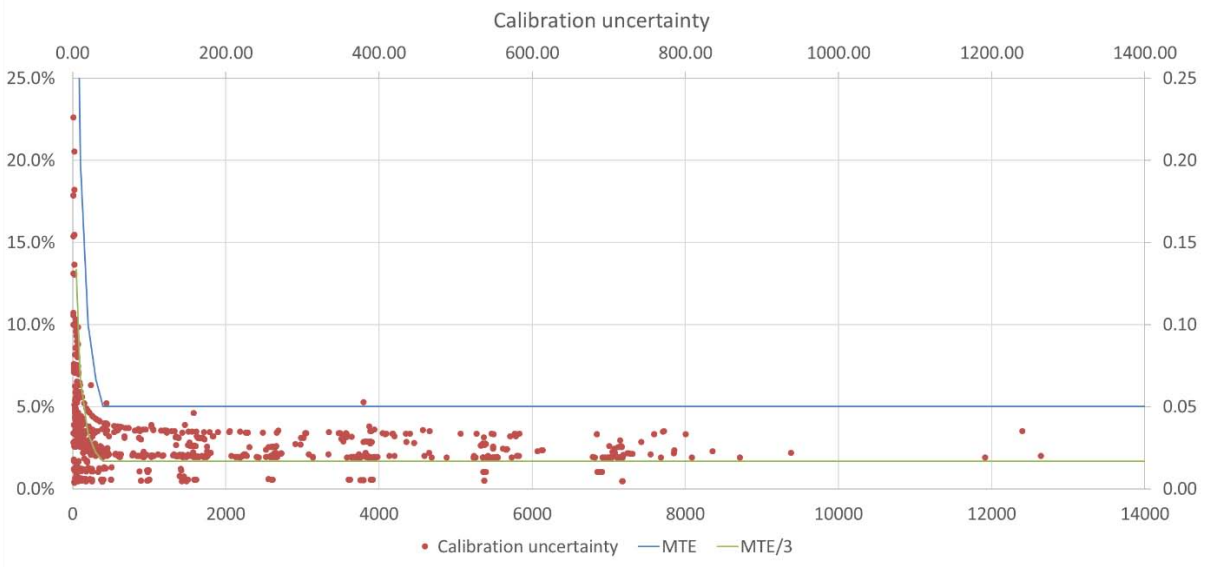

Figure 11: Calibration uncertainty according to the flowrate

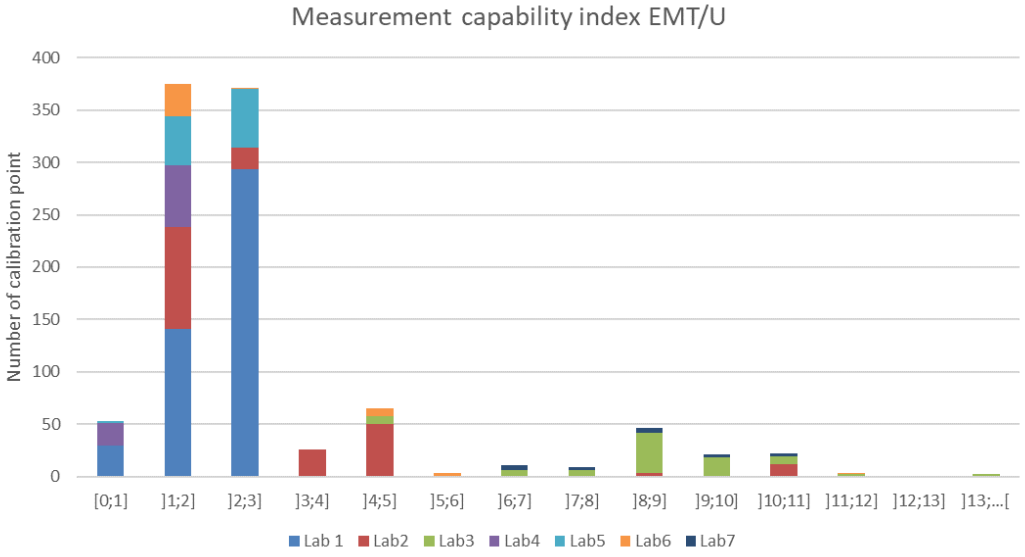

Figure 12: Distribution of measurement capability index per calibration laboratory

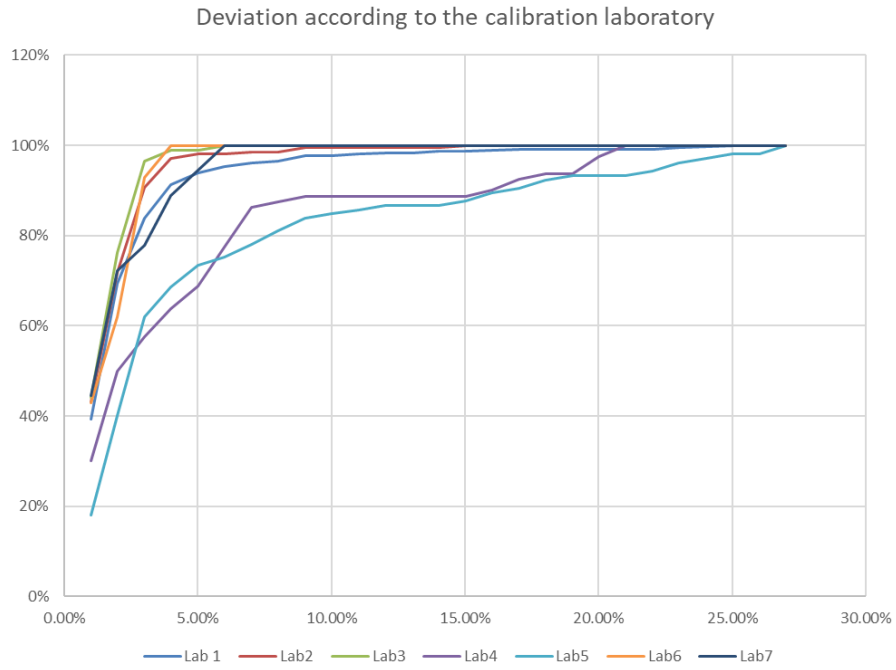

Figure 13: Cumulative frequency of observed deviation compared to manufacturer coefficients according per laboratory.

Laboratories which have low measurement capability index also have a higher deviation, therefore the observed deviation may not be an actual deviation of the device but may be due to calibration uncertainty. However, it has to be kept in mind that these results may be biased by the fact that these laboratories may also check only certain kind of products.

4 DISCUSSION

The observed deviation is quite similar in the first and in the second sections. Table 5 summarizes the results.

Table 5: Comparison of the results for the two parts of the study

	Part 1: recalculation of coefficients	***Part 2: comparison with manufacturer coefficient***
10% vary of more than	6.5%	4.5 %
5% vary of more than	8 %	8.5 %

This deviation is low but not negligible as 4 configurations on 60 do not comply with the French requirements.
The two parts of the study cannot be compared to decide whether the British or the French approach is more appropriate as they don't cover the same sample of data. However, the first part of the study has shown that the pressure used to calculate the flowrate has a large impact on the observed deviation. This is probably because the calibration does not always cover the full range of pressure of the fan, therefore the linear regression leads to extrapolation outside the calibrated range and coefficient are less reliable than manufacturers ones.
Note: This paper does not cover the issue of linear regression but the ordinary least squares method is not always applicable to calibration. See ISO/TS 28037 for more information.
Therefore, it can be concluded that if a recalculation of coefficient is done, the calibration shall:

- cover the full range of possible pressure of the device

- probably be done on more than three points
- use a proper regression method.

Both the first and the second part of the study have shown that low-used and well-stored fans (as those from CEREMA) deviate less than daily used ones (as those from Syneole for example).

The study taking into account the sign of the deviation shows that the median and average of the deviation are close to 0% (0.5%) which means that the flowrate measured by fans tends to increase very slightly but vary mostly randomly.

Configurations measuring large flowrates deviate much less than configurations that measure small flowrates (in the 2 parts of the study). The second part has shown that medium and large flowrate remain conform to the regulation in 96% of cases.

In the second part of the study a significant difference of deviation is observed according to the background test pressure. This means that manufacturer fan coefficients are probably calculated for 50 Pa and vary when the background pressure changes. This means that, when performing a multiple test point on-site, the uncertainty due to the variation of the fan coefficient shall be added to the global uncertainty calculation (if not already included in the device uncertainty). This would need further investigation.

Even if the deviation is low, this study shows that calibration is necessary to establish the appropriate coefficients. However it does not stress the need of an high-frequency one. The first calibration is probably the most important one.
However, if a requirement is set on calibration or verification, first it shall define whether a calibration or verification of calibration has to be performed. It shall also include requirements on laboratories performing the calibration/verification such as:

- Provide at least the following data (in accordance with ISO 17025)
    - Both for calibration and verification of calibration:
        - Reference flowrate
        - Uncertainty on the reference flowrate
        - Device flowrate (calculated with fan coefficients)
        - Fan pressure
        - Uncertainty of fan pressure
        - Background pressure
        - Uncertainty on background pressure
        - Measurement error
        - Uncertainty on measurement error
    - In addition for verification of calibration
        - Maximal permissible error of the device
        - Probability of conformity
        - Measurement capability index
        - Decision rule
        - Conformity assessment
    - In addition for adjustments:
        - calibration function, calibration diagram, calibration curve, or calibration table with associated measurement uncertainty
- Having a measurement capability index above 3

Nevertheless, this study has not shown a significant difference of observed deviation for laboratory with high uncertainty and those with low uncertainty.
In addition to the calibration, it is good practice to check the state of the fan (fan position, vacuity of pressure taps, distortion of the case, broken elements, etc.) on a regular basis.

5 CONCLUSIONS

This study has shown that the fan deviation is low but not negligible with 5% of the fan varying of more than 8.5% in the second part of the study.
Therefore, calibration is necessary but this study does not stress the need of a high frequency calibration/verification nevertheless it insists on the importance to perform an accurate one. A requirement on calibration/verification shall include requirement on the laboratories performing this calibration.
The two parts of the study has not highlighted a large difference between the two approaches (calibration in UK and verification of calibration in France) when comparing results at an average fan pressure of 150 Pa for calibration. However, it seems that new calculated coefficients are less reliable than manufacturers ones on a large scale of pressure. Therefore, when only few points are available, a verification seems more relevant than a calibration. The observed deviation is randomly positive or negative so it is probably not due to the apparition of leakage in the device.
However, statistics have shown that the deviation is correlated with the use of the fan and with the flowrate, highly used fan and small flowrates configurations deviate more than others.
A significant difference of deviation is observed according to the background test pressure (30 or 50 Pa) further investigations are needed to explain it.

6 ACKNOWLEDGEMENTS

The authors would like to thank the Belgian Construction Certification Association (BCCA) for its support.
The views and opinions of the authors do not necessarily reflect those of BCCA. The published material is being distributed without warranty of any kind, either expressed or implied. The responsibility for the interpretation and use of the material lies with the reader. In no event shall the authors or BCCA be liable for damages arising from its use. Any responsibility arising from the use of this report lies with the user.

The AIVC of the 20th Century

Martin Liddament

Reading, UK
mwliddament@gmail.com

SUMMARY

This report reviews the activities of the AIVC during its first twenty years of operation. It identifies key projects and addresses them in the context of research activities and associated issues of the time. Early issues included the need for energy conservation and reducing air infiltration loss. Much work concentrated on assessing the performance of numerical models and acquiring input and validation measurement data. Towards the end of the period attention focused towards energy efficient ventilation systems for good indoor air quality and comfort. Calculation and measurement needs of the time are described.

KEYWORDS

Air infiltration, calculation methods, measurement methods, historical review.

1 BACKGROUND

In the wake of uncertainty over oil supply, the International Energy Agency (IEA) was established in 1974 as an autonomous body within the Organisation for Economic Cooperation and Development (OECD). One element of its activities was for participants to undertake cooperative activities in energy research, development and demonstration with the primary objective of reducing dependency on fossil fuel.

Energy consumption in buildings was identified as a significant consumer of energy and was an area offering the potential for a considerable reduction in energy use. To address this an Executive Committee for Energy Conservation in Buildings and Community Systems (ECBCS) was formed with a responsibility for encouraging various exercises to predict, more accurately, energy use within buildings through a series of task based Annexes.

Air infiltration into buildings was quickly identified as an area about which least was known. To address this, Annex 5 the Air Infiltration Centre (AIC), was established by the ECBCS in 1979. Its aim was to provide an understanding of the complex behaviour of air flow in buildings and to advance the effective application of associated energy saving measures in both the design of new buildings and the improvement of the existing building stock. These activities were extended to the field of ventilation, as a whole, and became the Air Infiltration and Ventilation Centre (AIVC) in August 1986. Funding was provided by member countries who chose to join the Centre. Many Annexes have subsequently been established within the ECBCS with several associated with the work of the AIVC. The AIVC fulfilled its objectives through a programme of technical activities, the provision of an information centre and dissemination.

This report summarises the work and outcomes of the AIVC between 1979-2000, as well as its interaction with associated Annexes and other projects. It further attempts to outline the progression of interest from minimising energy use to interests in improving knowledge about air and pollutant transport as well as improving health, comfort and indoor air quality.

1.1 The AIVC Steering Group

The work of the Centre was assisted through a Technical Steering Group appointed by member Countries. This Group provided expertise and assistance to the staff of the Centre as well as providing a conduit to relevant research and activities in member countries. This approach has undoubtedly been instrumental in the success of the AIVC.

2 INFORMATION ACTIVITIES

Without access to Google and modern bibliographic information systems, finding relevant information in 1979 was not a as simple as in 2019. To overcome this, a computerised bibliographic database, AIRBASE, was established on a 'mainframe' computer in 1980. This could be interrogated through keyword or free text searching on author, title or abstract fields. Initially this was only accessible at the AIVC and searches were undertaken, internationally, by request, usually by telex. In 1985 the AIVC acquired two IBM AT desktop personal computers and were able to transfer AIRBASE to floppy disks running on the DOS operating system. These disks were updated quarterly and sent to any organisation in member countries that wanted direct access to AIRBASE. Also, direct searching was possible via a modem link established in February 1983. Subsequently, AIRBASE was made available on CD-ROMs. Information for AIRBASE was derived from data and resources provided by the Steering Group, regular surveys of research and by direct library research.

3 DISSEMINATION ACTIVITIES

The AIVC disseminated information through a strong publication programme.
Publications included:

- Technical Notes based on work undertaken at the Centre and by associated Annexes within ECBCS;
- Technical Guides;
- Bibliographic Reviews based on topical information contained within AIRBASE;
- Quarterly Newsletter Air Infiltration Review (AIR);
- AIVC Website, the AIVC Website was established in September 1995.

The Centre also organised annual conferences and workshops and hosted visiting specialists.

4 TECHNICAL ACTIVITIES

4.1 Model Validation

A fundamental initial task of the AIVC was to undertake a programme to 'validate' mathematical models of air infiltration. This progressed in five stages, these being to:

- Select appropriate mathematical models;
- Establish the data needs of each model;
- Prepare suitable high-quality datasets based on measurements made on site;
- Use the available data to compare modelled results with actual infiltration measurements;
- Identify key parameters.

It is through this activity and the activities of related research organisations and universities that developments in ventilation in the AIVC's early years can best be reviewed.

To 'validate' a model substantial monitoring data are required including:

- Building dimensions and layout;
- Building permeability or leakage value (airtightness test data);
- Continuous monitoring of actual infiltration rate (tracer gas measurements);
- Simultaneous monitoring of driving forces (indoor temperature, outdoor temperature and wind speed).

These were difficult data to obtain since very few projects simultaneously monitoring all these had been undertaken. A total of ten 'physical' models were selected which were based on the solution of the equations of flow through openings in the building structure. Complexity ranged from simplified single zone methods, in which the interior of the building was assumed to be at a single uniform pressure, to multizone approaches, in which the interior was divided into individual rooms or zones. Not surprisingly, very few complete datasets were available, and analysis was restricted to three naturally ventilated dwellings, each of which was configured for whole building ventilation monitoring (i.e. with internal doors open). Within the limitations of measurement errors, all the models produced results that were consistent with measured ventilation rates (mostly within 25%) for these fairly simplistic configurations. Full details of the work and results are described in AIVC TechNote 11 (Liddament and Allen 1983).

4.2 Air Infiltration Calculation Techniques Guide

The numerical modelling activity spawned many associated activities that governed the early technical work of the Centre. The first was compiling the background and basic theory of mathematical model themselves into an Applications Guide published in 1986 (Liddament 1986). The intention was to provide both researchers and designers with a detailed background to air infiltration modelling and to give guidance on the application of modelling techniques in design. Associated calculations included infiltration heat loss, air flow rates, pressure distribution and pollutant concentrations.

4.3 AIVC's Numerical Database

Numerical data, collected as part of the Centre's mathematical studies, were subsequently compiled into a numerical database. This was developed in response to a need to establish a core numerical data source, suitable for design purposes and model validation.

The database was presented in three sections i.e.

- Component leakage data;
- Whole building leakage data
- Wind pressure evaluation.

A full description of the database and an analysis of the data was published as a technical note (Orme et al 1994).

5 RELATED NUMERICAL MODELLING

Advancing mathematical modelling of air infiltration and ventilation was a theme that continued throughout the 1980's, much of which involved related Annexes. These included the following:

5.1 The COMIS Multizone Project (ECBCS Annexes 20 and 23)

In 1988 an international project COMIS (Conjunction of Multlzone Infiltration Specialists) was initiated at Lawrence Berkeley Laboratory's Applied Science Division. Its task was to develop a detailed multizone infiltration program taking crack flow, HVAC-systems, single-sided ventilation and transport mechanisms through large openings into account. The final aim was to produce an up-to-date user-friendly program suitable for researchers and building professionals.

This task was subsequently incorporated into ECBCS Annex 20 Airflow patterns in buildings and then, ECBCS Annex 23 Multizone airflow modelling. Multi-gas tracer measurements and wind tunnel data were used to check the model. Monitoring and comparisons were made on nine buildings, each presenting several cases.

From comparisons with measurement, it was concluded that:

- When proper input is provided, air and contaminant flows, resulting from infiltration through cracks and ventilation systems, are properly predicted by COMIS and similar programs.
- Air and contaminant flows through large openings (that is openings presenting two-way flows) can be calculated, but the result may not be close to reality. This is especially true in case of wind and when the building structure acts as a thermal reservoir.
- In general, global air flow rates through the building are predicted more accurately than inter-zonal flow rates.

A major difficulty identified by the work of Annex 23 was the tendency of modelling programs to user error. This is partly due to the complexity of the required input data but may also be due to the lack of understanding by users of the underlying mechanisms of air flow, resulting in an incorrect definition of the problem to be solved. COMIS attempted to overcome this with a carefully designed user interface. A technical summary of this work is presented by Warren (Warren 2000).

5.2 CONTAM

A second major international multizone model originating from the 1980's is CONTAM. This began with work by Walton (1983) on a computer algorithm for predicting inter room air flow as well as flow through small and large openings. This then evolved into the National Bureau of Standards (now NIST) "General Indoor Air Pollution Concentration Model Project" initiated in 1985 (Axley 1985). This first incarnation version became CONTAM86. Since then CONTAM has gone through many iterations and is in current use today.

5.3 Computational Fluid Dynamics (CFD) IEA Annex 20 airflow patterns within buildings

Computational fluid dynamics to predict air flow patterns in rooms and other spaces had its beginning in the late 1970's. As affordable computer power became more available CFD became an attractive observation and design tool. The Centre published a short summary Technical Note on the topic in 1991 (Liddament 1991) but it became a main task for IEA Annex 20 which was completed in 1992.

An objective of this work was to determine the reliability of computer prediction of the flow field within a room. To resolve this, a test room was set up with identical instrumentation in five countries. Tests were performed for various flow regimes and measurement results were compared with CFD simulations. From this it was concluded that CFD simulations are useful when:

- Values of difficult to measure variables are needed in all points of the flow field;
- Studying the sensitivity of small changes of conditions;
- predicting airflow patterns for critical projects.

It was also concluded that CFD predictions can predict room air movement with sufficient realism to be of use to design practice (Lemaire 1993). At the time of this work, it was concluded that further work was required to model supply jets, turbulence and thermal wall functions. The application of CFD has since significantly expanded within the building sector across the entire research and practitioner field.

6 MEASUREMENT TECHNIQUES

In all the above studies measurement were essential and measurement methods made significant advances during the 1980's and 90's. Key measurement parameters included:

6.1 Tracer gas to measure air infiltration rate and ventilation

Tracer gas monitoring is an essential method for measuring ventilation and infiltration under ambient conditions. In essence the process is fairly straight forward: an inert, non-toxic gas is released into a space and its concentration is monitored as it disperses and eventually leaves the building through the ventilation process. Throughout the 1980's real time monitoring in test houses, as well as occupied spaces, took place. Techniques included tracer decay, constant concentration, constant emission and multi tracer methods. There were also long-term monitoring techniques using 'passive emission' samplers. Simpler methods included monitoring the concentration of metabolic carbon dioxide emissions from building occupants.

Common tracer gasses were:

- Nitrous oxide;
- Carbon dioxide;
- Per Flouro Compounds (PFCs);
- Sulphur hexafluoride (SF_6);
- Freon.

The complexity of monitoring systems generally restricted applications to the research sector, making it unattractive for general application. Also, SF_6, PFC's and Freon are significant greenhouse gasses with no significant decomposition. Consequently, their use is now restricted. Similarly, nitrous oxide is no longer considered as non-toxic. As a consequence, the use of tracer gas monitoring has declined. The exception is the monitoring of carbon

dioxide, which is now inexpensive and can be used to assess the adequacy of ventilation in occupied spaces.

6.2 Whole building and component airtightness measurements

The airtightness or permeability value of a building is essential for modelling and design purposes.

In the late 1970's, whole building leakage monitoring was relatively uncommon. However. towards the end of the 1970's, the Swedish Government introduced airtightness requirements for housing (SBN 1980). The requirement for single houses was that airtightness should not exceed 3 air changes/hour at an induced indoor-outdoor pressure difference of 50 Pa (3 ac/h_{50}). Typically, this was measured by removing an external door and replacing it with a fan that could drive enough air to monitor the required airtightness value. The 50 Pa pressure standard has largely remained the same to this day, although the use of air change rate has given way to permeability (which expresses leakage in terms of the surface area of the building façade). A pressure difference of 50 Pa was primarily selected because it was generally above the value of natural driving forces (at least for low rise buildings) but not so high that it could force joints in the façade to open or close. Also, it sets a reasonable flow capacity for fans. Initially, blower fans were laboratory designed but, by 1983, 'blower doors', as recognised today, were in use. Giant trailer born fans for larger buildings were also in use by 1980.

Pressurisation techniques had additionally been developed during this period to measure leakage across specific components or facades. These include multiple fans and component test rigs. Although novel in the early 1980's blower door methods are now in common use.

6.3 Wind Pressure

The wind induced pressure across infiltration openings is a key component of an infiltration calculation. It is not possible to measure this directly but, instead, it is commonly related to wind speed (at a specified reference height) in terms of a wind pressure coefficient. These are derived from wind tunnel testing. Throughout the 1980's much wind tunnel analysis was undertaken to derive wind pressure values. In the early days of the AIVC mathematical modelling study, wind pressure coefficient data were largely derived from the wind tunnel testing of Bowen (1976) and Wiren (1985).

6.4 Air Infiltration Measurement Techniques Guide

Information on tracer gas testing, airtightness measurements and associated techniques was compiled into an AIVC measurement techniques guide, published in 1988 (Charlesworth 1988). This was subsequently updated to include further measurement detail, covering a wider range of cases and theory, by Roulet and Vandaele in 1991 (Roulet and Vandaele in 1991).

7 HANDBOOK: AIR INFILTRATION CONTROL IN HOUSING – A GUIDE TO INTERNATIONAL PRACTICE

A handbook (Elmroth 1983) was prepared by the Swedish participant of the AIVC to review international practice on airtight construction. Its objective was to understand air leakage

routes through construction joints and to identify mechanisms for securing airtightness. Each construction joint was identified and an airtightness solution presented. This publication followed an earlier Swedish handbook on airtightness and thermal insulation (Carlsson et al 1981) that defined the future building air tightness design practice for new housing in Sweden.

8 ASSOCIATED VENTILATION ANNEXES AND RESEARCH

During the 1980's and 90's other important topics and projects evolved, many of which have important applications today. Several of these were picked up by associated Annexes of the ECBCS and some of the final reports were subsequently published by the AIVC as Technical Notes. These topics included the growing interest in indoor air quality and comfort as well as energy efficient ventilation systems. Topics included:

8.1 Inhabitants behaviour with respect to ventilation, Annex 8

This occupational study was managed by TNO in The Netherlands and was aimed at identifying the motivation of occupants in controlling their indoor climate, as well as assessing potential energy savings if behaviour could be modified. There are numerous important conclusions but results showed that there were considerable differences between household in sensitivity to temperature variation, on the whole ventilation behaviour was found to be highly weather dependent and the greater the interest of inhabitants in controlling energy use the more positively they responded to advice. Results are presented by Dubrul (1988).

8.2 Minimum ventilation rates and measures for controlling indoor air quality, Annex 9

This project focused on researching the minimum ventilation rate needed to maintain good air quality for a range of common indoor pollutants. It considered the source characteristics and adverse effect of pollutants, along with control measures for limiting concentrations and appropriate ventilation strategies. The details and results are reported by Trepte and Haberda (Trepte and Haberda, 1989).

8.3 Ventilation efficiency and pollutant removal effectiveness

Once buildings became more airtight, attention turned to indoor air quality and comfort. Improved ventilation systems were designed that were aimed at providing clean air more efficiently, such as by using displacement rather than conventional mixing ventilation. In turn this meant that, in certain climates, heating and cooling could be provided using chilled ceilings and 'low' temperature heating systems. Issues included the supply and spread of clean air and removal of polluted air from occupied spaces. Various definitions that quantify these concepts began to emerge in the mid 1980's. Explanations of these evolving definitions were compiled into a series of Technical Notes (Sutcliffe 1990, Brouns and Waters 1991 and Liddament 1993).

8.4 Demand controlled ventilation - intelligent ventilation systems for indoor air quality control, Annex 18 demand controlled ventilation systems

As air quality sensors became less expensive, interest increased in developing demand control ventilation systems. The principle objective of this task was to develop an efficient ventilating

system by a demand control based on analysis of the ventilation effectiveness and proposed ventilation rates for different users in different cases in domestic, office and school buildings. The project also involved work on field studies, sensor location and ventilation strategies. Details and results are published by Mansson et al (Mansson et al 1997).

8.5 Other ECBCS ventilation related projects

There were several other ECBCS projects that were related to the activities of the AIVC. These included:

Annex 25 Realtime HEVAC simulation, Annex 26 Energy efficient ventilation of large enclosures and Annex 27 Evaluation and demonstration of domestic ventilation systems. Project reports for these activities as well as recent projects (and all past activities) can be found on the ECB (formerly ECBCS) website (www.iea-ebc.com).

8.6 European NatVent Project - Overcoming barriers to low energy natural ventilation

This EU project was supported by the AIVC and was aimed at encouraging the use of natural ventilation in moderate to colder climates. Of interest was the targeting of buildings and countries where summer overheating from solar and internal gains could be significantly reduced by low energy design and good natural ventilation. It also addressed buildings in noisy and polluted locations. NatVent's main objective was to provide practical solutions and guidance and thus encourage the wider uptake of natural ventilation technologies. As part of the project, hourly monitoring of indoor climate took place in nineteen mainly large commercial and public buildings located in participating countries. A detailed summary of the project is presented by Kukadia (1999).

8.7 AIVC Guide to Energy Efficient Ventilation

A task of the AIVC, towards the end of this period, was to produce a Guide to Ventilation (Liddament 1996). This was aimed at providing background knowledge, in the form of an easy to read primer, for policy makers and practitioners that needed basic information. The structure was a descriptive approach with equations restricted to a minimum and only included in the final chapter. Some summary data were included as appendices, along with a simple algorithm to allow basic infiltration and ventilation calculations. Topics covered basic definitions, indoor air calculations, comfort, energy impact, design criteria, ventilation, cooling, filtration, ventilation efficiency, maintenance, measurement methods and calculation techniques.

9 CONCLUSIONS

The AIVC presented a unique opportunity to develop and promote an understanding in energy efficient ventilation. In its early years it established a bibliographic and numerical database to assist researchers and practitioners. Much of the compiled data has been used in practice and incorporated into computer codes.

Initially, the Centre's task focused on minimising air infiltration energy loss. Over time, however, the AIVC evolved to respond to indoor climate, comfort and air quality concerns.

During the 1980's, there were considerable advances in mathematical model development and measurement techniques. Tracer gas was especially important for infiltration measurements, while pressurisation techniques were developed for airtightness testing. Mathematical model development included advances in multi-zone methods and CFD. Towards the end of this period, demand for tracer gas monitoring reduced. In part, this was, perhaps, as a consequence of limitations on permitted tracer gas as well as expense and complexity. Possibly, the increasing availability of low cost carbon dioxide sensors enabled rudimentary tests on the adequacy of ventilation to be made without the complication of a full tracer gas test.

By the 1990's computational fluid dynamics had grown in popularity and may have began to replace measurement methods for some applications. Work by Annex 20 has done much to understand and develop approaches to secure reliable results.

Throughout the 1990's, interest expanded into indoor air quality, health and thermal comfort. Particularly, parameters evolved to quantify the quality of ventilation in relation to these issues.

Throughout this period, the Centre interacted with IEA and other groups undertaking ventilation related activities.

The active technical support provided by the Steering Group was instrumental to the success of the AIVC.

10 REFERENCES

Allen, C. (1981) *Reporting format for the measurement of air infiltration in buildings.* AIVC TN 6.

Axley, J. (1987) *Indoor air quality modeling phase2 report CONTAM 86 including User Manual.* NBSIR 87-3661 NIST (Formerly NBS).

Bowen, A. J. (1976) *A wind tunnel investigation using simple building models to obtain mean surface wind pressure coefficients for air infiltration estimates.* Report no. LTR LA 20N, National Aeronautical Research Establishment, Canada.

Brouns, C., Waters J.R. (1991) *A guide to contaminant removal effectiveness.* AIVC TN 28.2.

Carlsson, B., Elmroth, A., Engvall, P-A. (1981) *Airtightness and thermal insulation –building design solutions,* Svensk Byggtjänst.

Charlesworth, P. S., (1988) *Air Exchange rate and airtightness measurement techniques – an application guide.* AIVC ISBN 0 946075 38 7.

Dubrul, C. (1988*) Inhabitants' behaviour with regard to ventilation.* AIVC TN 23.

Elmroth, A. (1983) *Air infiltration control in housing – A guide to international practice*. AIVC Handbook HNBK.

Feustel, H. E. et al. (1990) *Fundamentals of the multizone air flow model- COMIS.* AIVC TN 29.

Kukadia, V. (1999) *European NatVent Project. Air Infiltration Review* Vol 20 No2. AIVC.

Mansson, L. G., Svennberg S. A. (1997) Annex 18: *Demand controlled ventilation systems – Annex 18,* Technical Synthesis Report, IEA-EBC.

Lemaire, A. D. (1993) *Annex 20: Room air and contaminant flow evaluation of computational methods. Subtask 1 Summary Report*, ISBN 90-6743-298-9, TNO, The Netherlands.

Liddament, M.W. (1991) *A review of building air flow simulation. AIVC* TN 33.

Liddament, M.W., Allen, C. (1983) *The validation and comparison of mathematical models of ventilation.* AIVC TN11.

Liddament, M.W. (1993) *A review of ventilation efficiency.* AIVC TN 39.

Liddament, M.W. (1986) *Air infiltration calculation techniques – an application guide.* AIVC

Liddament, M.W. (1996) *A guide to energy efficient ventilation.* AIVC

Orme, M. et al (1994) *An analysis and summary of the AIVC's numerical database*. AIVC TN 44.

Roulet, C.A., Vandaele, L. (1991) *Air flow patterns: measurement techniques.* AIVC TN 34.

SBN (1980) *Thermal insulation and airtightness Chapter 33.* Svensk Byggnorm med Kommentarer, Statens Planverk, Sweden.

Sutcliffe, H. (1990) *A Guide to air change efficiency.* AIVC TN 28.

Trepte, L., Haberda, F. (1989) *Minimum ventilation rates and measures for controlling indoor air quality*. AIVC TN 26.

Walton, G. (1983) *A computer algorithm for estimating Infiltration and inter room air flows.* Report NBSIR 83-2635 NIST (Formerly NBS).

Warren, P. (2000) *Summary of IEA Annex 23 Multizone Airflow Modelling (COMIS) within the Energy Conservation in Buildings and Community Systems Programme*. Document TSR-06-2000 ISBN 1902177 155. IEA-ECB Energy in Buildings and Community.

Wiren, B.G. (1985) *Effects on surrounding buildings on wind pressure distributions and ventilation losses for single-family houses. Part 1: 1 1/2-storey detached houses.* Nat. Swed. Inst. for Build. Res., Bulletin M85:19, 1985.

40 Years of Modeling Airflows

Iain Walker

Lawrence Berkeley National Laboratory
1 Cyclotron Road
Berkeley, CA, USA
iswalker@lbl.gov

SUMMARY

The modelling of air flows to investigate indoor air quality and energy issues has been a topic at the AIVC for all of its 40 years. Models have been developed that range in complexity from single-zone algebraic expressions that can be calculated by hand to complex multi-zone approaches that integrate contaminant transport and other functions. Key advancements have come in terms of increased computer speed and storage capabilities, (leading to more complex multi-zone approaches and smaller time-step/longer simulation periods), improved used interfaces, and better input data (e.g., wind pressure coefficients).

KEYWORDS

Infiltration, ventilation, modelling, energy, indoor air quality

1 INTRODUCTION

The ability to model infiltration using physics-based engineering calculations grew from the desire to know more about the energy associated with heating (and sometimes cooling) loads driven by the first "energy crisis" starting in about 1973. Researchers in Europe, Canada and the USA began investigating these air flows. Experiments showed that the air exchange increased with building envelope leakage and with harsher weather and efforts were begun to model the infiltration using the measured envelope leakage and weather conditions. Two types of ventilation model have emerged: simple models that use semi-analytical approaches and simplifying assumptions to allow for hand calculation and complex models that require computation to solve the non-linear mass balance equations.

2 CALCULATING BUILDING ENVELOPE AIR FLOWS

The nature of the relationship between flow through building cracks and the pressure difference across the crack and the crack geometry has been thoroughly debated in AIVC publications (e.g., Liddament (1987) and Etheridge (1987) published on both sides of the discussion in Air Infiltration Review). There are essentially two alternative viewpoints (Walker et al. (1997) give a more detailed summary in the Proceeding of the 17th AIVC Conference). The first assumes that we can combine fully developed laminar flow with entry and exit losses to describe the pressure-flow relationship. The other uses a semi-empirical approach based on measured characteristics and developing flow experiments called the power law. The two governing equations are:

$$\text{Laminar + entry/exit (usually called a quadratic approach): } Q = A\Delta P + B\Delta P^2 \quad (1)$$

$$\text{Power law: } Q = C\Delta P^n \quad (2)$$

Where, A, B, C and n are parameters that are fitted to measured pressure and flow data. Over time the power law has been used more and is the basis of most infiltration modeling.. Some

models use a special case of the power law and assume that the pressure exponent, n, is equal to 1/2 (e.g., the LBNL Model (Sherman and Grimsrud 1980).

3 SIMPLE MODELS

Simple models are single zone and calculate wind and stack effects separately, which are then combined using various semi-empirical approaches to account for their non-linear interactions. Many of the first ventilation models were purely empirical based on correlating measured ventilation rates to wind and temperature. However, most subsequent models have been more physics-based and follow the following general format. "Stack" flows (Q_s) are driven by the difference in air density between inside and outside a building that causes pressure differences across the building envelope. This depends on the indoor-outdoor temperature difference (T_{in}-T_{out}), air density (ρ_{out}), the gravitational constant (g), the building height H, and the location of building leaks (represented in this case by the stack factor, f_s) first introduced by Sherman and Grimsrud (1980).

$$Q_s = Cf_s\Delta P_s^n \tag{3}$$

$$\Delta P_s = \rho_{out}\, gH\left(\frac{|T_{in} - T_{out}|}{T_{in}}\right) \tag{4}$$

Wind flows have a similar functional form where the wind pressure depends on windspeed (U), a factor to account for shelter (S_w) and the location of building leaks (represented by f_w).

$$Q_w = Cf_w\Delta P_w^n \tag{5}$$

$$\Delta P_w = \frac{\rho_{out}(S_w U)^2}{2} \tag{6}$$

Various approaches have been used to combine stack and wind effects to obtain the total natural infiltration. Quadrature (squaring, adding and square-rooting) has proved to be a reasonable approach for many buildings, although attempts at pressure addition and pressure addition with empirically determined correction factors have also been used (Walker and Wilson (1998)).

$$\text{Quadrature } Q_{total} = \sqrt{Q_s^2 + Q_w^2} \tag{7}$$

$$\text{Pressure addition with correction: } Q_{total} = \left(Q_s^{\frac{1}{n}} + Q_w^{\frac{1}{n}} + B(Q_s Q_w)^{\frac{1}{2n}}\right)^n \tag{8}$$

Similarly, various non-linear empirical approaches have been used to combine natural infiltration with mechanical ventilation (Li (1990), Modera and Peterson (1985) and Wilson and Walker (1990) summarize these approaches) For balanced systems, simple addition is adequate as the mechanical systems do not interact with the envelop pressures. For unbalanced mechanical ventilation several approaches have been suggested, such as the "half-fan" approach for stack-dominated buildings (Palmiter and Bond 1991) and quadrature. More recent work by Hurel et al. (2015) developed more sophisticated approaches that, while retaining simplicity, work well for large range of conditions.

4 COMPLEX AND MULTIZONE MODELS

More complex single-zone and all multizone models are based on developing an air flow network of envelope (and internal for multi-zone) air flow paths and combining this with inputs for mechanical system air flows, weather, and assumptions about leak locations and surface wind pressure coefficients. The air flow for each individual leak is calculated using the same principles as those for simplified models – with the exception that the pressure across each flow path is a function of the weather, operation of mechanical systems and

pressure shifts that act to balance mass flows in and out of the building. The resulting set of equations are solved to perform a mass balance. AIVC Tech Note No. 11 (Liddament and Allen (1983)) was the first comprehensive attempt to compare several single and multi-zone model predictions of infiltration to measured data. Tech note No.11 found that all the models gave reasonable predictions (+/- 25%) compared to measured data and that the biggest source of uncertainty was estimating wind pressure changes due to shielding and different building shapes. The next major step for multizone modelling was the development of COMIS - Conjunction of Multizone Infiltration Specialists (Feustel and Raynor-Hoosen (1990)). COMIS included relatively sophisticated approaches for creating wind pressure coefficients, and introduced an inter-zonal pollutant transport model. Since then other multizone models have been developed including CONTAM, BREEZE and AIOLOS, together with single zone and simplified models. These newer models build on the basic principles discussed here and include things like more advanced wind pressure modling, improved user interfaces and integrated thermal modelling. These advances are summarized, together with an update for simplified models in AIVC Tech Note No. 51 Orme ((1999).

5 RECENT DEVELOPMENTS

Over the past 20 years infiltration modelling has seen small incremental improvements (such as better superposition techniques for simplified models) and integration of these models developed in the 80's and 90's into specific applications, such as building energy and IAQ regulations. The modelling of ventilation has successfully transitioned from a research tool to develop a better understanding of building physics into a well-accepted part of energy and IAQ regulation. Current ventilation modeling advancements are into highly specific applications, such as developing smart ventilation control strategies (e.g., Clark et al. 2019) and ventilation of semi-conditioned spaces (e.g., attics) that have unique goemetries or wind pressures.

6 REFERENCES

Clark, J., Less, B., Dutton, S., Walker, I. and Sherman, M. (2019). Efficacy of occupancy-based smart ventilation control strategies in energy-efficient homes in the United States. Building and Environment, Vol. 156, https://doi.org/10.1016/j.buildenv.2019.03.002. LBNL 201199

Etheridge, D.W., (1987), "The Rule of The Power Law - An Alternative View", Air Infiltration Review, Vol. 8, No.4.

Feustel , H., & Raynor-Hoosen, A. (1990). AIVC Tech Note 29: Fundamentals of the Multizone Air Flow Model- COMIS.

Hurel, N., Sherman, M.H. and Walker, I.S. (2015). Simplified Methods for Combining Natural and Mechanical Ventilation. Proc. 2015 AIVC Conference.

Li, Y. (1990). Simplified Method of Combining Natural and Exhaust Ventilation. *Climate and Buildings vol.2*, 29-35.

Liddament, M.W., (1987), "Power Law Rules - OK?", Air Infiltration Review, Vol. 8, No.4.

Liddament, M., & Allen , C. (1983). AIVC Tech Note 11: The Validation and Comparison of Mathematical Models of Air Infiltration.

Modera, M., & Peterson, F. (1985). *Simplified Methods for Combining Mechanical Ventilation and Natural Infiltration.* Lawrence Berkeley National Laobratory report no. LBL-18955.

Orme, M. (1999). AIVC *Tech Note 51: Applicable Models for Air Infiltration and Ventilation Calculations.*

Palmiter, L., & Bond, T. (1991). Interaction of mechanical systems and natural infiltration. *12th AIVC Conference - Air Movement and Ventilation Control Within Buildings,* (pp. 285-295). Ottawa, Canada.

Sherman, M.H. and D.T. Grimsrud. 1980. Measurement of Infiltration Using Fan Pressurization and Weather Data. Report #LBL-10852. Lawrence Berkeley Laboratory, Berkeley, California.

Walker, I.S., Wilson, D.J., and Sherman, M.H., (1997), "Does the Power Law Rule for Low Pressure Building Envelope Leakage". Proc. 17th AIVC Conference.

Walker, I.S. and Wilson, D.J., (1998), "Field Validation of Equations for Stack and Wind Driven Air Infiltration Calculations", ASHRAE HVAC&R Research Journal, Vol. 4, No. 2, pp. 119-140. April 1998. ASHRAE, Atlanta, GA. LBNL 42361

Wilson, D., & Walker, I. S. (1990). Combining Air Infiltration and Exhaust Ventilation. *IndoorAir '90*, (pp. 467-472). Toronto, Canada

The Role of Carbon Dioxide in Ventilation and IAQ Evaluation: 40 years of AIVC

Andrew Persily

National Institute of Standards and Technology
100 Bureau Drive, MS8600
Gaithersburg, MD 20899 USA
**Corresponding author: andyp@nist.gov*

SUMMARY

The purpose of this summary is to review Air Infiltration and Ventilation Centre activities, as reflected in its publications, related to indoor carbon dioxide over the 40 years that have transpired since its creation. These activities, like most applications of indoor CO_2 to the fields of ventilation and indoor air quality, have focused on the following: control of outdoor ventilation rates, i.e., demand control ventilation; use as a tracer gas to measure outdoor air change rates; providing an indicator or metric of IAQ; and, directly impacting human health, comfort and performance. More recent work on CO_2 generation rates from building occupants and CO_2 concentrations in standards and building regulations is also covered. This summary was generated by searching on Air Infiltration and Ventilation Centre publications, though the findings also reflect the evolving application and understanding of indoor CO_2 in the broader literature.

KEYWORDS: carbon dioxide; indoor air quality; metrics; ventilation

GENERAL DISCUSSIONS OF INDOOR CO_2

One of the earliest Air Infiltration and Ventilation Centre (AIVC) publications on the application of indoor CO_2 is a short article covering a range of topics, including tracer gas applications, indoor air quality (IAQ) evaluation, and CO_2 as an indicator of occupancy (Liddament, 1996). Another short paper was published more recently, which focused on CO_2 as an IAQ indicator and for ventilation control (de Gids and Wouters, 2010). No other general reports or publications on CO_2 have been issued by the AIVC over its 40 years. The application of CO_2 has been covered mostly by individual conference papers on the topics covered below. For each of the topics, a table of references is provided at the end of this summary. These tables are not exhaustive but provide a sense of the issues covered for each topic.

DEMAND CONTROL VENTILATION

Indoor CO_2 has been discussed as a control parameter for outdoor air ventilation for decades, with the goal being to provide sufficient ventilation for the occupants in a space. Ventilating for the actual occupancy rather than a maximum design value provides an opportunity to reduce energy used for space heating and cooling, as well as assuring that the ventilation is sufficient to meet the needs of the occupants. In 2001 the AIVC generated a literature list (LL) that identified about 50 publications on the topic of CO_2 demand control ventilation, many of them not published by the AIVC itself. Additional work on the topic has continued in subsequent publications on sensor performance, energy and IAQ impacts, case studies in a variety of building types and other subtopics as noted in the table below.

CO_2 AS A TRACER GAS

Carbon dioxide has long been recognized as a useful tracer gas for studying building ventilation and airflow given its low reactivity and toxicity, relative ease of measurement and, in some applications, building occupants serving as a convenient tracer gas source. CO_2 was identified

as a potential tracer gas in an early AIC publication (Liddament and Thompson, 1983). Since that time, CO_2 has been used as a tracer gas in many studies, with several noted below.

IAQ ASSESSMENT

Indoor CO_2 concentrations have long been used as part of IAQ assessments with the oldest reference listed in the table below dating back to 1985. Some of these assessments measure CO_2 concentrations as one of many pollutants monitored, though many assessments do not explain the significance of the measured concentrations or compare them to a reference or guideline value. Such measurements are still common as part of IAQ investigations; the explicit consideration of CO_2 concentration metrics is a more recent development and is discussed next.

IAQ METRIC

The AIVC has focused on IAQ metrics in recent years, with the topic being a major theme of its 2016 conference held in conjunction with the ASHRAE IAQ conference series. Only two papers on the topic of CO_2 as an IAQ metric are listed in the table below, but the issue has been discussed in recent AIVC workshops and conference sessions without any papers being published and those discussions are likely to continue.

CO_2 GENERATION RATES

The use of CO_2 as a tracer gas for quantifying building and space ventilation rates requires a value of the rate of CO_2 generation by the building occupants. For many years, default values from ASHRAE and other sources have been used without evaluating their accuracy or the sources on which they were based. Recent publications have developed more well-documented and robust methods for estimating these generations rates, with three AIVC conference papers included in the table below.

STANDARDS AND REGULATIONS

While indoor CO_2 has been considered in ventilation and IAQ studies for decades, most standard or guideline values were only for industrial environments. More recently a number of standards and building regulations have been promulgated with specific indoor CO_2 concentration limits. Several of these are covered by the publications listed in the table below, though other countries and localities appear to also be setting such limits.

CO_2 IMPACTS ON BUILDING OCCUPANTS

Finally, a number of recent studies have taken a new look at how CO_2 impacts building occupants both physically and mentally. Many of these studies have been looking at concentrations that are typical of indoor spaces. However, the studies in the broader literature are not consistent as to the human effects observed. The three studies listed in the table below are just an example of such work that has been presented in recent AIVC conferences.

REFERENCES

de Gids, WF and Wouters, P. (2010). *CO_2 as Indicator for the Indoor Air Quality - General Principles*, Air Infiltration and Ventilation Centre.

Liddament, M and Thompson, C. (1983). *Techniques and Instrumentatoin for the Measurement of Air Infiltration in Buildings - A Brief Review and Annotated Bibliography*, Air Infiltration Centre, Bracknell, Great Britain., Technical Note 10.

Liddament, MW. (1996). Why CO_2? *Air Infiltration Review*, 18, 1-4.

Demand Control Ventilation
H. Han, K-J Jang, C. Han and J. Lee. 2013. Occupancy estimation based on CO2 concentration using dynamic neural network model, 34th AIVC Conference.
A. Persily, A. Musser, S. Emmerich, M. Taylor. 2003. Simulations of indoor air quality and ventilation impacts of demand controlled ventilation in commercial and institutional buildings. 24th AIVC and BETEC Conference.
Villenave J.G., Bernard A.M., Lemaire M.C. 2003. Simulations of indoor air quality and ventilation impacts of demand controlled ventilation in commercial and institutional buildings. 24th AIVC and BETEC Conference.
Chan G Y, Chao C Y, Lee D C, Chan S W, Lau H. 1999. Development of a demand control strategy in buildings using radon and carbon dioxide levels. Indoor Air 99 and 20th AIVC Conference.
Fleury B. 1992. Demand controlled ventilation: a case study. 13th AIVC Conference.
Zamboni M, Berchtold O, Filleux C, Fehlmann J, Drangsholt F. 1991Demand controlled ventilation - an application to auditoria. 12th AIVC Conference.
Fahlen P, Andersson H. 1991. Demand controlled ventilation: full scale tests in a conference room. 12th AIVC Conference.
Donnini G, Haghighat F, Van Hiep Nguyen. 1991. Ventilation control of IAQ, thermal comfort and energy conservation by CO2 measurement. 12th AIVC Conference.
Fahlen P, Ruud S, Andersson H. 1991. Demand controlled ventilation - evaluation of commercially available sensors. 12th AIVC Conference.
Raatschen W. 1988. Market analysis of sensors for the use in demand controlled ventilating systems. 9th AIVC Conference.
Smith B E, Prowse R W, Owen C J. 1984. Development of occupancy-related ventilation control for Brunel University Library. 5th AIVC Conference.

Use of CO_2 as a Tracer Gas
J.D. Carrilho, M. Mateus, S. Batterman, M. Gameiro da Silva. 2014. Measurement of infiltration rates from daily cycle of ambient CO_2. 35th AIVC Conference.
D. Kraniotis, T. Aurlien, T.K. Thiis. 2013. On investigating instantaneous wind-driven infiltration rates using CO2 decay method. 35th AIVC Conference.
Bong C, Kim S, Lee J, Lee H. 1999. Ventilation demand in a subway train - based on CO2 bioeffluent from passengers. Indoor Air 99 and 20th AIVC Conference.
Federspiel C. 1996. Ventilation performance evaluation using passively-generated carbon dioxide as a tracer gas. 17th AIVC Conference.
Ekberg L E, Strindehag O. 1996. Checking of ventilation rates by CO2 monitoring. 17th AIVC Conference.
Kohal J S, Riffat S B, 1993. Computer modelling & measurement of airflow in an environmental chamber. 14th AIVC Conference.

IAQ Assessment
J. Sifnaios, P.V.Dorizas, M. Assimakopoulos. 2014. A study of carbon dioxide concentrations in elementary schools. 35th AIVC Conference.
Weinlader H, Beck A, Fricke J, 2000. Demand controlled ventilation in schools - energetic and hygienic aspects. 21st AIVC Conference.
Parent D, Stricker S, Fugler D, 1996. Ventilation in houses with distributed heating systems. 17th AIVC Conference.
Donnini G, Nguyen V H, Molina J, 1994. Occupant satisfaction and ventilation strategy - a case study of 20 public buildings. 15th AIVC Conference.
Weinlader H, Beck A, Fricke J, 2000. Demand controlled ventilation in schools - energetic and hygienic aspects. 21st AIVC Conference.
Parent D, Stricker S, Fugler D, 1996. Ventilation in houses with distributed heating systems. 17th AIVC Conference.
Donnini G, Nguyen V H, Molina J, 1994. Occupant satisfaction and ventilation strategy - a case study of 20 public buildings. 15th AIVC Conference.
Grelat A, Cohas M, Lemaire M C, Fauconnier R, Creuzevault D, Loewenstein J-C, 1992. Correlation between carbon dioxide concentration and condensation in homes. 13th AIVC Conference.
Nielsen J B, 1992. A new ventilation strategy for humidity control in dwellings. 13th AIVC Conference.
Croome D J, Gan G, Awbi H B, 1992. Field evaluation of the indoor environment of naturally ventilated offices. 13th AIVC Conference.

Fehlmann J, Wanner H U, 1990. Air change rate and indoor air quality in bedrooms of well tightened residential buildings. 11th AIVC Conference.
Grot R A, Persily A, Hodgson A T, Daisey J M, 1988. Ventilation and indoor air quality in a modern office building. 9th AIVC Conference.
Baumgartner T, Bruhwiler D, 1987. Simulation of CO2 concentration for determining air change rate. 8th AIVC Conference.
Fecker I, Wanner H U, 1986. Measurement of carbon dioxide of the indoor air to control the fresh air supply. 7th AIVC Conference.
Lundqvist G R, 1985. Indoor air quality and air exchange in bedrooms. 6th AIVC Conference.

IAQ Metric
A. Persily. 2018. Development of an Indoor Carbon dioxide metric. 39th AIVC Conference.
A. Szczurek, M. Maciejewska, T. Pietrucha. 2015. CO2 and volatile organic compounds as indicators of IAQ. 36th AIVC Conference.

CO_2 Generation Rates
M. Tajima, T. Yorimitsu, Y. Shimada. 2018. Accuracy Improvement for Estimating Indoor Carbon Dioxide Concentration Produced by Occupants. 39th AIVC Conference.
A. Persily, L. de Jonge, 2017. A New Approach to Estimating Carbon Dioxide Generation Rates from Building Occupants. 38th AIVC Conference.
M. Tajima, T. Inoue, Y. Ohnishi. 2014. Derivation of equation for personal carbon dioxide in exhaled breath intended to estimation of building ventilation. 35th AIVC Conference.

Standards and Regulations
S. Caillou, J. Laverge, P. Wouters. 2018. IAQ in working environments in Belgium: alternative approaches to CO2 requirement. 39th AIVC Conference.
A. Persily. 2015.Indoor Carbon Dioxide Concentrations in Ventilation and Indoor Air Quality Standards. 36th AIVC Conference.
P. Paulino. 2015. Impact of the new rite 2013 (regulation on thermal installation) on indoor air quality. 36th AIVC Conference.

CO_2 Impacts on Building Occupants
L. Yoshimoto, T. Yamanaka, A. Takemura, K. Ikeda. 2018. Subjective Evaluation for Perceived Air Pollution Caused by Human Bioeffluents. 39th AIVC Conference.
P. Wargocki, J.A. Porras-Salazar, W.P. Bahnfleth, 2017. Quantitative relationships between classroom CO2 concentration and learning in elementary schools. 38th AIVC Conference.
X. Zhang, P. Wargocki, Z. Lian, 2015. Effects of Carbon Dioxide With and Without Bioeffluents on humans. 36th AIVC Conference.

HVAC and VOCs: interaction between building systems and indoor VOC concentrations

Klaas De Jonge[1,*], Jelle Laverge[1]

Research group of Building Physics,
Department of Architecture and Urban Planning,
Ghent University
Sint-Pietersnieuwstraat 41 B4
9000 Ghent, Belgium
Corresponding Author: klaas.dejonge@ugent.be

SUMMARY

HVAC systems in newly built or extensively renovated dwellings were all developed with the aim for energy saving with equal or better comfort. However, these systems (floor heating and DCV systems) have certain characteristics which increase the emissions of Volatile Organic Compounds (VOCs) and give VOCs the chance to accumulate to higher concentrations. This interaction is investigated based on dynamic simulations using a temperature and humidity dependent VOC emission model.

KEYWORDS

Indoor Air Quality, IAQ, HVAC, Floor heating, Demand Controlled Ventilation, DCV, Volatile Organic Compounds, VOC

1 INTRODUCTION

New technologies for the building and HVAC industry are being implemented in every type of building at a fast rate. These technologies typically aim for less energy but equal or better indoor comfort. Buildings are getting built more airtight, high temperature radiator heating is being replaced by low temperature surface heating and continuous flow ventilation systems make way for demand controlled ventilation (DCV) systems.

The assessment of the impact of such a system is typically only done based on potential energy saving and the comfort aspect of Indoor Air Quality (IAQ). E.g. in Belgium, the assessment method for DCV systems only considers CO2, H2O and a tracer representing smell from the toilet [1]. By doing so, the health aspect of IAQ related to VOC emissions to the indoor environment is neglected.

The relation of indoor VOC levels to humidity and temperature combined with the higher airtightness and (sometimes) lowered ventilation rates in DCV systems make is increasingly important to consider this additional aspect in order to be sure the long term health consequences do not pose a significantly higher risk

2 METHODOLOGY

A temperature and humidity based VOC emission model is implemented in the simulation software CONTAM [2]–[4]. Based on dynamic simulations with or without floor heating and with or without DCV systems, the interaction between the HVAC system and the VOC exposure of the occupants is analyzed.

3 MAIN RESULTS AND CONCLUSION

For DCV systems, the risk of prolonged exposure to high VOC levels is observed. Especially in spaces with limited occupation or spaces with long periods of absence like the bedroom. The impact of floor heating is also significant, heat is supplied directly to the floor, heating up the floor to temperatures higher than it would have been with radiator heating. The higher emission

rates due to the temperature dependence of the VOC emissions make for higher VOC exposure of the occupant.
VOC exposures are higher, but the energy saving potential of these new technologies should off course not be overlooked. The way the VOC exposure changes with regards to the new HVAC technologies are as expected, thus can be managed. By choosing low VOC-emitting surface finishing when floor heating is begin used, the VOC exposure could be reduced significantly and the new generation of DCV systems could be further developed taking into account this risk of exposure to higher VOC concentrations.

4 ACKNOWLEDGEMENTS

The author, K. De Jonge, would like to acknowledge FWO and Ghent University for respectively supporting and hosting the work he does in his role as SB PhD fellow at FWO (1SA7619N).

5 REFERENCES

[1] N. Heijmans, N. Van Den Bossche, and A. Janssens, 'Berekeningsmethode gelijkwaardigheid voor innovatieve ventilatiesystemen in het kader van de EPB-regelgeving', WTCB, Ghent University, Mar. 2007.
[2] W. S. Dols and B. J. Polidoro, 'CONTAM User Guide and Program Documentation Version 3.2', National Institute of Standards and Technology, NIST TN 1887, Sep. 2015.
[3] K. De Jonge, 'The impact of demand controlled ventilation on indoor VOC exposure in Belgian dwellings', Master dissertation, Ghent University, 2018.
[4] J. Laverge, 'Design strategies for residential ventilation systems', PhD dissertation, Ghent University, 2013.

Alternative ducting options for balanced mechanical ventilation systems in multifamily housing

Gabriel Rojas[*1], Rainer Pfluger[1]

1 Unit for Energy Efficient Buildings, University of Innsbruck
Technikerstr. 13
Innsbruck, Austria
** Corresponding author: gabriel.rojas-kopeinig@uibk.ac.at*

SUMMARY

Duct routing often poses a great challenge when planning the installation of a mechanical ventilation system with heat recovery. This is particularly true for retrofits, where the necessary space for supply and exhaust ducts was originally not accounted for. This extended summary presents an alternative approach for duct routing avoiding ducts in the dwelling, while allowing the installation of a centralized MVHR unit and the implementation of a cascading airflow through the dwelling. The general advantages as well as some implementation details within a refurbishment case study are presented.

KEYWORDS

Mechanical ventilation, heat recovery, duct routing, external insulation, insulation integrated ducting

1 INTRODUCTION

Duct routing often poses a great challenge when planning the installation of a mechanical ventilation system with heat recovery (MVHR). This is particularly true for retrofits, where the necessary space for supply and exhaust ducts was originally not accounted for. If the floor plan as well as the room height allows, a false ceiling can be installed in the hallway and/or the bathroom of the apartment enabling the installation of the ducts, the silencers and the flow control valves (in case of a centralized system) or the MVHR unit for the apartment. However, in practice this solution is often difficult to implement, resulting in a cost intensive installation and operation, e.g. due to the need to install many fire dampers and suspended ceilings. In fact, spatial requirements and duct routing has been identified as one of the barriers for widespread implementation of MVHR in various countries (Bocanegra-Yanez et al. 2017). As a consequence, many housing refurbishment projects opt for the installation of an exhaust air system (if space for the exhaust ducting exists), giving away the potential for substantial energy savings by heat recovery. Alternatively, the use of room-based decentralized ventilation unit with heat recovery are used. However, room-based systems result in lower ventilation efficiency, since the air cannot be cascaded from supply to extract air rooms, requiring nearly twice the total air exchange. In general, these solutions often fall short also in terms of thermal or acoustic comfort as compared to a cascading MVHR system due to sound emission of the units and reduction of sound insulation of the exterior walls by multiple wall openings. They also lack the possibility to install good air filters.
The herein presented approach avoids ducting within the dwelling, while allowing the installation of a centralized MVHR unit and the implementation of a cascading airflow through the dwelling. It has been applied in several refurbishment projects within the FP7-project “Sinfonia”, see (Music 2018) and https://passivehouse-database.org under the project ID 5673, 5674, 5675 and 5676.

2 RESULTS

The principal idea of this ducting solution is simple: install the central ventilation unit in the attic and run the supply and extract air ducts down into each apartment and each room on the outside of the external walls through the insulation layer (see Figure 1). This approach requires a core hole (or a window integrated opening) in each room where air is supplied or extracted. However, it has several advantages. The major advantage being that duct routing within the apartments can be avoided. The other advantage is related to necessary fire protection measures. When ducts are routed through the interior of the building, fire safety codes in Austria (and other countries) prescribe the installation of fire dampers and/or other fire protection measures, whenever the ducting penetrates walls of declared fire zones. Such dampers are costly and need regular inspection. Their easy accessibility often poses a major issue for property managers, if they are installed in the false ceiling within the flat. In the presented case study the number of required fire dampers could be greatly reduced with all of them being easy accessible in the attic of the building. The MVHR unit was placed within a fire protected housing only needing four (easy accessible) fire dampers at its penetration points, see Figure 2 (left). From there, the supply and extract air ducts are split and routed to the exterior wall. After the splitting, manual flow valves and silencers were installed, see Figure 2 (right).

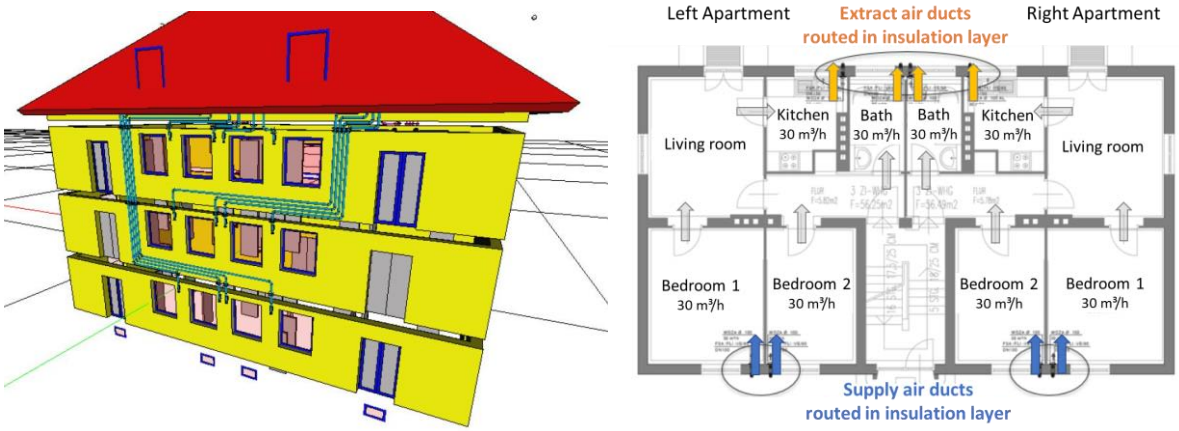

Figure 1: Left: 3D sketch of one of the case studies installing the supply and extract air ducts in the exterior wall insulation. Source: (Music 2018). Right: Floor plan of the case study where all supply and extract air ducts are integrated in the external wall insulation. Note that the living rooms are ventilated with overflowing air (extended cascade principle).

All together, this ducting solution simplifies centralized MVHR systems, which are generally considered advantageous in terms of maintenance/accessibility for non-owner occupied housing. To fully exploit the advantages of this approach all bedrooms and wet rooms should have access to an exterior wall where ducts can be integrated. Nevertheless, this concept was also advantageously applied in projects by combining external and internal duct routing, see (Music 2018). Ideally, the supply air rooms are on one side and the extract air rooms on the other side, e.g. see Figure 1. In the presented case studies the 7 cm diameter ducts were installed within the existing cork insulation layer (6 cm). They were covered by the new 20 cm thick EPS insulation layer. However, an existing insulation layer is not a prerequisite, since the slots for the ducts could also be included within the new insulation layer. Basic calculations suggest the remaining insulation thickness should be roughly >2/3 of the total insulation layer to avoid significant heat losses. Other projects investigated the use of pre-formed EPS elements to ease the integration of air ducts in the insulation layer (Hauser and Kaiser 2013; Schwerdtfeger 2018).

Figure 2: Left: *Central unit with fire protected housing and fire dampers at the top. The fire protected maintenance cover at the front is not mounted in the picture. Right: Supply air ducts in attic with flow regulation dampers, silencers and penetration to the outside of the exterior wall.*

3 CONCLUSIONS AND OUTLOOK

This case study presents an attractive alternative for routing the supply air and extract air ducts for centralized MVHR during a deep energy retrofit of multifamily housing. The main advantage is the fact that no ducting is needed within the dwelling, thus saving space and minimizing disturbance of dwelling occupants. The layout of these case study buildings allowed a very simple planning, in particular in terms of fire protection, and resulted in a smooth installation process. Due to it simple and low tech design (manual flow regulation valves, few fire dampers, no false ceilings, etc.) the costs could be kept at roughly €2500 per apartment, which less than half of the costs for installing the MVHR system in comparable projects. As it worked well for deep retrofit, this concept could also be adapted for new buildings as well. Up to now, it was only applied for centralized MVHR. The University of Innsbruck is currently investigating a decentralized concept (one unit per dwelling), further reducing necessary fire protection measures.

4 REFERENCES

Bocanegra-Yanez, Maria, Gabriel Rojas, Daria Zukowska-Tejsen, Esfand Burman, Guangyu Cao, Mathieu Pierre Hamon, and Jakub Kolarik. 2017. “Design and Operation of Ventilation in Low Energy Residences – A Survey on Code Requirements and Building Reality from Six European Countries and China.” in *AIVC Proceedings*, edited by AIVC.

Hauser, Gerd and Jan Kaiser. 2013. “Dämmstoffintegrierte Kanäle Für Zentrale Lüftungsanlagen Mit Wärmerückgewinnung.” *Bauphysik* 35(6):367–76.

Music, Admir. 2018. “Luftverteilung: Erschließung Über Die Fassade - Erfahrungen Aus Dem Forschungsprojekt Sinfonia (A).” Pp. 127–35 in *AKKP 54: Neue Konzepte der kontrollierten Lüftung: Fassadenintegrierte Lüftung*, edited by W. Feist. Darmstadt, Germany: Passive House Institute.

Schwerdtfeger, Peter. 2018. “Luftverteilung: Erschließung Über Die Fassade. Erfahrungen Aus Dem Projekt Nauheimer Straße.” Pp. 137–50 in *AKKP 54: Neue Konzepte der kontrollierten Lüftung: Fassadenintegrierte Lüftung*, edited by W. Feist. Darmstadt, Germany: Passive House Institute.

Lessons learned from a ten-year monitoring in residential buildings equipped with humidity based demand controlled ventilation in France

Gaëlle Guyot[1,2*]

1 Cerema, BPE research team,
46 rue St Théobald
38081 L'Isle d'Abeau cedex
**Corresponding author: gaelle.guyot@cerema.fr*

² Univ. Grenoble-Alpes, Univ. Savoie Mont Blanc,
CNRS, LOCIE, 73 000 Chambéry, France

SUMMARY
Humidity-based DCV systems have been widely used in France for 35 years and are considered as a reference system, including for low-energy residential buildings. Indeed, most of the new residential buildings, which must be low-energy buildings to comply with the RT 2012 energy performance regulation, are equipped with such systems. Feedbacks from two long-term studies show the durability of the humidity sensitive components and show the robustness of this system to bad maintenance or use by occupants. The on-going Performance 2 project delivers the first results of a ten-year monitoring in thirty social housing apartments. In the context of the increasing awareness about smart ventilation, from these feedbacks, it seems very important consider the durability of the systems and its components (including the sensors) and the robustness of the systems to a lack of maintenance by occupants.

KEYWORDS
Ventilation, performance, DCV, humidity, residential buildings

1 INTRODUCTION

1.1 Regulatory context
The French dwellings airing regulation (J.O. 1983) requires a general and continuous airing system, describes the compulsory general layouts of ventilation installation and requires exhaust airflows in each humid room, depending on the total number of rooms in the dwelling. This regulation has been modified in 1983 in order to reduce these airflows in case of demand-controlled ventilation system (DCV), for instance based on humidity. In this case, manufacturers must follow a compliance procedure to ensure adequate ventilation, with a performance-based approach. Indeed, the procedure (CCFAT 2015) describes the common scenario used to evaluate the DCV systems using the multizone software MATHIS (Demouge, Le Roux, and Faure 2011) and calculating two IAQ performance indicators: a condensation risk (number of hours with relative humidity higher than 75%) and a cumulative CO_2 exposure exceeding 2000 ppm, further described in (Guyot, Walker, and Sherman 2018). Each room of the dwelling is modelled as single zone, with a time-step of 15 min. Once a system receives certification of compliance via this procedure, called "Avis technique", it can be used in new dwellings according to its specifications. For each type and size of dwelling, the agreement gives the references of inlets and outlets and the input data for energy calculation.
As a result, humidity-based DCV systems have been widely used in France for 35 years. Most of the new residential buildings, which must be low-energy buildings to comply with the RT 2012 energy performance regulation, are equipped with such systems (Mélois et al. 2019). They are also considered today as a reference system.

1.2 Technological context: presentation of the reference humidity based DCV system
RH-MEV is a Demand Control Ventilation (DCV) system adjusting the airflows according to the estimated needs of the building and its occupants, with a direct relative humidity (RH) measurement in both the wet and dry rooms. The extensions and retractions of a hygroscopic

fabric modify the cross-section of inlets and outlets upon hygrometric changes in their environment without the need for motors or electronic sensors.
The reference system used in France includes as air terminal devices, humidity sensitive trickle ventilators in the dry rooms and humidity sensitive exhaust units in the wet rooms, except in the toilets which are equipped with an occupancy.
Energy savings have been estimated about 30% to 50 % of the heating energy compared to constant airflows exhaust-only ventilation (Savin and Bernard 2009).
They could be considered as a type of smart ventilation system, according to the definition given by (Durier, Carrié, and Sherman 2018).

2 FIRST FEEDBACKS ON ROBUSTNESS AND DURABILITY AFTER PROLONGED IN SITU OPERATION

In 2006, before generalizing the usage of humidity based ventilation in French residential buildings, the French Ministry for Housing ordered an evaluation of these systems after prolonged on-site operation. For this purpose, after 6 years of in-situ functioning, an independent laboratory collected 57 exhaust units in 21 social housings (Berthin and Parsy 2018). Despite an absence of sufficient maintenance observed for 75% of the units (dust), tests in laboratory conditions showed that 46 % of the kitchen units complied with factory specifications despite the absence of maintenance, 100 % of the bathroom exhaust units showed an airflow reduced by 5 m^3/h. 100 % of the non-damaged exhaust units exhibited a conform hygroscopic behavior or showed a slight shift of their characteristic when still soiled.

Once the devices have been cleaned and properly re-assembled, 75 % of the units complied with factory specifications. Among the other 25 %, the kitchen elements showed an increase of volume flow lower than 3 m^3/h, while bathroom units exhibited a decrease lower than 2 m^3/h. Results are further described in

These first results show the reliability of the components including humidity sensors and the robustness of their operation to a bad maintenance and use by occupants.

3 FIRST RESULTS FROM THE PERFORMANCE 1&2 PROJECTS

The Performance 2 project is based on a 10 years' follow-up study on a large-scale monitoring on thirty occupied social housing apartments in two residential buildings. The former Performance project was an on-field evaluation of the reference humidity-based components and systems from an energy performance and an indoor air quality point of view, over two heating seasons (2007-2009) (Bernard 2009). The ventilation terminals were instrumented, and the buildings were equipped with sensors during the construction phase, including temperature, humidity, and CO_2 in the different rooms of the dwellings, as well as pressure and volume flow sensors for monitoring the ventilation system. The Performance project showed the good IAQ in terms of CO_2 and humidity provided by the ventilation system, despite the over-occupation of some apartments.
Ten years later, in the framework of the Performance 2 project, the data acquisition system is turned back on with the intention to assess the ventilation system behaviour/performance after a prolonged in-situ functioning period (Jardinier et al. 2018). This preliminary study results shows:

- At start-up, more than 80 % of the metrology sensors is still in working conditions.
- Using this rough data, the average in-situ drift of the hygroscopic devices after 9 years of operation is estimated below ± 1.5 %RH and is lower than the announced accuracy of the electronical humidity sensors at installation (± 1.8 %RH).
- The observed drift of volume flows on some of the exhaust units is typical of an absence of maintenance.

- The battery of the presence-based toilet exhaust is often (90 %) discharged.

In July 2019, we organized a first meeting with the occupants, and got their first feedbacks. These first promising results on the durability and robustness of these systems need to be confirmed by the end of the Performance 2 project which shall include:

- The collection of the ventilation devices for a full quality control before and after the recommended cleaning.
- The collection of the metrology sensors for re-calibration and drift-correction on the measurements.
- A new set-up for each apartment including particle sensors to follow the latest interests of IAQ research.

4 PERSPECTIVES

In the context of the increasing awareness about smart ventilation, from these feedbacks, it seems very important to include in this definition the durability of the systems and its components (including the sensors) and the robustness of the systems to a lack of maintenance by occupants.

5 REFERENCES

Bernard, Anne-Marie. 2009. *Performance de La Ventilation et Du Bâti - Phase 3 - Performance Énergétique et QAI Des Systèmes Hygroréglables*. Projet PREBAT ADEME.

Berthin, S, and F Parsy. 2018. “Feedback on Installation, Maintenance, and Aging of Mechanical Humidity-Controlled Ventilation Exhaust Units.” In *Smart Ventilation for Buildings*. Juan les Pins, France.

CCFAT. 2015. “VMC Simple Flux Hygroréglable - Règles de Calculs Pour l’instruction d’une Demande d’avis Techniques - GS14.5 - Equipements / Ventilation et Systèmes Par Vecteur Air.” http://www.ccfat.fr/groupe-specialise/14-5/.

Demouge, François, Nicolas Le Roux, and Xavier Faure. 2011. “Numerical Validation Fo Natural Ventilation Design.” In *32nd AIVC Conference “ Towards Optimal Airtightness Performance.”* Brussels, Belgium. https://www.researchgate.net/profile/Francois_Demouge/publication/232621659_Numerical_validation_for_natural_ventilation_design/links/542123d50cf241a65a1e606b.pdf.

Durier, François, F. Rémi Carrié, and Max Sherman. 2018. “VIP 38: What Is Smart Ventilation?” *AIVC*, March. http://aivc.org/sites/default/files/VIP38.pdf.

Guyot, Gaëlle, Iain S. Walker, and Max H. Sherman. 2018. “Performance Based Approaches in Standards and Regulations for Smart Ventilation in Residential Buildings: A Summary Review.” *International Journal of Ventilation* 0 (0): 1–17. doi:10.1080/14733315.2018.1435025.

Jardinier, E, F Parsy, G Guyot, S Berthin, and S Berthin. 2018. “Durability of Humidity-Based Demand-Controlled Ventilation Performance: Results of a 10 Years Monitoring in Residential Buildings.” In *Smart Ventilation for Buildings*. Juan les Pins, France.

J.O. 1983. *Arrêté Du 24 Mars 1982 Relatif à l’aération Des Logements*.

Mélois, Adeline Bailly, Bassam Moujalled, Gaëlle Guyot, and Valérie Leprince. 2019. “Improving Building Envelope Knowledge from Analysis of 219,000 Certified on-Site Air Leakage Measurements in France.” *Building and Environment*, May. doi:10.1016/j.buildenv.2019.05.023.

Practical use of the Annex68 IAQ Dashboard

Marc Abadie[1]

1 Laboratoire des Sciences de l'Ingénieur pour l'Environnement (LaSIE) - University of La Rochelle
Pôle Sciences et Technologie
Avenue Michel Crépeau
17042 La Rochelle Cedex 1, France

SUMMARY

The present paper aims at illustrating the practical use of the Annex68 IAQ Dashboard. To this end, numerical simulations have been performed to provide useable data about the Indoor Air Quality (IAQ) of a low-energy detached house. The dashboard has been used to compare three possible solutions of ventilation systems commonly found in French residential buildings i.e. natural ventilation using vertical ducts for extraction, self-regulated exhaust and balanced mechanical ventilation. The analysis shows that a 50% IAQ improvement can be achieved with a balanced system compared to other ventilation systems.

KEYWORDS

Indoor Air Quality, IAQ metrics, low-energy building, ventilation system.

1 ANNEX68 IAQ DASHBOARD

IEA Annex 68 Subtask 1 aimed at setting up the metrics to assess the performance of low-energy buildings as regards indoor air quality (IAQ) combining the aspirations to achieve very high-energy performance without compromising indoor environmental quality (Abadie and Wargocki, 2017). We proposed IAQ sub-indices based on acute (short-term) and chronic (long-term) effects as the ratio of the concentrations to the guideline levels; for chronic effects, we also proposed the DALY approach (Disability-Adjusted Life Years) as an IAQ index. As for the multipollutant index, we proposed the maximum of the calculated indices acknowledging limitations and inaccuracies introduced by aggregation methods. Finally, the value of the index, or set of sub-indices, for IAQ ultimately needs to be weighed against the additional use of energy needed to improve IAQ in comparison with current standard practice. Figure 1 presents the graphical representation of IAQ indices along with energy consumption. All indices for single pollutants are seen for long-term (LT) and short-term (ST) effects using two approaches (based on Exposure Limits and DALY). Energy consumption is displayed in the lower right corner.

2 METHODOLOGY

As an example, we use the time-varying pollutant concentrations obtained by Cony-Renaud-Salis et al (2018) by numerical simulations by coupling a building energy simulation software with a multi-zone indoor air quality and ventilation program. The case study is two-storey low-energy house with one living room and three bedrooms located in La Rochelle, France (small city, low pollution). See the references for more details regarding wall compositions, furniture quantity and everyday objects such as books, shoes, computers, TV monitor, etc. Ventilation rates have been calculated according to the French standards (180 m^3/h during 30 min. at noon and 19:30, 105 m^3/h otherwise). The goal of this study is to evaluate the IAQ of three possible

solutions of ventilation systems commonly found in French residential buildings using the IAQ dashboard: natural ventilation using vertical ducts for extraction (NAT), self-regulated exhaust (EXH) and balanced mechanical ventilation (BAL). We considered here 9 out of the 16 target pollutants identified in Subtask 1: acetaldehyde, acrolein, benzene, formaldehyde, nitrogen dioxide, particulate matter (PM2.5, PM10), styrene and toluene. The time-varying pollutant concentrations have been integrated according to the occupancy schedule in order to calculate the exposure to each pollutant during one week in winter.

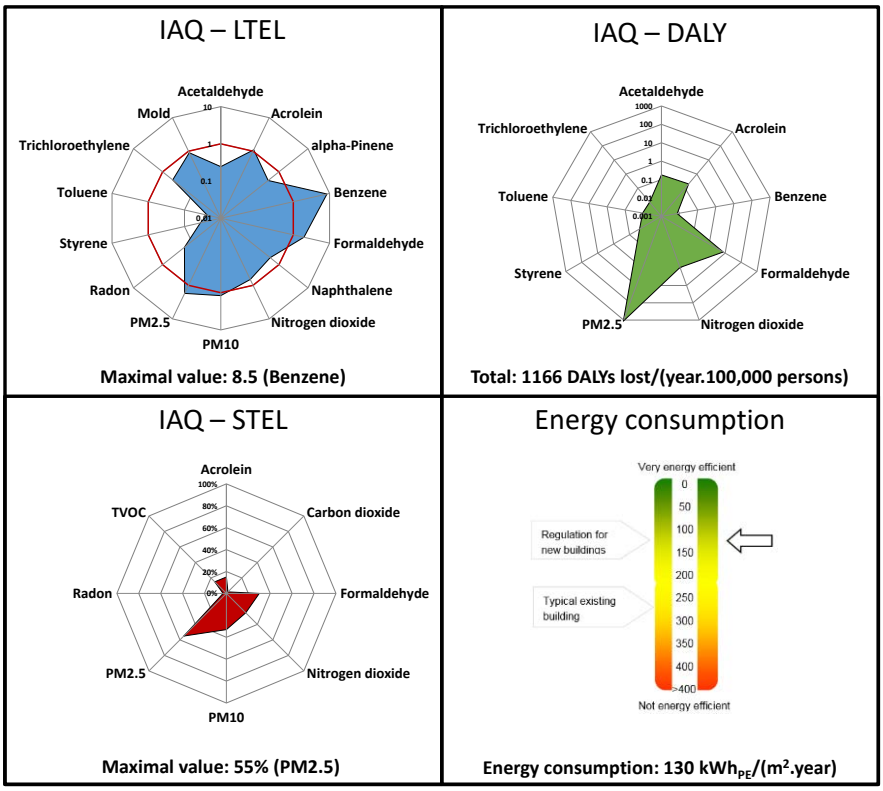

Figure 1: *IAQ/Energy dashboard for low-energy residential buildings – IAQ-LTEL is for Indoor Air Quality – Long-Term Exposure Limit, IAQ-STEL is for Indoor Air Quality – Short-Term Exposure Limit and IAQ-DALY is for Indoor Air Quality – Disability-Adjusted Life Years (data represented here are just for display and do not represent actual situation).*

3 MAIN RESULTS AND FINDINGS

Among the four quadrants of the IAQ dashboard, only the one relative to Long-Term Exposure Level is represented here because no energy consumption calculation has been carried out here (fourth quadrant), there is no exceedance of short-term exposure levels (third quadrant) and DALY representation (second quadrant) does not allow clear comparison between the cases. Figure 2 presents the IAQ-LTEL for the three ventilation systems compiled in one graph to ease the comparison. Overall, the results obtained by these numerical simulations confirmed the trend observed with real experimental data such as those used in Subtask 1: LTEL is higher than 1 (i.e. pollutant concentration higher than the Exposure Limit Value) for acrolein, benzene, formaldehyde, nitrogen dioxide and particulate matter (PM2.5, PM10) and lower than 1 for the other pollutants. In this example, benzene is identified as the pollutant of higher index; actions to improve the IAQ should then focus in reducing indoor benzene sources that are here the building materials. Regarding the performance of the three ventilation systems, it should be noted that, even if the systems were sizing (ducts and fans) with the same objective in terms of exhausted airflow rates, the simulation results show 20% higher airflow rates for the balanced system compared to the self-regulated exhaust; those for the ventilation natural system tend to

be the lowest. This fact explains why LTEL is lower for the BAL and higher for the NAT systems for pollutants of only indoor emissions (acetaldehyde, acrolein, benzene, formaldehyde, styrene and toluene). The role of the filtration regarding the BAL system is clearly observed for PM2.5 and PM10 (PM2.5 LTEL values are 0.6, 1.1 and 1.2 for BAL, EXH and NAT systems, respectively). Outdoor gaseous pollutant concentration (nitrogen dioxide) is almost not affected by the ventilation systems.

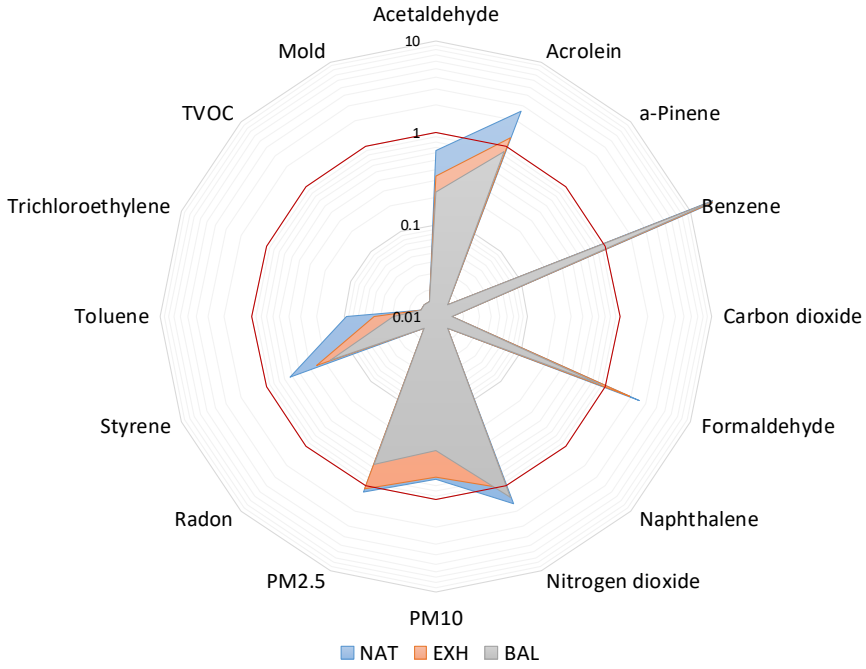

Figure 2: *IAQ-LTEL quadrant for the studied case.*

4 CONCLUSION

This exercise shows that, for the ventilation cases studied here that comply with ventilation regulations in terms of permanent airflow rates, the assessment of system performance can be limited to the long-term LTEL index. Its value for PM2.5 demonstrates that a 50% IAQ improvement can be achieved with a balanced system compared to other ventilation systems.

5 ACKNOWLEDGEMENTS

The authors would like to thank the French Environment and Energy Management Agency (ADEME) supported research reported in this paper under convention n°1504C0157.

6 REFERENCES

Abadie, M., Wargocki, P. (2017). CR 17: Indoor Air Quality Design and Control in Low-energy Residential Buildings- Annex 68 | Subtask 1: Defining the metrics. AIVC Contributed Report 17, 116p.

Cony-Renaud-Salis, L., Ramalho, O., Abadie, M. (2018). Development of a Numerical Methodology to Assess Indoor Air Quality in Residential Buildings, *Proceedings of the 15th Conference of the International Society of Indoor Air Quality & Climate (ISIAQ)*, July 22 to 27, Philadelphia, USA.

Lessons learned from design and operation of ventilation systems in low-energy dwellings in the UK

Esfand Burman

UCL Institute for Environmental Design and Engineering, 14 Upper Woburn Place, London, WC1H 0NN, United Kingdom

SUMMARY

This presentation will cover the key lessons learned from post-occupancy evaluation of the ventilation strategies in several new-build dwellings in the UK. Two ventilation strategies often used for new dwellings in the UK are mechanical extract ventilation (MEV) and whole-house balanced mechanical ventilation with heat recovery (MVHR). Few examples of the design and operation of these systems will be presented identifying the best practice and improvement opportunities for mechanical ventilation systems that are increasingly used in airtight low-energy dwellings.

Issues around system installation and commissioning may compromise energy efficiency of the air distribution system and the airflows supplied to dwellings. Measurement of air flows in new-build dwellings with MEV system showed that actual flow rates may be significantly lower than design intents if the systems are not commissioned effectively. Actual flow rates measured in boos ventilation mode were up to 30% lower than the design target.

The study also found examples of under-ventilation in dwellings with MVHR systems. In addition to system commissioning, maintenance of MVHR system including regular filter replacement is crucial to ensure adequate fresh air is provided to a dwelling. There are improvement opportunities in provision of information and training to building users about MVHR systems. It is suggested that Landlords and housing association can also take more responsibility for system inspection and maintenance in rented accommodation and social housing similar to the requirement for annual inspection of heating systems.

Finally, measurements of concentration levels of several pollutants, identified as high risk in low-energy dwellings in IEA-EBC Annex 68 programme, identified improvement opportunities for source control and enhanced ventilation to reduce concentration level of Formaldehyde to the best-practice exposure limit value. The current regulatory framework in the UK covers major outdoor sources of pollution and TVOC as a proxy for indoor sources related to construction material. However, TVOC is not the best indicator of indoor sources of air pollution and their potential health effects. It is necessary to adopt a more refined approach and address specific volatile organic compounds with potentially high adverse impact on health and well-being to protect building users and strike the right balance between energy efficiency and indoor air quality.

KEYWORDS

Post-occupancy evaluation, low-energy dwellings, Mechanical extract ventilation (MEV), Mechanical ventilation with heat recovery (MVHR), Indoor Air Quality (IAQ)

Figure 1: Examples of dwellings covered in the study: terraced houses with MEV system (left), apartments with MVHR system (right)

Table 1: Measured air flows in sample dwellings with MEV systems against design targets

Dwelling	**Total trickle extract flow rate / design target (l/s)**	**Total boost flow rate / design target (l/s)**
Mid-terrace House 1	11.7 / 30.5	34.9 / 35
Mid-terrace House 2	12.2 / 30.5	30.2 / 35
End of Terrace House	2.2 / 30.5	24.1 / 35

Table 2: Concentration levels of ley contaminants and air change rates in dwellings with MVHR system during heating season

VOC concentration (µg/m³) & Air Change rates per Hour for each zone	**APT. 3 (Block A, 9th Floor)**			**APT. 4 (Block B, Ground Floor)**			**IEA EBC Annex 68 Long Term ELV**
	Living room	Kitchen	Sample bedroom	Living room	Kitchen	Sample bedroom	
Benzene	**1.3**	**1.0**	**1.2**	**1.5**	**2.1**	**1.6**	0.2
Formaldehyde	**29.25**	**26.87**	**29.53**	**21.23**	**31.35**	**27.44**	9
Trichloroethylene	<0.5	<0.5	<0.5	<0.5	<0.5	<0.5	2
Styrene	1.5	2.2	3.0	0.8	0.7	1.7	30
Naphthalene	**5.4**	**5.4**	**5.0**	0.9	0.9	1.3	2
Toluene	2.7	2.9	3.1	2.2	2.6	2.4	250
Tetrachloroethylene	0.6	<0.6	<0.6	1.5	1.2	1.8	100
ACH (PFT measurements)	0.50	0.52	0.76	1.02	1.14	0.6	n/a

ACKNOWLEDGEMENTS

This presentation is based on the findings of research projects funded by the Innovate UK Building Performance Evaluation Programme (project reference no.: 17973-111184) and EPSRC (TOP project, reference no.: EP/N009703/1).

REFERENCES

Burman, E., Shrubsole, C., Stamp, S., Mumovic, D., & Davies, M. (2018). Design and operational strategies for good Indoor Air Quality in low-energy dwellings:

performance evaluation of two apartment blocks in East London, UK. *the 7th international Building Physics Conference (IPBC 2018).* Syracuse, USA.

Innovate UK. (2013). *Centenary Quay Fabric and Distric Heating Performance Study , Phase 1 : Post construction and early occupation, Building Performance Evaluation programme, Domestic Buildings.* London: Innovate UK.

Innovate UK. (2014). *Centenary Quay Fabric and Distric Heating Performance Study , Phase 2 : In-use performance & post occupancy evaluation, Building Performance Evaluation programme, Domestic Buildings.* London: Innovate UK.

Moisture in indoor air: findings of 40 years

Paula Wahlgren

Chalmers University of Technology
Building Technology
SE- 412 96 Gothenburg, Sweden
paula.wahlgren@chalmers.se

SUMMARY

This extended summary is a part of a more extensive summary (technote to be published) that compiles a number of AIVC publications that deal with ventilation and health in relation to moisture in air, and the development over time.

KEYWORDS

AIVC publications, moisture, iaq

1 MOISTURE IN INDOOR AIR

AIVC has over the years had focus on air infiltration and ventilation. This is a brief review of the work, primarily within AIVC, that relate to moisture in buildings, connected to ventilation and indoor air quality.

Moisture in the air is one of the reasons for ventilating a building, as is removing contaminants and odours, and maintaining desired temperature and air movement (Parfitt, 1985). Liddament (1996) describes that moisture is often the dominant pollutant in dwellings, generated by occupants and occupant activities, such as cooking and washing. Since there are major health issues related to high moisture levels in buildings, moisture is an important aspect to consider in the design of buildings. In the history of AIVC publications and conference papers, moisture was discussed in combination with pollutants that influence the need for ventilation. In the 1980's moisture problems appeared in relation to the effects of weather-stripping actions and inadequate energy saving measures which resulted in thermal bridges, air gaps, increased humidity indoors and various types of moisture damage.

These problems have been discussed in several AIVC conference publications. Technical Note 26 (1989) summarized the findings of Annex IX about pollutant sources, effects and control of indoor pollutants, in order to define ventilation rates that meet the requirements of energy use as well as the demands of an adequate indoor environment. One of the seven pollutants discussed in the publication was indoor humidity, in relation to condensation problems and mould growth. Apart from the presence and activities of occupants as the main source of water vapour production, three other sources were mentioned: construction moisture, ground water and seasonal storage of water vapour. The incidence of mould growth was related to the relative humidity in a room, with 70% as a limiting value below which the incidence was found to be small. Ventilation was defined a necessary but not a sufficient method to maintain relative humidities below this value, the level of heating and thermal

insulation being equally important. In a later technote, Liddament (2001) provides statistics on moisture production from Annex 27.

Technical note 20 (1987) reports on a workshop in New Zealand addressing the specific problem of moisture accumulation in the building envelope as a result of air leakage. The publication showed that moisture control in light weight building envelopes is predominantly related to air movements, often in small amounts, and not to water vapour diffusion controlled by vapour barriers as was the general understanding in construction practice at the time. The understanding of the consequences of airborne moisture transfer led to recommendations to design ventilation systems that create a slight underpressure in dwellings in cold climates to prevent indoor water vapour from penetrating and condensing in the building fabric (Liddament 1996).

Currently, the moisture itself should not be considered a pollutant, but too high exposure to moisture can initiate processes that can lead to elevated exposure levels (Borsboom et al., 2016). Most building materials subjected to high moisture levels are affected by this. In case of wood based material, there is risk of mould growth, fungal growth, hydrolysis of resin in particle boards and plywood. High moisture levels are also favourable for some bacteria and viruses, and mites. It should also be mentioned that low moisture levels also have drawbacks. These include growth of some other bacteria and viruses, of respiratory infections, and ozone production. Low moisture levels can result in dimensional changes of wooden buildings with a resulting decrease in airtightness. Cold attic constructions are particularly sensitive to moisture convection and a large amount of cold attic have mould growth.

A valuable source of information with regards to ventilation and humidity is the guidebook by Liddament (1996), and with regards to health and humidity Technical note 68 by Borsboom et al. (2016), is recommended. Additional information on moisture in indoor air will be published in a new technote during 2019.

2 ACKNOWLEDGEMENTS

The compilation of AIVC work on moisture in indoor air has been performed by Paula Wahlgren and Arnold Janssens in preparation for the 40th AIVC conference and as a part of a new AIVC technote.

3 REFERENCES

AIVC. (1987). *TN 20: Airborne Moisture Transfer: New Zealand Workshop Proceedings and Bibliographic Review.*

Borsboom, W., de Gids, W., Logue, J., Sherman, M., & Wargocki, P. (2016). *TN 68: Residential Ventilation and Health.* AIVC.

Parfitt, Y. (1985). *TN 17: Ventilation Strategy - A Selected Bibliography.* AIVC.

Liddament, M. (1996). *GV: A Guide to Energy Efficient Ventilation.* AIVC.

Liddament, M. (2001). *TN 53: Occupant Impact on Ventilation.* AIVC.

Trepte, L., & Haberda, F. (1989). *TN 26: Minimum Ventilation Rates and Measures for Controlling Indoor Air Quality IEA Annex IX.* AIVC.

Issues on humidity environment and health problem

Hiroshi Yoshino*[1], and Kenichi Hasegawa[2]

1 Emeritus Professor, Tohoku University
Kasuga-machi Fine Bldg. 4F, Kasuga-machi, Aoba, Sendai,Japan
** yoshino@sabine.pln.archi.tohoku.ac.jp*

2 Akita Prefectural University
84-4 Ebinokuchi, Yurihonjo, AKita, Japan

ABSTRACT

Japan is characterized by high humidity in summer and low humidity in winter. Therefore, summer is in a climatic condition where mold is easy to grow, and in fact, mold damage is occurring. Due to improvement of the thermal insulation and airtightness of houses, the temperature in the room is maintained high even in winter, and mold damage occurs. We will introduce the research we have conducted regarding humidity environment and health problems, and discuss future subjects. The outline is as follows.

1. The results of long-term measurements on the temperature and humidity environment of houses in regions with different climatic conditions are shown, and it is stated that the humidity environment is significantly different in each region and house. In addition, the mold index was used to investigate the possibility of mold generation.
2. A survey was conducted on approximately 5,000 homes nationwide regarding the relationship between dampness and children's health. Condensation and mold often occur on the surfaces of the outer walls, window glass, and windows frames. It was found that the higher the dampness index based on condensation and mold occurrence, the more the prevalence of allergic diseases such as allergic rhinitis and atopic rhinitis.
3. A survey on relationship of low humidity with dryness and health effects in winter was conducted on approximately 4,000 houses nationwide. As a result, the rate of feeling dryness was about 60%, and the rate of responding that health was affected was 23% of the whole. However, there are occupants that feel dryness even in houses with high relative humidity, and it is found that the feeling of dryness is not always due to low humidity. It is also found that the effect of air pollution cannot be ignored.
4. From the above, it is necessary to improve the thermal insulation performance to solve the problem of dampness, and controls of humidity and air quality are important to prevent a sense of dryness. Also it is noted that the factors affecting the feeling dry need to be further studied.

KEYWORDS

Humidity, Dry, Indoor, Environment, Health

1 INTRODUCTION

The climatic conditions of Japan are characterized by high temperature and humidity in summer, but low temperature and humidity in winter. Therefore, summer has a situation where mold is easy to grow, and the issue of mold damage is commonly found in many houses. In addition, due to the influence of thermal insulation and airtightness in modern building design, the room temperature in winter is often maintained at a relatively high level, and this also causes the mold damage occurred even in winter. As a result, health problems caused by mold are a big concern throughout the year. On the other hand, the problem of being too dry in a well-insulated house has been pointed out.

In this paper, based on the research conducted by the current authors regarding humidity environment and health problems, the actual indoor environmental conditions, especially temperature and humidity, of houses in various parts of Japan are firstly described. The results of a large-scale questionnaire survey on the relationship between indoor humidity and children's allergic diseases will be given. In addition, the relationship between dryness and health/comfort will be presented, and finally the problems of humidity environment and health will be summarized as well as future research directions will be described.

2 INDOOR TEMPERATURE/HUMIDITY ENVIRONMENTS OF HOUSES IN JAPAN

2.1 Outline of the survey

The Research Committee established in the Architectural Institute of Japan had conducted a survey on the energy consumption and the indoor thermal environment of the houses from 2002 to 2004. The targets were 80 houses in 6 areas: Hokkaido, Tohoku, Hokuriku, Kansai, Kinki, and Kyushu. Indoor temperature and humidity were measured using a temperature and humidity logger. The measurement interval was 15 minutes, except for the case of Hokkaido where 10 minutes measuring interval were adopted. The authors had analyzed the temperature and humidity, which were measured throughout the year of 2003, of the living room in 51 detached houses and 21 apartments. Two journal papers have been published based on the results of this database. In this chapter, some of the important results will be outlined.

2.2 Annual frequency distribution of indoor relative humidity

Figure 1 shows the frequency distribution of annual relative humidity of the living room in six houses, which have typical characteristics. The relative humidity of detached houses Tohoku D01 and Hokuriku D06 are distributed in a wide range with almost constant frequency. For the Hokuriku apartment (i.e. Hokuriku D03), two peaks are found at 40-45% and 65-70%, indicating that summer is humid and winter is dry. In cases of Hokkaido A03and Kanto D07; although the width of distribution is different, the range shows a bell-shaped trend. In Hokkaido A03, the distribution is rather narrow with 50-70%, because the unvented space heater is used in winter and hence the absolute humidity is high. In the case of Kansai D04, the relative humidity is found over 60%, because the room temperature in winter is low with less than 15 °C, consequently the relative humidity is also high even in winter.

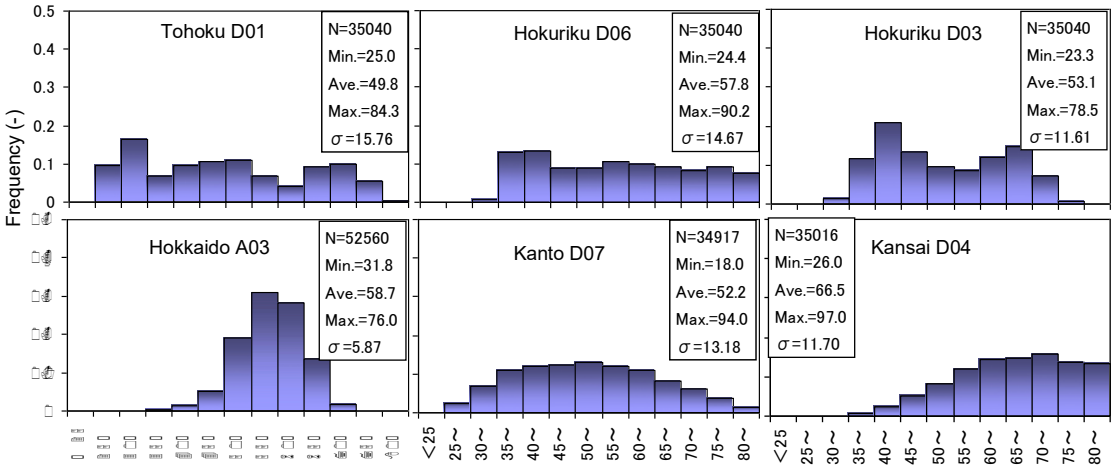

Figure 1: Frequency distribution of the annual relative humidity of 6 houses

2.3 Characteristics of relative humidity in winter

(1) Time variations of temperature and humidity

Figure 2 shows the time variations of temperature and humidity over 5 consecutive days in winter, with 2 houses of low relative humidity (Tohoku D01 and Kanto D07) and 2 houses of high relative humidity (Kanto A02 and Kansai D04). The temperature of Tohoku D01 is constantly around 24 °C by continuous operation of space heating. Reflecting the continuous heating, the relative humidity is almost below 30%. The temperature of houses in Hokkaido, which is not shown in the figures, is almost constant due to continuous heating operation. With the exception of the houses in Hokkaido and Tohoku D01, space heating is commonly adopted and operated intermittently, therefore the temperature varies significantly. In particular, when heating is not operated at night, the room temperature deceases and then the relative humidity increases. Although the temperature changes due to intermittent heating operation in Kanto D07, the absolute humidity is very low and the room air is dry. The relative humidity is high in both the Kansai D04 and the Kanto A02, in which the temperature of the former case is observed low and the absolute humidity of the latter case is found high.

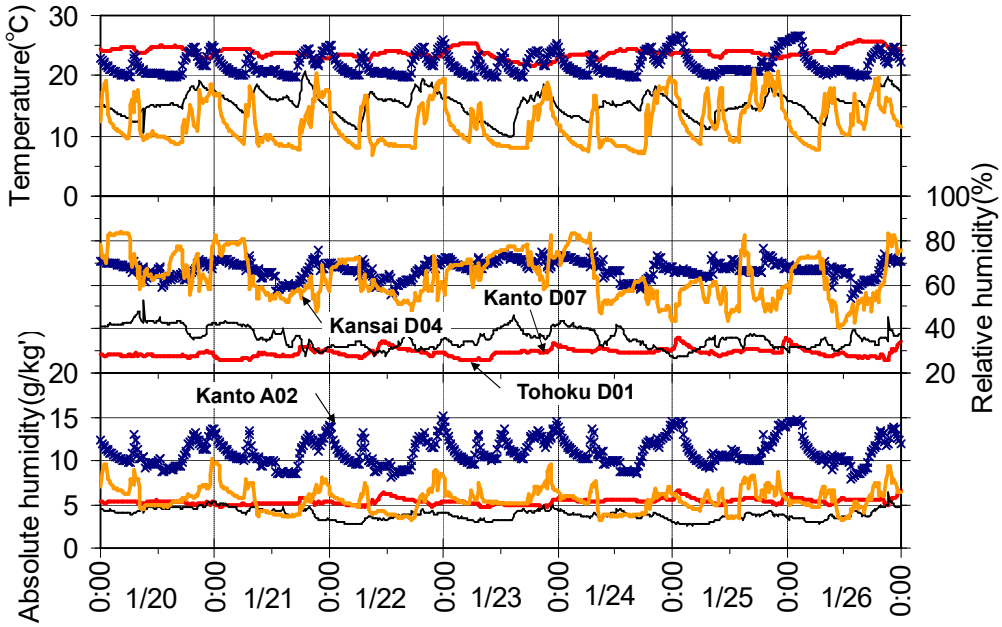

Figure 2: Time variations of indoor environment of four houses in winter

(2) Characteristics of overall relative humidity in January and February

The average relative humidity is less than 40% and the room air is dry, in 50% of the investigated houses in Hokkaido, and nearly 40% of the investigated houses in Tohoku and Hokuriku. Elsewhere, the average values of most of the houses are over 40% and some of them are more than 60%. In houses of Hokkaido, the fluctuation range of relative humidity is small because of the continuous heating operation. In the houses of other areas, the rooms are in general intermittently heated and the range of fluctuation is large. Therefore, there are hours when the relative humidity exceeded 80%.

2.4 Characteristics of relative humidity in winter

(1) Time variations of temperature and humidity

Figure 3 illustrates the time variations of temperature and humidity over a 5-day period in summer, with 2 houses of low relative humidity (Kansai A01 and Kansai D02) and 2 houses of high relative humidity (Kyushu D05 and Hokuriku D06). In each of the house, the room temperature rises during the daytime, and there are some cases where the room temperature exceeds 30 °C. In the cases of Kansai A01 and Kansai D02, the absolute humidity drops sharply during nighttime because these houses are air-conditioned at those hours. The absolute humidity is high and the temperature is low in Hokuriku D06 and Kyushu D05, among which some houses have high relative humidity exceeded 80%.

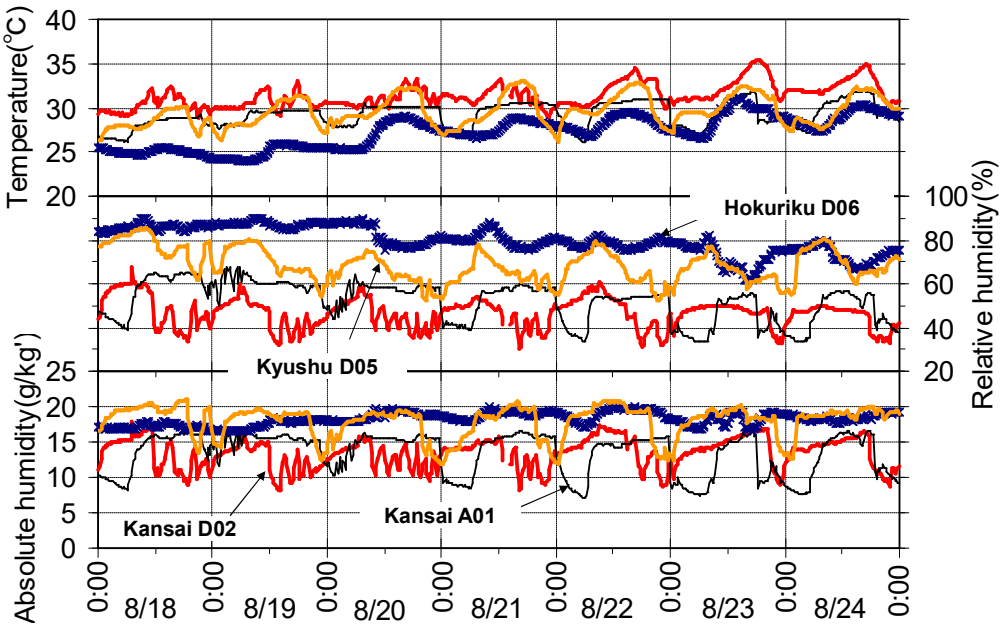

Figure 3: Time variations of indoor environment of four houses in summer

(2) Characteristics of relative humidity in July and August

Except in Hokkaido where the outside air humidity is low, the average relative humidity in most of the houses is distributed between 60-80%, and the room is humid. About 25% of the total houses, except Hokkaido, space cooling is often used and there are cases where the absolute humidity of the room is lower than that of the outside air.

2.5 Prediction of indoor mold contamination

The mold index was used to assess the possibility of mold contamination. The mold index is an index quantitatively representing the degree of growth of mold mycelium per week at a certain temperature and relative humidity, and if it is 3.0 ru/week or more, the possibility of mold contamination becomes high.

Figure 4 shows the number of hours when the mold index is found 3.0 ru/week or more. The bar charts are arranged from the one where summer relative humidity is high, and the number of days with missing data is indicated in parentheses. The houses in Hokkaido have a maximum of 328 hours, while some others houses, especially half of houses in Kansai and Kyushu, have more than 1000 hours. Questionnaire survey was conducted for the houses in the Tohoku region, where the number of hours with the mold index is more than 3.0 ru/week. As a result, it was confirmed that molds were visible in the living rooms of D06, A01 and A03, but mold

was not visible in the living room of D08 (with many houseplants), and in D01 and D03 the mold was visible in the rooms other than the living room.

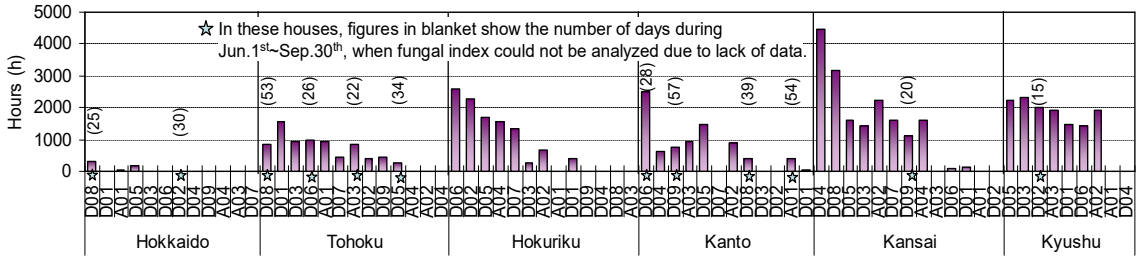

Figure 4: Cumulative hours when fungal index exceeded 3ru/week in each house

2.6 Summary

With regard to the indoor humidity environment in Japanese homes, the relative humidity is generally 60% or more in summer, which creates an environment prone to mold. However, in houses where cooling is frequently operated, the relative humidity is rather low with less than 50%.

On the other hand, in winter, the humidity environment varies between houses greatly and depends on the type of space heating equipment, the way of heating operation, the setting temperature, etc. In the houses of Hokkaido where the temperature is maintained high by space heating in all rooms, the humidity is as low as 30% or less. Hence, in the houses of other areas, the relative humidity is over 60% when the room temperature is low due to the intermittent heating operation. Especially, when the room is not heated at night, the relative humidity exceeds 80%,

Although we did not mention the situation in the rooms other than the living room, it is clear, from the database, that in most of the houses, except Hokkaido, the bedrooms are not heated enough and the relative humidity is high because the temperature is low.

3 SURVEY ON THE RELATIONSHIP BETWEEN DAMPNESS AND CHILDREN'S HEALTH

3.1 Outline of the survey

The authors conducted a questionnaire survey for elementary school students in the fourth and fifth grades from 2007 to 2010, with the aim of clarifying the relationship between dampness and children's health problems, especially on allergic diseases. The survey was divided into two stages; the first stage was to investigate the presence and type of allergic diseases. Questions for allergic diseases were answered by parents based on the doctor's diagnosis. For the method of survey, we asked prefectural educational authorities throughout the country to randomly select elementary schools situated in the urban areas and the suburbs where the prefectural office was located. The number of distributions was 30,332, the number of responses was 8,336, which means the recovery rate was about 27.5%. As the second step, the present authors examined the relationship between allergic symptoms and the living environment for the houses selected from the first survey in which occupants agreed to cooperate detailed investigation. The number of distributions was 2,865 and the number of responses was 1846, that means the recovery rate was 64.4%. The results of this survey were summarized and reported in a journal paper. This chapter abstracts and introduces the key findings from the journal paper.

3.2 Actual situation about allergic diseases of children in the first stage of the survey

Allergic diseases are classified into asthma, allergic conjunctivitis, allergic rhinitis, allergic dermatitis, digestive tract allergy and others, in this research. The ratio of the children with any allergies accounted for 49.9% overall, with little difference between regions. In addition, the prevalence rate of boys is higher than that of girls in any area, with 55.3% boys and 44.8% girls overall.

It was revealed that, among the abovementioned allergic diseases, the prevalence of allergic rhinitis was the highest in all regions, following with asthma and allergic dermatitis. The prevalence of allergic rhinitis was found as high as 37.2% in Tokai, around 30% in other regions, and 33.3% overall. There were no regional differences in other diseases.

The causes of allergic diseases are generally attributed to pollen, mites and house dust. The results indicated that pollen was a cause for 25.1% of children in all regions, and it was observed high with 36.4% in Tokai. In terms of regional characteristics, the proportion of house dust, ticks and molds which were listed as the causes, was about 3% to 10% higher in the eastern part of Japan than in the western portion of Japan. Due to the differences in housing performance and thermal environment, the adverse effects of microbes on children's health had become serious in the northern regions where the houses were well insulation.

Figure 5 presents the relationship between the different allergic diseases and their causes. Ticks and house dust were found in high rate as the cause of asthma. And pollen (followed with house dust) was mostly responsible for the cause of allergic rhinitis and allergic conjunctivitis, as high as 60% or more. House dust was indicated as the main cause for atopic dermatitis, in more than 50%.

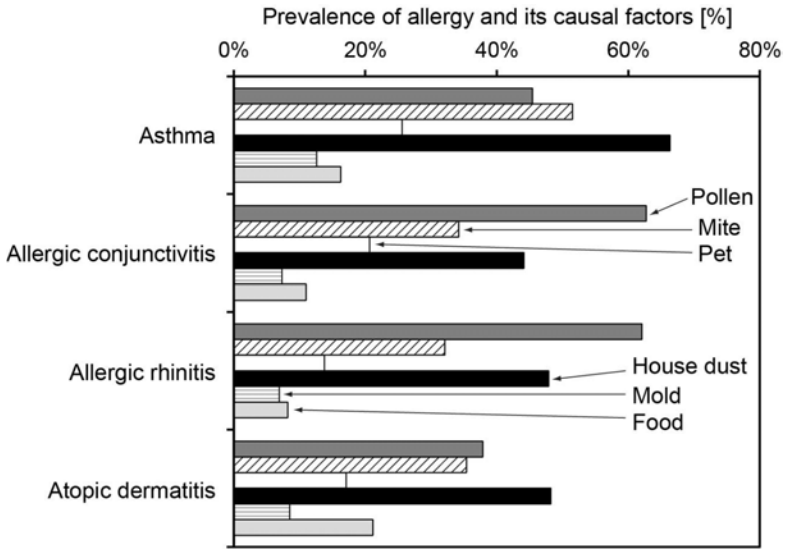

Figure 5: Causes of various allergic symptoms

3.3 Relationship between residential environment and allergic symptoms in the second stage of the survey

According to the results obtained from the second stage of the questionnaire survey, the percentage of children with allergic symptoms was 61.2%. The ratio of pollen symptom was over 49.0% in Hokkaido and over 50% in all the investigated regions. Especially in Kanto, the ratio showed high with 62.2%. The prevalence ratios of wheezing, airways hyperresponsiveness, asthma-like symptoms (severe) and asthma-like symptoms (not severe) were 5.5%, 12.5%, 5.4% and 11.9%, respectively.

Regarding the indoor environment related to humidity, about 10% and 20% of respondents stated that condensation did not occur in Hokkaido and other areas, respectively. This implied that condensation occurred in many houses, and it was found especially on windows and sashes. The ratio of houses with mold was more than 50%, and mold also appeared often on windows and sashes.

According to the analysis of the relationship between the indoor environment related to moisture and the allergic symptoms, there revealed a significant association between prevalence of all symptoms and the occurrence of mold on the internal surfaces other than window sash in the living room and bedroom. In particular, for airway hyperresponsiveness and asthma-like symptoms Adjusted Odds Ratio (AOR) were 3.05 ($p < 0.01$) and 3.76 ($p < 0.01$), respectively, in comparison to the case without mold. As for the relationship between each symptom and the Dampness Index, which indicates the degree of dampness (zero when there is no condensation, no mold, and no water stains; three when there are three phenomena), AOR is significantly greater than 1.0 when the Dampness Index is 3 for all symptoms except wheezing.

In order to find out which factors have strong influence on the occurrence of allergic symptoms to children, a further analysis was necessary. Thus, a multivariate model was constructed using the living environmental factors including the Dampness Index as explanatory variables. From the analysis of factors related to airway hyperresponsiveness and asthma-like symptoms, the findings are as follows; 1) In terms of surrounding environment, industrial areas increase the risk of symptoms, 2) The use of humidifiers and/or aquariums affects allergic symptoms, 3) The installation of a television and/or personal computer affects the symptoms, 4) The risk of occurrence increases when the Dampness Index is at 3 ru/week.

3.4 Summary

The prevalence of children allergic diseases in children in Japan reaches about 50%. Considering the bias that respondents are parents of children with allergic disease, it is a large figure. Allergic diseases include conjunctivitis, rhinitis and dermatitis, which are caused by pollen, mite, house dust and so on. According to the correlation analysis between the Dampness Index and the allergic disease, the relationship between the Dampness Index and the prevalence rate of allergic diseases, except wheezing, was clearly indicated.

In addition, according to the multivariate analysis including various environmental factors (without considering the Dampness Index), living in an industrial area, use of a humidifier and/or a aquariums, installation of a television and/or a personal computer are the influencing factors that enhance symptoms. In terms of indoor environment, it can be concluded that measures to prevent high humidity and measures against condensation are important.

The present authors conducted a similar nationwide questionnaire survey on January 2015 in the other opportunity, and analyzed the relationship between dampness and allergic symptoms based on 3,262 reliable responses. Dampness index was rated from 0 to 24 based on condensation, mold growth and mold odor in the living room, bedroom, bathroom, washroom and kitchen in this study. Figure 6 shows the distribution of the dampness and the rate of reported allergic symptoms. From this figure, it is clearly indicated that the larger the dampness index is, the greater the proportion of reported symptoms.

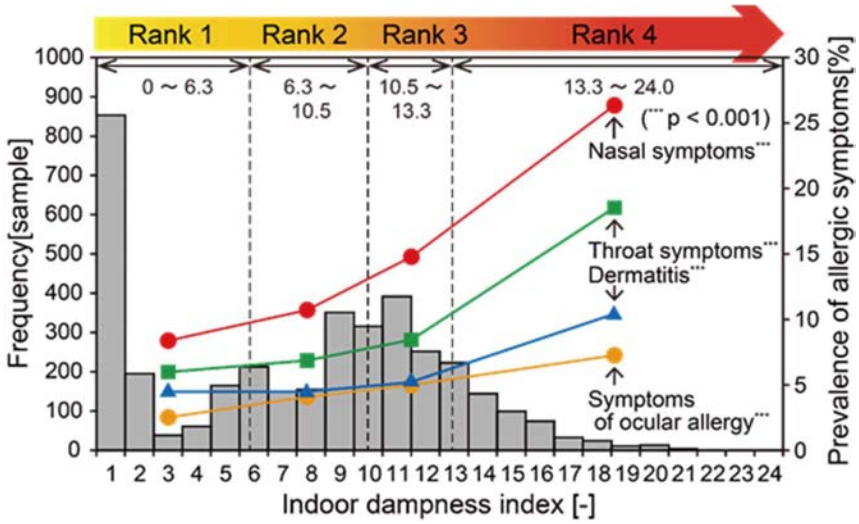

Figure 6: Distribution of dampness index and prevalence of allergic symptoms

4 SURVEY ON THE SENSE OF DRYNESS AND THE HEALTH EFFECTS OF DRYNESS

4.1 Outline of the survey

We conducted a nationwide questionnaire survey and measurement survey, looking into the actual condition of dryness in the houses and the health effect by dryness. The questionnaire survey was conducted via Internet in January 2011 for households living within 10 years. The number of valid responses was 3,879 and the response rate was 83.3%. The contents of the survey include residents' characteristics and types, as well as their operation style of the heating equipment, with/without the presence or absence of ventilation equipment and its way of operation, indoor environmental problems in winter, and so on. The measurement of indoor temperature and humidity was conducted to the households who suffered from health problems due to dryness and damage to buildings. The number of houses for the measurement was 102. The survey period was from February to March 2011. The results were reported in a journal paper. In this chapter, the main conclusions will be summarized.

4.2 Results of questionnaire survey

According to the questionnaire survey, the percentage of the households who felt dryness was over 50% in all regions of Japan, and it was over 70% in Hokkaido and South Kanto. Overall, the percentage was found higher in the northern territory. In addition, the percentage of households who felt dryness and pointed out a health problem was 30.2% in Hokkaido, and 25-27% in Tohoku, South Kanto and Shikoku. Percentage of households feeling dryness as well as having problems with comfort or damage to buildings ranged from 9% to 19% depending on location.

Figure 7 shows the analysed results of whether occupants felt dryness or whether they felt health problems, and other specific health effects. The percentage of occupants who actually felt dryness was 61.1%, and 37.1% of occupants thought that the dryness was a problem. Furthermore, the percentage of occupants suffering from health problem was 22.8% of the total. Health problems included: easy to catch cold (12.3%), sore throat (9.0%), allergy worsened (2.4%). The percentages of dry skin (16.6%) and dry throat (15.8%) were relatively high. On

the other hand, the percentages of occupants citing the loss of comfort as a problem and the damage to buildings were 17.4% and 2.4% of the total, respectively.
The analysis of the relationship between the feeling dryness and the residential environment factors indicated that the longer the operation time of space heating and ventilation, the higher the rate of reporting feeling dryness and health problems.
Furthermore, according to the results of detailed statistical analysis, the case that occupants have a health problem and feel dry only at the upper airway, is associated with a long heating time. The effect on the upper airway is likely to be related to low humidity, because a longer heating time creates a dry environment. On the other hand, it was found that occupants had odor perception when they felt dry on all parts of the upper respiratory tract, eyes and skin; these are the symptoms affecting health problems.

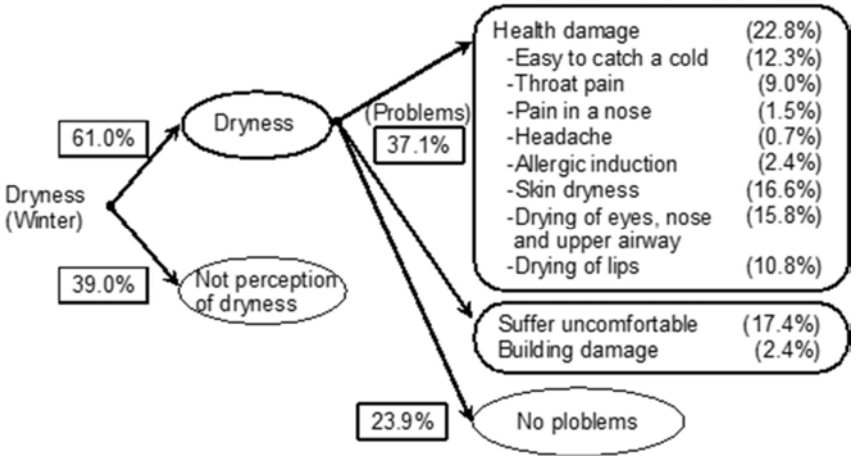

Figure 7: Ratio of dryness perception and claims of health problems

4.3 Analysis of dryness and related factors based on actual measurements

It was found that there was not clear correlation between the declaration of dryness and environmental conditions such as temperature, relative humidity, and absolute humidity. For example, in houses where occupants replied "slightly dry" or “dry” or "very dry", the relative humidity was largely distributed in a range below 50%, and the absolute humidity was also distributed in a range less than 7 g/kg. No relationship was found with the concentration of chemical substances.

4.4 Summary

The proportion of occupants who felt dryness was 61.1%, and the proportion that felt dryness was a problem was 37.1%. In addition, the proportion of occupants who had health problems due to dryness was 22.8% of the total, with susceptible to colds (12.3%), dry skin (16.6%), and dry throat (15.8%) reported at a relatively high rate. According to the measurement survey, the relationship between the feeling of dryness and the relative humidity is not clear, and even in a house with high relative humidity, occupants also feel dryness. Moreover, the relationship between the feeling of dryness and the concentration of chemical substance was also not clear. This is also concluded by Wolkoff (2018) that the cause of dryness is not yet elucidated.

5 CONCLUSIONS AND FUTURE DIRECTIONS

Generally, the climatic conditions of Japan are hot with high temperature and humidity in summer, low temperature and dryness in winter. But the conditions are quite different from the north to the south because it is a long island country. Especially in Hokkaido, the winter is severe and summer is relatively low humidity. Looking at the heating conditions alone, while all rooms are heated all day long in Hokkaido, many houses in other regions are intermittently heated and operated mainly in the living room. Therefore, the characteristics of the indoor temperature and humidity vary greatly depending on the heating and cooling conditions, and also depending on the location.

In addition, there is a large variation in dampness among houses. In houses where dampness is evaluated as a problem, it is found that dampness may be related to allergic diseases to children, especially airway hyperresponsiveness and asthma-like symptoms.

Therefore, it is necessary to keep an environment away from high relative humidity. In order to do so, the following measures can be considered;

1) To prevent the decrease in surface temperature of inside wall by installing thermal insulation
2) To equalize spatial and temporal distribution of indoor temperature during the operation of heating
3) Appropriate use of humidity control materials (further research is needed on how to install them)
4) Proper installation of the dehumidifier (further research is needed on how to install it) On the other hand, 61% of occupants feel about dryness in the winter, and 25-30% of the occupants describe that dryness is a health problem. A clear relationship between dryness and relative humidity has not been obtained, and the cause of dryness must be studied further.

6 REFERENCES

Zhang, H., Yoshino, H., Murakami, S., Bogaki, K., Tanaka, T., Hayama, H., Akabayashi, S., Inoue, T., Iio, A., Hokoi, S., Ozaki, A., Abe, K. (2007). Investigation of Actual Humidity Conditions in Houses and Evaluation of Indoor Environment by Fungal Index, Proceedings of IAQVEC 2007.

Zhang, H., Yoshino, H., Murakami, S., Bogaki, K., Tanaka., Akabayashi, Abe, K. (2009). Analysis of Indoor Humidity Environment in Nationally Residential Houses of Japan, AIJ Journal of Technology and Design, Vol.15 (30), 453-257.

Hasegawa, K., Yoshino, H., Mitamura, T. (2019). Investigation of Feeling Dryness and Its Adverse Health Effect in Residential Buildings of Japan, Journal of Environmental Engineering, Vol.84 (760), 587-596.

Wolkoff, P. (2018). The mystery of dry indoor air – An overview, Environmental International, 121, 1058-1065.

Fungal growth on timber frame houses

Michiel Vanpachtenbeke[*1,2], Liselotte De Ligne[2], Jan Van den Bulcke[2], Jelle Langmans[3], Joris Van Acker[2] and Staf Roels[1]

1 KU Leuven, Department of Civil Engineering, Building Physics Section
Kasteelpark Arenberg 40 – box 2447
BE-3001 Heverlee, Belgium
**Corresponding author:*
michiel.vanpachtenbeke@kuleuven.be

2 UGent, Department of Environment, Laboratory of Wood Technology (UGent-Woodlab)
Coupure Links 653
BE-9000 Ghent, Belgium
**Corresponding author:*
michiel.vanpachtenbeke@ugent.be

3 Bauphi bvba
Stropkaai 55
BE-9000 Ghent, Belgium

KEYWORDS

Onset and progress of fungal growth, timber frame constructions, fibre saturation point

1 EXPERIMENTAL RESEARCH ON FUNGAL GROWTH

Due to the increasingly stringent energy efficiency requirements, timber frame houses are becoming more and more popular across Europe. Since wood is an organic material, susceptible to mould growth and wood rot, an effective moisture control strategy is required to keep the moisture levels inside the building components to an acceptable level. Moisture related problems may affect the health of the inhabitants, or even jeopardize the building's structural integrity. To determine the acceptable moisture level inside a construction, a clear view on the development of fungal growth is essential.

Therefore, tests have been described in literature examining the critical moisture contents for decay. In a so-called pile test, executed by different researchers (a. o. Brischke & Meyer-Veltrup 2015; Stienen et al. 2014), a moisture gradient within a pile of small wood samples is created. After inoculation and an incubation period of 3-4 months, the relationship between moisture content and fungal growth is assessed. Main disadvantage of this test, however, is that moisture content and fungal attack is only evaluated at the end of the experiment, while fungal growth is a dynamic process. Furthermore, since this test includes a malt agar medium, results only apply in case a moisture and nutrition source is nearby, and RH is high.
Consequently, different researchers conducted experimental research without an external moisture and nutrition source (Brischke et al. 2017; Saito et al. 2012; Viitanen 1997). These tests amount to inoculate small wood samples with fungal mycelium or feeder blocks (= previously infested wooden specimens). The samples were then incubated at different levels of RH. These tests concluded that, without an external moisture source, progress of fungal growth can only occur at very high levels of relative humidity. However, the tests also resulted in contradictory findings whether progress of fungal growth can occur below fibre saturation point (FSP; point when there is a maximum of hygroscopic bound water in the wood cell walls, but no free liquid water in the cell lumen).
All laboratory experiments described above take advantage of sterile conditions and bring only the wood-degrading test fungus into the set-up by inoculation. In reality, however, fungal spores first need to colonize the wooden substrate. A significant time lag may occur between **onset**

and **progress** of fungal growth. Moreover, higher moisture levels may be required for the onset compared to the progress of fungal growth. The FSP might be a critical level in this regard. Furthermore, next to the exposure conditions, also design details may influence the service life of a timber construction. Hence, next to experiments without inoculation, experiments based on realistic conditions occurring during the specific end use of a timber product should be performed as well. So-called field tests are described in several European standards (a.o. CEN 2014). However, in these tests, wood samples are exposed to Use Class (UC) 3-4 (CEN 2013), whereas wood inside a timber frame construction is typically exposed to UC 1-3 conditions, which are less extreme. Tests examining the onset of fungal growth and the risk of fungal attack for a timber frame construction exposed to UC 1-3 are still lacking.

The present study aims at a contribution to the understanding of the influence of wood moisture content on the onset and progress of fungal growth. Based on the information that is still lacking in international literature, different specific experiments are executed at Woodlab-UGent and the Building Physics Section of KU Leuven. In a first experiment, the goal is to study the relation between moisture content and **progress** of fungal growth throughout the degradation process and in different climatic conditions, when an external moisture source is nearby. In a second experiment, the determination of the minimal moisture threshold and required exposure time for the **onset** of fungal growth is envisaged. In a last experiment, the risk of fungal growth in a timber frame wall exposed to UC 1-3 is studied.

2 CONCLUSION

The first results from the experiments conducted in this work show that, as long as no liquid water source is available, timber will only suffer from mould growth. The reliability of current mould growth prediction models depends on the considered wood species. Further, with the current set-up, progress of decay below FSP was not observed. Nevertheless, the relative humidity of the surrounding air clearly had an impact on the process. Further tests with an adjusted set-up should be conducted to further study the relation between moisture content and progress of fungal growth.

3 REFERENCES

Brischke, C. & Meyer-Veltrup, L., 2015. Modelling timber decay caused by brown rot fungi. *Materials and Structures*.

Brischke, C., Soetbeer, A. & Meyer-Veltrup, L., 2017. The minimum moisture threshold for wood decay by basidiomycetes revisited. A review and modified pile experiments with Norway spruce and European beech decayed by Coniophora puteana and Trametes versicolor. *Holzforschung*, 71(11), pp.893–903.

CEN, 2014. EN 252: Field test method for determining the relative protective effectiveness of a wood preservative in ground contact.

CEN, 2013. EN 335: Durability of wood and wood-based products - Use classes: definitions, application to solid wood and wood-based products.

Saito, H., Fukuda, K. & Sawachi, T., 2012. Integration model of hygrothermal analysis with decay process for durability assessment of building envelopes. *Building Simulation*, 5(4), pp.315–324.

Stienen, T., Schmidt, O. & Huckfeldt, T., 2014. Wood decay by indoor basidiomycetes at different moisture and temperature. *Holzforschung*, 68(1), pp.9–15.

Viitanen, H., 1997. Modelling the Time Factor in the Development of Brown Rot Decay in Pine and Spruce Sapwood - The Effect of Critical Humidity and Temperature Conditions. *Holzforschung*, 51, pp.99–106.

Big humidity data from smart ventilation systems

Loes Lokere[1], Arnold Janssens[1], Steven Vandekerckhove[2], Ivan Pollet[2], Marc Delghust[1], Klaas De Jonge[1] and Jelle Laverge[*1]

1 Building Physics group, Ghent University
Jozef Plateaustraat 22
9000 Gent, Belgium
**Corresponding author: jelle.laverge@ugent.be*

2 Renson Ventilation NV
Maalbeekstraat 10
Waregem, Belgium

SUMMARY

A smart ventilation system is generally equipped with a range of sensors. The data – or data derived from it - collected by these sensors can be used by both building owners, occupants and managers. A new generation of IoT enabled residential ventilation systems allows collecting and analysing this data at scale to get a better view on typical IAQ conditions in dwellings. In this paper, the results from such an analysis on the first 900 installed devices of a new model with respect to moisture in relatively new Belgian dwellings is presented.

KEYWORDS

Smart Ventilation, Moisture, Humidity, Residential, Big Data

1 CASE STUDY

The case study is based on the initial roll-out of new smart ventilation model by Renson, Healthbox 3.0, in Belgium. It is a centralised exhaust-only DCV system, a demand-controlled system with mechanical extraction of polluted air and natural supply of fresh air. Natural supply of the fresh air occurs by window mounted trickle vents in dry rooms. At the end of each extraction duct, sensors measure several parameters (temperature, humidity, CO2 and VOC). The ventilation rate is adjusted based on the measured air quality for each roomThe basic configuration of the unit can connect up to seven rooms and can be extended to eleven rooms via the use of up to two valve collectors.
The (anonimised) monitoring data related to moisture of 900 of the first installed units was analysed and is presented below. The sample mostly includes recent (EPB compliant) construction.

2 RESULTS

From the observed temperature and humidity conditions, we can conclude that the systems, sized according to the Belgian standard NBN D 50-001 effectively protects the indoor environment against excessive moisture levels, as assessed by the mould growth risk in accordance with the VTT isopleth model proposed by Hukka & Viitanen (1999). The results for bathrooms and laundry rooms are shown in figure 1. In total, only 1.15%, 0.63%, 1.14%, 0.52%, 2.39% of the processed datapoints were above the risk threshold for bedrooms, kitchens, bathrooms, laundry rooms and toilets respectively.

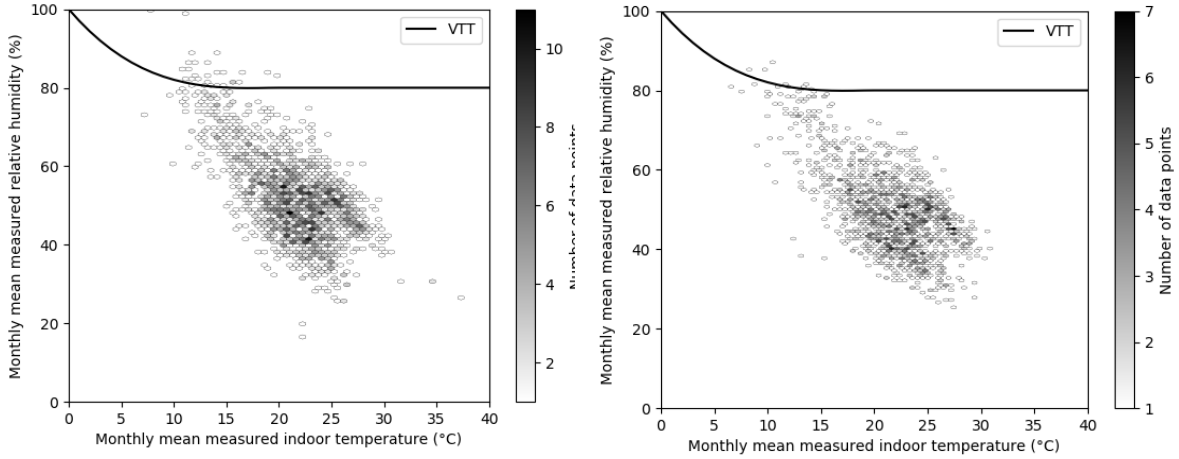

Figure 1: Mould growth risk based on the Hukka and Viitanen isopleth in the bathrooms (left) and laundry rooms (right) in the case study sample

Based on the available data and the weather data for Brussels provided by the Royal Meteorological Institute, the moisture load with respect to the indoor climate classes as defined by Hens (1992) were assessed. This shows that the dependency of moisture loads on outdoor temperature has decreased over the last 25 years.

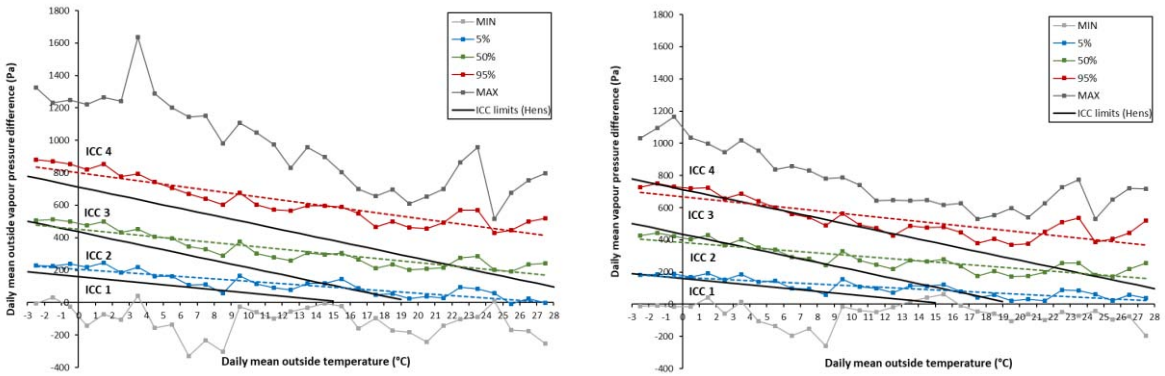

Figure 2: Moisture load based on the Hens indoor climate classes in the bathrooms (left) and laundry rooms (right) in the case study sample

3 REFERENCES

A. Hukka and H. A. Viitanen (1999) "*A mathematical model of mould growth on wooden material*," Wood Science and Technology, vol. 33, no. 6, pp. 475–485, https://doi.org/10.1007/s002260050131

Hens, S.L.C. (1992) Indoor Climate Classes, Intern Rapport IEA-Annex 24 T2-B_92/02 International Energy Agency; Heat, Air and Moisture Transfer through new and retrofitted Insulated Envelope parts (HAMTIE).

ByggaF - A Method to Include Moisture Safety in the Construction Process

Kristina Mjörnell[*1] and Thorbjörn Gustavsson[2]

1 RISE Research Institutes of Sweden
Sven Hultins Plats 5
412 58 Göteborg, Sweden
**Corresponding author: kristina.mjornell@ri.se*
Presenting author: Kristina Mjörnell

2 RISE Research Institutes of Sweden
Box 857
501 15, Borås, Sweden

ABSTRACT

ByggaF is a methodology for including moisture safety in the construction process that was developed and presented in 2007. ByggaF comprises methods to secure, document and communicate moisture safety throughout the construction process, from planning to management. The methods involve a standardized way of working designed to meet the demands of society and the client's requirements for moisture safety. It contains tools and routines for all actors in the building process; building developers' requirements, moisture safety design routines, risk evaluation, moisture plans, routines for moisture rounds at the building site, routines for commissioning and moisture safety documentation. On request from the Swedish construction sector, ByggaF has been transformed into an industry standard. ByggaF was used in the first pilot projects more than ten years ago and since then it has been frequently used by the building sector in a number of Swedish construction projects. One reason for the broad implementation of ByggaF is that it is referred to in the Swedish building regulations, another is that the Swedish environmental assessment tool "Miljöbyggnad" demand for using ByggaF in order to reach "silver level" or "gold level". To this date 144 moisture experts have been trained to use ByggaF and apply the standardized way of working to assure a moisture safe building process. It is difficult to quantify the effect of using ByggaF in terms of time and cost savings since moisture damages are never accounted for when planning a project, but based on our experience, many risk constructions and shortcomings during the construction have been avoided when using ByggaF. There has also been interest in using ByggaF expressed from other countries, both by Swedish contractors working with projects abroad but also from researchers in other countries. The industry standard has been translated into English, but in order to be applied in other countries, it needs to be adjusted to country specific conditions, such as regulation and building practices. In Finland, the Swedish version of ByggaF has been adapted to Finnish regulations and used for including moisture safety in real construction projects. ByggaF has also been adapted to specific applications such as construction of prefabricated single-family houses and renovation of multifamily houses.

KEYWORDS

Moisture safety, moisture management, building process, industry standard,

1 INTRODUCTION

Working with moisture is even more important than ever. Many buildings, both new and old, suffer from moisture-related problems, with negative consequences on health, comfort and wellbeing, costs for refurbishment and lost confidence in the building sector. A recently published report from the Swedish Board of housing building and planning (Boverket 2018) points out moisture damage as the single dominant factor to the major building faults and costs. At the same time there is an increased interest in building in wood or wood-based materials, for example cross laminated timber, for environmental reasons. Wood must be handled with extra care to avoid damage caused by moisture. Building moisture-proof is also more sustainable because moisture damage is a major environmental impact, as moisture-damaged material must be demolished, discarded and replaced with new material which causes an environmental impact. In case extra drying out is needed as a result of leakage if

weather protection has not been used, this causes an environmental impact, extended time and cost in the construction project. These problems could have been avoided if moisture issues had been focused on and dealt with throughout the building process. In Sweden the authorities' requirements increases concerning moisture safety in the building process. Today all new constructions need special planning regarding moisture safety, according to the Building regulations (Boverket 2019). To fulfil the requirements regarding a moisture safe building process, it is recommended to use the ByggaF method for including moisture safety in the entire building process. For this reason, ByggaF has been widely used in construction industry. Another reason for the broad implementation of ByggaF is that the Swedish environmental assessment tool "Miljöbyggnad" demand for using ByggaF in order to reach "silver level" or "gold level" (Swedish Green Building Council 2019). There has also been interest in using ByggaF expressed from other countries, both by Swedish contractors working with projects abroad but also from researchers in other countries. In Finland, the Swedish version of ByggaF has been adapted to Finnish regulations and used for including moisture safety in real construction projects.

2 DESCRIPTION OF THE BYGGAF METOD

A method for including moisture safety in the building process has been developed. In Sweden, the method is called ByggaF which is short for "Build moisture safe". The purpose of the method is to support all actors involved to work with moisture safety activities and to document them in a structured way. The method includes several tools and aids for building developers to specify requirements for moisture safety early on in the project, and to follow up and document the measures employed by different participants.

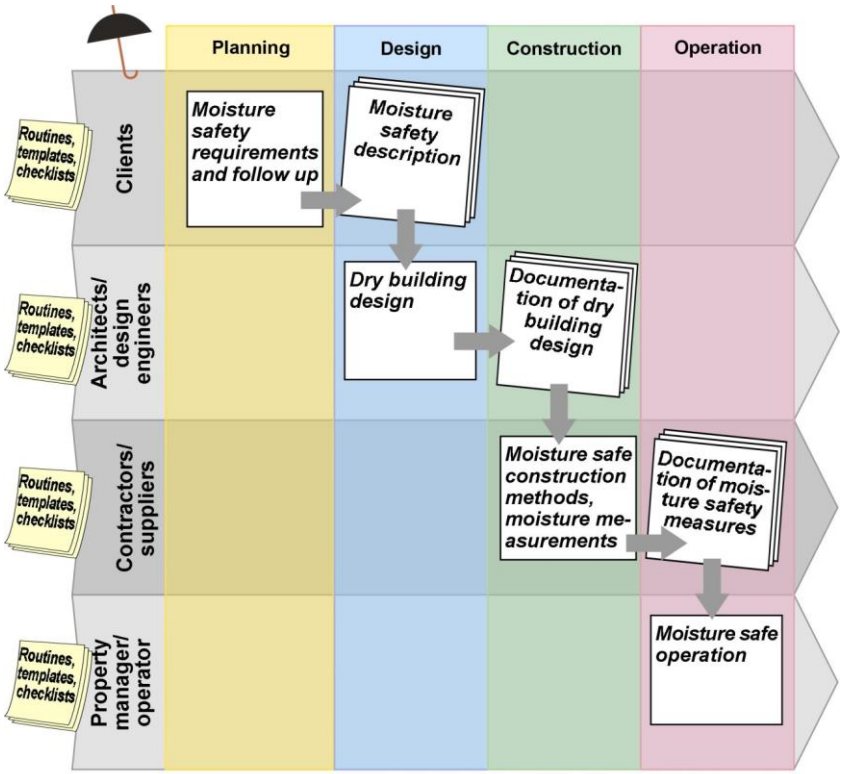

Figure 1 A schematic figure of the ByggaF method.

There are also tools for architects and design engineers, such as lists of references to literature, check lists and design examples to use for dry building design. For contractors, routines have been developed for setting up a moisture plan and moisture control during

construction. The method has been used by the building sector and applied in several construction projects both for residential, public and commercial buildings. Based on experience from these projects, the method and the tools have been evaluated and revised, (Mjörnell and Arfvidsson 2008, Mjörnell et al 2012, Mjörnell 2016, Fuktcentrum 2013).

2.1 Industry standard ByggaF

When the ByggaF method had been used for a couple of years, it was requested from the building sector to transfer it into an Industry standard. The reason was to clarify what activities and controls that should be included to ensure that ByggaF was applied, to define the responsibility when of moisture experts and to specify requirements in tender documents for procurements. The Industry standard ByggaF includes a methodology to ensure, document and communicate moisture safety in the entire building process, from planning to operation and management. The method involves an approach to meet the demands of society and the property developer's requirements for moisture control. The Industry standard is formulated as a technical standard starting with a section with terms and definitions, a section describing the method, legislation and regulations, responsibilities and organization for the moisture safety work, followed by sections for activities to be carried out in each stage of the building process; planning stage, detailed planning and design, production stage, end of production stage and management stage. Each activity is described with a specific heading and the text is divided into "the requirements" that must be met and “guidance text” to clarify, explain or give examples of what the requirement means. The guidance also contains advice.
The division of responsibility for moisture safety issues within a building project is organized as in figure 2. The moisture expert has regular meetings with the design- and production managers to follow up the moisture safety work and regular meetings with the property developer to communicate the results and support decisions how to proceed with the moisture safety work.

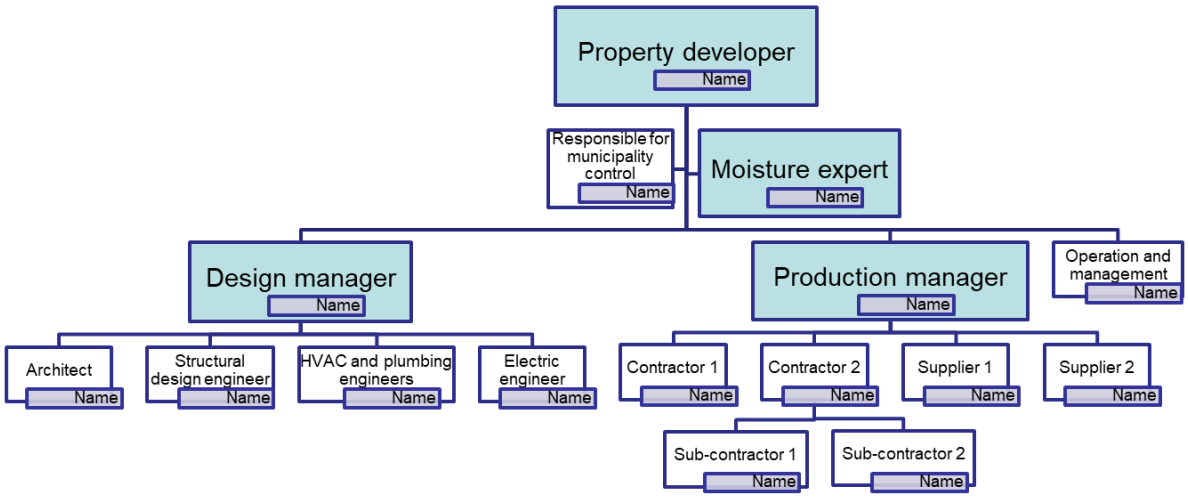

Figure 2 Organisation of responsibility of moisture safety issues in a building project.

The main required activities included in the Building Industry standard are listed in Table 1.

Table 1: Activities included in the Industry Standard ByggaF.

Stage	Activities included in the Industry standard
Moisture safety in the programme stage	• Appoint a moisture expert • Early moisture risk analysis • Decide on the developer's moisture safety requirements • Decide on measures in cases of non-conformance • Decide on procedures for monitoring • Formulate moisture requirements and requirements for activities in the contract documents
Moisture safety in the planning stage	• System planning o Information to planners about the developer's moisture safety requirements and methods for monitoring o Appoint moisture safety officer for planning o Present a procedure for moisture safety planning o Moisture safety planning o Moisture risk analysis o Inspection and documentation of system selections for moisture safety o Decision on specific moisture safety requirements in the production stage • Moisture safety specification • Detailed planning o Information to planners about the developer's moisture safety requirements and methods for monitoring o Appoint moisture safety officer for planner o Procedure for moisture safety planning o Monitoring meetings with planners o Review of moisture safety planning o Collect supporting data for moisture safety documentation
Moisture safety in the production stage	• The results of moisture safety planning are communicated to production • Information to contractors and suppliers about the developer's moisture safety requirements and methods for monitoring • Appoint a moisture safety officer for production • Identify moisture-sensitive elements, structures and installations • Prepare a moisture safety plan • Developers' monitoring meetings with contractors and suppliers • Moisture inspection rounds • Measurement and inspections • Document non-conformance in relation to the moisture safety plan • End of production stage o Collect and establish supporting data for operation and maintenance instructions for moisture safety o Collect supporting data for moisture safety documentation • Moisture safety documentation
Moisture safety in the management stage	• Review of property organisation • Moisture inspection rounds in the management stage

A number of guiding documents and templates have been developed to support the actors in their activities and documentation of the moisture safety work. These includes:

1. ByggaF industry standard
2. Risk identification and evaluation at early stage
3. Moisture Inventory of existing building
4. The developer's moisture safety requirements and activities
5. Job description for moisture expert

6. Moisture Safety Description (template)
7. Moisture Safety Planning and Risk Management (template)
8. Moisture Plan (template)
9. Moisture Round Protocol (template)
10. Deviation Report (template)
11. Content for moisture safety documentation (template)

All material can be downloaded from: www.fuktcentrum.se

2.2 Moisture safety design and risk assessment

Each participant who selects, designs, draws and constructs materials, building elements or installations that affect the moisture safety of the building must comply with the procedures for moisture safety planning and design. The planning and design engineers' group must jointly conduct and document a moisture risk analysis. In case the design conditions are changed a new moisture-risk analysis should be performed. The planning- and design manager is responsible for the coordination of the moisture risk analysis. A template is developed to support the designers to perform moisture safety design and risk evaluation. The document is however perceived as difficult for designers to use. One of the problems is that designers cannot judge the probability and consequence in a risk evaluation One reason is that there are lack of routines, tradition and system for experience feedback in the construction sector, which in turn make it difficult for designers to information about what is high and low risk constructions. ByggaF suggests that qualified assessments should be used for the risk analysis, but the guidance does not explain how to carry out the assessment. Instead, there is a description in how a proper risk analysis is done, which does not help the designer to evaluate the risks at this stage. There is a need for a better description of how a qualified assessment should be carried out. This has been identified as one of the areas of improvements.

2.3 Management and administration of ByggaF

Swedish Moisture Centre (SMRC) is responsible for management and administration of ByggaF. This involved updating documents as regulation changes and to develop and improve the method to better suit the users and the building process. SMRC has, since about ten years ago, arranged training courses for Moisture Experts. More than 150 persons from industry and academia have been participating and until today 144 persons have received a diploma for passing the exams. Every year SMRC arrange a day to share experience aimed for the Moisture Experts Alumni and in 2017 they took the initiative to form a network of Moisture Experts in Sweden and in 2018 an interest association was established. The association in an important collaboration partner in managing and further development of ByggaF since the members represent the everyday users of the method and tools. SMRC is still responsible for development and management of ByggaF.

2.4 Adaption to the renovation process

Even though ByggaF is a general method that could be applied on all buildings and both new and renovation of existing buildings, the sector sometimes asks for more specific tools. Therefore, two initiatives to adapt ByggaF for specific use, one is renovation of buildings and the other is single family houses were initiated. The adaptation to renovation process was done based on eighteen interviews with moisture experts and four building owners in the sector. In addition to existing documents and template they suggested a more profound inventory of the existing building. To ensure than a more profound inventory is carried out,

there must be a forcing requirement in the Industry standard ByggaF. The document should state the requirements to do an inventory in the program stage as well as a guidance of possible procedure to carry out an inventory. Another aspect of implementing the inventory in the industry standard is to ensure proper communication of the results to the designers and contractors. The result of the inventory should give indications about necessary investigations, which can be important for the designers. This is something that should be described in future versions of ByggaF. (Olsson and Tjäder 2017)

2.5 Adaption to prefabricated production of single-family housing

The generality of the ByggaF method constitutes a disadvantage when applied to prefabricated manufacturing of single-family homes due to differences from general construction in the building process and building techniques. The purpose of the second initiative was to adapt ByggaF into a modified method ByggaF-PST applicable to prefabricated manufacturing of single-family homes with timber frame. The prefabricated manufacturing building process requires adjustments in ByggaF because the building process involves construction of modules and elements in a factory. For this reason, ByggaF-PST includes a new stage: Factory production. Another difference with this building technique is that the client in most cases chooses a house from a catalogue. This means that the house already is more or less planned when the client gets involved in the project. For this reason, there is an essential difference between the prefabricated and the general building process. This affects the activities, stages, and parties in the presented method ByggaF-PST. The adjustments in ByggaF that were made regarded constructions, parties and stages that are relevant to prefabricated manufacturing of single-family homes. In addition to these adjustments some parts have been added to the documents and the method. Among these changes a more detailed checklist for risk assessment was made. Other changes regard supplemented moisture safety requirements and activities in the factory concerning moisture safety. (Johansson and Bengtsson 2015)

3 APPLICATION IN CONSTRUCTION PROJECTS

Our impression and experience from meeting moisture experts in training courses and in the alumni network, that ByggaF is used in all ongoing projects. There is no statistics solely on which projects have been using ByggaF, but there is statistics on the number of buildings certified according to the environmental assessment system Miljöbyggnad, this is a reasonably good estimation since there is a requirement to follow ByggaF to reach gold or silver level. Since 2012 to today, there are 1375 buildings certified according to Miljöbyggnad, of which 975 at silver and 165 at gold level.

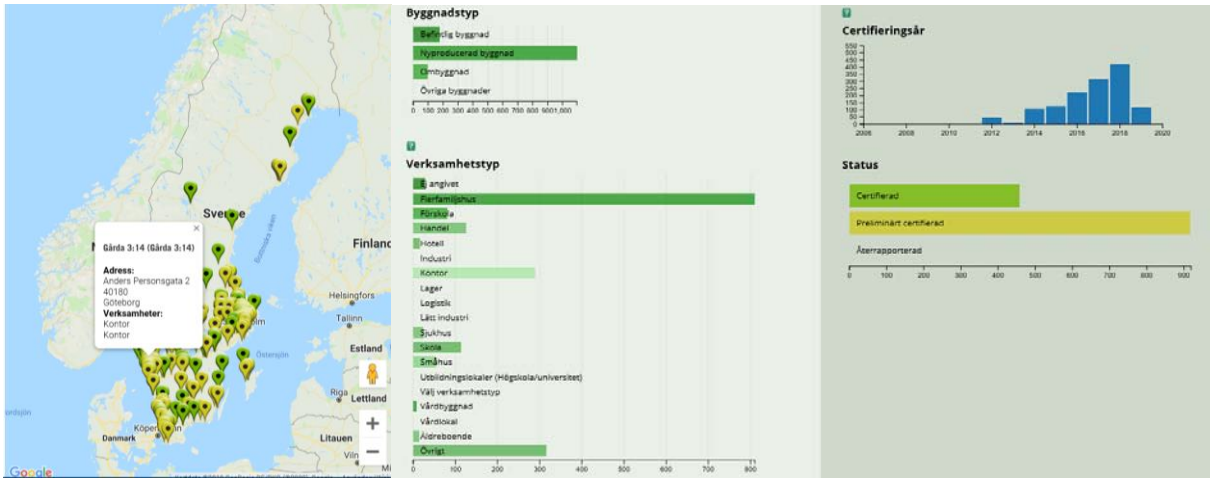

Figure 3 Today 1375 buildings are certified according to Miljöbyggand silver and gold level. Green dot is certified (457) and yellow is preliminary certified (918), Statistics from SGBC 2019.

Most of the certified buildings are multi-family housing followed by office buildings, commercial buildings, pre-schools and schools. The buildings are mainly new construction but also renovated and reconstruction. Information of the actual building can be found on the SGBC's website. In addition, there are building owners who use ByggaF but not Miljöbyggnad. For example, the city of Borås has followed the procedures of ByggaF for more than ten years and one school in Finland has used a version of ByggaF adjusted to Finnish conditions.

4 CONCLUSIONS

A method for including moisture safety in the construction process has been developed and successfully adopted by the Swedish construction industry. One reason is that it is an advice in the building regulation to use ByggaF, but it is also required to follow ByggaF to reach silver and gold level in the Swedish environment assessment system Miljöbyggnad. The ByggaF method was transferred into an industry standard to enforce that necessary activities are carried out and routines have been followed and documented in a standardized way. It is possible to adapt ByggaF to other countries, if national conditions and regulations are considered and accounted for in the requirements and in the templates. Some routines and templates are however perceived as difficult for designers to use, such as the moisture risk assessment. This procedure must be explained in more detail and supplemented with practical examples to be useful. ByggaF is a general method that can be applied in construction of all types of buildings, both new and existing, but adjustments have been made to better suit specific applications. ByggaF has been adapted for renovation of buildings by supplemented by a more detailed template for inventory. ByggaF has also been adjusted to new construction prefabricated manufactured single-family homes with timber frame. Although several changes have been made in ByggaF to achieve this, ByggaF-PST requires further adjustments based on feedback from the industry. Based on the statistics from buildings certified according to Miljöbyggnad, 1375 buildings should have been used ByggaF in the construction, renovation or reconstruction of multifamily buildings, office buildings, commercial buildings, pre-schools and schools.

Quality assurance is difficult and heavy-duty work, but digitization opens up new opportunities for smart systems to capture the right control points, to ensure that people get the right information and documentation can be made more accessible and tracked. There are great development opportunities to digitize ByggaF.

5 ACKNOWLEDGEMENTS

The research which form the basis of the results presented in this paper was carried out within the research project *Fuktsäkerhet i Byggprocessen* financed by SBUF Development Fund of the Swedish Construction Industry and within The Swedish Moisture Research Centre.

6 REFERENCES

Boverket (2019). Kartläggning av fel, brister och skador inom byggsektorn, Mapping of faults, deficiencies and damages in the construction sector. https://www.boverket.se/sv/om-boverket/publicerat-av-boverket/publikationer/2018/kartlaggning-av-fel-brister-och-skador-inom-byggsektorn/

Mjörnell, K, Arfvidsson, J, (2008). ByggaF A Method for Including Moisture Safety in the Building Process – Experience from Pilot Projects, Nordic Building Physics Symposium in Copenhagen, 2008. Proceedings of the 8th Symposium on Building Physics in the Nordic Countries. Volume 3, p 1181-1188.

Mjörnell, K., Arfvidsson, J., & Sikander, E. (2012). A Method for Including Moisture Safety in the Building Process. *Indoor and Built Environment*, 21(4), 583–594. https://doi.org/10.1177/1420326X11428340

Mjörnell, K. (2016). ByggaF- A Method to Include Moisture Safety in the Construction Process. Proceedings of the CIB World Building Congress 2016 in Tampere, Finland.

Boverket (2019). Boverkets byggregler – föreskrifter och allmänna råd, BBR https://www.boverket.se/contentassets/a9a584aa0e564c8998d079d752f6b76d/konsoliderad_bbr_2011-6.pdf

Swedish Green Building Council (2019). Miljöbyggnad 3.0, version 170510, indicators. https://www.sgbc.se/app/uploads/2018/07/Milj%C3%B6byggnad-3.0-Nyproduktion-vers-170915.pdf

Fuktcentrum (2013). *Industry standard ByggaF - method for moisture safety of construction process.* Available at: http://www.fuktcentrum.lth.se/fileadmin/fuktcentrum/PDF-filer/ByggaF_Branschstandard/1_ByggaF_branschstandard_--oeversaettning_av_version_130508_ENG.pdf (accessed: 26-06-2019).

Olsson, P., Tjäder, E., Suggestions for adjustment of ByggaF to improve the current use and suit the process of renovation, Energy Procedia, Volume 132, October 2017, Pages 921-926

Johansson, J. and Bengtsson, M., (2015) Anpassning av ByggaF till prefabricerade småhus med trästomme, Adjustment of ByggaF to prefabricated single-family housing with wood frame. Master thesis, Lund University. http://lup.lub.lu.se/student-papers/record/7451403.

Swedish Green Building Council (2019b) https://www.sgbc.se/statistik/

Analysis of the Effects of Ventilation Method on Indoor Humidity Distribution and Condensation by CFD method

Fangyuan Zhang [*1], Yuji Ryu [2]

1 Graduated Student, The University of Kitakyushu.
Address :Hibikino 1-1,Wakamatsu-ku Kitakyushu,Fukuoka, Japan .
**Corresponding author:*
E-mail: y7dbb408@eng.kitakyu-u.ac.jp

2 Professor, The University of Kitakyushu,Dr.Eng.
Address :Hibikino 1-1,Wakamatsu-ku Kitakyushu,Fukuoka, Japan .

ABSTRACT

People spend 70% -90% of their time indoors. Indoor air quality and human body's health have a close relationship. With the advance of society, user comfort requirements for thermal environment are rising. Humidity is an important parameter for evaluating indoor air quality, which not only affects the thermal comfort of the human body but also seriously restricts the function of the building. In winter, the indoor humidity is dry. When using humidifier, the humidity around the humidifier is higher, but there is still a dry area in the room. It is necessary to study the placement, blowing direction and capacity of the humidifier. In addition, when the room air supply method is different, the indoor humidity distribution is also slightly different. In recent years, with the development of large capacity, high speed of computer, CFD technology has been used to simulate air flow organization. It is possible to simulate the airflow organization, temperature and humidity of the building air conditioning system by using CFD technology.

This paper the effects of different ventilation methods and different humidifier placement positions on the indoor humidity distribution of single room. And exploring the effects of condensation on different ventilation modes.

1)The model can realistically simulate the effect of ventilation on the condensation distribution.
2) Within the scope of the nearby, the air just can hold limited capacity water vapor. The humidifier working efficiency was infected by the different position of humidifiers.
3) The humidity distribution in the room is related to the ventilation mode, and the flow pattern of the indoor airflow affects the distribution of indoor humidity.

KEYWORDS

Thermal environment, humidity, humidifier, ventilation mode, simulation

1 INTRODUCTION

Most people spend their lives indoors, and indoor air quality is inseparable from human life. With the improvement of the quality of life, more and more people are paying attention to the comfort of the indoor thermal environment. Humidity is an important part of the thermal environment. For human which is not only related to human comfort, but also to the health. During the winter time, indoor humidity is dry. There are major impacts on the health when

indoor humidity falls outside the appropriate range. We found that when using the humidifier there are some parts which are still dry in the room. So, the humidifier reasonable placement and effective humidification range need to be researched. Humidity condition of each space is influenced by individual variation and the use of humidifier. Condensation is a serious phenomenon while using humidifier. Bacterium and virus will enhance greatly in condensate water. There is also tremendous impact for people's health. The way of using of humidifier also influenced a lot to people's health. We need to place humidifier in an appropriate location for maximizing its effectiveness. In addition, when the room air supply method is different, the indoor humidity distribution is also slightly different. So in this paper the effects of different ventilation methods and different humidifier placement positions on the indoor humidity distribution of single room were simulated.

2 THE SUMMARY OF CFD SIMULATION

2.1 Establishment of a basic physical model

This paper simulated the effects of two different ventilation method and different placement of humidifier on condensation. The simulation is dedicated to single room(5m*5m*2.8m).The room plan is shown in Figure 1. The case number and humidifier position comparison are shown in Table 2. There are two type of air conditioning system. The way of A type is air supply and air outlets at the same direction. The B type is the air supply and air outlets on the opposite of

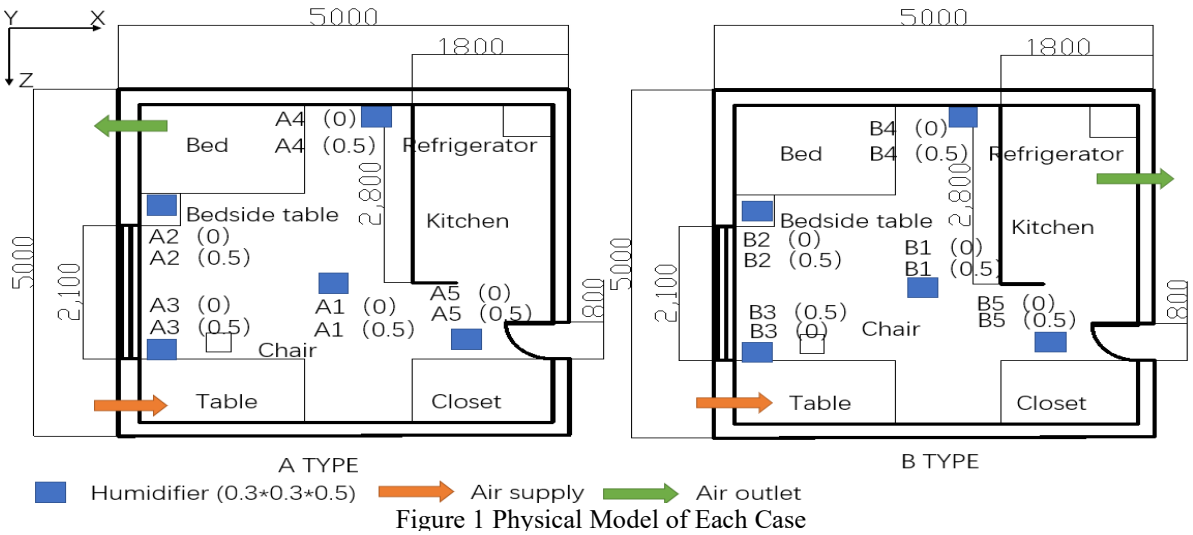

Figure 1 Physical Model of Each Case

Table 1: Model Boundary Conditions

Boundary	Parameter Setting
Air supply	Air volume： 216m^3/h, Temp.: 30℃, Relative Humidity: 20%
Air Outlet	Outflow
Wall	Dehumidification, overall heat transfer coefficient 1.74W / (m^2 • K), Outdoor temperature 5 ℃
Ceiling and Floor	Insulation
window	heat transfer coefficient 0.63W / (m^2 • K)
Initial environment	Temp. 23℃ RH Φ=20%
Penetrating wind	0.2m/s
Humidifier	Amount of moisture 300ml/h

Table 2: Case number and the humidifier position

case 1	no humidifier		
case 2	A1(0)	case 12	B1(0)
case 3	A1(0.5)	case 13	B1(0.5)
case 4	A2(0)	case 14	B2(0)
case 5	A2(0.5)	case 15	B2(0.5)
case 6	A3(0)	case 16	B3(0)
case 7	A3(0.5)	case 17	B3(0.5)
case 8	A4(0)	case 18	B4(0)
case 9	A4(0.5)	case 19	B4(0.5)
case 10	A5(0)	case 20	B5(0)
case 11	A5(0.5)	case 21	B5(0.5)

the room.A total of 10 placement for the humidifier in the simulation experiment is shown in the Figure 1. In the model, the humidifiers are placed in five locations, two heights, in short ten places. The letters indicate two different ways of ventilation(A,B). The height is indicated in parentheses. For example, A1(0) and A1(0.5) indicate that the humidifier is placed on the ground at position 1 of the ventilation mode A and placed at the height of 0.5 m from the ground at position 1 of the ventilation mode A.

In the model the wall on the side of window are made by concrete with overall heat transfer coefficient of 1.74W/m^2 · K. The heat transfer coefficient of the window is 0.63 W/m^2 · K. The other walls are insulated and desiccated. A humidifier was placed in the room to simulate humidification. The model boundary conditions are set in the Table.1

2.2 Simplification of the physical model

5 points simplifying assumption were made for the model：

1.The effects of gravity fields on air and water vapors are ignored;

2.Both air and water vapor are considered to be incompressible fluids with a constant density;

3.When the water vapor evaporates from the water surface, only latent heat exchange is performed, and sensible heat exchange is not considered;

4.When water vapor condenses on the wall, the heat release ignored from the phase change process;

5.Wall surfaces moisture absorption capacity is not considered during wall condensation.

2.3 Mathematical model

The FLUENT 14.0 turbulence module (Standard k-ε) is used to analyze the flow field characteristics. The component transport module (Species Transport) and the multiphase flow module (Multiphase) simulated the mass transfer phase transition of water vapor in the air. The governing equation is as follows:

$$\frac{\partial（\rho\phi）}{\partial\tau} + div(\rho u\phi) = div(\Gamma grad\phi) + s \quad (1)$$

Where: $\phi$is a general variable;

Γ is a generalized diffusion coefficient;

s is a generalized source term.

2.4 Criterion of wall condensation

Wall condensation conditions: When the absolute humidity D_{air} of the air node around the wall surface is higher than the saturated absolute humidity D_{wall} corresponding to the wall temperature, the wall surface is considered to be condensation.

Conditions for no condensation on the wall: Any time τ, when the absolute humidity D_{air} of the air node around the wall is less than the saturated absolute humidity D_{wall} corresponding to the wall temperature, the wall is not considered to be condensation

$$D_{wall} < D_{air} \quad (2)$$

3 SIMULATION RESULTS AND ANALYSIS

3.1 The result of the simulation without humidifier and the humidity diagram of each case.

For the first time, the simulation without a humidifier has been completed. The indoor humidity distribution is shown in Figure 2. It can be seen that the indoor humidity is about 25%

when the humidifier is not used in winter, which is lower than the indoor humidity comfort range.

This simulation verifies that the indoor humidity range is not in the comfort range without using a humidifier in winter and verifies the need for a humidifier in winter. In addition, it is necessary to study the placement position of the humidifier.

A total of 21 simulations were performed. Figure 3 shows the humidity of each simulation case. It can be seen that after using the humidifier, the indoor humidity environment is

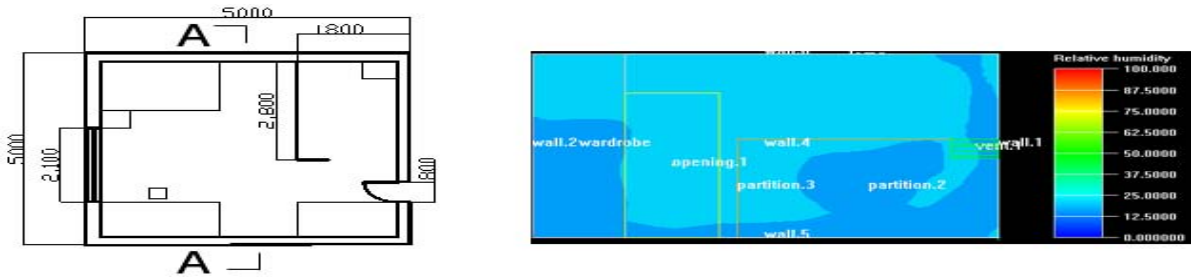

The Humidity Plane Cut of Section A

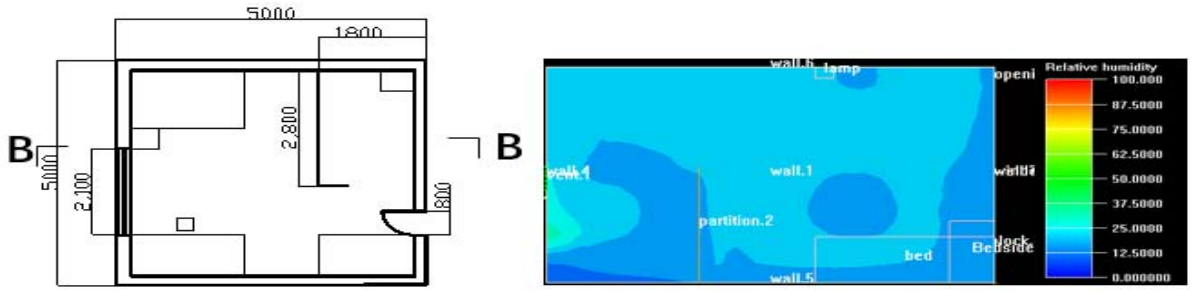

The Humidity Plane Cut of Section B

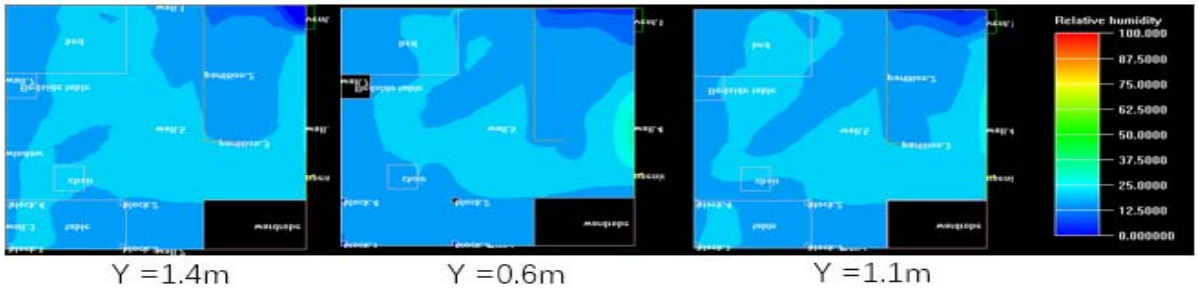

The Humidity Plane Cut of Height Section

Figure 2 The Humidity Plane Cut of Case 1 (Initial conditions)

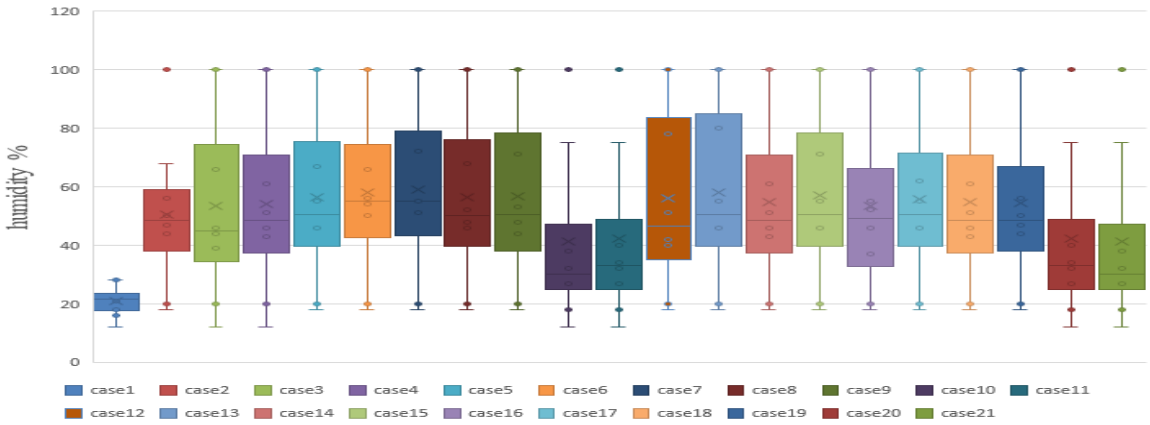

Figure 3 The Humidity Box Diagram of Each Case.

significantly improved. Under the ventilation mode of B, the indoor humidity is better than the ventilation mode A.

3.2 Influence of different ventilation methods on indoor humidity distribution

In Figure 3, it can be seen that the humidity environment of case 2 is very good, between 40% and 60%. However, in case 12 there are many parts of the humidity above the comfort range. The humidity plane distribution of case 2 and case 12 is shown in Figure 4.

Figure 4 is a good illustration of the effect of different ventilation methods on the indoor humidity distribution with the same placement of the humidifier. In case 2, the indoor humidity is between 40% and 60%. The average humidity is around 50%. No obvious condensation in the room occurred. In case 12, the humidifier position is the same as in case 2, and the ventilation is different. Indoor humidity is mostly distributed between 40% and 60%. However, there is obvious condensation in the area around the humidifier, and the humidity in the centre of the room is high. The humidity in the room varies greatly. It can be concluded that the humidity distribution in the room is related to the ventilation mode, and the flow pattern of the indoor airflow affects the distribution of indoor humidity.

3.3 Influence of humidifier placement height on indoor humidity distribution

In Figure 4, case2 and case3 are used to analyse the effect of humidifier placement height on indoor humidity distribution under the same ventilation mode. Comparing case2 and case3, the humidifier is placed 0.5 meters away from the ground, and water mist gathers around the humidifier, which may cause condensation. The indoor average humidity of case3 is higher than the indoor average humidity of case2. and at the same time, the humidity in the near-ground area is low.

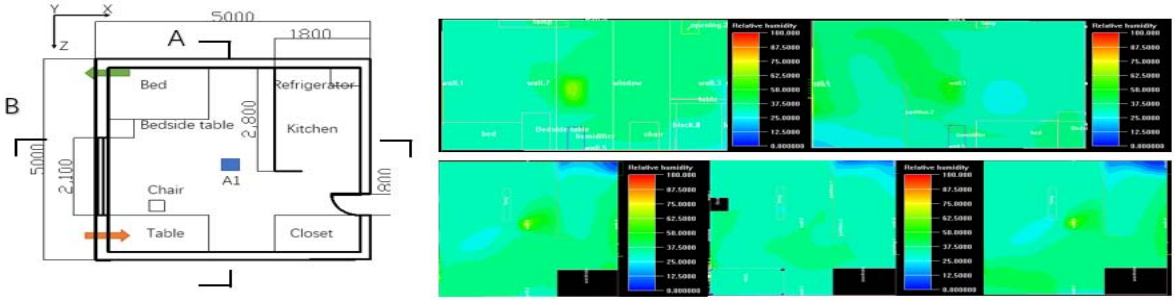

The Humidity Plane Cut of Case 2

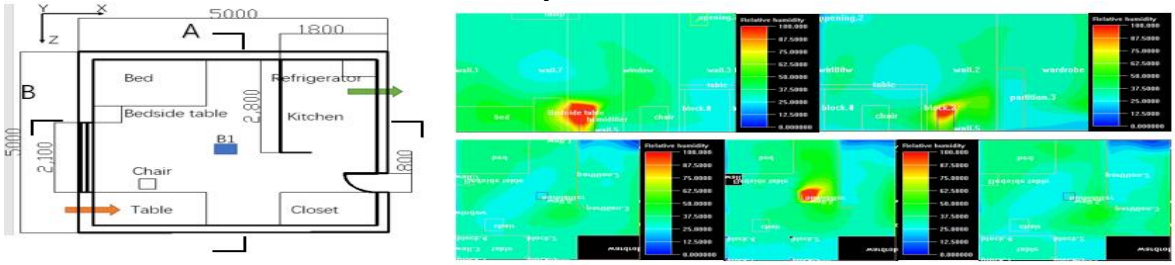

The Humidity Plane Cut of Case 12

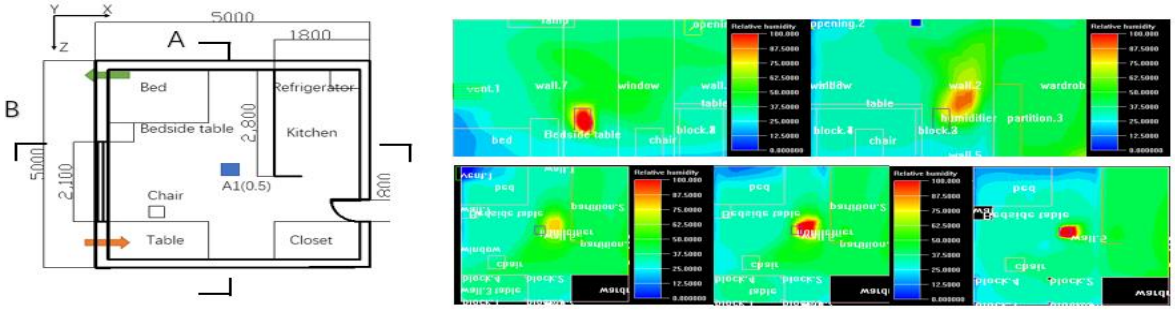

The Humidity Plane Cut of Case 3

Figure 4 The Humidity Plane Cut of Case 2, Case 3 and case12

3.4 Influence of different humidifier placement positions on indoor humidity distribution

In addition, it can be clearly seen in Figure 3 that there are four cases of simulations and other significant differences. The humidity plane cut for these four cases are shown in Figure 5.

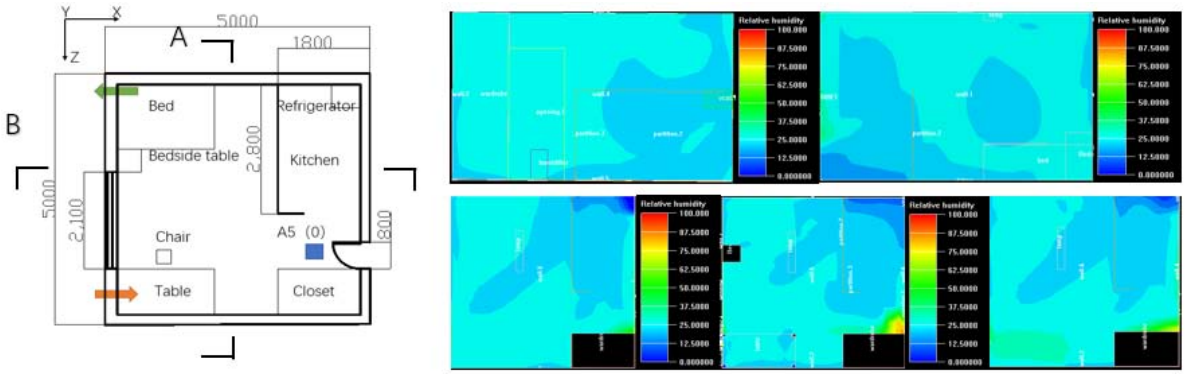

The Humidity Plane Cut of Case 10

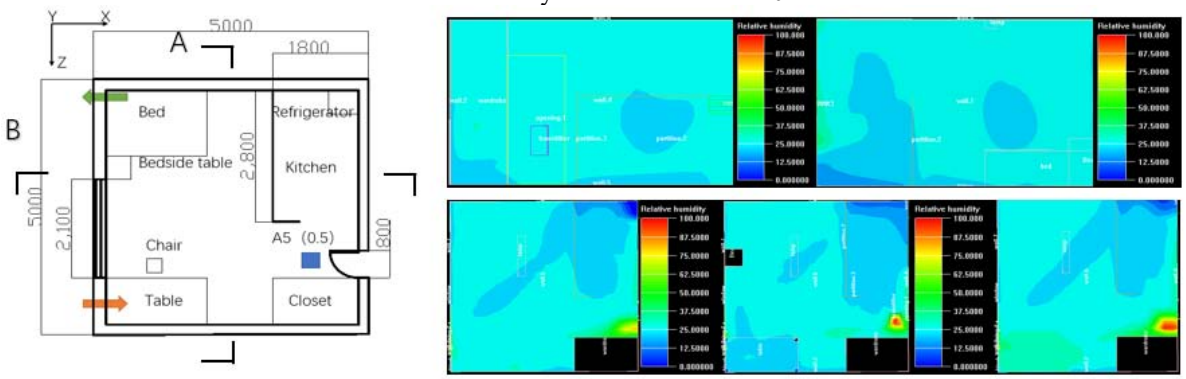

The Humidity Plane Cut of Case 11

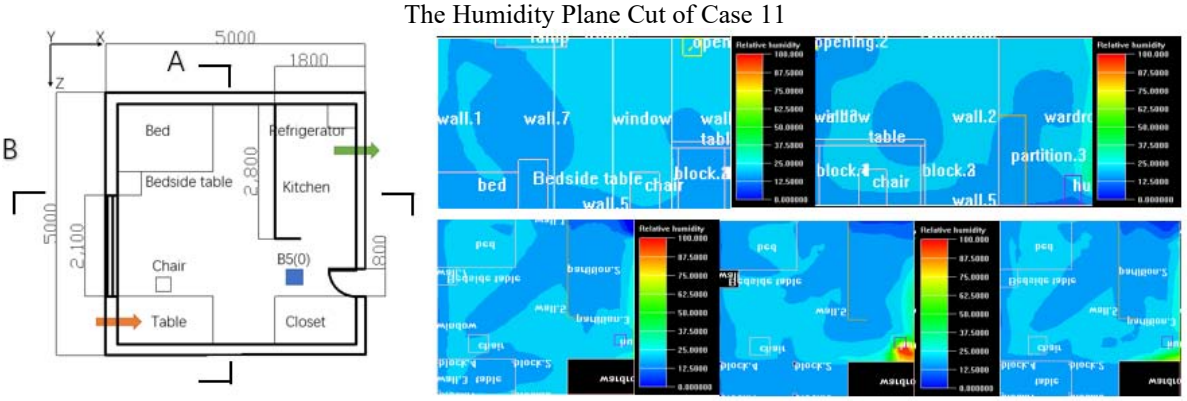

The Humidity Plane Cut of Case 20

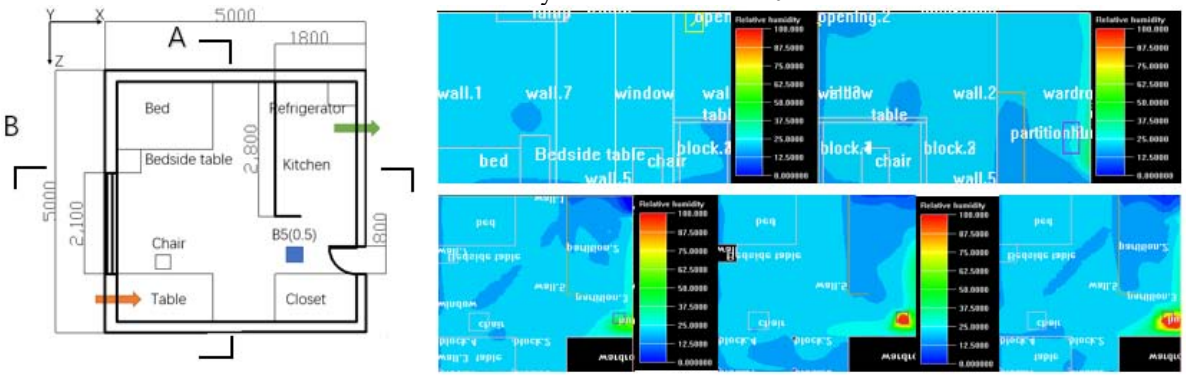

The Humidity Plane Cut of Case 21

Figure 5 The Humidity Plane Cut of Case 10,11,20,21.

As can be seen from Figure 5, when the humidifier is placed beside the door, the humidifier does not improve the indoor humidity. The humidity in ventilation mode A is higher than the humidity in ventilation mode B. And when the humidifier is placed 0.5 meters above the ground, condensation may occur on the surface of the wardrobe of the room. The reason why the indoor humidity environment is not improved can be considered in the direction of air flow. When the humidifier is placed beside the door, the air at the door of the room is not well mixed. At the same time, the air flow on the refrigerator side is also poor. However, as can be seen from Figure 5, when the humidifier is placed 0.5m from the ground, the humidity of the room is slightly higher than the humidifier placed on the ground.

4 CONCLUSION

This paper establishes a mathematical model and uses FLUENT software to simulate the effects of ventilation on indoor humidity and condensation. The simulation results show that the ventilation mode and the placement of the humidifier have a great influence on the condensation distribution. The results can be summarized as follows:
1) The model can realistically simulate the effect of ventilation on the condensation distribution.
2) Within the scope of the nearby, the air just can hold limited capacity water vapor. The humidifier working efficiency was infected by the different position of humidifiers.
3) The humidity distribution in the room is related to the ventilation mode, and the flow pattern of the indoor airflow affects the distribution of indoor humidity. The room with the air supply and the return air outlets in the same direction, there is a difference in humidity on both sides of the room, and when the humidifier is used, the humidity on the other side of the room changes little. 4) The placement height of the humidifier also affects the indoor humidity distribution. When the humidifier is placed in a slightly higher position, the average humidity in the room will increase, and it will be easier to reach a comfortable humidity environment at a sleep height of 0.6 meters. But at the same time, there will be condensation of water near the humidifier.
5) The placement of the humidifier also has a great influence on the indoor humidity and humidity distribution. when the humidifier is placed beside the door, the humidifier does not improve the indoor humidity. When the humidifier is placed in the centre of the room, the humidity in the room is evenly distributed. When the humidifier is placed close to the wall, condensation occurs near the ground due to the low wall temperature.
6) From this simulation, it can be concluded that in the dry winter season, by arranging the position of the indoor vents and placing the humidifier reasonably, the humidity can reach a comfortable range while reducing the possibility of condensation.

5 ACKNOWLEDGEMENTS

We would like to express our deep appreciation to all those who helped us during the writing of this paper. Many people have made invaluable contributions, both directly and indirectly to our research.

First and foremost, we would like to express our warmest thanks to the assistant Mrs.Dian of the laboratory, for her instructive suggestions and valuable comments on the writing of this article and the examination of grammar. Without her invaluable help and generous encouragement, the present paper would not have been accomplished.

Besides, we would like to thank Ms. Lu, a student of our lab, for providing us with relevant data for the initial period of the experiment. Last but not least, thanks also to the other laboratory mates, who helped us work out the problems during the difficult course of the paper

6 REFERENCES

[1] Zhang Fangyuan, Analysis of the Effects of Ventilation Method on Indoor Humidity Distribution and Condensation by CFD method, AIJ Kyushu Chapter Architectural Research ‘Meeting ： 2019.3

[2] Zhang Fangyuan, Study on the Distribution of Indoor Humidity using CFD Method, AIJ Kyushu Chapter Architectural Research ‘Meeting ： 2018.3

[3]Ma Xiaotong. Ventilation and air conditioning room temperature and humidity and pollutant distribution law and its application [D]. Beijing: Tsinghua University, 2012: 58-59.

[4] Igarashi, Yuriko: Study on Thermal Environment in Houses for the Aged Couples and Singles in Niigata Prefecture Part 1 and Part 2, SUMMARIES OF TECHNICAL PAPERS OF ANNUAL MEETING ARCHITECTURAL INSTITUTE OF JAPAN 2001/9

[5]"Indoor Air Facts No. 8: Use and Care of Home Humidifiers". Environmental Protection Agency. 1991.

[6]Wang Chunxu (2011), Study on Humid Environment and Humidifier Using Situation in Elderly Health Facility in the North of Kyushu Region, The Yellow Sea Rim International Exchange Meeting on Building Environment and Energy.

[7] Wagner, J. A., Robinson, S., and Marino, R. P.: Age and Temperature Regulation in Neutral and Cold Environments, J. Appl. Physiol., 37, 562-565(1974)

[8] Guo Xingguo, Chen Youming. Analysis of internal condensation of walls in hot and humid climate areas [J]. Civil and Environmental Engineering, 2011, 33(5): 121-124.

[9]Wang Yiding. Numerical simulation of airflow organization in air-conditioned rooms with different air supply speeds [J]. Building Energy Efficiency, 2017(5): 33-36

[10]M. Homes, M. Jaafar, B. Croxford, Adapting to technology: the case of air conditioning use, Proceedings of Conference: Adapting to Change: New Thinking on Comfort, WINDSOR 2010 (2010)

[11]Hiroshi Yoshino, Teruaki Mitamura and Ken-ichi Hasegawa: ANNEX41 Subtask 1 Common Exercise 2 “Small chamber test (THU test room) in the climate chamber”, IEA ANNEX41 meeting report, 2006.

[12]Mamoru Matsumoto, Simultaneous heat and moisture transfer in porous wall and analysis of internal condensation, Energy Conservation in Heating, Cooling and Ventilating Building, Hemisphere, 1978, pp.45 – 58 M.

[13]Matsumoto, Moisture, Physics of Environment, Architectural Science series, Vol.10, Shokokusya, 1984, (in Japanese)

[14]M. Kumar KUMARAN, IEA ANNEX24 Heat, Air and Moisture Transfer Through New and Retrofitted Insulated Envelope Parts (Hamtie) Final Report Volume 3 TASK 3: MATERIAL PROPERTIES

Performance of a Heat Recovery Ventilation System in the Canadian Arctic

Justin Berquist[*1], Carsen Banister[1], and Dennis Krys[1]

1 National Research Council Canada

1200 Montreal Road, Ottawa, Ontario, K1A 0R6

Canada

**Corresponding author:*
justin.berquist@nrc-cnrc.gc.ca

ABSTRACT

A demonstration house was previously built and commissioned in Iqaluit, Nunavut, Canada. The purpose of the overall effort is to evaluate the performance of a high-performance building located in the Canadian Arctic, while considering the unique social, economic and logistical challenges associated with its remote location. Previous work consisted of monitoring and reporting on the energy consumption due to heating between April 2016 and April 2017. The purpose of this ongoing research is to contribute experimental data regarding the functionality of ventilation systems in cold climates. This paper outlines the development, implementation and monitoring of a carbon dioxide-based demand-controlled heat recovery ventilation system that took place between April 2017 and April 2019. The system was equipped with two electric preheaters to ensure that frost build-up did not occur in the heat recovery ventilator (HRV) and adequate fresh air ventilation could be maintained. An electric heater was included after the HRV to control the supply air temperature. Monitoring of the ventilation system's performance took place between December 2018 and February 2019. During this period the electricity consumption of the HRV, preheaters, and supply air heater were measured for the fresh air required for two "theoretical" occupants. Flow rate and important temperatures in the ventilation system were also monitored to assess the system's performance. A comparison of the sensible recovery efficiency (SRE) of the HRV and overall system is presented. Experiments displayed that on average the SRE of the system and HRV was 35% and 72%, respectively. The total energy consumption of the ventilation system was 390 kWh over the two months, which translates to 6.30 kWh/day, an energy use intensity of 0.27 kWh/m^2/day and 4.49 Wh per L/s of fresh air.

Keywords: heat recovery ventilator, ventilation, demand control, energy performance, and cold climate.

1 INTRODUCTION

There are multiple challenges associated with housing in northern Canada. Firstly, the cost of supplies and labour are increased in remote locations (Roszler, 2005) and the cost of heating is substantially higher due to the cold climate (Minich, et al., 2011). Furthermore, extremely cold climates result in durability issues with houses and their systems, which can result in health problems (Minich, et al., 2011). An Inuit Health Survey was conducted to evaluate the living conditions in a total of 1,901 households. From the survey it was concluded that approximately 40% of the homes were in need of major repairs, 30% were overcrowded and 20% contained mould (Minich, et al., 2011).

The occurrence of mould growth in these homes suggests a need for better building envelopes and proper ventilation. The research outlined by Banister et al. (2018) presented a better building envelope solution in cold climates. However, a limited amount of research has been directed at solving ventilation issues in cold climates. The large difference between outdoor and indoor temperatures during much of the year in these locations makes it highly valuable to control ventilation rates effectively and have a system that manages ventilation air heating energy well. Equipment for air to air heat/energy recovery is an effective method of reducing the cost associated with ventilating the home (Nasr, Kassai, Ge, & Simonson, 2015). Heat recovery ventilators (HRVs) were utilized by Kovesi et al. (2009) and successfully allowed for a reduction of indoor air pollutants and in the number of reported respiratory infection symptoms in Inuit children. However, the extreme temperature difference between the fresh air and indoor temperature can cause problems, such as frosting, in the mechanical equipment, which can cause the performance of equipment to degrade (Nasr, Kassai, Ge, & Simonson, 2015), or system failure (Kragh, Rose, & Svendsen, 2005).

While these challenges are difficult to overcome, they need to be addressed for the living standards and occupant health to be increased in northern communities (Minich, et al., 2011). Therefore, this paper aimed to address this gap in research through the development and implementation of a ventilation system within the Iqaluit demonstration house which combines effective use of low-cost CO_2 sensors for demand-controlled ventilation, ventilation system modifications to enable more fan speeds, preheaters to reduce the need for defrost cycles when desired, and a supply air heater to achieve satisfactory thermal comfort. Moreover, this paper provides experimental data regarding the operation of a ventilation system in a cold climate, an area that is limited in literature.

2 LITERATURE REVIEW

Due to the high energy costs in the Arctic it is very beneficial to ventilate on an “as needed” basis. For this reason, literature related to residential demand control ventilation (DCV) strategies was reviewed. Furthermore, literature pertaining to ventilation systems in cold climates was also reviewed due to the difficulties associated with ventilating in extreme cold.

2.1 Residential Demand Control Ventilation Strategies

Kim & Park (2009) studied eight ventilation strategies in a 5-story apartment building in Jeju, Korea. The eight strategies consisted of either constant air volume (CAV) or CO_2-based DCV systems, and varying locations of the supply and CO_2 sensors. CONTAMW 2.4 simulations revealed that the CAV systems are more advantageous in terms of initial cost, when compared to the CO_2-based DCV systems. They were also most advantageous in terms of percent dissatisfied and CO_2 concentration because of the constant supply of sufficient outdoor air. However, the CO_2-based DCV methods have a lower energy cost, and the investment payback periods are short.

Cho, Song, Hwang & Yun (2015) evaluated the energy saving potential of a demand-control ventilation system with an air-cleaning unit in a multi-residential building. The ventilation system operates based on the indoor CO_2 and HCHO concentrations. The ventilation and air-cleaning modes operate independently or simultaneously to optimize the energy usage for ventilation. Results obtained through TRNSYS displayed that the proposed ventilation system, when compared to continuous ventilation methods, decreases the introduction of fresh air approximately 50% of the operating time and the energy use by approximately 20%.

Cleveland & Schuh (2010) designed an automated thermostat that operates based on the occupancy of the ecoMOD1 house. The occupancy of the house was determined by utilizing a combination of carbon dioxide sensors and motion detectors on each floor. When an occupant was detected in the house the thermostat would adjust the set-point temperature accordingly. It was determined that a concentration level of 525 ppm was necessary to denote the house

as occupied. However, the time needed to reach this level can range up to twenty minutes, therefore the system also considered the rate of change of the carbon dioxide.

Guyot, Sherman & Walker (2018) reviewed 38 studies related to smart ventilation systems, which operate based on CO_2, humidity, combined CO_2 and total volatile organic compounds (TVOC), occupancy and outdoor temperature. The literature review displayed that ventilation energy savings of up to 60% can be achieved without jeopardizing the IAQ of the space. However, the meta-analysis revealed studies that resulted in a 26% increase in energy consumption. The literature review presents a well-documented table outlining the type of home, utilized controls strategy, the main findings, and the resulting IAQ performance and energy savings of each reviewed research study.

2.2 Ventilation Systems in Cold Climates

Liu, Alonso, Mathisen & Simonson (2016) built and tested a novel quasi-counter-flow membrane energy exchanger during cold operating conditions. A moisture transfer diffusive resistance of dense and porous membrane was derived for cold climates. The sensible and latent effectiveness was found to vary between 88.5% to 94.5% and 73.7% to 83.5%, respectively.

Nielsen, Rose & Kragh (2009) developed a dynamic model of a counter flow air to air heat exchanger in Simulink. The model took into account condensation, frosting and melting, in order to accurately simulate its performance in cold climates. It is shown through experimentation and simulation that ice will begin to form in a heat exchanger, unless defrosting methodologies are deployed.

Nasr, Kassai, Ge & Simonson (2015) experimentally tested two cross-flow heat/energy exchangers during frosting and defrosting cycles. The effect of two defrosting methods (preheating and bypassing), on energy consumption of ventilation in three locations was evaluated. It was determined that preheating the fresh air performs better than the heat exchanger bypass method. Also, it was found that cold weather conditions impact heat recovery ventilators more than energy recovery ventilators.

Further, more in depth reviews of heat and energy recovery ventilators, and frosting in cold climates were completed by Nasr, Fauchoux, Besant & Simonson (2014) and Alonso et al. (2015). Nasr et al. (2014) provided a detailed review regarding frosting in heat and energy recovery ventilators. Alonso et al. (2015) summarized literature pertaining to key technologies that are ideal for zero energy buildings located in cold climates.

2.3 Summary of Literature Findings

The review on literature pertaining to DCV revealed that careful consideration to the control strategy is required to obtain positive indoor air quality and energy savings. Due to low occupant densities CO_2 may be a poor indicator of occupancy in residential applications. However, it is believed that the over-crowding associated with northern housing makes this a viable option. The review on literature regarding ventilation systems in cold climates revealed that defrosting methods are necessary for heat and energy recovery ventilators to maintain functionality in cold climates (Zeng, Liu, & Shukla, 2017). The literature revealed that the cost of novel defrosting methods can be high, the equipment can be bulky and there is limited experimental data (Zeng, Liu, & Shukla, 2017) and that other defrosting techniques cut off the supply of fresh air for an extended period of time, defeating the purpose of a ventilation system. As a result, preheating was considered an effective method for preventing frosting in this research due to its low initial cost, non-invasiveness and the added benefit of a continuous supply of fresh air.

3 METHODS AND MATERIALS

This section describes the design of the ventilation system, the ventilation system controls strategy for the DCV system and preheaters, and the sensors utilized to monitor the performance of several aspects of the ventilation system.

3.1 Ventilation System Design

The system was designed with two 1 kW preheaters to make use of an off-the-shelf HRV and avoid inadequate ventilation from occurring. To avoid or remove frost build up, the HRV has a factory-set defrost strategy which switches the unit into recirculation mode on an increasing proportion of time as the HRV inlet temperature decreases below -5 °C. The supply air temperature that exits the HRV will vary based on the indoor temperature set point and the outdoor temperature. Furthermore, the supply air temperature could also be low relative to the indoor

temperature, resulting in cold drafts within the spaces, as was found to be the case in (Kragh, Rose, & Svendsen, 2005). To ensure a comfortable supply air temperature would be reached prior to entering the space, a 1 kW electric heater was included on the supply air stream to control the delivered temperature. The fresh air and exhaust ducts were insulated with R4 reflective insulation to reduce heat gains from the space.

3.2 Ventilation System Controls

Having established the equipment required to achieve desired indoor conditions through ideal ventilation rates, a control strategy was developed for the DCV system and the preheaters.

Demand Control Ventilation Strategy

New HRV fan speeds were enabled to allow the CO_2-based DCV system to meet a wider range of occupant densities, without excessive over-ventilation. The HRV was modified by replacing the standard transformer with an alternative supplied by the manufacturer. A relay control board was also integrated to allow the system to switch between the speeds of the new transformer. An Arduino microcontroller was used to control the system based on CO_2 concentration measurements in the main room of the building. The Arduino collects the data from a CO_2 sensor and controls the speed of the fan in the HRV according to the predefined carbon dioxide concentration thresholds. Table 1 shows the operational modes of the HRV, the corresponding airflow rate, and the CO_2 concentrations that trigger each flow rate when the CO_2 concentration is rising and falling.

Table 1: HRV control modes and corresponding airflow rates

HRV mode	Airflow rate (L/s)	CO_2 concentration thresholds (ppm)	
		When rising	When falling
Fan speed 1	13.5	-	700
Fan speed 2	21.0	700	1000
Fan speed 3	40.5	1300	-

Preheater Control Strategy

The analysis of measurements from an existing ventilation system with heat recovery used in single-family houses in Denmark and a test of a standard heat recovery unit in the laboratory have clearly shown that problems occur when the outdoor temperature gets below approximately –5 °C (Kragh, Rose, & Svendsen, 2005). For this reason, and to avoid the built in defrost mode of the HRV the preheater strategy was set to a static minimum temperature of -5 °C. Although the moisture content of the return air could be considered an input to the preheater temperature control, it was determined at this time that the added complexity and reliance on a humidity sensor, which could fail, was not warranted.

3.3 Monitoring of System Performance

The system was equipped with several sensors to allow for the performance of several components to be monitored. This section outlines the various parameters and corresponding sensors that were utilized to monitor the performance of the CO_2-based DCV strategy and the performance of the HRV, preheaters and supply air heater.

CO_2-based DCV control strategy performance

The performance of the CO_2-based DCV system was monitored On November 26th and 27th, 2018. These two dates were selected for performance monitoring as the demonstration house was unoccupied for an extended period of time, starting November 28th. Occupancy was recorded manually and the operation of the DCV system was monitored through the utilization of two CO_2 sensors located in the space and an airflow sensor in the fresh air duct. The HRV mode and airflow measurement can then be analyzed to verify if the system was operating as expected.

HRV performance

The current and voltage that is supplied to the HRV is measured by a WattsOn power meter, allowing for the power and energy consumption of the HRV to be recorded. In addition to the power and energy consumption information, six thermocouples located on the HRV's core are utilized to measure the HRV's performance. The intake and return air streams are assumed to be well mixed, and thus one thermocouple for each stream was utilized. During the heat exchange a temperature distribution arises for each air stream. For this reason, thermocouples were placed on the bottom, center and top of the core's exhaust side. This allowed for a quadratic temperature distribution to be fit to the exhaust air stream, leading to the determination of the average exhaust temperature. The core's supply side

temperature distribution was assumed to be the same as the exhaust side, allowing for an approximation of the average supply air stream temperature.

The performance of the HRV was monitored by evaluating its sensible recovery efficiency (SRE). Equation 1 represents the equation utilized to calculate the SRE of the HRV and accounts for the energy added to the supply air stream via electrical consumption, HRV case heat gains, cross flow leakage and the energy used to defrost.

$$SRE_{HRV} = \frac{\dot{m} \times c_p \times (T_s - T_I) - \dot{Q}_{sf} - \dot{Q}_C - \dot{Q}_L - \dot{Q}_D}{\dot{m} \times c_p \times (T_R - T_I) + \dot{Q}_{ef}} \quad (1)$$

where

SRE_{HRV} = sensible recovery efficiency of heat recovery ventilator
$\dot{m}$ = mass flow rate of air (kg/s)
c_p = specific heat capacity of air (J/kgK)
T_s = supply temperature (K)
T_I = inlet temperature (K)
T_R = return temperature (K)
$\dot{Q}_{sf}$ = energy added to the supply stream by the supply fan (W)
$\dot{Q}_{ef}$ = energy added to the exhaust stream by the exhaust fan (W)
$\dot{Q}_C$ = energy added to the supply stream due to heat transfer through casing (W)
$\dot{Q}_L$ = energy added to the supply stream due to cross flow leakage (W)
$\dot{Q}_D$ = energy transferred to the HRV core during defrost, from the space (W)

The HRV power data is utilized to determine when the HRV is operating in defrost mode. The HRV operates at the maximum fan speed when it is in defrost mode, and thus will consume the most electricity at this time. For this reason, it is assumed that the HRV is in defrost mode when it is consuming over 50 W.

Preheater and supply air performance

The current and voltage that is supplied to the three electric heaters (two preheaters and one supply air heater) is measured by a WattsOn power meter, allowing for the power and energy consumption of the HRV to be recorded. In addition to the power and energy consumption information, the outdoor temperature and temperature after the electric preheaters is measured, allowing for the functionality of the preheater control strategy to be monitored.

System Performance

The performance of the system is monitored by evaluating its SRE. Equation 2 represents the equation utilized to calculate the SRE of the system and is the energy required to raise the fresh air temperature from the outdoor temperature to the supply temperature, adjusting for the energy added to the system via electrical consumption, duct heat loss/gain, HRV case heat loss/gain, cross flow leakage and the energy used to defrost.

$$SRE_{Sys} = \frac{\dot{m} \times c_p \times (T_s - T_O) - \dot{Q}_{ph} - \dot{Q}_{sf} - \dot{Q}_{sd} - \dot{Q}_C - \dot{Q}_L - \dot{Q}_D - \dot{Q}_{sh}}{\dot{m} \times c_p \times (T_{Room} - T_O) + \dot{Q}_{ef} + \dot{Q}_{ed}} \quad (3)$$

where

SRE_{Sys} = sensible recovery efficiency of system
$\dot{m}$ = mass flow rate of air (kg/s)
c_p = specific heat capacity of air (J/kgK)
T_s = supply temperature (K)
T_O = outdoor temperature (K)
T_{Room} = room temperature (K)
$\dot{Q}_{sf}$ = energy added to the supply stream by the supply fan (W)
$\dot{Q}_{ef}$ = energy added to the exhaust stream by the exhaust fan (W)

$\dot{Q}_{ph}$ = energy added to the supply stream by the preheater (W)
$\dot{Q}_{sh}$ = energy added to the supply stream by the post HRV heater (W)
$\dot{Q}_{sd}$ = energy added to the supply stream due to heat transfer/leakage from the duct (W)
$\dot{Q}_{ed}$ = energy added to the exhaust stream due to heat transfer/leakage from the duct (W)
$\dot{Q}_{C}$ = energy added to the supply stream due to heat transfer through casing (W)
$\dot{Q}_{L}$ = energy added to the supply stream due to cross flow leakage (W)
$\dot{Q}_{D}$ = energy transferred to the HRV core during defrost, from the space (W)

4 RESULTS

The functionality of the CO_2-based DCV system was verified on November 26th and 27th, 2018, Afterward, the performance of the HRV, preheaters and supply air heater were monitored for two months, starting on December 1st, 2018 and ending on February 1st, 2019.

4.1 CO_2-based DCV system performance monitoring

A two-day experiment was conducted on November 26th and 27th, 2018 to verify the functionality of the CO_2-based DCV system. The occupancy was varied from no occupancy to up to five occupants during these two days. Figure 1 shows the measured CO_2 concentration, fresh air supply rate and number of occupants present in the space.

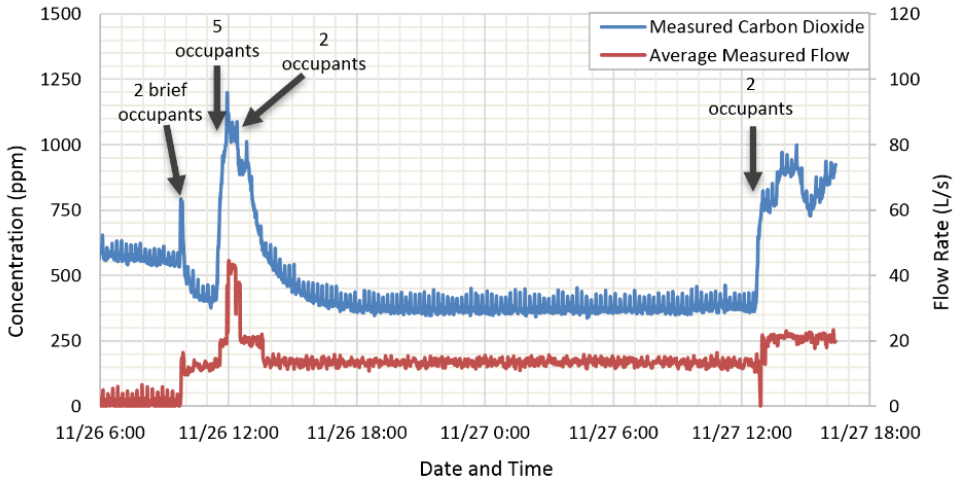

Figure 1: Sample data of demand-controlled ventilation system operation

Initially, the measured CO_2 concentration was above outdoor ambient as a result of previous occupancy and no fresh air supply. Two occupants briefly entered the space to enable the system. Their presence caused the CO_2 levels to increase, and enabling the system caused the HRV to enter fan speed 1 (13.5 L/s of fresh air). The occupants leaving, combined with the increase in fresh air supply caused the CO_2 concentration to decrease back to outdoor ambient. When five occupants entered the space, the CO_2 levels increased, causing the HRV to enter fan speed 2 (21 L/s of fresh air), followed by fan speed 3 (40.5 L/s of fresh air). The CO_2 concentration stabilized at approximately 1050 ppm until three occupants left. The three occupants leaving caused fan speed 3 to decrease the concentration in the space to below 1000 ppm, causing the fan to switch to speed 2. After the two occupants left, the CO_2 levels decreased below 700 ppm, which caused the fan to switch to speed 1. Eventually ambient CO_2 concentrations were reached in the space once again. The next day two occupants entered the space, causing the CO_2 concentration to increase above 700 ppm. This caused the HRV to enter speed 2, stabilizing the CO_2 levels below 1000 ppm.

4.2 System energy and SRE performance

The energy performance and SRE of the system was monitored between December 1st, 2018 and February 1st, 2019.

Energy performance monitoring

While monitoring the system the average outdoor temperature was -26.9 °C and the daily energy consumption of the HRV, preheaters, supply air heater and total system was 0.55 kWh, 3.19 kWh, 2.56 kWh and 6.30 kWh, respectively. Although two months of monitoring data is available, one week will be presented for clarity purposes. Figure 2 shows the energy consumption of the preheaters, supply air heater and the HRV, as well as the HRV inlet and outdoor temperature during the first week of December. The energy data provided in **Error! Reference source not found.** consists of a 10-minute moving average of 1-minute data.

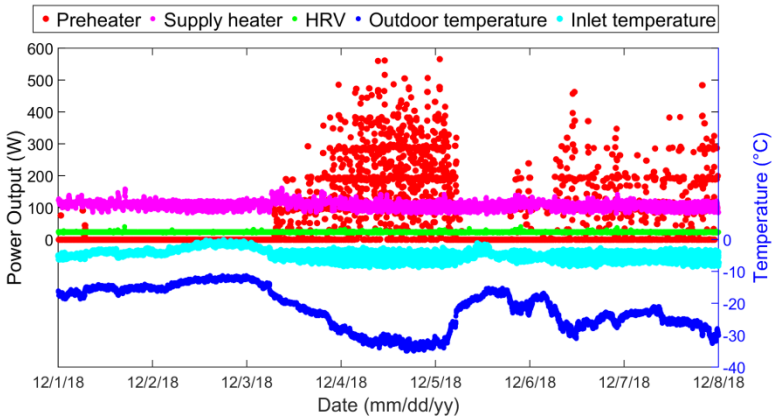

Figure 2: Energy consumption of system from December 1st to December 8th, 2018

Figure 2 shows that the supply air heater constantly provided heat to maintain a supply air temperature of 18 °C. Since the building was unoccupied during this time, the DCV system mainly operated in fan speed 1, the lowest available fresh air supply rate. The HRV operated in defrost mode a few times in January, even though preheat was available. Figure 2 shows that the preheater control strategy was functional, however, minimal preheat was utilized during the week. Figure 2 shows that as a result of an increase in outdoor air temperature, the preheaters stopped supplying heat to the fresh air. The increase in outdoor air temperature did not exceed -10 °C. However, the fresh air was warmed up in the duct before the HRV, by the space. This was a result of the low 13.5 L/s flow rates and 3 m length of fresh air duct, which was found to heat fresh air by as much as 12 °C, without the utilization of preheat.

Sensible recovery efficiency (SRE) monitoring

While monitoring the system the average outdoor temperature was -26.9 °C, the average SRE of the HRV was 72%, the average SRE of the system was 35% and the system delivered fresh air 98% of the time. Although two months of monitoring data is available, one week will be presented for clarity purposes. Figure 3 shows the SRE of the system and HRV, and the HRV inlet and outdoor temperature for the first week of December. The SRE of the system and HRV was not calculated when the HRV was operating in defrost mode (i.e., when there was no fresh air flow) to ensure validity and accuracy of the calculations, instead these times are displayed as 0 in Figure 3.

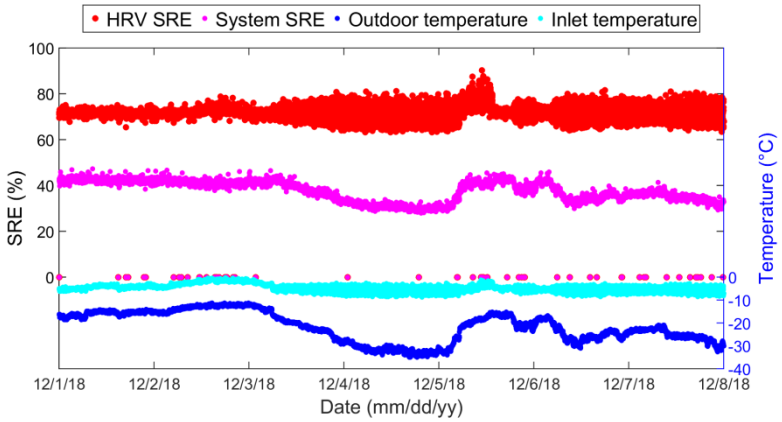

Figure 3: SRE of the system and HRV from December 1st to December 8th, 2018

Figure 3 shows a significant drop in the SRE of the system from the SRE of the HRV. The large discrepancy is a result of the extremely low temperatures causing the preheaters to consume more energy and the fresh air duct to gain excessive energy from the space. The SRE of the system constantly changes, whereas the SRE of the HRV is fairly constant. The SRE of the system is dependent on the outdoor temperature and follows an almost identical trend. As a result of the preheaters, the SRE of the HRV is not dependent on the outdoor temperature. Instead, it is dependent on the inlet temperature. Since the preheaters are unable to maintain a steady inlet temperature for the HRV, the calculated SRE for the HRV is scattered. Although the SRE of the HRV is dependent on the inlet temperature, this dependency is likely exaggerated as a result of the simultaneous measurements in the HRV, when in fact there is a time delay between the supply temperature that results from the inlet and return temperatures.

5 DISCUSSION

5.1 CO_2-based DCV system performance

The two-day testing of the DCV system proved the viability of using low-cost CO_2 sensors for ventilation control. Further testing will be conducted in the future to develop a more in-depth analysis of the DCV system's performance. However, the two-day study sufficed for testing the demand-control strategies and showed that if occupants were to enter the space temporarily, sufficient fresh air would be supplied to them.

The detection of occupancy is important for health reasons; accurate occupancy detection allows for appropriate fresh air supply rates to the space. In addition to health reasons, occupancy detection is important for energy conservation purposes. Ventilation systems can be made more efficient by selecting the defrosting method based on the DCV system. For example, recirculating indoor air to defrost the core of the HRV temporarily stops fresh air from being supplied to the space, which is undesirable during high occupancy. However, it utilizes less energy than preheating, and thus at times when no or less fresh air is required during no or low occupancy, recirculation could be utilized instead of preheating. On the other hand, when occupancy is detected, preheat can be used to ensure that continuous fresh air is being supplied to the occupants, albeit, with slightly higher energy consumption.

CO_2-based DCV for residential applications has had negative findings as a result of low occupant densities being difficult to detect. However, CO_2-based DCV seems more appropriate in the Arctic as housing can become much more overcrowded in the north, negating this reported disadvantage. Moreover, the necessity to supply fresh air on demand is exemplified in Arctic locations given the extreme, cold temperatures.

5.2 System energy and SRE performance

The system operated well during the two-month period. The preheaters consistently maintained HRV inlet temperatures around -5 °C, resulting in 3.19 kWh of heating energy used daily. However, the HRV entered defrost 2% of the time, which shows that the preheaters allowed the inlet temperature to drop below -5 °C as the HRV's defrost settings initiate at temperatures below -5 °C. The reason the HRV entered defrost was likely a result of unsteady control of the preheaters, which allowed for the inlet temperature to fluctuate slightly. The energy consumed by the HRV was minimal, at 0.55 kWh per day. To limit drafts of cool air in the building, the supply air was heated to 18 °C after the HRV, resulting in 2.56 kWh of daily heating energy use. The total energy associated with tempering and supplying the building's fresh air was 4.49 Wh per L/s during the two-month testing period.

When the HRV was supplying fresh air to the building it was, on average, recovering sensible energy at a rate of 72%. However, as a result of electrical consumption and duct gains from the space, the SRE of the system was, on average, only 35%. Although insulation was installed on the fresh air duct, the fresh air was able to be heated by as much as 12 °C, without the utilization of preheat, as a result of the low, 13.5 L/s flow rates and 3 m length of R4 insulated duct. This finding indicates an even stronger need for proper installation of exceptional insulation on the fresh air duct, in cold climates. In addition, better insulation should be installed on the exhaust duct to avoid unnecessary system losses, which will be exemplified in extremely cold climates. Moreover, the lengths of the ducts that penetrate through the building envelope should be limited as much as possible.

5.3 Comparison of system performance of recirculation vs. preheat

It is often believed that preheating consumes an excessive amount of energy when compared to other defrosting methodologies and is not economical for long cold seasons (Nasr, Kassai, Ge, & Simonson, 2015). However, a

theoretical analysis can be conducted to show that the energy consumption of preheating vs. recirculating for frost prevention is relatively comparable.

Consider an outdoor air temperature of -25 °C, fresh air supply rate of 10 L/s, HRV effectiveness of 67%, and a return and supply temperature of 20 °C. Without preheating, the HRV would warm up the outdoor air to 5 °C. To get the air to 20 °C, the supply air heater would have to deliver approximately 150 W of heat to the air. On the other hand, if the air is preheated to -10 °C, the preheater would also consume approximately 150 W. The HRV will then warm up the air to 10 °C, requiring an additional 100 W to be added to the air to get it to the desired 20 °C setpoint. Therefore, without preheat, the system consumes roughly 40% less energy. However, this does not consider the additional costs of defrosting the core via increased fan speeds and heat lost from the space to the core of the HRV during recirculation. Thus, the energy savings of frost prevention via recirculation are slightly lower than calculated.

Although it is recognized that preheat as a frost prevention technique causes the ventilation system to consume more energy than other defrost methodologies, the purpose of the ventilation system is to provide the building and occupants with fresh air. Relying on recirculation as a defrost technique can cause the fresh air supply to be cut off for a high proportion of time, which goes against the purpose of the ventilation system. For periods of high occupancy or humidity, preheating is an important technique to ensure sufficient fresh air can be delivered to a space to maintain acceptable indoor air quality. Preheat also has the added benefit of reducing or avoiding cycles of condensation and/or frost build-up and removal from the core, which could result in less required maintenance.

Another strong reason for using preheating instead of recirculation is that it reduces noise from the ventilation system. For periods of moderate occupancy, it is likely more preferred by occupants for the fan to operate at a medium speed rather than the maximum. If preheat is not used, the HRV fan speed will alternate to a maximum flow rate during recirculation, which can occur every 23 minutes for this particular HRV model. These frequent alternations in fan speed and high levels of noise during recirculation could lead occupants to disable their ventilation system. Additionally, the system will be operating continuously at the highest fan speed at higher occupancy levels, whereas the system utilizing preheat would be able to run continuously at lower fan speeds at the same occupancy levels.

6 CONCLUSION

A demonstration house in Iqaluit was equipped with a ventilation system consisting of a heat recovery ventilator, two preheaters and a supply air heater. The system was instrumented with thermocouples, an airflow sensor and current transducers to perform long term monitoring of the system performance. While long term monitoring is ongoing, short term experimental data regarding the functionality of the ventilation system is provided in this paper. The two-day testing of the DCV system proved the viability of using low-cost CO_2 sensors for ventilation rate control. While two-months of monitoring the system displayed the systems functionality in the extreme cold. Contrary to some belief that preheating is an undue approach for frost prevention in heat/energy recovery ventilators, this research finds that this method can be acceptable if controlled well. It is important to design building systems as efficient as possible; however, these systems must function and effectively serve their purposes. In the case of a ventilation system, the purpose is to provide fresh air to the building and defrosting reduces the proportion of time when fresh air is delivered, possibly to an unacceptable point to the occupants.

7 FUTURE WORK

The development of efficient and comfortable residential buildings in cold climates will continue to be a focus of future work. In the future, measured indoor CO_2 concentrations could be used to influence the setpoint of the preheaters. When the building is unoccupied, the preheaters could be disabled, and a lower effective fresh air delivery rate could be accepted, i.e., permit recirculation. When occupants are present, the preheater setpoint would be re-enabled, avoiding the need for defrost cycles. This would restore the effective fresh air delivery rate to the supply air rate, i.e., avoid recirculation. This strategy allows for heat recovery to be maximized and the energy consumption minimized, as the air will only be preheated when the space is occupied, and frosting is possible. Additionally, future experiments will be conducted to build on the theoretical comparison of preheating and recirculating for frost prevention and evaluate the system performance at various fresh air flow rates. The energy

consumption of each methodology per unit of fresh air delivered to the space will be utilized to measure the performance of each technique at the respective operational fresh air rate.

REFERENCES

Alonso, M. J., Liu, P., Mathisen, H. M., Ge, G., & Simonson, C. (2015). Review of heat/energy recovery exchangers for use in ZEBs in cold climate countries. *Building and Environment*, 228-237.

Banister, C., Swinton, M., Moore, T., Krys, D., & Macdonald, I. (2018). Energy consumption of an energy efficient building envelope in the Canadian Arctic.

Cho, W., Song, D., Hwang, S., & Yun, S. (2015). Energy-efficient ventilation with air-cleaning mode and demand control in a multi-residential building. *Energy and Buildings*, 6-14.

Cleveland, M. A., & Schuh, J. M. (2010). Automating the Residential Thermostat Based on House Occupancy. *Systems and Information Engineering Design Symposium.* Charlottesville.

Guyot, G., Sherman, M. H., & Walker, I. S. (2018). Smart ventilation energy and indoor air quality performance in residential buildings: A review. *Energy & Buildings*, 416-430.

Kim, Y.-J., & Park, C.-S. (2009). Comparative Study of Ventilation Strategies in Residential Apartment Buildings Under Uncertainty. *Eleventh Internation IBPSA Conference.* Glasgow.

Kovesi, T., Zaloum, C., Stocco, C., Fugler, D., Dales, R. E., Ni, A., . . . Miller, J. D. (2009). Heat recovery ventilators prevent respiratory disorders in Inuit children. *Indoor Air*, 489-499.

Kragh, J., Rose, J., & Svendsen, S. (2005). Mechanical ventilation with heat recovery in cold climates. *Proceedings of the 7th Symposium on Building Physics in the Nordic Countries*.

Liu, P., Alonso, M. J., Mathisen, H. M., & Simonson, C. (2016). Performance of a quasi-counter-flow air-to-air membrane energy exchanger in cold climates. *Energy and Buildings*, 129-142.

Minich, K., Saudny, H., Lennie, C., Wood, M., Williamson-Bathory, L., Cao, Z., & Egeland, G. (2011). Inuit housing and homelessness: results from the International Polar Year Inuit Health Survey 2007-2008. *International Journal of Circumpolar Health*, 520-531.

Nasr, M. R., Fauchoux, M., Besant, R. W., & Simonson, C. J. (2014). A review of frosting in air-to-air energy exchangers. *Renewable and Sustainable Energy Reviews*, 538-554.

Nasr, M. R., Kassai, M., Ge, G., & Simonson, C. J. (2015). Evaluation of defrosting methods for air-to-air heat/energy exchangers on energy consumption of ventilation. *Applied Energy*, 32-40.

Nielsen, T. R., Rose, J., & Kragh, J. (2009). Dynamic model of counter flow air to air heat exchanger for comfort ventilation with condensation and frost formation. *Applied Thermal Engineering*, 462-468.

Roszler, S. (2005). *Building skills: a construction trades training facility fo rthe eastern Canadian Arctic.* Massachusetts Institute of Technology.

Zeng, C., Liu, S., & Shukla, A. (2017). A review on the air-to-air heat and mass exchanger technologies for building applications. *Renewable and Sustainable Energy Reviews*, 753-774.

Long-term performance and resiliency testing of a dual core energy recovery ventilation system for the Arctic

Boualem Ouazia[*1], Chantal Arsenault[1], Yunyi Li[1], Michael Brown[2], Gerald Kolsteren[2], and Christopher Chisholm[2]

1 National Research Council Canada
1200 Montreal road, Building M-24
Ottawa, Ontario K1A 0R6, Canada
**Corresponding author: Boualem.ouazia@nrc-cnrc.gc.ca*

2 Polar Knowledge Canada
Canadian High Arctic Research Station (CHARS)
1 Uvajuq Road, PO box 2150
Cambridge Bay, Nunavut X0B 0C0, Canada

ABSTRACT

The Arctic environment is challenging for housing ventilation and heating systems. Energy consumption and demand for space heating for northern remote community residential buildings are very high. Airtight built northern homes require energy efficient and effective ventilation systems to maintain acceptable indoor air quality and comfort, and to protect the building envelope from moisture damage. Conventional single core heat/energy recovery ventilation systems are a mature and proven technology for modern and energy-efficient Canadian homes; but underperform and are plagued with problems when operating in high-arctic locations north of 60°. Their performance achieved to date has been inadequate due to equipment failures (freezing of cores, etc.) and their defrost strategies can undermine ventilation rate requirement and the energy saving. Inadequate ventilation in northern communities contribute to poor indoor air quality, and this contribute to increased cases of serious health issues; tuberculosis and asthma, specifically asthma infections among young Inuit children. To overcome these issues, a novel dual core energy recovery system designed with two heat exchangers could address frost protection by periodically directing warm air through one core of the two cores while outside air gains heat from the other. By employing a cycling heat exchanger, frost doesn't have a chance to form, and one heat exchanger is always delivering conditioned air to the space. This paper presents results from a repeated side-by-side winter testing using NRC's twin research houses comparing whole house performance of a reference house equipped with a single core ERV with a test house equipped with a dual core energy recovery unit, and some results from the long-term monitoring of the technology deployed in a triplex located in Canada's Arctic. The side-by-side testing was undertaken in the NRC twin-houses research facility of the Canadian Centre for Housing Technology (CCHT) over four weeks in winter 2019. In comparison with a conventional single core ERV, the dual core energy recovery system had much higher apparent sensible effectiveness, a difference of 12 percentage points, and had much higher apparent total effectiveness, a difference of 9 percentage points. The dual core design showed no sign of frost problems after 4 weeks of testing and continued to provide outdoor air throughout winter days without stopping to defrost, unlike the conventional single core ERV which had to spend up to 7.5 hours defrosting per day. It also provided a higher supply air temperature (up to 3°C) to indoor and the house with dual core ERV had a whole-house heating and ventilation energy saving of 5% over the winter testing period. The long-term performance testing was undertaken in a mechanical room of a triplex on the Canadian High Arctic Research Station (CHARS) in Cambridge Bay (Nunavut) to assess the resiliency and durability of the technology in harsh cold climate. The monitoring period included two heating seasons 2017-18 and 2018-19 and showed that the dual core technology was very frost-tolerant and capable of withstanding temperature below -40°C for long periods without deteriorating its thermal and ventilation performances, and providing constant and continuous supply of outdoor air. The proven performance and resiliency to harsh Arctic operating conditions demonstrates that the dual core design ERV is a solution to ventilation of northern housing, in providing continuous ventilation that will improve indoor air quality and health in Northern communities.

KEYWORDS

Residential, Ventilation, ERV, Dual core, Arctic

1 INTRODUCTION

The extremes of the Arctic climate pose severe challenges on housing ventilation and heating

systems. In the Arctic and northern regions of Canada, the average temperature during winter is -25°C or below, and many northern homes are heated to above 25°C resulting in significant loads on systems (Zaloum, 2010). As a part of the overall effort to reduce space heating requirements, homes are built air tight to reduce infiltration or exfiltration heat losses. However, airtight homes require energy efficient, effective and resilient ventilation systems to maintain acceptable indoor air quality and comfort, and to protect the building envelope from moisture damage. A balanced mechanical ventilation system with heat or energy recovery is an ideal way to meet both National Building Code (NBCC, 2015) and the ventilation requirements of standards (ANSI/ASHRAE 62.2, 2016, CAN/CSA-F326-M91, 2013). Heat recovery ventilation (HRV) and energy recovery ventilation (ERV) are well-known and effective methods to improve energy and ventilation efficiency of residential heating, ventilating and air conditioning (HVAC) systems when designing energy efficient homes, because they allow adequate outdoor ventilation air without excessive energy consumption. The performance of the conventional single core HRV/ERV units achieved to date has been inadequate due to equipment failures and conventional problems created by the formation of frost in heat exchangers. Freezing of cores can cause partial or full blockage of air flow passages, increased pressure drop through the heat exchanger or decreased airflow rate, increased electrical power consumption for the fans, decreased heat transfer rate between the two airstreams, and cold draughts within the space due to low supply air temperatures [Rafati et al., 2014). Conventional single core HRV/ERV units are usually equipped with frost protection systems such as pre-heating of outdoor air or recirculating of return air across the heat exchanger and back into the supply air to the house. These defrost strategies can undermine ventilation standards (ventilation rate requirement not being met) and the energy saving of the HRV or ERV unit. Surveys conducted in Canada's north found that at present, there are no HRVs/ERVs specifically designed, manufactured and certified to meet rigorous requirements for operation in the North [CMHC, 2016). This paper presents some results from a project employing an innovative dual core design energy recovery system and its applicability for housing in the Arctic. One alternative technology that can overcome problems faced by conventional single core HRV/ERV units installed in extreme cold climates is a dual core ERV unit designed to address frost protection concerns and provide continuous ventilation.

2 SINGLE CORE HEAT OR ENERGY RECOVERY VENTILATORS

The exhaust air heat loss is a considerable part of the total heat loss in cold climates. Since typical ventilation systems introduce unconditioned outdoor air and exhaust conditioned indoor air, there is potential for energy savings by incorporating heat transfer between the two airstreams. This could be achieved by installing a heat or energy recovery ventilator. The core of a conventional HRV or ERV is constructed of a series of parallel plates that separate the exhaust and outdoor air streams. These plates are typically fabricated of metal or plastic. They simultaneously supplies and exhausts equal quantities of air to and from a house while transferring heat or energy between the two air streams. The heat or energy is transferred from exhaust to outdoor air stream during the heating season. The heat exchange process is reversed during cooling season. In cold winter conditions, the condensation inside the core can freeze and block the exhaust air stream. HRVs or ERVs are designed to protect against freezing and clear the core of ice going automatically into defrost mode. This is typically accomplished by a damper that closes of the outdoor air supply and allows warm indoor air into the HRV to heat the core and melt any ice on the exhaust side. Frost control strategies for conventional single core HRV/ERV are presented in Table 1 (Rafati et al., 2014). When operating in defrost mode, there is a temporary discontinuation in the indoor-outdoor air exchange. Another common method of defrost is to use a pre-heater, which is more applicable in colder climates where more

constant defrost is required. Pre-heater increase energy costs and reduces the heat recovery efficiency of the HRV or ERV.

Table 1: Frost control strategies for HRVs/ERVs

Technique	Control Parameter	Capital Cost	Operating Cost	IAQ	Pros	Cons
Preheating the outdoor air	Temperature	↔	↑	↑	Simple, used as frost prevention	Not economical in cold climates
Reducing or closing the supply air	Flow rate	↔	↔	↓	Simple	Increases infiltration
Recirculating warm exhaust air	Flow rate	↔	↔	↓	Simple, high flow rate enhances the melting process	No supply of outdoor air
Bypassing the supply air partially or fully	Flow rate	↔	↑	↔	Simple	Reduced energy recovery

In North America, residential HRVs and ERVs are tested and rated using a standard test procedure that is described in the certification standard for heat/energy recovery ventilators (CSA-C439-09, 2015). The certification standard identifies a standard indoor condition of 22°C, 40% RH and an outdoor (supply) temperature of 0°C. The standard also provides a test procedure for an optional low temperature performance/endurance test. The duration of the low temperature test is 72 hours, with the performance ratings determined from measurements recorded during the final 12 hours. The standard allows for the low temperature test to be performed at any temperature specified by the manufacturer; although the industry has since adopted -25°C as the default temperature. Rating tests are performed at the air flows specified by the submitter. As noted above, cooling tests and a low temperature performance/endurance test are optional.

3 DUAL CORE ENERGY RECOVERY SYSTEM

A dual core ERV unit comes equipped with a regenerative cyclic dual core heat exchanger, based on the cyclic storage and release of heat in the corrugated plates alternately exposed to exhaust and intake air. It includes a supply and exhaust fan and two plate heat exchangers, which act as heat accumulators. In between the cores is a patented damper section which changes over every 60 seconds to periodically direct warm air through one of the two cores while outside air gains heat from the heated plates in the other core. In front of each fan is a filter section to filter the air. The schematic of the dual core unit is presented in Figure 1, where OA is the outdoor air, EA is the exhaust air to outdoor, RA is the return air from indoor and SA is the supply air to indoor.

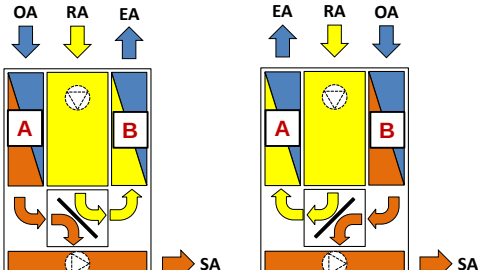

Figure 1. Principle of function – sequence 1 (left) and sequence 2 (right)

The description of the two sequences of the unit is as follow. During *Sequence 1*, exhaust air charges Core B with heat from exhausted warm air from indoors and Core A discharges heat to the supply air: During *Sequence 2* the exhaust air charges Core A with heat from exhausted warm air from indoors and Core B discharges heat to the supply air. The damper is controlled by two internal thermostats (thermostat 1 in the supply air is set to 15°C and thermostat 2 in the

exhaust air is set to 20°C) to ensure that comfortable air delivery temperatures are achieved under all conditions. When the exhaust air temperature is below 20°C, the unit runs in energy recovery mode (cycling every 60 seconds). When the exhaust air temperature is above 20°C and the supply air temperature is higher than 15°C, the unit runs in free cooling mode (cycling every 3 hours). Finally, when the exhaust air temperature is above 20°C and the supply air temperature is below 15°C, the unit runs in energy recovery mode until the supply air temperature exceeds 15°C, at which point it will revert to free cooling mode.

4 SIDE-BY-SIDE TESTING

The Canadian Centre for Housing Technology's (CCHT) twin research houses shown in Figure 2 (left) were used for the comparative side-by-side testing between a dual core ERV (installed in the test house) and a conventional single core ERV (installed in the reference house). These houses are typical 2-storey wood-frame houses with their characteristics presented in Figure 2 (right). The twin-house research facility features a "simulated occupancy system". The simulated occupancy system, utilizes home automation technology to simulate human activity by operating major appliances (stove, dishwashers, washer and dryer), lights, water valves, fans, and other sources simulating typical heat gains. The schedule is typical of activities that would take place in a home with a family comprised of two adults and two children. Electrical and water consumption are typical for a family of four. The heat given off by humans is simulated by two 60 W (2 adults) and two 40 W (2 children) incandescent bulbs at various locations in the house. The CCHT research houses are equipped with a data acquisition system (DAS) consisting of over 250 sensors and 23 metering devices (gas, water and electrical). A computer reads the sensors every 5 minutes and provides hourly averages. Meter data and a few other measurements are recorded on a 5 minute-basis. The DAS captures a clear history of the house performance in terms of temperature, humidity and energy consumption.

Feature	Details
Construction Standard	R-2000
Liveable Area	210 m^2 (2260 ft^2), 2 storeys
Insulation	Attic: RSI 8.6, Walls: RSI 3.5, Rim joists: RSI 3.5
Basement	Poured concrete, full basement. Floor: Concrete slab, no insulation. Walls: RSI 3.5 in a framed wall. No vapour barrier.
Garage	Two-car, recessed into the floor plan; isolated control room in the garage
Exposed floor over the garage	RSI 4.4 with heated/cooled plenum air space between insulation and sub-floor.
Windows	Low-e coated, argon filled windows Area: 35.0 m^2 (377 ft^2) total, 16.2 m^2 (174 ft^2) South Facing
Air Barrier System	Exterior, taped fiberboard sheathing with laminated weather resistant barrier. Taped penetrations, including windows.
Airtightness	1.5 air changes per hour @ 50 Pa (1.0 lb/ft^2)
Furnishing	Unfurnished

Figure 2. CCHT twin houses (left) and their characteristics (right)

The side-by-side testing involved first benchmarking the houses for set operating conditions and simulated occupancy, using existing high efficiency single core ERVs originally installed in each house. The test house was modified by installing the dual core ERV unit in the basement and making no other modifications to the house, then programing the dual core unit to match the single core ERV supply and exhaust airflows in the reference house. Finally, whole-house performance was monitored for four weeks during the 2019 heating season.

5 EXTENDED MONITORING IN THE ARCTIC

The dual core ERV unit tested in the Lab and the twin housing has been deployed and monitored in Canada's Arctic to prove its long-term performance and resilience. The monitoring in the Arctic was structured around instrumenting one dual core ERV installed in a mechanical room of a Triplex on CHARS campus in Cambridge Bay (Nunavut) with a dedicated data logging system, as shown in Figure 3. The extended monitoring was undertaken with measurement of the following parameters; 4 relative humidity and temperature probes installed at four locations (supply inlet and outlet, and exhaust inlet and outlet) in the duct, two differential pressure

through each heat exchanger, two multipoint air flow sensors were installed in-duct to measure supply and exhaust airflows, and three signals to monitor damper position and fan speeds.

Figure 3. Triplex and deployed dual core ERV on CHARS campus in Cambridge Bay, NU

6 RESULTS AND DISCUSSION

6.1 Ventilation

The typical daily single ERV and dual core ERV supply and exhaust airflows are presented in Figure 4 for a cold day with an outdoor temperature below -10°C (January 17th 2019). The plot of the single core ERV airflows excluded the defrost cycle as shown on the left plot of Figure 4. Both single and dual core ERVs presented balanced supply and exhaust flows. The dual core ERV showed no sign of frost problems and continued to provide outdoor air throughout a cold testing day (outdoor temperature ranging between -20.1°C and -11.8°C) without stopping to defrost, unlike the single core ERV that had to spend hours defrosting as shown in the plot on the left side of Figure 4.

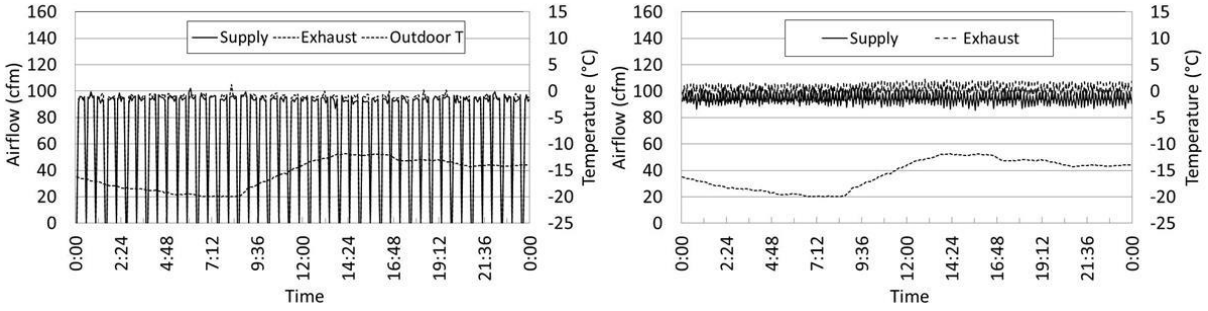

Figure 4. Measured airflows from side-by-side testing, Reference House (left) and Test House (right)

The single core ERV uses a defrosting method presented in Table 2. The amount of time the single core ERV spent in defrost mode ("defrost time") per day during the winter test period is presented in Figure 5 along with the minimum and mean outdoor temperatures.

Table 2. Defrosting method

Outside Temperature [°C]	Defrost Cycle Defrost [min] / Operating [min]
Warmer than -10	No Defrost
-10 to -27	7 / 25
-27 and less	10 / 22

The duration of the de-icing cycle is strongly dependent on outdoor temperature. The single core ERV spent between 0 and 7.5 hours per day defrosting, during which time it did not provide fresh air to the reference house. Due to its design, the dual core ERV did not require defrosting, and provided fresh air continuously throughout the winter test period. The frequent defrost cycles of the single core ERV led to a reduced volume of outdoor air being delivered to the reference house, leading to under ventilation of the reference house (compared to the test

house), and it not meeting the ventilation requirement. This is a common situation for single core HRV/ERV units installed in extremely cold climates.

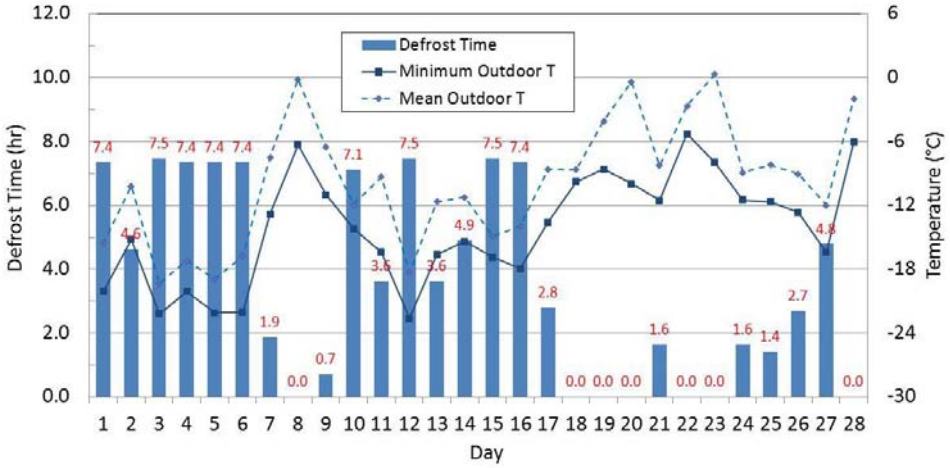

Figure 5. Daily single core ERV defrost time during winter 2019 testing

6.2 Supply air temperature

The temperature of the supply air from the single and dual core units to indoors (to return air plenum upstream of the furnace) measured during the side-by-side testing (January 17 to February 12, 2019) are presented in Figure 6 with the measured outdoor temperature. The supply outlet air temperature from the single core ERV in reference house varied between 7.5°C and 18.8°C and the test period mean value was 13.5°C. The supply outlet air temperature from the dual core ERV in test house varied between 9.9°C and 19.8°C and the mean value over the same testing period was 16.1°C. The mean temperature of the supplied air to the house was higher by 2.6°C from the dual core ERV than the single ERV. This was due to the much higher ASE of the dual core unit (higher than 80%) from regenerative cyclic dual cores. The supply air to the test house required less tempering by the furnace to meet the thermostat set point of 22°C, which means that a dual core unit provided more pre-heating than a single core ERV and would lead to additional energy savings.

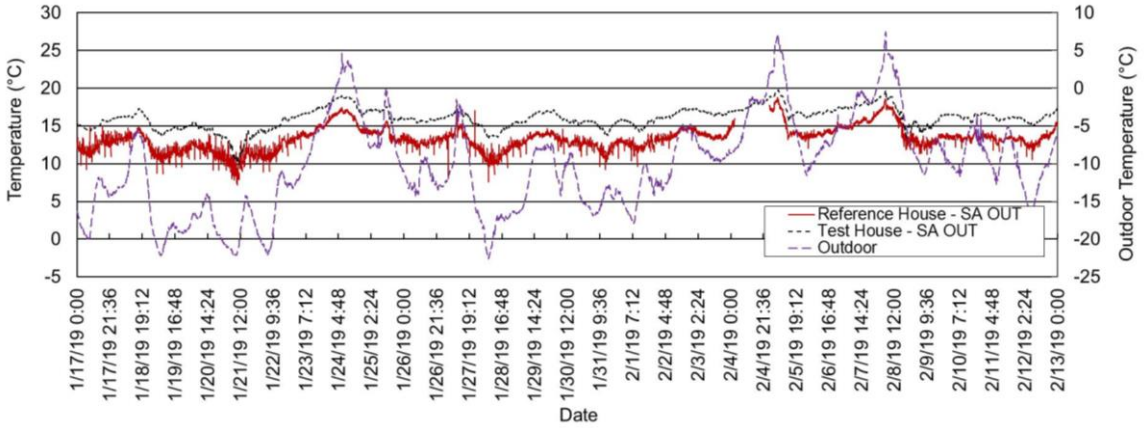

Figure 6. Measured supply air temperature from side-by-side testing

6.3 Effectiveness

The performance of the innovative dual core ERV unit was primarily determined by its apparent sensible effectiveness (ASE) and apparent total effectiveness (ATE) as described in ASHRAE testing standard [6] and Canadian testing standard [7], airflow characteristics, supply air

temperature, frosting occurrence and whole-house energy consumption. The measured temperatures and relative humidities across the tested unit were used to calculate the ASEs and ATEs. The ASE and ATE were calculated using Equation 1.

$$\varepsilon = \frac{m_s(X_{SI} - X_{SO})}{m_{min}(X_{SI} - X_{EI})} \quad (1)$$

where, ε is the sensible, latent, or total heat effectiveness. X is either the dry-bulb temperature, T, humidity ratio, w, or total enthalpy, h, respectively, at the supply inlet and outlet and at the exhaust inlet of the unit. m_s *is the* mass flow rate of the supply and m_{min} *is the* minimum value of either mass flow rate of the supply or mass flow arte of the exhaust.

The calculated ASE and ATE of a single core ERV and dual core ERV using data obtained from the side-by-side testing in the CCHT twin houses are presented in Figure 7 and Figure 8. The calculated ASE of the dual core ERV (installed in the test house) had a mean value of 85.1% and ranged from 63.2% to 99.4%. The single core ERV (installed in the reference house) had a mean value of ASE of 73.2% during the same testing period of four weeks and ranged from 62.3% to 94.2%, a mean difference over reference house of 12 percentage points. The ATE, which takes into account the latent heat of the single core ERV, varied between 58.4% and 91.4%, with a mean value of 69.9%. The dual core ERV unit had an ATE between 64.16% and 98.9%, with a mean value of 79.1%, a mean difference over the reference house of 9 percentage points. These results show clearly that the dual core ERV unit over perform the conventional single core ERV in terms of sensible and totale efficiencies.

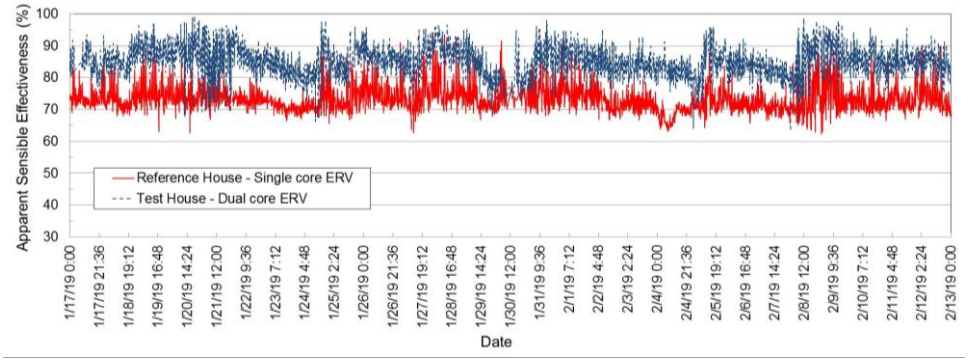

Figure 7. Calculated apparent sensible efficiencies

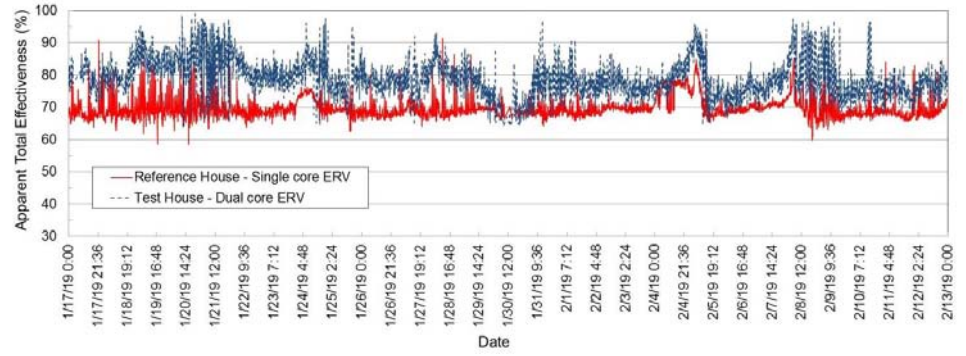

Figure 8. Calculated apparent total efficiencies

6.4 Energy

Changes in whole-house energy performance due to the innovation were addressed through comparison of the test house performance (with dual core ERV) to that of the reference house (with single core ERV). The recorded whole-house energy consumption of both reference house and test house included; heating energy consumption (furnace natural gas consumption), furnace fan electrical consumption, single core ERV fan electrical consumption and dual core

ERV fan electrical consumption. The expected test house energy consumption in benchmark configuration (i.e. operating the benchmark ERV equipment, both houses with single core ERV) was first calculated, and from this the overall energy savings when the dual core ERV system was operating in the test house was calculated. Savings were calculated by subtracting the measured test house (with dual core ERV experiment consumption from the calculated test house (with single core ERV) benchmark consumption, as shown in Figure 9. The average whole-house energy saving when operating the dual core ERV compared to the benchmark ERV over the period of the study was 5.0%.

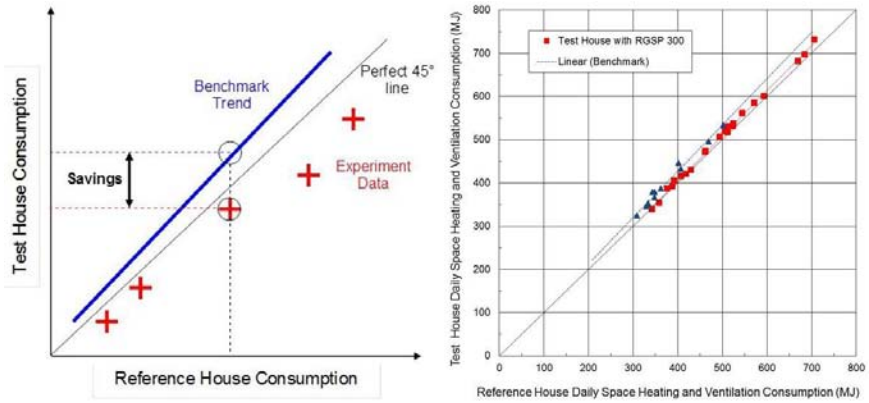

Figure 9. Energy saving, method (left) and results (right)

6.5 Performance in the Arctic

The monitoring of the dual core ERV in the Arctic started June 2017 and continue to April 2020, already tested over two winters 2017-18 and 2018-19. Through this extended field monitoring in the Arctic, we were able to verify the performance and resilience of the technology in a real northern environment, advance confidence in northern applications of this new technology and collect the operational evidence that northern housing corporation and stakeholders require deploying this innovative technology in the north.

The measured supply and exhaust airflows from extended monitoring of the dual core ERV unit in Cambridge Bay (Nunavut) are shown in Figure 10**.** The plot was for the week of December 31st, 2018 – January 6th, 2019 where the outdoor temperature was between -19°C and -36°C. The dual core ERV was slightly unbalanced, experienced very few air exchange reductions, but in general was frost-tolerant, capable of withstanding an outdoor temperature as low as -35°C without deteriorating its ventilation performance (no significant supply flow reduction) and able to provide a continuous supply of outdoor air.

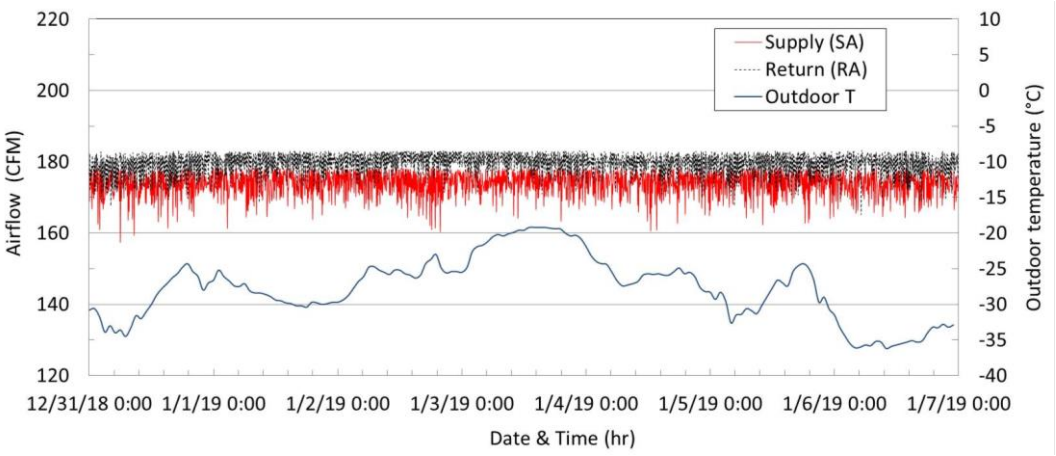

Figure 10. Measured airflows from extended monitoring in Cambridge Bay (Dec. 31, 2018 to Jan. 06, 2019)

A typical measured air temperature at the inlet/outlet of supply and exhaust airstreams and outdoor temperature are presented in Figure 11. The plot was for the week of December 31st, 2018 – January 6th, 2019. The supply air temperature from the dual core ERV to indoor ranged from 14.5°C to 19.2°C with a mean value of 17.2°C. The cycling of the outdoor air (OA) and exhaust air (EA) is caused by cycling damper periodically directing warm air and exhaust air through one of the two heat exchangers. The exhaust air temperature was below 20°C, the unit ran in energy recovery mode with damper cycling every 60 seconds, periodically directed warm air through one of the two cores while outside air gained heat from the heated plates in the other core.

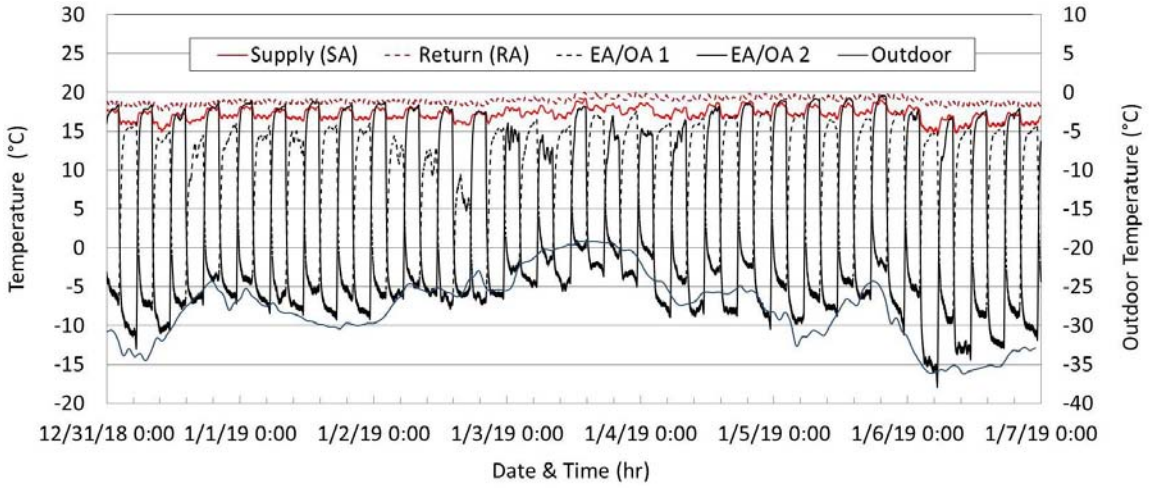

Figure 11. Measured air temperatures in Cambridge Bay (Dec. 31, 2018 to Jan. 06, 2019)

7 CONCLUSIONS

In comparison with conventional single core ERV, the dual core ERV designed with two parallel regenerative heat exchangers and a controlled cycling damper had higher ASE (a difference of 12 percentage points) and ATE (a difference of 9 percentage points) from side-by-side testing than the single core ERV. It was more frost-tolerant, showing no signs of frost problems, and was capable of withstanding an outdoor temperature down to -23°C without degrading its thermal performance, and provided a continuous supply of outdoor air without stopping to defrost, unlike the conventional single core ERV which spent many hours per day (up to 7.5 hours) defrosting during cold days (outdoor temperature below -10°C) of the side-by-side testing. The dual core technology was capable of providing air at the supply outlet at a temperature 2.6°C higher than the air temperature supplied by a single core ERV. Its incorporation into the test house showed a saving in heating and ventilation energy consumption of approximately 5% (24.6 MJ/day). The ongoing extended monitoring of the dual core ERV in the Arctic over already two heating seasons (2017-18 and 2018-19) showed that the technology was frost-tolerant and capable of withstanding temperature below -40°C for long periods without deteriorating its thermal and ventilation performances, and provided continuous supply of outdoor air. The proven performance and resiliency to harsh Arctic operating conditions demonstrated that the dual core design ERV is a viable solution for ventilation of northern housing that will improve indoor air quality and health in Northern and remote communities.

8 ACKNOWLEDGEMENTS

This research project on "*Air Ventilation Systems for housing in the Arctic"* was supported by funding provided by NRCan's Panel of Energy Research & Development (PERD) and NRC's

Arctic Program. The research team is grateful to the Canadian Centre for Housing Technology (CCHT) team (Heather Knudsen, Patrick Tardif and Daniel Lefebvre) for giving us access to the twin houses and technical support, and to Canadian High Arctic Research Station (CHARS) team (Robert Cooke, Matt Wallace and Bryan Vandenbrink) for giving us access to the triplex in Cambridge Bay (Nunavut) and technical support in the Arctic.

9 REFERENCES

ANSI/ASHRAE 62.2 (2016). Ventilation for acceptable indoor air quality. ASHRAE, Atlanta, GA.

CAN/CSA-C439 (2015). Standard Laboratory Methods of Test for Rating the Performance of Heat/Energy Recovery Ventilators. Canadian Standard Association.

CAN/CSA-F326-M91 (2013). Residential Mechanical Ventilation Systems. National Standard of Canada, Canadian Standards Association, Rexdale, Ontario.

CMHC (2016). Research Report: Survey of HRV/ERV performance issues in Canada's near north and far north.

National Building Code of Canada (NBCC) (2015).

Rafati, M.N., Fauchoux, M., Besant, R., Simonson, C. (2014). A review of frosting in air-to-air energy exchangers. Renewable and Sustainable Energy Reviews, 30, 538-554.

Zaloum, C. (2010). Technical advice to task force on Northern mechanical ventilation equipment design and testing. Ottawa, Canada Mortgage and Housing Corporation.

Experimental investigation of frost formation on air to air counter flow heat exchanger in air handling unit and climatic influence on dry, wet, frost operation condition

Michal Pomianowski*, Rasmus Lund Jensen, Dzhanan Osman Metin, Nils Kristian Kure Rasmussen and Diana State

Aalborg University
Thomas Manns Vej 23
Aalborg, Denmark

ABSTRACT

The work presented in this paper investigates frosting problem on high efficient air to air counter flow heat exchanger. The presented investigation consists of two main activities.
Firstly, experimental tests on a counter flow plate heat exchanger in a climatic chamber have been performed to better understand under which exhaust condition frost starts forming in the exit region of the exhaust port. A special experimental set-up to investigate frost formation on the air to air heat exchanger was developed. Set up consists of a cold chamber that could maintain freezing temperatures and a warm chamber imitating indoor condition. Both temperature and relative humidity could be controlled. Experimental tests have indicated that the temperature gradient on the exhaust port is very significant. While in one part of the exhaust port occurs frosting the other part has still positive temperature. Observed temperature difference across exhaust port was up to 6.8 ^{O}C. From the experiments, it is observed that the frost starts to form when mean temperature of the exhaust air is at 0°C. Furthermore, it can be stated that even though frost formation depends greatly on the outdoor temperature, the level of indoor humidity also plays some role in location of frost formation.
Secondly, the percentage of operation condition of the exchanger – dry, wet and frost - has been analyzed for four geographical locations – Southern Scandinavia, Central Europe, Southern Germany and Austria, and Scotland. Regarding indoor conditions, data has been created using dynamic simulation software BSim with loads representative for classrooms and offices. This investigation has shown that for the respected regions risk of frosting can occur but would not be higher than 5.8 % of operational time in the most severe investigated location. Finally, for the investigated high heat recovery efficient exchanger, it is discovered that heat recovery efficiency drops below required by Ecodesign 73% when outdoor temperature would drop below -14 °C.

KEYWORDS

Air to air heat exchanger, frost formation, climate chamber, dry, wet, frost operation

1 INTRODUCTION

Legal requirements regarding energy efficiency and rational exploitation of the energy resources [1] are getting stricter in countries with cold climates due to high space heating consumption [2] and rising environmental awareness. For space heating in cold climates is consumed between 40-60 % of the total building energy demand [2] and 30-60 % from the total space heating consumption is due to heating up the incoming fresh air [3]. For that reason, from January 2018 the minimum demand for heat recovery in ventilation units has been increased from 67 % to 73 % by [4] in EU Member States. Although there is a big energy saving potential in ventilation units with high heat recovery, in cold climates it can lead to frost formation on the plate surface of the warm side. During winter, when the plate surface temperature falls below freezing point, there is a risk of condensation and frost formation. Consequently, when the highest heat recovery efficiency is needed, it cannot be provided. Frosting leads to reduction

of the heat recovery efficiency, increase in pressure drop in the return airflow channels, higher electricity consumption for the fans, and draught in the space due to low supply air temperature. In case of severe frosting, there is also a risk of damage of the heat exchanger [5] [6]. Even though the topic has raised concerns for the past 35 years, the published papers related to frost formation in heat exchangers are limited. Frost formation has been detected by many researchers, but only few have investigated frost prevention or defrost methods. Due to that, literature states that the problem of frost is still unresolved and even the most commonly used defrost methods face challenges in cold climates [5].
In counter flow heat exchangers, the supply and return airstreams flow along each other, separated by thin aluminum/ plastic plates. Heat is transferred from the return to the supply air. The heat exchanger is sealed, and therefore, the two flows are unmixed. They are very popular in the northern countries because of their reliability, long service-life due to no moving parts, operation with unmixed fluids and high heat recovery efficiency [6].
The purpose of the paper is:

- To investigate where and under what condition frost starts forming in the exit region of the exhaust port.
- To investigate percentage of operation condition of the exchanger – dry, wet and frost for preselected geographical locations – Southern Scandinavia, Central Europe, Southern Germany and Austria, and Scotland.

Additionally, the influence of different indoor conditions on frost formation and temperature distribution across the ports is analyzed. Loads typical for office and class room are investigated.. Furthermore, the required minimum heat recovery efficiency is analyzed taking account for efficiency in freezing conditions.

2 METHODOLOGY

2.1 Experimental investigation

A schematic plan view of the experimental setup is shown in Fig.1. The setup is designed to achieve outdoor temperatures corresponding to winter conditions and typical indoor conditions. It consists of an insulated shipping container divided into two environmental chambers: a warm chamber where the temperature and humidity is controlled by a duct electric heater and a humidifier and a cold chamber where the temperature is controlled by a cooling unit.
To achieve indoor conditions of a typical classroom or office, the temperature for the extracted air should be maintained at 22 °C. For that reason, a circular electric duct heater is used to maintain the air temperature at the desired set point [7]. The heater that is installed in the warm chamber is connected to a fan, that has the purpose to circulate the air in the room so that stratification does not occur. Moreover, in terms of control, the fan also helps to better control the temperature, as the sensor is measuring a uniform temperature of the well mixed chamber. In Fig.1, the placement of the fan (no. 4) and the duct with the electric heater (no. 5) is shown. Both are placed at the ceiling level and the duct has a 90-degree bend towards the floor, so that the flow does not influence the extraction.
The humidification system consists of a domestic water pump (no. 1), a water heater (no. 2) and the Vapac Minivap Humidifier (no. 3), as shown in Fig. 1. The pump provides water to the small water heater. After the water gets heated it is pumped to the humidifier, where it gets heated further until it boils. The steam is released into the ventilation duct after the circular

electric duct heater (no. 5) [8]. The desired relative humidity that should be maintained stable is in the range 25 - 65 %.
The cooling unit consists of an evaporator placed in the cold chamber. The compressor and condenser are placed outside - on the roof of the container. The evaporator is connected to a duct system (no. 4) that provides cold air to the room, without influencing directly the air that is being supplied to the warm room. In addition, a circular electric duct heater is installed (no. 5) to defrost the evaporator and to maintain the ambient temperature in case higher set points are desired. The cooling unit is shown in Fig. 1.

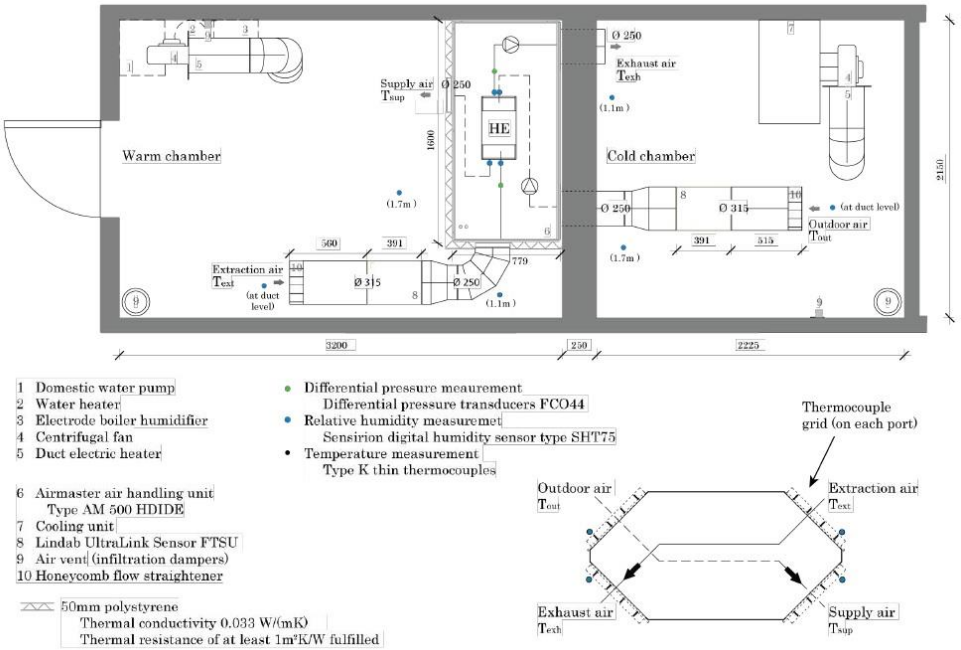

Figure 1: Schematic of test chamber layout and equipment.

The decentralized ventilation unit is placed in the warm chamber and it is tightly connected to the cold chamber through ducts. The operation principle of the unit is as following: air at outdoor conditions (tout) moves by suction in the ventilation unit passing through the heat exchanger and then is provided to the room (tsup), while the warm extraction air (text) moves by suction in the ventilation unit passing through the heat exchanger and then is exhausted (texh) on the cold side, as shown in the 3D drawing in Fig 2.

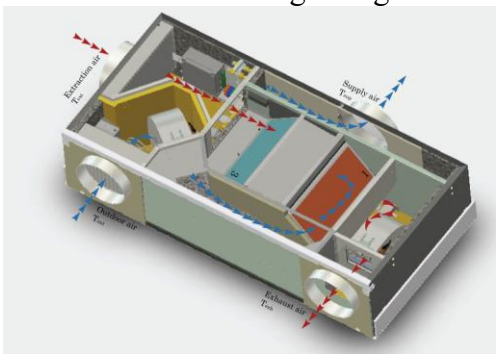

Figure 2: 3D graphic of tested heat exchanger in air handling unit.

The parameters that are measured in order to test the performance of the heat exchangers are air temperature, relative humidity, air flow and differential pressure. For both air streams of the heat exchanger, the parameters are measured at different locations, as shown in Fig. 1.

The air temperature is measured with a type K thermocouples (Chromel /Alumel) that are gold coated, through sputtering technique. In this case, radiative heat exchange that can influence the measurement is decreased by using coating [9]. The temperature is measured with four grids of thermocouples on all ports of the heat exchanger. Since there is a risk of uneven temperature distribution, 16 temperature measuring points are distributed evenly across each grid. The recommended number of temperature sensors for rectangular ducts is 9, according to ASHRAE [10].
The relative humidity is measured with a Sensirion digital humidity sensor type SHT75. In the ventilation unit, as shown in Fig. 1, the relative humidity is measured with the Sensirion sensor. To monitor the temperature and relative humidity in the two chambers, 3 sensors are used, in each room.
The airflow rate is measured on both airstreams: for the outdoor - supply airstream the measurement is performed on the outdoor side, while for the extraction - exhaust airstream the measurement is performed on the extraction side, see Fig. 1. The device used is an UltraLink FTSU with a diameter of 315 mm and a length of 391 mm. The flow is measured with and angled ultrasonic beam that provides high accuracy.
The pressure difference is measured using a pressure transducer FCO44 manufactured by Furness Control Limited that has a range of ±500 Pa. The measurement is performed on the extraction - exhaust side (warm side) of the heat exchanger. The aim is to detect pressure drop increase caused by frost growth on the plates of the exhaust side of the heat exchanger. Pressure taps are drilled on the surfaces on which flow passes, therefore measuring static pressure.
Before running the experiments, analysis on indoor relative humidity - outdoor temperature relation was done. The purpose was to find out which indoor air relative humidity ranges (for typical indoor loads) correspond to outdoor negative temperature during the working hours. The findings from this investigation helped defining the relative humidity ranges that need to be tested for the frost formation experiments. The results were obtained using dynamic simulation tool BSim and provide the relation between the indoor relative humidity (at 22 °C) and outdoor temperature. For classrooms and offices, indoor relative humidity does not reach above 41 % and 37 %, respectively, for the outdoor temperatures below 0 °C. This relative humidity limits are the same for the investigated locations – Gothenburg (Southern Scandinavia), Groningen (Central Europe), Innsbruck (Sounth Germany and Austria) and Leuchar (Scotland). The last location, Leuchar, has almost no negative temperatures, therefore this location and the area it is representing (Scotland) can be considered as out of risk for frost formation.

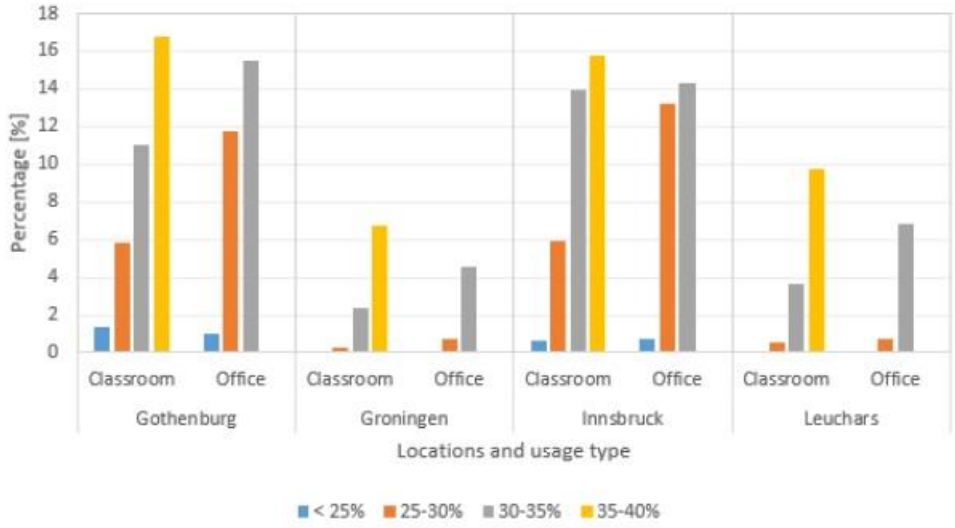

Figure 3: Percentage of critical indoor relative humidity ranges from the total number of yearly working hours with 22 °C as indoor temperature.

The pre-defined extraction temperature for the tests is 22 °C and the relative humidity range is determined based on the results presented in Fig 3. Due to the discovered not sufficient cooling capacity on the cold site of the chamber the indoor temperature had to be decreased from 22 °C and as consequence indoor relative humidity had to be adjusted to compensate for that. Table 1 presents both indoor conditions as scheduled based on loads and climate analysis (temperature and relative humidity) and equivalent indoor conditions for lowered temperature matching the available cooling capacity that corresponds to indoor temperature at 22 C.

Table 1: Frost formation test condtion - actual tested and equivalant to them.

Experiment	Equivalent conditions to ind. temp. 22 °C	Indoor scheduled conditions
Condition 1	22 _C and 22 %	RH 22 _C and 22 % RH
Condition 2	16 _C and 38 %	RH 22 _C and 27 % RH
Condition 3	15 _C and 46 %	RH 22 _C and 30 % RH
Condition 4	16 _C and 58 %	RH 22 _C and 40 % RH

2.2 Operation condition – dry, wet, frost

Due to the varying outdoor conditions during the year, the dynamic temperature efficiency of the heat exchanger is looked into. It is compared with the minimum heat recovery efficiency required by the Ecodesign [4], which is currently at 73 %. Moreover, the duration of the periods with dry, wet and frost operation conditions for the heat exchanger are also investigated for the chosen four geographical locations. Yearly (hourly) data for outdoor, supply, extraction and exhaust air temperature, based on BSim simulations and validated software to calculate performance of investigated heat exchanger is analyzed. Only working hours are investigated. Depending on whether the exhaust temperature is below the dew point for extraction air or below the frost limit temperature of 0 °C, the periods with dry, wet and frost conditions are sorted.

The temperature efficiency for the different conditions is calculated using the formula in equation 1. When it comes to calculating the efficiency under freezing conditions, the supply temperature is calculated taking into account the maximum possible heat transfer before frost occurs. The formula which is used can be seen in equation 3.

$$\eta_t = \frac{t_{sup} - t_{out}}{t_{ext} - t_{out}} \; [-] \tag{1}$$

t_{out} - outdoor air temperature [°C]
t_{sup} – supply air temperature [°C]
t_{ext} – extraction air temperature [°C]

$$Q_{\max possible} = m_h \cdot (h_{ext} - h_{exh'}) \tag{2}$$

$$t_{sup,frost} = \frac{Q_{\max possible}}{m_c \cdot Cp_c} + t_{out} \; [°C] \tag{3}$$

$Q_{max\ possible}$ – maximum possible heat flow based on freezing point threshold [W]
m_h – mass flow rate on the warm side [kg/s]
m_c – mass flow rate on the cold side [kg/s]
h_{exh} – exhaust air enthalpy [kJ/kg]
$h_{exh'}$ – freezing limited threshold air enthalpy [kJ/kg]
Cp_c – air heat capacity on the cold side [(J*kg)/K]

3 RESULTS

3.1 Experimental investigation

Fig. 4 shows the test conditions on an I-x diagram. The lines for the different conditions indicate the air treatment process and correspond to mean temperature values. During the experiments, it was observed that for all the relative humidity levels, frost on the exit region of the exhaust side appears at 0 °C mean exhaust temperature. Still, it is not possible to tell whether frost starts to form inside the heat exchanger sooner. Moreover, significant temperature gradient on the exhaust port for all the test conditions was observed. As a consequence on the heat exchanger exhaust port that is below 0 °C is formed frost and the part with positive temperatures remains free of frost.

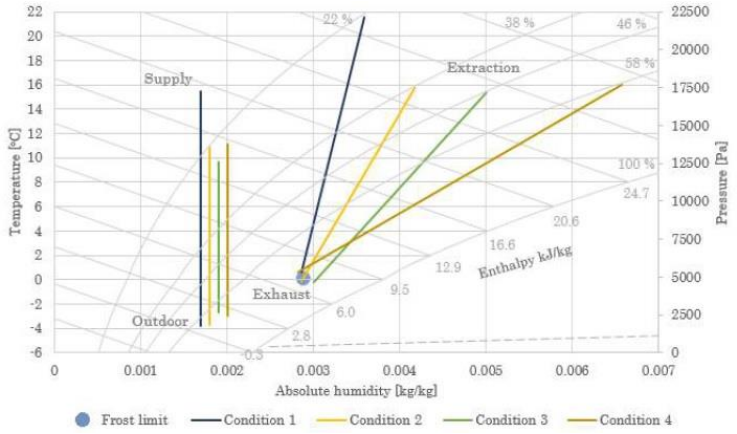

Figure 4: Frost formation test conditions presented on an I-x diagram - for mean temperatures.

Figure 5: Temperature gradient on exhaust port for all 4 test condition.

During the experiments it was observed that due to the low level of water vapour in the air with 22 % relative humidity (condition 1), frost formation started without condensation. The water vapour in the air turned directly into a very thin layer of frost on the coldest part of the port. The reason for that is because the dew point for that condition (-0.8 °C) is below the triple point (0 °C). The triple point (gas-liquid-solid point) corresponds to the pressure at 0 °C below which liquid cannot exist [11]. Due to low vapor content in the air it would take more time for frost to build up with relative humidity ranges corresponding to dew point value of below 0 °C.

The low temperature on the outdoor port (intake) decreases the temperature on the top part of the exhaust port. Additionally, the temperature gradient increases when there is more

condensation, as with condition 4 (58 % relative humidity). Compared to the other cases, the temperature at the bottom of the port is significantly higher. In this case, the greater condensation rate keeps the plate surface warmer and maintains higher air temperature values.

Depending on the relative humidity, frost formation starts in different places on the port. With low relative humidity (22 %), it starts on the coldest part of the port (the top side). With higher relative humidity, it starts a bit lower, though still in a spot with a local negative temperature value. As condensation occurs, it drips down along the plates of the heat exchanger. The more condensation there is, the lower on the port the condense droplets reach before they freeze. Fig. 6 indicates where frost starts forming with the different relative humidity ranges. The frost formation location is marked with a red circle to indicate where frost starts to occur.

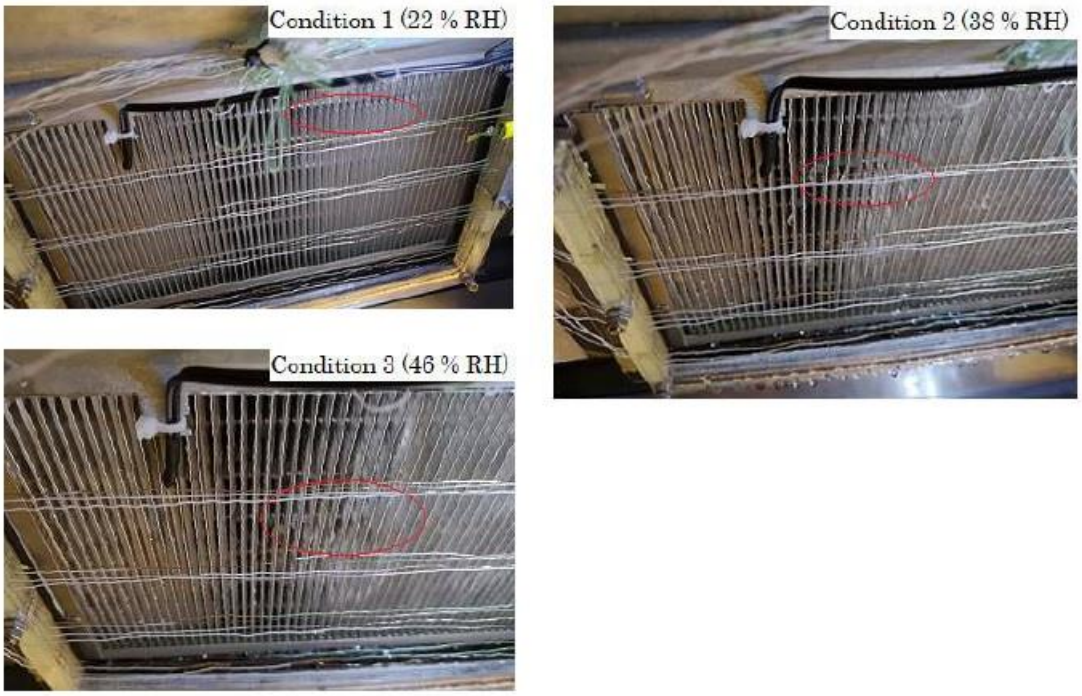

Figure 6: Frost formation location at 1-3 condition.

3.2 Operation condition – dry, wet, frost

Yearly (hourly) data for outdoor, supply, extraction and exhaust air temperature, based on BSim simulations and outcomes from validated software to calculate performance of investigated heat exchanger, was analyzed for three selected locations with the frost risk. Only working hours were investigated. Depending on whether the exhaust temperature is below the dew point for extraction air or below the frost limit temperature of 0 °C, the periods with dry, wet and frost conditions are sorted. When it comes to calculating the efficiency under freezing conditions, the supply temperature was calculated taking into account the maximum possible heat transfer before frost occurs.

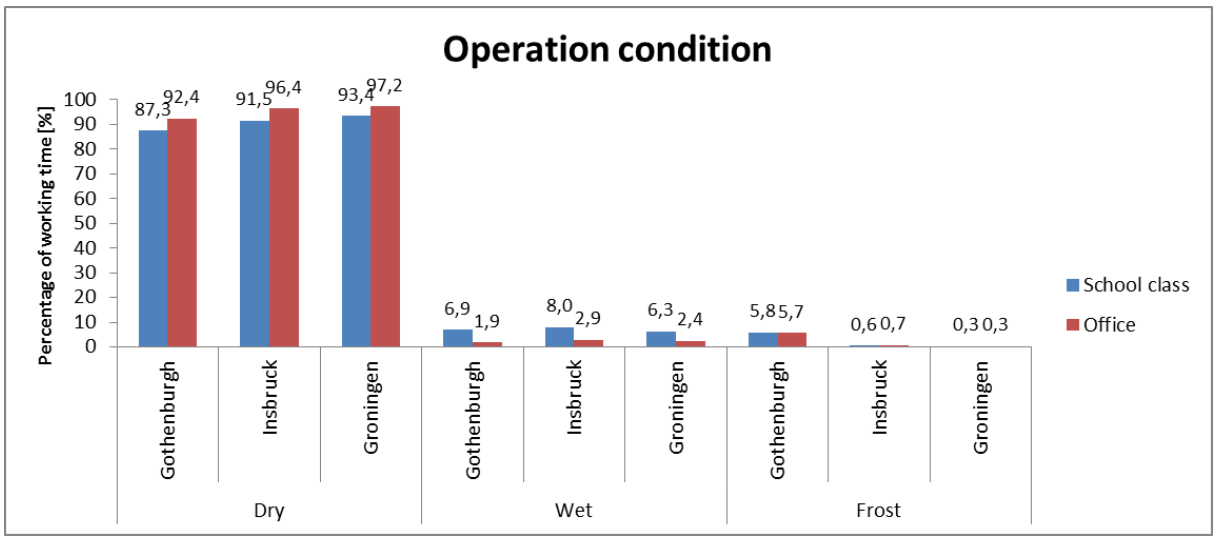

Figure 7: Operation condition – dry , wet, frost.

4 CONCLUSIONS

The focus of this paper is the frost formation on air to air counter flow heat exchangers. To investigate this topic an experimental setup with a decentralized ventilation unit containing the high efficiency counter flow heat exchanger was built and equipped with sensors. The setup consists of a cold room that could maintain freezing temperatures and a warm room where both temperature and relative humidity could be controlled.
To observe when frost occurs in the heat exchanger, a video camera was mounted inside the ventilation unit as well as pressure sensors to measure the pressure increase on the warm side of the heat exchanger. Even though frost formed, it was not possible to detect it with pressure increase nor with the camera. Therefore, visual inspection of frost formation was necessary.
From the experiments it can be concluded that the mean temperature of the exhaust air is 0 °C when frost occurs on the heat exchanger. Furthermore, it can be stated that even though frost formation depends greatly on the outdoor temperature, the level of indoor humidity also plays a significant role. It has been observed that the temperature gradient of the exhaust port can be 6.8 °C from warmest to coldest area. The coldest point is the area close to the outdoor port and the gradient is greater when indoor humidity is also higher.

At last, the risk of frost in the investigated geographical locations has been evaluated. Investigation indicates that the highest risk of all investigated areas is in Southern Scandinavia, but still do not exceed approx. 6% of working time. In the rest of the investigated locations the risk of frost formation is insignificant.

5 REFERENCES

[1] Andrzej Jedlikowski, S. Anisimov, J. Danielewicz, M. Karpuk, and D. Pandelidis. Frost formation and freeze protection with bypass for counter-flow recuperators. International Journal of Heat and Mass Transfer, 108:585–613, May 2017.

[2] Natasa Nord. Building energy efficiency in cold climates. Reference Module in Earth Systems and Environmental Sciences, December 2017.

[3] Jesper Kragh, J. Rose, and S. Svendsen. Mechanical ventilation with heat recovery in cold climates. Proceedings of the 7th Symposium on Building Physics in the Nordic Countries, January 2005.

[4] Ecodesign. Regulation (EU) No 1253/2014 with regard to ecodesign requirements for ventilationunits.
https://ec.europa.eu/energy/sites/ener/files/documents/implementation_guide_ventilation_units_with_cover.pdf, 2016.

[5] Mohammad Rafati Nasr, M. Fauchoux, R. W. Besant, and C. J. Simonson. A review of frosting in air-to-air energy exchangers. Renewable and Sustainable Energy Reviews, 30:538–554, February 2014.

[6] Sergey Anisimov, A. Jedlikowski, and D. Pandelidis. Frost formation in the cross-flow plate heat exchanger for energy recovery. International Journal of Heat and Mass Transfer, 90:201–217, November 2015.

[7] VEAB Heat Tech AB. CV Circular electric duct heaters. https://veab.com/documents/cv/broschyr/CV_VEAB_Heat_Tech_GB.pdf, 2018.

[8] Vapac Humidification Ltd. Minivap Humidifier Model DV4.
https://www.vapacparts.com/manuals/vapac-dv4-owners-manual.pdf, 2006.

[9] Larsen, Olena Kalyanova, F. Zanghirella, M. J. Heiselberg, Perino, and R. Lund. Measuring Air Temperature in Glazed Ventilated Facades in the Presence of Direct Solar Radiation. Proceedings of Roomvent 2007 FINVAC, January 2007.

[10] ASHRAE. ASHRAE Standard - Standard Method for Temperature Measurement. American Society of Heating, Regrigerating and Air-conditioning Engineers, Inc., 2001.

[11] A. og Aage Bredahl Eriksen. Termodynamik - teoretisk grundlag, praktisk anvendelse. Nyt Teknisk Forlag, 2017.

Efficiency of heat recovery ventilation in real conditions: feedback from several measurement campaigns

Sébastien Pecceu*[1], Samuel Caillou[1]

1 Belgian Building Research Institute (BBRI)
Avenue P. Holoffe 21
1342 Limelette, Belgium
**Corresponding author: sebastien.pecceu@bbri.be*

ABSTRACT

Heat recovery ventilation (HRV) is one of the usual techniques (next to demand controlled) to reduce the energy impact of ventilation in buildings. For a given air change rate, the energy savings of HRV are in the first place dependent of the heat-exchanger efficiency, usually measured in standardized laboratory conditions. However, many other factors can have an impact on the overall system performance in practice. Through three different projects in the last years, BBRI had the opportunity to monitor about 15 systems during several months, allowing to (try to) evaluate their performance in real operation.

Before going into the details of the measurement campaigns, this paper gives a short overview of the various factor that can negatively affect the actual energy recovery compared to what could be expected from the heat-exchanger efficiency only. This overview will help to interpret and explain the monitoring results.

What concerns the monitoring campaigns, the temperature in the 4 flows of the heat exchangers were measured with a few minutes time step during several months. The frequency and the duration of the measurement allowed to compute the supply and exhaust efficiencies and derive statistics (mean efficiency, …), but also to observe more localized events like the triggering of frost-protection systems. In the two first campaigns, these temperatures were measured directly within the ventilation groups at the vicinity of the heat exchanger so that the measurements were not impacted by the heat released by the fans. For the last measurement campaign, the temperatures were measured in the ducts just before and after the ventilation unit. The outcomes of this measurement campaign are twofold:

- For most installations, the average efficiencies of the ventilation units (as computed in the Belgian EP calculation) are between 70% and 90%. These are quite in line with the declared product values (as published on www.epbd.be).
- Some of the results in the first two campaigns showed that a non-negligible temperature heterogeneity exists in some of the fluxes leading to biased evaluation of the efficiency. Furthermore, the monitored data of the third campaign showed less noise of unexplainable variations than in the first two campaigns. Even if the sample was quite reduced for this last campaign (5 installations), the trend seems quite clear and we would thus recommend this measurement method for future measurement campaigns.

KEYWORDS

Heat Recovery Ventilation, Efficiency, Field measurements

1 INTRODUCTION

Heat Recovery Ventilation (HRV) is one of the common techniques to reduce the energy footprint of ventilation in buildings in Belgium and more generally in northern Europe. This footprint becomes more and more important (in relative terms) as the requirements on building insulation become stronger with the evolution of the various building energy performance regulations.

The heat quantity that can be recovered through a HRV unit depends in the first place of the heat-exchanger efficiency, usually measured in lab conditions following appropriate standards. On-site operation is however different from idealized lab measurement, and one can expect a performance gap between lab and on-site measurements. A lot of factors can negatively impact the real heat recovery such as flow unbalance, leaks, insulation defect, fouling, etc. (Rouleta C. , 2001), (Rouleta C. A., 2001-2). Some field experiments at the building scale also show that the energy savings due to HRV seem lower than predicted by the applicable EPB calculation methods (Janssens, 2017).

In this context of questioning over real HRV energy efficiency, we had the opportunity to perform measurements on about 15 HRV units operating on-site in the frame of various research projects. Our target was first to verify if the efficiency claimed by the manufacturers were reached or approached in practice, and second to have an overview on how these systems were operating in practice: are their efficiencies constant? ; do the frost-protection correctly trigger ? ; is there any sign of malfunctioning ? ; etc.

2 HRV EFFICIENCY

2.1 Effectiveness, efficiency and temperature ratios

Strictly speaking, the effectiveness of a heat exchanger (ε) is the ratio of the actual transferred heat over the theoretical transferred heat if the heat-exchanger was perfect (counter-current and with infinite heat-exchange area). This maximum transferrable heat is determined by the side with the lower thermal capacity $\left(q_m C_p\right)_{min}$ (with q_m the mass flow [kg/s] and C_p the specific heat of the circulating fluid). If the fluid is the same on both sides of the heat exchanger, the lower mass flow determines the maximum heat transfer.

Applied to heat recovery ventilation, one can write:

$$\varepsilon = \frac{q_{m,eta}(T_{eta} - T_{eha})}{\min(q_{m,eta}, q_{m,sup})(T_{eta} - T_{oda})} = \frac{q_{m,sup}(T_{sup} - T_{oda})}{\min(q_{m,eta}, q_{m,sup})(T_{eta} - T_{oda})}$$

with q_m the mass flow rates and T the temperatures of the flows, with the following suffixes (illustrated in Figure 1).

- eta : ‘extracted air’
- eha : ‘exhausted air’
- sup : ‘supply air’
- oda : ‘outdoor air’

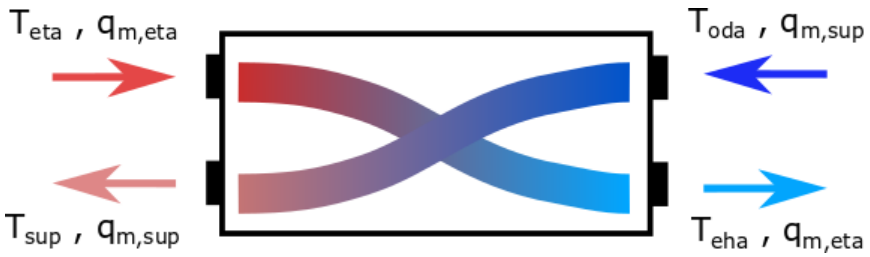

Figure 1 Flow and temperatures at the bounds of a heat exchanger or a HRV unit

In the context of (heat recovery) ventilation, the term "efficiency" is generally used instead of effectiveness; the term of "ventilation effectiveness" being used to quantify the quality of the air renewal. Further in this paper, we'll use the term "efficiency" (written η) to refer to the fraction of the heat that is recovered.

If the flows are perfectly balanced, the efficiency simplifies a temperature ratio that can be computed on both sides (supply or exhaust) of the heat exchanger.

$$\eta_{sup} = \frac{T_{eta} - T_{eha}}{T_{eta} - T_{oda}} = \eta_{eha} = \frac{T_{sup} - T_{oda}}{T_{eta} - T_{oda}} = \eta$$

Theoretically, η_{sup} and η_{eha} are perfectly equal, but generally not in practice for several reasons due to the ventilation unit itself or due to global ventilation system (flow balance, heat released by the fans, etc.).

In the field of ventilation, efficiency is often calculated using temperatures only, not considering these perturbating effects. Further in this paper, η_{sup} and η_{eha} will be named temperature ratios to make a clear distinction with the real efficiency.

2.2 Factors influencing HRV Energy efficiency at system or building scale

The heat exchanger efficiency is the most influencing factor on the energy that is recovered. However, a lot of other factors can have a significant impact. The global energy efficiency at system or building scale is in practice different from the lab-measured efficiency of the heat-exchanger or the unit. The most influencing factors are shortly described here below.

Flow imbalance

The flow imbalance between supply and exhaust is always negative regarding the energy efficiency at building or system scale. The energy that is recovered in the heat exchanger is limited by the smallest flow rate.

The flow imbalance is then compensated by extra in- or exfiltrations through the building envelope (whose energy loss is not compensated by the heat recovery).

- If the supply is higher that the exhaust (overpressure), more hot air leaves the building by exfiltration
- If the exhaust is higher than supply (underpressure), more cold air enters the building by infiltration

In both cases, this leads to an extra energy loss. Roughly, if the highest flow rate is considered as reference, the recovered energy decreases linearly with the imbalance. This is illustrated by

a theoretical calculation using a e-NTU model in Figure 2. The temperature of the low flow side increases and tends to 1 as the flows become unbalanced. This determines the maximum transferable heat quantity as described in the formal definition of "effectiveness". However, if considering that the flows are in any case balanced at the building scale (by extra in- or exfiltrations), the recovered energy decreases with imbalance. The real 'energy efficiency' is the temperature ratio of the high flow side (that decreases with imbalance).

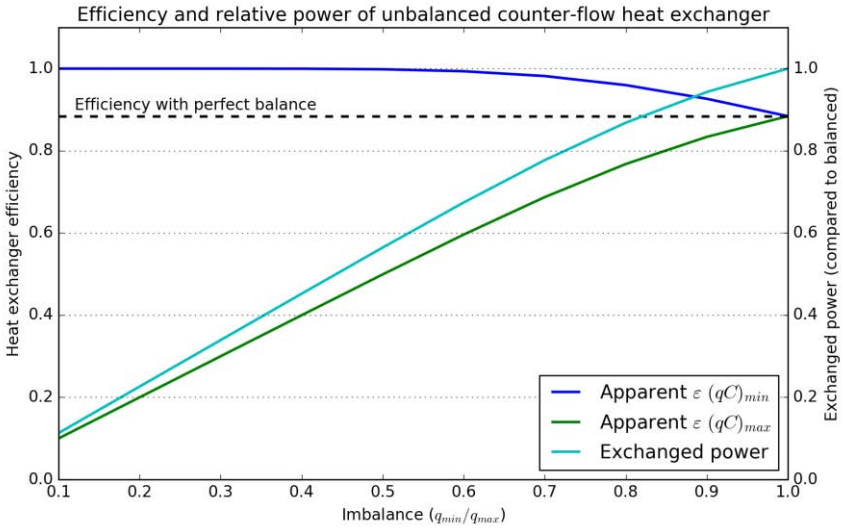

Figure 2 Temperature ratios (left axis) and exchanged energy (right axis) for an imbalances heat-exchanger.

Leaks

Duct leaks or leaks within the ventilation unit either lead to imbalance at the heat exchanger or lead to extra in- or exfiltrations. In both cases, this is an energy loss.

Absence or lack of duct insulation

There are globally two temperature levels: hot side (supply and extract) and cold side (exhaust and outdoor). Part of the recoverable energy is lost if there are:

- Non isolated cold ducts within heated spaces
- Non isolated hot ducts in unheated spaces

For a typical residential installation (250 m³/h, main duct of 200 mm diameter), we computed that 3 to 4 m non isolated ducts can reduce the heat recovery potential of 10%.

Thermal insulation of the unit

The energy balance and efficiency calculations suppose that the system is closed and that there is no heat loss towards outside, which is naturally not perfectly the case in practice.

Building dynamics and temperature difference between zones

Some research works (Janssens, 2017) (Faes, 2016) showed through theoretical models and thermal dynamic simulations that all the energy recovered by a HRV unit does not necessarily lead to a reduction of the heating demand.

Without entering into the details, these demonstrations rely on the fact that all the rooms are not necessarily heated at the same temperature and that the heat recovery is not always synchronous with the presence of occupants and the heating needs (in the latter case, energy recovery 'looses' part of its interest).

2.3 HRV in Belgian EP-regulations

To be used in the EP calculations in Belgium, the heat-exchangers or ventilation units must be tested following a specific test method (Méthode PER - Annexe G - Détermination du rendement themrique d'un récupérateur de chaleur), mostly following NBN EN 308 standard.
During the test, even in lab conditions, there are several factors influencing the apparent efficiency:

- The perfect flow balance (see §2.2) is very difficult to reach
- The heat released by the fans changes the temperatures levels
- Leakages or transmission heat losses of the units

It has been shown (Caillou, 2009) (Caillou, 2012) that most of these issues tend to increase the supply efficiency and to decrease the exhaust efficiency. That's why a specific test method and calculation procedure has been developed in the frame of the Belgian energy performance regulations. One of the key points of the method is that the final efficiency from the test is the average of apparent η_{sup} and η_{eha}.

This way of doing was demonstrated as robust to the various uncertainties listed above (Caillou, 2009), (Caillou, 2012) and representative of the HX or HRV unit true efficiency in balanced conditions. Further in this document, the mean efficiency (mean of 'supply' and 'exhaust') will be named η_{epbd} in reference to Belgian EP-regulation.

To illustrate this rationale, Figure 3 re-uses the example of imbalanced flow with a theoretical model. Until an unbalance of 20% (flow rate ratio of 0.8) , making an average of the supply and exhaust efficiency remains very close to the 'balanced' efficiency of the heat-exchanger. This rationale can be applied to other perturbations that have a symmetric effect like the fan heat for example.

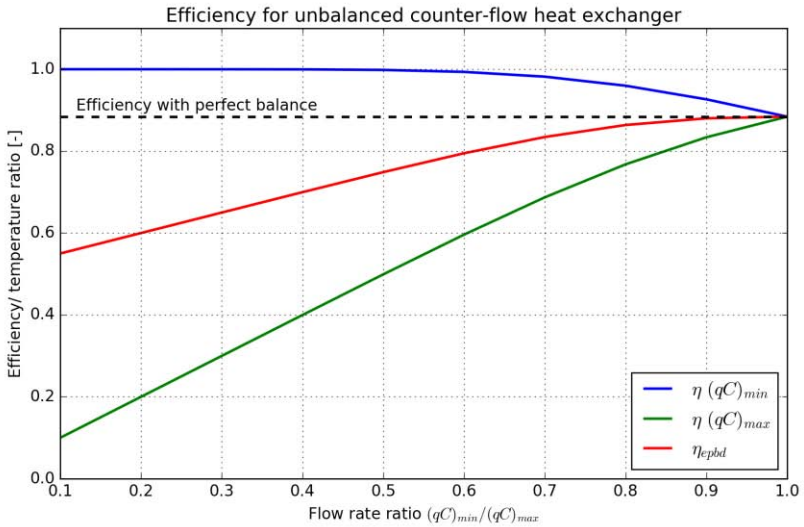

Figure 3 Theoretical example of apparent efficiency for imbalanced heat-exchanger. The 'epbd' efficiency remains close to the 'balanced efficiency' up to a flow rate ratio of 0.8 (20% imbalance).

Note that the test procedure has for target to determine the efficiency of the ventilation units in perfectly balanced conditions. The impact of possible imbalance at the system scale is taken into account in a later stage in the EP calculation method, with correction factors that depends on the whole ventilation system.

3 MEASUREMENT CAMPAIGNS AND RESULTS

In the frame of various research projects, 16 different HRV units have been monitored in situ for several months by measuring the temperatures at the four bounds of the units. For each unit, these four temperatures allow to compute both supply and exhaust apparent efficiency as defined in §2.1.

The initial objectives of these successive campaigns were on one side to verify if the heat-exchanger efficiency were equal or close to the lab-measured efficiency, and on the other side to see if there were any malfunctioning, and if relevant, try to identify the most common ones. These campaigns were also an opportunity to learn about the measurement methodology itself.

3.1 First campaign

The first measurement campaign occurred in the frame of the OPTIVENT project (funded by VLAIO - Flanders Innovation and Entrepreneurship Agency). Nine operating installations were monitored during one to three months.

In this campaign, the data loggers (measuring temperature and humidity) were placed directly inside the unit at the bounds of the heat exchanger, downstream of the fans so that the calculated temperature ratios are representative of the heat exchanger only and not perturbated by the fans heat. The used data loggers had been calibrated (for temperature) in lab conditions before being installed on site.

Figure 4: Example of temperature logger placement for the first measurement campaign. The heat-exchanger has been removed to place the sensors

We have also performed flow measurement for some of the units. This was a single measurement performed at nominal operation point at the beginning of the project. This allow to evaluate the flow imbalance, that can help explaining some of the results.

We consider this evaluation of (im)balance as qualitative since:

- The flows have been measured by summing the measured flow at the terminal devices. They may not be exactly equal to the flow through the heat exchanger if the ductwork airtightness is not perfect
- The balance of the installation may have changed during the monitoring period (fouling, cleaning or replacement of the filters during the monitoring period)

For this campaign, we choose to present more in detail the measurement results on 3 out of the 9 monitored installations. These results are representative of 3 types of results we observed in the campaign.

Normal situation

Monitoring results for the first site are presented in Figure 5. Results were available with a 10 minutes frequency and have been averaged over 1 hour. Both the supply and exhaust temperature ratios show 'high frequency' oscillations, but their average value is very close to 70%. By definition, the 'epbd' efficiency (average of the two ratios) is also about 70%.

The frequency of the oscillations is about a few hours. A closer analysis showed that these variations occur with indoor or outdoor temperature variations, but with no systematic correlations. Overall, the behavior of this unit seems quite normal.

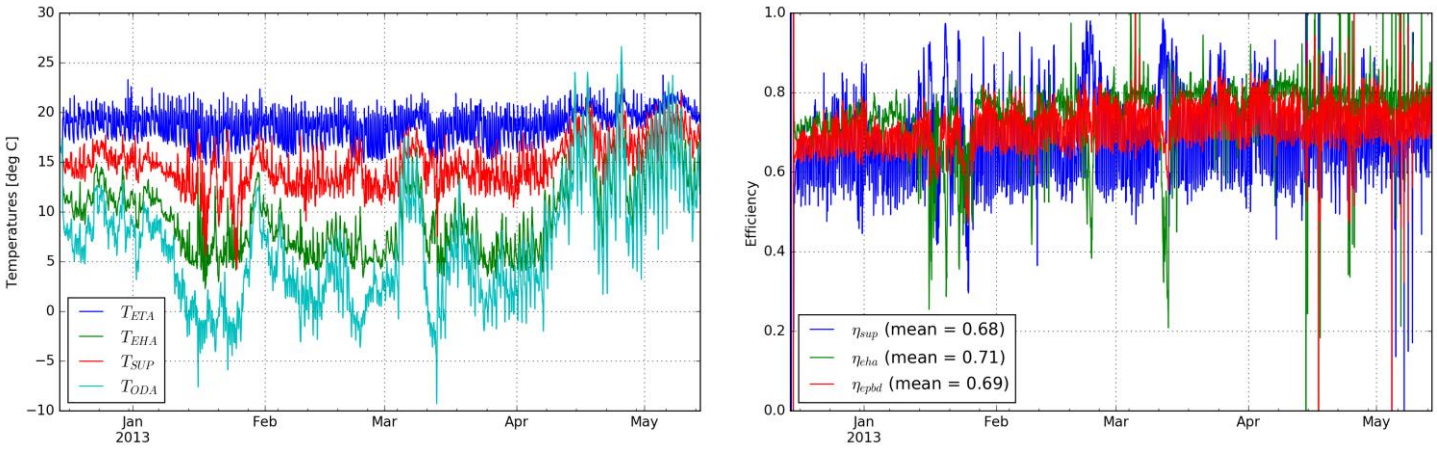

Figure 5 Measured temperatures and apparent efficiency for site 1

Almost normal situation

Results for a second installation are given in Figure 6. For this second case, one can first observe a systematic difference between the two temperature ratios. The 'exhaust' ratio is systematically higher than the 'supply' one, and this difference increases with time. Some possible explanations for this difference have been listed in §2.1 (flow unbalance, location of the sensor close to a thermal bridge, etc), but we do not have enough information to accurately identify

the issue. One will also note that the difference between ratios occurs at higher external temperatures, which is less impacting in terms of yearly energy recovery.

It is interesting to note that the 'epbd' efficiency remains more or less constant (between 70% and 80%) during the whole test period.

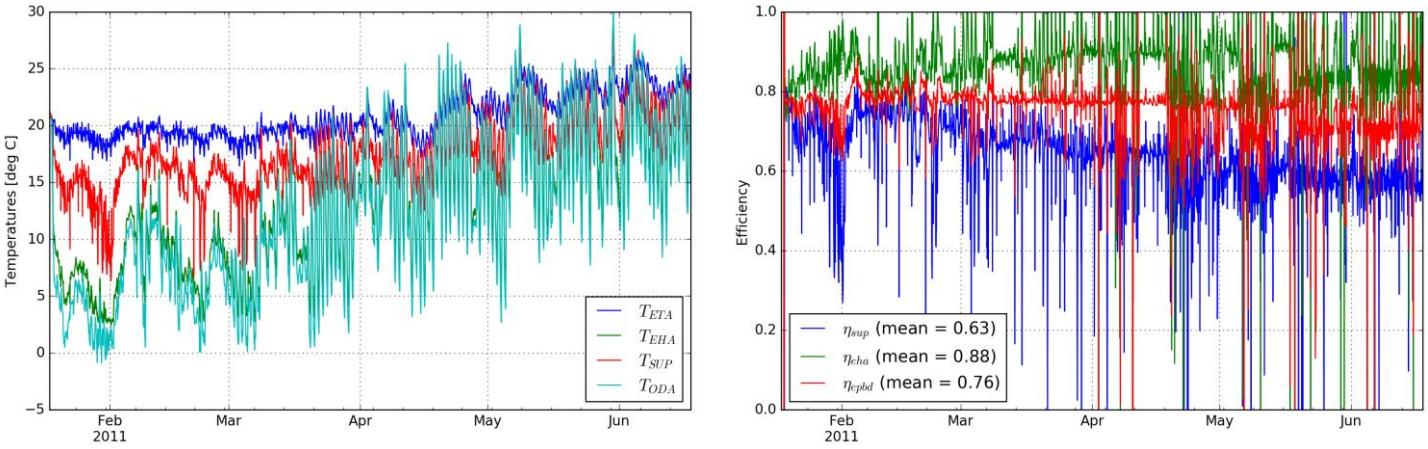

Figure 6 Measured temperatures and temperature ratios for site 2

Abnormal situation

Results for the third analyzed case are given in Figure 7. One observes a very high exhaust temperature (EHA), close to the supply one. When computing the temperature ratios, this leads to a very low value on the exhaust side while the supply value seems quite normal around 0.8.

For this installation, we know from air terminal devices measurements that the extracted flow was about 30% higher than the supply flow. This can explain a part of the difference, but not in this order of magnitude. The location of the sensors in the wake of the heat exchanger could also have an impact (see §3.3).

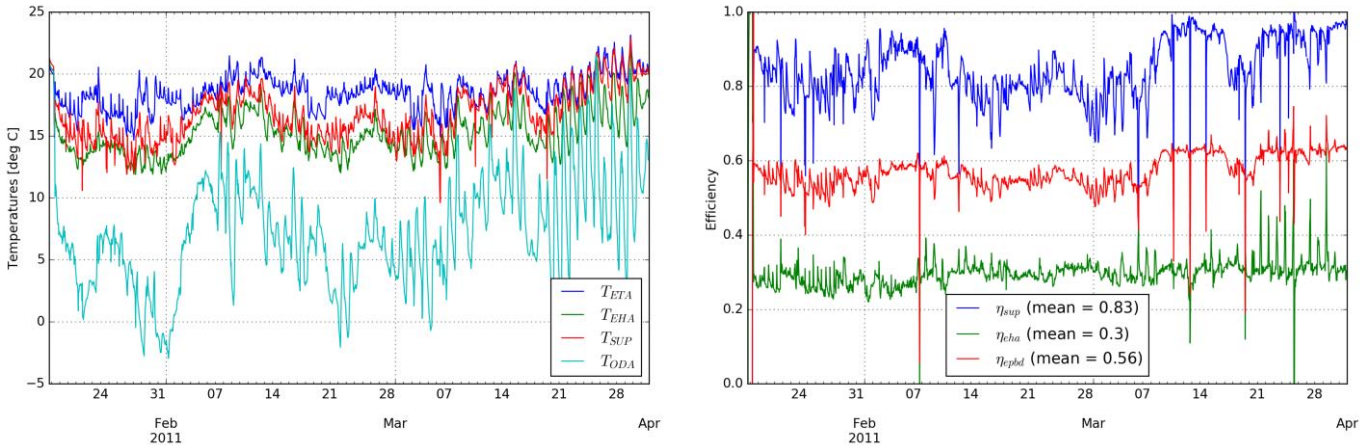

Figure 7 Measured temperatures and apparent efficiency for site 3

Overview of other results

Only 3 out of 9 cases have been presented here. They were selected to show an overview of all kind of encountered results.

If looking at the 9 installations globally, there were only 2 “abnormal” cases on the whole set. The 7 other cases can be considered as “normal” or “almost normal”. For these, the average ‘epbd’ efficiency was between 0.7 and 0.8. Out of these 7, the difference between the two temperature ratios was higher than 0.2 for only one case (but with an average > 0.7). This could possibly be explained by a flow imbalance, as illustrated in Figure 3 (but it could not be verified).

3.2 Second campaign

The second campaign was performed with similar conditions and material as the first one. This time, only 4 installations were monitored, among which 2 were already part of the first campaign. For 3 of the measurements, the calculated ‘epbd’ efficiency was once again between 0.7 and 0.9 and are very comparable to the results of the first campaign.

The last installation that was monitored is the same as Case 3 of the 1st campaign, i.e. the “abnormal case”. For this second period of monitoring, the temperature loggers were doubled, i.e. two sensors were placed at each bound of the heat-exchanger. This test was done to test if there was some temperature heterogeneity in the flow close to the heat exchanger. The position of the dataloggers for this experiment are visible on the different pictures in Figure 8.

Figure 8 Positioning of the data loggers for the experiment with doubled sensors

Monitoring results are given in Figure 9. The left plot shows the temperature difference between the two sensors of each position (SUP, ETA, EHA, ODA). The right plot shows the temperature ratios and epbd efficiency. One observes significant difference between the ratios, that are due to temperature differences between sensors at the SUP and mostly at the EHA position.

The average difference on the SUP side is 0.15°C on the monitoring period, and 2.3°C on the EHA side. Sensors have an accuracy of 0.2°C and are regularly calibrated, so such large measurement error is excluded.

The only possible explanation is that there are effectively temperature differences in the flow rate in the unit, either due to very nonhomogeneous flow out of the heat exchanger, either due to local effect of the unit insulation. In the EHA flow rate, there can also be an effect of the condensation of water during some periods.
It is particularly interesting to observe that the temperature differences are very low in the flow position upstream of the heat exchanger (ETA and ODA) and quite higher downstream of the heat exchanger and close to the fan (EHA and SUP). One possible explanation could be that the proximity of the fan has higher impact on the non-homogeneity of the flows after the heat exchanger, while the flow before the heat exchanger would be more homogeneous.
Note that the results of the worst series (suffix '2') are comparable with the results of the first campaign on this installation.

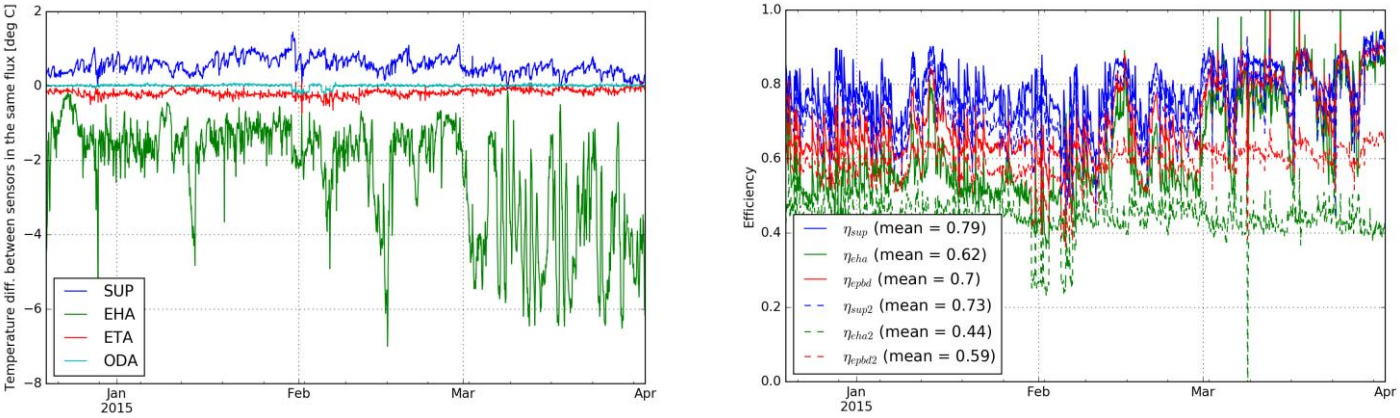

Figure 9 Experiments with doubled sensors: temperature difference between sensors at the same position and temperature ratios

3.3 Third campaign

In the frame of a third project (MEASURE – Funded by the Walloon Region), we had the opportunity to measure the heat recovery efficiency of 5 other HRV units on-site. Given the feedback from first campaigns, the sensors have been placed in the ducts just upwards and downwards of the ventilation unit, and not in the unit itself. These measurement conditions are similar to those used for laboratory measurement of ventilation unit according NBN EN 308 in the context of EPB regulation.

Flow measurement were performed by measuring the air flow rates at the supply and extract air terminal devices, but not necessarily at the same period as the temperature were measured. Temperature ratios were computed without the correction for fan power. This is different from what is done in the context of EPB regulation (where the efficiency is corrected for fan heat). However, the calculated average efficiency is less affected because the average neutralizes this effect symmetrically for the supply and exhaust efficiencies.

Table 1 summarizes the average efficiencies for the various dwellings on the measurement period. One observes for all the dwellings that the η_{sup} ratios higher than η_{eha}. This may be partially due to fan heat, as explained here above. For dwelling 4 for which the η_{sup} is 1, one can probably suspect strong flow unbalance as it was illustrated by a theoretical model in Figure 3.

The average values are all close to 80% in average, which is reasonably close to the values from the lab-tests for the concerned models (in the sample of 5 units, there were 2 different models with a declared value of 0.84 for both).

Figure 10 and Figure 11 illustrate the temperature and temperature ratios measurements for dwelling 1 and dwelling 3 of this campaign. Similar curves were obtained for all dwellings of this campaign. Compared to results of the two first campaigns, the curves are less noisy and seem more stable in time. Part of this difference could maybe be explained by a better quality or commissioning of these 5 units, but we have no objective reason to suppose these are better than the previous ones. More probably, we believe that the new measurement method (in the ducts upwards and downwards the ventilation unit) provides more representative results than the previous one (sensors upwards and downwards the heat-exchanger, within the ventilation unit) due to a more homogeneous temperature in the ducts than at the vicinity of the heat-exchanger.

Table 1 Average temperature ratios (sup,eha) and epbd efficiency on the whole measurement period for the 3rd measurement campaign

Dwelling	**1**	**2**	**3**	**4**	**5**
$\eta_{sup,av}$	0.89	0.85	0.86	1.01	0.83
$\eta_{eha,av}$	0.8	0.76	0.69	0.7	0.76
$\eta_{epbd,av}$	0.85	0.8	0.78	0.85	0.8

Next to the average values and the general shape of the curves, one could observe some punctual phenomena like the triggering of the frost protection or the by-bass. An example of it is visible in Figure 10. At two different moments (begin and mid-January) the ODA temperature drops below 0°C. At these periods, one can clearly see that the asymmetry between supply and exhaust ratios increases. This is probably explained by reduction of the supply flow, in order to prevent the exhaust (EHA) temperature to drop. One observes that this temperature never decreases below 5°C even though the outdoor temperature continues decreasing. We observed this kind of punctual phenomena several times in the different monitoring results, but it is not the main focus of the present paper. It will not be further developed here.

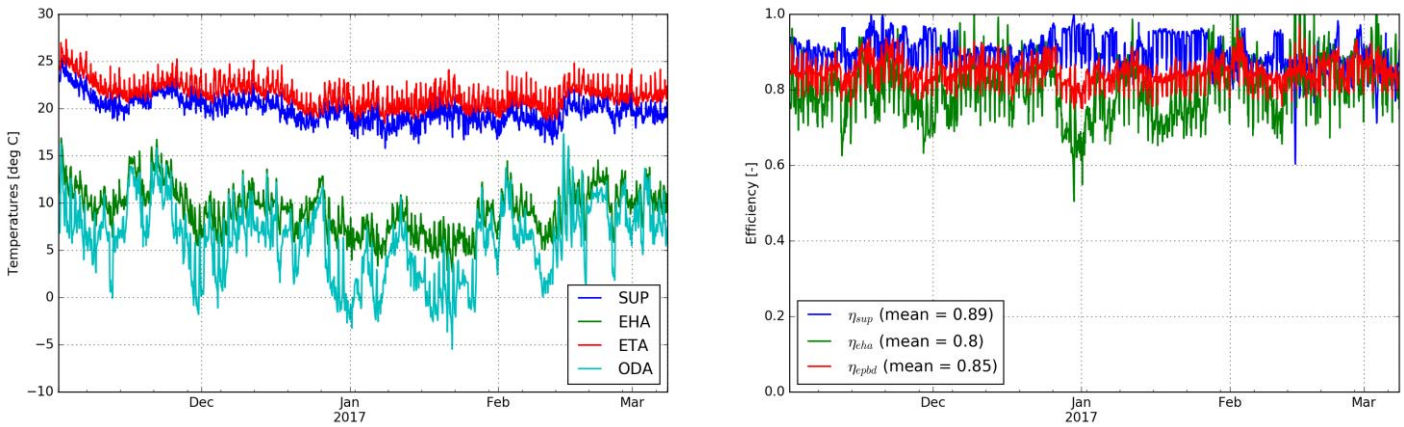

Figure 10 Measurement results for dwelling 1 of the 3rd campaign (from November 2017 to March 2017)

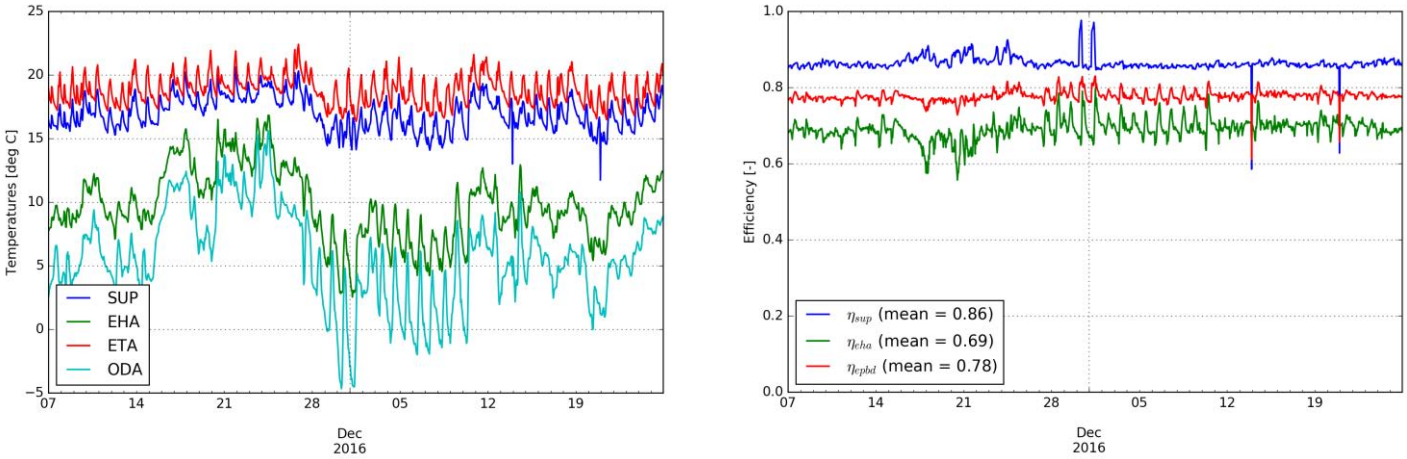

Figure 11 Measurement results for dwelling 3 of the 3rd campaign (from 7 November to 26 December 2016)

4 CONCLUSIONS

The main objective of this paper was to verify if the efficiency of HRV units operating on-site was consistent with the values obtained in lab-measurements.

We also recalled that heat-exchanger or ventilation unit efficiency is not the global energy efficiency and gave a short overview of the main issues that can negatively impact it. These reminders also highlighted that it is not that easy to decorrelate both, since some phenomena at the system scale (e.g. flow imbalance) can impact the temperature ratios measurements at the unit scale.

Regarding the on-site measurement itself, we showed that if computed the same way as in the lab-conditions (average of the supply and exhaust temperature ratios, following the Belgian EPB approach), the efficiency of the tested units was between 70 and 85% for most of them. Over the 16 different tested units, two of them showed problematic behaviour.

One experiment performed with doubled sensors showed that measurements directly within the unit (upwards and downwards the heat-exchanger) were highly sensitive to the sensor location. This is probably explained by temperature heterogeneity of the flow at the heat-exchanger outlet, even if there are other possible explanations (local condensation, thermal bridge). The last campaign with measurement in the ducts showed less noise and more stability in the results. In this last (and more trustworthy) results, the calculated efficiencies are around 80%, i.e. quite close to lab measured values We would recommend using this method in the future for such measurements.

5 ACKNOWLEDGEMENTS

Some of the experimental measurements presented in this report were performed in the frame of the OPTIVENT project (funded by VLAIO, the Flemish Innovation and Entrepreneurship Agency) and the MEASURE project (funded by SPW DGO4; the Walloon Public Service for Energy).

6 REFERENCES

Belgian EPB Regulation. (2018). Méthode PER - Annexe B2 - Le facteur de réduction pour préchauffage.

Belgian EPB Regulation. (sd). Méthode PER - Annexe G - Détermination du rendement themrique d'un récupérateur de chaleur.

Caillou, S. (2009). Towards Comparable And Relevant Heat Recovery Efficiencies. *Passivehouse Symposium.* Brussels.

Caillou, S. (2012). Heat Recovery Efficiency: Measurement and Calculation Methods. *The 33rd AIVC and 2nd TightVent Conference.* Copenhagen.

Faes, W. (2016). *Useful energy transfer in air-to-air heat recovery units in low energy buildings.* UGent - Faculty of Engineering and Architecture.

Janssens, A. (2017). Of Heat Recovery Ventilation: Problem Statement Based On Steady-State Two Zone Analysis and Field Studies. *38th AIVC conference.* Nothingham,UK.

NBN EN 308. (1997). Echangeurs thermiques – Procédures d'essai pour la détermination de la performance des récupérateurs de chaleur air/air et air/gaz.

Rouleta, C. (2001, 5). Real Heat Recovery With Air Handling Units. *Energy and Buildings*, pp. 495-502.

Rouleta, C. A. (2001-2). Is Heat Recovery in Air Handling Units Efficient? *Universisty of Siegen, Germany*.

Impact of ductwork leakage on the fan energy use and sound production of central mechanical ventilation units in houses

Valérie Leprince[1*], Marcus Lightfoot[2], Jelmer de Jong[3]

1 PLEIAQ
84 C Av de la Libération
69330 Meyzieu, France
**Corresponding author: valerie.leprince@pleiaq.net*

2 Ubbink - Centrotherm
Verhuellweg 9
6984 AA Doesburg, the Netherlands

3 Brink Climate Systems
Wethouder Wassebaliestraat 8
7951SN Staphorst, the Netherlands

ABSTRACT

Various studies demonstrate a significant impact of ductwork leakage on the fan power consumption of ventilation systems. They have shown that the total energy used by fans can be reduced by 30-50% by improving the airtightness of the ductwork system. However, most of those studies focused on non-residential and multi-family buildings. This study focuses on single-family dwellings; specifically houses.
This paper first explains why fan energy use increases with ductwork leakage and then presents a model, which is based upon (Leprince & Carrié, 2018), that is used to estimate the impact of ductwork leakage on the fan energy use of central mechanical ventilation units with heat recovery in three houses and with a DCV system in one house. The calculations have shown that fans connected to leaky ductwork (3*Class A) in the four houses use 57-169% more energy than fans connected to very airtight ductwork (Class D), if they ventilate to provide the hygienic flowrate at Air Terminal Devices.
Obviously, the harder a mechanical ventilation unit has to work to displace more air to achieve the hygienic flowrate at the Air Terminal Devices, the more sound it will produce. It is estimated that a mechanical ventilation unit with heat recovery will produce at least 2.5 dB(A) more sound pressure level in the habitable rooms whith leaky ductwork.

KEYWORDS

Ductwork airtightness, fan energy use, single houses, sound pressure

1 INTRODUCTION

There are a number of studies that demonstrate a significant impact of ductwork leakage on fan energy use (Soenens & Pattijn, 2011) (Stroo, 2011) (Berthault, Boithias, & Leprince, 2014) (D.F., 2011) (Bailly, Duboscq, & Jobert, 2014) (Levinson, Delp, Dickerhoff, & Modera, 2000) (Carrié, Bossaer, Andersson, Wouters, & Liddament, 2000) (Krishnamoorthy & Modera, 2016) (Leprince & Carrié, 2018).
(Soenens & Pattijn, 2011) concluded that more than 30% of the energy used by the fans in the ventilation systems in a hospital wing, care home and office building could be saved using airtight ventilation systems (Soenens & Pattijn, 2011). Those results are consistent with (Stroo, 2011) and with the experimental study of Berthault in a multi-family building (Berthault, Boithias, & Leprince, 2014), which concluded up to 50% energy savings with class C airtight ductwork compared to 1.5*class A.
However, recent measurements performed in France in the context of the Effinergie + label (Moujalled, Leprince, & Mélois, 2018) have shown that almost 50% of the ductwork systems in the tested houses have ductwork airtightness 2.5*class A or worse. This stresses the need to

change construction habits because the ductwork in most of the tested buildings was designed to achieve at least class A (required by the Effinergie + label), but missed the target. Unfortunately, the negative impact of ductwork leakage on fan energy use and sound production is still neglected in most countries (Leprince, Carrié, & Kapsalaki, 2017), particularly in residential buildings.
This paper aims to:

- explain the impact of ductwork leakage on flowrate and pressure drop;
- calculate the impact of ductwork leakage on the fan energy use of central mechanical ventilation units with heat recovery in 4 houses with different ductwork systems, hygienic flow rates and pressures drops;
- estimate the impact of ductwork leakage on the sound pressure in bedroom and living-rooms

2 IMPACT OF DUCTWORK LEAKAGES ON FAN ENERGY USE AND SOUND PRESSURE

2.1 Fan energy use

The fan power consumption depends upon the flowrate produced by the fan and the pressure difference on either side of the fan.
The nominal efficiency of the fan is defined by the following equation:

$$\eta = \frac{\Delta P * Q}{P_{el} * 3600} \qquad (1)$$

η	-	Efficiency of the fan
ΔP	Pa	Pressure difference at fan
Q	m^3/h	Flowrate at fan
P_{el}	W	Electrical power of the fan

This efficiency may not be constant according to the pressure difference and flow rate.
The higher the pressure drop (resistance) in the ductwork, the higher the pressure difference the fan needs to produce to overcome this resistance and achieve the hygienic flow rate. Generally, axial fans are able to produce high flowrates, but cannot generate enough large pressure difference to overcome any resistance without running at higher speeds and producing more sound. On the other hand, centrifugal fans are able to generate large pressure differences, but their flowrates are limited.

2.2 Pressure losses

Pressure drop in ductwork systems is due to the irreversible transformation of mechanical energy into heat (ASHRAE, 2013). There are two types of losses:

- friction losses (occurring along the ductwork)
- and dynamic losses (occurring at bends and junctions)

Friction losses
Friction losses occur along the entire length of duct. They are due to fluid viscosity. Friction loss can be calculated using the Darcy equation (ASHRAE, 2013)

$$\Delta p_f = \frac{1000 f L}{D_h} * \frac{\rho V^2}{2} \qquad (2)$$

Δp_f	Pa	Friction losses in terms of total pressure
f	-	Friction factor
L	m	duct length
D_h	m	hydraulic diameter
V	m/s	velocity
ρ	kg/m^3	air density

Friction losses are proportional to the flow velocity to the power of 2 so also to the square of the flowrate.

Dynamic losses

Dynamic losses result from flow disturbance caused by duct accessories, which change the direction of the flow (bends) and of the hydraulic diameter (adaptors) and at converging/diverging junctions.

Dynamic loss can be calculated using the following equation (ASHRAE, 2013):

$$\Delta p_t = \frac{C\rho V^2}{2} \qquad (3)$$

C	-	Total loss coefficient
Δp_t	Pa	Total pressure loss
V	m/s	velocity
ρ	kg/m^3	air density

Total pressure loss in the ductwork

Total pressure loss in a duct section is calculated by combining friction and dynamic losses.

$$\Delta p = \left(\frac{1000f}{D_h} + \sum C\right)\left(\frac{\rho V^2}{2}\right) \qquad (4)$$

Therefore, the pressure loss in the ductwork system is proportional to the square of the flowrate and the higher the flowrate to overcome ductwork leakage, the higher resistance in the ductwork.

Fan and pressure losses

The fan needs to compensate for the additional flowrate due to ductwork leakage and also the additional pressure drop to maintain the hygienic flowrate. Therefore, both the flowrate and the pressure at the fan needs to be increased.

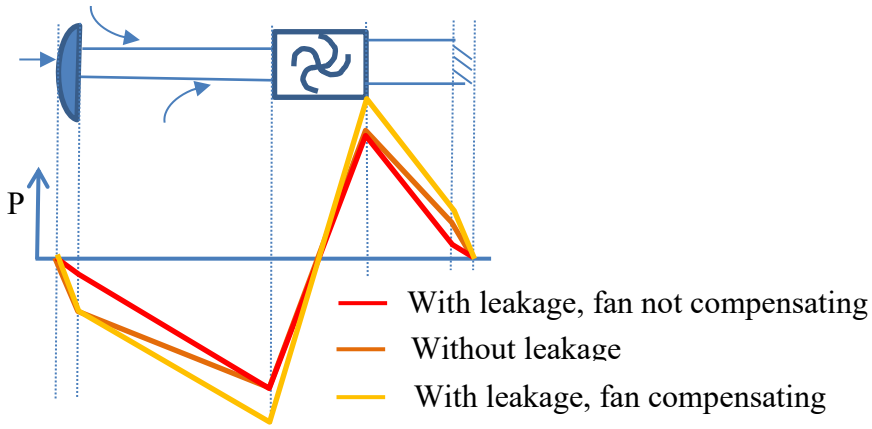

Figure 1: Pressure profile within the system with and without leakages according to the fan pressure drop

The flowrate (Q) at the Air Terminal Devices (ATD) depends upon the pressure at the ATD according to a power law.

$$Q = C\,\Delta P^n \qquad (5)$$

C and n depend upon the air terminal device (n is close to 0.5).

Therefore, the lower the pressure drop at ATD's, the lower the flowrate.

Therefore, as shown in Figure 1, if the fan is not compensating for the additional pressure drop due to ductwork leakage, the pressure drop and flowrate at ATD's will decrease.

Generally, the pressure drop at a fixed ATD providing the hygienic flowrate is around 10 Pa. Self-adjusting ATD's generally need 50-70 PA to function properly.

2.3 Calculation method

To estimate the additional energy used to overcome ductwork leakage the additional flowrate and the additional pressure drop shall be calculated using the calculation model developed by (Leprince & Carrié, 2018), which is based upon EN 16798-5-1 (CEN, 2016).
If the fan compensates for leakages the flowrate at the fan shall be:

$$q_{v;ahu} = q_{v;dis;req} + q_{lea} \quad (6)$$

$$q_{lea} = A_{du} * c_{lea} * \Delta P_{du}^{ep} * 3600 \quad (7)$$

With

$q_{v;ahu}$	m^3/h	Required flowrate at Air Handling Unit
$q_{v;dis;req}$	m^3/h	Sum of required flowrates at Air Terminal Devices
q_{lea}	m^3/h	Flowrate through leakages
A_{du}	m^2	Area of the ductwork
c_{lea}	$m^3/s/m^2$ at 1Pa	Airtightness factor of the ductwork
ep	-	pressure difference exponent, default value: 0.65
ΔP_{du}	Pa	Average pressure difference between inside and outside the ductwork

Leakage only creates an additional pressure drop in the ductwork (not at the ATD), so to estimate the additional pressure drop due to ductwork leakage the pressure drop at the ATD's shall be deduced from the total pressure drop.

$$\Delta P_{fan} = \Delta P_{ATD;req} + \left(\frac{q_{v;dis;req}+q_{lea}}{q_{v;dis;req}}\right)^2 * \Delta P_{du;noleak} \quad (8)$$

ΔP_{fan}	Pa	Required pressure at fan to provide required pressure at ATD
$\Delta P_{ATD;req}$	Pa	Required pressure at ATD to provide required flowrate
$\Delta P_{du;noleak}$	Pa	Pressure drop in the ductwork when there are no leakages (when flowrate in the ductwork is the hygienic flowrate). This pressure drop does not include pressure drop at ATD.

To simplify the calculation and avoid cross-references, it can be assumed that ΔP_{du} is constant whatever the leakage is and equal to:

$$\Delta P_{du} = \Delta P_{ATD;req} + \frac{\Delta P_{du;noleak}}{2} \quad (9)$$

In this study, any leakage inside the AHU itself and the heat exchanger have been neglected to only show the impact of leakage in the ductwork system.

2.4 Impact of leakages on sound level

The more flowrate and pressure the fan is producing the more casing radiation (sound power) is produced by the fan.
For a given Air Handling Unit, the sound Power transmitted to the dwelling is measured in laboratory according to EN ISO 5135:1999 (Determination of sound power levels of noise from air-terminal devices, air-terminal units, dampers and valves by measurement in a reverberation room). Data are provided by manufacturers.
Usually in single-houses the fan is directly connected to a silencer, the sound attenuation of this device is laboratory tested according to ISO 7235 (Acoustics -- Laboratory measurement procedures for ducted silencers and air-terminal units -- Insertion loss, flow noise and total pressure loss).

The flow then goes through an air distribution box where the sound is split. The sound reduction depends upon the number of habitable rooms. If there are 2 rooms a reduction of 3 dB is assumed, if there are 4 rooms the reduction is of 6 dB.

To estimate the sound pressure level in the room the following equation is used:

$$L_p = L_w + 10 * \log\left(\frac{Q}{4\pi r^2} + \frac{4}{A}\right) \qquad (10)$$

With:

L_p	dB(A)	Sound pressure in the room
L_w	dB (A)	Sound power after the distribution box (neglecting the attenuation of ductwork)
Q	-	Coefficient depending of the angle of radiation, Q=2 for an Air Terminal Device on a wall
r	m	Distance to the source (r=1.5 m in the following example)
A	m²	Reference sound absorption area (20 m² Sabin for a furnished living-room and 8.5 m² Sabine for a small furnished bedroom)

3 RESULTS AND DISCUSSIONS : CASE STUDY

3.1 Fan energy use

Hypothesis

The following four scenarios have been simulated:

- House 1 is a medium-sized house with a central mechanical ventilation system with heat recovery. The ductwork system is a radial air distribution system using semi-rigid plastic ductwork. The diameter of the ductwork is 75mm and the total length is 125m. It is assumed that the ductwork is equally split between supply and extract.
- House 2 is also a medium sized house with a central mechanical ventilation system with heat recovery. The ductwork system is a trunk and branch air distribution system using metal or rigid plastic ductwork with 6m of ductwork DN160mm and 40m of ductwork DN125mm. It is assumed that the ductwork is equally split between supply and extract.
- House 3 is a large house with a central mechanical ventilation system with heat recovery. The ductwork system is a radial air distribution system using semi-rigid plastic ductwork. The diameter of the ductwork is 75 mm and the total length is 200 m. It is assumed that the ductwork is equally split between supply and extract.
- House 4 is a large house with a humidity-based extract only ventilation system, with self-adjusting ATD. The average flowrate is 100 m^3/h. The required pressure at the ATD is 70 Pa. The ductwork area is assumed to be 7.4m² (radial air distribution system).

Table 1 summarises the hypothesis of the ventilation system in each house used for the calculation.

Table 1: Hypothesis for cases studies

	House 1	House 2	House 3	House 4 (specific to the French market)
Hygienic flowrate (m^3/h)	**225**	**225**	**300**	**100**
Required pressure at ATD's (Pa)	**10**	**10**	**10**	**70**
Ductwork area of each airflow (m²)	**14.72**	**9.36**	**23.6**	**7.4**
Pressure drop in ductwork (without leakages) (Pa) for each airflow	**100**	**100**	**150**	**80**

Results

Table 2 shows the required flowrate and pressure of ***each*** airflow (supply and extract) and fan in each house and for the various airtightness classes. The required pressure at the fan includes the pressure drop in the ductwork plus the required pressure at the ATD's.

Table 2: Required pressure and flowrate for each fan according to the ductwork leakages for the 3 houses tested

Required flowrate of each fan (m^3/h)				
	House 1	House 2	House 3	House 4 (specific to the French market)
3*class A	286	264	424	146
1.5*class A	256	245	362	123
Class A	245	238	341	115
Class B	232	229	314	105
Class C	227	226	305	102
Class D	226	225	302	101
No leakage	225	225	300	100
Required pressure at each fan (Pa)				
3*class A	172	148	309	240
1.5*class A	139	128	228	191
Class A	129	122	204	176
Class B	116	114	174	158
Class C	112	111	165	153
Class D	111	110	162	151
No leakage	110	110	160	150

The fan power consumed to produce this pressure and flowrate can either be calculated by assuming a constant efficiency or read in the fan curves provided by the ventilation unit manufacturer.

The annual fan energy use shall be estimated assuming that the fans in both airflows work continuously that is to say 8,760 hours per year.

Table 3 shows the annual energy use of both fans assuming a constant fan efficiency of 0.27.

Table 3: Annual energy use of both fan (kWh) assuming an efficiency of 0.27

Annual energy use of both fans (kWh)				
	House 1	House 2	House 3	House 4 (specific to the French market)
3*class A	888	703	2359	315
1.5*class A	641	565	1488	211
Class A	571	523	1255	183
Class B	485	471	984	150
Class C	459	454	904	140
Class D	450	449	878	137
No leakage	446	446	865	135

Figure 2 and Figure 3 compare the annual energy use of both fans in the 4 houses according to the various airtightness classes. It shows that fans connected to leaky ductwork (3*Class A) in the four houses use 57-169% more energy than fans connected to very airtight ductwork (Class D), if they ventilate to provide the hygienic flowrate at Air Terminal Devices.

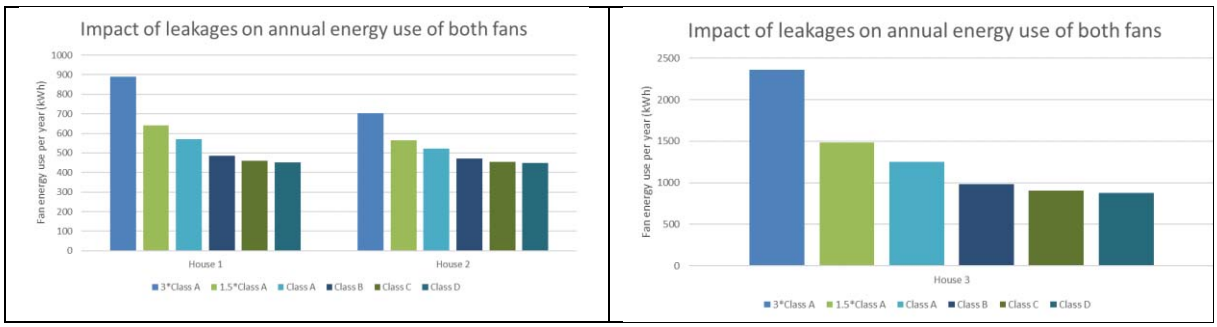

Figure 2: Annual energy use of both fans in houses 1 and 2 (left) and in house 3 (right) (estimated assuming a fixed fan efficiency of 0.27)

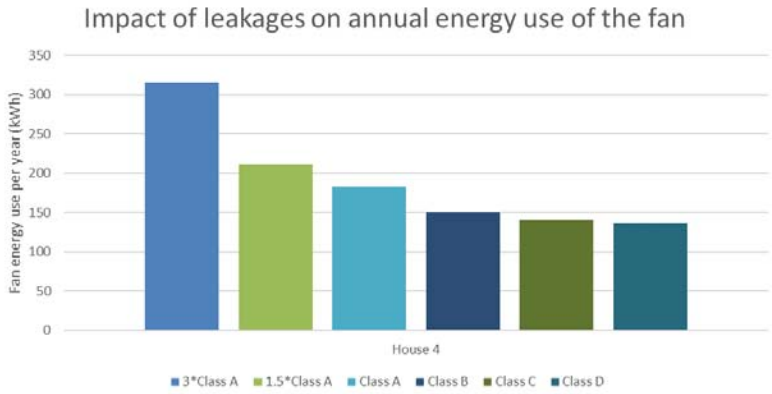

Figure 3: Annual energy use of the fan in house 4 (estimated assuming a fixed fan efficiency of 0.27)

3.2 Sound pressure

The sound pressure in bedrooms and living rooms has been calculated for houses 1 to 3 (with heat recovery system).

The sound power to dwelling (supply) measured according to ISO 5135 for the Residential Air Handling Unit Excellent 400 of Brink has been used (provided by manufacturer). The values are given in Table 4.

The sound reduction (or attenuation) of the silencer Brink (ISO AKS 1m, diam 160 mm) is provided for each frequency by the manufacturer. The impact on the total sound power is given in Table 4.

The sound power to each room and the sound pressure in bedrooms and living-rooms are calculated according to assumptions explained in § 2.4.

Table 4: Sound power in the ductwork and sound pressure in the rooms for the 3 houses for leaky and airtight ductworks

	HOUSE 1		HOUSE 2		HOUSE 3	
	3*Class A	Class D	3*Class A	Class D	3*Class A	Class D
Required flowrate (m^3/h)	286	226	264	225	424	302
Required pressure (Pa)	172	111	148	110	309	162
Sound power to dwelling (dB)	78.7	73.1	75.5	73.1	80.4	78.7
Sound power to dwelling with A correction and silencer dB(A)	43.9	38.5	41	38.5	46.8	43.9
Sound power to each room (- 6dB)	37.9	32.5	35	32.5	40.8	37.9

Sound pressure in bedrooms dB(A) according to equation (9)	35.2	29.8	32.3	29.8	38.1	35.2
Sound pressure in living rooms dB(A) according to equation (9)	32.2	26.8	29.3	26.8	35.1	32.2

<30 dB(A)	Quiet
30-35 dB(A)	Audible sound
>35 dB(A)	Loud

The impact is of 5.4 dB in the first house, 2.5 dB in the second and 2.9 dB in the third one, making the sound pressure from quiet to loud in house 1. In dB a difference of 3 dB corresponds to twice the noise level: it is equivalent to have two identical systems working at the same time.

4 CONCLUSION

The first part of this study has demonstrated the impact of ductwork leakage on both the flowrate and pressure drop at the fan. It has provided equations to calculate the impact according to

- the required hygienic flowrate
- the required pressure at ATD
- ductwork properties (surface area, leakage coefficients and pressure drop without leakage).

In, the second part of this study these equations were applied to central mechanical ventilation systems with heat recovery in three houses and with a single exhaust DCV system in one house. It has shown that fans connected to leaky ductwork (3*Class A) can use 57-169% more energy than fans connected to very tight ductwork (Class D) to produce the required hygienic flowrate.
If the fans have to work harder to produce the required hygienic flow rate, then they will produce more sound through the casing and in the ductwork and therefore noise hindrance. Calculation made from fan manufacturer data have shown a difference from 2.5dB(A) and up to 5.4 dB(A) in the habitable rooms according to the ductwork airtightness.

5 ACKNOWLEDGEMENTS

This work was funded by Ubbink. The views and opinions of the authors do not necessarily reflect those of Ubbink. The published material is being distributed without warranty of any kind, either expressed or implied. The responsibility for the interpretation and used of the material lies with the reader. In no event shall PLEIAQ, Ubbink and Brink be liable for damages arising from its use any responsibility arising from the use of this document lies with the user.

6 REFERENCES

ASHRAE. (2013). *2013 ASHRAE Handbook: Fundamentals.*
Bailly, A., Duboscq, F., & Jobert, R. (2014). Impact of a poor quality of ventilation systems on the energy efficiency for energy-efficient houses. *35th AIVC Conference "*

Ventilation and airtightness in t (pp. 108-118). Poznań, Poland, 24-25 Septembe: AIVC.

Berthault, S., Boithias, F., & Leprince, V. (2014). Ductwork airtightness: reliability of measurements and impact on ventilation flowrate and fan energy consumption. *35 TH AIVC-4 TH TIGHTVENT & 2 ND VENTICOOL CONFERENCE , 2014* (pp. 478-487). Poznań, Poland, 24-25 September: AIVC.

Carrié, F., Bossaer, A., Andersson, J., Wouters, P., & Liddament, M. (2000). Duct leakage in European buildings: Status and perspectives. *Energy and Buildings, 32*(3), 235-243.

CEN. (2016). *EN 16798-5-1:2016 Energy performance of buildings - Ventilation of buildings - Part 5-1: Calculation methods for energy requirements of ventilation and air conditioning systems.*

Crowe, K. (1974). *A History of the Original Peoples of Northern Canada.* Montreal: McGill/Queen's University Press for the Arctic Insitute of North America.

D.F., D. (2011). Case study: effect of excessive duct leakage in a large pharmaceutical plant. *32th AIVC Conference. Towards Optimal Airtightness Performance* (pp. 55-56). Brussels, Belgium: AIVC.

Krishnamoorthy, S., & Modera, M. (2016). Impacts of duct leakage on central outdoor-air conditioning for commercial-building VAV systems. *Energy and Buildings, 119*, 340-351.

Leprince, V., & Carrié, F. (2018). Impact of ductwork airtightness on fan energy use: Calculation model and test case. *Energy and Buildings, 176*, 287-295.

Leprince, V., Carrié, F., & Kapsalaki, M. (2017). Building and ductwork airtightness requirements in Europe – Comparison of 10 European countries. *38th AIVC Conference. Ventilating healthy Low-energy buildings* (pp. 192-201). Nottingham, UK: AIVC.

Levinson, R., Delp, W., Dickerhoff, D., & Modera, M. (2000). Effects of airflow infiltration on the thermal performance of internally insulated ducts. *Energy and Buildings, 32*(3), 345-354.

Moujalled, B., Leprince, V., & Mélois, A. (2018). Statistical analysis of about 1300 ductwork airtightness measurement in new French buildings: impact of the type of ducts and ventilation systems. *39th AIVC conference.* Juan les pins.

Soenens, J., & Pattijn, P. (2011). Feasibility study of ventilation system air-tightness. *32th AIVC Conference. Towards Optimal Airtightness Performance* (pp. 51-54). Brussels, Belgium: AIVC.

Stroo, P. (2011). Class C air-tightness: Proven roi in black and white. *32th AIVC Conference. Towards Optimal Airtightness Performance2* (pp. 96-97). Brussels, Belgium: AIVC.

Zaslow, M. (1988). The Northward Expansion of Canada. *The Journal of Canada, 2*(3), 216-222.

The contribution of a solar air heater collector to the cooling load in a Building

Pavlos Toumpoulidis[*1], Argiro Dimoudi[1], Panos Kosmopoulos[2], and Stamatis Zoras[1]

1 Laboratory of Environmental and Energy Design of Buildings and Settlements, DUTH
Xanthi, Greece
**Corresponding author: ptoumpou@env.duth.gr*

2 K-eco Projects co, f. Director of the Laboratory of Environmental and Energy Design of Buildings and Settlements, DUTH
Thessaloniki, Greece

ABSTRACT

Over the last few decades, there is a clear target for reducing energy needs in the building sector. The above objective can be achieved both by renovating the existing building stock and/or by constructing new buildings that will meet the characteristics of zero or nearly zero energy buildings. In order to construct or renovate a building into a zero or almost zero energy building, different passive, active and hybrid systems can be used. One such system is a solar air heater collector. The above system was installed in the south facade of the outdoor test cell (ZED-KIM (Zero Energy Demand – Kimmeria)), located at the Campus of the Environmental Engineering School, DUTH at Xanthi (Greece). In the present study, the monitoring results of the solar air heater collector and its contribution to cover the cooling load of a building will be presented. The system was monitored under real weather conditions for the period June 2017 to August 2017. This period was separated in two sub-periods. In the first one, the system operated as a solar air heater and with the appropriate modifications air from inside the test cell was passed through solar collector and hot air was rejected out. In the second sub-period, a ventilation inlet was added in the north facade of the test cell, and the system operated as a solar chimney. The heating load that rejected out in the first sub-period was 12 KWh and in the second sub-period was 58.5 KWh. In other terms the cooling load of the test cell was reduced by 70.5 KWh for the whole period of measurements. In addition the cooling load for the specific climate zone of Greece and for 20m^2 cooling space was 488 KWh so there was a reduction of 15 percent. Furthermore, it was noticed that the thermal efficiency of the system increased above 50 percent between 1st and 2nd sub period, with values being 16% and 34% respectively. Based on the above results, it is concluded that even in hot weather conditions prevailing in northern Greece, the use of a solar air heater collector with the appropriate modifications can cover, in a significant degree, the cooling load of a building and in conjunction with other passive and active systems it can lead at a nearly zero energy building.

KEYWORDS

Hybrid Systems, Solar Air Heater Collector, Thermal Efficiency, Solar Chimney

1 INTRODUCTION

In the building sector, different active, passive and hybrid systems can be used in order to reduce energy needs and achieved thermal comfort. Several studies have been carried out on solar systems in order to improve their performance and to integrate on buildings. For instance, the International Energy Agency (IEA) has launched in 1977 a program on solar heating and cooling (SHC) which aims, among others, to provide guidelines for the use of

such systems. In addition, both in the world and in the Mediterranean countries due to the prevailing weather conditions, the study of solar thermal systems is quite well developed. However, solar air collectors have not been adequately studied as solar water collectors are predominant. The study of solar air collector systems focuses mainly on improving their performance with the researchers studying both experimentally and theoretically a range of parameters such as the effect of the use of baffles and fins on the absorber surface ((Bayraka et al (2013), Chabane et al (2011), El-Sebaii et al (2011), Yeh (2012)), the effect of roughness on the ducts or the absorber surface ((Akpinar and Koçyiğit (2010), Bopche and Tandale (2009)),different coatings of the absorber surface ((El-Sebaii and Al-Snani (2010)), and using heat storage media (Aboul-Enein et al., 2000). In contrast, the bibliography is limited to the application of solar air collector systems in the building sector ((Oikonomidis G., Davliakos N. and Botsios-Valaskakis A. (2014), Toumpoulidis et al., 2018)) and referred mainly on covering of the heating loads of a building. Additionally, the already limited literature is old enough with no access to relevant studies. Instead, as shown above, solar collector systems have been studied in depth only in terms of improving their performance through various techniques, and combining the use of such systems with other passive and active systems, emphasizing only the energy benefits that have emerged. Therefore one of the main objectives of the present study is to study solely a solar air collector system as far it concerns the energy performance in conjunction with the weather conditions prevailing in the study area. Finally, an additional objective which will be also presented in this study is to study the use of the solar collector as a mean of reducing the cooling load of a building in cooling period.

2 METHODOLOGY

2.1 Description of ZED-KIM (Zero Energy Demands–Kimmeria)

The prefabricated test cell ZED-KIM (Zero Energy Demand - Kimmeria), located at the Campus of the Engineering School, DUTH, 4 km east of the city of Xanthi, in Greece. The ZED-KIM consists of an imitation of an average household on a scale of 1:5, has been constructed in such a way so as to conform to bioclimatic design principles (Kosmopoulos and Galanos. (2006)).The ground plan is rectangular and 20 m^2 in total, the house faces south with an azimuth angle of 0^o. It has two windows, one on the south and one on the east side, which allow sun light to enter, thus increasing thermal energy. It is worth mentioning that this pilot house is very well insulated, its roof provides additional thermal insulation and sound proofing (Papadopoulos 2000). The roof is tilted at 42^o which is considered the most appropriate slant for the latitude of the city of Xanthi, in order to exploit the greatest levels and intensity of solar radiation during the sunny months (Hussein et al. 2004). Two photovoltaic arrays, one with 2 axis tracker, with a total power of 2120 Watt have been installed on the roof and near the test cell. On the west side of the house a wind generator of 900Watt has been installed, in order to function alongside the hybrid system in connection with the photovoltaic modules and to help considerably in the production of energy during seasonal fluctuations. With all the above-mentioned active systems, the total power of installed RES exceeds 3 kW. At this point it is worth noting that in the ZED-KIM a complete system has been installed to follow and record meteorological conditions, this system consists of a wind cup anemometer, rain gauge, temperature and humidity gauge, barometer, and one pyranometer to measure the intensity of total solar radiation. The general image of ZED-KIM is presented in figure 1.

Figure 1: The test cell ZED-KIM

Finally on the south façade of the test cell, as shown in figure 2, a solar air collector system have been installed in which carried out the present study.

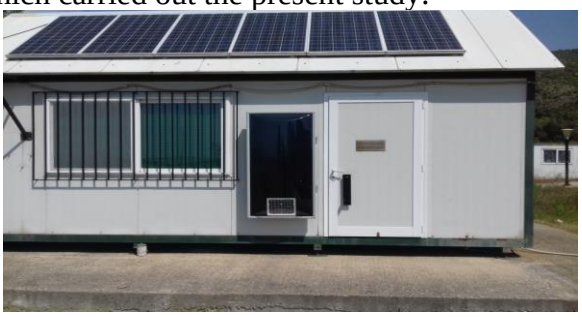

Figure 2: Solar air collector

2.2 Description of the solar air collector system

2.2.1 Technical specification of solar air collector

The solar air collector used is a single-flow hybrid solar collector. Its total surface area is 1.08m^2, of which 0.97m^2 is the absorbing surface. The absorbent surface of the collector is made of 0.4mm thick aluminum and has a titanium (TiO_2) oxide coating that is blue in color, which contributes substantially to improving collector performance. The cover of the collector is made of cast 3mm thick acrylic sheet with 92% permeability coefficient. The frame is made of aluminum, resulting in a weight of 20kg, with special attention being paid both to the sealing of the individual materials and to the insulation of the system using 20mm rock wool on the back side and 20mm glass wool on the side panels. Finally at the bottom of the system there is a small 10-watt photovoltaic panel, in which a small low-power fan is installed. At this point it is worth noting that for maximum solar radiation of 1000W / m^2 the maximum calculated power is 700W with a maximum air flow of 100m^3 / h and a maximum surface temperature of 155 ° C (Sole, 2017).

2.2.2 Solar air collector system function

The solar collector system is driven through adjustable air ducts, with 10 cm diameter, inside the house as shown in figure 3.

Figure 3: Installed solar air collector

In winter, with the air ducts open the system takes off the cool air, through the intake duct, and driven to the absorbing surface of the collector. After that, the heated air is reintroduced by the upper duct into the test cell at a higher temperature. Thus, both space heating and dehumidification are achieved. On the other hand, in summer air ducts are closed and they do not let the system to function. In transition periods, like spring, if both fresh air and heating is needed, the ducts can be adjusted from 0 to 100%. Also, the air ducts are insulated with fiber glass with 5cm width, this insulation diminishes thermal losses during the procedure of transition of the air from the collector to the inside of test cell. Finally, there is a small solar panel at the bottom of the system with maximum power equal to 10W, in which a small power fan is installed. So in sunny hours the system will be more efficient due to faster air exchange. In the reference system, sensors of air temperature and relative humidity have been installed at the center of the two ducts and at a height of a sitting person at the center of the test cell. The sensors are connected with a data logger, which also records weather data from the meteorological station. Finally, the recording system is connected with a computer from both the recording and saving the measurements. The whole experimental scheme is illustrated in figures 4a and 4b.

Figure 4a: Measurements points at the air duct

Figure 4b: Measurements point at the center of area

The experimental set up during cooling period is not differed from that of heating as it concerns the procedures of measuring and storing data. The difference, though, in system operation lies in the fact that the air is being rejected out, instead of reintroduced after being heated from the absorbing surface. Thus, instead of placing sensors of air temperature, humidity and air velocity in the upper duct, the sensor were placed at a modified air outlet of the collector, well insulated with fiberglass, shown presented in figures 5a and 5b.

Figure 5a: Modified air outlet

Figure 5b: Measurements point at the modified air outlet

The sensors were placed in a special structure. At the same time, the upper duct remained closed, preventing in that way the entry of hot air. The cooling period is divided into two time intervals. Those time intervals are different each other only in the way the air inlet from the outdoor environment to indoor one. Therefore, a rectangular ventilation inlet was created at a height of 30cm. This inlet is 7.5 times bigger than ducts, with 30cm long and 20cm height, as shown in figure 6a. An instrument that measures and records air temperature, humidity and air velocity inlet in the indoor area was placed at the center of the ventilation inlet as shown in figure 6b.

Figure 6a: Ventilation inlet

Figure 6b: Measurements point at ventilation inlet

2.3 Measurements period

Greece is divided in four climatic zones, A,B,C and D, in order to specify the time periods round the year for heating and cooling. The study area belongs in climatic Zone C and the cooling period is from 1st of June to 31st of August. As already mentioned, the cooling period is divided into two sub-periods. The first sub-period concerns the operation of the system as a solar collector system and the second as a solar chimney system. The first sub-period was from 1st of June to 28th of July 28, 2017 and the second from 29th of July to 31st of August, 2017. At this point need to mentioned that was absent from measurements taken from 11th of June to 13th of June, 2017 and from 10th of August to 15th of August, 2017 as the data logger was not recording during technical problem.

2.4

The useful thermal power delivered by a solar air collector according to can be calculated from the equation 1.

$$Q_u = \dot{m} C_p (T_o - T_i) \quad (1)$$

Where Q_u the useful heat output of the collector in kW, $\dot{m}$ the air flow in kg / s, C_p the specific heat capacity in kJ / Kg * K, while T_i and T_o the temperature in K at the system inlet and outlet respectively. At this point, it is worth to mention the assumptions that had made. The collector operated in a permanent state, the air flow was one dimensional and there is mass preservation. Also, regarding the collector's losses to the environment was assumed that they were included in the equation as the temperatures measured were experimental. On the above basis and knowing the inlet and outlet temperatures of the collector, the useful thermal power can be calculated by taking a coefficient of specific heat capacity equal to 1,005 kJ / Kg * K and calculating the air flow from the equation 2.

$$\dot{m} = \rho V D \quad (2)$$

Where $\dot{m}$ the air flow in kg / s, ρ the air density in kg / m^3, V the average fluid velocity is perpendicular to the duct inlet cross section in m / s and D the cross sectional area of the duct inlet in m^2. The calculation of the output of thermal energy in the space derived by multiplying the thermal power by the time it takes. Finally, the equation 3 is proposed by authors to calculate the efficiency of a solar collector system.

$$n = \frac{E}{\mathrm{H}_\tau \mathrm{A}_c} \quad (3)$$

Where n the collector efficiency, E the mean daily energy output of solar collector in kWh, H_τ the mean daily solar radiation incident to collector surface in kWh / m^2 and A_c the active surface or the absorbing surface of the collector in m^2.

3 RESULTS

The results which presented in this study referred to the energy that system reject out of the test cell and also the energy efficiency of the system regarding the whole period of measurements and the two sub-periods separately. Daily average values of solar radiation, incident to collector surface, thermal energy and energy efficiency presented in Table 3.1.

Table 3.1 Mean value of solar radiation, thermal energy and energy efficiency of the solar air collector- June 2017

Day	Solar Radiation* (kWh/m^2)	Thermal Energy (kWh/ m^2)	Energy Efficiency (%)
1/6	3.0	0.4	15
2/6	2.7	0.5	18
3/6	2.9	0.6	21
4/6	2.4	0.4	16
5/6	2.9	0.6	22
6/6	2.9	0.4	15
7/6	2.9	0.5	18
8/6	1.9	0.2	11
9/6	2.8	0.4	14
10/6	2.8	0.4	14
14/6	2.8	0.5	17
15/6	2.3	0.2	9
16/6	2.9	0.5	19
17/6	1.9	0.0	0
18/6	2.4	0.2	6
19/6	2.7	0.5	19
20/6	2.7	0.3	11
21/6	2.9	0.5	16
22/6	2.8	0.6	20
23/6	2.9	0.6	20
24/6	2.6	0.3	13
25/6	2.9	0.7	24
26/6	2.9	0.6	20
27/6	2.9	0.5	19
28/6	2.9	0.6	21
29/6	2.9	0.6	21
30/6	2.9	0.7	22

*Solar radiation incident to collector surface

Based on the above table the maximum thermal energy which is 0.7 kWh/ m^2, and energy efficiency which is 24%, observed to the 25th June in which the solar radiation, equal to 2.9 kWh/ m^2 approach the maximum value of 3 kWh/ m^2. The minimum thermal energy which is 0 kWh/ m^2 and energy efficiency which is 0 kWh/ m^2 noticed on the 17th June in which the solar radiation incident to collector surface has the minimum value of that period which is 1.9 kWh/ m^2. In addition, the daily mean thermal energy and energy efficiency values were 0.5

kWh/ m^2 and 16% respectively, while solar radiation was equal to 2.7 kWh/ m^2. Also, the total thermal energy for June 2017 was about 12.0 kWh. Finally, both the daily mean thermal energy values and the energy efficiency values presented in figure 3.1 and 3.2 respectively.

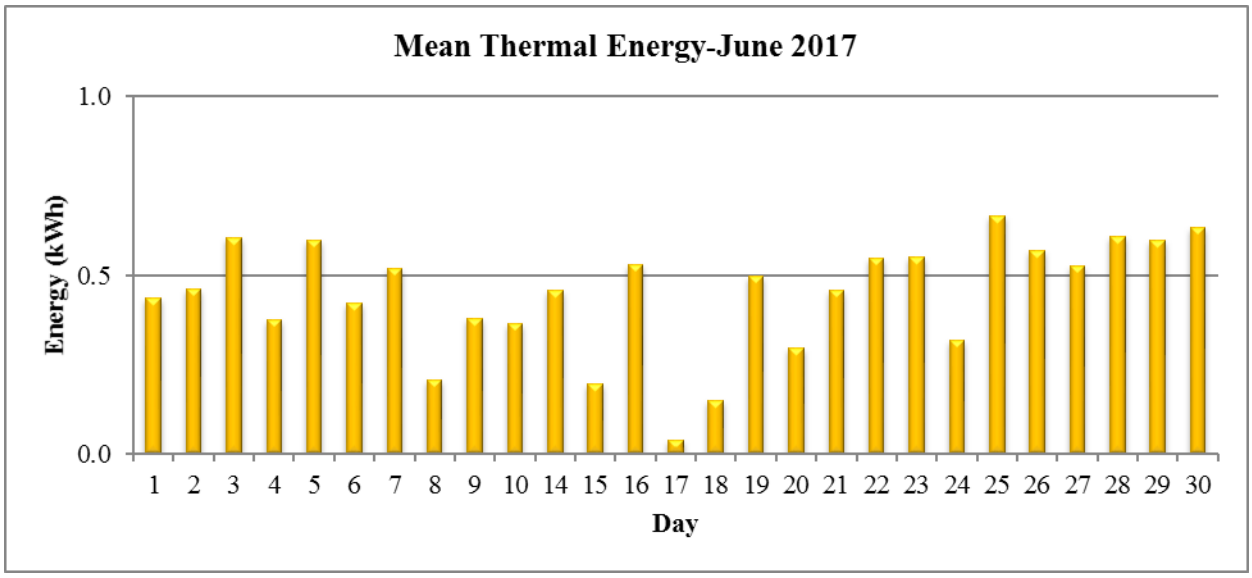

Figure 3.1: Mean Thermal Energy-June 2017

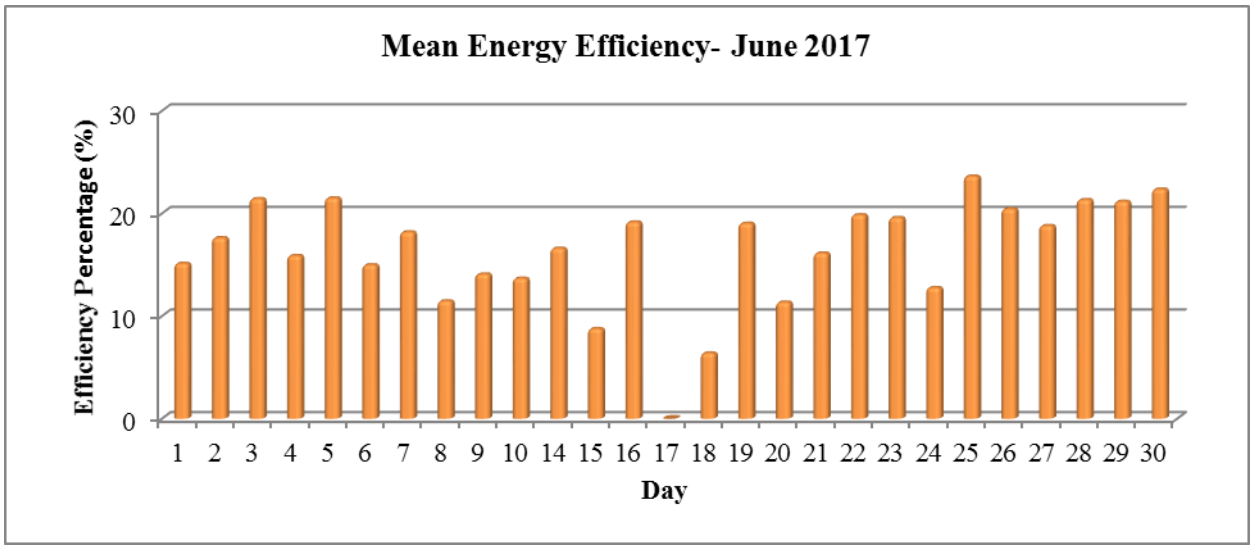

Figure 3.2: Mean Energy Efficiency -June 2017

Similar results observed both July and August 2017. Both thermal energy and energy efficiency daily mean values, depends on solar radiation incident to collector surface, showed in Table 3.2.

Table 3.2 Mean value of solar radiation, thermal energy and energy efficiency of the solar air collector

Month	Solar Radiation* (kWh/m2)	Thermal Energy (kWh/ m2)	Energy Efficiency (%)
June	2.7	0.5	16
July	2.8	0.9	32
August	3.3	1.2	36

*Solar radiation incident to collector surface

From the above table, noticed that the maximum energy efficiency observed at August, equal to 36%, while the minimum value 16% noticed in June. Also, the average energy efficiency during measurements was equal to 28%. These results were expected while the contribution of ventilation inlet lowering the temperature on the test cell and therefore at the inlet duct of the system. Based on the above the air flow as well as the difference between inlet and outlet of the system, was maximized. In addition, in August there was better angle of incidence solar radiation at the collector, with daily average 3.3 kWh/ m^2, which guide to increase the performance of the solar air collector. On the other hand, in June the lack of the external air supply in conjunction to the low levels of the incidence of the solar radiation at the collector, equal to 2.7 kWh/ m2, lead to significantly reduce of system performance almost 50 %. Furthermore, it has to be mentioned that the thermal energy is strongly depends on thermal energy performance of the system and therefore cannot be excluded. The 25 days measurements during August showed that the results of thermal energy was quite closed to those of July, with 30.1 kWh total energy and 1.2 kWh/ m^2 daily average and, 28.4 kWh total energy and 0.9 kWh/ m^2 average respectively. On the other hand the 27 day measurements during June showed that the thermal energy was equal to 12 kWh total energy and 0.5 kW daily average. As it can be concluded, the thermal energy produced during June was generally low, almost the half production among period measurements. The total thermal energy rejected out from the test cell during cooling period was 70.5 kWh. Also the aforementioned heat load rejected out at the first sub-period was 12 kWh and at the second sub-period was 58.5 kWh. Finally according to Droutsa et al (2016), for climate zone where the study area belongs, the average consumption, regarding the cooling load, of a typical household is equal to 2440kWh/year. According to reference, the cooling load for the total area of 20m^2 was 488 KWh. We conclude that there is a reduction of 15% of cooling load, while the solar collector's energy production was equal to 70.5kWh. Based on this the cooling load for 20m^2 calculated at 488 KWh, so there was a reduction of 15 percent while the solar air collector thermal energy as previously referred was in total 70.5kWh.

4 CONCLUSIONS

As part of this study, it has been shown that the solar air collector system has an important role about the thermal loads that rejected out of the test cell in cooling period. Taking into account the fact that was the only cooling systems that function on the test cell a significant reduced in cooling loads had been achieved. The results obtained from the pilot house lead to the conclusion that in conjunction with other interventions both on building shell and using other passive and active systems, even in climatic conditions such as those that prevailed during the measurement period, it can be lead at a nearly zero energy building Finally, the simplicity of the construction of the system makes its installation as a mild intervention in the building shell, while the maintenance cost is zero, resulting in a quick economic damping.

5 REFERENCES

Aboul-Enein S., El-Sebaii A.A., Ramadan M.R.I., El-Gohary H.G., (2000). *Parametric study of a solar air heater with and without thermal storage for solar drying applications.* Renewable Energy, pp. 505-522

Akpinar E.K., Koçyiğit F.,(2010). *Experimental investigation of thermal performance of solar air heater having different obstacles on absorber plates.* International Communications in Heat and Mass Transfer, pp.416-421

Bayraka F., Oztopb F. H., Hepbaslic A., (2013).*Energy and exergy analyses of porous baffles inserted solar air heaters for building applications.* Energy Build, pp. 338-345.

Bopche S.B.,Tandale M.S.,(2009).*Experimental investigation on heat transfer and friction characteristics of a turbulator roughened solar air heater duct.* International Journal of Heat and Mass Transfer, pp.2834-2848

Bouadila S., Kooli S., Lazaar M., Skouri S., Farhat A., (2013).*Performance of a new solar air heater with packed-bed latent storage energy for nocturnal use.*Applied Energy pp. 267-275

Chabane F., Moummi N., Benramache S., (2014).*Experimental study of heat transfer and thermal performance with longitudinal fins of solar air heater.* Journal of Advanced Research, pp. 183-192.

Davliakos N., Botsios-Valaskasis A., (2014), Problems and Prospects in Social Residence Renovation: *The Solar Village Case*, Presentation, available on www.cres.gr/kape/publications/pdf/12.pdf

Droutsa, K. G., Kontoyiannidis, S., Dascalaki, E.G. Balaras, C.A. (2016) *Mapping the energy performance of hellenic residential buildings from EPC (energy performance certificate) data*. Energy, pp. 284-295

Economidis G., *Bioclimatic Office of Low Energy Consumption*, Presentation, available on www.cres.gr/kape/publications/pdf/27.pdf

El-Sebaii A.A., Aboul-Enein S., Ramadan M.R.I., Shalaby S.M., Moharram B.M., (2011).*Thermal performance investigation of double pass-finned plate solar air heater.* Applied Energy, pp. 1727-1739

El-Sebaii A.A., Aboul-Enein S., Ramadan M.R.I., Shalaby S.M., Moharram B.M., (2011).*Investigation of thermal performance of-double pass-flat and v-corrugated plate solar air heaters.* Energy, pp. 1076-1086

El-Sebaii A.A., Al-Snani H., (2010).*Effect of selective coating on thermal performance of flat plate solar air heaters.* Energy, pp. 1820-1828

Hussein, H.M.S., Ahmad, G.E. and H.H. El-Ghetany. (2004).*Performance evaluation of photovoltaic modules at different tilt angles and orientations.* Energy Conversion and Management, 45: 2441–2452

Kosmopoulos, P. and D. Galanos. (2006).*The use of renewable energy source in houses (ZED-KIM).*The 3rd Conference on Passive and Low Energy Architecture. Geneva, Switzerland, 6-8 September

Papadopoulos, A. (2000).*Feasibility of energy saving measures in multi-use building*. Congress on heating, refrigerating and air-conditioning. Belgrade, Pages 233-241.

Sole 2017, *Use of solar air collectors for heating*, Sole, viewed 21 June 2017, <https://www.eurostar-solar.com/solar-air-conditioning-gr.html>

Toumpoulidis P., Dimoudi A., Kosmopoulos P., Zoras S., 2018, *Heat gains from the use of a solar air heater.* The 11th National Conference on Renewable Energy Sources. Thessaloniki, Greece, 14-16 March

Yeh H.M.,(2012). *Upward-type flat-plate solar air heaters attached with fins and operated by an internal recycling for improved performance.* Journal of the Taiwan Institute of Chemical Engineers, pp. 235-240

Evolution of ventilation strategies in air-conditioned buildings in Singapore – IAQ and Energy perspectives

Chandra Sekhar

National University of Singapore
Department of Building,
School of Design and Environment
4, Architecture Drive, Singapore 117566

SUMMARY

Situated 1º North of the equator, Singapore has a year-round hot and humid climate with temperatures in the range of 25 and 32º C and relative humidity around 70%. In view of these environmental conditions, there is really no need for "Heating (or simply "H") in the traditional Heating, Ventilating and Air-Conditioning (HVAC) terminology. Consequently, the term Air-Conditioning and Mechanical Ventilation (ACMV) is used in the local industry. Air-conditioning has over the years become a necessity across the entire building sector, and in particular, in commercial, office, institutional, hotel and hospital buildings. With rising affluence levels, air-conditioning has also become more prevalent in the residential building sector. This presentation tracks the evolution of ventilation strategies in ACMV systems as well as the associated ventilation and IAQ guidelines and standards in Singapore since the 70s. Whilst the early years in Singapore's built environment evolution and development (70s through 90s) were primarily driven by energy considerations, ventilation and IAQ requirements were not ignored. In fact, ventilation provisions were always integral to the building regulations even from those early years. Since the nineties, IAQ awareness rose considerably that also led to the launch of IAQ guidelines in 1996, followed by two related standards in 2009, one on ventilation and the other on IAQ, both of which are part of the design specifications for the built environment. Singapore's own building rating system, called the Green Mark scheme launched in 2005, started with a primary focus on energy and has, since 2015, incorporated an enhanced IEQ and well-being criteria. The fundamental philosophy of ensuring a good balance between energy and IEQ is key to the whole notion of designing and operating energy-efficient healthy buildings.

KEYWORDS

Air-Conditioning and Mechanical Ventilation; Hot and Humid Climate; Ventilation Strategies; High Recirculation Rates; IAQ; Energy

1 INTRODUCTION

The high energy penalty associated with air-conditioning in hot and humid climates has always been a challenge and, hence, a driver for the design of such systems for different types of buildings. Inherent in these designs for energy conservation and energy efficiency are also the considerations for good Indoor Air Quality (IAQ) in the built environment. As "heating" is not needed for comfort air-conditioning in hot and humid climates, the industry term is Air-Conditioning and Mechanical Ventilation (ACMV) rather than the more commonly used Heating, Ventilating and Air-Conditioning (HVAC). This presentation traces the origin of the typical air-conditioning system design concept in Singapore buildings with a particular focus on the ventilation strategies of the various systems adopted and its evolution over the past four decades to the present-day notion of creating and sustaining energy efficient healthy buildings. Singapore introduced its building rating system, called the Green Mark scheme in 2005, which started with a primary focus on energy and has, since 2015, incorporated an enhanced Indoor Environmental Quality (IEQ) and well-being criteria.

2 ACMV CONCEPT AND EVOLUTION IN SINGAPORE

Since the 70s, the most commonly employed ACMV systems in Singapore include the following:

1. Constant Air Volume (CAV)
2. Variable Air Volume (VAV)
3. Primary Air Fan Coil Units (PA-FCU)

VAV systems and PA-FCUs are still popular in current designs. In view of the high energy penalty associated with air-conditioning in hot and humid climates, a high amount of recirculation up to 90% is generally used. This leads to the design and operation of air-conditioned buildings having minimum ventilation provisions, and by design, would not have the possibility of free-cooling or economiser cycle operation.

PA-FCUs are commonly used in designs of hotel buildings as it provides ventilation to all guest rooms at all times and gives considerable flexibility in the operation of the secondary FCUs for additional cooling on demand. A related concept, called the Pre-cooled AHU has also been used in some high-rise building designs with the view of a centralised means of conditioning all the outdoor air needed in a building and distributing through a vertical shaft to the various secondary AHUs at each level. It is, however, to be noted that the Pre-cooled AHU located on the roof-top of a building only caters to partial cooling and dehumidification of the outdoor air and the secondary AHUs need to be designed for additional cooling and dehumidifying capacities.

The 90s also saw the entry of refrigerant modulation systems in buildings in Singapore, which continues to be popular to this day. Although the energy benefits of such systems are fairly well established, it is important to acknowledge the potential IAQ challenges involved if a separate ventilation system or strategy is not considered. The designer needs to ensure that adequate ventilation is provided in these buildings.

The above systems could be considered as typical ACMV systems for Singapore and cover almost the entire sector of commercial, office, institutional, hotel and hospital buildings.

The energy issues and indoor humidity concerns in air-conditioned buildings have also been addressed by employing technologies to better handle the cooling and dehumidification processes. Heat pipes have begun to be used in some buildings since the 90s as they provide significant energy savings and simultaneously achieve good humidity control, especially in applications needing 100% Outdoor Air.

Within the past decade or so, the concept of DOAS integrated with chilled beams or other means of providing secondary localised cooling is drawing considerable attention. Some examples of such recent applications will be presented.

Since the 70s, there has been a gradual evolution of the ACMV concept in buildings in Singapore. Energy, ventilation and IAQ criteria have been the primary drivers for this evolution and the current thinking encompasses the following key considerations:

- High Temperature cooling and dehumidification
- Move only as much air as is needed for ventilation

- It is much more energy efficient to move water/fluid to occupied zones for heat transfer/cooling
- Elevated space temperature and elevated air speed for Thermal Comfort

3 EVOLUTION OF VENTILATION AND IAQ STANDARDS

Ventilation requirements have been an integral part of the Singapore Building Regulations since the early 80s. As mentioned earlier, energy considerations were the prime mover and minimum ventilation provisions were specified (CP13, 1980), which underwent one revision in 1999. It was only in 1996 that IAQ guidelines were first introduced in Singapore. In 2009, CP13 was further revised and redesignated as SS553 and a new standard on IAQ was also simultaneously launched (SS553, 2009; SS554, 2009). These two standards are now to be used in tandem for specifying indoor environmental requirements in buildings.

4 REFERENCES

CP 13, 1980. *Code of Practice for Mechanical Ventilation and Air-conditioning in Buildings* Singapore

SS 553, 2009. Singapore Standard. *Code of Practice for air-conditioning and mechanical ventilation in buildings,* Singapore.

SS 554, 2009. Singapore Standard. *Code of Practice for indoor air quality for air-conditioned buildings,* Singapore.

Dynamic performance of displacement ventilation in a lecture hall

Natalia Lastovets[*1], Kai Sirén[1], Risto Kosonen[1,2], Juha Jokisalo[1], Simo Kilpeläinen[1]

1 Aalto University
Department of Mechanical Engineering
Sähkömiehentie 4
Espoo FI-00076, Finland
**Corresponding author: natalia.lastovets@aalto.fi*
Presenting author: Natalia Lastovets

2 Nanjing Tech University
College of Urban Construction
P.O. Box 76, No. 200 North Zhongshan Rd
210009, Nanjing, China

ABSTRACT

An accurate temperature gradient calculation is essential for displacement ventilation (DV) system design, since it directly relates to the calculation of the required supply air flow rate. Inaccurate temperature prediction can cause the poor thermal comfort and w sizing of the ventilation and cooling systems. Several simplified nodal models were developed and implemented in the various building simulation software to estimate the temperature stratification in rooms with DV. Recent studies reveal that the multi-nodal models provide the most accurate temperature gradient prediction. However, the most building simulation software uses the air models with only one air node. The present study introduces the dynamic temperature gradient model for DV and investigates the effect of thermal mass on the temperature stratification. The model was validated with the experimental results of the lecture room with displacement ventilation. The room air temperature measurements were conducted during three weeks at 20 different heights. The supply air temperature and occupancy rate were recorded during each scheduled lecture. The developed dynamic nodal model is able to accurately calculate the air temperatures in occupied zone. The effect of the thermal mass and varied heat loads on the indoor air temperature stratification is analysed for the lecture room with DV.

KEYWORDS

Displacement ventilation, RC-model, building simulation, thermal mass, thermal comfort

1 INTRODUCTION

In displacement ventilation (DV) systems, cool air is supplied into the occupied zone of the room near the floor at low velocity and then entrained by buoyant plumes over any warm objects. As a result, a two layer profile of room air temperature, stratified and mixed, is developed. Ideally, the air movements induced by thermal plumes transport heat and pollutants up to the occupied zone, promoting a vertical temperature and contaminants stratification. The transition level between a mixed upper layer and stratified layer is called mixing height, which is related to the height where the inflow rate matches the airflow induced by the thermal plumes in the occupied zone. Controlling the mixing height position is one of the most challenging tasks in DV system design, since it directly related to the calculation of supply air flow rate.
The temperature gradient in DV systems is usually calculated with the nodal approach. (Griffith and Chen, 2004). The multi-nodal models provide a promising method for the temperature gradient prediction (Kosonen et al, 2016). Some of the simple and multi-nodal models are applied in DV design and available in thermal energy simulation tools, such as IDA-ICE (Mundt, 1995) and EnergyPlus (Mundt, 1995 and Mateus, 2015, Mateus and da Graça, 2017)..

Nowadays, building energy simulation methods are applied to study the dynamic behaviour of heat and mass balance. They have been developed starting from engineering steady-state analytical models through simplified dynamic balance methods to the modern validated energy modelling programmes (Wang and Zhai 2016). The programs could use simplified dynamic method, for instance response function methods, or numerical finite difference method. Having been driven by the increase of computational power, the use of building simulation software is getting widespread in the design and consulting communities. However, simplified models are still applied in building energy analysis due to their user-friendliness, straight forward calculation and suitability for optimisation and demand control calculations (Kramer et al., 2012). The simplified models are classified to physical and mathematical data-driven models (Foucquier et at., 2013; Ji et al, 2016). Among the simplified model RC models are the most popular, since their parameters have obvious physical meanings and the models require less data than data-driven models. Based on circuit principles and Kirchhoff electric current theory, constructing building models with RC-networks implies representing every element of the building with resistors and capacitors. The simplest one-capacity models are not able to represent accurately the indoor air temperature dynamics, since the real physical process behaves like a two- or higher order system. In addition, several studies show that higher order models are more accurate than the first order RC models in capturing thermal behaviour of a building (Fraisse et al., 2002; Tindale, 1993). The RC models can be focused mainly on the dynamic thermal behaviour in building envelope or in the whole building. The building envelope RC models usually consist of at least three wall resistances and two (Gouda et al, 2002) or four (Fraisse et al., 2002) capacitances. These models are usually suitable to predict dynamic indoor and outdoor heat pulses and working insufficiently with lasting thermal loads (Antonopoulos & Koronaki, 2001).

Lumped parameter methods can also be applied for modelling the whole zone instead of individual construction elements (Crabb, 1987; Dewson, 1993; Neilsen, 2005 Kämpf, 2007). In this approach, all the thermal capacities of the different construction elements that the zone is composed of are concentrated in a single equivalent capacitance, and another additional capacitance is added for the air of the zone. The accuracy of these methods highly depends on the value of their characteristic capacities, so they need to be adjusted using different methods. Values of the characteristic parameters of the model be obtained with simple configurations (Seem et al., 1989) or analytically by comparing the response with a high-order reference model using optimization with single objective (Wang and Xu, 2006; Gouda et al, 2002; Fraisse et al., 2002) or multi-objective (Underwood, 2014) function.

This study introduces simplified 2-capacity R2C2 model, where the capacities and conductances are calibrated against the results taken from the advanced building simulation model IDA-ICE. The 2-capacity model structure and the calibration methodology was initially created by Kai Sirén (Sirén, 2016) and implemented for the space heating using model predictive control in an office building (Mäki, 2018) for one air node. The initial model was modified with calculate the temperature gradient in rooms with DV with the use of the multi-nodal model (Lastovets et al., 2018). The presented calibrated two-capacity model was validated with the measurements in the lecture hall.

2. METODS

2.1 Simplified 2-capacity model

The structure of the proposed model is shown in Fig.1. The initial model was modified to calculate the indoor air temperature gradient in rooms with displacement ventilation to calculate three air temperatures: along the floor at the height 0.1 m $t_{0.1}$, at the level of mixing height t_{mx} and the exhaust temperature tex. The first two temperatures were counted with following

assumptions: the supply air temperature reflects the temperature along the floor; there is a load division between the mixing height level and the height of exhaust air.
The inputs of the models are the outdoor air temperature T_{out} and the supply air temperature T_s. T_{mx} is the air temperature at the mixing height that is calculated using the plume theory (Lastovets et. al, 2018).
In the model, there is two capacities: conductances of room air C_a and building thermal mass C_m. The mass capacity C_m is related to the thermal mass in the walls, ceiling and floor. The model includes the heat capacity flow through ventilation H_{as}, heat conductances of window H_{ae}; between mass node and outdoor air node point H_{ms} and between mass node and indoor air node point Ham.

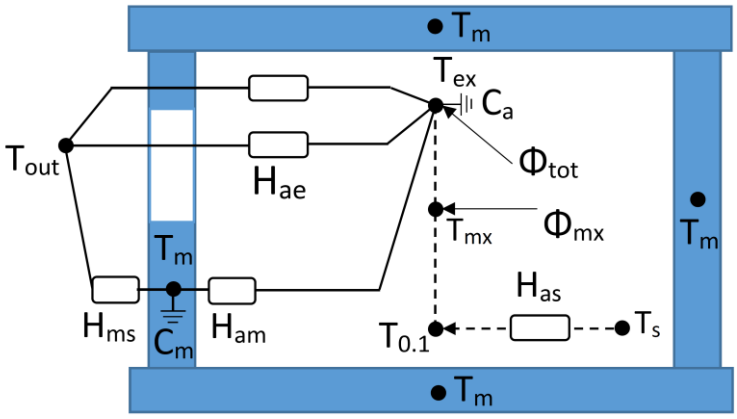

Figure 1: Structure of the simplified 2-capacity

Both conductances H_{ms} and H_{am} contain heat conduction in the solid wall material as well as convection on the surfaces. The mass node point is located in an undefined depth inside the building structure and represents a kind of mean temperature of the active building mass.
The total heat load in the zone heat balance in the model Φ_{tot} consists of low Φ_{mx} and high Φ_{high} heat loads.
Low heat loads are related the ones that occur in the occupied zone of the room, whereas high heat loads are located near the ceiling. The examples of low heat loads are the ones from people and office equipment. The high heat loads in practice could be from lighting units or solar gains through high-located windows. When heat load occurs in the middle of the room, it depends on the mixing height whether consider them high or low heat loads. If the mixing height is located within the occupied zone, it refers to low heat loads, and vice versa (Lastovets et al., 2018).

2.2 Experimental study of the lecture room

Measurements were carried out between 27th of October and 1st of December 2017 in the lecture room of Aalto University. A sketch of the layouts are provided in Figure 1. The exhaust grilles are near the ceiling height and located along the back walls. The supply air flow rate has maximum value when occupancy sensors detect any presence though ventilation rate does not change with number of students present.

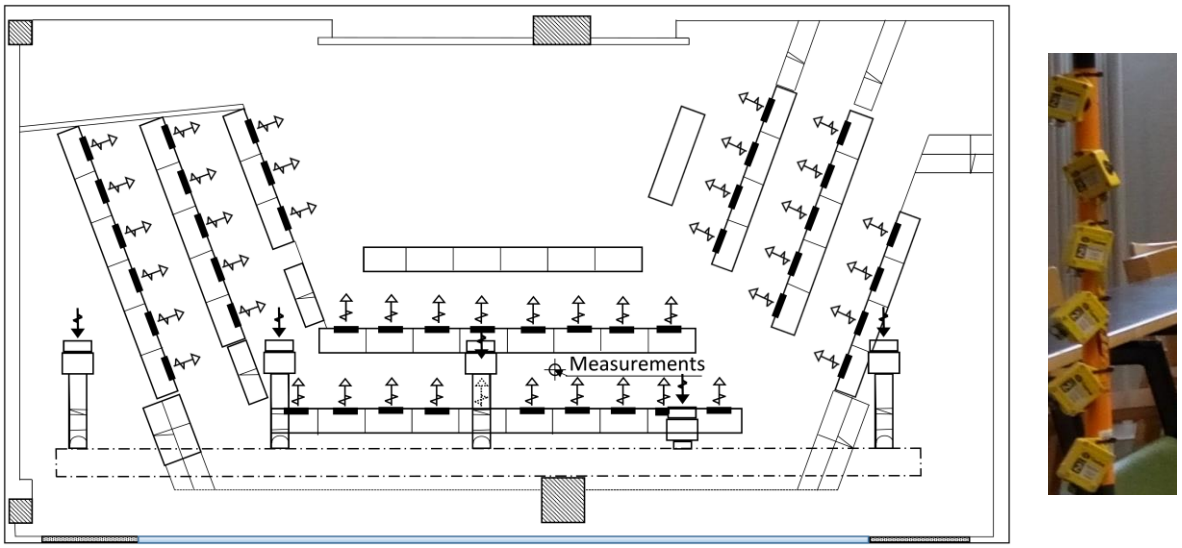

a) b)

Figure 2: The layout of the classroom and the location of the measurement mast a) and the image of it b).

For measuring temperature at different heights, floor to ceiling, the measuring mast was assembled with 20 TinyTag Plus 2 Dual Channel loggers. Seventeen TinyTags were located at 10 cm separation, starting from 0.1 to 1.7 m, followed by three more at 2, 2.5, and 3 m respectively. A Swema 3000md manometer was used for measuring flow rates from individual diffusers

Table 1: Table Caption

Column Title	Column Title	Column Title	Column Title	Column Title
Table content				

2.3 IDA-ICE building simulation as a source of the reference data

The building model was formed using IDA indoor Climate and Energy 4.0 (IDA-ICE) building simulation software. This software allows modelling of the building, HVAC-systems, internal loads, outdoor climate, etc. and provides simultaneous dynamic simulation of heat transfer and mass flows. It is a suitable tool for the simulation of thermal comfort, indoor air quality, and energy consumption in complex buildings. A modular simulation environment, IDA-ICE, has been developed by the Division of Building Services Engineering, KTH, and the Swedish Institute of Applied Mathematics, ITM (Shalin et al. 1996, Björsell et al. 1999). The mathematical models are described in terms of equations in a formal language using non-negative matrix factorization. The IDA-ICE simulation software was validated both empirically (Bjorsell at al., 1999; Moinard and Guyon, 1999; Jokisalo at al., 2007; Travesi et al, 2001) and via several independent inter-model comparisons (Achermann and Zweifel, 2003; Loutzenhiser et al, 2009). In addition, IDA-ICE was validated according to the European Standard prEN 13791 by Kropf and Zweifel (2001). The standard defines the test cases: heat conduction through opaque walls, internal long wave radiation exchange, shading of windows by external constructions, and a test case for the whole calculation method, for which the IDA-ICE simulations gave the results as demanded by the standard. The robustness and reliability of IDA-ICE building simulating program to perform building energy calculations allows using it as a reference for the calibration of the 2-capacity model.

Since the software does allows building only “show box” rooms, the sizes of the model was adjusted from the volume of the room (Table 1). The internal staircase massive was also shrimped to equal floor thickness (Figure 3).

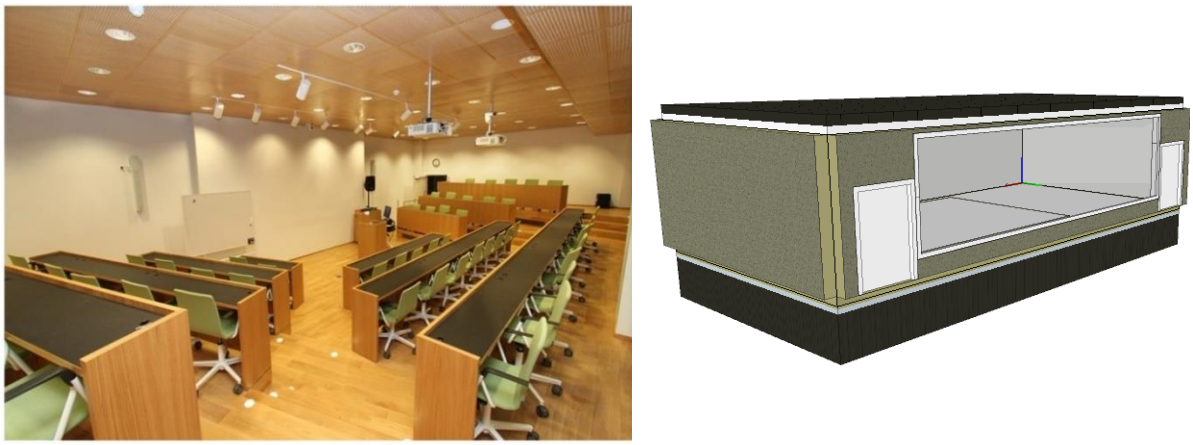

Figure 3: The photo of the studies lecture room and the IDA-ICE model of it

Table 1: Constructional and system parameters of the study case

Parameter	Value	Dimension
Net floor area	A_f	86.4
Total internal surface area	A_{int}	289.2
Internal volume	V_{int}	256.5
Internal heat loads	Φ_t	0.0
Window conductance	H_{ae}	45.4
Leakage air flow	q_{inf}	0.0
Supply air flow	q_s	0.6
Supply air temperature	t_s	18.0
Room air temperature	t_a	21.0

3. CALIBRATION METHOD OF THE TWO-CAPACITY MODEL

In the RC model , the heat conductances and heat capacitances are needed to determine. The characteristic parameters of the presented R2C2 model are calibrated against IDA-ICE simulation results. In the method, the thermal behaviour in RC-model matched with the results of the detailed model of IDA ICE. The methodology of the model calibration was performed for one air node ta by using the methodology developed by Kai Sirén (Sirén, 2006). The calibration consists of steady-state and dynamic set response parameter identification (Figure 4).

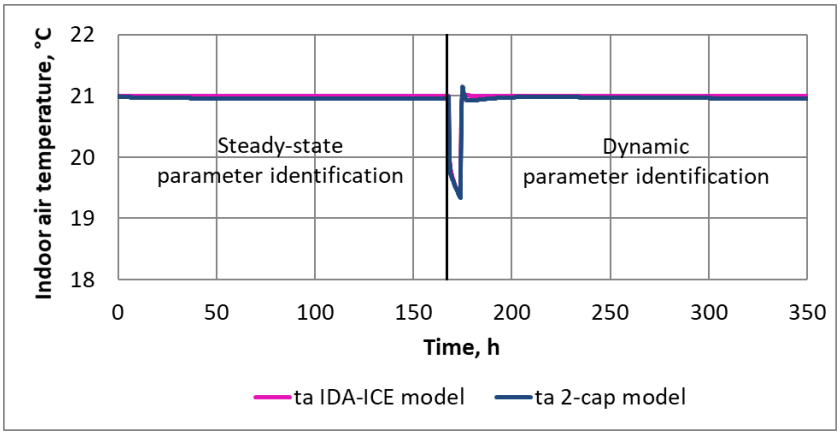

Figure 4: Steady-state and dynamic parameter identification in RC-model calibration with constant T_{out} = 18 °C.

3.1 Steady-state parameter identification

In steady state parameter identification, the steady state energy balance was matched with the indoor air node point to fix the conductance values of the 2-capacity model. The internal heat loads were not applied in the models since they are not needed in the calibration. The IDA-ICE simulation program generates the reference data for the steady state conditions. Conductance values were calculated by running the IDA ICE model with artificial weather file were all the parameters, such as outdoor air temperatures, wind speed, had constant values. Three different values of outdoor temperatures (+18 °C, +19 °C, +20 °C) were used to get an average performance that are outdoor temperature dependent such as heat transfer coefficients and window U-values.

The simulation with the IDA ICE model with constant outdoor parameters has to carry out long enough, so that the building reached steady-state condition, from which the conductance values and the heat capacity flows could be determined. In order to keep the indoor air set point temperature 21 °C, the ideal heater is applied with the maximum power 5 kW.

The conductance values of window H_{ae} and room constructions H_{ams} and as are inserted directly from the IDA-ICE model. The conductance H_{ams} in steady-state parameter identification is combined from the conductances on both side of the mass node point (H_{am} and H_{ms}), which are determined in the dynamic identification stage.

The correct value for H_{ams} was searched so that the error in heating powers resulting from air node energy balance between the IDA ICE and the RC-model at the three different outdoor temperatures was at the minimum with the use of nonlinear optimization using the generalized reduced gradient method.

Parameters from the steady-state identification together with the calibration parameters are presented in Table 2.

Table 2: 2-capacity model parameter values from steady-stare identification

t_{out} , °C	Φ_{hc}, W	H_{as}, W/K	H_{ae}, W/K	H_{ams}, W/K
18	2714			
19	2573	726	45	146
20	2439			

3.2 Dynamic parameter identification

The dynamic parameter identification was performed after the steady-state one. The purpose of the dynamic parameter identification was to determine the air and mass heat capacities Ca and Cm and the conductance between mass node and indoor air node point Ham. The conductance between mass node and outdoor air node point H_{ms} is determined from the Eq 9.

Three model parameters H_{am}, C_m and C_a were searched in a dynamic state by applying an excitation influence the system based on the IDA reference simulations. The excitation can be achieved by a sudden change in the external temperature, solar intensity, internal loads or heating power. Since the 2-capacity model was intended to forecast the indoor heat gains and temperature stratification, the heating power was chosen as a variable when the time-dependent change was made.

In the presented calibration, the simulated identification sequence had first a 167-hour one-week period for stabilizing the temperatures, a 6 hours interruption in the heating power and a second one-week period to check the final temperature level and the heating power will reach steady-state values. The IDA-ICE reference simulations were again performed in three different

outdoor air temperatures (18 °C, 19 °C, 20 °C) with the correspondent recording of the air temperatures and heating powers.
Indoor air temperature was chosen as identification criterion the difference between simulated reference and model produced values of a chosen quantity in the system is used. The room air temperatures calculated in the 2-capacity model and IDA model were compared for parameter identification. The dynamic calibration was defined as a minimization problem, where the average absolute differences between air temperatures in IDA model and 2-capacity model from the simulations with three different outdoor temperatures were minimized. The minimization problem was solved by using a sequential search algorithm supplemented with a local refinement procedure. Table 2 shows the calibrated parameter values.

Table 3: The parameters of the calibrated 2-capacity

H_{am}, W/K	H_{ms}, W/K	C_a, kJ/K	C_m, kJ/K	$\lvert t_a - t_{ar} \rvert$, °C
1453	162	1581	48158	0.04

The indoor air temperatures in the IDA model and in the 2-capacity model after the calibration with three constant outdoor air temperatures are showed at the Figure 5.

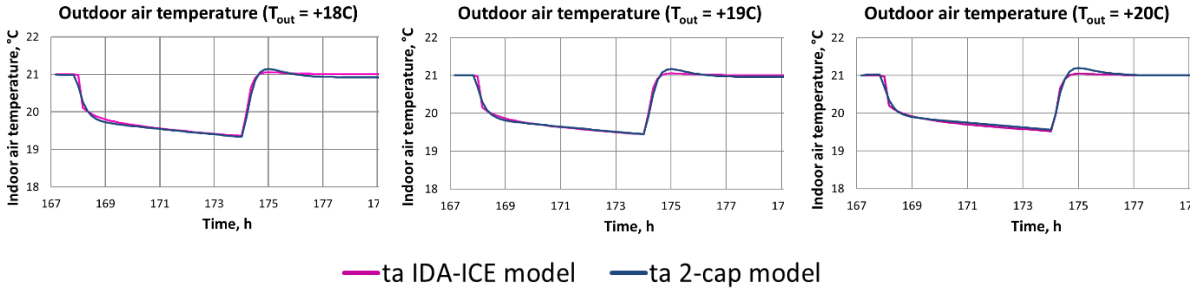

Figure 5: Comparison of the two-capacity model and IDA-ICE simulation indoor air temperature with tree different outdoor temperatures

The decay curves depict first a rapid change when the air is cooling down and then after that a more slow decay when the building mass thermal mass is activating. The indoor air temperatures calculated with the IDA-ICE model and 2-capacity model demonstrate a reasonable fit to describe the thermal mass effect of the room air and structures. That makes possible to use the celebrated parameters (Tables 2 and 3) to calculate indoor air temperatures in 2-capacity model.

4. VALIDATION OF 2-CAPACITY MODEL

This section presents the validation of the 2-capacity model based on the air temperature measurements in the lecture hall for two conditions (Table 4). The heat gains of people were estimated to be 100 W per person. The high-levelled heat gains consisted of the lighting units. Figure 5 presents the measured indoor temperature gradients and the comparison between two-capacity model simulations and indoor temperature measurements for the cases with different heat loads and load profiles.

Table 4: The parameters of the two validation cases

	Φ_{tot}, W	Φ_{mx}, W	Φ_{high}, W	$\lvert t_s \rvert$, °C
Case 1	8000	5000	3000	19

Case 2	5000	3000	2000	21

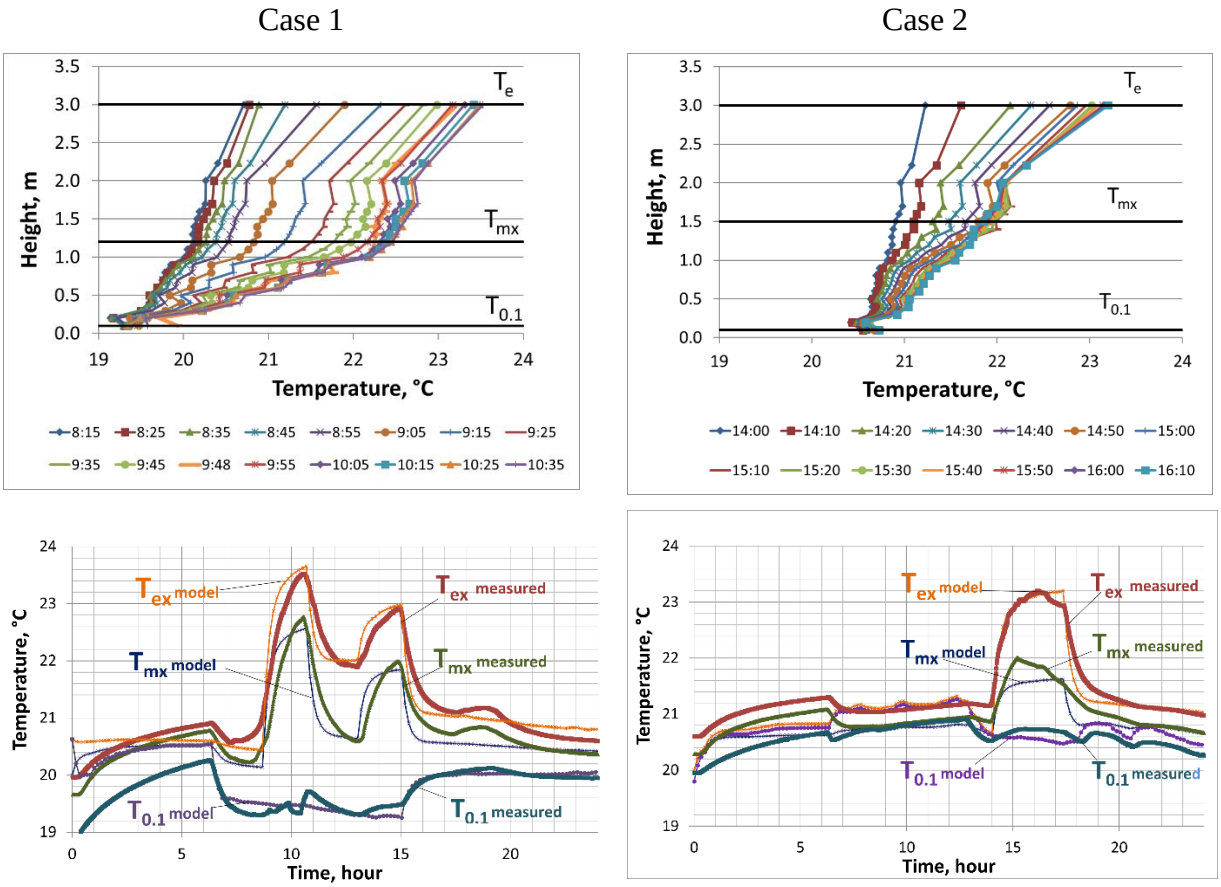

Figure 5: The measured indoor temperature profiles (upper) and the comparison of the two-capacity model three temperatures with measurements (lower).

In both cases, the 2-capacity DV model predicted well the trends of the indoor air temperatures in all three studied heights. The model was able to account the changing supply temperatures and heat loads. Thus, the calibrated capacities are applicable to the presented R2C2 model. The important temperatures for displacement ventilation, such as a mixing height temperature tmx and a temperature along the floor $t_{0.1}$, were calculated with the high average level of accuracy. In the Case 2, the mixing height temperatures were slightly underestimated. However, in this case it could be related to the uneven internal load distribution.

5. CONCLUSIONS

The accurate dynamic model to calculate the temperature gradient in rooms with DV is crucial in the design process, since it reflects the close to the reality conditions. The introduced calibration procedure allows accounting the thermal mass effect on the internal air temperatures. The presented model is able to take into account time schedules of heat loads and thermal mass of building. The results show that the trained two-capacity model can predict the indoor air temperature gradient in dynamic conditions. The model has good robustness to predict the thermal performance under different operation conditions by capturing the dynamic characteristics of the building system correctly. The good robustness of the model is due to the parameters of the building internal mass model and the model structure, which not only

describes the behaviour or performance of the building internal mass but also represents the building thermal mass physically. The procedure to estimate the lumped thermal parameters of the building internal mass model is presented in the study can be effectively used to identify the parameters using short-term operation data. The model can be applied in design DV in various dynamic conditions.

6. REFERENCES

Antonopoulos, K. A., & Koronaki, E. P. (2001). *On the dynamic thermal behaviour of indoor spaces*. Applied Thermal Engineering, 21(9), 929-940.

Björsell N., Bring A., Eriksson L., Grozman P., Lindgren M., Sahlin P., Shapovalov A., Vuolle M. (1999). I*DA indoor climate and energy*, in: Proceedings of the IBPSA Building Simulation Conference, Kyoto, Japan.

Braun, J. E., & Chaturvedi, N. (2002). *An inverse gray-box model for transient building load prediction*. HVAC&R Research, 8(1), 73-99

Crabb, J. A., Murdoch, N., & Penman, J. M. (1987). *A simplified thermal response model*. Building Services Engineering Research and Technology, 8(1), 13-19.

Dewson, T., Day, B., & Irving, A. D. (1993). *Least squares parameter estimation of a reduced order thermal model of an experimental building*. Building and Environment, 28(2), 127-137.

Foucquier, A., Robert, S., Suard, F., Stéphan, L., & Jay, A. (2013). *State of the art in building modelling and energy performances prediction: A review*. Renewable and Sustainable Energy Reviews, 23, 272-288.

Fraisse, G., Viardot, C., Lafabrie, O., & Achard, G. (2002). *Development of a simplified and accurate building model based on electrical analogy*. Energy and buildings, 34(10), 1017-1031.

Gouda, M. M., Danaher, S., & Underwood, C. P. (2002). *Building thermal model reduction using nonlinear constrained optimization*. Building and environment, 37(12), 1255-1265.

Griffith, B., & Chen, Q. Y. (2004). *Framework for coupling room air models to heat balance model load and energy calculations (RP-1222)*. Hvac&R Research, 10(2), 91-111

Ji, Y., Xu, P., Duan, P., & Lu, X. (2016). *Estimating hourly cooling load in commercial buildings using a thermal network model and electricity submetering data*. Applied Energy, 169, 309-323.

Jokisalo, J., Kalamees, T., Kurnitski, J., Eskola, L., Jokiranta, K., & Vinha, J. (2008). *A comparison of measured and simulated air pressure conditions of a detached house in a cold climate*. Journal of Building Physics, 32(1), 67-89.

Kosonen, R., Lastovets, N., Mustakallio, P., da Graça, G. C., Mateus, N. M., & Rosenqvist, M. (2016). *The effect of typical buoyant flow elements and heat load combinations on room air temperature profile with displacement ventilation*. Building and Environment, 108, 207-219.

Kramer, R., Van Schijndel, J., & Schellen, H. (2012). *Simplified thermal and hygric building models: A literature review*. Frontiers of architectural research, 1(4), 318-325.

Kämpf, J. H., & Robinson, D. (2007). *A simplified thermal model to support analysis of urban resource flows*. Energy and buildings, 39(4), 445-453.

Lastovets, N., Kosonen, R., & Mustakallio, P. (2018). *Comparison of simplified models to estimate vertical temperature gradient in rooms with displacement ventilation*. In Proceedings Roomvent & Ventilation 2018 (pp. 499-504)

Loutzenhiser, P., Manz, H., Maxwell ,G. (2007). *Empirical Validations of Shading /Daylighting / load Interactions in building energy simulation tools, A Report for the International energy Agency SHC Task 34*, ECBCS Annex 43 Project C.

Mateus, N. M., & da Graça, G. C. (2015). *A validated three-node model for displacement ventilation*. Building and Environment, 84, 50–59.

Mateus, N. M., & da Graça, G. C. (2017). *Simulated and measured performance of displacement ventilation systems in large rooms*. Building and Environment, 114, 470-482.

Moinard S.,Guyon G. (1999). *Empirical validation of EDF ETNA and GENEC test-cell models*, in: Subtask A.3, A Report of IEA Task 22. Building Energy Analysis Tools.

Mundt, E. (1995). *Displacement ventilation systems – Convection flows and temperature gradients.* Building and Environment, 30(1), 129–133.

Mäki A. (2018). *Demand response of space heating using model predictive control in an office building. Doctoral thesis*. Espoo, Finland: Aalto Univer-sity.

Nielsen, T. R. (2005). *Simple tool to evaluate energy demand and indoor environment in the early stages of building design*. Solar Energy, 78(1), 73-83.

Seem, J. E., Klein, S. A., Beckman, W. A., & Mitchell, J. W. (1989). *Transfer functions for efficient calculation of multidimensional transient heat transfer.* Journal of heat transfer, 111(1), 5-12.

Shalin, P. (1996). *Modelling and simulation methods for modular continuous system in buildings. PhD Thesis*. Royal Institute of Technology (KTH), Stockholm, Sweden.

Sirén Kai (2016). *Course material: A simple model for the dynamic computation of building heating and cooling demand*. Espoo, Finland: Aalto University.

Tindale, A. (1993). *Third-order lumped-parameter simulation method*, Build. Serv.Eng. Res. Technol. 1487–97

Travesi, AJ., Maxwell, G., Klaassen, C., Holtz M. (Eds.) (2001). *Empirical Validation of Iowa Energy Resource Station Building Energy Analysis Simulation Models*, IEA, 2001.

Wang, H., & Zhai, Z. J. (2016). *Advances in building simulation and computational techniques: A review between 1987 and 2014*. Energy and Buildings, 128, 319-335.

Wang, S., & Xu, X. (2006). *Parameter estimation of internal thermal mass of building dynamic models using genetic algorithm*. Energy conversion and management, 47(13-14), 1927-1941.

Zweifel, G., & Achermann, M. (2003). *RADTEST–the extension of program validation towards radiant heating and cooling*. Building Simulation ‘03, Eindhoven, Netherlands, 1505-1511.

Crowe, K. (1974). *A History of the Original Peoples of Northern Canada.* Montreal: McGill/Queen's University Press for the Arctic Insitute of North America.

Zaslow, M. (1988). The Northward Expansion of Canada. *The Journal of Canada, 2*(3), 216-222.

Numerical Modelling of Large Air-Conditioned Space: Comparison of Two Ventilation Systems

Ali Alzaid*[1], Maria Kolokotroni*[1], Hazim Awbi[2]

1 College of Engineering, Design and Physical Science, Brunel University London
Uxbridge, Middlesex UB8 3PH, UK
AliMohammadA.Alzaid@brunel.ac.uk
Maria.kolokotroni@brunel.ac.uk

2 School of Built Environment, University of Reading
Reading RG6 6AY, UK

ABSTRACT

This paper presents a comparative study based on CFD simulation between the performance of Impinging Jet Ventilation (IJV) and Mixing Ventilation (MV) systems in providing indoor air quality and thermal comfort for a mechanically ventilated occupied large open plan office (floor-to-ceiling height > 5m). Large spaces differ from spaces with standard heights because of the significant upward stratification. The evaluation was carried out using the Air Distribution Index (ADI) which combines several parameters, such as overall ventilation effectiveness for removing pollutants and for temperature distribution ($\overline{\epsilon_c}$,$\overline{\epsilon_t}$), percentage of dissatisfied (PD) and predicted percentage of dissatisfied (PPD). ADI has been used to characterize ventilation systems in spaces with typical floor-to-ceiling heights, but it has not been studied for large spaces to-date. In this study, different test conditions were considered for two cooling loads (48 W/m^2, 68 W/m^2) with full and half occupancy respectively. The model was validated via spot measurements of air temperature, air speed and CO_2 concentration in a large office located in south east England which, is supplied by a mechanical cooling with overhead diffusers providing mixing ventilation. The predicted results were generally in good agreement with measured values of air temperature, air velocity and CO_2 concentration.
The calculated (ADI) for (IJV) and (MV) systems using the validated CFD model showed that the (IJV) system is more effective than (MV) system in removing both pollutants and heat from the occupied zone. It is concluded that using (ADI) to assess the effectiveness of different ventilation systems in large enclosures can provide useful information that combines both indoor air quality and thermal comfort.

KEYWORDS

Large space, Ventilation system, Air Distribution Index (ADI), Numerical model

1. INTRODUCTION

Large single cell spaces have become a considerable characteristic of modern buildings. Examples include shopping malls, lecture theatres, airports terminals, gymnasiums and large open plan offices. They are considered to be large when the floor-to-ceiling height is more than 5 meters (Li *et al.*, 2009). Ventilation of such spaces needs more careful attention by design engineers than spaces with a small volume, i.e. those with a ceiling height of 3 meters or less. This is because the volume of the occupied zone is generally small compared to the entire volume. Therefore specific ventilation strategies which direct the ventilated air and thermal conditioning to the occupied zone are needed to achieve energy efficiency (International Energy Agency (IEA), 1998). Heating, ventilation and air conditioning systems (HVAC) are used to supply the spaces with acceptable levels of air temperature, humidity, air velocity and acceptable indoor air quality by removing the contaminants from the spaces. Therefore, the implementation of a suitable air distribution system will have a significant impact on the air flow patterns and indoor air quality within the ventilated space. To characterise the combined thermal environment and indoor air quality in buildings, Awbi and Gan (1993) and Awbi (1998) developed the concept of the ventilation performance (VP) which

was re-named later the Air Distribution Index (ADI) (Awbi, 2003; Karimipanah, Awbi and Moshfegh, 2008). This index is used to assess the thermal comfort, indoor air quality and energy performance of an air distribution system. In 2017, an extensive literature survey was carried out on studies of HVAC systems' performance in large rooms, which found that only three types of room air distribution strategies are used in large rooms. These are displacement ventilation (DV), mixing ventilation (MV) and underfloor air distribution systems (UFAD) (Mateus and Carrilho da Graça, 2017). Also, a fourth system, impinging jet ventilation (IJV) which has been evaluated only in two recent studies by Ye *et al.* (2016) and (Ye *et al.*, 2019) when it was used in the ventilation of a large space. It is traditionally used in typical spaces and described as having promising potential for large spaces.

This paper aims to evaluate the performance of two different ventilation systems: Impinging Jet Ventilation (IJV) and Mixing Ventilation (MV) systems in providing indoor air quality and thermal comfort and consequently energy performance for a mechanically ventilated occupied large open plan office (floor-to-ceiling height > 5m). The Air Distribution Index (ADI) will be used to characterize ventilation systems in large spaces for the first time since it has been studied only in spaces with typical floor-to-ceiling heights.

2. NUMERICAL METHOD

2.1 Physical Models

The large space under consideration is a large open plan office used by research staff and students which has floor-to-ceiling height of 6m is the CSEF Building at Brunel University London. The enclosure has dimensions of 15.5m x14m x 6m and a floor area of 201 m^2 with brick external walls and metallic roof which includes two large skylights. Two big rectangle windows are located on the south side wall of the building with dimensions 3.5m x 1.1m and 4.2m x 1.1m. There is one door on each end wall of the building. For the MV simulation, the external air is delivered into the building interior through a 13m long cylindrical supply duct with a 0.7m diameter. This duct has eight air diffusers located at a height of 3.7 m above the floor with a dimension of 0.8m x 0.15m. Air exhaust is via two return grills located at a height of 3.7m with dimensions 1.0m x 0.5m each, see Figure 1. For the IJV simulation, the supply air is delivered into the building interior through 21 IJV ducts each with a supply opening area of 0.03 m^2 and a distance of 0.7 m above the floor were uniformly distributed inside the office, as recommended by Awbi (2003). 17 IJ diffusers were attached to the walls while the remaining 4 were attached to a column at the centre of the office, as shown in Figure 2.

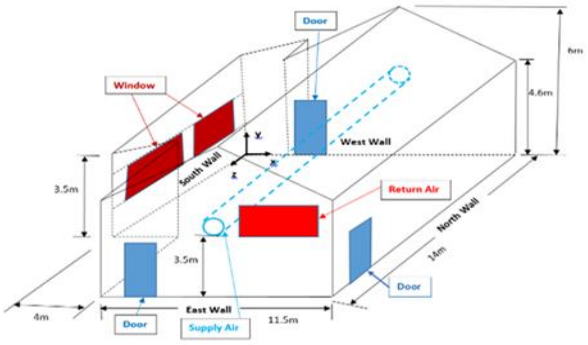

Figure 1: Sketch of the researchers' office with the MV

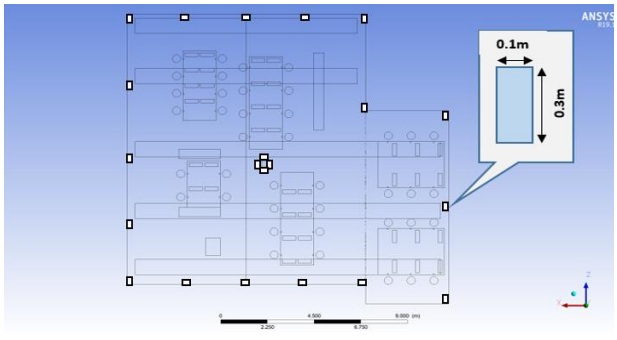

Figure 2: Plan sketch of the researchers' office with the IJV

In this study two different test cases were considered for two occupancy capacity loads; full occupancy (Case F) and half occupancy (Case H) for summer conditions. On this basis, the office was modelled to have 40 and 20 researchers as a full and half occupancy loads along with their computers respectively.
ANSYS Workbench Design Modeller 17.1 with Fluent 17.1 (ANSYS Fluent, 2016) was used to simulate the large space case-study (the researchers' office) at CSEF building. Some simplification of the geometrical model was made to save computing time and power while still preserving the most relevant physical aspects of the geometry. For instance, The body of the occupant was presented as a cylinder of height 1.4m and diameter of 0.4m giving a body surface area of approximately 1.8 m^2 according to (Pinkel, 1958).

2.2 Numerical Model

The finite-volume solver Fluent 17.1 was used to simulate the flow field of the ventilated enclosure, the governing equations were solved with a segregated scheme, and the SIMPLE algorithm was used for coupling the pressure and velocity. In the discretization scheme, the non-linear and the viscous terms were calculated with the second order upwind scheme while the BODY FORCE WEIGHTED scheme was used to reveal convergence when two consecutive iterations for the local airflow variable was less than 10^{-3} whereas for energy when it was less than 10^{-6}. Besides that, the net heat flow rate imbalance was less than 0.003% of the total flux through the system, and the net heat imbalance was less than 0.3% of the total energy flux through the system too.
Several turbulence models can be used for the simulation of turbulent flow. Reynolds-averaged Navier-Stokes (RANS) equation simulation using one or two-equation turbulence models such as RNG k-ε models, SST k-ω model and Reynolds Stress model (RSM) are often used. In fact, the performance of both RNG k-ε and SST k-ω models were compared in the large space by utilising the temperature and air velocity measurements in our previous study (Alzaid, Kolokotroni and Awbi, 2017). The prediction from SST k-ω shows better agreement with measurements in comparison with RNG k-ε model. Hence, the SST k-ω model was used in the present study to predict the turbulent features of air flow within the researchers' office.
Since CO_2 cannot be absorbed or filtered, it can be utilised as a good index for indoor air quality (Oke *et al.*, 2008). The CFD model was developed to predict the metabolic CO_2 distribution within the case-study building. The rate of production of carbon dioxide CO_2 by the human's respiratory system is associated with the metabolic rate as given by the following equation (MacIntyre, 1980):

$$G = 4 \times 10^{-5}\, MA \qquad (1)$$

where G is the CO_2 production in (L/s), M is the metabolic rate in (W/m^2) and A is the body surface in (m^2). In this study, an average sedentary adult produces around 0.005 L/s of CO_2 by the respiratory system.
To represent the CO_2 production per person in the CFD model, a separate cell zone shaped as a cube (5 x 5 x 5 cm) was used for modelling species transport. One mass CO_2 source term was added to that cells zone. Therefore, for G = 0.005 L/s ≈ 9.9×10^{-6} kg/s and as it was presented by a cube with a volume of 1.25×10^{-4} m^3, then the CO_2 production per person in the CFD model is 9.9×10^{-6} kg/s divided by 1.25×10^{-4} m^3 which leads to 0.0792 kg/m^3s. Consequently, the CO_2 source term is added in the conservation of the CO_2 mass fraction equation.

2.3 Boundary Conditions

The required supply air flow rates for the modelled office of full and half occupancy were calculated from the following equation (Tymkow *et al.*, 2013; BS EN 16798-3, 2017):

$$\dot{m} = \frac{\dot{q}}{c_p(t_e - t_\infty)} \quad (2)$$

where $\dot{q}$ is the thermal load in (W), $\dot{m}$ is the mass rate of air flow (kg/s), c_p is the specific heat of air (J/kg.K), t_e is the air temperature of air exhaust (°C) and t_∞ is the air temperature of air supply (°C).

To use the above equation, the thermal load $\dot{q}$ can be calculated using HAP 4.9 (hourly analysis program) which is a microcomputer program developed by Carrier Corporation (Carrier, 2010). Therefore, from HAP the cooling loads for the modelled office were calculated to be 68 W/m^2 and 48 W/m^2 for full and half occupancy respectively. Consequently, the calculated supply air flow rates using equation (2) are 2.6 m^3 /s (65 l/s) and 1.7 m^3 /s (85 l/s) for full and half occupancy, respectively.Thus, for the mixing ventilation system, the corresponding diffuser supply velocities were 2.7 m/s for full occupancy and 1.8 m/s for half occupancy. For the impinging jet ventilation system, the corresponding supply velocities were 4.1 m/s for full occupancy and 2.7 m/s for half occupancy.

Due to the high demand of energy needed to cool and dehumidify the outdoor air, recirculating part of the conditioned air is recommended as an essential aspect of energy conservation strategies in many parts of the world (Fadeyi et al. 2009). Many HVAC designers use the recirculated air after mixing it with fresh air then supply it to space after it has been filtered and cooled. In this study, the recirculating air that was contaminated with CO_2 was considered in both cases presented in this section. To find the CO_2 concentration for recirculating air, the supply flow rate (2.6 m^3/s) was used for this study after adding CO_2 source terms in the model to represent the CO_2 production per person. At the start, only fresh air (10 L/s) per person as recommended by ASHRAE standard 62.1 (American Society of Heating, 2016) with 400 ppm CO_2 concentration was used as a supply air flow rate. Then, the CO_2 concentration of the air at the exhaust was determined from the CFD output, which was 808 ppm. Consequently, the CO_2 concentration of the new supply air, which is a mixture of fresh and recirculated air was calculated to be 745 ppm, as shown in Figure 3.

A similar procedure was used to find the CO_2 concentration for recirculated air for the modelled office with half occupancy. The CO_2 concentration of the recirculated air was 686 ppm; while it was 652 ppm for the new supply air, which is a mixture of fresh and recirculated air.

Table 1 summarises the two cases which were used to compare the performance of the MV and IJV systems. It is worth mentioning that according to BS EN 16798-1 (BSI, 2019), the recommended range of the mean design operative temperature for energy saving in open plan offices is (20 – 24 °C) and (22 – 27 °C) for heating and cooling seasons respectively. Moreover, a study by (Seppanen, Fisk and Lei, 2006) recommended that the highest productivity in the office environment is at a temperature of around 22°C. Therefore, in this study, the air supply temperatures presented in the table below were set by an iterative procedure to achieve a rather steady temperature condition of 22.3°C ± 0.4°C in the occupied zone of the office building for providing accurate comparisons.

Therefore, the boundary conditions of Case F and Case H for both MV and IJV systems as flowing:

a. The condition of the air supply is set in the CFD model at values, as shown in Table 1.
b. The boundary conditions for the surfaces temperature of all the office walls were (28 °C), ceiling (35°C), windows (39°C), occupants clothing (33.7°C), personal computers (40°C),

lighting (40°C) and photocopier (40°C) which have been derived from the measurements by (Alzaid, Kolokotroni and Awbi, 2017).

Table 1: CFD cases used for the MV and IJV system performance comparison

Case name		Case F		Case H	
Occupancy		Full		Half	
Distribution system		MV	IJV	MV	IJV
Flow rate (m^3/s)		2.6	2.6	1.7	1.7
Diffusers	Number	8	21	8	21
	Area (m^2)	0.12	0.03	0.12	0.03
	Velocity (m/s)	2.7	4.1	1.8	2.7
	Temperature (°C)	18	19	19	20
	CO_2 (ppm)	745	745	652	652

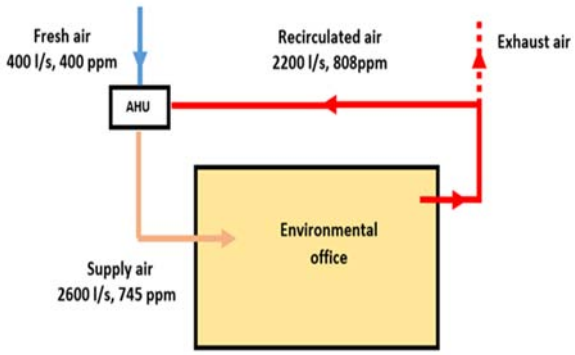

Figure 3: Recirculation system of the modelled office for full occupancy

2.4 Validation of the CFD Model and Computational Grid

The current CFD model for predicting the thermal and airflow fields in a large space is validated with experimental data in our previous study (Alzaid, Kolokotroni and Awbi, 2017). The ANSYS code was used to construct the three-dimensional geometry and generate the mesh. The present study adopted the same mesh strategy as the one used in the validation study, see (Alzaid, Kolokotroni and Awbi, 2017), i.e., non-uniform grid strategy was utilised to cover the whole computational domain for the room. The finer grid was used close to air inlets, outlets and walls, and also in the areas that were anticipated to have steep velocity gradients. Based on that, the total grid size generated for case F and Case H was (16,853,380) and (15,824,322), respectively.

2.5 Air distribution Index (ADI)

The overall ventilation effectiveness for the removal of pollutants ($\bar{\varepsilon_c}$) and the removal of heat ($\bar{\varepsilon_t}$) are used to evaluate the effectiveness of an air distribution system and are defined as (BS EN 16798-3, 2017):

$$\bar{\varepsilon_c} = \frac{C_e - C_\infty}{C_m - C_\infty} \quad (3) \qquad \bar{\varepsilon_t} = \frac{t_e - t_\infty}{t_m - t_\infty} \quad (4)$$

where C is contaminant concentration (p.p.m), t is the temperature (°C), subscripts e, ∞ and m denote exhaust, supply and mean value in the occupied zone. Even though high values of both the overall ventilation effectiveness for the removal of pollutants ($\bar{\varepsilon_c}$) and for heat removal ($\bar{\varepsilon_t}$) state a high efficiency of the ventilation system, they do not alone offer a strong indication of the air quality and thermal comfort in the occupied zone (Awbi, 2003). Awbi and Gan (1993) combined ($\bar{\varepsilon_c}$) with Fanger's Percentage of Dissatisfied (PD) for air quality and ($\bar{\varepsilon_t}$) with Fanger's Predicted Percentage of Dissatisfied (PPD) to define two new numbers that include the percentage of dissatisfied for air quality and thermal comfort, thus

$$N_c = \frac{\bar{\varepsilon_c}}{PD} \quad (5) \qquad N_t = \frac{\bar{\varepsilon_t}}{PPD} \quad (6)$$

where N_c and N_t are air distribution number for air quality and thermal comfort respectively.
The expression for PD and PPD are as follow (Fanger 1988; BSI 2007)

$$PD = 395 \times EXP(-1.83\dot{v}^{0.25}) \quad (7)$$

$$PPD = 100 - 95 \times EXP - \{0.03353(PMV)^4 + 0.2179(PMV)^2\} \quad (8)$$

Where $\dot{v}$ is the outdoor air flow rate (L/s) per standard person and PMV is the Predicted Mean Vote as defined in ISO 7730 (BSI, 2005). The two numbers N_c and N_t have been combined to produce what they called the Air Distribution Index (ADI)(Awbi and Gan, 1993):

$$ADI = \sqrt{(N_c \times N_t)} \quad (9)$$

Achieving a value of $ADI \geq 10$ by a ventilation system designed for an acceptable value of 10% for both PD and PPD can be assumed to be a good air distribution system. However, a large value of ADI would not ensure the existence of a good air distribution system as unwanted local conditions might be still present. Consequently, ADI should be applied along with room temperature distribution and air movement measurements or predictions to evaluate the global and the local conditions particularly the presence of high or low temperature or local draughts regions within the occupied region (Awbi & Gan 1993; Awbi 1998).

3. RESULTS AND DISCUSSION

3.1 Comparison between the Performance of the MV and IJV Systems for Case F

Figures 4 to 6 illustrate the air velocity vectors, air temperature contours, CO_2 concentration contours on a lateral plane located in the middle of the office at Z=6.6m for the MV and Z=7.2 m for the IJV systems for Case F.

From Figure 4 (a) it can be seen that the left supply jet for the MV system is spreading over the floor towards the south (external) wall after impinging on it. In addition, the hot sources and heat gain through the window generate thermal plumes causing considerable buoyancy forces which move the air up to the ceiling. This large and robust air circulation produces the least stratification level by the MV system compared to the IJV system. A cross-recirculation is created in different parts of the occupied zone for both the MV and IJV systems due to partitions and furniture, as shown in Figure 4 (a) and (b). The supplied air from two IJV diffusers spreads along the floor for about 3 m and decays as it moves onto the office floor, as can be seen in Figure 4 (b).

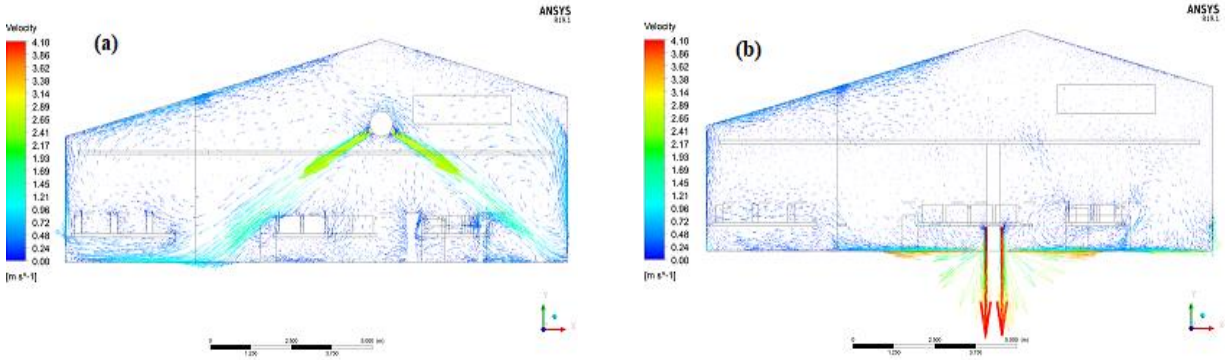

Figure 4: Velocity vector plots on a lateral plane located in the middle of the office for Case F: (a) MV system at Z=6.6 m and (b) IJV system at Z=7.2 m.

Figure 5 (a) and (b) show that with the different supply air temperatures used, 18°C for the MV and 19°C for the IJV, the temperature field in both the MV and IJV systems are somewhat similar when the average temperature in the occupied area was maintained at the same level (22°C). Also, temperature stratification for the office is observed in both contours, which was very significant for IJV supplies, as shown in Figure 5 (b).

The predicted CO_2 concentration on a vertical plane located in the middle of the office for the MV and IJV systems are shown in Figure 6 (a) and (b), respectively. In Figure 6 (a), the concentration of CO_2 in a part of the occupied zone is higher than its mean value in that zone. This is because the supplied air is displaced downward and mixes with the office air apart from that areas covered by the obstructions such as tables. However, for IJV system, the concentration of CO_2 is generally uniform in the occupied zone within the range 750 and 800 ppm. Therefore the IJV system was more efficient in providing fresh air to the breathing zone than the MV system.

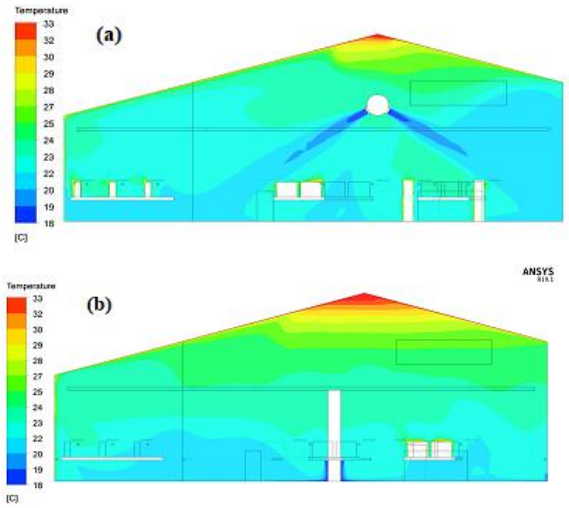

Figure 5: Temperature contour plots on a plane located in the middle of the office for Case F: (a) MV system at Z=6.6 m and (b) IJV system at Z=7.2 m

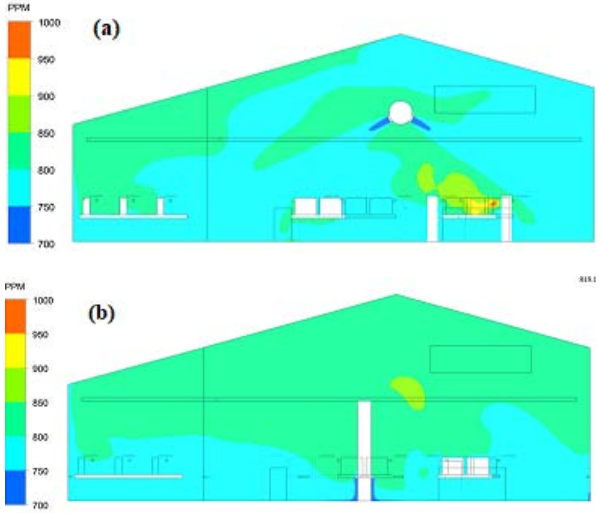

Figure 6: CO_2 concentrations contours on a plane located in the middle of the office for Case F: (a) MV system at Z=6.6 m and (b) IJV system at Z=7.2m

.

The predicted parameters were used to calculate the Air Distribution Index (ADI) for this case, as shown in Table 3. The IJV system was able to remove contaminants and heat ($\bar{\varepsilon_c}$,$\bar{\varepsilon_t}$) from the ventilated space more effectively than the MV system. Also, both air distribution numbers for air quality and for thermal comfort (N_c,N_t) were higher (better) for the IJV than for the MV system and consequently, it shows higher (better) ADI value. However, PPD values for both systems were too high because of dumping of cold and high velocity jet into the occupied zone.

Table 3: The predicted ADI for the MV and IJV systems for Case F

systems	Diffusers					$\bar{\varepsilon_c}$	PD (%)	N_c	$\bar{\varepsilon_t}$	PPD (%)	N_t	ADI
	No.	A (m^2)	V (m/s)	T (°C)	CO_2 (ppm)							
MV	8	0.12	2.7	18	745	1.2	15.2	7.7	1.5	40	3.8	5.4
IJV	21	0.03	4.1	19	745	1.8	15.2	11.7	2.2	31	7.2	9.2

3.2 Comparison between the Performance of the MV and IJV Systems for Case H

Figure 7 to 9 show the air velocity vectors, air temperature contours, CO_2 concentration contours on a lateral plane located in the middle of the office at Z=6.6 m for the MV system and Z=7.2 m for the IJV system for case H. As can be seen from Figure 7 (a), a large clockwise air circulation is present on the left side of the office. The stable thermal stratification near the ceiling tends to slow down this circulation. Also, on the right side of the office, another extensive air recirculation was created with counter clockwise direction. In Figure 7 (b) for the IJV case, the heat sources

from the window and the left part of the ceiling created a strong buoyancy force which pushes the air up to the highest part of the office.

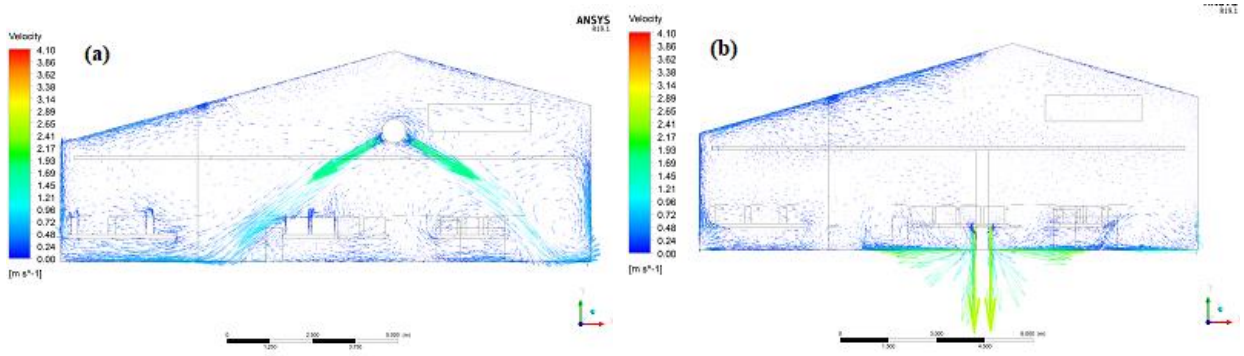

Figure 7: Velocity vectors on a lateral plane located in the middle of the office for Case H: (a) MV system at Z=6.6 m and (b) IJV system at Z=7.2 m.

Figure 8 (a) and (b) shows the temperature contours in the middle of the office and the temperature stratification in the case of MV and IJV systems. The mean air temperature in the occupied zone for the MV system is higher than that for the IJV system. This is because, in the IJV system, the cold jet over the floor has sufficient momentum to continue along the floor despite the heat sources due to the occupants. As for the MV system case, the cold jet momentum was not strong enough to produce good air mixing inside the office. Thus, $\overline{\varepsilon_t}$ value was 1.75 for the MV system compared to 3.5 for IJV system (see table 4).

It is noticed that the occupied zone has a low and uniform CO_2 concentration for IJV system compared to that for the MV system, as shown in Figure 9 (a) and (b). As evidence of that, the overall ventilation effectiveness for contaminant removal ($\overline{\varepsilon_c}$) value is 1.16 for the MV system compared to 2.35 for the IJV system (see table 4).

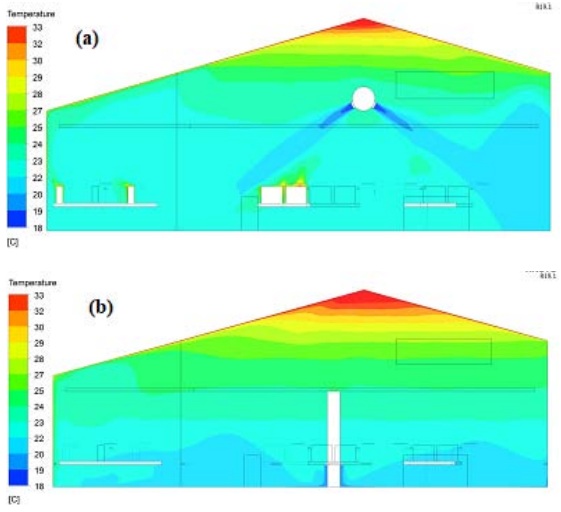

Figure 8: Temperature contour plots on a plane located in the middle of the office for Case H: (a) MV system at Z=6.6 m and (b) IJV system at Z=7.2 m

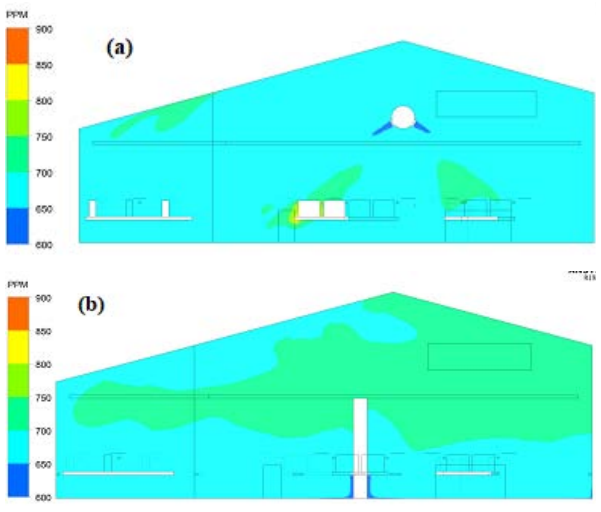

Figure 9: CO_2 concentrations contour on a plane located in the middle of the office for Case H: (a) MV system at Z=6.6 m and (b) IJV system at Z=7.2 m.

Table 4 shows the predicted ADI parameters for the MV and IJV systems for this case. From the table, it can be seen that the air distribution numbers for air quality, N_c, and thermal comfort, N_t, for the MV system were 7.7 and 6.7 respectively while they were double these values for the IJV system. Hence, the results reveal that the highest value of ADI was produced by the IJV system which was 15.

Table 4: The predicted ADI for the MV and IJV systems for Case H

systems	Diffusers					$\bar{\varepsilon_c}$	PD (%)	N_c	$\bar{\varepsilon_t}$	PPD (%)	N_t	ADI
	No.	A (m^2)	V (m/s)	T (°C)	CO_2 (ppm)							
MV	8	0.12	1.8	19	652	1.2	15.2	7.7	1.8	26	6.7	7.2
IJV	21	0.03	2.7	20	652	2.4	15.2	15.4	3.5	24	14.6	15.0

4. CONCLUSION

The ventilation performance of the two air distribution systems used (MV and IJV) were examined by applying the Air Distribution Index (ADI) for the first time in large spaces. Based on the results obtained, the IJV system performed better than the MV system for all the conditions considered as it provided higher ADI values. Since the occupied zone temperature for the two systems was maintained at 22℃, the IJV system performed better than the MV system where the air supply temperature for the IJV system was higher by 1 ℃ than that for the MV system for both thermal load cases. Thus, the IJV system uses less power than the MV system and also performs better. In general, the ADI concept presented in this work could be a beneficial tool for evaluating a ventilation system performance in large spaces as it provides assessments for both air quality and thermal comfort.

5. REFERENCE

Alzaid, A., Kolokotroni, M. and Awbi, H. (2017) 'Experimental and Numerical Investigation of Air Distribution in a Large Space', in. 38th AIVC International Conference.

American Society of Heating, R. and A.-C. E. (2016) *Standard 62.1 User's Manual: Based on ANSI/ASHRAE Standard 62.1-2016, Ventilation for Acceptable Indoor Air Quality*. ASHRAE.

ANSYS Fluent (2016) 'Thory guide'. ANSYS Inc,.

Awbi, H. (2003) *Ventilation of buildings*, *Zhurnal Eksperimental'noi i Teoreticheskoi Fiziki*. doi: 10.1080/02786820490519234.

Awbi, Hazim B. (1998) 'Calculation of convective heat transfer coefficients of room surfaces for natural convection', *Energy and Buildings*, 28(2), pp. 219–227. doi: 10.1016/S0378-7788(98)00022-X.

Awbi, H B (1998) 'Energy efficient room air distribution', *Renewable Energy*. Elsevier, 15(1), pp. 293–299.

Awbi, H. B. and Gan, G. (1993) 'Evaluation of the overall performance of room air distribution', in *Proceedings of the 6th International Conference on Indoor Air Quality and Climate, Helsinki*, pp. 283–288.

BS EN 15251 (2007) 'Indoor environmental input parameters for design and assessment of energy performance of buildings- addressing indoor air quality , thermal environment , lighting and acoustics Contents', 3(BS EN 15251), pp. 1–50.

BS EN 16798-3 (2017) *Energy performance of buildings — Ventilation for buildings Part 3: For non-residential buildings - Performance requirements for ventilation and room-conditioning*

systems (Modules M5-1, M5-4).
BSI (2005) 'BS EN ISO 7730: 2005: Ergonomics of the thermal environment Analytical determination and interpretation of thermal comfort using calculation of the PMV and PPD indices and local thermal comfort criteria', *Management*, 3, pp. 605–615. doi: 10.1016/j.soildyn.2004.11.005.
BSI (2019) 'BS EN 16798-1: 2019: Energy performance of buildings - Ventilation for buildings-Part 1:Indoor environmental input parameters for design and assessment of energy performance of buildings addressing indoor air quality, thermal environment, lighting and aco', (BS EN 16798-1).
Carrier (2010) 'hourly analysis program and system design load program'. NY: Syracuse.
Fadeyi, M. O., Weschler, C. J. and Tham, K. W. (2009) 'The impact of recirculation, ventilation and filters on secondary organic aerosols generated by indoor chemistry', *Atmospheric Environment*. Elsevier, 43(22–23), pp. 3538–3547.
Fanger, P. O. (1988) 'Introduction of the olf and the decipol units to quantify air pollution perceived by humans indoors and outdoors', *Energy and Buildings*, 12(1), pp. 1–6. doi: 10.1016/0378-7788(88)90051-5.
International Energy Agency (IEA) (1998) 'IEA Annex 26: Energy Efficient Ventilation of Large Enclosures - Technical Synthesis Report'.
Karimipanah, T., Awbi, H. B. and Moshfegh, B. (2008) 'The Air Distribution Index as an Indicator for Energy Consumption and Performance of Ventilation Systems', *Journal of the Human-Environment System*, 11(2), pp. 77–84. doi: 10.1618/jhes.11.77.
Li, Q. *et al.* (2009) 'CFD study of the thermal environment in an air-conditioned train station building', *Building and Environment*. Elsevier Ltd, 44(7), pp. 1452–1465. doi: 10.1016/j.buildenv.2008.08.010.
MacIntyre, F. (1980) 'The absorption of fossil-fuel CO 2 by the ocean', *Oceanologica Acta*, 3, pp. 505–516.
Mateus, N. M. and Carrilho da Graça, G. (2017) 'Simulated and measured performance of displacement ventilation systems in large rooms', *Building and Environment*. Elsevier Ltd, 114, pp. 470–482. doi: 10.1016/j.buildenv.2017.01.002.
Oke, S. A. *et al.* (2008) 'A mathematical modelling of the intensity of contaminants (C02) on occupancy level of a spacein continuous use'. Inderscience Enterprises Limited.
Pinkel, D. (1958) 'The use of body surface area as a criterion of drug dosage in cancer chemotherapy.', *Cancer research*, 18(3), pp. 853–856.
Seppanen, O., Fisk, W. J. and Lei, Q. H. (2006) *Effect of temperature on task performance in officeenvironment*. Ernest Orlando Lawrence Berkeley NationalLaboratory, Berkeley, CA (US).
Tymkow, P. *et al.* (2013) *Building services design for energy efficient buildings*. Routledge.
Ye, X. *et al.* (2016) 'Heating energy consumption of impinging jet ventilation and mixing ventilation in large-height spaces: A comparison study', *Energy and Buildings*. Elsevier B.V., 130, pp. 697–708. doi: 10.1016/j.enbuild.2016.08.055.
Ye, X. *et al.* (2019) 'Comparison study of contaminant distribution and indoor air quality in large-height spaces between impinging jet and mixing ventilation systems in heating mode', *Building and Environment*. Elsevier, p. 106159.

Proposal of Optimal Control Method in order to reduce Mutual Interference of Air Conditioning Indoor Units

Yuga Urata*[1], Yasuyuki Shiraishi[2]

1 Graduate Student, The University of Kitakyushu
1-1, Hibikino, Kitakyushu shi, Wakamatsu Ku
Fukuoka Ken, 808-0135, Japan
**e-mail address:z8mbb003@eng.kitakyu-u.ac.jp*

2 Professor, The University of Kitakyushu, Dr. Eng.
1-1, Hibikino, Kitakyushu shi, Wakamatsu Ku
Fukuoka Ken, 808-0135, Japan

ABSTRACT

In recent years, many multi-type package air conditioning systems for buildings have become widespread in office buildings in Japan, and there are many cases where one air conditioning space is shared by using several indoor air conditioning units. The advantages of multi-type package air conditioning system are that it is possible to operate and control individually for each indoor unit, and that the user can arbitrarily change the temperature setting of the indoor unit. On the other hand, these advantages cause air conditioning control problems such as air quality deterioration and mutual interference between adjacent indoor units. Therefore, this study aims at developing a new air conditioning control method that reduces air quality deterioration and influence of mutual interference by using model predictive control (hereinafter MPC) when sharing one air conditioning space with multiple air conditioning indoor units. In this paper, we carried out CFD (Computational Fluid Dynamics) analysis incorporating multiple-input multiple-output (hereinafter MIMO) MPC that controls each zone while considering the thermal environment between adjacent zones in an office where the set temperature differs between zones. Furthermore, we showed the effectiveness of this method (MIMO MPC) by comparing the single-input single-output (hereinafter SISO) MPC.

The following results were obtained: 1) when comparing the outlet air temperature, SISO MPC had a large fluctuation range of the outlet air temperature in the zone where the set temperature was 26 degree, but MIMO MPC was small. 2) The averaged room air temperature in the zone where the set temperature was 27 degree showed almost the same behavior in both control methods, but comparing the behavior of room air temperature at each point, the temperature fluctuation of SISO MPC was large, and the MIMO MPC was small. The reason for this is presumed that the fluctuation range of the room air temperature was suppressed in MIMO MPC in accordance with the difference in the behavior of the outlet air temperature in the adjacent zone. From the results of 1) and 2), the improvement of control performance and the reduction effect of mutual interference were confirmed by the introduction of MIMO MPC for the office with different set temperatures among each zone.

KEYWORDS

Mutual Interference, Model Predictive Control, Coupled Analysis, CFD Analysis, MATLAB/Simulink

1 INTRODUCTION

Multi-split packaged air-conditioning systems have recently become commonplace in office buildings in Japan, and in many cases one space is served by several indoor air-conditioning units. The advantage of a multi-split packaged air-conditioning system is that each indoor unit can be operated and controlled individually, with users being able to change the temperature settings of the indoor units as desired. However, this can cause air-conditioning control problems such as a deterioration in air quality and mutual interference between adjacent indoor units[1)]. In particular, when each air-conditioned zone has a different internal load and set temperature, the sensor temperatures are influenced by disturbances, the indoor units are driven harder than they need be, energy consumption increases[2)~4)], and indoor air quality worsens[5)~7)].

Given the aforementioned problems, the aim of this study was to develop a new air-conditioning control method that reduces the deterioration in air quality and the influence of mutual interference by using model predictive control (MPC) when one space is served by multiple indoor air-conditioning units. We carried out computational fluid dynamics (CFD)

analyses incorporating multiple-input–multiple-output (MIMO) MPC that controls each zone while considering the thermal environment between adjacent zones in an office space in which the set temperature differs between zones. Furthermore, we showed the effectiveness of this method by comparing it with single-input–single-output (SISO) MPC.

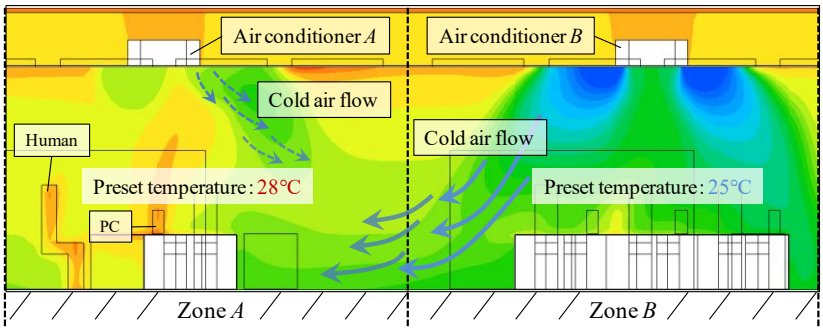

Fig.1 Image of mutual interference between adjacent indoor units

2 MUTUAL INTERFERENCE BETWEEN INDOOR AIR-CONDITIONING UNITS

According to previous research, when one space is served by several indoor air-conditioning units, those units behave differently depending on the uneven distribution of the internal load and differences in the set temperatures among the zones. As such, it is obvious that adjacent indoor units can experience mutual interference. Therefore, in this study we compare the influence of indoor units with different behaviors on their respective adjacent zones by means of a case study in which SISO MPC and MIMO MPC are incorporated separately in the air-conditioning control. We also show the effectiveness of the proposed method by comparing how the two control methods perform and how the room temperature changes.

3 OUTLINE OF CFD ANALYSIS

3.1 Analysis Model

Figures 2 shows the floor plan of analysis model. The analysis model simulates a general office space that has six zones in the form of two perimeter zones (hereinafter periES, periWS) and four interior zones (hereinafter inE01, inE02, inW01, and inW02). A ceiling-cassette air conditioner with four blowing directions is installed in the center of each zone. Furthermore,

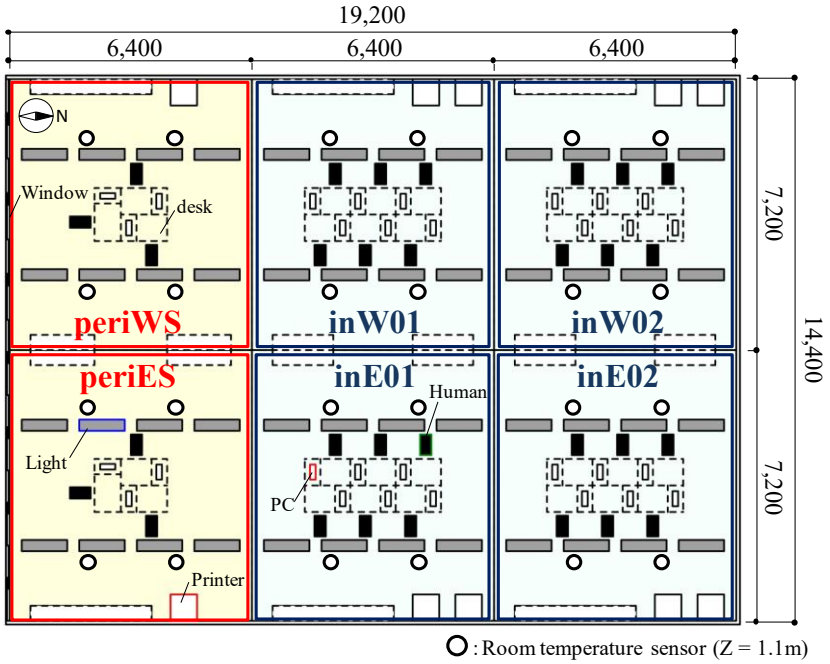

Fig.2 Floor plan of analysis model

four temperature sensors are installed at a height of 1.1 m in each zone, and their average value is taken as the room temperature in the zone.

3.2 Analysis Conditions

The CFD analysis conditions are listed in Table 1. The analysis period was 7,200 s during summertime, and analysis was performed under the conditions of the set temperature in each case. Regarding the control methods, conventional thermal ON/OFF control was used for the first 3,600 seconds, and SISO MPC or MIMO MPC was used for the second 3,600 seconds. As internal loads, a human body, office automation equipment, and lighting were installed as shown in Fig. 2; the load amounts are listed in Table 1[1), 8)]. In addition, the amount of heat received from solar radiation on the south- facing side of the building was calculated as the solar heat gain, and the thermal load due to absorption and transmission was given to the windows and blinds.

3.3 Analysis Cases

Table1. Analysis conditions for CFD analysis

Domain	19.2m *(X)* × 14.4m *(Y)* × 4.0m *(Z)*
Mesh	278 *(X)* × 235 *(Y)* × 55 *(Z)* = 3,593,150
Outlet boundary conditions	Temperature: Control by MATLAB/Simulink [°C], Flow rate: 1,680m^3/h, $k_{in} = (U_{in}/10)^2$, $\varepsilon_{in} = C_u^{3/4} \cdot k_{in}^{3/2}/l_{in}$
Inlet boundary conditions	Fixed velocity, zero-gradient condition
Turbulence model	Standard k-ε model
Wall boundary conditions	Velocity: Logarithmic law, Temperature: Convective heat transfer coefficient (= 4.6 W/m^{2}K)
Adjacent room boundary	27°C (Overall heat transfer coefficient: 9.0 W/m^{2}K)
Outdoor side boundary	30°C (Overall heat transfer coefficient: 23.0 W/m^{2}K)
Heat generation	Human: 36W/person(3.9W/m^2), Lighting: 13.4W/m^2, Solar radiation: 60.3W/m^2, OA equipment and PC: 60W/unit(6.4W/m^2), Printer: 151.2W/unit(5.4W/m^2),

U_{in}: Outlet air wind speed [m/s], k_{in}: Outlet air turbulence energy [m^2/s^2], ε_{in}: Dissipation rate of k_{in} [m^2/s^3], C_μ: Model constant (=0.09) [-], l_{in}: Length scale [m]

By means of coupled analysis using CFD and MATLAB/Simulink[9), 10)], we verified the effectiveness of MIMO control when the set temperatures of adjacent zones are different. In the analysis, case 1 involves SISO MPC, case 2 involves MIMO MPC, and we compared the control performance and behavior of outlet air temperature and room temperature in two cases.

3.4 Flow of Control in Coupled Analysis

In this study, we performed a coupled analysis using CFD for the office space with multi-split air conditioning and MATLAB/Simulink for the air-conditioning control. The flow of the coupled analysis is described below. First, the CFD receives data for outlet air volume, outlet air temperature, and outlet air humidity (hereinafter manipulating variables) from MATLAB/Simulink. Next, the CFD sets the read operation amount as a boundary condition, performs three-dimensional thermal fluid analysis, calculates the sensor temperature of each zone, outputs it to an intermediate file, and waits. MATLAB/Simulink then reads the sensor temperature of each zone and sets this as the initial value of the sensor temperature $y(t)$ at the current time t. From there, MATLAB/Simulink predicts the sensor temperature and optimizes the outlet air temperature so that the error between the set temperature and the room temperature is minimized. Finally, MATLAB/Simulink outputs the current outlet air temperature that was calculated by optimization to the CFD. As described above, the coupled analysis was performed by optimizing the manipulating variable and repeating these data transfers at the calculation time interval Δt of CFD.

3.5 Obtain Step Response used for SISO Control

First, an internal load is generated in each zone to create a steady state. After that, the outlet air temperature of periES is changed from 27°C to 16°C, and the prediction model of periES, is obtained. Finally, the prediction model inE01, inE02, periWS, inW01, and inW02 of the other five zones are also obtained in the same flow. In the SISO MPC, control is performed by incorporating these six step responses in the control law (Fig. 3). The predicted output model of each zone obtained at time $t+j$ is represented by Equation (1) because SISO MPC does not consider the influence from the adjacent zone.

$$y_{n_{SISO}}(t+j) = \sum_{k=1}^{\infty} a_n(k)\Delta u_n(t+j-k) + \sum_{k=1}^{\infty} b_n(k)\Delta d_n(t+j-k) \quad (1)$$

n: Zone position($n = 1 \sim m$), t: Current time
j: Prediction horizon, k: Sampling time of step response
$a_n(k)$: Step response factor to air-conditioner output in n zone
$b_n(k)$: Step response factor for disturbance output in n zone
$\Delta u_n(t+j-k)$: Step input of air-conditioner in n zone
$\Delta d_n(t+j-k)$: Step input of disturbance in n zone

3.6 Obtain Step Response used for MIMO Control

As described above, in the SISO MPC (e.g., a zone of periES), control is performed using only the step response. However, in reality the sensor temperature of periES is affected by air conditioners inE01, inE02, periWS, inW01, and inW02 in the same space. Therefore, the SISO MPC cannot consider the influence of air conditioners in adjacent zones, and it is difficult to perform control that reproduces the heat transfer phenomenon with mutual interference between the zones. Therefore, in the MIMO MPC of this research, each zone was controlled using a step response that considered the influence of the air conditioners in all zones. The step response used in the MIMO MPC was obtained by the following method. First, as with the SISO MPC, an internal load is generated in each zone to create a steady state. The outlet air temperature of the control target zone was then changed from 27°C to 16°C, and the step responses of the sensor temperatures of both the target zone and all the other zones are obtained. For example, when the outlet air temperature of periES is changed, the step responses of the other five zones are obtained simultaneously in addition to the step response of periES. In the same flow, the

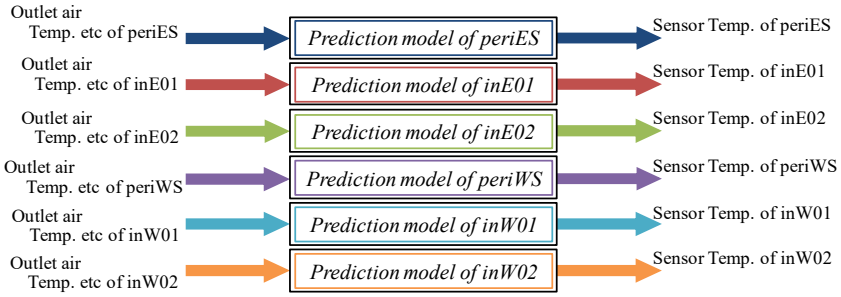

Fig.3 Image of SISO MPC prediction model

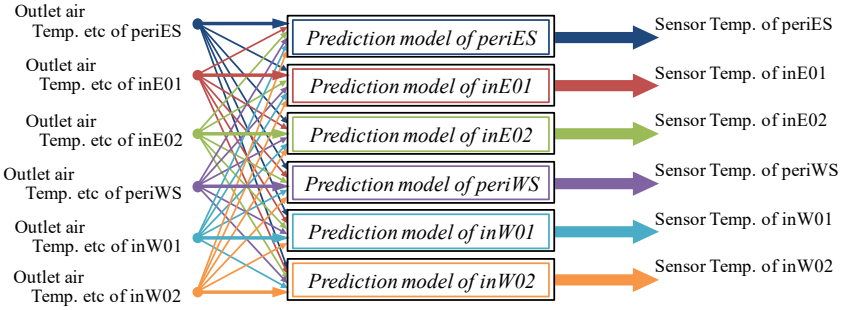

Fig.4 Image of MIMO MPC prediction model

step responses of inE01, inE02, periWS, inW01, and inW02 are obtained, and MIMO control is performed by incorporating a total of 36 step responses into the prediction model (Fig. 4). The predicted output model of each zone obtained at time $t+j$ is represented by Equation (2) because MIMO MPC considers the influence from the adjacent zone.

$$y_{n_MIMO}(t+j) = \sum_{i=1}^{m}\left\{\sum_{k=1}^{\infty} a_{ni}(k)\Delta u_i(t+j-k) + \sum_{k=1}^{\infty} b_{ni}(k)\Delta d_i(t+j-k)\right\} \quad (2)$$

n: Zone position ($n = 1 \sim m$), i: Zone number ($i = 1 \sim m$)
$a_{ni}(k)$: Step response factor to air-conditioner output of i zone in n zone
$b_{ni}(k)$: Step response factor for disturbance output of i zone in n zone
$\Delta u_i(t+j-k)$: Step input of air-conditioner in i zone
$\Delta d_i(t+j-k)$: Step input of disturbance in i zone

4 ANALYSIS RESULTS

4.1 Control Performance and Follow Ability at Room Temperature

Figures 5 and 6 show the room temperature and the outlet air temperature of representative zones in Cases 1 and 2, respectively, and Fig. 7 shows the control error (Root Mean Squared Error) of the room temperature in all zones in both cases. As shown in Figs. 5 and 6, when comparing the outlet air temperatures of the respective cases, the fluctuation range of the outlet air temperatures of the periWS and inW02 zones where the set temperature is 26°C, is large in Case 1 but small in Case 2. This is because while the control in Case 1 considers only the target zone, the control in Case 2 also considers the influence of the air conditioner and internal load of the adjacent zone. Moreover, the three east zones of periES, inE01, and inE02 show the same tendency as the three west zones, and consequently in Case 2 the control error of the zone whose set temperature is 27°C is reduced by approximately 0.4°C (Fig. 7).

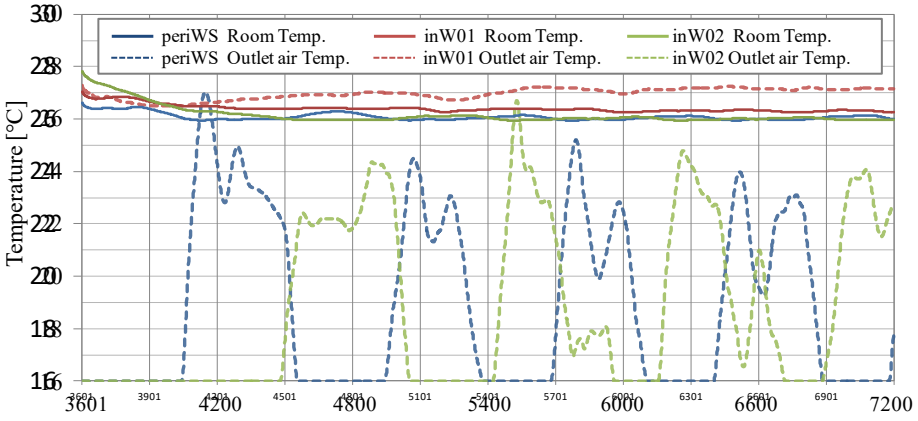

Fig.5 The room temperature and the outlet air temperature of representative zones in Case1(SISO MPC)

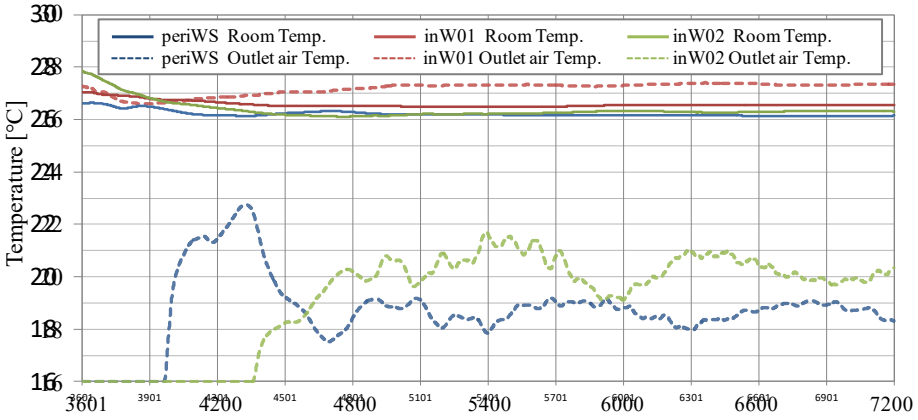

Fig.6 The room temperature and the outlet air temperature of representative zones in Case2(MIMO MPC)

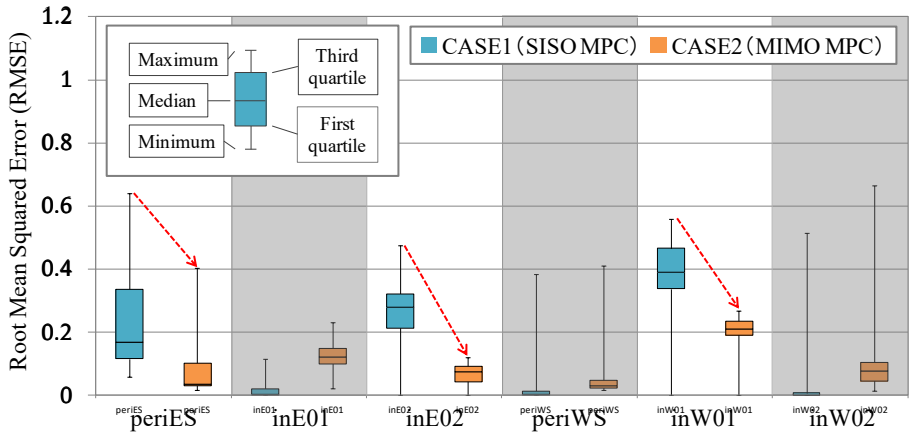

Fig.7 A temperature control error of the room temperature in all zones in Cases1 and 2

4.2 Mutual Interference due to Air Supply of Adjacent Indoor Units

Figures 8 and 9 shows the room temperature (each point) of the inW01 zone in Cases 1 and 2. Furthermore, Fig. 10 shows a temperature control error in the average temperature of the room in the inW01 zone, and Fig. 11 shows the temperature fields and flow fields of the vertical surface and horizontal surface at 5,400 s in Case 2. As shown in Figs. 5 and 6, the outlet air temperature and the room temperature of the inW01 zone have almost the same behavior in Cases 1 and 2. However, comparing the behavior of the occupancy-area sensor temperature (each point) in the inW01 zone shown in Figs. 8 and 9, the temperature fluctuation range in Case 1 is large but that in Case 2 is small. The reason is presumed to be that the fluctuation of the room temperature is suppressed in Case 2 in accordance with the difference in the behavior of the outlet air temperature of the adjacent zone of inW01. Furthermore, in Fig. 10 it is

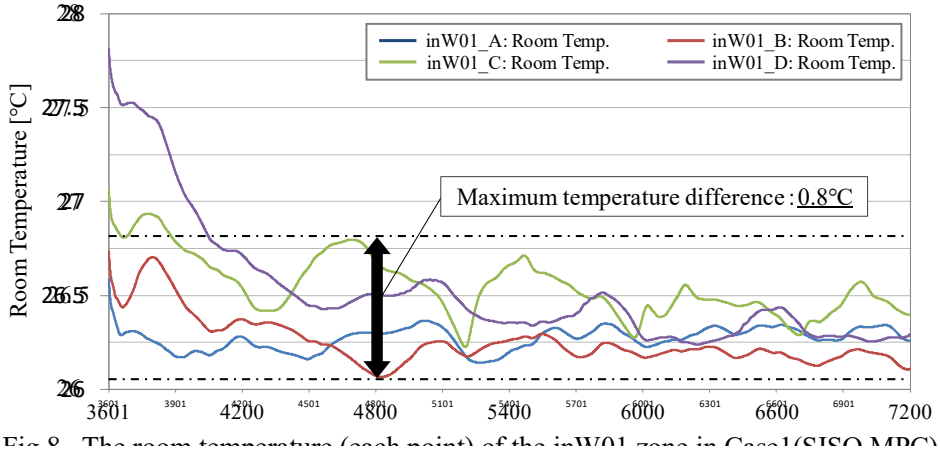

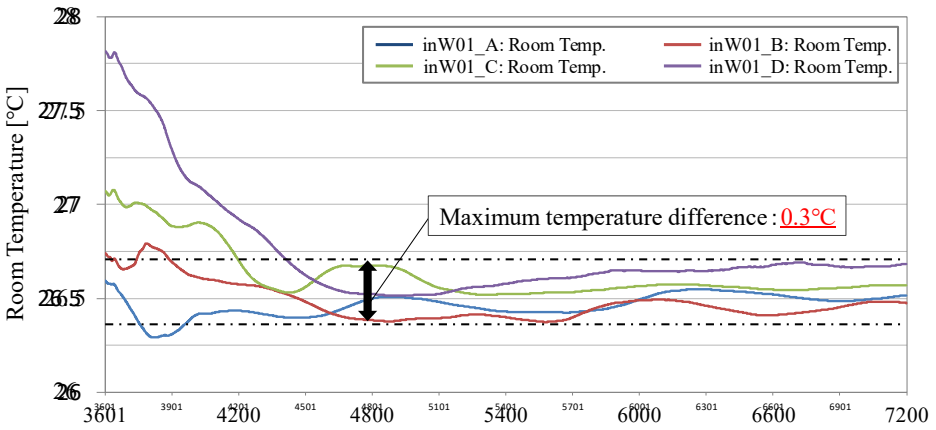

Fig.9 The room temperature (each point) of the inW01 zone in Case2(MIMO MPC)

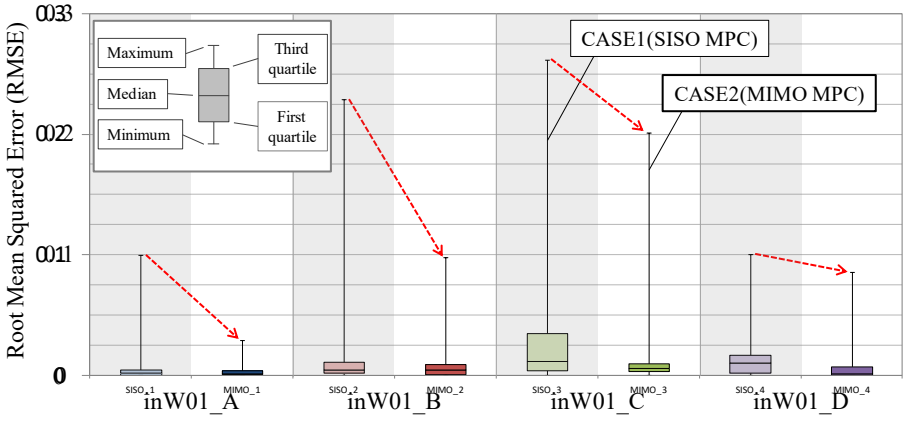

Fig.10 A temperature control error in the average temperature of the room in the inW01 zone

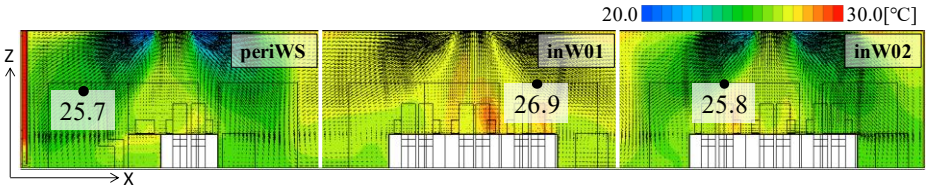

(a) The vertical surface

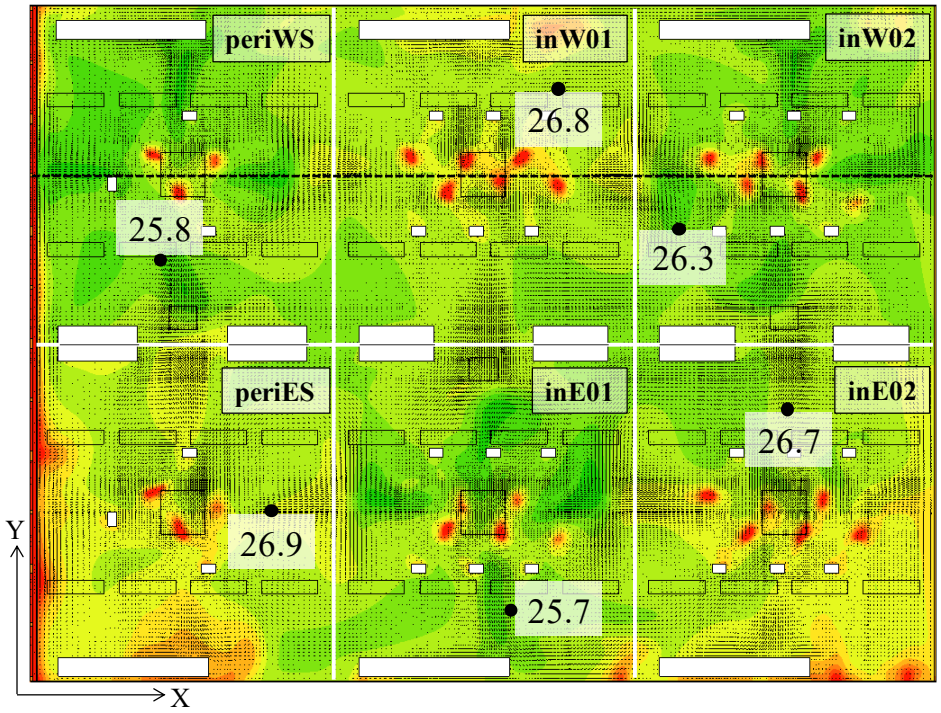

(b) The horizontal surface

Fig.11 The temperature fields and flow fields at 5,400 s in Case 2 (MIMO MPC)

confirmed that the fluctuation of the room temperature is suppressed at all four points in Case 2. It is also confirmed in Fig. 11 that the temperature of not only each sensor but also the entire office space is generally controlled to the set temperature of each zone. From the above results, the effectiveness of the MIMO MPC proposed in this research is confirmed.

5 CONCLUSION

In this study, we carried out CFD analyses incorporating MIMO MPC that controls each zone while considering the thermal environment between adjacent zones in an office space in which the set temperature differs between zones. Furthermore, we showed the effectiveness of this

method by comparing it with SISO MPC. The following results were obtained: 1) when comparing the outlet air temperatures of the respective cases, the fluctuation range of the outlet air temperatures of the periWS and inW02 zones where the set temperature is 26°C is large in Case 1 but small in Case 2. 2) The averaged room air temperature in the zone where the set temperature was 27 °C showed almost the same behavior in both control methods, but comparing the behavior of the occupancy-area sensor temperature at each point, the temperature fluctuation range in SISO MPC was large but that in MIMO MPC was small. The reason is presumed to be that the fluctuation of the room temperature was suppressed in MIMO MPC in accordance with the difference in the behavior of the outlet air temperature of the adjacent zone. From the results of 1) and 2), the improvement of control performance and the reduction effect of mutual interference were confirmed by the introduction of the MIMO MPC for the office space with different set temperatures among each zone.

6 REFERENCES

1) K.Sato.(2008). A Study on the Energy Performance Evaluation of Multiple Packaged Air-conditioning System, The Tokyo University, doctoral dissertation (in Japanese).
2) M.Sasaki.(2012). Performance Evaluation of Multi-Split Air Conditioning Systems by Coupling CFD and HVAC System Simulations Part1. Outline of coupled analysis method and the simulated results of indoor environment, Heating, Air-Conditioning and Sanitary Engineers of Japan, No.43, pp.2175-2178, 2012.9 (in Japanese).
3) G.Yoon.(2012). Performance Evaluation of Multi-Split Air Conditioning Systems by Coupling CFD and HVAC System Simulations Part2. Case study for evaluation of indoor environment and energy performance, Heating, Air-Conditioning and Sanitary Engineers of Japan, No.43, pp.2179-2182, 2012.9 (in Japanese).
4) S.Yang.(2018). A State-space Thermal Model Incorporating Humidity and Thermal Comfort for Model Predictive Control in Buildings, Energy and Buildings, Vol.170, pp.25-39, 2018.4.
5) P.MacNaughton.(2015). Economic, Environmental and Health Implications of Enhanced Ventilation in Office Buildings, International Journal of Environmental Research and Public Health, pp14709-14722, 2015.12.
6) R.Maeda.(2012). The Influence of Ventilation Rate on Memorization Performance of the Occupants, Part1, Experimental Method and the Results of the Performance, Architectural Institute of Japan, Summaries of Technical Papers of Annual Meeting, pp.897-898, 2012.9 (in Japanese).
7) T.Hibino.(2012). The Influence of Ventilation Rate on Memorization Performance of the Occupants, Part2, Discussion on Mistakes of Memorization, Architectural Institute of Japan, Summaries of Technical Papers of Annual Meeting, pp.899-900, 2012.9 (in Japanese).
8) H,Matsunaga.(2015). A Proposal of Operation Scheme for a Multi-split Air-conditioning System During a Power-Saving Period in Summer: Study on Energy Simulation Coupling with CFD for HVAC System Part3, Journal of Environmental Engineering (Transactions of AIJ), Vol.80, No.715, pp.775-783, 2015.9 (in Japanese).
9) http://jp.mathworks.com/products/matlab/.
10) Y,Manda.(2018). Feasibility Study on various Air Conditioning Control Methods using CFD Analysis and Air Conditioning System Part1. Study on Multiple Input Multiple Output Control for VAV System, Architectural Institute of Japan Kyushu Chapter Architectural Research Meeting, Vol.57, pp.273-276, 2018.03 (in Japanese).

Minimising the influence of the stack effect and wind on the operation of mechanical exhaust ventilation systems

Romy Van Gaever*[1], Samuel Caillou[1] and Sébastien Pecceu[1]

1 Belgian Building Research Institute (BBRI)
Avenue P. Holoffe 21
1342 Limelette, Belgium
**Corresponding author: romy.van.gaever@bbri.be*

ABSTRACT

Ventilation systems play an important role in providing a good indoor air quality in dwellings. Mechanical exhaust ventilation systems implement natural vents, also called trickle vents, to supply outdoor air to the dwelling. The airflow through these natural supply vents depends on the natural driving forces, i.e. wind and the stack effect, which vary in time.

This study examines several interventions to minimise the influence of the stack effect and wind on the operation of a classical mechanical exhaust ventilation system as defined by the current Belgian standard NBN D50-001 (1991). These interventions contain the overall use of smaller natural supply vents, additional mechanical extraction in the bedrooms, the use of natural supply vents only in the hallway, the use of mechanical transfer openings, balanced airflow rates per building level, increased air flow rates and the use of larger transfer openings. This paper covers a simulation study using CONTAM to investigate the effectiveness of the different interventions on the operation of a mechanical exhaust ventilation system in two types of single-family dwellings, i.e. a detached 3-bedroom dwelling and a terraced 2-bedroom dwelling. The operation of the mechanical exhaust ventilation system is evaluated in terms of the exposure of the occupants to CO_2 in the living spaces.

All of the above described interventions have a positive effect, to a greater or lesser extent, on minimising the influence of wind and the stack effect on the operation of the mechanical exhaust ventilation systems in both types of dwellings. However, some of the interventions are not as efficient to be considered as a valid solution to minimise the influence of the stack effect and wind.

KEYWORDS

Natural ventilation, Mechanical exhaust systems, IAQ

1 INTRODUCTION

Mechanical exhaust ventilation systems supply outdoor air to the dwelling by using natural supply vents and extract the indoor air from the dwelling mechanically using (a) fan(s) (AIVC, 1996). Currently, the Belgian standard NBN D50-001 (1991) permits the use of mechanical exhaust systems to supply air in the living spaces (ex. living room or bedrooms) by natural vents and to mechanically extract air from the service spaces (ex. kitchen, bathroom). The standard refers to these systems as C-systems.

The Belgian standard also defines that the airflow rate (capacity) of a fully opened naturally supply vent must be designed at a pressure difference of 2 Pa. However, the actual pressure differences over the supply vents fluctuate in time due to natural driving forces, i.e. wind and the stack effect. Therefore, the actual supply flow rates through the vents vary in time depending on the weather conditions.

The conference paper 'The effectiveness of mechanical exhaust ventilation systems in dwellings', presented at the AIVC conference in 2017, discussed the influence of the wind and the stack effect on the airflow rate through the natural vents by taking the sizing of the natural vents and the airtightness of the dwelling envelope into account. This paper concludes that due to wind and the stack effect the flow rates vary in time and are not as designed. Wind is responsible for higher flow rates in the rooms at the windward side and lower or even negative flow rates at the leeward side. The stack effect is responsible for higher supply flow rates downstairs (living room) and lower supply flow rates upstairs (bedrooms). In a leaky dwelling, these negative effects are even bigger than in an airtight building: air will enter the dwelling through the leakages in both the living and service spaces, leading to more variable flow rate through the natural supply vents and the total supply flow rate in the living room and bedrooms will decrease and an additional supply flow rate in the service spaces will occur. Smaller natural supply openings, designed at e.g. 10 Pa, lead to less variable and more controlled flow rates, closer to the desired design flow rate in airtight dwellings. However, in leaky dwellings these smaller vents are not as favourable: lower flow rates through the natural vents occur compared to the airtight dwelling.

This paper discusses several interventions to minimise the influence of the stack effect and wind on the operation of mechanical exhaust ventilation systems in airtight as well as more leaky buildings. This influence is investigated based on multi-zone flow rate simulations in CONTAM and is evaluated by the exposure of the occupants to CO_2.

2 METHOD

The simulation study uses the multi-zone airflow and contaminant transport calculation software CONTAM to determine the occupants exposure levels to CO_2 during the whole heating season in two reference dwellings.

The first reference dwelling used in this study represents a two-storey detached, three-bedroom house with a total living area of 117 m². The day zone (living room, kitchen, utility room, toilet, entranceway) is located downstairs and the night zone (bedrooms, bathroom, hallway) upstairs (Figure 1).

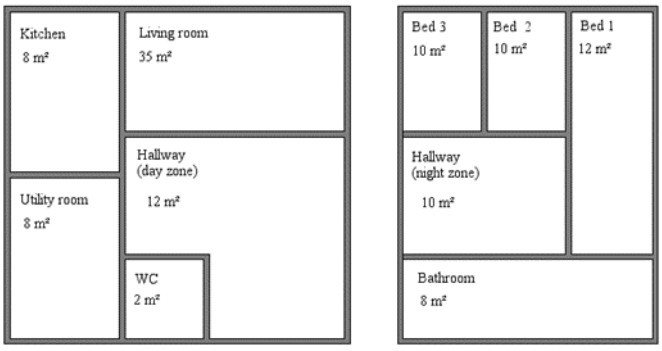

Figure 1: The first reference dwelling is a two-storey dwelling with the day zone downstairs and the night zone upstairs

The second reference dwelling is a two-storey, terraced house with a limited total living area of 63 m². The downstairs contains a small living room and open kitchen, a toilet and the entrance; the first floor two small bedrooms, a bathroom and the hallway.(Figure 2).

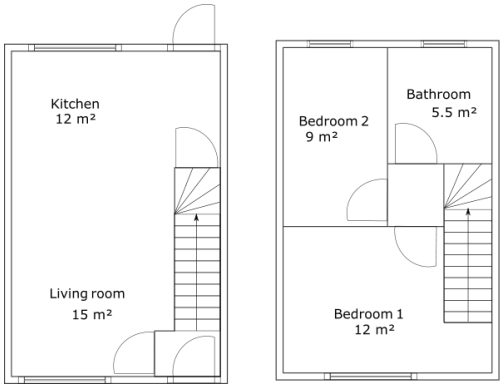

Figure 2: The second reference dwelling is a two-storey dwelling with a limited total living area

Dwelling 1 and 2 are occupied by respectively four (2 adults and 2 children) and three (2 adults and 1 child) persons. The occupants are always at home (fixed occupation schedule), representing the 'worst case' scenario regarding the production of and the exposure to contaminants.

The CO_2-production rate in the house depends on the emission rates of humans and their activities. The occupant's CO_2-emission rates are based on CEN/TR 14788:2006 (European Committee for Standardization, 2006):

- CO_2 awake: 16 l/h
- CO_2 asleep: 10 l/h

The design airflow rate for each room in these dwellings are listed below. The supply and extraction airflow rates are balanced.

	Dwelling 1	**Dwelling 2**
Supply (natural)	Flow rate [m³/h]	Flow rate [m³/h]
Living room	100	75
Bedroom 1	50	42
Bedroom 2/3	25	32
Extraction (mechanical)	Flow rate [m³/h]	Flow rate [m³/h]
Kitchen	50	75
Bathroom	50	50
Utility room	50	n.a.
Toilet	25	25
Hallway day zone	-	-
Hallway night zone	25	-

Both dwellings are equipped with a C-system, i.e. mechanical exhaust ventilation with natural supply vents in the living room and bedrooms and mechanical extraction in the service spaces. Two sizes of natural vents are studied: class P3 designed at 2 Pa and class P0 designed at 10 Pa.

The natural supply vents of class P3 designed at 2 Pa are self-regulating, while the class P0 vents designed at 10 Pa are non-self-regulating. The design flow rates of the self-regulating vents of class P3 occur at 2 Pa, while by closing the valve the flow rate at 4.5 Pa is maximum 1.5 times the flow rate at 2 Pa. The non-self-regulating vents of class P0 don't include a closing valve.

The airtightness, defined as the airflow through the dwelling envelope per m² at a pressure difference of 50 Pa ($_{v50}$) for reference dwelling 1 and as the air change rate at a pressure difference of 50 Pa (n_{50}), also varies throughout the study.

The airtightness is simulated by 2 cracks in the outer wall of each room. The first crack is located at ¼ of the height of the wall and the second at ¾. The in-/exfiltration rate through each crack is determined according to the surface area that each crack represents (uniform airtightness/air permeability). The in/exfiltration rate through the roof is evenly divided over the cracks in the walls.

The hourly Test Reference Year Uccle (Brussels) is used to determine the outdoor conditions. This file contains, among other parameters, the wind speed, the wind direction and the outdoor temperature of an entire 'reference' year in Uccle. The indoor temperature is 20°C. The simulation reporting time is set to each minute, corresponding to the simulation time step.

3 RESULTS AND DISCUSSION

The simulation study investigates four interventions which minimize the influence of the stack effect and wind on the operation of mechanical exhaust ventilation systems in comparison with the classical system C. This results in the following five schemes (including the reference one):

1. Classical C-system with P3@2Pa supply vents (reference)
2. C-system with smaller P0@10Pa natural vents
3. C-system with additional mechanical extraction in the bedrooms
4. Natural supply with P3@2Pa vents in the entrance way and mechanical extraction in the living room, bedrooms and service spaces.
5. C-system with mechanical transfer openings in the living room and bedrooms

The simulation results show the cumulative occupant exposure to CO_2 for the whole heating season for the four intervention (scheme 2-5) in relation to the classical C-system (scheme 1).

3.1 Classical C-system with P3@2Pa supply vents (reference)

The simulations investigate the influence of a classical C-system with class P3 natural vents designed at 2 Pa on the occupant exposure levels in both reference dwellings with varying airtightness (Figure 3).

Reference dwelling 1 **Reference dwelling 2**

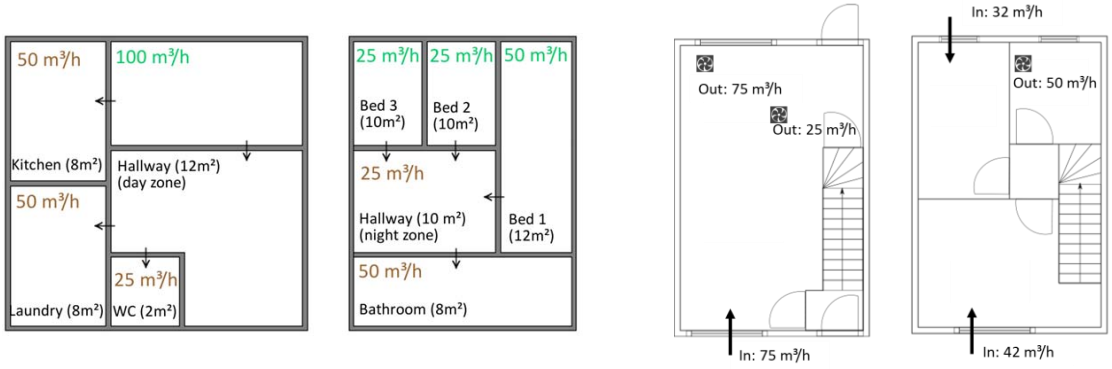

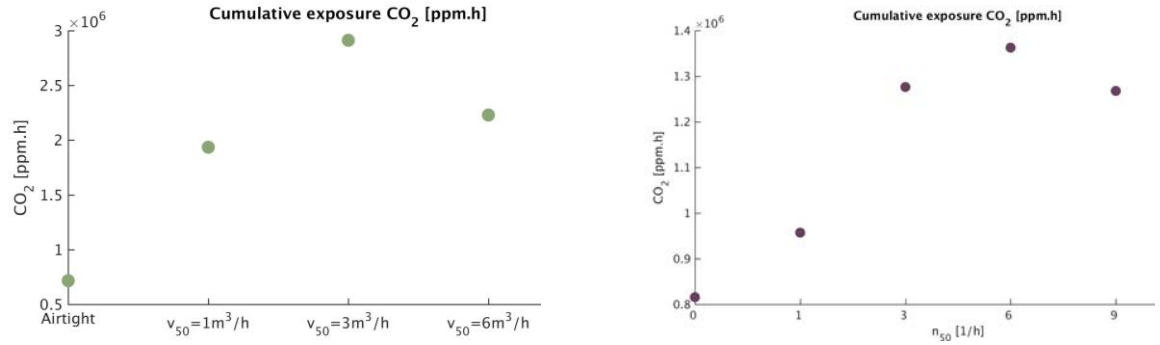

Figure 3: Both reference dwellings are equipped with a classical C-system (above). The graphs (below) show the occupant exposure levels to CO_2 of this ventilation system for different airtightness levels.

In both reference dwellings and with decreasing airtightness, the occupant exposure to CO_2 increases as a result of less airflow supplying the living spaces as a consequence of more airflow through leakages in the service spaces due to the mechanical driving force of the extraction. However, at very low airtightness the occupant exposure decreases again as a result of high airflow through all leakages in all spaces. Notice that the leakages are uniformly distributed over the surface area of the building envelope.

3.2 C-system with smaller P0@10Pa natural vents

The simulations investigate the influence of a C-system with smaller class P0 natural vents designed at 10 Pa on the occupant exposure levels in both reference dwellings with varying airtightness in relation to the classical C-system (Figure 4).

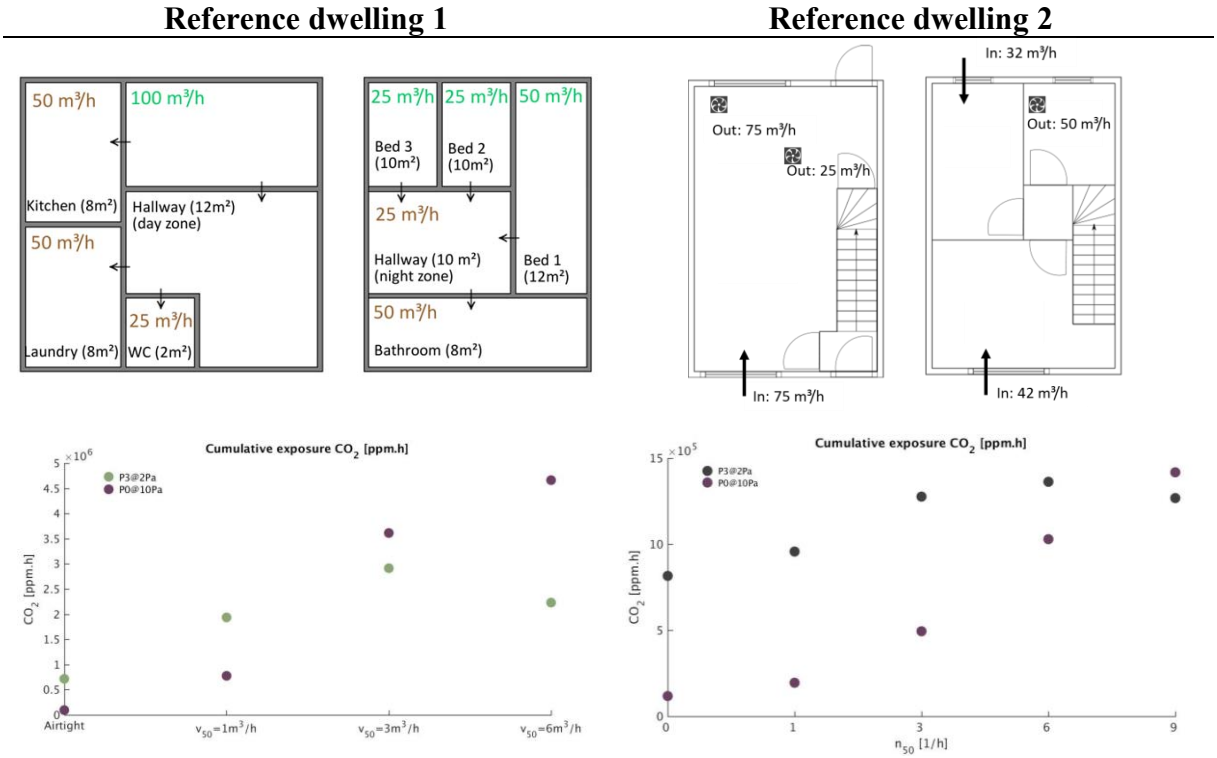

Figure 4: Both reference dwellings are equipped with a C-system with smaller class P0 vents designed at 10 Pa (above). The graphs (below) show the occupant exposure levels to CO2 of this ventilation system for different airtightness levels. The results for classical supply vents designed at 2 Pa are shown for reference dwelling 1 and 2 in respectively green and grey; for the smaller vents designed at 10 pa in purple.

For high levels of airtightness, the smaller natural vents designed at 10 Pa lead to lower levels of occupant exposure to CO_2. The smaller vents are less sensible to the wind and the stack effect resulting in less variable airflow rates. However, at lower airtightness levels the smaller vents lose their advantage, resulting in higher exposure levels in comparison with the larger vents designed at 2 Pa.

Furthermore, Figure 5 shows that the smaller vents designed at 10 Pa are less sensible to the wind direction compared to the vents designed at 2 Pa (similar results for dwelling 1).

Reference dwelling 2 (n_{50} = 3/h)

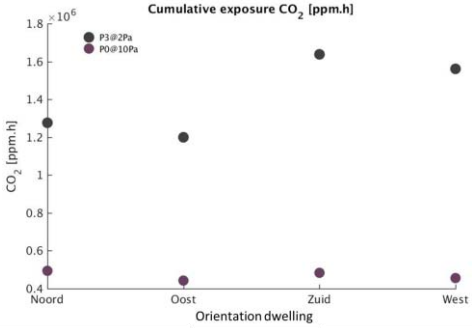

Figure 5: The graph shows the occupant exposure levels to CO_2 for different orientations of the reference dwelling 1 for an airtightness of n_{50} = 3/h. The results for the classical vents designed at 2 Pa are shown in grey and results for the smaller vents designed 10 Pa in purple.

3.3 C-system with additional mechanical extraction in the bedrooms

The simulations investigate the influence of a C-system with class P3 natural vents designed at 2 Pa with additional mechanical extraction in the bedrooms on the occupant exposure levels in both reference dwellings with varying airtightness (Figure 6).

Reference dwelling 1 **Reference dwelling 2**

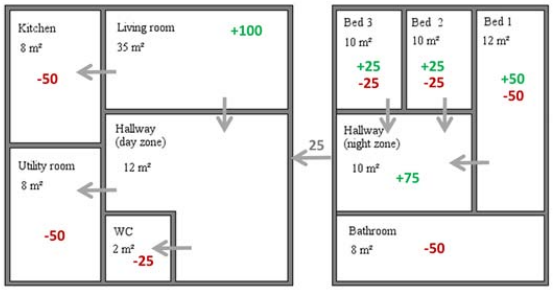

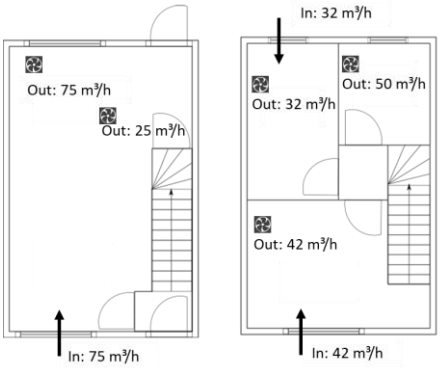

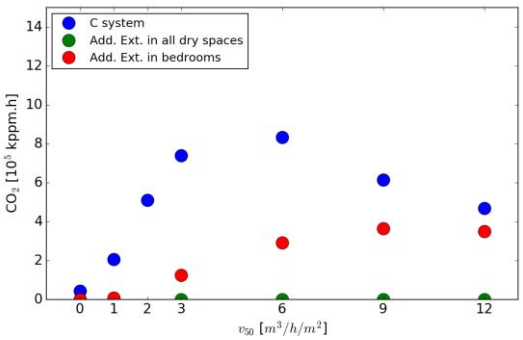

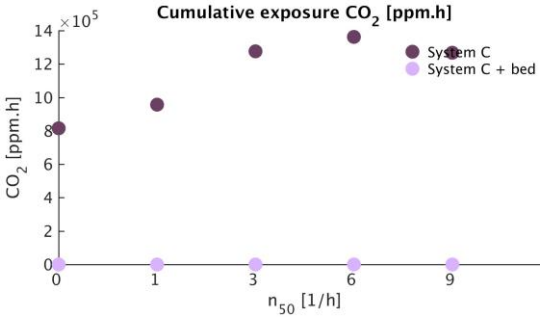

Figure 6: Both reference dwellings are equipped with a C-system with class P3 natural vents designed at 2 Pa with additional mechanical extraction in the bedrooms (above). The graphs (below) show the occupant exposure levels to CO_2 for different airtightness levels. The results for the classical C-system are shown for reference dwelling 1 and 2 in respectively blue and dark purple; for the ventilation system with additional mechanical extraction in the bedrooms respectively in red and light purple; for additional mechanical extraction in the living room and bedrooms in green (reference dwelling 1).

For both reference dwelling, adding mechanical extraction to the bedrooms, greatly decreases the occupant exposure to CO_2, leading to (very) low exposure levels due to the more controlled airflow rates in the bedrooms. However, in the reference dwelling 1 is adding an mechanical extraction only in the bedrooms not as efficient as in the reference dwelling 2 because of the closed kitchen. An additional mechanical extraction in the bedrooms and living room does leads to very low occupant exposure levels in dwelling 1.

Please note that the total airflow rate of the C-system with additional extraction is higher than the classical system. Therefore, a demand control system could be recommended in this case.

3.4 Natural supply with P3@2Pa vents in the entrance way and mechanical extraction in the living room, bedrooms and service spaces

The simulations investigate the influence of a ventilation system with class P3 natural vents designed at 2 Pa in the entrance way and with mechanical extraction in the living room, the bedrooms and the service spaces on the occupant exposure levels in both reference dwellings with varying airtightness (Figure 7).

Reference dwelling 1 **Reference dwelling 2**

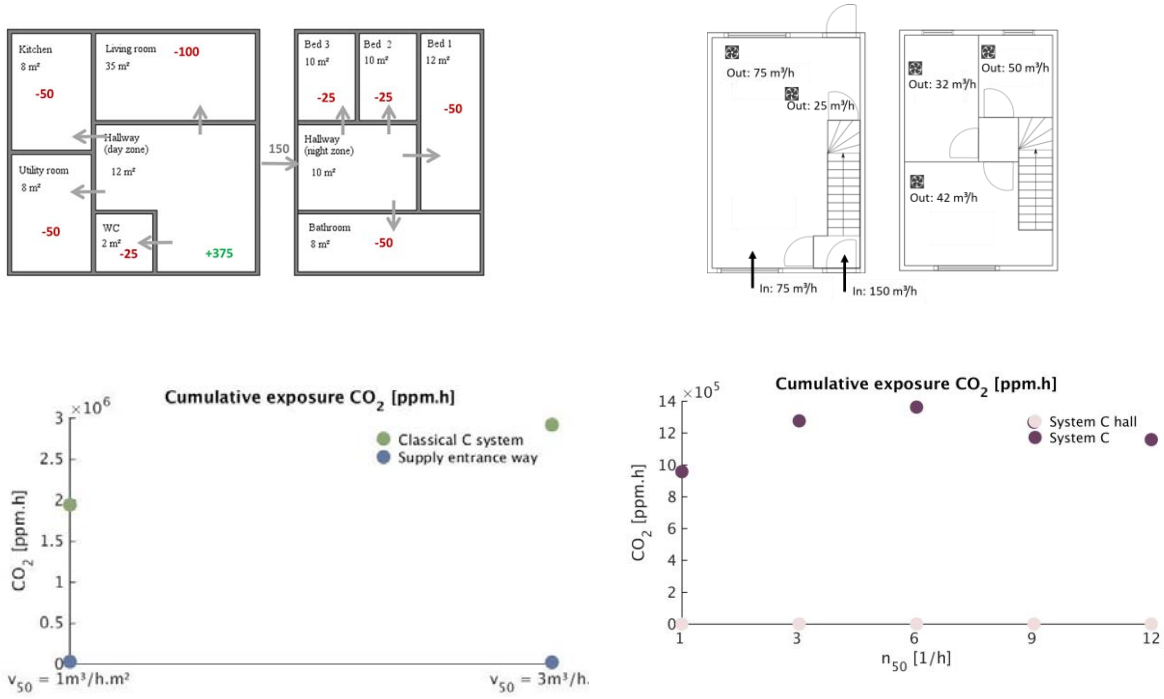

Figure 7: Both reference dwellings are equipped with a ventilation system with class P3 natural vents designed at 2 Pa in the entrance way and with additional mechanical extraction in all other spaces (above). The graphs (below) show the occupant exposure levels to CO_2 for different airtightness levels. The results for the classical C-system are shown for reference dwelling 1 and 2 in respectively green and dark purple; for the ventilation system with natural supply vents in the entrance way respectively in blue and light pink.

For both reference dwelling, implementing only natural supply vents in the hallway (for reference dwelling 2 in hallway and living room) greatly decreases the occupant exposure to CO_2, leading to very low exposure levels. The supply flow rate is less dependent to both the wind (direction) and the stack effect, as the natural vents are situated on only one side of the building and only on the ground level. However, the total airflow rate of the C-system with additional extraction is higher than the classical system. Therefore, a demand control system could be recommended.

3.5 C-system with mechanical transfer openings in the living room and bedrooms.

The simulations investigate the influence of a classical C-system with natural supply vents designed at 2 Pa and mechanical transfer openings between the living room/bedrooms and respectively the entrance and the hallway of the night zone on the occupant exposure levels in reference dwelling 1 with varying airtightness in relation to the classical C-system (Figure 8).

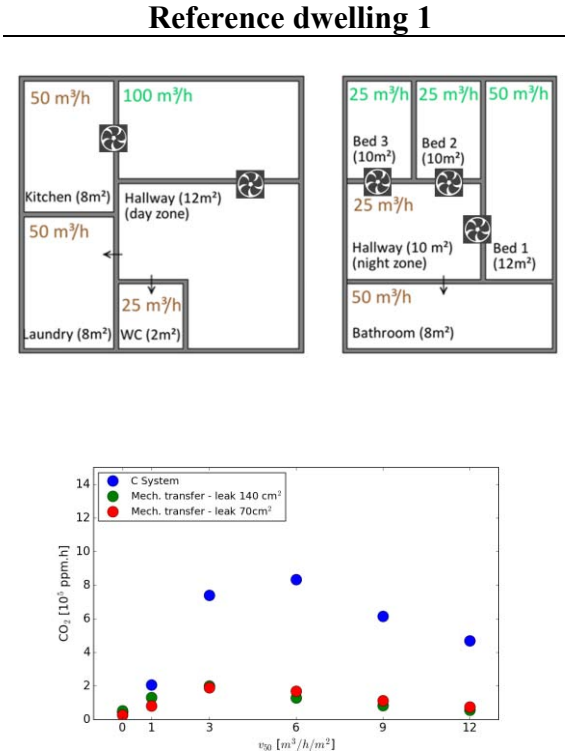

Figure 8: Reference dwelling 1 is equipped with a classical C-system with mechanical transfer opening in the living room and bedrooms (above). The graphs (below) show the occupant exposure levels to CO_2 for different airtightness levels. The results for the classical C-system are shown in blue; for the ventilation system with mechanical transfer openings in green and red for respectively large and smaller leakages between the rooms .

Applying mechanical transfer openings between the living room and entrance hall and kitchen and between the bedrooms and the hallway of the night zone leads to lower occupant exposure levels to CO_2, even if there are leakages between the spaces in the dwelling. Although this intervention is not as efficient as the previous ones because of the recycling of air that can occur, this intervention remains a valid solution to decrease the occupant exposure to a sufficient level.

3.6 Inefficient intervention to minimize the influence of the stack effect, wind and the airtightness on the operation of mechanical exhaust ventilation systems

This study also investigated other interventions to minimize the influence of the stack effect and wind on the operation of mechanical exhaust ventilation systems in comparison with the classical system C, such as:

1. Increasing the mechanical extraction airflow rates
2. Balancing the airflow rates per floor level
3. Decreasing the internal resistance by using larger transfer openings between the spaces in the dwelling

Without presenting the actual results, following conclusion can be drawn: all of the above interventions don't lead to an efficient decrease of the occupant exposure levels to CO_2. Increasing the mechanical extraction airflow rates and balancing the airflow rates per floor level only lead to a small decrease; decreasing the internal resistance even leads to slightly higher exposure levels in dwellings with a good airtightness.

4 CONCLUSIONS

The first four presented interventions lead to considerably lower exposure levels of the occupants to CO_2 for both types of dwellings. However, implementing smaller natural supply vents is only effective in dwellings with high airtightness levels.

Adding mechanical extraction to the bedrooms, implementing the natural supply vents only in the entrance hallway or adding mechanical transfer openings lead to very low levels of exposure and are therefore very effective solutions to minimise the influence of the stack effect and wind on the operation of mechanical exhaust ventilation systems.

These solutions are even very effective in less airtight dwellings, where a negative impact of the leakages in the building envelope occurs in addition to the effects of wind and the stack effect, by enhancing the effective air renewal in the living and bedrooms

However, these solutions require higher total ventilation design flow rates whereby demand control ventilation is advised.

5 ACKNOWLEDGEMENTS

This paper is based upon work supported by the Federal Public Service Economy (FPS Economy) in Belgium for reference dwelling 1 and by Innoviris (the Brussels Capital Region) for reference dwelling 2

6 REFERENCES

Belgisch Instituut voor Normalisatie (BIN). (1991). *NBN D 50-001: ventilatievoorzieningen in woongebouwen.* Brussel.

AIVC. (1996). *A Guide to Energy Efficient Ventilation.*

Van Gaever, R., et al. (2017). The effectiveness of mechanical exhaust ventilation in dwellings. *AIVC Conference 2017.*

Multi-Objective Optimization of Energy Saving and Thermal Comfort in Thermo Active Building System based on Model Predictive Control

Ogawa Yohei[1], Shiraishi Yasuyuki[*2]

1 Graduate student, The University of Kitakyushu
〒808-0135
1-1 Hibikino Wakamatsu-ku Kitakyushu city
Fukuoka prefecture, Japan
shiraishi@kitakyu-u.ac.jp

2 Professor, The University of Kitakyushu
〒808-0135
1-1 Hibikino Wakamatsu-ku Kitakyushu city
Fukuoka prefecture, Japan
shiraishi@kitakyu-u.ac.jp

ABSTRACT

Japan will have to further reduce CO_2 emissions to meet its obligations under the Paris Agreement negotiated at the 2015 United Nations Climate Change Conference. Society is increasingly demanding higher energy-efficiency standards and zero-energy buildings because general commercial buildings have high energy costs, especially for air conditioning. Furthermore, it is just as important to consider the productivity of the people working in these buildings; therefore, there is an urgent need for air-conditioning systems and control methods that are both energy efficient and provide thermal comfort. Radiant heating and cooling has been introduced in Japan in recent years. This is a means of creating an indoor thermal environment that balances energy efficiency and comfort in the office. A thermo-active building system (TABS) is an example of an advanced radiant heating and cooling system. TABS utilizes the building frame, which is mainly concrete slab, to store and radiate heat. Compared with a conventional radiant system, TABS offers higher energy efficiency, a more comfortable environment for workers, and cost advantages. ON/OFF or PID controls are commonly used to control conventional air conditioning; however, to optimize air-conditioning control, it is essential to include load prediction because the thermal response of the ceiling surface temperature is slow due to the ceiling's large thermal mass. The problem is that either energy consumption increases or thermal comfort decreases in cases where these controls are applied to TABS. In a previous study, we proposed using model predictive control (MPC), which takes into consideration thermal response, as a way of optimizing the control of TABS in an existing office building that also had an outdoor air processing unit. We verified the effectiveness of MPC by performing a coupled analysis using MATLAB/Simulink and CFD as a single-objective optimization method for optimizing thermal comfort; however, energy consumption was not considered in this previous study. Therefore, in the present study, we conducted a fundamental examination of multi-objective optimization of thermal comfort and energy efficiency by performing numerical simulations using MATLAB/Simulink. As the result this study suggests that it is possible to reduce the water flow rate of TABS while maintaining comfort by performing multi-objective optimization. A reduction effect of up to 68.3% was obtained in comparison with reference case.

KEYWORDS

Radiation air conditioning, Building thermal storage, TABS, MPC, CFD

1 INTRODUCTION

Japan will have to further reduce CO_2 emissions to meet its obligations under the Paris Agreement negotiated at the 2015 United Nations Climate Change Conference. Society is increasingly demanding higher energy-efficiency standards and zero-energy buildings because general commercial buildings have high energy costs, especially for air conditioning. Furthermore, it is just as important to consider the productivity of the people working in these buildings; therefore, there is an urgent need for air-conditioning systems and control methods that are both energy efficient and provide thermal comfort.

Radiant heating and cooling has been introduced in Japan in recent years. This is a means of creating an indoor thermal environment that balances energy efficiency and comfort in the office. A thermo-active building system (TABS) is an example of an advanced radiant heating and cooling system. Compared with a conventional radiant system, TABS offers higher energy

efficiency, a more comfortable environment for workers, and cost advantages. ON/OFF or PID controls are commonly used to control conventional air conditioning; however, to optimize air-conditioning control, it is essential to include load prediction because the thermal response of the ceiling surface temperature is slow due to the ceiling's large thermal mass[1].

Previous studies[2] have attempted to dynamically control TABS using MPC by targeting half spans of a standard floor, and the effectiveness of this control method has been demonstrated by CFD analysis and numerical simulation using MATLAB/Simulink[3]. However, only single-objective optimization for thermal comfort was conducted in these analyses and energy consumption was not considered. Therefore, in the present study, we conducted a fundamental examination of multi-objective optimization of thermal comfort and energy efficiency by performing numerical simulations using MATLAB/Simulink.

2 MULTI-OBJECTIVE OPTIMIZATION

Previous studies have determined the optimal operating conditions in an indoor environment using an air handling unit (AHU) and TABS together. The ceiling surface temperature was controlled using MPC with the optimal operating conditions being the target values.

With multi-objective optimization, energy consumption increases when thermal comfort is prioritized and, conversely, thermal comfort decreases when energy consumption is reduced. Therefore, there is a trade-off between energy consumption and thermal comfort. This trade off means that multi-objective optimization is achieved by minimizing or maximizing multiple objective functions within given constraints[4].

2.1 An optimization method[5]

Multiple objective functions can be unified by using the multi-objective formulation shown in equation (2.1) in the multi-objective optimization problem. The optimal solution of the unified objective function is found using an optimization method.

$$\min f = \sum_{i=1}^{k} f_i \tag{2.1}$$

Furthermore, there is an infinite number of solutions in the solution space, as shown in Fig. 1. There will always be a set of solutions (Pareto solution) that are superior to other solutions for any of the objective functions where there is a trade-off. A set of such solutions, called a Pareto frontier, is a rational solution to multi-objective optimization problems. However, the preferred Pareto solution (e.g., optimizing energy consumption and comfort) differs according to what a given building is used for and what its design concept is; therefore, weighting[6] is used in the optimization method in this research. In the method we used, each of the Pareto solutions is obtained by solving the weighted sum shown in equation (2.2) as a single objective function. A

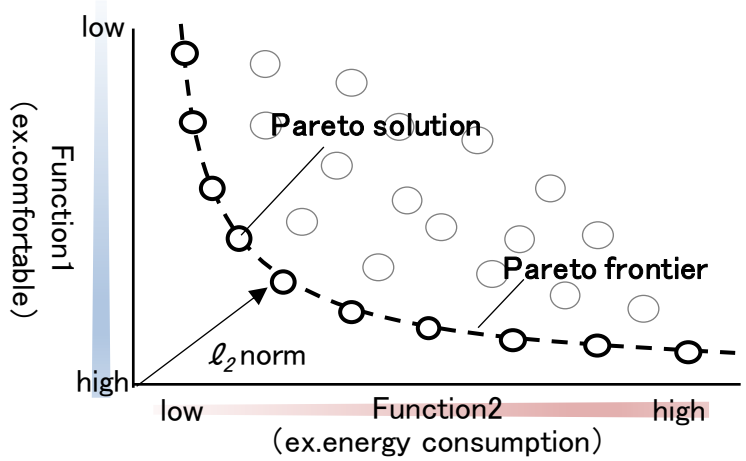

Figure 1: Image of Multi-Objective Optimization

decision maker determines the Pareto solution by setting a weighting for each objective function by using the weighting factor w.

$$\sum_{i=1}^{k} w_i = 1 \tag{2.2}$$

$$w_i \geq 0 \tag{2.3}$$

3 OUTLINE OF OPTIMAL CONTROL METHOD[7,8)]

We used MPC as the optimal control method in this report. MPC is a control method that determines the current value of the optimal manipulated variable pattern (i.e., the water flow rate) while predicting the behavior of a future controlled variable (i.e., the ceiling surface temperature). Equation (3.1) shows the evaluation function of MPC. As shown in Fig. 2, H_p represents a prediction horizon, H_u represents a control horizon, and $w^y, w^u, w^{\Delta u}$ represent different weightings. The first term indicates the deviation of the prediction control output $\mathrm{y}(k+i|k)$ from the reference trajectory $y_{ref}(k+i|k)$, and any deviation is penalized. The initial point of $\mathrm{y}(k+i|k)$ is the output measurement value $y(k)$. The second term is penalized for its deviation from the ideal static value of the input. The third term is penalized for deviating from the control move $\Delta\mathrm{u}(k+i|k)$. In addition, constraints of equations (3.5) and (3.6) are required in order to use the weighting method. Equation (3.1) is a convex function, which is a standard optimization problem known as a quadratic programming problem. z_k shows the manipulated variable in each step within a prediction horizon. An optimal solution is obtained by minimizing the evaluation function $J(z_k)$ by using the least squares method. Each term is an *l2* norm (Euclidean norm) and also called an *l2* norm optimal control problem[9)].

$$J(z_k) = J_y(z_k) + J_u(z_k) + J_{\Delta u}(z_k) \tag{3.1}$$

Where

$$J_y(z_k) = \sum_{j=1}^{n_y} \sum_{i=1}^{H_p} \{\frac{w_{i,j}^y}{S_j^y}[y_{ref}(k+i|k) - y_j(k+i|k)]\}^2$$

$$J_u(z_k) = \sum_{j=1}^{n_u} \sum_{i=0}^{H_p-1} \{\frac{w_{i,j}^u}{S_j^u}[u_j(k+i|k) - u_0]\}^2$$

$$J_{\Delta u}(z_k) = \sum_{j=1}^{n_u} \sum_{i=1}^{H_p-1} \{\frac{w_{i,j}^{\Delta u}}{S_j^u}[u_j(k+i|k) - u_j(k+i-1|k)]\}^2$$

$$z_k^T = [u(k|k)^T \;\; u(k+1|k)^T \;\; \cdots \;\; u\big(k+H_p-1\big|k\big)^T]$$

Subject to

$$\Delta\underline{u} \leq \Delta u(k) \leq \Delta\overline{u} \tag{3.2}$$

$$\underline{u} \leq u(k) \leq \overline{u} \tag{3.3}$$

$$H_p > H_u \tag{3.4}$$

$$w_{i,j}^y + w_{i,j}^u + w_{i,j}^{\Delta u} = 1 \tag{3.5}$$

$$w_{i,j}^y, w_{i,j}^u, w_{i,j}^{\Delta u} \geq 0 \tag{3.6}$$

n_v: Number of plant output variables, n_u: Number of manipulated variables,
k: Current control interval, y_{ref}: Reference value for jth plant at ith prediction horizon step
y_j: Predicted value of jth plant output at ith prediction horizon step, u: manipulated variables
u_0: Initial value of manipulated variables(MV), S_j^y, S_j^u: Scale factor tor jth output, MV(= 1)
$w_{i,j}^y, w_{i,j}^u, w_{i,j}^{\Delta u}$: Tuning weight for jth output, MV, MV movement movement at ith prediction horizon step
H_p: Prediction horizon, H_u: Control horizon,
z_k : MV of each step in the predction horizon at current control interval

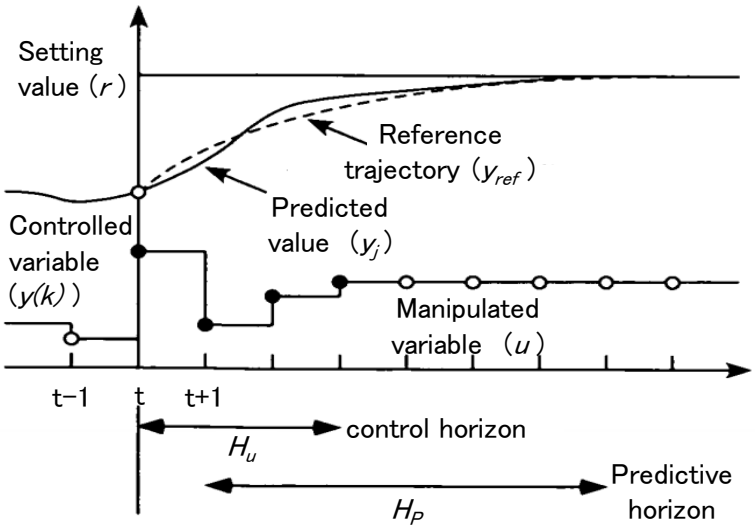

Figure 2: Image diagram of Model Predictive Control (MPC)

4 OUTLINE OF ANALYSIS

First, we used a Simulink analysis model whose effectiveness was demonstrated in previous research[2)] to conduct case studies in which multi-objective optimization using MPC was performed with manipulated and controlled variables that had been given various weightings.

4.1 Analysis case

The cases analyzed are shown in Table 1. Case 0 is a case that prioritizes comfort. Case 1 is a case in which the objective functions of comfort and the integrated water flow rate have the same weighting. Case 2 is a case in which the integrated water flow rate is prioritized by increasing the weighting of the manipulated variable. The weighting factor of manipulated variable movement is the same in all cases.

Table 1: Analysis cases

	Weighting factor			Remarks
	Control variable	Manipulated variable	Manipulated variable movement	
	w^y	w^u	$w^{\Delta u}$	
Case0	0.9	0.0	0.1	Comfort priority
Case1	0.45	0.45	0.1	—
Case2	0.3	0.6	0.1	Energy efficiency priority

4.2 Analysis model

A prediction model was created from a step response using CFD analysis that reproduced the office space. The CFD analysis model is shown in Fig. 3. The radiating part of the CFD analysis model has piping that was laid out at a 150-mm pitch on a 125-mm thick slab and was held in place with mortar and insulation. To improve the analysis accuracy, a multi-block, which is a mesh generation technique, was inserted only around the embedded piping. A time delay, which is a fluctuation that often occurs in the step response to a step input, was observed when acquiring the step response of TABS. Therefore, a prediction model that took into account this time delay was created to reproduce this actual phenomena with Simulink. Because TABS and an AHU thermally affect the ceiling surface temperature and room temperature, respectively, in real space, they are reproduced similarly in the Simulink analysis model. Lighting is not considered in this analytical model because the heat load is low.

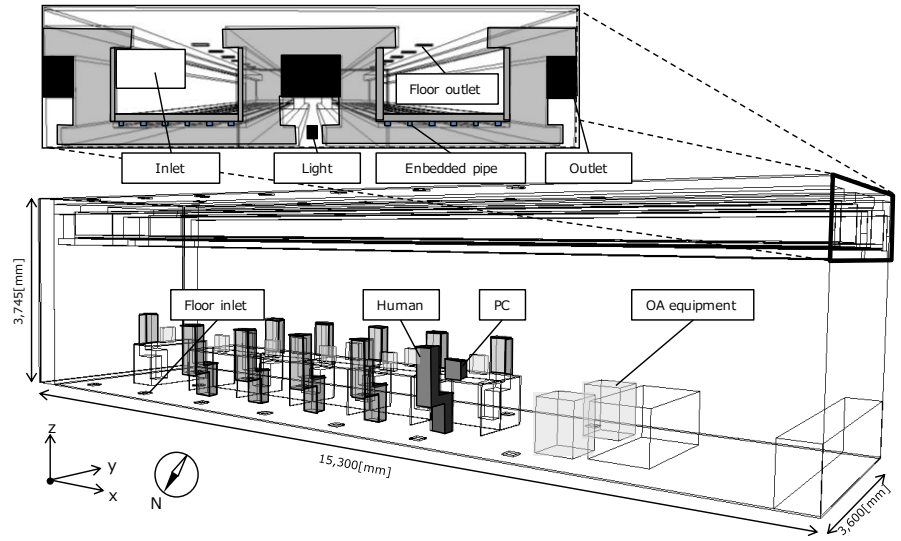

Figure 3: CFD analysis model

4.3 Analysis conditions

The analysis conditions in the Simulink are shown in Table 2. The load schedule is shown in Fig. 4. For the analysis period, the approaching period and the analysis period were each set to 1 day. PMV is used as an indicator of comfort. The average radiant temperature is affected by the ceiling surface temperature.

Table 2: Analysis conditions in Simulink

Prediction Model		Transfer function model
Sample time		TABS:1,800s, AHU:5s
H_p(Prediction horizon)		48step
H_u(Control horizon)		24step
Internal load	Human	6.8W/m^2
	OA equipment	5.6W/m^2
	Lighting	8.8W/m^2
Under floor air conditioning system	Flow rate	430~1,040m^3/h
	Air flow temperature	26℃
TABS	Water flow temperature	16℃
Constraints		
u(TABS)		$0 \leq u(k) \leq 4$
Δu(TABS)		$0 \leq \Delta u(k) \leq 4$
Weighting factor		$w^y + w^u + w^{\Delta u} = 1$
		$w^y, w^u, w^{\Delta u} \geq 0$

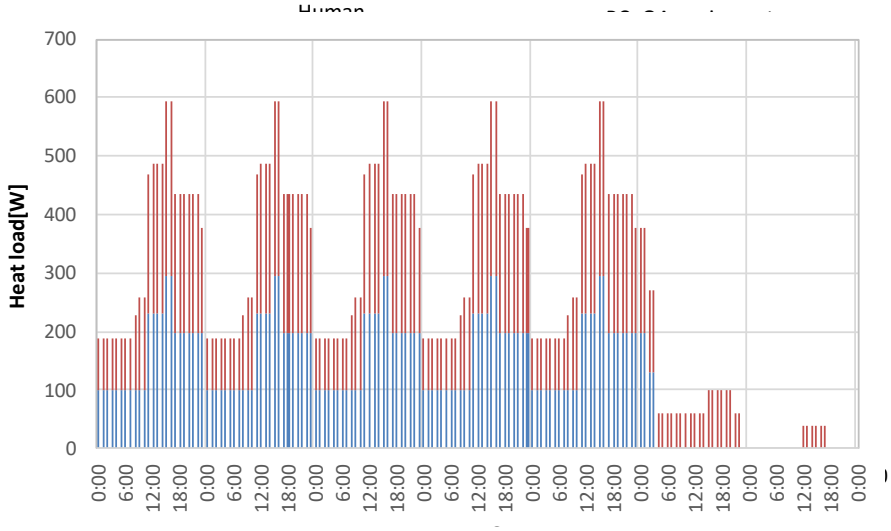

Figure 4: Load schedule

4.4 Analysis result

The results for the ceiling surface temperature and water flow pattern are shown in Fig. 5. The water flow rate is the largest in Case 0 because the weighting of the controlled value is large, but the ceiling surface temperature is controlled such that it is a constant target value of 24°C. The ability to maintain the target value becomes impaired as the weighting, w^u, of the controlled variable becomes larger. It was confirmed that, in all cases, the ceiling surface temperature stayed within the comfort range even though the water flow rate decreased. This suggests that the minimization of the water flow rate became important when the weighting of the controlled valuable was reduced. The control error in the target value of the ceiling surface temperature and the effect of reducing the water flow rate are shown in Fig. 6. The control error is the same as in Fig. 5. In addition, Case 2 has the lowest integrated water flow rate because the weighting of the manipulated valuable became large. A reduction effect of 30% in Case 1 and of 68% in Case 2 were obtained in comparison with Case 0. The above suggests that it is possible to reduce the water flow rate of TABS while maintaining comfort by performing multi-objective optimization using MPC.

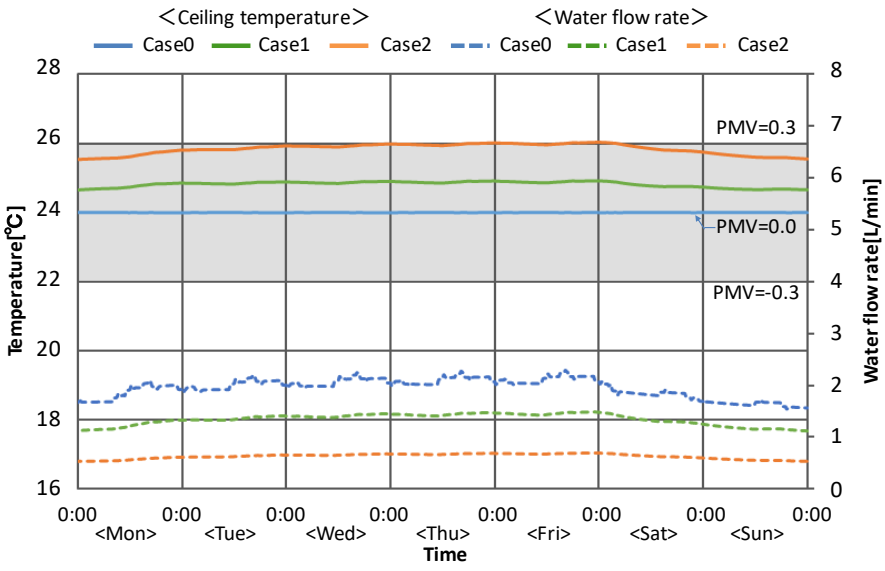

Figure 5: Analysis results on Simulink

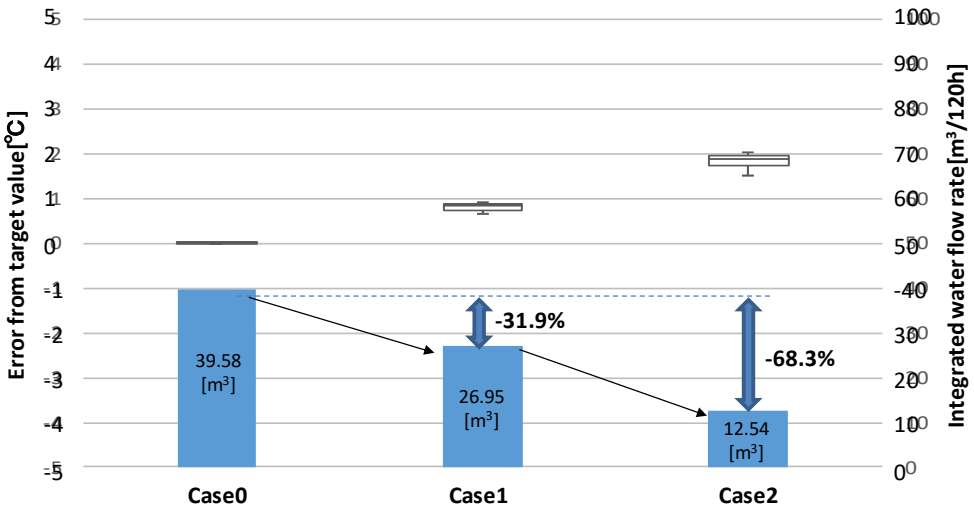

Figure 6: Control error and reduction effect of energy consumption

5 CONCLUSION

In the present study, we conducted a fundamental examination of multi-objective optimization of thermal comfort and energy efficiency by performing numerical simulations using MATLAB/Simulink. As a result, it is possible to reduce the water flow rate of TABS while maintaining the comfort by multi-objective optimization using MPC.

6 ACKNOWLEDGMENTS

This work was supported by Kosuke Sato, Eri Kataoka and Kosuke Yoshida in NIKKEN SEKKEI LTD. The authors would like to thank them and the company for a research grant and helpful.

7 REFERENCES

1)Yongjun Sun, Shengwei Wang, Fu Xiao, Diance Gao, Peak load shifting control using different cold thermal energy storage facilities in commercial buildings: A review. Energy Conversion and Management 71 (2013) 101-114

2)Yohei Ogawa et all, Radiation Cooling and Heating using Building Thermal Storage for outside Insulation Building Part8. Proposal of Optimal Control Method using Model Predictive Control, Hearing,Air Conditioning and Sanitary Engineers of Japan, No.69(2018),pp.401-404 (in Japanese)

3) http://jp.mathworks.com/products/matlab/

4)Masatoshi Sakawa (1984), Linear System Optimization -From One Purpose to Multiple Purposes, Morikita Publishing Co., Ltd. (in Japanese)

5)Masatoshi Sakawa (1986), Optimization of Discrete System, -From One Purpose to Multiple Purposes, Morikita Publishing Co., Ltd. (in Japanese)

6)Hirokazu Kobayashi et all, Introduction of a Weighting Factor Setting Technique for Multi-Objective Optimization, Journal of the institute of systems, control and information engineers, Vol.31, No.8, 2018, pp.281-294

7)Jan M.Machiejowski(2015), Predictive Control with Constraints, Pearson Education Limited

8)Ge Yu, Harutoshi Ogai, Haoyang Deng:Offset-free Model Predictive Control of Diesel Engine by Combined Design of Disturbance Model and Observer, IEEJ Transactions on Industry Applications, 2018, Vol.14, No.1, pp.1-11

9)Masaaki Nagahara (2017), Sparse Modeling-Fundamentalls and Its Applications to Dynamical Systems-, CORONA PUBLISHING CO., LTD. Tokyo Japan (in Japanese)

Two Case Studies on Ventilation for Indoor Radon Control

Justin Berquist*, Liang Grace Zhou, Jeffrey Whyte, Yunyi Ethan Li, Mark Vuotari and Gang Nong

National Research Council Canada
1200 Montreal Road
Ottawa, Ontario, Canada
**Corresponding author: Justin.Berquist@nrc-cnrc.gc.ca*

ABSTRACT

Health Canada's cross-Canada residential radon survey report from 2012 demonstrated that roughly 7% of Canadian homes contain radon levels above the Canadian guideline of 200 Bq/m^3. The research outlined in this paper evaluates the effect of ventilation rates on radon levels in two homes located in Ontario, Canada. The first case study consisted of short-term (2 day) radon monitoring in a home using three ventilation strategies; one heat recovery ventilator (HRV) running, two HRVs running, and both HRVs turned off. The results displayed the potential benefits of increasing the ventilation rate in an airtight home to reduce occupants' radon exposure. When both HRVs were off the measured air exchange rate was 0.05 h^{-1} and maximum radon concentration was 222 Bq/m^3. When both HRVs were operating, the air exchange rate was 0.40 h^{-1}, and within four hours the lowest radon concentration measured was 33 Bq/m^3. The first case study provided justification for conducting longer-term radon monitoring (2.5 months) in a second home using three ventilation strategies. During this time period, an energy recovery ventilator (ERV) was successively operated in three different modes: continuously, running 20 minutes per hour, and turned off. When the ERV was off, the average basement radon concentration was 872 Bq/m^3 and the air exchange rate was 0.16 h^{-1}. When the ERV in the house was operating continuously, the air exchange rate rose to 0.28 h^{-1}. However, possibly a result of the second home being leakier and the initial radon concentration being higher than in the first home, it was not possible to reduce the average radon concentration (242 Bq/m^3) below the Canadian guideline of 200 Bq/m^3 solely via ventilation. The results obtained in both homes suggest, 1) studies using a larger number of homes would be beneficial for evaluating ventilation as a solution for radon control and 2) when considering ventilation as a radon reduction technique, both the initial radon concentration and the natural ventilation rate of the home should be considered.

KEYWORDS

Radon, mitigation, and ventilation

1 INTRODUCTION

Radon is a naturally occurring radioactive gas. It is the direct decay product of radium-226, stemming from the decay of uranium-238 (Shammas and Wang 2009). As such, radon originates below the ground and migrates to the earth's surface (Zhukovsky and Vasilyev 2014). This is problematic because of the risks associated with the inhalation of radon and radon decay products. Radon decay products are not gases, as such, it is common for them to lodge in the lining of the lungs (American Cancer Society 2015). As further decay of these products occur, alpha particle radiation is given off that can cause various cellular damage, leading to the development of lung cancer (American Cancer Society 2015).

Outside, radon dilutes to concentrations that do not pose a significant risk (Shammas and Wang 2009). However, the accumulation of radon in buildings is problematic (Shammas and Wang 2009). Radon is the second leading cause of cancer, after smoking (American Cancer Society 2015). Between 3 and 14% of a country's lung cancer occurrences can be attributed to

radon, although the severity in each country depends on the national average radon level and smoking prevalence (World Health Organization 2016).

Due to the danger of high radon levels, many countries around the world have implemented guidelines and regulations for indoor radon. Canada and the United States have national *guidelines* of 200 Bq/m^3 and 148 Bq/m^3, respectively. Meanwhile, European Union mandates that Member States enforce *regulations* to ensure indoor radon concentrations are below 300 Bq/m^3, as required by the Basic Safety Standards 2013 Directive. In addition, the World Health Organization has established a national *reference level* of 100 Bq/m^3 (World Health Organization 2009).

The risk associated with indoor radon is a major threat to Canadians as they spend over 90% of their time indoors (Khan et al. 2018) and 7% of Canadian homes have been found to contain radon levels above the Canadian guideline of 200 Bq/m^3 (Health Canada 2012). There are several methods to prevent and reduce radon entry into buildings. The most common methods are active soil depressurization, passive soil depressurization, increasing overall ventilation rates, avoiding depressurization inside the building, and sealing soil gas entry routes into the building.

In this research, two case studies explore the effectiveness of using ventilation for radon control. This paper begins by outlining previous, relevant case studies, followed by a description of the case study and the presentation of the obtained results. The paper then finishes with a discussion of the obtained results and conclusions.

2 LITERATURE REVIEW

This section provides a review of various worldwide case studies that evaluated the effectiveness of ventilation as a solution for radon control. All of which were conducted outside of Canada; New Jersey, USA (Turk et al., 1988), New Jersey, USA (Socolow and Varma., 1994), Czech Republic (Jiranek and Kacmarikova., 2014), Sweden (Akbari and Oman., 2013), Hong Kong (Chao and Hu., 2004), and Washington (Turk et al., 1991).

Jiranek and Kacmarikova (2014) monitored radon in four rooms, for 1 year, before and after an energy-saving retrofit. Although the retrofit reduced the annual heat demand 2.8 fold, it also reduced the air exchange rate to below 0.1 h^{-1}. The authors suggested that this caused the average annual radon concentration to increase from 337 to 1117 Bq/m^3. Akbari and Oman (2013) studied the impact of ventilation on energy consumption and radon concentrations in a house. When inducing an air exchange rate of 0.25, 0.5 and 1 h^{-1}, the average radon concentration was 150, 65, and 36 Bq/m^3, respectively. Chao and Hu (2004) developed a dual-mode (carbon dioxide and total volatile organic compound) demand controlled ventilation strategy for a lecture hall. In the study, the radon concentration decreased below 100 Bq/m^3 when ventilation rates were increased. However, low ventilation rates caused radon concentrations to rise above 700 Bq/m^3 at times. Socolow and Varma (1994) studied radon mitigation by natural and mechanical ventilation. They found the ground floor living area's outdoor air supply had no effect on radon concentration. Turk et al. (1991) studied the long-term performance of two houses that used ventilation to reduce the indoor radon concentration. The radon levels were inversely proportional to the ventilation rates. Moreover, after modifying the ventilation system in one home, a further reduction in radon occurred. Turk et al. (1988) increased ventilation capacity in one home by approximately 0.5 h^{-1}. As a result, the basement and first floor radon levels decreased from 1036 to 592 Bq/m^{3}and 666 to 518 Bq/m^3, respectively.

There is a need to evaluate the effectiveness of many ventilation systems worldwide since an optimal mitigation strategy largely depends on the building type, soil conditions, and climate (Rahman and Tracy 2009). However, the literature review revealed a limited number of research papers (6) pertaining to ventilation as a solution for radon control, all of which were conducted outside of Canada. Therefore, this research will build on previous studies that used ventilation for radon control with two case study homes located in Ontario, Canada.

3 METHODOLOGY

This section provides a description of the measurements and two case study homes used to evaluate the effectiveness of ventilation as a solution for radon control.

3.1 Measurement Description

This subsection outlines the equipment used to monitor the radon concentration and measure the air exchange rate in the two case study homes.

3.1.1 Radon Measurements

The two case studies measured radon concentration with different devices, the AlphaGUARD PQ 2000 Pro (Home #1) and Corentium Plus (Home #2) radon monitors. The AlphaGUARD PQ 2000 Pro uses an ionization chamber to detect radon (Saphymo 2012), while the Corentium Plus uses digital detector technology (Airthings 2019).

The AlphaGUARD PQ 2000 Pro has a range of 2 to 2,000,000 Bq/m^3 and is accurate to ± 3%. The AlphaGUARD PQ 2000 Pro has measurement cycles of 10 or 60 minutes. The duration that the device can measure depends on the interval of the measurement cycle. Data collection capacity is approximately 21 days when using a 10-minute measurement cycle and approximately 4 months when using a 60-minute measurement cycle.

The Corentium Plus radon monitor has a range of 0 to 9,999 Bq/m^3 and is accurate to within 5% ± 5 Bq/m^3. The Corentium Plus continuously monitors radon concentrations in a space and outputs a short and long-term average of the radon concentrations in the space. However, data can only be stored internally at 1-hour intervals. At this time interval, the internal memory storage capacity will last approximately 10 years.

3.1.2 Air Exchange Rate Measurements

In both case studies, tracer gas decay tests were performed to determine the ventilation rate during each control strategy. In tracer gas decay tests, a small amount of tracer gas (SF_6 in this case) is released into the house, and its concentration is recorded as a function of time. The air exchange rate of a building can be determined based on the decay in the tracer gas concentration. An exponential trendline equation can be used to characterize the obtained decay, and the exponent within this equation represents the air exchange rate.

The current study used SF_6 as the tracer gas for the following reasons:

- SF_6 is very inert and relatively low in toxicity
- the environment does not naturally contain SF_6; therefore, ambient background levels are low, and although background levels have been steadily rising due to its use in many fields, it is present at a fraction of the level being measured in this research
- SF_6 is readily available in compressed cylinders, and the research team has been using an in-house developed dosing unit on a routine basis

In the two case study homes, the tests were conducted when the pressure differential across the building envelope could be assumed insignificant (i.e. limited wind). The tests used an INNOVA 1303 Multipoint Sampler and Doser unit to sample SF_6 at six locations in each home and an INNOVA 1312 Photoacoustic Multi-gas Monitor to analyse the samples.

3.2 Case Study Description

This subsection describes the two case study homes monitored in this research. Described first is Home #1, which consisted of short-term (two-day) radon monitoring. Described second is Home #2, which expanded the study to long-term (monthly) radon monitoring.

3.2.1 Home #1

The first home consists of a basement, ground and second storey floor. The total floor area and volume of the home, excluding the basement, is 133.4 m^2 (1,435 ft^2) and 549 m^3 (19,380 ft^3), respectively. The house contains two heat recovery ventilators (HRVs), one along the main ductwork into and out of the furnace and a second stand-alone unit in the basement. This allowed for the effect of three ventilation strategies to be analysed: one HRV on, both HRVs off, and both HRVs on.

The tracer gas concentration was measured at six locations within the house. The six sampling locations included the basement general area, basement stairwell, ground floor kitchen, ground floor front entrance, second floor hallway, and second floor bedroom. The basement was equipped with an AlphaGUARD radon monitor. Radon concentration measurements started July 11th, 2017 at 8:45 am and continued at 10-minute intervals until July 12th, 2017 at 1:00 pm. Table 1 shows the tracer gas decay test and radon monitoring schedule for the three ventilation strategies implemented in Home #1.

Table 1: Home #1 tracer gas decay test and short-term radon monitoring schedule for each ventilation strategy

Control Strategy	Start Date	Start Time	End Date	End Time
1 HRV on	July 11th, 2017	9:45 am	July 11th, 2017	2:00 pm
Both HRVs off	July 11th, 2017	2:22 pm	July 12th, 2017	8:45 am
Both HRVs on	July 12th, 2017	9:00 am	July 12th, 2017	1:00 pm

3.2.2 Home #2

The second home also consists of a basement, ground and second storey floor. The total floor area and volume of the home, including the basement, is 227.6 m^2 (2,450 ft^2) and 736 m^3 (26,000 ft^3), respectively. It has a variety of features found in energy efficient homes. The house is equipped with continuous building envelope insulation and foam board insulation underneath the concrete slab. There is also an energy recovery ventilator (ERV) located in the basement of the house, supplying outdoor air to the return air plenum of the furnace. In addition, there is an active soil depressurization radon mitigation system within this home. However, for the purposes of this ventilation case study, the active soil depressurization system was disabled. This allowed for three ventilation strategies to be analysed: ERV operating continuously, 20 minutes per hour, and turned off.

The tracer gas concentration was measured at six locations within the house. The six sampling locations included the basement recreation room, basement stairwell, ground floor kitchen, ground floor front entrance, second floor hallway, and second floor master bedroom. Due to equipment availability, the tracer gas decay tests were conducted at different times than radon monitoring. Table 2 shows the tracer gas decay test schedule for the three ventilation strategies implemented in Home #2.

Table 2: Home #2 tracer gas decay test schedule for each ventilation strategy

Control Strategy	Start Date	Start Time	End Date	End Time
ERV 20/60	January 29th, 2019	3:00 pm	January 30th, 2019	7:00 am
ERV On	January 30th, 2019	3:00 pm	January 31st, 2019	9:00 am
ERV Off	January 31st, 2019	9:00 am	January 31st, 2019	3:30 pm

During the long-term radon monitoring, the basement was equipped with a Corentium Plus continuous radon monitor. The Corentium Plus continuous radon monitor measured radon concentrations between March 6th, 2018 and May 22nd, 2019. Table 3 shows the radon monitoring schedule for the three ventilation strategies implemented in Home #2.

Table 3: Home #2 long-term radon monitoring schedule for each ventilation strategy

Control Strategy	Start Date	End Date
ERV 20/60	March 6th, 2018	March 23rd, 2018
ERV On	April 15th, 2018	May 6th, 2018
ERV Off	May 6th, 2018	May 22nd, 2018

4 RESULTS

This section displays the results obtained for the two case study homes. Presented first are the short-term test results for Home #1, followed by the long-term test results for Home #2.

4.1 Home #1

The first case study monitored short-term radon concentrations in a home using three ventilation strategies; one HRV on, both HRVs off, and both HRVs on. Presented first are the tracer gas decay test results, followed by the short-term radon monitoring results.

4.1.1 Tracer Gas Decay Testing

To determine the ventilation rate for each ventilation strategy, tracer gas decay tests were performed. The average concentration from six locations in the house was used to approximate the overall ventilation rate of the house. Figure 1 shows the average tracer gas decay and exponential line of best fit for each control strategy. Note that for clarity purposes, the entire decay period of SF_6 while both HRVs were off was not included in Figure 1; however, the displayed exponential line of best fit does consider the entire decay period.

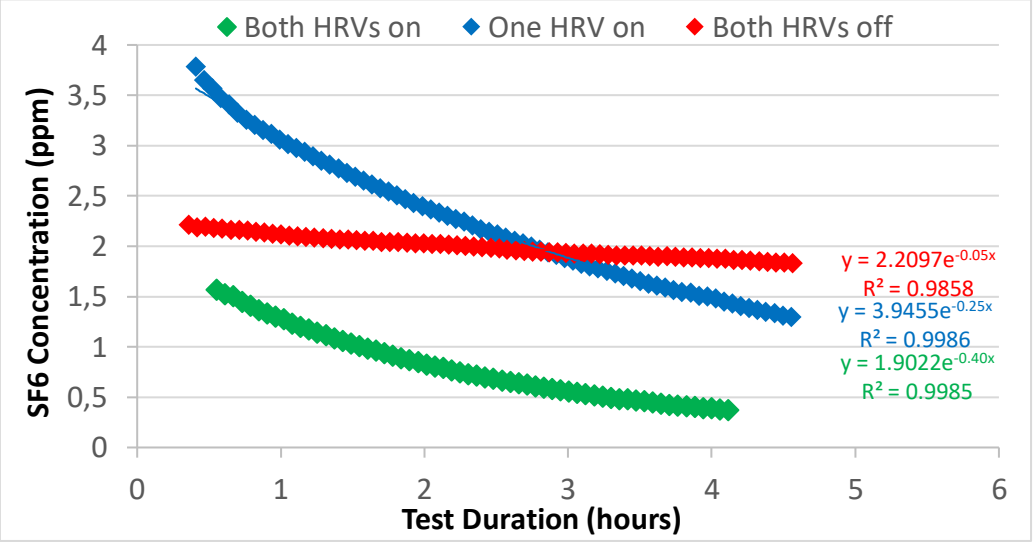

Figure 1: Home #1 tracer gas decay test results for each ventilation strategy

Figure 1 shows the air exchange rates for each ventilation strategy. When one HRV was on, the air exchange rate was 0.25 h^{-1}. When both HRVs were off, the air exchange rate was 0.05 h^{-1}. When both HRVs were on, the air exchange rate was 0.40 h^{-1}.

4.1.2 Radon Monitoring

Short-term radon monitoring was used to evaluate the effectiveness of each ventilation strategy in Home #1. Figure 2 shows the radon concentration measurements in the basement general area during each ventilation strategy on July 11th and 12th, 2017.

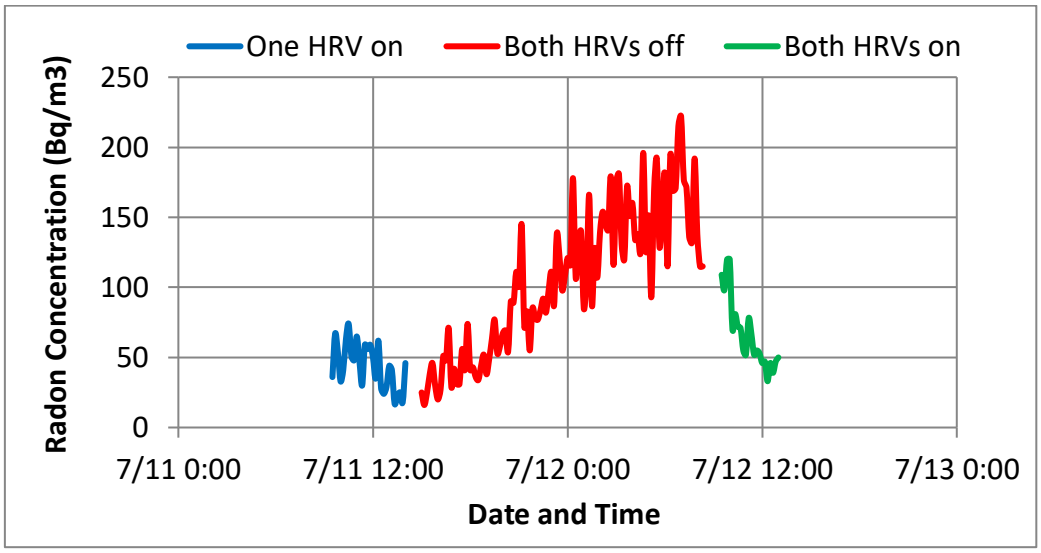

Figure 2: Home #1 short-term radon monitoring results for each ventilation strategy

Initially, the operation of one HRV limited the average radon concentration in the basement to 44 Bq/m^3. Within 15 hours of the HRVs being turned off, the basement radon concentration increased to a peak of 222 Bq/m^3. Within 4 hours of the HRVs being turned on, the basement radon concentration dropped to 33 Bq/m^3.

4.1.3 Summary of Results

Table 4 summarizes the key results obtained from the tracer gas decay tests and short-term radon monitoring within Home #1. Included in Table 4 are the average, maximum, and minimum basement radon concentrations, as well as the air exchange rates for the home, for each ventilation strategy. However, the short duration that each ventilation strategy was implemented should be considered when viewing the average, minimum, and maximum radon concentrations and drawing conclusions related to causality.

Table 4: Home #1 short-term radon monitoring results for each ventilation strategy

Control Strategy	Average (Bq/m^3) AlphaGUARD	Minimum (Bq/m^3) AlphaGUARD	Maximum (Bq/m^3) AlphaGUARD	ACH (h^{-1})
Both HRVs off	106	16	222	0.05
1 HRV on	44	17	74	0.24
Both HRVs on	66	33	120	0.40

The two-day study displayed the potential benefits of providing additional ventilation for radon mitigation. When both HRVs were off, the basement radon concentration ranged between 16 and 222 Bq/m^3, with an average concentration of 105 Bq/m^3. When one HRV was on, the basement radon concentration ranged between 17 and 74 Bq/m^3, with an average

concentration of 44 Bq/m^3. When both HRVs were on, the basement radon concentration ranged between 33 and 120 Bq/m^3, with an average concentration of 66 Bq/m^3.

4.2 Home #2

A second case study monitored radon concentrations long-term within Home #2. Three ventilation control strategies were implemented: no mechanical ventilation (ERV off), ventilation supply for 20 minutes per hour (ERV 20/60), and constant mechanical ventilation (ERV on). Presented first are the tracer gas decay test results, followed by the long-term radon monitoring results.

4.2.1 Tracer Gas Decay Testing

Performing tracer gas decay tests in the case study home allowed for the determination of ventilation rates when the ERV was off, supplying outdoor air for 20 minutes per hour, and constantly supplying ventilation. Tracer gas samples were taken at six locations in the house and the average concentration was used to approximate the overall ventilation rate of the house. Figure 3 shows the average tracer gas decay and exponential line of best fit for each ventilation strategy.

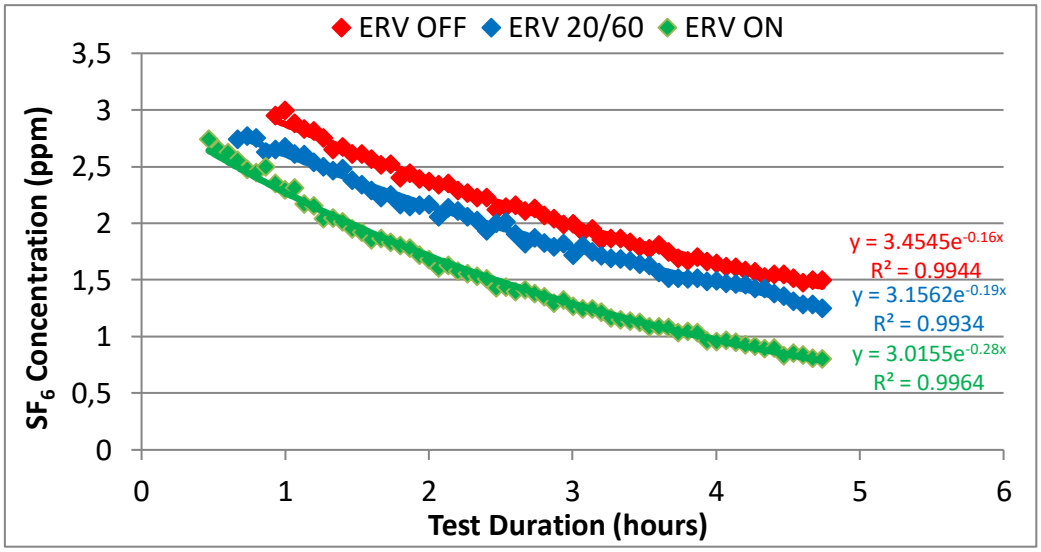

Figure 3: Home #2 tracer gas decay test results for each ventilation strategy

Figure 3 shows the air exchange rates for each control strategy. When the ERV was off, the air exchange rate was 0.16 h^{-1}. When the ERV was supplying outdoor air for 20 minutes per hour, the air exchange rate was 0.19 h^{-1}. When the ERV was on continuously, the air exchange rate was 0.28 h^{-1}.

4.2.2 Radon Monitoring

Long-term radon monitoring was used to evaluate the effectiveness of each ventilation strategy in Home #2. Figure 4 shows the radon concentrations in the basement recreation room during each ventilation strategy between March 6th and May 22nd, 2018.

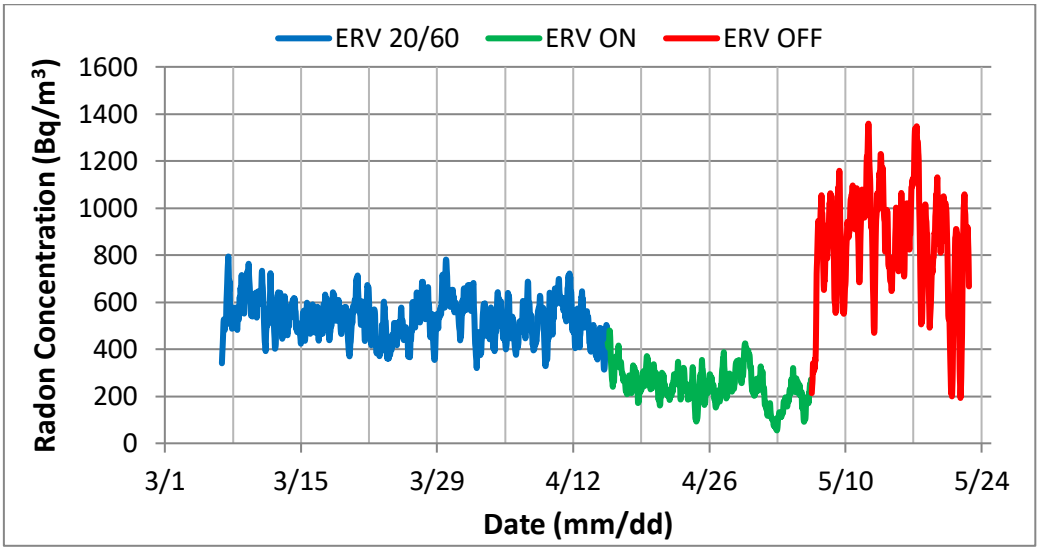

Figure 4: Home #2 long-term radon monitoring results for each ventilation strategy

For the period when the ERV was supplying outdoor air for 20 minutes per hour, the average radon concentration was 537 Bq/m^3. For the period when the ERV was constantly on, the average radon concentration was 242 Bq/m^3. For the period when the ERV was off, the average radon concentration was 872 Bq/m^3.

4.2.3 Summary of Results

Table 5 summarizes the key results obtained from the tracer gas decay tests and long-term radon monitoring. Included in Table 5 are the average, maximum, and minimum basement radon concentrations, as well as the air exchange rates for the home, for each ventilation strategy.

Table 5: Home #2 long-term radon monitoring results for each ventilation strategy

Control Strategy	Average (Bq/m^3) Corentium	Minimum (Bq/m^3) Corentium	Maximum (Bq/m^3) Corentium	ACH (h^{-1})
ERV 20/60	537	314	767	0.19
ERV On	242	58	424	0.28
ERV Off	872	193	1359	0.16

Table 5 shows the benefits of increasing the ventilation rate for radon control. When the ERV was off the air exchange rate of home #2 was low, 0.18 h^{-1}. This low air exchange rate resulted in a high average radon concentration, 872 Bq/m^{-3}, and a maximum concentration of 1359 Bq/m^{-3}. However, after increasing the ventilation to the home the measured radon concentrations lowered. Compared to no ventilation, periodic ventilation (ERV 20/60) increased the air exchange rate to 0.19 h^{-1} and decreased the average radon concentration to 537 Bq/m^{-3}, while constant ventilation increased the air exchange rate to 0.28 h^{-1} and decreased the average radon concentration to 242 Bq/m^{-3}

5 DISCUSSION

The first case study home displayed a positive effect of household ventilation for radon control. This provided justification to conduct long-term radon monitoring in a second home. Although it was valuable for the progression of this research, it was a short-term study, which can provide unreliable information, since indoor radon concentrations exhibit large temporal variability. For this reason, the second case study home will be the focus of this discussion, as long-term radon monitoring allows more reliable information to be obtained.

Constantly supplying ventilation with the ERV increased the air exchange rate from 0.16 h^{-1} to 0.28 h^{-1} and reduced the average radon concentration from 872 Bq/m^3 to 242 Bq/m^3. Due to the high initial air exchange rate (0.16 h^{-1}) and radon concentration (872 Bq/m^3) of the home, the ERV was unable to reduce the average radon concentration below the Canadian guideline of 200 Bq/m^3. However, the addition of the ERV did cause the air exchange rate to increase by a factor of almost 2 and reduced the radon concentration by approximately 72%. This shows that ventilation can effectively reduce radon concentrations in homes; however, it implies that when considering ventilation as a radon reduction technique, both the initial radon concentration and the natural ventilation rate of the home should be considered.

The researchers acknowledge the limitations of the conducted research. Due to equipment availability, the tracer gas decay tests were conducted at a different time than the radon monitoring in Home #2, this is a limitation, as the outdoor air temperature affects the air exchange rate of each ventilation strategy. In addition, it is not possible to make concrete conclusions regarding the effectiveness of ventilation for radon control with a small sample of case study homes, one of which consisted of only short-term monitoring. However, this research supports the long-term objective of the research team and lays the foundation for future work.

This research has supported the long-term objective of the research team with regards to ventilation for radon control; to consider both the initial radon concentration and the natural ventilation rate of the home. To accomplish the objective a better understanding of the impacts of building air exchange rate on radon in homes is required. Therefore, future work will focus on long-term radon monitoring in homes having various natural ventilation rates, radon concentrations, and mechanical ventilation strategies.

6 CONCLUSION

In this research, the ventilation rates in two homes were mechanically varied and the corresponding reduction in radon concentration was measured. In the first home, three ventilation strategies were implemented using two HRVs over a two-day span. This case study provided promising results, displaying benefits of ventilation for radon control. However, short-term radon measurements can be unreliable since indoor radon concentrations exhibit large temporal variability. For this reason, an additional case study was performed to evaluate the long-term effects of increasing the overall ventilation rate in homes. In the second home, three ventilation strategies were implemented using an ERV for approximately one month each. The second case study revealed two key findings: 1) studies using a larger number of homes would be beneficial for evaluating ventilation as a solution for radon control and 2) that when considering ventilation as a radon concentration reduction technique, both the initial radon concentration and the natural ventilation rate of the home should be considered. In the future, the research team will conduct long-term radon monitoring in a larger sample of air tight and leaky homes with elevated radon levels to better understand the impacts of building air exchange rates on radon levels in homes.

7 ACKNOWLEDGEMENTS

The authors of this publication gratefully acknowledge that this study was enabled by funding through the Canadian Government's initiative "Taking Action on Air Pollution".

8 REFERENCES

Airthings. 2019. "Corentium Plus - Specification." Retrieved May 30, 2019

(https://www.corentium.ca/ca_en/corentium-plus/).

Akbari, Keramatollah and Robert Oman. 2013. “Impacts of Heat Recovery Ventilators on Energy Savings and Indoor Radon in a Swedish Detached House.” *Management of Environmental Quality: An International Journal* 9(1):682–94.

American Cancer Society. 2015. “Radon and Cancer.”

Chao, C. Y. H. and J. S. Hu. 2004. “Development of a Dual-Mode Demand Control Ventilation Strategy for Indoor Air Quality Control and Energy Saving.” *Building and Environment* 39:385–97.

Health Canada. 2012. *Cross-Canada Survey of Radon Concentrations in Homes Final Report*.

Khan, Selim M., Daniel Krewski, James Gomes, and Raywat Deonandan. 2018. “Radon, an Invisible Killer in Canadian Homes: Perceptions of Ottawa-Gatineau Residents.” *Canadian Journal of Public Health*.

M. Jiranek and V.Kacmarikova. 2014. “Dealing With the Increased Radon Concentration in Thermally Retrofitted Buildings.” 160(1):43–47.

Saphymo. 2012. “AlphaGUARD - Portable Radon Monitor.”

Shammas, Nazih K. and Lawrence K. Wang. 2009. “Shammas 2009.Pdf.” in *Handbook of Advanced Industrial and Hazardous Waste Treatment*.

Socolow, Robert H. and Matesh N. Varma. 1994. *Exposure to Radon and Radon Progeny in the Indoor Environment*.

Turk, B. H., J. Harrison, R. G. Sextro, L. M. Hubbard, K. J. Gadsby, T. G. Matthews, C. S. Dudney, and D. C. Sanchez. 1988. “Evaluation of Radon Reduction Techniques in Fourteen Basement Houses: Preliminary Results.” Pp. 1–22 in *81st Annual Meeting of the Air Pollution Control Association*.

Turk, Bradley H., Richard J. Prill, William J. Fisk, David T. Grimsrud, Bradley H. Turk, Richard J. Prill, William J. Fisk, David T. Grimsrud, Bradley H. Turk, Richard J. Prill, William J. Fisk, David T. Grimsrud, and Richard G. Sextro. 1991. “Effectiveness of Radon Control Techniques in Fifteen Homes Effectiveness of Radon Control Techniques in Fifteen Homes.” *Journal of the Air & Waste Management Association* 723–34.

World Health Organization. 2009. *WHO Handbook on Indoor Radon: A Public Health Perspective*.

World Health Organization. 2016. “Radon and Health.” Retrieved (https://www.who.int/news-room/fact-sheets/detail/radon-and-health).

Zhukovsky, M. V. and A. V. Vasilyev. 2014. “Mechanisms and Sources of Radon Entry in Buildings Constructed with Modern Technologies.” *Radiation Protection Dosimetry* 160(1–3):48–52.

Influence of Ventilation on Radon Concentration in a Study Case in Spain

Pilar Linares-Alemparte[1*], Sonia García-Ortega[1]

1 Eduardo Torroja Institute for construction sciences-CSIC
4, Serrano Galvache St.
Madrid, Spain
plinares@ietcc.csic.es

ABSTRACT

Radon gas is a well-known building´s pollutant which can affect negatively people´s health (WHO, 2009). Radon´s source is the soil underneath buildings. Radon moves from the soil to the buildings by advection through cracks and joints, and diffusion through porous materials. Once radon enters buildings it can accumulate in lower areas due to lack of ventilation. Ventilation is one of the main ways to prevent radon from accumulating in enclosed spaces in the case of moderate radon concentrations up to 600 Bq/m^3 (Collignan, 2008).

This paper presents the research that has been conducted in a building with moderate levels of radon, using precisely ventilation to reduce these levels. The building is placed in a granitic area at the North of Madrid (Spain) with a high presence of radon (García-Talavera, 2013). The results show how even little ventilation can lower radon concentration up to acceptable levels.

KEYWORDS

Ventilation. Radon, Case, Spain

1 INTRODUCTION

One of the objectives of the research project: *Proyecto Radón Cero (Proyecto Radón Cero,* 2018), is the study of the efficiency of ventilation as a way to mitigate moderate indoor radon concentration in an existing building.

Moderate levels of radon concentration were measured in an existing building so it was chosen to perform the corresponding tests The methodology conducted in the research is based on the study of the existing building (initial measurement of radon concentration, building elements, airtightness), proposal of mitigation solution, final measurement of radon concentration and analysis of results.

2. STUDY OF THE EXISTING BUILDING

2.1. Description

The case study is a social centre that belongs to the City Council of Torrelodones, Madrid (Spain). The building is placed above granite rock which is common in the area.

The studied rooms are the kitchen and the fireplace room (Fig. 1). The kitchen presents a high level of airtightness whereas the fireplace room does not due to the chimney, the configuration of windows and an opening above the door to the corridor.

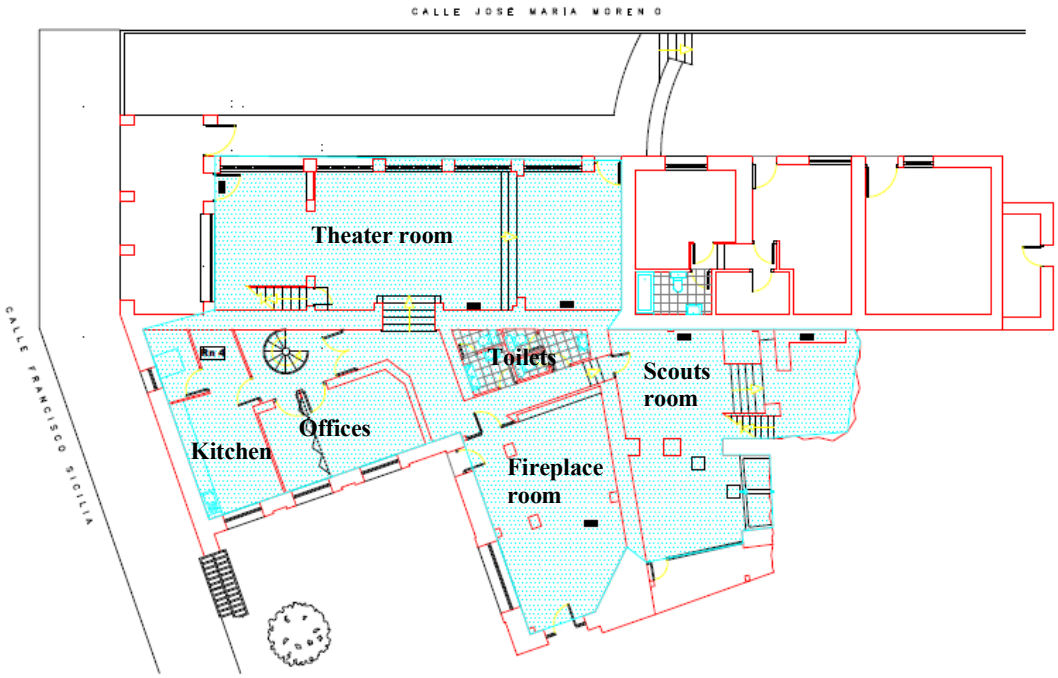

Fig. 1 Ground floor.

2.2. Radon concentration

During 2016 and 2017 radon concentration integrated measurements were carried out using trace detectors CR-39 with the collaboration of *Universidad de Cantabria*. These measurements revealed that some areas presented moderate radon concentrations (Table 1).

Table 1. Radon concentration (Bq/m^3)

	Period of time	
Room	**01/03-05/04/2016**	**19/09/2016 - 27/01/2017**
Theater room	677 ± 55	471 ± 37
Scouts room	78 ± 26	304 ± 29

3. PROPOSAL OF RADON MITIGATION SOLUTION

In order to reduce the moderate levels of radon concentration, a mechanical ventilation system with heat recovery was designed and installed in the building.

The system consists of mechanical extraction in wet rooms and corridor, and mechanical supply in the habitable rooms (Fig. 2). It can provide air flows up to 400 m^3/h and be programmed hourly and daily.

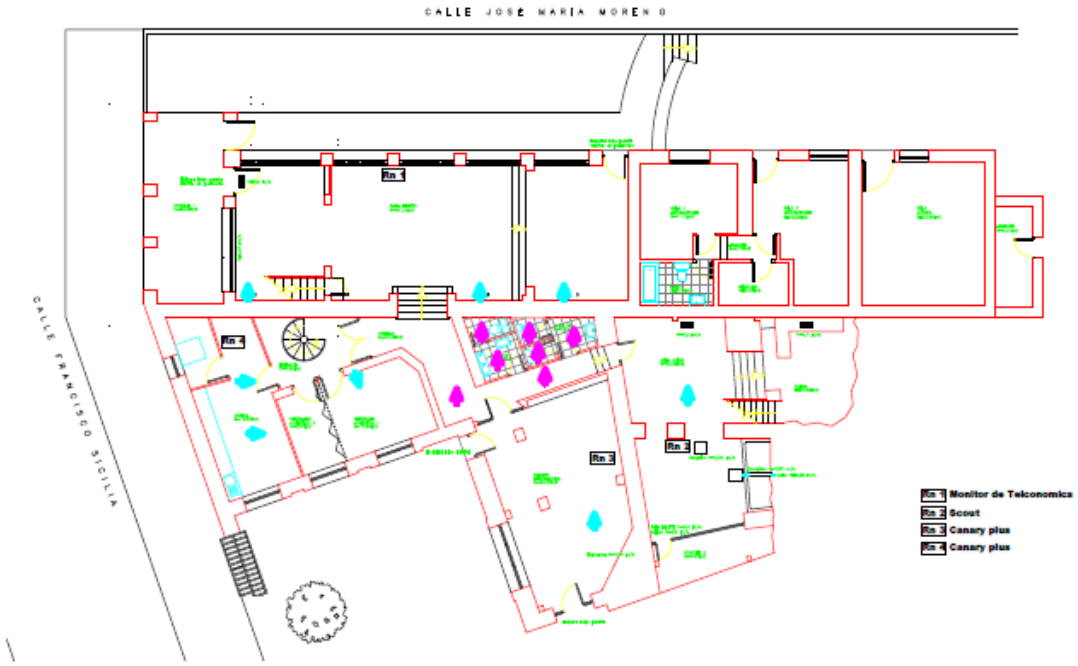

Fig. 2. Air inlets (blue) and outlets (pink).

4. MEASUREMENT OF RADON CONCENTRATION AND RESULTS

After the installation of the mechanical ventilation system, radon concentration was continuously monitored with different levels of ventilation using Canary Pro by Corentium detectors to assess the efficiency on the reduction of radon concentration.

Tables and figures were made to analyse the results. In the tables, values below 300 Bq/m^3 have been marked in green, from 300 to 400 in yellow, from 400 to 500 in orange and above 500 in red. 300 Bq/m^3 is the Spanish reference level for indoor radon concentration.

4.1 Initial test: 75 m^3/h

A short test with 75 m^3/h ventilation flow was performed in November (Table 2) to calibrate the ventilation flow needed for the tests.

Table 2. Average radon concentration (Bq/m^3) without ventilation and with 75 m^3/h constant flow

Room	No ventilation	Constant ventilation 75 m^3/h
Fireplace room	566	547
Kitchen	437	370

It was observed a marginal change in the radon concentration in the fireplace room, however it was relevant in the kitchen, perhaps because of the higher level of air tightness of the envelope of the latter room.

1.1 Constant ventilation flow: 350 m^3/h

Further research was conducted with an increased level of ventilation such as 350 m^3/h, which was scheduled alternating periods of time with and without ventilation. This was performed during several months (from February to December) to take into account the effect on the radon concentration of climatic and seasonal variations. Doors and windows were kept closed most of the time to facilitate concentration of radon.

Figure 3 shows the variations of radon concentration from 5 March to 30 August 2018, and Table 3 the average values for each period of time as well as the global ones to take into account the climatic and seasonal conditions. The period of time from 3 to 20 June was not included in this study because a different type of ventilation was tested.

Table 3. Average radon concentration (Bq/m^3)

	Fireplace room		**Kitchen**	
Period of time	**No ventilation**	**Constant ventilation 350 m^3/h**	**No ventilation**	**Constant ventilation 350 m^3/h**
05-19/03	171		81	
20/03-24/04		168		68
25/04-02/05	258		245	
03-16/05 (1)		206		66
17/05-03/06	414		196	
20/06-01/07		341		63
02-17/07	473		319	
18/07-01/08		351		62
02-13/08	543		207	
14-30/08		469		44
Total	372	307	209	60
Reduction (%)	17.4		71	

(1) An accidental disconnection of the system occurred at an unknown time within this period of time.

On 5 June 2018, the opening above the doorway to the fireplace room was covered. This may explain the increase of radon concentration in this room after this date (with and without ventilation) due to the reduction of air exchange with the corridor.

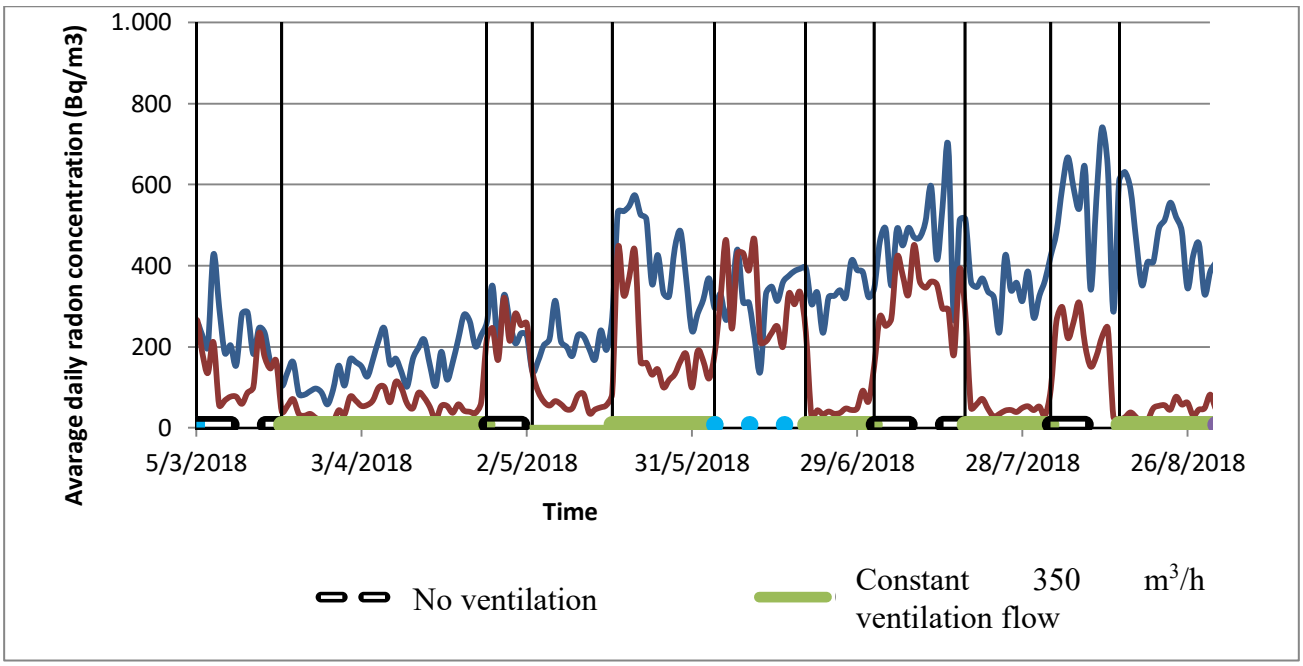

Fig. 3. Average daily radon concentration levels (Bq/m^3) in fire place room (blue) and kitchen (red)

It was observed that the radon concentration is always lower with ventilation in each period of time, and consequently the total value of radon concentration is lower as well.

The total reduction of the radon concentration is 17% in the fire place room and 71% in the kitchen. The bigger reduction in the kitchen could be explained because of the airtightness of this room that is probably contributing to create a pressurization that prevents radon gas from penetrating from soil.

1.2 Constant ventilation flow: 200 m^3/h

With the aim to optimize the ventilation flow able to reduce the radon concentration, a further test was performed with a lower ventilation flow of 200 m^3/h from 2 October to the end of December. Figure 4 and table 4 show the results.

Table 4. Average radon concentration (Bq/m^3)

	Fireplace room		**Kitchen**	
Period of time	**No ventilation**	**Constant ventilation 200 m^3/h**	**No ventilation**	**Constant ventilation 200 m^3/h**
02-17/10		341		140
18-30/10	495		359	
31/10-15/11[(1)]		338		260
16/11-02/12		390		364
03-21/12	329		364	
Total	412	356	361	254
Reduction (%)	13.5		30	

[(1)] An accidental disconnection of the system occurred at an unknown time within this period of time.

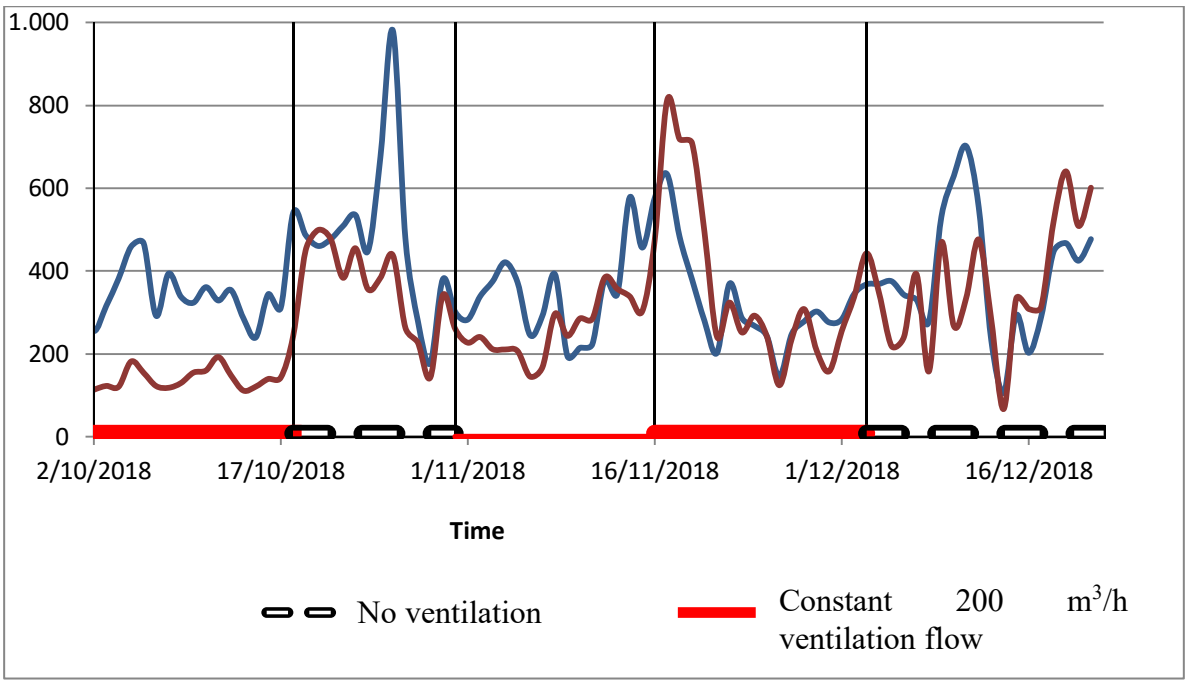

Fig. 4. Average daily radon concentration levels (Bq/m^3) in fire place room (blue) and kitchen (red)

It was observed that the radon concentration is always lower with ventilation in each period of time, and consequently the total value of radon concentration is lower as well. Although in this case the difference between both situations is not as remarkable than with 350 m^3/h, as expected.

The total reduction of the radon concentration is 13.5% in the fire place room and 30% in the kitchen. Even with a smaller ventilation flow, the kitchen keeps providing the better results due to its higher airtightness and the pressurization.

It is worth remarking that in both cases (350 and 200 m^3/h) total values related to constant ventilation include the periods when an accidental disconnection of the system is believed to have occurred, so it is quite likely that these values are higher than expected.

5 CONCLUSIONS

Mechanical ventilation system helped reducing moderate levels of indoor radon in an existing building. Two ventilation rates were tried: 200 and 350 m^3/h. With 350 m^3/h, reductions of 17% and 71% were achieved in the fire place room and in the kitchen, respectively. With 200 m^3/h, reductions of 13.5% and 30% were achieved in the fire place room and in the kitchen, respectively. The reduction was more efficient with a higher ventilation rate, as expected.

Rooms in which the mitigation was conducted where submitted to air supply, whereas extraction was performed in adjacent wet rooms. This air supply was particularly efficient in the kitchen, because of its airtightness that helped to create a pressurization preventing radon from entering the building from the soil.

In the fire place room pressurization was not achieved, so it was more efficient to have a less airtight room, ventilating to other parts of the building.

Ventilation could be used to reduce moderate radon concentration, but it is important:

- to achieve a minimum airtightness of the building,
- to assess the energy performance of the building with the increased ventilation level and to use systems that improve it like heat recovery.

6 ACKNOWLEDGEMENTS

We wish to acknowledge the help provided by Francisco Saro (Torrelodones Council), Alberto Rodríguez (Siberzone) and Borja Frutos (IETcc-CSIC).

7 REFERENCES

WHO (2009). *Handbook on indoor radon, a public health perspective*.

Collignan, B. (2008). *Le radon dans les bârtiments. Guide pou la remédiation dans les constructions existantes et la prevention dans les constructions neuves.* CSTB

García-Talavera, M. et al. (2013). Mapping radon-prone areas using Č-radiation dose rate and geological information. *Journal of radiological protection*, 33 (3), 605-20.

Proyecto radon cero (2018): Optimizacion de soluciones constructivas frente a la inmision de gas radon en edificios y desarrollo de metodologias de diseño de soluciones (BIA2014-58887-R) - Zero radon: optimization of building solutions against radon gas and development of solutions design methods https://proyectoradoncero.ietcc.csic.es/

Energy and Indoor Air Quality Analysis of Mixed Air and Displacement Ventilation Systems

Walid Chakroun*[1], Sorour Alotaibi[1], Kamel Ghali[2], and Nesreen Ghaddar[2]

1 Kuwait University
Alfardous St
Khaldiya, Kuwait
**Corresponding author: wchakroun@gmail.com*

2 American University of Beirut
Riad El-Solh
Beirut, Lebanon

ABSTRACT

Indoor pollutants and particles pose a threat to human health as people spend 90% of their time in indoor spaces. A proper ventilation system should be able to remove indoor air pollutants, reduce particle depositions, at the lowest energy consumption by that system. In this work, particle concentrations and depositions are presented for two ventilation configurations (1) Displacement Ventilation (DV) and (2) the conventional ceiling supply and return. From previous work, energy analysis conducted showed that DV systems supported by chilled ceilings were able to supply cooling and reduce the total energy demand by 53% than the conventional system. Nonetheless, with this energy reduction, the DV system cannot remove as much particles as the conventional ceiling supply and return, causing more particles to deposit which is a problem as deposited particles can resurface again when there are floor disturbances like walking and vacuuming. To benefit from the energy reductions of the DV system supported by the chilled ceiling, a recommendation of a reversed DV system was numerically studied, showing lower particle depositions and concentration.

KEYWORDS

Indoor air quality, Particle Exposure, Ventilation systems

1 INTRODUCTION

Most heating, ventilation and air conditioning engineers and designers (HVAC) focus on indoor air quality (IAQ) and thermal comfort when designing any HVAC system for either commercial or residential buildings. Providing an appropriate IAQ to indoor spaces and occupants remain to be an important parameter and challenge to any HVAC system to limit contaminant formation or transport in those spaces with reducing the energy consumed by that system.

Commercially, introducing outdoor ventilation air, and adding more filtration are two methods of maintaining a suitable IAQ. The flow rate of outdoor air being to be supplied to an indoor space is specified in ASHRAE Standard 62.1, depending on the number of occupants, the floor surface area, and the human activity level of individuals in indoor spaces or zones. Outdoor ventilation air maintains an acceptable IAQ by diluting pollutants in indoor spaces. The higher the ventilation rate the more dilution there is for pollutants, the healthier indoor air is for occupants (Dimitroulopoulou, 2012). Nonetheless, this method is challenging due to the unpredictable variations in indoor spaces occupancy. This could result in engineers overdesigning the HVAC system to accommodate more people than needed. Higher outdoor ventilation rates will result in more energy consumption, which opposes the current need to have energy efficient buildings (Sheng et. al. 2018). Hesaraki et al. (2015) studied the effects of changing the fresh airflow rates, considering the corresponding CO_2 concentrations within indoor spaces, to limit the outdoor airflow rates, reducing energy consumption in cooling fresh air.

The other method of providing a suitable IAQ, is filtration. Filters now have different efficiencies and capabilities of removing contaminants, defined in the minimum efficiency

reporting value (MERV). Most ventilation systems are equipped with filters to reduce particle concentrations in indoor air. Nonetheless, Weschler, (2003) reported that surface area of filters is always changing, depending on the particle sizes that are being trapped and time of which the filter was used. As the filter is trapping more particles the pressure difference through the filter increases, resulting in a drop of air flow to indoor spaces if not adequately and periodically cleaned. Researchers investigated an air-handling unit, equipped with several pocket filters and found that the indoor particle concentration levels decreased by 34% (Jamriska et al. 2000). Moreover, using high efficiency particulate air filters (HEPA) with MERV ratings of 19 and 20, have an extremely high-pressure drop, and require blowers with high static pressure supplies that are only present in air handling units, and commercial air package units to be able to supply air to indoor spaces (Rudnick, 2004). Such applications maybe suitable for commercial buildings and hospitals, but is unfit for residential applications, that have a lower cooling load and energy consumption demand.

Airborne particles removal from indoor spaces requires an in depth understanding of transport activities of micro particles under various ventilation systems. While ventilation systems are installed to ensure thermal comfort to residents and occupants, they are also designed to decrease the concentration of the pollutants in indoor spaces and ensure minimal deposition and re-deposition fractions over surfaces and floors (Gradon 2009), while including the likelihood of the direct inhalation of these particles by the occupants breathing close to these surfaces. For this reason, it is important to remove the particles from indoor environments by installing the proper ventilation systems (Makhoul et al. 2013).

The aim of this paper is to study the effect of mixed air (MA) and displacement ventilation (DV) systems capacity to remove indoor particles and pollutants, when particles were generated on the floor level and considering the energy consumption of both systems. A review on energy analysis of the DV system aided by chilled ceiling cooling will be explained from (Bahman et al. 2009). Furthermore, an experimental setup was built to test the particle removal capacities of both systems, and the coil load for the MA system was determined from experimental data. Later a new system bas on the DV system was suggested and the particle removal capacities of this system was also determined.

2 PARTICLE REMOVAL EFFECTIVENESS FOR DIFFERENT VENTILATION SYSTEMS

To determine the capability of each ventilation configuration in removing indoor contaminants, a ducting system was built to accommodate different ventilation systems, in a room of dimensions (4.95 m × 4.5 m × 2.5 m). The systems are (1) Mixed air ceiling supply and return, and (2) Displacement Ventilation (Floor Supply and Ceiling Return). The ducting system was designed and manufactured to ensure that each system operates separately, by adding volume control dampers (VCD) in each supply and return vent, to control the air-flow rate, and to shut the air supply and return when needed. (Figure 1)

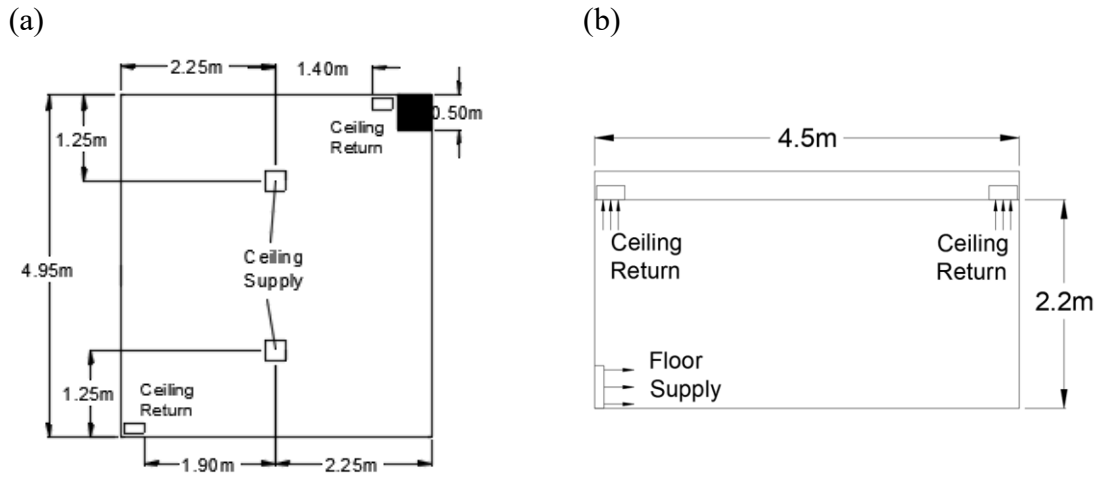

Figure 1: Schematic for both systems (a) Mixed air ceiling supply and return (b) Displacement Ventilation

For each ventilation configuration, the room temperature and humidity were maintained at 24℃ and 50%, respectively. The lighting load of the room was at 10 W/m^2. A roof load of 222 W and a uniformly distributed walls load of 10.96 W/m^2 were present. System (1) has two supply diffusers each supplying 200 CFM and system (2) has one supply providing 400 CFM. To avoid infiltration through the building envelope, the total supply air flow is 400 CFM at 18℃, the return flow rate is 360 CFM, and the indoor pressure was maintained at 102.5 kPa. In addition, 40 CFM of fresh air mixed with the return air in accordance with ASHRAE Standard 62.1, for the flow per floor unit area and the assumption of two occupants in the room with activity corresponding to two seated adults.

Particles with known sizes and densities were generated via a Condensation Aerosol Monodisperse Generator. The generator was set to constantly produce particles of 2.5 μm diameter and 912 kg/m^3 density at a rate of 4 L/min with an aerosol geo-metric standard deviation lower than 1.1 (Figure 2a). The particles were generated simultaneously at different locations of the room on the floor level, to simulate the effect of having more than one source of indoor pollution. This was done by the means of a conductive tubing network composed of seven outlets was attached to the floor. Each outlet was equipped with a valve to control and equate the output flow rate of the particles (Figure 3). Particles where generated for 1 hour until steady state condition were reached. The Optical Particle Sizer (OPS) was used to measure the particle concentration by sampling 1 L/min of air at the desired location (Figure 2b).

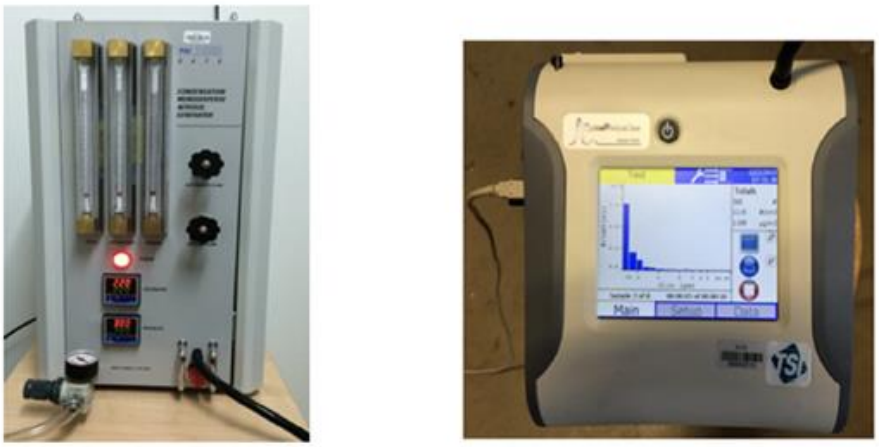

(a) (b)

Figure 2: (a) Condensation Aerosol Generator and (b) Optical Particle Sizer

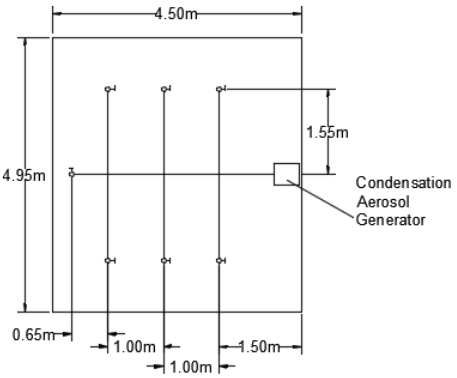

Figure 3: Position of particle outlets with valves on the floor

3 RESULTS AND DISCUSSION

Average normalized particle concentrations (AOC) is the ratio of the particle concentrations at a given position to the total particle concentration generated. The AOC percentages distributions for each ventilation system were compared at the floor level (Figure 4) and in the occupied zone (Figure 5). The occupied zone is the average concentrations from 20-cm to 180-cm from the floor level. The AOC percentages are in both figures as contour plots around the room.

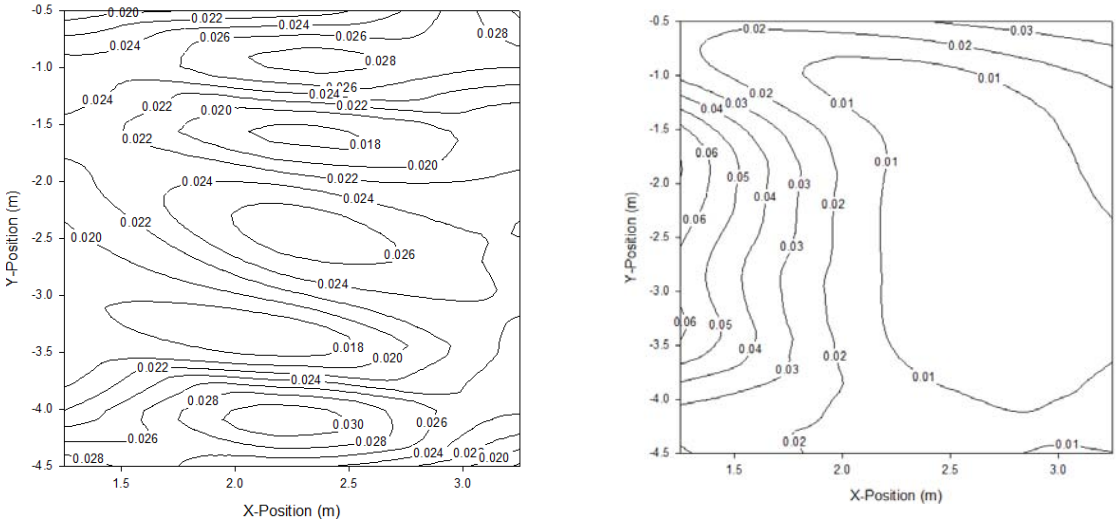

Figure 4: AOC percentages on the floor for (a) MA ceiling supply and return and (b) DV

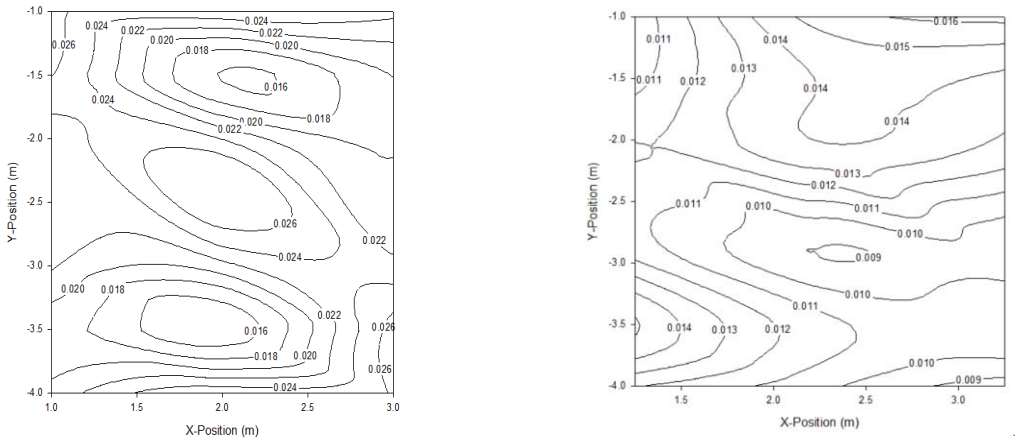

(a) **(b)**

Figure 5: AOC percentages in the occupied zone for (a) MA ceiling supply and return and (b) DV

From Figures 4 and 5, it can be seen that the DV system has a higher AOC percentage on the floor than the MA ceiling supply and return. Whilst on the other hand, the AOC is higher in the MA within the occupied zone than the DV. This is not due the DV removing more particles the MA, but rather the fact the DV system is confining more particles below the 20 cm height from the floor, forcing them to deposit on the floor. To validate that, the AOC within the return vents are shown in Table 1, where the return AOC for MA is higher than the DV one, showing that less particles are going toward the return vents. So the DV system is incapable of removing particles from indoor air and is confining them to the floor, which is dangerous when floor disturbances occur due to walking, vacuuming, and movement of toddlers.

Table 1: AOC x 10^{-4} in the return vents for both configurations

Ventilation System	**AOC x 10^{-4}**
MA Ceiling Supply and Return	3.612
DV Displacement Ventilation	1.193

With that being said, a good ventilation system is able to provide a suitable IAQ to indoor spaces and occupants, with the least energy consumption. By looking at previous work, a suggestion of a suitable system that meets both criteria is needed. Firstly, studying the DV system assisted with the chilled ceiling (CC) has the several characteristics. The DV system here solely supplies 100% fresh to the room on the floor level, displacing the warmer air to the top part of the room, placing fresh cool air at the occupied zone of the room. All contaminated air is exhausted out of the room with non-recirculated back to the room. Designing the DV with the CC requires simultaneous knowledge and meeting several parameters including thermal comfort and IAQ in the room, avoiding presence of any humidity condensate on the CC. To achieve this the supply air conditions and the CC temperature need be continuously monitored and controlled. Figure 6 shows the DV system assisted by CC from Bahman et al. (2009).

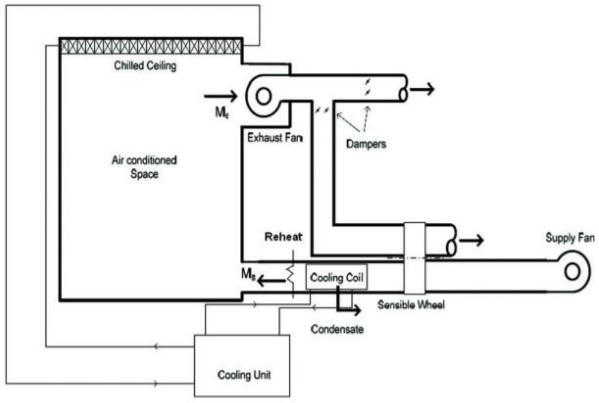

Figure 6: Schematic for the DV system with chilled ceiling system (Bahman el al. 2019)

Figure 7 compares the conventional system at 100% fresh air, with DV assisted by CC, in the month of July. As it can be seen, the conventional system has used almost twice as more energy than the DV assisted by CC. An estimated 53% reduction in energy consumption is recorded for the DV/CC system. Nonetheless, when the DV/CC is compared to 30% fresh air conventional system, the conventional system reported lower energy consumption rates. However, there will be lower air quality in the conventional 30% fresh air system than the DV/CC, as the DV/CC has 100% fresh air supplied to the occupied zone of the room.

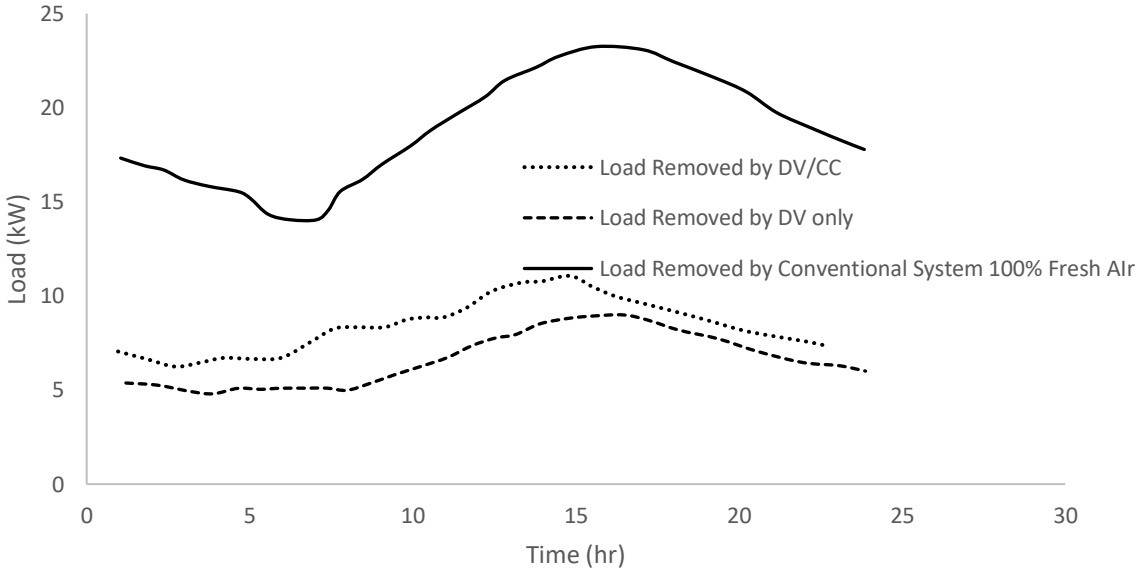

Figure 7: Hourly variation of system cooling load in July at 100% fresh air supply for conventional system and DV/CC system (Bahman et al. 2009)

Despite the good results of the DV/CC system, it is still expensive to have any ventilation system supplying cooled 100% fresh air, especially in hot and dry climates like Kuwait where HVAC consumes 70% of Kuwait's load in the summer, using low fresh air supply conventional mixed air systems. In this work, it is out of question to use 100% fresh air, so to save energy, ASHRAE standard 62.1 was used to determine fresh air quantity, which accounts for 10% of the room supply air flow rate.

The daily average coil load was evaluated for the MA ceiling supply and return and found to be 7.35 kW. When compared with the average coil load for the DV/CC, it was found to be 9.69 kW. However, keep in mind the the DV/CC is 100% fresh air, and if the fresh air is lowered and recirculated air is introduced, the coil load with significantly decrease.

A proposed solution is to obtain an energy efficiency similar to DV/CC, and provide a decent IAQ, while implementing a reversed displacement system that can remove more particles than both DV and MA ventilation systems. The DV systems assisted by chilled ceiling was more capable in cooling than DV working solely (Figure 7). DV/CC systems was capable of to reduce the energy consumption by 53% compared to the conventional system. Chakroun et al. (2019) numerically investigated a validated CFD model the reversed DV system and compared it to the MA ventilation system during vacuuming. Due to the difficulty and expenses of rebuilding the testing facility to accommodate a reversed DV, a validated CFD model on ANSYS/Fluent was more suitable to for this application. Figure 8 shows the drop in particle concentrations of 1 μm sizes between the MA ventilation system and the reversed DV system, where the drop is significant from the floor to the 180-cm. This shows that reversed DV systems can be used to improve indoor air quality, and if there is collaboration between the reversed DV and CC, then similar coil load reductions to the DV/CC can be achieved.

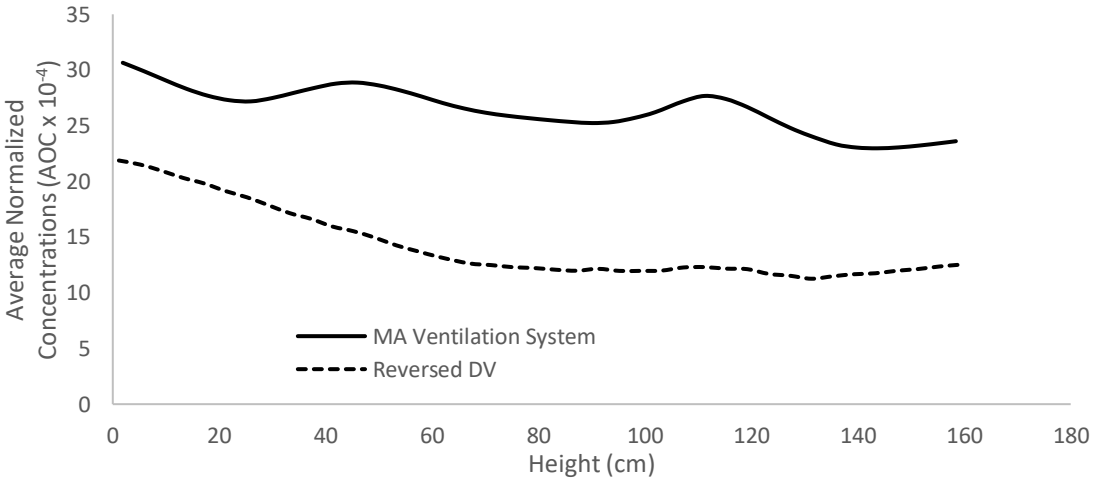

Figure 8: Comparison between MA system and reversed DV AOC's (Chakroun et al. 2019)

4 CONCLUSIONS

The effect of mixed air (MA) and displacement ventilation (DV) systems capacity to remove indoor particles and pollutants, and energy performance was investigated. A review on energy analysis of the DV system aided by chilled ceiling cooling will be explained from Bahman et al. (2009) and found that an estimated 53% reduction in energy consumption is recorded for the DV/CC system compared to conventional MA systems at the same fresh air rate. Nevertheless, it is still expensive to have any ventilation system supplying cooled 100% fresh air, especially in hot and dry climates like Kuwait where HVAC consumes 70% of Kuwait's load in the summer, using low fresh air supply conventional mixed air systems. DV system is confining more particles below the 20 cm height from the floor, forcing them to deposit on the floor, unlike the MA ventilation system which is allowing more particles to escape to the return vents, A proposed reversed DV system was able to remove far more particles, and a lower energy consumption if applied with chilled ceiling.

5 REFERENCES

Bahman, A., Chakroun, W., Ghaddar, N, Saade R., and Ghali, K. "Performance Comparison of Conventional and Chilled Ceiling/ Displacement Ventilation Systems in Kuwait" *ASHRAE Transaction*. 155, 587, 2009.

Chakroun, W., Alotaibi S., Habchi C., Ghali, K. and Ghaddar, N. “Comparison of removal effectiveness of mixed versus displacement ventilation during vacuuming session.” *Building and Environment*. 155, pp. 118-126 2019.

Dimitroulopoulou C. “Ventilation in European Dwellings: A Review.” *Building and Environment* 47 (2012) pp.109-125

Gradoń, Leon. "Resuspension of Particles from Surfaces: Technological, Environmental and Pharmaceutical Aspects." *Advanced Powder Technology* 20.1 (2009): pp 17-28.

Herasaki A., Myhren J. A., Holmberg S. “Influence of Different Ventilation Levels on Indoor Air Quality and Energy Savings: A Case Study of a Single-Family House” *Sustainable Cities and Society* 19(2015) pp. 165–172

Jamriska M, Morawska L, Clark BA. “Effect of ventilation and filtration on sub-micrometre particles in an indoor environment.” *Indoor Air* 2000;10:19e26.

Makhoul, A., K. Ghali, and N. Ghaddar. “Low-mixing coaxial nozzle for effective personalized ventilation,” *Indoor and Built Environment*. 24 (2), pp. 225-243 2015.

Rudnick SN. “Optimizing the Design of Room Air Filters for the Removal of Sub-micrometer Particles.” *Aerosol Science and Technology* 2004;38:861e9.

Sheng Y., Fang L. Sun Y. “An Experimental Evaluation on Air Purification Performance of Clean-Air Heat Pump (CAHP) Air Cleaner.” *Building and Environment* 127 (2018): pp. 69–76

Weschler C. J. “Indoor/Outdoor Connections Exemplified by Processes that Depend on an Organic Compound’s Saturation Vapor Pressure” *Atmospheric Environment* 37 (2003): pp. 5455–5465

Investigation of The Combined Effect of Indoor Air Stability and Displacement Ventilation on Pollutant Transport in Human Breathing Microenvironment

Xiaorui Deng[1], Guangcai Gong[*2]

1 Hunan University
Lushannanlu Road
Changsha China
Presenting author

2 Hunan University
Lushannanlu Road
Changsha China
**Corresponding author: gcgong@hnu.edu.cn*

ABSTRACT

The ventilation system removes pollutants effectively, and the resultant vertical temperature difference in the room greatly affects the indoor air distribution. A reasonable air distribution system is essential to provide a satisfying indoor air quality (IAQ) for the occupants, of which air quality in the breathing microenvironment plays a major role in occupant health, as they are exposed to this region directly. With a view to ultimately optimize the air quality in the breathing microenvironment, indoor air stability, namely, the background temperature effect, integrated with a displacement ventilation system, is analyzed in this study. Experiments were conducted in a full-scale test room with a test subject performing normal breathing activity. The concentration of the carbon dioxide (CO_2) was measured as a proxy for the pollutant concentrations in the breathing microenvironment. The results indicate that the vertical movement of the exhaled air is inhibited in a displacement ventilation system combined with a stable condition, so the inefficient dispersion leads to a severely polluted breathing microenvironment, increasing the infection risk of the occupants. It is also shown that with the same displacement ventilation system, the unstable condition causes the indoor air to undergo significant mixing, which to some extent destroys the stratification resulting from the displacement ventilation. A much greater irregularity appears in the exhaled airflow, so the pollutants travel widely beyond the breathing microenvironment, contributing to a less polluted region. It is concluded that indoor air stability will affect the ventilation systems performance and the unstable condition is advisable for minimizing the amount of pollutants in the breathing microenvironment, reducing the risk of infection and providing a better air quality for the occupants.

KEYWORDS

Indoor air stability; Displacement ventilation; Human exposure; Breathing microenvironment

1 INTRODUCTION

People spend 80-90% of their time indoors, so their health greatly depends on the indoor air quality (Godish & Spengler, 1996). To obtain a high IAQ, ventilation has been considered an effective way to bring fresh air into the room and remove the polluted air. When compared with mixing ventilation, displacement ventilation has the potential to provide higher air quality (Coffey & Hunt, 2007) while consuming less energy, so it is regarded as a promising approach to improve IAQ.

There are many sources of pollutants in indoor environments, the most common of which are the occupants themselves. Human respiration activities generate bio-aerosols that may carry pathogens (Douwest, Thorne, Pearce, & Heederik, 2003), leading to the airborne transmission of infectious substances in indoor spaces (Nielsen, 2009). This is rather remarkable in the occupied zone where human exposure to the indoor pollutant mostly often occurs (Melikov, 2015). When people is in a displacement ventilated room, the temperature gradient confines the vertical movement of the exhaled air, so instead of dispersing, the exhaled air could penetrate a long distance along the initial exhaled direction (Qian et al., 2006). This confinement would lead to pollutants accumulating at a certain height in the breathing zone, which has a negative impact on the occupants health.

Despite in the displacement ventilated room, temperature gradients are also common in the built environment when installed with other HVAC (Heating, Ventilation and Air-Conditioning) systems, for example, radiant air conditioning rooms (Olesen, 2002; Zhou et al., 2019; Schiavon, Bauman, Tully, & Rimmer, 2012; Li, Yoshidomi, Ooka, & Olesen, 2015; Peng, Gong, Mei, Liu, & Wu, 2019). Different vertical temperature or, equivalently, density gradients in a room are referred as the indoor air stability which is defined as a measure of the ability of an air parcel to keep its initial inertia state (Gong & Deng, 2017). The indoor air stability is classified into three categories, namely, stable, neutral and unstable conditions. In the stable condition, buoyancy force inhibits the vertical movement of air and the inertia force dominates the pollutant transport, so pollutants are more likely to maintain the initial inertia state and remain in the mainstream direction. In the unstable condition, the intensified instability of the ambient air would promote the entrainment of the pollutant with the ambient air and thus enhance the vertical movement of the exhaled pollutant. The pollutant is more likely to depart from its original state and dissipates widely. Indoor air stability has been shown to influence pollutant distribution in the indoor environment (Wang, Gong, Xu, & Yang, 2014; Xu, Nielsen, Gong, Jensen, & Liu, 2015a; Gong & Deng, 2017), however, no studies has been concluded with regard to the the feature of air distribution when indoor air stability is combined with the ventilation system.

The purpose of this study is to analyze the combined effect of displacement ventilation and indoor air stability on pollutant transmission in the breathing microenvironment. Exposure intensities (definition is given in 3.3) of different combinations are compared. The results demonstrate that in a displacement ventilated room the indoor air stability has significant effect on pollutant transport in the breathing microenvironment and reduces human exposure to pollutant.

2 METHOD

A whole experiment lasted 1 hour and was divided into two parts. The first part was the 30-minute respiration process. The test subject was asked to perform a steady breathing activity while standing by inhaling through the nose and exhaling through the mouth. The second part was a 30-minute pollutant decay process with no subject presenting in the test room. Figure 1a illustrates the full-scale test room, with length, width, and height equal to 4 m, 3.9 m, and 2.4 m, respectively. To create different indoor air stability conditions, the test room was equipped with an air carrying energy radiant-air-condition system on the ceiling to control the temperature of the top area. Four electrical blankets, with a dimension of 2 m × 2 m, were laid over the floor to control the temperature near the floor. The radiant air conditioning system and the electric blankets were operated at least 6 hours before each experiment was commenced in order to ensure a steady temperature distribution. The walls of the room were considered to be adiabatic. Twenty-five mini data loggers with an accuracy of ± 0.5 °C were distributed evenly on five poles (L1, L2, L3, L4, L5) to record the temperature at heights of 0.1 m, 0.6 m, 1.1 m, 1.7 m and 2.3 m. Two additional loggers were hung at the return and exhaust.

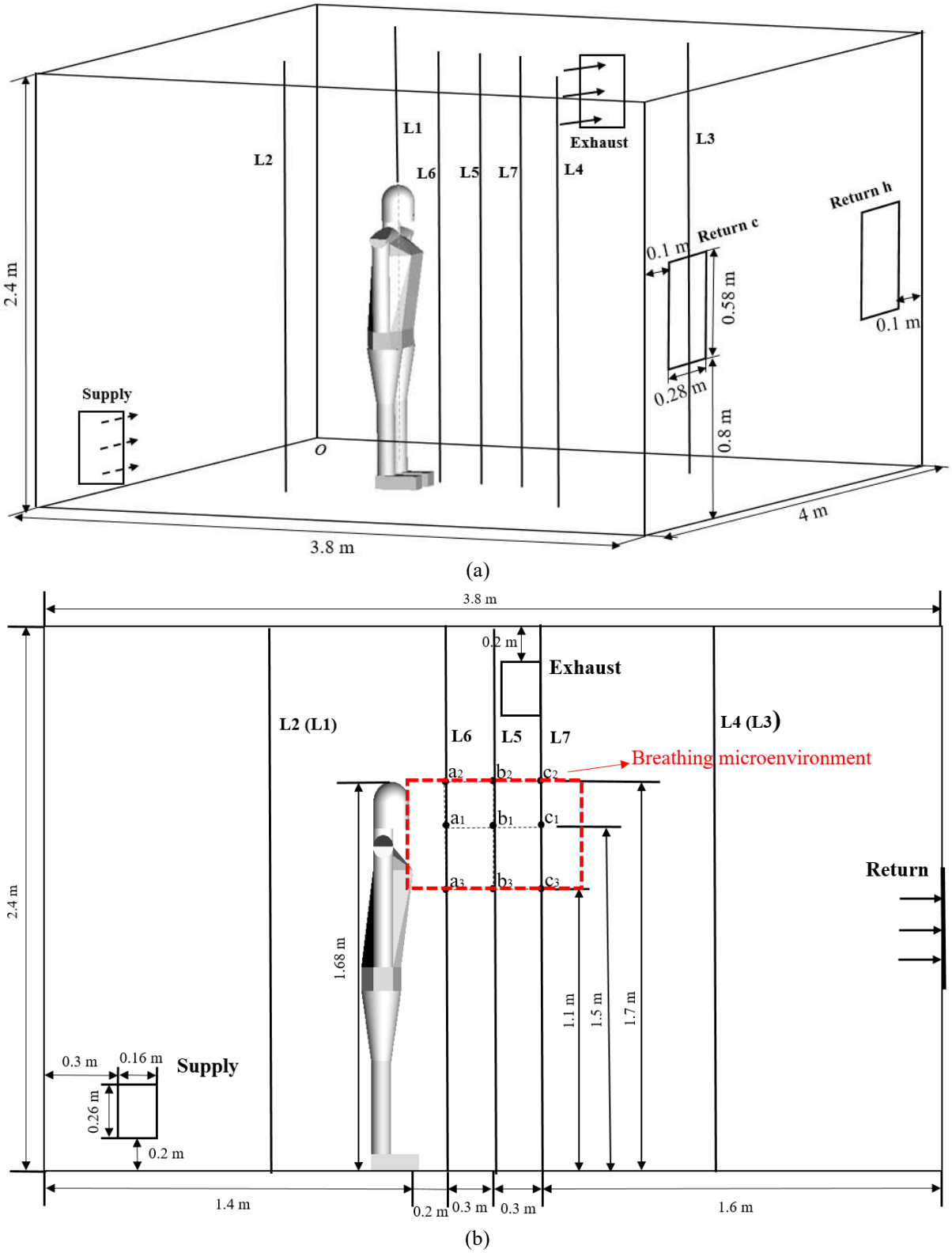

Figure 1: (a) Configuration of the three-dimensioned test room. (b) Layout of the displacement ventilation system and the measuring points

Figure 1b shows the layout of the displacement system. A wall-mounted air supply was installed neat the base of the sidewall with a ventilation rate of 7.75 ACH. The exhaust was of the same size as the supply and was installed near the top of the opposite sidewall. Two air returns were mounsted on the wall on the right hand side. When the radiant air conditioning system was in

heating mode, Return h was opened and Return c was closed; when in cooling mode, Return c was opened and Return h was closed.
In this study, the breathing microenvironment was defined as a region, see Figure 1b, which is 1 m in front of the human body between the height of 1.1 m and 1.7 m (Bjørn & Nielsen, 2002; Xu et al., 2015a; Olsen, 2016; Liu, Li, Nielsen, Wei, & Jensen, 2016). CO_2 has been acknowledged as a good indicator in IAQ studies for more than one century (Billings, 1893), and is still being widely used in recent studies (Zhang, Wargocki, Lian, & Thyregod, 2017; Ramalho et al., 2014; Sundell et al., 2011;), so here, the CO_2 concentration from natural respiration was measured to indicate the pollutants level in the breathing microenvironment. Nine CO_2 sensors, with an accuracy of ± 30 ppm, were installed along three poles (L5, L6, L7) at stomach height (1.1m), mouth height (1.5 m) and head height (1.7 m), see Figure 1b. Before each experiment, the background CO_2 concentration was measured by a CO_2 meter. The CO_2 sensors and the CO_2 meter were cross-calibrated before each experiment. The air velocities at the supply, exhaust, and return were measured before each experiment by an anemometer with an accuracy of ± (0.1m/s + 5% of measured velocity).

3 RESULTS AND DISCUSSION

3.1 Temperature distribution in the test room

The measured temperature at different heights are shown in Table 1, which gives a temperature difference between the ceiling and the floor for the stable and unstable condition, respectively. In the stable condition, the floor temperature was 19.8 ℃ and the ceiling temperature was 26 ℃, forrming a temperature difference of 6.2 ℃ in the room; in the unstable condition, the temperature for the floor and the ceiling was 31.0 ℃ and 25.5 ℃, respectively, forming a temperature difference of – 5.5 ℃. The vertical temperature profiles are not a linear function of the height. It might be explained by the existence of heat source in the room (the test subject and the effect of the displacement ventilation.

Table 1: Temperature (℃) at different heights

Indoor air stability	**Height（m）**						
	0	**0.1**	**0.6**	**1.1**	**1.7**	**2.3**	**2.4**
Stable	19.8	20.5	21.6	23.6	24.2	25.3	26.0
Unstable	31.0	28.2	27.8	27.6	27.2	26.8	25.5

3.2 CO2 concentration distribution in the microenvironment

The CO_2 concentrations in the breathing microenvironment were obtained from the 9 measurement points (between the heights of 1.1 m and 1.7 m) ,see Figure 1. To eliminate the effect of the slight differences of the background CO_2 concentration at the beginning of each experiment, the CO_2 concentrations were normalized as follows

$$C=\frac{C_i-C_0}{C_0} \quad (1)$$

In (1) C_i is the concentration of instantaneous CO_2 (ppm), C_0 is the concentration of background CO_2 of each experiment (ppm). The normalized results are shown in Figure 2.

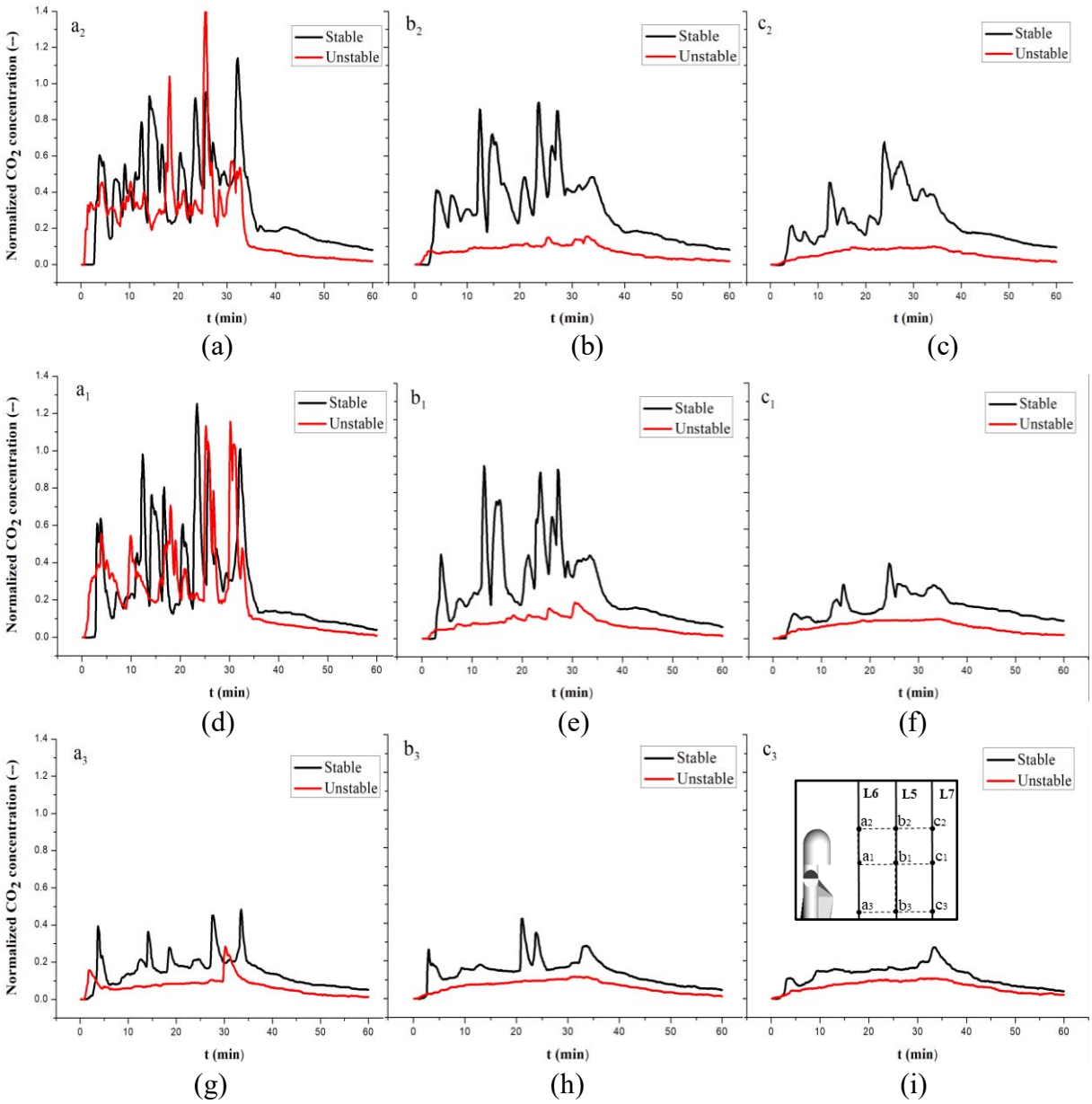

Figure 2: The variation of the normalized CO_2 concentration with time at different measuring points in the displacement ventilated room with stable and unstable conditions

During the first 30 minutes, periodic oscillations of CO_2 concentration were observed. These oscillations are in line with the normal breathing mode found by Villafruela et al. (2016) and Xu et al. (2015b). CO_2 concentration reaches a peak during the exhaling process where a relatively large amount of CO_2 is produced, then it drops significantly. This drop is partly because the test subject re-inhales the exhaled CO_2, and partly because the CO_2 has been dispersed into the ambient environment. This phenomenon is evident at most measuring points in the stable condition, except that point c_3 (Figure 2i) has a rather smooth concentration curve; while in the unstable case, the occurrence of this oscillation is greatly reduced. Only at points a_1 and a_2 (Figures 2d and 2a) can the phenomenon be observed. This indicates that when compared with the unstable condition, the pollutant is more likely to retain its initial state of motion in the stable condition.

As revealed from the concentration distribution at different measuring heights in Figure 2, the CO_2 flow is initially exhaled horizontally from the mouth with a relatively high momentum, and gradually deflects from its initial mainstream direction, turning upwards. The CO_2 concentrations at points a_1 and a_2 (Figures 2d and 2a) are the highest when the distance from the

test subject is 0.2 m (L6). This is mainly due to the fact that CO_2 is released from the test subject themselves, the thermal boundary layer of the human body carries the CO_2 flow towards head height, resulting in a high concentration near the human body, both at mouth height and head height. As the CO_2 flow travels further, in the stable condition, for example, at 0.5 m (L5) from the test subject, the concentration of CO_2 at point b_2 (Figure 2b) begins to exceed that at point b_1 (see Figure 2e), indicating that more exhaled flow has been transported to the upper breathing microenvironment. At 0.8 m (L7), this difference becomes more pronounced. The factors that are responsible for this increase are, firstly, the temperature of the exhaled air is higher than that of the ambient air, so the buoyancy force drives the exhaled air upwards. Secondly, the supplied air in the displacement ventilation system rises up after being heated by the heat source (here the test subject). When this supplied air reaches the breathing microenvironment, the exhaled airflow acquires the vertical momentum from the supplied air and thus bends upward. This upward movement is less obvious in the unstable condition as the CO_2 concentrations drop dramatically and eventually lie in the range within 0.0 and 0.1 with much less fluctuation.
Noticeably, the concentrations of CO_2 within the breathing microenvironment tend to be relatively high in the stable condition and relatively low in the unstable condition, except two abnormal peak values of the unstable condition at point a_2 when the respiration lasts for 19 min and 26 min, respectively. This presumably happens by the occasionally unsteady expiration of the test subject, such as a sudden deep breath or an unavoidable cough. The higher concentration in the stable condition is probably because, in the stable air, the temperature in the upper area is higher than the lower part, the buoyancy of the exhaled airflow decreases as it rises. The exhaled CO_2 will be suppressed and can not be dispersed effectively, causing a more severe polluted area in the breathing microenvironment. The occupants is at a higher risk of getting infected in this stable environment. The confinement of the exhaled flow has been also reported by Bjorn and Nielsen (2002). They concluded this confinement as a 'lock-up' phenomenon as the stably stratified environment can lock the exhaled flow at a certain height, causing a high concentration locally. Conversely, in unstable air, the buoyancy of the exhaled air increases as it rises, increasing the ultimate deviation and propagation distance. Any variation will have a noticeable effect on the state of the exhaled air (Pellew & Southwell, 1940) which would in return cause the disturbance to grow in amplitude in such a way that the exhaled air progressively departs from the initial state. Regardless of the distance from the test subject, the CO_2 concentrations at stomach height (see Figures 2g, 2h and 2i) were always the lowest, which indicates less CO_2 has travelled to the lower part of the breathing microenvironment, which is also found by Licina et al. (2015), Qian et al. (2006) and Olsen et al. (2016).

3.3 Exposure assessment

This breathing mode adopted in this study (inhale through the nose and exhale through the mouth) is normally seen in this cases where people smoke or suffer from a nasal congestion, and the exhaled air normally contains a high concentration of infective aerosols. These pople are regarded as the pollutant sources, meanwhile they are also exposed to the polluted breathing microenvironment as they would re-inhale a fair amount of their exhaled air. To assess human exposure under stable and unstable condition, exposure intensity E, is adopted in this study, which is defined by the National Research Council (National Research Council, 1991) as

$$E = \int_{t_1}^{t_2} C(t)\, dt \qquad (2)$$

In (2), C(t) is pollutant concentration, and $t_2 - t_1$ is the duration of exposure. Figure 3 plots the exposure intensity in the first 30 minutes of the experiments. In the first 5 minutes after the test subject began to breathe, no significant difference of the exposure intensity between the stable condition and the unstable condition is observed, with E = 6 in stable and E = 4 in unstable. At later times, the differences become more apparent and at the end of the breathing experiments,

the exposure intensity is E = 80 in the stable condition and only E = 40 in the unstable condition. It is straightforward to see that the stable exposure intensity is always double that of the unstable condition at different times, which indicates the occupants in a stable environment have a significant greater possibility of being infected if exposing themselves to an indoor environment with existing desease carriers.

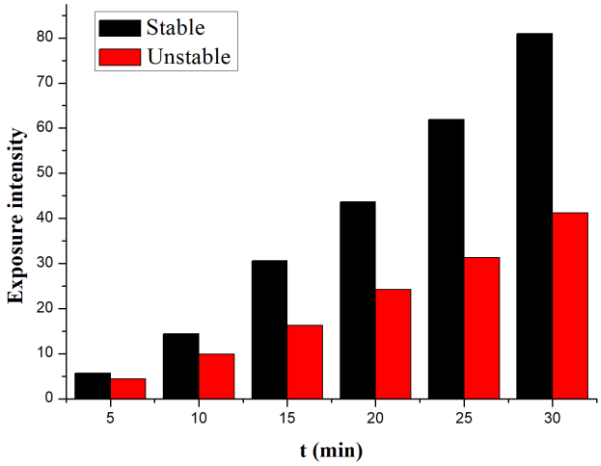

Figure 3: Exposure intensity E from (2) in the microenvironment in a displacement ventilated room for stable and unstable conditions

Figure 3 demonstrates that in the stable condition, the strong stratification inhibits the vertical motion of the airflow, so the movement of the air is confined to a certain region and gradually settles down in the breathing microenvironment, resulting in a higher exposure intensity. People exposed to this area will be at a higher risk of becoming infected. In addition, it may also aggravate the illness condition of the source person as they might re-inhale exhaled air remaining in their breathing microenvironment area (Bjørn & Nielsen, 2002). In the unstable condition, the vertical motion is promoted by Rayleigh-Bernard convection (Getling, 1998)) which is formed by the warm floor and cool ceiling in the test room. This arrangement of heating and cooling causes instability in the background environment, so the airflow experiences an enhanced mixing effect and thus disturbs the air stratification in the breathing microenvironment. As the exhaled air continuously entrains the ambient air, the pollutant has been correspondently well dissipated before it travels further in the breathing microenvironment. The resultant lower exposure intensity is in line with the finding by Olesen et al.(2016), who reported that floor heating would destroy the stratification of the displacement ventilation and thus reducing human exposure.

It is notable that the exposure intensity also depends on the duration of the stay. When people stay in the indoor space for a very short time, the stable condition would not lead to a worse situation of human exposure than an unstable condition would. The negative impact would only be prominent when people stay indoors for a considerable time.

3.4 Limitation of the work

The movement of people can create strong local air movement due to the wake behind the person, which breaks down the stratification of exhaled air (Bjørn & Nielsen, 2002). Tang, Li, Eames, Chan, & Ridgway (2006) pointed out that a person walking forward at about 1 m/s would create a volume flux of 225 L/s, with an attached wake of 76-230 L. Compared with the test room volume here of approximately 36 m^3, the wake could cause a significant mixing in the room. This local airflow is of great value in studying the pollutant distribution in certain areas (Bjørn & Nielsen, 2002). However, the research interest of this study primarily focuses on the pollutant concentration in the breathing microenvironment when the occupant is in a stationary standing posture. With this in mind, the test subject was asked to walk out of the test

room as gently as possible (at approximately 0.2 m/s) at the end of the experiments to avoid causing a strong wake. It is thus assumed herein that occupant movement does not affect the pollutant distribution.

4 CONCLUSIONS

A combination of indoor air stability and displacement ventilation has been experimentally studied.

The full scale study has shown that indoor air stability influences the performance of displacement ventilation systems. A displacement ventilation system integrated with a stable condition will cause a more stagnant air environment in the breathing microenvironment. Under such environments, occupants have a larger exposure intensity and are more likely to be infected by the polluted air.

The unstable indoor air caused an instability of the indoor air, and to some extent destroys the stratification associated with the displacement ventilation. The exhaled flow is less likely to keep its initial state and tends to disperse beyond the breathing microenvironment, resulting in lower concentrations in this region. Occupants may have a lower infection risk. In conclusion, the unstable condition is advisable for minimizing the amount of pollutants in the breathing microenvironment, reducing the risk of cross infection and providing a better IAQ for the occupants.

Air distribution under the combination of indoor air stability and displacement ventilation could be affected by moving objects, which is worthy of future investigation.

5 ACKNOWLEDGEMENTS

This study was funded by the National Natural Science Foundation of China (No.51378186) and the National Science & Technology Supporting Program (No.2015BAJ03B00). The authors gratelfully acknowledge financial support from China Scholarship Council at the University of Cambridge (No. 201806130150). Xiaorui Deng would like to express her gratitude to Prof. Gary R. Hunt at Department of Engineering, University of Cambridge for hosting her stay and giving all these corrections and comments on this paper, as well as special thanks to Mr. Tom Newton for providing language and structure suggestions on this paper.

6 REFERENCES

Bjørn, E., & Nielsen, P. V. (2002). Dispersal of exhaled air and personal exposure in displacement ventilated rooms. *Indoor Air,*12(3), 147-164.

Billings, J.S. (1893) Ventilation and Heating, New York, The Engineering Record.

Coffey, C. J., & Hunt, G. R. (2007). Ventilation effectiveness measures based on heat removal: Part 1. Definitions. *Building and Environment,* 42(6), 2241-2248

Douwest, J., Thorne, P., Pearce, N., & Heederik, D. (2003). Bioaerosol Health Effects and Exposure Assessment: Progress and Prospects. *The Annals of occupational hygiene,* 47(3), 187–200.

Godish, T. and Spengler, J. D. (1996). Relationships Between Ventilation and Indoor Air Quality: A Review.

Indoor Air, 6(2), 135-145.

Getling, A.V. (1998). *Rayleigh - Bénard Convection: Structures and Dynamics.* Singapore: World Scientific.

Gong, G., & Deng, X. (2017). Nature and characteristics of temperature background effect for interactive respiration process. *Scientific Reports,* 7(1), 8549.

Licina, D., Melikov, A., Sekhar, C., & Tham, K. W. (2015). Air Temperature Investigation in Microenvironment Around a Human Body. *Building and Environment,* 92, 39-47.

Li, R., Yoshidomi, T., Ooka, R., & Olesen, B.W. (2015). Field Evaluation of Performance of Radiant Heating/Cooling Ceiling Panel System. *Energy and Buildings,* 86, 58-65.

Liu, L., Li, Y., Nielsen, P. V., Wei, J., & Jensen, R. L. (2016). Short-range airborne transmission of expiratory droplets between two people. *Indoor Air,* 27(2), 452-462.

Melikov, A.K. (2015). Human Body Micro-environment: The Benefits of Controlling Airflow Interaction. *Building and Environmen*t, 91, 70-77.

National Research Council. (1991). *Human Exposure Assessment for Airborne Pollutants: Advances and Opportunities*. Washington, DC: The National Academies Press.

Nielsen, P.V. (2009). Control of Airborne Infectious Diseases in Ventilated Spaces. *Journal of the Royal Society, Interface,* 6(6), S747-S755.

Olesen, B.W. (2002). Radiant Floor Heating in Theory and Practice. *ASHRAE Journal,* 44(7), 19-26.

Olesen, B. W., Simone, A., KrajcĺIik, M., Causone, F., & Carli, M. De. (2016). Experimental Study of Air Distribution and Ventilation Effectiveness in a Room with a Combination of Different Mechanical Ventilation and Heating/Cooling Systems. *International Journal of Ventilation,* 9(4), 371-383.

Pellew, A and Southwell,R. V. (1940). On maintained convective motion in a fluid heated from below. *Proceedings of the Royal Society of London. Series A. Mathematical and Physical Sciences,* 176(966), 312-343.

Peng, P., Gong, G., Mei, X., Liu, J., & Wu, F. (2019). Investigation on Thermal Comfort of Air Carrying Energy Radiant Air-Conditioning System in South-central China. *Energy and Buildings,* 182, 51-60.

Qian, H., Li, Y., Nielsen, P. V., Hyldgaard, C. E., Wong, T. W., & Chwang, A. T. (2006). Dispersion of Exhaled Droplet Nuclei in A Two-Bed Hospital Ward with Three Different Ventilation Systems. *Indoor Air,* 16(2), 111-128.

Ramalho, O., Wyart, G., Mandin, C., Blondeau, P., Cabanes, P., Leclerc, N., …Redaelli, M. (2014). Association of carbon dioxide with indoor air pollutants andexceedance of health guideline values. *Building and Environment,* 93, 115-124

Schiavon, S., Bauman, F., Tully, B., & Rimmer, J. (2012). Room Air Stratification in Combined Chilled Ceiling and Displacement Ventilation Systems. *HVAC&R Research,* 18(1-2), 147-159.

Sundell, J., Levin, H., Nazaroff, W.W., Cain, W. S., Fisk, W.J., Grimsrud, D. T.,…Weschler, C. J. (2011). Ventilation Rates and Health: Multidisciplinary Review of the Scientific Literature. *Indoor Air,*21 (3),191-204.

Tang, J. W., Li, Y., Eames, I., Chan, P. K., & Ridgway, G. L. (2006). Factors Involved in the Aerosol Transmission of Infection and Control of Ventilation in Healthcare Premises. *Journal of Hospital Infection,* 64(2), 100-114.

Villafruela, J. M., Olmedo, I., & San José, J. F. (2016). Influence of human breathing modes on airborne cross infection risk. *Building and Environment,* 106, 340-351.

Wang, Y., Gong, G., Xu, C., & Yang, Zu. (2014). Numerical investigation of air stability in space capsule under low gravity conditions. *Acta Astronautica,* 103, 81-91.

Xu, C., Nielsen, P. V., Gong, G., Jensen, R. L., & Liu, L. (2015a). Influence of air stability and metabolic rate on exhaled flow. *Indoor Air,* 25(2), 198–209.

Xu, C., Nielsen, P. V., Gong, G., Liu, L., & Jensen, R. L. (2015b). Measuring the exhaled breath of a manikin and human subjects. *Indoor Air,* 25(2), 188-197.

Zhang, X., Wargocki, P., Lian, Z., & Thyregod, C. (2017). Effects of Exposure to Carbon Dioxide and Bioeffluents on Perceived Air Quality, Self-assessed Acute Health Symptoms, and Cognitive Performance. *Indoor Air,* 27(1),47-64.

Zhou, X., Liu, Y., Luo, M., Zhang, L., Zhang, Q., & Zhang, X. (2019). Thermal comfort under radiant asymmetries of floor cooling system in 2 h and 8 h exposure durations. *Energy and Buildings,* 188-189, 98-110.

Indoor environment and adverse health symptoms among children under home damp conditions

Kenichi Hasegawa*[1], Naoki Kagi[2], Nobuhiro Kanazawa[3], Jun Sakaguchi[4], Naohide Shinohara[5], Yasuyuki Shiraishi[6], Teruaki Mitamura[7] Jun Fukushima[8]

1 Akita Prefectural University
84-4 Ebinokuchi, Yuhonjo city, Akita, Japan
** haseken@akita-pu.ac.jp*

2 Tokyo Institute of Technology
2-12-1 Ookayama, Meguro-ku, Tokyo, Japan

1 Akita Prefectural University
84-4 Ebinokuchi, Yuhonjo city, Akita, Japan

4 University of Niigata
471, Ebigase, Higashi-ku, Niigata City, Niigata, Japan

5 National Institute of AIST
1-1-1 Umezono, Tsukuba, Ibaraki, Japan

6 The University of Kitakyusyu
1-1 Hibikino, Wakamatsu-ku, Kitakyushu, 1-2 Fukuoka, Japan

7 Maebashi Institute of Technology
460-1, Kamisadori, Maebashi-City, Gunma, Japan

8 Akita Prefectural Uni. & Bio Technology Center
241-438 Kaidobata-Nishi Nakano Shimoshinjo, Akita City, Akita, Japan

ABSTRACT

Building dampness and mouldy indoor environments are associated with the increase of approximately 30-50% in variety of respiratory and asthma-related health outcomes through a meta-analysis. The indoor environment related to indoor dampness is not be revealed yet, however it is important to provide the architectural techniques and optimal occupant behavior for prevention of dampness in buildings. The authors previously proposed an estimation method for home dampness using occupants self-reported answers to questions about visible vapor condensation, visible mould growth during winter. This dampness index ranges from 0 to 24, and its values were classified into four ranks (Rank 1 to Rank 4) based on quartiles from the results of a national questionnaire survey of about 5,000 houses in Japan. In order to clarify the association between home dampness and indoor environmental quality, questionnaire survey was conducted and several physical environmental items such as indoor temperature, humidity and microbial flora from the floor dust were measured in 120 detached houses located in East Japan.
This paper firstly describes the quantitative estimation of indoor dampness through the dampness index and the surveyed results from measured houses. The questionnaires also included items regarding the following health-related symptoms onset within 3 months among children. The dampness index is not following to normal distribution like a previous large scale questionnaire survey. And the prevalence of nasal symptoms (chi-square test: $p < 0.01$) and ocular symptoms increased as rank of dampness index was rising.
Secondary, the characteristics of indoor temperature, humidity and microbial flora due to home dampness were clarified by comparing dampness index and measured results of these physical items. The microorganisms were genetically analysed to evaluate the population diversity of microbial species through the DNA analysed technologies. The median relative humidity in each dampness rank was higher at higher rank of indoor dampness. This tendency was statistically significant for both a living room and a bed room, and humidity ratio at rank 1 was significantly lower than that at rank 3 and rank 4. The fungal species of which the detection rate was increasing with ranks 1 to 4 of indoor dampness index were considered to be associated with indoor environmental problems of dampness. This paper indicates the association between indoor dampness and fungal species of *Wallemia sebi* and *Rhodotorula glutinis*.
Finally, the association between adverse health effect and influencing factors related to indoor dampness was estimated using a multivariable logistic regression model. As results, it was revealed that children who were living in dampness are at significant risk for health-related symptoms such as nasal symptoms and dermal symptoms.

KEYWORDS

Home dampness, Health-related symptoms, Indoor temperature and humidity, Microorganism flora

1 INTRODUCTION

Building dampness and mouldy indoor environments are associated with the increase of approximately 30-50% in variety of respiratory and asthma-related health outcomes through a meta-analysis. The indoor environment related to indoor dampness is not be revealed yet, however it is important to provide the architectural techniques and optimal occupant behavior for prevention of dampness in buildings. The causal structure from dampness to adverse health effect seems to be estimated as shown in Figure 1. Based on these causalities it is expected to reveal prevention methodologies for serious problems related to indoor dampness. The authors previously proposed an estimation method for home dampness using occupants self-reported answers to questions about visible vapor condensation, visible mould growth during winter. This dampness index ranges from 0 to 24, and its values were classified into four ranks (Rank 1 to Rank 4) based on quartiles from the results of a national questionnaire survey of about 5,000 houses in Japan. The houses in the Rank 4 represents the most serious problems related to indoor dampness. In addition, it is expected to reveal the actual condition of indoor dampness. In order to clarify the association between home dampness and indoor environmental quality, questionnaire survey was conducted and several physical environmental items such as indoor temperature, humidity and microbial flora from the floor dust were measured in 120 detached houses located in East Japan during winter.

This paper firstly describes the quantitative estimation of indoor dampness through the dampness index proposed by authors and the surveyed results from measured houses. The questionnaires also included items regarding the following health-related symptoms onset within 3 months among children: ocular symptoms, nasal symptoms, respiratory symptoms, dermal symptoms and mental symptoms. The prevalence of these symptoms was presented in each dampness index rank.

Secondary, the characteristics of indoor temperature, humidity and microbial flora due to home dampness were clarified by comparing dampness index and measured results of these physical items. The microorganisms were genetically analysed to evaluate the population diversity of microbial species based on the length of ITS. In this paper, fungal diversity included in the floor dust of surveyed 120 houses was analysed and then these samples were also performed comprehensive analysis using the next generation sequencer.

Finally, the association between indoor dampness and health-related symptoms among young children was presented by statistical analysis method.

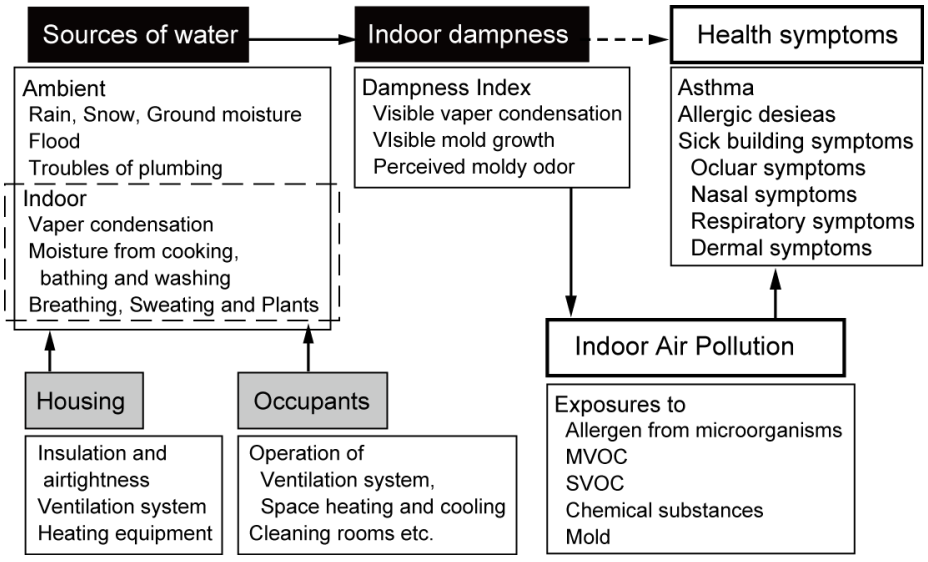

Figure 1: Dampness, indoor environment and health

2 METHODOLOGIES OF SURVEY

2.1 Outline of survey

A cross-sectional study has been conducted to 6 - 12 years old children through the internet survey in the winter of 2017. The subjects to meet the requirements for respondent were recruited from the customers which a Japanese internet research company held. The investigated houses were detached houses which occupants had lived for more than one year and had parents and more one child who was 6 -12 years old. Questionnaires were distributed on the web to the 120 houses in Japan during winter season, and continuously the indoor temperature, humidity and microorganisms in sampling dust were measured in five days. The occupants answered several questions on the internet web site for five days of the investigation period and measured indoor temperature and humidity in a living room and bed room using small thermo-hygrometer. In addition, the occupants were asked to collect floor dust in a living room and bed room with a vacuum cleaner. The investigated areas were belonging to the northern portion of Japan, which were snowy and cold regions.

The questionnaire included information regarding gender, age, housing location, housing type, installed equipment for space heating, type of ventilation system, indoor environmental quality, pattern of operating space heating and mechanical ventilation systems, the performance of the building envelope, and others. Questions about indoor environmental quality addressed the occurrence of visible vapour condensation, visible mould growth indoors and perception of odours. Questions regarding thirteen health-related symptoms among children, which reflected respiratory symptoms, dermal symptoms, ocular symptoms, nasal symptoms and mental symptoms. Respiratory symptoms addressed cough and shortness of breath, dermal symptoms dryness, itch, rash, eczema and erythema, ocular symptoms addressed redness, dryness, itch and irritation and nasal symptoms addressed sneezing, stuffy and runny nose. Answers indicated every symptom onset from indoor environment in three months.

The microorganisms were genetically analysed to evaluate the population diversity of microbial species based on the length of ITS. The fungal DNA of each house was obtained from the floor dust of 50mg which was collected in a living room and bed room using a vacuum cleaner. The ITS regions are located among the ribosomal RNA genes that are a part of genome of microorganisms, and is hyper-variable, suggesting its length is a unique signature in each microorganism. In this paper we analysed spacers ITS2 using the fungal-specific primers ITS3 and ITS4. Fungal diversity included in the floor dust of surveyed 120 houses was analysed and then these samples were also performed comprehensive analysis using the next generation sequencer. All base sequence data sets were clustered using more than 97% sequence similarity and the fungal species were identified with UNITE database v7.2.

2.2 Evaluation method of indoor dampness

Authors have already proposed the estimation method of indoor dampness using the results of occupants self-rated answers to questions about visible vapor condensation, mould growth, perception of mouldy odor and so on during winter season (Hasegawa, 2016). This dampness index was calculated as the value from 0 to 24 points and its values classified into four kinds of rank on the basis of the quartile. Rank 4 presented the house which had the most serious problems related to dampness. Figure 2 presents the results from large scale national survey (N=3,765, conducted on February of 2014). A distribution of dampness index from this survey approximately has a normal distribution. In addition the dampness index revealed an association between indoor dampness and health-related symptoms among children.

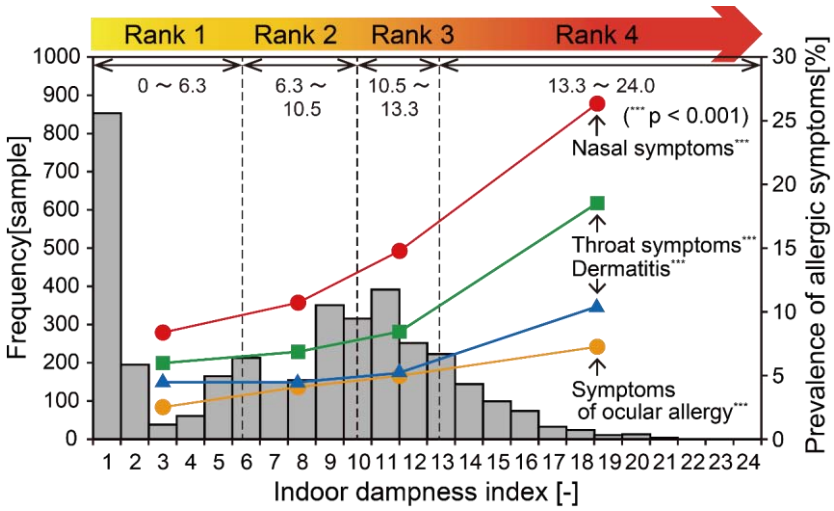

Figure 2: Distribution of dampness index and prevalence of allergic symptoms from the last survey

3 INDOOR ENVIRONMENT OF DAMPNESS IN HOUSES

3.1 Indoor dampness index

Figures 3 present surveyed dampness index distribution and the prevalence of health-related symptoms among children for each rank from 119 houses. The dampness index ranged from 1 to 22 and it is not following to normal distribution like a previous large scale questionnaire survey. The prevalence of nasal symptoms (chi-square test: $p < 0.01$) and ocular symptoms increased as rank of dampness index was rising. In particular the prevalence of nasal symptom in Rank 4 was more 50% among children. The prevalence of throat symptoms and dermatitis was the biggest in Rank 3, and there is no clear association between dampness index and health-related symptoms.

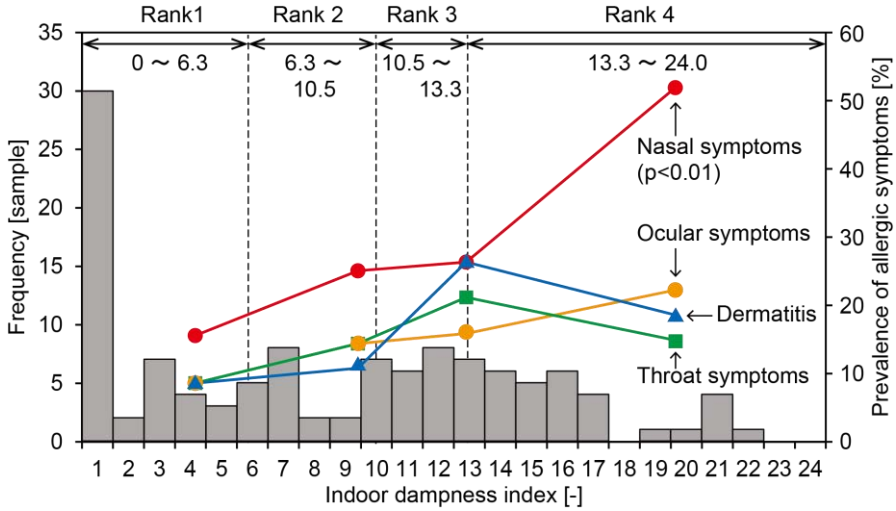

Figure 3: Distribution of dampness index and prevalence of allergic symptoms

3.2 Indoor temperature and humidity

Figures 4 to 6 present the statistical values of temperature, relative humidity and humidity ratio during staying in a living room and bed room for each rank of indoor dampness. The values in every rank of indoor dampness index include the median, the first and third quartiles, and the

maximum and minimum values of temperature and humidity during measuring periods from 119 houses. In order to test the significance of these associations, Kruskal-Wallis test, which is one of non-parametric method, was performed to evaluate whether samples in each rank of indoor dampness index originate from the same distribution. Moreover, the significant difference among samples of each rank was tested by multiple comparison.

As for the result of temperatures in Figure 4, no significant association was found among each rank of indoor dampness index. This tendency is presumed that the temperature in a living room was affected by the heating behaviour at the time of occupancy. Although an association between the temperature in a bedroom and dampness index was not statistically significant, p value (p=0.084) in a bed room was lower than that in a living room and the temperature tended to be decreasing for Rank 4.

On the other hand, the relative humidity and the humidity ratio associated significantly rank of indoor dampness index though the Kruskal-Wallis test as shown in Figure 5 and 6. It was indicated that the higher the rank of indoor dampness index, the higher the humidity in a living room and bed room. In addition, the relative humidity and humidity ratio in a living room at Rank 2, 3 and 4 were significantly increasing in comparison with at Rank 1. As the humidity ratio at Rank 4 was found to be significantly the highest among surveyed houses, it was expected that these houses at Rank 4 had severe environmental problems for indoor dampness. There was the significant difference between humidity ratio in a bed room among each rank, and the humidity ratio at rank 4 was not the highest.

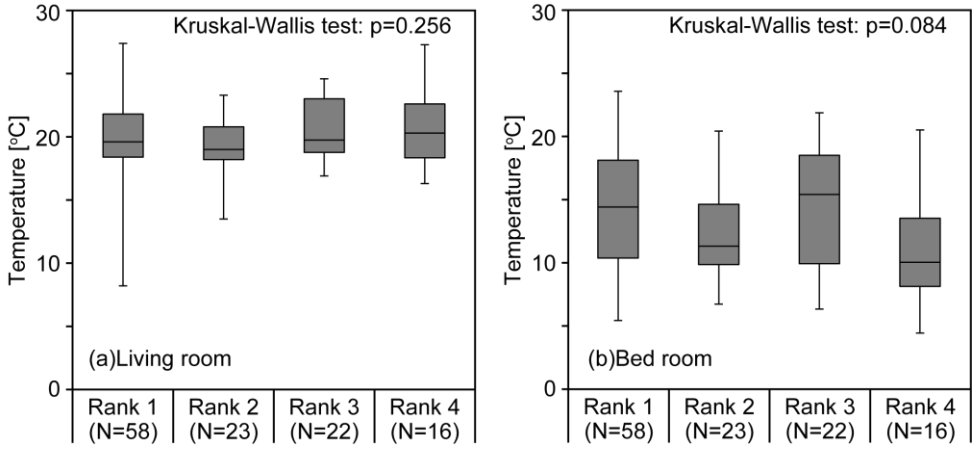

Figure 4: Dampness rank and temperature in a living room and bedroom

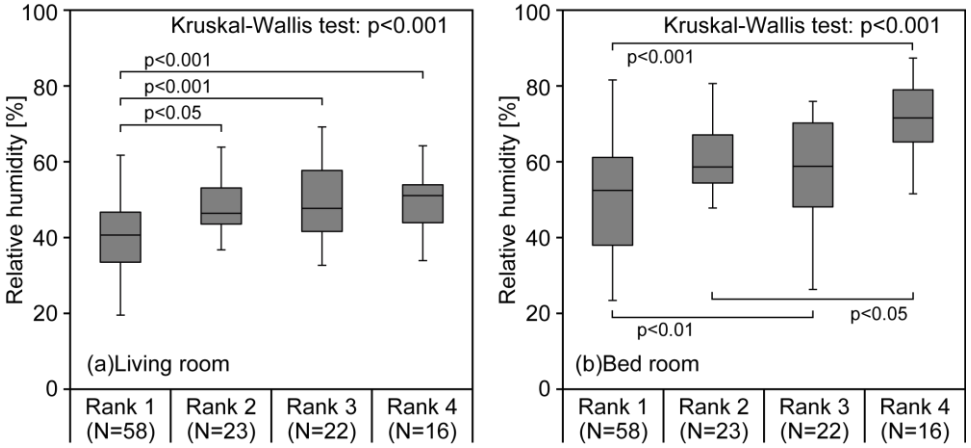

Figure 5: Dampness rank and relative humidity in a living room and bedroom

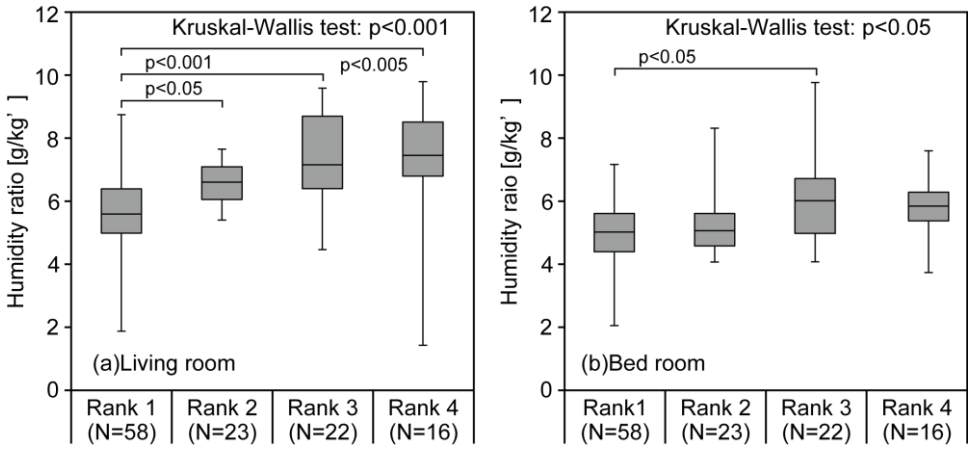

Figure 6: Dampness rank and humidity ratio in a living room and bedroom

3.3 Microorganisms flora

In the surveyed houses though DNA analysis method, 1,522 kinds of fungal species were detected. Table 1 presented the detection ratio of several fungal species at ranks of indoor dampness index.

Table 1: The detection ratio of microbial species

Fungal species	Rank of dampness index				Fungal species	Rank of dampness index				Fungal species	Rank of dampness index			
	1	2	3	4		1	2	3	4		1	2	3	4
Aspergillu sappendiculatus	96.4	95.5	93.8	100.0	*Graphiolaphoenicis*	54.5	63.6	87.5	71.4	*Trametes versicolor*	40.0	63.6	37.5	52.4
Aspergillus conicus	98.2	100.0	93.8	100.0	*Hortaea werneckii*	52.7	68.2	62.5	71.4	*Yamadazyma triangularis*	30.9	22.7	18.8	52.4
Aspergillus penicillioides	100.0	100.0	100.0	100.0	*Mycosphaerella tassiana*	58.2	81.8	68.8	71.4	*Aspergillus hongkongensis*	25.5	50.0	25.0	47.6
Cladosporium sphaerospermum	94.5	100.0	100.0	100.0	*Trichosporon insectorum*	61.8	77.3	75.0	71.4	*Candida zeylanoides*	52.7	54.5	68.8	47.6
Mycosphaerella punctiformis	96.4	95.5	93.8	100.0	*Aureobasidium pullulans*	76.4	72.7	62.5	66.7	*Exophiala cancerae*	60.0	90.9	81.3	47.6
Penicillium jiangxiense	96.4	90.9	81.3	100.0	*Hypsizygus marmoreus*	50.9	77.3	43.8	66.7	*Gibellulopsis nigrescens*	29.1	59.1	37.5	47.6
Penicillium kongii	94.5	90.9	100.0	100.0	*Knufia epidermidis*	52.7	63.6	81.3	66.7	*Grifola frondosa*	49.1	50.0	68.8	47.6
Toxicocladosporium rubrigenum	94.5	100.0	100.0	100.0	*Penicillium decumbens*	34.5	59.1	56.3	66.7	*Lentinula edodes*	56.4	63.6	68.8	47.6
Verrucocladosporium dirinae	100.0	100.0	100.0	100.0	*Penicillium digitatum*	50.9	77.3	62.5	66.7	*Panellus serotinus*	40.0	27.3	43.8	47.6
Alternaria betae-kenyensis	100.0	95.5	100.0	95.2	*Phlebia radiata*	63.6	59.1	75.0	66.7	*Paraphaeosphaeria sardoa*	41.8	59.1	43.8	47.6
Aspergillus parasiticus	87.3	95.5	100.0	95.2	*Talaromyces veerkampii*	60.0	59.1	43.8	66.7	*Pestalotiopsis trachicarpicola*	36.4	18.2	31.3	47.6
Cyphellophora europaea	94.5	95.5	100.0	95.2	*Arthrocatena tenebrio*	45.5	77.3	62.5	61.9	*Pholiota microspora*	45.5	40.9	37.5	47.6
Rhodotorula mucilaginosa	96.4	95.5	93.8	95.2	*Cutaneotrichosporon jirovecii*	36.4	63.6	37.5	61.9	*Sagenomella griseoviridis*	21.8	31.8	56.3	47.6
Schizopora ovispora	74.5	77.3	68.8	95.2	*Fusarium oxysporum*	54.5	68.2	68.8	61.9	*Sistotrema sernanderi*	30.9	63.6	25.0	47.6
Filobasidium magnum	94.5	86.4	87.5	90.5	*Gibberella tricincta*	61.8	59.1	68.8	61.9	*Vishniacozyma carnescens*	38.2	54.5	37.5	47.6
Penicillium armarii	83.6	77.3	87.5	90.5	*Guehomyces pullulans*	45.5	68.2	56.3	61.9	*Acremonium charticola*	21.8	31.8	37.5	42.9
Sphaerulina rhabdoclinis	83.6	90.9	93.8	90.5	*Metschnikowia reukaufii*	60.0	50.0	68.8	61.9	*Aureobasidium subglaciale*	32.7	54.5	31.3	42.9
Sterigmatomyces halophilus	54.5	72.7	75.0	90.5	*Neoascochyta desmazieri*	78.2	63.6	68.8	61.9	*Calycina marina*	36.4	36.4	37.5	42.9
Wallemia mellicola	54.5	81.8	81.3	90.5	*Penicillium onobense*	45.5	50.0	43.8	61.9	*Camptophora hylomeconis*	45.5	54.5	50.0	42.9
Wallemia sebi	43.6	77.3	75.0	90.5	*Plectosphaerella alismatis*	74.5	81.8	75.0	61.9	*Candida parapsilosis*	56.4	31.8	56.3	42.9
Penicillium ornatum	74.5	86.4	81.3	85.7	*Clavispora lusitaniae*	63.6	68.2	87.5	57.1	*Cladosporium halotolerans*	56.4	31.8	56.3	42.9
Pyrenochaeta keratinophila	70.9	68.2	68.8	85.7	*Didymella aurea*	43.6	68.2	43.8	57.1	*Cryptococcus uniguttulatus*	25.5	36.4	37.5	42.9
Wallemia tropicalis	60.0	77.3	68.8	85.7	*Exophiala equina*	45.5	59.1	68.8	57.1	*Cutaneotrichosporon curvatus*	23.6	45.5	31.3	42.9
Capnobotryella renispora	69.1	77.3	75.0	81.0	*Hannaella oryzae*	56.4	68.2	75.0	57.1	*Exophiala xenobiotica*	29.1	45.5	31.3	42.9
Neocatenulostroma abietis	74.5	77.3	81.3	81.0	*Malassezia restricta*	67.3	63.6	56.3	57.1	*Flammulina velutipes*	54.5	45.5	43.8	42.9
Penicillium corylophilum	76.4	77.3	62.5	81.0	*Malassezia sympodialis*	50.9	31.8	62.5	57.1	*Kondoa aeria*	29.1	31.8	37.5	42.9
Rhodotorula glutinis	67.3	81.8	75.0	81.0	*Neodevriesia imbrexigena*	47.3	59.1	50.0	57.1	*Magnusiomyces capitatus*	38.2	13.6	37.5	42.9
Saccharomyces cariocanus	89.1	95.5	87.5	81.0	*Ochroconis mirabilis*	47.3	54.5	62.5	57.1	*Mycosphaerella handelii*	49.1	31.8	56.3	42.9
Alternaria infectoria	69.1	63.6	62.5	76.2	*Penicillium roqueforti*	40.0	63.6	31.3	57.1	*Penicillium citrinum*	27.3	45.5	25.0	42.9
Aspergillus restrictus	60.0	77.3	68.8	76.2	*Aspergillus conversis*	41.8	63.6	43.8	52.4	*Phyllotopsis nidulans*	30.9	27.3	50.0	42.9
Fusarium asiaticum	74.5	77.3	62.5	76.2	*Candida albicans*	36.4	45.5	31.3	52.4	*Schizopora flavipora*	34.5	31.8	43.8	42.9
Pseudotaeniolina globosa	65.5	54.5	62.5	76.2	*Candida etchellsii*	27.3	36.4	12.5	52.4	*Sistotremastrum guttuliferum*	41.8	36.4	43.8	42.9
Sporobolomyces phaffii	70.9	54.5	75.0	76.2	*Candida magnoliae*	32.7	31.8	31.3	52.4	*Symmetrospora foliicola*	52.7	54.5	56.3	42.9
Stemphylium herbarum	70.9	81.8	87.5	76.2	*Candida parapsilosis*	40.0	68.2	37.5	52.4	*Trametes hirsuta*	40.0	31.8	37.5	42.9
Trichosporon debeurmannianum	54.5	86.4	81.3	76.2	*Cystobasidium lysinophilum*	38.2	63.6	43.8	52.4	*Vermiconia calcicola*	41.8	31.8	25.0	42.9
Aspergillus niger	85.5	72.7	100.0	71.4	*Malassezia dermatis*	45.5	31.8	56.3	52.4	*Vishniacozyma victoriae*	54.5	31.8	56.3	42.9
Aureobasidium melanogenum	56.4	77.3	68.8	71.4	*Malassezia globosa*	56.4	68.2	50.0	52.4	*Xerochrysium dermatitidis*	38.2	40.9	37.5	42.9
Bjerkandera adusta	69.1	59.1	75.0	71.4	*Meyerozyma guilliermondii*	30.9	50.0	31.3	52.4	*Yarrowia lipolytica*	63.6	68.2	62.5	42.9
Cystofilobasidium macerans	54.5	77.3	62.5	71.4	*Neofabraea vagabunda*	54.5	54.5	31.3	52.4	*Apiotrichum montevideense*	30.9	59.1	31.3	38.1
Debaryomyces hansenii	47.3	77.3	68.8	71.4	*Papiliotrema flavescens*	47.3	36.4	56.3	52.4	*Ascosphaera atra*	14.5	31.8	25.0	38.1

The fungal species of which the detection rate was increasing with ranks 1 to 4 of indoor dampness index were considered to be associated with indoor environmental problems of dampness. For example, this trend was found on fungal species of *Wallemia sebi* and

Rhodotorula glutinis. Also, the association between the OTU ratio of fungal species in each house and the rank of indoor dampness index was statistically analysed though Kruskal-Wallis test. As results, it was estimated that the higher the rank of indoor dampness index, the higher the detection ratio such as *Aspergillus* spp., *Trichosporon* spp., *Wallemia mellicola*, and *Wallemia sebi*. If the major fungal species related to indoor dampness in houses of Japan were clarified from the population diversity of microbial species, we could understand the indoor microbial contamination related to indoor dampness.

4 ADVERSE HEALTH EFFECT AND DAMPNESS INDEX

4.1 Outline of statistical analysis

The associations between indoor dampness and health-related symptoms among children were estimated using a multivariate logistic regression analysis with adjustment for gender, age and parents health condition. Adjusted odds ratios were estimated including the 95% confidence interval (CI). We analysed the data using the Statistical Package for the Social Sciences (SPSS version 23).

4.2 Analysed results

Associations between four kinds of health-related symptoms among children and indoor dampness are presented in Table 2. Adjusted ORs of nasal symptoms (AOR = 5.25, $p < 0.01$) was statistically significant in rank 4 of the dampness index. In this analysed results, the increased risk of nasal symptoms due to indoor dampness was estimated (p for trend <0.05). The dose-response relationships between indoor dampness and nasal symptoms was presented using the dampness index proposed by authors. In addition, adjusted ORs of dermal symptoms in rank 3 of dampness index (AOR = 4.26, $p < 0.05$) was statistically significant. There were not meaningful associations for other health-related symptoms with indoor dampness. In this paper, we could conclude that children who were living in dampness are at significant risk for health-related symptoms such as nasal symptoms and dermal symptoms.

Table 2: AORs for ocular symptoms, nasal symptoms, throat symptoms and dermal symptoms

Factors	Frequency	Adjusted OR[a] (95%CI)			
		Ocular symptoms	Nasal symptoms	throat symptoms	Dermal symptoms
Rank of dampness Index					
Rank 1	71	1.00 (*Ref.*)	1.00 *(Ref.)*	1.00 *(Ref.)*	1.00 *(Ref.)*
Rank 2	28	2.03 (0.51-8.14)	1.42 (0.47-4.28)	1.57 (0.39-6.29)	1.51 (0.32-7.20)
Rank 3	19	1.92 (0.43-8.66)	2.16 (0.62-7.59)	2.82 (0.68-11.7)	4.26* (1.02-17.7)
Rank 4	27	3.39† (0.96-12.0)	5.25** (1.88-14.7)	1.69 (0.26-2.00)	3.23 (0.82-12.7)
p for trend		0.302	<0.05	0.544	0.166

[a] Adjusted for age, gender and parents health condition related to allergies.
CI = confidence interval; †<0.1, *<0.05, **<0.01

5 CONCLUSIONS

The indoor dampness was associated with allergic symptoms among children, however the causal mechanisms was not be revealed yet. This paper describes the quantitative estimation of indoor dampness using dampness index proposed by authors and measured results such as indoor temperature, humidity and microorganisms. The microorganisms were genetically analysed to evaluate the population diversity of microbial species through the DNA analysed technologies. The results from this survey are shown as follows.

1) The dampness index is not following to normal distribution like a previous large scale questionnaire survey. The characteristics of indoor temperature, humidity and microbial flora due to home dampness were clarified by comparing dampness index and measured results of these physical items. The median relative humidity in each dampness rank was higher at higher rank of indoor dampness. This tendency was statistically significant for both a living room and a bed room, and humidity ratio at rank 1 was significantly lower than that at rank 3 and rank 4.
2) The fungal species of which the detection rate was increasing with ranks 1 to 4 of indoor dampness index were considered to be associated with indoor environmental problems of dampness. This paper indicates the association between indoor dampness and fungal species of *Wallemia sebi* and *Rhodotorula glutinis*.
3) The association between adverse health effect and influencing factors related to indoor dampness was estimated using a multivariable logistic regression model. As results, it was revealed that children who were living in dampness are at significant risk for health-related symptoms such as nasal symptoms and dermal symptoms.

6 ACKNOWLEDGEMENTS

The authors would like to thank the residents who were involved in this study for their helpful cooperation. This survey was supported partly by JSPS KAKENHI Grand Number JP17H03356 and Research Project selected by President in Akita Prefectural University.

7 REFERENCES

Fisk WJ, Lei-Gomez Q, Mendell MJ. (2007). Meta-analyses of the associations of respiratory health effects with dampness and mold in homes. *Indoor Air '07*, 17(2):84-96.

Hasegawa K et al, 2016. National survey on home dampness and children's allergic symptoms during consecutive survey periods in Japan, *Proceedings of Indoor Air 2016*, ID400:1-2.

Relationship between indoor allergen and occupants' allergic symptoms before and after moving in the house with the countermeasure against allergy

Teruaki Mitamura*[1], Kunio Dobashi[2], and Hiroki Harasawa[3]

1 Maebashi Institute of Technology
460-1 Kamisadori-machi,
Maebashi, Gunma 371-0816, Japan
**Corresponding author: mitamura@maebashi-it.ac.jp*

2 Jobu Hospital for Respiratory Diseases
586-1 Taguchi-machi,
Maebashi, Gunma 371-0048, Japan

3 Harasawa Homes Co., Ltd.
565 Araicho,
Ota, Gunma 373-0852, Japan

ABSTRACT

Allergic symptoms are closely related to indoor allergens, such as airborne particulate matter, fungi, and house dust mite. This paper introduces a central air-conditioning system integrated with an electrical dust collector developed as a countermeasure against allergy. Here, it was demonstrated that this air-cleaning system can remove fine particles of PM2.5. Objectively, this study aims to elucidate the relationship between indoor allergens and occupants' allergic symptoms. Thereby, the concentrations of fine particles, airborne fungi, and the amount of mite allergen in the dust were measured before and after the subject occupants moved into the house installed with an air-cleaning system. In addition, the ratio of active CD4+ T cells in the occupants' blood was measured as an indicator of their allergic symptoms. The results showed that the concentrations of fine particles, airborne fungi, and the amount of mite allergens in the houses with a countermeasure against allergy, as well as the ratio of active CD4+ T cells, were significantly reduced after the occupants have moved in, demonstrating an improvement in the state of the occupants' allergic symptoms with the installation of the air-cleaning system in their houses.

KEYWORDS

Air-cleaning system, Indoor allergen, Filed survey, CD4+ T cells, Allergic symptom

1 INTRODUCTION

The promotion of highly insulated and airtight houses in Japan since the 1980s has been a parallel move with the reduction of CO_2 emissions in the region. Consequently, indoor chemical pollution has become a social problem since the 1990s. To address the issue, the Building Standard Law of Japan on sick house syndrome concerns was revised in July 2003, and various countermeasures, such as the mandatory installation of ventilation system, were carried out. Nonetheless, it was pointed out that allergic diseases, i.e., asthma and atopic dermatitis, are related to the indoor environment. Despite the increasing number of allergic patients, countermeasures against allergens in houses were not enough. One of the reasons points to the inadequate elucidation of the relationship between indoor environment and allergic symptoms in the patients' houses. In this study, a central air-conditioning system integrated with an electrical dust collector was developed as a countermeasure against allergy. This air-cleaning system is capable of removing fine particles of PM2.5. Practically, this study aims to clarify the relationship between indoor allergens and occupants' allergic symptoms. To date, the efficient performance of the system has been verified based on the measurement results in 31 houses investigated (Mitamura, T. et al., 2013). Specifically, this paper presents a comparative study

of indoor allergens and the ratio of active CD4+ T cells, as an indicator of allergic symptoms prior to and after moving into the houses, with a countermeasure against allergy.

2 METHODS

2.1 Air-cleaning system

Figure 1 shows an outline of the central air-conditioning, ventilation, and air-cleaning system installed in the house as a countermeasure against allergy. Outside air (OA) is supplied from the air inlet and passes through the air-cleaning unit that consists of a net pre-filter, a medium efficiency particulate air (MEPA) filter. A large size of particles is caught by this unit. Returned air (RA) from the stair hall on the second floor is mixed with OA after passing through the air-cleaning unit. Subsequently, RA passes through the electric precipitator, which consists of an aluminium mesh filter and an electronic cell. It then moves through the collector part of the electronic cell where alternate parallel plates are charged positively and negatively, creating a uniform electronic field. The charged small particles are attached to and collect on the plates that have the opposite electrical charge. The fractional efficiency of the electric precipitator for a small size of particle E1 (from 0.3 to 1.0 μm) based on the ASHRAE Standard 52.2-1999 is 73%. Next, the fresh air passing through the electric precipitator is air-conditioned by the heating/cooling coil and is supplied (SA) to each residential room. Dirty air is exhausted (EA) from the air outlet in the toilet, bathroom, and kitchen.

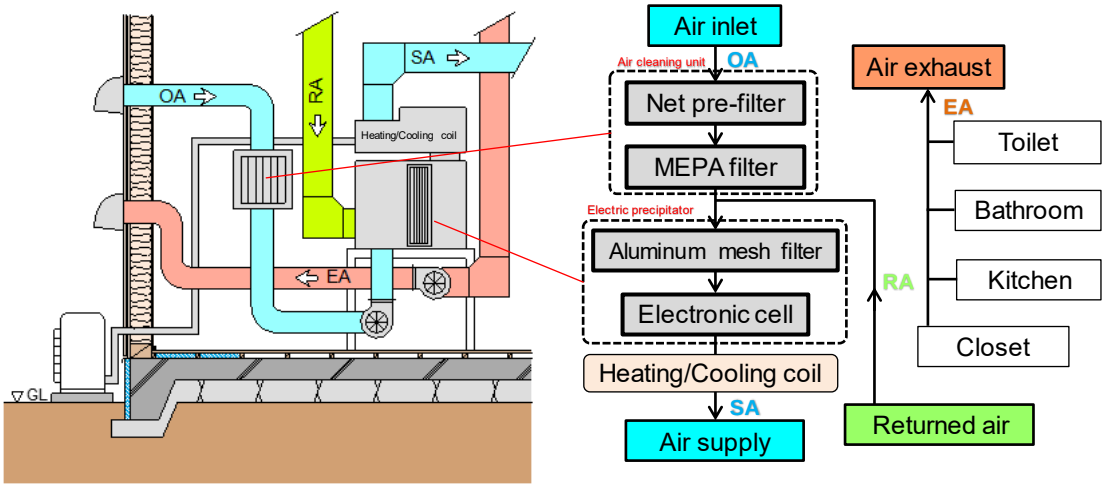

Figure 1: The whole house air-conditioning, ventilation and air-cleaning system

2.2 Investigated houses

A total of 40 family units and 107 houses were subjected to the investigation and measurements. In these targets, at least one family member has an allergic disease. Measurements were performed prior to and after the subjects moved into the house installed with a countermeasure against allergy. In some of the houses, measurements were repeated twice in roughly 1 month and 6 months after moving in. Before being occupied, most of the houses were apartment buildings used for over 10 years. Houses with a countermeasure against allergy were highly insulated and airtight.

2.3 Measurements

Indoor allergens were measured according to the concentrations of fine particles, airborne fungi, and the amount of mite allergen. Fine particle concentrations were measured 1.0-m above floor

level for both the living room and bedroom. The light-scattering particle counter for aerosol was used. Fine particles at six size levels, from >0.3 to >5.0 μm, were measured. Sampling air volume was set at 1.0 L/min; a portable air sampler blew 50 L of air to potato dextrose agar medium. The airborne fungi were cultured in the incubator for more than 5 days at 25 °C, and then the number of fungal colonies was counted. An electric vacuum cleaner was used to collect household dust on the living room floor and on the bottom mattress in the bedroom in a 1-m^2 area for 2 min. The amount of mite allergen in the household dust was analysed by enzyme-linked immunosorbent assay (ELISA). All measurements were carried out with an opening in the closed room. Additionally, CO_2 concentration was measured in an area of the houses to determine the indoor ventilation characteristics. Mann–Whitney U test was used to compare the differences in these values before and after occupying a house with a countermeasure against allergy.

Accordingly, the occupants were examined medically in Gunma University Hospital. The ratio of active CD4+ T cells was measured through a blood test as an indicator of the occupants' allergic symptoms. Here, a lower value of the ratio of active CD4+ T cells indicates less allergic symptoms. These examinations, along with the measurements of indoor allergens, were performed before and after the occupants moved into the house with a countermeasure against allergy. Comparison of the differences before and after occupying the house was carried out via the Wilcoxon signed-rank test.

3 RESULTS AND DISCUSSION

Figure 2 shows the box-and-whisker plots of the average CO_2 concentration in the living room and bedroom before and after the occupants moved into the house with a countermeasure against allergy. After occupancy, there were significantly lower concentrations in both rooms ($p < 0.01$). Specifically, the average CO_2 concentration after the occupants moved in was 645 ppm in the living room and 720 ppm in the bedroom. Prior to the occupancy, the mechanical ventilation equipment was not often installed, and ventilation airflow seemed insufficient. In addition, some of the houses had heating appliances, such as an oil stove used in winter.

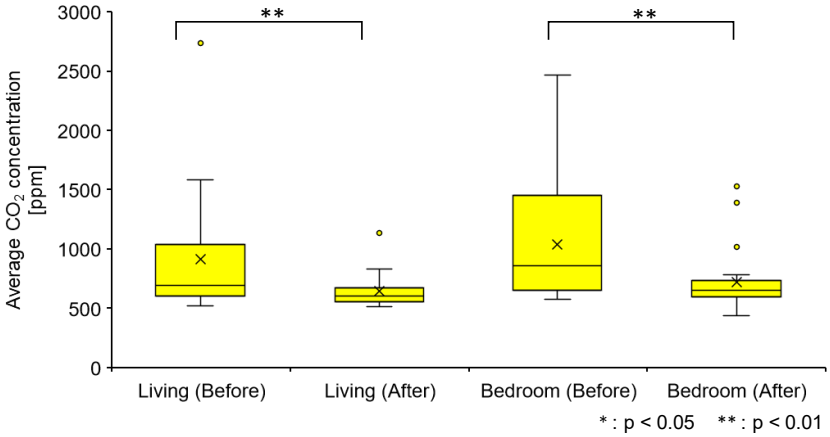

Figure 2: Average CO_2 concentration

Figure 3 shows the box-and-whisker plots of the concentration of fine particles in the living room and bedroom before and twice after the occupants moved into the house with a countermeasure against allergy. Notably, significantly lower concentrations of six levels of particle sizes were recorded after the occupants moved in ($p < 0.01$). In particular, the smaller the particle size, the lower the concentration. Fine particles causing asthma, within the size range of 1.0 to 5.0 μm, were suggested to have been effectively removed with the air-cleaning

system. Based on the first and second measurements made after the occupants moved in, the concentration was kept low except for particle sizes greater than 5.0 μm. Moreover, such fine particles were settled in the floor, which indicates that they may not have been sufficiently removed through the air-cleaning system.

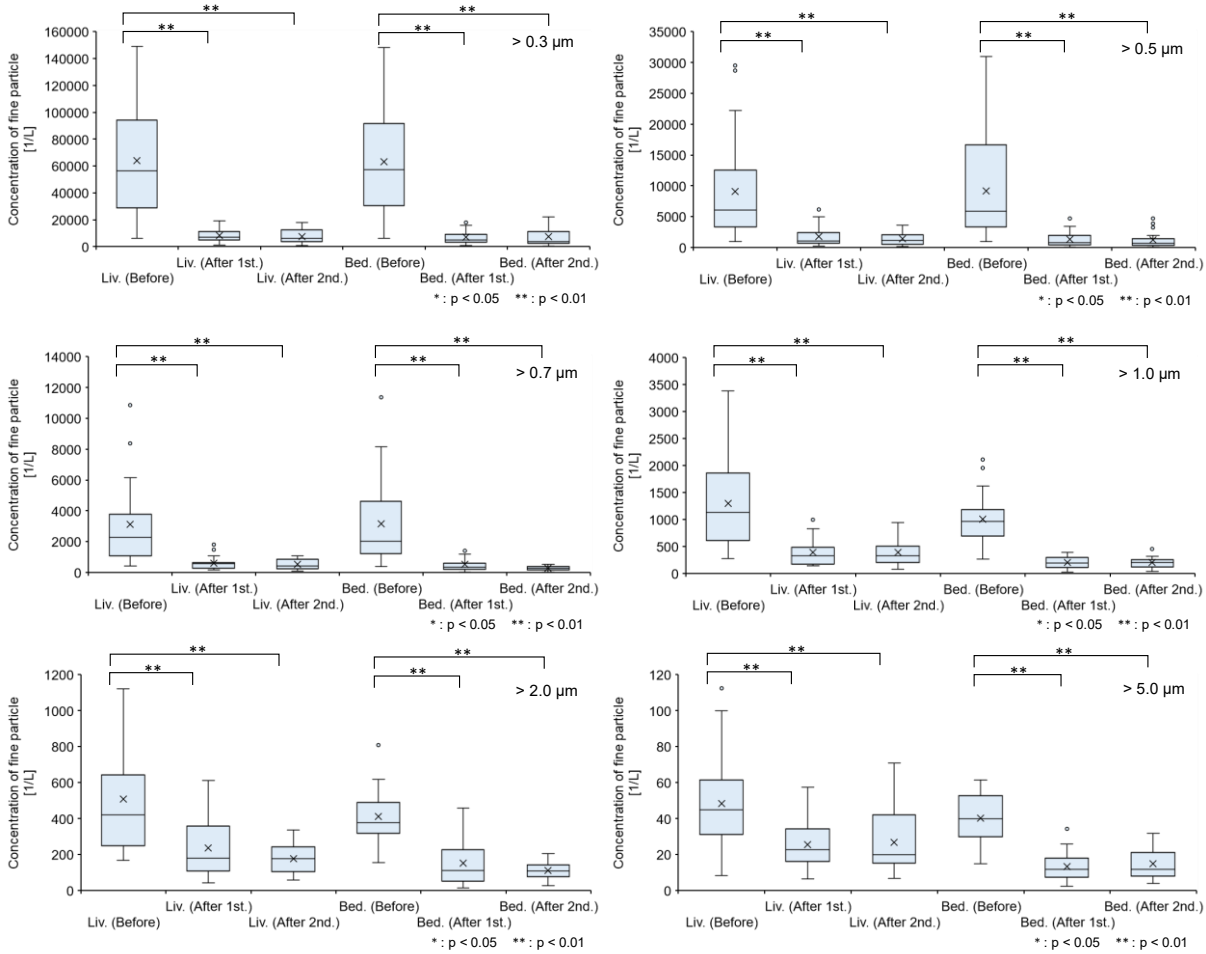

Figure 3: Concentrations of fine particles

Similarly, Figure 4 shows the box-and-whisker plots of the concentration of airborne fungi in the living room and bedroom before and twice after the occupants moved into the house with a countermeasure against allergy. After the occupants moved in, significantly lower concentrations of airborne fungi ($p < 0.01$) were recorded. The average concentrations of airborne fungi prior to occupancy were 365 CFU/m^3 in the living room and 296 CFU/m^3 in the bedroom, and these values varied widely. In contrast, the average concentrations of airborne fungi after the occupants moved in were below 100 CFU/m^3, much lower than 1,000 CFU/m^3 specified as the standard by the Architectural Institute of Japan.

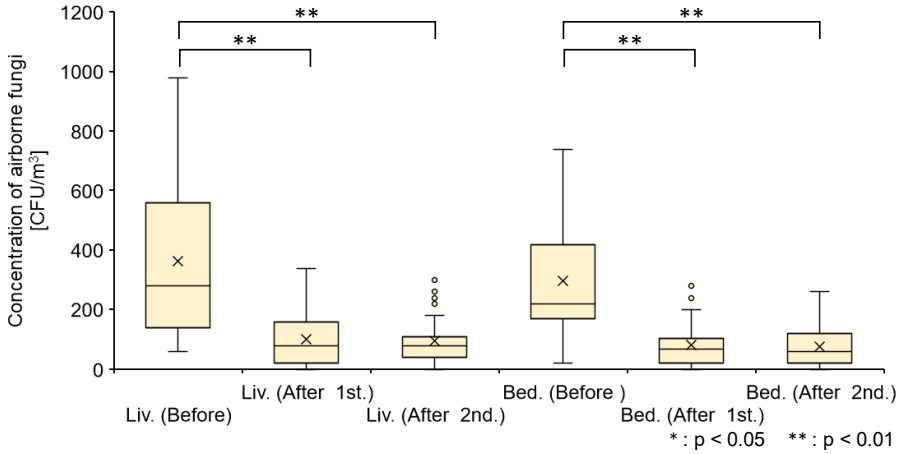

Figure 4: Concentration of airborne fungi

Figure 5 shows the box-and-whisker plots of the amount of mite allergen (Der 1) in the living room and bedroom before and twice after the occupants moved into the house with a countermeasure against allergy. After the occupants moved in, the amount of mite allergen became significantly lower ($p < 0.01$). Additionally, the amount of mite allergen in the bedroom tended to be lower than in the living room. Specifically, the average amounts of mite allergen before occupancy were 2.6 µg/g dust in the living room and 6.8 µg/g dust in the bedroom, which exceeded the average sensitization threshold of 2.0 µg/g dust.

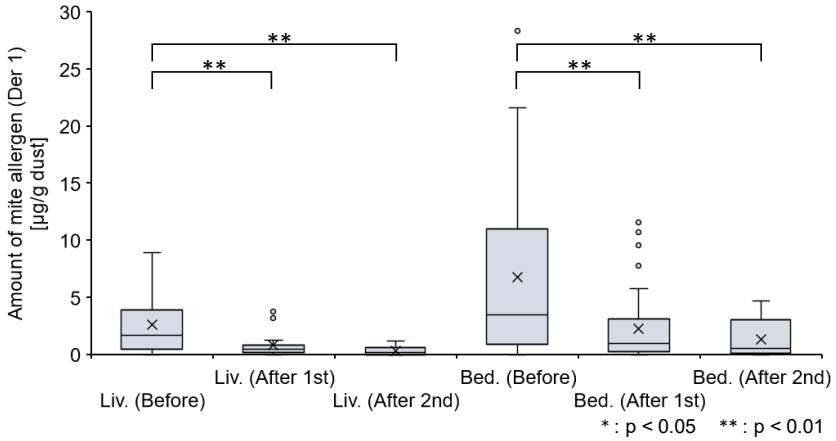

Figure 5: The amount of mite allergen (Der 1) in household dust

Figure 6 shows the box-and-whisker plots of the ratio of active CD4+ T cells for healthy subjects before and after they moved into the house with a countermeasure against allergy. The ratio of active CD4+ T cells after under 3 and 4–6 months of occupancy was not significantly lower compared with that prior to the occupancy. On the contrary, the ratio of active CD4+ T cells after over 7 months of occupancy was significantly higher ($p < 0.05$). However, the difference between both average values was not significant.

Figure 7 shows the box-and-whisker plots of the ratio of active CD4+ T cells for allergic patients before and after they moved into the house with a countermeasure against allergy. After under 3 months of occupancy, the ratio of active CD4+ T cells was not significantly lower compared with that prior to the occupancy. In contrast, after 4–6 months and over 7 months, the ratios became significantly lower ($p < 0.01$ and $p < 0.05$, respectively). Thus, the allergic symptoms of allergic patients improved with a countermeasure against allergy after moving into the house.

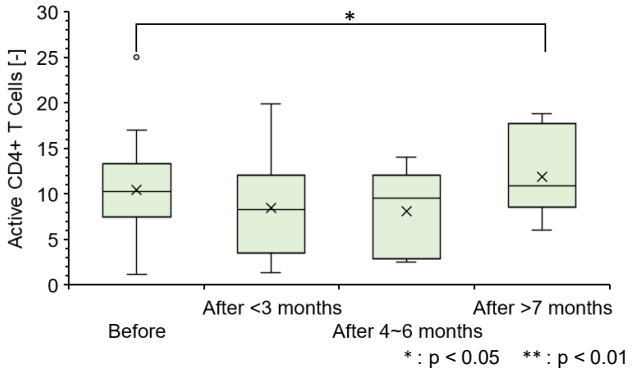

Figure 6: The ratio of active CD4+ T Cells for healthy subjects

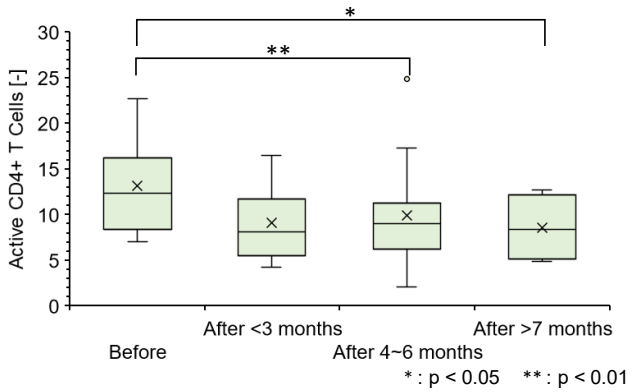

Figure 7: The ratio of active CD4+ T Cells for allergic patients

4 CONCLUSIONS

This paper presented a comparison of the concentrations of fine particles, airborne fungi, and the amount of mite allergen, prior to and after the subjects' occupancy in the house with a countermeasure against allergy. Based on the results, the amount of indoor allergen was significantly reduced after the occupants moved in. In addition, the measured ratio of active CD4+ T cells from the blood of the occupants indicated no significant reduction for the healthy subjects but was considerably reduced for the allergic patients, given a time frame of after 4–6 months and over 7 months of occupancy. Such results indicate that improvement of indoor environment led to the reduction of allergic symptoms.

5 ACKNOWLEDGEMENTS

A part of this research work was supported by the Ministry of Land, Infrastructure, Transport and Tourism of Japan in 2009, and from 2013 to 2015. The authors would also like to acknowledge the occupants of the investigated houses.

6 REFERENCE

Mitamura, T. *et al.* (2013). *Verification of Indoor Air Quality Before and After Moving in the House with the Countermeasure Against Allergy*. 11th REHVA World Congress and the 8th International Conference on IAQVEC Clima2013 Congress.

Learning Performance in Odor Environment with aroma oils: Influence of Odor of Essential Oils on Learning Performance in Classroom

Aya Eto[*1], Narae Choi[1], Toshio Yamanaka[1],
Akihisa Takemura[2] and Tomohiro Kobayashi[1]

1 Osaka University
Suita 565-0821
Osaka, Japan
**eto_aya@arch.eng.osaka-u.ac.jp*

2 Setsunan University
Neyagawa 572-8508
Osaka, Japan

ABSTRACT

There is no doubt that odor is also an important factor to evaluate indoor air quality. Since the olfactory system was proven to be closely related to the limbic structures which support emotion, long-term memory and motivation, the psychological and the physiological effects of the essential oils have been widely researched in various fields. The odor environment formed by essential oils is popularly used in commercial facilities to make customers have special mood. On the other hand, there are also some studies about its effects on workplace productivity or learning performance in actual spaces such as office buildings and schools.

The purpose of this research is to examine whether the odor environment with essential oils has positive effects on learning performance in classroom and how students feel about the environment. In this paper, the influences of "rosemary" essential oil on learning performance and mood in healthy participants are tested. Participants were all graduate or undergraduate students and were divided into two groups randomly and assigned to conditions of rosemary aroma or no aroma (control).

Learning performance was assessed using two methods, and one is reading task and the other is verbal memory task. The number of letters participants read during the specified time and a percentage of correct answers of the comprehension test were used to evaluate the performance in reading task. For verbal memory task, Esperanto words were adopted. In order to assess memory retention, these tests were conducted again about one month after the first task unexpectedly for the same participants. Additionally, the subjective evaluations were done by participants before and after tasks with several mood scales: intensity of odor, hedonic scale, preference, acceptability of odor environment, evaluation of impression on odor and impression of experimental room.

As a result, under the condition of rosemary aroma, the number of letters in reading task was significantly larger than control group without aroma odor. From the t-test, however, there was no significant difference between two samples in terms of memory retention. Analysis of subjective evaluation revealed that the mood of participants is greatly affected by the preference of the odor of rosemary aroma. It was found that the participants tend to select negative words among many SD scales for odor they dislike in the impression evaluation of odor.

KEYWORDS

Odor, Sensory Evaluation, Rosemary, Learning Performance

1 INTRODUCTION

Indoor climate affects individual performance [1]. It is known that poor indoor environment derived from high indoor temperature and low ventilation rate has a negative effect on working performance [2, 3]. As improving workplace productivity is directly related to the economic benefit, the influence of indoor environment on performance in office work has been widely studied. On the other hand, there are relatively fewer studies on learning performance in school.

Wargocki et al. [4] examined children's learning performance under different temperature and ventilation rate conditions. As a result, it was proven that increasing the outdoor supply air rate and appropriate temperature can improve the performance of schoolwork. Like temperature, humidity and ventilation rate, odor is also an important factor to evaluate the indoor environment. However, the influence of odor on learning performance is still not well understood. Since it was revealed that the olfactory system is directly connected to the limbic structures which are known to control human's mood and memory, the effects of the odor environment have been actively discussed and studied recently. Although there are some studies about its effects on office productivity [5], little information exists concerning its effects on learning performance in study spaces.

This research investigates whether the odor environment has positive effects on learning performance of university students and how students feel about studying in an environment fragranced by essential oils. In this paper, the influence of "rosemary" essential oil, which is known to improve memory and concentration [6], on learning performance and mood are investigated using two tasks; reading task and verbal memory task. Subjective evaluation is also analysed considering preference for the odor.

2 EXPERIMENT

2.1 Participants

Participants were comprised of seventeen males and fourteen females, healthy university students, aged 19-26 years (mean age, 21.7±1.9 years). All the recruited participants were engineering majors in order to reduce individual effect due to knowledge differences. Thirty-one participants were randomly assigned to one of two groups: a group under the odor environment with rosemary essential oil (Rosemary), and a control group using water vapor (No Atomizing). All of them were non-smokers and passed the screening test of using five kinds of standard odor ("T&T olfactometer": the standard olfactory test for selecting participants in Japan), and they received reward for participating in the experiments. Experimental conditions are shown in **Table1**.

Table 1: Experimental conditions

	Number of Participants						**Elapsed Days**	
	First Test			**Second Test**				
	Male	Female	Total	Male	Female	Total	Average	Min / Max
Control (No Atomizing)	7	8	15	7	7	14	38.9	31 / 44
Rosemary	10	6	16	7	5	12	40.2	37 / 44

2.2 Experimental setup

The experiment was carried out in the meeting room of Osaka University from December 2018 to February 2019. A heat exchange ventilating unit (100 m^3/h airflow rate from the catalog value) and a packaged air conditioner were installed on the ceiling. In order to distribute the aroma odor evenly in the whole room, four circulators were placed at the four corners of the room, and the aroma diffuser was set on one of the circulators (**Fig.1**).

The detailed time schedule for each experimental session is shown in **Fig.2**. Aroma atomization from the diffuser was started twenty minutes in advance of experiment. The participants were given instructions outside the room and started subjective evaluation right after they entered the room.

In this experiment, Rosemary cineole (produced by Tree of Life Corp.) was used to provide the odor environment. Rosemary was chosen for its effects of enhancing memory and concentration. Rosemary essential oil was atomized for 10 seconds in every minute, from the nebulizing aroma diffuser.

Due to the concern that the thermal environment affects learning performance as well, PMV was measured using PMV meter (AM-101 manufactured by Kyoto Electronics Manufacturing CO., Ltd). CO_2 concentrations were also measured by portable CO_2 recorder (TR-76Ui manufactured by T&D Corp.), to make sure that the room air was mixed evenly.

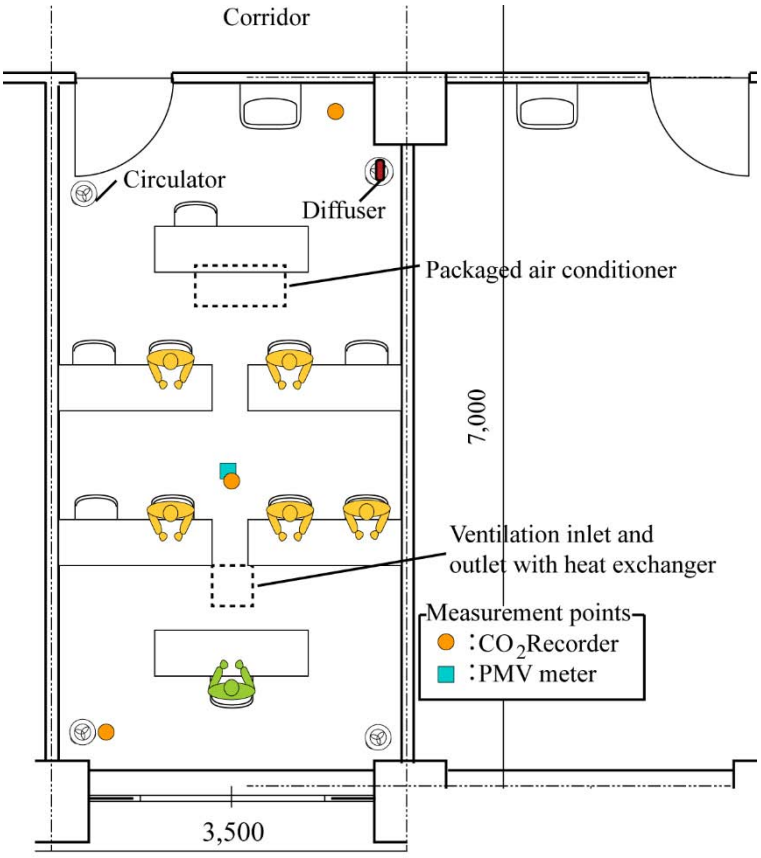

Figure 1: Plan view of the experimental room

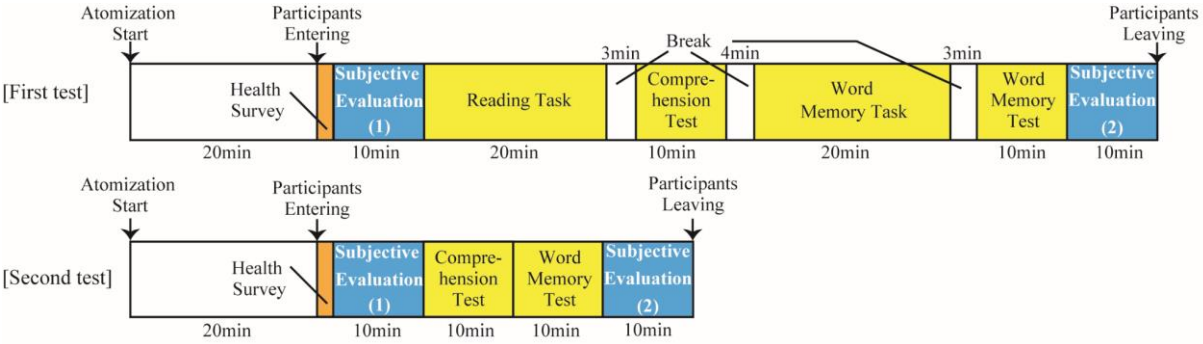

Figure 2: Experimental time schedule

2.3 Subjective Measurements

The questionnaire was used to obtain subjective evaluation included questions regarding perceived odor environment. All items of the questionnaire are shown in **Fig.3**. The perceived odor environment assessed using categorical scales describing the intensity of odor, odor pleasantness, preference, and impression of odor. In addition, acceptability of odor environment and acceptability assuming that participants study in the lecture room with the odor environment for 90 minutes were also assessed.

The odor intensity was measured using the 6-point category scale, and odor pleasantness and preference were measured using the 9-points category scales [7]. Both acceptability of the odor were assessed using continuous scales [8,9]. The twenty-one sets of odor impression were measured by Semantic Differential (SD) scale method with 7-points category [7]. All scales were presented in Japanese in the experiment.

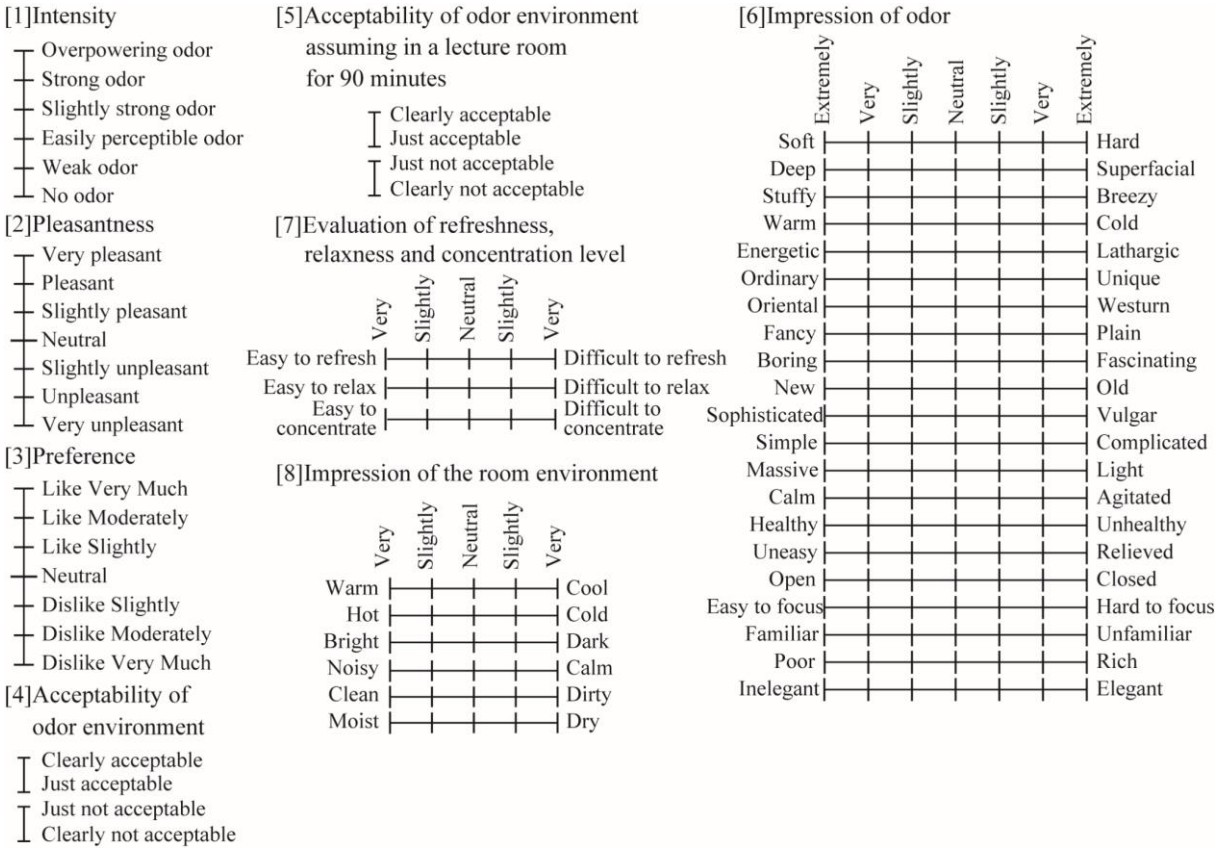

Figure 3: Scales for subjective evaluation

2.4 Subjective Measurements

Two types of tasks which simulated actual learning behaviors were adopted to evaluate the learning performance: a reading task and a memory task [10, 11]. The reading task was assessed by how many letters participants could read in 20 minutes and the score of comprehension test. Even though the answer was correct, it was not counted toward the score if the question was from the unread part. In addition, five-option two-choice questions were used to avoid a lucky guess.

The verbal memory task was evaluated by the score of vocabulary quiz. The Esperanto vocabulary list of 69 words and Esperanto dialogue with Japanese translation was offered to every participant. Participants memorized the vocabulary list for 20 minutes and took the word memory quiz. The Esperanto language was selected because it is written in alphabets and participants are less likely to have studied this language before. During the task, participants

were not informed what language it was. After the task, participants answered the question of what language it was. One participant knew about the Esperanto language and the data of the participant was excluded from the evaluation.

In order to examine the influence on memory retention, after a month, participants retook the same tests without being informed in advance. Maximum, minimum and average elapsed days from the first test to the second test are shown in **Table 1**.

3 RESULT AND DISCUSSION

3.1 Odor Intensity, odor pleasantness, preference and acceptability of odor

The measured results of odor intensity, odor pleasantness, preference and acceptability of odor are shown in **Fig.4(1)**. It was assumed that the preference of the odor would affect subjective evaluation; hence, the "Rosemary" group was further classified into two subgroups: a group of participants who like the scent of rosemary ("like" group, N=9) and a group of participants who dislike it ("dislike" group, N=5). The mean value of the Rosemary group tends to be close to neutral compared with control group. However, it was revealed that there were significant differences between evaluation of the "like" group and the "dislike" group. The "like" group evaluated the odor environment produced by the rosemary essential oil as more pleasant and more acceptable. In the second subject evaluation, all results got close to neutral. Olfactory adaptation could be the reason.

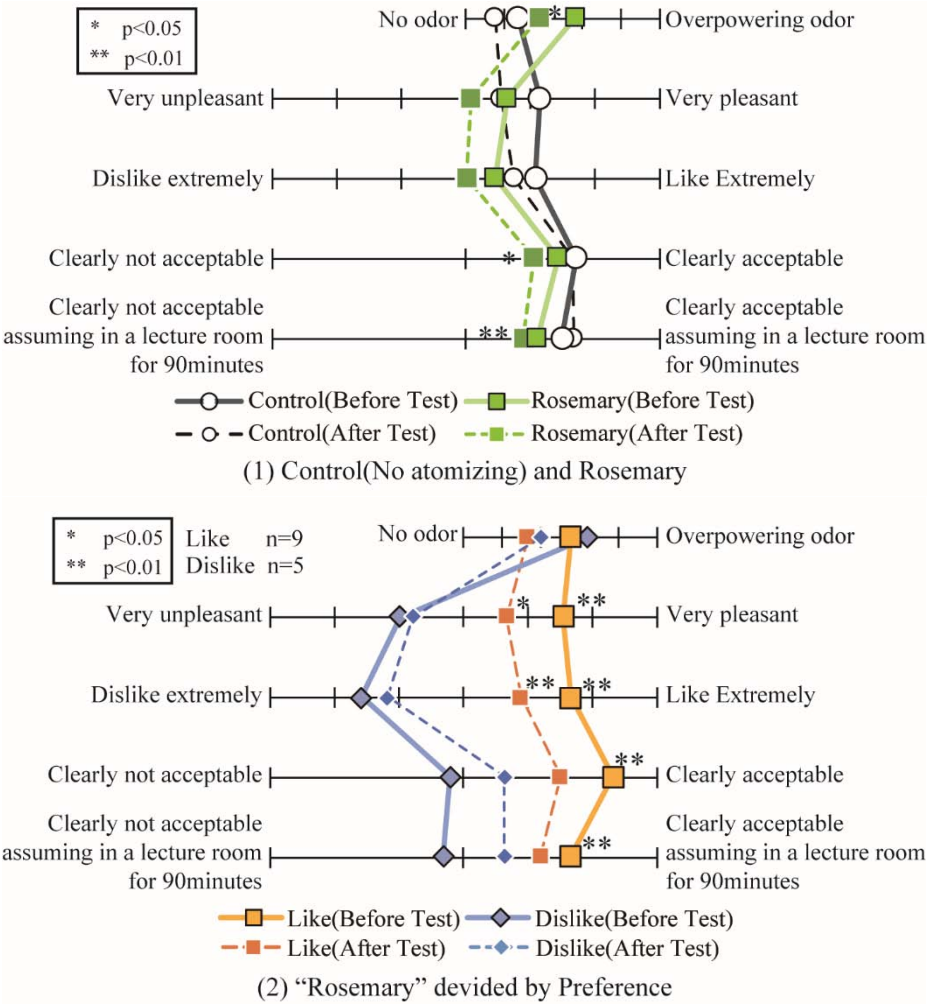

Figure 4: Intensity, Pleasantness, Preference and acceptability of odor. The results of the t-test are indicated by ''*'' for 5% statistical significance and by ''**'' for 1% statistical significance in figures.

3.2 Percentage of dissatisfied

Percentages of dissatisfied (PD) were calculated using the evaluations on the acceptability scale. PD of the rosemary odor in the environment itself, as well as assuming learning in a lecture room with an odor, are shown in **Fig 5**. The environment with the odor of rosemary tends to be acceptable. However, PD increased when it was assumed that the rosemary odor exists in the lecture room. Participants may feel that studying in the room under the aroma environment is an unfamiliar situation. PD for both questions decreased with each subjective evaluation. One reason for decreasing of PD was that there were fewer participants in the second test than in the first test. Another reason could be the influences of olfactory adaptation and habituation.

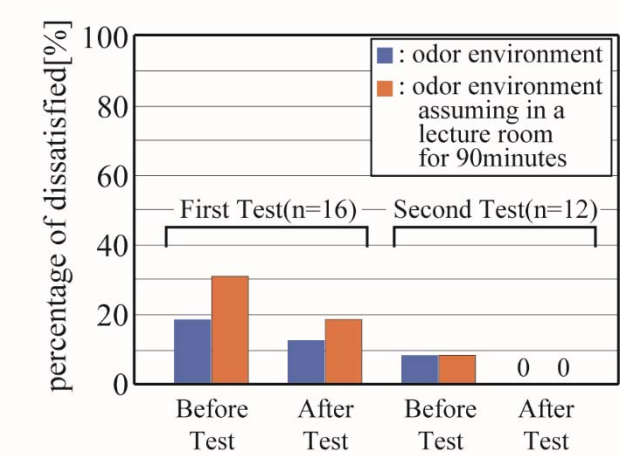

Figure 5: Percentage of dissatisfied of rosemary

3.3 Percentage of dissatisfied

The impression of the odor in the experimental room was evaluated using the SD method (**Fig. 6**). There were significant differences between the control and rosemary groups in the adjective pairs of "Energetic-Lethargic", "Unique-Ordinary", "Plain-Fancy", "Simple-Complicated" and "Easy to focus-Hard to focus". It was also revealed that the preference for the odor considerably affected the impression of odor. In most of the adjective pairs, the "like" and "dislike" groups selected opposite sides. The participants who liked rosemary tended to have a more positive impression than those who disliked it. However, interestingly, concerning the adjective pair "Unique–Ordinary," both the "like" and "dislike" groups considered rosemary odor slightly unique.

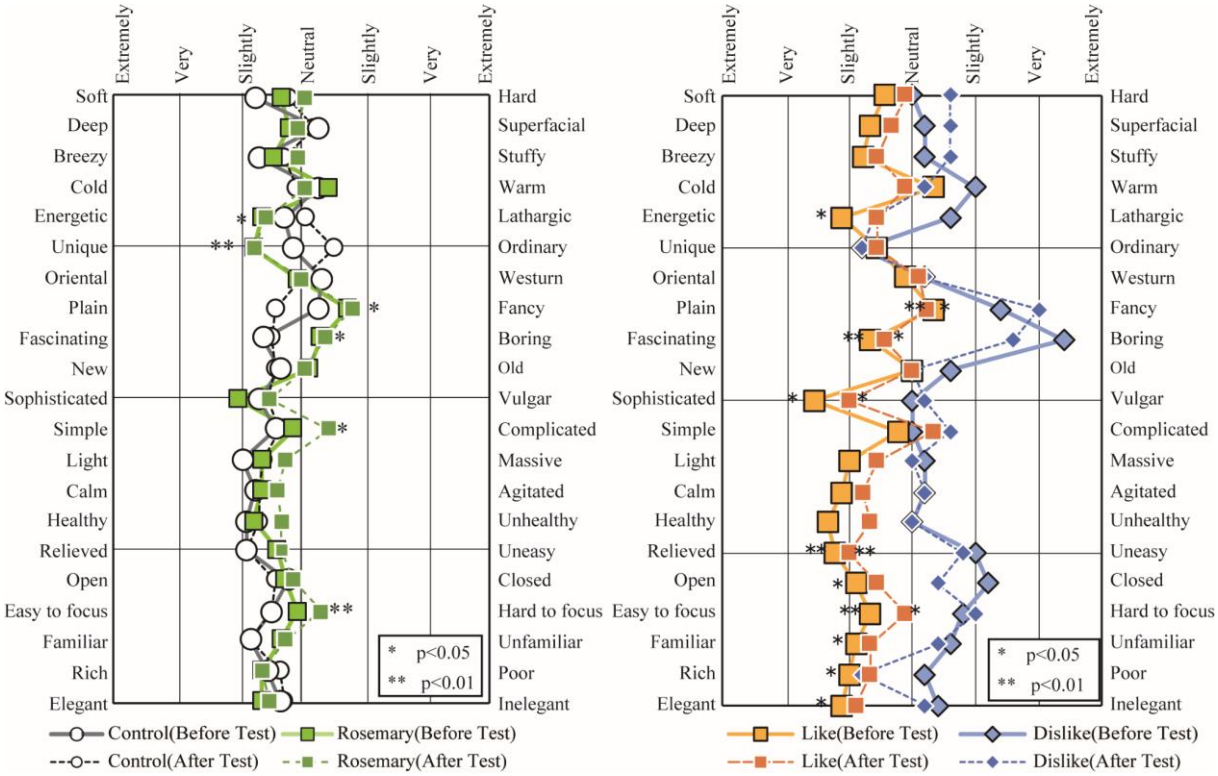

Figure 6: Impression of odor. The results of the t-test are indicated by ‘‘*’’ for 5% statistical significance and by ‘‘**’’ for 1% statistical significance in figures.

3.4 Impression of the room environment

As shown in **Fig.7**, the impression of the room did not differ significantly between control and rosemary groups. Participants, however, who dislike rosemary evaluated the experimental room as hotter and dirtier compared with participants who like rosemary in the first subjective evaluation (Before test). However, there was no significant difference in the second evaluaiton (After test). The odor may not make a considerable difference to the impression of the room, especially in terms of light and acoustic environments.

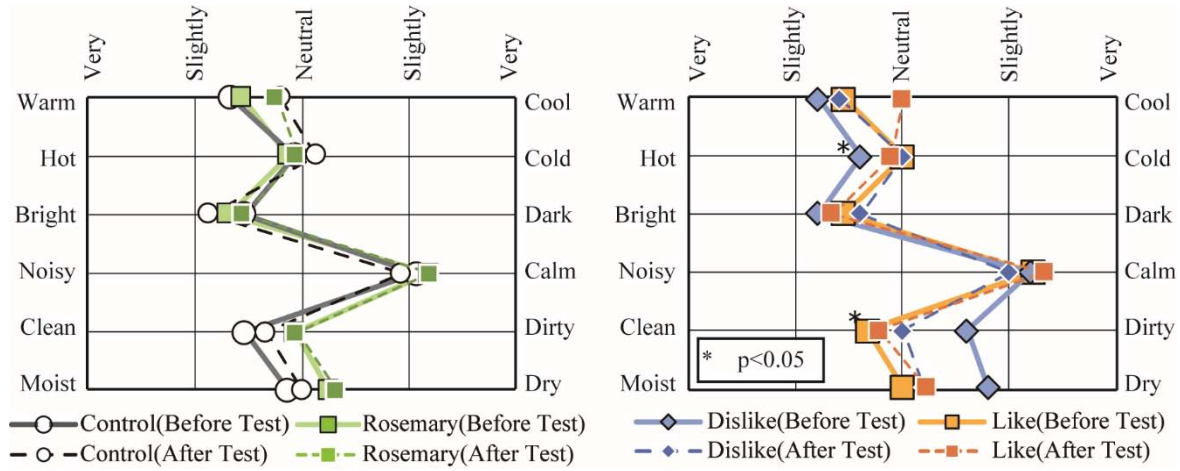

Figure 7: Impression of the conference room. The results of the t-test are indicated by ‘‘*’’ for 5% statistical significance and by ‘‘**’’ for 1% statistical significance in figures.

3.5 Impression of the room environment

Fig.8 shows the subjective evaluation results of the impression of odor environment. The mean value of the rosemary group was close to neutral in every item. However, considering the preference for the odor, participants who like the rosemary odor evaluated the odor as easier to refresh, relax, and concentrate than the "dislike" group. The results indicate that the preference for the odor has a great influence on how people feel and act.

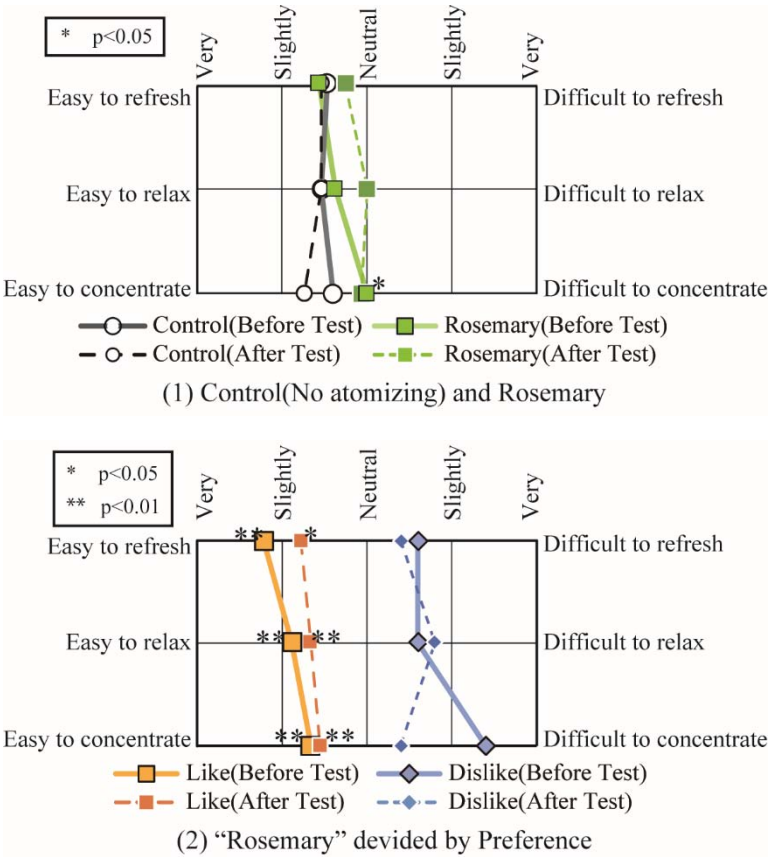

Figure 8: Impression of the odor environment. The results of the t-test are indicated by ''*'' for 5% statistical significance and by ''**'' for 1% statistical significance in figures.

3.6 Tests Scoret

Test scores of two methods are shown in **Fig.9**. The rosemary group read a larger number of letters than the control group ($p<0.05$). However, there was no significant difference in the correct answer rate of the comprehension test after reading between two conditions (**Fig.9(2)**). The result indicates that the rosemary group could read faster than the control group without decreasing the comprehension level. Furthermore, the average number of read letters was larger with the "like" group, compared with the "dislike" group. Hence, the preference for odor may also influence reading speed.

On the other hand, there was no difference between the rosemary and the control group in terms of the scores of the verbal memory test (**Fig.9(3)**). **Fig.9(4)** presents the measured results of the memory retention rate, which is the ratio of the second test score to the first test score. The average scores of two groups (rosemary and control) were nearly equal in the two tests. The odor environment of rosemary hardly had an effect on both short-term and long-term memories in this experiment.

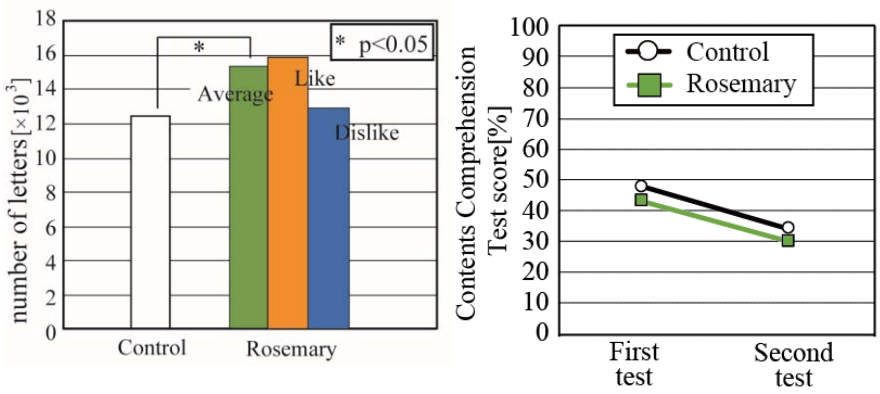

(1) Number of letters (2) Test score: Reading task

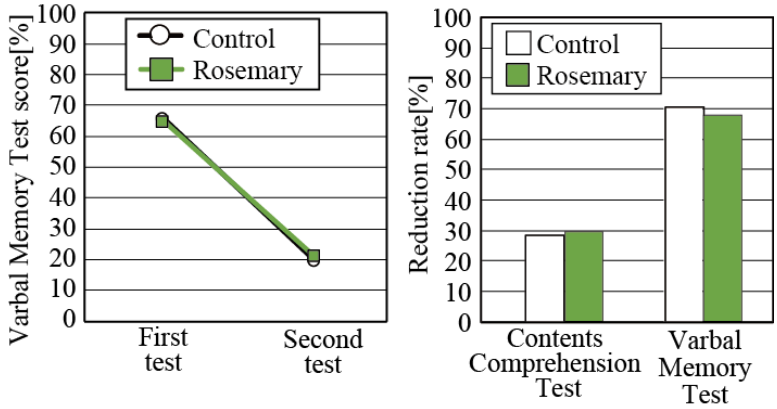

(3) Test score: Verbal Memory (4) Memory retention rate

Figure 9: The results of learning performance tasks

4 CONCLUSIONS

・In this experiment, the reading speed of the rosemary group was faster than the control group, without any effect on reading quality. Rosemary essential oil may have a positive effect on enhancing concentration.

・There were no significant differences between rosemary and control groups in terms of memory retention.

・The preference for the odor affects the impression of the odor environment greatly. Participants who like rosemary tend to evaluate the odor environment positively.

・The percentage of dissatisfied decreased during the experiment, and the possible reason could be the influence of adaptation and habituation.

5 ACKNOWLEDGEMENTS

This research was supported financially by Daikin Industries, Ltd.

6 REFERENCES

[1] S. P. Corgnati, M. G. Da Silva, R. Ansaldi, E. Asadi, J. J. Costa, M. Filippi, J. Kaczmarczyk, A. K. Melikov, B. W. Olesen, Z. Popiolek, P. Wargocki, “Indoor Climate Quality Assessment”, REHVA Guidebook No.14, 2011

[2] D.P. Wyon, P. Wargocki, “Room temperature effects on office work.” In: Clements-

Croome, D. (ed.) Creating the Productive Workplace, 2nd ed., 181 – 192. London: Taylor & Francis, 2006a
[3] D. P. Wyon, P. Wargocki, "Indoor air quality effects on office work" In: Clements-Croome, D. (ed.) Creating the Productive Workplace, 2nd ed., 193 – 205, London: Taylor & Francis, 2006b
[4] P. Wargocki, D. P. Wyon, "Research report on effects of HVAC on student performance", ASHRAE Journal Vol. 48, pp.23-28, 2006
[5] D. E. Gaygen, A. Hedge, "Effect of acute exposure to a complex fragrance on lexical decision performance", Chemical Senses, 34, pp.85-91, 2009
[6] M. Moss, J. Cook., K. Wesner, P. Docket, "Aromas of rosemary and lavender essential oils differentially affect cognition and mood in healthy adults", International Journal of Neuroscience Vol.113, pp. 15-38, 2003
[7] M. Matsuo, T. Yamanaka, H. Kotani, T. Tomita, "Sensory Evaluation of Odor from Building Materials (Part3) Effect of Odor Concentration on Odor Intensity, Comfort, Taste and Acceptability", Journal of Architectural Institute of Japan, D-2, pp. 957-958, 2001 (In Japanese)
[8] P. Wargocki, D. P. Wyon, Y. K. Baik, G. Clausen, P. O. Fanger, "Perceived air quality, sick building syndrome (SBS) symtoms and productivity in an office with two different pollution loads", Indoor Air, 9, pp.165-179, 1999
[9] L. Gunnarsen, P. O. Fanger, "Adaptation to indoor air pollution", Energy and Building, 16, pp.43-54, 1992
[10] S. Tsujimura, K. Ueno, "Effect of Sound Environment on Learning Efficiency in Classrooms", Journal of Environmental Engineering (Transactions of AIJ) Vol.75, pp. 561-568, 2010 (In Japanese)
[11] G. Iwashita, Y. Hanada, T. Gohara, "The impact of the room temperature on occupant productivity", Journal of Environmental Engineering (Transactions of AIJ) Vol.69, pp. 55-60, 2004 (In Japanese)

A large-scale longitudinal indoor air quality study: is low-cost sensor deployment a viable approach?

James A. McGrath*[1], Alison Connolly[2] and Miriam A. Byrne[3]

[1]*National University of Ireland Galway,*
University Road,
Galway,
H91 CF50,
Ireland.
Corresponding author: james.a.mcgrath@nuigalway.ie

ABSTRACT

To date, the vast majority of indoor air quality studies have relied on repeated visits to dwellings to obtain data derived from short-term monitoring exercises, a time-consuming process that places considerable constraints on personnel, equipment and costs. These studies have focussed on the use of research-grade instrumentation; however, recent developments in the field of consumer-grade indoor air quality sensor technology offers new opportunities. Several studies have reported that these devices provide sufficient accuracy to be utilised in longitudinal studies and collect data via remote transmission. This new development means that it is now possible to collect longer-term data and larger sample sizes than was previously possible. However, additional factors need to be considered that did not represent issues when short-term sampling methodologies were employed. Factors that influence occupant engagement and data transmission need to be considered. With reference to three customer-grade sensors, this current study focusses on reviewing a set of parameters that should be considered for longitudinal studies. .

One customer-grade sensor device was selected for demonstrative purposes and its capability to remotely transmit data was assessed. To date, the device has recorded data for 86 consecutive days from March to June 2019. In addition to compiling summary statistics, it was possible to download all the raw data and analyse indoor environmental quality parameters which exceeded baseline scenarios. The results showed that while the average temperature was 20.4°C; the average hourly temperatures exceeded 24°C for a cumulative time of 1512 hours and exceeded 26°C for a cumulative time of 509 hours over the period. Similarly for CO_2, the average concentration was 546 ppm; however, the hourly average of the CO_2 concentrations exceeded 1000 ppm for 100 hours over the period.

While several factors need to be considered when selecting a device, and it is possible that a single device will not fit all scenarios, preliminary results indicate that customer-grade instruments have the potential for applications in conducting longitudinal based indoor air quality studies. Further work is planned to evaluate the effectiveness of larger-scale deployment within indoor environments for extended periods.

KEYWORDS

- Indoor air quality
- Large scale data collection
- Low-cost sensors
- Indoor built environment

1 INTRODUCTION

The personal exposure of an individual to air pollution has a negative impact on their health (WHO, 2010). Residential exposures to air pollutants are of particular concern, as occupants spend more than half of the time spent in their residence (Klepeis et al., 2001, Broderick et al., 2015), with elderly and children spending up to 100% of their time in dwellings (Torfs et al., 2008). Numerous studies have highlighted that indoor activities contribute to air pollution through combustion events such as smoking, frying, solid fuel fires and use of candles and incense (Broderick et al., 2017, Semple et al., 2012, He et al., 2004, Morawska et al., 2013) and resuspension activities such as cleaning, walking, and vacuuming (Ferro et al., 2004, Boor et al., 2015).

Volatile Organic Compounds (VOCs) are gases emitted from different solid or liquid materials that include a variety of chemicals compounds. VOCs can be generated from a range of sources: furnishings, construction materials, paints, adhesives, cleaners, frying foods, smoking, dry cleaned clothing, deodorisers, showering, moulds and pesticides (Torfs et al., 2008, Hiscock et al., 2012, Brown et al., 2015). In a recent study, Svanes et al. (2018) reported that inhalation exposure to cleaning products could be as harmful as smoking 20 cigarettes per day. The study found that among women who used sprays or other cleaning products at least once per week, there was an associated decline in lung function.

Numerous studies highlight the potential for large spatial variations in pollutant concentrations even within the same dwelling due to the presence of doors and walls (Ferro et al., 2009, Du et al., 2012, McGrath et al., 2014b). These factors have important implications for exposure estimations and factors that influence ventilation controls (temperatures and humidity sensors). Spatial variations can also occur due to different requirements for mechanical ventilation; habitable rooms, kitchen, utility room, bathroom and sanitary accommodation (no bath or shower) can have varying minimum extract rates (DHPLG, 2019, DHPLG, 2009). The temporal variation in indoor air quality, due to building-, occupant- and environment- related factors, has been widely recognised (Tsai, 2018, McGrath et al., 2014a). In a study of seasonal indoor air quality variations, Bekö et al. (2016) noted that while building regulations require a minimum outdoor air supply rate, moisture generation typically will not be constant, and varies significantly with occupant activities. The authors expressed concern about the criteria surrounding a minimum outdoor air supply rate and its ability to account for varying moisture generation. While moisture, CO_2 and temperature can be strongly linked to occupants' activities (cooking, washing clothes, showering) (Yik et al., 2004, Persily, 2015), there is a need to also consider pollutants that can be generated without an occupant, such as radon (McGrath and Byrne, 2019, Collignan et al., 2016).

Reliable estimates of indoor environmental quality require sample sizes with larger datasets due to the complex nature of the indoor built environment (where some of the influencing factors on air quality are building characteristics, occupant behaviour, ventilation type, and ventilation system maintenance). The IEA's Energy in Buildings and Communities Programme established Annex 68 to discuss "*Indoor Air Quality Design and Control in Low Energy Residential Buildings".* As part of this Annex, Cony Renaud Salis et al. (2017) noted that there are very limited data available regarding pollutant concentrations in low-energy residential buildings. The issue is complicated as the data are usually reported only as aggregated pollutant concentrations (average, min, max), which lack detail for an individual building.

The relative cost of research-grade indoor environmental quality (IEQ) instruments has placed considerable constraints on conducting large-scale monitoring campaigns. The vast majority of relevant studies to date have relied on repeated visits to dwellings to obtain data derived from short-term monitoring exercises, a time-consuming process that places constraints

on both personnel and equipment resources. However, recent advancements in the development of customer-grade (low-cost) sensors with the capability for remotely transmitting information means that there is now a unique opportunity to gather large-scale monitoring data without the traditional constrictions.

A number of studies show that customer-grade sensors have the potential to reasonably measure indoor air quality. Moreno-Rangel et al. (2018) compared a Foobot FBT0002100 with GrayWolf instruments (GrayWolf Sensing Solution, Shelton, CT, USA), where the GrayWolf probes represented high-grade research equipment. The study reported a significant agreement with temperature (r_s= 0.832–0.871), relative humidity (r_s= 0.935–0.948), *t*VOC (r_s= 0.827–0.869), and $PM_{2.5}$ (r_s= 0.787–0.866) data. However, the Foobot device lacked a specific CO_2 sensor and instead estimated CO_2 based on a percentage of TVOC measurements. Singer and Delp (2018) compared the accuracy of seven low-cost IEQ devices (AirBeam 1, Air Quality Egg, AirVisual Node, Awair, Foobot, Purple Air PA-II, and Speck) with two research-grade optical aerosol monitors (pDR-1500, MetOne BT-645). The study generated fine particulate matter based on common residential sources in laboratory conditions and analysed time-resolved measurements. Four of the devices measured were deemed suitable to have sufficient accuracy and reliability to detect large PM sources within the residential environment; although the devices were not considered suitable for detecting all sources of ultrafine particle emissions (below 0.3 μm diameter).

Developments in low-cost sensor technology, combined with the capability for remotely transmitting information, means that there is now a unique opportunity to gather large-scale monitoring data without the traditional constrictions. Longitudinal studies have the potential to overcome, through continuous monitoring, the traditional uncertainties associated with occupant behaviour and short-term changes in the built environment that are a current limitation in short-term monitoring studies. The objective of this study is to evaluate the conditions under which consumer-grade monitors can optimally perform large-scale data collection.

2 METHODOLOGY

2.1 Review of devices

For the purposes of this study, the focus was not on the accuracy and analysis of the sensors, as earlier studies have already quantified these factors. The current study instead concentrated on parameters that need consideration when conducting a longitudinal-based monitoring study. Several factors need specific attention that would not be necessary during traditional-short-term monitoring exercises.

Occupants' willingness to participate in monitoring studies was deemed the highest priority, and as such, it was felt that off-the-shelf products were designed to be visually more appealing, while custom-made devices are unlikely to achieve the same level of aesthetics. For this reason, custom-made devices controlled by micro-controllers (Arduino, Raspberry Pi, etc.) were not considered in the scope of this review.

This study focussed on factors including: wireless data transmission protocols; continuous recording and transmission of information; occupants' behaviour and willingness to maintain engagement. The use of battery vs mains power supply is a factor which has varying importance depending on the sampling duration, as occupants may or may not be willing to leave devices plugged in for extended periods. The size, mounting option and visual appeal need to be considered to ensure that the occupants do not move the devices during the course of the study.

The strengths of longitudinal-based studies are the ability to collect long-term measurements; therefore, consideration must be given to ensure that the raw data can be obtained over the sampling period. Several devices store the data on a cloud-based server;

however, some devices display the data via a smartphone and the ability to access the raw data via an online-portal needs to be considered.

Three IEQ sensors were identified; uHoo (uHoo Air, Hong Kong, Hong Kong), Airthings Wave Plus (Oslo, Norway) and Foobot (Foobot, Belvaux, Luxembourg). These devices were reviewed based on the factors discussed above.

2.2 Pilot study of a selected device

One sensor, the Airthings WavePlus, was selected for demonstrative purposes to assess the capability and potential application ofthese devices during monitoring campaigns. The device was placed in a naturally-ventilated office (approximate volume 28 $m^{3,}$ and dual occupancy) from March 2019 until June 2019 The device was mounted on the wall, as shown in Figure 1.

Figure 1. A IEQ sensor mounted on the wall in an office.

3 RESULTS

Table 1 summarises some of the characteristics that should be considered when selecting a device for monitoring in a longitudinal based study. Occupants' willingness to maintain engagement with the study becomes a greater challenge the longer the desired sampling period; power consumption, sampling location and position of the sensor are factors that require greater consideration for long term monitoring.

The data transmission protocol is a factor that needs particular care. While some devices operate via a mobile-phone app, this ultimately requires the occupant to login into the app on a regular basis to allow the data to upload to the servers; this can pose challenges in terms of long-term engagement, but also has the potential to introduce bias as the occupant becomes aware of their air quality conditions. While uHoo and Footbot connect directly to a Wi-Fi network, they currently do not support secondary authentication login portals, managed login networks or networks protected by firewalls. While these networks are considered to be less common in the residential environment, they may occur in some localised situations.

Table 1: A summary of key factors for three different customer-grade IEQ sensors.

Parameters	Wave Plus	uHoo	Foobot
Internal storage	Yes		No
Remote data transmission protocols	Only uploads data to cloud via smartphone (Bluetooth connectivity). Alternatively, can connect directly to the cloud via additional hub (Bluetooth connectivity)	Connects to the clould via a private WiFi network	Connects to the clould via a private WiFi network
Monitoring Parameters	Radon, Humidity, TVOCs, Temperature, CO_2 and Air Pressure	Temperature, Humidity, VOC, CO_2, Air Pressure, Particulate Matter (PM2.5), Nitrogen Dioxide, Carbon Monoxide and Ozone	Fine Particles, Total VOC, Carbon Dioxide, Temperature and Humidity
Sampling Resolution	5-minute resolution for Humidity, TVOCs, Temperature, CO2 and air pressure: Hourly for radon	1-minute intervals	5-minute intervals
Power Supply	Battery Operated - 2 AA batteries	Micro USB power adapter and 5V DC external power adapter	AC-DC 5V 0.5A USB power adaptor
Cloud base storage	Cloud-based with iOS and Android mobile applications include online dashboard	Cloud-based with iOS and Android mobile applications	Stores data in a cloud based server
Access to the raw data	Downloadable CSV files	Downloadable CSV files (with Uhoo Pro)	Downloadable
Warranty on the devices	1-year warranty	1-year warranty	1-year warranty
Position / Mounting	Supports wall or ceiling mount	Rests on a horizontal surface	Rests on a horizontal surface
Dimensions	12 cm (diameter) x 3.6 cm (height)	16.5 cm (height) x 85 cm (diameter)	7.1cm (diameter) x 17.2 cm (height)
Weight	219 grams	210 grams	475 grams
Restricted access	Assigned to a smartphone via an app log in.	Assigned to a smartphone via an app log in.	Assigned to a smartphone via an app log in.

Table 2: A summary of the indoor environmental parameters collect by the AirThings WavePlus over an 86 days period.

	Radon ($Bq\ m^{-3}$)	Temperature (°C)	Relative Humidity (%)	Air Pressure (Pa)	CO_2 (ppm)	VOCs (ppb)
Average	17	20.4	42.7	101,377	546	207
Standard Deviation	9	2.4	6.6	1,119	105	165
Minimum	0	11.2	21.5	97,610	399	0
Maximum	76	29.5	58.0	103,670	1288	659

The IEQ device recorded temperature, humidity, carbon dioxide, TVOCs and air pressure at 5-minute intervals and the radon concentration at hourly intervals. Table 2 summarises the raw data exported from the Airthings dashboard over the entire 86-day period. In total, 125,538 data points were collected over the sampling period.

Figure 2 shows the time-series trends collected by the WavePlus over a month-long period. The figure represents a screenshot of the dashboard taken from the web browser. While the averages are displayed on the left-hand side, the time-series data displayed on the right-hand side provides a more-detailed analysis of the conditions within the room. Pre-defined conditions established by Airthings determined the colour coding on the graphs; for example, the red spikes in the temperature data corresponds to when the temperature exceeds 25°C, while the blue portions indicate where the temperature fell below 18°C.

Figure 2: A screenshot showing the dashboard containing the data collected using an AirThings WavePlus. The figure shows data for a month-long period for radon, TVOCs, carbon dioxide, humidity, temperature and air pressure measurements

Based on the quantity of data collected, it was possible to further analyse the raw data. While the average temperature was 20.4°C, further analysis determined that the average hourly temperatures exceeded 24.0°C for a cumulative of 1,512 hours and exceeded 26.0°C for a cumulative of 509 hours over the period. Similarly, the average CO_2 was 546, while the hourly average of the CO_2 concentrations exceeded 1,000 ppm for 100 hours over the period.

4 CONCLUSIONS

The traditional approaches to monitoring indoor air quality in residential environments rely upon repeated visits to dwellings, and this poses considerable constraints on personnel, equipment and costs. These constraints limit the capability of obtaining comprehensive data sets, including the number of houses and the sampling duration. Recent developments in the field of consumer IEQ sensor technology offers the possibility to conduct longitudinal studies. The current study identified factors that need to be considered when using customer-grade sensors for longitudinal studies that are not associated with traditional monitoring using research-grade instrumentation. Three different customer-grade sensors were selected and reviewed in this context. Each device has advantages and disadvantages that facilitate their use in longitudinal studies. The circumstances that surround the monitoring campaign (duration, location, occupants, air quality parameters, Wi-Fi transmission) will influence the device that is selected for the monitoring campaign.

One sensor was selected to assess its potential application in longer-term monitoring. The device recorded six indoor environmental parameters (temperature, humidity, carbon dioxide, TVOCs, radon and air pressure) and collected data in an office environment for 86 days. Average, standard deviation, minimum and maximum values were calculated based on the raw data. In addition, it was possible to identify periods and durations during which environmental conditions were exceeded.

The results show promising trends where customer-grade instruments could be used to conduct longitudinal based indoor air quality studies; these have been significantly constrained to date. The next stage of the current project is to deploy the sensors in 10 residential environments and assess the ability to remotely collect and analyse the data from these dwellings. The longitudinal approach will capture changes in occupants' behaviour, seasonal variations, meteorology conditions and varying spatial variation within a dwelling.

5 ACKNOWLEDGEMENTS

This work represents research funded by Sustainable Energy Authority of Ireland (SEAI) under the Research, Development and Demonstration (RD&D) Funding Programme 2018 (RDD00284) 'Assessment of VentilAtion effectiveness via a Longitudinal indoor environmental study in 'A' rated Irish Dwellings: VALIDate'.

6 REFERENCES

BEKÖ, G., GUSTAVSEN, S., FREDERIKSEN, M., BERGSØE, N. C., KOLARIK, B., GUNNARSEN, L., TOFTUM, J. & CLAUSEN, G. 2016. Diurnal and seasonal variation in air exchange rates and interzonal airflows measured by active and passive tracer gas in homes. *Building and Environment,* 104**,** 178-187.

BOOR, B. E., SPILAK, M. P., CORSI, R. L. & NOVOSELAC, A. 2015. Characterizing particle resuspension from mattresses: chamber study. *Indoor Air,* 25**,** 441-456.

BRODERICK, Á., BYRNE, M. A., MCGRATH, J. A. & COGGINS, A. M. Indoor Air Quality and Thermal Comfort in Irish Retrofitted Energy Efficient Homes. *In:* CENTRE., A. I. A. V., ed. 38th AIVC - 6th TightVent & 4th venticool Conference,, 13-14 September 2017 2017 At Crowne Plaza Hotel, Nottingham UK.

BRODERICK, B., BYRNE, M., MCNABOLA, A., GILL, L., PILLA, F., MCGRATH, J. & MCCREDDIN, A. 2015. PALM: A Personal Activity-Location Model of Exposure to Air Pollution. Environmental Protection Agency, Wexford, Ireland.

BROWN, T., DASSONVILLE, C., DERBEZ, M., RAMALHO, O., KIRCHNER, S., CRUMP, D. & MANDIN, C. 2015. Relationships between socioeconomic and lifestyle factors and indoor air quality in French dwellings. *Environmental Research,* 140**,** 385-396.

COLLIGNAN, B., LE PONNER, E. & MANDIN, C. 2016. Relationships between indoor radon concentrations, thermal retrofit and dwelling characteristics. *Journal of Environmental Radioactivity,* 165**,** 124-130.

CONY RENAUD SALIS, L., ABADIE, M., WARGOCKI, P. & RODE, C. 2017. Towards the definition of indicators for assessment of indoor air quality and energy performance in low-energy residential buildings. *Energy and Buildings,* 152**,** 492-502.

DHPLG 2009. Buildings Regulations 2009 - Technical Guidance Document F - Ventilation. *In:* DEPARTMENT OF HOUSING, P. A. L. G. (ed.).

DHPLG. 2019. *Buildings Regulations 2019 - Technical Guidance Document F - Ventilation* [Online]. Available: https://www.housing.gov.ie/housing/building-standards/tgd-part-f-ventilation/technical-guidance-document-f-ventilation [Accessed].

DU, L., BATTERMAN, S., GODWIN, C., CHIN, J. Y., PARKER, E., BREEN, M., BRAKEFIELD, W., ROBINS, T. & LEWIS, T. 2012. Air change rates and interzonal flows in residences, and the need for multi-zone models for exposure and health analyses. *Int J Environ Res Public Health,* 9**,** 4639-61.

FERRO, A. R., KLEPEIS, N. E., OTT, W. R., NAZAROFF, W. W., HILDEMANN, L. M. & SWITZER, P. 2009. Effect of interior door position on room-to-room differences in residential pollutant concentrations after short-term releases. *Atmospheric Environment,* 43**,** 706-714.

FERRO, A. R., KOPPERUD, R. J. & HILDEMANN, L. M. 2004. Source strengths for indoor human activities that resuspend particulate matter. *Environmental science & technology,* 38**,** 1759-1764.

HE, C., MORAWSKA, L., HITCHINS, J. & GILBERT, D. 2004. Contribution from indoor sources to particle number and mass concentrations in residential houses. *Atmospheric Environment,* 38**,** 3405-3415.

HISCOCK, R., BAULD, L., AMOS, A., FIDLER, J. A. & MUNAFÒ, M. 2012. Socioeconomic status and smoking: a review. *Annals of the New York Academy of Sciences,* 1248**,** 107-123.

KLEPEIS, N. E., NELSON, W. C., OTT, W. R., ROBINSON, J. P., TSANG, A. M., SWITZER, P., BEHAR, J. V., HERN, S. C. & ENGELMANN, W. H. 2001. The National Human Activity Pattern Survey (NHAPS): a resource for assessing exposure to environmental pollutants. *Journal of Exposure Analysis and Environmental Epidemiology,* 11**,** 231-252.

MCGRATH, J. & BYRNE, M. 2019. UNVEIL: UNderstanding VEntilation and radon in energy efficient buildings in IreLand. *Environmental Protection Agency, Wexford, Ireland.* http://www.epa.ie/pubs/reports/research/health/Research_Report_273.pdf.

MCGRATH, J., BYRNE, M., ASHMORE, M., TERRY, A. & DIMITROULOPOULOU, C. 2014a. Development of a probabilistic multi-zone multi-source computational model and demonstration of its applications in predicting PM concentrations indoors. *Science of The Total Environment,* 490**,** 798-806.

MCGRATH, J. A., BYRNE, M. A., ASHMORE, M. R., TERRY, A. C. & DIMITROULOPOULOU, C. 2014b. A simulation study of the changes in PM2.5 concentrations due to interzonal airflow variations caused by internal door opening patterns. *Atmospheric Environment,* 87**,** 183-188.

MORAWSKA, L., AFSHARI, A., BAE, G., BUONANNO, G., CHAO, C., HÄNNINEN, O., HOFMANN, W., ISAXON, C., JAYARATNE, E. & PASANEN, P. 2013. Indoor aerosols: from personal exposure to risk assessment. *Indoor air,* 23**,** 462-487.

MORENO-RANGEL, A., SHARPE, T., MUSAU, F. & MCGILL, G. 2018. Field evaluation of a low-cost indoor air quality monitor to quantify exposure to pollutants in residential environments. *J. Sens. Sens. Syst.,* 7**,** 373-388.

PERSILY, A. K. Indoor Carbon Dioxide Concentrations in Ventilation and Indoor Air Quality Standards. 36th AIVC Conference Effective Ventilation in High Performance Buildings, Madrid, Spain, September 23, 2015. 810-9.

SEMPLE, S., GARDEN, C., COGGINS, M., GALEA, K. S., WHELAN, P., COWIE, H., SANCHEZ-JIMENEZ, A., THORNE, P. S., HURLEY, J. F. & AYRES, J. G. 2012. Contribution of solid fuel, gas combustion, or tobacco smoke to indoor air pollutant concentrations in Irish and Scottish homes. *Indoor Air,* 22**,** 212-223.

SINGER, B. C. & DELP, W. W. 2018. Response of consumer and research grade indoor air quality monitors to residential sources of fine particles. *Indoor Air,* 28**,** 624-639.

SVANES, Ø., BERTELSEN, R. J., LYGRE, S. H. L., CARSIN, A. E., ANTÓ, J. M., FORSBERG, B., GARCÍA-GARCÍA, J. M., GULLÓN, J. A., HEINRICH, J., HOLM, M., KOGEVINAS, M., URRUTIA, I., LEYNAERT, B., MORATALLA, J. M., MOUAL, N. L., LYTRAS, T., NORBÄCK, D., NOWAK, D., OLIVIERI, M., PIN, I., PROBST-HENSCH, N., SCHLÜNSSEN, V., SIGSGAARD, T., SKORGE, T. D., VILLANI, S., JARVIS, D., ZOCK, J. P. & SVANES, C. 2018. Cleaning at Home and at Work in Relation to Lung Function Decline and Airway Obstruction. *American Journal of Respiratory and Critical Care Medicine,* 197**,** 1157-1163.

TORFS, R., BROUWERE, K. D., SPRUYT, M., GOELEN, E., NICKMILDER, M. A. & BERNARD, A., . 2008. Exposure and risk assessment of air fresheners. *Flemish Institute for Technological Research NV (VITO).*

TSAI, W.-T. 2018. Overview of Green Building Material (GBM) Policies and Guidelines with Relevance to Indoor Air Quality Management in Taiwan. *Environments,* 5**,** 4.

WHO 2010. WHO guidelines for indoor air quality: selected pollutants. http://www.euro.who.int/__data/assets/pdf_file/0009/128169/e94535.pdf?ua=1: World Health Organization.

YIK, F. W. H., SAT, P. S. K. & NIU, J. L. 2004. Moisture Generation through Chinese Household Activities. *Indoor and Built Environment,* 13**,** 115-131.

An argument for a reality check in the ventilation industry: We still have an energy crisis, in practice, and are not generally, in practice, achieving better indoor climate

Sergio George Fox [1]

[1] *AWE*
Consulting Engineers
Munkesøvej 1
4000 Roskilde,
Denmark

ABSTRACT

In 2017 the Danish Building and Property Agency started a project titled **"Avoiding energy waste in ventilation systems"** by tracking the actual energy use in a sample of their 4 million m^2 portfolio of buildings through on-line energy management tools. The project is not complete, but the key preliminary findings described in this paper are:

1. The energy consumption of ventilation systems is a much higher **proportion** of the total energy consumption of the buildings than expected.

2. The ventilation system **components** are generally well maintained, but the ventilation **systems** as a whole are not well maintained, which results in poor indoor climates in buildings, despite the high energy costs.

3. Although a component was possibly checked, it was found that an important distinction between component function and component quality caused operational problems if the component was not **calibrated,** or its real function was not **tested**.

4. Original design or installation **mistakes** not discovered at the time, often complicated by changes to the systems over time, led to additional ad-hoc attempts at system repairs over many years, which often did not address or correct the original faults.

5. The **control** systems are extensive and have developed - or mutated - over many years into webs of complexity that are difficult to analyse, understand or operate effectively, so that user complaints often lead to systems being "adjusted" inappropriately.

6. A growing tendency is the apparent abandonment of faith in existing ventilation systems and investment in several small **decentral** cooling or ventilation systems, often installed in the same areas served by the central ventilation systems, thus adding to the energy burden and also adding to the complexity of the indoor climate control systems.

7. Re-creating ventilation system **documentation** and design information combined with installing indoor climate data loggers allowed **analysis** of system performance, and thus revealed possibilities for simple indoor climate **improvement** as well as energy **savings**.

8. The overall results appear to confirm that the old saying **"Keep it simple"** is still true, and that the use of intelligent user-friendly data monitoring tools should be combined with simpler user-friendly control tools so that Facility managers and other operators can achieve a better correlation between energy use and indoor climate.

9. The overall **conclusion** of this study is that our ventilation industry is still too focused on theoretical project design and construction delivery, with an overall belief in complex controls. Combined with a lack of attention

to durability and operational performance, most ventilation systems degenerate within a short period of time into systems with high energy costs providing low indoor climatic quality.

10. The overall **recommendation** of this article is that our ventilation industry reduces its attachment to traditional business goals of growth and turnover and instead focuses on **quality** of the delivered product through simplification and durability.

KEYWORDS

Ventilation, Maintenance, Operation, Sustainability, Energy

1. INTRODUCTION

1.1. "From energy crisis to sustainable indoor climate"?

This conference title *"From energy crisis to sustainable indoor climate"* reflects the complacency, or possibly, some may say, the cynical marketing strategy, of our ventilation industry. Most engineers involved in the practical side of the industry, working with real systems in real buildings with real people, will probably smile at the title too. Don't we have **more** of an "energy crisis" now than ever before? What exactly is meant by "sustainable indoor climate"?

1.2. Time for real change in our industry?

From my previous work at the Danish Energy Authority, and now as a Consulting Engineer currently working on numerous building projects for the Danish Building and Property Agency, it does not seem that we in the ventilation industry produce much sustainability at all, and we certainly seem to be adding to the weight of the energy burden, not lightening it. One of the problems is that there seems to be a lack of real support from the ventilation industry for real change towards sustainability. As Fanger (Reference 7) once said of our ventilation industry's design methodology: **"What a waste!"**. That was in 2003.

1.3 Do the results match the image?

All this should be viewed within the framework of the image, expectations and ambitions of consecutive Danish Governments towards energy effectiveness and climate goals. Denmark prides itself on sustainable energy systems, and its advances in renewable energy **supply** systems, such as offshore wind power, have been a model for many nations. However, the net energy **consumption** in commercial and domestic buildings has not matched the transformation of the energy supply systems. In the period 1980 to 1990 energy consumption did fall, in all buildings, but since 1990, energy consumption has risen, and our ventilation industry is a major contributor to this problem. This problem is reflected throughout the EU, and indeed the world. See Figure 1.

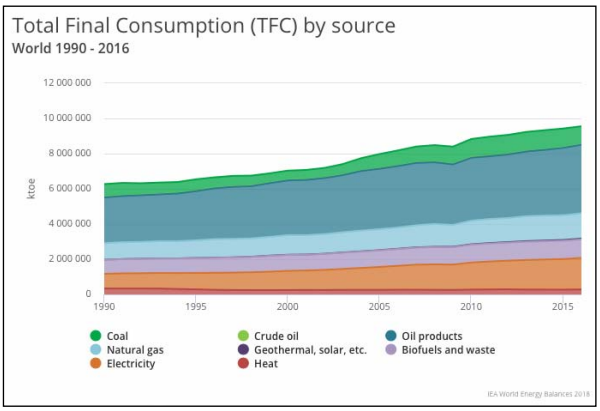

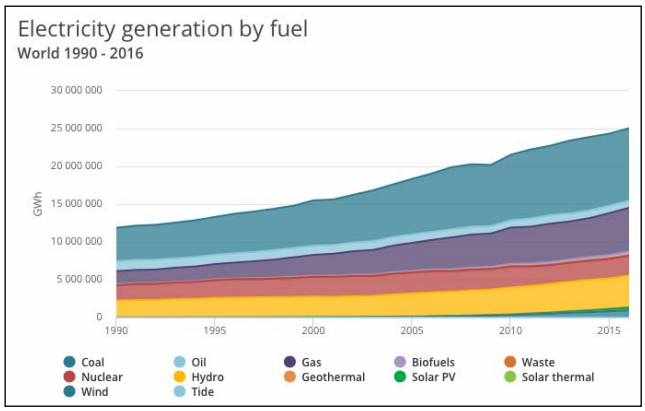

Figure 1: World Energy Consumption, IEA data. Electricity is one of the highest rising energy "sources".
https://www.iea.org/statistics/?country=WORLD&year=2016&category=Energy%20consumption&indicator=TFCbySource&mode=chart&dataTable=BALANCES

1.4 Our industry can do a lot better!

The hope with this paper is that it can contribute towards a "reality check" within the ventilation industry so that the very real challenges of climate change can be addressed seriously. Our children and grandchildren deserve more from us. Our industry can do a lot better, and we know it.

2. STATISTICS

2.1 National energy consumption data (Denmark)

It can be seen, with hard-core energy statistics, that most good intentions regarding energy savings do not seem to give results. See Figure 2 (from Reference 1). Energy consumption in all Danish buildings fell from 1980 to 1990, but has since been rising steadily, despite national and EU legislation and other initiatives.

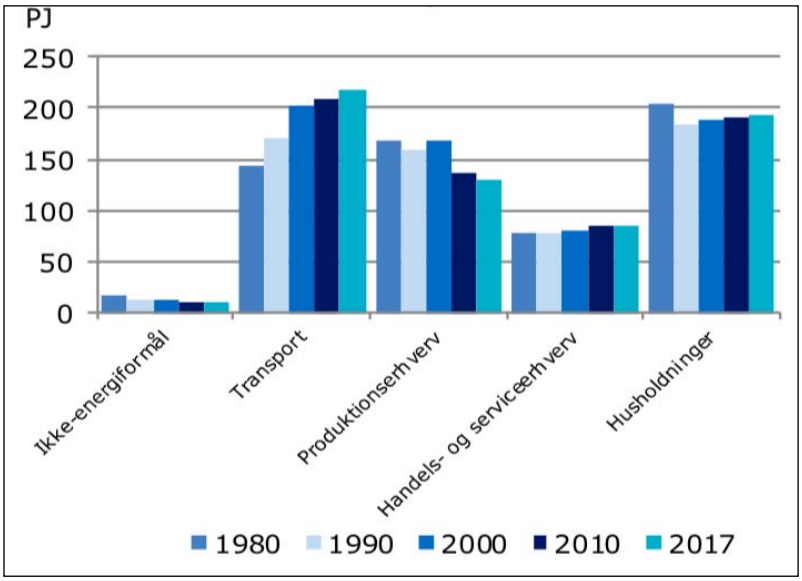

This figure from the Danish Energy Authority is only officially available in the Danish language.

The areas of interest for the ventilation industry are the two sets of columns on the right:

"Handels- og serviceerhverv" is ***"Commercial and Public Services"*** *and "Husholdninger" is* ***"Households"***

Figure 2: The **development in energy consumption** in Denmark from 1980 to the latest available statistics (2017) showing a rise in energy consumption in buildings for the past 30 years. (Reference 1).

2.2 Increase in energy consumption in buildings

Specifically, the percentage changes in the markets most served by the ventilation industry show very high energy consumption **increases** in the very period when energy saving initiatives were supposed to be taking effect. See Figure 3 (Reference 2). In particular, despite all the very real warnings about climate change, there are also increases in all categories in the latest statistical period 2016-2017. The EUs "Energy Performance of Buildings" Directive (Reference 3), has been in force for many years, but the message does not seem to have filtered down to the people actually responsible for running and using ventilation systems.

Change %		
1980-2017	1990-2017	2016-2017
50,5	-0,6	2,4
57,7	14,7	0,1
115,0	53,2	8,1
47,5	14,9	2,4

Electrical energy consumption changes in the following categories:

Wholesale.

Retail trade.

Private Service.

Public Service.

Figure 3: A detailed statistic from Figure 2, with numbers. The **percentage increase** in development in electrical energy consumption in commercial and public buildings in Denmark from 1980. (Reference 2).

2.3 Cost of energy in buildings run by the Danish Building and Property Agency

Getting away from statistics and moving into the area that most building Facility Managers are concerned with, that is, actual costs of providing (good) indoor climates, one can see in Figure 4 that electrical energy costs are the highest, and as we saw from Figure 3, are also rising at the highest rate. Our ventilation industry, including cooling and related components

such as pumps etc., are one of the main reasons for this electrical energy consumption in buildings.

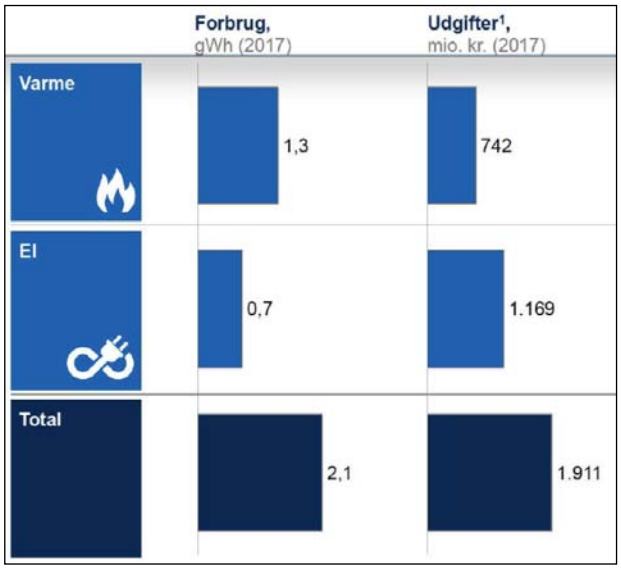

Heating ("Varme") is the highest consumption at 1.3 GWh, but electricity is the highest cost at 1,169 million kroner per year (157 million €/year (2017)).

Figure 4: A further breakdown from statistics, the heating and electricity consumption data and costs for the 4,1 million m^2 portfolio of the Danish Building and Property Agency (Reference 4).

3. ANALYSIS

3.1 The project "Avoiding energy waste in ventilation systems"

In 2017 the Danish Building and Property Agency started a project titled "Avoiding energy waste in ventilation systems". The Agency had for some years been tracking the actual energy use in their portfolio of buildings through on-line energy management tools such as "EnergyKey" and "WebTools". Although there was no clear quantifiable data about the extent of this ventilation system energy "waste", if in fact there was any, the hypothesis from the experienced Project Managers in the Agency was, that there was "something wrong".

3.2 First results: Phase 1 energy savings by simulated demand control.

After two years of investigations and tests, including pilot projects, there are clear indications that there is indeed "something wrong", and that customers, the users of the buildings, are not really getting what they pay for. In 2017 indoor climate dataloggers were set up in properties 3 and 8 in Figure 5, and after analysis of the actual use (CO2 levels and acoustic data) simple software changes to the control system to simulated demand controlled ventilation for one

ventilation system at each location gave measured energy savings of 9 %.

Figure 5: A detailed analysis of the energy consumption statistics: The electricity consumption data and pilot project results for the 10 buildings in the 2017-2019 project "Avoiding energy waste in ventilation systems" of the Danish Building and Property Agency (References 5 and 6).

3.3 Phase 2: Energy savings by wireless demand control.

In 2018 real demand controlled ventilation was installed for property nr. 10 for one ventilation system (out of five at the property) and gave 33 % measured savings (Figure 5). This was a surprisingly high result and indicated that the proportion of energy in total going to the ventilation systems was much higher, based on a rough analysis of the before and after performance (Figures 6 and 7). A programme of measuring the specific electrical consumption of the ventilation systems alone has now been implemented, with results expected in 2020.

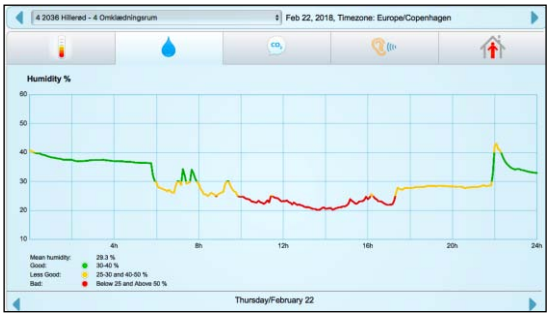

Figures 6 and 7: At the left, Fig. 6, showing the actual moisture levels in Property nr. 10 (Figure 5) before any changes (February 2018), with the ventilation system running at full power from 5.30 am to 5.30 pm. User complaints of "sauna-like" conditions were received sporadically, and confirmed by service personnel. One year later, January 2019, the system is performing according to demand - BMS trend-diagram at the right, Figure 7.

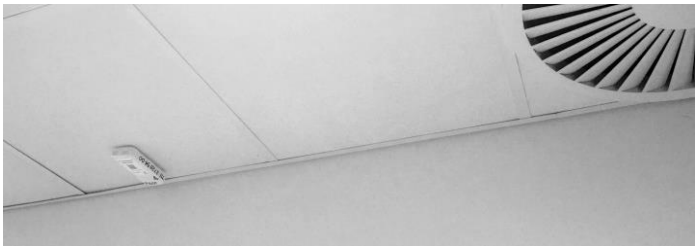

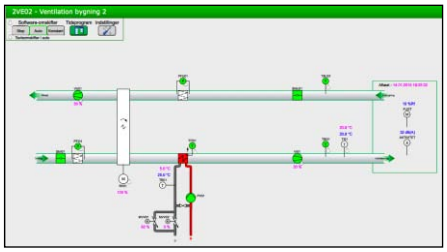

Figures 8 and 9: At the left, Fig. 8, showing the indoor climate data logger providing the wireless signal for the control of fan speed. System diagram from the BMS showing control parameters at the right, Figure 9.

3.4 Phase 2 challenges: System imbalance and blockages.

However, the physical ventilation system required an overhaul before any intelligent control system could be effective. The system had last been commissioned in 1994 and although checks of total air quantities were made at yearly service intervals, there was no control of where the air actually went to, or, more importantly, where it did not go. There had been many physical building changes since 1994, without corresponding adjustments to the ventilation system (Figure 10), and accumulated dirt (Figure 11) had also reduced air quantities, so that system cleaning, physical duct checking, measurements, and re-commissioning were required.

3.5 Phase 2 results and consequences of the hidden extra expenses.

However, despite the extra expenses, the simple payback time for Phase 2 was under 3 years (Reference 6) and the users achieved a better indoor climate (Figure 7). This problem with hidden expenses related to basic system performance was both a benefit and a concern moving into Phase 3. An advantage was that an apparent lack of ventilation could often be related to system defects that could be relatively easily remedied, although sometimes difficult to identify, instead of requiring "new systems". The disadvantage of course is that costs of intelligent improvements such as wireless demand control could not be estimated owing to the uncertainty about basic system assumptions, such as design air volumes.

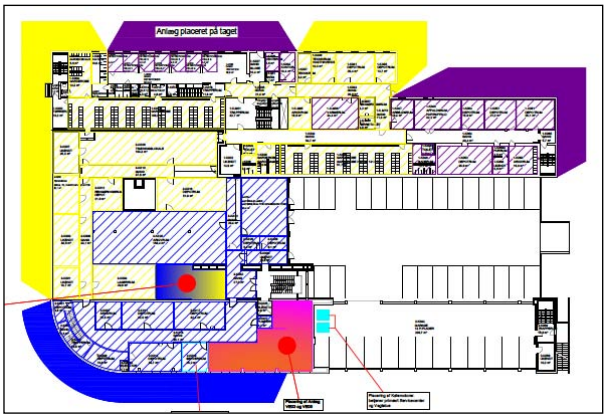

Figures 10 and 11: At the left, Fig. 10, showing an example of the ventilation system mapping that was necessary to determine which areas were served by which systems. At the first location studied in 2018 it was discovered that the Facility Manager was having IAQ issues with some offices, but he was adjusting the wrong ventilation system, because there were no drawings, and the assumptions about ventilation zones used in the BMS control software turned out to be incorrect.
On the right, Fig. 11, a well known issue with duct cleanliness. In this particular case, air volume was down to 35 % of design volume and simply cleaning the system gave considerably improved IAQ.

3.6 Hidden expenses: Ventilation system anarchy

The project goal of simplifying existing ventilation system control with intelligent wireless demand control systems had met some challenges, as mentioned above, but as the project proceeded the extent of these hidden expenses began to mount, revealing, on the one hand, simple possibilities for energy saving and indoor climate improvement, but on the other hand, delaying the project considerably. In almost all cases the standard response from the Service companies involved was a recommendation to completely renew the systems, which of course is a possibility, but an expensive option, and one which does not address the reason that the original systems got into such a bad state in the first place, or provide an answer to the question of why it will not just happen again.

4. EXAMPLES FROM THE CURRENT PROJECT PHASE 3

The following figures illustrate the real life challenges met during Phase 3 here in 2019, which partly provided the motivation for this article, since they show that, despite good intentions on the side of politicians and academics, our industry is just not meeting modern requirements for sustainability, neither energy savings, durability, or good indoor climates.
Figures 12 and 13: Fresh air intake problems. On the left, Fig. 12, an example of a blocked fresh air inlet grille.

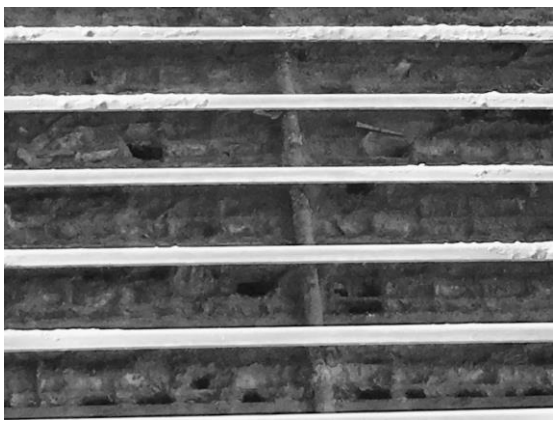

Both the ventilation service company and the cleaning contractor “assumed” that the other party had responsibility for these grilles.
On the right, Fig. 13, a fresh air intake box right next to the air exhaust box, both with horizontal louvres, such that there is considerable mixing of the two airstreams, depending on wind directions.

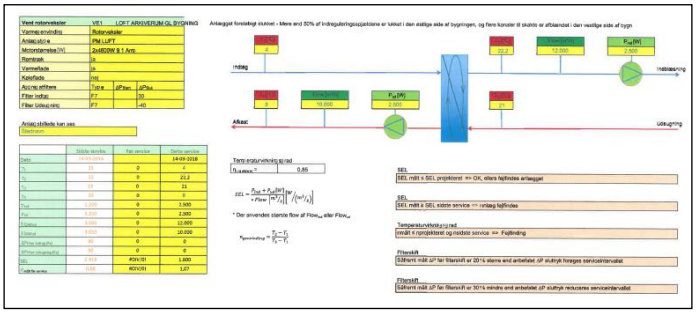

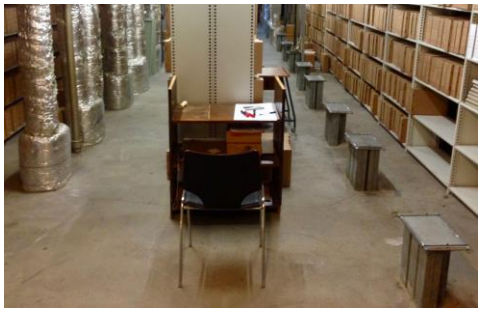

Figures 14 and 15: Ventilation system non-alteration problems. On the left, Fig. 14, the service chart for the ventilation system serving a five story office building. The original system supplied 12.000 m^3/h air to all offices in the building. Over the course of 30 years the ventilation unit itself has been upgraded several times, and the areas served have been modified considerably. On the right, Fig. 15, can be seen a photo of the blocked off vertical ducts from the ventilation unit that used to supply offices. The delivered capacity is in 2018 down to

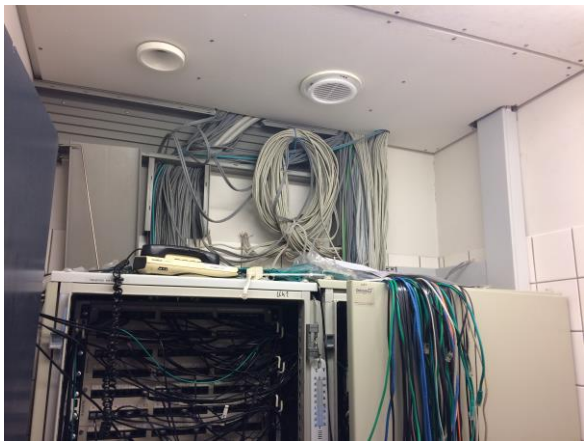

approx. 4.000 m^3/h, but no-one was sure which areas in the building were actually supplied by this system.
Figures 16 and 17: Consequences of alteration problems: Some offices that are no longer supplied with air from the ventilation unit (Fig. 14 and 15) are overheating, but because the tenants just think that the ventilation system is inadequate (instead of just not being connected) they install split air conditioners (Fig. 16, left photo) adding to the energy burden, at the same time as the ventilation system is running inefficiently and is underused. The photo on the right, Fig. 17, shows a small server room with ventilation connected to the system shown in figure 14. It needs ventilation constantly, 150 m^3/h 168 hours/week, but it is connected to the same system supplying

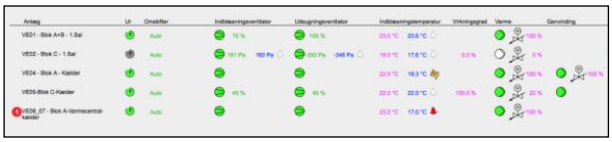

offices that only need ventilation 40 hours/week, so that the the ventilation unit designed for 12.000 m^3/h runs inefficiently and constantly at 4.000 m^3/h just to supply one room with 150 m^3/h.
Figure 18: The project group is currently (summer 2019) having to check just about everything. At a separate location with five ventilation systems (CTS picture above) we have found that several of the temperature detectors are measuring incorrectly, the outdoor temperature detector is defect, the rotary heat recovery units are running manually, there is only 30 % of design air quantity available, the night-cooling function was disabled, and there were very high pressure drops in the system.

Figure 19 on the right shows an example of the physical investigations. The ventilation unit and ductwork has been replaced at some time, but apparently without knowledge of system design conditions. The open duct in the photo is attached (incorrectly) to the side of the sound attenuator and has an air velocity of 26 m/s and a pressure drop of 250 Pa. Once found, resizing and reconnecting (correctly) the duct reduced system pressure considerably, giving an electrical energy saving of approx. 2.000 €/year and delivering twice as much air to the users. Energy savings and IAQ improvements for very little work - once the problem was found.

5. CONCLUSIONS

"We need a paradigm shift" wrote P. Ole Fanger in 2003 (Reference 7). He was writing in terms of increasing the quality of air *"while maintaining the same or even a lower ventilation rate and energy consumption"*, as he concludes in his paper.

This 2019 paper ***"An argument for a reality check"*** illustrates the current poor state of our ventilation industry, in practice, at the level of users and service personnel, with all manner of small problems, accumulated over many years, resulting in low IAQ and high energy consumption. Exactly the opposite of what Fanger wrote about 16 years ago.

In fact, the project ***"Avoiding energy waste in ventilation systems"*** indicates that our ventilation industry is responsible for a much higher proportion of the rising electricity use in buildings than is usually expected, and this hypothesis is currently the subject of analysis in Phase 4 of the current project.

One of the main problems seems to be the extremely **low durability and weak robustness of our ventilation systems**. Ventilation systems seem to "mutate" and degenerate, very soon after the project team has left, into "monsters" that Facility Managers, Service Personnel and users have no control over, often leading to the bizarre situations described above.

The **examples** of many problems can easily be dismissed as exceptions, but unfortunately, the exception seems to be the opposite, as existing ventilation systems that meet good industry standards are very rare in the current project with a sample size of 10 buildings. The current Phase 4 of this project is starting to systematically collect data so that we can statistically identify the extent of each problem, but one can ask if this is not something our industry should be doing themselves for our own reputation's sake?

Well meaning academics, altruists and civil servants have for many years been trying to improve our ventilation industry with **top-down measures** that seem to have very little effect at on-site level. At the on-site level consultants, producers and contractors seem to be getting away with, at worst bad-practice. and at best systems with extremely low practical durability.

There is still a need for a paradigm shift, but it would seem that this shift can start at a very low level, just by simplifying the complex mess that our industry has been selling for decades, and getting back to basics: selling the customer something she can use, and not selling her all manner of stuff that she does not really need, and that does not really work.

"Keep it simple", as well as **"keep it durable"**, even if this means not so much turnover, is the message of this paper. Quality, not quantity. And as an industry we should be much more honest with our customers about the realities of what we are selling. I am sure that many of the examples shown above will not surprise the practical people in our industry, and perhaps it is time that the practical people starting leading the industry again?

6. ACKNOWLEDGEMENTS

Mr. Bjarne Dalgaard of the Danish Building and Property Agency, Project Manager for the project: "Avoiding energy waste in Ventilation Systems".

7. REFERENCES

1. Danish Energy Authority (2019). Annual energy statistics 2017. https://ens.dk/service/statistik-data-noegletal-og-kort/maanedlig-og-aarlig-energistatistik Final net energy consumption, Table 31 in official PowerPoint presentation. Only available in the Danish Language.

2. Danish Energy Authority (2019). Annual energy statistics 2017: https://ens.dk/en/our-services/statistics-data-key-figures-and-energy-maps/annual-and-monthly-statistics Table "Final energy consumption in the commercial and public services" Percentage changes.

3. EU Directive https://ec.europa.eu/energy/en/topics/energy-efficiency/energy-performance-of-buildings/energy-performance-buildings-directive first introduced in 2002, consolidated in 2010 and revised in 2018.

4. Danish Building and Property Agency. Energy saving lecture material, internal material, 14-1-2019. https://www.bygst.dk/english/about-us/property-portfolio/

5. Danish Building and Property Agency. Final report 10-5-2017 from Phase 1 of the project "Avoiding energy waste in ventilation systems" Only in the Danish language ("Undgå energispild i ventilationsanlæg".) AWE 10-5-2019.

6. Danish Building and Property Agency. Final report 4-4-2018 from Phase 2 of the project "Avoiding energy waste in ventilation systems" Only in the Danish language ("Undgå energispild i ventilationsanlæg").

7. P. Ole Fanger, 2003, "Providing Indoor Air of High Quality: Challenges and Opportunities" https://www.aivc.org/resource/providing-indoor-air-high-quality-challenges-and-opportunities

Status of Air filter energy performance and product characteristics

Kiyan Vadoudi*, Gregory Kelijian

Eurovent Certita Certification
50 Rue de la Victoire
Paris, France
k.vadoudi@eurovent-certification.com
**Corresponding author: k.vadoudi@eurovent-certification.com*
Presenting author: Kiyan Vadoudi

ABSTRACT

Throughout the certification process of air filters, the major technical characteristics are evaluating. Both theoretical models and experimental methods, proves some relationships between the parameters and the performance of product. In this article we present the statistical analysis of certified products according to EN ISO16890:2016. A sample of 1800 certified products by Eurovent Certita Certification is analysed to highlight products characteristics based on quantitative approach. The results could be useful for manufactures to find out the important characteristics and their relationships in terms of product performance and certification process.

KEYWORDS

Air Filter, Fin Qir Filter; Product Characteristics, Energy Efficiency, Certification

1 INTRODUCTION

Nowadays, the quality of indoor and outdoor air is an important topic anywhere in the world and especially indoor air that is typically two to five times more polluted than outdoor air (United States Environmental Protection Agency). Thus, air filters could perform an important function in commercial and institutional facilities to remove respirable particles such as microorganisms, dust and allergens from the breathing air. In fact, air filters provide the primary protection for building occupants and HVAC equipment against air pollutants (Filtration + Separation - the online magazine).

When considering different types of air filters, it is important to look at the performance of the filter. According to EN ISO16890:2016, there are three major components to filter performance; (1) Efficiency that presents the percentage of airborne particulate the filter will remove, (2) Dust-Holding Capacity, which presents the amount of dust the filter will hold before being changed and (3) The resistance to airflow, measured in inches of water gage (Pa), of the filter.

The efficiency depends on several factors such as pore size, fiber size, mat thickness, filter density, size and density of the entrained particle, and the velocity of air movement through the filter. The most effective filters depend primarily on the retention of particles through the sieve action of small pores developed through compaction or other processes, or through the interception of the particles by a mat of fine fibers as the result of either a diffusion or impaction mechanism. In most cases combinations of the above are operating (Lockhart Jr. et al., 1964).

Throughout the certification process, the major technical characteristics of air filters such as initial pressure drops, basic design, depth/length, face dimensions, filter Media, nominal airflow rate and particulate matter efficiency (ePMx) are evaluating. Both theoretical models and experimental methods, proves some relationships between these parameters and the performance of product. For instance, decreasing fibre charge density, filter thickness and

packing density, increases aerosol penetration through the electret filter media. However, these studies are of a limited significance for the relationships between these parameters and the results of the air filters standards. In this article we discuss the relationships between all those parameters with the air filter classes according to EN ISO16890:2016. A sample of 1800 products will be analysed based on quantitative approach and the result could be useful for manufactures to find out the important characteristics and their relationships in terms of product performance and certification process.

2 PARTICULATE MATTER EFFICIENCY

Years ago, it was difficult for end users to choose the right filtration solution for a given environmental situation. But, the new global standard for general filtration solve this because ISO 16890 directly links the outdoor air pollution measurements PM_1, $PM_{2.5}$ and PM_{10} to the filtration removal efficiency of air filters, which called particulate matter efficiency (ePMx) (Sundvik A., 2017). Particulate matter in the context of the EN ISO 16890 series describes a size fraction of the natural aerosol (liquid and solid particles) suspended in ambient air. The symbol ePMx describes the efficiency of an air cleaning device to particles with an optical diameter between 0,3 µm and x µm. In simple terms, this means that a filter rated ePM_1[60%] removes 60% or more of the particulates in the PM_1 range. In other words, the filter provides 60% protection against PM_1 air pollution. Different classes of particulate matter can be defined according to the particle size range. The most important ones are PM_1, $PM_{2.5}$ and PM_{10}.
As the precise definition of PM_1, $PM_{2.5}$ and PM_{10} are quite complex and not simple to measure, public authorities, like the U.S. EPA or the German Federal Environmental Agency, increasingly use in their publications the simpler denotation of PM_{10} as being the particle size fraction less or equal to 10 µm. Since this deviation is complex, the EN ISO 16890 series refers to this simplified definition of PM_1, $PM_{2.5}$ and PM_{10}. The following particle size ranges are used in the EN ISO 16890 series for the listed efficiency values.

Table 1: Optical particle diameter size ranges for the definition of the efficiencies, ePMx

Efficiency	Size Range, µm
ePM_{10}	$0,3 \leq x \leq 10$
$ePM_{2,5}$	$0,3 \leq x \leq 2,5$
ePM_1	$0,3 \leq x \leq 1$

The average and minimum efficiency values are both used to classify a product. To classify a filter as an ePM_1 or $ePM_{2.5}$ product, the minimum efficiency must be above 50%. If the minimum efficiency is above 50%, the reported efficiency value will be the average efficiency value between the minimum and virgin efficiency. For ePM_{10}, there is no threshold demand for minimum efficiency, but the average efficiency has to stay above 50%. If a filter's efficiency drops below 50% on ePM_{10}, it will be classified as a "coarse" filter and only dust arrestance in percent [%] is reported:

Table 2: Filter Groups

Group Designation	Requirement			Class Reporting Value
	$ePM_{1,\,min}$	$ePM_{2,5,\,min}$	ePM_{10}	
ISO Coarse	–	–	< 50%	Initial grav. Arrestance
ISO ePM_{10}	–	–	≥ 50%	ePM_{10}
ISO $ePM_{2,5}$	–	≥ 50%	–	$ePM_{2,5}$
ISO ePM_1	≥ 50%	–	–	ePM_1

3 EUROVENT FINE FILTER CERTIFICATION PROGRAM

As an independent institution the Eurovent Certification Company has developed an international certification program for fine filters (https://www.eurovent-certification.com/fr). The evaluation and classification of fine filters is based on the EN ISO 168900:2016 test standard. Viledon fine filters are all certified by Eurovent, giving users complete peace of mind. The aim of this guideline is to assess the yearly energy consumption based on a laboratory test procedure which can be the basis for an energy efficiency classification, to give the user of air filters guidance for the filter selection.
This Certification Program applies to Air Filter elements rated and sold as ISO PM_1, $PM_{2.5}$ and PM_{10} according to EN ISO 16890-1:2016, referring to a front frame size of 592x592mm according to standard EN 15805:2010 and with a nominal airflow between 0.24 and 1.5 m^3/s. When a company joins the program, all relevant ISO ePM_1, ISO $ePM_{2.5}$ and ISO ePM_{10} air filter elements shall be certified". As manufacturers may produce a large number of filters with different length/depth there is an acceptance criteria for the declaration of filters belonging to the same filter family as already certified filters with the same nominal airflow and with different length/depth of the overall filter element within an acceptance criteria of +/- 10% or 50 mm (whatever is the smaller). Outside of this acceptance criteria the filters shall be declared.

Table 2: Filter Groups

M_X = 200 g (AC Fine)	**AEC in kWh/y FOR ePM1**					
	ePM_1 and $ePM_{1,\,min} \geq 50\%$					
	A+	A	B	C	D	E
50% & 55%	800	900	1050	1400	2000	>2000
60% & 65%	850	950	1100	1450	2050	>2050
70% & 75%	950	1100	1250	1550	2150	>2150
80% & 85%	1050	1250	1450	1800	2400	>2400
> 90%	1200	1400	1550	1900	2500	>2500

M_X = 250 g (AC Fine)	**AEC in kWh/y FOR ePM2.5**					
	$ePM_{2.5}$ and $ePM_{2.5,\,min} \geq 50\%$					
	A+	A	B	C	D	E
50% & 55%	700	800	950	1300	1900	>1900
60% & 65%	750	850	1000	1350	1950	>1950
70% & 75%	800	900	1050	1400	2000	>2000
80% & 85%	900	1000	1200	1500	2100	>2100
> 90%	1000	1100	1300	1600	2200	>2200

M_X = 400 g (AC Fine)	**AEC in kWh/y FOR ePM10**					
	$ePM_{10} \geq 50\%$					
	A+	A	B	C	D	E
50% & 55%	450	550	650	750	1100	>1100
60% & 65%	500	600	700	850	1200	>1200
70% & 75%	600	700	800	900	1300	>1300
80% & 85%	700	800	900	1000	1400	>1400
> 90%	800	900	1050	1400	1500	>1500

Each filter family should include the information about; Model, product category (e.g. Bag, V-type), filter media, number of pockets, filter depth, face dimensions, nominal flow rate, initial pressure drop at nominal air flow rate, ePMx, ePMx min, Eurovent Energy Efficiency Class according to RS 4/C/001 2 (Table 3), annual Energy Consumption according to Eurovent Document 4/21 and filter frame material.
The Annual Energy Consumption calculated using the method described in Eurovent Document 4/21 - 2018 shall be compared to the class limits defined in the table below for the different energy efficiency classes to classify the filter under concern, depending of its filter class to EN ISO 16890:2016. For instance, if a declared value for ePM_1 is 66% and the measured value is 59%, the status will be "Passed", but if the declared value is 54% and measured one is 48%, then the status will be "Failed" and product will be rerated in group $ePM_{2,5}$.

4 RESULTS

In this research work, a mathematical analysis is implemented about existing data on Eurovent website [8]. The data is collected for 1800 certified air filters from 22 different manufactures. In this section the results are presented in two section; (1) the statistical analysis about product characteristics and (2) analysis on the energy efficiency of air filters.

4.1 Filter Media

Filter media are the granular filtering materials which are installed in the filters and Their function are to retain the suspended solids during the filtration process. Based on our statistical analyis, the major material of certified products is Glass with 63,16% and later Synthetic with 31,09% is the most used material through different models (Figure 1). There are other minor materials like combination of carbon with glass or synthetic that are used in the structure of less than 7% of filters.

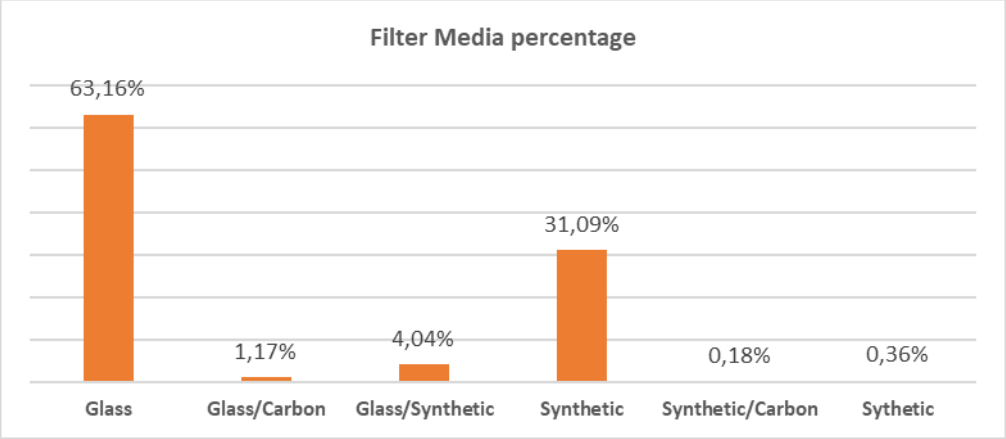

Figure 1: Filter Media percentage

4.2 Design Type

Several types of air filters are common in commercial HVAC systems; (1) Bag filter or named Glass or synthetic media bags which are made in a metal, plastic or wooden frame, (2) Pleated filter which are deep pleated filters in a metal, plastic, aluminum, MDF or wooden frame (> 150 mm depth), (3) V-type filters that are rigid filters with media pleats in a Vshaped design. 1, 2, 3, 4 … V´s, (4) Panel filter is a type of filter made in glass media pleat or synthetic media pleat in a cardboard, plastic or metal frame. <150 mm depth and (5) Filter mats that are

manufactured from silicon- and PVC-free Polyester (PES) or Polyethylene terephthalate (PET) non-woven materials. Through our existing analysis, Bag filter is the major design type (60,65%) and later the V-type with 18,69% and Panel filters with 16,53% are the most designed filters.

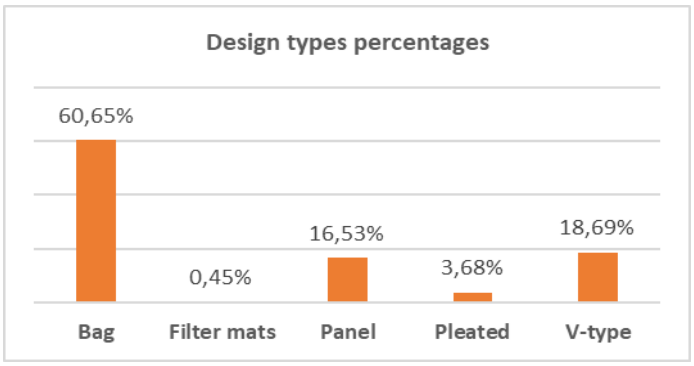

Figure 2: Design Types percentage

4.3 Depth/Length

This parameter corresponds to the Depth or Length of air filters in mm with the frame (complete filter), which are only calculated for bag, Panel, V-type and Pleated. In our analysis we define seven different categories (Figure 3) for existing certified product that start from the range {0 - 100} mm up to {600 - 700} mm. The study presents the range {500-600} mm as the major group with 23,8% and later the ranges {600 - 700} mm and {200 – 300} mm with 20,7% as the second most range groups. The minimum range belongs to {100 – 200} mm and {400 – 500} mm. Very small percentages of declared filters do not include their depth sizes which are presented as NA.

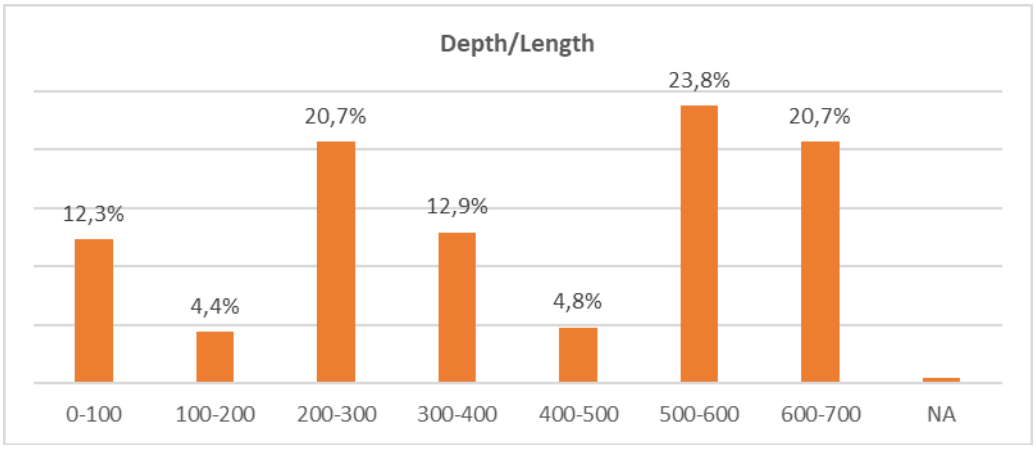

Figure 3. Depth/Length categories percentage

4.4 Number of Bags

Nowadays there are different types of air filters and one of the parameters that makes the filters different is the number of bags to for the clarification/filtration of fluids. Our analysis (Figure 4) proves that 33,50% of the air filters in HVAC systems are including eight filters. In second level there are certified filters with ten bags (26%), which is not far in terms of quantity with

eight bags. Later there are filters with four (15,86%) and six bags (11,86%). The minor quantity of bags through these kinds of filter include five (0,42%) and seven bags (0,08%).

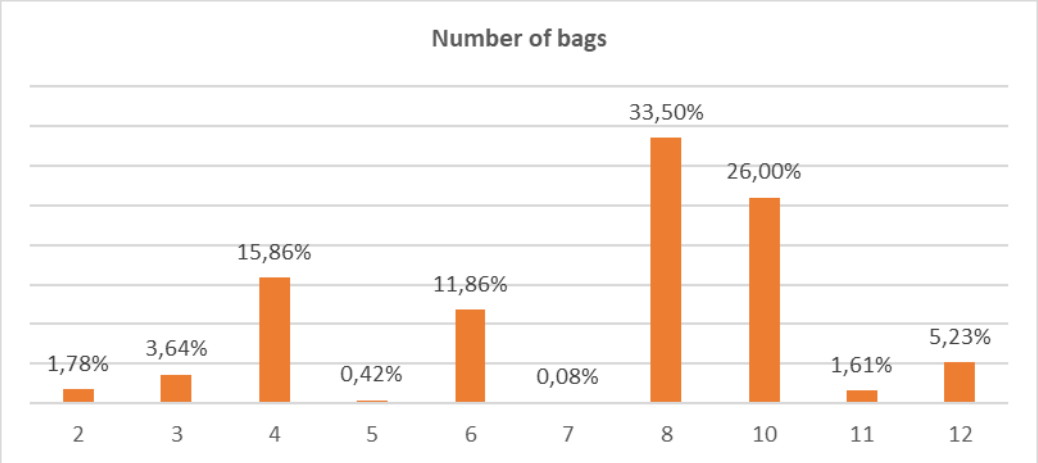

Figure 4. Number of bags percentage in certified filters

4.5 Eurovent Energy efficiency classes

Eurovent Energy Efficiency Class according to RS 4/C/001 2 (Table 3), annual Energy Consumption according to Eurovent Document 4/21 and filter frame material, shows that 24%, 23,8 and 22,8% of filters as the received Energy class C, D and E. Unfortunately, a minor percent of filters (3,1%) received energy class A+ that could motivate other manufactures to improve their quality of manufacturing (Figure 5).

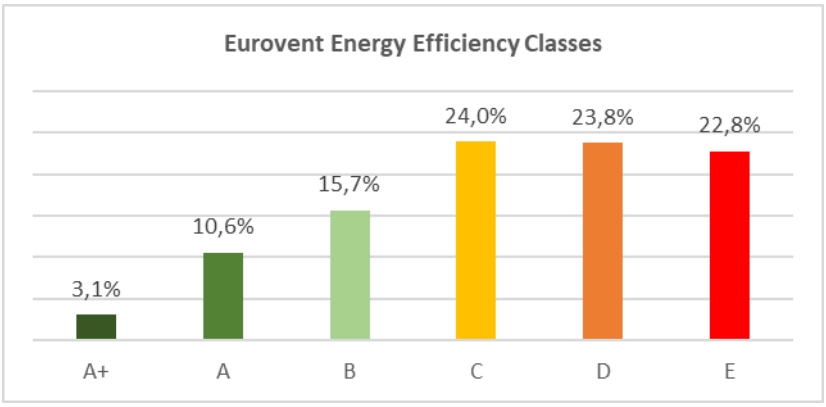

Figure 5. Eurovent energy efficiency class percentage

Particulate matter in the context of the EN ISO 16890 series describes a size fraction of the natural aerosol (liquid and solid particles) suspended in ambient air. Since this deviation is complex, the EN ISO 16890 series refers to this simplified definition of ISO ePM_1, $ePM_{2.5}$ and ePM_{10}. The following figure (Figure 6) describes the relation between ISO Class rating according to EN ISO16890: 2016 and Eurovent energy efficiency classes. Based on this figure, ISO ePM_1 is as the major percentage (56,2%) of certified products that includes 15,8% as C class, 13,6% as D class, 9,3% and 9,2% as E and B classes, 6,3% as A Class and only 2% as A+. Later, 30,6% of certified products considered as ISO ePM_{10} and in this category, 10,5% of products received class E as the major class, 6,4% class D, 5,6% class B, 4,5% class C and few

percentages (2,6% and 0,9%) classes A and A+. Minor percentages of certified products contain ISO ePM$_{2.5}$ with 13,1% and in this category classes C, D and E are the major classes.

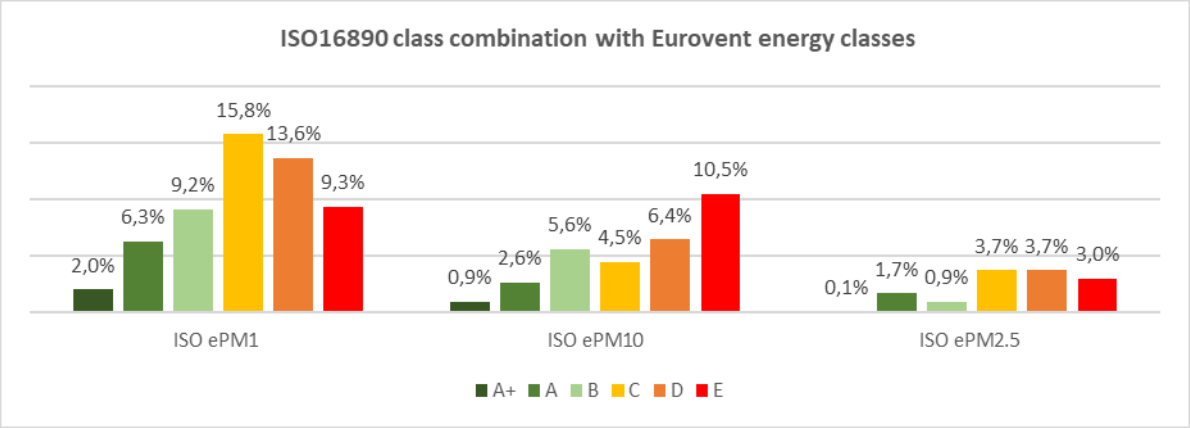

Figure 6. ISO Class rating acc. to EN ISO16890: 2016 and Eurovent energy efficiency class percentage

5 CONCLUSIONS

The objective of this article is to present some results from analyzed data that exists on Eurovent website. A part of these results is about product characteristics in terms of their structure that could give an overview to manufactures about the major physical parameters of existing certified products in the market. And other part is about the certification process and status with a comparison between Eurovent certification program and EN ISO 168900:2016.
The results above prove that only a minor portion of certified air filters have proper energy performance and the rest are certified as Classes C, D and E. As this product is applying in different HVAC products, and could have important impact in final energy performances. Therefore, needs more efforts and attention from manufactures to work on the improvement of their products. In the next article, the correlation between energy performance and product characteristics will be presented.

6 REFERENCES

A. SUNDVIK, “EN-ISO 16890:2016 New global standard links filtration performance to outdoor air pollution.”
European Standard EN ISO 16890-1:2016: “Air filters for general ventilation - Part 1: Technical specifications, requirements and classification system based upon particulate matter efficiency (ePM)”
European Standard EN ISO 16890-2:2016: “Air filters for general ventilation - Part 2: Measurement of fractional efficiency and air flow resistance”
European Standard EN ISO 16890-3:2016: “Air filters for general ventilation - Part 3: Determination of the gravimetric efficiency and the air flow resistance versus the mass of test dust captured”
European Standard EN ISO 16890-4:2016: “Air filters for general ventilation - Part 4: Conditioning method to determine the minimum fractional test efficiency”
https://www.eurovent-certification.com/en
https://www.epa.gov/
https://www.filtsep.com/
L. B. Lockhart Jr, R. L. Patterson Jr, and W. L. Anderson, “Characteristics of air filter media used for monitoring airborne radioactivity,” Naval Research Lab., Washington, DC, 1964.

Influence of Building Envelope's Solar Reflectivity, Wind Speed and Building Coverage Ratio on Urban Heat Environment

Haruto KITAKAZE[*1], Jihui YUAN [1],
Toshio YAMANAKA[1] and Tomohiro KOBAYASHI [1]

1 Osaka University
Suita 565-0871
Osaka, Japan
**:kitakaze_haruto@arch.eng.osaka-u.ac.jp*

ABSTRACT

In recent years, especially, the climate change (CC) and urban heat island (UHI) effects are becoming serious problems, affecting people's life and health, especially in hot summer. For large cities such as Tokyo or Osaka in Japan, the UHI effect is particularly intense. It is known that about 40% of urban anthropogenic heat comes from buildings in large cities. To reduce the anthropogenic heat from buildings is an important countermeasure to this problem.

Strategies for UHI mitigation include urban ventilation, urban greening, green roof, highly reflective (HR) roads, and HR building envelopes, etc. In order to mitigate the urban heat island phenomenon and reduce the building cooling heat load, it has been common to apply the building envelopes because it is easy to apply and free of maintenance.

However, the effect of HR coating materials on urban outdoor thermal environment have not been thoroughly studied. In addition to the HR coatings, it is considered that the outdoor airflow and building coverage ratio possibly affect the outdoor thermal environment. This study aims to use Computational Fluid Dynamics (CFD) analysis method to predict the outdoor thermal environment, including three thermal sensation index: 1) outdoor temperature, 2) wet bulb globe temperature (WBGT), and 3) new standard effective temperature with consideration of outdoor solar radiation (hereinafter abbreviated as OUT_SET*) by varying the parameters of solar reflectivity, wind speed and building coverage ratio, and the results are reported in this study.

KEYWORDS

CFD simulation, Outdoor thermal environment, Outdoor temperature, WBGT, OUT_SET*

1 INTRODUCTION

The urban heat island (UHI) effect is a well-known climate change phenomenon in recent years and is becoming very serious, especially in summer, due to the rapid increase of urban anthropogenic heat [1]. While it has a profound effect on the cooling energy consumption of the building, the strength of UHI in hot climates can raise the temperature by as much as 10^{o}C, which can increase discomfort and have a major impact on human lives [2]. It is reported that there is much research has focused on defining the relationship between rising temperatures and various elements of the city to reduce the impact of UHI. A reviewed paper indicated that there are mitigation strategies such as: HR and radioactive light colored materials, cool colored materials, phase-change materials (PCM), dynamic cool materials used for building roofs or facades, urban albedo increase, and green roofs etc [3]. Furthermore, other studies have focused on the microscale, which shows the impact of urban design on climate [4]. A study showed that increasing the percentage of urban green cover and urban albedo can lower the temperature of the city, reduce the energy consumption of the building, and improve the outdoor thermal

comfort [5]. HR coatings are widely studied in a strategy to reduce the UHI effect. The higher the total solar reflectivity, the lower the painted surface temperature, thus indicating that it can be used to reduce the cooling load of buildings, directly related to energy conservation in buildings.

However, since the influence of the HR building envelope on the outdoor environment temperature has not been widely discussed in Japan, this study aims to evaluate the effect of solar reflectivity of building envelopes on the outdoor thermal environment which includes air temperature, wet bulb globe temperature (WBGT), and new standard effective temperature with consideration of outdoor solar radiation (hereinafter abbreviated as OUT_SET*) with ~~in~~ consideration of the variation of the solar radiation reflectivity of the building envelope. In addition to the solar reflectivity, the other factors such as wind speed and building coverage ratio of the city are also used to evaluate the outdoor thermal environment by using computational fluid dynamics (CFD) analysis method.

2 MATERIALS AND METHODOLOGY

2.1 Analysis Target

The analysis target is assumed to be the architectural blocks located in Chuo Ward, Osaka City of Japan (34.4 ºN, 135.31 ºE). As shown in **Fig.1**, the dimension of one block model with a rectangular shape is set to a variable size of 75 m, 80 m and 85 m in east-west direction, a variable size of 75 m, 80 m and 85 m in north-south direction, and a constant size of 40 m in height direction, and a total of nine such blocks are in the CFD simulation. As shown in **Fig.2**, the analysis area is set to be 4800 m × 900 m × 400 m.

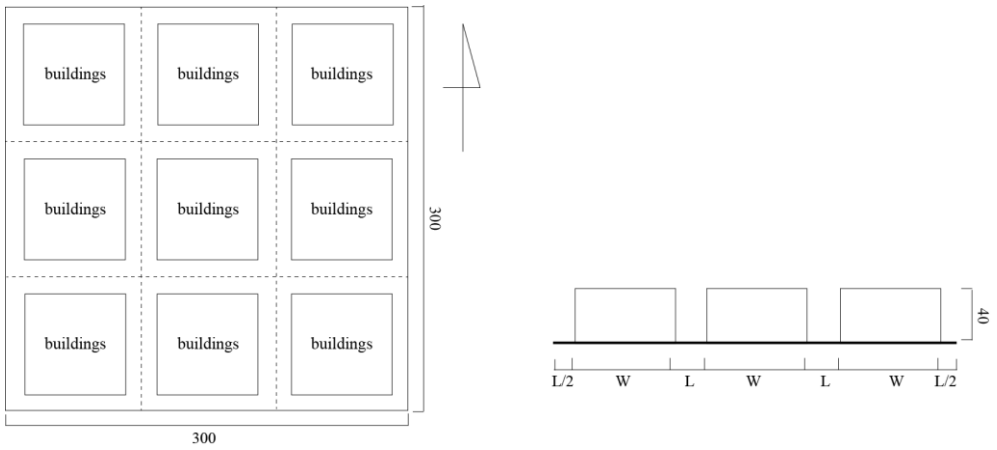

Fig. 1 Plane and Elevation of Target Area

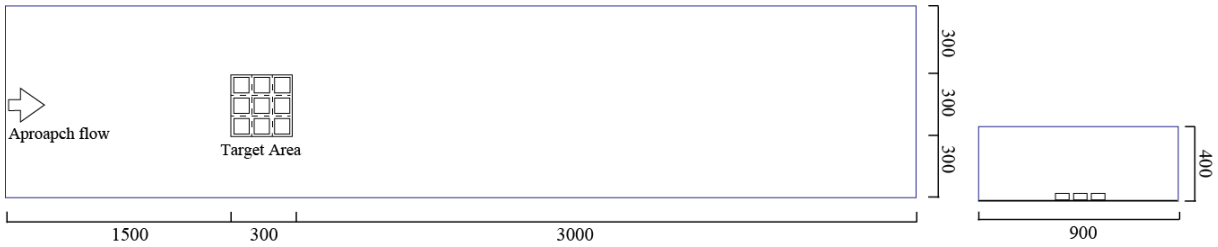

Fig. 2 Plane and Elevation of Analysis Area

2.2 Analysis Condition

The same as ANSYS Fluent, the software STREAM [7] often used in Japan is adopted to evaluate the outdoor thermal environment. The condition of CFD analysis is shown in **Table 1**. The room temperature of the block model is set to a fixed value of 24°C. According to NEDO

database [6], the initial outdoor temperature is set to a daily average value of 30.6°C on July 31st, the solar radiation (direct and diffuse) is set to the value at culmination time of July 31st, and the wind direction is set to west. For the thermal boundary condition, the convective heat transfer coefficients between air and solids (ground and building surface) are given by the generalized power law.

Table 1 Analysis Condition

CFD code		STREAM V14(RC2)
Turbulence model		Standard k-ε model
Algorithm		SIMPLER
Discretization scheme		QUICK
Area of CFD analysis		X(4800m)×Y(900m)×Z(400m)
Boundary condition	Xmin	Fixed temperature, Power law (Exponent recipracal(n)=4)
	Xmax	Natural outflow boundary
	Ymin	Fixed temperature, Free slip
	Ymax	Fixed temperature, Free slip
	Zmin	Fixed temperature, Free slip
	Zmax	Fixed temperature, Free slip
	Fluid-Solid	Temperature power law, No slip
Weather condition		June 21st ,12:00, in Osaka Sunny Day
Solar condition	Solar position	Altitude:79.04°, Azimuth:0.00°
	Direct solar radiation	658W/m^2
	Diffuse solar radiation	236W/m^2
Indoor preset temperature		24°C
Outdoor temperature		30.6°C
Wind direction		West

2.3 Analysis Case

In this research, as shown in **Table 2**, a total of nine analysis cases were analyzed. The solar reflectivity is varied from 0.3 to 0.7 with the interval of 0.1, the wind speed is varied from 1m/s to 5m/s with the interval of 2m/s, and the building coverage ratio is varied from 0.56 to 0.72 with the interval of 0.08. The basic case is set as the condition that the solar reflectivity of ~~on~~ the block (building) surface is 0.5, the wind speed is 3 m/s, and the building coverage ratio is 0.64. According to the database of Japan Meteorological Agency (JMA) [8], the external wind speed at the height of 24 m from the ground surface is set in this study. In addition, the solar reflectivity of the ground surface is set to a constant value of 0.75 [9], and the long wavelength emissivity of the building exterior and the ground surface is set to a constant value of 0.9.

Table 2 Analysis Case

Analysis parameter	**Solar reflectance[-]**	0.3	0.4	0.5	0.6	0.7
	Wind speed[m/s]	1		3	5	
	Coverage ratio[-]	0.56 (L=25,W=75)		0.64 (L=20,W=80)	0.72 (L=15,W=85)	

2.4 Thermal sensation index

In this study, three thermal sensation index which includes outdoor temperature, WBGT and OUT_SET*, are evaluated by CFD under nine cases (see **Table 2**).

The WBGT is an index developed for the purpose of heatstroke prevention in field military training, and it is considered to be dangerous when it exceeds 31°C. In this study, the relative humidity is fixed at constant value of 68%. The WBGT can be calculated using equation (1).

$$WBGT = 0.7T_{nwb} + 0.2T_g + 0.1T_a \tag{1}$$

As for MRT, long wavelength radiation is considered only when used indoors, but solar radiation must be considered when used for outdoor thermal environment evaluation. The spatial distribution of global solar radiation (GSLR) and the long wavelength radiation temperature (MRT) can be calculated from the analysis software. GSLR is the amount of solar radiation received in the upward horizontal plane, taking direct, diffuse and scattered solar radiation into consideration. The distribution of GSLR at 1.5m above the ground is shown in **Fig. 3**. In this study, OUT_MRT is calculated by separating direct solar radiation and diffuse (scattered) solar radiation. The separation of them was done by calculating the cases separately in the case of the sunshine and the sunshade.

The case of sunshade is judged as the condition that GSLR is more than $S\downarrow_{input}$. Thus, the case of sunshade can be expressed as equation (2),

$Case\ of\ the\ sunshine$:

$$S\downarrow = \frac{S\downarrow_{input}}{sin\beta},\ D\downarrow = GSLR - S\downarrow_{input} \tag{2}$$

The case of sunshade is judged as the condition that GSLR is less than $S\downarrow_{input}$. Thus, the case of sunshade can be expressed as equation (3),

$Case\ of\ the\ sunshade$:

$$S\downarrow = 0, \qquad D\downarrow = GSLR \tag{3}$$

OUT_MRT is calculated by equation (4),

$$OUT_MRT = \left[\frac{f_p(1-\alpha_{cl})S\downarrow}{F_{eff}\sigma} + \frac{(1-\alpha_{cl})\{D\downarrow+(D\downarrow+S\downarrow)\alpha_{GND}\}}{\sigma} + T_{MRT,L}^4\right]^{0.25} \tag{4}$$

The albedo of clothes (α_{cl}) is 0.4, the effective radiation area ratio (F_{eff}) is 0.75, and the projected area ratio of the human body to direct solar radiation is calculated by equation (5) [10],

$$f_p = 0.42cos\beta + 0.43sin\beta \tag{5}$$

OUT_SET* was calculated by using OUT_MRT in the calculation of SET* proposed by Gagge et al [11]. The calculation conditions for SET* are assumed to be a human body with a height of 1.77 m, a weight of 81.7 kg, a surface area of 2.0 m^2, the amount of clothes of 1 clo, and the amount of metabolism ~~is~~ of 1.5 met for the real environment.

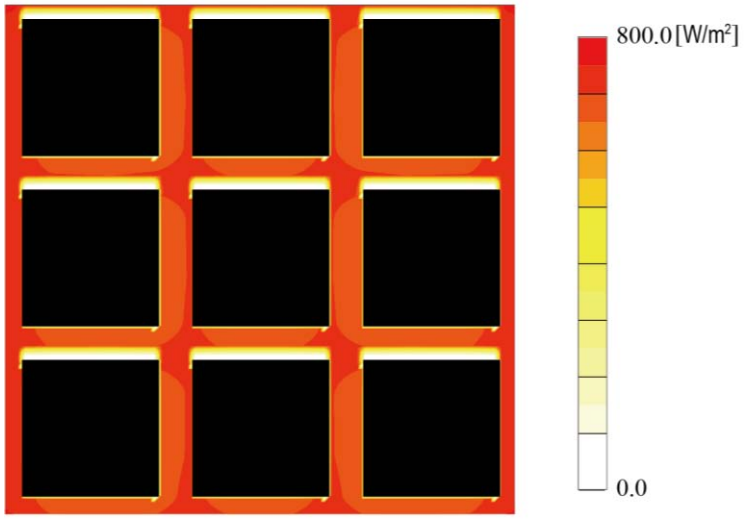

Fig. 3 Horizontal distribution of GSLR at height of 1.5m above the ground under solar reflectivity of 0.5

3 RESULTS AND DISCUSSION

The horizontal distribution for ~~of~~ each index shows a relatively similar distribution under either condition, thus as a representative, the wind speed and thermal sensation index (outdoor temperature, WBGT and OUT_SET*) distributions of horizontal section at height of 1.5 m above the ground under the basic case set as solar reflectivity of 0.5, wind speed of 3 m/s, and building coverage ratio of 0.64 are shown in Figs.4-7.

3.1 Wind speed distribution

The distribution of wind speed contour and vector at a height of 1.5 m above the ground under the basic case is shown in **Fig. 4**. It is shown that the wind speed is slower on the windward side of the building and faster on the leeside of the building.

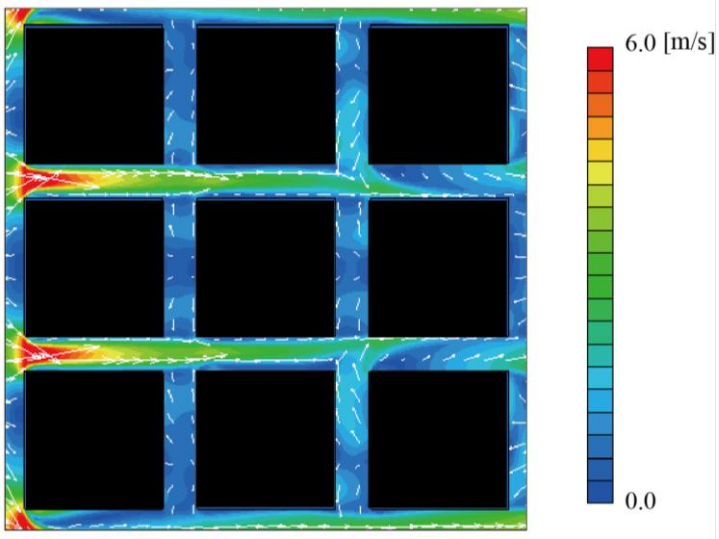

Fig. 4 Wind speed distribution of horizontal section at height of 1.5m above the ground under wind speed of 3 m/s

3.2 Outdoor thermal sensation index

The distribution of outdoor temperature at a height of 1.5m above the ground under the basic case is shown in **Fig. 5**. The horizontal distribution of outdoor temperature is almost the same as that of wind speed. It is shown that the stronger the wind (see **Fig.4**), the lower the outdoor temperature. In addition, since the temperature does not decrease in the shaded area, it may be said that the effect of solar radiation on the outdoor temperature is small.

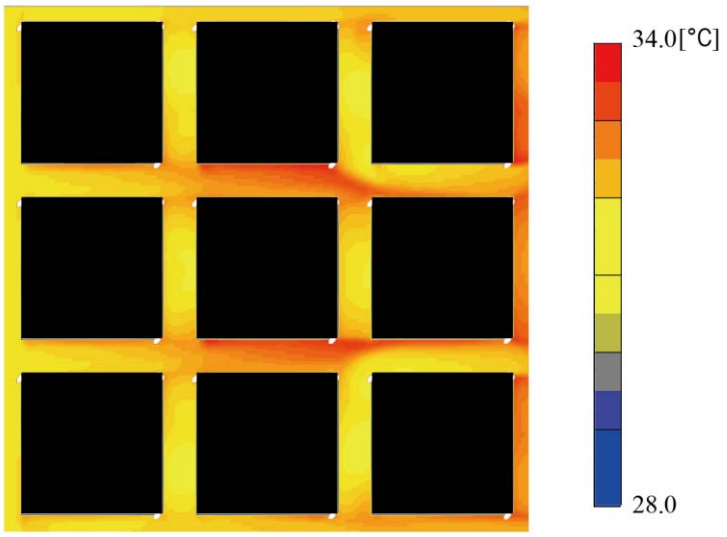

Fig. 5 Outdoor temperature of horizontal section at height of 1.5m above the ground under the basic case

The distribution of WBGT at height of 1.5m above the ground under the basic case is shown in **Fig. 6**. The result showed that the WBGT is higher while the wind speed is weaker. Unlike distribution of outdoor temperature, the WBGT of the shaded area is decreasing, thus it may be considered that the effect of solar radiation on WBGT is more significant, compared with outdoor temperature. In the shadow area, the WBGT is between 28-30^{o}C, thus the shadow area is considered to be a thermal comfort zone. However, in the sunshine area, the WBGT is exceeding 31^{o}C or more, thus the sunshine area is considered to be a dangerous area for the human body.

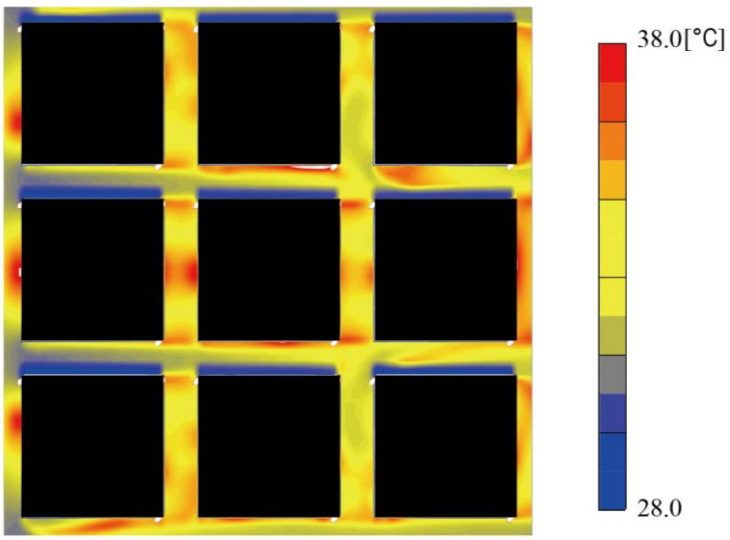

Fig. 6 WBGT of horizontal section at height of 1.5m above the ground under the basic case

The distribution of OUT_SET* at height of 1.5m above the ground under the basic case is shown in **Fig.7**. It is shown that the horizontal distribution of OUT_SET* is almost the same as that of WBGT. However, it also indicated that the range of OUT_SET* is about 6 ºC higher than WBGT.

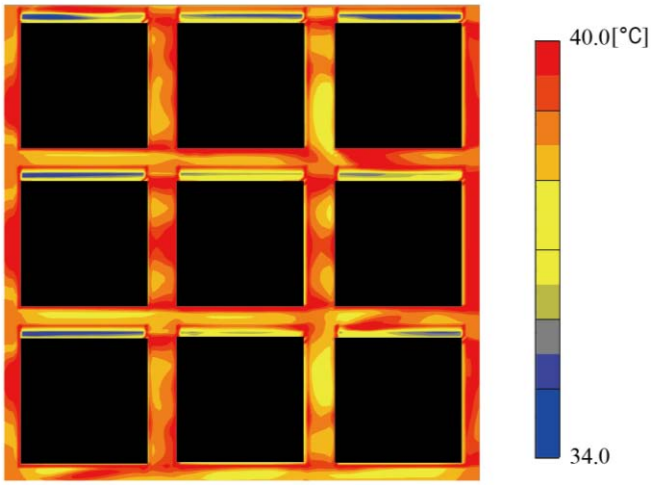

Fig. 7 OUT_SET* of horizontal section at height of 1.5m above the ground under the basic case

3.3 Correlation between thermal sensation index and analysis parameters

In order to investigate the influence of analysis parameters (solar reflectivity, wind speed and building coverage ratio) on three thermal sensation index (outdoor temperature, WBGT and OUT_SET*) in more detail, the change in the three thermal sensation index under each analysis condition (detailed in **Table 2**) are shown in Figs.8-10.

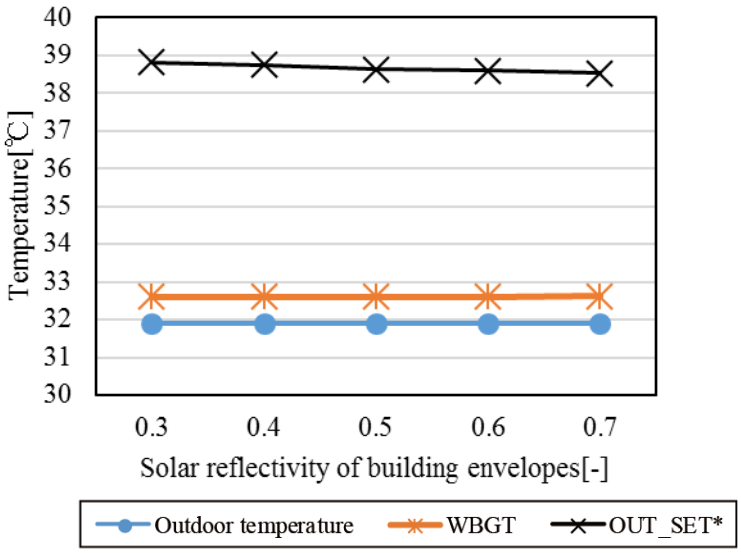

Fig. 8 Correlation between thermal sensation index and solar reflectivity

Correlation between thermal sensation index and solar reflectivity of building envelopes is shown in **Fig. 8**. The results show little effect of solar reflectivity on both outdoor temperature and WBGT. However, it is shown that the change in solar reflectivity has relatively larger effect on the OUT_SET*, compared to other two thermal sensation index. The OUT_SET* is slightly

decreasing by about 0.5°C when increasing the solar reflectivity of building envelopes from 0.3 to 0.7.

Therefore, it is concluded that the HR building envelope may give an effective impact on the OUT_SET*. However, the effect is relatively small and further study such as more detailed CFD analysis and field experiment is necessary.

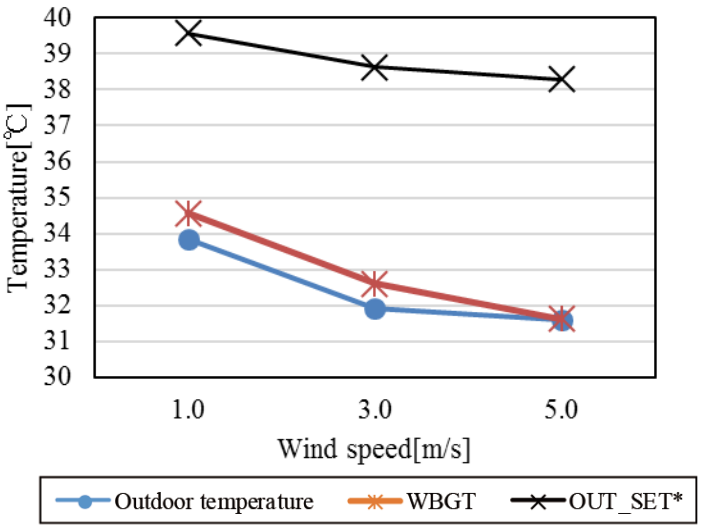

Fig. 9 Correlation between thermal sensation index and wind speed

Correlation between thermal sensation index and wind speed is shown in **Fig. 9**. It was found that as the wind speed became stronger, all of thermal sensation index substantially decreased. When the wind speed is varied from 1m/s to 5m/s, the outside temperature and WBGT decreased by about 3°C respectively, and OUT_SET* decreased by about 1.5°C. Therefore, it is concluded that the wind speed has a great influence on the thermal environment around the building.

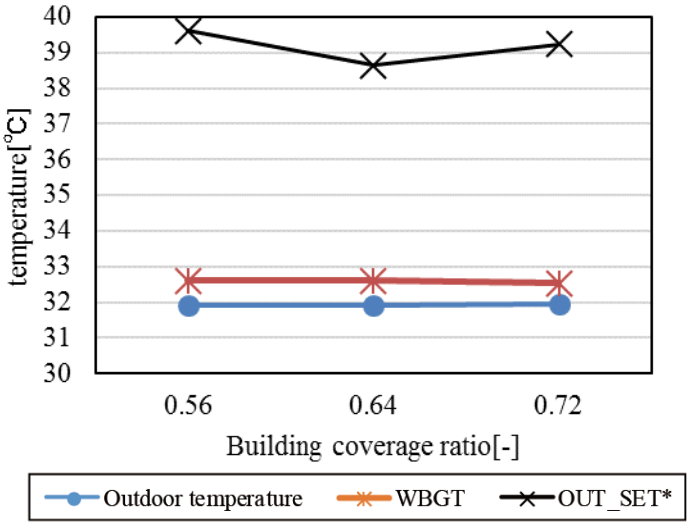

Fig. 10 Correlation between thermal sensation index and building coverage ratio

Correlation between thermal sensation index and building coverage ratio is shown in Fig. 10. Results showed that both outdoor temperature and WBGT are constant for changes in building coverage. The effect of building coverage ratio on the OUT_SET* showed that the OUT_SET* decreased by about 0.9oC when the coverage ratio is varied from 0.56 to 0.64, however it increased by about 0.4oC when the coverage ratio is varied from 0.64 to 0.72.

The reason for such change is considered to be the result of the interaction of short-wavelength and long-wavelength radiations. It is considered that short-wavelength radiation of solar plays a leading role when the building coverage ratio is small, and long-wavelength radiation of building envelopes plays a leading role when coverage ratio is large. Thus, we can see a decreasing trend in OUT_SET* when the coverage ratio is varied from 0.56 to 0.64, and an increasing trend in OUT_SET* when the coverage ratio is varied from 0.64 to 0.72.

4 CONCLUSION

This paper used CFD analysis method to evaluate the effect of solar reflectivity, wind speed and building coverage ratio on the outdoor thermal sensation index (outdoor temperature, WBGT and OUT_SET*).

The knowledge are obtained and summarized as following,

- Except for the effect of sunshade, the horizontal distributions of outdoor temperature, WBGT and OUT_SET* show the similar contours with that of wind speed.
- It is indicated that the WBGT and OUT_SET * are largely affected by the effect of sunshade.
- It is found that HR building envelopes are effective for hot environment mitigation by this CFD analysis, however the effect is small.
- It is concluded that the wind speed has a great influence on the thermal environment around the building.

For the future work, the research will be focused on comparison between CFD analysis and field measurement. In addition, the future work is also aimed at implementing the research on the reflective directional characteristic of building envelope materials and evaluating the effect of reflective directional envelope (i.e., retro-reflective glass film [12]) on the outdoor thermal environment by using CFD analysis method.

Nomenclature

$D\downarrow$	Diffuse solar radiation [W/m^2]
F_{eff}	Effective radiation area factor [-]
$S\downarrow$	Direct solar radiation [W/m^2]
$S\downarrow_{input}$	Input value of direct solar radiation [W/m^2]
$T_{MRT,L}$	Mean radiant temperature [K]
T_a	Outdoor temperature [°C]
T_g	Globe temperature [°C]
T_{nwb}	Wet-bulb temperature [°C]
OUT_MRT	Mean radiant temperature considering short wavelength radiation of the sun [-]
α_{cl}	Albedo of the clothed body surface [-]
α_{GND}	Ground albedo [-]
f_p	Projected area ratio of the human body to direct solar radiation [-]
β	Solar altitude [°]
σ	Stefan-Boltzmann constant (=5.67 x 10^{-8}) [W/ (m^{2}K^4)]

5 REFERENCES

[1] M, Santamouris. "Energy and Climate in the Urban Built Environment", James and James Science Publishers: London, UK, 2001.

[2] I, Livada, M, Santamouris, K, Niachou, N, Papanikolaou, G, Mihalakakou. "Determination of places in the great Athens area where the heat island effect is observed", J. Theor. Appl. Climatol., 2002, 71, 219–230.

[3] M, Santamouris, A, Synnefa, T, Karlessi. "Using advanced cool materials in the urban built environment to mitigate heat islands and improve thermal comfort conditions", Solar Energy, 2011, Vol.85, Issue 12, pp.3085-3102.

[4] M, Idczak, D, Groleau, P, Mestayer, J, Rosant, J, Sini. "An application of the thermo-radiative model SOLENE for the evaluation of street canyon energy balance", Building and Environment, 2010, 45(5), pp.1262-1275.

[5] J, Yuan, K, Emura, C, Farnham. "Is urban albedo or urban greening covering more effective for urban microclimate improvement: A simulation for Osaka", Sustainable Cities and Society, 2017, Vol.32, pp.78-86

[6] NEDO database HP: http: //app0.infoc.nedo.go.jp/

[7] Cradle (n.d.). Retrieved July 14, 2019, from https://www.cradle-cfd.com/

[8] HP of Japan Meteorological Agency (JMA): http://www.jma.go.jp/jma/index.html

[9] M, Nishioka, M, Nabeshima, T, Wakama, J, Ueda. "Effects of Surface Temperature Reduction and Thermal Environment on High Albedo Coating Asphalt Pavement", *Journal of Heat Island Institute International Vol.1 (2006)*

[10] J, Pickup and R, de Dear. "AN OUTDOOR THERMAL COMFORT INDEX (OUT-SET)- PART I –THE MODEL AND ITS ASSUMPTIONS", available at:* https://www.researchgate.net/profile/Richard_De_Dear/publication/268983313_An_outdoor_thermal_comfort_index_OUT-SET_-_Part_I_-_The_model_and_its_assumptions/links/567a4b6308ae40c0e27e9397.pdf

[11]A.P, Gagge."An Effective Temperature Scale Based on a Simple Model of Human Physiological Regulatory Response", ASHRAE Trans. 77, 247-262, 1971.

[12] S, Yoshida, A, Mochida. "Evaluation of effects of windows installed with near-infrared rays retro-reflective film on thermal environment in outdoor spaces using CFD analysis coupled with radiant computation", Building Simulation,Vol.11,No. 5

The influence of external environment characteristics on the heating and cooling load of super-tall residential building

Hyoeng-Tae Kim[1], Hee-Gang Kim[1], Chang-Ho Jeong[2], and Myoung-Souk Yeo[*3]

1 Department of Architecture and Architectural engineering, Graduate school, Seoul National University
39-418 Seoul National University, 1 Gwanakro, Gwanak-gu, Seoul, 08826, S. KOREA

2 Institute of construction and Environmental Engineering, Seoul National University
135-302 Seoul National University, 1 Gwanakro, Gwanak-gu, Seoul, 08826, S. KOREA

3 Department of Architecture and Architectural engineering, Seoul National University
39-428 Seoul National University, 1 Gwanakro, Gwanak-gu, Seoul, 08826, S. KOREA
**Corresponding author: msyeo@snu.ac.kr*

ABSTRACT

Upper floors of super-tall residential buildings have different characteristics of the exterior environment as compared to their low floors or low-rise residential buildings due to the high-rise. Upper floors are more affected by direct solar radiation due to the reduced number of adjacent shading buildings and by reflected solar radiation from rooftops. Super-tall buildings also have high level of airtightness because of higher wind speed with high-rise. Therefore, upper floors of super-tall residential buildings are expected to have different heating and cooling load characteristics as compared to low-rise residential buildings. In this study, the influence of external environment characteristics due to the high-rise on the heating and cooling loads of super-tall buildings were analysed. EnergyPlus was used for dynamic load analysis simulation, which showed that upper floors of super-tall residential building would have different heating and cooling load characteristic compared to low-rise building and low floors of super-tall building due to solar radiation and airtightness. In addition, it was expected that upper floor of super-tall residential building had different sensible heat ratio than low-rise residential building.
.

KEYWORDS

Super-tall building, Residential building, Solar radiation, Airtightness, Heating and cooling load

1 INTRODUCTION

1.1 Background and objective

Upper floors of super-tall residential buildings have different characteristics of exterior environment with respect to outside temperature, effect of solar radiation and wind speed as compared to low-rise buildings because of high-rise. Also, they have higher level of airtightness due to increased wind speed with high-rise than low-rise residential buildings. Therefore, upper floors of super-tall buildings should have different heating and cooling load characteristics as compared low-rise buildings. The objective of this study was to analyse the effect of the characteristics due to the high-rise on the heating and cooling loads of super-tall buildings for determining architectural and mechanical alternatives suitable for super-tall residential buildings.

1.2 Scope and methodology

Considering the external environment, temperature decrease while wind speed increase with high-rise. As buildings are concentrated in urban areas, solar radiation would affect the heating and cooling load. Also, Super-tall buildings have high level of airtightness and difficulty for ventilation due to change of exterior environment.

EnergyPlus, a heat balance based simulation program, was used for analysing heating and cooling load with respect to transient characteristics of the dynamic load. The influence of solar radiation and infiltration on the heating and cooling loads of super-tall building and low-rise building were analysed for a period of one year. The load of upper floor of super-tall building was compared with that of low floor, middle floor of super-tall building and low-rise building.

Both peak load and annual energy should be considered to estimate the required capacity of mechanical systems. In order to determine the cooling capacity, room latent cooling load should also be analysed. The sensible and latent load ratio are expected to be different due to the exterior environment (such as solar radiation and moisture of infiltration). Therefore, for efficient the system selection, sensible heat ratio (SHR) when peak cooling load occurred were analysed

2 SIMULATION FOR HEATING AND COOLING LOAD ANALYSIS

For the analysis of heating and cooling load, super-tall building and low-rise building were selected satisfying building code in Korea as shown in Table 1. Considering layout of city, high density of buildings, adjacent buildings were placed around the selected buildings. It was assumed that the super-tall building and low-rise building were built in the same location. The input data for the simulation were summarized as shown in Table 2. Heating and cooling load in the living room were analysed.

Table 1: Super-tall residential building and low-rise residential building for simualtion

	Super-tall building	**Low-rise building**
Floors(Height)	74 Floors(222m)	24 Floors(72m)
Airtightness (Effective Leakage Areas) [㎠/㎡]	1.4	2.8
Ventilation	No ventilation	Window open according to temperature in May, September and October (18℃~26℃)
Classify for load analysis	Upper floor: 70 Floor Middle floor: 50 Floor Low floor: 10 Floor	10 Floor

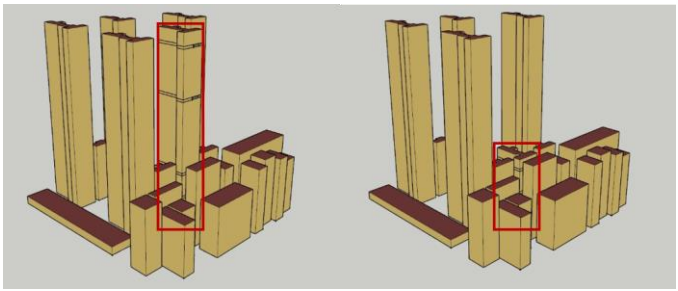

Figure 1: Layout of super-tall residential building and low-rise residential building

Table 2: Summary of input data for simulation

		Input Data
Model House	Orientation	South
	Area and height	140 ㎡ / 3m
	Weather Data	Standard weather data for Seoul
Internal Loads	Number of Occupants	4 people
	Occupancy schedule[6]	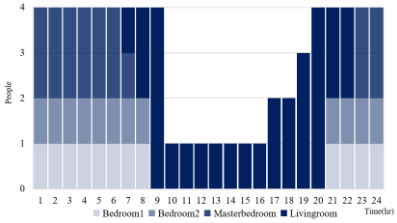
	People	120 W/person
	Light	6.19 W/㎡
	Equipment	Sensible heat: 160W Work: 15W(Sensible heat 11.25W, Latent heat 3.75W)

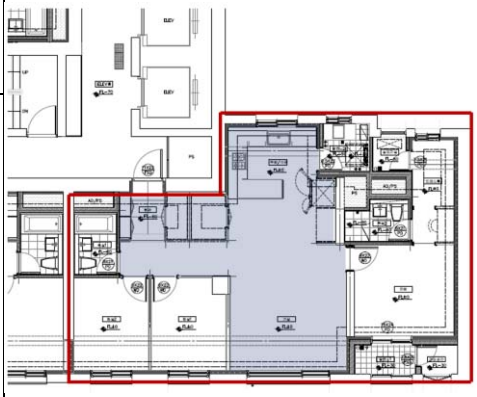

Figure 2: Plan of the simulation model

3 HEATING AND COOLING LOAD CHARACTERISTIC IN SUPER-TALL RESIDENTIAL BUILDING

Heating and cooling load analysis with respect to external environment characteristics and different airtightness was done. Table 3 shows the results for peak load and annual energy of the buildings.

According to the analysis, upper floor of super-tall building has larger peak heating and cooling load but lower annual heating energy than its low floor. As shown in Figures 3 and 4, upper floor of super-tall building has larger monthly peak heating energy than its low floor during winter. However, monthly heating energy less occurs in upper floor of super-tall building than in its low floor.

Table 3: Heating and cooling load of residential super-tall building and low-rise residentail building

	Cooling Load		Heating Load	
	Peak Load W/㎡	Annual Energy Wh/㎡(a)	Peak Load W/㎡	Annual Energy Wh/㎡(a)
Upper floor of super-tall building	**25**	**63,141**	**11**	**759**
Middle floor of super-tall building	**25**	**66,459**	**10**	**531**
Low floor of super-tall building	**21**	**42,227**	**6**	**906**
Low-rise building	**29**	**44,759**	**21**	**3,441**

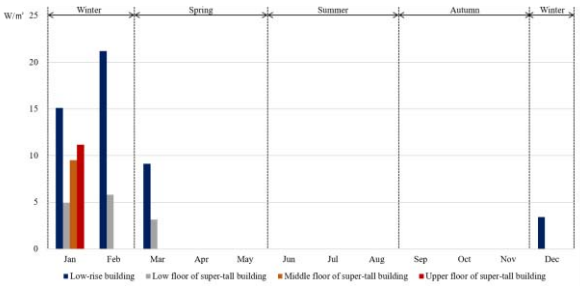

Figure 3: Monthly peak Heating load

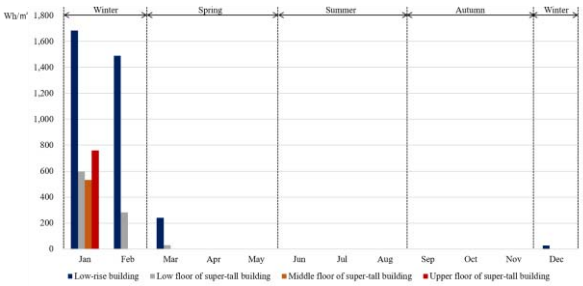

Figure 4: Monthly Heating Energy

Upper floor of super-tall building has lower peak heating and cooling load but larger annual cooling energy than low-rise building. Figures 5 and 6 shows that upper floor of super-tall building has lower monthly peak cooling load than low-rise building. However, upper floor of super-tall building has higher monthly cooling energy than low-rise building during all seasons except summer. In addition, monthly cooling energy more occurs in upper floor of super-tall building than in low-rise building.

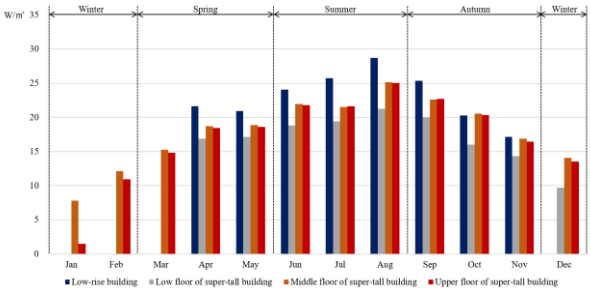

Figure 5: Monthly peak Cooling load

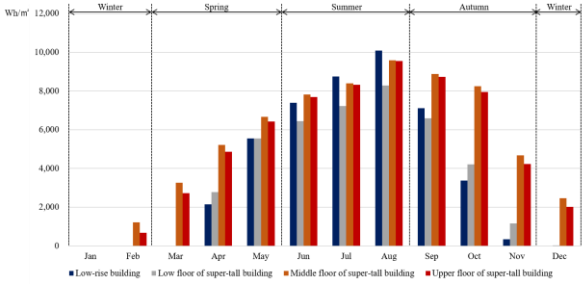

Figure 6: Monthly Cooling Energy

The result shows that the annual cooling energy is larger in upper floor of super tall building than low floor of super-tall building and low-rise building. Moreover, upper floor of super-tall building has larger annual cooling energy than annual heating energy.

4 INFLUENCE OF SOLAR AND INFILTRATION ON HEATING AND COOLING LOAD

According to table 4, upper floor of super-tall building has more beam and diffuse solar radiation than low floor of super-tall building and low-rise building. This would be due to reduction of adjacent shading buildings and reflections from adjacent rooftops. As average infiltration increases with high-rise in super-tall building, upper floor of super-tall building has more infiltration heat gain and heat loss than low floor of super-tall building but smaller heat gain than low-rise building due to high level of airtightness.

According to Figures 7 and 8, upper floor and middle floor of super-tall building have larger solar heat gain energy than low floor of super-tall building and low-rise building. Since outside temperature decreases and infiltration increases with high-rise, infiltration heat loss and heat gain are higher in upper floor of super-tall building than in low floor of super-tall building. Due to lager solar heat gain, upper floor of super-tall building has smaller annual heating energy but larger cooling energy than low-floor of super-tall building. Also, upper floor of super-tall building has smaller annual heating energy but larger annual cooling energy than low-rise building because of larger solar heat gain and smaller infiltration heat gain.

Table 4: Heating and cooling load of residential super-tall building and low-rise residentail building

	Annual Solar Radiation Wh/m²(a)		Infiltration Energy Wh/m²(a)	
	Beam Solar Radiation	Diffuse Solar Radiation	Heat gain	Heat loss
Upper floor of super-tall building	**6,125**	**10,135**	**25**	**4,883**
Middle floor of super-tall building	**6,125**	**9,868**	**25**	**4,165**
Low floor of super-tall building	**907**	**2,511**	**19**	**2,227**
Low-rise building	**907**	**2,704**	**43**	**3,968**

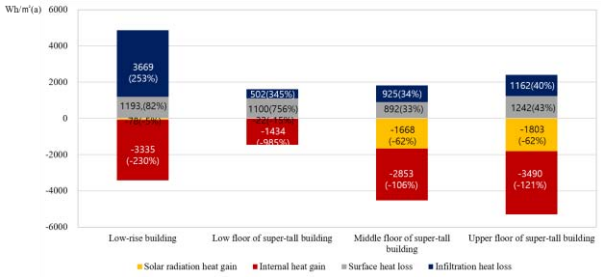

Figure 7: Annual Heating Energy components

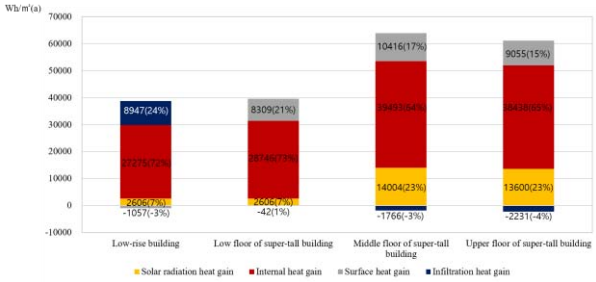

Figure 8: Annual Cooling Energy components

According to Figures 9 and 10, upper floor of super-tall building has larger infiltration heat loss and heat gain than low floor of super-tall building. This would be due to increased wind speed at the high-rise. However, upper floor of super-tall building has smaller infiltration heat loss and heat gain than low-rise building due to high level of air tightness. Therefore, upper floor of super-tall building has larger peak heating and cooling load than low floor of super-tall building but smaller than low-rise building due to infiltration.

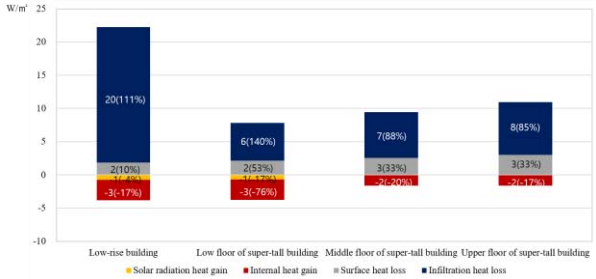

Figure 9: Peak Heating Load components

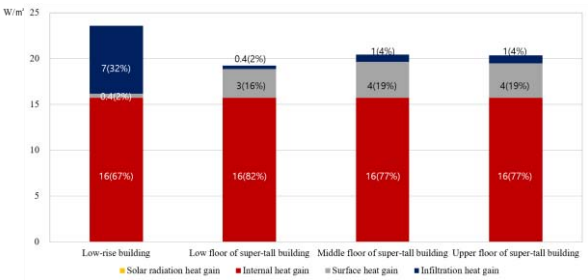

Figure 10: Peak Cooling Load components

With respect to change of solar radiation and infiltration, Figures 11 and 12 shows the difference in SHR when peak cooling load appeared in super-tall building and low-rise building. During the daytime, upper floor of super-tall building has larger sensible cooling load but during night time, it has smaller sensible and latent cooling load than low-rise building. In summer, solar radiation is expected to make larger sensible cooling load during daytime but under hot and humid weather, large amount of infiltration makes large sensible and latent cooling load in night time. It is the reason why upper floor of super-tall building has larger SHR than low-rise building but has smaller than low floor of super-tall building. Since variation of the SHR in the super-tall building is larger than that in the low-rise building, cooling system capable of coping with a change in sensible heat would be advantageous in the super-tall building.

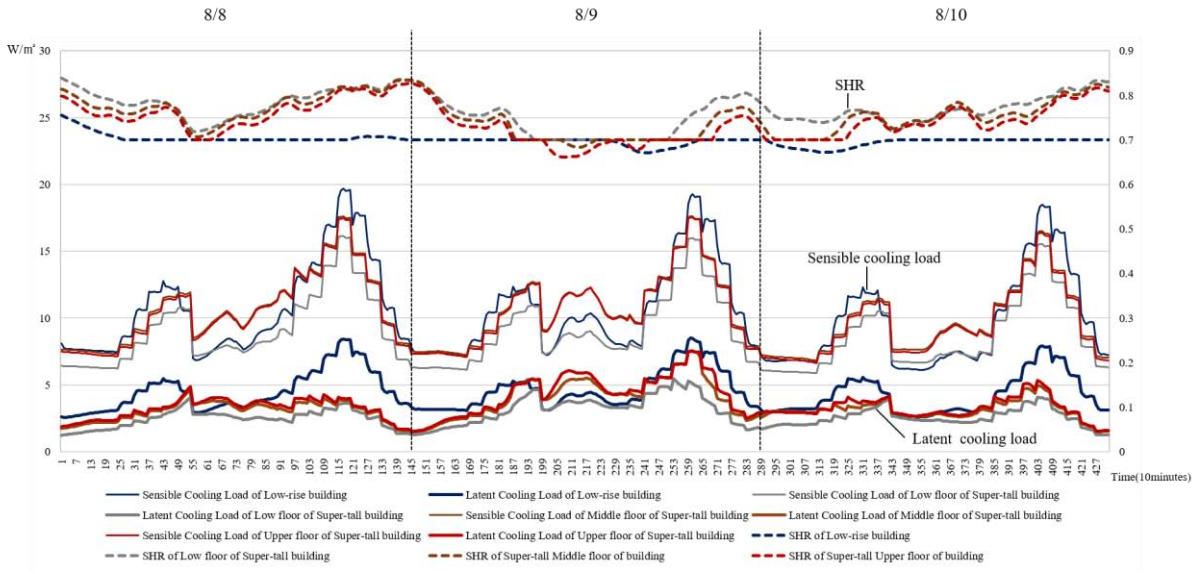

Figure 10: Cooling load and SHR when Peak Cooling load appeared in upper floor of super-tall building

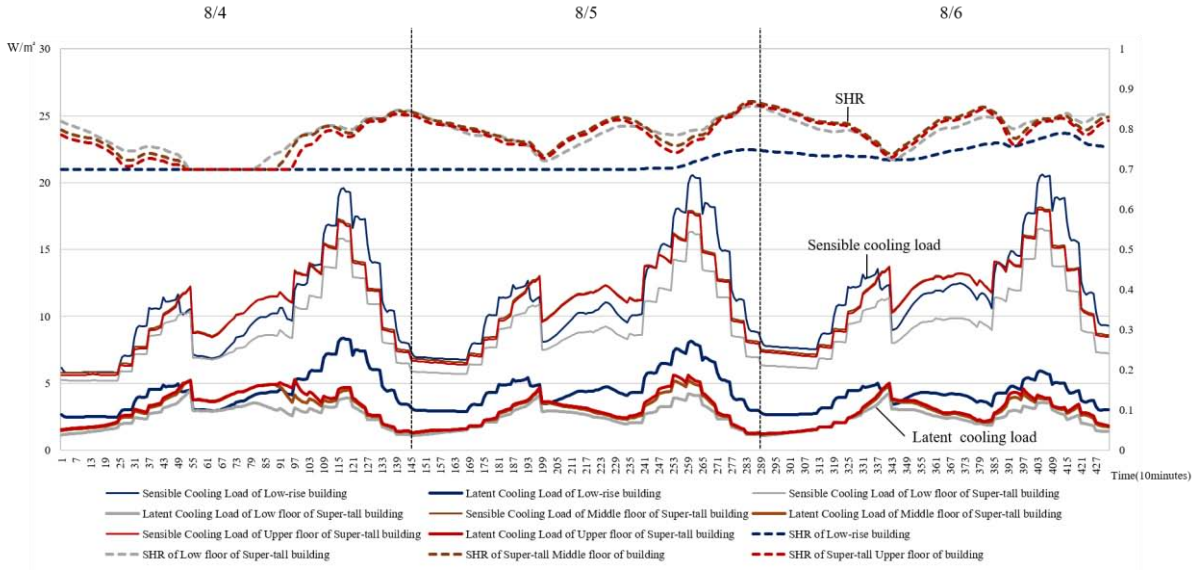

Figure 11: Cooling load and SHR when Peak Cooling load appeared in low-rise building

5 CONCLUSIONS

The objective of this study was to analyse the influence of external environment on heating and cooling load of super-tall building due to high-rise. Through a dynamic load analysis, heating and cooling load of super-tall residential building and low-rise residential building was examined.

The simulation results showed that upper floor of super-tall building has different heating and cooling load characteristic as compared low-rise building and low floor of super-tall building due to solar radiation and airtightness. Since solar radiation affect the annual heating and cooling energy, upper floor of super-tall building has larger annual cooling energy and smaller heating energy than low floor of super-tall building and low-rise building. Infiltration affect the peak heating and cooling load. Therefore, upper floor of super-tall building has larger peak heating and cooling load than low floor of super-tall building but smaller the peak loads than low-rise building.

It is considered mechanical operation plan for annual cooling energy is necessary in upper floor of super-tall building because cooling load more occurs in upper floor of super tall building than in low floor of super-tall building and low-rise building. Also, for cooling system, it is considered upper floor of super-tall building has larger SHR and variation of the SHR than low-rise building.

6 ACKNOWLEDGEMENTS

This research was supported by a grant (18AUDP-B106327-05) from Architecture & Urban Development Research Program funded by Ministry of Land, Infrastructure and Transport of Korean Government.

7 REFERENCES

Ellis, P. G., & Torcellini, P. A. (2005). Simulating Tall Buildings Using EnergyPlus: Preprint (No. NREL/CP-550-38133). National Renewable Energy Lab., Golden, CO (US).

Kim, K. W., Yeo, M. S., Ryu, S. R., Shin, M. S. (2007). Planning consideration for High-rise Buildings. Magazine of the SAREK, 36(2), 4-19

Kim, Y. S., Song, D. S. (2010). A building load analysis of ultra high-rise building under the effect of vertical microclimate change. 2010 The Society of Air-conditioning and Refrigerating Engineers of Korea Conference, 407-412

ASHRAE. (2013). 2013 ASHRAE Handbook Fundamentals. American Society of Heating, Refrigerating and Air-Conditioning Engineers, Inc

M. S. Jung, Y. J. Choi, D. S. Song. (2006). A Study on Hybrid AC System Coupled with Natural Ventilation and Cooling System. 2006 The Society of Air-conditioning and Refrigerating Engineers of Korea Conference, , 351-358.

Yoon, D. W. (2011). Development of high-rise residential ventilation integrated HVAC system, Korean Institute of Architectural Sustainable Environment and Building Systems, 5(2), 57-65

Jeong, C. H., Lee, J. Y., Yeo, M. S., & Kim, K. W. (2007). Cooling load analysis of residential buildings for dehumidification/sub-cooling system in radiant cooling. *Sustainable Buildings (SB)*, *1*, 505-512.

Jo, J. H. (2010). Measurements of the Dwelling Unit Airtightness in High-rise Residential Buildings. JOURNAL OF THE ARCHITECTURAL INSTITUTE OF KOREA Planning & Design, 26(10), 337-344.

S, H. S., Kim, B. S. (2011). A Comparative Analysis of Energy Simulation Results and Actual Energy Consumption on Super High-rise Apartments. Journal of the Korean Solar Energy Society, 31(4), 34-40.

Improvement Method of Thermal Environmental Near Windows During Heating Period -Thermal and Air Flow Characteristics of Two-Dimensional Jet from Breeze Line Diffuser in Free Field

Shaoyu Sheng*[1], Toshio Yamanaka[1], Tomohiro Kobayashi[1], Jihui Yuan [1], Masahiro Katou[2] and Saori Yumino[2]

1 Osaka University
2-1 Yamadaoka
Suita, Osaka, Japan
Sheng_shaoyu@arch.eng.osaka-u.ac.jp

2 KAJIMA Technical Research institute
2-19-1 Tobitakyu
Chofu, Tokyo, Japan

ABSTRACT

The perimeter space near windows usually has some problems with the thermal environment which is easily affected by heat transfer and radiation from windows. Compared to interior space of the room, the airflow in this area usually has different characteristics due to the effect of buoyancy, thus it may reduce thermal comfort of perimeter space. To improve the thermal environment in perimeters, breeze line diffusers are widely used in Japan as the terminal equipment of air conditioning and ventilation systems. This diffuser is the same as so-called ceiling slot diffuser. In this research, the authors analysed the performance of breeze line diffuser for heating usage by experiment. The airflow rate and temperature around the breeze line diffuser was also obtained to define boundary conditions of CFD (Computational Fluid Dynamics) model of breeze line diffuser, which will be simulated in our future work.

For the full-scale experiment, the breeze line diffuser is set up in a free field. The air supply temperature under isothermal and non-isothermal conditions, and the length of the outlet of the diffuser are adjusted as parameters. Temperature and wind velocity distribution not only around the diffuser but also the other part of the free field were measured by hot wire anemometer, ultrasonic anemometer, and thermocouple in this study.

The results of the experiment are compared. The breeze line diffuser has a limited heating effect in the occupant zone (height below 1.7m) due to the effect of buoyancy, but heating effect can be decreased if the outlet velocity is fast enough. Install some deflection plane inside the breeze line diffuser to adjust the outlet area can help to enhance diffuser's heating effect. And the authors will use these data to decide the location of P.V. Method's boundary. The airflow rate and temperature distribution will also be used as comparison data to examine the accuracy of the CFD model in further study.

KEYWORDS

Perimeter environment, Breeze line diffuser, Free field, Airflow distribution

1 INTRODUCTION

Breeze line diffusers are widely used in Japan as the terminal equipment of air conditioning and ventilation systems to improve the thermal environment of the perimeter area near the window. This diffuser is the same as so-called ceiling slot diffuser. With the buoyancy's effect, warm air outflow has very different characteristics while compared to the condition of cooling air, and the research on efficiency of the diffuser for heating usage is limited [1]. Furthermore, in recent years, designs like glass curtain wall make the glazing ratio much larger, and the equipment with higher efficiency contributes to less heat generation than before, thus these problems like temperature distribution and cold draft in perimeter area during heating period are arising. It is

important to examine the performance of breeze line diffuser and improve its efficiency for heating usage.

According to the user's feedback and the results of some simple smoke test, the perimeter performance of breeze line diffuser in winter is occasionally poor because warm airflow jetting from the breeze line diffuser cannot reach the occupancy zone below 1.7m height when the outlet velocity is not high enough. Although raising the air volume can increase the outlet velocity, and the outlet temperature should also be balanced with the heat load, it may complicate the operation and decrease the total efficiency of the air conditioning system. Thus, without replacing the breeze line diffuser to a new type, two deflection panels are installed inside the diffuser to change the area of outlet. Under the same air volume condition, the velocity of outlet airflow can be varied by adjusting the panel angle of diffuser.

CFD simulation is considered as the most efficient way to examine the efficiency of breeze line diffuser with deflection panels in different outlet temperatures and operational environment, because the parameter conditions can be changed easily. As the first step of a CFD simulation, it is necessary to obtain enough data through experiment to precisely reproduce the diffuser's property in CFD simulation.

With the full-scale experiment carried out in the free field, the authors had meant to use the vector velocity and temperature data respectively measured by ultrasonic anemometer and thermocouples at the surface area of the diffuser as the boundary condition of CFD simulation. However, the frequency of ultrasonic anemometer (max 10Hz) cannot provide enough data to calculate the turbulence kinetic energy and turbulence eddy dissipation accurately. Additionally, the probe size of the ultrasonic anemometer (3cm) is larger than the diffuser's size (2.55cm wide), thus the vector velocity at the surface area of diffuser can't be well measured. These will decrease the reliability of the CFD model, and may even give incorrect prediction in further research.

The shape of the diffuser is always oversimplified in CFD though the actual breeze line diffuser has complex geometry. It is considered that simple CFD diffusers will lead to inaccurate predication. On the contrary, establishing a complex geometry model of breeze line diffuser may increase the accuracy of prediction, however huge computer capacity and long calculation time are required. Fortunately, it is generally acknowledged that using P.V. Method (Prescribed Velocity Method) to displace the model into some layer's boundary condition to reproduce the diffuser's outlet airflow has satisfactory accuracy in CFD simulation [2], [3] and fewer numbers of meshes is needed to help reduce the computational load.

The aim of this study is to obtain the data of airflow and temperature distributions both near the diffuser and whole outlet space by experiment. Based on the experimental data obtained in this study, the authors will decide the measurement layer's location of X-type probe hotwire anemometer. Furthermore, the velocity and temperature data of outlet space will be used to examine the accuracy of the CFD simulation in the future.

2. FULL SCALE EXPERIMENT

2.1 Experiment facilities

- **Breeze line diffuser**

The breeze line diffuser used for experiment in this study is shown in Fig.1 and Fig.2. Two deflection panels are installed inside the diffuser to change the outlet area of diffuser with 1/1 outlet or 1/2 outlet by adjusting the panel angle. Thus, the velocity of outlet airflow can be varied under the same air volume condition.

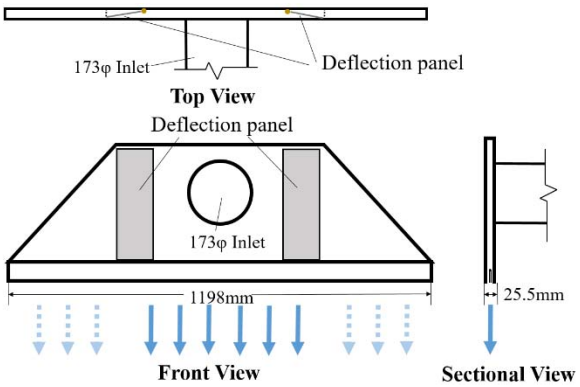

Fig.1 Detail view of the breeze line diffuser

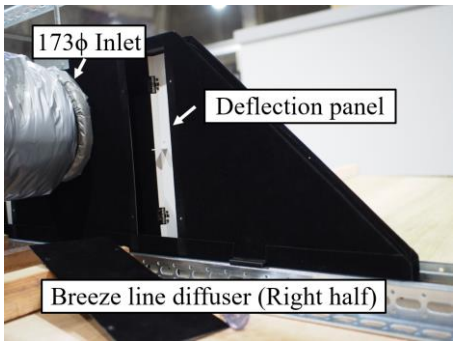

Fig.2 Photograph of the breeze line diffuser

■ Experiment space

The experiment was conducted in the Laboratory of Building Environment (hereinafter abbreviated as LBE) at Osaka University in February 2019. The experiment space with a dimension of 3 m (L) x 3 m (W) x 3 m (H), is a free field with ceiling but no surrounding exterior walls structure. The detailed are shown in Fig.3 and Fig.4. In addition, the LBE can provide enough experiment space without obvious disturbance like natural convection or heating element, and it can be regarded as a free field.

■ Air-conditioning and ventilation system

As shown in Figs.3 and 4, a breeze line diffuser is connected to a duct fan and electronic heater by spiral duct. A volume damper is set in the inlet area to control the airflow volume, and an ultrasonic flowmeter is set between fan and diffuser to measure the airflow volume. In order to control the temperature difference between inlet and outlet of air-conditioning and ventilation system, the thermocouples are fixed both on the inlet area of duct near the damper and diffuser's outlet surface. The temperature difference between inlet and outlet can be controlled by adjusting the output efficiency of electronic heater. In addition, all the spiral ducts are thermal insulated by using glass wool.

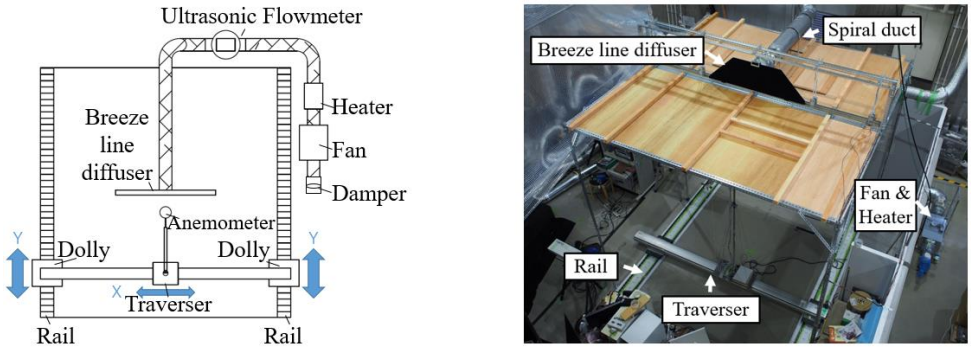

Fig.3 Top view of outlet and measurement system

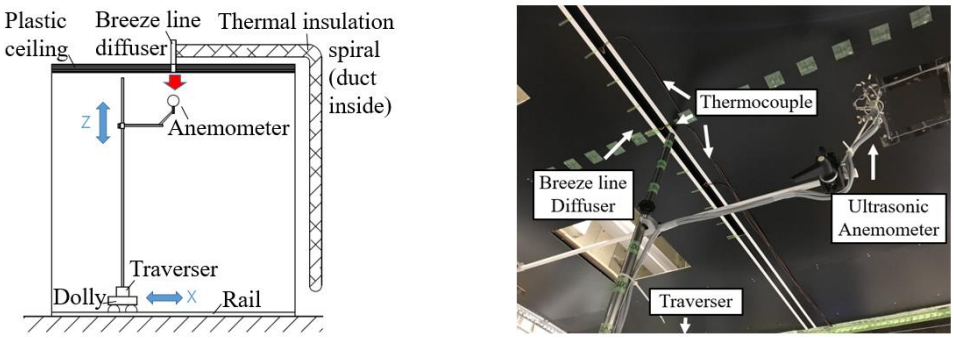

Sketch Photograph

Fig.4 Side view of outlet and measurement system

2.2 Measurement method & measurement point

■ Temperature and wind speed of diffuser's outlet surface

To measure the outlet temperature continuously, three thermocouples were stacked on diffuser's outlet surface in equal divided area. Measurement points of these thermocouples were adjusted (40cm intervals when 1/1 outlet, 20cm intervals when 1/2 outlet), depending on the length of the main flow outlet (120cm or 60 cm).

The scalar wind speed of the outlet surface (5mm below the diffuser) was measured by hot wire anemometer. All the diffuser's outlet surface was measured regardless of the location of the jet airflow. The locations of measurement points are shown in Fig.5, with 100 mm intervals in the horizontal direction and 8.5 mm intervals in vertical direction. A total of 60 data was taken for 1 minute for 1 measurement point.

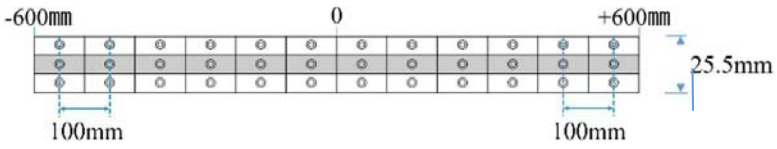

Fig.5 Overview of measurement points of scalar wind speed in outlet surface of the diffuser

■ Temperature and vector velocity of outlet space

Ultrasonic anemometer (10 Hz) and thermocouples of Type-T (1Hz) were respectively used to movement measure the vector velocity and temperature distribution in outlet space. Locations of the measurement points are shown in Fig.6.

■ Vertical temperature distribution

The vertical temperature distribution in the LBE was measured by eight thermocouples, at the height of 0.1m, 0.6m, 1.1m, 1.7m, 2.2m, 2.5m, 2.7m, and 2.9m. Measurement location is near the experiment space (thermocouples are stuck on the vertical flame of experiment space).

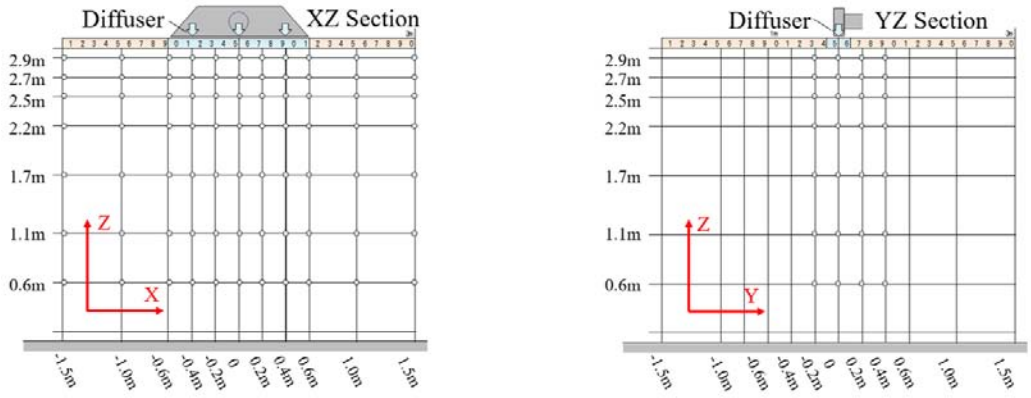

Fig.6 Overview of measurement point in outlet space

2.3 Temporal temperature change & correction method

The temperature measurement of the outlet area in this research is in order from the height near the diffuser to the ground. Including preparation time, it took at least 8 hours for each case to finish all the measurement points. Because the indoor temperature of LBE is susceptible to outdoor temperature, the indoor air temperature varied about 2~3℃ for each measurement height during measurement time (as shown in Fig.7).

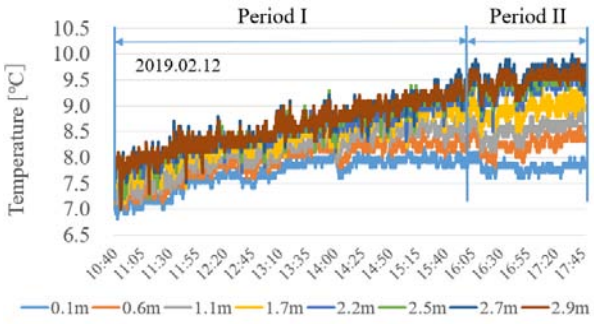

Fig.7 temperature distribution in laboratory

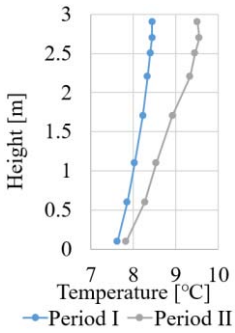

Fig.8 Average temperature distribution

The movement measurement time was divided into two periods to correct-temporal errors. During Period I (10:30~16:00), the temperature of measurement points at the height of 1.7m~2.9m was measured. As shown in Fig.7, the temporal temperature change during this period can be regarded as a process of constant speed raise (about Δ1.5℃ for this case). Thus, the time when measurement started of every point was recorded and temperature correction was accrued in proportion to time. The time-based correction formula is as follows (1).

$$\theta_P^* = \theta_P + \frac{t_{16} - t}{t_{16} - t_0} \times (\theta_{Pr16} - \theta_{Pr0}) \quad (1)$$

θ_P^* : corrected temperature at point P [℃]
θ_{Pr} : the temperature of reference point at the same height as measurement point P [℃]
t : elapsed time from the start of section I[s]
16 : 16:00pm (data is corrected when they was measurement before 16:00pm)
0 : start time of measurement

The temperature for measurement points at the height of 0.6m and 1.1m was measured during Period II (16:00~17:40). Compared to Period I, the temporal temperature change during Period II is less, thus the temperature data of Period II was recorded without correction.

2.4 Experiment case and parameter

The experiment cases and parameters are shown in Table 1. As shown in Fig.9 and Fig.10, the airflow rate and temperature difference between inlet and outlet are well maintained around 200 m^3/h and Δ8℃ respectively. In addition, using the result of measured scalar velocity of diffuser outlet surface (as shown in Fig.11), the airflow rate was also calculated by average scalar wind speed measured at diffuser's outlet surface by hotwire anemometer. It is shown that the calculated result (1/1 outlet: 2.04m/s×0.0305m^2=223 m^3/h; 1/2 outlet: 1.99m/s×0.0305m^2=218 m^3/h) is generally consistent with the measurement value of ultrasonic flowmeter.

Table 1: Experiment case & parameter

Case	Outlet area	Thermal condition	Δ℃	Air volume
Case 1	1/1 outlet	Isothermal	-	200Nm^3/h
Case 2	1/1 outlet	Heating supply	Δ8℃	200Nm^3/h
Case 3	1/2 outlet	Heating supply	Δ8℃	200Nm^3/h
Case 4	1/2 outlet	Isothermal	-	200Nm^3/h

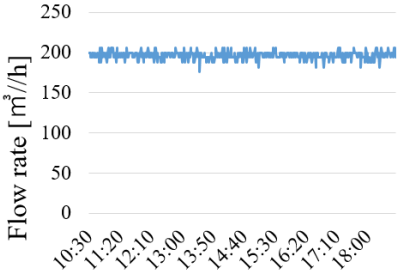

Fig.9 Airflow rate measured by flowmeter

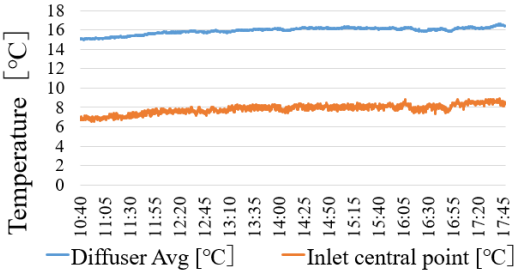

Fig.10 Inlet (Damper) & outlet (Diffuser) temperature

3. RESULTS AND DISCUSSION

3.1 Wind velocity distribution

Fig.11 shows the scalar wind speed of outlet surface for 1/1 outlet and 1/2 outlet conditions. The number (1~12) of X-axis represents the position of measurement in the long side, and the wind speed is averaged by 3 measurement points in the wide side of the diffuser (see Fig.5).
In order to make the airflow velocity distribution in the outlet space easier to understand, the alphabetic symbols (X_n and Y_n) was used to represent the position of measurement in horizontal and longitudinal directions. For example, X_0 and Y_0 mean the horizontal and longitudinal sections passing through the central point of the outlet. Scalar wind speed and vector velocity in X_n and Y_n sections are shown in Fig.12~Fig.19.

■ Scalar wind speed distribution of diffuser's outlet surface

All the scalar wind speed was measured in the isothermal condition.Fig.11(1) shows the outlet wind speed when the deflection panels inside the diffuser were opened (1/1 outlet). It is shown that the airflow is jetting from the whole surface of the diffuser at the average speed of 2.04m/s. Due to the geometry of the breeze line diffuser, outlet wind speed in the two sides area is about 0.5m/s faster than the central area of the diffuser.

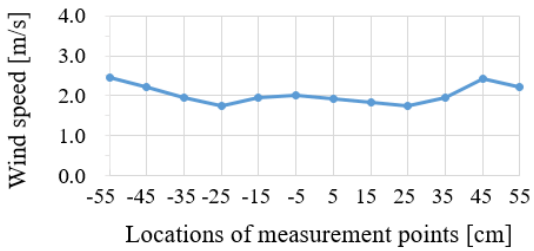

(1) Outlet wind speed (1/1 outlet)

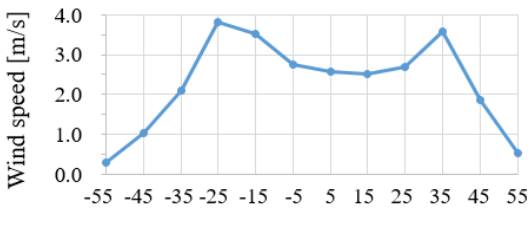

(2) Outlet wind speed (1/2 outlet)

Fig.11 Scalar wind speed of diffuser's outlet surface

For the case when the deflection panels were closed (1/2 outlet), as shown in Fig.11(2), the vast major of airflow is jetting from the central area of the diffuser (60cm in range with the total length of the diffuser is 120cm), at an-average wind speed of 3.57m/s which is about 1.7 times faster than the case when deflection panels were opened (1/1 outlet). In the area outside of the deflection panels (above 30cm away from the center of diffuser, outside the dotted line in Fig.1), some airflow was observed as the result of air leak. Similar to Fig.11(1), outlet wind speed in the two sides of the mainstream is about 1.3m/s faster than that in central area.

■ **Airflow velocity distribution of section Y**

Fig.12 and Fig.14 respectively show the scalar wind speed and vector velocity in section Y_0 for Case 1 (isothermal & 1/1 outlet) and Case 2 (heating supply & 1/1 outlet). Fig.13 and Fig.15 respectively show the scalar wind speed and vector velocity in section Y_0 for Case 3 (isothermal & 1/2 outlet) and Case 4 (heating supply & 1/2 outlet).

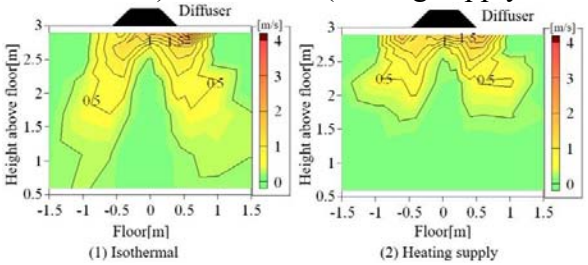

Fig.12 Scalar wind speed of section Y_0 (1/1 outlet)

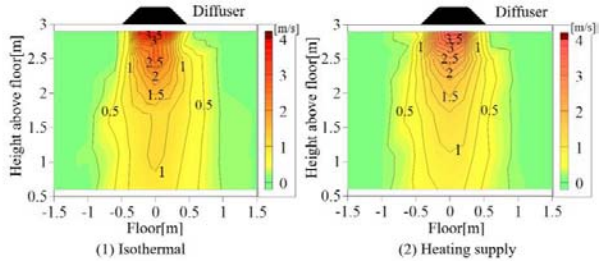

Fig.13 Scalar wind speed of section Y_0 (1/2 outlet)

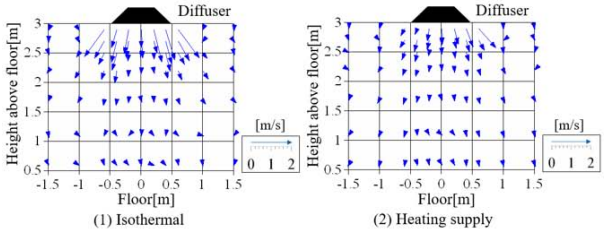

Fig.14 Vector velocity of section Y_0 (1/1 outlet)

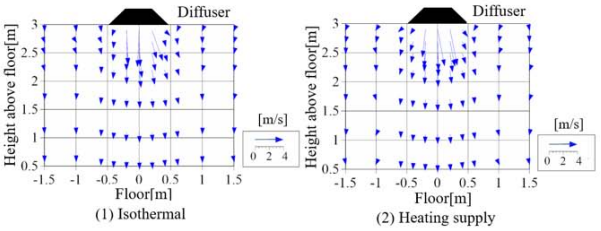

Fig.15 Vector velocity of section Y_0 (1/2 outlet)

When the outlet airflow is jetting from the whole outlet surface, it has a reversed "V" shape (see Fig.12) that the arrival ranges in the side of diffuser are much vaster than that in the center, which is similar to the outlet wind speed's distribution at the outlet surface of diffuser (Fig.11). For the isothermal case, outlet airflow can reach the occupancy zone (below 1.7m height) at wind speed of around 0.3m/s. For heating supply case, heating airflow can't reach the space below 1.7m height mainly due to the effect of buoyancy. However, heating airflow has larger diffusion ranges than isothermal airflow near the ceiling (above 2m height). When the outlet airflow is jetting under the case of 1/2 outlet, it can see that outlet airflow goes straight down to the floor without spreading around whether it's under isothermal or heated conditions from Fig.13 and Fig.15. The airflow on center of diffuser has the fastest wind speed, and reached the occupancy zone at speed of above 1m/s. The difference between the case of isothermal and heating supply outlet is the range of 1m/s speed in the heating supply case is smaller due to the buoyancy.

■ **Airflow velocity distribution of section X**

Figs.16 and 17 show the scalar wind speed of section X (3 sections: X_0, $X_{-0.4}$, $X_{-0.6}$) respectively under the cases of 1/1 outlet and 1/2 outlet. Figs.18 and 19 show the vector velocity of section X (3 sections: X_0, $X_{-0.4}$, $X_{-0.6}$) respectively under the cases of 1/1 outlet and 1/2 outlet.

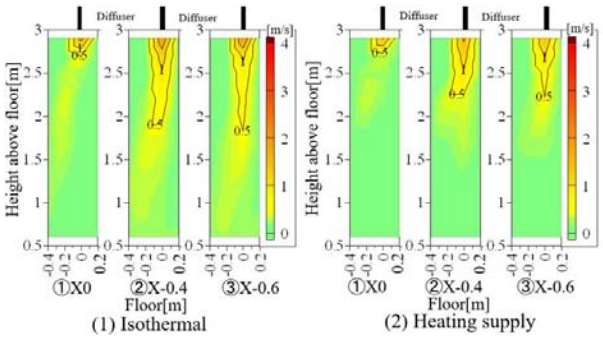

Fig.16 Scalar wind speed of section X (1/1 outlet)

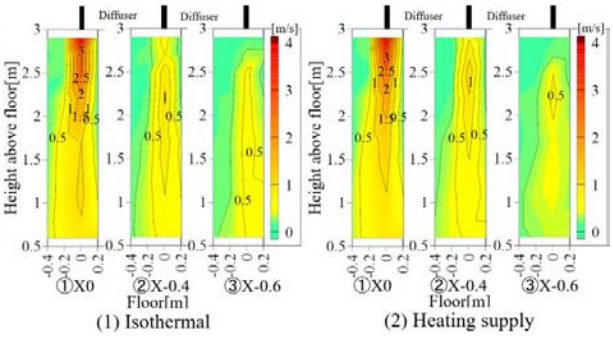

Fig.17 Scalar wind speed of section X (1/2 outlet)

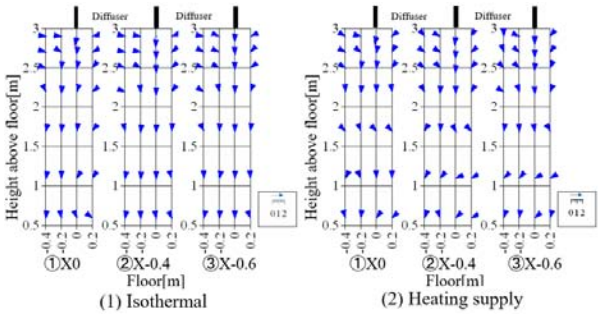

Fig.18 Vector velocity of section X (1/1 outlet)

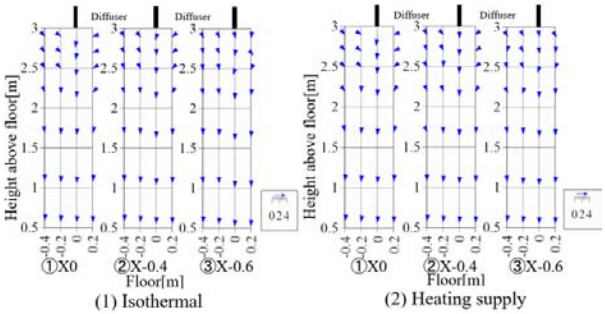

Fig.19Vector velocity of section X (1/2 outlet)

For the case of 1/1 outlet, the airflow from diffuser has the tendency of deviating aside under isothermal condition, and the deviation range becomes farther when under heating supply condition. For the case of 1/2 outlet, it is shown that the airflow is going straight from the diffuser to the floor with relatively higher wind speed, in comparison with to the case of 1/1 outlet.

Regardless of the outlet temperature condition (ΔT=8℃ and ΔT=0℃) or outlet area condition (1/1 outlet and 1/2 outlet), wind direction near the ceiling is aimed at the center part of airflow (Fig.18 & Fig. 19, 2.5m~2.9m height) due to the reason of induction.

3.2 Temperature distribution

As shown in Fig.20, for the case of 1/1 outlet, when the airflow is jetting from the diffuser with 16℃, the outlet airflow temperature dropped to about 11℃ at 0.5m away from diffuser, then the outlet airflow dropped to 9℃ at about 2.5m away from diffuser. In addition, the result of Fig.20 also showed that the temperature stratification has been observed obviously for above Δ2℃ in the occupancy zone, however very limited heating effect (less than 1℃) can be seen in this study.

The result of temperature distribution under the case of 1/2 outlet is shown in Fig.21. It is seen that the warm airflow is jetting from the diffuser with 23℃, and is reaching to the occupancy zone by much higher outlet speed, compared with the case of 1/1 outlet. The temperature in the occupancy zone just below the diffuser is about 17℃ without stratification. Furthermore, an obvious heating effect (above Δ2℃) has been observed at the range of 2m in long below the diffuser.

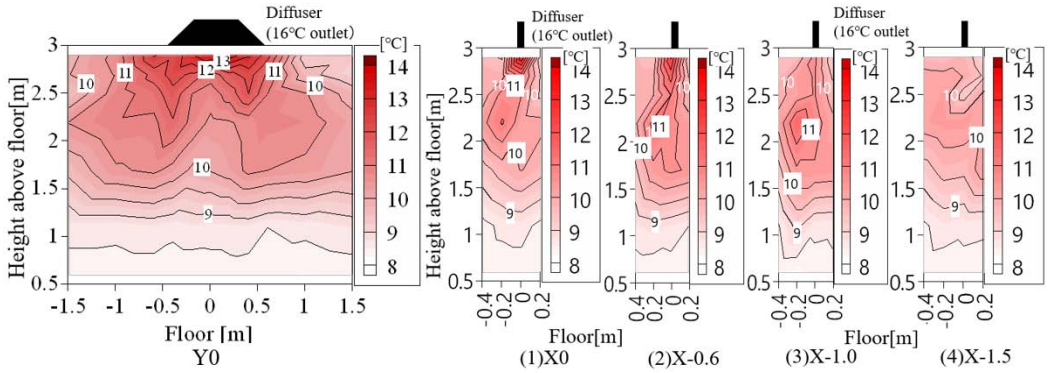

Fig.20 Temperature distribution in section (1/1 outlet)

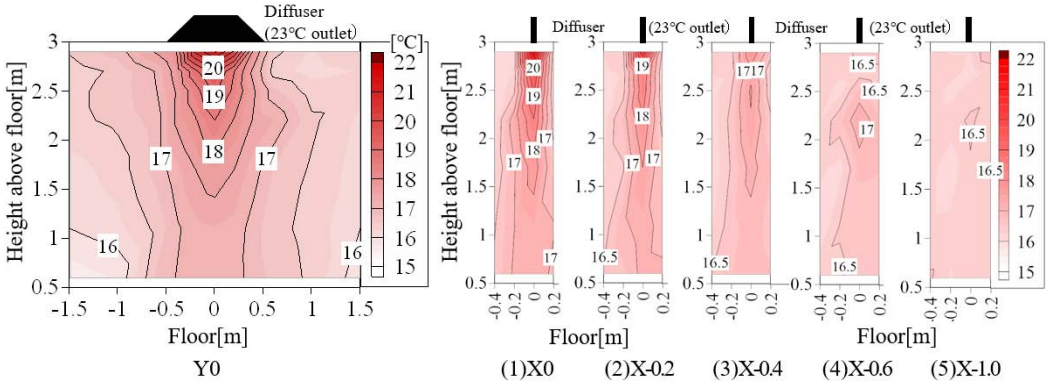

Fig.21 Temperature distribution in section (1/2 outlet)

Seeing from the side of the diffuser, from the result for the case of 1/1 outlet (Fig.20), it can see that the temperature distribution at the height of around 2.2m is higher than that closer to celling. The reason is considered to be the influence of warm air buoyancy. From the farthest section X ($X_{-1.5}$), it can see that very limited airflow arrived in this area, however there is about Δ1.5°C temperature stratification in this area.

From the result for the case of 1/2 outlet (Fig.21), it can see that the temperature distribution of the section $X_{-1.0}$ (1.0m away from the diffuser centre in X direction) has almost no stratification, about 17°C, and almost the same as the indoor temperature of LBE. The reason is considered as that the airflow can't reach to this area.

3.3 Effect of buoyancy on airflow velocity

The CFD simulation analysis on the breeze line diffuser will be planned in our future work. To decide the location of boundary conditions for the P.V. method of CFD, the scalar wind speed and wind direction angle in isothermal and heating supply conditions for both the 1/1 outlet and 1/2 outlet cases, have been measured and compared. The results are detailed in Figs.22-25.

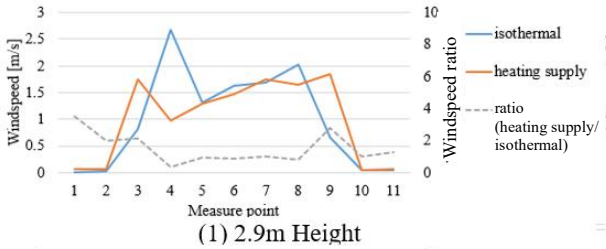

(1) 2.9m Height

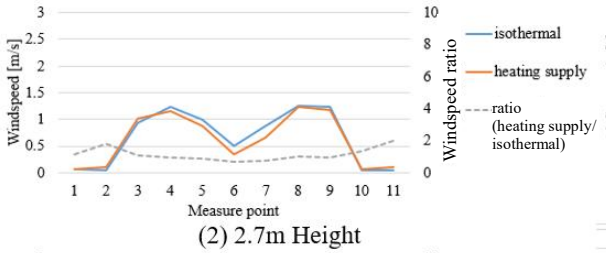

(2) 2.7m Height

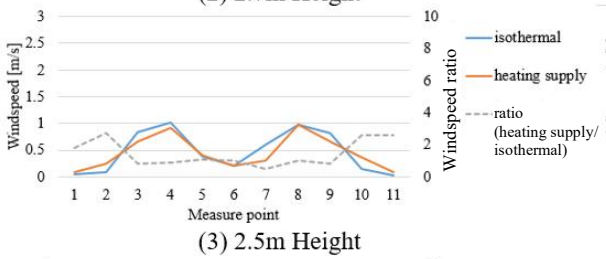

(3) 2.5m Height

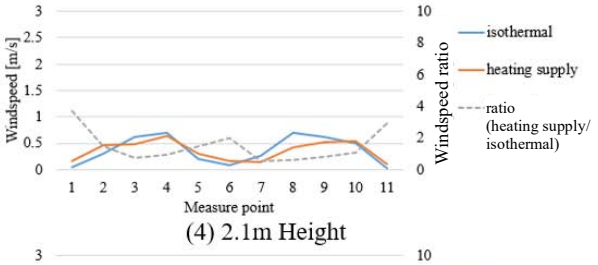

(4) 2.1m Height

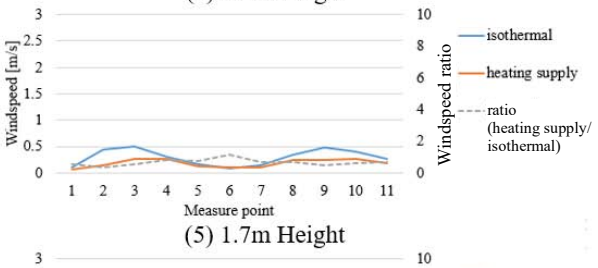

(5) 1.7m Height

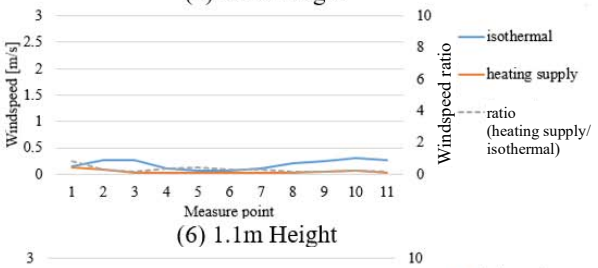

(6) 1.1m Height

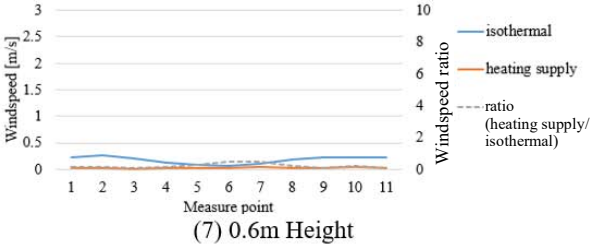

(7) 0.6m Height

Fig.22 Wind speed ratio
(Heating supply/isothermal, Section Y 1/1 outlet)

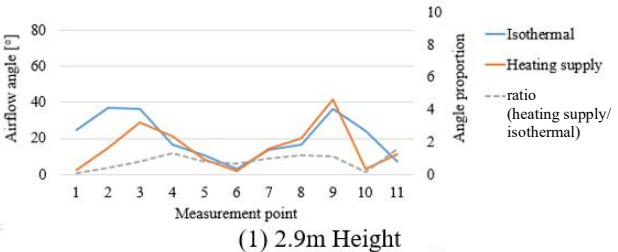

(1) 2.9m Height

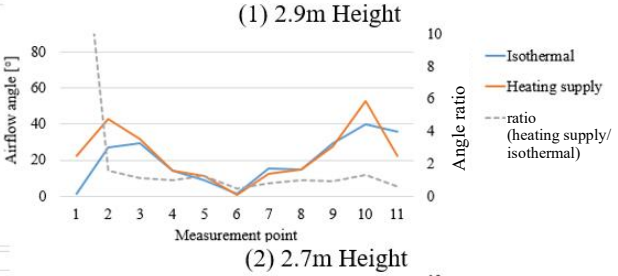

(2) 2.7m Height

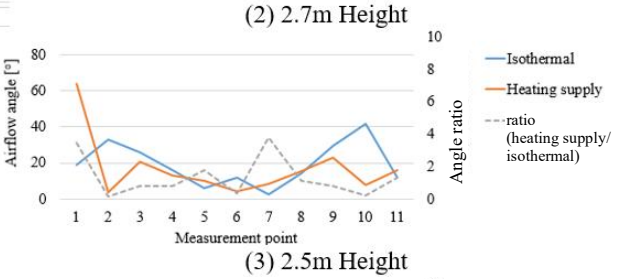

(3) 2.5m Height

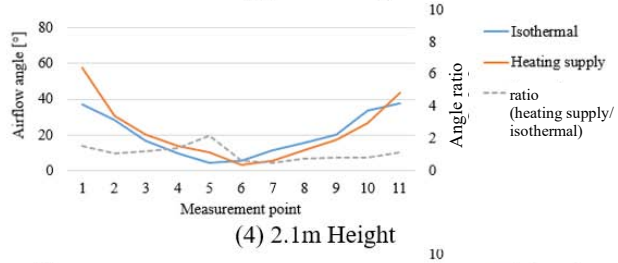

(4) 2.1m Height

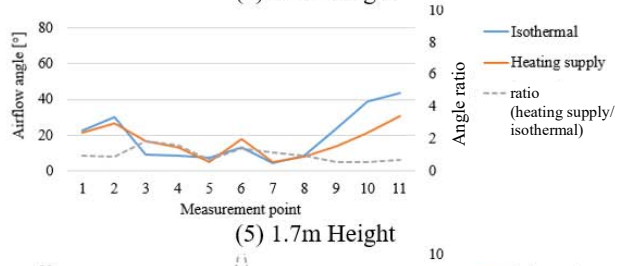

(5) 1.7m Height

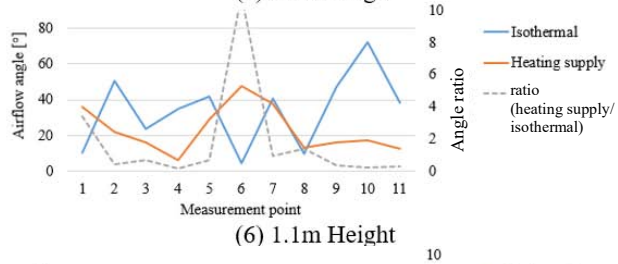

(6) 1.1m Height

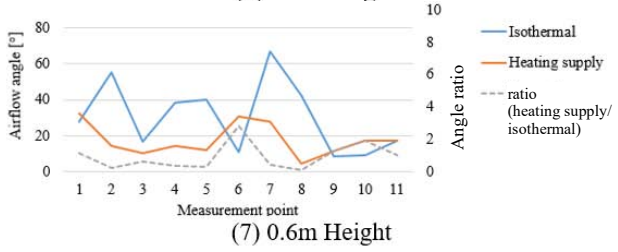

(7) 0.6m Height

Fig.23 Airflow angle ratio
(Heating supply/isothermal, Section Y 1/1 outlet)

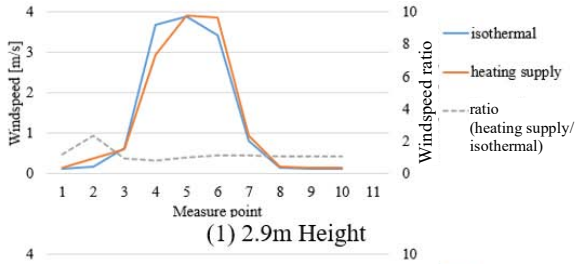

(1) 2.9m Height

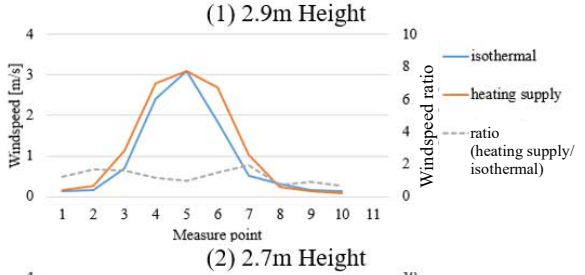

(2) 2.7m Height

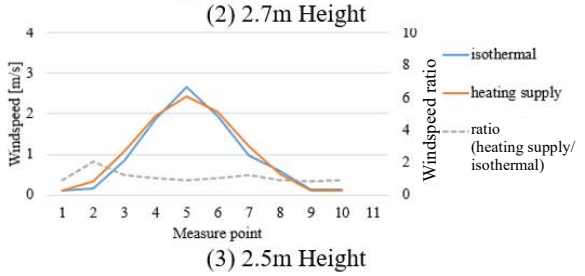

(3) 2.5m Height

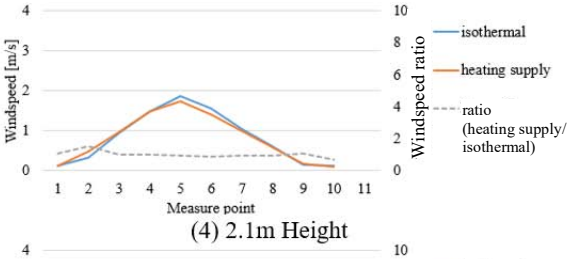

(4) 2.1m Height

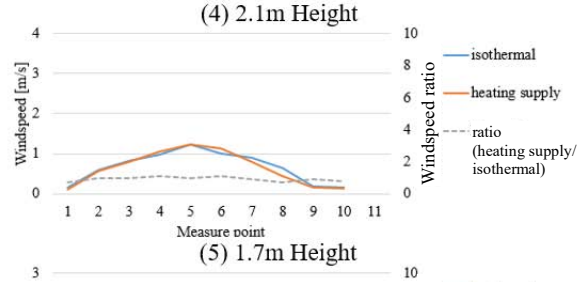

(5) 1.7m Height

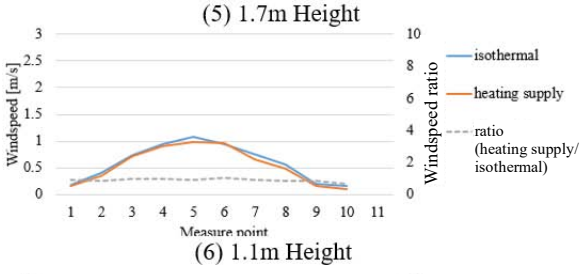

(6) 1.1m Height

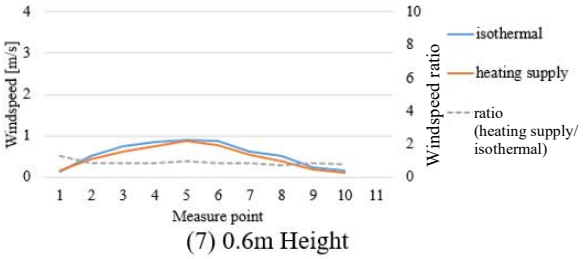

(7) 0.6m Height

Fig.24 Wind speed ratio
(Heating supply/isothermal, Section Y 1/2 outlet)

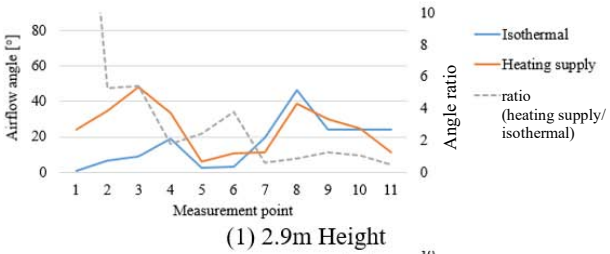

(1) 2.9m Height

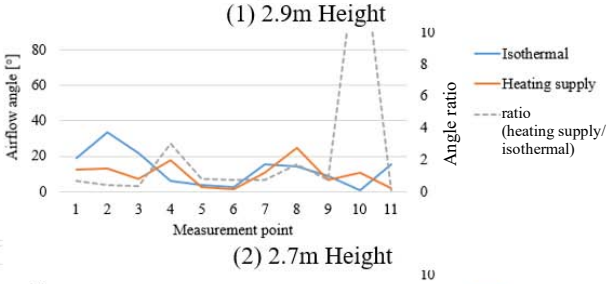

(2) 2.7m Height

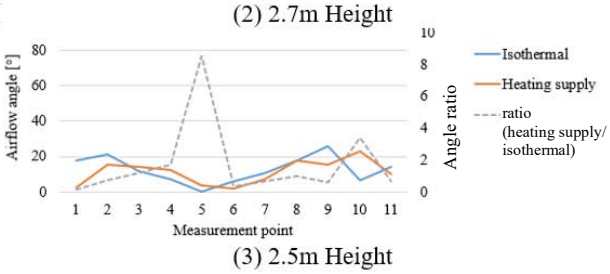

(3) 2.5m Height

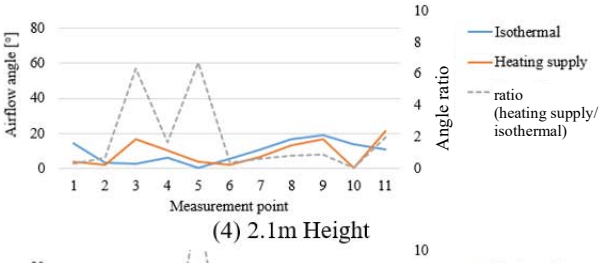

(4) 2.1m Height

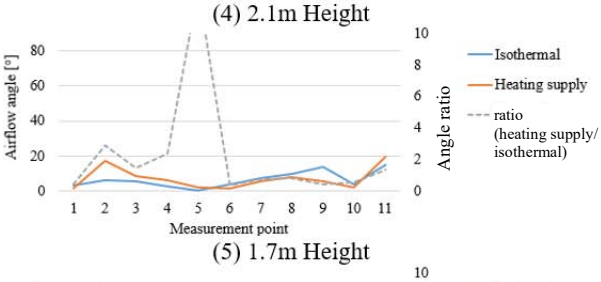

(5) 1.7m Height

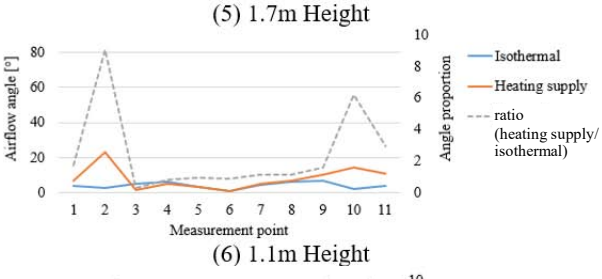

(6) 1.1m Height

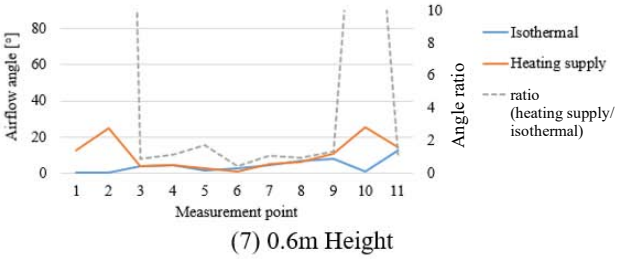

(7) 0.6m Height

Fig.25 Airflow angle ratio
(Heating supply/isothermal, Section Y 1/2 outlet

4 CONCLUSIONS

In this research, the full-scale experiment of breeze line diffuser was carried out. The size of the outlet surface was changed by adjusting the deflection panel inside the diffuser. The knowledge obtained in this study are shown as follows.

- Buoyancy can affect the arrival area of outlet airflow (case of 1/1 outlet), however, when the outlet velocity is fast enough (case of 1/2 outlet), this influence is limited.
- The breeze line diffuser has limited heating effect in the occupancy zone (below 1.7m) when the warm air is jetting from the whole outlet surface (1/1 outlet) at a common outlet volume of about 200m^3/h.
- Without increasing the outlet volume, to adjust the deflection plane inside of the diffuser can make the heated airflow reach the occupancy zone at a certain speed (case of 1/2 outlet).
- It is indicated that there is almost no temperature stratification, but heating effect has been observed in the occupancy zone near the diffuser under case of 1/2 outlet.
- It is worth looking forward to enhancing the heating effect of breeze line diffuser by set deflection panels inside it.

For the future work, the figure of the ratio of wind speed and airflow angle will be used to decide the location of the boundary condition for the P.V. method. A vector velocity measurement by X-type probe hotwires anemometer will be carried out at these boundary layers, and all the data obtained from this experiment will be used to examine the accuracy of the CFD model in further study.

5 ACKNOWLEDGEMENTS

The authors are sincerely grateful to the KUKEN KOGYO. Co. Ltd for providing the breeze line diffuser used in this study.

6 REFERENCES

[1] M. KATOH, T. SHINOZUKA, Y. ARAI Y, S. YUMINO, T. YAMANAKA, T. KOBAYASHI: Prediction Method of Thermal Environment during Heating in Winter for Spaces with Large-Area Window(Part 1)Measurement Results and Simplified Evaluation method for Vertical Temperature Difference in Office buildings, Transactions of the Society of Heating, Air-conditioning and Sanitary Engineers of Japan (266), 11-21, 2019.05 [in Japanese]

[2] Chen Q and Srebric J: Simplified Numerical Models for Complex Air Supply Diffusers, HVAC&R RESEARCH Volume 8, pp.277-294,2002

[3] P.V. Neilsen: DESCRIPTION OF SUPPLY OPENINGS INUMERICAL MODELS FOR ROOM AIR DISTRIBUTION, ASHRAE Transactions Part1, pp.963-971, 1992.2.

Airtightness and energy impact of air infiltration in residential buildings in Spain

Irene Poza-Casado*[1], Alberto Meiss[1], Miguel Ángel Padilla-Marcos[1], and Jesús Feijó-Muñoz [1]

1 GIR Arquitectura & Energía
Universidad de Valladolid
Avda/ Salamanca, 18 - 47014
Valladolid, Spain

**Corresponding author: irene.poza@uva.es*

Presenting author: Irene Poza-Casado

ABSTRACT

Addressing the airtightness of the building envelope is key to achieve thermal comfort, good performance of ventilation systems and to avoid excessive energy consumption. Previous studies have estimated an energy impact on infiltration on the heating demand between 2 and 20 kWh/(m^2·y) in regions with temperate climates. In Spain, this issue has not yet been addressed in depth. This study aims to assess the energy impact of uncontrolled air flows through the building envelope in residential buildings in Spain. For this purpose, airtightness results of more than 400 blower door tests have been analyzed. Multi-family and single-family dwellings built in several periods and located in 9 regions with different climate characteristics have been studied. Infiltration was found to have an energy impact in the range 2.43 – 19.07 kWh/(m^2·y) for the heating demand, whereas it is not so significant regarding the cooling demand. The obtained results show great potential for energy saving in the country.

KEYWORDS

Air leakage; Blower Door, energy impact; residential buildings; fan pressurization test

1 INTRODUCTION

The European Union is committed to reducing greenhouse gas emissions, establishing a sustainable, competitive and decarbonised energy system by 2050. It is estimated that buildings are responsible for approximately 36% of all CO_2 emissions and that almost 50% of the final energy consumption of the Union is used for heating and cooling. 80% of it is consumed in buildings (European Parliament 2018). Therefore, it seems essential to establish strategies that support the renovation of national buildings stocks, facilitating their transformation into nearly zero energy buildings (nZEB).

In this context, one of the factors that have a great impact is the presence of air infiltration. The constant improvement and EPB-requirements in the transmittance of the construction elements has led to the grown relevance or the entrance of outdoor air in the total energy consumed by the residential sector.

In Mediterranean countries, however, airtightness has still not been broadly addressed. The fact that ventilation is not controlled and normally done by manually opening the windows, means that air infiltration is the only continuous air inlet. It has already been estimated that the energy impact of air infiltration on the heating demand can account for around 10 kWh/(m^2·y) in regions with a moderately cold climate (2500 degrees-day) (Carrié and Wouters 2013), or an increase on the heating demand from 5 to 20 kWh/(m^2·y) in countries with temperate climates (Spiekman 2010). In Spain, it has been

estimated that air infiltration can be responsible for up to 27.4% of the energy demand (Meiss and Feijó-Muñoz 2014).
National building regulations in Spain are gathered in the National Building Code (CTE), which was first released in 2006 and updated several times so far (Ministerio de Fomento del Gobierno de España 2017). Requirements regarding the limitation of energy demand are gathered in DB HE. Concerning airtightness, there is only a limitation on the permeability of windows depending on the climate zone. That means that global airtightness is not taken into account in spite of the increasing weight of the energy impact of air leakage on the overall energy performance of buildings. A new update of CTE is expected to be released in 2019. Although measures are taken to implement nZEB following European Directive 2018/844 (European Parliament 2018) on the energy performance of buildings and energy efficiency, no update regarding airtightness is expected.
However, even though regulations in Spain do not include airtightness requirements of the whole building envelope, the official tools for the EPB-requirements verification consider air infiltration as a parameter. Global permeability is calculated considering permeability of doors and windows, air leakage of the opaque part of the envelope and air inlets. Since tests performance is not mandatory, default values are almost always used: 0.63 h^{-1} for residential buildings and 0.80 h^{-1} for tertiary.
Given the relevance of airtightness from an energy point of view, the purpose of this paper is to analyze the energy impact of air infiltration in Spain from real airtightness measurements in order to evaluate its importance in the total energy consumption in dwellings.

2 METHODOLOGY

2.1 Sample

Since airtightness is not mandatory in Spain, there is a lack of data on air infiltration in buildings. Tests are only performed to comply with specific energy programmes (Passivhaus, BREEAM, LEED, etc.), by constructors who wish to ensure the quality of construction or as a diagnostic tool in case of poor energy performance of the building or before retrofitting actions. In any case, this data is scarce, not publicly available and belong to a very specific type of buildings, which are not representative of the housing stock of the country. Some studies on airtightness in Spain have already been carried out so far focused on the specific type of dwellings (Meiss and Feijó-Muñoz 2014; Jiménez Tiberio and Branchi 2013; Fernández-Agüera et al. 2016). Recently, another study established a database with more than 400 representative cases (Feijó-Muñoz et al. 2018), which will constitute the sample for this study.
The considered database includes cases in different climate zones, built in different periods of time and gathers both single and multi-family dwellings. The dwellings tested were chosen based on a representative sample of the existing housing stock in Spain by means of a non-probabilistic quota sampling scheme.
The most represented climate areas were Mediterranean (209 cases located in Barcelona (BCN), Alicante (ALC), Málaga (MAL) and Sevilla (SEV)) and Continental (129 cases located in Madrid (MAD) and Valladolid (VLL)), but also Oceanic (47 cases located in Bilbao (BIL) and La Coruña (COR)) and the Canary Islands (16 cases located in Las Palmas de Gran Canaria (LPA)) were included in the sample. The age of the cases tested was proportional to the existing building stock, being the periods 1960-1979 (37%) and 1980-2006 (39.5) the most represented ones. Concerning typology, 325 cases were apartments (81%) and 76 cases were single-family houses (19%).

2.2 Testing method

The assessment of the building airtightness was approached by means of the fan pressurization method, according to ISO 9972 (International Organization for Standardization 2015). Regarding building preparation, any intentional opening in the building envelope was closed or sealed (Method B). The correct calibration of the equipment was ensured to maintain accuracy specifications of 1% of reading, or 0.15 Pa. On the other hand, according to ISO 9972, the overall uncertainty is highly dependent upon the environment during the test, being lower than 10% in most cases in calm conditions.

The infiltration curve is calculated as follows (Equation 1):

$$V_{env} = C_{env}(\Delta p^n) \quad (1)$$

where:

V_{env}: air flow rate through the envelope of the dwelling [m^3/h]

C_{env}: air flow coefficient [$m^3/ (h \cdot Pa^n)$]

Δp: induced pressure difference [Pa]

n: pressure exponent [-]

In order to compare air leakage rates, the air flow rate values were normalized by the building thermal envelope area, A_E [m^2] and internal volume V [m^3], and reported at 50 Pa, q_{50} [$m^3/(h \cdot m^2)$] and n_{50} [h^{-1}] respectively, interpolated from measurements. However, operational pressure differences are typically an order of magnitude lower than 50 Pa at around 4 Pa (Jones et al. 2015). There have been many studies in this regard so far. The first studies that first assessed the relationship between n_{50} and n_{nat} (air change rate in natural conditions) where carried out in the 70' and 80' (Kronvall 1978), (Persily and Linteris 1983). Subsequently, Sherman (Sherman 1987) reported a linear relationship (Equation 2), which is often refered as the *Sherman's ratio*:

$$n_{nat} = \frac{n_{50}}{20} \quad (2)$$

Sherman developed this model, maintaining the assumption of a linear relationship between the air change rate at a pressure difference of 50 Pa and under natural conditions but considering an empirical correction factor N scaling it according to local climate, air leakage path size, dwelling height and shielding (Equation 3).

$$n_{nat} = \frac{n_{50}}{N} \quad (3)$$

This model has been broadly applied in national building codes and standards, although it must be emphasized that the use of a scaling factor is a simplified treatment of a complex reality (Chan et al. 2005). Furthermore, it is worth mentioning that it does not allow to distinguish the origin of air infiltration in the case of apartments in buildings. In this case, given that the study is a first approximation to the energy impact of air infiltration in Spain, a simplified model has been addressed and the most unfavourable situation was approached, considering that the whole air infiltration is produced in the surface in contact with the outdoor environment.

2.3 Energy impact assessment

Infiltration can contribute a significant amount to the overall heating or cooling load of a building (Buchanan and Sherman 1998). Several models have been developed so far but there is no common criterion about the appropriate model to evaluate the energy impact of infiltrations. The energy load was obtained by means of a simplified model using the classical infiltration calculation (Equation 4).

It is obtained as a product of the air infiltration flow, the specific air capacity and the temperature difference between the inside and the outside of the dwelling. The concept of degree-day was applied, relating the average temperature outside the tested dwelling and the comfort indoor temperature (21℃ for heating and 25℃ for cooling). It is important to note that this estimation is theoretical and real energy consumption depends on the particular temperature conditions of the dwellings (Feijó-Muñoz et al. 2019). Some authors have emphasized that this method might be well acceptable when calculating the load due to concentrated leakage (through large openings, short paths), but it could entail a considerable overestimation of the energy impact in the case of diffuse leakage (small cracks, where heat exchange between the infiltrating air and the wall may occur) (Younes, Shdid, and Bitsuamlak 2012).

$$Q_{inf} = C_p \cdot G_t \cdot V_{inf} \quad (4)$$

where:

Q_{inf} is the annual energy loss [kWh/y] due to air infiltration for heating Q_{inf-H} and cooling Q_{inf-C}. Annual energy losses are expressed per unit area

C_p is the specific heat capacity of the air, which is 0.34 Wh/(m^3·K)

G_t are the annual degree days [kKh/y], both for heating (G_{t-C}) with a base comfort temperature of 21 ℃, and for cooling (G_{t-R}) with a base comfort temperature of 25 ℃

V_{inf} is the air leakage rate [m^3/h]

3 RESULTS AND DISCUSSION

Averaged main results sorted by location of the dwellings are shown in Table 1. The energy impact estimation of the air infiltration was obtained, both for the heating and cooling demand (Figure 1). Furthermore, the relative impact of air infiltration on the heating and cooling demand has been approached based on reference demand values used in energy certification of existing buildings (IDAE 2011) (Figure 2).

Table 1: Airtightness results and energy impact due to air infiltration

Parameter	unit	COR	BIL	VLL	MAD	BCN	ALC	MAL	SEV	LPA
n_{50}	h^{-1}	4.61	4.67	4.99	7.29	9.73	7.78	6.89	8.88	5.43
q_{50}	m^3/(h·m^2)	3.58	3.47	3.76	5.93	7.49	6.26	5.16	6.81	4.60
n	-	0.62	0.62	0.64	0.61	0.59	0.61	0.60	0.58	0.59
Q_{inf-H}	kWh/(m^2·y)	11.10	11.15	16.41	19.07	16.44	10.02	8.61	14.21	2.43
Q_{inf-C}	kWh/(m^2·y)	0.02	0.26	0.80	2.47	0.73	1.60	0.78	3.06	0.54
$\%_{-H}$	%	11	11	10	15	18	18	20	25	0
$\%_{-C}$	%	0	0	9	12	5	5	2	6	2

Figure 1: Anual energy impact due to air infiltration

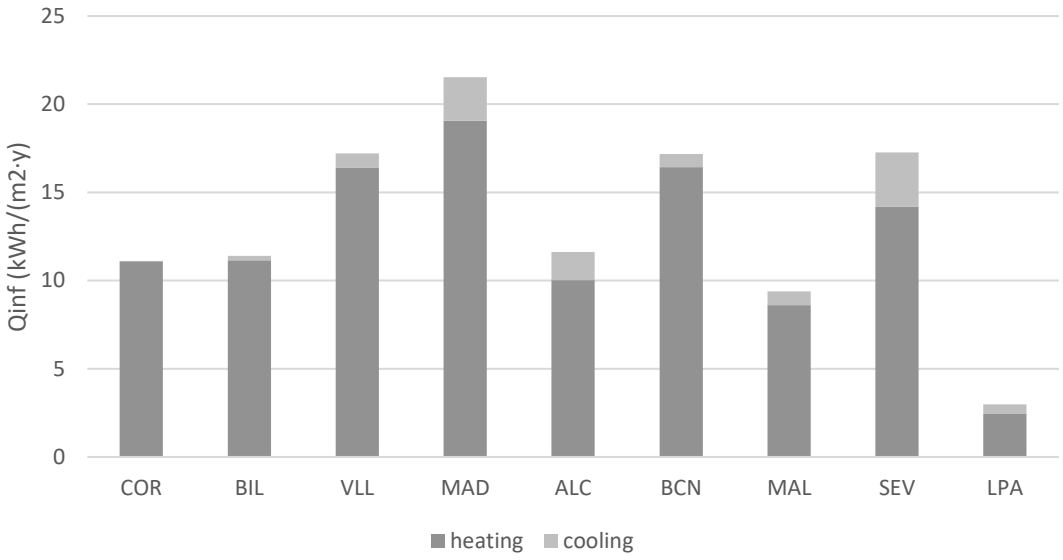

Maximum permeability values (q_{50}) were found in Mediterranean areas such as Barcelona, Sevilla and Alicante, whereas dwellings with a better airtightness performance were located in the north of the country (A Coruña, Bilbao and Valladolid). The pressure exponent, n, is in all the locations close to 0.6.
Air infiltration has a greater impact on the heating demand, especially in cities with a continental climate such as Madrid or Valladolid. Values of up to 19.07 kWh/(m^2·y) have been obtained in the case of Madrid, while in cities with a milder climate such as Las Palmas de Gran Canaria, the value is reduced to 2.43 kWh/(m^2·y). In the case of the cooling demand, the energy impact of air infiltration is lower, with maximum values of 3.06 kWh/(m^2·y) in the case of Sevilla. In other locations such as A Coruña or Bilbao, the impact on the demand for refrigeration becomes residual.

Figure 2: Relative impact of air infiltration on the heating and cooling demand

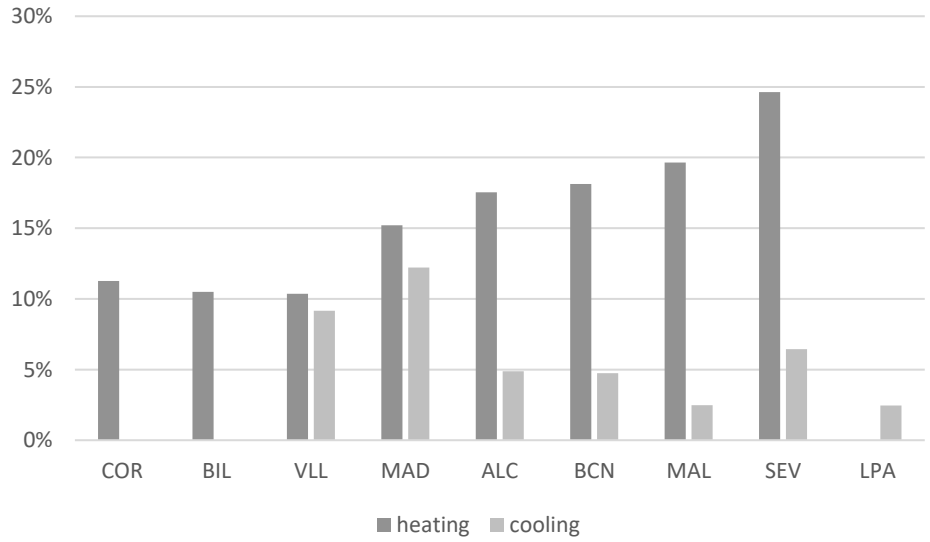

Regarding the relative impact of air infiltration, values up to 25% corresponding to the heating demand or 12% for cooling demand were obtained.

4 CONCLUSIONS

In Mediterranean countries with mild climates and where ventilation has traditionally been done in a natural way, the concern regarding airtightness is still scarce. However, air infiltration cannot be ignored any more in a context where huge efforts are being made to transform the existing stock into nZEB. It seems to be time to face a change in building construction traditions and regulations, addressing airtightness properly.

From the results obtained in the present study, it can be derived the enormous impact that air infiltration through the building envelope has in Spain. The impact is greater on the heating demand, while the impact for cooling can be residual in Atlantic areas. Maximum values of up to 19.07 kWh/(m^2·y) for the heating demand have been obtained in the case of Madrid, or up to 3.06 kWh/(m^2·y) in the case of the cooling demand in Sevilla. In relative terms, air leakage entails up to 25% of the heating demand and up to 12% of the cooling demand. These results are in line with the values previously stated in other studies.

Therefore, the energy impact of air infiltration in existing residential buildings of Spain is a question to consider necessarily given its demonstrated relevance. Consequently, compliance with the European Directive 2018/844 seems only possible by paying special attention to airtightness, implementing limitations in this respect applicable both to the design of new buildings and to the renovation of the existing housing stock.

Nevertheless, a larger sample and a deeper analysis of the data should be considered in order to draw more accurate conclusions.

5 ACKNOWLEDGEMENTS

The test campaigns that allowed this work were supported by the Spanish Ministry of Economy and Competitiveness (BIA2015-64321-R) under the research project *INFILES: Repercusión energética de la permeabilidad al aire de los edificios residenciales en España: estudio y caracterización de sus infiltraciones*. The attendance to this conference has been possible thanks to the program *Movilidad de Doctorandos UVa 2019*.

6 REFERENCES

Buchanan, C. R., and M. H. Sherman. 1998. “CFD Simulation of Infiltration Heat Recovery.” In *19th AIVC Annual Conference*, 1–10. Oslo, Norway.

Carrié, Rémi, and Peter Wouters. 2013. “Building and Ductwork Airtightness.” *REHVA European HVAC Journal*. http://tightvent.eu/wp-content/uploads/2012/02/TightVent-book2013-REHVA-TOC1.pdf.

Chan, Wanyu R., William W. Nazaroff, Phillip N. Price, Michael D. Sohn, and Ashok J. Gadgil. 2005. “Analyzing a Database of Residential Air Leakage in the United States.” *Atmospheric Environment* 39 (19): 3445–55. doi:10.1016/j.atmosenv.2005.01.062.

European Parliament. 2018. *European Directive 2018/844 Amending Directive 2010/31/EU on the Energy Performance of Buildings and Directive 2012/27/EU on Energy Efficiency*. *Official Journal of the European Union*. Vol. 156.

Feijó-Muñoz, Jesús, Cristina Pardal, Víctor Echarri, Jesica Fernández-Agüera, Rafael Assiego de Larriva, Manuel Montesdeoca Calderín, Irene Poza-Casado, Miguel Ángel Padilla-Marcos, and Alberto Meiss. 2019. “Energy Impact of the Air Infiltration in Residential Buildings in the Mediterranean Area of Spain and the Canary Islands.” *Energy and Buildings* 188–189: 226–38. doi:10.1016/j.enbuild.2019.02.023.

Feijó-Muñoz, Jesús, Irene Poza-Casado, Roberto Alonso González-Lezcano, Cristina Pardal, Víctor Echarri, Rafael Assiego de Larriva, Jesica Fernández-Agüera, et al. 2018. “Methodology for the Study of the Envelope Airtightness of Residential Buildings in Spain: A Case Study.” *Energies 2018, Vol. 11, Page 704* 11 (4). Multidisciplinary Digital Publishing Institute: 704. doi:10.3390/EN11040704.

Fernández-Agüera, Jesica, Samuel Domínguez-Amarillo, Juan José Sendra, and Rafael Suárez. 2016. “An Approach to Modelling Envelope Airtightness in Multi-Family Social Housing in Mediterranean Europe Based on the Situation in Spain.” *Energy and Buildings* 128. Elsevier B.V.: 236–53. doi:10.1016/j.enbuild.2016.06.074.

IDAE. 2011. “Escala de Calificación Enegética Para Edificios Existentes.”

International Organization for Standardization. 2015. *ISO 9972:2015 Thermal Performance of Buildings. Determination of Air Permeability of Buildings. Fan Pressurization Method*. https://www.iso.org/standard/55718.html.

Jiménez Tiberio, Alberto, and Pablo Branchi. 2013. “A Study of Air Leakage in Residential Buildings.” In *2013 International Conference on New Concepts in Smart Cities: Fostering Public and Private Alliances (SmartMILE)*, 1–4. Gijón. doi:10.1109/SmartMILE.2013.6708180.

Jones, Benjamin, Payel Das, Zaid Chalabi, Michael Davies, Ian Hamilton, Robert Lowe, Anna Mavrogianni, Darren Robinson, and Jonathon Taylor. 2015. “Assessing Uncertainty in Housing Stock Infiltration Rates and Associated Heat Loss: English and UK Case Studies.” *Building and Environment* 92. Elsevier Ltd: 644–56. doi:10.1016/j.buildenv.2015.05.033.

Kronvall, Johnny. 1978. “Testing of Houses for Air Leakage Using a Pressure Method.” *ASHRAE Transactions* 84 (1): 72–79.

Meiss, Alberto, and Jesús Feijó-Muñoz. 2014. “The Energy Impact of Infiltration: A Study on Buildings Located in North Central Spain.” *Energy Efficiency* 8 (1): 51–64. doi:10.1007/s12053-014-9270-x.

Ministerio de Fomento del Gobierno de España. 2017. *Código Técnico de La Edificación (CTE) (in Spanish)*. Spain. https://www.codigotecnico.org/.

Persily, A.K., and G.T. Linteris. 1983. “A Comparison of Measured and Predicted Infiltration Rates.” *ASHRAE Trans.* 89 (June).

https://www.osti.gov/biblio/6499412-comparison-measured-predicted-infiltration-rates.
Sherman, Max H. 1987. “Estimation of Infiltration from Leakage and Climate Indicators.” *Energy and Buildings* 10 (1): 81–86. doi:10.1016/0378-7788(87)90008-9.
Spiekman, Marleen. 2010. “ASIEPI. The Final Recommendations of the ASIEPI Project: How to Make EPB-Regulations More Effective?” https://ec.europa.eu/energy/intelligent/projects/sites/iee-projects/files/projects/documents/asiepi_access_the_results._en.pdf.
Younes, Chadi, Caesar Abi Shdid, and Girma Bitsuamlak. 2012. “Air Infiltration through Building Envelopes: A Review.” *Journal of Building Physics* 35 (January): 267–302. doi:10.1177/1744259111423085.

Exist'air: airtightness measurement campaign and ventilation evaluation in 117 pre-2005 French dwellings

Sylvain Berthault*[1], Lucille Labat[1], Cédric Delahais[2], Elodie Héberlé[3] and Sabrina Talon[1]

1 Cerema Centre-Est
Département Laboratoire d'Autun
1 Bd Giberstein, BP141
71405 Autun cedex, France
**Corresponding author:*
Sylvain.berthault@cerema.fr

2 Cerema Normandie-Centre
Département Aménagement Durable des Territoires
10 chemin de la poudrière CS 90245
76121 Le Grand Quevilly cedex,France

3 Cerema Est
Laboratoire Régional de Strasbourg
11, rue Jean Mentelin, BP9
67035 Strasbourg Cedex 2, France

ABSTRACT

Between 2017 and 2018, the Centre for Studies and Expertise on Risks, the Environment, Mobility and Planning (Cerema) organized an airtightness measurement campaign in 117 multi-family collective and single-family French dwellings. These dwellings were built before 2005, that is, before the release in 2005 of the fifth French thermal regulation for new dwellings, that was the first to introduce specific requirements for airtightness. The aim of this campaign was to give a clear picture to the French Ministry of Sustainable Development of airtightness and ventilation performance of the existing building stock. To do so, the dwellings were selected to constitute a representative panel that represented the French residential building of the stock. First, a diagnostic protocol was defined to evaluate the state of deterioration of the building, the ventilation performance and the building airtightness. All this information and other details about the dwellings were compiled into a database to be processed.

Air change rates at 50 Pa (n_{50}) were very variable and ranged from 0.44 hr^{-1} to 13.7 hr^{-1}.

The results showed that some air leakages paths influenced the airtightness of the panel more than others. Some of them could not be observed before the airtightness measurement and were therefore not easily predictable. Results also highlighted the fact that some building characteristics were highly correlated to high air change rates. These characteristics were different between collective and single-family dwellings. Unfortunately, the size of the panel (67 houses and 50 apartments), compared with the number of characteristics, did not allow to propose some robust models for airtightness prediction. To address this issue, it was decided to expand the panel with a second airtightness measurement campaign in 2019.

In the same time, ventilation systems of these dwellings were recorded and their performance were qualitatively assessed without making any measurement. A lack of ventilation was detected in 84% of the houses and 64% of the apartments, either because the system installations were out of date, or because they were too incomplete or if not inexistent. Yet, when analysing the global air exchange rate, it appeared that it was sufficient in two-thirds of the dwellings, thanks to high air change rate that compensated the low ventilation performance. The good aeration habits of the inhabitants also limited the risk of condensation on and into the walls and poor indoor air quality.

Those results could be used to update the air change rates used in the French thermal regulation for the rehabilitation of existing buildings, which dated from 2007. In addition, this campaign helped to develop the "A+V+P-"indicator. This is a simple evaluation of the aeration, the ventilation and the airtightness of a dwelling, which could also be promoted by the Ministry to building contractors, as it gives a quick overview of the global air exchange before and after retrofitting.

KEYWORDS

Airtightness, air leakage, air change rate, ventilation, existing building stock.

1 INTRODUCTION

Existing buildings are not as airtight as new ones, even if airtightness value vary widely depending on the year of construction. Air leakages are also quite different as those found in new buildings.

(Stephen, 2000) studied the airtightness of 471 dwellings in the UK, built during the 20th century. n_{50} values ranged from 7 to 14 h^{-1} and the average value was about 11,5 h^{-1}. Dwellings built between 1930 and 1960 were less airtight than those built before 1930, whereas the most recent dwellings were as airtight as those built at the beginning of the century. These results are due to the variability of building techniques and design, building materials and regulations, changing over the years (Barbisan & Altan, 2012).

(Sinnott & Dyer, 2013) analysed the airtightness of 28 Irish single-family dwellings built between 1944 and 2008. In average, the dwellings built before 1975 were more airtight than those built in the 80's and in 2008 (respectively: q_{50} = 7.5, 9.4 and 10.5 $m^3/h/m^2$). Main air leakages are located at the junction between walls and floors, trapdoors for attic access, windows and doors surrounds, ductworks (plumbing, electricity, etc.) passing through walls, floors or ceilings and mail boxes.

A database of 135 000 American single-family dwellings was analysed in (Chan, Joh, & Sherman, 2012). Unlike the two studies above, the authors showed that the oldest dwellings were the leakiest ones. They considered that the evolution of construction techniques made it possible to build more airtight buildings and that airtightness deteriorated over the years, especially if dwellings weren't retrofitted.

(McNeil, 2012) reached the same conclusion on 36 New Zealander single-family dwellings built before 2011 and explained also this result by the evolution of construction techniques: (Chan, Joh, & Sherman, 2012) no more floorboards or panels, seals at windows and doors, no more fireplaces, etc.

Retrofitting could be the solution to get all these dwellings airtight. Nevertheless (Földvary et al, 2017) and (Collignan et al, 2016) mentioned the risk of drastically lowering the global air change rate and, by this way, of affecting indoor air quality.

In France,

- available airtightness data of existing residential buildings do not well represent the French residential building stock;
- parameters such as building characteristics or retrofitting works already carried out are not available, so it is difficult to study the influence of these parameters on measured airtightness values;
- information about the airtightness and the ventilation of a dwelling is rare: therefore, the air change rate in French existing buildings is not clearly defined.

So the airtightness of existing buildings and the impact of retrofitting were never studied precisely in France. That is why the French Ministry of Sustainable Development commissioned the Exist'air measurement campaign about this topic to the Cerema.

2 METHOD

2.1 Selection of the representative panel

117 dwellings were selected to constitute a panel that represented the French residential building stock. (Bureau d'études POUGET Consultants, 2012) showed that the French residential building stock was composed of 55% of houses and 45% of apartments.

About 1/3 of the stock was built before 1948 (heritage buildings, built with traditional techniques and materials), 1/3 between 1949 and 1974 and 1/3 after 1975 (the year of the first French thermal regulation), as shown in Figure 1.

The Cerema sent a call for volunteers. Dwellings were selected in order to respect the composition of the global residential building stock. There were no criteria about the retrofitting works that had already been done.

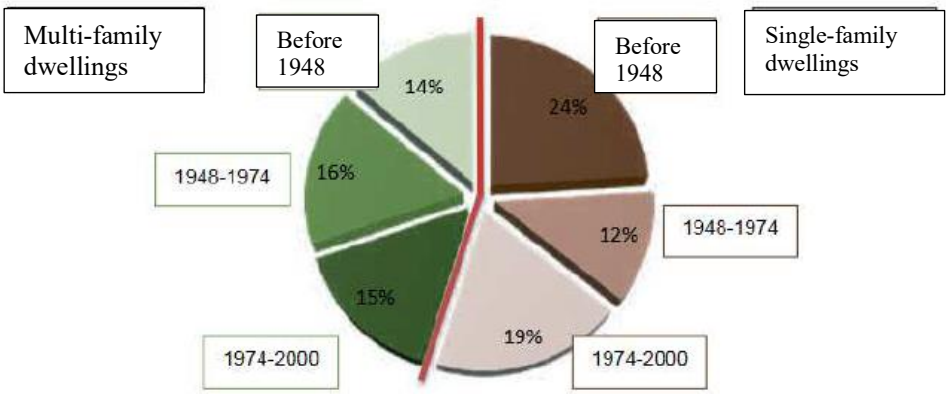

Figure 1: Composition of the French residential building stock (Bureau d'études POUGET Consultants, 2012)

2.2 Protocol for the in-situ campaign

A diagnostic protocol was defined to assess the state of deterioration of the building, the ventilation performance and the building airtightness.

2.2.1 Description of the characteristics of the dwellings

Information about dimensions and geographical context of the dwellings, composition of building elements like walls, floors and ceilings, nature and number of windows, doors and trapdoors, type of heating system and number of fireplaces were collected in a database. The state of deterioration of the building was evaluated by three possible levels for each element: good, intermediate or bad state.

The worst evaluation was always chosen. For walls, floors and ceilings, it depended on cracks, humidity, holes and aspect of finish.

For windows and doors, it depended on the state of deterioration of the seals, handle systems and aspect of the frame.

2.2.2 Evaluation of the ventilation systems

The evaluation method depended on the ventilation system:

- mechanical ventilation: evaluation of the state of deterioration of the extraction ventilator and ventilation network;
- natural ventilation: evaluation of the state of deterioration and number of vents and ductworks;
- no permanent air outlet (no mechanical or natural air outlet): there could however be air inlets.

Whatever the case, the method determined:

- if the dwelling had, at least, one air inlet in each dry room (living room, bedroom, desk, etc.), one air outlet in each damp room (kitchen, toilets, bathrooms, laundry, etc.);
- if it had 1 cm free cross-section under each inner door;
- if each inlet and outlet was clean;
- and if an airflow rate could be perceived each time.

A global score was determined for each dwelling, depending on the method. Table 1 presents the three possible scores.

Table 1: Evaluation of the ventilation score for each dwelling

Ventilation Score	Qualitative evaluation	Criteria
V3	Good ventilation	All rooms had an air inlet or an air outlet that was clean and an airflow rate was perceived each time. AND ventilation ductworks were well installed (no bend, no pinch and good connection to the ventilator) and in good state (no tear, no hole and good connection between two sections). AND exhaust air was rejected outside. AND ventilation system was independent of other systems and ran all the time. Some cross-section under inner doors could be narrower than 1cm.
V2	Medium ventilation	Some air inlets or air outlets were dirty or broken. OR there was an air inlet in a damp room or an air outlet in a dry room. OR ductworks were in bad state. OR exhaust air was rejected in the attic. OR ventilation system was not independent of other systems.
V1	Bad ventilation	Ventilator was not operating or not connected to the ventilation network. OR some air inlets or air outlets were missing. OR no airflow rate was perceived near an inlet or an outlet.

2.2.3 Airtightness measurement method

Airtightness was measured in accordance with (ISO 9972, 2015). Intentional openings in the building envelope were conditioned in accordance with method 3. These are detailed in Table 2.

Table 2: Conditions of intentional openings in the building envelope (method 3)

	Intentional openings	Conditions of intentional openings
Openings for natural ventilation	Air outlets: vents or ductworks	Sealed
	Air inlets: vents or inlets on windows or shutter casings	If the dwelling had at least one natural air outlet: sealed. If not: closed (if a closing device exists, open otherwise)
Openings for whole building mechanical ventilation	Air outlets: exhaust air openings	Sealed
	Air inlets: vents, supply air openings or inlets on windows or shutter casings	If the dwelling had at least one permanent mechanical air outlet: sealed. If not: closed (if a closing device exists, open otherwise)
Openings for mechanical ventilation (only intermittent use)	Air outlets: exhaust air openings	Closed (if a closing device exists, open otherwise)
	Air inlets: vents, supply air openings or inlets on windows or shutter casings	If the dwelling had at least one air outlet (natural ventilation or permanent mechanical ventilation): sealed. If not: closed (if a closing device exists, open otherwise)
Openings not intended for ventilation	Fireplaces and stoves	Closed (if a closing device exists, open otherwise)
	Boilers	Exhaust gas ductwork: closed (if a closing device exists, open otherwise) Air supply: open
	Kitchen hoods, tumble dryers, etc.	Open
	Water traps in plumbing systems	Filled with water or sealed
Windows, doors and trapdoors	-	Closed

In some cases, airtightness was measured with air inlets remained open.

2.3 Method for the analysis

The method employed in the Exist'air project is inspired from the one used in (Bramiana, Entrop, & Halman, 2016), which studied relationship between buildings characteristics and airtightness in Dutch dwellings.

2.3.1 Correlation between air leakages and dwellings characteristics

Some features as sliding windows, rolling shutter casings, trapdoors, false ceilings, kitchen hoods, etc. are deemed to be leaky. The frequency of air leakages on a feature (F, equation 1) provides guidance to project managers, when choosing to conserve or replace it.

$$F = \text{Number of dwellings with a given feature and with an air leakage on it} / \text{Number of dwellings with this feature} \quad (1)$$

It could be useful to get information about the risk of observing an air leakage by a simple evaluation of the state of deterioration of the building. The correlation between the state of deterioration of a building element (walls, floors, ceilings, windows, doors, trapdoors) and a type of air leakage was evaluated by the relative risk (RR, equation 2).

$$RR = \text{Frequency of air leakage on a building element in a bad state} / \text{Frequency of air leakage on a building element in a good or medium state} \quad (2)$$

A Fisher test was used to calculate the p-value of RR: if it is lower than 5%, the relative risk is significant, which means that the air leakage is correlated with the state of deterioration the building element.

2.3.2 Correlation between air leakages and airtightness values

Reducing important air leakages should be one of the objectives of project managers. To determine such leakages, a linear regression between the n_{50} and binary variables defined by the absence or the presence of an air leakage (equation 3) was calculated.

$$n_{50} = a*x + b + res \quad (3)$$

where:

- x is the binary variable;
- b is the mean value of n_{50} when x=0, i.e. when the air leakage is absent;
- a is the difference between the mean value of n_{50} when x=0 and the mean value of n_{50} when x=1;
- *res* is the residual; its distribution shall be normal to validate the linear regression.

A Student test was used to calculate the p-value of a. If a is positive and its p-value is lower than 5%, then the average value of n_{50} is significantly higher when the air leakage is present.

2.3.3 Correlation between airtightness values and dwellings characteristics

Information about dwellings characteristics that are associated with high n_{50} values can be useful for project managers when choosing an airtightness target. For this analysis, multi-family (49) and single-family (66) dwellings were studied separately. The database contained 42 variables, with many categorical variables, which was too extensive by comparison with the number of dwellings. First, an analysis of the correlations between variables was performed to get a set of independent variables. Then, for each numerical or binary variable, a linear regression as in equation (3) was calculated. For categorical variables, an ANOVA analysis was realised (equation 4).

$$n_{50} = a_1*x_1 + a_2*x_2 + a_3*x_3 + \ldots + b + res \quad (4)$$

where:

- b is the mean value of n_{50} when all x_i are null, i.e. when the dwelling is featured with all the reference categories (categories the most represented in the panel);
- x_i is a binary variable; x_i = 1 when the dwelling is featured with the category i;

- a_i is the coefficient associated to the variable x_i.

If a_i is positive with a p-value (Student test) lower than 5%, then n_{50} is significantly higher in dwellings featured with category *i* than the ones featured with the reference category.

2.3.4 Evaluation of the global air change rate

Global air change rate was qualitatively evaluated using an overall score:

- Score V+ (see §2.2.2)
- Score A+: frequency of aeration by opening windows: every day (A3), every week (A2), or rarely (A1)
- Score P-: depending on the n_{50} value (3) (values detailed in Table 3)

Table 3: Evaluation of the P- score for each dwelling

P- score	Impact of airtightness on global air change rate	n_{50} limit value
P3	The building was very leaky. Airflow rate participated highly to the global air change rate.	$n_{50} > 3\ h^{-1}$
P2	The building was quite airtight. Airflow rate participated significantly to the global air change rate.	$1,5\ h^{-1} < n_{50} < 3\ h^{-1}$
P1	The building was airtight. Airflow rate did not participate significantly to the global air change rate.	$n_{50} < 1,5\ h^{-1}$

n_{50} lower than 1,5 h^{-1} agrees with Minergie A and Minergie Passiv labels for retrofitting and with the German thermal regulation for retrofitted buildings with mechanical ventilation (Erhorn-Kluttig & Erhorn, 2012). n_{50} not higher than 3 h^{-1} agrees with German thermal regulation for retrofitted buildings with natural ventilation.

3 MAIN RESULTS AND DISCUSSION

3.1 Airtightness levels

Apartments were more airtight (n_{50} = 4.9 h^{-1}) than houses (n_{50} = 7.2 h^{-1}), Figure 2 (a) and the evolution over the periods of construction was similar, Figure 2 (b). Average values were much lower than n_{50} values presented in (McNeil, 2012) and (Stephen, 2000) at the same period of construction.

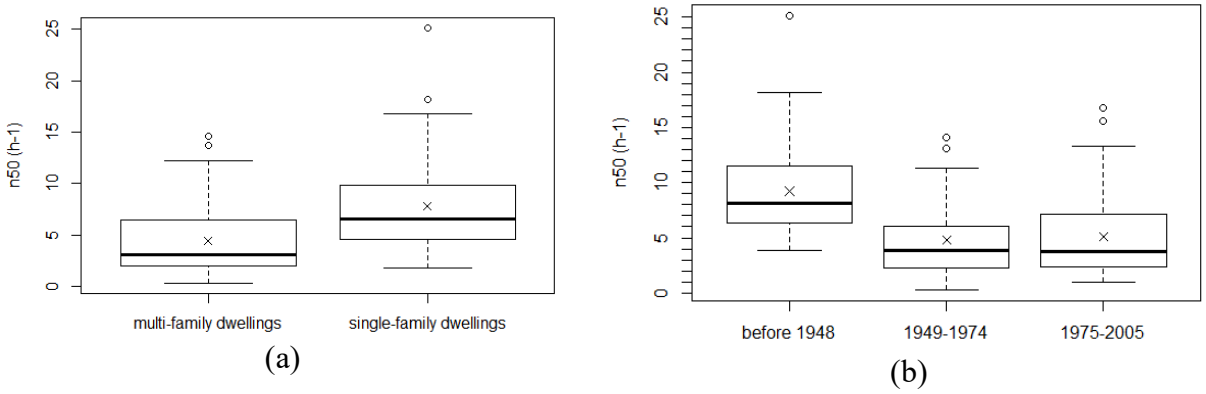

Figure 2: Airtightness of 117 dwellings depending on the type of building (a) and the period of construction (b)

When observing the nature of air leakages (Figure 3), the most frequent ones were due to missing or failing seals at windows (C2), ductworks crossings walls, floors and ceilings (D3) and electrical wall outlets (F3). These air leakages were present in more than 60 % of the panel.

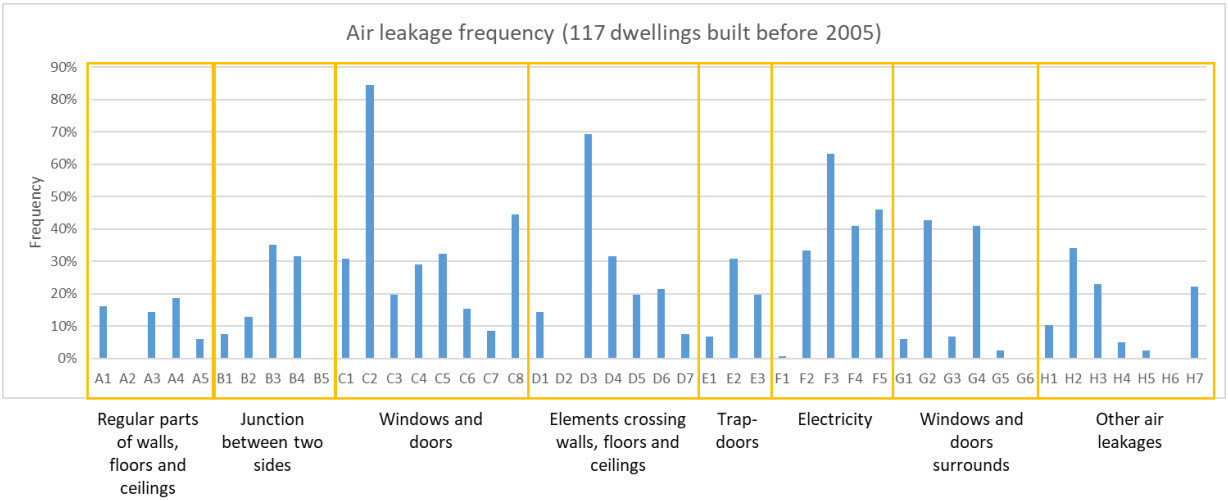

Figure 3: Air leakage frequency for 117 dwellings

3.2 Correlation between air leakages and dwellings characteristics

Data (detailed in Table 4) confirmed that false ceilings, sliding windows, shutter boxes, trapdoors, boilers, stoves, fireplaces and kitchen hoods were often leaky.

Table 4: Air leakages correlated with a dwelling characteristic

Air leakage types	Dwelling characteristics	Frequency or relative risk
Trapdoors	At least one trapdoor in the dwelling	F=91%
Air leakages on shutter casings	At least one shutter casing in the dwelling	F=86%
Leakage on a boiler or a stove	At least one boiler or stove	F=81%
Leakage on a kitchen hood	Presence of a kitchen hood	F=71%
Junction between suspended ceiling tiles	Ceilings were mainly suspended ceilings	F=66%
Air leakages on sliding windows	At least one sliding window in the dwelling	F=62%
Air outlets surrounds	Mechanical ventilation	F=15%
Junction between a floor or a wall and a staircase	Floors in a bad state	RR=4,7
Windows and doors surrounds	Bad state of windows and doors	RR=4,6
Junction between two walls	Walls in a bad state	RR=4
Little holes (fixing holes, etc.)	Ceilings, floors and walls in a bad state	RR=2,4 RR=3,6 RR=3,0
Various leakages on regular parts of walls and floors (cracks, junctions between floorboards or panels, etc.)	Ceilings in a bad state	RR=2,7
Junction between a wall and the floor	Floors in a bad state	RR=2,7

Unfortunately, the method to evaluate the state of deterioration of the building elements was not precise enough to predict air leakages on windows hinges, ductworks and electrical devices. Yet, those air leakages are common in existing dwellings (Figure 3).

3.3 Correlation between air leakages and airtightness values

Table 5 lists air leakages correlated with airtightness values.

If some types of air leakages were not often observed, they had yet an important effect on n_{50} value.

It highlights that several important air leakages were typically localised on the ceiling, which provides guidance to take special caution with this building element when retrofitting.

It also shows that predictable air leakages (see Table 4) had not always an important effect on n_{50}. Furthermore, some important air leakages were not detected by the evaluation of the state of deterioration of the building. It was the case for air leakages between building blocks, at the junction between a wall and a ceiling, between a beam and a wall or a ceiling and air leakages near light fittings.

Table 5: Air leakages correlated with airtightness values (n_{50})

Air leakage types	b (h^{-1})	a (h^{-1})	p-value of a (%)	Number of dwellings (presence of the air leakage)	Number of dwellings (absence of the air leakage)
Junction between building blocks	5,65	4,61	0,0%	17	98
Junction between suspended ceiling tiles	6,13	3,96	2,8%	6	109
Junction between a wall and a ceiling	5,47	2,77	0,1%	36	79
Junction between a beam and a wall	5,61	3,62	0,0%	23	92
Junction between a beam and a ceiling	5,67	3,04	0,2%	25	90
Surrounds of trapdoors to the attic	5,74	1,93	2,7%	35	80
Light fittings (recessed luminaires, surface-mounted fixtures, pendant-mounted fixtures)	5,59	1,60	4,7%	53	62
Junction between doors and walls	6,08	3,58	2,3%	8	107
Air inlet and air outlet that were not sealed during the airtightness test	5,83	2,32	1,7%	25	90

3.4 Correlation between airtightness values and dwelling characteristics

3.4.1 Single-family dwellings

As seen in Table 6, for the 66 houses of the panel, the nature and the type of insulation of walls and the type of insulation of ceilings were correlated with n_{50} values. The effect of ventilation system and specific equipment (as kitchen hoods) can be explained by the measurement method and the conditions of intentional openings in the building envelope.

Table 6: Houses characteristics correlated with airtightness values (n_{50})

Characteristic	Value	Coefficient (vol/h)	p-value (%)	Number of houses
Wall and outer materials	Blockwork with rendering (reference category)	6,18	0,0%	20
	Brickwork	3,27	2,8%	15
	Brickwork with rendering	0,98	51,9%	13
	Stone	2,73	10,2%	10
	Other	2,03	25,8%	8
Wall insulation	Insulated (reference category)	6,81	0,0%	48
	Non-insulated	3,56	0,2%	18
Ceiling insulation	Exterior insulation (reference category)	6,24	0,0%	29
	Interior insulation	2,74	2,0%	26
	No insulation	3,40	4,9%	8
	Unknown	-	-	3
Ventilation	Mechanical ventilation (reference category)	6,48	0,0%	38
	Natural ventilation	1,34	38,2%	7
	None	3,51	0,3%	21
Number of specific equipment (kitchen hoods, intermittent air outlets, etc.)	1 (reference category)	6,28	0,0%	33
	At least 2	3,30	3,0%	10
	None	2,86	1,3%	23

3.4.2 Multi-family dwellings

As seen in Table 7, for the 49 apartments of the panel, the structure of the building, the type of separation walls between apartments and the type of wall insulation were correlated with n_{50} values. The effect of ventilation system and open fires can be explained by the measurement method and the conditions of intentional openings in the building envelope.

Table 7: Apartments characteristics correlated with airtightness values (n_{50})

Characteristics	Values	Coefficients (vol/h)	p-value (%)	Number of apartments
Nature of separation walls	Load-bearing walls (reference category)	3,89	0,0%	43
	At least one lightweight partition wall	4,04	0,7%	6
Ventilation	Mechanical ventilation (reference category)	3,42	0,0%	35
	Natural ventilation	2,62	3,2%	9
	None	4,71	0,3%	5
Closed off open fire	None (reference category)	3,82	0,0%	42
	At least one	3,94	0,5%	7
Wall insulation	None or interior insulation (reference category)	5,43	0,0%	31
	Exterior insulation	-2,88	0,9%	15
	Unknown	-	-	3
Structure (walls, floors and ceilings)	Concrete (reference category)	2,13	0,1%	22
	Stone walls (whatever the floors type)	5,38	0,0%	11
	Other	3,21	0,1%	16

3.5 Evaluation of the global air change rate

Overall, dwellings were well aerated, bad ventilated and the air permeability contributed highly to the global air change rate (see Table 8). Lack of ventilation and bad-managed ventilations (V1) were more often observed in houses than in apartments.

Table 8: A+V+P- score for the whole dwellings panel (a) and V+ score depending on the building type (b)

(a) Score	3	2	1	(b) Score	V3	V2	V1
Aeration A+	83	18	1	Houses	7%	9%	84%
Ventilation V+	10	19	88	Apartments	10%	26%	64%
Permeability P-	88	21	8				

Only two dwellings were A3V3P1, i.e. the ideal configuration for a good air change rate with little energy consumption. 11 dwellings were quite airtight and correctly ventilated (V3P1, or V3P2, or V2P2). 57% of the dwellings were V1P3, which means air change rate was mainly provided by air leakages. In 22% of dwellings, ventilation was failing and building was quite airtight, but this lack of air change was often compensated by inhabitant good practice of aeration by opening windows.

4 CONCLUSIONS

In a panel of 117 dwellings built before 2005, airtightness measurement results were very variable and ranged from 0.44 h^{-1} to 13.7 h^{-1}. The analysis of correlation between n_{50} values and air leakages showed that several leakages at the ceilings influenced strongly the airtightness of existing buildings. Unfortunately, it seems impossible to anticipate those important leakages by a simple evaluation of the state of deterioration of the building. Furthermore, the analysis of the correlation between n_{50} and buildings characteristics highlighted that the type of walls and ceilings and their insulation were highly correlated to airtightness values.

The measurement method had also a strong influence on results (mainly because of the way to condition intentional openings in the building envelope). The size of the panel (67 houses and 50 apartments), compared with the number of parameters, did also not allow to propose some robust models for airtightness prediction. This limit argued for pursuing the measurement campaign in 2019.

In the same time, a lack of ventilation was detected in 84% of houses and 64% of apartments, either because installations were out of date, or because they were incomplete or inexistent. Nevertheless, the global air exchange rate was enough in two-thirds of the dwellings, thanks to high airtightness values that compensated low ventilation performance. The good aeration practices of the inhabitants limited also the risk of condensation and poor indoor air quality.

Those results should be used to improve the airtightness indicators of the French thermal regulation for existing buildings.

5 ACKNOWLEDGEMENTS

This measurement campaign was funded by the French Ministry for Sustainable Development. Authors would like to thank all airtightness operators from the Cerema, without whom the Exist'air project would not have been possible: Emmanuel Roux, Philippe Dunez, Christophe Lozurowicz, Fabien Meley, Jean-Yves Fosse, Sébastien Aubry, Julien Chédru, Stéphane Baudrouet, Didier Meaux, Eddy Handtschoewercker, François Marconot, Jean-Paul Dorr, Laurent Crouzet, Antoine Cuny, Yaneck Zajkowski, Laurent Decouche, Jocelyne Ponthieux, Alexis Huet, Pascal Pelte, Christophe Carella.

6 REFERENCES

Barbisan, R., & Altan, H. (2012). Energy retrofit of the existing housing stock in England,. *33rd AIVC Conference.*

Bramiana, C., Entrop, A., & Halman, J. (2016). Relationship between building characteristics and airtightness of Dutch dwellings. *Energy Procedia 96*, 580-591.

Bureau d'études POUGET Consultants. (2012). *Programme Règles de l'Art Grenelle Environnement (RAGE) - Analyse détaillée du par résidentiel existant.*

Chan, W., Joh, J., & Sherman, M. (2012). Air leakage of US homes: regression analysis and improvements from retrofit. *33rd AIVC Conference.*

Collignan, B., Le Ponner, E., & Mandin, C. (2016). Relationship between indoor radon concentrations, thermal retrofit and dwelling characteristic. *Journal of environmental radioactivity*.

Erhorn-Kluttig, H., & Erhorn, H. (2012). Phylosophy and approaches for airtightness requirements in Germany. *AIVC International Workshop.*

Földvary, V., Bekö, G., Langer, S., Arrhenius, K., & Petras, D. (2017). Effect of energy renovation on indoor air quality in multifamily residential buildings in Slovakia. *Building and Environment*.

ISO 9972. (2015). *THermal performance of buildings - Determiantion of air permeability of buildings - Fan presurization method.*

McNeil, S. (2012). A survey of airtightness and ventilation rates in post 1994 NZ homes. *33rd AIVC Conference.*

Sinnott, D., & Dyer, M. (2013). Airtightness and ventilation of social housing in Ireland - a review of field measurements and occupant perspectives pre- and post-retrofit. *34th AIVC Conference.*

Stephen, R. (2000). *Airtightness in UK dwellings.* Building Research Establishment.

New findings on measurements of very airtight buildings and apartments

Stefanie Rolfsmeier

BlowerDoor GmbH
Zum Energie- und Umweltzentrum 1
31832 Springe, Germany
rolfsmeier@blowerdoor.de

ABSTRACT

The trend in European countries, such as Belgium, France and Germany is that the quality of the airtightness of the building envelope is getting better and better. This is true for small, airtight apartments, Passive houses and some large buildings with an excellent airtightness due to special requirements, e.g. oxygen reduction or fire protection. This good quality leads to new challenges in the performance of airtightness tests: Knowledge about an adapted way of measuring with a lot of patience.

What has to be taken into account in order to perform measurements of very airtight buildings? The different causes, solutions and tips are presented in this paper.

KEYWORDS

airtightness test, very airtight buildings, apartments, blowerdoor, test procedure, air permeability measurement, very low air-change rate

1 INTRODUCTION

Over the last decades, airtightness has become a necessary and important characteristic of the building envelope. Extensive experience as well as expertise in the production of good air barriers frequently lead to building airtightness of excellent quality. Large buildings with specific airtightness requirements, as for example oxygen reduction in warehouses for chemicals or food items, show air-change rates as low as 0.03 h^{-1}. Passive houses and apartments in some instances achieve n_{50}-values significantly below 0.03 h^{-1}.
It can be observed that the usual measuring procedures for airtightness tests are coming up against their limits when measuring these extremely airtight objects, creating new challenges for measuring technology and technicians alike.

This article will look at the measuring procedure in such cases and give recommendations on how to achieve reliable and repeatable measuring results.

2 DESCRIPTION OF THE PROBLEM

There is little experience as to how long it takes to establish a stable and constant pressure differential when testing air permeability of buildings with very low air-change rates, in some instances even starting with a n_{50}-value below 0.6 h^{-1}. The automated measurement in such objects may reach its limits. One indication is when the desired building pressure cannot be achieved, and the measurement is interrupted. If the individual measuring points are widely scattered around the line of best fit (the correlation coefficient in this case is significantly

lower than 0.98), this is further indication, because sometimes the measuring values are recorded before achieving the target pressure.

Using calculations and experience from measurements, the following section will show which waiting times have to be planned when building up pressure in buildings with very low air-change rates (n_{50}-values).

3 TESTING VERY AIRTIGHT OBJECTS

3.1 Real-time display of the measuring values from an airtightness test of a very airtight building

In order to explore the reasons behind the limitations we recorded the measurements of different buildings with low and extremely low air-change rates with a data-logging program (TECLOG). This program shows the building pressure differentials and the measuring values of the BlowerDoor fan (air flow and fan pressure) over time in real time. The progression of the curves with measuring intervals of one second allow you to understand how the building pressure is established. This makes it possible to adequately react to specific measuring situations.

3.2 Example of a very slow pressure build-up

The following object is an example of how the building pressure of a measuring point is built up in a very airtight building. Figure 1 shows a warehouse with an interior volume of V = 46,600 m³. At 0.03 h^{-1}, the air-change rate n_{50} is impressively low. For reasons relating to food technology, the necessary input of nitrogen must be kept at a minimum. This allows for keeping the oxygen-reduction equipment small and for minimizing electricity consumption.

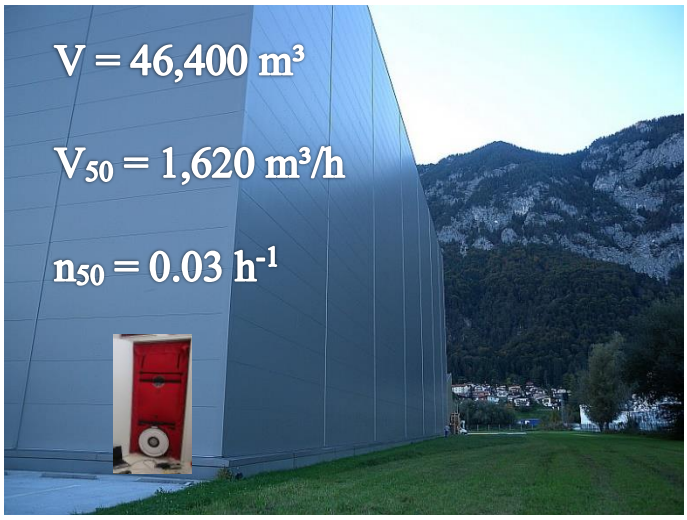

Figure 1: Warehouse for herbs with an air-change rate n_{50} = 0.03 h^{-1}

How the building pressure is built up after turning on the measuring fan can be seen in the following diagram (Fig. 2). The horizontal timeline runs the time during the measurement and the y-axis shows the pressure differential in Pascal. The green curve shows the progression of the building pressure differential and the red one the fan pressure at the measuring fan resulting in the air flow as a function of the measuring ring.

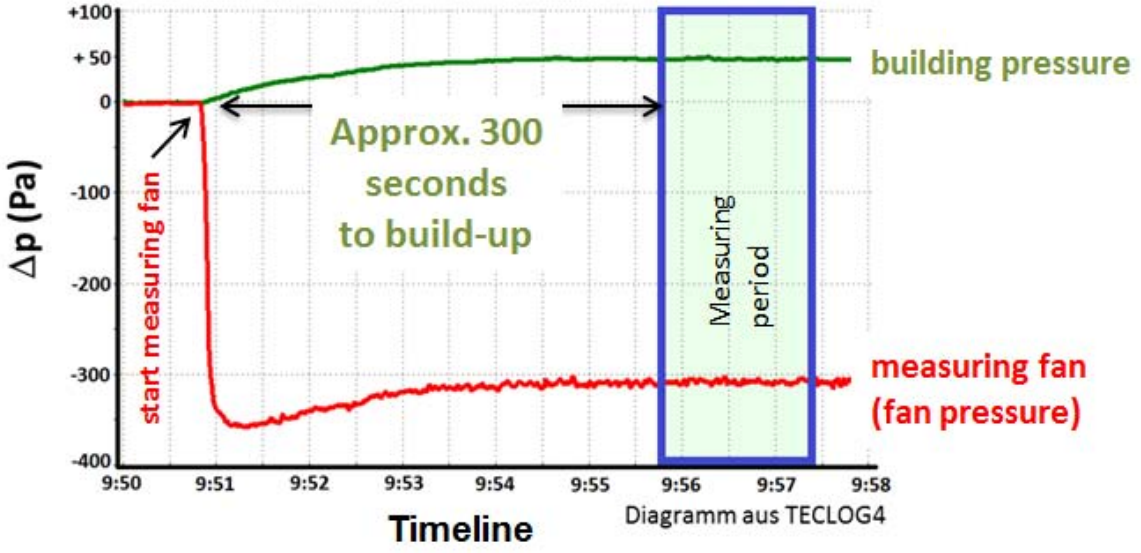

Figure 2: Approx. 300 seconds build-up time from 0 Pa starting pressure to 50 Pa building pressure (green curve from approx. 9:51 to 9:56)

Slightly before 9:51, the red curve for the fan pressure strongly declines from 0 Pa to ca. -350 Pa, indicating that the measuring fan (Minneapolis BlowerDoor Model 4, B Ring) has been turned on. The green curve for the building pressure increases comparatively slowly from the 0 Pa starting pressure to the target pressure of approx. 50 Pa. The closer the curve comes to the 50 Pa, the flatter it becomes (asymptotic progression).
At 9:56, after about 5 minutes (300 seconds), the target pressure has been reached and is sufficiently accurate, because both measuring curves are now running parallel to the timeline and indicating that no further serious changes are to be expected. Only as of this moment can we assume stable and constant conditions.
The measuring values for this measuring point that will later be included in the regression calculation can now be recorded.

3.3 Calculating the time for establishing building pressure differential

In order to optimally control the measurement, it is necessary to know the build-up times for the pressure differential of very airtight objects. Calculations by [Zeller] on the basis of the ideal gas equation, the equation for the leakage curve of a building, and assuming a constant air flow (independent of the building pressure) show that the time for reaching a specific pressure differential is inversely proportional to the air-change rate at 50 Pa (n_{50}). Figure 3 shows the build-up times from a starting pressure of 40 Pa to the target pressure of 50 Pa for different air-change rates. The flow exponent n of the leakage curve is 0.67.

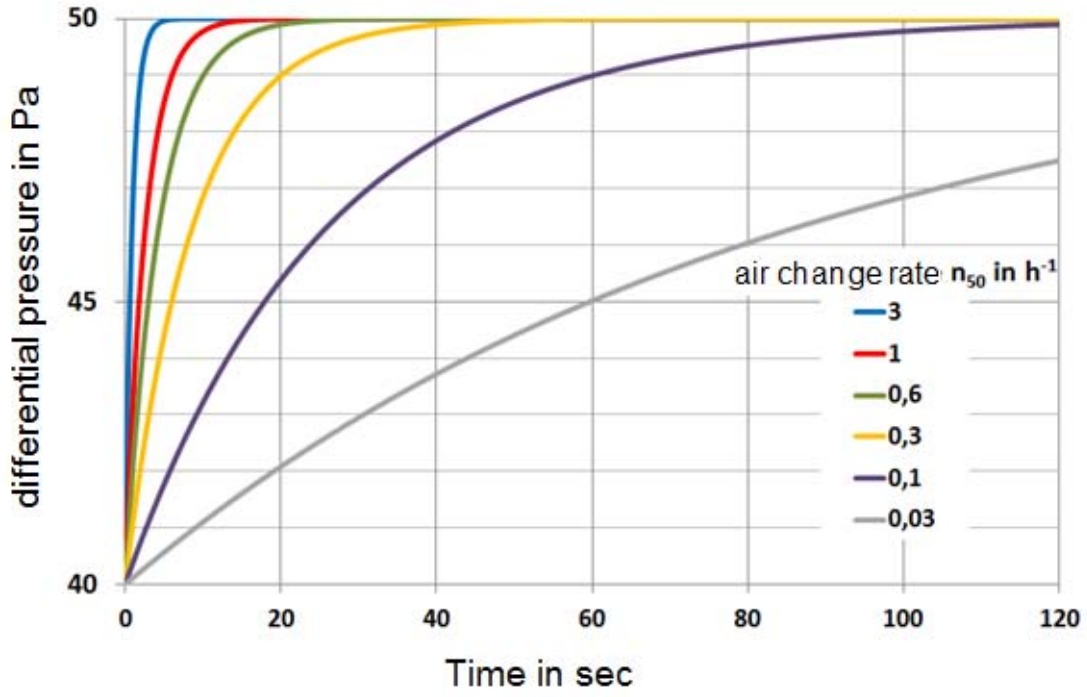

Figure 3: Build-up times from 40 Pa to 50 Pa building pressure differentials for different air-change rates at 50 Pa (n50). Boundary condition: The flow exponent n of the leakage curve is 0.67 [Zeller]

The diagram clearly shows that small air-change rates lead to an increase in the time for reaching a stable building pressure differential. At a n_{50}-value of 3 h^{-1} (blue curve), the 50 Pa differential pressure is established within a few seconds. In comparison, at 0.03 h^{-1} (grey curve), and after the 120 seconds displayed here, the target pressure is still far from being reached.

For the measuring practice, the following equation [Zeller], helps you to estimate the minimum waiting time that must be planned for achieving repeatable and robust results.

$$t\,(s) = \frac{9\,(s/h)}{n_{50}(h^{-1})}$$

t: waiting time in seconds
n_{50}: air-change rate in h^{-1}

Boundary conditions:
- The pressure differentials for the measuring series are ca. 10 Pa apart.
- The flow exponent is 0.67.
- The target pressure is reached with a tolerance of +/- 0.5 Pa.

Example:
The desired air-change rate is 0.1 h^{-1}.

t = 9 s/h / n_{50} (1/h)
= 9 s/h / 0.1 h^{-1}
= 90 s

The calculated times may deviate from the actual waiting times during the measurement. The time for building up the pressure differential is actually reduced, when the measuring steps of 10 Pa (70 Pa, 60 Pa, 50 Pa, etc.) are decreased to 5 Pa (70 Pa, 65 Pa, 60 Pa, etc.). A smaller flow exponent of the leakage curve increases the time.

3.4 Comparing the calculations with the real-life example

For comparisons, the pressure build-up time for the building presented before is calculated. The air-change rate is 0.03 h^{-1} and the flow exponent of the leakage curve n is 1. The diagram in Figure 4 shows the pressure build-up from 0 Pa starting pressure to a building pressure of 50 Pa.

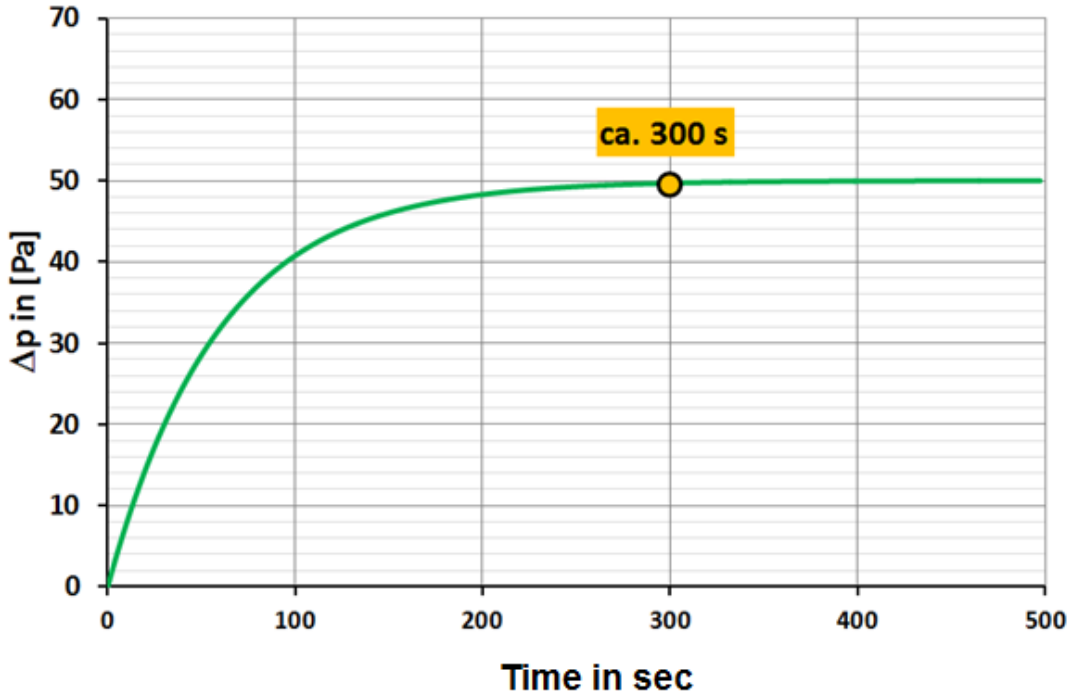

Figure 4: Calculated time for building up the building pressure differential from 0 Pa to ca. 49.5 Pa

The 49.5 Pa are reached after a good 300 seconds. In the actual measurement, we had started recording the measuring values for this target pressure after approx. 300 seconds. This means that the calculations correspond very well to the experience in real life.

4 WIND IMPACT

Variations in the pressure at the building envelope caused by wind make it more difficult to determine the time, when a sufficiently accurate target pressure has been achieved. It is thus absolutely necessary to follow the recommendations given in the testing standards [EN 13829 and ISO 9972] to conduct air permeability measurements preferably at wind speeds of 6m/s or less or a maximum wind force of 3 Beauforts. The stronger and gustier the wind, the larger and more irregular the fluctuations. The diagram in Figure 5 shows the oscillations of the natural pressure differentials at a median wind speed of 4.5m/s.

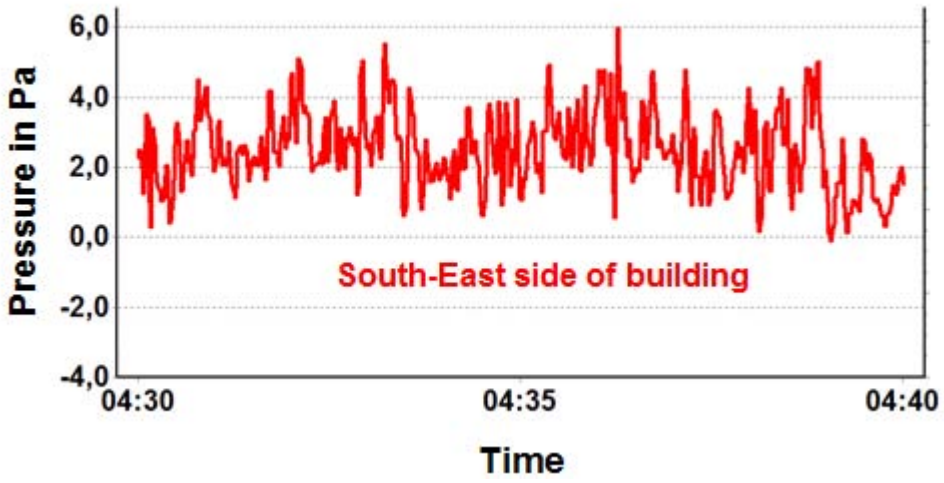

Figure 5: natural pressure differentials at one side of the building caused by wind with a median speed of 4.5m/s

These fluctuations reoccur at all pressure stages of the measuring series. This makes it more difficult to achieve a stable and constant pressure differential. In windy conditions, it helps to place the measuring location for the reference pressure on the downwind side (lee side) [Brennan et al.] and to increase the measuring time for each measuring point. The latter improves the accuracy of the leakage curve. The rapidly changing pressure fluctuations can also be compensated by a lower reaction speed of the measuring fan.

5 IMPACT OF MOVING FOILS

Another factor of influence sometimes making the measurement more difficult are large foils inside the building like the PE vapor barriers on the top floor of passive houses or in penthouse apartments, which at the time of measurement have not yet been covered by gypsum board. Another example are PE vapor barriers above the suspended ceilings in supermarkets.

Other than, for example, a fix brick wall, the foil will move when building up pressure. At negative pressure, it will slowly bulge until stretched. This flexibility may disrupt the automated control of the measuring fan. However, this effect can also be compensated by longer waiting times.

6 RECOMMENDATIONS

6.1 Build-up times for a pressure differential (target pressure) at low air-flow rates

In order to obtain reliable and repeatable results, you should plan with the times for establishing specific pressure differentials listed in Table 1.
At very low air-change rates, it is enough to wait until the target pressure is reached with a ±0.5 Pa tolerance.

Table 1: Minimum times for building up a pressure stage with a tolerance of ± 0,5 Pa as a function of the air-change rate of 50 Pa, based on calculations by [Zeller].

Air-change rate at 50 Pa	Build-up time for pressure stage
1.0 h^{-1}	> 9 s
0.8 h^{-1}	> 12 s
0.6 h^{-1}	> 15 s
0.4 h^{-1}	> 23 s
0.3 h^{-1}	> 30 s
0.2 h^{-1}	> 45 s
0.1 h^{-1}	> 90 s
0.08 h^{-1}	> 115 s
0.06 h^{-1}	> 150 s
0.04 h^{-1}	> 225 s
0.03 h^{-1}	> 300 s
0.02 h^{-1}	> 450 s
0.01 h^{-1}	> 900 s

The build-up times have been determined for the following boundary conditions: change of pressure stage from 70 Pa to 60 Pa plus a flow exponent of 0.67.

When controlling pressure stages in extremely airtight buildings (n_{50}-values < 0.1 h^{-1}), any change in the measuring fan settings will lead to significantly longer build-up times for the pressure stages. Any interventions in the control basically mean a new start for the build-up. This is why it makes sense not to readjust the measuring fan.

6.2 Measuring at very low air-change rates

At very low air-change rates, the usual measuring programs with the standard settings come up against their limits. In comparison to the testing volume, the required air-flow rate is extremely low, and it is difficult to control the measuring object to obtain stable and constant measuring values.

At air-change rates between 1 h^{-1} and 0.6 h^{-1} it helps to slow down the fan.

At air-change rates between 0.6 h^{-1} and 0.3 h^{-1} a semiautomated measurement will provide good results. During these types of measurements, the user can adjust the fan and determine when the building pressure is sufficiently stable to begin with recording the measuring values [BlowerDoor Standard Manual].

If the n_{50}-values are smaller than 0.3 h^{-1}, it helps to display the curve progressions for building pressure and air-flow rate in a data-logging program. They can be observed in real time and the measuring points can be selected as required [BlowerDoor Multiple Fan Manual].

6.3 Recommendations for wind

At windy conditions, it helps to install the measuring equipment on the downwind side (lee side) of the building and to measure the outside building pressure there. The measuring series

should also include several measuring points above 50 Pa [EN 13289 and ISO 9972]. To compensate the irregular pressure fluctuations, the different pressure stages should be controlled more slowly and possibly allow for a greater tolerance. To increase the accuracy of leakage curves, the measuring time for each measuring point is extended. The usual measuring times for a measuring point are 10 to 15 seconds. They can be extended to 30 seconds without any problem and during gusty winds even to 60 to 120 seconds.

6.4 Recommendations for foils (vapor barrier)

The target pressures are to be adjusted more slowly, so that the foil can slowly bulge until stretched.

7 CONCLUSIONS

Airtightness tests of very airtight objects like large warehouses with air-change rates of 0.03 h^{-1} due to oxygen reduction or passive houses and apartments with n_{50}-values below 0.6 h^{-1} require a different approach for recording the measuring values than buildings with high air-change rates. The time for setting up a stable pressure differential suitable for recording measuring values is significantly longer. The user may sometimes have to wait several minutes until the pressure differential is sufficiently accurate.
If it is also windy during the time of measurement, the building pressure differentials will fluctuate. A slower control of the pressure stages and a longer measuring time for each measuring point will help to record a measuring series with sufficiently accurate results.
Another influencing factor is a building envelope with large, moving foils like vapor barriers. A careful control of the measurement will also help in this case.

8 REFERENCES

Brennan, T., Nelson, G., Olson, C. (2013): Repeatability of Whole-Building Airtightness Measurements: Midrise Residential Case Study. In: Workshop on Building and Ductwork Airtightness Design, Implementation, Control and Durability: Feedback from Practice and Perspectives, Washington D.C.

Leprince, V. (2018): Mesure d'étanchéité à l'air à petit débit

Zeller, J. (2019): unveröffentlichte Studie zum zeitlichen Verlauf des Druckaufbaus

DIN EN 13829 (2001): Wärmetechnisches Verhalten von Gebäuden. Bestimmung der Luftdurchlässigkeit von Gebäuden. Differenzdruckverfahren (ISO 9972: 1996, modifiziert), deutsche Fassung EN 13829: 2000. Berlin: Beuth.

DIN EN ISO 9972 (2018): Wärmetechnisches Verhalten von Gebäuden - Bestimmung der Luftdurchlässigkeit von Gebäuden - Differenzdruckverfahren (ISO 9972:2015); deutsche Fassung EN ISO 9972:2015

Reference Guide BlowerDoor Standard and MiniFan (2018) sowie Reference Guide BlowerDoor MultipleFan (2018)

Comparison between infiltration rate predictions using the divide-by-20 rule of thumb and real measurements.

Alan Vega Pasos[1], Xiaofeng Zheng[1], Mark Gillott[1] and Christopher J. Wood*[1]

1 Buildings, Energy and Environment Research Group, Faculty of Engineering, University of Nottingham, University Park, Nottingham NG7 2RD, United Kingdom.
**Corresponding author:*
christopher.wood@nottingham.ac.uk

ABSTRACT

Across different territories there are various normative models for assessing energy demand of domestic dwellings, which use simplified approaches to account for the heat loss due to the air infiltration of a building. For instance, the United Kingdom uses a dwelling energy model, known as the Standard Assessment Procedure (SAP), and this utilises a process where the measured air permeability value (q_{50}), is simply divided by 20 to provide an infiltration rate (subsequent modification factors are then used for factors such as sheltering etc.). This rule is commonly known as the divide-by-20 rule. As a starting point, building air leakage rate is measured through a steady pressurisation (blower door) test, and normalised by envelope area to provide a value of air permeability. In this study the air infiltration rate of five dwellings based in Nottingham, UK was investigated. Air infiltration was measured and calculated using the conventional approach with the divide-by-20 rule and also with tracer gas methods, which directly assessed air infiltration at ambient pressure levels. Results showed that for the test dwellings, a divide-by-39 (q_{50}/39) rule would predict air infiltration more accurately (than the divide-by-20). It was also seen that the air change rate is overestimated by SAP when modifying factors are added. The errors in more than half of the properties are higher than 225%. The most significant differences were seen in the dwellings with more airtight building envelopes.

KEYWORDS

Air infiltration, airtightness, blower door, pulse, permeability

1 INTRODUCTION

Energy efficiency of buildings plays a crucial role in the efforts to tackle climate change (Lapillonne, Pollier, & Samci, 2015). The energy used for heating and/ or cooling of the internal air represents the largest source of energy usage in a building in many territories, therefore, reducing the loss of conditioned air is key to achieving an energy efficient building. In the UK for instance, one third of a dwellings heat loss can come from air infiltration (Etheridge , 2015). Air infiltration (h^{-1}) is the unintended ventilation of a building, and is not only important for energy efficiency, but also for indoor air quality and thermal comfort.

Correspondingly, building airtightness is the property that impacts the most on the air infiltration rate. The first step to understand the infiltration properties of a building is to measure its airtightness. Airtightness can take units of: air change rate (h^{-1}), air permeability ($m^3h^{-1}m^{-2}$) when the flow (m^3/s) is normalised by volume and envelope area.

1.1 UK context

As mentioned, airtightness is measured prior to obtaining the heat losses attributed to air infiltration. Air permeability (q), or air change rate (n), are airtightness metrics and regularly

are quoted at a certain pressure difference; for example, British legislation requires the measurement of air permeability to be quoted at 50 Pa, thus this metric is shortened as q_{50}, the subscript 50 references the 50 Pa of pressure difference obtained by the pressurisation method when measuring air permeability.

The steady pressurisation method, most commonly known as "blower door", is an airtightness measuring technique which increases the pressure difference of a building by pressurising or depressurising the internal space with aid of a fan mounted in a doorway. Measurements are taken while the building covers a range of pressure differences, typically between (-)10 to (-)60 Pa (The British Standards Institution, 2015).

This pressure difference is correlated with the airflow through the fan, the technique quotes the results at 50 Pa. Flow and pressure difference are related by the power law in equation 1 (The British Standards Institution, 2015).

$$Q = C\Delta p^n \tag{1}$$

where:
Q= fan air flow rate (m^3h^{-1});
C = air flow coefficient ($m^3h^{-1}Pa^{-n}$);
Δp = Indoor-outdoor pressure difference (Pa);
n= flow exponent (dimensionless), in the range from 0.5 to 1 (turbulent to laminar flow).

Due to the nature of the method (pressurising), which increases the pressure difference experienced by the building; some authors have questioned that the pressurisation method results do not represent the air change rate occurring under natural conditions (Cooper & Etheridge, 2007), which usually lie between 1-4 Pa of pressure difference. To obtain a value in a lower pressure range, an extrapolation is needed.

Air infiltration prediction models are the tool to estimate an infiltration rate (under natural conditions) from airtightness measurements (Orme & Leksmono, 2005). Models vary in complexity; the simplest way to predict an infiltration rate (n_1) is to use an airtightness – infiltration ratio (equation 2).

$$n_{50}/n_1 = N \tag{2}$$

where:
n_{50} = air change rate at 50 Pa (h^{-1});
n_1 = air infiltration rate (h^{-1});
N = ratio constant (dimensionless).

Research in the United States (Jones, Persily, & Sherman, 2016; Sherman, 1987; Persily, 1982) determined that the value of N in equation 2 can be taken as 20, and it should be modified by a number of environmental factors. In other words, if the air change rate obtained in a pressurisation test is divided by 20, the obtained result is the air infiltration rate under natural conditions; this was called the divide-by-20 rule of thumb (equation 3).

$$n_{50}/20 = n_1 \tag{3}$$

Even when this rule was created, tested and validated in the United States, the United Kingdom adopted it as the way to predict the infiltration rate (Building Research Establishment, 2013). The usage of this ratio in the UK has been questioned before due to its simplicity (Keig, Hyde, & McGill, 2016; Johnston & Stafford, 2016). Furthermore, UK legislation does not utilise an

air change rate at 50 Pa (n_{50}) to predict the infiltration rate, air permeability (q_{50}) is the airtightness metric used. Then, for UK legislation, equation 3 turns into equation 4. This change assumes that a building has a volume – envelope to area ratio of 1.

$$q_{50}/20 = n_1 \quad (4)$$

1.2 Measurement of air infiltration

Air infiltration rate is usually predicted from airtightness measurements, nevertheless the possibility of measuring it does exist. This is regularly carried out through tracer gas methods. Several tracer gas methods have been standardised (American Society for Testing and Materials, 2011; British Standards Distribution;, 2017), yet the tracer gas concentration decay method is the most popular one due to its simplicity, low cost, and relatively good accuracy (Sherman, 1989).

In a standard concentration decay test, the gas is released and mixed in the test space, and the concentration decay is monitored over time. Different gases can be used, however carbon dioxide is probably the most widely used. Normally, fans are employed to ensure a good mix of tracer gas and air. Time, and the natural logarithm of the concentration are placed on a linear regression. The infiltration rate is given by the slope in the linear best fit of the time-$\log_e$ relationship. Furthermore, to comply with the standards, a minimum time for testing is required, depending on the airtightness of the building. Table 1 lists the approximate testing time required for buildings with various levels of airtightness.

Table 1: Minimum durations of tracer gas decay method
(American Society for Testing and Materials, 2011)

Air Change Rate (h^{-1})	Minimum duration (h)
0.25	4
0.5	2
1	1
2	0.5
4	0.25

Tracer gas methods have been proved accurate when measuring air infiltration rate, yet they are not commonly utilised because they are invasive, time taking, costly and the tested property has to be unoccupied during the test.

The objective of this paper is to assess the UK building regulation's method of predicting air infiltration heat losses, which utilises the divide-by-20 rule of thumb (equation 4). The study involves pressurisation and tracer gas concentration decay tests in five dwellings located in Nottingham, United Kingdom.

2 METHOD

This project is part of a large airtightness testing campaign using different technologies in dwellings in the United Kingdom. Five houses located near the University of Nottingham in Nottingham, United Kingdom were selected to be tested using the tracer gas concentration decay method; in addition, pressurisation tests and weather monitoring were carried out in the houses. The characteristics of each dwelling are described in Table 2.

Pressurisation (and depressurisation) tests were carried out according to the British Standard (The British Standards Institution, 2015). The tracer gas tests and the calculations were carried

out according to the British and ASTM standards (British Standards Distribution;, 2017; American Society for Testing and Materials, 2011). The equipment utilised in the tests is listed in Table 3.

Table 2: Description of dwellings

Dwelling	Date of test	Form	Main construction type	Volume (m^3)	Envelope area (m^2)
1	25/04/2018	Detached	Cavity	278	269
2	03/08/2018	Detached	Timber frame	188	227
3	16/08/2018	Detached	Solid	478	435
4	07/06/2018	Semi-detached	Solid	264	252
5	18/01/2018	Detached	Cavity	285	290

Table 3: Testing equipment

Airtightness		Minneapolis blower door model 4. (BD-4)
Tracer gas	Gas:	Carbon dioxide
	Sensor:	Sontay CO_2 sensor GS-CO2-1001 accuracy ±30ppm ±5% of scale
Other		Fans Datataker DT85 data logger WindSonic Ultrasonic anemometer Temperature sensors PT100 RTD

The selected tracer gas was carbon dioxide; each dwelling was divided into six different "zones". A set of CO_2 and temperature sensors were placed in each dwelling, one sensor for each zone. The sensors were connected to a data logger which recorded the temperature and gas concentration at a sampling rate of 1 *Hz*. The gas was released into each zone until the concentration was close to 5000 *ppm* and to ensure adequate mixing of the CO_2 with the bulk air volume, a floor fan located in each zone was used to achieve homogeneity. The CO_2 was left to decay for as long as possible, considering the minimum times stated in Table 1. Figure 1 shows part of the equipment utilised for the tracer gas tests. In addition, an ultrasonic anemometer connected to the same data logger recorded every second the wind speed and direction during the tracer gas decay period.

a) *b)* *c)*

Figure 1. Equipment utilised for tracer gas decay method tests. a) Data logger with sensors connections, b) carbon dioxide canisters, c) example of a building zone, with a temperature sensor, a carbon dioxide sensor and a fan.

3 RESULTS AND DISCUSSION

In the following analysis two aspects will be investigated to test the appropriateness of the so-called 'divide by 20 rule' in relation to the test dwellings. The ratio of air permeability (at 50 *Pa*) to infiltration rate (as per the UK's requirement under the Standard Assessment Procedure, SAP) and also in the original form of air changes rate per hour (at 50 *Pa*) to infiltration rate. Pressurisation tests, results were obtained in the form of air permeability at 50 *Pa* ($q_{50,}\ m^3h^{-1}m^{-2}$) and also the air change rate at 50 *Pa* ($n_{50,}\ h^{-1}$). The air infiltration rates, determined by the concentration decay tests and by calculation from pressurisation tests (via the 'divide-by-20 rule) are given in air changes per hour ($n_{1,}\ h^{-1}$).

3.1 Pressurisation tests results

Table 4 includes the mean value of pressurisation and depressurisation tests for each dwelling tested, in air change rate (n_{50}) and air permeability units (q_{50}). It is believed that in the UK, dwellings have a volume – envelope area ratio close to one (as per its application in SAP). It can be seen that this is true for most of the test properties, as relatively similar values of air change rate and air permeability confirm this.

Table 4. Blower door tests results

Dwelling	ACH @50 Pa (n_{50}) h^{-1}	Air Permeability @50 Pa (q_{50}) $m^3h^{-1}m^{-2}$	Volume (m^3)	Envelope area (m^2)
1	7.62	7.88	278	269
2	5.31	4.40	188	227
3	3.51	3.86	478	435
4	5.77	6.04	264	252
5	7.73	7.60	285	290

The data set showed that property number 3 is the most airtight; furthermore, all the properties comply with the UK standard that requires a minimum air permeability of 10 $m^3h^{-1}m^{-2}$. The average air permeability of all five dwellings is 5.96 $m^3h^{-1}m^{-2}$.

3.2 Tracer gas results

Each CO_2 sensor measured the concentration decay in each zone. Figure 2 shows an example of the concentration decay of the average of the concentration from all the zones; this example shows a decay from (circa) 4200 *ppm* to 2000 *ppm*.

ASTM E741-11 (American Society for Testing and Materials, 2011) requires a least square regression performed between the elapsed time and the natural logarithm of the concentration. The best linear fit is produced, and, the slope of the equation represents the air infiltration rate of the building. Figure 3 shows the time against natural logarithm of the concentration regression in dwelling 4; it also shows the equation of the best fit and the r^2 value. The infiltration rate was $0.1645\ h^{-1}$. Both Figure 2 and Figure 3 are examples of how the air infiltration rate is obtained from a tracer gas decay test.

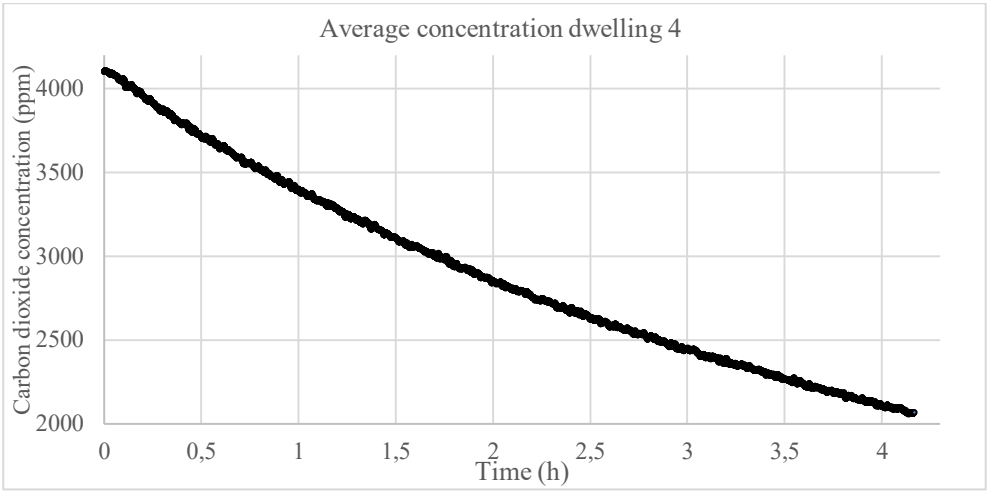

Figure 2. Concentration decay of dwelling 4.

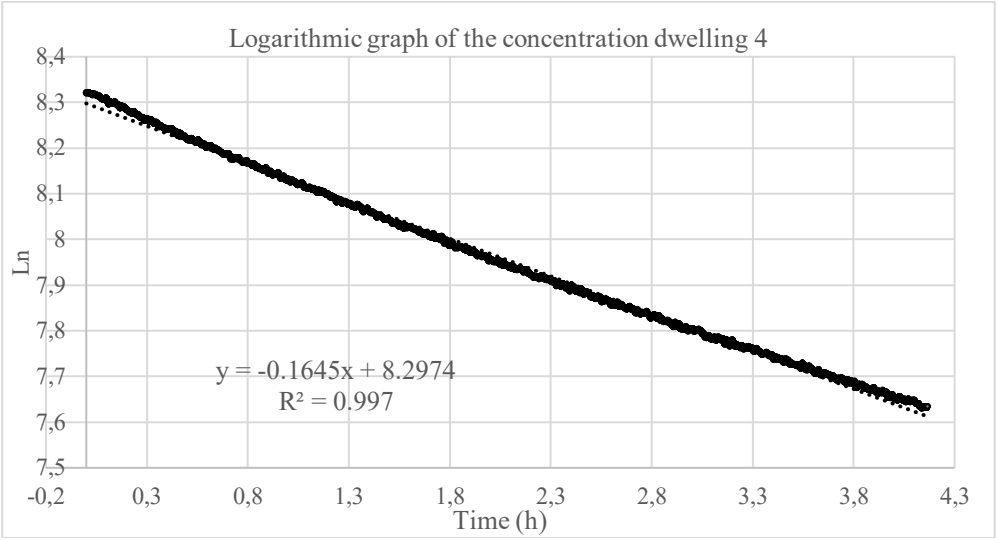

Figure 3. Natural log of the concentration decay for dwelling 4 and the best fit linear regression, and equation where the slope represent the air infiltration rate in h^{-1}.

Pressurisation tests were carried out prior to the tracer gas tests, and all building conditions were kept as per the pressurisation test standard for both tests: all windows and external doors were closed, internal doors were opened, vents, flues and trickle vents were closed and sealed. Therefore, the obtained infiltration rate was only due to adventitious openings and represents a direct comparison with the airtightness tests. All the results and characteristics of the concentration decay tests are presented in Table 5. The valid duration of test is shown, the uncertainty of the regression is given, and finally, the average weather conditions during the tests are presented.

Table 5. Tracer gas decay method results

Dwelling	Date of test	infiltration rate (n_1, h^{-1})	r2	Test duration h	Uncertainty $\pm h^{-1}$	Wind m/s	Δt K
1	25/04/2018	0.1484	0.99	7.32	0.0009	2.736	4.73
2	03/08/2018	0.1241	0.999	8.5	0.0019	1.08	3.69
3	16/08/2018	0.0787	1	8.00	0.0036	0.710	3.39

4	07/06/2018	0.1645	1	4.17	0.0020	1.700	0.94
5	28/02/2018	0.3618	0.99	7.64	0.0007	0.350	11.00

As per the duration, all tests fulfilled the standard ASTM E741-11 (American Society for Testing and Materials, 2011), the regressions had high correlation values of both variables, and the uncertainty created was low (less than 5% in all cases), within the limits given by other authors (Sherman, 1989); proving the validity of the tests. The average infiltration rate of all five dwellings was $0.1755\ h^{-1}$. Regarding the measurement of the on-site wind, the anemometer was positioned near the houses in spaces, as open as possible, however, this was not always achieved due to various site conditions, the anemometer's height varied from 1.8 to 2.5 metres. Finally, the indoor-outdoor temperature difference was calculated by averaging all the measured internal temperatures (one sensor was placed next to each CO_2 sensor) and, subtracting the measured outdoor temperature, which was placed next to the anemometer.

3.3 Air Infiltration ratios

To obtain the air infiltration rate from airtightness measurements, the British Standard Assessment Procedure (SAP) requires to use the divide-by-20-rule. The new calculated value is then modified by certain factors. Table 6 presents the calculated infiltration rates using equation 4 and how it compares with the real measurements, finally, the last column gives the real value of *N* if a divide-by-N rule is to be utilised.

Table 6. Air permeability – air infiltration

Dwelling	Air Permeability @50 Pa $m^3h^{-1}m^2$ q_{50}	$q_{50}/20$	ACH h^{-1} n_1	Error	q_{50}/n_1
1	7.88	0.3938	0.1484	165%	53.07
2	4.40	0.2200	0.1241	77%	35.46
3	3.86	0.1930	0.0787	145%	49.05
4	6.04	0.3020	0.1645	84%	36.72
5	7.60	0.3798	0.3618	5%	21.00
				Average	39.06
				Min	21.00
				Max	53.07
				Std dev	11.32
				Std error	5.06

Dividing the air permeability by 20 creates a large error compared to the measured infiltration rate. There is an overestimation of air infiltration, therefore if heat losses are calculated using the divide-by-20 rule this will result in a larger prediction of heat loss than that experienced by the dwelling in reality. The last column suggests that a much larger value is required; for these five properties a divide-by-39 value would be more accurate, which agrees with Vega Pasos (Vega Pasos, et al., 2018). The estimated average value of *N* is almost twice the figure used in SAP. For dwelling five, it can be seen that the figure for N is close to 20, this is the only property where this happens.

Table 7. Air change rate – air infiltration

Dwelling	ACH @50 Pa $m^3h^{-1}m^2$ q_{50}	$n_{50}/20$	ACH h^{-1} n_1	Error	n_{50}/n_1
1	7.62	0.3810	0.1284	157%	51.35
2	5.31	0.2656	0.1076	114%	42.81
3	3.51	0.1756	0.0700	123%	44.63
4	5.77	0.2883	0.1442	75%	35.05
5	7.73	0.3865	0.2426	7%	21.37
				Average	39.04
				Min	21.37
				Max	51.35
				Std dev	10.25
				Std error	4.58

Table 7 shows results when the divide-by-20 rule is used in its original form, (using n_{50} instead of q_{50}, or equation 3). Results do not differ much from those given in Table 6, because the volume-envelope area ratio is close to 1, it can be seen that the figure of *N* is still 39, and the minimum error created by using the divide-by-20 ratio is 7%.

Using the divide-by-20 rule in the United Kingdom does not deliver accurate results for most of the properties, this is because the rule is rather crude and, the housing stock is different than the United States one where it was originally created. The authors recommend using different ways to predict infiltration rates. Continuing the testing campaign with more dwellings will give a more accurate vision of the usage of leakage-infiltration ratios.

3.4 Calculations using SAP

The SAP uses the divide-by-20 rule with the objective of estimating the infiltration heat losses in a building, after using it, the resulting value is modified by shelter, wind and ventilation factors. The wind factors depend on the location of the dwelling, for this study, all dwellings were in the East Pennines area of the United Kingdom.

Table 8 includes the -calculated by SAP- air infiltration rates (air change rates) after the modifying factors; two cases are considered: first, during the month when the tracer gas test was carried out and, second, an annual average of the air change rate. Errors calculated when comparing measured and predicted values are listed in the last two columns.

Table 8. Air change rates (h^{-1}) calculated using SAP, values of N from values calculated, and their error compared to measured values

Dwelling	SAP n_1 during test month	SAP n_1 annual average	N SAP during test month	N SAP annual average	ACH, tracer gas	Error SAP during test month	Error SAP annual average
1	0.6000	0.6000	13.1256	13.1261	0.1484	304%	304%
2	0.5150	0.5212	0.5444	8.4428	0.1241	315%	320%
3	0.5161	0.5228	7.4792	7.3838	0.0787	556%	564%
4	0.5352	0.5472	11.2852	11.0380	0.1645	225%	233%
5	0.6174	0.5873	12.3050	12.9340	0.3618	71%	62%

The values calculated by SAP overestimate the air change rate, thus the infiltration heat losses; the error is larger than 300% in some cases. First, the divide-by-20 rule makes an over-prediction, and second, the correction factors make this over-prediction even larger, this is

because when a house is tight, the correction gives a minimum infiltration of $0.5h^{-1}$ (hence why all values are higher than 0.5). It is recommended to revise these correction factors, to avoid the large error and to design with ventilation rates closer to reality.

4 CONCLUSION

Five houses in the East Pennines region of the UK were tested by means of pressurisation. Air permeability ($m^3h^{-1}m^{-2}$) and air change rate (h^{-1}) quoted at 50 Pascals were presented. Tracer gas concentration decay tests were carried out, following the pressurisation tests in the same dwellings to directly determine the air infiltration rate.

Pressurisation tests showed that all the houses comply with the British building standard requirement with air permeability rates lower than 10 $m^3h^{-1}m^{-2}$. Tracer gas tests showed an average infiltration value of 0.1755 h^{-1}.

Standard Assessment Procedure (SAP) evaluates the energy efficiency of dwellings in the UK. An important factor in SAP is the air change rate and it is obtained through dividing the air permeability (q_{50}) value of the house (obtained by a pressurisation test) by 20. This rule is known as the divide-by-20 rule of thumb. The rule of thumb was evaluated and results suggest that, if a ratio is used, a number closer to reality is 39 for the test dwellings in this study. This was true for both, q_{50} and n_{50}. Errors between 5% and 165% were found; the rule overestimated the infiltration rate for all tested dwellings. After adding the modifying factors, SAP overestimated the air infiltration rate creating errors larger than 500%. The fact that dwellings are getting tighter might not be reflected by SAP.

Suggestion of the revision of the modifying factors and the utilisation of the rule of thumb were given. A larger testing campaign in different areas of the country would deliver a better vision on whether the rule should still be used, or a more accurate model must be included in the regulation.

5 ACKNOWLEDGEMENTS

Part of this work was funded by the Mexican Council of Science and Technology (CONACYT), and the European Union's Horizon 2020 research and innovation programme under grant agreement No 637221. ['Built2Spec': www.built2spec-project.eu/];and their full support is acknowledged by the authors. The authors also thank the support of Build Test Solutions ltd.

6 REFERENCES

American Society for Testing and Materials. (2011). *Standard Test Method for Determining Air change in a Single Zone by Means of Tracer Gas Dilution.* ASTM designation E741-11.

British Standards Distribution;. (2017). *BS EN ISO 12569:2017 Thermal Performance of Buildings ans Materials - Determination of Specific Aiflow Rate in Buildings - Tracer Gas Dilution Method* . United Kingdom: BSI Standards limited .

Building Research Establishment. (2013). *The Government's Standard Assessment Procedure for Energy Rating of Dwellings.* Watford, United Kingdom.: Building Research Establishment on behalf of the Deparment of Energy and Climate Change.

Cooper, E., & Etheridge, D. (2007). Determining the Adventitious Leakage of Buildings at Low Pressure, Part 1: Uncertainties. *Building Services Engineers Research Technology , 28*, 71-80.

Crowe, K. (1974). *A History of the Original Peoples of Northern Canada.* Montreal: McGill/Queen's University Press for the Arctic Insitute of North America.

Etheridge , D. (2015). A perspective of fifty years of natural ventilation research. *Building and environment, 97*, 51-60.

Johnston, D., & Stafford, A. (2016). Estimating the background ventilation rates in new-build UK dwellings - Is n50/20 appropriate? *Indoor and Built Environment, 26*(4), 502-513.

Jones, B., Persily, A., & Sherman, M. (2016). The Origin and Application of Leakage-Infiltration Ratios. *ASHRAE AIVC IAQ 2016, Defining Indoor Air Quality: Policy, standards and Best Practices.* Alexandria, Virginia, U.S.A.

Keig, P., Hyde, T., & McGill, G. (2016). A comparison of the estimated natural ventilation rates of four solid wall houses with the measured ventilation rates and the implications flor low-energy retrofits. *Indoor and Built Environment, 25*(1), 169-179.

Kronvall, J. (1978). Testing of houses for air leakage using a pressure method. *ASHRAE Transactions*, 84:72-9.

Kronvall, J. (1980). Correlating pressurization and infiltration rate data - tests of an heuristic model. *1st AIVC Conference on instrumentation and measuring techniques.* Windsor, U. K.

Lapillonne, B., Pollier, K., & Samci, N. (2015). Energy efficiency trends for households in the EU. 1-51.

Orme, M., & Leksmono, N. (2005). *AIVC guide 5: Ventilation modelling data guide.* Brussels, Belgium: International Energy Agency, AIVC.

Persily, A. (1982). *Understanding air infiltration in homes.* Princeton University: Report PU/CEES=129.

Sherman, M. (1987). Estimation of Infiltration from Leakage and Climate Indicators. *Energy and Buildings, 10*, 81-86.

Sherman, M. (1989). Uncertainty in air Flow Calculations Using Tracer Gas Measurements. *Building and Environment, 24*(4), 347-354.

The British Standards Institution. (2015). *BS EN ISO 9972:2015 Thermal Performance of Buildings - Determination of Air Permeability of Buildings- Fan Pressurization Method.* United Kingdom: BSI Standards.

The British Standards Institution. (2015). *Thermal Performance of Buildings - Determination of Air Permeability of Buildings - Fan Pressurization Method.* United Kingdom: BS EN ISO 9972:2015.

Vega Pasos, A., Zheng, X., Sougkakis, V., Gillott, M., Meulemans, J., Samin, O., . . . Wood, C. J. (2018). Experimental study on the measurement of Building Infiltration and Air Leakage rates (at 4 and 50 Pa) by means of Tracer Gas methods, Blower Door and the novel Pulse technique in a Detached UK Home . *39th AIVC Conference Proceedings.* Juan-les-Pins/Antibes, France.

On the experimental validation of the infiltration model DOMVENT3D

Alan Vega Pasos[1], Xiaofeng Zheng[1], Benjamin Jones[1], Mark Gillott[1] and Christopher J. Wood[*1]

1 Buildings, Energy and Environment Research Group, Faculty of Engineering, University of Nottingham, University Park, Nottingham NG7 2RD, United Kingdom.
**Corresponding author:*
christopher.wood@nottingham.ac.uk

ABSTRACT

Buildings represent approximately 40% of global energy demand and heat loss induced by uncontrolled air leakage through the building fabric can represent up to one third of the heating load in a building. This leakage of air at ambient pressure levels, is known as air infiltration and can be measured by tracer gas means, however, the method is disruptive and invasive. Air infiltration models are a non-disruptive way to calculate predictive values for air infiltration in buildings. DOMVENT3D, is an infiltration model that predicts the infiltration rate from air permeability measurements quoted at 50 Pa. The model has been used to calculate the English housing stock infiltration rates, however, it has not been experimentally verified. The objective of this study is to compare DOMVENT3D's predictions with real measurements. Air permeability measurements using a blower door (50 Pa) and the Pulse method (4 Pa) were carried out in three domestic dwellings in Nottingham, U.K. DOMVENT3D was calibrated to predict infiltration from air permeability measurements taken at 4 Pa. This paper presents a comparison of results for both the blower door and pulse methods predicted values and real infiltration measurements. Initial results show discrepancies (from 34 to 107%) in the predictions between blower door and pulse methods and also with the real infiltration measurements. Nevertheless DOMVENT3D presented results close to the measurements. Further validation is needed before a final conclusion about the model is given.

KEYWORDS

Air infiltration, airtightness, infiltration modelling, permeability, heat loss

1 INTRODUCTION

Buildings represent approximately 40% of the global energy demand. The heat losses induced by the uncontrolled air leakage through the building fabric can represent up to one third of the building heating load (Etheridge , 2015). This uncontrolled leakage at ambient pressure levels is commonly known as air infiltration (h^{-1}).

Air infiltration is a parameter which is difficult to measure. The common method to measure air infiltration is by tracer gas means, however these are disruptive, invasive, costly and time consuming. The most used tracer gas methods are the constant concentration, constant emissions and concentration decay, out of which the last is the most used one. Hence, a practical way of obtaining the infiltration rate is by predicting it based on a measurement of building airtightness. Airtightness is the parameter that affects the most on air infiltration; and is defined as a flow of air passing through adventitious openings in the building envelope at a given pressure difference. Airtightness can be given as a rate of flow Q (m^3/s, kg/s), an air change rate n (h^{-1}), or an air permeability q ($m^3h^{-1}m^{-2}$), when normalised by building volume and envelope area.

The way to predict air infiltration is to use air infiltration predicting models. Models have changed over the years. The simplest models are the airtightness-infiltration ratios which have been questioned by their crude simplicity (Jones, et al., 2016). Simplified models have been used since the 1980's, the most widely used simplified models are the LBL (Sherman & Grimsrud, 1980) and the AIM-2 (Walker & Wilson, 1990) models, both created in North America. Through the years more complex models with improved accuracies were developed such as CONTAM (Dols, et al., 2000). In the UK, the infiltration predicting model DOMVENT3D (Jones, et al., 2013) has been used to predict the infiltration of the English housing stock, however it has not gone through experimental validation.

The objective of this paper is to field validate the predictions made by DOMVENT3D from measurements of airtightness quoted at 50 Pa. In addition, DOMVENT3D will be calibrated to give predictions from airtightness measurements quoted at 4 Pa. Both results (at 50 and 4 Pa of pressure difference) are compared herein to assess the feasibility of including different airtightness measuring methods in air infiltration prediction.

2 DOMVENT3D

DOMVENT3D is an infiltration model which is based on research undertaken by Lyberg (Lyberg, 1997) and Lowe (Lowe, 2000), which proved that superposition techniques used in simplified models are not physically correct.

DOMVENT3D is a modification from Lowe's (Lowe, 2000) model (DOMVENT2D). In this new model, flows from every façade are accounted for. It used the power law (equation 1) as governing equation to predict infiltration rate.

$$Q = C\Delta P^b \tag{1}$$

Where
Q is the air flow (m^3/s),
C is the flow coefficient ($m^3/h/Pa^n$),
ΔP is the differential pressure experienced (Pa), and,
b is the flow exponent (dimensionless) which varies from 0.5 to 1 (turbulent to laminar), typically taken as 0.66.

Lowe identified four zones in a building, windward and leeward exfiltration (a and b), and windward and leeward exfiltration (c and d), shown in Figure 1. Δh_0 is the differential of the mean heights of the neutral planes of each façade.

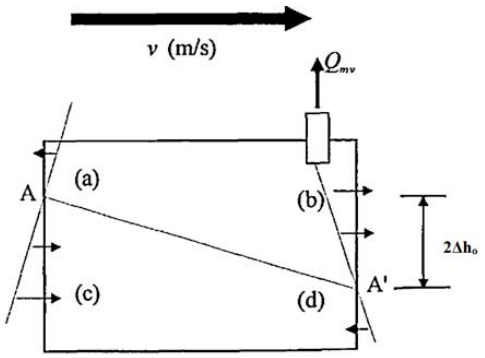

Figure 1. From (Lowe, 2000) Vertical cross section through dwelling, showing direction and magnitude of infiltration and exfiltration across envelope. AA' is the neutral plane.

Lowe formulated a single integral for each zone from Figure 1, and once solved, the resulting equations are as shown in equation 2.

$$Q_{inf} = \frac{LEC(\rho g\, \Delta T/T)^b}{n+1}\begin{bmatrix} +(h_0+\Delta h_0)^{b+1} \\ -(h_0+\Delta h_0-H)^{b+1}|_{h_0+\Delta h_0>H} \\ +(h_0-\Delta h_0)^{b+1}|_{\Delta h_0<h_0} \\ -(h_0-\Delta h_0-H)^{b+1}|_{h_0-\Delta h_0>H} \end{bmatrix} \quad (2)$$

L and *H* (*m*) are the length and height of the building respectively; *E* is the relative leakage area (dimensionless); *g* is the gravitational acceleration (m/s^2); ΔT is the temperature difference (K) and; h_0 (*m*) is the mean height of the neutral plane (no flow).

Jones (Jones, et al., 2013) modified the model when testing the effect of infiltration if party walls are considered fully permeable or impermeable. This model, named DOMVENT3D considers flow from every façade; the power law (equation 1) is applied to an infinitesimal section of a vertical façade. The flow rates ($\dot{Q}_f$) from DOMVENT3D can be simplified in equation 3.

$$\dot{Q}_f = E\alpha W\varepsilon(\rho_0-\rho_i)\{|(\rho_0-\rho_i)|g\}^b \begin{bmatrix} +\int_0^{minh_{0.H}} (h-h_0)^b dh \\ -\int_{maxh_{0.H}}^{H} (h-h_0)^b dh \end{bmatrix} \quad (3)$$

Where
α is taken as $(2/\bar{\rho})^b$, and $\bar{\rho}$ is the mean air density (indoor-outdoor) in kg/m^3,
ρ_o and ρ_i are the outdoor and indoor air densities respectively in kg/m^3,
W is the width of the façade (*m*) and,
h is the height of the selected opening (*m*).

The solution of the integrals in equation 3 leads to equations 4 and 5.

$$Q_1 = \frac{E\alpha W\varepsilon(\rho_0-\rho_i)}{b+1}\{|(\rho_0-\rho_i)|g\}^b \begin{bmatrix} +h_0^{b+1}|_{h_0>0} \\ -(h_0-H)^{b+1}|_{h_0>H} \end{bmatrix} \quad (4)$$

$$Q_2 = \frac{E\alpha W\varepsilon(\rho_0-\rho_i)}{b+1}\{|(\rho_0-\rho_i)|g\}^b \begin{bmatrix} +(H-h_0)^{b+1}|_{h_0<H} \\ -(-h_0)^{b+1}|_{h_0<0} \end{bmatrix} \quad (5)$$

DOMVENT3D predicts air infiltration in each façade using only two equations from 1, 4 and 5 depending on the air densities. The major shortcoming of the model is that is only valid for low rise buildings because it does not account for temperature stratification. The model, has been used to predict the infiltration rate of the English housing stock (Jones, et al., 2015). Nonetheless, it had not been field validated until this study.

3 AIRTIGHTNESS AND AIR INFILTRATION MEASURING

Air infiltration is the parameter needed to calculate the infiltration heat losses of a building. To obtain the infiltration rate of a building, first its airtightness has to be measured.

The steady pressurisation method, commonly known as “blower door” (Energy Conservatory, n.d.), is the most common way of measuring the airtightness of a building. The blower door test is implemented by creating a pressure difference across the building by pressurising or depressurising the building by a fan mounted in an existing doorway. This pressure difference, commonly between 10-60 Pa, is correlated to the airflow exchange rate. Results are quoted at 50 Pa; high pressures are used to minimize the noise of natural phenomena occurring at low pressure difference, namely wind and buoyancy effect. The method is well known, developed and standardised internationally (The British Standards Institution, 2015; American Society for Testing and Materials;, 2019). A picture of a typical blower door is give in Figure 2.

Despite the long development process that the blower door has gone through, some authors argue that measuring at high pressure differences create high uncertainty when extrapolating to the lower pressures (Cooper & Etheridge, 2007), and that measuring airtightness at low pressure should be more accurate. For this reason the Pulse method was developed; Pulse measures building airtightness at low pressure difference.

Pulse generates an instantaneous pressure rise in a building, whilst at the same time the variations in tank and building pressures are monitored and used to determine the airtightness. This pressure rise in the building is created by releasing air from a compressed air tank. The pressure rise in the building typically lies between 1 - 10 Pa. The method quotes the airtightness at 4 Pa (Cooper, et al., 2014). The latest PULSE-60 equipment is shown in Figure 3.

Despite the shorter time that has been developed, the Pulse has shown good repeatability and reproducibility; and, is considered as a future alternative of measuring airtightness (Cooper, et al., 2016; Zheng, et al., 2018; Zheng, et al., 2019).

Figure 2. Standard Minneapolis blower door unit (photo source: Wikimedia)

Figure 3. Latest version of the Pulse unit

On the other hand, to measure the air infiltration rate of a building directly, is through tracer gas methods. Different methods have been standardised, however, the concentration decay method is the one most frequently used due to its simplicity in operation and required equipment. The tracer gas concentration decay method is carried out by increasing the gas concentration, commonly carbon dioxide (CO_2), and monitoring its decay for a certain period.

Standards describe the minimum test period and the optimum conditions for a decay test (American Society for Testing and Materials, 2011; British Standards Distribution;, 2017).

In order to obtain the air infiltration rate (h^{-1}) from the tracer gas decay method, a plot of time vs natural logarithm of the average concentration graph is produced. The slope in the equation of the best fitting line from that regression is the average air infiltration rate; valid for that period and the encountered environmental conditions.

4 METHOD

Three houses in Nottingham, United Kingdom were tested with the objective of validating the infiltration model DOMVENT3D. Table 1 describes the characteristics of the houses tested.

Table 1. Description of dwellings

Dwelling	Date of test	Dwelling type	Main construction type	Volume (m^3)	Envelope area (m^2)
1	03/08/2018	Detached	Timber frame	188	227
2	16/08/2018	Detached	Solid	478	435
3	07/06/2018	Semi-detached	Solid	264	252

The first step was to measure the airtightness conditions of the houses, therefore blower door tests were carried out. A pressurisation and a depressurisation test were performed and the average result of both tests was reported. As an alternative three different Pulse tests were undertaken, with the average also reported.

All airtightness tests were carried out according to standard *BS EN ISO 9972:2015*(The British Standards Institution, 2015). This means that internal doors were left open, outdoor openings were closed, flues, vents, and trickle vents were sealed. These considerations applied for both, the blower door and the Pulse tests.

After the airtightness testing, the infiltration rate was measured using the tracer gas concentration decay method. Any sealing applied to the house was maintained. Before the test, the houses were divided in different zones according to volume and distribution of the house. One CO_2 sensor was placed in each zone; the sensors were connected to a data logger sampling every second. To ensure the right mixture of the gas fans were placed in every internal zone. Tracer gas was spread until the concentration was close to 5000 ppm. The concentration was left to decay for as long as possible, trying to comply with the minimum time specified in the standard ASTM designation E741-11. (American Society for Testing and Materials, 2011).

During the airtightness and tracer gas tests, the environmental conditions were measured. An ultrasonic anemometer was placed outside the tested dwelling. Meanwhile, a temperature sensor was placed in each internal zone (next to the CO_2 sensor) and next to the anemometer which was installed in an open outdoor area. Both the anemometer and the temperature sensors were connected to a data logger sampling every second throughout the test. A summary of the equipment used is listed in Table 2.

Table 2. Equipment

Airtightness measuring	Minneapolis blower door model 4. (BD-4) Pulse-60
Tracer gas	Carbon dioxide Sontay GS-CO2-1001 CO_2 sensors ±5%
Environmental	WindSonic Ultrasonic anemometer Temperature sensors PT100 RTD
Data logging	Datataker DT85 data logger
Other	Fans

DOMVENT3D model was re-coded using MATLAB; the input parameters included the dimensions of the dwellings, blower door test result, wind and temperature measurements. The output was the predicted air infiltration rate (h^{-1}). DOMVENT3D was designed to work with a pressure difference of 50 Pa, due to the assumption of using the blower door for airtightness tests. In order to use the Pulse method measurements as an input value, DOMVENT3D was recalibrated. Therefore a second set of predictions was made using the Pulse measurements.

The predictions given by DOMVENT3D using the blower door results were compared against the measured infiltration rates from the tracer gas test. In addition, the predictions using the Pulse measurements were compared with the measured infiltration rate and the DOMVENT3D predictions based on blower door measurements. Discussions were made according to the performance of the model and how the input values changed the predictions.

5 RESULTS AND DISCUSSION

Dwelling parameters (dwelling type, volume, envelope area), shielding conditions and terrain conditions have to be defined before entering to an infiltration model. Table 3 describes these parameters from the tested dwellings. The shielding conditions vary depending on the surroundings of the property and the natural and artificial barriers can obstruct the flow of wind or, change the microclimate. Terrain conditions are bound to the infrastructure in the area where the dwelling is located. In addition, the measured environmental factors are presented in Table 3. Wind speed, wind direction and temperature difference were measured while the airtightness and tracer gas tests were being carried out; an average value is reported. Finally, the exposed facades are presented, 0° represents the north orientation, moving clockwise, 90° represents the east orientations and so on.

Table 3. DOMVENT3D inputs.

Dwelling number	Shielding conditions	Terrain conditions	Wind speed (m/s)	Wind direction (°)	ΔT (K)	Dwelling type	Exposed Facades			
							0°	90°	180°	270°
1	Light	Suburban	1.080	250	3.69	Detached	✓	✓	✓	✓
2	Moderate	Suburban	0.712	216	3.40	Detached	✓	✓	✓	✓
3	Light	Suburban	1.700	195	1.71	Semi detached	✓	✗	✓	✓

Table 4 includes the measured air change rate (h^{-1}) obtained from blower door tests (average from pressurisation and depressurisation) quoted at 50 Pa; another important result of the airtightness tests is also the flow exponent (*b*); both are key parameters to input in the DOMVENT3D model.

As mentioned before, DOMVENT3D was calibrated to predict infiltration values from airtightness measurements quoted at 4 Pa. Table 4 includes the airtightness results obtained from Pulse tests in each dwelling.

Table 4. Air infiltration (n_1) and airtightness results from blower door (n_{50}, b_{50}) and Pulse (n_4, b_4).

Dwelling number	Air infiltration, n_1 (h^{-1})	Air infiltration uncertainty (h^{-1})	Blower door		Pulse	
			n_{50} (h^{-1})	b_{50}	n_4 (h^{-1})	b_4
1	0.1241	0.0019	5.3128	0.659	1.0098	0.707
2	0.0787	0.0036	3.5310	0.596	0.7167	0.675
3	0.1645	0.0020	5.7654	0.626	1.2267	0.604

The measured air infiltration given by the tracer gas method is included in table 4. An uncertainty of the data and the regression was calculated. It can be seen that all the tests have uncertainties lower than 5%.

Aided by information from Tables 1, 3 and 4, DOMVENT3D was able to predict infiltration rates for each dwelling. The results are presented in Table 5. The first column shows the predicted infiltration rates from blower door measurements, and, the second from Pulse measurements.

Table 5. DOMVENT3D air infiltration rate predictions (DVn_1).

Dwelling number	DOMVENT3D predictions from n_{50} (h^{-1})	DOMVENT3D predictions from n_4 (h^{-1})
1	0.2091	0.1941
2	0.1628	0.1289
3	0.2203	0.2346

There are discrepancies between DOMVENT3D's predicted values, however, except for property two (133%), the values are not large. Nevertheless, there is not a specific pattern, i. e. for property number one and two, the predicted values are higher when the n_{50} is used, whereas for property number three, the opposite occurs. This is probably due to the nature of the tests and their own uncertainties during the measurements.

In Table 6, the predicted values (DVc), using blower door and Pulse are given and each are separately taken into account with the tracer gas value (n_1) to provide a statistical standard error assuming a normal distribution for any results.

There are clear differences between the measured and predicted values, for the blower door the standard error reaches up to 18% and up to 14% for the Pulse. It can be seen that the discrepancies from property to property are smaller for the results obtained using the Pulse method (11-14%), though this does not mean that the Pulse method gives better predictions, but suggests the range of uncertainty of the predictions using this model is smaller when using measurements taken at 4 Pa. However, these results need to be validated by further tests in more properties.

Table 6. Standard error between measured and predicted infiltration values.

Dwelling number	n_1 (h^{-1})	Blower door (ΔP=50 Pa)			Pulse (ΔP=4Pa)		
		DVn_1 (h^{-1})	Standard Error (h^{-1})	Standard Error (%)	DVn_1 (h^{-1})	Standard Error (h^{-1})	Standard Error (%)
1	0.1241	0.2091	0.0301	14%	0.1941	0.0248	13%
2	0.0787	0.1628	0.0297	18%	0.1289	0.0177	14%
3	0.1645	0.2203	0.0197	9%	0.2346	0.0248	11%

Regarding the precision of DOMVENT3D's prediction, Table 7 shows the difference in percentage between the measurements of air infiltration and the predictions (based on both airtightness measurement methods).

Table 7. Percentage difference between measurements of air infiltration and DOMVENT3D's predictions.

Dwelling number	DVn_1 (ΔP=50 Pa) difference (%)	DVn_1 (ΔP=4 Pa) difference (%)
1	68%	56%
2	107%	64%
3	34%	43%
Average	**70%**	**54%**

As mentioned there are discrepancies between the predictions and measurements; it is important to remark that the environmental conditions during the airtightness measurements were used as the input to the infiltration model. This suggests that the measured and predicted infiltration rates are valid only for those scenarios. The differences between using a standard pressurisation method as an input for DOMVENT3D and tracer gas measurements, range from 34 to 107%. For the Pulse method the differences lie in a much tighter range (43-64%).

Despite the lower average difference obtained by the Pulse method, the results seem inconclusive. The difference in the third property is lower when predicting from the blower door than the Pulse. DOMVENT3D's predictions overall generate an error, nevertheless this error is smaller than when using infiltration ratios (Vega Pasos, et al., 2019) and modifying factors, as used in UK's legislation (Building Research Establishment, 2013). Therefore, for more accurate calculations of heat losses, infiltration models should be used.

Assuming that the Pulse method is as repeatable and accurate as the conventional pressurisation method, DOMVENT3D, or other infiltration model can be employed to predict infiltration rates. Nevertheless, this study is rather short (limited number of properties) for the capabilities of the model which has been used to predict full housing stocks. More properties in different climates in different seasons need to be studied in order to give a realistic validation of the results; and, to make conclusive statements about the model. A larger testing and modelling campaign is underway led by the authors, future results will be compared with the ones reported in this paper.

6 CONCLUSION

Three houses located in Nottingham, United Kingdom were used to validate the infiltration rate predictions given by the infiltration model DOMVENT3D. Airtightness tests using the pressurisation and the Pulse methods were carried out in those dwellings. In addition, the infiltration rate was measured using the tracer gas concentration decay method. Real measurements were used to compare against predictions. DOMVENT3D was also calibrated to produce an infiltration rate prediction when inputting airtightness measurements at 4 Pa (using Pulse). During those tests the environmental conditions were monitored. The test were considered as successful.

Results from the tracer gas tests delivered valid results with low uncertainty, therefore it was concluded that they were representative of the infiltration rate for that period. Input parameters were defined for each dwelling and logged into DOMVENT3D including the air change rate obtained from airtightness measurement methods.

DOMVENT3D predictions differed from 34% to 107% when using the blower door's measurements; and, from 43% to 64% when using the Pulse measurements. Despite these figures, it cannot be concluded that an airtightness measurement method is better than the other to predict infiltration rate, however, results suggested that the nature of Pulse (low pressure measurement), led to a lower uncertainty, or a more repeatable one. In addition, the Standard error between measurements and predictions was lower in general when using the Pulse method. Despite these, it is concluded that these results are only a first step to experimentally validating the model. This same method has to be used in a larger testing and modelling campaign including different dwellings, locations and environmental conditions.

Although the difference between measurements and predictions might seem large, in some cases, the model showed more accurate results than those ones obtained when using UK's legislation method. Finally, assuming that both airtightness testing techniques give accurate results, it can be concluded that they both can be used to measure airtightness and predict air infiltration rates.

7 ACKNOWLEDGEMENTS

Part of this work was funded by the Mexican Council of Science and Technology (CONACYT), and the European Union's Horizon 2020 research and innovation programme under grant agreement No 637221. ['Built2Spec': www.built2spec-project.eu/];and their full support is acknowledged by the authors. The authors also thank the support of Build Test Solutions ltd.

8 REFERENCES

American Society for Testing and Materials;, 2019. *Standard test method for determining air leakage rate by fan pressurisation,* U.S.A.: American Society for Testing and Materials;.

American Society for Testing and Materials, 2011. *Standard Test Method for Determining Air change in a Single Zone by Means of Tracer Gas Dilution,* s.l.: ASTM designation E741-11.

British Standards Distribution Princeton University; 2017. *BS EN ISO 12569:2017 Thermal Performance of Buildings ans Materials - Determination of Specific Aiflow Rate in Buildings - Tracer Gas Dilution Method ,* United Kingdom: BSI Standards limited .

Building Research Establishment, 2013. *The Government's Standard Assessment Procedure for Energy Rating of Dwellings,* Watford, United Kingdom.: Building Research Establishment on behalf of the Deparment of Energy and Climate Change.

Cooper, E. & Etheridge, D., 2007. Determining the Adventitious Leakage of Buildings at Low Pressure, Part 1: Uncertainties. *Building Services Engineers Research Technology ,* Volume 28, pp. 71-80.

Cooper, E. et al., 2014. *A Nozzle Pressurization Technique for Measurements of Building Leakage at Low Pressures.* Poznan, Poland, s.n.

Cooper, E. et al., 2016. Field Trialling of a New Airtightness Tester in a Range of UK homes. *International Journal of Ventilation,* 18(1), pp. 1-18.

Dols, W. S., Walton, G. N. & Denton , K. R., 2000. *CONTAMW 1.0 user manual,* Gaithersburg, MD, USA: NISTIR 6476, National Institute of Standards and Technology.

Energy Conservatory, n.d. *Minneapolis Blower Door Operation Manual for Model 3 and Model 4*

Etheridge , D., 2015. A perspective of fifty years of natural ventilation research. *Building and environment,* Volume 97, pp. 51-60.

Jones, B. et al., 2013. *A Stochastic Approach to Predict the Relationship between Dwelling Permeability and Infiltration in English Apartments.* Athens, Greece, s.n., pp. 199-209.

Jones, B. et al., 2015. Assessing uncertainty in housing stock infiltration rates and associated heat loss: English and UK case studies. *Building and Environment,* Volume 92, pp. 644-656.

Jones, B. et al., 2013. The effect of party wall permeability on estimations of infiltration from air leakage. *International Journal of Ventilation,* 12(1), pp. 17-29.

Jones, B., Persily, A. & Sherman, M. H., 2016. *The Origin and Application of Leakage-Infiltration Ratios.* Alexandria, Virginia, U.S.A., s.n.

Lowe, R. J., 2000. Ventilation Strategy, Energy Use and CO2 Emissions in Dwellings - a Theoretical Approach. *Buildin Services Engineering Research and Technology,* 21(3), pp. 179-185.

Lyberg, M. D., 1997. Basic air infiltration. *Building and Environment,* 32(2), pp. 95-100.

Sherman, M. H. & Grimsrud, D., 1980. *Infiltration-Pressurization Correlation: simplified Physical Modelling.* Denver, Colorado, s.n.

The British Standards Institution, 2015. *BS EN ISO 9972:2015 Thermal Performance of Buildings - Determination of Air Permeability of Buildings- Fan Pressurization Method,* United Kingdom: BSI Standards.

Vega Pasos, A., Wood, C. J., Zheng, X. & Gillott, M., 2019. *Comparison between infiltration rate predictions using the divide-by-20 rule of thumb and real measurements.* Ghent, Belgium., AIVC.

Walker, I. S. & Wilson, D. J., 1990. *AIM-2 The Alberta Air Infiltration Model,* s.l.: The University of Alberta Department of Mechanical Engineering. Report 71.

Zheng, X. et al., 2019. Experimental Studies of a Pulse pressurisation technique for measuring building airtightness. *Future Cities and Environment,* 5(10), pp. 1-17.

Zheng, X. F., Wallis, I. & Wood, C. J., 2018. *Experimental study of enclosure airtightness of an outdoor chamber using the pulse technique and blower door method under various leakage and wind conditions.* Juan-les-Pins, France, AIVC.

How Accurate is our Leakage Extrapolation? Modeling Building Leakage Using the Darcy-Weisbach Equation

Steven Rogers[1]

1 The Energy Conservatory
2801 21st Avenue South
Suite 160
Minneapolis, MN, USA 55407

ABSTRACT

This study used a mathematical model to explore the accuracy of extrapolating multi-point blower door test results down to lower pressures at which building infiltration usually occurs naturally. The mathematical model was applied to leaks of five different widths. The leakage of the five different widths was then combined in different distributions to simulate total building leakage. The calculated total building leakage was then compared to an extrapolation from the test pressures using a power law curve fit. The results showed that depending on the distribution of the leaks from widest to narrowest, extrapolation of the power law fit may significantly over-estimate or under-estimate the building leakage. At a building pressure of 1 Pa, one simulation the power law fit under-estimated the leakage by 19%, while another over-estimated the leakage by 78%. At pressures below 1Pa, the deviations were even larger.

KEYWORDS

Leakage modelling, natural infiltration, blower door test, laminar and turbulent leakage

1. INTRODUCTION

Since the earliest days of blower door tests in the 1970's, multi-point tests have been commonly used to characterize building leakage over a range of test pressures. Soon thereafter, a power law fit ($Q_v = C*\Delta p^n$) of the pressure vs. flow rate points was employed to estimate the leakage at pressures other than those tested. Such a fit is useful since it allows an estimate of the leakage behavior by extrapolating from test pressures, which are usually 15 – 100 Pa, to pressures that are most common under natural leakage conditions, about 0 – 20 Pa.

However, the accuracy of such extrapolations is not well understood. Accuracy is important because one of the primary motivations for air tightness testing is provide data for energy loss models of buildings. Since buildings lose energy from air infiltration and exfiltration due to the pressure difference created by wind and the stack effect, the test data from higher pressures must be extrapolated to the lower pressures at which air infiltration and exfiltration occur naturally.

It should be acknowledged that in addition to the extrapolation of the power law fit, there are other known problems in estimating natural infiltration. The distribution of leaks vertically in the building and the distribution of pressure differences due to wind are two other important sources of error in estimating natural building infiltration. This paper will only discuss errors due to the extrapolation of the power law fit.

2. METHOD

The Darcy-Weisbach equation is used due to its simplicity and because it characterizes the pressure vs. flow behavior in both the laminar and turbulent flow regimes, which are known to exist in building leakage. The Darcy-Weisbach equation was developed for cylindrical pipes, and may not be regarded as applicable to long, narrow cracks with corners like those found in a leaky building. However, in this study, it will be shown that the model does not need to predict the magnitude of the leakage, but only how it changes with pressure and Reynolds number. For this purpose, the Darcy-Weisbach equation and the Darcy friction factor are useful and instructive.

The leakage model consists of cracks with five different widths: 16, 7, 5, 2.2, and 1.6 mm, where width is defined as shown in Figure 1. What is most important about the choice of these dimensions is the flow regime that will occur under conditions of test pressures and conditions of natural infiltration. For long, thin cracks the flow regime (laminar or turbulent) is determined by this width, and to a lesser degree the roughness of the building materials. In the case of the largest width, 16mm, flow is turbulent at all pressures where testing would occur (above about 3 Pa) and is approximately the largest width of a crack that can be expected to frequently occur in residential construction. With the smallest width, 1.6 mm, flow is laminar at all pressures of interest, up to 100 Pa. So this smallest leak can represent all leaks 1.6mm or smaller, since they will all remain laminar at all pressures of interest.

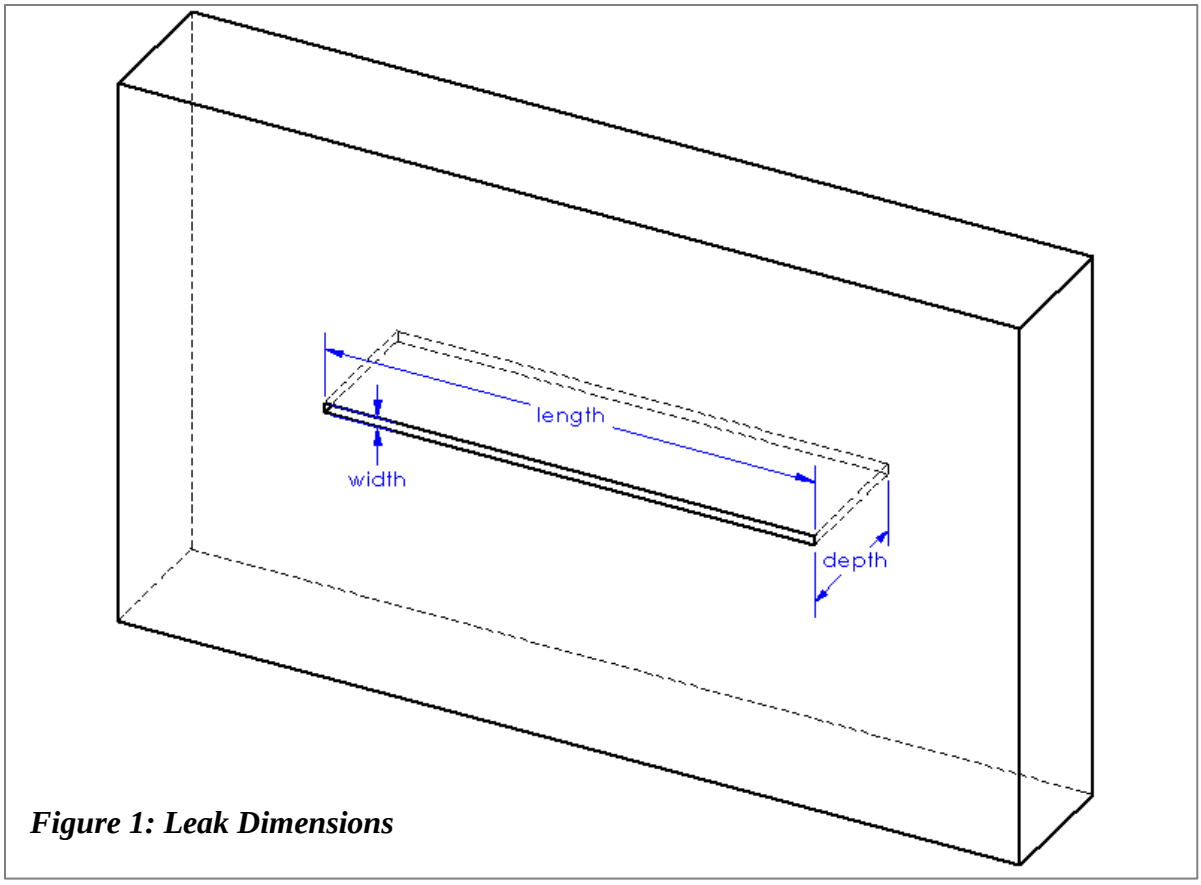

Figure 1: Leak Dimensions

The flow through each of the cracks is modeled over a range of 0.1 Pa to 100 Pa using the Darcy-Weisbach equation and Darcy friction factor. Most of the cracks change from laminar flow at low pressure differences through transitional flow and into the turbulent flow regime at higher pressure differences. Next, an arbitrary number of leaks (or leakage area) may be assigned to each of the five characteristic lengths, such that a total volume of air leakage is divided up into the five characteristic lengths. Finally, the sum of all leaks is computed at each pressure difference to calculate the total building leakage.

This approach allows the comparison of buildings with similar total leakage due to a smaller number of larger sized leaks, or a larger number of smaller sized leaks. By distributing the leaks carefully, one can even create two very different leakage distributions that result in exactly the same power law fit.

2.1 Five Leak Sizes

Initially, each of the five leaks is assumed to have an equal cross sectional area of 2500 mm^2, but each one has a different length to width aspect ratio, ranging from 10:1 to 1000:1. The widest leak is 16 x 158 mm, and the narrowest leak is 1.6 x 1580 mm. Each leak is assumed to be 100 mm in depth, where depth is the distance the air travels through the thickness of the wall (see figure 1). However, this depth has no impact on the results, since the total pressure loss is proportional to this depth and each leak will be multiplied by an arbitrary area. Again, this investigation is

interested in relative differences of one leak width to another as they change over a range of pressures.

The roughness of all leaks is required to calculate a Darcy Friction Factor in the turbulent region. The roughness, ε, of the three wider leaks was assumed to be 0.25 mm. The 0.25 mm value is given from several sources as the roughness of cast concrete pipe, and was assumed to be similar to many building materials. The two narrowest leaks were assumed to be smoother at 0.135 mm and 0.111 mm.

2.2 Darcy Friction Factor

Using the roughness values above, the Darcy Friction Factor was calculated over the range of Reynolds Numbers of interest. The width, as previously defined, is the characteristic linear dimension used in the calculation of Reynold number. In the laminar flow region for Re < 2300, the Darcy friction factor is known to be equal to 64/Re. In the turbulent flow region, Re > 4000, the friction factor becomes dependent on both relative roughness and Reynolds number, and eventually becomes nearly constant at high Reynolds numbers. A numerical approximation called 'Serghides's solution' is used to calculate the turbulent friction factor.

In the transition flow region, 2300 > Re > 4000 the flow is unsteady; it varies grossly with time and space within the flowing fluid. For simplicity, the friction factor has been modeled as a straight line connecting the friction factor from the laminar to the turbulent flow regime. In reality, there is considerable uncertainty in this Reynolds number range and it is indicated by the shaded region of Figures 2 and 3.

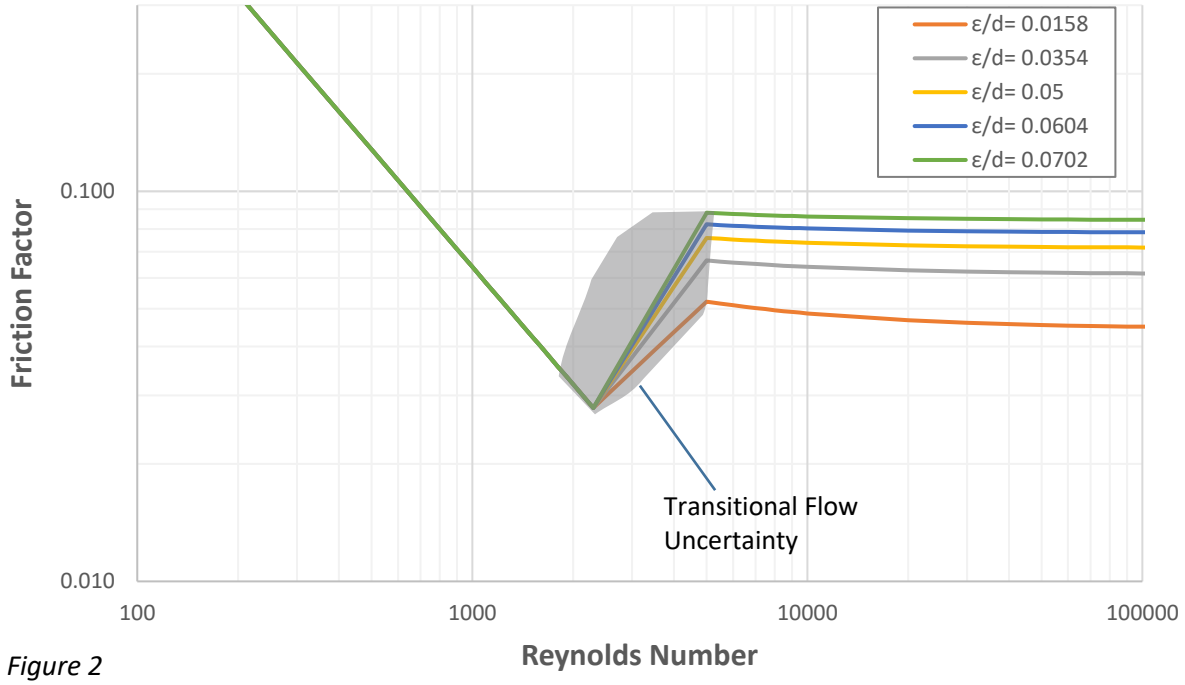

Figure 2

2.3 Flow vs. Pressure Difference

Once we have friction factors, the air velocity through each leak size can be calculated using the Darcy-Weisbach Equation, shown here solved for velocity.

$$v = \sqrt{\frac{2 * D_h * \Delta p}{\rho * f_D * L}} \quad (1)$$

Where:

v = the average velocity of air through the leak

D_h = the hydraulic diameter of the leak

Δp = the pressure difference inside to outside the building

ρ = the density of air

f_D = the Darcy friction factor

L = the depth of the leak (as shown in Figure 1)

Since the Darcy friction factor depends on the Reynolds number, which depends on the velocity, the solution is iterative. Once the average air velocity through each leak is calculated, the volumetric flow rate is obtained by multiplying velocity by the cross-sectional area of the leak.

Figure 3 shows the relationship between the pressure difference and the volumetric flow through a leak. The 7mm leak was chosen since it passes through all three flow regimes between 1 and 100 Pa pressure difference. Notice that in the laminar region where flow rate is proportional to pressure (n=1), the slope is the steepest, and in the turbulent region the slope is flatter where (n=0.5). The figure also shows the range of pressures at which blower door tests are usually run (between 15 and 100 Pa), and the pressures at which natural infiltration usually occurs (under 20 Pa).

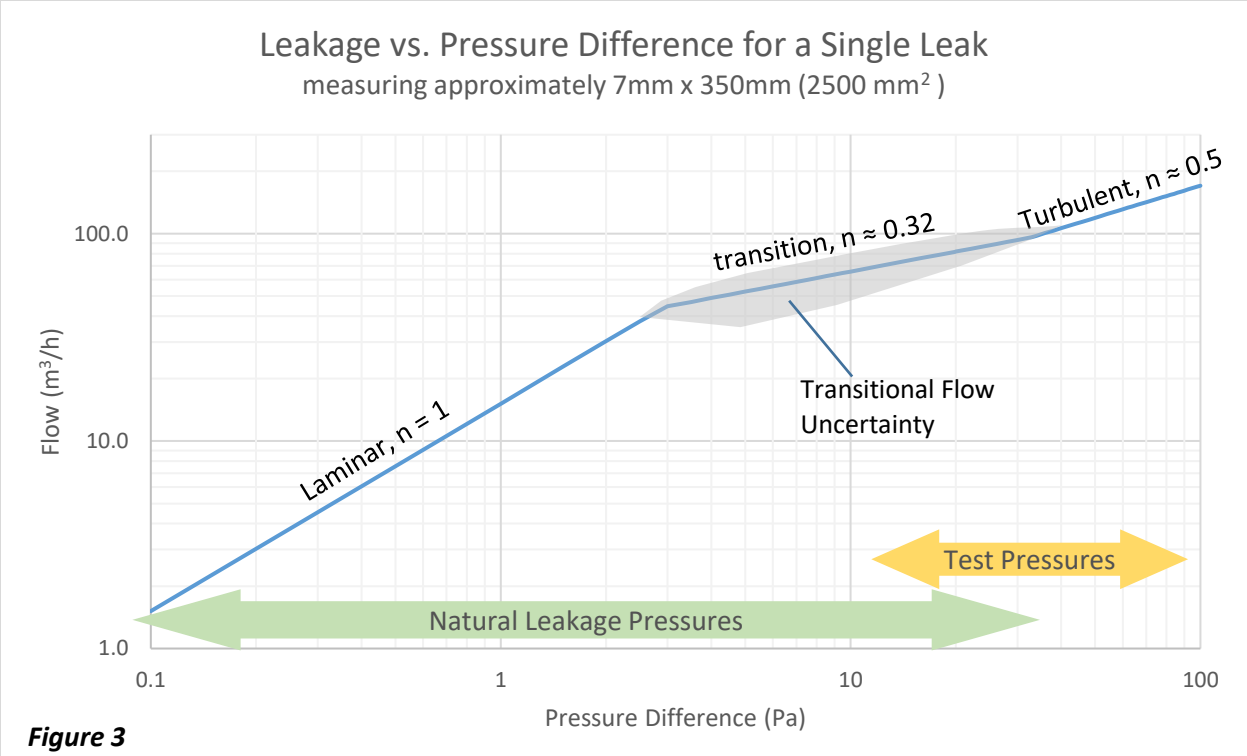

Figure 3

Figure 4 shows the leak rate vs. pressure difference behavior for all the leak sizes modeled. Notice that in some cases a narrower leak may have the same or more flow than a wider leak.

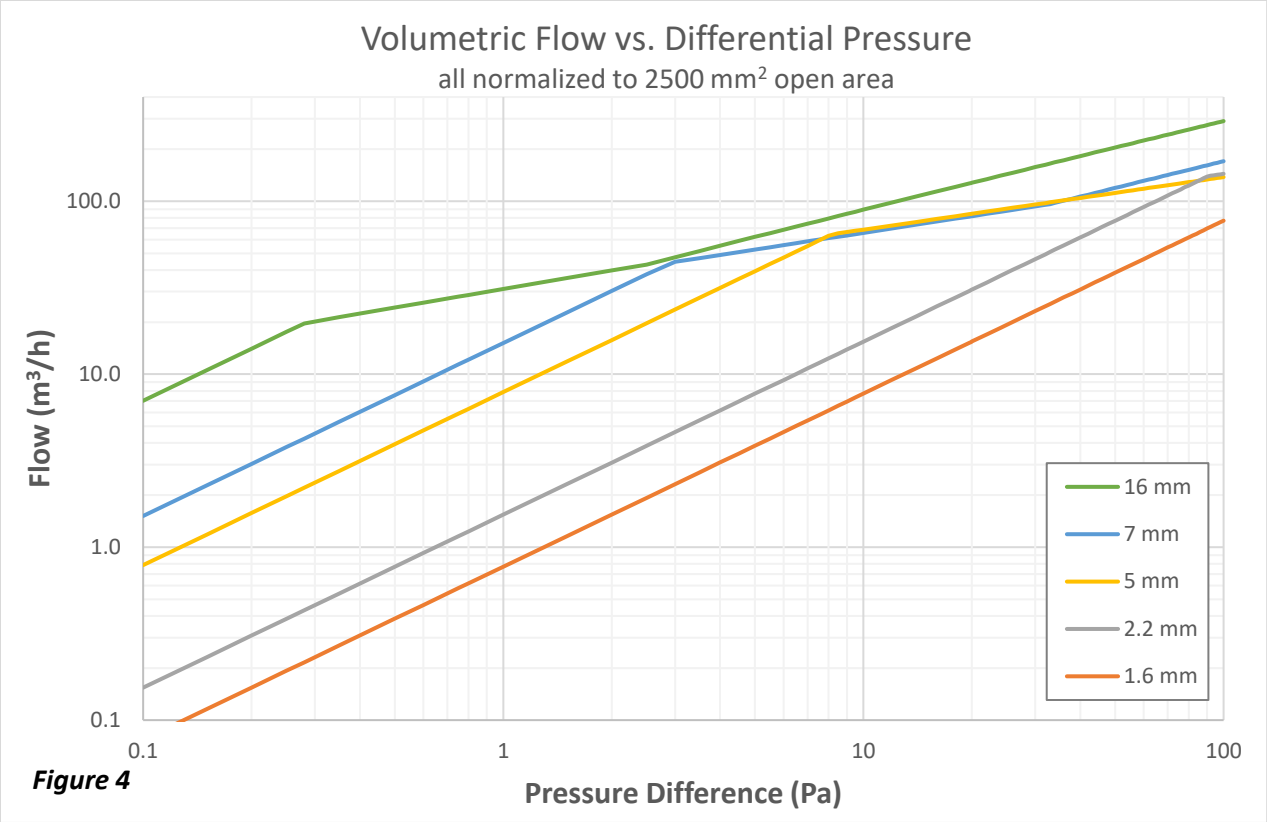

Figure 4

2.4 Combining Individual Leaks into Total Leakage

Once the pressure difference vs. leakage behavior is characterized, multiple sizes of leaks can be combined into a total. Originally, all the leaks were normalized to an open area of 2500 mm^2. Now we replace these areas with new areas that are somewhat arbitrary. The objective is to iteratively adjust these areas until the calculated leakage results are similar to what we find by field testing buildings.

This adjustment of leakage areas is the reason why our model does not need to accurately predict the magnitude of leakage for the various leak sizes, but only their relationship to each other and how they change over the pressure range. In this study, we are interested in understanding how the sum of many individual building leaks of various sizes changes with pressure, particularly at lower pressures. The pattern of flow as it changes from laminar to turbulent in building leaks is likely to follow a pattern very similar to the Darcy friction factor and Darcy-Weisbach equation, since they both result from the same fundamental physics described by the Navier-Stokes equations.

In a first example, we can begin by allocating the leakage areas so that the total leakage at 50 Pa is about 1200 m^3/h, and each of the five leak sizes accounts for 20% of the leakage. This gives the following results.

Table 1: Equal Leakage Distribution, Flow @ 50 Pa = 1206 m^3/h

Leak Size	16 mm	7 mm	5 mm	2.2 mm	1.6 mm
Leakage Area (mm^2)	2950	5045	5572	7834	15590
% of Total Leakage @50Pa	*20.0%*	*20.0%*	*20.0%*	*20.0%*	*20.0%*

When the leakage from all leaks is equal at 50 Pa, a power law fit of a multi-point test yields the following: $Q_v = 117.4*\Delta p^{0.595}$. However, our experience with real-world building leakage tests tells us that the exponent *n* is usually closer to 0.65. So our leakage distribution should be adjusted to have more leakage from the smaller leaks in proportion to the larger ones, in order to better reflect our experience with real-world leakage.

2.5 Comparing Three Different Distributions

Next, we will modify the leakage areas until we have a distribution that gives us a coefficient *n* close 0.65. To achieve this we progressively increase the leakage area as the leak size gets smaller, which results in the following proportions of leakage.

Table 2: Leakage Distribution A, Flow @ 50 Pa = 1219 m^3/h

Leak Size	16 mm	7 mm	5 mm	2.2 mm	1.6 mm
Leakage Area (mm^2)	1875	3375	6075	10935	19683
% of Total Leakage @50Pa	*12.6%*	*13.2%*	*21.6%*	*27.7%*	*24.9%*

The Power Law fit is: $Q_v = 94.410*\Delta p^{0.653}$

We can then plot the total leakage at pressures from 0.1 Pa up to 100 Pa. We can assume 9 test pressures of 12, 18, 22, 28, 36, 42, 50, 56, and 64 Pa. Figure 5 shows the leakage at all pressures in orange, and the test points in blue. The blue dotted line is the power law fit of the test points. It has an exponent of 0.653, which was the objective. Notice that total leakage is very close to the power law fit at pressures near the test points, but it deviates markedly as pressures get further from the test pressures.

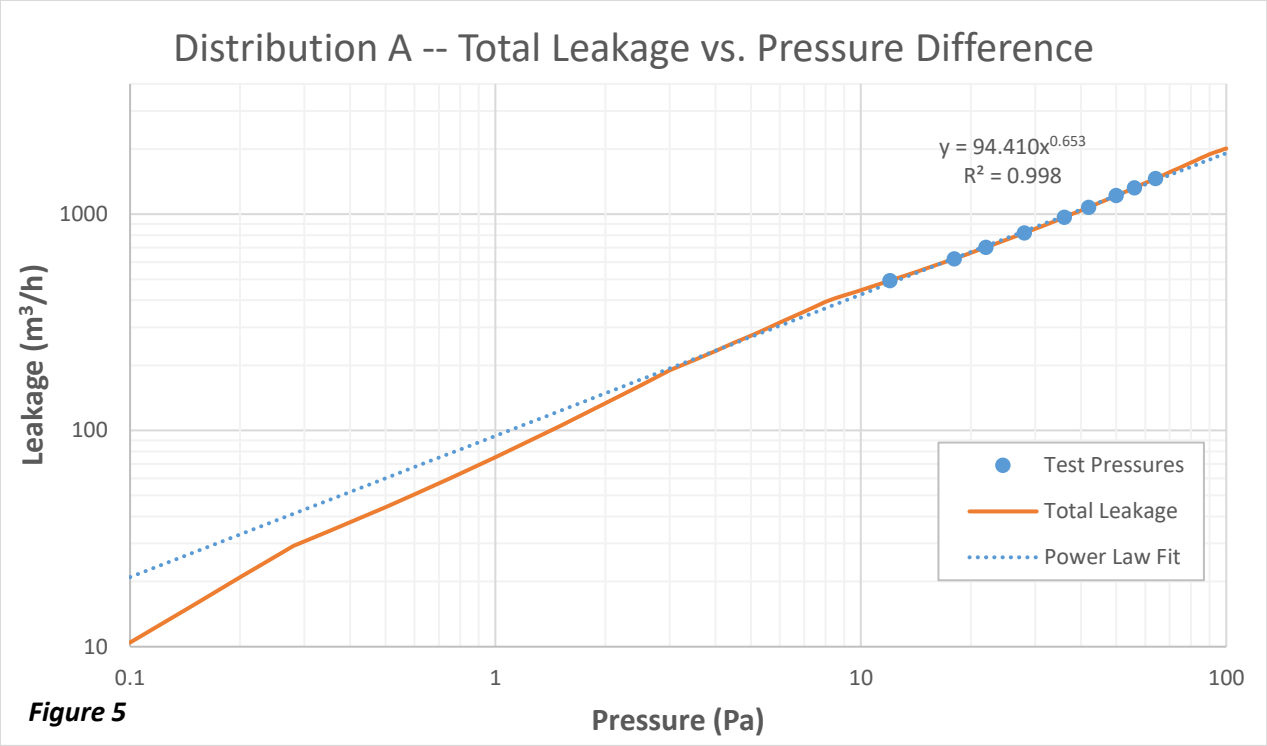

Figure 5

Next, we consider whether a significantly different distribution of leaks could also give the same resulting flow and exponent. Leakage Distribution B shows another possible distribution of leaks in which most of the leakage is 1.6 mm or 16mm with much less leakage in between. By adjusting the leakage area of small and large leaks, a total leakage can be calculated which results in a power law fit that is almost identical to Leakage Distribution B.

Table 3: Leakage Distribution B, Flow @ 50 Pa = 1217 m^3/h

Leak Size	**16 mm**	**7 mm**	**5 mm**	**2.2 mm**	**1.6 mm**
Leakage Area (mm^2)	7663	1120	1400	1750	27410
% of Total Leakage @50Pa	*51.4%*	*4.4%*	*5.0%*	*4.4%*	*34.8%*

The Power Law fit is: $Q_v = 94.401 * \Delta p^{0.653}$

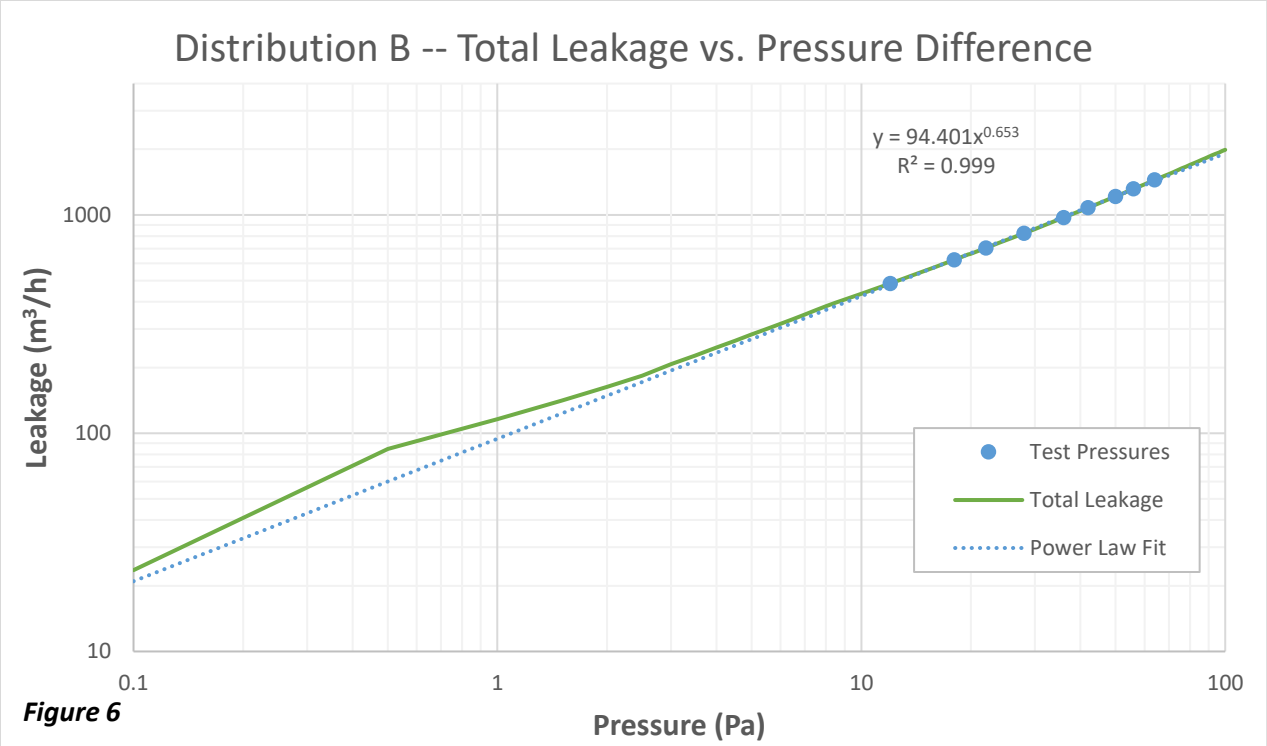

Figure 6

Just as with distribution A, the power law fit of Distribution B is very close to the calculated total leakage around the test pressures. However in this case, the Total Leakage is greater than the power law predicts, whereas with Distribution A, the Total Leakage was less than the power law predicts. So the "error" could be positive or negative.

A third distribution of leaks was also created which also results in the same total leakage at 50Pa and the same exponent: 0.653. In this case, most of the leakage was assumed to be from the 5 mm and 2.2 mm leaks, with very little from the smaller or larger leaks.

Table 4: Leakage Distribution C, Flow @ 50 Pa = 1219 m^3/h

Leak Size	**16 mm**	**7 mm**	**5 mm**	**2.2 mm**	**1.6 mm**
Leakage Area (mm^2)	250	250	10764.05	23175	250
% of Total Leakage @50Pa	*1.7%*	*1.0%*	*39.0%*	*58.0%*	*0.3%*

The Power Law fit is: $Q_v = 94.403 * \Delta p^{0.653}$

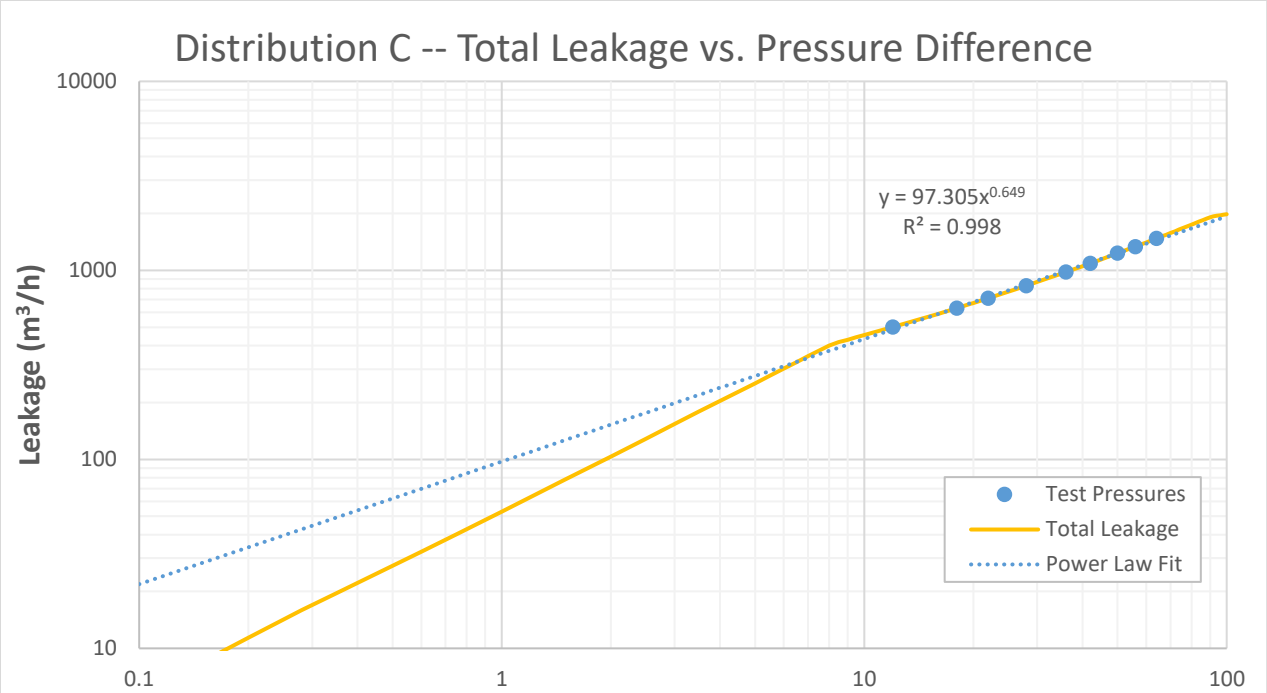

Figure 7

Like the others, distribution C deviates significantly from the power law fit model at lower pressures.

3 RESULTS

Now we return to the original question: how accurate is an extrapolation from leakage measurements taken at higher pressures to leakage occurring naturally at a few Pascals? Figures 8 shows a comparison of the results from Distributions A, B and C. Here, the vertical axis is the percent deviation of the flow estimated using the power law fit from the calculated total leakage. This makes it easier to compare the three results and understand the percent "error" that might be implied by extrapolating a power law fit from the test pressures down to lower pressures. At a pressure of 1 Pa, we have deviations of -19%, +26%, and +78% for distributions A, B, and C respectively.

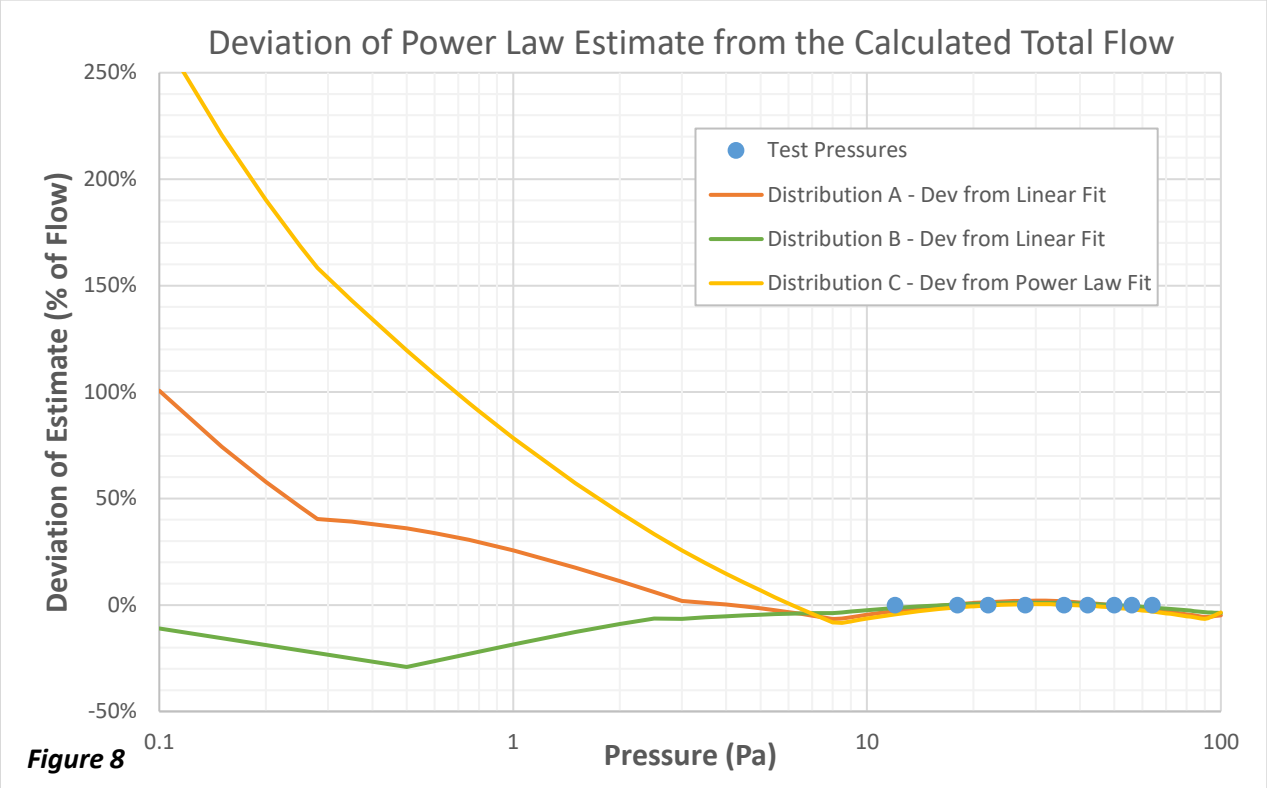

Figure 8

4 Necessary Assumptions

It is important to review the assumptions necessary for these results to be informative and useful. The first assumption is that real-world building leaks are of sizes that include both laminar and turbulent leaks. This is almost certainly true since real-world power law fits of measured leakage do not have exponents close to 1.0 or 0.5, which would be the case if all building leaks were laminar or turbulent respectively. Real world power law exponents are usually between 0.6 and 0.75.

The second assumption is that some leak sizes transition from laminar flow to turbulent flow as pressure increases within the pressure range of interest. This is also almost certainly true since the width of real-world leaks is continuously variable and the width of the leaks will determine the Reynolds number in the leak.

The third assumption is that in real-world building leaks, the relationship between pressure and flow changes in a way similar to that in round pipes. Since the Darcy-Weisbach equation was developed to describe flow in round pipes, we must consider whether it can be applied to long, narrow leakage geometries. This assumption is probably valid since the fundamental boundary layer physics that govern transitions from laminar to turbulent flow in round pipes are the same as those that govern flow through other geometries. The relationship between pressure and flow is best understood by referring to Figure 3. When viewed on a log-log plot, the change in the flow vs pressure appears as a straight line with a different slope as the flow changes from laminar to

turbulent. If real-world leaks change slope in a similar way, then these results are useful irrespective of the accuracy of the calculated leakage flow rate.

To look at it another way, we can use the 7mm wide leak as an example. In our simulation, we calculated that a leak 7mm wide, having a total open area of 2500 mm^2 has a leakage of 66 m^3/hr at a building pressure of 10 Pa. But for the purposes of this study, it doesn't matter if the actual leakage from a leak this size is 33, 66, or 133 m^3/hr. What is important is only that the flow regime will transition from laminar through transitional flow to turbulent flow at pressures somewhere between 0.1 Pa and 100 Pa. When this occurs, the slope of the line will change on the log-log plot and this will introduce error in the power law fit.

5 Discussion and Conclusions

These simulations can give us some idea of the shapes and inflections we might see in the error curves of a power law fit. They can also show what order of magnitude the errors might be at various pressures. They also seem to indicate that the true errors might be either positive or negative.

What cannot be determined from these results is which of the three simulations is most similar to buildings in the real world. Further study would be required to determine this.

The well-known and widely used power-law fits accurately predict leakage near the test pressures. However, at much lower pressures the true leakage might be higher or lower than the power law fit predicts and the error associated with this extrapolation might be quite large.

6 REFERENCES

Wikipedia contributors. (2019, August 7). Darcy–Weisbach equation. In *Wikipedia, The Free Encyclopedia*. Retrieved 12:56, August 15, 2019, from

https://en.wikipedia.org/w/index.php?title=Darcy%E2%80%93Weisbach_equation&oldid=909769707

Wikipedia contributors. (2019, July 5). Darcy friction factor formulae. In *Wikipedia, The Free Encyclopedia*. Retrieved 13:30, August 15, 2019, from

https://en.wikipedia.org/w/index.php?title=Darcy_friction_factor_formulae&oldid=904919914

Vertical Distribution of Temperature and Contaminant Concentration in a Room with Impinging Jet Ventilation System

Mako Matsuzaki*[1], Tomohiro Kobayashi[1], Toshio Yamanaka[1], Narae Choi[1], Haruna Yamasawa[1]

1 Osaka University
Suita 565-0871
Osaka, Japan
**matsuzaki_mako@arch.eng.osaka-u.ac.jp*

ABSTRACT

The impinging jet ventilation system (hereinafter referred to as IJV) has been proposed as a new air conditioning ventilation system. Properties of indoor environment with this system using impinging jet are complicated. The present paper reports fundamental properties of indoor air with distributed interior heat generation load assuming an office.
The experiment was conducted in the climate chamber of which floor area was 27.0 m^2, and basic properties of temperature and CO_2 distributions were investigated. Heat load within a room was simulated by black lamps (incandescent bulb covered with dark purple glass) distributed uniformly. As for contaminant, CO_2 was generated from 4 locations. The temperature and CO_2 concentration were measured by changing the combination of supply air temperature and supply air flow rate, and four cases were studied. In addition, the number of IJV supply terminals was also changed as a parameter to understand the effect of supply air momentum. Two cases (1 or 2 terminals) were studied without changing total supply airflow rate, i.e., only supply momentum was changed. In total eight cases were studied in the experiment. The specific Archimedes number was defined and evaluated based on experimental results, and relationship between temperature/concentration stratification and Archimedes number was investigated. It was shown that the temperature/concentration stratification become clear when the supply airflow momentum is small. Moreover, a correlation between Archimedes number and vertical temperature difference was shown. To propose a simplified calculation model, further parametric study is required, and CFD analysis seems to be beneficial because it enables numerical experiment easily. To do this, however, CFD calculation method for IJV system needs to be validated. Therefore, one case of full-scale experiment was simulated. Here, the effect of turbulence model was evaluated, and three turbulence models (standard k-ε model, RNG k-ε model, and SST k-ω model) were studied, and the accuracy of CFD analysis is finally verified.

KEYWORDS

Impinging Jet, Temperature Stratification, Full-scale Experiment, Quasi Displacement Ventilation, Thermal Stratification, CFD analysis

1 INTRODUCTION

As an air distributing system with high ventilation efficiency, a displacement ventilation system is well known. However, this supply system can only be used for cooling mode, and may generate excessive vertical temperature difference. To overcome these disadvantages, the IJV system *[1]* has been proposed. IJV system is an air distributing strategy that supplies air horizontally from the bottom of the room by using impinging jet. The impinging jet is generated by blowing the jet downward from ducts installed on the wall and impinging on the floor surface. To date, however, few studies have been done on the indoor environment created by IJV system. In previous studies *[2] [3]*, in order to understand the fundamental tendency of the

thermal environment created by IJV system in a large space with high heat load such as a factory, where IJV system seems to be beneficial, the laboratory experiment, CFD analysis and model calculation were conducted for a room model with high heat generation load at the center of the room. In order to investigate the performance of the IJV system for more general environment like an office, a full-scale experiment and CFD analysis were conducted for a room with uniformly distributed heat load. The final purpose of this study is to propose a simplified calculation method of vertical distribution of temperature and contaminant concentration that can be used in the design phase. This paper first presents the results of the full-scale experiment. Then, the CFD analysis which simulates the experiment is conducted to verify its accuracy.

2 FULL SCALE COOLING EXPERIMENT

2.1 Experimental Room

The experiments were conducted from January 29th, 2019 to February 14th, 2019 at a full-scale climate chamber (5,450(d)×5,000(w) ×2,770(h)[mm]) in Osaka University, Japan. The floor plan and cross-section of the chamber are shown in Figure 1 and 2, respectively. Two round ducts whose diameter were 150 mm were provided as IJV supply terminals, and the height of their bottom end was set at 600 mm above the floor level. These IJV supply ducts were insulated by foamed polyethylene sheets. The supply air flow rate was adjusted using a volume damper and an orifice flow meter (Iris Damper, Continental Fan). The room air was sucked out from an exhaust opening located on the ceiling. To simulate four occupants and all other interior heat generation in an office, 20 black lamps (50W × 20) were distributed in the chamber. The details of the assumed indoor heat load are shown in Table 1.

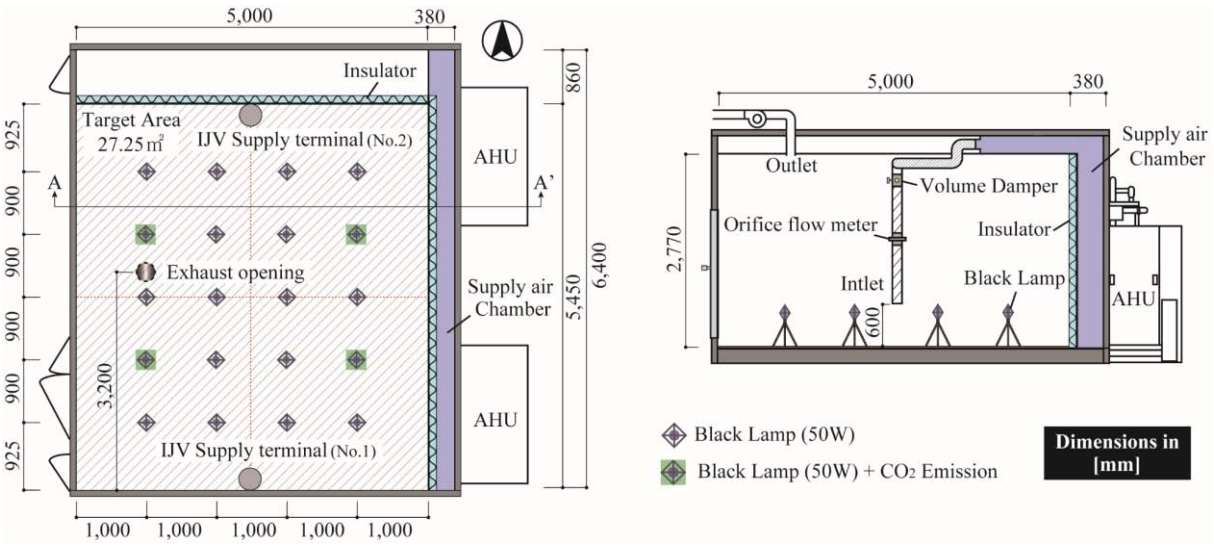

Figure 1: Floor plan and A-A' Cross-Section of the climate chamber

Table 1: Details of heat load

Sensible heat load of occupants (60[W/person])	Other heat load (28[W/m^2])	Total heat load [W]	Total heat load per unit area [W/m^2]
240	760	1000	36.7

2.2 Experimental Conditions

In the chamber, steady-state non-isothermal experiments were conducted to understand the effect of the correlation between supply airflow momentum and buoyancy (temperature difference from supply to ambient air) on the temperature and CO_2 concentration distribution. To investigate this under the same condition of input heat rate, both supply air temperature and supply airflow rate were varied. The experimental conditions are shown Table 2. Here, supply air temperature was set by assuming perfectly insulated enclosure and 17 °C of the exhaust temperature for all cases. Additionally, the number of IJV inlet terminals was changed, which enables the comparison of different supply momentum conditions under the same total supply airflow rate. Since the experiments were conducted in winter, the outside temperature of the climate chamber (the chamber is a large space laboratory not air conditioned) was 7-12 °C. Generally, the setting point temperature for cooling is approximately 26 °C. However, it might cause excessive continental fan heat loss through the wall of the climate chamber because of large temperature difference if this temperature was assumed as the experimental condition of exhaust temperature. Therefore, to decrease the heat loss through the walls, assumed exhaust temperature was set at 17 °C.

Table 2: Experimental conditions

No	Number of IJV terminal	Assumed Exhaust Temperature [°C]	Heat Load [W]	Supply Temperature [°C]	Total Supply flow rate [m^3/h]				Supply velocity [m/s]
					250	300	375	500	
1	2	17	1000	5	X				1.96
2	2	17	1000	7		X			2.36
3	2	17	1000	9			X		2.95
4	2	17	1000	11				X	3.93
5	1	17	1000	5	X				3.93
6	1	17	1000	7		X			4.72
7	1	17	1000	9			X		5.89
8	1	17	1000	11				X	7.86

2.3 Measurement item

In the experiments, the distribution of temperature and CO_2 concentration were measured. The measurement points are shown in Figure 3. Temperature measurement was conducted by T-type thermocouple. The vertical temperature profile was obtained at 7 poles, where 24 measurement points were provided vertically for each, including the surface temperature of ceiling and floor. The measurement points on the north-south line is shifted by 200 mm from the center, so as not to barrier the development of the jet along the floor. The wall surface temperature was measured at 24 points for each wall. The CO_2 concentration was measured using 9 portable CO_2 concentration recorders provided vertically for each pole. CO_2 concentration was also recorded at the supply air chamber, the exhaust duct, and outside the climate chamber. After the temperature got to the steady state, CO_2 gas started to be emitted continuously with 15 L/h at each of the four emission points shown in Figure 1. Flow rate of CO_2 was regulated by the pressure reducing valve, and was emitted by inserting the tube into the sponge placed above the black lamp to decrease the initial velocity. The steady state result of both the temperature and CO_2 concentration was averaged for 30 minutes. (measurement interval:1 min)

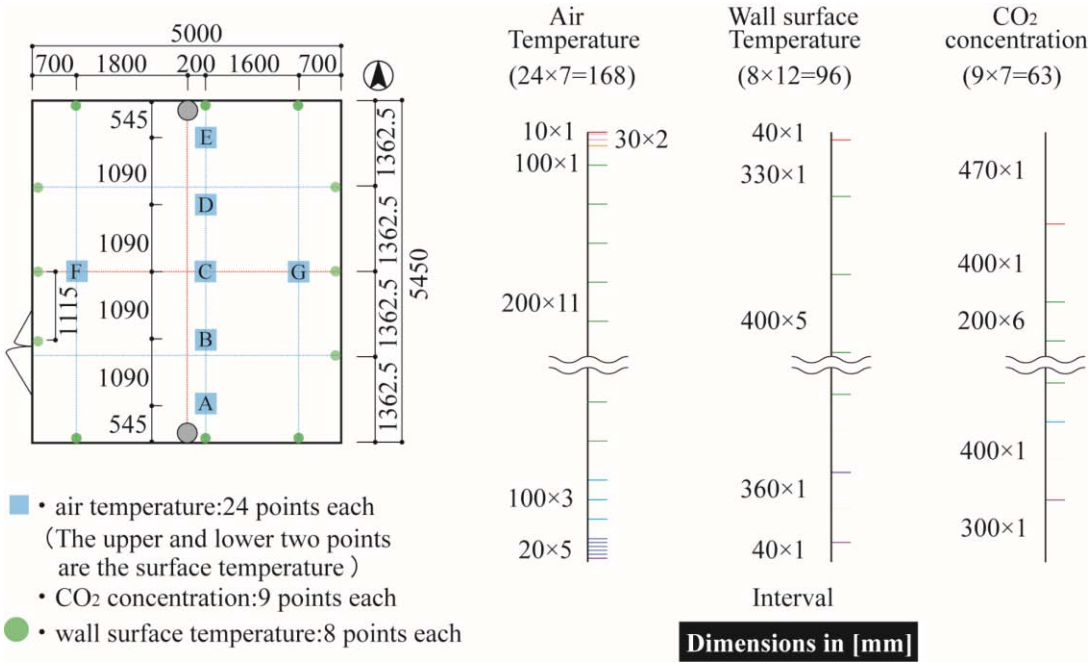

Figure 2: Measurement point of Temperature and CO_2 concentration

2.4 Experimental result

2.4.1 Temperature distribution

Temperature contours of the north-south central cross-section and vertical distribution of horizontal-averaged room temperature are shown in Figure 4 and 5, respectively. Under the condition of small supply air flow rate, indoor air temperature was vertically stratified. As the supply air flow rate increases, indoor air temperature distributed uniformly. Regarding the number of IJV terminal, the temperature distribution in the room was more uniform at single IJV terminal conditions, whose supply air momentum was relatively high, than two IJV terminal conditions. Supply temperature, exhaust temperature, external temperature, heat loss due to heat transmission through the wall calculated from the heat balance, heat load measured using a watt meter and heat loss ratio (ratio of heat loss and heat load) are summarized in Table 3. The temperature difference of the exhaust air for each condition seems to be caused by the effect of the external temperature. In most cases, the heat loss tended to increase as the external temperature decreased, and the maximum heat loss ratio was 18 %, which cannot be regarded as negligible. Although the insulation needs to be improved for further detailed study, we interpreted that the experiment was helpful for understanding the fundamental physics.

Table 3: Supply/Exhaust/External Temperature, and Heat loss

No	Number of IJV terminal	Supply Temperature [°C]	Exhaust Temperature [°C]	External Temperature [°C]	Heat Load [W]	Heat loss [W]	Heat loss ratio [%]
1	2	4.61	16.08	9.56	993	38	4
2	2	6.70	16.32	10.59	997	34	3
3	2	8.67	15.60	9.42	1001	135	13
4	2	10.83	16.31	11.81	995	81	8
5	1	4.61	14.43	6.78	991	173	17
6	1	6.58	15.21	9.18	979	116	12
7	1	8.45	15.13	7.93	1005	170	17
8	1	10.77	15.67	9.66	990	177	18

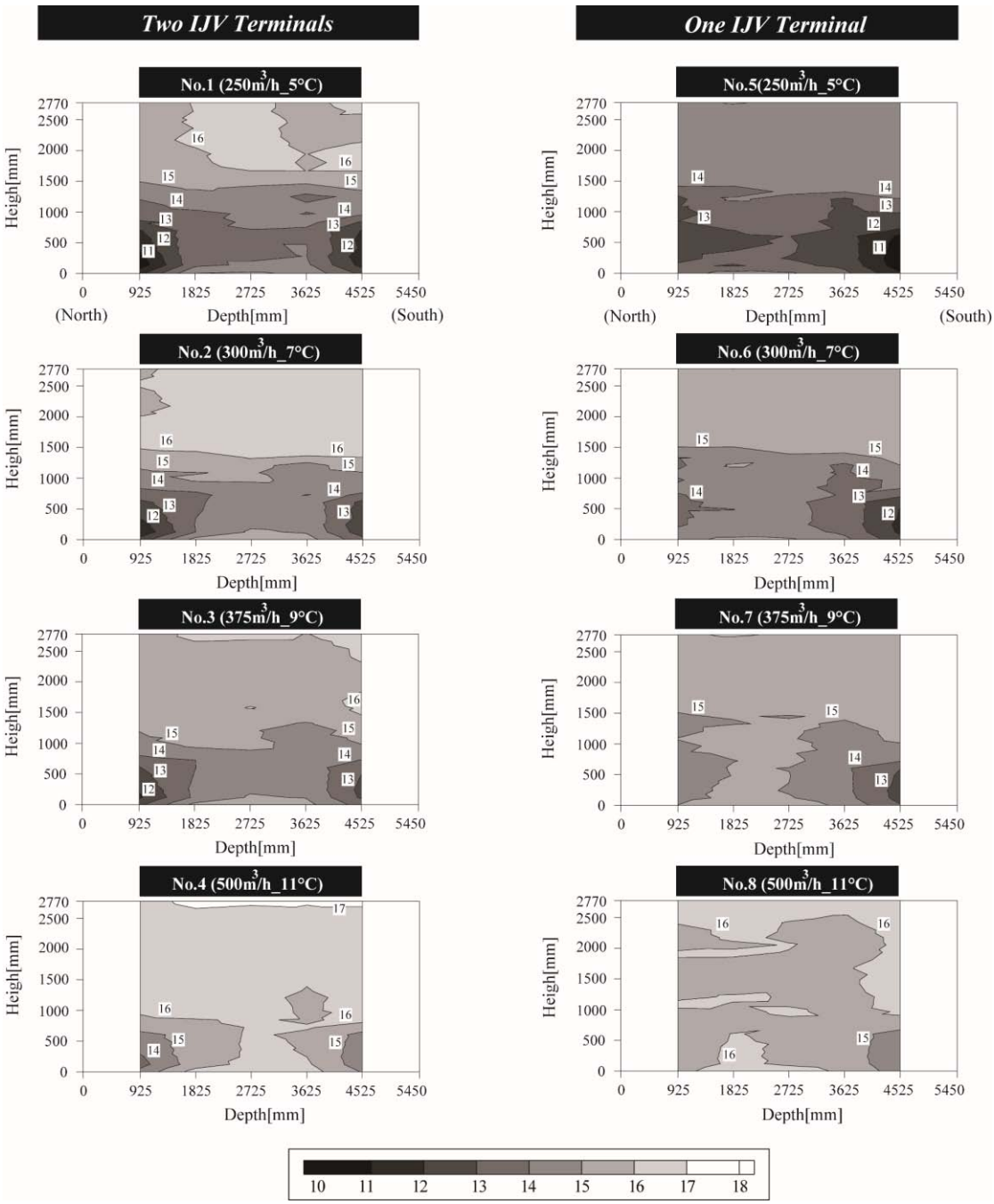

Figure 3: Temperature Contour

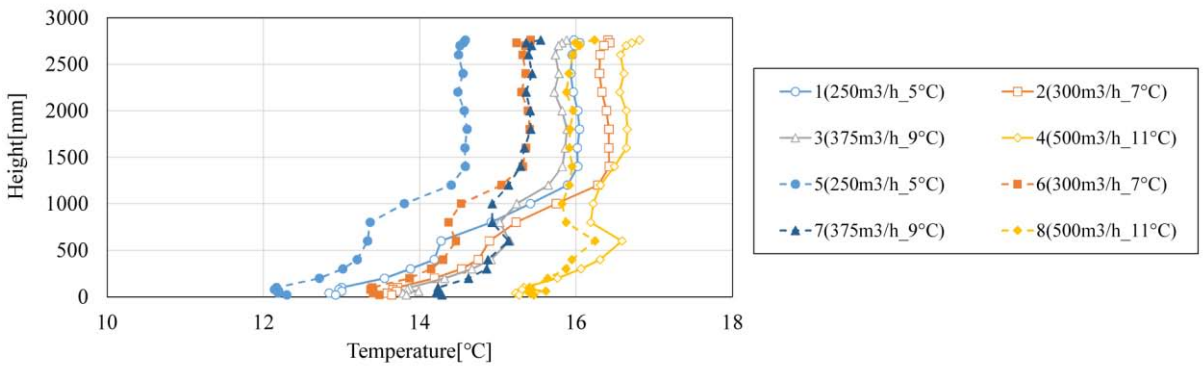

Figure 4: Vertical distribution of horizontal-averaged room Temperature

2.4.2 Normalized CO_2 concentration distribution

The normalized CO_2 concentration contours on the north-south central cross-section and vertical distribution of horizontal-averaged room normalized CO_2 concentration are shown in Figure 5 and 6, respectively. For normalization, CO_2 concentration at each measurement points were subtracted by that of supply air, and divided by the concentration difference between exhaust and supply air. As shown in Figure 5, CO_2 concentration generally stratified vertically. As the supply air flow rate decreases, the CO_2 concentration stratification inside the room got more clear. In addition, it was found that the stratification of CO_2 concentration is clearer than that of temperature because CO_2 works like passive contaminant.

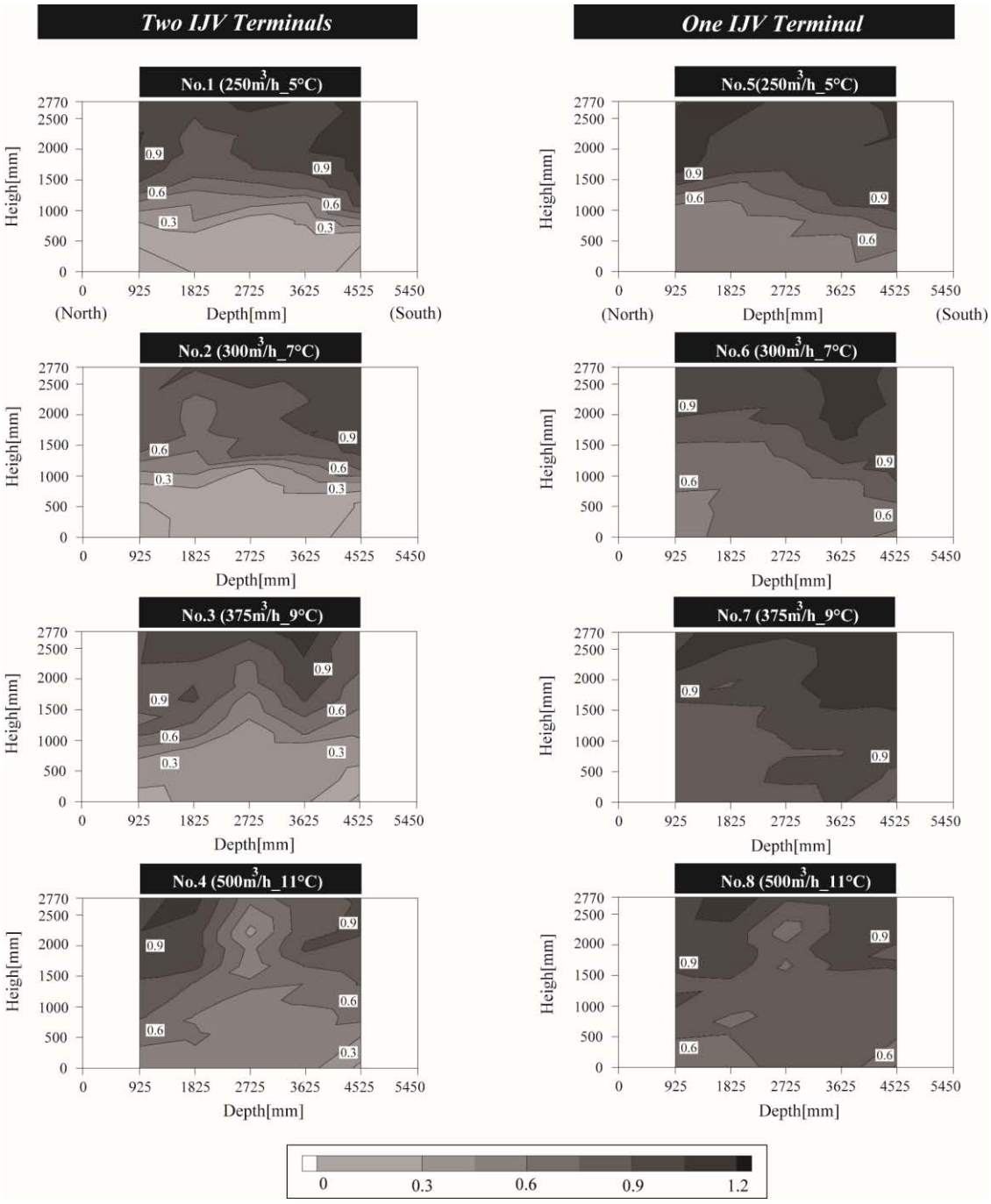

Figure 5: Normalized CO_2 concentration Contour

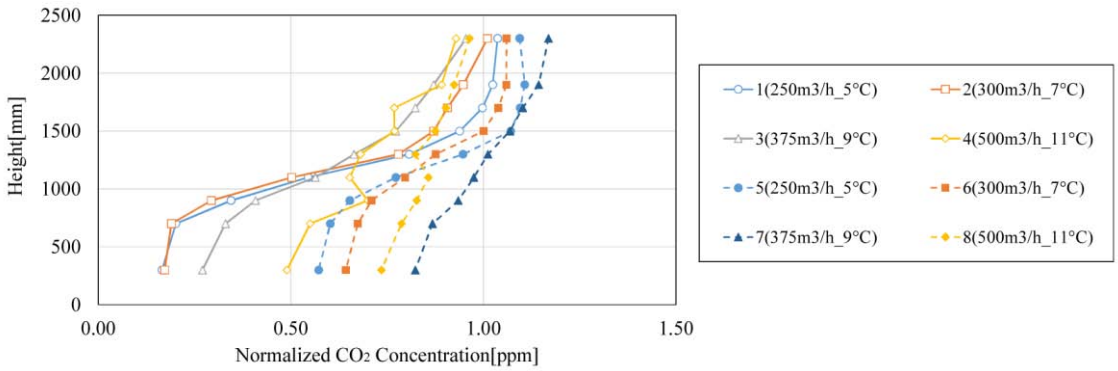

Figure 6: Vertical distribution of horizontal-averaged room Normalized CO_2 concentration

2.5 Archimedes number

It is considered that the ratio of buoyancy and supply airflow momentum has more or less influence on the formation of thermal stratification. Thus, the "Inlet Archimedes number" around the IJV supply terminal was defined in this paper:

$$A_{r(in)} = \frac{g\beta(T_\ell - T_s)D}{U^2} \tag{1}$$

where T_ℓ [°C] is the average temperature in the lower part of the chamber (20 to 100 mm above the floor), T_s [°C] is supply air temperature, T_e [°C] is exhaust air temperature, D [m] (=0.15) is the diameter of the terminal, g [m/s^2] (=9.81) is acceleration of gravity, U [m/s] is supply air velocity, and β [1/K] is volume expansion coefficient. The variables and Archimedes numbers are shown in Table 4, and the correlation between Archimedes number and dimensionless temperature difference is shown in Figure 6. The dimensionless temperature difference was defined as:

$$\Delta T^* = \frac{T_e - T_\ell}{T_e - T_s} \tag{2}$$

where, ΔT^* is a measure of temperature distribution, i.e. ΔT^* approaches to 1 when the temperature stratification was formed, and ΔT^* approaches to 0 when the temperature distribution was uniform. In Figure 6, it is shown that ΔT^* approaches to the constant value which depends on the chamber insulation and the outside temperature of the chamber, as $A_{r(in)}$ increases, thus it was confirmed that $A_{r(in)}$ has correlation with ΔT^*. Therefore, air temperature distribution varies by changing the number of supply inlet and supply air condition, even if the heat load is the same.

Table 4: Value of variable and Archimedes number

No	U[m/s]	T_e[°C]	T_s[°C]	T_ℓ[°C]	β[1/K]	Ar×10^{-3}[-]	Δ T*[-]
1	1.96	16.08	4.61	12.95	0.00360	11.43	0.27
2	2.36	16.32	6.70	13.66	0.00357	6.59	0.28
3	2.95	15.60	8.67	13.86	0.00355	3.12	0.25
4	3.93	16.31	10.83	15.31	0.00352	1.50	0.18
5	3.93	14.43	4.61	12.20	0.00360	2.60	0.23
6	4.72	15.21	6.58	13.41	0.00357	1.62	0.21
7	5.89	15.13	8.45	14.24	0.00355	0.87	0.13
8	7.86	15.65	10.77	15.46	0.00352	0.39	0.04

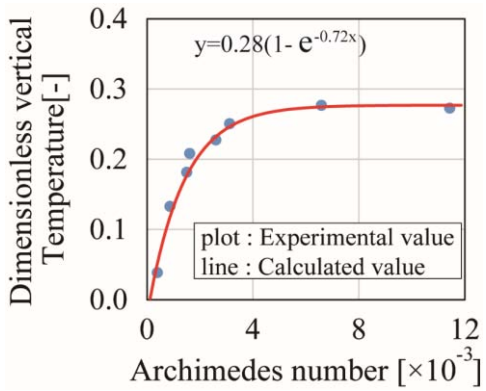

Figure 7: Correlation between Inlet Archimedes number and dimensionless vertical temperature difference

3 ACCURACY VERIFICATION OF CFD ANALYSIS

3.1 Computational domain

It seems beneficial to use CFD because it facilitates the parametric study regarding several important parameters. As the preliminary step, the accuracy of CFD analysis needs to be verified by comparing the results with experiment. The computational domain was assumed to be indoor space of the chamber in the previous chapter, and a full-scale model was constructed as shown in Figure 7.

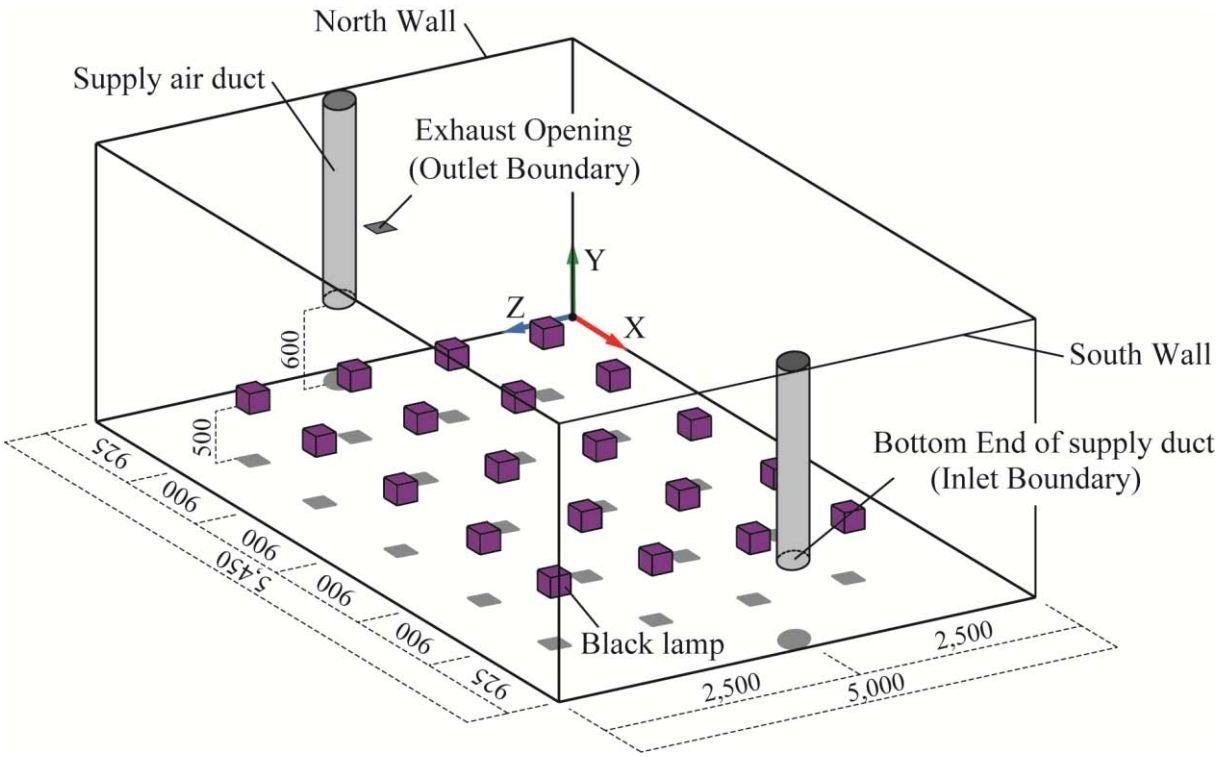

Figure 8: Computational domain

The analysis was conducted under the experimental condition 1 in Table 3. The distributed indoor heat loads were 1,000 W in total, and two IJV terminals were placed at the center of walls, one at the north wall and the other at the south wall. The inlet boundary was set at the bottom end of the supply duct (600 mm above the floor) with the supply air flow rate of 250 m^3/h, which corresponds to 1.96m/s of the inlet velocity, and the supply air temperature was set at 4.61 °C. The analysis was conducted in a non-isothermal condition, and the buoyancy was expressed by Boussinesq approximation. The heat load was simulating by considering spatial energy source term (=50,000[W/m^2]). The thickness, heat conductivity and external temperature were given as the thermal boundary condition at the wall and ceiling. Since the floor was located on the ground, the boundary condition was set as insulation. The radiation was also solved based on surface to surface radiative heat transfer model, and the analysis was steady state. Total number of cells was 3,250,474. Three types of turbulence model, which were SST k-ω, Standard k-ε and RNG k-ε, were compared. The summary of the CFD calculation setting is summarized in Table 5.

3.2 Examination of turbulence model dependency

The temperature profiles along five vertical lines in north-south central line (z=2,500[mm]), which correspond to the poles in the experiment, obtained from different turbulence models were compared with experimental result in Figure 8. As shown in Figure 8, analysis results agreed relatively well with experimental result at the upper part of the room, while there were large errors at the lower part. It may be due to the adiabatic boundary condition at the floor. Since the supply air temperature is very low in the experiment, the heat came into the room through the floor when the supply air was impinging on the floor. However, the boundary condition of the floor was set as adiabatic, thus the analysis results underestimated the heat transmission through the floor, which resulted in difference in the lower part. Regarding the turbulence model, the standard deviation of the temperature difference between experimental and analysis was the smallest in the case of SST k-ω model. It was shown that the boundary condition at the floor needs to be reconsidered for improving the accuracy of CFD.

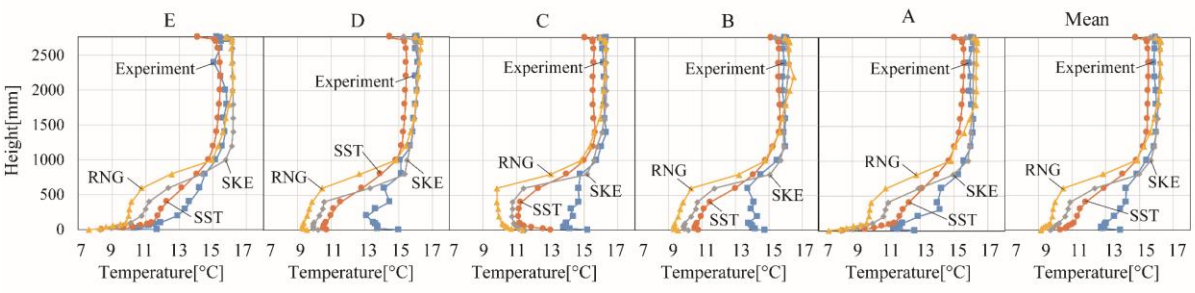

	Turbulence model	Standard Deviation
No1	SST k-ω(SST)	1.688
No2	Standard k-ε(SKE)	2.047
No3	RNG k-ε(RNG)	2.556

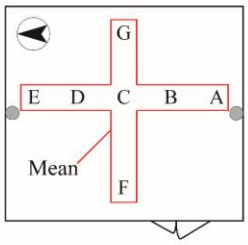

Figure 9: Experimental values and calculated values with different turbulence model and standard deviation

Table 5: Summary of the CFD Calculation Setting

Studied Case			No.1	No.2	No.3
CFD code			Ansys Fluent 19.2		
Turbulence Model			SST k-ω	Standard k-ε	RNG k-ε
Radiation Model			Surface-to-Surface Model		
Algorithm			SIMPLE		
Discretization scheme for Advection Term			QUICK	Second order upwind	QUICK
Boundary Condition	Inlet		Velocity Magnitude U=1.96[m/s]		
			Turbulent Intensity I=10[%]		
			Turbulent Length Scale L=10.5[mm]		
			Temperature T=4.61[°C]		
	Outlet		Velocity Magnitude U=-6.94[m/s]		
	Walls	Velocity	Linear-Logarithmic Blending Law	Standard Wall Function	
		Floor	Adiabatic Boundary (0[W/m^2])		
		Other walls	External Temperature		
Cell Zone Condition	Black Lamp		Energy source 50,000[W/m^3]		
Total Number of cells			3,250,474		

4 CONCLUSIONS

In order to understand the environment formed by IJV system in a room with uniformly distributed heat generation load, both the experiment and CFD analysis were conducted. The supply air conditions were changed as a parameter in this paper. The findings obtained in this paper are summarized follows:

- In the experiments, under the condition of small supply air flow rate, indoor air temperature distribution was vertically stratified, while under the condition of large supply air flow rate, indoor air temperature distributed uniformly.
- The distribution of CO_2 concentration stratified clearer than that of temperature.
- Air temperature distribution varies by changing the number of supply inlet and supply air condition, even if the heat generation load is the same.
- In CFD analysis, results agreed relatively well with experimental result at the upper part of the room, while there were large errors at the lower part. This may be due to the adiabatic boundary condition at floor. Consequently, it seems necessary to change the boundary conditions considering heat loss to improve the accuracy.

5 REFERENCES

[1] T.Karimipanaha, H.B.Awbi (2002) Theoretical and experimental investigation of impinging jet ventilation and comparison with wall displacement ventilation. Building and Environment, Vol.37, pp.1329‑1342.

[2] Tomohoro KOBAYASHI, Kazuki SUGITA, Noriko UMEMIYA (2016) A Study on Semi-Displacement Ventilation using Impinging Jet Flow. Journal of Environmental Engineering (Transactions of AIJ), Vol.81, No.730, pp.1117‑1125. (In Japanese)

[3] Atsushi TOMITA (2014) Fundamental Study onTemperature and Airflow Distribution in Semi-Displacement Ventilation using Radial Wall Jet, Part 3. Proceedings of Annual Meeting of SHASE Kinki Chapter, pp.413‑416. (In Japanese)

Analysis of convective heat transfer coefficient correlations for ventilative cooling based on reduced-scale measurements

Katarina Kosutova[1], Christina Vanderwel[2], Twan van Hooff[*1,3], Bert Blocken[1,3], Jan Hensen[1]

1 Eindhoven University of Technology
PO Box 513
5600 MB, Eindhoven, the Netherlands

2 University of Southampton
Bldg 13, Highfield Campus
SO16 7DY, Southampton, United Kingdom

3 KU Leuven
Kasteelpark Arenberg 40, bus 2447
3001 Leuven, Belgium
**Corresponding author: twan.vanhooff@kuleuven.be*

ABSTRACT

Ventilative cooling can be used as a passive cooling measure to reduce the cooling energy demand of buildings. It can be used during the day, directly removing excessive heat gains, or during the night (i.e. night flush), in which cold outdoor air flows through the building and cools down the indoor air volume and subsequently the thermal mass of the building. Night flushing reduces the indoor air temperatures at the beginning of the next day and the cooling demand over the day. To assess the impact of ventilative cooling on the temperatures in a building and the resulting cooling energy demand, building energy simulations (BES) can be performed. An important parameter to set in BES is the convective heat transfer coefficient (CHTC) (or CHTC correlation) for the interior surfaces to calculate convective heat transfer from these surfaces to the indoor environment and vice versa. The majority of the available CHTC correlations for internal surfaces in BES are based on natural convection, with a temperature difference as the driving force for convection. However, in case of night flush the airflow rates through the building can be quite large and mixed convection can occur due to the possible presence of relatively high indoor air velocities. A solution to this problem could be the use of convective heat transfer correlations for forced convection, or correlations for external surfaces subjected to the atmospheric boundary layer (ABL) wind flow, which generally calculate the convective heat transfer based on a reference wind speed at a certain location.
This paper presents reduced-scale experiments (ABL wind tunnel measurements) of velocities, turbulence levels, air temperatures, surface temperatures and convective heat fluxes in a generic cubical cross-ventilated enclosure. One of the walls of the enclosure is heated and has a higher temperature than the ambient air, resulting in convective heat exchange between this surface and the air inside the enclosure. The experimental results are used to calculate the values of CHTC for this mixed convection case, in which the contribution of forced convection dominates, as indicated by the calculated Richardson number. The measurement results are subsequently compared with both CHTC correlations for natural and forced convection. The results indicate that the average CHTC values from the experiments generally show a fair to good agreement with the values obtained using CHTC correlations for forced convection, while the agreement with the CHTC values from the CHTC correlations based on natural convection is, as expected, much worse (72-91% difference). This finding is in line with earlier publications in which the use of CHTC correlations for ventilative cooling assessment in BES is discussed. A proper definition of the CHTC correlations for ventilative cooling applications is required to correctly estimate the reduction in cooling energy demand and is part of a larger ongoing research effort.

KEYWORDS

Convective heat transfer coefficients, mixed convection, wind tunnel experiments, ventilative cooling

1 INTRODUCTION

An energy-efficient method to reduce the cooling demand in buildings is the use of ventilative cooling (e.g. Carrilho da Graça et al. 2002, Geros et al. 2005, Wu et al. 2006, Artmann et al. 2007, Santamouris et al. 2010). Ventilative cooling refers to the use of natural ventilation through openable elements in the building envelope to remove excessive heat from a building, and can be used either during the day (directly removing excessive heat gains) or during the night time (night flushing) when outdoor air with a lower temperature than the indoor air flows through the building and cools down the indoor air volume and subsequently the thermal mass of the building. An analysis of the effect of this passive measure with respect to the reduction of cooling energy demand can be made using building energy simulations (BES). The BES results depend heavily on the input provided by the user; more realistic, detailed and high quality input will increase the reliability and quality of the BES results. One of the input parameters that can influence the results of the simulations conducted is the convective heat transfer coefficient (CHTC) for the interior surfaces (e.g. Goethals et al. 2011, Leenknegt et al. 2013). Normally, CHTC correlations are used to predict convective heat transfer between these interior surfaces and the air in a room, but often these correlations are based on natural convection; i.e. the driving force is a temperature difference. However, in ventilative cooling applications relatively high indoor velocities due to higher volume flow rates through the building can be present, implying that the CHTC correlations based on natural convection as commonly used are not, or less, suitable and one must resort to CHTC correlations for forced or mixed convection. The disadvantage of the CHTC correlations for forced convection is that only one CHTC value is obtained for an entire wall/floor/ceiling. In addition, depending on the conditions either natural or mixed convection can be present, both of which would require other CHTC correlations.

This paper presents the results of an experimental study on convective heat transfer in a cross-ventilated generic building model. The experiments included measurements of velocities, turbulence levels, air temperatures, surface temperatures and heat fluxes and were conducted in the open-circuit wind tunnel at the University of Southampton. The objective is to generate an experimental data set which can be used for CFD model validation. The validated CFD model can subsequently be used to assess CHTC distributions in ventilative cooling cases in more detail. In addition, the experimental data can be used to analyze the suitability of interior CHTC correlations as commonly used in BES. Section 2 presents the experimental setup as used in the wind tunnel. Section 3 contains the results of the experimental campaign and a comparison between the experimentally obtained values of CHTC and the values based on existing CHTC correlations. Sections 4 and 5 present the discussion and conclusions of this paper.

2 EXPERIMENTAL SETUP

The reduced-scale experiments were performed in the open-circuit wind tunnel at the University of Southampton (UK), which has dimensions 0.9 × 0.6 × 4.5 m^3 (W × H × L). A neutral atmospheric boundary layer (ABL) was created using 427 mm high spires in combination with three different types of roughness elements (32, 16 and 7 mm high), and a carpet (see Taddei et al. 2016). The resulting mean streamwise velocity profile matched the logarithmic equation:

$$U = \frac{u^*_{ABL}}{\kappa} \cdot ln \frac{y}{y_0} \tag{1}$$

with κ the von Karman constant (0.42), u^*_{ABL} (= 0.195 m/s) the ABL friction velocity and y_0 (= 0.0024 m) the aerodynamics roughness length. The reference velocity (U_{ref}) was equal to 1.9 m/s at building height H (= 0.15 m). The streamwise turbulence intensity I_u at the location of the building was about 10%. The air temperature of the approach-flow during the measurements was 25.5 °C (= T_{ref}). The building Reynolds number, defined as $Re = U_{ref}H/\nu$, with $\nu = 1.56 \times 10^{-5}$ m²/s the kinematic viscosity of air at an air temperature of 25.5°C, was equal to 19,000. Finally, the experiments reported were carried out for one wind direction (perpendicular to the facade with the openings).

The model of the generic building (scale 1:50) used in the experiments was a single-zone cubic building ($0.15 \times 0.15 \times 0.15$ m^3, Fig. 1a,b), with one opening in both the windward and leeward facade and a heated wall (left hand side when looking in streamwise direction; Fig. 1c). The model was made of polymethyl methacrylate (PMMA) sheets (0.01 m thick) and the window openings are 0.04×0.035 m^2 ($W_O \times H_O$), resulting in a facade porosity of about 6%. The wall opposite to the heated wall was equipped with a 0.75 mm thick clear polypropylene sheet to allow thermal camera measurements of the heated wall. A detailed schematic of the heated wall (brass plate) including materials and thicknesses for all layers is shown in Figure 1d. The Richardson number ($Ri = Gr/Re^2$) in these experiments was around 0.03, indicating that forced convection is dominant over natural convection.

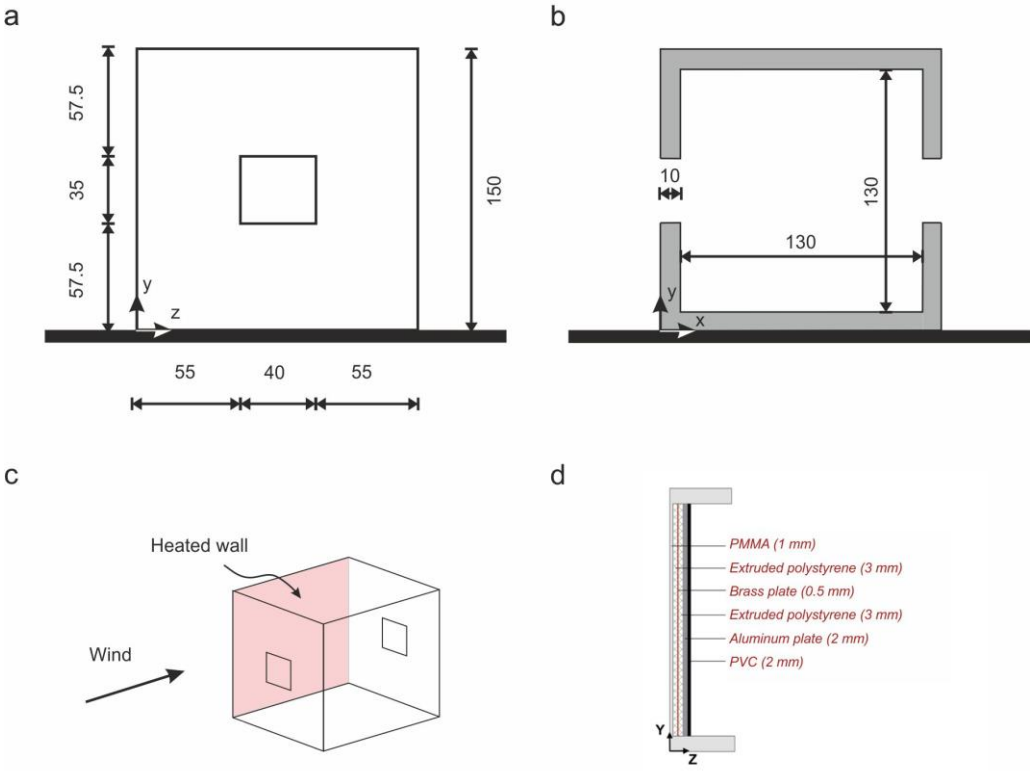

Figure 1: Geometry of the building model used in the wind-tunnel experiments (6% facade porosity). (a) Facade with window opening. (b) Vertical cross section along flow direction. All dimensions are in mm. (c) Isometric view of the building model indicating the position of the heated wall. (d) Vertical cross section of the heated wall with wall composition.

Velocities in the vertical centerplane (parallel to flow direction) were measured using a 2D particle image velocimetry (PIV) system. Two double pulse 200-15 PIV Nd:YAG lasers were used to create a laser sheet. The flow is seeded using a solution of demineralized water and glycol, and a fog machine. A charged coupled device camera (CCD) was used to capture images, and was located normal to the laser sheet. A set of 500 uncorrelated images was taken

at a rate of 0.7 Hz, resulting in a total measuring time of 12 minutes. The PIV results were processed using 50% overlap and an interrogation window size of 32 × 32 pixels. The uncertainty of the measurement results is around 1-5.5%.

Measurements of surface temperatures at the heated wall were taken using a mid-range infrared camera (FLIR SC7000). NTC U-type sensors with a diameter of 2.4 mm and precision of 0.05 °C were used to measure the indoor air temperatures at 27 locations (9 along each of the three horizontal lines) (Fig. 2a). The air temperatures were measured for 120 s to obtain stationary results. Six gSKIN-Xp 26 9C heat flux sensors (greenTeg) with a size of 10 × 10 mm^2 measured the surface heat fluxes on the heated wall (see Fig. 2b) (precision of ± 3%). The measured heat fluxes are time-averaged over a period of 120 s to obtain stationary values.

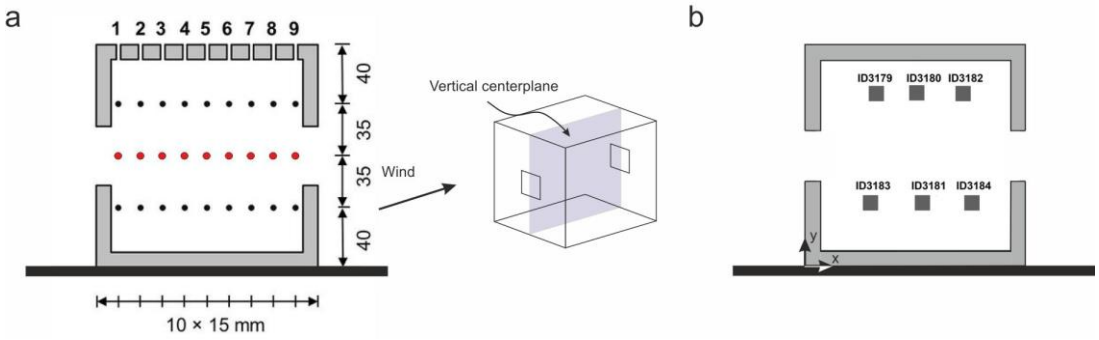

Figure 2: (a) Positions for indoor air temperature measurements in the vertical centerplane (z/H = 0.5). Only the results at mid height (red dots) are included in this paper for the sake of brevity. The probes for the air temperature measurements were inserted through closable openings in the ceiling of the building. All dimensions are in mm. (b) Positions of heat flux sensors at interior surface of heated wall.

3 RESULTS

Figure 3 provides the dimensionless time-averaged streamwise velocity (U/U_{ref}) along three vertical lines (x/H = 0.3, x/H = 0.5, x/H = 0.7) in the vertical centerplane (z/H = 0.5). A clear incoming jet is visible, with velocities higher than U/U_{ref} = 0.6 in the center of the jet (around y/H = 0.4; Fig. 3a). The jet is directed downwards and the maximum velocity decreases in downstream direction (U/U_{ref} < 0.4 at x/H = 0.7; Fig. 3c).

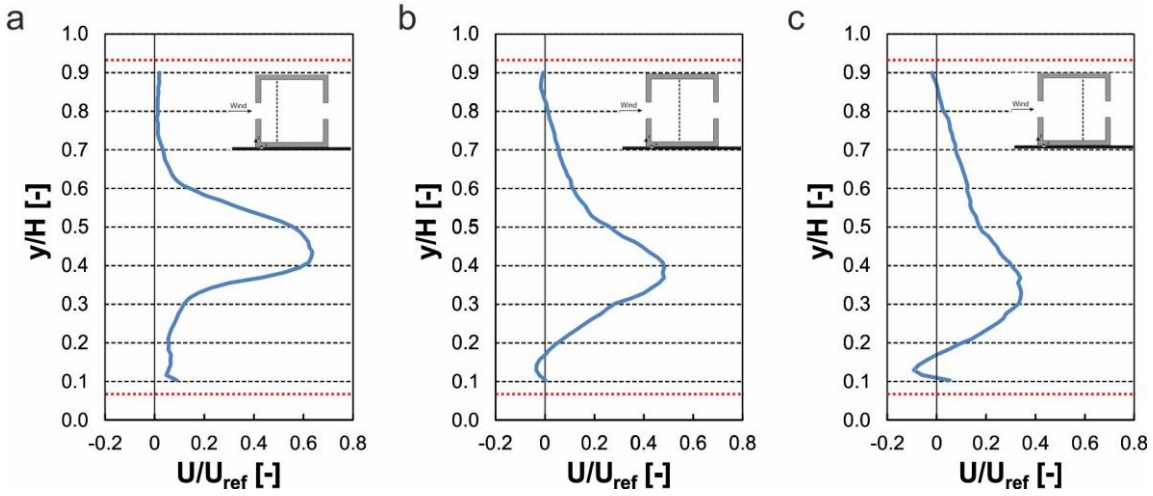

Figure 3: Dimensionless time-averaged vertical profiles of streamwise velocity component, U/U_{ref}, along three lines in the vertical centerplane (z/H = 0.5): (a) x/H = 0.3, (b) x/H = 0.5, (c) x/H = 0.7. H = 0.15 m, U_{ref} =1.9 m/s. The red dotted lines indicate the location of the floor and ceiling.

Figure 4 shows the measured dimensionless time-averaged air temperatures ($(T-T_{ref})/T_{ref}$) along a horizontal line in the vertical centerplane (y/H = 0.5, z/H = 0.5). Air temperatures are generally lowest behind the window opening, i.e. at x/H = 0.2 until x/H = 0.4, where the incoming jet provides cool air to the enclosure. Higher air temperatures are present further downstream (x/H > 0.5); the downward direction of the jet mainly provides cool air in the lower part of the enclosure (y/H < 0.5) from this point onwards (not shown here for the sake of brevity).

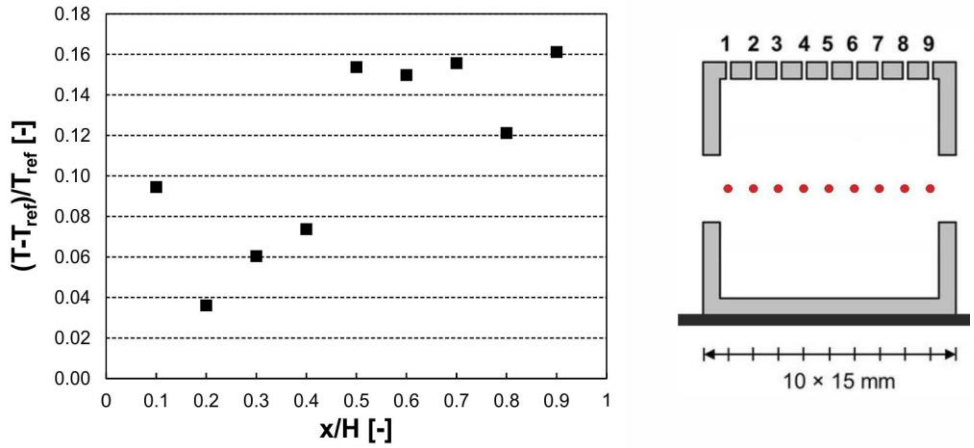

Figure 4: Time-averaged air temperatures ($(T-T_{ref})/T_{ref}$), measured along the horizontal line at mid height of the enclosure (y/H = 0.5) in the vertical centerplane (z/H = 0.5), T_{ref} = 25.5°C. The locations are indicated on the right-hand side with red dots.

Figure 5 presents the measured heat fluxes at the six locations on the heated wall. The highest heat fluxes (500 W/m^2 < Q < 570 W/m^2) are measured at the three locations in the lower part of the enclosure, i.e. by sensor ID3181, ID3183, ID3184. These higher values can be explained by the particular flow pattern, as described above, with the downward directed jet from the windward window opening. The maximum difference between two locations (ID 3179 vs. ID3184) is 46%.

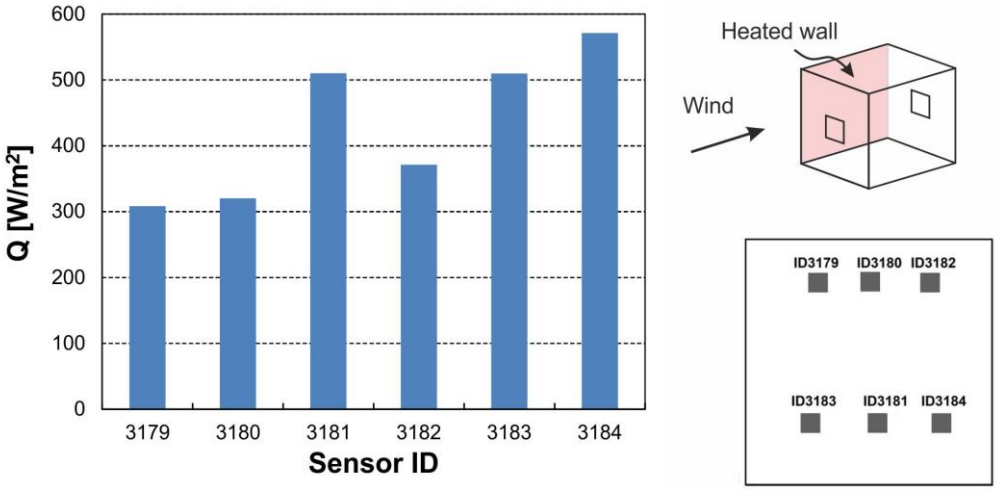

Figure 5: Measured surface heat flux (W/m^2) at the six different locations at the interior surface of the heated wall. The locations are indicated on the right-hand side.

Figure 6 presents a comparison of the CHTC values obtained from the experiments presented in this paper with CHTC values based on some of the available CHTC correlations for BES

(Table 1). The CHTC correlation for vertical surfaces which is provided by TRNSYS (Klein et al. 2010) is defined based on the temperature difference between the surface and the surrounding air, while the correlation from Khalifa (1989) uses the average room temperature in their experiments as reference temperature to calculate CHTC. Spitler et al. (1991) performed experiments to develop a CHTC correlation for situations with large volume flow rates, i.e. forced convection, as present in ventilative cooling cases. Their correlations use the velocity of the supply jet to determine CHTC and is thus not location dependent. Finally, Loveday and Taki (1996) developed a CHTC correlation for the outdoor surfaces of facades of a building based on full-scale experiments. Their correlation based on the combined measurement data for both the windward and leeward facade (see Table 1) is used in the current comparison with the data from the wind tunnel experiments described above.

Table 1: Convective heat transfer coefficient (h_c) correlations.

Source	**Correlation***	**Remarks**	**Type#**
TRNSYS (Klein et al. 2010)	$h_c = 1.5\left(T_s - T_{air}\right)^{0.25}$	Temperature of surrounding air	N
Khalifa (1989)	$h_c = 1.98\left\|\Delta T\right\|^{0.32}$	Average room temperature	N
Spitler et al. (1991)	$h_c = 1.6 + 92.7\left(\frac{\dot{m}U_0}{\rho g V_{room}}\right)^{0.5}$	Side wall inlet. High flow rates. J is outside limits (> 0.011)	F
Loveday and Taki (1996)	$h_c = 16.21 V_{loc}^{\ 0.452}$	Average for windward and leeward facade	F

*T_s and T_{air} the surface and air temperature, respectively, $\dot{m}$ the mass flow rate, U_0 the supply velocity, ρ the density, g the gravitational acceleration constant, V_{room} the volume of the enclosure, V_{loc} the local velocity. #: N and F indicate whether correlation is developed for natural or forced convection, respectively.

Figure 6 indicates the mismatch in CHTC values when one would employ the correlations based on natural convection (i.e. temperature differences) for interior CHTC in a ventilative cooling case. The underprediction of CHTC, with 72-91%, will lead to an erroneous prediction of heat transfer at the surfaces and thus an unreliable prediction of the effect of ventilative cooling on the overall building energy demand and/or thermal comfort. The CHTC obtained with the correlations by Spitler et al. (1991) (28.8 W/m^{2}K) is about 15% higher than the average CHTC from the six measurements (25.1 W/m^{2}K). However, the differences between the CHTC obtained from this correlation and the experimentally obtained local values can be as high as 62% (i.e. for ID3179). Note that the value of J in the correlation by Spitler et al. (1991), which is equal to the term in brackets in Table 1, is higher than the limits mentioned in their paper (J > 0.011), however, the correlation is included for the sake of comparison. The correlation by Loveday and Taki (1996), which is developed for exterior building surfaces, provides CHTC values close to the lowest values obtained from the measurements, i.e. around 17 W/m^{2}K. However, the difference in CHTC at locations with high measured values of CHTC is large as well for this correlation, up to 48% for ID3184, while the average difference is about 31%. Note that a disadvantage of the correlations by Spitler et al. (1991) and Loveday and Taki (1996) is that it is based on the supply or local velocities and thus results in one value for all locations on a particular surface. In addition, it is not always clear at which location to select the value of the velocity as input for the correlation.

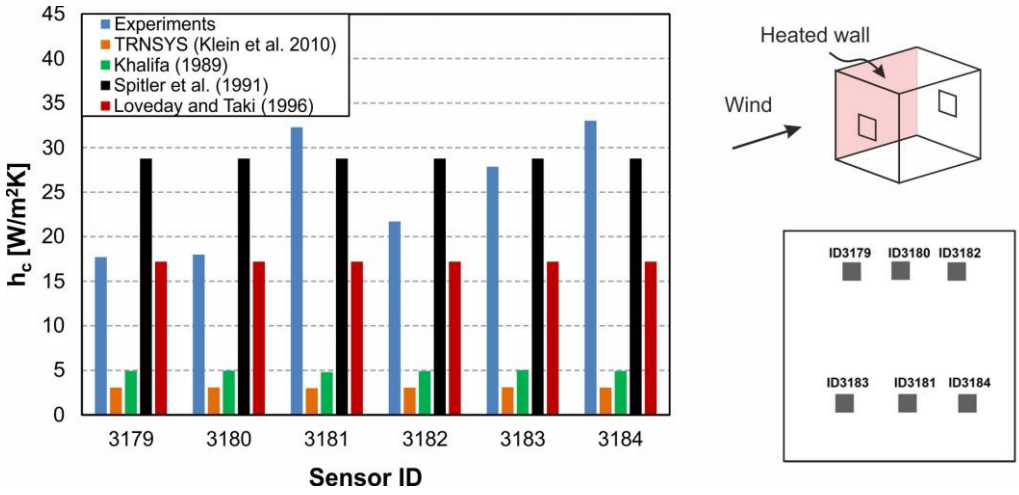

Figure 6: Convective heat transfer coefficients h_c (W/m^2K) based on experiments and convective heat transfer correlations at the six positions at the interior surface of the heated wall. Note that the experiments were conducted in a reduced-scale model, while the CHTC correlations were developed for real-scale cases.

4 DISCUSSION AND FUTURE WORK

The main goal of the research presented in this paper is the collection of data for detailed validation studies of non-isothermal CFD simulations of cross-ventilation. In addition, the aim is to analyze the flow and heat transfer in the enclosure and to provide a comparison with existing CHTC correlations from literature. This research is part of a larger research effort on the modeling and optimization of ventilative cooling. Future work will include CFD simulations that will be validated using the experimental data presented in this paper. Subsequently, the CFD simulations can be used to provide detailed data on CHTC distributions in buildings subjected to ventilative cooling, with the aim to develop more accurate CHTC correlations for these cases. Eventually, the new correlations could be used later in BES models to assess their influence on the calculated cooling demand and thermal comfort.

The CHTC values from the experiments indicated the large spatial differences that can occur, even in a very simple geometry subjected to cross-ventilation. Note that the experiments were conducted in a reduced-scale model, while the CHTC correlations were developed for real-scale cases. Irrespective of this difference, most correlations for forced convection provide one single value for an entire wall, floor or ceiling and the information provided is thus limited. In addition, temperature differences are often neglected. On the other hand, although the correlations for natural convection take into account temperatures and can predict local values of CHTC, their results do show large differences with the measured values and thus appear to be not suitable in case of ventilative cooling.

5 CONCLUSIONS

This paper presented results of an experimental campaign in the wind tunnel of the University of Southampton. The experiments were conducted for a cross-ventilated generic enclosure with a heated wall, and included measurements of velocities, turbulence levels, air temperatures, surface temperatures and heat fluxes. From these experiments the CHTC values on the heated wall were calculated and these values were subsequently compared with existing CHTC correlations from literature. The results indicated a clear influence of the indoor airflow pattern on air and surface temperatures, and heat fluxes. For example, the six measured heat fluxes on the heated wall differ up to 46%. The CHTC correlations based on temperature differences strongly underpredict the CHTC on the heated wall. The CHTC calculated using the correlation

by Spitler et al. (1991) for enclosures with high volume flow rates shows a good agreement with the averaged values obtained from the experiments (15% difference), although local differences can still be as high as 62%. The correlation by Loveday and Taki (1996) provides a good agreement for locations with low values of CHTC, however, large difference (up to 48%) are present for other locations. On average, the difference with the correlation by Loveday and Taki (1996) is 31%. One must note that the experiments were conducted in a reduced-scale model, while the CHTC correlations were developed for real-scale cases; this difference in scale can contribute to the observed discrepancies.

6 ACKNOWLEDGEMENTS

Twan van Hooff is currently a postdoctoral fellow of the Research Foundation – Flanders (FWO) and acknowledges its financial support (project FWO 12R9718N). Moreover, the authors are thankful to Geert-Jan Maas and Jan Diepens (Laboratory of the Unit Building Physics and Services, Eindhoven University of Technology) for their help in the construction and development of the experimental building model and to Neil Gillam from the University of Southampton for his help and support during the wind-tunnel experiments.

7 REFERENCES

Artmann, N. Manz H., Heiselberg, P., 2007. Climatic potential for passive cooling of buildings by night-time ventilation in Europe. *Applied Energy* 84, no. 2, 187–201.

Carrilho da Graça, G., Chen, Q., Glicksman, L., Norford, L., 2002. Simulation of wind-driven ventilative cooling systems for an apartment building in Beijing and Shanghai. *Energy and Buildings* 34, no. 1, 1–11.

Geros, V., Santamouris, M., Karatasou, S., Tsangrassoulis, A., Papanikolaou, N., 2005. On the cooling potential of night ventilation techniques in the urban environment. *Energy and Buildings* 37, no. 3, 243–257.

Goethals, K. Breesch, H., Janssens, A., 2011. Sensitivity analysis of predicted night cooling performance to internal convective heat transfer modelling. *Energy and Buildings* 43, no. 9, 2429–2441.

Khalifa, A.J.N., 1989. *Heat transfer processes in buildings*. PhD Thesis, University of Wales, College of Cardiff.

Klein, S.A., et al., 2010. *TRNSYS 17: Volume 4, Mathematical Reference*.

Leenknegt, S. Wagemakers, R., Bosschaerts, W., Saelens, D., 2013. Numerical study of convection during night cooling and the implications for convection modeling in Building Energy Simulation models. *Energy and Buildings* 64, 41–52.

Loveday, D.L., Taki, A.H., 1996. Convective heat transfer coefficients at a plane surface on a full-scale building façade. *International Journal of Heat and Mass Transfer* 39, 1729-1742.

Santamouris, M., Sfakianaki, A., Pavlou, K., 2010. On the efficiency of night ventilation techniques applied to residential buildings. *Energy and Buildings* 42, no. 8, 1309–1313.

Spitler, J., Pedersen, C., Fisher, D., 1991. Interior convective heat transfer in buildings with large ventilative flow rates. *ASHRAE Transactions* 97(1), 505-515.

Taddei, S., Manes, C., Ganapathisubramani, B., 2016. Characterisation of drag and wake properties of canopy patches immersed in turbulent boundary layers. *Journal of Fluid Mechanics* 798, 27–49.

Wu, L.X., Zhao, J.-N., Wang, Z.-J., 2006. Night ventilation and active cooling coupled operation for large supermarkets in cold climates. *Energy and Buildings* 38, no. 12, 1409–1416.

Overheating reduction in a house with balanced ventilation and postcooling

Bart Cremers

Zehnder Group Zwolle
Lingenstraat 2
8028 PM Zwolle, The Netherlands
bart.cremers@zehndergroup.com

ABSTRACT

The outdoor climate is changing and the airtightness and insulation levels of residential buildings are improving. During the warmer season this can lead to overheating problems, especially when the house is situated in urban areas. In order to reduce overheating problems, ventilative cooling can be used to keep the indoor conditions at a comfortable level. Natural ventilation is not always a feasible solution, for the risk of burglary, and when the outdoor temperatures are not suitable for cooling the house, for instance in urban heat islands.
This document describes the monitored performance of a ventilation system in a nearly zero energy building in Modena, Italy. The house is ventilated with a balanced ventilation system in combination with a water/air heat exchanger in the supply air from the ventilation unit, hereafter named postconditioning system. The water in the exchanger comes from a heat pump, activated by a room thermostat that defines whether there is a request for cooling or heating. In summer, the system cools and dehumidifies the fresh air (postcooling) and in winter the system heats the fresh air (postheating). The resulting cooling and heating is the only conditioning means in the house, there is no other cooling or heating system installed in the house.
The monitored performance is shown with example weeks in summer, autumn and winter. In these weeks the functional modes of balanced ventilation and postconditioning are shown, together with the resulting temperatures in the relevant air streams. The modes of indoor heat recovery, indoor heat extraction and outdoor heat rejection, in combination with postcooling or postheating, can clearly be observed. The overall performance during a 7 month period is shown in a correlation graph where extract, supply and postconditioned supply temperatures are given as a function of outdoor temperature.
The postconditioning system does not only show the cooling effect in a sensible way (temperature decrease of supply air) but also in a latent way (humidity decrease of supply air). This is indicated by the monitored temperatures when the water temperature in the postconditioning system is dropping below the dew point of the fresh air in summer. The resulting condensation on the postconditioning exchanger decreases the absolute humidity of the fresh air, which adds to the comfort of the fresh air supply even further.
The ventilative cooling as a result of indoor heat extraction, outdoor heat rejection, in combination with postcooling is discussed looking at the resulting extract air temperatures (indication of indoor temperatures). It is shown how the overheating problem in this house is reduced by the mechanical ventilation system, even when summer outdoor air temperature and humidity are higher than indoors. Both the hygiene in terms of guaranteed fresh air, and the comfortable supply air temperatures, make this ventilation system a comfortable, and energy efficient solution for all seasons of the year.

KEYWORDS

Nearly zero energy house, balanced ventilation, overheating reduction, postcooling

1 INTRODUCTION

The outdoor climate is changing towards more extreme temperatures and the airtightness and insulation levels of residential buildings are improving. During the warmer season this can lead to overheating problems, especially when the house is situated in urban areas. In order to reduce overheating problems, postcooling of ventilation air can be used to keep the indoor conditions at a comfortable level. Natural ventilation is not always a feasible solution, for the risk of burglary, and when the outdoor temperatures are not suitable for cooling the house, for instance in urban heat islands.

2 MONITORING SET-UP

This document describes the monitored performance of a ventilation system in a nearly zero energy building in Formigine, near Modena, Italy (fig. 1). The house is ventilated with a balanced ventilation system (type ComfoAir Q600) equipped with enthalpy exchanger. The flow rates in the fan positions low, middle and high are set at 180, 250 and 420 m^3/h.

Figure 1: Nearly zero energy house in Modena, Italy

The balanced ventilation system is equipped with a water/air heat exchanger in the supply air of the ventilation unit, hereafter named postconditioning system. The water in the postconditioning system comes from a 4 kW heat pump, activated by a room thermostat that defines whether there is a request for cooling or heating. In summer, the system cools and dehumidifies the fresh air (postcooling) and in winter the system heats the fresh air (postheating). The resulting cooling and heating is the only conditioning means in the house, there is no other cooling or heating system installed in the house.

3 MONITORING RESULTS

The monitored performance is shown in figure 2 with example weeks in summer, autumn and winter. In these weeks the functional modes of balanced ventilation and postconditioning are shown, together with the resulting temperatures in the relevant air streams. In summer, the outdoor heat (temperatures up to 40°C) is rejected because of the cold recovery from the colder indoor air of 27°C. The ventilation air is postcooled during daytime to a supply temperature between 11°C and 20°C, when requested by the room thermostat.
In autumn the indoor temperature of 22°C is fairly constant because the indoor heat is recovered. In this example week the outdoor temperatures between 10°C and 15 °C lead to supply temperatures of the fresh air of about 20 °C.
In wintertime the outdoor temperature in the example week are between 0°C and 10°C. The indoor heat is recovered and postheated to a supply air temperature of about 25 at nighttime and up to 50°C temperature during daytime.

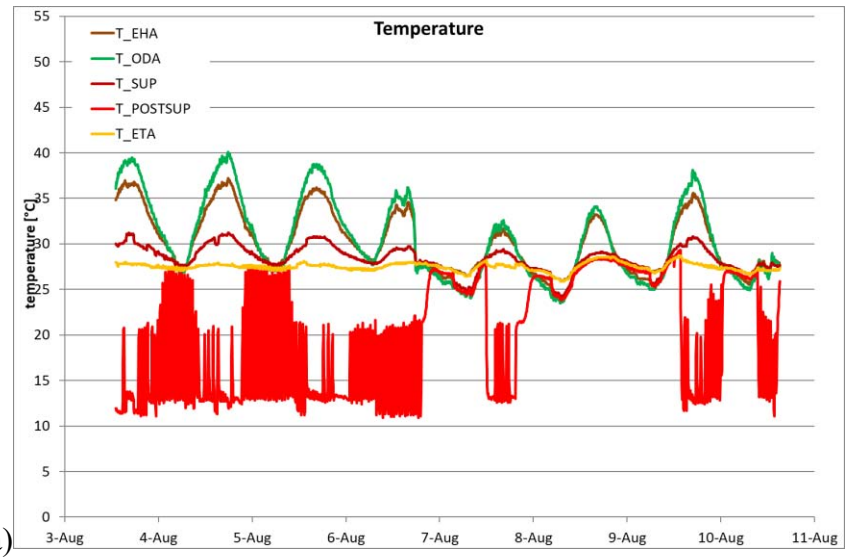

a)

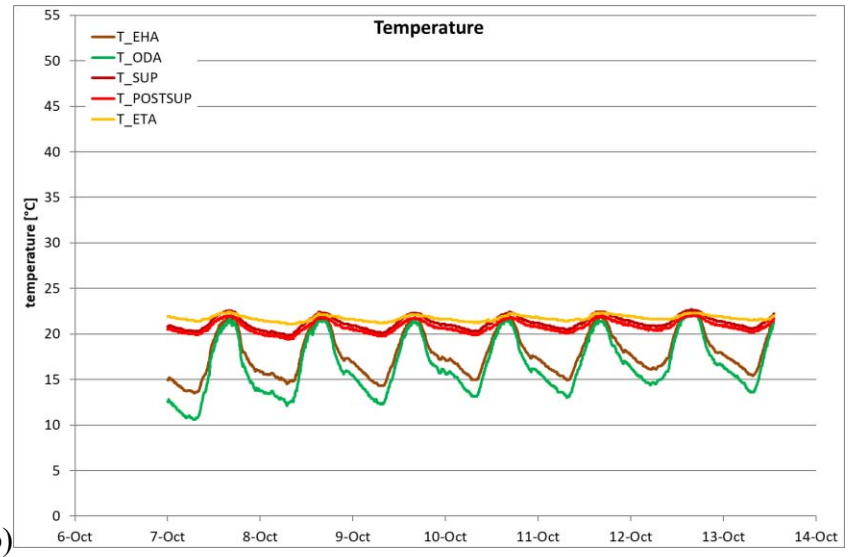

b)

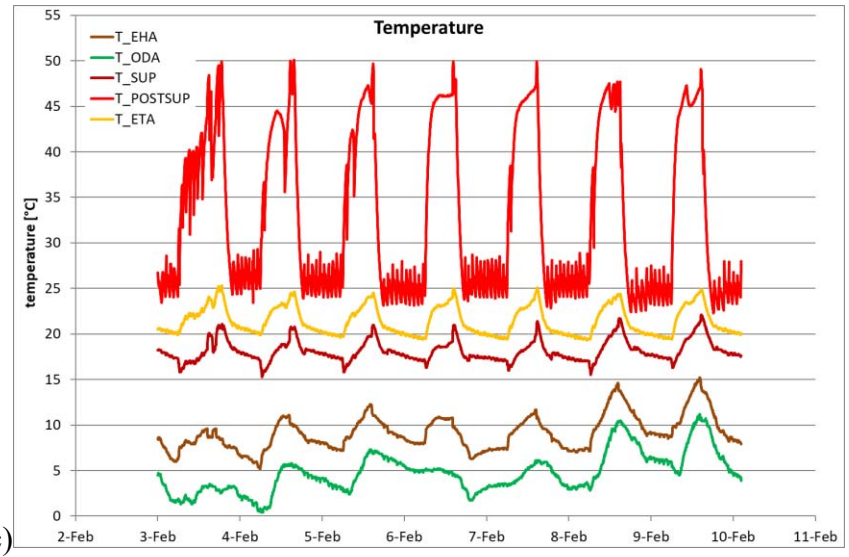

c)

Figure 2: Air temperatures in exhaust air (brown), outdoor air, (green), supply air (dark red), postsupply air (light red) and extract air (yellow) for an example summer week (a), autumn week (b) and winter week (c).

The overall performance during a 7 month period is shown in a correlation graph where extract, supply and postsupply temperatures are given as a function of outdoor temperature. In this graph the function modes can be observed for the whole ventilation system. Heat recovery with possible postheating in the cold season and heat rejection with possible postcooling in the warm season. In the intermediate season there is no postconditioning and the heat is either recovered (bypass not active) or removed from the house (bypass activated). The extract air temperatures in the correlation graph show that in summer, the extract air temperatures (indicative for indoor air temperature) are kept below 27 °C because of the postcooling effect.

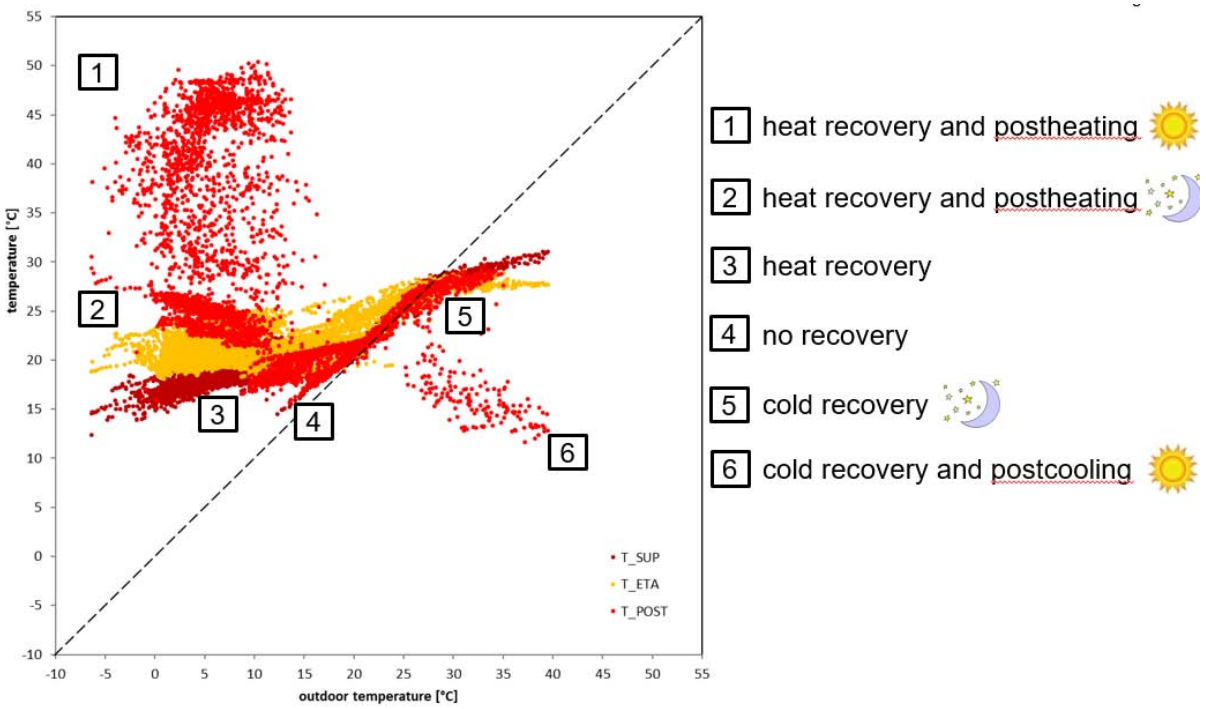

Figure 3: Hourly averages of extract air temperature (yellow), supply air temperature (dark red) and postsupply air temperature (light red) as a function of outdoor air temperature.

The postconditioning system does not only give a cooling effect in a sensible way (temperature decrease of supply air) but also in a latent way (humidity decrease of supply air). This is indicated in fig. 4 by the monitored temperatures.
For a period of one summer month, the water temperature is estimated by the measured postsupply air temperature (for a well dimensioned heat exchanger in the postconditioning system this estimation is valid). The dewpoint of the air before it enters the postconditioning is calculated from the supply air temperature and supply air humidity as measured in the balanced ventilation unit.
It can be observed in fig. 4 that with an active postcooling, the water temperature is dropping below the dew point of the fresh air in summer. As a result of this, the condensation on the postconditioning exchanger is expected to lower the absolute humidity in the supplied fresh air, which adds to the comfort of the fresh air supply even further.

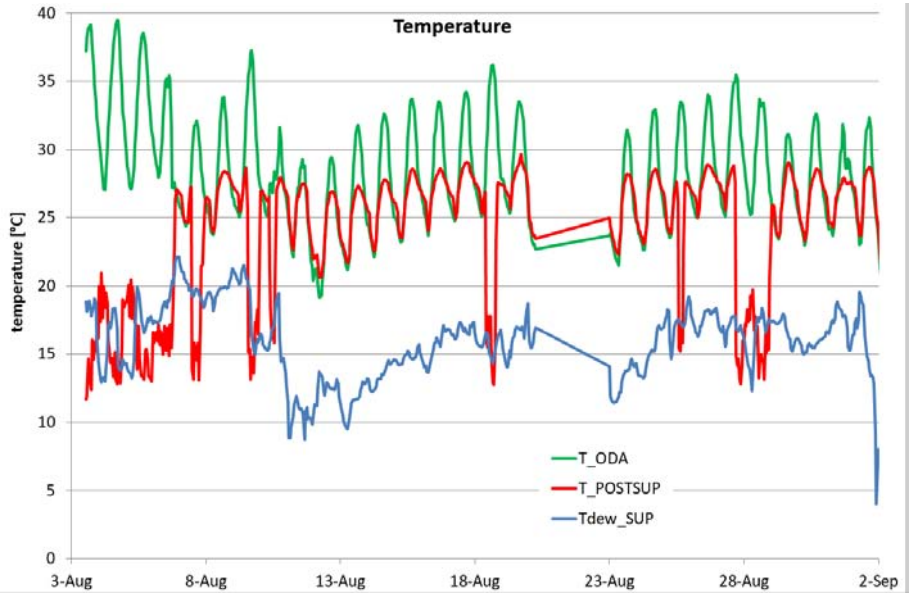

Figure 4: Monitored values during a summer month of outdoor air temperature (green), postsupply air temperature (light red) and dewpoint of the supply air (blue).

4 CONCLUSIONS

The ventilative cooling as a result of indoor heat extraction (activated bypass) and outdoor heat rejection (bypass not activated) reduce the overheating effect in a nearly zero energy house in summer. In combination with postcooling with chilled water from a heat pump, it is shown how the overheating problem in this house is reduced by the mechanical ventilation system, even when summer outdoor air temperature and humidity are higher than indoors. The results show that the extract air temperatures are about 27°C for outdoor air temperatures as high as 41°C.
Both the hygiene in terms of guaranteed fresh air, and the comfortable supply air temperatures, make this ventilation system a comfortable, and energy efficient solution for all seasons of the year.

Modelling thermal comfort and energy consumption of a typical mixed-cooling apartment in Guilin, China

Jie Han*[1,2], Wenheng Zheng[1], Guoqiang Zhang[3]

1 Guilin University of Electronic Technology
1Jinji Road, Guiln, China
**Corresponding author: hanjie@guet.edu.cn*

2 Aalborg University
Thomas Manns VEJ 23, Denmark

3 Hunan University
2 Lushan road,Changsha, China
Presenting author: Jie Han

ABSTRACT

Many studies have shown that the use of mixed-mode cooling can bring down the cooling load significantly while maintaining satisfactory in door air quality and thermal comfort. But there is little information available concerning mixed-mode cooling in China. Thus, basing on design parameters of design standard, A series of computer simulation of a typical mixed-cooling apartment in Guilin, lies south-west of China, was conducted by Eneryplus and Climate Consultant software. Analysis of the results indicates natural ventilation can burden part air conditioning load but is not enough to satisfy the requirement of indoor thermal comfort, mechanical cooling and heating systems are needed. For the whole year, the running days of individual natural ventilation, heating and cooling are very seldom, and hybrid operation is available for most of the year. There are difference using Fanger model and adaptive model to assess thermal comfort in mixed-mode spaces. Which one is the most suitable methods need to further research. The current design parameters of fully air-conditioning and natural ventilation buildings can not be simply used in mixed-mode cooling design. People's behaviour in mixed-mode spaces have an major influence to energy consumption. The study will contribute to a deep understanding of thermal comfort and energy consumption of mixed-mode buildings. At the same time, it will also enlighten to optimize suitable design parameters and control strategies of mixed-cooling apartments in south-west of China.

KEYWORDS

Mixed-mode cooling; Apartments; Energyplus; Thermal comfort; Energy consumption

1 INTRODUCTION

Air-conditioning systems for space cooling is responsible for more than half the energy consumption in buildings for Chinese climates. According to statistics, the total building energy consumption in China accounts for 21% of the total national energy consumption (Tsinghua, 2013). Many studies have shown that the use of mixed-mode cooling can bring down the cooling load significantly while maintaining satisfactory in door air quality and thermal comfort(Daaboul, et al., 2018; Barbadilla-Martin, et al.,2018).Mixed-mode cooling refers to a hybrid approach to space conditioning that uses a combination of ventialtive cooling and mechanical cooling that provide air distribution and some form of cooling(Heiselberg, 2002; Brager, 2006). Mixed-mode cooling system has been researched extensively in the University of California, Berkeley. However, to the best of our knowledge, there is little information available concerning mixed-mode cooling buildings in China. Thus, the purpose of this study was to conduct a simulation on thermal comfort and energy consumption in a mixed-cooling apartment in Guilin, lies in hot summer and warm winter zone of China. The building construction for the case, lighting and other inter gains data about the building can be found in the design standard(Ministry, 2003). The study will contribute to a deep understanding of

thermal comfort and energy consumption of mixed-mode buildings. At the same time, it will also provide suitable control strategies of mixed-cooling apartments.

2 METHODOLOGY

Guilin city is located in the south-west of China and belongs to the hot summer and warm winter climate zone. The climate data of Guilin city, which was downloaded from Energyplus website (Energyplus, 2019), is analysed using Climate Consultant software version 6.0 to gain knowledge into the mixed-mode design. EnergyPlus is used as the simulation tool in the study for modelling thermal comfort and energy consumption of a typical apartment for a family with three people-parents and one child. EnergyPlus, developed by U.S. Department of Energy, is an open-source whole-building energy simulation program built upon sub-hourly zone heat balance and integrated solutions of building loads, HVAC systems, and central plant equipment. Generally, a typical apartment includes three rooms- a living room, a master room and a secondary room. Figure 1 shows the model of the typical apartment. A multi-zone variable air volume (VAV) system, with a single-speed direct-expansion (DX) cooling coil and a gas burner, is used to provide cooling and heating for the living room and the master room. Natural ventilation is applied to the secondary room. Temperature-based control strategy is used to control mixed-cooling systems**.** EnergyPlus Airflow network is used to simulate airflow movement through multizone wind driven airflows with hybrid ventilation control. Energy management system (EMS) in EnergyPlus is used to implement different control strategies for mixed-mode systems.

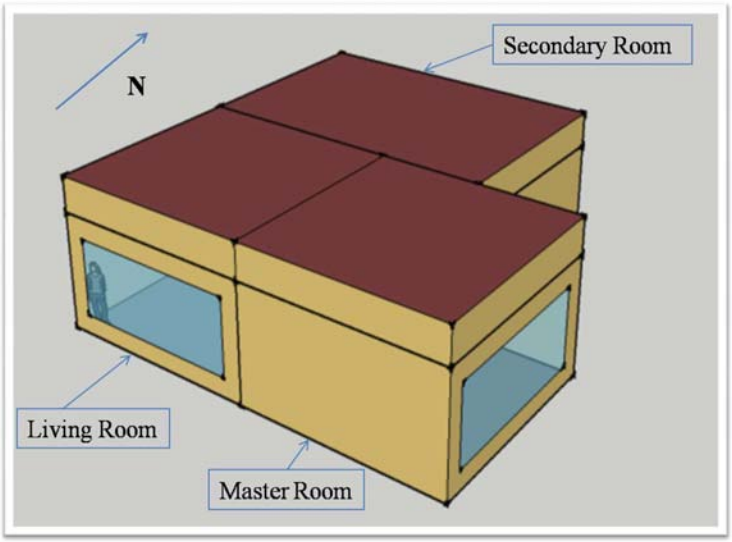

Fig.1 Model of the typical apartment

3 RESULTS AND DISCUSSION

3.1 Climate analysis

The climate data of Guilin is analysed using Climate Consultant software version 6.0 to gain insights into the mixed-mode cooling design. The timetable plot in Fig.2 shows that natural ventilation a day before10:00 a.m. may work in summer months, air-conditioning would be required in the afternoon of summer time and night ventilation with thermal mass may work in the summer and transition months. The psychrometric chart in Fig. 3 shows that different design strategies are utilized to available thermal comfort. The main measures under the weather

conditions include adaptive comfort ventilation (28.2%), heating with dehumidification (25.3%) ,internal heat gain(23.6%), and dehumidification only(20.9%), which also indicate that natural ventilation is not enough to conditioned the temperature, mechanical cooling and heating systems are needed.

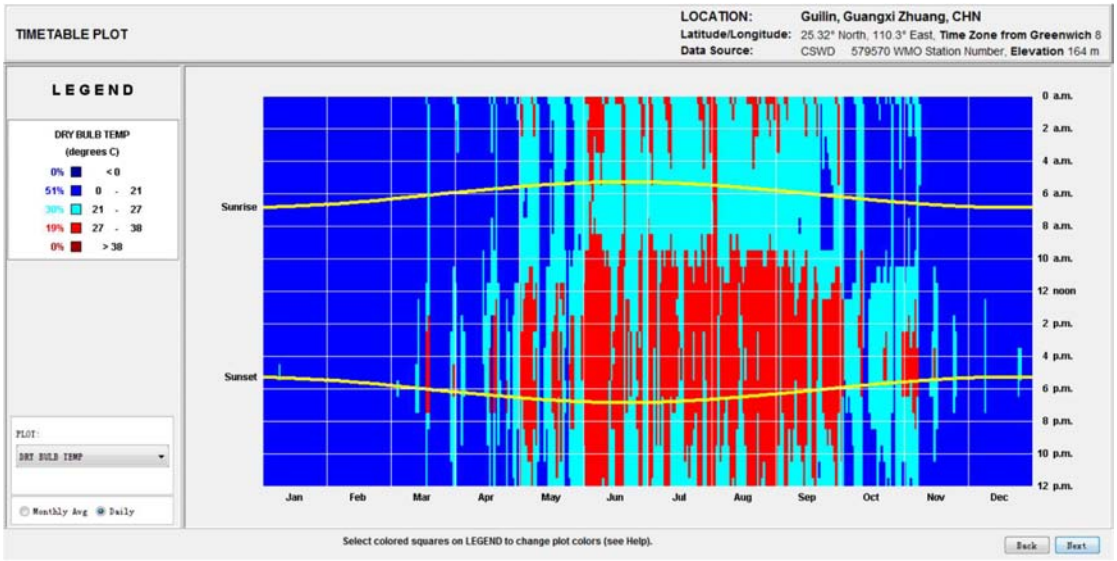

Fig.2. Timetable plot for temperature on a monthly basis

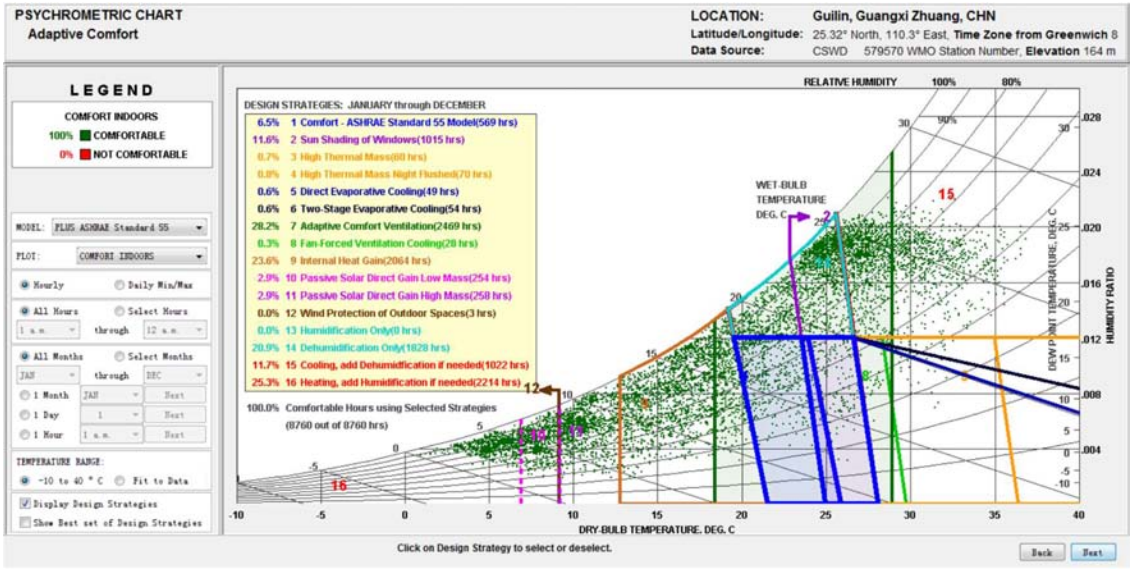

Fig.3. Psychrometric chart of Guilin climate

3.2 Schedule of hybrid operation

Figure 4 shows the hybrid operation days of the living Room. The hybrid ventilation control status is represented by three integer values: 0, 1, and 2.A zero value indicates no hybrid ventilation control. A value of one indicates that natural ventilation is allowed. A value of two denotes that the natural ventilation is not allowed, so all window/door openings are closed. A value of one for Availability Manager Hybrid Ventilation Control Mode means temperature control for either cooling or heating, which is determined internally based on thermostat set point and temperature control type. when the room temperature is above the given set point the active cooling system takes over and the windows are closed. This corresponds to the transition

in the figure between the two systems, natural ventilation taking place in the morning on warm days and on cooler days it continues in to the afternoon. It must be noted that irrespective of the design option active cooling is always required. In Figure 4 it can be observed, for the whole year, the running days of individual natural ventilation is very seldom. The running days of individual heating and cooling exists in winter and summer time. Hybrid ventilation is available for most of the year.

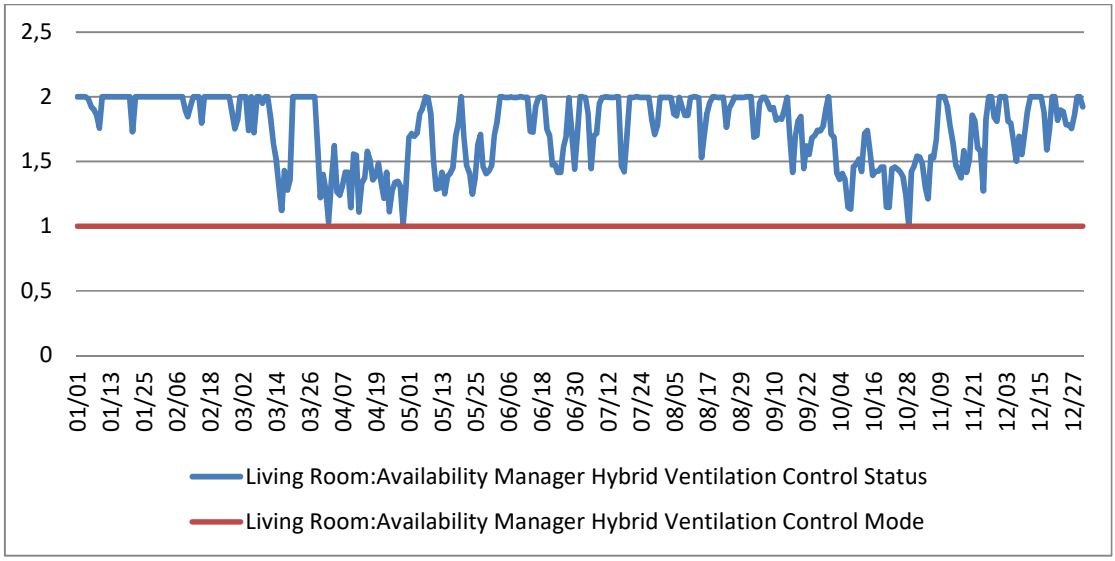

Fig.3. Operation days

3.3 Thermal comfort

Two methods were chosen to assess thermal comfort. These methods were selected because they are widely used in scientific researches and by thermal comfort professionals:
(1) Method for determining acceptable thermal conditions in occupied spaces by Fanger model (ASHRAE, 2004); (2) Method for determining acceptable thermal conditions by thermal adaptive model (ASHRAE55, 2010).
The number of Frequency days of PMV calculated by Fanger Model are shown in Fig.4. Thermal comfort days ($-0.5 \leq PMV \leq 0.5$) to the living room, the master room and the secondary room are 99, 101 and 105 respectively.Fig.5 shows whether the operative temperature falls into the 80% acceptability limits of the adaptive comfort in ASHRAE 55-2010. A value of 1 means within (inclusive) the limits, a value of 0 means outside the limits, and a value of -1 means not applicable. From the figure 5, we can find that there are the same days (59) of the living room, the master room and the secondary room satisfying the limits. According to the Fig 4 and Fig 5, we can conclude three rooms of the apartment do not satisfy the requirement of thermal comfort basing on current design parameters and control schedules from design standards or codes. Secondly, there are difference using the two methods to assess thermal comfort of mixed-mode spaces. Which one is the most suitable method need to be further research.

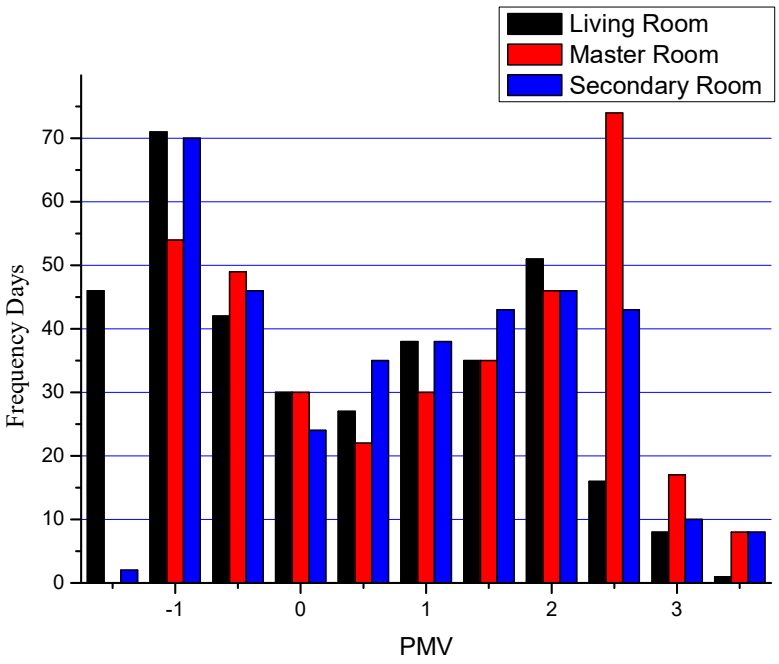

Fig.4. Frequency days of PMV

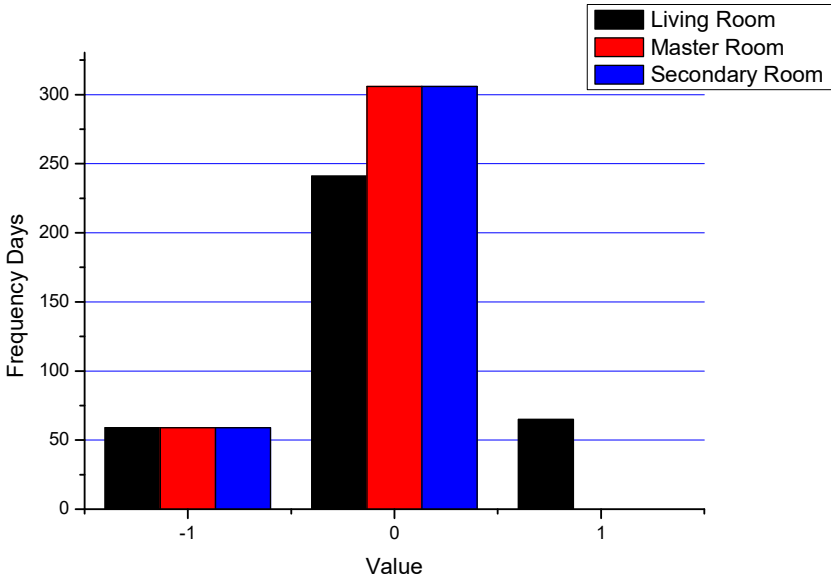

Fig.5. Frequency days of adaptive thermal comfort

Energy consumption

Fig.6 shows the plant energy consumption of main heating and cooling. From the figure, we can find the heating period is approximate from 1 April to 1 October, the cooling period from 1 January to 31 March and from 11 November to 31December.the cooling values are much less than heating value because of ventilative cooling burdening part of air conditioning load, which indicate mixed-mode cooling can reduce air conditioning load effectively. Fig.7 shows the plant energy consumption of reheat in the living room and master room, and we can find the reheat energy consumption in master room are much higher than the living room, which

might attribute to different schedules of people's behaviour in the two rooms. It indicates that people's behaviour in mixed-mode spaces have an major influence to energy consumption.

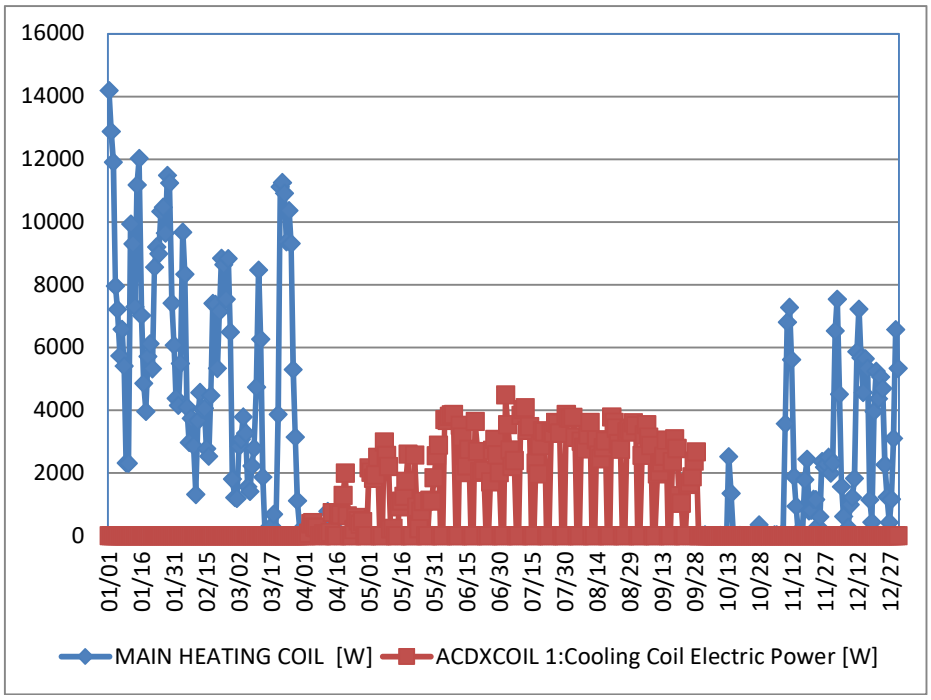

Fig.6. Plant energy consumption of main heating and cooling

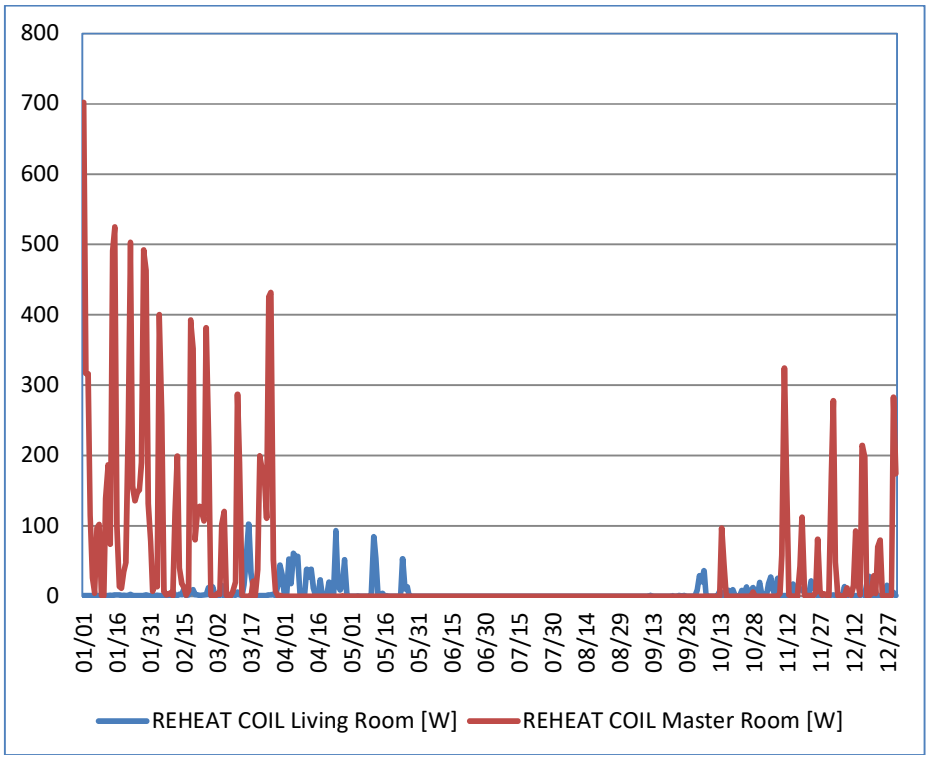

Fig.7. Plant energy consumption of reheat in living room and master room

4 CONCLUSIONS

Many studies have shown that the use of mixed-mode cooling can bring down the cooling load significantly while maintaining satisfactory in door air quality and thermal comfort. But there is little information available concerning mixed-mode cooling in China. Thus, basing on design parameters of design standard, A series of computer simulation of a typical mixed-cooling apartment in Guilin, lies south-west of China, was conducted by Eneryplus and Climate Consultant software. The following main conclusions can be drawn:

1) Natural ventilation can burden part air conditioning load but is not enough to conditioned the temperature, mechanical cooling and heating systems are needed.

2) For the whole year, the running days of individual natural ventilation, heating and cooling are very seldom. Hybrid operation is available for most of the year.

3) There are difference using Fanger model and adaptive model to assess thermal comfort in mixed-mode spaces. Which one is the most suitable methods need to further research.

4) The current design parameters of fully air-conditioning and natural ventilation buildings can not be simply used in mixed-mode cooling designs. people's behaviour in mixed-mode spaces have an major influence to energy consumption.

5 ACKNOWLEDGEMENTS

The project is supported by Natural Science Foundation of Guangxi (2018GXNSFAA281212) and Joint Cultivation Fund of Guangxi (No.2018GXNSFAA138071), Demonstration and Research on Key Technologies of Low Carbon Green Intelligent Zone in Guilin City (No.20180107-2).

6 REFERENCES

ASHRAE Stand 55.(2004).Thermal environmental conditions for human occupancy. American society of heating, refrigerating and air-conditioning engineers inc. Atlanta.

ASHRAE Stand 55.(2010).Thermal environmental conditions for human occupancy. American society of heating, refrigerating and air-conditioning engineers inc. Atlanta.

Brager, G.S. (2006). Mixed-Mode Cooling. ASHRAE Journal, 48, 30-37.

Barbadilla-Martin E, Martin J.G, Lissen J.M.S, Ramos J.S, Dominguez .A.(2018).Assessment of thermal comfort and energy saving in a field study on adaptive comfort with application for mixed mode offices. Energy and Buildings,2018,167,281-289.

Daaboul J, Ghali K, Ghaddar N. (2018). Mixed-mode ventilation and air conditioning as alternative for energy savings: a case study in Beirut current and future climate. Energy Efficiency,11(1),13-30.

Energyplus. 2019. https://energyplus.net/weather.

Heiselberg, P.(2002). Principles of Hybrid Ventilation, Aalborg, Department of Building Technology and Structural Engineering, Aalborg University, Denmark.

Ministry of Housing and Urban-Rural Department of The People's Republic of China. 2003.Design standard for energy efficiency of residential buildings in hot summer and warm winter zone JGJ 75-2003, Beijing (In Chinese).

Tsinghua University Building Energy Conservation Research Center. 2013. Annual report on energy efficiency in buildings in China 2013, China construction industry press, Beijing.

Comfort at hospital reception desks

R.M.J. Bokel*. P.J.W. van den Engel, A.M. Eijkelenboom, M.A. Ortiz Sanchez

Delft University of Technology
Julianalaan 134
2628 BL Delft, The Netherlands
**Corresponding author:r.m.j.bokel@tudelft.nl*

ABSTRACT

For several years indoor comfort is measured in halls of hospitals by architecture students from the Delft University of Technology. Questionnaires and interviews have shows that patients and visitors have very few complaints about the indoor comfort in hospital halls.
This, in hindsight, is not so very surprising. Patients and visitors usually come out of the cold into the hallway. A hallway which is at least marginally warmer, a hallway where it does not rain and hallway that is sheltered from the outside wind. Secondly, the indoor comfort is not the main concern of the patients and visitors entering the hospital. The patient's and visitor's upcoming consults with the doctors or nurses is much more important. Coming from the consult, patients and visitors always have the choice to immediately leave the hospital if they do not like the indoor comfort. Complaints from staff, however, are very common. Staff personnel usually complain about low temperatures and draught.

A reception desk is the main workplace in a hospital hall. A reception desk can be closed, i.e. physically separates the personnel from the environment of the hall. A reception desk can also be open, thus without a physical separation between personnel and patients and visitors. In a hospital, in general, an open reception desk is favoured for a more welcoming atmosphere for patients and visitors. This more open reception desk, however, often causes the personnel to experience low temperatures and draught.

From this study it is clear that it is very difficult design a thermally comfortable reception desk in a hospital. The quest for a reception that expresses openness and transparency clearly hinders the design for a comfortable reception desk. On the other hand, the small number of people at the reception desk is in no comparison to the hundreds of staff and patients for which the hospital is also designed.

Many solutions to improve thermal comfort at a reception desk are already known. The exact cause of the experienced draught and the best solutions, however, are difficult to determine. Scale models or CFD simulations should be used as a guide for design a reception desk in a hospital or when solving thermal comfort problems.

A new cause of draught, people moving past the reception desk, was identified and quantified. As a result, a completely open reception desk inside a large atrium with a lot of people moving past might not be possible without either closing off the reception desk, or increasing the temperature at the reception desk.

KEYWORDS

Hospital, Comfort, Draught, Reception

1 INTRODUCTION

A reception desk is an important part of a hospital. The reception desk is often the first contact between the patients and visitors with the hospital. Anxious patients are welcomed at the reception desk. Reception desk personnel helps patients and visitors to find their way around the hospital. Happy reception personnel increase the effectiveness of a hospital. To keep the reception desk personnel content, the indoor climate at the reception desk should be comfortable. Masters students from the Delft University of Technology in Delft have investigated if the indoor climate at three hospitals reception desks is comfortable within the master course AR0125 [2018, 2019]. The encountered indoor climate is given in this paper and possible improvements are presented when the indoor climate is not found to be comfortable.

2 LITERATURE

There is very little scientific literature about thermal comfort at reception desks or hospital reception desks [Eijkelenboom, Bluyssen, 2019]. Searching for "reception" in the AIVC database only yields one unrelated paper. Searching the Scopus database is not much better. That does not mean that nothing is known about reception desks in large hospital halls. Common sense and practical experience is available (berkela.home.xs4all.nl, kikk-recreatie.dearbocatalogus.nl, www.arbocatalogusmobiel.nl, www.arbo-online.nl)

2.1 Type of receptions

A reception desk can be either closed or open. A closed reception desk physically separates the personnel from the environment of the hall. An open reception desk has no physical separation between personnel and patients and visitors.

The most important reasons to choose a closed reception desk are: Safety, privacy, thermal comfort and noise. A closed desk ensures the safety of the employees and the products handles at the reception desk such as money and legal documents, but can also raise aggression by visitors. Reception desks that are positioned close to the entrance of a building or are positioned in large atria can suffer from cold airflows that are difficult to control. A closed reception desk can protect the desk from these airflows. The last reason to choose a closed reception desk is to prevent acoustic discomfort by acoustically insulating the reception desk from a lot of background noise. In a hospital, in general, an open reception desk is favoured for a more welcoming atmosphere for patients and visitors.

2.2 Comfort at receptions

Temperatures

A receptionist usually performs a number of tasks, from giving information, answering the telephone to performing light administrative work. According to the literature, see tables 1 and 2, a temperature above 21 °C and air velocities lower than 0.15 m/s is comfortable. The literature also mentions that there is a difference in comfort between men and women and that thermal comfort depends on the tiredness of people. These last two aspects are not taken into account in this paper.

Draught

Fanger defines draught as "an unwanted local cooling of the human body caused by air movement". Most people are affected by draught at locations that are not covered by clothing, such as head, neck and ankles. The air temperature, the turbulence intensity and the average air velocity together define the degree of discomfort due to draught (ISSO 74, 2014).

At the moment the most used draught equation is the draught ratio (DR) by Fanger:

$$DR = (34 - T)(u - 0.05)^{0.62}(3.14 + 0.37uI) \quad (1)$$

Where I is the local turbulence intensity, u the local air velocity and T is the local temperature in ˚C (combined air and radiation temperature). The thermal state of the body also has impact on the degree of disturbance by draught. The activity level has an impact on the maximum acceptable air velocity, see table 2.

Table 1: Comfort temperatures from literature

Reference	Building function	Temperature winter (°C)	Comments
ISSO 74, 2014	not distinguished	> 20	alpha building
CIBSE, 2007	entrance halls/ lobbies/ corridors/ general waiting areas	19-21	max air velocity 0.15 m/s, Met = 1.4, clo = 1.0.
ISSO 7730	office, auditorium, restaurant	22 ± 2	Normal level of expectation, class B, max 10 % dissatisfied, max velocity 0.16 m/s, Turbulence intensity 40 %, Activity 70 W/m^2.
Hospitals 2 and 3	reception	> 21	personal communication

Table 2: Maximum acceptable air velocities at different air temperatures and at different activity levels [AR0125, 2018]

Air Temperature (°C)	maximum acceptable mean air velocity (m/s) at activity level			
	Metabolic rate 85-105 W	Metabolic rate 130 W	Metabolic rate 160 W	Metabolic rate 200 W
20	0.15	0.15	0.20	0.20
22	0.15	0.20	0.20	0.20
24	0.20	0.20	0.20	0.30
26	0.30	0.30	0.30	0.40
28	0.30	0.40	0.40	0.40

2.3 General solutions of problems at receptions

The main causes of thermal comfort complaints are the following according to the Dutch ARBO-online [www.arbo-online.nl]: the position of the reception desk, limited air circulation under the reception desk, unbalanced airflows produced by the heating and ventilation system, the position of the heating elements and the inability of the personnel to influence the temperature themselves. Radiation of a cold floor or from the front of the reception desk can be solved using floor heating or radiators (but beware of uneven heating).

Draught problems can be prevented by separating the personnel from the outside air when the entrance doors are opened. This can be done using an air curtain, a revolving door, a draught lobby and enough distance between the reception and the entrance door.

3 METHOD

3.1 Case study receptions

Three hospital reception desks were investigated.

Hospital 1 [AR0125, 2018]: The entrance hall, which is an atrium consisting of large glass surfaces. The hall is oriented northeast and has, partly, a double storey height of over 7.3

meters. The ground floor of the hospital houses a restaurant, espresso-bar, and small giftshop for the visitors. When people enter the hall through a revolving door, they directly see the welcome desk which is placed centrally in the hall. The hall leads to a long corridor which leads to all different departments situated on the ground floor. The main source of heating during winter, and cooling during summer is the mechanical ventilation system. Several service desks also have their own local heating devices. During warm summer days, the revolving door is fully opened to let in as much fresh air as possible.

Hospital 2 [AR0125, 2019]: The patients, visitors and staff members enter the building through the main entrance. After entering the building, the user must go through a long hallway to go to the reception area. The areas surrounding this reception area are several waiting areas, a coffee corner and a long hallway to the parking garage.

Hospital 3 [AR0125, 2019]: The patients, visitors and staff members enter the building through the main entrance. After entering the building, the user finds a hallway which is were the reception area is situated. The areas surrounding this reception area are a waiting area, a working area and a commercial area.

3.2 Measurements

Eltek Squirrels, HOBO dataloggers, I-buttons and EXTECH air velocity meters were used to measure the temperature, the relative humidity the air velocity and the CO2 concentration, see figure 1. The researcher's nose was used to track and identify any interesting smells at the reception desk and in the surrounding areas. The outdoor temperatures of the nearest airport were taken from the KNMI website. The perceptions of the people from the reception desk were investigated using a questionnaire and additional small talk. The questionnaire consisted of questions about personal characteristics and thermal comfort.

Figure 1: Equipement Eltek Squirrels, Hobo Dataloggers, I-buttons and air velocity meter, images from the producers.

4 RESULTS

4.1 Measurements

***Hospital 1*:** The measurements were taken between the 5th of May 2018 and the 12th of May 2018. The average outdoor temperature was between 5.0 and 9.0 °C, see figure 2.

Measurement day	*day*	t_{start}	t_{end}	$T_{outside}$ (°C)
1	05/03/2018	11:09	12:30	6.4
2	07/03/2018	9:36	12:33	5.0
*3**	12/03/2018	9:34	12:18	8.6

Figure 2: Outside temperatures (KNMI, closest weather station) of hospital 1.

The temperature at the reception desk was generally between 21 and 23 °C, see measurements 1 and 3 in figure 3. This means that the temperature should in general be comfortable. The personnel of the reception desk had a personal heating system. The air velocities were

measured on the 21 of March 2018. The average air velocity (0.1 m, 0.6 and 1.1. m) in front of the reception desk was 0.26 m/s at an average temperature of 20.5 °C and an average turbulence intensity of 0.84.

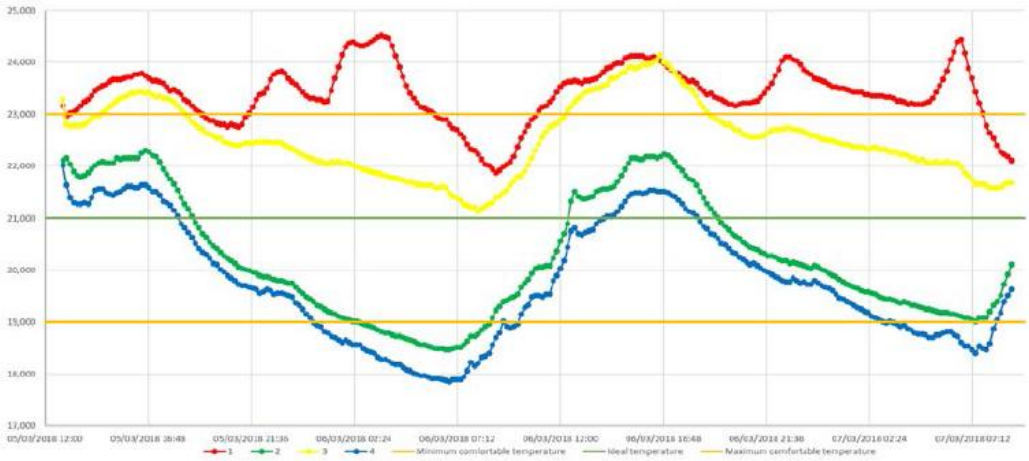

Figure 3: Temperature measurements (red and yellow line) at the reception desk in hospital 1.

***Hospital 2*:** The measurements were taken on the 6th of May 2019 between 9.00 and 14:30. The outdoor temperature was between 9.5 and 12 °C with a North wind speed of 11 km/h, see figure 4. The temperature at the reception was between 22.5 and 23.5 °C measured with Eltek, I-button and Hobo's, see figure 6. The CO_2 concentration was below 800 ppm.

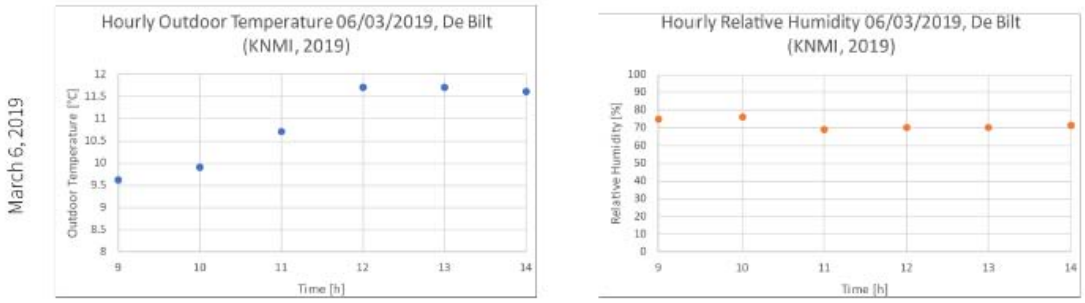

Figure 4: Outside temperatures (KNMI, closest weather station) of hospital 2.

***Hospital 3*:** The measurements were taken on the 7th of May 2019 between 9.00 and 14:30. The outdoor temperature was between 9.5 and 10.5 °C with a North East wind speed of 18 km/h, see figure 5. The temperature at the reception was again between 22.5 and 23.5 °C measured with Eltek, I-button and Hobo's, see figure 7. The CO_2 concentration was below 800 ppm and is not further investigated.

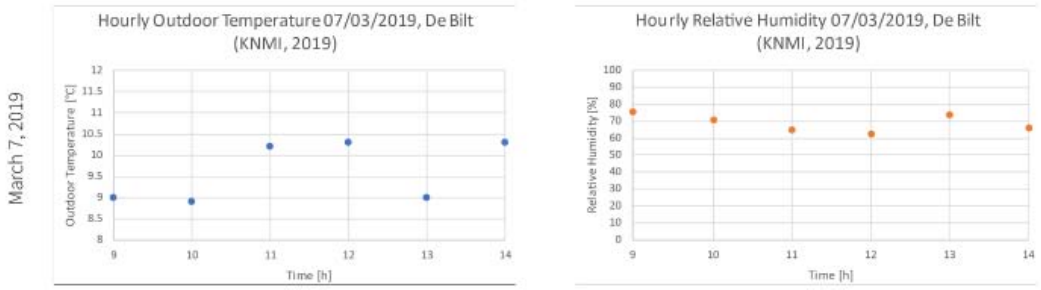

Figure 5: Outside temperatures (KNMI, closest weather station) of hospital 3.

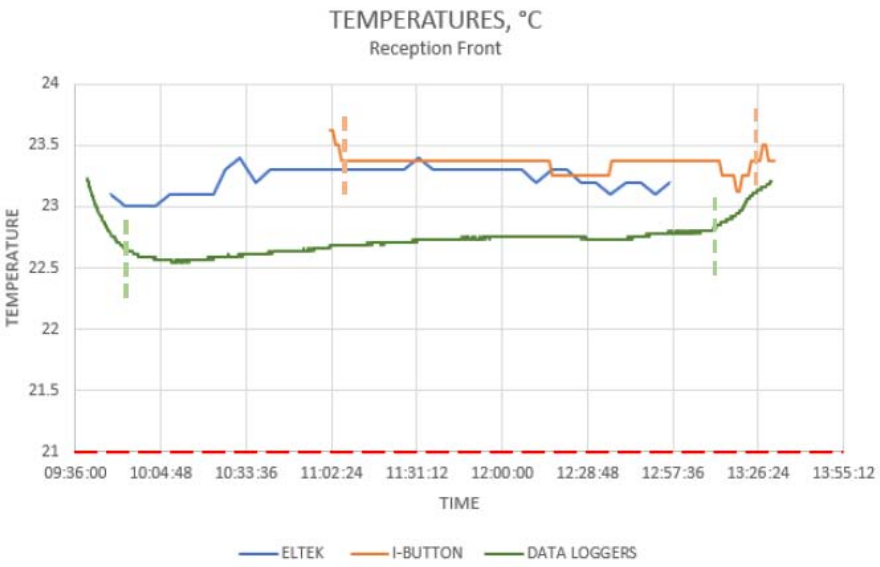

Figure 6: Indoor Temperature at the reception desk in hospital 2.

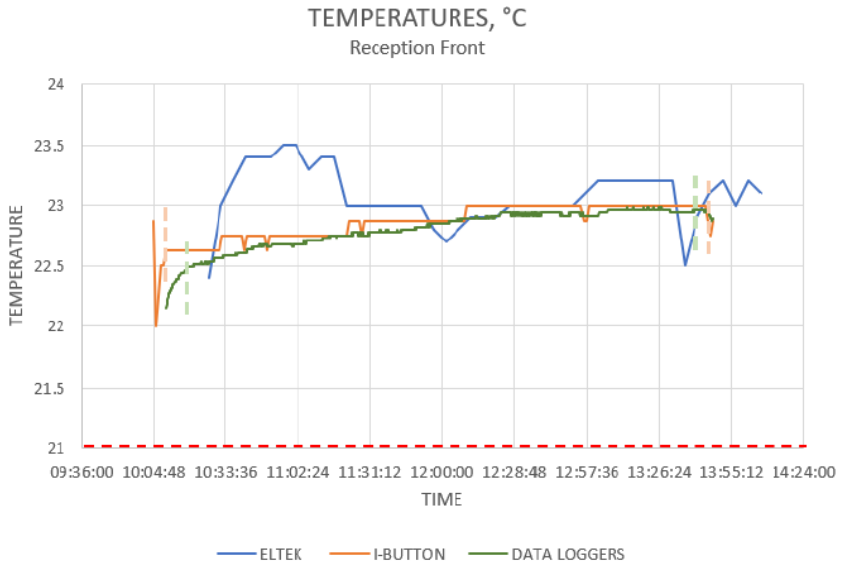

Figure 7: Indoor Temperature at the reception desk in hospital 3.

4.2 Questionnaires

Hospital 1: 24 employees were surveyed, 60 patients and 36 visitors. 43.8% of the employees were feeling (slightly) cool or cold (where only 12.5% felt slightly warm or hot); and a lot of employees felt draught (68.4%). Those two ways of expressing thermal discomfort are likely to be related. For people that are feeling cool, together with high turbulence intensities – draught can be a serious cause of discomfort, even at locations were no high values are measured for the air velocity.

The main outcome of the questionnaires in hospitals 2 and 3 is that the reception desk personnel (9 responses in hospital 2 and 6 responses in hospital 3) found the temperature at the reception desk to be slightly cool and that the personnel suffered from draught. 80 % of the people in hospital 2 and 100 % in hospital 3 often suffered from draught. In hospital 2 the personnel thought the draught came from the parking garage and in hospital 1 from the entrance near the reception area.

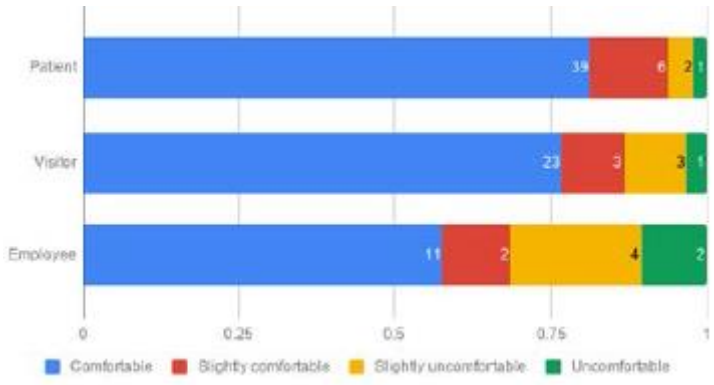

Figure 8: Level of comfort according to patients, visitors and employees in hospital 1.

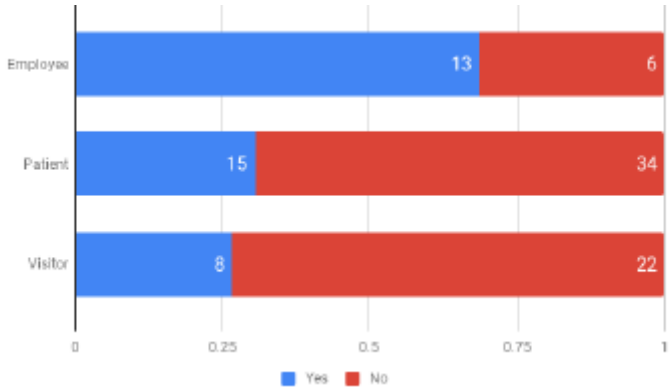

Figure 9: Perception of draught by employees, patients and visitors in hospital 1.

4.3 Conclusion

All three reception desks suffered from low perceived thermal comfort. The air temperatures were not the problem, they were generally above the comfortable 21 °C. Personnel mainly complained about draught, which was supported by measurements in hospital 1.

5 INVESTIGATION INTO THE CAUSE OF THE COMFORT PROBLEMS

5.1 General causes of discomfort

Hospital 1:

The main source of draught is probably the revolving door. Revolving doors increase the energy efficiency of the building and prevent draught, while allowing lots of people to enter a building in a short amount of time. Nevertheless, air leakages are inevitable and occur in two ways: when the door is closed through its seals and cracks, and when opened through the passage of people. Those air leakages can cause discomfort.

The air infiltration when the door rotates depends on the type of revolving door, the rotation speed of the door, the size of the opening, the temperature differential and to a certain extent on the outdoor wind speed and direction and the air velocities indoors. Revolving the door causes an exchange of indoor air and outdoor air of approximately equal volume. If more people are entering, the infiltration decreases with about the volume of the people occupying the space in the revolving door. According to Humphreys et al. this impact is only small [Humphreys et al., 1961]. Figure 10 shows that a higher wind speed outside, and a higher indoor air velocity, lead to a higher infiltration rate.

The air flows close to the revolving door in the hospital were measured. The average air temperature was 20.0 °C, the average air velocity was 0.38 m/s and the average turbulence intensity was 0.40. These values show that the revolving door is a source of unwanted air flows. When the distance between the revolving door and the reception area is small, the effect of the revolving door on the perceived draught is high. Fortunately the high temperature measured is caused by the air curtain included in the revolving door.

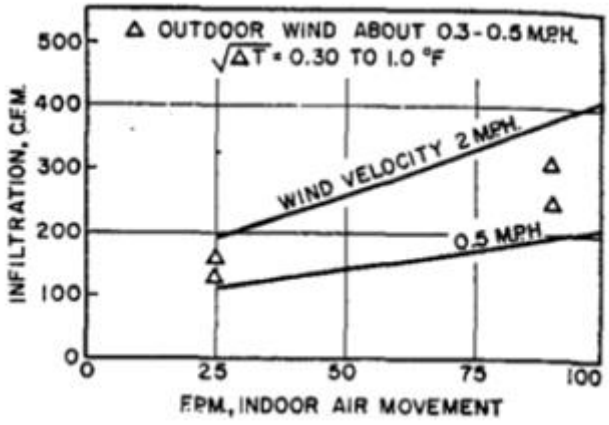

Figure 10: Effect of wind and indoor air movement on infiltration for small tempreature differences and indoor speed of 5 rounds per minute [Humpheys et al,, 1961].

Hospitals 2 and 3:
The draught problems for hospital 2 and 3 were investigated using both a physical model and a CFD (Phoenics) simulation model. The physical model was made from cardboard. The air flow was simulated with a computer fan and the air flow was visualised with a smoke tube.

Hospital 2: The physical model showed a possible discomfort in hospital 2. The air from the parking garage passes the reception to the entrance or the other way around. The CFD model showed that the air current from the entrance and the parking garage does not seem to influence the reception area. The diffusers appear to have a big influence in the microclimate of the reception. The diffusers reach the desks and contribute to the cold draught. There are numerous diffusers at the reception area and they are placed directly next to each other, creating discomfort. Besides this, there is an emergency stairway door located directly in front of the reception area. This door constantly opens and closes creating sudden currents of air as it sucks the air from the outside. This scenario includes an open door, sucking the air from the hallway.

Hospital 3: The physical model showed no discomfort in hospital 3, neither from the air inlets nor from the entrance. The reception desk is positioned in such a way that the main air flow does not pass the reception desk directly. The CFD model of hospital 3 shows that the current coming from the entrance is not a source of discomfort in the reception desk.

5.2 Other causes of discomfort

Due to the fact that in hospital 3 still no explicable source could be found for the draught, the possibility of people being the source of the draught was investigated. To be able to show that people's movement can cause draught felt by the receptionist, an experiment was conducted. In this experiment, the air velocity was tracked of an area, first without people's movements, second with some movement and third with a lot of people moving. The area where the

experiment was conducted is the hallway at the Building Technology studio. Figure 11 shows a scheme of how and where the experiment was conducted.

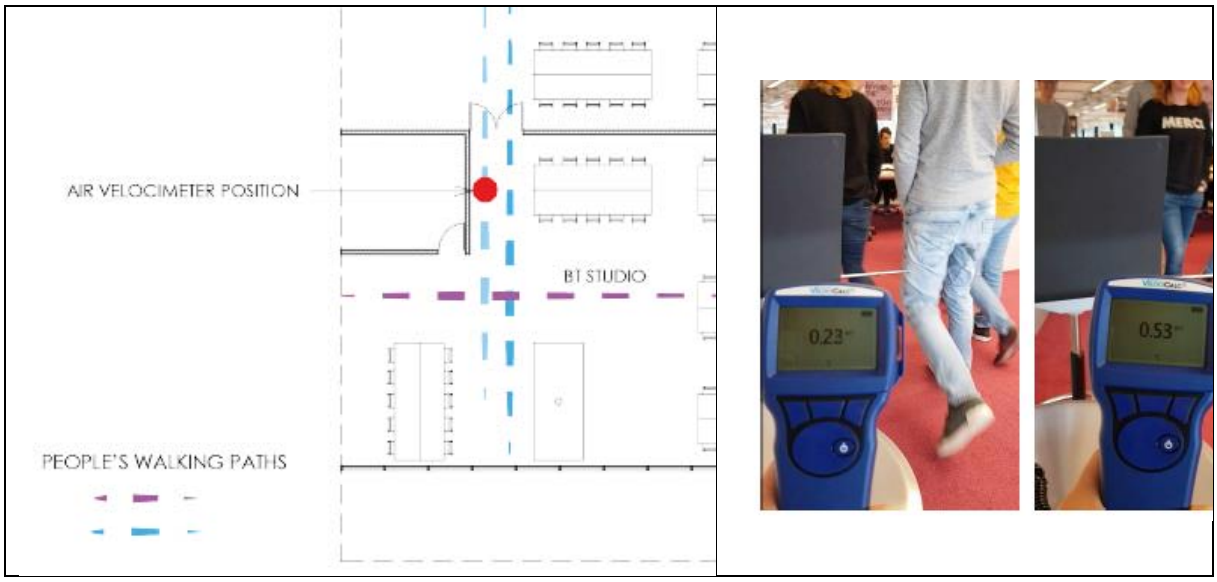

Figure 11: Building Technology Studie Floor plan, left, and group of four people walking from and towards the air velocity meter right [AR0125, 2019]

The air velocity in the hallway when there is no movement of people is 0.01 m/s, which means that there is practically no movement of air. Figure 11 shows the air velocity at the hallway when there is movement of a group of four people walking. In this case the air velocity is 0.23 m/s, measured when the group is walking by and 0.53 m/s, measured when the group is walking back. This experiment shows that when people move, they attract the air around them and that this follows the same path as the people moving. Therefore, it can be concluded that people's movement can be the cause of the air draught felt by the receptionist and the source of discomfort.

5.3 Solutions

From this study it is clear that it is very difficult to make a reception desk thermally comfortable. The quest for a reception that expresses openness and transparency clearly hinders the design for a comfortable reception desk. On the other hand, the few people at the reception desk are in no comparison to the hundreds of staff and patients for which the hospital is also designed.

The solutions given in section 2.3 are a good start to improve the thermal comfort at the reception desk. A different position in hospitals 1 and 2 might help to move the reception desk out of the main airstream. The main cross ventilation airflow through the hospitals can be reduced by rearranging the entrance and exit areas through air curtains, obtaining a different position of the revolving door, adding a revolving door, or creating a draught lobby. Further closing up the reception desk should help in all three hospitals, although this will challenge the openness and transparency of the reception desk design.

6 LIMITATIONS AND DISCUSSIONS

This research is performed by Master students from the faculty of Architecture of the Delft University of Technology. This means that there was limited time for the measurements. Besides limited time, the outside temperature in March can be either cold, as in 2018, or warmer, as in 2019, making comparisons between the hospitals more difficult. There is also limited equipment to do the measurements because equipment needed to be shared with other

students. The air flow measurements at the height of the reception desk of hospitals 2 and 3 are sadly missing.

7 CONCLUSIONS

From this study it is clear that it is very difficult design a thermally comfortable reception desk in a hospital. The quest for a reception that expresses openness and transparency clearly hinders the design for a comfortable reception desk. On the other hand, the few people at the reception desk are in no comparison to the hundreds of staff and patients for which the hospital is also designed.
Many solutions to improve thermal comfort at a reception desk are already known. The exact cause of the draught and the best solutions, however, are difficult to determine. Scale models or CFD simulations should be used as a guide for design a reception desk in a hospital or when solving thermal comfort problems..
A new cause of draught, people moving past the reception desk, was identified and quantified. As a result, a completely open reception desk inside a large atrium with a lot of people moving past might not be possible without either closing off the reception desk more, or increasing the temperature at the reception desk.

8 ACKNOWLEDGEMENTS

The following students are thanked for their active participation in the course: Andri Lysandrou, Nadine Mocking, Linda Vos, Aviva Opsomer, Javier Montemayor Leos, Sasha Rodriguez Arambatzis, Yarai Zenteno Montemayor. The three hospitals are thanked for their hospitality.

9 REFERENCES

AnneMarie Eijkelenboom & Philomena M. Bluyssen, (2019), *Comfort and health of patients and staff, related to the physical environment of different departments in hospitals: a literature review,* Intelligent Buildings International.

Andri Lysandrou, Nadine Mocking, and Linda Vos, (2018), *Report AR0125_Technoledge Climate Design*, Delft University of Technology.

Humphreys, C. M., Schutrum, L. F., Ozisik, N., & Baker, J. T. (1961). Air Infiltration through revolving doors. ASHRAE Journal.

Aviva Opsomer, Javier Montemayor Leos, Sasha Rodriguez Arambatzis, Yarai Zenteno Montemayor (2019), *Report AR0125_Technoledge Climate Design*, Delft University of Technology.

berkela.home.xs4all.nl/cad kantoor/cad kantoor balie.html, accessed June 28, 2019, in Dutch

kikk-recreatie.dearbocatalogus.nl/maatregel/klimaat-verbeteren-achter-de-receptie, accessed June 28, 2019, in Dutch

www.arbocatalogusmobiel.nl/content/files/Rapportage_Klimaatonderzoek_2010.pdf inventarisatie van recepties van een aantal garages, accessed June 28, 2019, in Dutch

www.arbo-online.nl/rie/artikel/2011/06/het-risico-baliewerk-1019987, accessed June 28, 2019, in Dutch

Prediction of the influence of solar radiation on adaptive thermal comfort using CFD simulation

Juti Hu*[1], Ge Song [1], Guoqiang Zhang[1]

1 Hunan Engineering Research Center for Intelligent Sunshading and High Performance Door and Window,National Joint Research Center for Building Safety and Environment,Department of Civil Engineering,Hunan University

Lushan South Road 2

Changsha, China

**Corresponding author: 15857168423.163.com*

ABSTRACT

Adaptive thermal comfort model has been widely used to evaluate the thermal comfort level of natural ventilation buildings.However, current adaptive standards offer a simple linear relationship between the outdoor temperature and the indoor comfort temperature， ignoring the influence of solar radiation. In this paper, CFD model is used to evaluate the thermal comfort of a residential building under natural ventilation conditions.Keeping the input parameters of outdoor temperature and wind speed and changing the input parameters of solar radiation to simulate the distribution of Indoor air temperature and velocity.the result are compared with adaptive thermal comfort temperatures to predict global and local indoor thermal comfort .The results show that the presence or absence of direct sunlight has a great influence on indoor thermal comfort at the same outdoor temperature; in the absence of direct sunlight, the thermal sensation is relatively more uniform, and solar radiation has a significant effect on local thermal sensation.

KEYWORDS

thermal comfort

CFD model

solar radiation

1 INTRODUCTION

The adaptive thermal comfort model proposes that people can adapt to environmental changes in a certain range by adding or subtracting clothes and opening and closing windows, which makes it possible to save unnecessary energy consumption of refrigeration and heating, and at the same time ensures the thermal comfort requirements by limiting the scope of application.Richard de Dear(Richard de Dear，2001) found a significant correlation between indoor comfort and outdoor air temperature through statistical analysis of large databases of comfort research results from all over the world.Thereafter, C. Bouden(G.Carrilho，2005) conducted a field survey of thermal comfort in five towns in two climate zones in Tunisia, and found that thermal sensation was related to the average outdoor temperature and the average outdoor operating temperature.The significance of outdoor parameters was further clarified.From that, the model describing the relationship between outdoor temperature and comfort temperature is widely used in the thermal comfort standard of natural ventilation in various countries.Therefore, it is possible to predict human thermal sensation under natural ventilation by using indoor and outdoor temperature parameters.

The CFD numerical simulation method fully considers the influence of actual factors on the ventilation process, and the simulation cost is low. It can obtain real-time three-dimensional data of the airflow characteristics in the ventilated room.It has become an indispensable tool for the study of natural ventilation.J.I. Peren et al.(J.I. Peren，2015) used CFD to simulate the effect of different positions of asymmetric openings on cross ventilation in buildings.H. Montazeri and F. Montazeri (H. Montazeri，2018)simulates the effect of the outlet opening of the roof windshield on the cross ventilation of buildings by CFD. The results show that the use of the outlet hole near the wind trap will not increase the induced air flow, but will lead to a significant decrease in indoor air quality.Because CFD software includes not only flow model, but also energy model and mass transfer model, CFD tools can also solve more complex problems of flow and heat transfer coupling. Xiufeng Yang and Ke Zhong (Xiufeng Yang，2015)used CFD to simulate the changes of transient temperature and wind speed fields of hot-pressure ventilation, and verified the number of transient hot-pressure ventilation. The results show that the transient development of airflow and temperature distribution are different under different indoor and outdoor temperature differences.Using CFD to simulate the temperature and velocity fields to obtain the environmental parameters needed for calculating thermal comfort index is a more convenient and fast way than the actual measurement, and its reliability has been verified by many researchers. Cinzia Buratti et al.(Cinzia Buratti，2017) used simulated temperature parameters in the classroom of the University of Perugia to calculate the predicted thermal sensation.Paige Wenbin Tien and John Kaiser Calautit (Paige Wenbin Tien，2019)used computational fluid dynamics CFD model to study the thermal comfort of high-rise buildings with different air courtyards. The results show that the design of air courtyards has little effect on the thermal comfort of buildings without considering vegetation.It is also suitable for local thermal comfort. Sally Shahzad et al. (Sally Shahzad，2017)analyzed the performance of the chair by CFD simulation, and analyzed the thermal distribution around the hot chair with cushion in detail. The results show that improving the local thermal sensation of human body can improve the overall thermal comfort of human body.In this paper, a three-dimensional steady-state computational fluid dynamics (CFD) model is established by using the renormalization group (RNG) k-e turbulence model to predict the air flow and temperature distribution. Combined with the adaptive thermal comfort model, the thermal comfort of each location in the natural ventilated residential space is evaluated, and the effects of solar radiation and ventilation on thermal comfort are studied.Firstly, the FLUENT software is used to simulate the indoor flow field and temperature field under different weather conditions, and the CFD model is validated by the measured data. The process of measurement and modeling will be described in detail in Chapter 2. Then, the influence of solar radiation and ventilation on thermal comfort is analyzed by comparing the simulation results with the indoor thermal comfort temperature predicted by the adaptive thermal comfort model. The part is discussed in Chapter 3.

2 METHOD

2.1 Measurement

This paper studies the thermal comfort of naturally ventilated residential buildings under different solar radiation. A residential building in Changsha was selected as the research object.The residence is one of the apartment buildings, and the horizontal distribution of the residence is shown in Figure 1. The out-of-plane normal of window one points to 45 degrees north-west. As shown in Table 1, the sizes of the interior doors are the same, and the sizes and forms of the three windows are different.

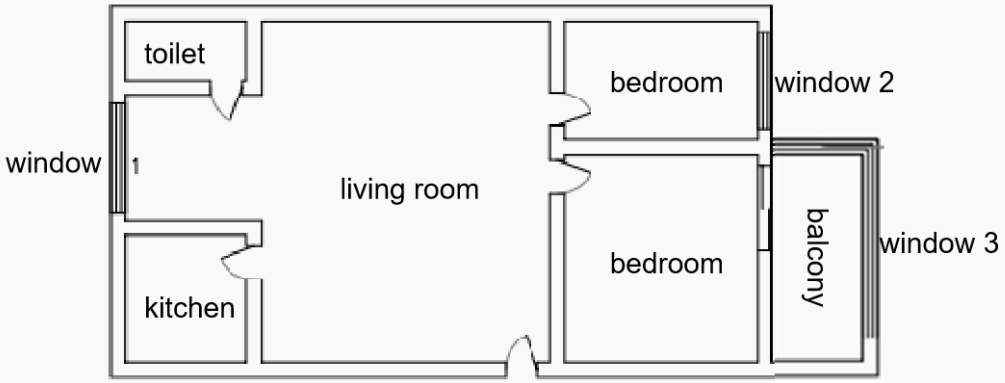

Figure 1: Residential plane

In order to obtain the actual indoor environmental parameters, HOBO was used to test and record the hourly temperature and humidity values from March 23 to May 13, 2019.HOBO is set to update and record data every 30 minutes. It is placed in the living room, bedroom and balcony room for testing. The test data will be used to validate the CFD model and thermal comfort analysis.

Table 1：Size and style of doors and windows

name	size	style
door	800mm*2000mm	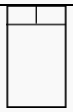
Window1	1460mm*1460mm	
Window2	1300mm*1650mm	
Window3	2800mm*1650mm+1400mm*1650mm	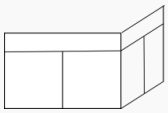

2.2 CFD simulation

Figure 2 is a physical model built by CFD ICEM according to the above residential dimensions.To study the CFD model of natural ventilation, it is necessary to determine the external computational domain. The selection of computational domain is three times as much

as that of the building according to the general requirements(Atish Dixit,2015). The grid division is shown in Figure 3. The height of computational domain is 8400 mm, the width is 19200 mm, the length is 40440 mm, and the distance between inlet and residence is 10110 mm.After trial calculation, the computational domain is sufficient for the full development of turbulence in the rear of the building, and the far-end air flow does not affect the indoor ventilation.Because the physical model is more standard, the structured grid is chosen.The size of the grid is related to the accuracy of computation and the amount of computing resources used. Different sizes are selected for grid division in different regions, and the grid in external computing domain is larger. The main object of study is the building part, which is refined. For the areas with complex flow and high wind speed, such as windows and doorframes, the grid is further refined.In order to avoid the influence of the number of meshes on the calculation results, grid independence verification was carried out. The initial number of meshes was 41594, the mesh quality was 0.98, the maximum draw ratio was 1.8, and the ventilation volume was calculated to be 1.263 kg/s.As shown in Table 2, when the number of grids exceeds 1 million, the calculation results are hardly affected by the number of grids, so the final grid is 1146 752.

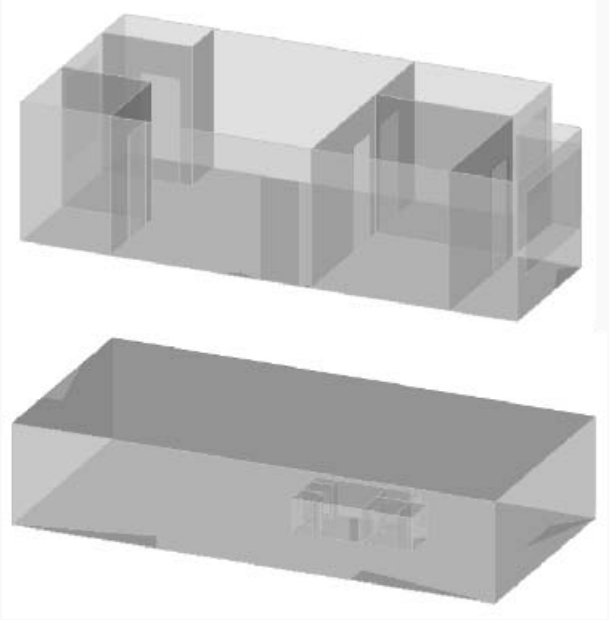

Figure 2：Physical model

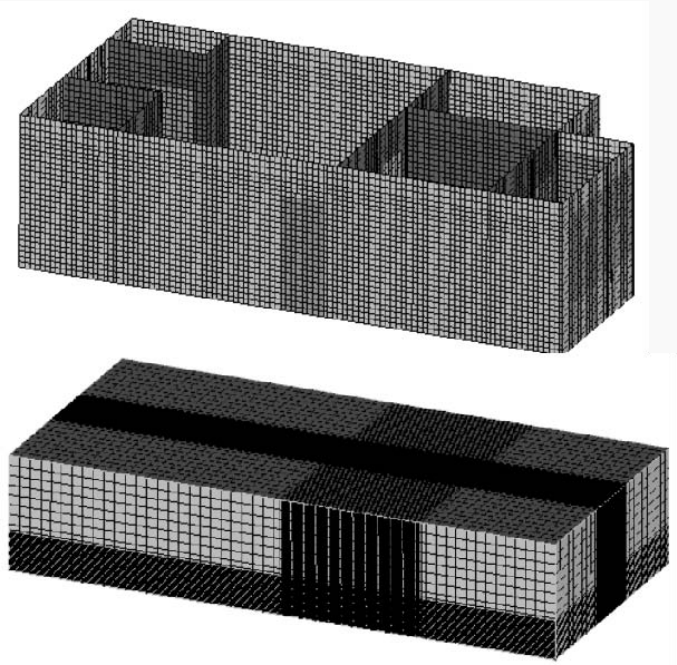

Figure 3：Mesh generation

Outdoor wind speed and direction change with time. Hourly wind speed monitored by meteorology can intuitively reflect outdoor weather change of natural ventilation, but the calculation cost is very large.The wind direction of natural ventilation is always changing, and the actual flow is transient. This brings difficulties to the determination of the entrance boundary conditions. Aiming at the exploratory study of the effects of simulation and solar radiation on thermal comfort in this paper, the representative outdoor wind speed is selected to simulate in steady state, which can achieve the purpose of this study.The front of the building is 45 degrees south to west. For the convenience of research, this paper chooses the direction of inflow parallel to the normal line of the front of the building, so the actual flow is simplified to steady flow with steady wind direction.

Table 2:Grid independence verification

	Test 1	**Test 2**	**Test 3**	**Test 4**
Number	415954	724389	1146752	1318247
Mass flow rate (kg/s)	1.263	1.524	1.654	1.683

Inlet boundary condition chooses the velocity entrance boundary condition, and the average velocity setting value takes the outdoor parameters of the hour. Turbulence intensity I and turbulence length size L are determined by formula(1) and (2).

$$I = 0.16 Re^{-1/8} \quad (1)$$

$$L = 0.07 D \quad (2)$$

Re is Reynolds number and D is pipe size.The pressure boundary condition is used for the outlet boundary condition. Pressure boundary conditions are used when flow details are not clear, but boundary pressures are known. When the outflow area is far from the backflow area and the flow direction does not change, the pressure boundary condition can be used. The outlet of the calculation area is natural outflow, and the outlet pressure is set as environmental pressure.

There is no indoor design temperature in the natural ventilation room, and the heat flow of the external wall can not be calculated as that of the air-conditioned room. Therefore, the known surface temperature of the external wall is used as the first kind of thermal boundary condition in CFD simulation. The outer wall is simplified as isotropic material, and the heat transfer from the outer surface to the inner surface is one-dimensional heat conduction. The thermal boundary condition is treated by steady state. The building maintenance structure is divided into inner wall and outer wall. The inner wall is considered as adiabatic boundary. The outer wall takes into account the influence of solar radiation and adopts outdoor comprehensive temperature.The outer walls and roofs in Southeast and southwest China are heated by solar radiation and outdoor air temperature. Considering the temperature rise caused by solar radiation, e.g. Formula 3, the outdoor comprehensive temperature is used to calculate the surface temperature of maintenance structures.

$$t_z = t_w + \frac{\alpha_s I}{\alpha_w} \tag{3}$$

Where， t_z is the outdoor comprehensive temperature;tw is the calculated temperature of outdoor air;α_s is the absorption coefficient of solar radiation on the outer surface of the maintenance structure;I is the total solar radiation illumination outside the maintenance structure;α_w is the heat transfer coefficient of the outer surface of the maintenance structure.Symmetrical boundary conditions are used for calculating domain boundaries; doors in the room are assumed to be open and set to interior; windows are set to wall according to the opening and closing state of windows, and solar ray tracing is performed if they are closed; and windows are set to interface to connect indoor and outdoor air.

The CFD simulation in this paper is based on pressure-based solution, and SIMPLE algorithm is used. The pressure and momentum are solved by two-stage upwind method. Using the renormalization group (RNG) k-e turbulence model, K and E are solved by the first-order upwind scheme.

2.3 Model Verification

Temperature changes over time were recorded at three sites on April 17. The positions of three measuring points in the model were A (1.82, 3.9, 1.35), B (7.21, 4.4, 1.35), C (8.71, 9.75, 1.35). Point A is in the living room, Point B is in the bedroom and Point C is on the balcony. The simulated instantaneous temperature is compared with the measured temperature, as shown in Figure 4. In the picture, the test temperature (light red line) and the simulated temperature (dark red line) at the bedroom measuring point B basically coincide with each other, and the deviation is the smallest. The average temperature difference between 0 and 23 points is 0.6, 0.3 and 0.45, respectively.

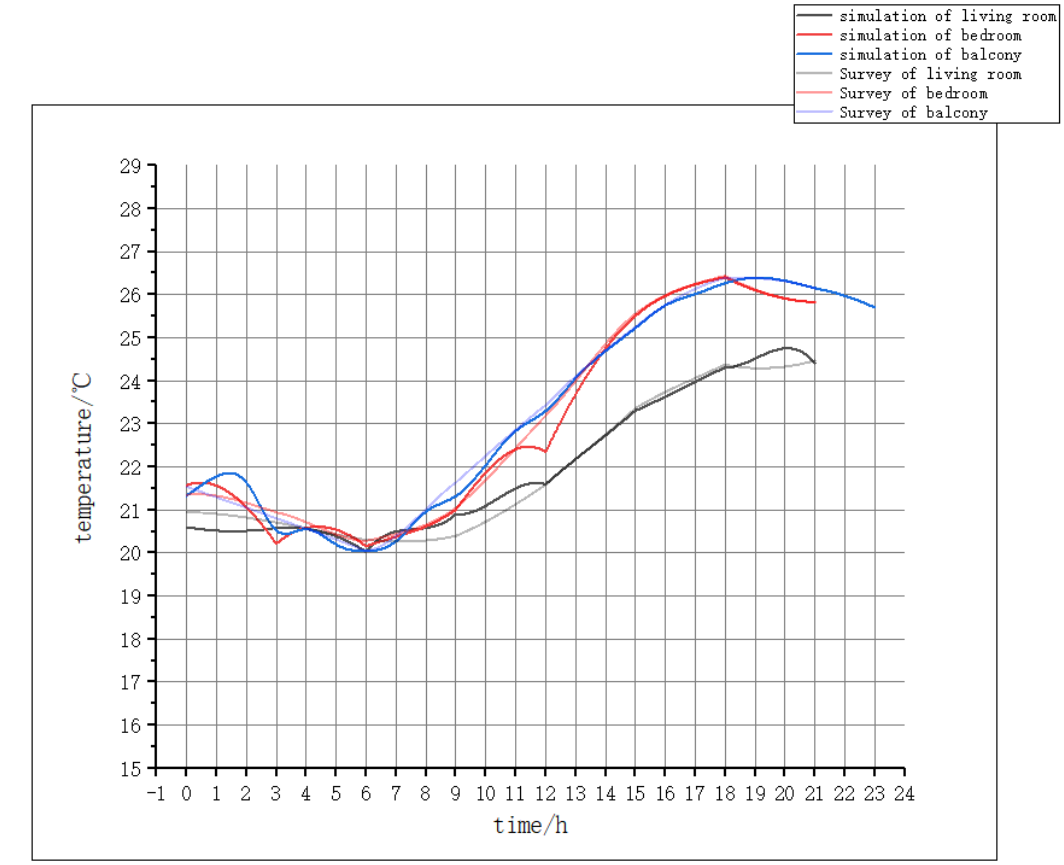

Figure 4：Comparison of test temperature with simulated temperature

2.4 Indoor Temperature Distribution

Figure 5 shows the temperature distribution in seven different rooms.Temperature fields at 8:00, 10:00, 12:00 and 2:00, 4:00 and 6:00 p.m. were simulated in different daytime considering the size of solar radiation and the direction of direct solar radiation. No solar radiation at night was considered as a typical case.Residential windows are located in the Northwest direction, and the walls of the gates are connected with other households. Therefore, the wall temperature in the southwest is maintained at 17 - 22 C, and there is no big fluctuation.The highest local temperature in a day is around 10:00 a.m., because the balcony is located in the Southeast direction, and the window openings are large, the direct sunlight makes the temperature of the southeast wall and balcony room rise sharply.During the day, the highest average air in the room is 12 o'clock. At this time, not only the solar radiation is stronger, but also the heat of the outer wall is released into the room after a morning's heating, which makes the indoor temperature rise.Temperature distribution is the most uniform point is 0, at this time the wall temperature difference is not big, so the temperature of each room will not be very different. The overall temperature in the room rises first and then decreases with time, which is consistent with the trend of outdoor temperature, mainly affected by solar radiation.

Fig. 6, the indoor velocity distribution is obtained under the conditions of maximum (v=4.3m/s) and minimum (v=0.9m/s) outdoor hourly wind speed in a day.When the wind speed is relatively high, the air flow enters from the balcony window and flows through the living room of the

bedroom and exhausts from the window. The indoor air flow velocity is very small, but the direction is basically the same, and there is no obvious eddy current. When the wind speed is small, the indoor air flow rate changes dramatically, forming many eddies which make the air flow in the living room and bedroom not smooth.In fact, 8 a.m. and 6 p.m. are the two time points with the highest wind speed. The horizontal zoning of the living room temperature occurs because the air flow makes the temperature in the central area drop faster than that near the wall.

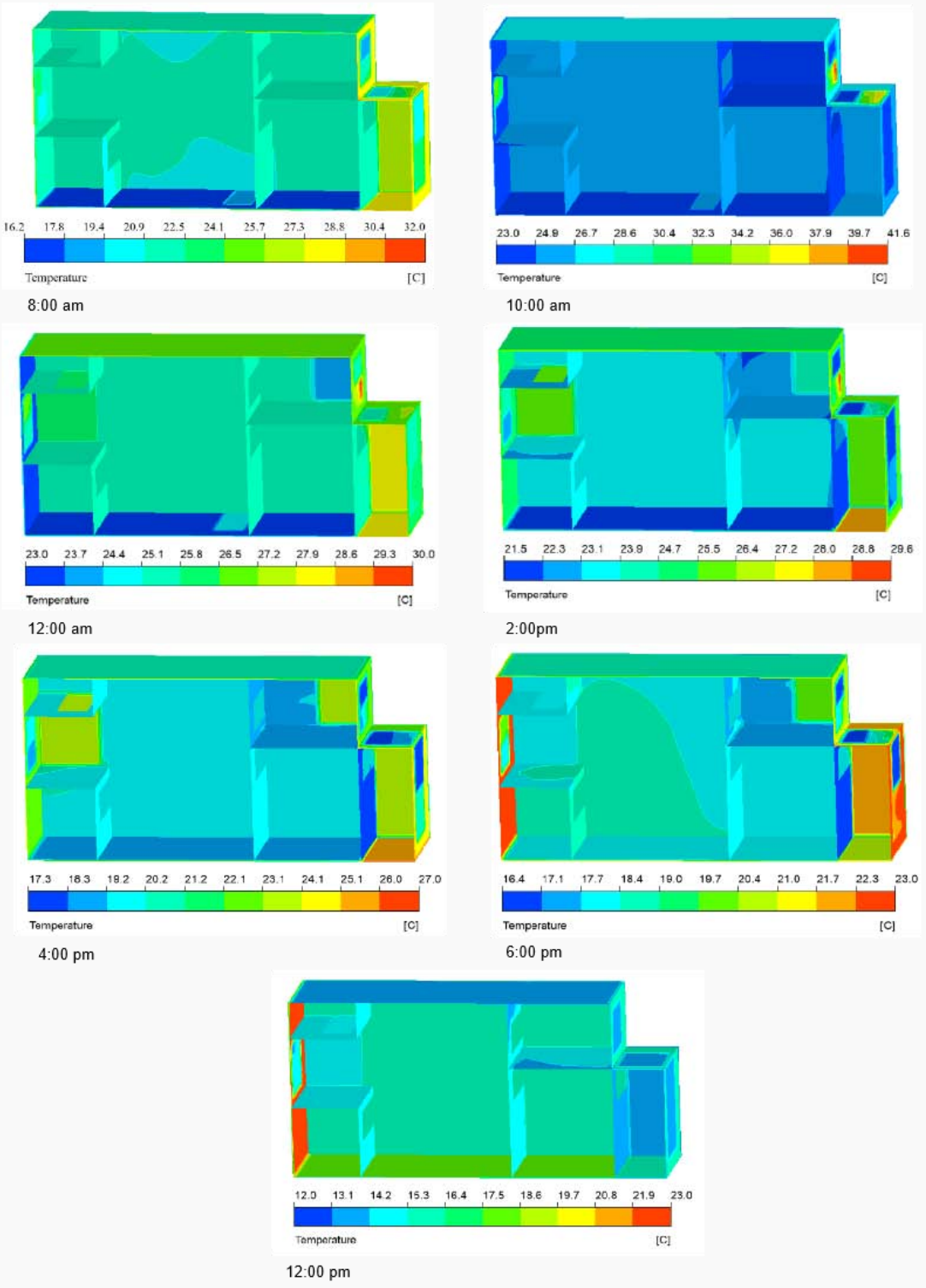

Figure 5:The Change of Temperature Field with Time

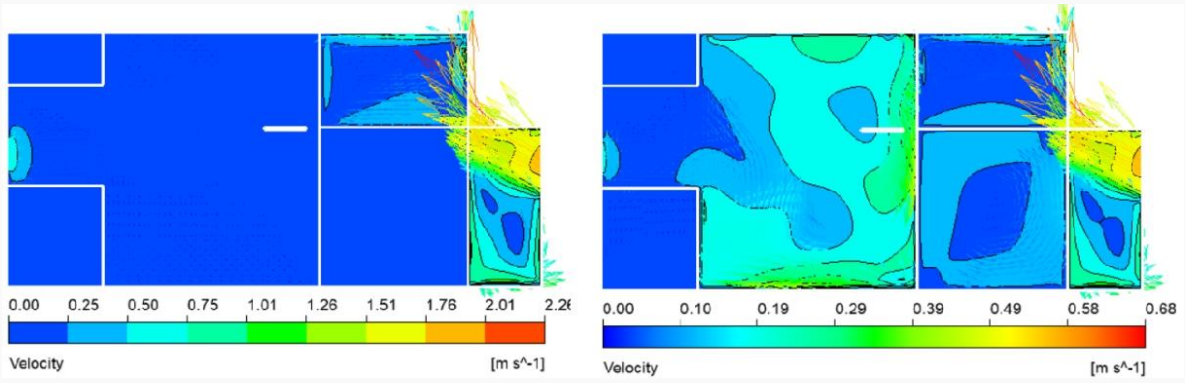

figure 6：Plane sketch of velocity field

2.5 Adaptive Thermal Comfort Index

The general method of evaluating with adaptive thermal comfort model is to calculate an average outdoor calculation parameter by using outdoor temperature of meteorological statistics. This parameter is called general average outdoor temperature or operating average outdoor temperature, e.g. formula (4) .The recommended value α=0.8 and $t_{e\,(d\text{-}n)}$ is the values of, the outdoor daily average temperatures from the date of calculation(ASHRAE，2017).

$$t_{pma(out)} = (1-\alpha)\cdot\left[t_{e(d-1)} + \alpha\cdot t_{e(d-2)} + \alpha^2\cdot t_{e(d-3)} + \alpha^4\cdot t_{e(d-4)} + ...\right] \quad (4)$$

The relationship between general average outdoor parameters or operating average outdoor temperature and upper and lower limits of indoor comfort temperature is a one-time function, that is, indoor comfort temperature conditions are determined by outdoor temperature. Figure 7 shows the relationship between indoor comfort temperature and general average outdoor temperature. The linear expression is shown in formula (5) and (6).

$$\begin{aligned} t_{up} &= 0.31t_{pma} + 21.3 \\ t_{lower} &= 0.31t_{pma} + 14.3 \end{aligned} \quad (5)$$

$$\begin{aligned} t_{up} &= 0.31t_{pma} + 20.3 \\ t_{lower} &= 0.31t_{pma} + 15.3 \end{aligned} \quad (6)$$

Formula(5) expresses the limit of 80% acceptance rate; and Formula(6) expresses the limit of 90% acceptance rate.

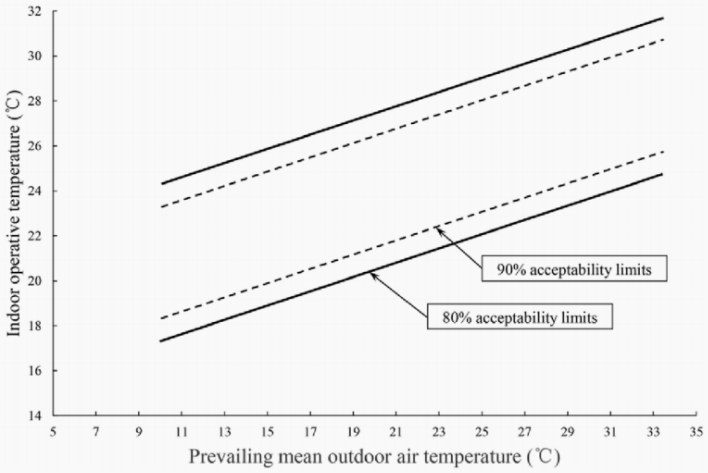

figure 7:Adaptive Thermal Comfort Model

From the above mathematical model, the range of comfortable temperature in the environment studied in this paper can be obtained. Figure 8 depicts the variation of acceptable comfort temperature in a day and the upper and lower limits of indoor temperature at different times. Obviously, we can judge the comfort by observing whether the indoor temperature is in the comfort zone.In the picture, the indoor temperatures from 21:00 to 23:00 and from 0:00 to 6:00 are all lower than the comfortable temperatures. However, because people should be sleeping during this period and have blankets and other insulation measures, they can not simply use the comfortable temperatures to judge, so this period of time will not be discussed.From 7:00 a.m. to 13:00 p.m. it's entirely within the comfort zone. From 14 p.m. to 20 p.m., part of the space is comfortable while the other part is uncomfortable. Next, we will distinguish the comfort zone from the uncomfortable zone in the room by analyzing the temperature field, and discuss what causes this.

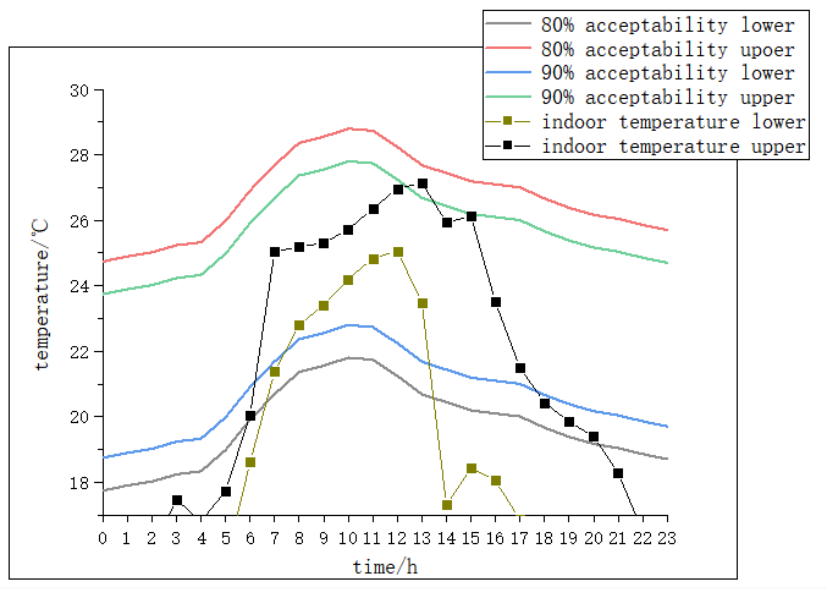

figure 8:Comparisons between Comfort Temperature and Simulated Temperature

Taking 15:00 as an example, Fig. 9 is a horizontal screenshot of temperature distribution at altitudes of 0.15m, 0.5m, 1.2m, 1.5m, 1.8m and 2.0m, respectively. These heights indicate the temperature of the ankle, knee, chest, head and upper region of the standing person,

respectively.The maximum vertical temperature difference is more than 7 ℃, because the house is located on the top floor and heat is transmitted into the room through the roof.

According to the relevant vertebrae, when standing, the temperature difference between head and foot should satisfy△t≤3℃. However, only the balcony and the corner of the bedroom in the Northeast have more than comfortable temperature difference, which can be ignored, that is to say, in this case, the temperature difference between the upper and lower parts will not cause uncomfortable feeling.However, only the balcony and the corner of the bedroom in the Northeast have more than comfortable temperature difference, which can be ignored, that is to say, in this case, the temperature difference between the upper and lower parts will not cause uncomfortable feeling.According to the thermal comfort model, the comfort temperature at this time is 20.19 - 27.19 ℃, and the temperature field at six altitudes is plotted within this temperature range.The area below the lower temperature limit is dark blue, and the area beyond the upper temperature limit is red.When Z < 0.5m, all areas of the room are below the comfortable temperature, reflecting a partial cold state. With the increase of height, the area with moderate temperature gradually enlarges, and the temperature gradually decreases from three outer walls to the inside. The room with transparent envelope structure, due to the role of solar radiation, the temperature change is faster and the difference is larger, the difference of local thermal comfort is more obvious; in contrast, the temperature distribution in the living room will be more uniform.

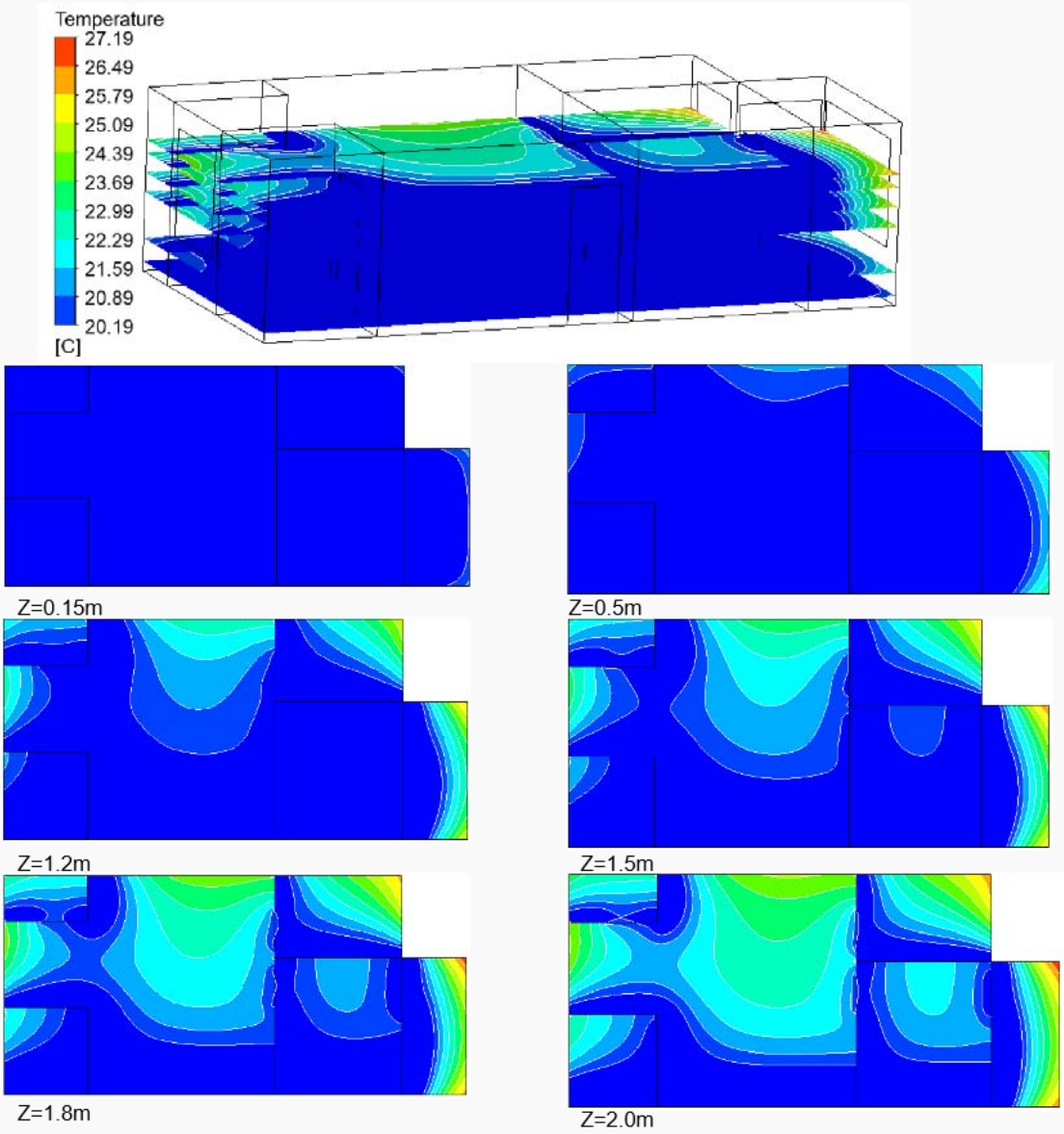

figure 9:Temperature Distribution at Different Heights

At the same time, that is, under the same conditions of solar radiation, the values of different thermal comfort indexes of ventilation volume are compared. Figure 10 depicts the relationship between thermal comfort and ventilation.There is no obvious consistency or relative relationship between the peak value and trend of curve describing comfort index and ventilation rate. Therefore, under the same solar radiation, the effect of ventilation rate on thermal comfort is not obvious, or there is no obvious linear relationship between them.

Figure 11 depicts the relationship between thermal comfort index and solar radiation. The value of solar radiation is determined by geographical location and time.According to the comparison of indoor temperature and comfortable temperature, thermal comfort index is evaluated with 1 as the most comfortable and 0 as the most uncomfortable. The changes of seven groups of data from 7:00 to 21:00 are counted and the trends of the two are observed. At first, the solar radiation gradually rises, and the thermal comfort index does not fluctuate significantly. They are basically in the most comfortable state. As the solar radiation begins to decrease, the thermal comfort is getting worse and worse. Until the solar radiation equals zero, the thermal comfort index is still getting lower and lower until it also drops to zero.It shows that the higher the solar

environment, and calculates the temperature and velocity distribution in the environment.Taking a unit house in Changsha as the research object, field tests were carried out to determine the parameters needed for thermal comfort and set input data.External air temperature, combined temperature and wind speed are used as input data in CFD program.The model was validated by checking the instantaneous temperatures at three different locations and applied to the prediction of indoor global and local thermal comfort.The thermal comfort evaluation method adopted in this paper is an adaptive thermal comfort model, and the thermal comfort index is obtained through the average parameters of outdoor temperature.The results show that during the transitional season, the whole indoor area is comfortable for about 6 hours a day, and only the part of the room whose exterior wall can be exposed to sunlight is comfortable for 6 to 8 hours.The temperature difference in the room is affected by the solar radiation, and increases with the increase of radiation. The maximum temperature difference is more than 8℃.The influence of solar radiation and ventilation rate on adaptive thermal comfort index is analyzed through data statistics. The results show that solar radiation has obvious influence on thermal comfort. In the case of this study, the higher the solar radiation is, the better the thermal comfort, but the difference of local thermal comfort will be greater; and the influence of ventilation rate on thermal comfort is not obvious.

4 REFERENCES

Richard de Dear (2001).*The adaptive model of thermal comfort and energy conservation in the built environment.* Int J Biometeorol (2001) 45:100–108

C. Bouden, N. Ghrab.(2005). *An adaptive thermal comfort model for the Tunisian context.Energy and Buildings 37 : 952–963*.

J.I. Peren (2015).*CFD analysis of cross-ventilation of a generic isolated building with asymmetric opening positions: Impact of roof angle and opening location.* Building and Environment 85: 263-276

H.Montazeri, F. Montazeri.(2018). *CFD simulation of cross-ventilation in buildings using rooftop windcatchers: Impact of outlet openings.*Renewable Energy 118：502-520.

Xiufeng Yang.(2015). *Numerical investigation on the airflow characteristics and thermal comfort in buoyancy-driven natural ventilation rooms.*Energy and Buildings 109：255–266.

Cinzia Buratti et al. (2017).*Prediction Of Indoor Conditions And Thermal Comfort Using CFD Simulations: A Case Study Based On Experimental Data.* Energy Procedia 126 :115 – 122

Paige Wenbin Tien (2019).*Numerical analysis of the wind and thermal comfort in courtyards"skycourts" in high rise buildings*. Journal of Building Engineering 24 : 100735

Sally Shahzad et al. (2017).*A user-controlled thermal chair for an open plan workplace: CFD and field studies of thermal comfort performance.* Applied Energy 207 : 283 – 293

Atish Dixit (2015).*A case study on human bio-heat transfer and thermal comfort within CFD.* Building and Environment 94:122-130

American Society of Heating, Refrigerating and Air- Conditioning Engineers (2017).*ANSI/ASHRAE, ANSI/ASHRAE Standard 55-Thermal Environmental Conditions for Human Occupancy.*

Developing a new passive tracer gas test for air change rate measurement

Sarah L. Paralovo*[1,2], Maarten Spruyt[2], Joris Lauwers[2], Borislav Lazarov[2], Marianne Stranger[2] and Jelle Laverge[1]

1 Universiteit Gent
Sint-Pietersnieuwstraat 25
B-9000 Gent, Belgium
**Corresponding author: sarah.limaparalovo@ugent.be*

2 VITO NV
Boeretang 200
2400 Mol, Belgium

ABSTRACT

Ventilation is critical in interpreting indoor air quality (IAQ), yet few IAQ assessments report ventilation rates; even when they do, the measurement method is often not fully described. Most ventilation assessments use a tracer gas test (TGT) to measure total air change rate. In a TGT, the indoor air is marked with an easily identifiable gas (tracer) so that the air change rate can be inferred by monitoring the tracer's injection rate and concentration. Passive sampling (adsorptive/absorptive samplers) is mostly preferred to monitor tracer concentration for its simplicity, practicality and affordability. Such samplers are commercialized by a range of companies and are widely used in IAQ studies to assess pollutants levels. Currently used passive TGTs present some limitations: inadequate tracer gas, disconnection from IAQ analysis (providing ventilation rates in a different time-scale than the pollutant concentrations) and possible bias arising from the perfect-mixing assumption. Thus, this paper proposes a new approach on the passive TGT method, which uses as tracer a suitable gas that can be co-captured and co-analysed using commercial passive samplers employed in common IAQ studies and which includes a more careful planning phase to account for imperfect mixing. A literature review was carried out in pursuit of such a gas. Considering that the most relevant compounds in IAQ studies are volatile organic compounds (VOCs), which are sampled separately from inorganic pollutants, the gases considered as possible tracers were the VOCs capable of being captured by the samplers commercialized by Radiello®, 3M and Gradko. They are composed by activated charcoal, which captures all VOCs in the targeted molar mass range by adsorption. The info-sheets for these samplers were consulted. Two options for alternative tracer gas are currently under consideration: 2-butoxyethyl acetate (EGBEA) and deuterated decane. Both present low-reactivity, usually negligible background indoor concentration, generally low toxicity and no links to chronic health effects. A preliminary field test was carried out in order to check EGBEA's measurability, and results showed insignificant background EGBEA concentration and good measurability by the Radiello® sampler. Two test chambers were also performed: TCP1 and TCP2. TCP1 tested a first option of tracer source for EGBEA; TCP2 tested a second option of source for EGBEA and decane (as proxy for deuterated decane). Results from both showed that the used sources yielded emission rates higher than targeted, but the concentration curves obtained for EGBEA in TCP1 and decane in TCP2 suggest emission rates stability. Future work includes further chamber testing in pursuit of an adequate source design and computer simulations using CONTAM software coupled to CFD to study the effects of source/samplers positioning on the accuracy of the resulting air change rate calculations.

KEYWORDS

Ventilation, air change rate, indoor air quality, tracer gas test, passive sampling.

1 INTRODUCTION

Air pollution in indoor environments has become a great concern in the last decades. People tend to spend the majority of their time indoors, where numerous known sources of substances with high potential to cause adverse effects to human health are present (Godish, 2005). Exposure to air pollution in indoor environments may be responsible for almost 2 million

premature deaths in developing countries and for about 4% of the global burden of disease (Bruce et al., 2000; Godoi et al., 2009).

A crucial factor in determining the accumulation of pollutants in indoor environments is ventilation, and its impacts on the health and comfort of occupants have long been recognized in standards and regulations (EPA, 1994). Simultaneously, ventilation is closely related to the energy efficiency of a building (Persily and Levin, 2011; Persily, 2015): the higher the building airtightness, the higher is its insulation, which saves heating/cooling costs. However, increased airtightness can also lead to lower total ventilation rates. Evidence shows that buildings with lower ventilation rates tend to present higher concentrations of indoor air contaminants (Flemish Government, 2012; 2014).

Although ventilation is critical in interpreting indoor air quality (IAQ) measurements, only few IAQ field studies report measured ventilation rates (Persily, 2015); and even when they do, the measurement methods are often not described in sufficient detail to evaluate their quality or applicability to the study design (Persily and Levin, 2011). Given the importance of ventilation in estimating pollutant sources impacts and proposing remediation actions if needed, it is crucial that IAQ assessments not only provide information on basic ventilation parameters (e.g. ventilation type, designed air change rate), but also report actual ventilation rate values, measured by means of a reliable and reproducible method.

Methods currently used for measuring ventilation rates either involve direct flow rate measurements at vent holes combined with pressurization tests, or a tracer gas dilution/dispersion test (TGT). The first type is used only under very specific circumstances, such as in extremely airtight buildings where all airflows occur mechanically in ductwork (Persily, 2015). Thus, most ventilation assessments use TGT as a method to measure the total air change rate of a building/indoor space (Persily, 2015). In a TGT, the air is marked by the injection of an easily identifiable gas and the air change rate is then inferred by monitoring the tracer emission rate and room concentration. This is a very simple and convenient method that can be carried out in occupied buildings, which allows for a greater accuracy since it takes into account the large effect occupancy has on a building's air change rate.

However, there are three important shortcomings related to TGTs. The first one is linked to the fact that most TGT techniques provide instantaneous results (due to the use of online monitors), which are very variable over time. The concentrations of indoor pollutants (also variable over time and significantly influenced by air change rate) are usually measured over a longer period using long-term sampling techniques that report time-averaged values, i.e. the link between the IAQ and the ventilation data is not direct, hindering their comparability.

The second shortcoming is connected to the substances currently used as tracer gases. Most TGTs employ sulfur hexafluoride (SF_6) or perfluorocarbons (PFTs) as tracers. Both substances are very potent greenhouse gases mentioned in the Kyoto protocol, with very long lifetimes in the atmosphere (IPCC, 20007). Therefore, even small atmospheric concentrations can have proportionately large effects on global temperatures and the release of any quantity of these substances should be avoided. Hence the importance of proposing alternative tracer gases, as it is possible that efforts to phase-out these substances may be done in the near future.

The third shortcoming is related to the perfect-mixing assumption. The application of a TGT assumes that the air in the assessed indoor space has a homogeneous spatial distribution. However, a perfect-mixing situation is rarely observed in real life, meaning that concentration levels of substances and airflows vary across the indoor space. Therefore, the placement of source/samplers can greatly impact the tracer concentrations measured and consequently the calculated air change rate. Studies show that this assumption can lead to severe bias in the air change rates measured by this method, even in single-zone measurements (Ott et al, 2002; Van Buggenhout et al, 2009; Liu et al, 2018).

Thus, a TGT which provides ventilation rates in the same timescale as the pollutant concentration measurements, uses a more adequate substance as tracer and includes a more

careful planning for placing sources/samplers to account for imperfect mixing would be more appropriate than the ones currently used. Furthermore, it is also important that the new method is suitable for use during normal occupancy, thus the TGT must not cause disturbance and the employed tracer must be scientifically proven harmless to the occupants' health. Also, a highly desirable characteristic for this new method is the non-dependence on electricity (i.e. a method based entirely on passive techniques for emitting and sampling the tracer), which lowers the utilization costs and broadens the range of buildings where it can be applied.

Taking all these desired characteristics into account, this project aims to develop a reliable and reproducible TGT using as tracer a substance that is safe for use during occupancy and that can be co-captured and co-analyzed with standard passive samplers used for common IAQ assessments. Additionally, this new method proposes the implementation of a pre-test planning phase in which the optimal physical placement of sources/samplers is determined by means of simulations, in an effort to minimize bias arising from imperfect mixing and possibly enabling the assessment of interzonal airflows.

2 MATERIALS AND METHODS

2.1 Selection of a new substance for use as tracer gas

The first step to propose this new TGT consists of finding an adequate substance to be used as a tracer, alternatively to the currently employed SF_6 and PFTs. This initial step was done by means of a comprehensive literature review. The thought process through which the literature review was carried out is explained below.

From an IAQ point of view, volatile organic compounds (VOCs) are the most relevant contaminants, since they are ubiquitous in indoor spaces, specially occupied ones, and several of them are knowingly harmful to human health (Uhde and Salthammer, 2009). This group of compounds is truly extensive and its constituents vary greatly in characteristics and properties. In IAQ assessments, such gases are sampled separately from inorganic pollutants due to their different physicochemical characteristics. The vast majority of researchers utilize passive sampling (i.e. purely diffusion-based, involving no pumps) to measure average VOCs concentration in common IAQ studies, for its simplicity, accuracy, practicality and suitability for use during normal occupancy. As one of the aimed characteristic for the new TGT is the matching timescale for air change rate and pollutant concentration measurements, the best option for a tracer is a gas which can be captured simultaneously by commercial passive VOC samplers. This approach also simplifies the process of ventilation measurement in IAQ studies, since only one sample simultaneously provides the information needed to infer both the air change rates and the indoor VOCs levels. Thus, the gases considered for use as tracer were the VOCs capable of being captured by the commercial passive VOC samplers most widely employed in common IAQ assessments. These samplers are composed by activated charcoal, in which organic gases are captured by adsorption. This process is essentially non-specific, meaning that any VOC in the targeted molar mass range may be captured and later analyzed in lab by applying the adequate extraction and analytical processes.

The information sheets for commercial passive VOC samplers were consulted. Radiello® and 3M samplers capture VOCs in the range C2-C12, and Gradko samplers capture compounds up to C28. Among the numerous VOCs in this range, paraffins initially stood out as possible candidates for use as tracer gas.

Paraffins are linear acyclic saturated hydrocarbons (alkanes). First four alkanes (methane to butane) are colorless, odorless gases at ambient conditions, C3 to C17 are colorless, nearly odorless, volatile liquids and higher alkanes are wax-like solids. Alkanes are the simplest class of organic compounds, extremely stable and inert, as they contain only carbon and hydrogen atoms (small electro negativity difference) and have no functional groups (Bano, 2007). C5-

C15 alkanes present no significant toxicological effects to humans, with the exception of n-pentanes, trimethylpentanes and n-hexanes. Alkanes of >C15 have lower vapor pressures, hindering their application as passive tracer gases (HSPA, 2015).

There is however a major problem regarding the applicability of paraffins as tracers. An ideal tracer should be absolutely absent in the ambient it is being placed. Alternatively, a tracer with non-zero background may be used provided that such background is stable and that the additional tracer concentration is significantly larger than it. Both background and added concentrations should be as low as possible in order not to oversaturate the passive sampler (when the adsorbed mass of analyte reaches the maximum capacity of the adsorbing medium, resulting in underestimation of the actual air concentration). Paraffins do not meet either of this criteria: they are largely present in the composition of a range of household products, thus their typical background concentration is significant in most indoor environments.

The option currently under consideration for use as tracer gas is the solvent 2-butoxyethyl acetate (also called ethylene glycol monobutyl ether acetate or EGBEA), mentioned by Radiello® in the VOC CS_2-desorption sampler info-sheet. EGBEA is a compound of the family of glycol ethers and has a relatively high production volume. Although EGBEA is present in various household products (ATSDR, 1999), its background indoor concentration is usually very low. A national survey for IAQ carried out in 490 French dwellings found EGBEA concentrations below the detection limit in 97% of the assessed houses (Billionnet et al, 2011). A similar assessment, carried out as part of the HABIT'AIR Nord – Pas de Calais program, monitored the presence of glycol ethers in 60 homes located in northern France, finding no trace of EGBEA in any of the assessed houses (Plaisance et al., 2008). More recently, Derbez et al. (2014) performed a field survey in 7 newly built energy-efficient houses, also in France, measuring a range of IAQ indicators and environmental parameters both before and during the first year of occupancy; EGBEA was not detected in any sample from any of the assessed houses. Regarding human health, EGBEA has generally low toxicity and has not been linked to any chronic effects (ATSDR, 1999; ECETOC, 2005; SCHER, 2006).

An alternative for EGBEA may be the use of stable isotope labeling, more specifically using deuterated compounds, not naturally present in the atmosphere or in any household product. Stable isotopes are chemical elements that occupy the same position in the periodic table, but differ in mass due to a different number of neutrons within the atomic nucleus. This difference makes isotopes analytically distinguishable yet chemically and functionally identical to the original compound (Wilkinson, 2016). Deuterium (D) is one of the most commonly used stable isotopes for tracing purposes. This approach allows revisiting the initial idea of using paraffins as tracers. Thus, the second option under consideration consists of deuterated paraffins in C8-C15 range. Deuterated decane (D-decane) is initially considered for its combination of lower flammability and higher volatility. Due to the high purchase cost of D-decane compared to EGBEA, its use as tracer gas has been considered as a backup plan in this project.

2.2 Preliminary test

A preliminary test was carried out in order to test EGBEA's measurability by Radiello® samplers in simplified field conditions. The Radiello® samplers were used to measure this compound's concentration in one room before and after the placement of a recipient containing the solvent. The room used was an office which was unoccupied at that time, although fully furnished (two desks with two chairs, two PCs, one wall cabinet and plastic blinds in the windows). Three sampling cartridges were used in total for this test: one as a lab blank, i.e. analyzed right out of the package; a second cartridge was used to measure the background EGBEA concentration in the office; the third and last cartridge was used to measure the air concentration of EGBEA after the placement of a source of this solvent in liquid phase. This so-called source consisted of a simple glass beaker filled with approximately 11 ml of EGBEA

(9.536 g) left uncapped so the solvent could freely volatilize into the room air, acting therefore as a completely passive source. Both these samplers were exposed in the room for a period of consecutive 4 days. Figure 1 shows the setup of the experiment.

Figure 1: Preliminary test setup

2.3 Chamber tests

To this date, two chamber tests (TCP1 and TCP2) were performed to evaluate the behavior of EGBEA when released from a source to the air under standard and constant conditions. From that baseline, it will then be possible to compare the substance's behavior under varying conditions and circumstances in future chamber tests. Testing under standard/constant conditions also enables the determination of the concentration curve of the tracer, allowing to know when it will reach steady state.

Efforts for determining this baseline started in the Test Chamber Phase 1 (TCP1), in which liquid phase EGBEA was added to a glass recipient with an adjustable cap and then used as tracer source inside the test chamber. The test chamber used in TCP1 was a 117 dm^3 steel chamber, with temperature, relative humidity and air change rate set to constant standard conditions (23°C, 50% and 0.5 h^{-1}, respectively, according to ISO 16000-9). Three different measurement methods were used simultaneously to measure EGBEA concentrations in the chamber: passive sampling (Radiello® tubes, solvent desorption), active sampling (Tenax® tubes, thermal desorption) and online monitoring (with a flame ionization detector - FID). Figure 2 shows the chamber setup right before the beginning of the experiment. TCP1 had a whole duration of 8 hours, during which the FID was used to monitor the EGBEA concentration.

The FID measures the air concentration of total hydrocarbons (THC). In TCP1, since the airflow provided to the chamber was completely clean of THC and there was no other source of VOCs inside the chamber, the THC concentration measured was equivalent to the EGBEA concentration originating from the source placed inside the chamber. In order to determine specifically the absolute EGBEA concentration as the experiment proceeded, Tenax® tubes were used to collect one air sample each hour, and 2 Radiello® samplers were placed together inside the chamber. Both Tenax® and Radiello® samplers were analyzed by means of gas chromatography with mass spectrometry detection, which allows to differentiate between different VOCs and thus to confirm that the signal detected by the FID is in fact due to exclusively EGBEA presence. While the Radiello® sampler is passive and provides long-term averages, the Tenax® tubes need a pump for sampling and provide short-term averages. In TCP1, Tenax® samples were taken in 8 moments (the first before the source placement, for a chamber baseline concentration), one per hour, for a period of around 30min each. This sampling period was determined by the sampling pump flow and by the maximum volume of air that can be sampled by the tube. The Radiello® samplers, on the other hand, were placed

inside the chamber at the same time as the source and remained there until the chamber was opened, 3 days later.

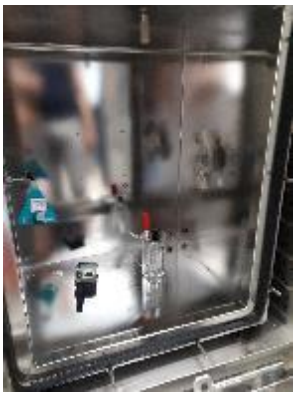

Figure 2: Setup of TCP1

A second phase of chamber testing was then carried out as a re-test of TCP1, under the same conditions. This re-test was called Test Chamber Phase 2 (TCP2) and its planning took into account some shortcomings observed in TCP1. The setup of TCP2 is shown in Figure 3.

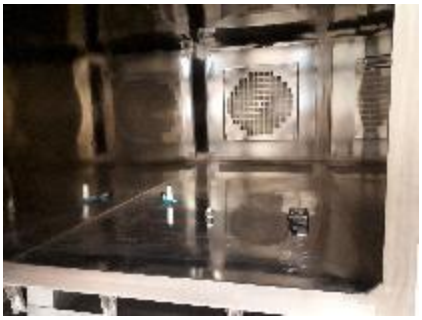

Figure 3: Setup of TCP2

There were four main differences between TCP1 and TCP2: 1) the glass recipient used as source in TCP1 was substituted by a different one in TCP2 (Figure 3), in an attempt to lower the tracer emission rate; 2) a bigger chamber was used in TCP2 (WEISS chamber, 1000 dm^3), to enable an increase in the airflow rate (to dilute more the tracer, in case the emission rate from the new source remained high) while still maintaining the same air change rate from TCP1; 3) the FID monitor yielded results below the detection limit due to a misconfiguration, thus no continuous FID data is reported for TCP2; and 4) two tracer options were tested, first EGBEA and then D-decane (in fact, normal decane was used as a proxy for D-decane, as an economy measure).

The EGBEA source was tested first, and then the decane source. Both tests lasted 3 days, with 8 Tenax® samples taken for each. In the EGBEA test, 1 sample was taken as blank, the following 6 were taken one per hour on the first day, and 1 was taken after 72h. In the decane test, 1 sample was taken as blank, the following 5 were taken one per hour on the first day, 1 was taken after 51h and 1 was taken after 70h. One Radiello® sample was taken per test, for a period starting with the tracer source placement and running until the reopening of the chamber at the end of the tests.

3 RESULTS AND DISCUSSION

3.1 Preliminary test

Results from the preliminary experiment are presented in Table 1.

Table 1: Preliminary field test results

Sample	Sampling start	Sampling finish	EGBEA mass
Lab blank	-	-	0,067
Background	15/01 – 17h25	19/01 – 17h39	0,059
With EGBEA source	19/01 – 17h40	23/01 – 17h34	3,324

Based on the values presented in Table 1, the background EGBEA concentration in the assessed room can be considered insignificant: the EGBEA mass desorbed from the cartridge placed before the recipient placement (background) was very similar to the mass desorbed from the blank cartridge, even slightly lower, meaning that virtually no EGBEA was adsorbed onto the cartridge. Furthermore, the relatively low volatility of EGBA (0.23 g evaporated in 4 days) did not hinder its measurability by the Radiello® sampler: the cartridge placed in the room after the addition of the EGBEA source adsorbed an EGBEA mass two orders of magnitude higher than the blank and background cartridges. The calculated average concentration in air corresponding to the adsorbed mass after 4 days exposure to the EGBEA source was 14.1 µg m^{-3}. The results observed in this primary experiment can be interpreted as clear indications of the potential suitability of EGBEA as tracer for the purposes of a new TGT approach: its background concentration in the assessed room was negligible and it was successfully captured by a commercial VOC sample at a measurable level.

3.2 Chamber tests

Figure 4 shows the results measured by the FID monitor during TCP1. Note that the FID acquisition started running approximately 30 minutes before the source placement, in order to have a background measurement.

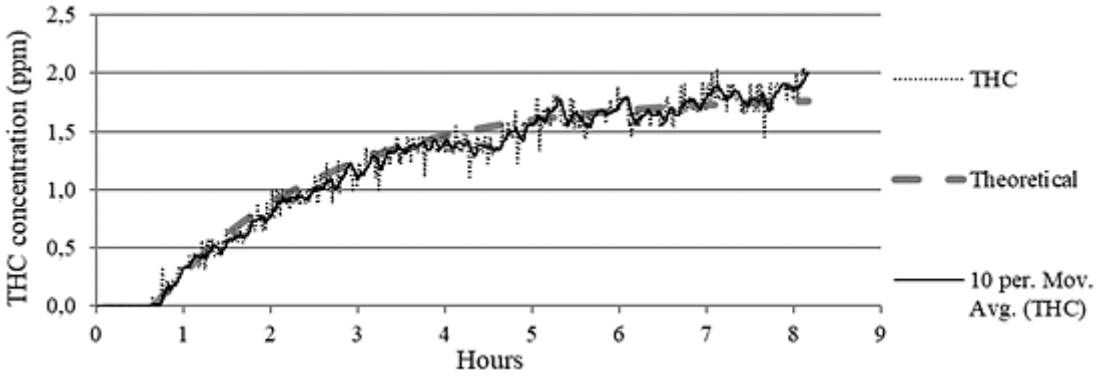

Figure 4: Results measured by the FID monitor during TCP1.

Results measured by the FID monitor presented a high noise signal even after smoothing (10 points moving average line), as it can be seen in Figure 4. The most likely reason for that is the fact that the sampling flow from the chamber to the FID had to be combined with another (clean) airflow in order to reach the working FID inlet flow. To reach the intended air change rate in the chamber, the inlet flow to the chamber had to be set at 1 l min^{-1}, the exact same as the inlet flow needed in the FID. Since the outlet flow from the chamber must correspond to less than 80% of the inlet flow, in order to maintain the equilibrium conditions inside the chamber (ISO 16000-9), the addition of an "extra" flow had to be done. This combination of flows implicates in 2 additional uncertainties: 1) the mixing may not be perfect and 2) the resulting concentration may be too diluted for the FID monitor. Nevertheless, the FID measurements followed the theoretical concentration trend quite well. The theoretical concentration ($C(t)$) of an emitted substance in a test chamber is given by:

$$C(t) = C_0(1 - e^{-Nt}) \quad (1)$$

In which C_0 is the substance concentration when it reaches steady state and N is the air change rate. Thus, even though the FID response was noisy, it can be considered realistic.

The analysis of the Tenax® and Radiello® tubes showed that the concentration of EGBEA inside the chamber was too high for the calibration curve ranges normally used. In the case of the Radiello® samples, it was possible to dilute them for reanalysis, which revealed a very high 3-day average EGBEA concentration in the chamber (1690 µg m^{-3}). The Tenax® samples could not be diluted for reanalysis due to the destructive nature of the thermal desorption process. The results obtained from both types of passive samplers cannot be trusted because 1) the calibration curve used was in a much lower range and 2) it is likely that the samplers oversaturated during the sampling period, incurring in the breakthrough effect (in which target substances present in the subsequent inlet flow are not captured by the sampler, yielding a result lower than the real one). These high passive sampling results, along with the also very high FID results (which reached values surpassing 13000 µg m^{-3}), indicate that the emission rate of the used source was too high for a TGT. Thus, the planning for TCP2 included the substitution of the source.

Figure 5 shows the results obtained with the Tenax® samplers in both test, with the EGBEA source and then with the decane source.

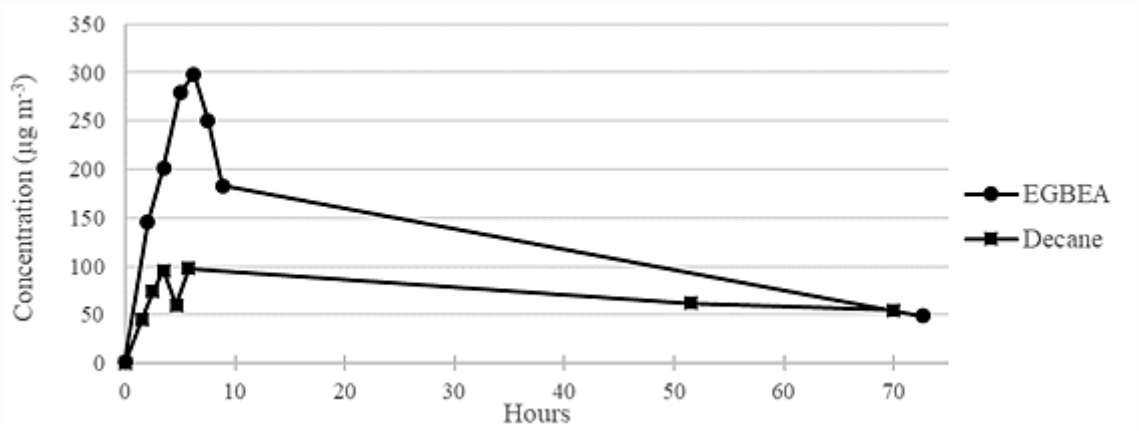

Figure 5: Results obtained with Tenax® samplers in TCP2.

In TCP2, the concentration levels reached inside the chamber were much lower than in TCP1. However, the EGBEA concentration curve deviated considerably from the expected pattern, raising rapidly in the initial 7 hours and then decreasing also rapidly in the following couple of hours. The last sample, taken after 2 days, shows that the concentration decrease deaccelerated, but the lack of samples in this in-between period does not allow to determine if a steady state was reached. Nevertheless, the shape of the EGBEA concentration curve itself indicates that either the emission rate of the source was not constant or there was a strong and variable sink system inside the chamber. Since the WEISS is a standard stainless-steel chamber specifically developed for source testing and the same problem was not observed in the decane test, it is more likely that the recipient used as EGBEA source was not able to hold a constant emission rate. The recipients used as decane and EGBEA sources were initially considered to be identical, but the different concentration curves show that in fact they are not.

The Radiello® samplers yielded average 3-day concentrations of 71.8 and 949 µg m^{-3} for EGBEA and decane, respectively. The EGBEA result makes sense if we assume that the last Tenax® sample represents the steady state concentration and that such concentration was reached not long after the 7th sample was taken. On the other hand, the decane concentration was extremely high compared to the Tenax® results, indicating a possible contamination of the Radiello® sample. Moreover, the analysis results from the GC-MS showed that the Radiello® samples yielded peaks with areas above the linearity range of the calibration curve, meaning

that the calculated concentrations should be considered with care, similarly to TCP1. Next chamber tests will employ a different source to lower the emission rate even more, and will use actual D-decane instead of decane as a proxy, to avoid possible contamination.

4 CONCLUSIONS

A TGT employing as tracer a harmless gas which is not commonly present in background indoor air, can be passively captured by commonly used commercial passive samplers and then co-analysed along with common IAQ pollutants is close to an ideal method to measure total average air change rate. Currently, EGBEA solvent and deuterated decane are considered as possible tracer candidates. A preliminary field test and two chamber tests were performed to evaluate the applicability of these substances as tracers, with promising results. Efforts will be continued with further chamber tests in pursue of an adequate source design. Future work also includes simulation of TGTs in imperfectly-mixed zones using CONTAM software coupled to CFD, in order to study the effects of source/samplers positioning on the accuracy of the resulting air change rate calculations.

5 REFERENCES

ATSDR - Agency for Toxic Substances and Disease Registry (1998) *Toxicological profile for 2-butoxyethanol and 2-butoxyethanol acetate.* U.S. Department of Health and Human Services, Atlanta, Georgia, 404 p.

Bano, S. (2007) *Alkanes, Alkenes, Alkynes, Alkyl Halides, Alicyclic Hydrocarbons, Alcohols, Ethers and Epoxides, Aldehydes and Ketones, Carboxylic Acids and their Functional Derivatives.* Jamia Hamdard, Department of Chemistry: NSDL project, NISCAIR. Chapter I.

Billionnet, C.; Gay, E.; Kirchner, S.; Leynaert, B.; Annesi-Maesano, I. (2011) Quantitative assessments of indoor air pollution and respiratory health in a population-based sample of French dwellings. *Environmental Research*, 111: 425-434.

Bruce, N.; Perez-Padilla, R.; Albalak, R. (2000) Indoor Air Pollution in Developing Countries: A Major Environmental and Public Health Challenge. *Bulletin of the World Health Organization*, 78(9).

Derbez, M.; Berthineau, B.; Cochet, V.; Lethrosne, M.; Pignon, C.; Riberon, J.; Kirchner, S. (2014) Indoor air quality and comfort in seven newly-built, energy-efficient houses in France. *Building and Environment*, 72: 173-187.

ECETOC - European Centre for Ecotoxicology and Toxicology of Chemicals (2005) *Technical report no. 95:* The toxicology of glycol ethers and its relevance to man. Volume I, 4th edition. Brussels, Belgium, 207 p.

EPA - U.S. Environmental Protection Agency. (1994) *Indoor air pollution: An Introduction for Health Professionals.* In association with: American Lung Association, the American Medical Association, The U.S. Consumer Product Safety Commission, and the U.S. Environmental Protection Agency. Available at: http://www.epa.gov/iaq/pubs/hpguide.html.

Flemish government. (2012) *Clean Air, Low Energy – Exploratory research on the quality of the indoor environment in energy efficient buildings: the influence of outdoor environment and ventilation*. VITO NV.

Flemish government. (2014) Renovair – *Explorative study on the quality of the indoor environment in buildings after (energy-efficient) renovations*. VITO NV.

Godish, T. (2005) *Air Quality*. Lewis Publisher, 4th edition.

Godoi, R. H. M.; Avigo Jr, D.; Campos, V. P.; Tavares, T.M.; de Marchi, M. R. R.; Van Grieken, R.; Godoi, A. F. L. (2009) Indoor Air Quality Assessment of Elementary Schools in Curitiba, Brazil. *Water, Air & Soil Pollution: Focus*, 9(3-4): 171-177.

HSPA - Hydrocarbon Solvents Producers Association (2015) *Background Documentation in Support of RCP Proposal*. Brussels.

IPCC - Intergovernmental Panel on Climate Change. (2007) 2.10.2 Direct Global Warming Potentials. Climate Change 2007: Working Group I: The Physical Science Basis.

Liu, Y.; Misztal, P. K.; Xiong, J.; Tian, Y.; Arata, C.; Nazaroff, W. W.; Goldstein, A. H. (2018) Detailed investigation of ventilation rates and airflow patterns in a northern California residence. *Indoor Air*, v. 28, p. 572-584. DOI: 10.1111/ina.12462

Ott, W.; McBride, S.; Switzer, P. (2002) Mixing characteristics of a continuously emitting point source in a room. *Proceedings: Indoor Air 2002*.

Persily, A. K. (2015) Field measurement of ventilation rates. *Indoor Air 2016*, 26: 97-111.

Persily, A. K. and Levin, H. (2011) Ventilation measurements in IAQ studies: problems and opportunities. In: *Proceedings of Indoor Air 2011*, 12th International Conference on Indoor Air Quality and Climate.

Plaisance, H.; Desmettres, P.; Leonardis, T.; Pennequin-Cardinal, A.; Locogea, N.; Galloo, J.-C. (2008) Passive sampling of glycol ethers and their acetates in indoor air. *Journal of Environmental Monitoring*, 10: 517–526

SCHER - Scientific Committee on Health and Environmental Risks (2006). *Risk Assessment report on 2-buthoxyethanol acetate.* Health & Consumer Protection Directorate-General, European Comission.

Uhde, E.; Salthammer, T. (2009) *Organic Indoor Air Pollutants*. 2nd Edition. WILEY-VCH Verlag GmbH & Co. KGaA, Weinheim. ISBN: 978-3-527-31267-2

Van Buggenhout, S.; Van Brecht, A.; Eren Özcan, S.; Vranken, E.; Van Malcot, W.; Berckmans, D. (2009) Influence of sampling positions on accuracy of tracer gas measurements in ventilated spaces. *Biosystems Engineering*, v. 104, p. 216 – 223. DOI: 10.1016/j.biosystemseng.2009.04.018

Wilkinson, D. J. (2016) Historical and contemporary stable isotope tracer approaches to studying mammalian protein metabolism. *Mass Spectrometry Reviews*, v. 37, p. 57–80.

Measuring the ventilation rate in occupied buildings and adapting the CO_2 tracer gas technique

Jessica Few*[1] and Clifford Elwell[1]

UCL Energy Institute
London
WC1H 0NN, UK
** Corresponding author: jessica.few.16@ucl.ac.uk*

ABSTRACT

Measuring ventilation rates in occupied dwellings is challenging but represents the conditions that occupants experience. This paper explores the constraints of existing methods when measuring the ventilation rate of occupied buildings and proposes a new method addressing some of them.

Ventilation rates in occupied buildings can change over short time scales due to changes in weather or window and door positions. PFT based methods measure average ventilation over an extended period. Similarly, an annualised ventilation rate based on the '20th rule of thumb' can be approximated using pressurisation tests. It is unclear how the results relate to the ventilation rate under any specific conditions. Conversely, measurement periods of less than an hour are possible with tracer gas techniques.

The spatial scale over which ventilation is measured is important. Whole dwelling estimates are obtained from pressurisation tests and tracer gas methods if the whole dwelling is dosed. In both cases internal doors must be open, affecting the airflow, which may or may not reflect the occupied configuration. Differences between whole dwelling and in-use ventilation could be important for IAQ and heat loss. Single zone tracer gas techniques have been applied to one room and assumed to represent the whole dwelling. Multi-zone methods using several different gases are not usually applied in occupied buildings because of the complexity of the experimental set-up.

Measurement techniques must be acceptable to occupants. Pressurisation tests are minimally disruptive, taking less than an hour. PFT measurements are unobtrusive, only requiring small sources and sorption tubes. Injection of tracer gases, such as SF_6, and concentration measurement can require pumped gas sampling which is noisy and bulky, causing inconvenience to the occupants. Metabolic CO_2 based methods do not require the injection of gas or pumped sampling and may be more acceptable to occupants.

CO_2 decay techniques require knowledge of occupancy; historically this has relied on occupant reports, assumed hours of occupancy, or hand-picked sections of data. Similarly, CO_2 equilibrium or accumulation techniques require knowledge of the CO_2 generation rate and occupant activities.

A new approach has been developed to address some of these issues, based on metabolic CO_2 tracer gas decay. An algorithm for identifying when a dwelling is occupied has been developed, agreeing with reported occupancy in 87% of cases, meaning that large volumes of data can be analysed automatically. CO_2 is measured in each room every 5 minutes, meaning that sub-hourly variations in ventilation rate, and variation between rooms, can be explored. Proximity sensors are used to monitor windows and doors, so that ventilation can be calculated during periods with constant conditions, and variation due to different configurations can be investigated. The proposed method represents a step towards appropriate measurement of ventilation and its variation in occupied buildings.

KEYWORDS

Ventilation, ventilation measurement, tracer gas, occupancy, occupied buildings

1 INTRODUCTION

Through the Paris Agreement, 185 countries have agreed to make efforts to tackle climate change (UNFCCC, 2015). Limiting excess ventilation improves the thermal efficiency of buildings; ventilation can account for 50% of the primary energy used in a UK dwelling (CIBSE, 2015). However, sufficient ventilation is required to maintain adequate indoor air quality (IAQ) in occupied buildings (Persily, 2006). Poor IAQ has been associated with various health implications, including: asthma, allergies, cancers, 'sick building syndrome' and respiratory tract infections (Sundell *et al.*, 2011). Fisk (2018) reviewed the literature and

concluded that there is likely to be an association between low ventilation rates and poor health outcomes. Additionally, the ventilation rate that the occupant experiences is likely to affect their thermal comfort and use of air conditioners (Iwashita and Akasaka, 1997).
Occupants can significantly influence the ventilation rate in their homes through their practices of window and door opening (external and internal) and use of mechanical ventilation (Kvisgaard and Collet, 1990). However, characterising the ventilation occupants experience is challenging due to the spatial and temporal variability of ventilation rate and the acceptability of the technique to the occupants. This can mean that it is difficult to understand the ventilation rates that the occupants are likely to experience.
This paper explores some of the challenges of measuring ventilation in occupied buildings, and suggests a method which addresses some of them. The following section reviews some of the issues with current ventilation measurement methods when used in occupied buildings, Section 3 introduces the proposed method, and describes the algorithm that has been developed to determine when a building is occupied, and the results of combining the measurement method and the occupancy algorithm. Section 4 discusses the strengths and weaknesses of the proposed method. Finally, Section 5 provides the conclusions and implications.

2 VENTILATION MEASUREMENT IN OCCUPIED BUILDINGS

Measurement of ventilation in occupied buildings can be complicated by factors including the weather, its spatial variability and the influence of occupants. These aspects are reviewed in relation to the most common methods used to characterise ventilation in this section.

2.1 Time Scale of Measurement

The ventilation rate estimated from a measurement is specific to the time for which the measurement took place. However, the weather conditions and building configuration will vary in occupied dwellings, thus the estimated ventilation rate only holds for the conditions during which the measurement took place (Persily, 2016). For example, changes in window or internal door position may alter the ventilation rate significantly, weather conditions particularly affect naturally ventilated buildings. Measurements taken in a specific configuration cannot easily be extrapolated to different conditions.
Methods to estimate ventilation may be broadly categorised as those which provide an average rate over a long duration (days to months), and those that provide a shorter-term ‘snapshot’ of the ventilation rate. Those methods estimating a long term ventilation rate are valuable in estimating the overall conditions in the space, but cannot distinguish the impact of factors such as door and window opening. This combined with the intermittent occupation of specific spaces by occupants means it can be challenging to interpret occupant exposure to pollutants using these methods. The physical interpretation of the calculated rate is also unclear in using these methods (Sherman, 1990). Perflourocarbon tracer gas methods (PFT) are commonly used to measure the average tracer gas concentration over varying time scales, examples range from two days (Bornehag *et al.*, 2005) to a month (Bekö *et al.*, 2016). In analysis of this data a constant ventilation rate over the period of measurement is assumed.
Another common method for estimating the average ventilation of a building is the ‘rule of thumb’ that the air change rate measured at 50 Pa divided by 20 is a rough estimate of the annualised air change rate under ‘normal’ conditions. Sherman (1998) stresses the limitations of this given the influence of variations in weather conditions and dwelling characteristics. Liddament (1996) suggests this can be particularly problematic for naturally ventilated buildings as the instantaneous ventilation rate can deviate significantly from the average.
Other methods provide a ‘snapshot’ of the ventilation rate in a space and specific configuration over a limited duration (minutes or hours). These may be useful to identify exposure to pollutants under specific conditions, but give relatively little information about general ventilation in a building. They are challenging to interpret if information about the weather,

doors and windows is missing (Persily, 2006). Tracer gas methods may be used to estimate the ventilation rate from the rate of release required to produce constant concentration, from its rate of accumulation given a known rate of release, or from its rate of decay. Tracer gas concentration is usually monitored over approximately 1-2 hours, assuming the ventilation rate to be constant over this period. Compared to the long term techniques above, the ventilation rate is much more likely to be stable on this shorter time scale. However, changes in doors, windows or operation of a ventilation system could still alter the ventilation rate significantly during the measurement period and the contextual information required to interpret such ventilation rates is considerable. Additionally, the relation of such estimated ventilation rates to those in different building configurations and weather conditions is not clear and may require extensive measurement and analysis to understand.

The number of measurement repeats carried out under different conditions varies considerably in the literature. Wallace, Emmerich and Howard-Reed (2002) carried out ventilation measurements every 2 to 4 hours in an occupied house over a year. They recorded weather conditions and fan use, but window use was inconsistently recorded and internal doors were not mentioned. A measurement period this long is extremely unusual, most measurements of ventilation rates using non-PFT tracer gas methods last less than a week (Guo and Lewis, 2007; Sharpe *et al.*, 2015; Keig, Hyde and McGill, 2016). Apart from Wallace, Emmerich and Howard-Reed's extremely extended study (whose method is unlikely to be acceptable to many building occupants, see section 2.3), little research has been published addressing the variation in ventilation rates of buildings, which may only be investigated using techniques requiring a short measurement duration.

2.2 Spatial Scale of Measurement

Air flows within buildings may be complex; dependent on the configuration of walls, the opening of internal doors and furniture. In addition, the air exchange with outdoors may be through both planned and unplanned ventilation paths. As a result, ventilation rates of different spaces within the building can be variable, due to the changes in door and window opening, amongst other factors. The IAQ may therefore vary substantially across the spaces that are occupied, resulting in an exposure to pollutants in individual spaces that may not reflect the whole house ventilation, or that in different rooms (Persily, 2006). It can also impact the thermal comfort of occupants and their consequent actions, for example in particularly still parts of a building occupants may increase their use of cooling in the summer (Iwashita and Akasaka, 1997), or in particularly draughty parts of the building may increase their use of space heating in the winter.

Some ventilation measurement methods are applied to the whole dwelling, such as the n/20 rule of thumb, which assumes that the building can be adequately described as a single zone (Sherman, 1998). Multiple blower doors can be used to characterise different parts of buildings, but this is uncommon and air leakage between internal spaces is challenging to characterise.

Single-zone tracer gas experiments can also be used to estimate whole building ventilation rates. A uniform concentration of tracer gas throughout the building is required (ASTM, 2011), meaning that internal doors are opened, which may alter the conditions compared to those experienced when the building is in use (Keig, Hyde and McGill, 2016). Fans are often used to ensure that uniform concentrations are achieved. However, Liddament (1996) suggests that fans should not be used if the aim of the measurement is to understand air quality, since areas of poor mixing are important in this context.

Multi-zonal tracer gas analysis can be used to investigate the effect of interzonal flows (e.g. Penman and Rashid, 1982; Smith, 1988; Harrje *et al.*, 1990). However, the analysis and experimental set-up is much more complex than for single zone measurements and this method is rarely carried out (Persily, 2006).

The ventilation rate of single rooms is often used to provide insight into IAQ and the exposure of occupants to pollutants. For example, Guo and Lewis (2007) and Sharpe *et al.* (2015)

measured a single room and assumed this to be representative of the whole building. However, in such cases the airflow between internal spaces has not been accounted for and the resultant estimate of the ventilation rate does not represent the indoor-outdoor ventilation (Persily, 2006). The complexity of airflow through and between spaces in buildings, and the resultant limitations in estimating and interpreting a ventilation rate to provide insight into the conditions experienced by occupants, is challenging and depends on the desired insights of the study. Averaging the ventilation over an entire building means that the ventilation the occupant experiences is unlikely to be understood, given that occupants will tend to move around rooms and close doors. However, it is technically challenging to adequately account for interzonal flows such that measurements can be taken in the building configuration that the occupant experiences.

2.3 Invasiveness of Equipment

The inconvenience associated with a measurement technique will likely influence how long people will tolerate its presence in their building. This section briefly reviews the invasiveness of different methods to estimate the ventilation rates of properties.

Pressurization tests can usually be completed in less than an hour and do not require any equipment to be left in a building. During testing occupants cannot use an external door and the test is noisy; however, they have been used in many studies of occupied buildings (e.g. Oreszczyn *et al.*, 2005).

Tracer gas methods are likely to vary in their acceptability to occupants. PFT equipment is small and silent so may be acceptable to occupants. Use of a safe tracer gas is essential, and using CO_2 (particularly metabolically generated) is likely to be more acceptable than other gases as it is naturally present in the air and does not involve the release of any gas for the purpose of measurements – a key motivation for the development of this method by Penman and Rashid (1982). CO_2 can be measured using NIR sensors, these are not excessively large and are silent so may be acceptable to occupants. By contrast pumped gas sampling requires tubes to be distributed around the building, increasing the spatial and visual burden to the occupant, as well as being noisy. Wallace, Emmerich and Howard-Reed (2002) used pumped gas sampling for a year, but this research took place in the home of one of the authors; recruitment of non-researcher participants may be challenging for an extended campaign with this method.

In order to ethically conduct ventilation measurements in occupied buildings, participants must be aware of any disruption likely to be caused, and must find this acceptable for the duration of the research. Less invasive techniques may be acceptable to a greater proportion of people, for example pressure testing may be more widely accepted than tracer gas experiments, but the insights gained may be reduced.

2.4 Knowledge of Periods of Occupancy

It is often important for the interpretation and analysis of measurements to know the times a building is occupied, this is essential for CO_2 based methods. However, methods to determine the occupancy status of dwellings during ventilation measurements have not been widely published. Guo and Lewis (2007) suggest that the difficulty in accurately determining when a dwelling is occupied is one of the reasons that there are few examples in the literature of the use of metabolic CO_2 as a tracer gas. In Guo and Lewis' study decay periods identified using an occupant-reported daily log-sheet; occupant diaries may not always be accurate and they increase the burden of the occupant participating in the research (Bryman, 2004). Roulet and Foradini (2002) monitored a single office-room and manually identified periods of decaying CO_2, implying that prolonged periods of decreasing CO_2 can be interpreted as indicating that there were no occupants present. However, this does not account for the possibility of leakage

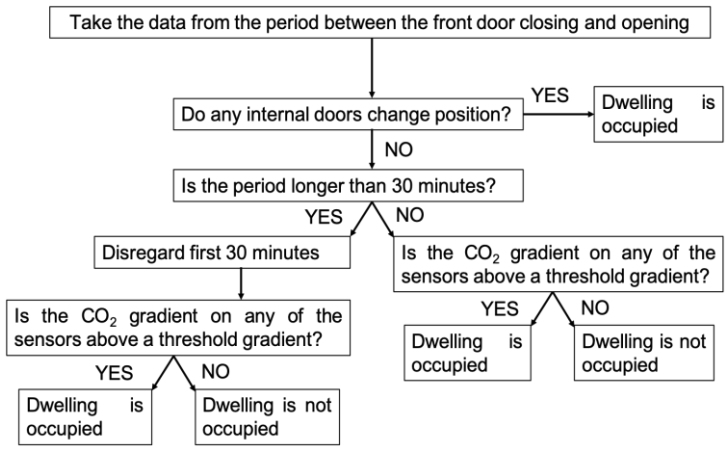

Figure 1. Flow chart of the decision making of the occupancy algorithm.

between zones and manual identification of unoccupied periods is a laborious process for long monitoring campaigns.

3 DEVELOPING A NEW TECHNIQUE TO ESTIMATE VENTILATION RATE

A new method has been developed, which refines the application of the CO_2 tracer gas decay method using metabolically generated CO_2. It is essential that the periods when the building is unoccupied are reliably known with this method; to achieve this state sensing of doors and windows is combined with an algorithm to determine the occupancy state.

The state of doors and windows was measured using binary magnetic contact sensors which record when a door or window is open or closed. Not only are these data required to determine occupancy, they also aid understanding of the configuration of the building during the unoccupied measurement. Additionally, measurements of the weather conditions and internal temperatures support the interpretation of the results.

3.1 Developing an algorithm for determining building occupancy

As discussed in Section 2.4, the ventilation literature has relatively few examples of methods for determining when a building is occupied. Where building occupancy has been recorded this has tended to be through occupant diaries, or by hand-picking sections of data for analysis.

Chen, Jiang and Xie (2018) reviewed the literature on determining occupancy in buildings, finding that different sensors have different results are often obtained when different sensors are combined. Dedesko *et al.* (2015) used beam-break sensors in an attempt to count the number of people passing in or out of the room. They also measured CO_2 concentrations and used estimated CO_2 generation rates to determine whether a beam-break event was associated with someone entering or leaving the room.

The algorithm developed in this research can be used to filter the data collected from the occupied buildings so that only those times which are identified as unoccupied are used in ventilation rate calculations; it is based on similar principles to the Dedesko method. The algorithm is based on the logic that if any of the internal doors or windows change state between the front door closing and the next time it opens, then the building must be occupied during that period. If none of the doors or windows change position, then the CO_2 concentration gradient is tested on the basis that if the CO_2 rises significantly then the building is highly likely to be occupied (or another significant source of CO_2 is present, which precludes use of the decay method). The first 30 minutes of data after the front door closes are disregarded if the period under investigation is sufficiently long to allow some stabilisation of the airflow. This ensures that if the door to a room with a high concentration of CO_2 is opened shortly before the building becomes unoccupied and causes the concentration of CO_2 to rise in adjacent rooms, this period isn't falsely identified as occupied. The flow chart in Figure 1 shows the decision making process used by the algorithm.

3.2 Testing the occupancy algorithm

A case study monitoring campaign was set-up in an occupied flat to provide data for developing the occupancy detection algorithm. The flat was monitored between February and July 2018. Three adults lived in the flat and it was unoccupied for several hours most days as all of the occupants worked full-time. CO_2 sensors were placed in every room except the bathroom. Door

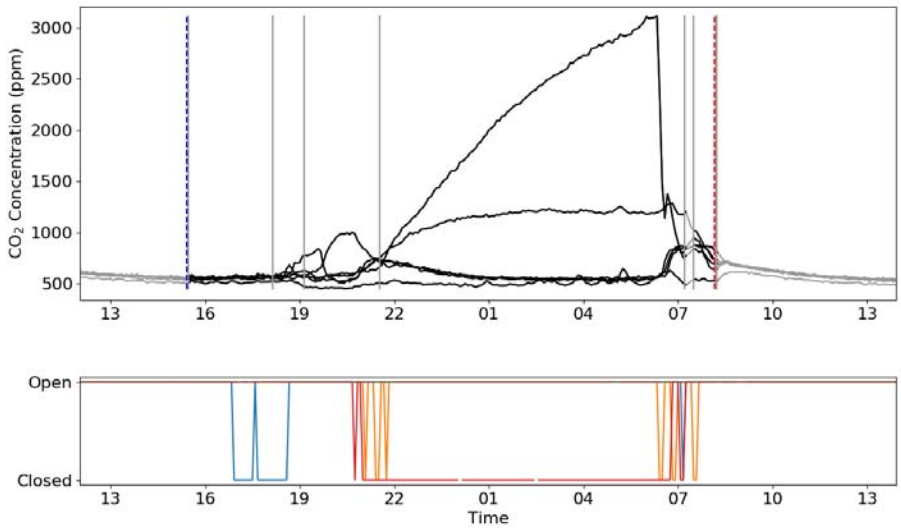

Figure 2. Example of the occupancy algorithm identifying the time at which the dwelling became occupied and unoccupied. The top part of the graph shows the measured CO_2 concentrations in each of the rooms, with the black sections of the CO_2 data indicate that the space has been identified as occupied. The grey vertical lines indicate the front door opening and closing. The blue (red) dashed vertical line indicates that the occupant reported the beginning (end) of the occupancy. The bottom part of the graph shows the internal doors changing between open and closed.

sensors were placed on all doors. The internal door sensors recorded the state (open or closed) every 5 minutes (state monitoring), whereas the front door sensor recorded every time the door opened or closed (event monitoring). The occupants were asked to record when the last person left the dwelling (occupancy ends) and when the first person entered the dwelling (occupancy begins). There were 62 reported start or end of occupancy times. Figure 2 shows an example of a reported occupancy start and end time with the door opening data and CO_2 concentrations in the dwelling.

The occupant records were compared to the results from the algorithm and these were in agreement in 87% of cases. To calculate this agreement the following logic was used: when the period before the occupant reported a start of occupancy event was identified by the algorithm as unoccupied this counted as one event of the algorithm correctly estimating the occupancy. Similarly, when the period after the occupant reported start of occupancy was identified by the algorithm as occupied this counted as another event of the algorithm correctly estimating the occupancy (and vice versa for end of occupancy data). The percentage of agreement was then calculated.

Disagreements between the occupant records and algorithm were investigated through detailed study of all the measured parameters. In some cases it is likely that the disagreement was due to window opening – the temperature rapidly dropped but the CO_2 did not rise. This highlights the need for window sensors to improve the algorithm performance. In other cases, the front door was in frequent use (likely because the occupants were arriving or leaving for work at similar times), in 10 of the 16 cases of disagreement the front door was opened with a frequency of more than 30 minutes. Since the door and window state was recorded every five minutes, the algorithm was sometimes unable to identify these periods as occupied; use of event logging equipment will resolve this issue. By recording windows and using event logging, the agreement would likely have been at or above 95%.

3.3 Measuring the ventilation rate

Calculation of the ventilation rate is based on the single zone approximation of the continuity equation in which no sources are present (Sherman, 1990):

$$CO_{2,Diff}(t) = CO_{2,Diff}(t = 0)\exp(-A.t) \quad (1)$$

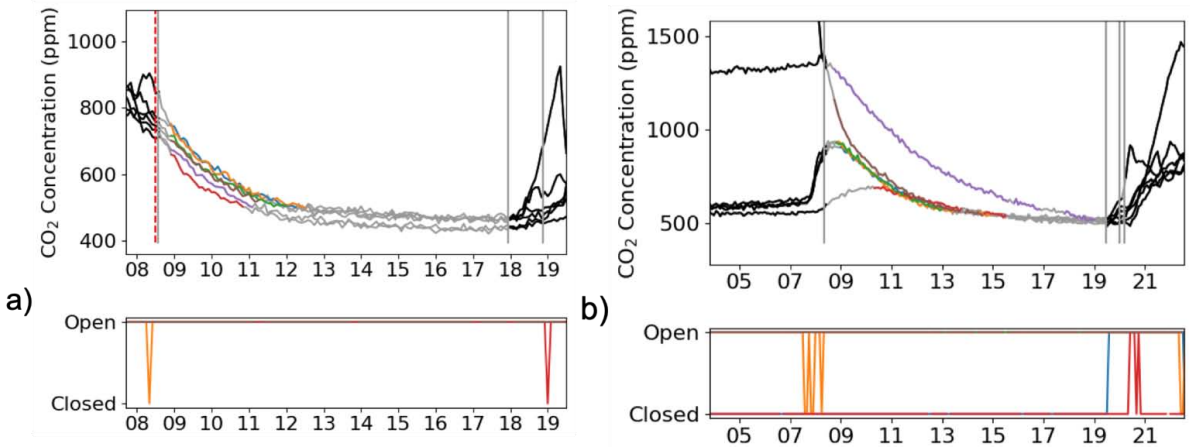

Figure 3. Examples of data collected in the test dwelling. The top part of each figure shows the CO_2 concentration against time of day in each room: occupied periods are shown in black, data suitable for decay analysis are shown in colour. The grey vertical lines show when the front door opened and closed. The bottom part of each graph shows the internal door states. In part a) all the internal doors are open and in figure b) some doors are closed.

Where $CO_{2,Diff}(t) = CO_{2,int}(t) - CO_{2,ext}(t)$, $CO_{2,int}(t)$ is the indoor CO_2 concentration, $CO_{2,ext}(t)$ is the outdoor CO_2 concentration, $CO_{2,Diff}(t = 0)$ is the concentration difference at the start of the decay period, A is the air change rate, and t is the time since the start of the decay.

Figure 3a shows an example of the data collected to test the occupancy algorithm: the transition from occupied to unoccupied and subsequent decay in CO_2 concentration can be seen. In this case, all internal doors were open and the CO_2 concentrations are closely matched in all rooms. In this case, $CO_{2,int}(t)$ would be the mean of the internal concentrations, as dwelling is behaving as a single zone.

Figure 3b shows a second example in which two of the rooms have their door closed. The CO_2 concentration decay is clearly different in different rooms. In this case, the dwelling does not behave as a single zone, so a single ventilation rate does not adequately describe the internal conditions, and the mean internal concentration should not be used in estimating the ventilation rate. However, the CO_2 concentration decay in different rooms can be used to estimate the ventilation rate in those rooms, with a systematic bias in a known direction. This is a significant advantage over measurements in which only a single room is measured, or in which the whole house is treated as homogenous. In this example, one room has higher CO_2 concentration throughout the decay (shown in purple). This room has a lower ventilation rate than the other rooms. To estimate the ventilation rate in this room $CO_{2,int}(t)$ would be the CO_2 concentration in this room only. The single room ventilation rate calculated would systematically larger than the 'true' indoor-outdoor ventilation rate of this room, because some of the reduction in CO_2 is likely due to air exchange with the other areas of the building.

Conversely, any ventilation rate calculated for the rest of the building using the concentration recorded in other rooms would be systematically higher than the 'true' indoor-outdoor ventilation rate of this space. This is because the rate of CO_2 decay would be reduced by any leakage of CO_2 from the first room. However, it is possible to see that the rest of the building eventually becomes well mixed, and then decays at the same rate throughout.

Figure 3b highlights the importance of the internal doors, in addition to ventilation to the outside, in determining the airflow in a dwelling. The implications of such issues on the data analysis and interpretation are discussed in the following section.

4 DISCUSSION

The method developed in this work may be used to estimate the ventilation rate in intermittently occupied properties. It does not account for interzonal flows as it uses the single zone approximation. However, collecting CO_2 and door opening data from each room supports

appropriate analysis and interpretation of the results. If the whole dwelling behaves as a single zone (Figure 3a) this technique gives the outdoor ventilation rate of the space in that configuration. When the building does not behave as a single zone (as in Figure 3b), the calculated ventilation rate of any particular room (using the concentration from that room only as $CO_{2,int}(t)$) is that assuming the decay in CO_2 is entirely due to exchange of air with outdoors (Mumovic *et al.*, 2009). By recording the concentration in all rooms, the direction of the systematic bias that the single zone assumption introduces to the ventilation rate calculated for particular rooms is known.

The calculated ventilation rate for a single room will be systematically higher than the indoor-outdoor ventilation rate when the room in question has CO_2 concentration higher than the adjacent spaces. This is because some of the reduction in CO_2 concentration is due to air exchange between indoor spaces rather than exchange with outdoors, so that the 'true' indoor-outdoor ventilation rate is lower than that measured. Conversely, the calculated value for a single room will be systematically lower when the CO_2 concentration in this room is lower than the adjacent spaces. This is because some additional CO_2 may be flowing into the room in question from the adjacent rooms, causing a reduction in the measured rate of CO_2 decay. The closer the indoor spaces to the concentration in the room in question, the closer the measured value will be to the indoor-outdoor ventilation rate. These measured ventilation rates in particular rooms might be considered 'effective' ventilation rates: when the CO_2 source is removed and given the distribution of CO_2 in the building, the capacity of the building to act as a fresh air reservoir and the configuration of the doors and windows, this quantifies how quickly the CO_2 decays to background concentrations.

Since the building is continuously monitored, the similarity of the configuration of the building during occupied times and unoccupied ventilation measurement periods can be assessed. This means it is possible to understand how the occupants use the building when they are present, and whether their use of internal doors means that the building is likely to behave as one single zone or if they are likely to experience different ventilation rates depending which room they are in during occupied times. This provides much more information on the ventilation conditions that occupants are likely to experience, and how this may vary, than is possible using standard single zone methods.

It should be noted that the binary nature of the window and door sensor limits the extent to which the occupied and unoccupied conditions can be compared – there is no record of whether doors or windows are ajar or fully open.

Weather conditions will also affect the ventilation in a building. The sensors required are silent and reasonably small, meaning that participants may be willing to accept the presence of the equipment for an extended period. An extended measurement campaign allows the variation of ventilation under different weather conditions to be explored. However, the cost of the equipment and management of the measurement campaign are important restrictions to the application of this method.

The proposed method allows detailed insights into the ventilation conditions in occupied buildings. The occupancy algorithm may be used to analyse large volumes of data over extended measurement campaigns with much reduced workload compared to manual selection. This method enables the investigation of the varying nature of ventilation rate, and an understanding of how the occupant's use of the building may affect the ventilation rates they experience.

5 CONCLUSIONS

Estimating the ventilation rate in occupied dwellings is challenging, and the method employed depends on the desired insights, occupant acceptance and resource limitations. Issues include the timescale over which estimates are required (e.g. average over a period, or only during

occupied hours), the spatial scale (e.g. specific room or whole building), the intrusiveness of measurements and occupant acceptance, and the researcher time required.

The method developed in this paper is based on metabolic CO_2 tracer gas decay, and uses an automated algorithm to detect occupancy. This method enables the variation in ventilation to be explored. The measurements may be acceptable to occupants since CO_2 is naturally present and the sensors can be silent and reasonably small. These sensors are not expensive, and are combined with sensors that determine the open/closed state of windows and doors, to investigate the differences in ventilation rates in different spaces and under different configurations. The window and door sensors also allow investigation into the extent to which different configurations are experienced in occupied and unoccupied times, and the impact that this has on the ventilation rate that the occupant experiences.

The proposed method uses an automatic algorithm for determining when the building is occupied. The algorithm has been shown to be agree with occupant records in over 80% of cases, which will increase with the use of window sensors and event rather than state loggers. This algorithm reduces burden on the researcher and occupant to manually record or interpret data, enabling the analysis of large volumes of data.

The proposed method represents a step towards appropriate measurement of ventilation and its spatial and temporal variation in occupied buildings. It may enable the measurement of buildings over an extended period, supporting ventilation rate estimation in many different configurations and weather conditions. Such results will support insights into the ways that a building is used by occupants and the ventilation rates that they are likely to experience given their use of the building. This will provide insight into the thermal comfort of occupants, as well as the IAQ they experience. The exposure of occupants to contaminants is complex, depending on ventilation rates, source strength, source location and exposure time: this method provides a detailed picture of the ventilation in occupied buildings, and could help to better understand the association between ventilation rates and health.

6 ACKNOWLEDGEMENTS

This research was made possible by support from the EPSRC Centre for Doctoral Training in Energy Demand (LoLo), grant numbers EP/L01517X/1 and EP/H009612/1.

7 REFERENCES

ASTM (2011) *E741-11: Standard Test Method for Determining Air Change in a Single Zone by Means of a Tracer Gas Dilution*. doi: 10.1520/E0741-11.

Bekö, G. *et al.* (2016) 'Diurnal and seasonal variation in air exchange rates and interzonal airflows measured by active and passive tracer gas in homes', *Building and Environment*, 104, pp. 178–187. doi: 10.1016/j.buildenv.2016.05.016.

Bornehag, C. G. *et al.* (2005) 'Association between ventilation rates in 390 Swedish homes and allergic symptoms in children', *Indoor Air*, 15, pp. 275–280. doi: 10.1111/j.1600-0668.2005.00372.x.

Bryman, A. (2004) *Social Research Methods*. 2nd edn. Oxford: Oxford University Press.

Chen, Z., Jiang, C. and Xie, L. (2018) 'Building occupancy estimation and detection: A review', *Energy and Buildings*. Elsevier B.V., 169, pp. 260–270. doi: 10.1016/j.enbuild.2018.03.084.

CIBSE (2015) *CIBSE Guide A: Environmental Design*. 8th edn. London.

Dedesko, S. *et al.* (2015) 'Methods to assess human occupancy and occupant activity in hospital patient rooms', *Building and Environment*. Elsevier Ltd, 90, pp. 136–145. doi: 10.1016/j.buildenv.2015.03.029.

Fisk, W. J. (2018) 'How home ventilation rates affect health: A literature review', *Indoor Air*, 28(4), pp. 473–487. doi: 10.1111/ina.12469.

Guo, L. and Lewis, J. O. (2007) 'Carbon dioxide concentration and its application on estimating the air change rate in typical Irish houses', *International Journal of Ventilation*, 6(3), pp. 235–

245. doi: 10.1080/14733315.2007.11683780.
Harrje, D. T. *et al.* (1990) 'Tracer Gas Measurement Systems Compared in a Multifamily Building', in Sherman, M. H. (ed.) *Air Change Rate and Airtightness in Buildings, ASTM STP 1067*. Philadelphia: American Society for Testing and Materials, pp. 5–20.
Iwashita, G. and Akasaka, H. (1997) 'The effects of human behavior on natural ventilation rate and indoor air environment in summer - a field study in southern Japan', *Energy & Buildings*, 25, pp. 195–205.
Keig, P., Hyde, T. and McGill, G. (2016) 'A comparison of the estimated natural ventilation rates of four solid wall houses with the measured ventilation rates and the implications for low-energy retrofits', *Indoor and Built Environment*, 25(1), pp. 169–179.
Kvisgaard, B. and Collet, P. F. (1990) 'The User's Influence on Air Change', in Sherman, M. H. (ed.) *Air Change Rate and Airtightness in Buildings*. American Society for Testing and Materials, pp. 67–76.
Liddament, M. (1996) *A Guide to Energy Efficient Ventilation*. Warwick: Air Infiltration and Ventilation Centre, International Energy Agency.
Mumovic, D. *et al.* (2009) 'A methodology for post-occupancy evaluation of ventilation rates in schools', *Building Services Engineering Research and Technology*, 30(2), pp. 143–152. doi: 10.1177/0143624408099175.
Oreszczyn, T. *et al.* (2005) 'The reduction in air infiltration due to window replacement in UK dwellings: Results of a field study and telephone survey', *International Journal of Ventilation*, 4(1), pp. 71–78. doi: 10.1080/14733315.2005.11683700.
Penman, J. M. and Rashid, A. A. M. (1982) 'Experimental determination of air-flow in a naturally ventilated room using metabolic carbon dioxide', *Building and Environment*, 17(4), pp. 253–256. doi: 10.1016/0360-1323(82)90017-8.
Persily, A. (2006) 'What we think we know about ventilation', *International Journal of Ventilation*, 5(3), pp. 275–290. doi: 10.1080/14733315.2006.11683745.
Persily, A. K. (2016) 'Field measurement of ventilation rates', *Indoor Air*, 26(1), pp. 97–111. doi: 10.1111/ina.12193.
Roulet, C.-A. and Foradini, F. (2002) 'Simple and Cheap Air Change Rate Measurement Using CO2 Concentration Decays', *International Journal of Ventilation*, 1(1), pp. 39–44. doi: 10.1080/14733315.2002.11683620.
Sharpe, T. *et al.* (2015) 'Occupant interactions and effectiveness of natural ventilation strategies in contemporary new housing in Scotland, UK', *International Journal of Environmental Research and Public Health*, 12(7), pp. 8480–8497. doi: 10.3390/ijerph120708480.
Sherman, M. (1998) *The Use of Blower-Door Data. Lawrence Berkley Lab Report 35173.* Berkelely, California: Lawrence Berkeley Laboratory. doi: 10.1111/j.1600-0668.1995.t01-1-00008.x.
Sherman, M. H. (1990) 'Tracer-gas techniques for measuring ventilation in a single zone', *Building and Environment*, 25(4), pp. 365–374. doi: 10.1016/0360-1323(90)90010-O.
Smith, P. N. (1988) 'Determination of ventilation rates in occupied buildings from metabolic CO2 concentrations and production rates', *Building and Environment*, 23(2), pp. 95–102. doi: 10.1016/0360-1323(88)90023-6.
Sundell, J. *et al.* (2011) 'Ventilation rates and health: Multidisciplinary review of the scientific literature', *Indoor Air*, 21(3), pp. 191–204. doi: 10.1111/j.1600-0668.2010.00703.x.
UNFCCC (2015) *Convention on Climate Change: Paris Agreement*.
Wallace, L. A., Emmerich, S. J. and Howard-Reed, C. (2002) 'Continuous measurements of air change rates in an occupied house for 1 year: the effect of temperature, wind, fans, and windows.', *Journal of Exposure Analysis and Environmental Epidemiology*, 12(4), pp. 296–306. doi: 10.1038/sj.jea.7500229.

Airtightness and non-uniformity of ventilation rates in a naturally ventilated building with trickle vents

Jessica Few*[1], David Allinson[2] and Clifford Elwell[1]

UCL Energy Institute
London
WC1H 0NN, UK
** Corresponding author: jessica.few.16@ucl.ac.uk*

School of Civil and Building Engineering
Loughborough University
Loughborough
LE11 3TU, UK

ABSTRACT

Infiltration is an uncontrolled contribution to ventilation in a building and can contribute significantly to the total ventilation rate, particularly in older, leaky, dwellings which can rely on infiltration to provide adequate indoor air quality. However, as explored in this paper, using a whole house airtightness metric to characterise ventilation rates can fail to identify low ventilation rates in specific rooms.

Measurements were undertaken in autumn and winter for a dwelling with an airtightness (by blower door) of 15.1 $m^3/hr/m^2$@50Pa. The dwelling was built in the 1930's: semi-detached, suspended timber floors, cavity walls and retrofitted throughout with double glazing incorporating trickle vents.

The whole dwelling ventilation rate (by CO_2 tracer gas decay) with the trickle vents closed was 0.7 ach, and 0.8 ach with the trickle vents open. However, the ventilation rate (by CO_2 tracer gas decay) in a single room with its internal door closed under different weather conditions was only 0.17 ach (standard deviation = 0.06 ach, number of measurements = 34), and with trickle vents open 0.32 ach (standard deviation = 0.13 ach, number of measurements = 40). This is below the 0.5 ach required for good indoor air quality. This is likely related to the closed internal door reducing cross-ventilation and the non-uniformity of air leakage paths in the dwelling. The leakage paths were investigated using smoke pens during a pressurisation test and significant air leakage paths were observed in other rooms: through the under stairs cupboard, around services in the kitchen and bathroom, and through the ceiling into the loft.

Low air change rates have been observed in a building with very low airtightness, typical of older stock in the UK. The dwelling was retrofitted with double glazing, which is likely to have significantly affected the airflow, but still left the dwelling with low total airtightness. The double glazing had trickle vents, but these did not provide adequate ventilation. Inclusion of trickle vents in replacement windows is 'good practice' according to English building regulations, but not compulsory if there were no vents in the previous windows. Similarly, undercuts are required for doors in new dwellings, but are only required for existing buildings in new wet rooms; the tested dwelling had undercuts half the size required for ventilation regulations in new buildings.

The difference in ventilation rates at different spatial scales is rarely discussed, but this research shows that there can be major discrepancies. This paper discusses the implications of this for appropriate measurement of ventilation, and the implications for ventilation regulations and guidance as well as the need for further research into the complexity of the manifestation of ventilation in occupied buildings.

KEYWORDS

Ventilation, airtightness, measurement, indoor air quality, building regulations.

1 INTRODUCTION

The Climate Change Act (2008) commits the UK to reducing carbon dioxide emissions to 80% of 1990 levels by 2050. In 2015, the domestic sector accounted for 29% of final energy consumption in the UK; space and water heating made up 80% of this energy use (BEIS, 2016). CIBSE (2015) state that heat loss through ventilation can account for up to 50% of the primary energy used in a building in the UK, so reducing heat lost through ventilation in dwellings is important. However, sufficient ventilation is required for good indoor air quality (IAQ). Fisk (2018) reviewed the literature and found that lower ventilation rates are likely to be associated with poor health outcomes, although the evidence is complicated by confounding factors and

associations are not universally observed. A ventilation rate of 0.5 ach is often considered to be sufficient for IAQ (Sundell *et al.*, 2011; Dimitroulopoulou, 2012; Fisk, 2018).

UK Building Regulations require that there 'shall be adequate means of ventilation provided for people in the building' (HMG, 2013b). The Approved Document to the UK Building Regulations Part F (ADF) specifies whole dwelling ventilation rates, dependent upon floor area and number of bedrooms, which should be achieved in new dwellings and details of ventilation systems which will be assumed to meet the requirements (HMG, 2013b).

The total ventilation in a building includes purpose-provided ventilation and ventilation through infiltration. Infiltration is uncontrolled airflow through unplanned breaks in the air barrier of the building (HMG, 2013b). Air permeability gives the average volumetric airflow through each unit area of the building envelope and characterises the infiltration.

The results of air permeability tests can be used to estimate the ventilation rate using the n/20 'rule of thumb' which states that the annualised whole dwelling ventilation rate is equal to the air change rate at 50 Pa divided by 20 (Sherman, 1987). In the UK, the Standard Assessment Procedure (SAP) – a method for estimating the energy efficiency of a building – uses a form of this rule to estimate the ventilation rate due to infiltration (BRE, 2014). The SAP method uses the air permeability rather than the air change at 50 Pa as the numerator. Sherman (1998) stresses the limitations of this approximation given variations in weather conditions and dwelling characteristics. Liddament (1996) suggests that this can be particularly problematic for naturally ventilated buildings as the instantaneous ventilation rate can deviate significantly from the average.

Air leakage paths are not evenly distributed throughout buildings (Johnston *et al.*, 2011). Breaks in the air barrier around services in kitchens and bathrooms, into roof voids or around poorly fitting windows or doors are common. So whole dwelling ventilation rates are unlikely to be evenly distributed and will depend on which doors are open or closed. However, little research has addressed the difference in ventilation rate measured on different spatial scales; for example Bekö *et al.* (2010) and Sharpe *et al.* (2015) measured only bedrooms, while Oreszczyn *et al.* (2005) and Keig, Hyde and McGill (2016) all characterised only the whole house ventilation rate, Johnston and Stafford (2017) compared the n/20 rule to the ventilation rate in two rooms, but did not discuss the different spatial scales of the measurement.

Differences in ventilation rate at different spatial scales could affect the occupants exposure to pollutants or their use of space heating, or both. This paper report on a case study dwelling that has been investigated to explore the ventilation rate in different spaces, and the research illustrates the possibility that occupants experience different ventilation rates depending on how they use internal spaces. The results are used to consider how guidance for providing adequate ventilation can be improved given spatial variation in ventilation rates.

This paper also considers the performance of trickle vents (background ventilators). Trickle vents are intended to ensure that buildings are adequately ventilated. They are an element in three of the four ADF approved systems for ventilation, and are recommended in existing buildings when windows are replaced (HMG, 2013b). Despite the prevalence of trickle vents there are limited studies on their performance. Low ventilation rates have been observed in naturally ventilated dwellings with trickle vents (Crump *et al.*, 2005; Sharpe *et al.*, 2014) and many occupants keep them closed (Sharpe *et al.*, 2015). This research gap is addressed here by investigating the effect of opening and closing trickle vents on the whole house and individual room ventilation rate.

The following section describes the case study building and the methods used to characterise the ventilation rates at different spatial scales using tracer gas analysis, then Section 3 presents the results. Section 4 discusses the implications for research and the need for further work to understand the implications of spatial variability in ventilation, as well as implications for ventilation regulations and the interacting factors at work in designing for adequate ventilation in occupied dwellings. Finally Section 5 provides the main conclusions and implications.

Figure 1. Photograph of the test dwelling.

2 METHODS AND CASE STUDY

2.1 Description of the test house

A single case study dwelling was studied: built in the 1930's, semi-detached, with suspended timber floors, cavity walls and retrofitted throughout with double glazing and trickle vents. Figure 1 shows the outside of the building.

ADF gives whole house ventilation rates which should be achieved only in newly built dwellings only. If this building were newly built, a ventilation rate of 28 L/s would be required, 0.4 ach assuming the whole house volume takes part in the ventilation. Since there will be dead-zones, the effective volume will be smaller than the physical volume and this would increase the required ach value.

The dwelling is naturally ventilated with no mechanical ventilation. The total geometric area of the trickle vents was 32,000 mm^2 for the whole house, 6,400 mm^2 for the single room studied in detail. The geometric area is provided because the slots inside the trickle vents were cut smaller than the manufacturer recommends, so the equivalent area is not known. If the dwelling were newly built, background ventilators with equivalent area of at least 5,000 mm^2 would be required in the single room, and 45,000 mm^2 in the whole house.

2.2 Pressurisation tests and smoke survey

Pressurisation tests use the flow rate required to maintain a given pressure difference between indoors and outdoors to measure air permeability. Pressurisation tests were conducted in line with the ATTMA protocol (ATTMA, 2016). Measurements were taken with a Minneapolis Model 3 and a Retrotec 6000 blower door on calm weather days in August 2018 and February 2019 respectively; one pressurisation and depressurisation test was carried out in each case and the mean value is reported below.

Additionally, while the house was pressurised, a qualitative survey of the dwelling was carried out using a smoke pen to visualise the air leakage paths.

2.3 Tracer gas tests

Tracer gas methods use a gas to 'tag' airflow and are based on the conservation of mass of tracer gas and air. The tracer gas concentration decay method was used with CO_2. Measurements were performed according to ASTM (2012) guidance.

The air change rate was calculated using the following equation (ASTM, 2012), and the analysis was carried out using a least squares curve fitting algorithm (curve_fit from SciPy):

$$CO_{2,Diff}(t) = CO_{2,Diff}(t = 0)\exp(-A.t) \quad (3)$$

Where $CO_{2,Diff}(t)$ is the difference between the indoor CO_2 concentration minus the outdoor CO_2 concentration, $CO_{2,Diff}(t = 0)$ is the concentration difference at the start of the decay period, A is the air change rate, and t is the time since the start of the decay.

Figure 2 shows a floor plan and locations of the CO_2 sensors in the test dwelling. The diamond in the corner of the back room represents three sensors: at floor level, at ceiling level and 1.2 m above floor; the diamond in the corner of bedroom 2 represents two sensors: at 1.2m above floor and ceiling level. All other sensors were all between 1.1 m and 1.3m above the floor. The CO_2 concentration was recorded every 5 minutes with Eltek GD-47 (NDIR) sensors. The outdoor CO_2 concentration for each sensor was taken to be the mean concentration during a

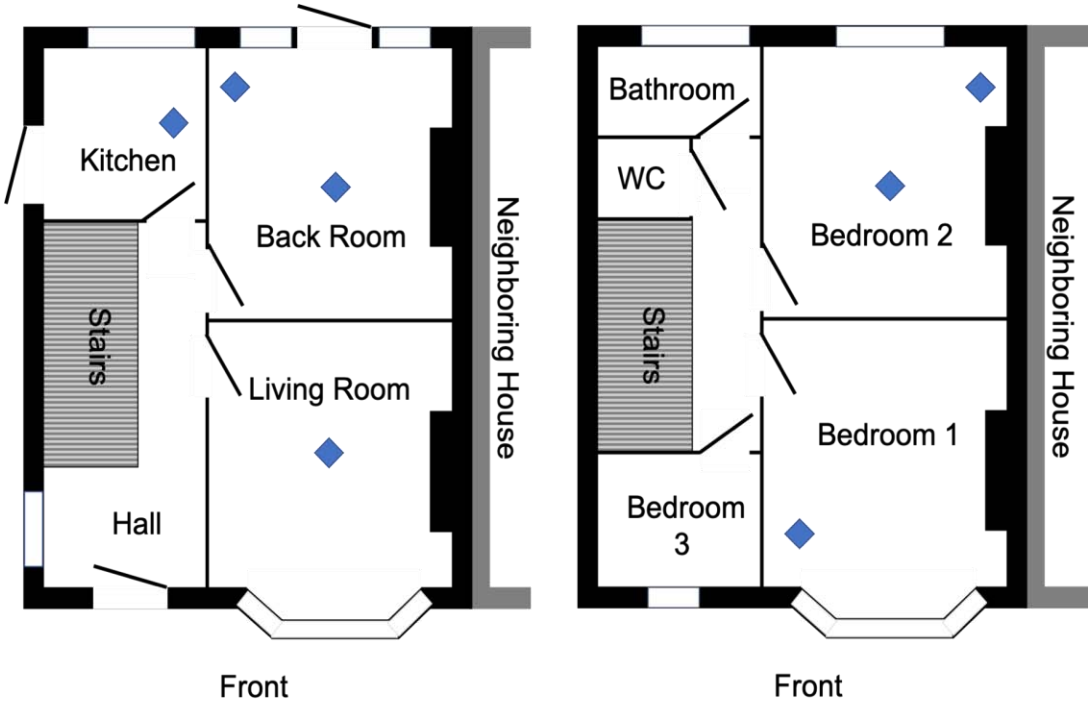

Figure 2. Layout of the test dwelling, ground floor on the left hand side, first floor on the right hand side. The CO_2 sensors are indicated by the blue diamonds. The single room tests took place in the downstairs 'back room'.

three-day period in which the dwelling was continuously unoccupied. Variation between sensors was less than 50 ppm and the mean of all sensors was 430 ppm during this time.

The tracer gas tests were carried out on two spatial scales: the whole house and a single room. These are described in more detail in the subsections below.

2.3.1 Whole house tests. Two whole house tests were carried out in February 2019: one with trickle vents open, the other with trickle vents closed. The temperature differences were 13 ºC and 15 ºC, the wind speeds were 10 mph and 14 mph for the measurement with the vents open and closed respectively. The wind direction was South-West in both cases.

CO_2 was released in each of the rooms and fans were used to encourage good mixing. However, it was not possible to maintain the CO_2 difference within 10% of each other in all the spaces as recommended by ASTM (2012). The downstairs sensors remained within 10% of each other, as did the upstairs sensors. There were differences of up to 30% between upstairs and downstairs. The volume-weighted average CO_2 concentration was used in the analysis.

2.3.2 Single room tests. The single room was on the ground floor and is identified as the 'back room' in Figure 2. The measurements took place between September and December 2018. Temperature differences ranged from -3 ºC to 18 ºC, the wind direction was predominantly North West to North East, and ranged from 3 mph to 23 mph. There were 34 tests with trickle vents closed and 40 with trickle vents open.

There were four CO_2 sensors in the single measurement room. These remained within 10% of each other throughout the single room tests and the mean concentration was used to calculate the air change rate. The sensors in adjacent rooms recorded CO_2 rises, suggesting inter-zone flows, but the concentration never exceeded the CO_2 concentration in the single room.

3 RESULTS

Table 1 summarises the results from each of the methods described above. The dwelling is leaky compared to modern properties, but is fairly typical of older dwellings - Perera and Parkins (1992). The qualitative smoke pen investigation revealed several significant air leakage

Figure 3. Photograph of the smoke pen survey, showing significant air leakage behind the kitchen cupboard.

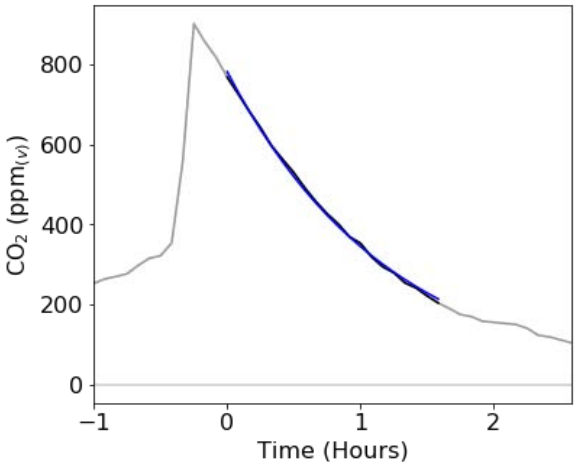

Figure 4. The whole house CO_2 decay with trickle vents open. The y-axis shows the volume weighted CO_2 difference. The black line shows the decay period, and the exponential model is shown in blue.

paths in the under stairs cupboard, around the services in the kitchen and bathroom, through several cracks in the walls and around the front door. The windows were well sealed. Figure 3 shows an example of the smoke being pulled into the space behind the kitchen cupboard, while the house is pressurised by blower door.

The whole house ventilation rate found using CO_2 decay is above the threshold of 0.5 ach with trickle vents open and closed, and the dwelling is therefore well ventilated from an IAQ perspective, but excessively inefficient to heat. Figure 4 shows an example of the CO_2 decay and log-linear fit of the data for the whole house measurement with the trickle vents open.

In contrast, the single room ventilation rate is below 0.5 ach with trickle vents open and closed. This suggests this individual room could have issues with poor IAQ when the door is closed. Figure 5 shows a histogram of the air change rates calculated for tests when the trickle vents are opened and closed. The ventilation in both configurations varies considerably because of the variety of weather conditions during the experiments, however none of the trickle vent closed rates are above 0.5 ach, and very few of the trickle vent open rates exceed this figure.

4 DISCUSSION

4.1 Limitations of the techniques

As with all methods to estimate ventilation rates, several limitation apply to this study. In particular, results from this case study may not be generalised to the wider stock. However, this building is of typical construction for a house built during the 1930s, and the available evidence suggests that the dwelling is not abnormal: the airtightness is typical of older stock (Perera and Parkins, 1992) and similar leakage paths locations have been found in other dwellings (Stephen, 2000). This study therefore identifies issues are that are likely to occur more widely in the stock, with unknown prevalence and highlights issues of policy and practice that may form the basis of further study.

Table 1: Summary of results characterising the case study dwelling from the pressurisation and CO_2 decay tests

	Trickle Vents Open	Trickle Vents Closed
Air Permeability	-	15.1 $m^3/hr/m^2$
ACH_{50}	-	15.1 ach
$N_{50}/20$	-	0.8 ach
Whole house CO_2 decay	0.8 ach	0.7 ach
Single room CO_2 decay (mean)	0.3 ach	0.2 ach

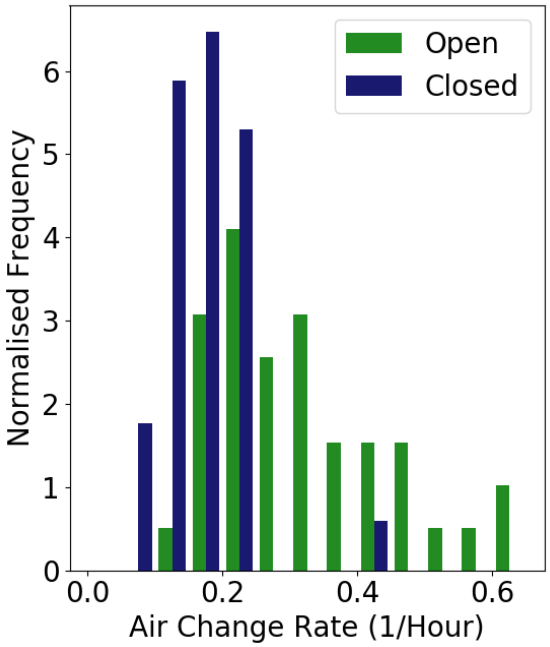

Figure 3. Normalised histogram of the measurement of air change rate measured in the single measurement room with the trickle vents opened and closed.

In application of the whole house tracer gas method it was not possible to maintain the CO_2 concentrations to within 10% between upstairs and downstairs. Analysis of the upstairs sensors resulted in a decay constant of 0.7 ach for trickle vents open and 0.5 ach for trickle vents closed. These values are systematically biased towards low values because the stack effect caused CO_2 to flow from downstairs to upstairs due to buoyancy effects. Given that these values are at or above the threshold of 0.5 ach, the finding that the whole dwelling is over-ventilated holds despite the inability to maintain uniform concentration.

The single zone approximation was used for the single room, neglecting flow between rooms. The CO_2 concentration in adjacent rooms was always below the measurement room, so any airflow to other internal spaces will have systematically biased the result towards higher values. The true indoor-outdoor ventilation rate is likely lower and therefore the IAQ worse.

Whole house tests were conducted once, while multiple tests were conducted in the single room. The distributions therefore cannot be compared, but since the whole house measurements took place with neither the highest temperature difference nor the highest wind speeds, the difference in ventilation rates between different scales is not due to more extreme weather conditions.

4.2 Difference in ventilation rate measured at different spatial scales

The results show that measurements of ventilation on different spatial scales can differ significantly. The whole dwelling value suggests that the dwelling is over-ventilated, while the single room with the door closed suggests poor IAQ due to a low ventilation rate. Whether this affects occupants would depend on how long occupants spend in a specific room, the ventilation rate and pollutant sources. For example: the use of candles, cleaning products, drying of clothes or simply the presence of several people are all events that could take place in a room with the door closed which could lead to poor IAQ (Satish *et al.*, 2012; Porteous *et al.*, 2014; Dimitroulopoulou *et al.*, 2015).

The difference in ventilation rates is likely to be caused by a range of factors, including the non-uniformity of air leakage paths and limited air exchange between spaces with closed doors. Inter-zone air flow may be encouraged by door undercuts; ADF requires undercuts of 7600 mm^2 in new buildings. However, the measured room had undercuts approximately half this size, which will have significantly reduced the airflow to the rest of the building.

4.3 Implications for research

It has been shown that the spatial scale on which ventilation is measured, and the closing of internal doors, can have a substantial effect on the ventilation rate that is calculated and consequently whether the ventilation appears to be adequate. This highlights the need to determine the purpose of ventilation measurements in study design, and identify the limitations to the values estimated in different ways.

To date there has been relatively little empirical work exploring how internal spaces are divided and used by occupants. Banfill *et al.* (2012) found that particular doors were opened and closed at regular times each day, while particular rooms were almost permanently closed off due to adult children moving away. McDermott, Haslam and Gibb (2010) found several reasons people opened or closed doors including: watching children in next door rooms, letting light in,

and blocking sounds. Sharpe *et al.* (2015) found that bedroom doors often closed overnight and doors were more likely to be open when a child is present.
Further work on how spaces and doors within buildings are used would support a better appreciation of the conditions that occupants experience, and their relation to whole house air change rates, or those in specific rooms. Such research would also support the application of appropriate techniques to estimate ventilation rates, according to the purpose of the measurement, in assessing whether spaces are under- or over-ventilated and the implication of this. For example, studies investigating the link between ventilation rate and health may be confounded if a whole building ventilation rate is measured, while occupants experience a very different rate (affecting their exposure to pollutants) in the spaces they use. Sundell *et al.*, (2011) and Fisk (2018) reviewed the literature and concluded that it is more likely than not that there is a detriment to health associated with low ventilation rates. Whilst neither author discusses the spatial scale of the measurements, Fisk suggested that greater clarity and uniformity in measurement of ventilation rate would be helpful for understanding and comparing results.

4.4 Implications for policy

At present, ADF specifies ventilation strategies for new buildings which will be assumed to meet the requirements for adequate ventilation. These provisions differ depending on the planned air permeability of the building. The results presented here suggest that this could be inappropriate, since the air permeability and subsequent ventilation through infiltration are unlikely to be evenly distributed around the building – a higher air permeability does not necessarily mean that more ventilation is provided in the places in which it is needed.
ADF recommends but does not require that trickle vents are installed when windows are replaced in existing buildings. The trickle vents improved the ventilation in the single room in this case study (though were unable to raise it to adequate levels). The installation of replacement UPVC glazing units is likely to increase the airtightness of a room and may result in reduced IAQ (Oreszczyn *et al.*, 2005). Requiring that all rooms contain adequate background ventilation whenever any change is made that could influence the air change rate in a space could mitigate this issue.
The trickle vents in this dwelling were unable to raise the single room ventilation rate to an adequate level. Further work is required to determine if this issue is widespread, but this result is in line with previous authors (Crump *et al.*, 2005; Sharpe *et al.*, 2015). Whilst increasing the number or size of trickle vents would improve the ventilation rate with the internal door closed, it would contribute to increased excess ventilation with the door open. Additionally, the ventilation rate for properties with natural ventilation through trickle vents is variable, depending on the weather conditions. This presents a challenge in devising appropriate policies and practice guidelines: appropriate ventilation depends on whether internal doors are open or closed. The problem is exacerbated by the findings of several authors that trickle vents are frequently closed in occupied dwellings (Crump *et al.*, 2005; Sharpe *et al.*, 2015), despite the stated intention in ADF that they are permanently open. The role of occupants on ventilation rate is therefore highly significant and measures designed to provide adequate ventilation must account for occupant behaviour. Strategies could include improving the design of trickle vents or raising public awareness such that occupants more readily understand their intended purpose, or providing trickle vents which cannot be closed.
This research has highlighted that the current building regulations are not designed to take into account differences between the behaviour of the whole building and individual rooms. Two measures that may address the observed disparity for naturally ventilated buildings are the use of undercuts for doors and vents between rooms. Undercuts with an area of 7600 mm^2 are required by ADF for new buildings and may improve flow between rooms with closed doors. However, there are no requirements for undercuts for existing buildings, except where a new wet room is added. Whilst the magnitude and scale of this issue is not known, requiring either undercuts or between room vents when doors are replaced, or when major building work is

completed on a property, could improve the single room ventilation rate without increasing the whole building ventilation rate with internal doors open.
Potential occupant acceptability issues arise for undercuts or vents: they allow cool draughts which may decrease thermal comfort, and they allow noise to travel between rooms. ADJ recommends noise attenuating vents when they are installed to provide adequate combustion air for flued appliances (HMG, 2013c), this may provide a partial solution.
Finally, in considering how to improve airflow through dwellings the need for buildings to be firesafe must be considered. Fire doors are tested for fire safety compliance with a particular undercut, up to a maximum of 25 mm (BSI, 2008). Any adjustment to the undercuts would require re-testing doors for their fire safety with a new undercut depth. Similarly, in order to comply with Approved Document B (HMG, 2013a), vents between rooms should not be used in fire-resisting walls and vents should be placed at low level to reduce the spread of smoke, this prevents placement of vents at high level to improve thermal comfort.
The above discussion has demonstrated the complexities involved in the design and regulations for adequate ventilation in occupied dwellings, especially those which are naturally ventilated. The research has shown that differences between individual rooms and whole house ventilation rates can affect whether the ventilation is adequate; research on the use of internal doors and the effect on internal environments is lacking. Neither is this difference adequately accounted for in current regulations. Trickle vents have been shown to be an unsatisfactory solution as the whole house became more over-ventilated and the individual room remained under-ventilated, compounding this, trickle vents are known to be shut in many occupied homes. Door undercuts and through-wall vents may mitigate this issue, though occupant concerns and fire regulations must be observed. The manifestation of ventilation in occupied buildings requires further research given that the way occupants use a building is influential yet challenging to account for when designing adequate, robust and safe guidance and regulations for ventilation.

5 CONCLUSIONS

Adequate ventilation is required to maintain good indoor IAQ, while excessive ventilation reduces the thermal efficiency of a building: a ventilation rate of 0.5 ach is considered to balance these issues (Sundell *et al.*, 2011; Dimitroulopoulou, 2012; Fisk, 2018). This paper addressed the differences in ventilation rates measured on different spatial scales in the same building. A case study building was measured with an air permeability of 15.1 $m^3/hr/m^2$@50Pa, the whole dwelling ventilation rate was 0.8 ach, while the ventilation rate was 0.3 ach in one room with the door closed (both ventilation rates with trickle vents open). The building is over-ventilated with all doors are open, but inadequate IAQ may be experienced in the single room when the door is closed. Although the dwelling has high air permeability, it cannot be assumed that the ventilation is adequate in the rooms with the door closed.
The differences in ventilation rates on different scales identified here are likely to be replicated in other dwellings in the stock as the locations of air leakage paths were not unusual (Stephen, 2000) and the air permeability was typical for a building of this age (Perera and Parkins, 1992), but the incidence and magnitude of the difference is unknown. More modern dwellings are built with a lower total air permeability and this issue may become more acute in these buildings as the ventilation through infiltration will be smaller so the single room ventilation rate could be even lower leading to a corresponding increase in indoor pollutant exposure.
Opening the trickle vents increased the whole dwelling ventilation rate in the case study property, worsening the heating efficiency, but did not provide adequate ventilation in the individual room with closed door, potentially leading to inadequate IAQ in this space. Additionally, previous research has shown that trickle vents often closed in occupied homes (Crump *et al.*, 2005; Sharpe *et al.*, 2015), despite permanently open trickle vents being the stated intention in ADF (HMG, 2013b). This shows that occupant actions have a significant

impact on the ventilation rate experienced and highlights the challenge of designing ventilation strategies and guidance which ensure appropriate ventilation in occupied dwellings.

The current building regulations do not adequately account for the differences between whole house and individual room ventilation rates. Strategies which may improve individual room ventilation rates, without increasing whole house ventilation, include increased undercuts beneath doors and vents between rooms. Undercuts are required for new buildings, but are only required in existing buildings when new wet rooms are fitted. Amending the regulations such that undercuts and vents between rooms are required when doors are replaced or major building work takes place may improve individual room ventilation rates. There are potential occupant acceptability issues with these measures: they may increase cold draughts and increase noise transmission around the dwelling. Noise attenuating vents provide a partial solution this issue. Fire safety concerns must also be addressed: between wall vents should not be placed in fire-resisting walls and should only be placed at low levels to reduce smoke transmission in the event of a fire; additionally, fire doors are rated for a particular depth of undercut so these may need to be retested if undercuts are adjusted.

This paper has shown that the spatial scale over which ventilation is measured can influence whether the ventilation appears to be adequate. This highlights the need to identify the purpose and limitations of a ventilation measurement when designing research. Further work on how occupants interact with buildings, including internal door opening behaviours, would support a better understanding of the appropriate scale over which to measure ventilation and appropriate measurement techniques for different purposes.

6 ACKNOWLEDGEMENTS

The data for this paper were collected using the Loughborough Matched Pair of 1930s Semi-detached test houses which are operated by the Building Energy Research Group (BERG) in the School of Architecture, Building and Civil Engineering at Loughborough University.

This research was made possible by support from the EPSRC Centre for Doctoral Training in Energy Demand (LoLo), grant numbers EP/L01517X/1 and EP/H009612/1.

7 REFERENCES

ASTM (2012) *D6245-12: Standard Guide for Using Indoor Carbon Dioxide Concentrations to Evaluate Indoor Air Quality and Ventilation*. doi: 10.1520/D6245-12.Copyright.

ATTMA (2016) *Technical Standard L1. Measuring Air Permeability in the Envelopes of Dwellings*. Amersham.

Banfill, P. *et al.* (2012) 'Energy-led retrofitting of solid wall dwellings: technical and user perspectives on airtightness', *Structural Survey*, 30(3), pp. 267–279. doi: http://dx.doi.org/10.1108/MRR-09-2015-0216.

BEIS (2016) *Energy Consumption in the UK: November 2016 Update*. London.

Bekö, G. *et al.* (2010) 'Ventilation rates in the bedrooms of 500 Danish children', *Building and Environment*. Elsevier Ltd, 45(10), pp. 2289–2295. doi: 10.1016/j.buildenv.2010.04.014.

BRE (2014) *SAP 2012: The Government's Standard Assessment Procedure for Energy Rating of Dwellings*. Watford, UK: BRE. doi: 10.1007/s13398-014-0173-7.2.

BSI (2008) *BS EN 1634-1:2008 Fire resistance and smoke control tests for door, shutter and openable window assemblies and elements of building hardware*. London: British Standards Institution.

CIBSE (2015) *CIBSE Guide A: Environmental Design*. 8th edn. London.

Climate Change Act (2008) *Climate Change Act*. United Kingdom.

Crump, D. *et al.* (2005) *Ventilation and indoor air quality in new homes*. Watford, UK: Building Research Establishment.

Dimitroulopoulou, C. (2012) 'Ventilation in European dwellings: A review', *Building and Environment*. Elsevier Ltd, 47(1), pp. 109–125. doi: 10.1016/j.buildenv.2011.07.016.

Dimitroulopoulou, C. *et al.* (2015) 'EPHECT II: Exposure assessment to household consumer products', *Science of the Total Environment*. Elsevier B.V., 536, pp. 890–902. doi: 10.1016/j.scitotenv.2015.05.138.
Fisk, W. J. (2018) 'How home ventilation rates affect health: A literature review', *Indoor Air*, 28(4), pp. 473–487. doi: 10.1111/ina.12469.
HMG (2013a) *Approved Document B: Fire safety. Volume 1 - Dwellinghouses. 2006 edition incorporating 2010 and 2013 amendments.*
HMG (2013b) *Approved Document F1: Means of ventilation. 2010 edition incorporating 2010 and 2013 amendments*. Her Majesty's Government.
HMG (2013c) *Approved Document J: Combustion appliances and fuel storage systems. 2010 edition incoprorating 2010 and 2013 amendments.*
Johnston, D. *et al.* (2011) *Airtightness of Buildings — Towards higher Performance Final Report — Domestic Sector Airtightness*. Department for Communities and Local Government.
Johnston, D. and Stafford, A. (2017) 'Estimating the background ventilation rates in new-build UK dwellings - Is n50/20 appropriate?', *Indoor and Built Environment*, 26(4), pp. 502–513. doi: 10.1177/1420326X15626234.
Keig, P., Hyde, T. and McGill, G. (2016) 'A comparison of the estimated natural ventilation rates of four solid wall houses with the measured ventilation rates and the implications for low-energy retrofits', *Indoor and Built Environment*, 25(1), pp. 169–179. doi: 10.1177/1420326X14540927.
Liddament, M. (1996) *A Guide to Energy Efficient Ventilation*. Warwick: Air Infiltration and Ventilation Centre, International Energy Agency.
McDermott, H., Haslam, R. and Gibb, A. (2010) 'Occupant interactions with self-closing fire doors in private dwellings', *Safety Science*. Elsevier Ltd, 48(10), pp. 1345–1350. doi: 10.1016/j.ssci.2010.05.007.
Oreszczyn, T. *et al.* (2005) 'The reduction in air infiltration due to window replacement in UK dwellings: Results of a field study and telephone survey', *International Journal of Ventilation*, 4(1), pp. 71–78. doi: 10.1080/14733315.2005.11683700.
Perera, E. and Parkins, L. (1992) 'Airtightness of UK Buildings: Status and Future Possibilities', *Environmental Policy and Practice*, 2, pp. 143–160.
Porteous, C. D. A. *et al.* (2014) 'Domestic laundering: Environmental audit in Glasgow with emphasis on passive indoor drying and air quality', *Indoor and Built Environment*, 23(3), pp. 373–392. doi: 10.1177/1420326X13508145.
Satish, U. *et al.* (2012) 'Is CO2 an Indoor Pollutant? Direct Effects of Low-to-Moderate CO2 Concentrations on Human Decision-Making Performance', *Environmental Health Perspectives*, 120(12), pp. 1671–1677.
Sharpe, T. *et al.* (2015) 'Occupant interactions and effectiveness of natural ventilation strategies in contemporary new housing in Scotland, UK', *International Journal of Environmental Research and Public Health*, 12(7), pp. 8480–8497. doi: 10.3390/ijerph120708480.
Sharpe, T. R. *et al.* (2014) 'An assessment of environmental conditions in bedrooms of contemporary low energy houses in Scotland', *Indoor and Built Environment*, 23(0), pp. 1–24. doi: 10.1177/1420326X14532389.
Sherman, M. (1998) *The Use of Blower-Door Data. Lawrence Berkley Lab Report 35173.* Berkelely, California: Lawrence Berkeley Laboratory.
Sherman, M. H. (1987) 'Estimation of infiltration from leakage and climate indicators', *Energy and Buildings*, 10, pp. 81–86. doi: 10.1016/0378-7788(87)90008-9.
Stephen, R. (2000) *Airtightness in UK Dwellings: information paper*. Watford: BRE.
Sundell, J. *et al.* (2011) 'Ventilation rates and health: Multidisciplinary review of the scientific literature', *Indoor Air*, 21(3), pp. 191–204. doi: 10.1111/j.1600-0668.2010.00703.x.

Effects of Outdoor Environment on Air Exchange Rate

Maria Marrero[*1], Manuel Gameiro da Silva[2], Leslie Norford[3]

1 ADAI LAETA, University of Coimbra
R. Luis Reis dos Santos
3030-788 Coimbra, Portugal
**Corresponding author:*
uc2016248508@student.uc.pt

2 ADAI LAETA, University of Coimbra
R. Luis Reis dos Santos
3030-788 Coimbra, Portugal

3 Department of Architecture, Massachusetts Institute of Technology,
77 Massachusetts Avenue,
02139, Cambridge, MA, United States

ABSTRACT

Indoor air quality is the chemical, physical and biological properties that indoor air must have to not cause any negative impact on occupants' health and provide comfort: feel fresh, pleasant and stimulating.
The indoor air quality is mainly determined by the indoor pollution sources and the outdoor air imported to the building. The indoor pollution sources are related to occupants, the building and their activities. The effect of the outdoor air in the indoor environment depends on its level of pollution and the amount entering the building through different ventilation systems and infiltrations. Ventilation and infiltrations are essential to ensure an optimal level of indoor air quality by refreshing the air. However, this can mean extra energy consumption because it can affect thermal comfort. Therefore, it is important to evaluate the efficiency of ventilation.
One way to characterize the ventilation rate, and the amount of air entering or leaving the indoor environment, is by the air exchange rate. The air exchange rate indicates the number of times that air in a fixed space is replaced by outdoor air in one hour. This study aims to determine the changes in the air exchange rate throughout the day depending on the weather conditions in the Mechanical Engineering Department building within the university campus located in the south of Coimbra city, Portugal. In line with this purpose, the air exchange rate determined using the metabolic CO_2 decay tracer gas technique, by measuring the CO_2 concentration inside and outside the building during a 3-month period. Meteorological observations were obtained from a weather station set in the car park. The variations and correlations of the air exchange rate against various outdoor meteorological factors, namely temperature, dew point, barometric pressure, wind speed and direction, precipitation and solar irradiation were tested using statistical regression techniques.
This paper concludes that the air exchange rate measured by the CO_2 tracer gas technique in an unoccupied building depends on meteorological conditions. Almost 80% of the variation in the air exchange rate can be explained by meteorological variables such as temperature, dew point, humidity, and wind speed and direction. Other parameters that affect air exchange rate are wind direction and precipitation. In these cases, the effects are conditioned to the situation. For example, only the wind coming from the direction in which the building is exposed has a noticeable effect. The precipitation episodes have different effects. Generally, it rains in cloudy skies, which reduces the amount of solar radiation that reaches the surface of the earth and the building. Thus, it can increase photosynthesis and the production of environmental CO_2 thanks to the extra contribution of water, an essential component in the respiration-photosynthesis process. All these parameters indirectly affect the air exchange rate.

KEYWORDS

Tracer gas method, air infiltration, atmospheric CO_2, Meteorological conditions

1 INTRODUCTION

We breathe air continuously, and the pollutants present in it can affect the respiratory system and accumulate in our body. Some symptoms related to poor indoor air quality are irritation in the eyes, nose, throat or bronchial tubes, or the appearance of rhinitis or asthma. The poor indoor air quality can produce mood swings, difficulties in concentration and a decrease in work performance (Mahbob N. S. et al., 2011, Satish U. et al., 2012). Therefore, air quality is not only a health problem but also an economic one.

Indoor air quality is the result of indoor emissions and the entry of outside air, through infiltration and ventilation. In general, the indoor air is more polluted than the outside, which makes the existence of infiltration and ventilation in the building necessary. Nevertheless, this can mean an additional energy consumption because it can affect thermal comfort. Therefore, it is important to evaluate the efficiency of ventilation.

A way of monitoring the rate in which air exchange occurs is the tracer gas method. This technique consists of releasing an inert gas in the room to be studied. When the gas is uniformly distributed in the room, its concentration is sampled to find a relationship with infiltration rates. A widely used tracer gas is CO_2, as it is safe (non-flammable, non-toxic, non-allergic ...), non-reactive, measurable and mixes well with the air. The presence of CO_2 in the air in small amounts is not a problem in the sampling if a large amount of CO_2 is injected during the test (Sherman, 1990). In addition, it has the advantage of its low cost, since the CO_2 generated naturally by the occupants of the building can be used as a source (Hänninnen, 2012). Although the use of metabolic CO_2 is simple and inexpensive, it has drawbacks that must be taken into account for good performance.

- Temperature, humidity and pressure can affect CO_2 sensors.
- The generation of CO_2 is rarely measured. The generation of CO_2 by the occupants is generally estimated through generic tables based on the activity and weight of the people.
- Outdoor CO_2 concentration varies daily and diurnal depending on traffic and weather (ECA, 2003, Batterman, 2017). In the tracer gas method, the outdoor concentration of CO_2 is considered as constant of 350-600 ppm depending on the site and year (Seppänen, 1999, Roulet et al., 2002, Xiaoshu Lu, 2011).
- Air exchange is generated by wind effect and stack effect and therefore depends on heating-cooling loads and weather: (Batterman, 2017, Roulet, 2002).

Previous research has addressed several aspects of the effects of meteorology conditions (air temperature, relative humidity, and wind speed and direction) on CO_2 concentration (Strong, 2011; Sreenivas, 2016) and on air exchange rate (Laschober and Healy, 1964, Shaw, 1981, Almeida, 2017). High temperature enhances the photosynthesis (Sreenivas, 2016) and the convection (Parazoo, 2008). Both processes decrease the atmospheric CO_2. Moisture in the soil greens the vegetation enhancing the photosynthesis and limiting the soil respiration. Both processes reduce the CO_2 concentration in the atmosphere (Sreenivas, 2016). Strong winds imply higher shear and more turbulence diluting the CO_2 in the atmosphere (Parazoo, 2008).

On the other hand, most of the studies have determined a linear relation between air change rate and both variables, indoor-outdoor temperature difference and wind speed. Malik (1978) went further and studied the relation with wind direction. He concluded that wind perpendicular to the wall is highly related to high air change rates. Montoya (2011) studied the relation in different conditions and determined the predominance of each variable. For example, in calm days the temperature difference dominates the change of the air change rate.

This paper proposes to determine the rate of air exchange from the instantaneous concentration of CO_2 in the environment. In addition, the relationship between the air exchange rate with different meteorological parameters is exposed. The meteorological parameters considered were air temperature, dew point, barometric pressure, relative humidity, precipitation, wind speed, wind direction, and solar irradiation.

2 MATERIALS AND METHOD

2.1 Theoretical formulation

The type of tracer gas test most widely used is the tracer decay. In a tracer gas decay test, the test space is initially loaded to a concentration of tracer gas appropriate for the instrumentation and then the injection is turned off. During the decay, the concentration is monitored. Since there are no sources or sinks of CO_2, the change in the concentration of CO_2 inside the zone is related to the airflow into and out of the zone:

$$\frac{dC_i}{dt} = -C_i\lambda + C_a\lambda \quad (1)$$

where C_i is CO_2 concentration in the room (ppm), λ is the air exchange rate (h^{-1}); C_a is the outdoor CO_2 concentration (ppm). In the decay case, the evolution of the indoor CO_2 concentration has an exponential behaviour described by the Eq. 2.

$$C(t) - C_{equi} = (C_0 - C_{equi})e^{-\lambda t} \quad (2)$$

where C(t) is the instant concentration in the room (ppm); C_{equi} is the equilibrium concentration that in the CO_2 decay tracer method equals to the outdoor concentration (ppm); C_0 is the initial concentration (ppm); λ is the air change rate (h^{-1}); t is the sample time (h). The indoor and outdoor CO_2 concentrations vary throughout the day and we measure them every 1 minute. The previous equation is discretized as indicated in Eq. 3.

$$C_{in_{n+1}} - C_{out_n} = (C_{in_n} - C_{out_n})\mathrm{e}^{-\lambda\Delta t} \quad (3)$$

This equation can be fit to the measured data using regression methods.

2.2 Experimental site description

The study site is the office of the PhD students in the building of the Mechanical Engineering Department located on the university campus at the southern end of the city of Coimbra, Portugal (40º11'4.31''N 8º24'46.5''W, elevation 37m). It is an educational building surrounded by large trees and isolated from the influence of the city by a hill (Fig. 1). The only existing traffic is from the department's faculty and students. The climate is Mediterranean with oceanic influence. Mediterranean climates (Cs) receive rain primarily during winter season from the mid-latitude cyclone. The average annual temperature is 16.5ºC. Over the course of the year, the temperature typically varies from 10ºC to 22ºC and is rarely below -5ºC or above 30ºC. Average monthly temperatures vary by 11.8ºC. Average annual rainfall amounts to 922 mm and the least amount of rain occurs in July when the average of this month is 10 mm. With an average of 129 mm, the most precipitation falls in January.

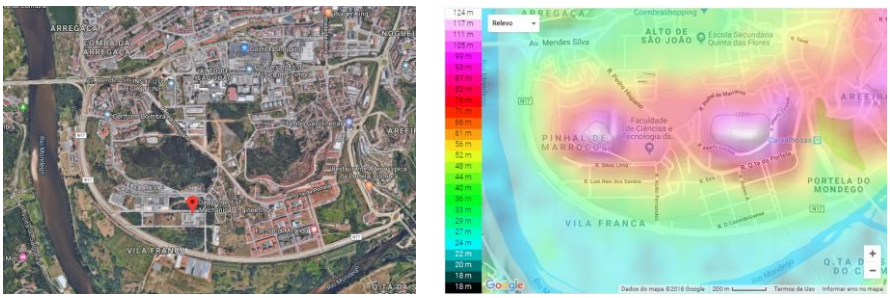

Figure 1: (a) Satellite image of the south of Coimbra. (b) Relief map of south of Coimbra, Portugal.

2.3 Measurements and Data Processing

The weather station measures the following parameters: air temperature, relative humidity, barometric pressure, wind speed and direction, solar irradiance. The anemometer and the pyrometer are mounted on poles at 5m over ground level. The sensors produce raw data each 0.1s, from which a 5 min average is calculated. The CO_2 concentrations were sampled with two Carbon Dioxide - Temp - RH Data Loggers, one place outdoor and the other in the PhD student office. The sampling time of the carbon dioxide sensors is 1 minute. For reducing random noise, the signal of the CO_2 concentrations were filtered using a Savitzky-Golay FIR filter with frame length of 6 hours.

Three months of data used, from February 27, 2019 to June 7, 2019. Multiple linear regression was performed to estimate relationships between the air exchange rate and the different meteorological parameters. In the section that follows, the results obtained will be discussed.

3 RESULTS AND DISCUSSION

This study focuses on the decay trace gas method. The metabolic CO_2 released by the occupants of the office is used as a tracer gas. Since the objective is the study of the influence of the external environment, the calculations are made at times when the office is unoccupied and approximately 3 hours immediately after the departure of all occupants. Figure 2 shows the indoor and outdoor CO_2 concentration for a 16 days period.

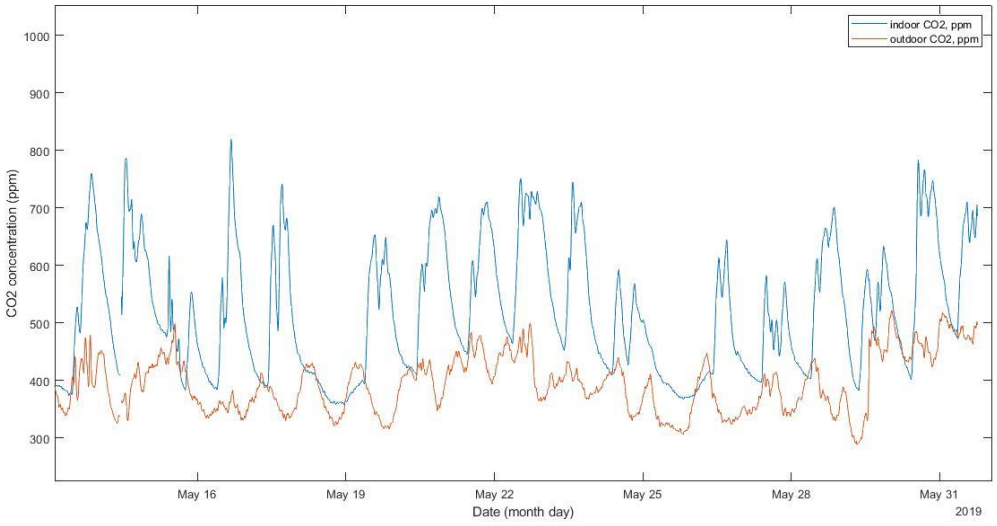

Figure 2: Indoor and outdoor CO2 concentration.

The air exchange rate (AER) from Equation 3 is determined by applying a linear regression to every period in which the office is unoccupied. The different values obtained in each period are shown in Figure 3. The average of results is 0.1965 ± 0.1206 h^{-1}. Applying the same process to the whole sample the air exchange rate is 0.1977 ± 0.0167 h^{-1}. Although both values are very close, the dispersion of the data with respect to the mean indicates that there are factors that affect the estimate.

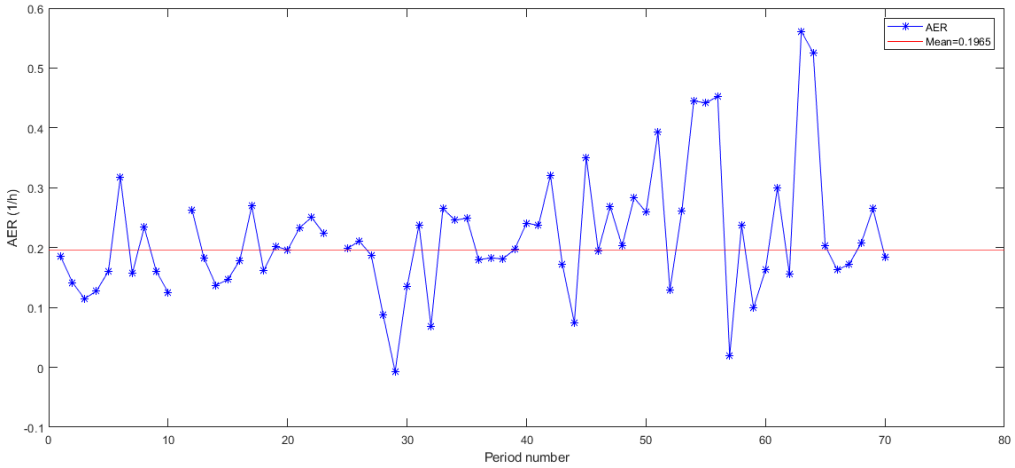

Figure 3: Estimated air exchange rate in different periods when the office is unoccupied.

3.1 Correlation between AER and different meteorological factors

The study of the correlation between AER and the different factors was carried out using multiple linear regression. By adding all the factors that describe different processes, we can explain 80% of the AER variation with a highly significant p-value = 4.4e-05. The statistics of this multiple regression are shown in Table 1. The most significant factors are the outdoor temperature, the outdoor relative humidity, and the difference between indoor and outdoor dew point. However, they are not the ones with high effect on AER prediction. The factors with highest effect on the estimation of AER are the difference between indoor temperature and the indoor dew point (iS in Table 1), the indoor relative humidity (iRH in Table 1) and outdoor temperature (oT in Table 1). Wind direction is not statically significant nor does it have a large effect on the AER estimate but it improves the model by 17%. The average value of the AER estimated by this model is 0.1592 ± 0.0675 h^{-1}, very close to values obtained by the mass balance.

The fact that wind direction has an effect on the amount of information provided by the model but is not statistically significant, is due to the lack of data. The building is located to the south of two hills, protected from the north and north-easterly winds. Many nights the winds are very gentle and there are no records.

On the other hand, this analysis is in agreement with the results of the aforementioned studies. The AER depends above all on temperature and humidity. In our analysis, the outdoor temperature plays a more important role than the indoor temperature. This is because the outdoor temperature varies more widely. In addition, it is a factor closely correlated with variations in ambient CO_2 concentrations.

Table 1: Statistics of correlation between AER and meteorological parameters: Indoor Temperature (iT), indoor Relative Humidity (iRH), outdoor Temperature (oT), outdoor Relative Humidity (oRH), difference between indoor and outdoor Dew Point (ΔDP), Wind Direction (WD), Wind Speed (WS), Daily Rain (Rain), Solar Radiation (SOL), and difference between indoor Temperature and Dew Point (iS).

Variables	Estimated Coef.	SE	t-Stat	pValue
Intercept	- 25.045	6.233	-4.0181	0.00067434
iT	+0.1123	0.03491	3.2168	0.0043268
iRH	+0.3395	0.07823	4.3392	0.00031834
oT	-0.1808	0.03088	-5.8559	9.9498e-06
oRH	-0.0310	0.00585	-5.2995	3.4663e-05
ΔDP	-0.1439	0.02864	-5.0246	6.4956e-05
WD	+0.0004	0.00032	1.1848	0.24997
WS	+0.0099	0.00445	2.2253	0.03773
Rain	-0.0688	0.02284	-3.0102	0.0069158
SOL	-0.0002	7.155e-05	-2.5701	0.01827
iS	+1.0179	0.25687	3.9627	0.00076769

In terms of humidity, the indoor humidity has a greater contribution to the prediction of AER due to the possibility of saturation inside the office.

4 CONCLUSIONS

The AER in the office is 0.1977 ± 0.0167 h^{-1}. It can be estimated from a model based on meteorological factors, particularly temperature and humidity. The temperature has different effects, direct and indirect, also affecting the concentration of CO_2. The effects of humidity are shown in different variables, from the relative humidity, the difference in the dew temperature and even in the rain. The wind also contributes to the variation of the AER, both its direction and its speed. Solar radiation contributes to a lesser extent, especially affecting the concentration of environmental CO_2.

5 ACKNOWLEDGEMENTS

The presented work was framed under two projects:
• The Energy for Sustainability Initiative of the University of Coimbra and LAETA (Associated Laboratory for Energy, Transports and Aeronautics) Project "SusCity: Modelação de sistemas urbanos para a promoção de transições criativas e sustentáveis". The first author wishes to acknowledge the Portuguese funding institution FCT – Fundação para a Ciência e Tecnologia, for supporting her research through the Ph.D. grant MITP-TB/CS/0026/2013
• The project TRAPHIC-"Traffic related air pollution impacts on historic city centres: an integrated approach" Supported by the Portuguese Foundation for Science and Technology (FCT) through national funds (PTDC/ECM-URB/3329/2014), and the co-funding of the European Regional Development Fund (POCI01-0145-FEDER-016729) and COMPETE2020.

6 REFERENCES

Almeida, M.S.F, Barreira, E., Moreira, P., (2017): *Assessing the variability of the air change rate through tracer gas measurements*, Energy Procedia 132 (2017) 831–836.

Batterman, S., (2017), *Review and Extension of CO2-Based Methods to Determine Ventilation Rates with Application to School Classrooms*, Int J Environ Res Public Health. Feb; 14(2): 145, 2017.

ECA (European Collaborative Action), (2003), *Urban Air, Indoor Environment and Human Exposure, Environment and Quality of Life* Report No 23 Ventilation, Good Indoor Air Quality and Rational Use of Energy, 2003.

Hänninen, O., 2012, *Combining CO2 data from ventilation phases improves estimation of air exchange rates*, Proceedings of Healthy Buildings Conference, Brisbane, July 8–12, 2012.

Laschober, R.R., Healy, J.H., *Statistical analyses of air leakage in split-level residences*, ASHRAE Trans (1964) 70: 364–374

Mahbob N. S. et al. (2011), *A Correlation Studies of Indoor Environmental Quality (IEQ) Towards Productive Workplace*, 2nd International Conference on Environmental Science and Technology IPCBEE vol.6 (2011) IACSIT Press, Singapore.

Malik N., (1978), *Field studies of dependence of air infiltration on outside temperature and wind*, Energy Build (1978) 1: 281–292.

Montoya, M. I., Pastor, E., Planas, E., (2011), *Air infiltration in Catalan dwellings and sealed rooms: An experimental study*, Building and Environment Volume 46, Issue 10, October 2011, Pages 2003-2011.

Parazoo N.C. et al., (2008): *Mechanisms for synoptic variations of atmospheric CO2 in North America, South America and Europe*, Copernicus Publications, Atmos. Chem. Phys., 8, 7239–7254, 2008.

Roulet Claude-Alain & Flavio Foradini (2002), *Simple and Cheap Air Change Rate Measurement Using CO_2 Concentration Decays*, International Journal of Ventilation, 1:1, 39-44, DOI: 10.1080/14733315.2002.11683620

Satish U. et al. (2012), *Is CO2 an Indoor Pollutant? Direct Effects of Low-to-Moderate CO2 Concentrations on Human Decision-Making Performance*: Environ Health Perspect 120: pp 1671–1677.

Shaw, C.Y., (1981): *A Correlation between Air Infiltration and Air Tightness for Houses in a Developed Residential Area*; National Research Council Canada: Ottawa, OT, Canada, 1981, 87, 333 –341.

Sherman, M. H. (1990), *Tracer-gas techniques for measuring ventilation in a single zone*. Building and Environment, 25, pp 365-374.

Seppänen, O. A. et al. (1999), *Association of Ventilation Rates and CO2Concentrations with Health and Other Responses in Commercial and Institutional Buildings*, Indoor Air 1999; 9: 226–252

Sreenivas, G. et al. (2016), *Influence of Meteorology and interrelationship with greenhouse gases*, Copernicus Publications, Atmos. Chem. Phys., 16, pp 3953–3967.

Strong, C. et al. (2011), *Urban carbon dioxide cycles within the Salt Lake Valley: A multiple-box model validated by observations*, J. Geophys. Res., 116, D15307.

Xiaoshu Lu, Tao Lu and Martti Viljanen (2011), *Estimation of Space Air Change Rates and CO2 Generation Rates for Mechanically-Ventilated Buildings*, Advances in Computer Science and Engineering, Dr. Matthias Schmidt (Ed.), ISBN: 978-953-307-173-2, InTech

Successive Indoor Air Pressure Calculation Method for Natural Ventilation Rate Prediction

Haruna Yamasawa[*1], Toshio Yamanaka[1],
Tomohiro Kobayashi[1], and Jihui Yuan[1]

1 Osaka University
Suita 565-0871
Osaka, Japan
**yamasawa_haruna@arch.eng.osaka-u.ac.jp*

ABSTRACT

Installing Natural Ventilation (NV) system in office buildings leads to the reduction of energy consumption of heating, ventilation and air conditioning (HVAC), which accounts for approximately 50% of total in an office building in Japan. However, it is difficult to estimate the NV performance before its completion, because the NV system is easily affected by the outdoor environment. Thus, its design method is not yet established. This study aims to easily estimate the NV performance by using transient airflow network calculation, and the wind pressure coefficient used in the method was obtained from Computational Fluid Dynamics (CFD). The theory of the model is described in detail by this study. Natural ventilation rate was calculated for two different models. Firstly, in order to learn about the availability of the calculation method, to know about available range of the time step and to calculate the transient conditions in a short period, a simple model, which consists of one node and two branches, was used. Secondly, in order to learn about the applicability of the method to actual buildings, an actual building was simulated as a complicated model, which consists of seven nodes and thirteen branches, and its natural ventilation rate was calculated by the method. As a result, at the simple model with the wind pressure coefficient that varies over time, the time-series change of the airflow rate was able to be obtained. In addition, at the actual building model, though its complexity, the time-series change of temperature and ventilation flow rate was obtained by the method. It was shown that the temperature changes are slower than that of pressure, because of the heat capacity of the air, which correspond the real phenomenon.

KEYWORDS

Natural ventilation, Network model, Transient calculation, Ventilation performance prediction

1 INTRODUCTION

Natural ventilation (NV) has long been used in Japanese buildings because of hot and humid climate in summertime [1]. It was mainly applied in residential buildings in the past years, and now it has been spread to non-residential buildings including office buildings. With the need of energy conservation and Business Continuity Planning (BCP) is on the rise, NV system, which basically does not use non-renewable energy, is attracting increasing attention. In Japanese commercial sector, energy consumption of Heating, Ventilation and Air-Conditioning (HVAC) accounts for approximately 30% of total energy consumption [2]. Subsector "Offices and buildings", which is a subsector in commercial sector, accounts for more than 20% of energy consumption in the sector. In the subsector, HVAC equipment is the largest consumer of energy, which accounts for 50% of all [3]. Furthermore, in western countries, it was shown that HVAC is the main end use in office buildings, whose proportion was close to 50% of the total energy consumption for non-residential buildings [4]. Thus, reducing energy consumption in

HVAC system has a large impact on running cost of the building as well. NV system uses renewable energy for driving force of ventilation, i.e. the air temperature difference (difference of air density) and wind pressure [5-8]. Using renewable energy saves expenses for ventilation, compared to mechanical ventilation systems. Yamamoto et al. [9] conducted a survey of natural ventilation system in 72 naturally ventilated buildings. It was shown that the reasons for installing NV system was divided as; saving energy and ensuring comfort. Most of the reasons for designers to install NV system are reducing the operation hours of air conditioning system. Since the range of acceptable thermal conditions seems to be wider under naturally ventilated condition, compared to centralized HVAC system [10], NV system can be used to enhance the satisfaction of thermal condition of buildings. Hummelgaard et al. [11] operated simultaneous field measurement in five mechanically and four naturally ventilated open-plan office buildings. It was reported that compared to the mechanically ventilated buildings, even though the air temperature and CO_2 concentration varied more and in some cases higher values were recorded, higher degree of satisfaction with the indoor environment and lower prevalence/intensity of symptoms among the occupants were obtained in the naturally ventilated buildings.

Chen [12] summarized methodology for predicting the performance of ventilation. The methods were classified into seven models; analytical model, empirical model, small-scale experimental model, full-scale experimental model, multizone model, zonal model and CFD model. However, this system causes unstable flow patterns [13] and fluctuation of airflow rate through NV apparatus. Because it is difficult to evaluate the NV performance before its completion, the method for estimating and predicting the NV performance has not yet been established. The designers are generally referring to the past cases, and are still designing it by rule of their thumb to some extent [14].

The aim of this study is to establish and propose a simplified prediction and estimation method of the NV performance for non-residential buildings, using a transient network model method and the wind pressure coefficient obtained from CFD analysis.

2 THE THEORY OF THE MODEL

In the airflow network model, each of the room is assumed to be a node of air pressure and temperature; each of the openings between rooms is assumed to be the branch connecting the rooms with the flow resistance. Air flow and heat transfer through the network are calculated by solving the balance equations. In the network model of NV, differential pressure Δp between ends of a branch was calculated considering the buoyancy and wind force. The airflow rate F through a branch is defined as:

$$F = sign(\Delta p) C_D A \sqrt{2/\rho \left| \Delta p \right|} \tag{1}$$

where C_D [-] is the discharge coefficient, A [m^2] is the area of the opening and ρ [kg m^{-3}] is the air density.

In many network model calculations, the air is commonly assumed to be incompressible fluid, so the density doesn't change by time. Thus, under the steady state, because of the law of mass conservation, the sum of mass flow rate and volumetric flow rate at a node is:

$$\sum \rho F = \Sigma F = 0 \tag{2}$$

However, the airflow rate was calculated over time and air is assumed to be compressible in the model in this paper. In other words, the model does not hold Eq. (2). The air flow rate, the air density, air temperature and the air pressure were calculated successively in the model.
Here, the density of the air in the room at $(k+1)\Delta t$ [s] is defined as:

$$\rho_i^{k+1} = \rho_i^k + \frac{\partial \rho}{\partial t}\Delta t = \rho_i^k + \frac{\partial M}{\partial t}\frac{\Delta t}{V_i} \approx \rho_i^k + \Sigma\left(\rho F_{i,j}^k \frac{\Delta t}{V_i}\right) \tag{3}$$

where, M_t [kg] is the mass of the air in a room and V [m^3] is the volume of the room. In this model, it is assumed that: the condition is kept isothermal during infinitesimal time interval Δt [s]; the temperature change occurs after the density change. The temperature of the air in a room at $(k+1)\Delta t$ [s] is defined as:

$$T_i^{k+1} = T_i^k + \Sigma\left\{\left(Q_{v_{i,j}}^{\ k} + Q_{h_i}\right)\Delta t \,/\, \left(C_p \rho_i^{k+1} V_i\right)\right\} \tag{4}$$

where T [K] is the temperature of the air in a room, Q_v [W] is the heat gain at the room caused by ventilation, Q_h [W] is the heat generation load at the room, and C_p [$J \cdot kg^{-1}K^{-1}$)] is the specific heat capacity of the air.

Here, the ideal gas law and the deformed equations are shown below:

$$pV = nRT \tag{5}$$

$$pm = \rho RT \tag{6}$$

$$p_i^{k+1} = \rho_i^{k+1}\, T_i^{k+1}\, R/m \tag{7}$$

where p [Pa] is the air pressure in a node, n [mol] is the number of moles, R [$J\ K^{-1}mol^{-1}$] is the gas constant and m [$g\ mol^{-1}$] is the molar mass. The air pressure of each node at $(k+1)\Delta t$ [s] was calculated by Eq. (6)' with using the values of density and temperature obtained by Eq. (3) and Eq. (4), respectively.

The flow of the model is shown in Table 1. The merit of this model is that: (1) the time-series results are able to be obtained, and (2) the air is assumed to be compressible in this model, thus this model is expected to be correspond to the real phenomenon. Moreover, this method can calculate the airflow network without convergence calculation. Here, in this paper, this model shall be called as "Successive Indoor Air Pressure Calculation Method".

Table 1: Flow of the calculation program

	Incident	**Cause**	**Eq.**
Step 0	Set the initial and boundary conditions		
Step 1	Differential pressure occurs between each end of the branch	*Step 0 & 5*	-
Step 2	Air flows into the branch	*Step 1*	(1)
Step 3	Total mass and density of air at a node change	*Step 2*	(2) & (3)
Step 4	Temperature change occurs because of the ventilation and other heat fluxes	*Step 2*	
Step 5	Pressure change occurs	*Step 3 & 4*	

3 TRANSIENT CALCULATION WITH A SIMPLE MODEL

At first, a simple rectangular room model was chosen to verify if the proposed method works well for the transient calculation of the fluctuating airflow. The results from the conventional method are compared with the new calculation method.

3.1 Calculation method and conditions

A simple single room model is shown in Figure 1. The model is a 3,000×3,000×3,000 cube with two openings at each side of the wall parallel to the approaching flow of 5 m s^{-1} at upper air. The wind pressure coefficient at each opening is required for the calculation as the boundary condition, thus the results of large eddy simulation (LES) by Kobayashi et al [15] were applied as input data. The CFD model analysed to obtain wind pressure coefficient by Kobayashi et al was a 200×200×200 sealed cube without any openings, which is 15 times smaller than the model used in this paper, with the approach flow of 10 m s^{-1} at upper air, which is 2 times larger than the calculation condition in this paper. The time-series result of wind pressure coefficient for two openings (Op-R and Op-L) is shown in Figure 2. Due to the scale difference and wind velocity difference, the data had to be modified. To make the time scale equal, the time was multiplied by 30 before the calculation, thus the data in Figure 2 was assumed to be the time-series result for 150 [s] (= 5 [s] × 15 × 2) in the calculation.

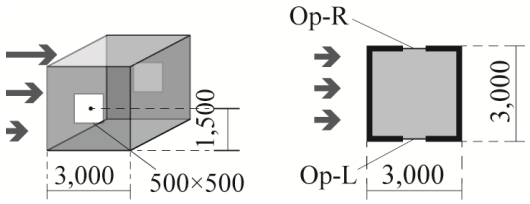

Figure 1: Single room Model

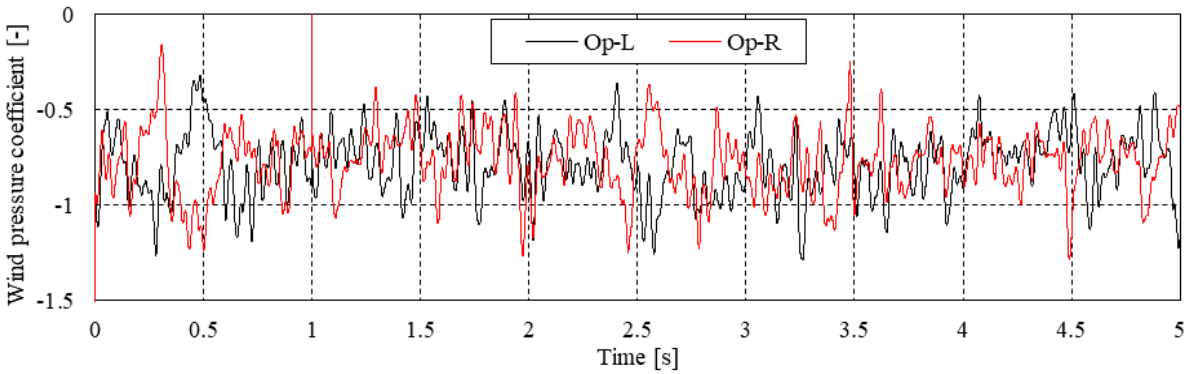

Figure 2: Time-series change of wind pressure coefficient

(Note: The figure shows the CFD result with measurement scale.)

With using the data of wind pressure coefficient, the following two transient calculations were conducted:

1) Successive Indoor Air Pressure Calculation Method

The model that has been explained in Chapter 2.

2) Instantaneous steady-state calculation assuming incompressible fluid

Resistance coefficients of two openings were summed up to evaluate "overall effective opening area" through flow path as follows:

$$\overline{(\mathrm{C_D A})} = \{(C_D A)_1^{-2} + (C_D A)_2^{-2}\}^{-0.5} \tag{8}$$

where $C_D A$ is the effective opening area for each opening (branch) [m^2]. Airflow rate through the room was also calculated by Eq. (1), and differential pressure in the equation is equal to the difference of static pressure across the openings in this method.

Air temperature and pressure were set as initial condition, and air density was calculated with the equation deformed from Eq. (6):

$$\rho = Pm/RT \tag{9}$$

where ρ [kg m^{-3}] is the air density, p [Pa] is the air pressure in a node, m [g mol^{-1}] is the molar mass, R [J $K^{-1}mol^{-1}$] is the gas constant and T [K] is the air temperature. The calculation condition is shown in Table 2.

Table 2: Calculation method and condition

Solution	**Time step [s]**	**Boundary condition**	**Initial condition**		
		Wind velocity of approach flow [m s^{-1}]	**Temperature [°C]**	**Pressure [Pa]**	**Density [kg m^{-3}]**
Explicit	5.0×10^{-6} (1×10^{6} cycles)	5.0 (constant)	24 (constant)	0 (Gauge pressure)	Calculated by **Eq. (9)**

3.2 Result and discussion

Figure 3 shows the calculation result of the airflow rate through each opening by method 1 (Successive Indoor Air Pressure Calculation Method). Outflow was defined to be positive at each opening. The calculation result of the airflow rate through the room by method 1 and method 2 (instantaneous steady-state calculation) are compared in Figure 4. The airflow from Op-L to Op-R was defined to be positive in method 2. The calculation results of airflow rate by method 1 was approximately the same with the results obtained by method 2. Thus, the calculation result of airflow rate by method 1 assumed to be reasonable. As shown in Figure 5, the difference between inflow/outflow rate was approximately 1.0% of the airflow rate, however it was expected that the compressibility may not be able to be avoided in larger room.

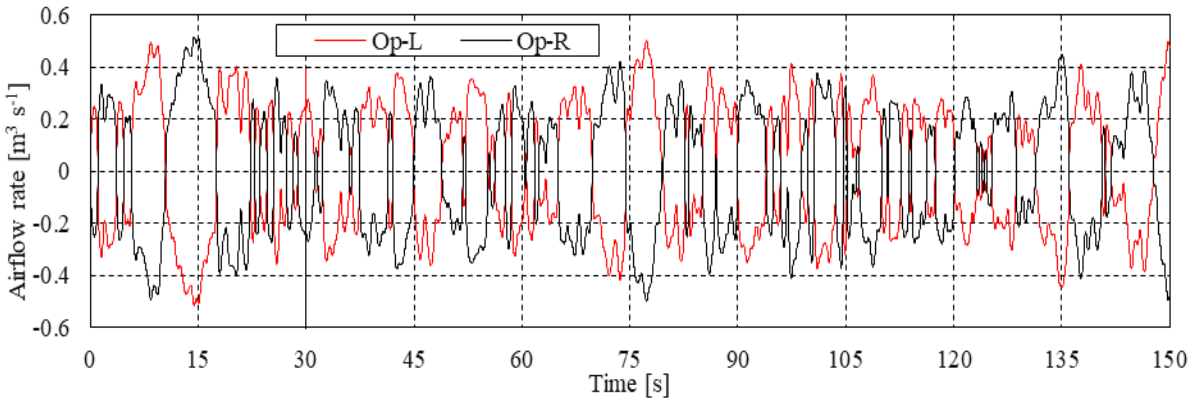

Figure 3: Airflow rate through openings by method 1 (Outflow was defined to be positive)

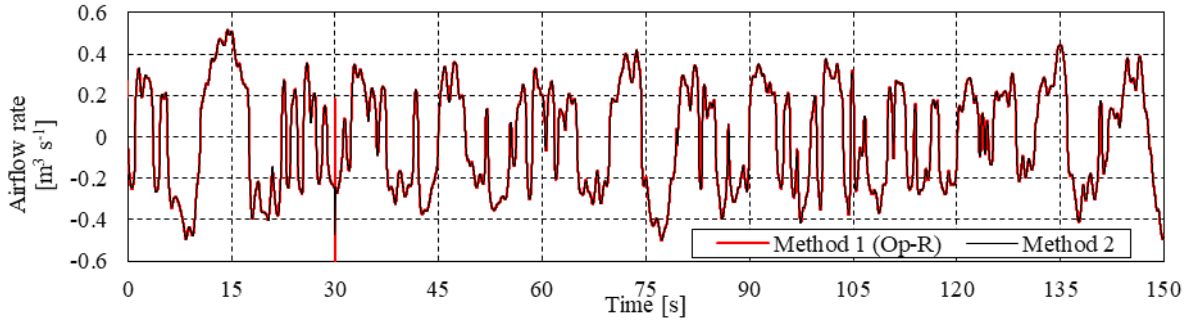

Figure 4: Airflow rate through the room by method 2 (Op-L → Op-R defined to be positive)

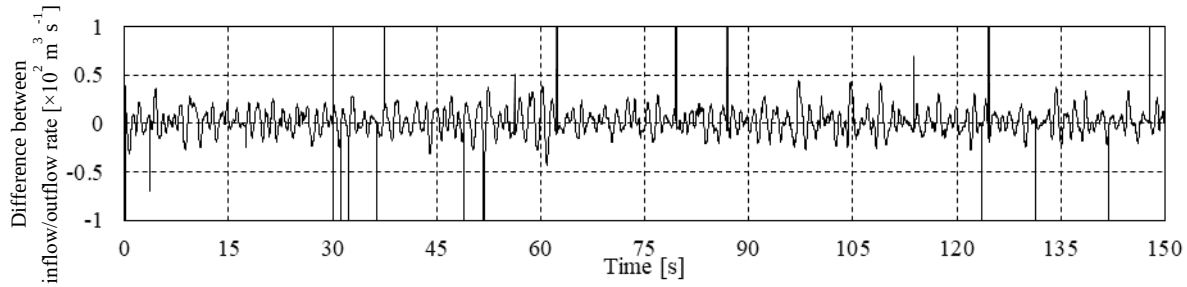

Figure 5: Difference between inflow/outflow rate by method 1 (Outflow was defined to be positive)

Air pressure inside the room at floor level calculated by method 1 and air pressure calculated by the result of airflow rate in method 2 are shown in Figure 6, where air pressure P of method 2 was calculated with the following equation based on the assumption of mass conservation, i.e. the assumption that the air is incompressible and the density is constant:

$$P = \left(\frac{F}{C_D A}\right)^2 \frac{\rho}{2} sign(F) + C_w \frac{1}{2} \rho V_o^2 \quad (10)$$

where P [Pa] is the pressure, F [$m^3\ s^{-1}$] is the airflow rate, $C_D A$ [m^2] is the effective area of the opening (Op-R), ρ [kg m^{-3}] is the density, C_w [-] is the wind pressure coefficient of the corresponding opening, and V_o [m^3] is the outside wind velocity [m s^{-1}].
The results of air pressure obtained by two methods were correspond to each other. Thus, the calculation results of air pressure also were reasonable. Therefore, it was expected that method 1 can be applied to the calculation for more complicated building flow network model, e.g. the room with several openings so the airflow direction is difficult to be determined. Air pressure varied around -12 [Pa] in both method 1 and 2, due to the negative wind pressure coefficient outside the openings.

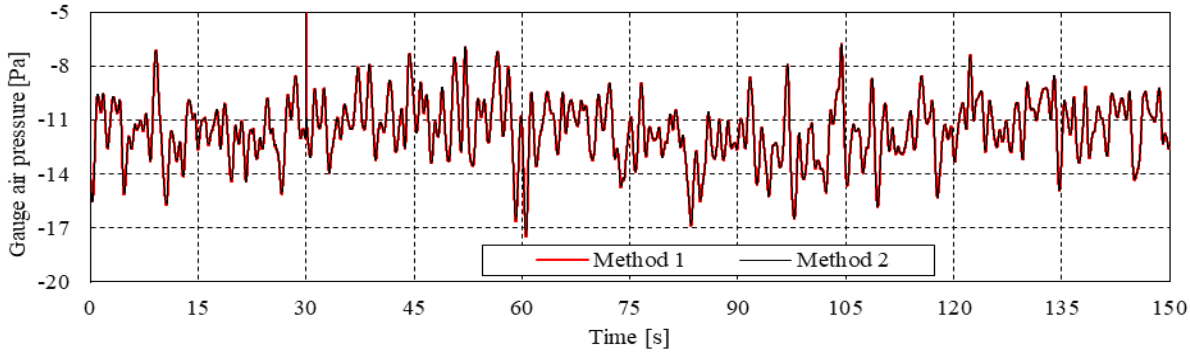

Figure 6: Gauge Air pressure at floor level

4 STEADY STATE CACULATION WITH BUILDING MODEL

A more complicated model, which simulates an actual building, was chosen to verify the validity of the calculation method for actual buildings. Additionally, this calculation is for verifying whether the model properly shows convergence to the steady result, if the boundary conditions are steady, and whether the time-series change correspond to the real phenomenon.

4.1 Calculation method and conditions

The measurement target building in the authors' previous study [16] was chosen to be the calculation target in this study. In order to obtain the wind pressure coefficient of the building, CFD analysis with the shear stress transport (SST) k-ω model was conducted. The CFD model of the target building is shown in Figure 7 (a). To facilitate the successive calculation, the building was simplified to be a model shown in Figure 7 (b). Using the results of wind pressure coefficient obtained from the CFD analysis, the successive calculation was conducted under the condition detailed in Table 3.

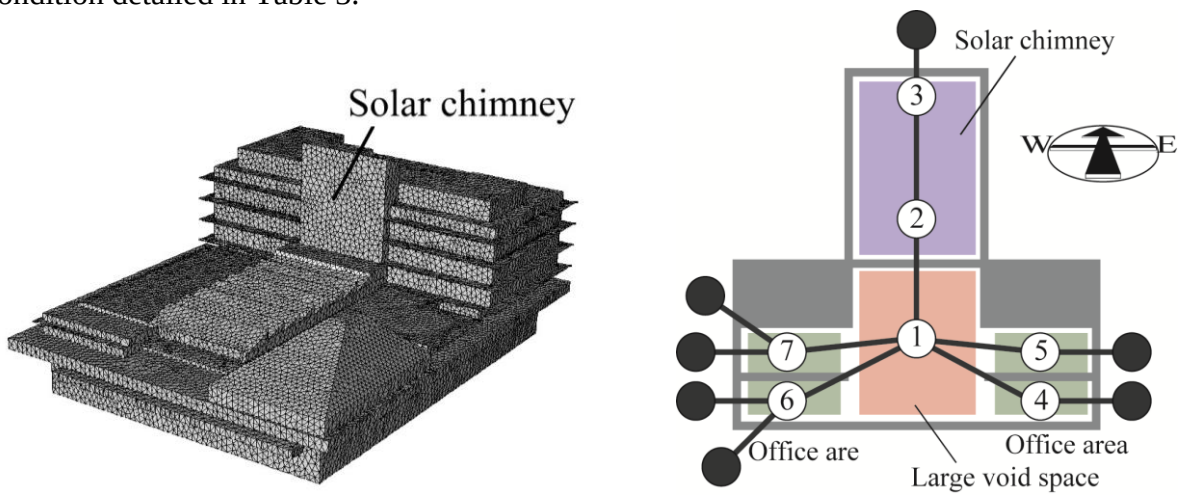

(a) Model of CFD analysis (b) Model of calculation

Figure 7: CFD Model and calculation model of Target Building

Table 3: Calculation condition

Programming Language		Fortran
Solution		Explicit
Time step		1.0×10^{-4} [s] (1×10^{7} cycles = 1,000 [s])
Initial Condition	Temperature	outdoor air: 24℃ (Constant), indoor air: 28℃
	Pressure	Gauge pressure: 0 [Pa] (Atmospheric pressure: 101,300 [Pa])
	Density	Calculated by Eq. (9)
Heat generation	Office area	60 [W m^{-2}] × Floor area [m^2]
	Solar chimney	500 [W m^{-2}] × Wall (glass) area [m^2]

4.2 Result and discussion

Calculation results of air pressure and temperature at each node are shown in Figure 8 and 9, respectively. The airflow rate through each branch are shown in Figure 10. As shown in Figures

8-10, air pressure and airflow rate reached to the steady state soon, while the air temperature took approximately sixteen minutes for reaching the steady state, which also occurs in the real phenomenon, because of the heat capacity of the air. The time-averaged airflow rate through the branches are shown in Table 4. Comparing the airflow rate with the time-series change of the temperature, the node with large airflow rate reached to the steady state more quick than the others, because of the large air change rate. These results show that the proposed calculation method has simulated the real phenomenon properly.

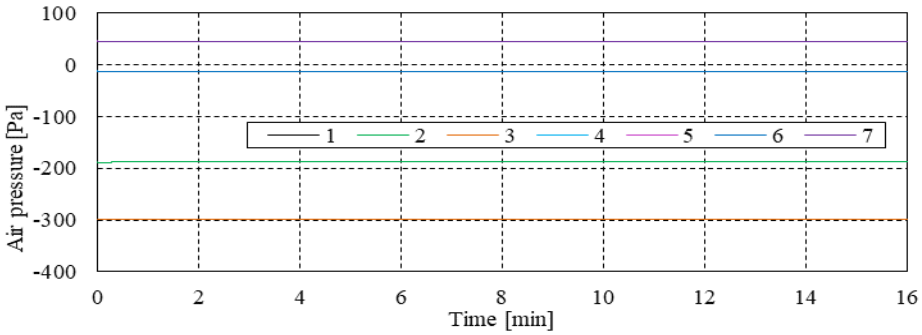

Figure 8: Air pressure at each node

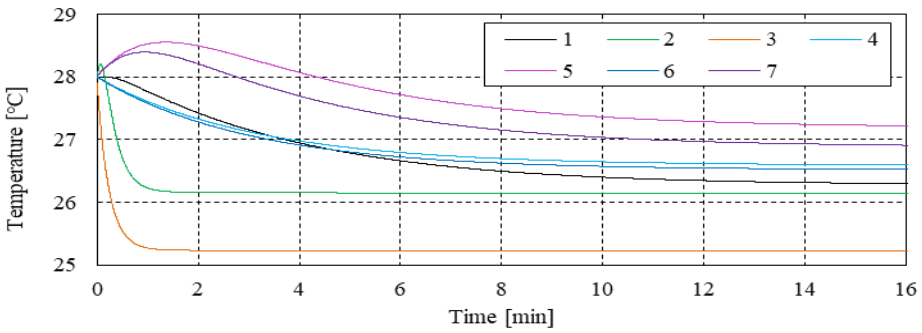

Figure 9: Air temperature at each node

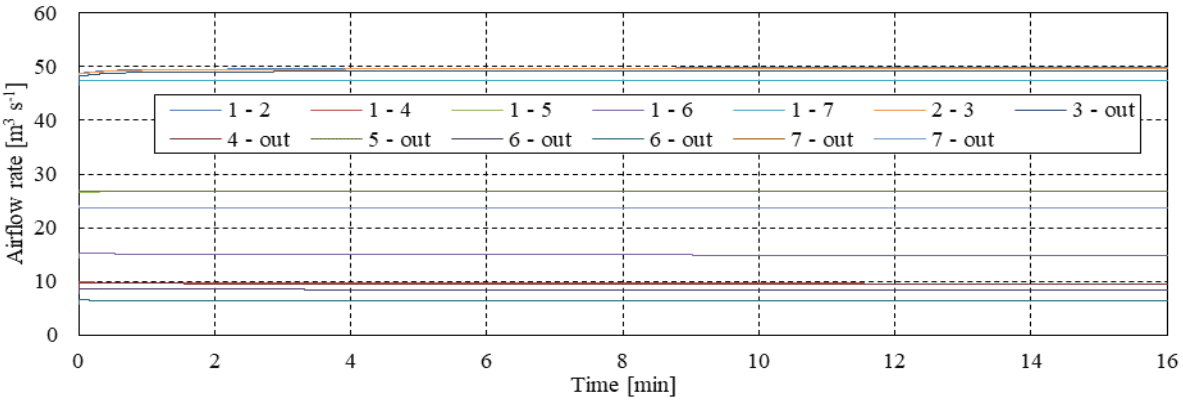

Figure 10: Airflow rate through each branch

Table 4: Averaged airflow rate through branches and difference between inflow/outflow at each node [$m^3 s^{-1}$]

Averaged airflow rate										
1 – 2	**1 - 4**	**1 - 5**	**1 - 6**	**1 - 7**	**2 - 3**	**3 - out**	**4 - out**	**5 - out**	**6 – out**	**7 - out**
49.7	9.6	26.7	15.0	47.5	49.6	49.2	9.5	26.8	14.8	47.5
Difference between inflow/outflow rate at each node (outflow was defined to be positive)										
		1			**2**	**3**	**4**	**5**	**6**	**7**

-0.0795	0.0990	0.3896	0.0925	0.0664	0.1403	0.0694

5 CONCLUSIONS

The theory of the "Successive Indoor Air Pressure Calculation Method" was explained, and two types of the calculation model was analyzed in this paper. One is the simple model to verify the applicability for the calculation with time-varying boundary condition, and the other is the complicated model for the actual buildings.

The main knowledge obtained in this study is summarized as follows:

- In a simple model with one node and two branches, the model calculation was conducted with transient condition with time-series change data of the wind pressure coefficient. However, there was no heat generation, thus the environment kept isothermal.

- By taking small time step, the vibration of the result was avoided, and it was confirmed that the model is able to calculate the time-series change of the pressure and airflow rate with the time-varying boundary condition.

- In a relatively complicated model, which is simulated by an actual NV building, the model calculation was conducted with steady state. However, there was heat generation, so the temperature time-series change of the air temperature was obtained.

- The result showed that the temperature took longer time for reaching the steady state, compared to the air pressure and airflow rate, due to the heat capacity, and it shows that the model has well simulated the real phenomenon.

The calculation result of this study showed the possibility of the calculation model to simulate the real phenomenon. The comparison between the calculation and experimental results is required as future prospects.

6 REFERENCES

[1] T. Kobayashi (2018). 130 Year History of Building Natural Ventilation Research in Japan – A Narrative Review. Journal of Environmental Engineering (Transactions of AIJ), 751, 749-759 (In Japanese)

[2] Japanese Ministry of Economy, Trade and Industry, Agency for Natural Resources and Energy (2018). FY 2017 Annual Report on Energy (Japan's Energy White Paper 2018). 139-140 (in Japanese)

[3] Japanese Ministry of Economy, Trade and Industry, Agency for Natural Resources and Energy (2015). Definition of ZEB and future measures proposed by ZEB Roadmap Examination Committee.

[4] L. Perez-Lombard, J. Ortiz, C. Pout (2008). A Review on Buildings Energy Consumption Information. Energy and Buildings, 40, 394-398

[5] T. S. Larsen, O. Heiselberg (2008). Single-sided natural ventilation driven by wind pressure and temperature difference. Energy and Buildings, 40, 1031-1040

[6] Y. Li, A. Delsante (2001). Natural ventilation induced by combined wind and thermal forces. Building and Environment, 36, 59-71

[7] M. Santamouris, P. Wouters (Eds.). (2006). Building Ventilation: The State of the Art. UK and USA: Earthscan Publications Ltd.

[8] T. Kurabuchi, M. Ohba, T. Endo, Y. Akamine, F. Nakayama (2004). Local Dynamic Similarity Model of Cross Ventilation Part 1 Theoretical Framework. International Journal of Ventilation, 2, 371-382

[9] Y. Yamamoto, M. Kumoki, H. Suzuki and S. Tanabe (2007). Investigation of Management of Natural Ventilation System. Journal of Environmental Engineering (Transactions of AIJ), 619, 9-16 (in Japanese)

[10] ANSI/ASHRAE Standard 55-2013 (2016) Thermal Comfort – Foundations and Analysis, Routledge

[11] J. Hummelgaard, P. Juhl, K.O. Sæbjornsson, G. Clausen, J. Toftum, G. Langkilde. (2007). Indoor air quality and occupant satisfaction in five mechanically and four naturally ventilated open-plan office buildings, Building and Environment, 42, 4051-4058

[12] Q. Chen (2009). Ventilation Performance Prediction for Buildings: A Method Overview and Recent Applications. Building and Environment, 44(4), 848-858.

[13] Y. Arinami, S. Akabayashi, Y. Tominaga, J. Sakaguchi, Y. Takano, M. Honda (2016). Proporsal of an Evaluation Method for Natural Cross-ventilation Performance Considering Flow Fluctuation – Study on Naturally Cross-ventilated House Using Large-Eddy Simulation (LES) Part 2. Journal of Environmental Engineering (Transactions of AIJ), 725, 589-597(In Japanese)

[14] Architectural Institute of Japan (Eds.). (2016). Natural Ventilation Design Handbook for Architects and Building Engineers (E-book). Translated by H. Kotani. Osaka: Gihodo Shuppan Co., Ltd.

[15] T. Kobayashi, M. Sandberg, T. Fujita, N. Umemiya (2018). Simplified Estimation of Wind-Induced Natural Ventilation Rate caused by Trbulence for a Room with Minute Wind Pressure Difference. Proceedings of Roomvent 2018, Track 4, pp.613-618

[16] H. Yamasawa, T. Yamanaka, Y. Momoi, S. Ito, K. Misuide and T. Fujii (2018). Ventilation Performance of Natural Ventilation Building with Solar Chimney. Air Infiltration and Ventilation Centre conference 2018 proceedings, 130-139

Using CFD simulation to improve estimation of wind pressure coefficient for naturally-ventilated buildings in tropical climate

Matthieu Zubialde-Elzaurdia*[1], Franck Lucas[1], Alain Bastide[2]

1 Laboratoire GEPASUD
University of French Polynesia
98702 Faa'a - Tahiti
French Polynesia
**Corresponding author:*
matthieu.zubialdeelzaurdia@doctorant.upf.pf

2 Laboratoire PIMENT
University of Reunion Island
117 rue du Général Ailleret
97430 Le Tampon – Reunion Island
France

ABSTRACT

Building energy simulation (BES) and Airflow network (AFN) programs generally incorporate wind pressure coefficients (C_p) estimated from secondary sources, namely data bases or analytical models. As these coefficients are influenced by a wide range of parameters, it is difficult to obtain reliable C_p data. This leads to uncertainties in BES-AFN models results, especially for naturally ventilated building studies, where air change rate which strongly depends on C_p, is a key value for thermal comfort and energy consumption results. This study focuses on naturally ventilated buildings in tropical climate and presents an alternative approach to estimate wind pressure coefficient. Computational fluid dynamics (CFD) simulations are performed to calculate wind-driven airflow rates at building opening level. Then wind pressure coefficient difference ΔC_p is calculated from large opening equation to be used as input data in BES-AFN program. Numerical simulations are performed for various wind directions on a typical cross-ventilated isolated building and a more complex building with opposite large openings. CFD results of wind pressure coefficient difference and airflow rate are compared to those obtained from AFN model using two different C_p sources. The results show that the calculated values vary greatly depending on the method used and highlight that an accurate estimation of wind pressure coefficient is a key parameter for evaluating natural ventilation in buildings.

KEYWORDS

Natural ventilation, computational fluid dynamics, airflow network model, wind pressure coefficient

1 INTRODUCTION

Tropical climate is characterized by relatively constant high temperature and humidity throughout the year, especially during summer (wet season). Providing thermally comfortable indoor environment in such conditions is seriously challenging. In most of the cases, building design response is based on active strategies to mechanically control indoor air temperature and humidity, thus resulting in a significant increase in the energy consumption of the buildings. Therefore passive strategies of sustainable architecture must be developed to reduce energy consumption in particular in tropical insular regions such as French Polynesia, where electricity production is highly polluting due to importation of fossil energy. In 2014, 279 000 tonnes of fossil fuels were imported, representing nearly 94% of the primary energy consumed by the country (ADEME, 2015).

Natural ventilation is a key strategy for the design of sustainable buildings in tropical climate. It addresses three distinct issues: thermal comfort, indoor air quality and energy savings. In order to quantify the impact of natural ventilation on thermal comfort and energy consumption, it is necessary to know the naturally driven ventilation rates. At building design stage, it is often

done by using Building Energy Simulation (BES) tools coupled with Airflow Network Models (AFN) which allow to perform annual simulation of the entire building, calculating coupled airflow and heat transfer.

Airflow network models are generally based on the large opening equation describing a steady incompressible flow through an opening (Bernoulli's assumption). This equation is valid under the following assumptions:

- the turbulent flow is fully-developed;
- the pressure distribution on the building facades is not affected by the presence of openings;
- the pressure drop across the inflow and outflow opening is equal to the static pressure difference, i.e. the dynamic pressure in the room can be neglected.

For wind-driven cross-ventilation, the large opening equation can be written as follows:

$$Q = C_D.A.U_{ref}.\sqrt{C_{p_W} - C_{p_L}} \quad (1)$$

Where A is the equivalent opening area (m^2), C_D is the discharge coefficient, U_{ref} is the reference wind speed at building height (m/s), C_{p_W} and C_{p_L} respectively the pressure coefficient on windward and leeward facade.

Wind pressure coefficient describes the pressure distribution on the building surfaces. It is defined by the equation:

$$C_p = \frac{P_x - P_0}{P_d} \; ; \; P_d = \frac{\rho.U_{ref}^2}{2} \quad (2)$$

Where P_x is the static pressure at a given point on the building facade (Pa), P_0 is the static reference pressure (Pa), P_d is the dynamic pressure (Pa), and ρ is the air density (kg/m3)

Wind pressure coefficient is influenced by a wide range of parameters, including building geometry, facade detailing, position on the facade, sheltering elements, wind speed, wind direction and turbulence intensity. Therefore it is difficult to obtain reliable C_p data. Cóstola et al. (Cóstola et al., 2009) identify two main sources of C_p data.

Primary sources including full-scale measurements, wind-tunnel measurements and Computational Fluid Dynamics (CFD) simulations are considered to be the most reliable but also the most expensive and complex to realize. As wind tunnel experiments can rarely be carried out during building design stage, CFD can be an interesting alternative.

Secondary sources including databases and analytical models, are most often used in BES–AFN programs. For example, EnergyPlus uses the analytical model proposed by Swami and Chandra. Databases compile C_p data generally obtained from wind-tunnel measurements with the main objective of providing an indication on the range of C_p values for various basic buildings geometries and orientations. Analytical models are also developed based on wind-tunnel and full-scale experiments, using regression techniques to analyse a large amount of C_p data. They consist of a set of equations to calculate averaged C_p values but are still limited to a narrow range of parameters taken into account. So, influence of environment is not considered by these sets of equations.

Comparing pressure coefficients from different data sources, Cóstola et al. (Cóstola et al., 2009) concluded that for the same building in the same conditions, C_p values show large variations, even for simple configurations like fully exposed cubic buildings. Pressure coefficients are generally calculated considering buildings without openings and averaging pressure surface values over the building facades. Cóstola et al. (Cóstola et al., 2010) highlighted that the use of surface-averaged pressure coefficients can lead to uncertainty in airflow rate calculations. Karava et al. (Karava et al., 2006) investigated internal pressure coefficient in naturally ventilated building and found that this parameter has a significant impact on airflow prediction.

Discharge coefficient is also a source of uncertainty in the calculation of airflow rates. It characterizes the local contraction of the flow at opening level and shear stress forces and therefore depends on the characteristics of the fluid and on the shape and dimensions of the opening. For small sharp-edged openings, typical values for discharge coefficient are within the range 0.60–0.65 and are considered independent of the Reynolds number (Re). These typical values are generally used as constant in BES-AFN programs. However Karava et al. (Karava et al., 2004) concluded after reviewing the literature that the discharge coefficient shows considerable variation with opening porosity, configuration (shape and location in the facade), wind angle and Reynolds number. Yi et al. (Yi et al., 2019) using CFD method found that discharge coefficient depends on the wind direction and its values show large variations in the case of large openings.

The use of the large opening equation for the study of naturally ventilated buildings shows limitations due to coefficients evaluation. The underlying assumptions of this equation are not compatible with the large openings encountered with naturally ventilated buildings. Large openings affect pressure distribution and kinetic energy may be not fully-dissipated at the downstream of the opening.

The objective of this study is to present an alternative approach to estimate pressure coefficients for use in BES-AFN programs. The traditional method consists in calculating pressure coefficients as intermediate values from primary or secondary sources and using them as input data in BES-AFN programs to calculate airflows rates. The approach proposed in this study is based on the opposite reasoning and on the use of conservative quantities: airflow rates at building openings level are directly calculated form the CFD. From the large opening equation, the artificial pressure field can be deduced. This value will be used as input data in AFN models. The objective of this method is to eliminate the various coefficients and their associated uncertainties in order to construct only one coefficient adapted to the geometry of the studied building.

Using numerical simulations, three methods to calculate airflow rates of two different cross-ventilated buildings are compared: (I) directly calculated from CFD; (II) calculated from AFN using C_p values from CFD; (III) calculated from AFN using C_p values from Swami and Chandra analytical model.

2 COMPUTATIONAL METHODS

Whole-domain CFD approach is considered in this study, as outdoor and indoor airflow are modelled simultaneously and within the same computational domain in order to calculate airflow through the ventilation openings.

Steady-RANS computations are performed for various wind speeds and wind incident angles using the open-source library OpenFOAM, with a finite volume method for solving the flow

equations. RNG k-e turbulence model is chosen based on previous work by Evola and Popov (Evola and Popov, 2006) who concluded that RNG model show good agreement with experimental data and thus "can be considered a useful tool for the study of air flow inside and around building when dealing with wind driven natural ventilation". Standard k-e model and Realizable k-e model are also tested on two configurations to quantify discrepancies between the different models. SIMPLE algorithm is used to solve pressure-velocity coupling. Second order schemes are employed until residuals decrease by at least four order of magnitude.

For this study, various wind incident angles are considered in the range of 0°-90°. In order to analyse the possible impact of wind speed on the CFD results, simulations are performed for different wind speeds corresponding to a Reynolds number range from 50,000 to 500,000.

Numerical simulations are carried out on two different cross-ventilated buildings. The first one is a typical cubic building with reduced scale dimensions W x D x H = 0.1 x 0.1 x 0.8 m³. Openings on opposite facades represent 10% wall porosity. Details of the geometry can be found in Figure 1. The second studied building is a typical school building that can be encountered in tropical climate, particularly in French Polynesia, with gable-roofed and large openings on opposite facades (representing more than 30% wall porosity) to favour natural ventilation. Building geometry is based on a rectangular floor plan with full-scale dimensions W x D x H = 9 x 7 x 4 m³.

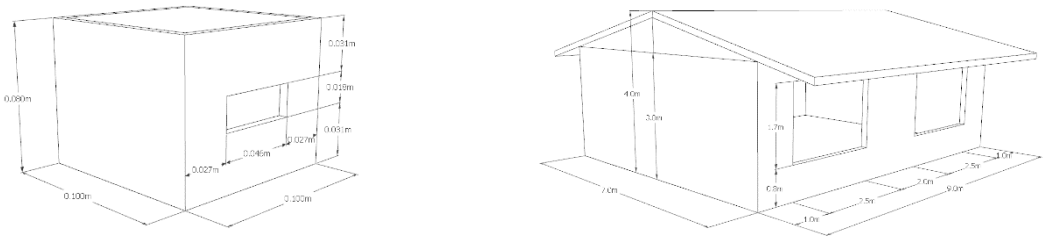

Figure 1: Building geometry description with on the left the cubic building and on the right the school building

Computational domain is constructed following the best practices proposed by Franke et al. (Franke et al., 2004): considering that H represents the height of the building, inlet, lateral and top boundary are 5H away from the building and outlet boundary is positioned at 15H behind the building.

Inlet boundary condition is imposed in order to generate an Atmospheric Boundary Layer (ABL). Velocity, turbulent kinetic energy and turbulence dissipation rate profiles are described by equations recommended by Richards and Hoxey (Richards and Hoxey, 1993):

$$U = \frac{u_*}{\kappa} ln\left(\frac{z+z_0}{z_0}\right) \quad (3)$$

$$k = \frac{{u_*}^2}{\sqrt{C_\mu}} \quad (4)$$

$$\varepsilon = \frac{{u_*}^2}{\kappa(z+z_0)} \quad (5)$$

Where κ is von Karman's constant, z_0 is surface roughness length (z_0 = 0.03m), C_μ is a model constant and u_* is the friction velocity usually calculated from a specified velocity U_h at a reference height h as:

$$u_* = \frac{\kappa\, U_h}{ln\left(\frac{h+z_0}{z_0}\right)} \quad (6)$$

Symmetry boundary conditions are imposed at the sides and the top of the domain, implying zero normal velocity and zero gradients for all the variables at these boundaries. The outlet of the domain is described by a zero static pressure boundary condition. Building surfaces are treated with non-slip boundary condition and specific wall function for ABL provided by OpenFOAM is used for ground boundary.

For the cubic building, the computational grid is composed of about 800 000 cells. As the school building geometry is complex and in order to describe accurately airflow at building openings level, the computational grid is composed of more than 4 200 000 cells, of which more than 90% are hexahedral cells. Special care is taken to limit the distance from the centre point of the wall-adjacent cell on the ground and building surfaces. For the entire range of simulated wind speed, the maximum value of y^+ does not exceed 300.

To calculate the volume flow rate through the building openings, the opening surfaces are decomposed into triangulated surfaces. Then velocity is interpolated onto the triangles and integrated over the surface area. Triangles are smaller than mesh cell size for an accurate result. Using the large opening equation, artificial ΔC_p can be deduced as:

$$\Delta C_p = \left(\frac{Q}{C_d * A_w * u_{wind}}\right)^2 * sgn(Q) \quad (7)$$

With:

$C_d = 0.65$

$$\frac{1}{{A_w}^2} = \frac{1}{(A_1 + A_2)^2} + \frac{1}{(A_3 + A_4)^2}$$

The previous calculated volume flow rate is compared to the one calculated by airflow network (AFN) using the large opening equation and mean pressure coefficient obtained from two different sources: (i) CFD results analysis of building with openings and (ii) the analytical model proposed by Swami and Chandra.

$$C_{p,n} = 0.6\, ln\begin{bmatrix}1.248 - 0.703\sin(\alpha/2) - 1.175\sin^2(\alpha) + 0.131\sin^3(2\alpha G) \\ +0.769\cos(\alpha/2) + 0.07G^2\sin^2(\alpha/2) + 0.717\cos^2(\alpha/2)\end{bmatrix} \quad (8)$$

Where:

$C_{p,n}$ = C_p value at a given angle between wind direction and the outward normal of the surface under consideration [dimensionless];

α = Angle between wind direction and outward normal of wall under consideration [deg];

G = Natural log of the ratio of the width of the wall under consideration to the width of the adjacent wall [dimensionless];

3 RESULTS OF NUMERICAL SIMULATIONS

The three different methods to calculate airflow rate and wind pressure coefficient differences ΔC_p are compared in this section according to the wind incident angle for the cubic building case and the school building case:

- method (1) corresponds to CFD results of airflow rate by integrating velocity over the opening surface of the building and calculating artificial pressure coefficient with equation (7);
- method (2) corresponds to AFN results of airflow rate with surface-averaged pressure coefficients calculated from CFD considering building with openings;
- method (3) corresponds to AFN calculation of airflow rate with surface-averaged pressure coefficients calculated from Swami and Chandra analytical model.

Figure 2 presents the variations of ΔC_p values and non-dimensional airflow rates as a function of wind direction for the cubic building case. Significant differences appear between the results of methods (1) and (2), particularly for wind direction normal to building openings where the discrepancy is about 40% on the ΔC_p value. As the angle of incidence increases the difference decreases to a minimum of 5% for a 45° wind direction and then increases again beyond this value. The consequence on the calculation of the airflow rate is an underestimation of the value calculated with method (2) compared to the actual flow rate calculated by the CFD for wind directions below 45° and on the contrary an overestimation of the flow rate for wind directions above 45°. Swami and Chandra's analytical model estimates a ΔC_p very similar to that of method 2 for 15° and 30° wind directions. Beyond a 30° wind direction the value of the ΔC_p is larger and therefore the air flow rate is greatly overestimated compared to the results of the other two methods.

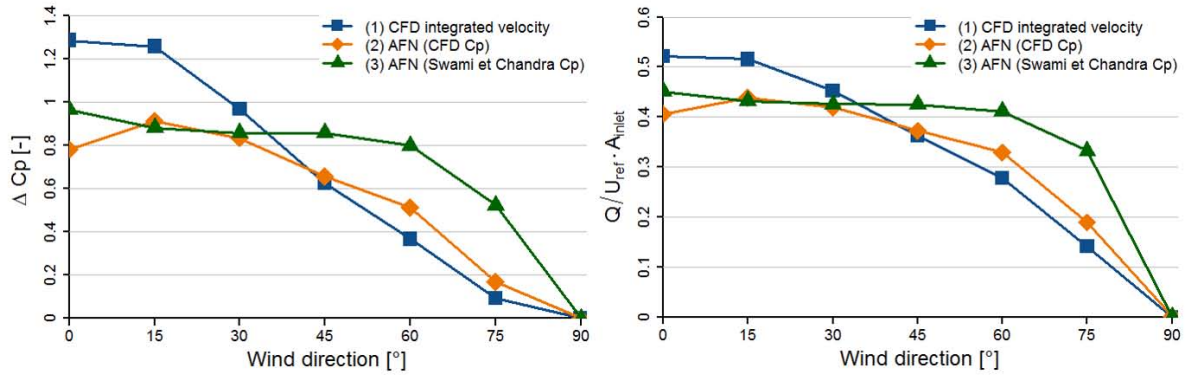

Figure 2: Wind pressure coefficient difference and non-dimensional airflow rate as a function of wind direction – results based on CFD simulation for the cubic building case

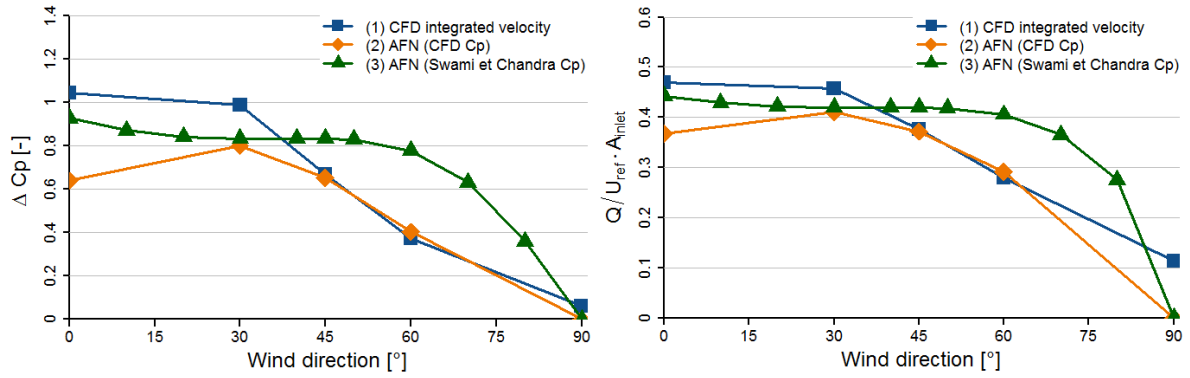

Figure 3: Wind pressure coefficient difference and non-dimensional airflow rate as a function of wind direction – results based on CFD simulation for the school building case

Figure 3 presents the results for the school building case. The same overall behaviour is observed for the evolution of the ΔC_p value and airflow rate as a function of wind direction. The differences between the results of methods (1) and (2) are of the same order for wind directions below 30°. Compared to method (1), method (2) still underestimates airflow rate by 20% for a 0° wind direction and by 10% for a 30° wind direction. For 45° and 60° wind directions, the results of these two methods are almost identical. For wind direction normal to the openings, results of method (1) are closer to those of method (3) for this building configuration compared to the cubic building configuration. For wind direction parallel to the openings, only method (1) is able to predict airflow rate through the building. Method (3) still calculates larger ΔC_p values for wind directions above 30° and thus overestimates airflow rates.

Turbulence models are compared in order to quantify the discrepancies about the calculation of the airflow rate through the school building openings. Table 1 presents the value of the non-dimensional airflow rate for a reference wind velocity corresponding to a Reynolds number Re ~ 50 000 and for two wind directions: 0° and 45°. For wind direction normal to the building openings, the three models calculate similar airflow values with a maximum difference of less than 5% between Realizable k-e model and RNG k-e model. For a 45° wind direction, Standard k-e and Realizable k-e calculate the same airflow value. This value differs by 5% from the value calculated by RNG k-e model.

Table 1: Comparison of results from various turbulence models for the calculation of non-dimensional airflow rate through the school building openings for a 0° and 45° wind direction.

		RNG k-e	Std k-e	Realizable k-e
Wind direction 0°				
$Q_{tot} / U_{ref} . A_{inlet}$	[-]	0.686	0.677	0.719
Discrepancy w/ RNG k-e	[%]		-1.3%	4.9%
Wind direction 45°				
$Q_{tot} / U_{ref} . A_{inlet}$	[-]	0.566	0.536	0.536
Discrepancy w/ RNG k-e	[%]		-5.3%	-5.3%

The influence of wind speed on the calculated artificial pressure coefficient ΔC_p from equation (7) is investigated for the school building case and shown on Figure 4. The results indicate that for all simulated wind directions the Reynolds number does not affect the value of the artificial pressure coefficient. Only very slight variations can occur for low Re values. This result supports what other studies have mentioned: pressure coefficient is normally assumed to be independent of wind speed.

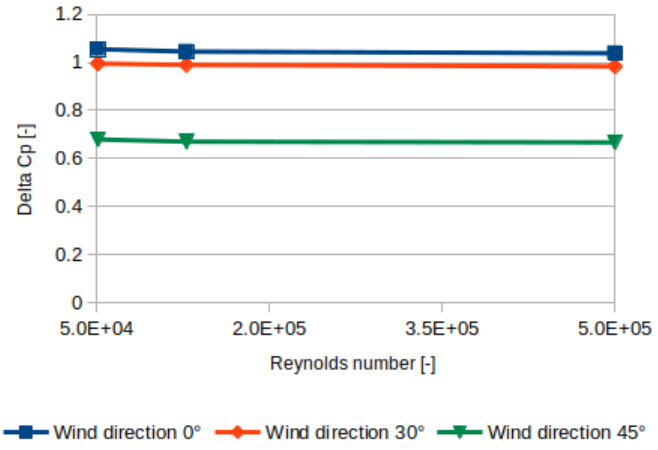

Figure 4: Wind pressure coefficient difference as a function of Reynolds number for three different wind directions – results based on CFD simulation

4 CONCLUSIONS

Large opening equation used in AFN models is not suitable for studying naturally ventilated buildings with large openings. In this equation, wind pressure coefficient is a key parameter and its estimation is a source of uncertainty in the calculation of airflow rates. This study proposes an alternative approach for estimating pressure coefficients that will be used as input data in BES-AFN programs. CFD RANS simulations are carried out on two different cross-ventilated buildings for various wind directions in order to calculate airflow rates at building opening level and wind pressure coefficient differences. The results are compared to AFN model calculation using C_p data from primary and secondary sources.

It can be concluded that airflow rates calculated from AFN model using surface averaged C_p values from CFD analysis (considering building with openings) are different from those directly calculated by CFD. In the case of wind direction normal to building opening, the discrepancy is more than 20% between the two calculated airflow rates. Such a difference can be significant on the estimation of thermal comfort of a naturally-ventilated building.

The alternative method proposed in this study has the advantage of calculating a ΔC_p value directly related to the flow rate calculated by the CFD. Therefore it avoids the uncertainties associated with the estimation of wind pressure coefficient and discharge coefficient. Future work will focus on experimental validation with PIV measurements to assess airflow rate calculation from CFD.

5 ACKNOWLEDGEMENTS

The author would like to acknowledge the *Service de l'énergie du gouvernement de la Polynésie française (SDE)* for the financial support of his PhD thesis.

6 REFERENCES

ADEME, 2015. Plan Climat Energie de la Polynésie française.

Cóstola, D., Blocken, B., Hensen, J.L.M., 2009. Overview of pressure coefficient data in building energy simulation and airflow network programs. Build. Environ. 44, 2027–2036. https://doi.org/10.1016/j.buildenv.2009.02.006

Cóstola, D., Blocken, B., Ohba, M., Hensen, J.L.M., 2010. Uncertainty in airflow rate calculations due to the use of surface-averaged pressure coefficients. Energy Build. 42, 881–888. https://doi.org/10.1016/j.enbuild.2009.12.010

Evola, G., Popov, V., 2006. Computational analysis of wind driven natural ventilation in buildings. Energy Build. 38, 491–501. https://doi.org/10.1016/j.enbuild.2005.08.008

Franke, J., Hirsch, C., Jensen, A.G., Krüs, H.W., Schatzmann, M., 2004. Recommendations on the use of CFD in wind engineering.

Karava, P., Stathopoulos, T., Athienitis, A.K., 2006. Impact of Internal Pressure Coefficients on Wind-Driven Ventilation Analysis. Int. J. Vent.

Karava, P., Stathopoulos, T., Athienitis, A.K., 2004. Wind Driven Flow through Openings – A Review of Discharge Coefficients. Int. J. Vent. 3, 255–266. https://doi.org/10.1080/14733315.2004.11683920

Richards, P.J., Hoxey, R.P., 1993. Appropriate boundary conditions for computational wind engineering models using the k-e turbulence model. J. Wind Eng. Ind. Aerodyn., Proceedings of the 1st International on Computational Wind Engineering 46, 145–153. https://doi.org/10.1016/0167-6105(93)90124-7

Yi, Q., Wang, X., Zhang, G., Li, H., Janke, D., Amon, T., 2019. Assessing effects of wind speed and wind direction on discharge coefficient of sidewall opening in a dairy building model – A numerical study. Comput. Electron. Agric. 162, 235–245. https://doi.org/10.1016/j.compag.2019.04.016

Experimental study of the combination of a positive input ventilation and active air vents on the air change rates of a house

Antoine Leconte[*1], Clément Lafféter[2], Thomas Fritsch[3], Nicolas Giordano[3], Julien Escaich[2] and Ophélie Ouvrier Bonnaz[1]

1 Univ Grenoble Alpes
CEA, LITEN, DTS, INES
F-38000 Grenoble, France
**Corresponding author: antoine.leconte@cea.fr*

2 Ventilairsec
16 rue des Imprimeurs
F-44220, Couëron, France

3 Bubendorff
24 rue de Paris
F-68220, Attenschwiller, France

ABSTRACT

This study aims to experimentally evaluate the influence of the combination of a supply only ventilation, called here positive input ventilation, and innovative active air vents on the Indoor Air Quality of a house. The positive input ventilation draws fresh air from the outside, filters and pre-heats it before blowing it in living areas. Active air vents are small motorised damper set up in upper parts of windows that can move according to local pollutants measurements or according to the measurements of the other active air vents in the house. This combination is expected to improve the Indoor Air Quality by increasing efficiently the air change rate of a room when it is too polluted. The goal of the tests presented in this paper is to evaluate quantitatively the air change rate in a real scale for different configurations of this combination. To do so, a positive input ventilation and active air vents are set up in an experimental house. The tests were carried out in 3 different rooms. For each room, the air change rate is evaluated for different configurations of the combination. CO2 is used as a trace gas to evaluate the air change rate. The results of 52 tests are used for those characterizations in order to take into account the possible variability of the results due to the real operation conditions. Results are promising and show that the studied combination enables to modulate significantly the air change rate of each room. An appropriate Demand Control Ventilation strategy based on the sensors of each active air vents and the communication between all the devices would thus lead to an efficient while simple improvement in the use of a positive input ventilation system.

KEYWORDS

Positive Input Ventilation, Active Air Vents, Real Scale Experimentation, Air Change Rate Estimation

1 INTRODUCTION

Indoor air pollution is one of the biggest environmental risks to public health. Most policies, at European scale (European Commission, 2013) and national scales ((Direction générale de la Santé, 2013) for the French case), agree on the importance of improving the indoor air quality and the related benefits. On the other hand, new buildings are more and more airtight

in order to reduce their energy consumption. Thus it is important to develop and use optimal Demand Control Ventilation (DCV) systems in order to ensure healthy and comfortable internal environment while keeping an appropriate level of energy consumption. Numerous DCV systems has been studied for decades, as reviewed by (Fisk & De Almeida, 1998) and (Guyot, Walker, & Sherman, 2018) for instance. Some DCV systems for dwellings are based on Indoor Air Quality (IAQ) sensors to modulate the air removal from wet rooms, like those introduced by (Faure, Losfeld, Pollet, Wurtz, & Ouvrier Bonnaz, 2018). However, most of them are only based on exhaust mechanical ventilation and can be complicated to set up if the control and the process of the supply air is also required.

This study aims to experimentally evaluate the influence of a new simple combination of a supply mechanical ventilation system with innovative active air vents on the IAQ of a house that would lead to an effective DCV system.

2 DESCRIPTION OF THE TESTED SYSTEM

2.1 Positive Input Ventilation (PIV)

The Positive Input Ventilation (PIV), also known as Supply-Only Ventilation, is a mechanical ventilation that draws fresh air from the outside, filters and pre-heats it before blowing it in one or several supply points in the building. Thus, the whole building is slightly pressurize which makes internal air leaks out through intentional vents. The U.S. Department of Energy (U.S. Department of Energy, 2002) introduces supply ventilation systems as relatively simple and inexpensive systems that allow a good control of the incoming air (including pollens and dust filtering) while discouraging the entry of pollutants from outside the living space and avoiding back drafting of combustion gases from fireplaces and appliances. The performance of such a system has been studied and optimized by (Rahmeh, 2014) in its PhD and by (Ouvrier-Bonnaz, Rahmeh, Stephan, & Potard, 2015) for instance. To the knowledge of the authors, the PIV has only been studied with passive air vents as evacuation points, which do not allow to significantly control and modulate the air removal between the rooms – as with the Active Air Vents introduced hereunder.

Figure 1: Pictures of the Positive Input Ventilation in the experimental house – Left: Central ventilation device in the attic, Right: Air diffusing unit in the first floor hall

2.2 Active Air Vents (AAVs)

Active Air Vents (AAVs) are small motorised damper, patented by BUBENDORFF (Europe Brevet n° EP3396267 A1, 2018). They are made up of:

- One main opened still plastic frame;

- One smaller opened metallic frame on the opening of the main frame, moved by an electric motor;
- One slat between the still frame and the mobile frame, independent so that it can close the opening when the mobile frame is opened to prevent the outside air from entering the house this way (like a double check valve);
- One electronic card that controls the motor, measures IAQ variables close to the opening, sends and receives information from the other AAVs.

As introduce in section 1, nowadays, some devices already use pollutants measurements in several rooms to adjust their air removal. However, most of them are implemented on exhaust mechanical ventilations which makes impossible to benefits from the advantages of the supply mechanical ventilation (see section 2.1). AAVs are easy-to-install and easy-to-use modules that would further improve the air quality management of a PIV.

For the tests presented in this paper, AAV prototypes were set up in upper parts of every window of the experimental house (see Figure 2).

Figure 2: Pictures of one AAV prototype in the experimental house – Left: From inside, Right: From outside

Thanks to its different parts, an AAV can have three different positions (see Figure 3, where the mobile frame is marked to clearly identify its position):

a) "Minimal position" – the mobile frame is completely closed on the main frame with an adjusting screw that leaves a slight opening;
b) "Maximal position" – the mobile frame is completely opened and the higher pressure inside the building than outside keeps the slat on the metallic frame;
c) "Non-return damper" – the mobile frame is completely opened but the higher pressure outside the building closes the slat on the opening so that the outside air can't enter the house this way.

(a) (b) (c)

Figure 3: Pictures of the 3 possible positions of a tested AAV – (a) Minimal position (b) Maximal position (c) Non-return damper

The control card measurements and communications enables the closing or opening of a AAV according to its own measurement and also according to the measurements of the other AAVs, creating this way as a possible concerted action.

2.3 Combination of PIV and AAV

The combination of PIV with AAVs is expected to improve the IAQ of the building by increasing efficiently the air change rate of a room when needed. The fresh air blown by the PIV in the building can be smartly directed to the more polluted rooms.

For instance, the operation steps could be as follow (see **Error! Reference source not found.**):

a) *Initial state – standby mode*: the IAQ is satisfactory in all rooms of the building, every AAV is in "Minimal position" so the fresh air from PIV is distributed in the different rooms in an almost balanced way.
b) *Foul air in one room – autonomous action*: the concentration of a pollutant is high in one room, the AAV of this room switches to the "Maximal position" so the fresh air from PIV is preferably directed to this room.
c) *Foul air in several rooms – autonomous actions*: the concentration of a pollutant is high in several rooms but still in a reasonable level, the AAV of those rooms are in "Maximal position" so the air change rate is increased in all those rooms in the same time.
d) *Foul air in several rooms – concerted actions*: the concentration of a pollutant is high in several rooms and especially in one room where the concentration is above a critical level, the AAV of this room holds the "Maximal position" while all others switch to "Minimal position", so the critical room is treated in priority until its pollutant level returns to an appropriate level. The warning signal can also be sent to the PIV in order to temporarily increase the fresh air flow rate.

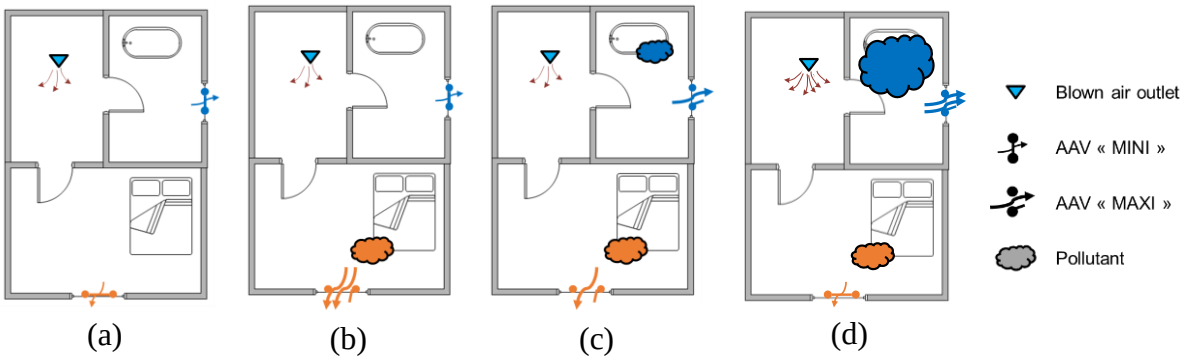

Figure 4: Different possible states of the combination of PIV and AACs to improve efficiently the IAQ of the building – (a) Steady State (b) Pollutants in one room with autonomous action (c) Pollutants in several rooms with autonomous actions (d) Critical level of pollutants in one room and concerted action

3 EXPERIMENTAL PROTOCOL

3.1 Goal of the tests and global approach

The goal of the tests presented in this paper is to quantify the impact of the studied PIV+AAVs combination and the different steps presented in section 2.3 on the air circulation in a building. No specific regulation is considered here (no specific pollutants levels for AACs opening for instance). The main idea is to assess the air change rate of different rooms of the building according to the possible positions of AAVs and fresh air flow rate in a real scale.

To do so, a PIV and AAVs are installed in an experimental house. For each test, the required configuration (mainly fresh air flowrate and AAVs position) is setup. The air change rate is estimated thanks to CO2 used as trace gaz. Each test is repeated several times in order to estimate the variability of the results.

3.2 Experimental setup

The equipped experimental house (see **Error! Reference source not found.**) is located in Le Bourget du Lac (France). It was built in 2011 with a recent constructive principle. The air tightness of the building was characterized thanks to blower door tests: the air change rate was 0.26vol/h at 50 pascal (69m^3/h) at the end of the construction work.

The living area is about 100m², on two levels:

- First floor : one large room (kitchen [KIT], dining [DIN] and living room [LIV]) and a cellar [CEL];
- Second floor: 3 bedrooms ([BED1], [BED2] and [BED3]), one bathroom [BATH], one toilet [WC].

Floors and rooms are represented on Figure 5 below.

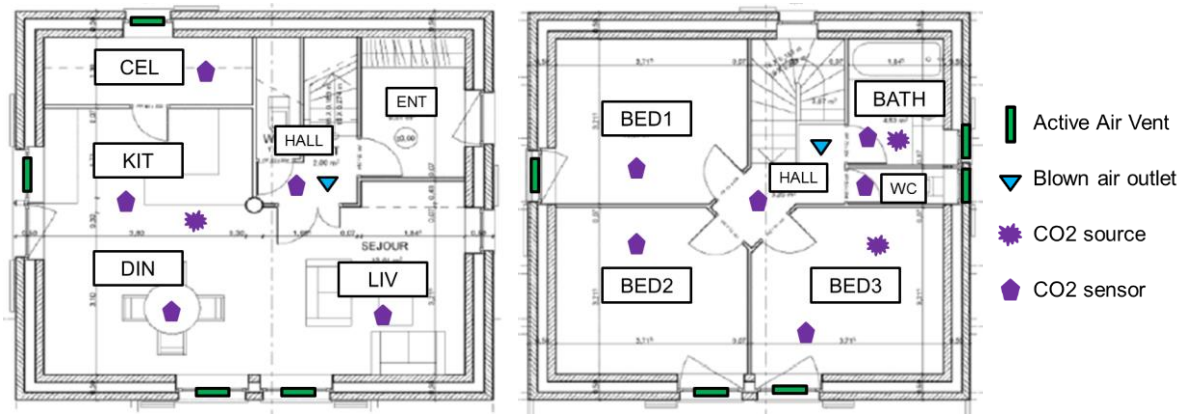

Figure 5: Introduction of the experimental house – Left: Plan of the first floor. Right: Plan of the second floor.

The PIV is set up in the attic. The fresh air is blown through two air outlets: one in the hall of each level (see Figure 5 and Figure 1 above). The global blown air flowrate is measured thanks to an ultrasonic air flow meter (*ULTRAFLUX 2000*). AAVs are set up in upper parts of every window of the experimental house (see Figure 5 and Figure 2 above). Sensors (*KIMO COT 212*) measure the CO2 concentration in the main rooms of the building. A set of CO2 bottles, pressure reducer and gas pipes enables to inject pure CO2 in the required room. A fan is used to homogenise the gas for the initialization of the test (see section 3.4). The complete experimental setup is summarized by the Figure 5.

3.3 Tested configurations

The tests are carried out in 3 different rooms:

- [BATH]: the bathroom (second floor – volume around 16m^3);
- [BED3]: One bedroom (second floor – volume around 39m^3);
- [KIT]: Kitchen + Dining + Living room (first floor – volume around 126m^3).

For each room, the air change rate is evaluated for different configurations of the combination:

- [REF]: With a classic static air vent (*ANJOS VM-G* self-regulation units);
- [MIN]: With all the AAVs of the room at the "Minimal position";
- [MAX]: With all the AAVs of the room at the "Maximal position".

For the first case, every window is equipped with a classic air vent (no AAV at all in the building). For all other tests, classic air vents are removed and the AAVs of the other rooms remains at the "Minimal position", except for some of the "concerted operation" tests which both bathroom's and bedroom's AAV are opened together to estimate the potential of the concerted action (see section 2.3 and 4.2). All internal doors are properly undercut and kept closed during the tests. All blinds are partially closed except for the tested room. The nominal speed of the PIV fan for this house (speed "2") is kept the same for all those tests except for some of the "concerted operation" tests: the speed is occasionally raised in order to estimate the impact of a possible communication (see section 2.3 and 4.2).

3.4 Air Change Rate estimation

The air change rate for each test is estimated thanks to CO2 used as a trace gas. The procedure is as follow:

- The experimental setup is tuned according to the room and the configuration to be tested;
- The studied room is filled with CO2 up to a high concentration, around 5000ppm, with the homogenisation fan turned on;
- The CO2 injection is stopped and so is the fan couple of minutes later;
- The decrease of the CO2 concentration is measured to estimate the air change rate.

As described by (Etheridge & Sandberg, 1996), the CO2 mass balance inside the studied room, taking into account the incoming and the outgoing CO2, links the air change rate and the CO2 concentration variation (see equation (1)).

$$\tau . dt = \frac{dC}{C_e - C} \tag{1}$$

According to equation (1), the air change rate (τ) can be estimated by computing the negative slope of the time evolution of the logarithm of the difference between the concentration in the studied room (C) and in its environment (C_e). In this case, the concentration C_e is considered as the measured concentration in the halls, where the PIV blows the fresh air (first floor hall for the tests in the kitchen, second floor hall for the tests in the bathroom and the bedroom). The inherent hypothesis is that the fresh air always goes from the halls to the studied room and then evacuated outside. The opposite case has never been observed on those tests. An example of the air change rate estimation is presented by Figure 6. For all the results selected for this analysis, the regression coefficient of the air change rate estimation is above 0.98.

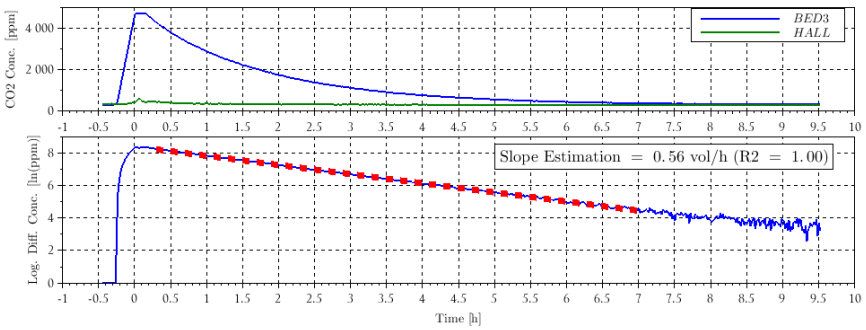

Figure 6: Estimation of the air change rate for one test – Upper: CO2 concentrations in the studied room and its environment. Lower: Logarithm of the differential concentration and slope estimation (red dots)

4 RESULTS

Results from 52 tests are used to characterize the air change rate in the different rooms, for the different configurations. Each configuration is tested several times in order to take into account the possible variability of the results due to the operation conditions, mainly the weather conditions during the tests. For each characteristic presented below (air change rate and global blown air flowrate), the number of tests considered and the standard deviation σ is presented (in brackets).

4.1 Autonomous operation of the AAVs in each room

Results of the tests for characterizing the AAVs' autonomous operation are presented in Table 1 and Figure 7. The autonomous operation in one single room is described by steps a) and b) in section 2.3 and **Error! Reference source not found.**. The tests were carried out between January and June 2018.

Table 1: Results of the tests for characterizing the AAVs' autonomous operation

Room	AAV Configuration	PIV fan speed	Number of tests	Global blown air flowrate [m3/h]	Air change rate [vol/h]
BED	REF	2	3	148 (σ=1)	0.58 (σ=0.02)
BED	MIN	2	7	159 (σ=2)	0.66 (σ=0.05)
BED	MAX	2	4	160 (σ=1)	1.53 (σ=0.04)
BATH	REF	2	3	150 (σ=3)	1.34 (σ=0.13)
BATH	MIN	2	4	157 (σ=6)	1.61 (σ=0.41)
BATH	MAX	2	4	157 (σ=6)	3.74 (σ=0.76)
KIT	REF	2	2	151 (σ<0.5)	0.85 (σ=0.03)
KIT	MIN	2	5	162 (σ=5)	1.03 (σ=0.17)
KIT	MAX	2	3	167 (σ=3)	1.51 (σ=0.13)

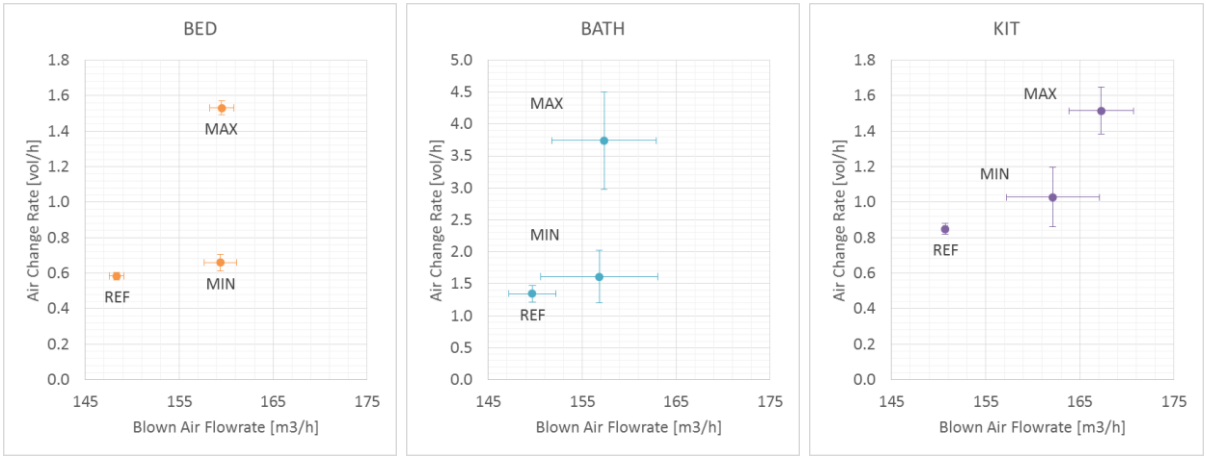

Figure 7: Evolution of the air change rate according to the AAV configuration in each tested room

The global blown air flow rate vary from 148 to 169m^3/h whereas the fan speed is the same for each test. This is due to the changing weather conditions that can naturally introduce variation on the volumetric flow rate of a fan even with the same speed. That is why Figure 7 shows air change rate estimations according to the measured global air flow rate. This representation enables to clearly distinguish the impact of the input air flow from the impact of the AAV configuration on the air change rate of each room.

Firstly, for each room, considering the global blown air flowrate changes and the standard deviations, the air change rate with the minimal position of the AAV is similar to the case with classic air vents. The gap could be even reduced by working further on the setup and the tuning of the AAVs in their "minimal position".

Comparing the results between "minimal position" and "maximal position", still including their standard deviation, it can be stated that the opening of the active air vent raises significantly the air change rate for each room : from 1.5 times more in the kitchen to 2.3 times more in the bathroom when considering the average values.

This means that in this case, an appropriate control of the autonomous action of the AAVs would treat basic IAQ issues very efficiently by changing significantly the air change rate of a room when needed.

4.2 Concerted operations between AAVs and the PIV

Additional tests were carried out in order to evaluate the relevance of a concerted action between the AAVs and with the PIV as well. The concerted operations in one single room is described from step a) to d) in section 2.3 and **Error! Reference source not found.**. For those tests, the trace gas is injected simultaneously in both the bedroom and the bathroom. The CO2 injection is then stopped at the same time and the air change rate estimated over the same period. The tests were carried out between July and August 2018. For this campaign, some AAV prototypes were changed and the bathroom and bedroom blinds were kept both opened. So the following results can't be strictly compared with the previous ones in section 4.1.

Table 2: Results of the tests for characterizing the AAVs' concerted operation

Step	AAV configuration in the bedroom	AAV configuration in the bathroom	PIV fan speed	Nb of tests	Global blown air flowrate [m3/h]	Air change rate in the bedroom [vol/h]	Air change rate in the bathroom [vol/h]
a)	MIN	MIN	2	4	168 (σ=2)	0.52 (σ=0.03)	1.27 (σ=0.14)
b)	MAX	MIN	2	3	171 (σ=1)	1.28 (σ=0.12)	1.31 (σ=0.10)
c)	MAX	MAX	2	3	168 (σ=3)	1.32 (σ=0.07)	3.59 (σ=0.28)
d)	MIN	MAX	2	3	165 (σ=4)	0.56 (σ=0.02)	4.52 (σ=0.37)
d')	MIN	MAX	4	4	236 (σ=18)	0.66 (σ=0.02)	5.71 (σ=0.25)

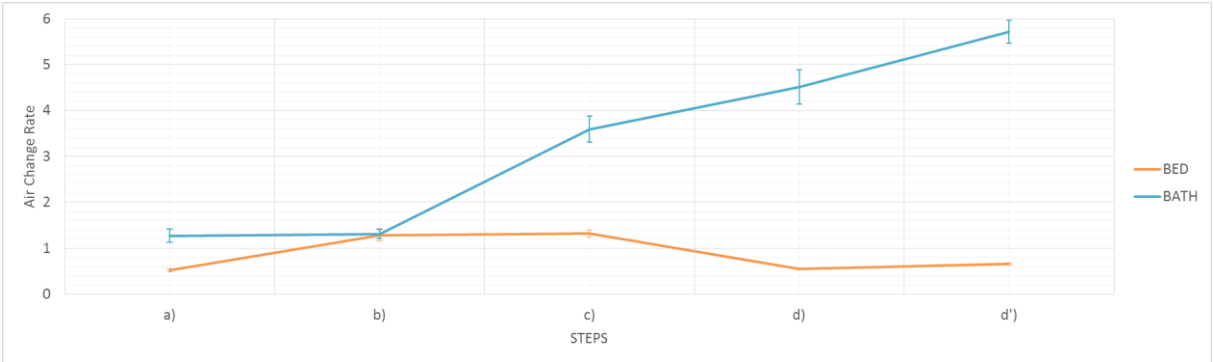

Figure 8: Evolution of the air change rate in the bedroom and the bathroom according to the possible steps of the AAVs and PIV concerted operation

The impact of the AAVs and PIV operations is clearly visible:

- From step a) to b) (pollution in the bedroom for example) :

The opening of the AAV in the bedroom increases the air change rate significantly in the bedroom but hardly impacts the air change rate in the bathroom.

- From step b) to c) (additional pollution in the bathroom for example):

The opening of the AAV in the bathroom highly increases the air change rate in the bathroom but hardly impacts the air change rate in the bedroom. The latter is a little increased in average but not significantly with regards to the standard deviations.

- From step c) to d) (critical pollution level in the bathroom for example):

The closing of the AAV in the bedroom brings a significant extra increase of the air change rate – around 25% in average in this case. The air change rate level in the bedroom is similar as the step a) case.

- From step d) to d') (PIV fan speed increased by 2 levels):

When the PIV fan speed is increased, the air change rate raises by another 25% in the bathroom in this case. And since the other AAVs are closed, the additional air flow rate is preferably led to the bathroom (the air change rate in the bedroom is hardly increased in this case).

Those results show that the communication between AAVs and the PIV could treat very efficiently critical pollution cases – when the bathroom is too humid for instance. In the latter configuration, the bathroom air would be completely removed in a few dozen minutes.

5 CONCLUSIONS

A combination of a central Positive Input Ventilation (PIV) and distributed Active Air Vents (AAVs) in each room were tested in an experimental house. Several tests were carried out to characterize the air change rate of different rooms with different combinations of AAVs and PIV. The results can be summarized as follows:

- The air change rate of minimal position AAVs is similar to classic ones,
- The opening of the AAV in a room raises significantly its air change rate when all others are in "MINI" position (from 1.5 times more in the kitchen to 2.3 times more in the bathroom),
- The closing of the bedroom air vent when the bathroom air vent is opened raises by around 25% the air change rate of the bathroom, which could be very helpful as a concerted action to treat critical situations, when the bathroom is exceedingly humid for instance.

Those results show the relevancy of using AAVs with a PIV to improve the IAQ of a house. The air change rate of each room can be significantly modulated when needed. So with an appropriate sensor based DCV strategy, the PIV + AAVs system could be very effective. The hysteresis opening of the active air vent - as autonomous operation - would have a significant impact on the pollution venting of a room. The concerted action could even enhance the pollution venting with appropriate critical thresholds. The tested system could then offer a lot of possibilities to smartly modulate the air change rate of each room (damp room as well as living room) according to its pollution level.

6 ACKNOWLEDGEMENTS

This work was supported by the French Unique Interministerial Fund (FUI).

7 REFERENCES

Direction générale de la Santé. (2013). *Plan d'actions sur la Qualité de l'Air Intérieur.* Obtido de https://solidarites-sante.gouv.fr: https://solidarites-sante.gouv.fr/IMG/pdf/Plan_Qualite_de_l_air_interieur_octobre_2013.pdf

Etheridge, D., & Sandberg, M. (1996). *Building Ventilation: Theory and Measurment.* John Wiley & Sons.

European Commission. (18 de 12 de 2013). *Environment: New policy package to clean up Europe's air.* Obtido de http://europa.eu/: http://europa.eu/rapid/press-release_IP-13-1274_en.pdf

Faure, X., Losfeld, F., Pollet, I., Wurtz, E., & Ouvrier Bonnaz, O. (2018). Resilient Demand Control Ventilation system for dwellings. *39th AIVC Conference.* Juna Les Pins, FRANCE.

Fisk, W. J., & De Almeida, A. T. (1998). Sensor-based demand-controlled ventilation: a review. *Energy and Buildings*, 35-45.

Fritsch, T. (2018). *Europe Patente Nº EP3396267 A1.*

Guyot, G., Walker, I. S., & Sherman, M. H. (2018). Performance based approaches in standards and regulations for smart ventilation in residential buildings: a summary review. *International Journal of Ventilation*, 1-17.

Ouvrier-Bonnaz, O., Rahmeh, M., Stephan, L., & Potard, M. (2015). Whole-house air distribution with a supply-only ventilation system VMI® for an optimum air change. *CLIMAMED 2015 Congress Sustainable Energy Performance of Buildings.* Juan Les Pins.

Rahmeh, M. (2014). *Etude expérimentale et numérique des performances de la ventilation mécanique par insufflation : qualité de l'air intérieur dans les bâtiments résidentiels.* La Rochelle: Université de la Rochelle.

U.S. Department of Energy. (2002). *Whole House Ventilation Systems - Improved control of air quality - Technology Fact Sheet.* Obtido de https://www.nrel.gov: https://www.nrel.gov/docs/fy03osti/26458.pdf

An investigation of ventilation control strategies for louver windows in different climate zones

Leonie Scheuring*[1], Bernhard Weller[1]

1 Institute of Building Construction, Technische Universität Dresden,
August-Bebel-Str. 30
01219 Germany
leonie.scheuring@tu-dresden.de

ABSTRACT

Guaranteeing high indoor air quality and high degree of user satisfaction at the same time is one of the challenges when improving the energy efficiency of a building. Current non-residential buildings mainly use mechanical ventilation systems to ensure high air quality. Mechanical ventilation systems are known for minimising heat losses but at the same time lead to higher installation, operating and maintenance costs. Furthermore, mechanically conditioned rooms may lead to the sick building syndrome caused by the lack of operable windows. Natural ventilation being more accepted by users has the potential to guarantee energy efficiency of buildings in conjunction with people satisfaction.
Present natural ventilated buildings pose the risk of higher energy demand and less indoor air quality due to user's behaviour. Controlled natural ventilation based on indoor CO_2-concentration and room air temperature is needed. However, the efficiency of a control strategy highly depends on climate zone and control parameters. This paper aims to explore the impact of different control strategies on the energy efficiency of an operable louver window. The most efficient strategy is then compared to a mechanical ventilation system
In a simulation four window opening strategies based on CO2 concentration were tested in Mediterranean, subtropical and moderate climate zone. Only at very cold and very warm conditions a difference in the different natural ventilation strategies was observed. When comparing the natural ventilation conditions to mechanical ventilation major differences were found. In almost all climate conditions natural ventilation outperformed the mechanical ventilation. In several climatic conditions energy consumption by the natural ventilation system was 10 fold lower than by mechanical ventilation, conflicting the common view that mechanical ventilation is the more efficient system.

KEYWORDS

Indoor air quality, natural ventilation, control strategies, louver window, energy performance.

1 INTRODUCTION

Natural ventilation still struggles against constraints about its energy efficiency and the lack of thermal comfort. Even some national energy standards demand for mechanical ventilation (EnEV, Minergie) to meet their requirements. Nevertheless, natural ventilation has been brought into the scientific focus during the last years (Prieto 2017) due to its potential to reduce the risk of the Sick Building Syndrom and its capacity to save energy by night ventilation (Becker 2002, Gratia 2004, Wang 2009). The results show that in moderately warm summer climates and warm Mediterranean climates (Becker 2002) as well as in cold climates of northern China (Wang 2009) natural ventilation at night substantially reduces cooling loads.
However, during daytime ventilation is difficult to control and inadequate user behaviour for manual natural ventilation poses the risk to not maintain the indoor air quality. This problem

can be overcome with controlled natural ventilation (automated window opening). For this purpose control strategies need to be established to define the window openings.
Control strategies for natural ventilation can control indoor air quality as well as indoor air temperature (Schulze 2013). However, whereas indoor air temperature can also be controlled by heating and cooling systems a controlled natural ventilation is necessary to regulate the indoor air quality. In office rooms the internal temperature gains are very high so that passive cooling by natural ventilation can effectively reduce the cooling loads. Therefore, the control strategies should have the indoor air CO_2- concentration as the main parameter and as a second parameter the indoor air temperature.
The main challenge defining the thresholds for the CO_2 control strategy is to overcome an overcooling or an overheating occurring by too long opening times. In this paper the lower CO_2 concentration, which defines the closing point of the window, will be examined. The performance of four different strategies will be analysed for the energy demands cooling, heating, lighting and auxiliary energy for ventilation. Furthermore, investigations of the influence of different climate zones on the efficiency of control strategies are still missing and will be examined in this publication.
In addition, this publication aims to compare the efficiency of natural and mechanical ventilation. Therefore a simulation of a mechanical ventilation under the same climatic conditions will be compared to the results of the natural ventilation.

2 METHODOLOGY

A simulation model is build up with Energyplus and evaluated for four control strategies and for three locations – Wiegendorf (central Germany), Madrid (Spain) and Hanoi (Vietnam). For these locations the energy performance will be evaluated. The analysis is performed in a time step of one second and results are shown as sums of every month individually. The control strategy with the lowest energy consumption is compared to a mechanical ventilated system for each of the three locations.

2.1 Case study

The investigations are carried out for an office room in a multistorey building. It is located in the ground floor, south orientated, surrounded above, beneath and besides by rooms conditioned equally. The office room is designed for four users with a net floor area of 32 m² according to the German industrial safety guideline ASR A1.2. The transparent area of the south-orientated wall is 3.85 m² designed in accordance with DIN 5034-1. The geometry is shown in figure 1. It consists of three parts: on the left side a non-operable window, in the middle an operable window and on the right side a non-operable window. For the operable window a louver window is used with an area of 2 m x 1.587 m. The louver window consists of three operable louvers, which open simultaneously. The louvers open fully to the outside with a nearly horizontal end position. This leads to a ventilation performance comparable with the performance of a casement window but at the same time there is no casement protruding into the room.

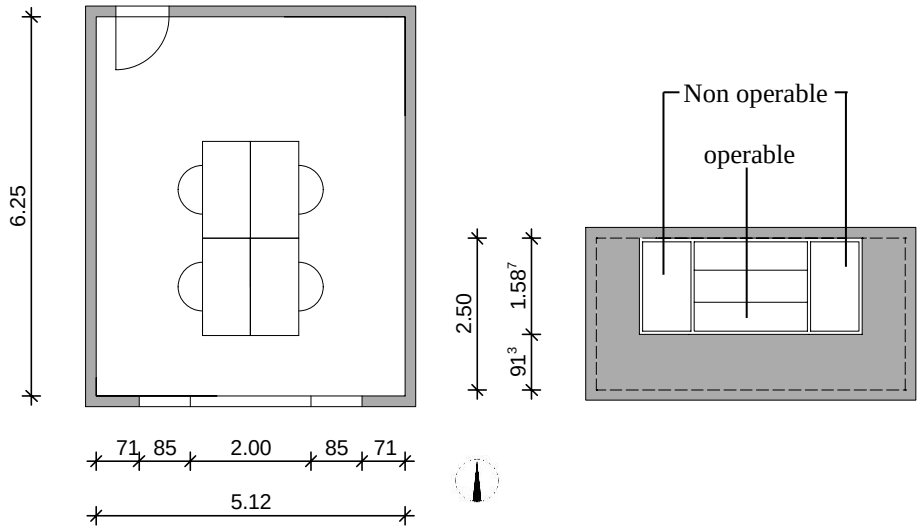

Figure 1 Case study office room – floor plan and south view.

The structural elements are made of concrete, nonstructural elements are made of sand-lime brick. The thermal properties go along the German Energy Saving Regulation 2016 (EnEV). The Solar Heat Gain coefficient is determined in accordance with the German standard for overheating in summer DIN 4108-2. The minimum value to satisfy the standard is chosen. The construction elements and the thermal properties are shown in table 1.

Table 1: Construction and thermal properties of the office room

Construction Element	U-Value	Solar Heat Gain coefficient (SHGC)	Material and thickness of the structural element
External wall	0.28 W/(m²K)	-	25 cm concrete
Louver window and non operable windows	1.27 W/(m²K)	0.54	-
Ceiling	adiabatic	-	20 cm concrete
Internal walls	adiabatic	-	11.5 cm sand-lime brick

The office room is designed for four people. However, it is not fully occupied during the working hours. The occupancy schedule is shown in Figure 2 and is based on the German standard DIN 18599 as well as the schedule for electric equipment and lighting hours. Lighting hours are from 7 am to 6 pm – during the working hours. The lights are equipped with a daylight sensor and are dimmed according to the required illumination level of 500 lux. The internal heat gains for people, lighting and electric equipment are shown in table 2.

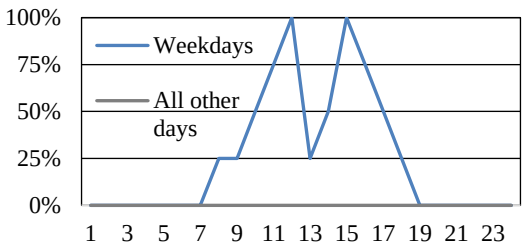

Figure 2 Occupancy and electric equip. schedule (100% = 4 people and 224 W from electric equip.)

Table 2: Internal gains

	Internal gains	Reference
People	126 W/person	DIN EN 15251
Lighting	10.63 W/m²	DIN 18599-10
Electric equip.	7 W/m²	DIN 18599-10
CO_2-production rate	$3.82 \cdot 10^{-8}$ m³/s·W	ASHRAE Standard 62.1-2007

2.2 Natural Ventilation Model

The model is built up in EnergyPlus. The single sided ventilation through the louver window is obtained using the EnergyPlus Design Flow Rate method. The method is based on Coblenz and Achenbach (Achenbach 1963) according to the following equation:

$$V = V_{design} \cdot F_{schedule} \cdot [A + B \cdot (T_{zone} - T_{odb}) + C \cdot (WindSpeed) + D \cdot (WindSpeed^2)] \quad (1)$$

The method uses a defined airflow volume (V_{design}) and modify it depending on the actual thermal difference between inside (T_{zone}) and outside (T_{odb}) temperature as well as the current wind speed. The coefficients A to D determine the effect of wind speed and temperature difference on the airflow volume. EnergyPlus offers to choose from several sets of predetermined coefficients. For the analysis BLAST coefficient set (A=0.606; B=0.03636; C=0.1177; D=0) was used because it distinguishes summer and winter conditions. (EnergyPlus 2018). Using these factors a typical summer day would result in the bracket term becoming 1, leading to:

$$V = V_{design} \cdot F_{schedule} \quad (2)$$

While for a typical winter day the bracket term is 2.75, resulting in:

$$V = V_{design} \cdot F_{schedule} \cdot 2.75 \quad (3)$$

V_{design} is determined by the equation described in Bäumler (Bäumler 2016) for a single sided ventilation.

$$V_{design} = ½ \cdot A_{geom} \cdot C_v \cdot \sqrt{\frac{\Delta p \cdot 2}{\rho_a}} \quad (4)$$

V_{design} is calculated to 0.2201 m³/s with A_{geom} of 2.32 m² and C_v of 0.58 for the louver window and Δp of 0.069 Pa for a an inside temperature of 20 °C and an outside temperature of 19 °C and a room located in the ground floor.

Control strategies

$F_{schedule}$ takes either the value 1 for the opened or the value 0 for the closed window. The decision if $F_{schedule}$ is 0 or 1 is triggered by the CO_2 concentration and the temperature in the room. In the control strategy the thresholds for these parameters are defined.
The window opens at the upper CO_2 limit of 900 ppm which is the maximum CO_2 concentration in the moderate category II of the European Standard DIN EN 15251. The lower limit, which indicates the window closure, varies from 500 ppm to 800 ppm with a step of 100 ppm so that four strategies will be analysed.
The passive cooling control strategy differs between occupancy time and non-occupancy time. During occupancy time the window opens for cooling if the indoor air temperature is above 25 °C and the outside temperature is more than 3 Kelvin below the inside air temperature. The window closes when the operative inside air temperature reaches 22 °C. During non-occupancy time the window opens when the inside air temperature is above 23 °C and the outside temperature is more than 3 Kelvin below the inside temperature and closes when inside air temperature drops under 18 °C. The strategies are implemented through the EnergyPlus Energy Management System (EMS).

2.3 Mechanical Ventilation Model

The most energy efficient natural ventilation strategy is compared to a mechanical ventilation system for each location. The mechanical ventilation should regulate the indoor air quality in the same way as the natural ventilation system. In order to achieve the required indoor air quality (900ppm CO2) a constant airflow volume of 7 l/(s pers) is defined by DIN EN 15251-12.

2.4 HVAC System

In both simulation models an ideal heating and cooling system is used. This ideal heating and cooling system is chosen in order to not have a dependency on specific heating and cooling energy losses due to a defined HVAC system. The heating set point temperature is defined to 21 °C from 6 am to 6 pm at weekdays and 17 °C during night and weekends. Cooling set point temperature is defined as 24 °C from 6 am to 6 pm during weekdays and 26 °C for all other times. For the natural ventilated system heating and cooling are switched off during window opening time.

3 RESULTS

In the simulation three locations were compared for their energy demand for lighting, heating and cooling. These locations differed in their climatic conditions. The first location, Wiegendorf (Germany), is in European continental climate with average temperatures of -0.3 °C in January and 17.2 °C in July. In the second location Madrid (Spain) Mediterranean climate with average temperature of 5 °C in January and 24 °C in July is found. In the third location subtropical climate leads to temperatures of 16.6 °C in January and 29.1 °C in July. The energy demand for these locations was simulated (time step one second) and values were summed up for each month.
Four strategies of natural ventilation were compared for each location individual (figures 3-5). These were based on the CO_2 concentration and the temperature within the room. Windows were opened according to the temperature thresholds described in part 2.2 of this paper and when CO_2 was above 900 ppm and were closed when either A: 500 ppm, B: 600 ppm, C: 700 ppm or D: 800 ppm CO_2 were reached. This leads to longer window opening phases with A and shorter but more frequent opening phases towards D.
These strategies were compared side by side in graphs 3-5 where strategy A is depicted with dark blue bars for cooling, red bars for heating and orange bars for lighting, while strategy D is shown in light blue (cooling), light red (heating) and yellow (lighting). The total height of a bar represents the sum of energy demand for lighting, heating and cooling.
In the simulation for Wiegendorf the majority of the energy is consumed for the heating, due to cold winters while demand for lighting is relatively low and stable during the year and energy needed for cooling is neglectable (figure 3).
The total energy demand for Wiegendorf is low between April and October (less than 2000 Wh/m² per month). During this period no substantial differences were observed between the different ventilation strategies. In contrast, energy demand in winter months (December-February) is high (4000 Wh/m² per month). The majority of energy consumed in these months is needed for heating (2000-3000 Wh/m² per month). A strong difference was observed between strategy A and the other three strategies. Energy demand for strategy A with windows closing at 500 ppm CO_2 is much higher than with the other strategies (heating energy in December for A: 4100 and D: 2900 Wh/m²). This trend is already visible in March and November but is less pronounced.

Thus for winter months with heating energy consuming more than 1000 Wh/m² the ventilation strategy with the shortest opening time should be chosen to achieve a reduction of up to 20 percent of the total energy demand. While in months with less than 1000 Wh/m² for heating the ventilation strategy has not an impact on the energy efficiency.

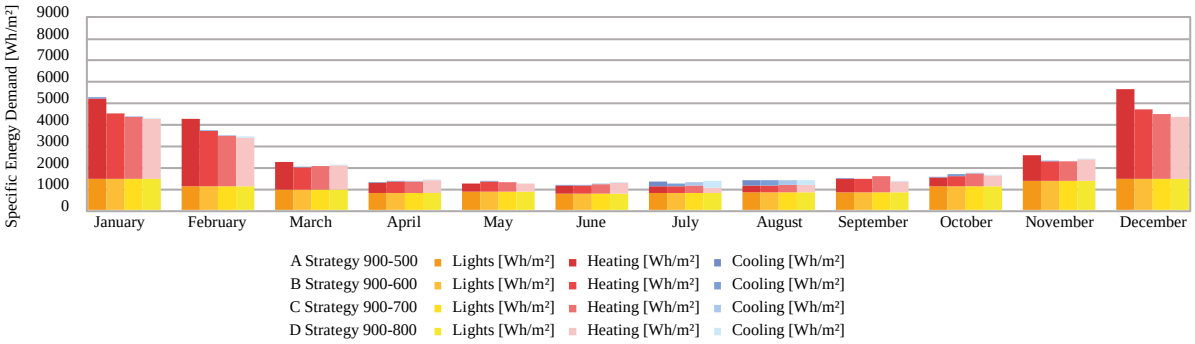

Figure 3 Specific energy demand for Wiegendorf – comparison of 4 ventilation strategies.

In the simulation for Madrid the total energy demand generally was low (~2000 Wh/m² per month) except for July and August where approximately 6000 Wh/m² per month were needed. This increase was due to energy needed for cooling. There is no obvious difference in the impact of the ventilation strategies on the energy consumption neither for cooling in summer nor for heating in winter. There is a minimal trend in December indicating that ventilation strategy A consumes more energy for heating than the other strategies. Interestingly, this is the only month for the Madrid simulation where heating energy consumption reaches approximately 1000 Wh/m² per month, confirming that 1000 Wh/m² per month might be threshold above which ventilation strategy effects become visible on the heating loads.

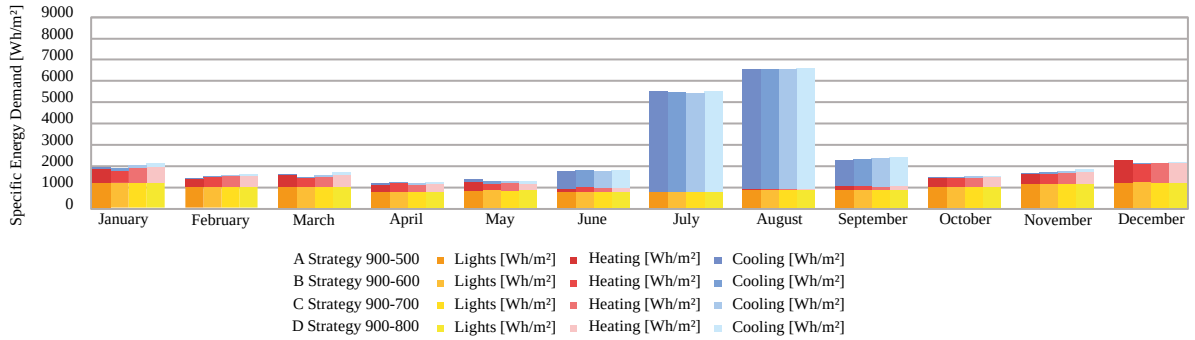

Figure 4 Specific energy demand for Madrid – comparison of 4 ventilation strategies.

Hanoi (figure 5) has a high energy consumption with the majority of energy being required for cooling. December, January and February have nearly no need for temperature regulation (less than 1000 Wh/m² per month) and therefore nearly no differences between the ventilation strategies were observed. From May to September, the highest energy consumption with cooling demands above 11000 Wh/m² per month were noted. For these months the ventilation strategy leads to a difference in energy performance indicating that strategy A uses the most and strategy D the least energy (approximately 1000 Wh/m² per month difference). In the months March, April, October and November there is still a relatively high demand for cooling energy (between 2000 and 10000 Wh/m² per month), however the differences between the ventilation strategies are low. In April and November energy demand for cooling is similar to that of Madrid in July and August. And in agreement to each other both simulation do not show a major impact of the ventilation strategy on the energy consumption.

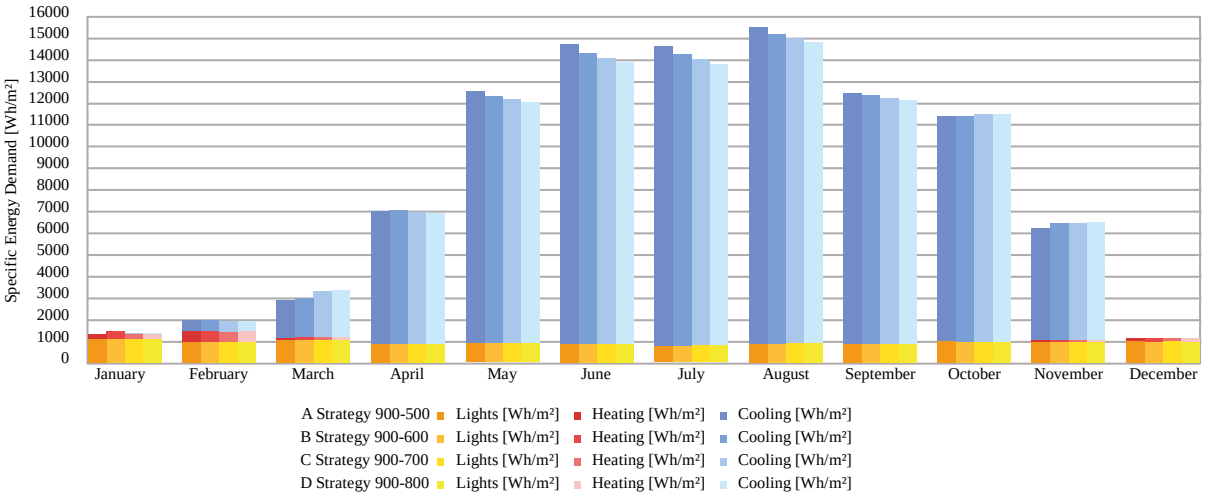

Figure 5 Specific energy demand for Hanoi – comparison of 4 ventilation strategies.

The results above (figure 3-5) were gained using a simulation of natural ventilation. These now were compared to a simulation of the same locations with mechanical ventilation to test if such system would be more efficient than the natural ventilation. For this purpose the energy demand of the best natural ventilation strategy of each month was compared to the energy demand by mechanical ventilation (e.g. for Hanoi in June strategy D and in November strategy A was used).

In the simulation of Wiegendorf from April to October natural ventilation is more energy efficient than mechanical ventilation (figure 6). The effect seems to depend on the outer temperatures and peaks in the summer months. In August mechanical ventilation consumes 8000 Wh/m² to cool down the room while by natural ventilation 550 Wh/m² is needed for heating and cooling. In the winter months (December-February) both systems are comparably efficient. Only in March and November the mechanical ventilation uses less energy than the natural ventilation. A difference of 500 Wh/m² are observed.

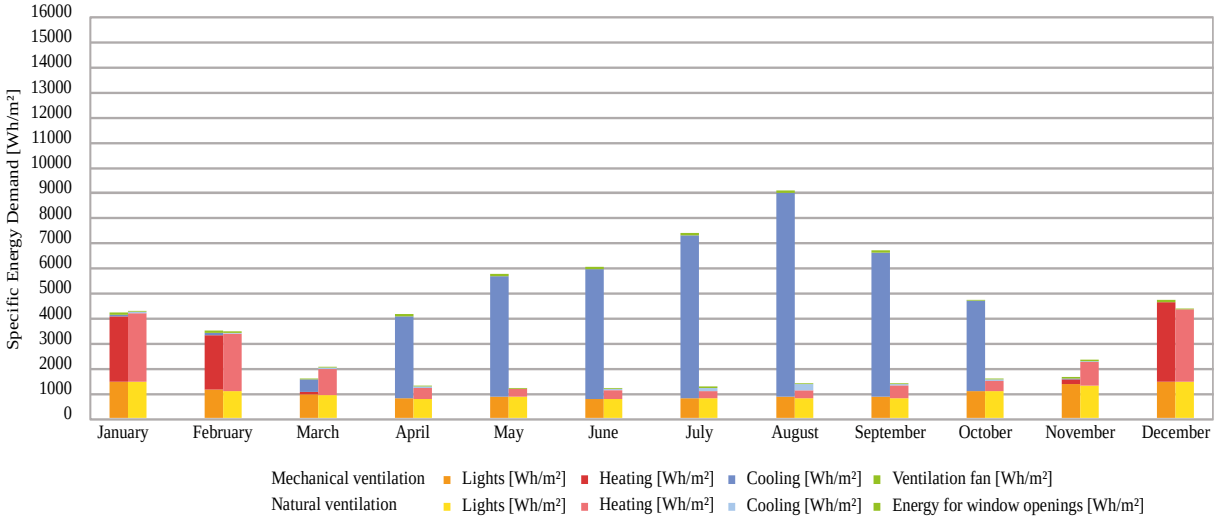

Figure 6 Specific energy demand for Wiegendorf – comparison of natural ventilation with mechanical ventilation.

In the Madrid simulation the natural ventilation is more efficient than the mechanical ventilation in all months. In the hottest months (July and August) mechanical ventilation consumes approximately 10000 Wh/m² for cooling while natural ventilation requires only 50 % of that. In milder months like September and October very little energy is needed (less than 1000 Wh/m²) for cooling by natural ventilation while mechanical ventilation still requires approximately 8000 Wh/m². For the other months similar effects are seen with natural ventilation requiring 10-20 % of energy that is needed by mechanical ventilation. Only in December both systems demand similar amounts of energy.

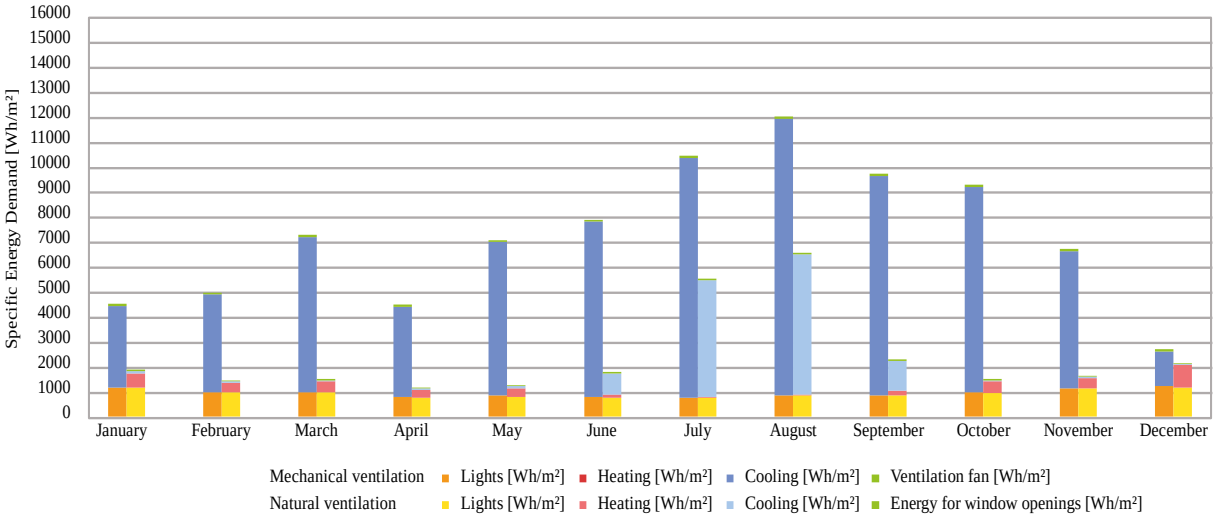

Figure 7 Specific energy demand for Madrid – comparison of natural ventilation with mechanical ventilation.

In the simulation of Hanoi in the summer months with extreme heat (June-August) there is little difference in the energy demand for natural and mechanical ventilation (with slight advantage of natural ventilation). However, in the colder months (November-March) natural ventilation is clearly more efficient than mechanical ventilation (e.g. Hanoi December 9000 Wh/m² per month for mechanical ventilation vs 3000 Wh/m² for natural ventilation). For the medium warm months (April, May, September and October) natural ventilation is more efficient but the effect is less pronounced.

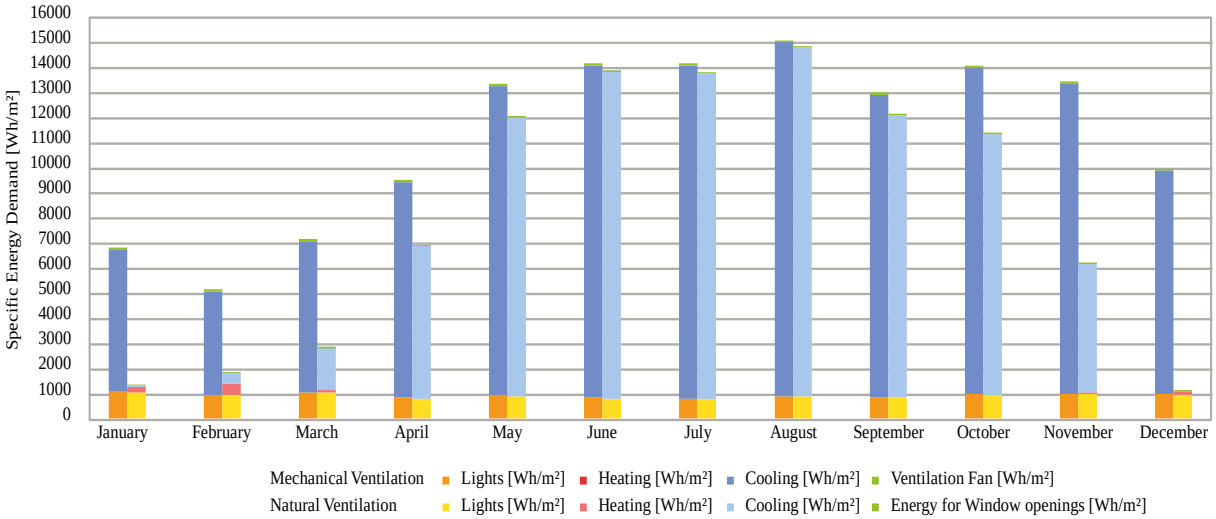

Figure 8 Specific energy demand for Hanoi – comparison of natural ventilation with mechanical ventilation.

4 DISCUSSION AND CONCLUSIONS

In the Mediterranean climate zone (Madrid) no difference in the efficiency of the natural ventilation was observed with the four different CO_2 parameters for window opening. For the moderate climate (Wiegendorf) in the months with high heating loads as well as for the subtropical climate (Hanoi) in the months with high cooling demand an improvement of the energy performance of about 20 % could be reached by using strategy D (900-800 ppm CO_2) instead of strategy A (900-500 ppm CO_2). The limits where varying the natural ventilation strategy come into effect are an energy demand higher than 11000 Wh/m² for cooling and more than 1000 Wh/m² for heating. Within these limits the open strategy does not have an impact on the energy demand therefore the personal preferences of the employees in the office can be given a higher priority.

In this simulation climate conditions that demand highest energy for cooling lead to a situation where natural and mechanical ventilation are comparable (e.g. Hanoi in June-August). When less cooling energy is required natural ventilation was more efficient than mechanical ventilation (e.g. 50 % less energy needed in July in Madrid or November in Hanoi). In climate conditions where the natural ventilation only uses little energy for cooling (e.g. September in Madrid) the mechanical ventilation still consumes very high amounts of energy for cooling. This leads to very high differences in the energy performance in such months. At colder climate conditions this effect becomes smaller (e.g. April in Wiegendorf) up to a point where mechanical ventilation is more efficient than natural ventilation (March in Wiegendorf). There seems to be only a small window for this turning point as in conditions where heating is needed both systems perform comparably well.

It is likely that this effect is an interplay of the outside temperature and the office temperature (simulations with more people might lead to shifted results). In the current simulation the month where natural ventilation performed better than mechanical ventilation lay in an average outside temperature range of 7 °C to 27 °C. Temperature below 2 °C lead to comparably results of both ventilation systems. While there likely is a small temperature range where mechanical ventilation outperforms natural ventilation. In our test this was between 2-7°C.

These results indicate that in the building design phase it would be useful to analyse the climatic conditions to decide on the most energy efficient ventilation system (e.g. in scandinavik locations mechanical ventilation might perform better).

This studies were performed under clearly defined conditions (e.g. south orientated office room, solid construction of building). Simulation with other conditions (e.g. lightweight construction) may lead to different results. Therefore more simulations are needed to be able to generalize the data described in this publication.

5 REFERENCES

Achenbach, P.R.; Coblenz, C.W. (1963). *Field measurement of air infiltration in ten electrically heated houses.* ASHRAE Trans., 69, 306-358.

Bäumler, A. (2016). *Experimentelle Quantifizierung des thermischinduzierten Luftwechsels in Abhängigkeit vonder Fensteröffnungsart sowie Beurteilung derPotenziale der Nachtlüftung.* Dissertation Universität Kassel.

Becker, R.; Pacuk, M. (2002). *Inter-related effects of cooling strategies and building features on energy performance of office buildings.* Energy and Building, 34, 25-31.

EnergyPlus (2018*). EnergyPlusTM Version 8.9.0 Documentation Input Output Reference.* Washington, DC, USA: U.S. Department of Energy.

Gratia, E.; Bruyère, A. (2004). *How to use natural ventilation to cool narrow office buildings.* Building and Environment, 39 (10), 1157-1170.

Prieto, A.; Knaack, U.; Klein, T.; Auer, T. (2017). *25 Years of cooling research in office buildings: Review for the integration of cooling strategies into the building façade (1990–2014).* Renewable and Sustainable Energy Reviews, 71, 89-102.

Schulze, T.; Eicker, U. (2013). *Controlled natural ventilation for energy efficient buildings*. Energy and Buildings, 56, 221-232.

Wang, Z.; Yi, L.; Gao, F. (2009). *Night ventilation control strategies in office buildings*. Solar Energy 83 (10), 1902-1913.

Cooling Performance of Air-Conditioning System with Ceiling Suspended Packaged Air Conditioning Unit over Divided-Type Membrane Ceilings in Large Classroom

Shogo Ito[*1], Toshio Yamanaka[1], Tomohiro Kobayashi[1], Jihui Yuan[1], and Narae Choi[1]

1 Osaka University
Suita 565-0871
Osaka, Japan
** ito_shogo@arch.eng.osaka-u.ac.jp*

ABSTRACT

The mainstream of air-conditioning system for medium and small sized buildings is conditionally air mixing ventilation with ceiling cassette unit of packaged air conditioner (PAC), however, it may bring a high cold-draught risk to occupants, due to the direct drop of the supply air jet. To solve this problem, the air mixing ventilation system can be improved into an air based radiant air-conditioning system by stretching the non-flammable membrane under the ceiling with PAC, thus the cold-draught of PAC could be substantially eliminated and the indoor environment could be improved easily. This air-conditioning system is named Membrane Ceiling Air-Conditioning System Using Ceiling Suspended PAC in this study. Many advantages of the system are (1) draught-less environment by inhibiting air velocity in occupation zone; (2) combination of the convective cooling by supplying micro airflow through a membrane ceiling and the radiative cooling from the cooled membrane ceiling; (3) the occupants' safety in case of the ceiling is collapsing because of its lightweight compared with the conventional ceiling materials; (4) the effect to avoid glare by diffusing illumination light. In addition, by dividing the membrane and making slits between them, that is divided-type, the convective airflow between the spaces across the membrane can be increased.
However, it isn't clear how the indoor environment will be affected by divided-type membrane ceiling air-conditioning system under various conditions. The aim of this study is to investigate the performance of this membrane ceiling air-conditioning system, and to conduct a Computational Fluid Dynamics (CFD) analysis on the airflows in the lecture room with this improved membrane ceiling air-conditioning system. The parameter in the CFD analysis is the membrane laying ratio, which is the ratio of membrane ceiling area to floor area.-Furthermore, room air temperature, air flow pattern and two evaluation indices (DR and ADPI), and exchange air velocity were evaluated by CFD analysis.
The result of this study shows that the improved membrane ceiling air-conditioning system can largely reduce the air velocity and thermal discomfort in occupied zone, compared with the traditional PAC. In addition, it is also shown that the membrane laying ratio would give a large effect on the indoor thermal environment, cooling efficiency and indoor air quality in the occupied zone.

KEYWORDS

Membrane, CFD Analysis, Draught, DR, ADPI

1 INTRODUCTION

In Japan, the mainstream of air-conditioning system for medium and small sized buildings is air mixing ventilation with ceiling cassette unit of packaged air conditioner (PAC). However, in cooling mode, there is a risk of cold draught due to the fall of supply air, and it may cause discomfort of the occupants. In order to solve this problem, the radiant air conditioning systems have attracted many people's interest. There are two types of radiant air-conditioning systems, water-based type or air-based type. It is usual to use water as refrigerant, because of due to the high capabilities of energy saving. Although, it is difficult to install this system and maintain system performance. Thus, the number of introductions example using air-based type has been increasing recently.

In addition, the new air-conditioning system, how non-flammable membrane has been installed underneath the ceiling at rooms with PAC, has been proposed. By installing the membrane, ventilation system of rooms with PAC can be easily changed to the air-based radiant air-conditioning system, which will improve the indoor environment by preventing draught risks in the occupied zone.

Here in this paper, the air-conditioning system shall be called membrane ceiling air-conditioning system. The characteristics of the system are; (1) draught-less environment by inhibiting air velocity in occupied zone; (2) combination of the convective cooling by the micro airflow through a membrane ceiling and the radiative cooling from cooled membrane ceiling *[1]*; (3) occupants are kept safe due to the lightweight of the membrane compared to the other materials, in case of collapsing of the radiant ceiling; (4) the effect to avoid glare by diffusing illumination light at the membrane *[2]*. As shown in Figure 1, in order to increase the amount of convective heat transmission and exchange flowrate, the membrane was divided, thus the airflow can go through the slit between the membrane.

However, the indoor environment of a room with divided-type membrane air-conditioning system has not yet been sufficiently studied. The aim of this study is to investigate the performance and to provide the design date of the membrane ceiling air-conditioning system. CFD analysis was conducted at the room with this new membrane ceiling air-conditioning system. DR and ADPI as indices of draught risk, exchange airflow rate as the index of indoor air quality (IAQ), and cooling effect, are evaluated by CFD and reported in this paper. Membrane laying ratio, which is defined as the ratio of membrane ceiling area to floor area, was changed as the parameter in this study.

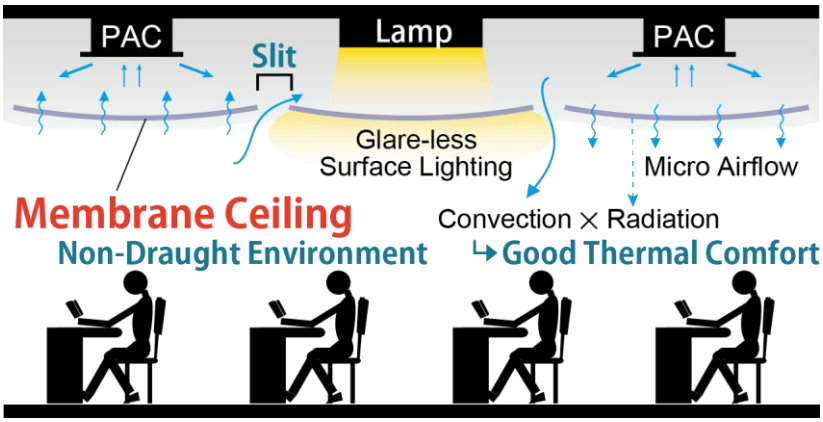

Figure 1: Outline of Divided Membrane Ceiling Air Conditioning System with PAC

Nomenclature

k	Turbulence kinetic energy [m^2/s^2]
Q_{ex}	Exchange airflow rate between attic to indoor space [m^3/s]
Q_{mem}	Exchange airflow rate through membrane [m^3/s]
Q_{op}	Exchange airflow rate through opening (not membrane) [m^3/s]
V_{ex}	Exchange air velocity between attic to indoor space [m/s]
n_{cell}	Number of cells [-]
A_{cell}	Area of a cell on the CFD analysis (= 0.5 ×0.5 = 0.25) [m^2]
t_{ed}	Effective draught temperature [°C]
t_o	Mean air temperature of occupied zone [°C]
t_r	Mean air temperature of room [°C]
t_{PAC}	Supply air temperature from PAC [°C]
t_p	Air temperature at a point P [°C]
Tu	Turbulent intensity [%]
$\overline{U_e}$	Estimated mean velocity [m/s]
$\overline{U_o}$	Estimated mean air velocity of occupied zone [m/s]
$\overline{U_p}$	Estimated mean air velocity at a point P [m/s]
$\overline{V}$	Mean velocity [m/s]
V_z	Velocity in z direction [m/s]
u_e^*	Estimated velocity standard deviation [m/s]

2 SIMULATION MODEL FOR CFD ANALYSIS

In order to investigate the applicability of the new membrane ceiling air-conditioning system to air-conditioned classroom in summer, the CFD analysis was conducted in this study. Cradle STREAM V14.1 *[3]* which is a CFD software was used. The outdoor condition and CFD settings are shown in Table 1 and Table 2, respectively. All of the cells are 50mm × 50mm× 50mm cubes. Table 3 summarises the boundary conditions, and the analysis domain and methods of modelling are shown in Figure 2 - 4.

Table 1: Outdoor Condition

Outdoor Temp. [°C]	35
Hallway Temp. [°C]	30
Solar Radiation [W/m^2]	160
Effective Temp. Difference [°C]	West : + 6

Table 2: Summary of CFD setting

Turbulence Model	Standard k-ε model
Algorithm	SIMPLER
Discretization Scheme	QUICK
Total Number of Cells	1,289,376

Table 3 : Boundary Conditions

a. Boundary Surface

Boundary Surface		Heat Transfer Condition	Wall Function
Ceiling		Log-law	Log-law
Wall	N・S	Symmetry	
	E・W	Log-law	
	W	Log-law	Log-law
Floor		Log-law	Log-law

b. Heat Load

Occupant		60 W×40 people
Window		83.627 W/m^2 × 11.88m^2
Wall	East	Heat Transfer
	West	4.10 W/m^2 × 39.6m^2

c. Flow

System		Airflow Rate [m^3/h]	Supply Temp.
PAC	Inlet	65.625 × 4	P Control Sensing Temp. : Return Air of PAC
	Outlet	262.5	
Total Heat Exchanger Ventilator	Inlet	500.0	Heat Exchange Efficiency 77 %
	Outlet	500.0	

The heat transmission through the east interior wall, whose opposite side is the hallway, and the slab of ceiling and floor, were calculated by setting the equivalent heat conductivity and air temperature outside each wall and slab. On the other hand, the heat load through the west exterior wall was simulated by setting the heat flux condition and was calculated, using effective temperature difference (ETD) of summer in Japan *[4]*. The heat load at the window was obtained by adding the heat transfer and the solar radiation heat, with consideration of the heat loss through the window, and was set on the room side window position.

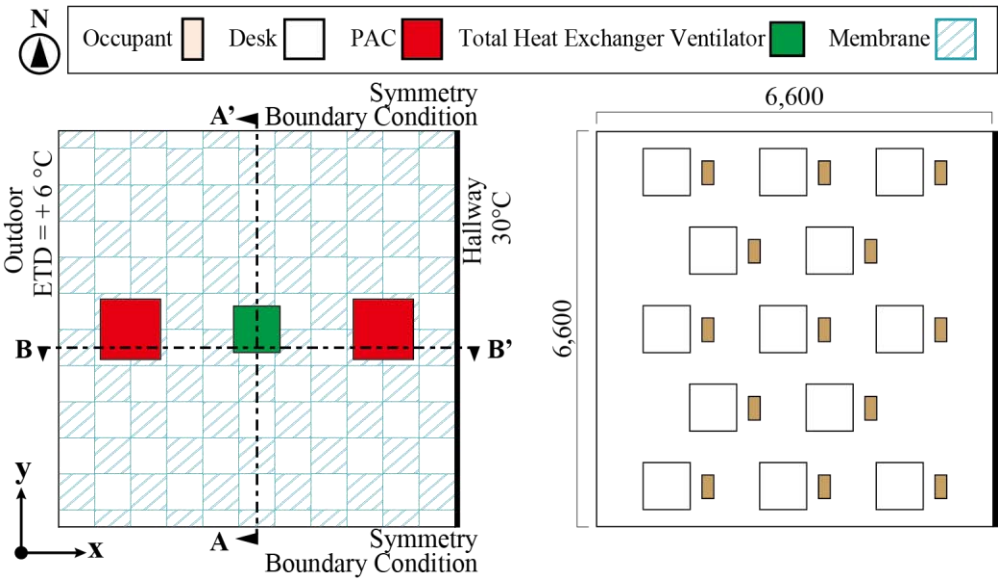

a. Air Conditioners and Membrane b. Occupants and Desks

Figure 2: Plan of Analysis domain of classroom

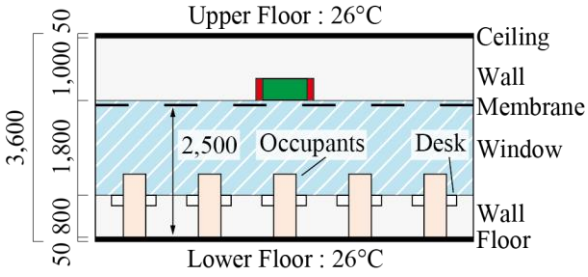

Figure 3: Cross Section at A-A'

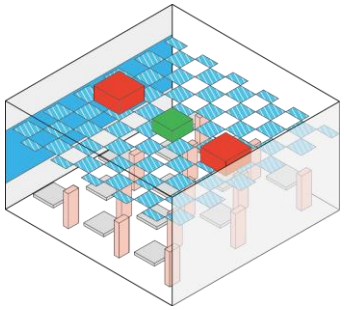

Figure 4: Isometric Drawing

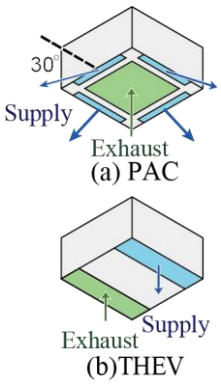

Figure 5: Model of Systems

As shown in Figure 5, two PACs and a total heat exchanger ventilator (THEV), which are introducing fresh air, were installed in the room as air conditioning system. It was assumed that PACs have the thermostats and can regulate the supply temperature to fix the exhaust temperature at 26°C and supply the cold air in the direction of depression angles formed with the ceiling surfaces of 30° from the size 50mm × 600mm inlet to the room. The THEV whose heat exchange effectiveness, which represents the ratio of exchange heat quantity between outdoor air and the room air returned, is 77% supplies the flesh air vertically downward and exhausts upward.

The characteristics of the membrane are shown in Table 4. This analysis took two steps; the first step is the investigation of membrane modelling in CFD analysis. Actually, one of the characteristics of membrane is air permeability. However detailed consideration in CFD analysis is so difficult due to too high calculation load that two simple membrane CFD models were used in the study; (1) Panel model (PM), (2) Pressure-Loss model (PLM). The former one is the PM where a membrane is simulated by non-thickness panel with the thermal conductance,

and its air permeability hasn't been simulated. The radiation heat exchange between the membrane panels and others is simulated. On the other hand, using the PLM, the membrane is simulated by the condition domain through which the air momentum is reduced, equal to the membrane with 20% aperture rate, and the simulation of air permeability is conducted, though it is the fault if the membrane is ignored in radiation analysis. From the above, it is examined which one would be better from the two methods. The first step of analysis was conducted by the case detailed in Table 5. The emissivity is set to 0.9 when radiation analysis is turned on.

Table 4 : Characteristics of the Membrane

Thermal Conductance	Aperture Rate
0.054 W/m	20 %

Table 5 : Examination Case of Memb. Modeling

Case	Membrane Model	Radiation Analysis
i	Panel	-
ii	Panel	X
iii	Pressure-Loss	-
iv	Pressure-Loss	X

The second step of the analysis is aimed to grasp the thermal comfort with different pattern of membrane laying ratios as shown in Figure 6. The 60mm square membrane panels installed in Case iv model due to above consideration were set at 2.5m height of the room.

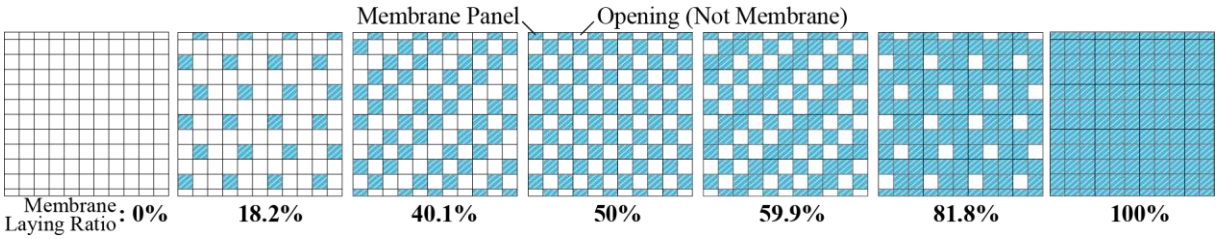

Figure 6: Layout of Membrane Panels of Analysis Case

3 EVALUATION OF THERMAL COMFORT IN THE ROOM

3.1 Equation to convert to scalar mean air velocity

To calculate thermal comfort indices used in the study, scalar mean air velocity and turbulent intensity as measured by low velocity thermal anemometers incorporating an omnidirectional velocity sensor should be applied, as the mean velocity field predicted by CFD simulation on the basis of RANS equation differs *[5]*. Thus, to quantify the improvement in determination of the indices when the air velocity field was estimated by CFD analysis, the following equations were used in the study.

$$\overline{U_e} = \begin{cases} \overline{V}(1 - 0.044Tu + 1.195Tu^2 - 0.329Tu^3), & Tu \le 1.3 \\ \overline{V}(0.287 + 1.502Tu), & Tu \ge 1.3 \end{cases} \quad (1)$$

$$u_e^* = \sqrt{(\overline{V}^2 + 2k - \overline{U_e}^2} \quad (2)$$

where

$$Tu = \frac{\sqrt{\frac{2k}{3}}}{\overline{V}} \quad (3)$$

Thus, estimated velocity field was used to evaluate the draught environment by two indices.

3.2 DR

Fanger et al. (1989) investigated the effect of turbulent intensity on sensation of draught *[6]*. In order to evaluate the draught risk (DR) i.e., the percentage of dissatisfied people due to draught in the occupied zone, the following equation can be used.

$$\mathrm{DR} = \left(34 - \mathrm{t_p}\right)\left(\overline{U_p} - 0.05\right)^{0.62}\left(0.37\overline{U_p}Tu + 3.14\right) \quad (4)$$

Here, the part of the room up to 1.8m above the floor was assumed as the occupied zone.

3.3 ADPI

The air distribution performance index (ADPI) was developed as a way to quantify the comfort level in a space conditioned by a mixed air system in cooling *[7]*. It originally represents the volume ratio of the occupied zone where the following (a) and (b) conditions in Equation (5) were simultaneously verified, however the conditions were altered (a) and (b) conditions to (a) and (b)' conditions in order to consider the influence of the cold draught only.

- $\overline{U_p} < 0.35$ (a)
- $-1.5 < t_{ed} < 1.0$ (b) → $-1.5 < t_{ed}$ (b)'

Where t_{ed} (effective draught temperature) can be calculated using the next equation:

$$\mathrm{t_{ed}} = \left(t_p - t_r\right) - 7.73\left(\overline{U_p} - 0.15\right) \quad (5)$$

4 RESULT AND DISCUSSION

4.1 Investigation of membrane modelling in CFD analysis

The air temperature and velocity distributions at the height of 1.3m on A-A' and B-B' cross sections depicted in Figure 2 for Case i-iv (detailed in Table 4), are shown in Figure 7 respectively. As for the air temperature distribution, by comparing Case i-iv, ~~in~~ under PM and PLM conditions, the temperature field in the room with PLM membrane was all cooler than that with PM membrane. It is considered that more amount of cold supply air from PACs reached the occupied zone by going through the PLM membrane, compared to PM membrane. Furthermore, when radiation analysis was conducted in CFD analysis, the temperature both in PM and PLM conditions got lower than that without consideration of radiation. On the other hand, it was indicated that there is almost no great difference for the velocity distribution regardless of radiant analysis. However, it was shown that the velocity in the room with PLM was higher than that with PM when ~~to~~ comparing the two modelling methods, and the maximum difference between them was approximately 0.2m/s, because the airflow goes through the membrane similarly. From the above, we can see that the temperature and velocity distributions is influenced by the permeability of the membrane substantially. Thus, the analysis method of Case iv was used in the study. However, it must be noted that the most appropriate radiation heat exchange between the membrane and the room was not able to simulate, because the PLM membrane is ignored in radiation analysis.

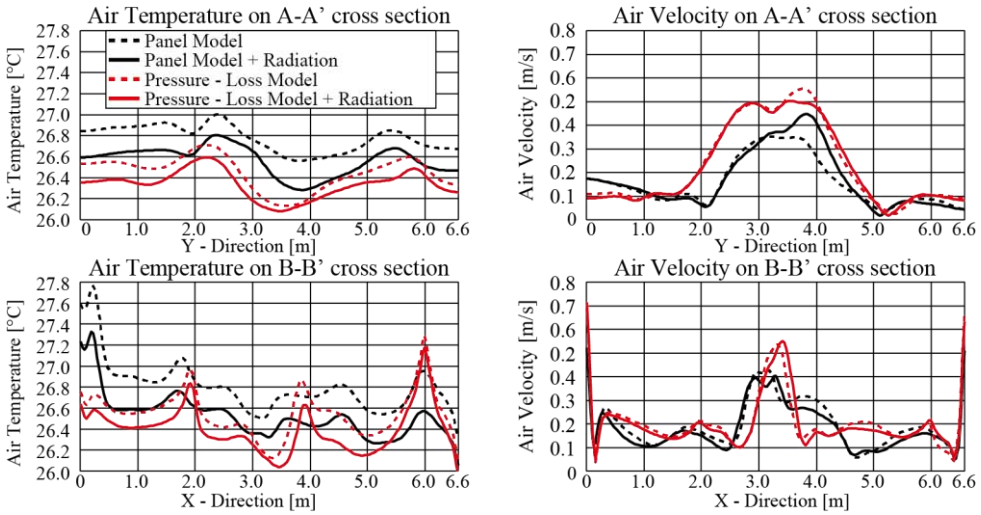

Figure 7: Compare of air temperature and velocity on A-A' and B-B' cross section at 1.3m height

4.2 Comparison of the indoor environment under various membrane laying ratio cases

4.2.1 Distribution of temperature, velocity, DR and ADPI

The average result for each case is shown in Table 6. The vertical distribution of air velocity and horizontal distribution of air temperature, velocity, DR and ADPI are respectively shown in Figure 8 and Figure 9. It is shown that the horizontal air temperature distribution became almost uniform in each case, and–the larger membrane laying ratio gets, the higher the temperature in occupied zone becomes. The reason is considered as that supply temperature from the PAC which includes the thermostat could not be appropriately controlled with high membrane laying ratio. Thus, the control system of PAC with a membrane ceiling may need to be considered in other ways.

On the other hand, when membrane laying ratio becomes higher and higher, the air velocity in occupied zone becomes much slower, and the DR and ADPI was evaluated to be a better result. Since the supply air jetting from the PAC lost momentum due to passing through the membrane. Therefore, we can conclude that the indoor environment can be improved by preventing draught risks as increasing the membrane laying ratio.

Table 6 : Average result value of air temperature, air velocity and indices

Case	Membrane Laying Ratio [%]	T_r [°C]	T_o [°C]	T_{pac} [°C]	U_o [m/s]	T_{ed} [°C]	DR [%]	ADPI [%]
1	0	26.3	26.2	23.7	0.311	-1.31	10.2	69.6
2	18.2	26.4	26.2	23.6	0.282	-1.15	9.4	76.6
3	40.1	26.4	26.3	23.6	0.240	-0.78	8.3	84.4
4	50.0	26.5	26.4	23.6	0.210	-0.57	7.4	90.1
5	59.9	26.6	26.4	23.6	0.197	-0.52	7.0	91.8
6	81.8	26.7	26.6	23.6	0.174	-0.24	6.1	94.5
7	100	26.8	26.8	23.6	0.164	-0.10	5.6	94.9

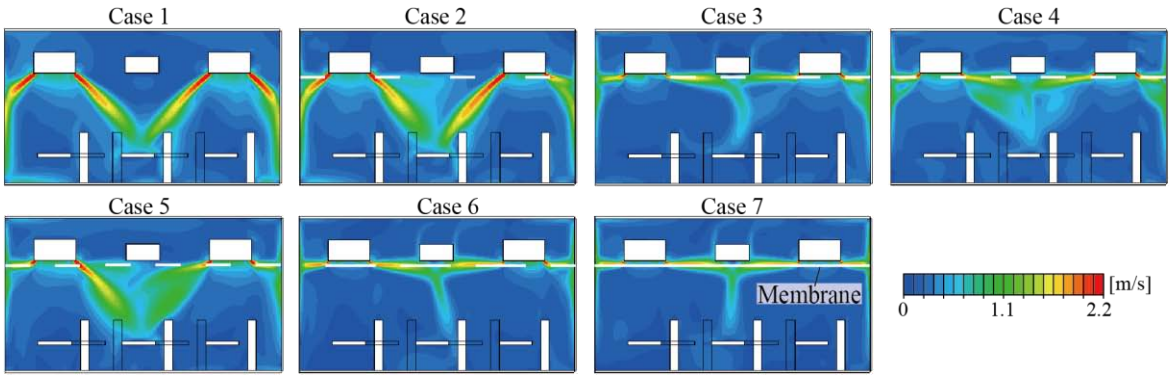

Figure 8: Vertical distribution of air velocity on B-B' cross section

4.2.2 Comparison between Exchange air velocity, DR and ADPI

To find an appropriate membrane laying ratio, the exchange air velocity, in other words, the amount of airflow rate exchanged from attic (space between ceiling and membrane) to indoor space divided by the floor area in the room, was used as an index. It is because increasing of exchange air velocity means increasing of convection flow and make a good effect for IAQ and cooling efficiency. The exchange air velocity can be estimated based on the following equations.

$$v_{ex} = \frac{Q_{ex}}{A_{floor}} \tag{6}$$

where

$$Q_{ex} = Q_{mem} + Q_{op} \tag{7}$$

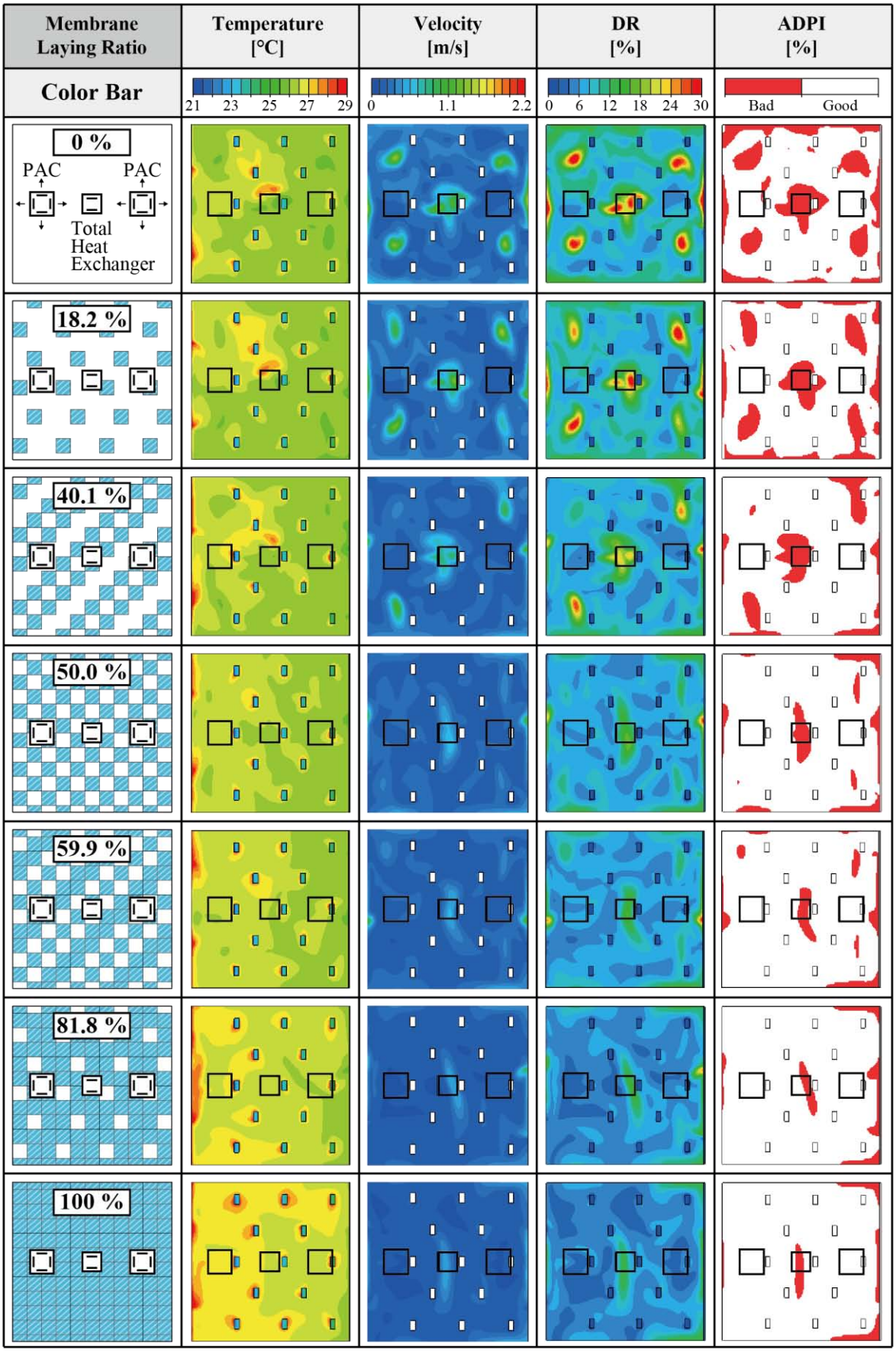

Figure 9: Horizontal distribution of air temperature, air velocity, DR and ADPI at 1.1m height

Furthermore, Q_{mem} and Q_{op} are calculated by the following equation.

$$Q_{mem}\ (\text{or } Q_{op}) = n_{cell} \cdot A_{cell} \times \mathrm{V_z} \tag{8}$$

Where, n_{cell} is the number of cells which are passed by exchange air. Therefore, when Q_{mem} is calculated, the number of the membrane and the velocity through the membrane is used.
The breakdown of exchange air velocity is shown in Figure 10. When the membrane laying ratio is about 70%, the velocity through the opening and the membrane may be same. The comparison between exchange air velocity, DR and ADPI are shown in Figures 11-12. It is shown that there was not much difference between upward and downward exchange velocity. On the other hand, we can also see that the exchange air velocity was decreased by increasing the membrane laying ratio. As mentioned in the preceding section, the draft risk could be prevented. Therefore, it is noted that the membrane laying ratio should be carefully decided because it will give large impact on the indoor environment.

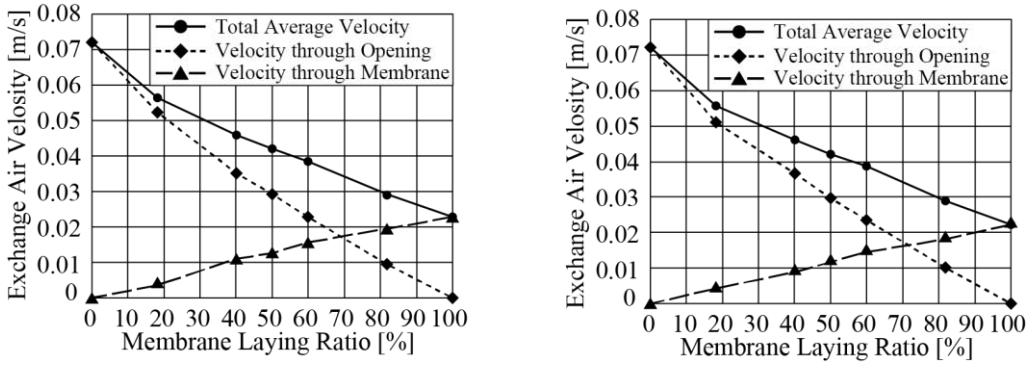

(a) Upward (b) Downward

Figure 10: Breakdown of Exchange Air Velocity

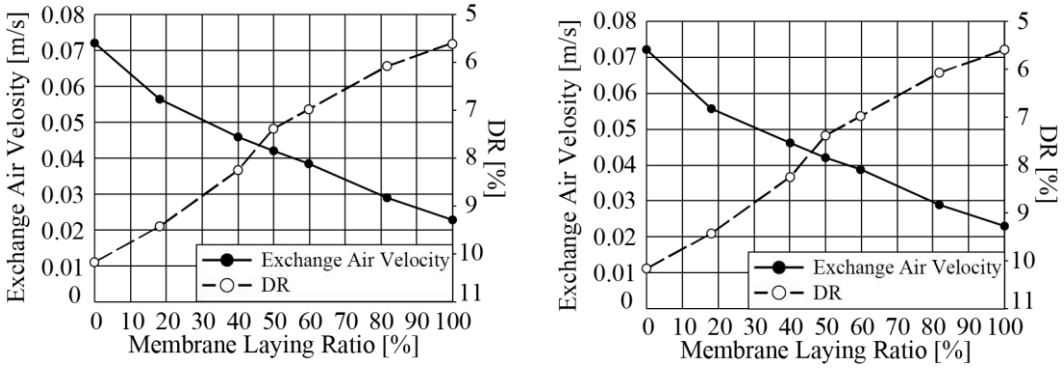

(a) Upward (b) Downward

Figure 11: Exchange Air Velocity vs. DR

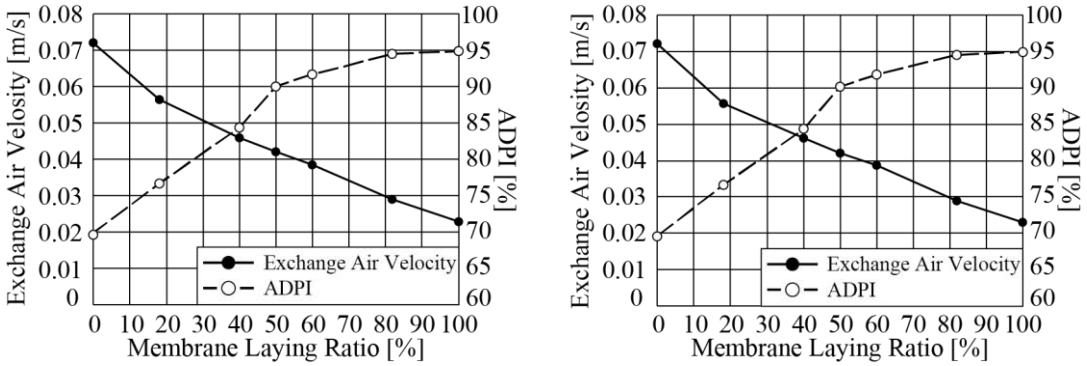

(a) Upward (b) Downward

Figure 12: Exchange Air Velocity vs. ADPI

5 CONCLUSIONS

In this study, the evaluation on the impact of membrane ceiling air-conditioning system using ceiling suspended PAC on the indoor environment is carried out by CFD analysis.

The main remarks obtained in this study is summarized as follows:

- In order to simulate a membrane in CFD analysis, it is examined that the pressure-less model may be better than the panel model, because the indoor environment is much influenced by the airflow through the membrane. However, further studies are need to be done in order to simulate high-accuracy for the system, because radiative heat transfer between the wall and membrane is ignored in the pressure model.

- By increasing the membrane laying ratio, the exchange air velocity was decreased, so that the draught risk was prevented. Therefore, it is noted that the membrane laying ratio should be carefully decided because it has an essential impact on the indoor environment.

As future prospects, we intend to conduct a full-scare experiment in order to grasp the actual phenomenon and confirm the consistency between the result of CFD analysis and the experiment. In addition, the effects of the amount of exchange velocity on the indoor air quality and the efficiency of the performance of air-conditioning system will also be evaluated in the next work.

6 ACKNOWLEDGEMENTS

This work was the joint study with Daikin Industries, Ltd., and the author deeply appreciate the fund from Daikin Industries, Ltd.

7 REFERENCES

[1] Wada, K. (2010). *Task Ambient KOOL System with Ceiling Radiation Membrane (Part 1) – Effectiveness Forecast based on CFD Analysis and Human Thermoregulation Model JOS* -, Japan : Summaries of Technical Papers of Annual Meeting, Architectural Institute of Japan, Environmental Engineering – 2, pp.1077-1078.

[2] Yamamoto,S.(2007). *Membrane Lighting System by Daylight*, Japan : Summaries of Technical Papers of Annual Meeting, Architectural Institute of Japan, Environmental Engineering, pp.415-418.

[3] Cradle (n.d.). Retrieved July 14, 2019, from https://www.cradle-cfd.com/

[4] SHASE Handbook Vol. 2 (1989). Japan, pp.40

[5] Popiolek,Z.(2008). *Improvement of CFD predictions of air speed turbulence intensity and draught discomfort* : 11th International conference on Indoor Air Quality and Climate – Indoor Air 2008; Vol. Paper 718

[6] Fanger,P.O.(1988). *Air Turbulence and Sensation of Draught* : Energy and Buildings 12, pp.21-39

*[7]*ASHRAE HANDBOOK HVAC Applications SI Edition(2011), pp. 57.5

Modelling of Supply Air Jet from Diffusers of Four-way packaged Air-conditioner for CFD Analysis on Unsteady Airflow in Room

Norikazu Yasuda*[1], Toshio Yamanaka[1], Tomohiro Kobayashi[1], Jihui Yuan[1] and Choi Narae[1]

1 Osaka University
Suita 565-0871
Osaka, Japan
**: yasuda_norikazu@arch.eng.osaka-u.ac.jp*

ABSTRACT

Recently in Japan, many buildings introduce packaged air-conditioner (hereinafter, this is called "PAC") as an air conditioning equipment. Most of the PACs can change the direction of supply air blown from the unit and the "Swinging Mode" can change airflow direction periodically as one of the airflow direction setting of PAC. Before constructing the building, appropriately predicting the indoor environment (e.g. temperature distribution or air velocity distribution and so on) is important for indoor environment design. CFD analysis is one of the simulation technique based on the fluid dynamics and have been used to predict the building environment. However, it will take long time to finish non-steady analysis while analysing swinging airflow with non-steady analysis in CFD, it may cause trouble in design situation.

In order to shorten the analysis time and acquire more precise result, the purpose of this research is to establish a CFD model to possibly analyse the swinging airflow in non-steady condition, using dynamic Prescribed Velocity (P.V.) method. In this paper, the experiment to understand the characteristics of the airflow blown from the PAC was carried out. The results of airflow direction measured by an anemometer, airflow volume measured by a cardboard duct, airflow velocity near air supply opening measured by hot-wire anemometer with X-type probe are obtained to establish the CFD model of analysing the swinging airflow with unsteady condition in this study.

KEYWORDS

Packaged Air Conditioner, Hot-wire Anemometer, CFD Analysis, Dynamic P.V. Method

1 INTRODUCTION

Currently, packaged air conditioner (hereinafter referred as PAC) as air conditioning equipment has been introduced to many buildings in Japan, i.e. office building. In indoor environment design phase, predicting the indoor environment is considered as one of the most important things to do. To predict the indoor environment, for example, temperature distribution, air velocity distribution, pollutant distribution, CFD analysis is often used. However, while analysing CFD model in non-steady situation, the time to finish CFD analysis is sometimes too long. One of the way to shorten the analysing time of CFD is to establish a simpler model to calculate the equally large meshes while compared to the original model. In the past, a CFD model of various kind of diffuser or supply opening was conducted (Nielsen,1976, Skovgaard,1991, Kondo,2002, Niwa,2016). Many operation modes i.e. cooling mode and warming mode with different airflow direction and airflow volume, can be set in PAC. Therefore, various kinds of airflow blown from PAC need to be predicted by CFD.

The purpose of this study is to make a simpler airflow model of the PAC based on dynamic Prescribed Velocity (P.V.) method, which can be applied to the all airflows blown from PAC. Thus, the time of analysing CFD could be shortened, and the accuracy of the CFD analysis would be better by using the simpler model.
In addition, airflow direction, airflow volume and airflow velocity were measured by experiment for the purpose of reproducing the airflow by CFD analysing using P.V. method in this study.

2 PROFILE OF EXPERIMENTAL ROOM

The cross section and reflecting ceiling plan of the experimental room are detailed and shown in Figure 1.

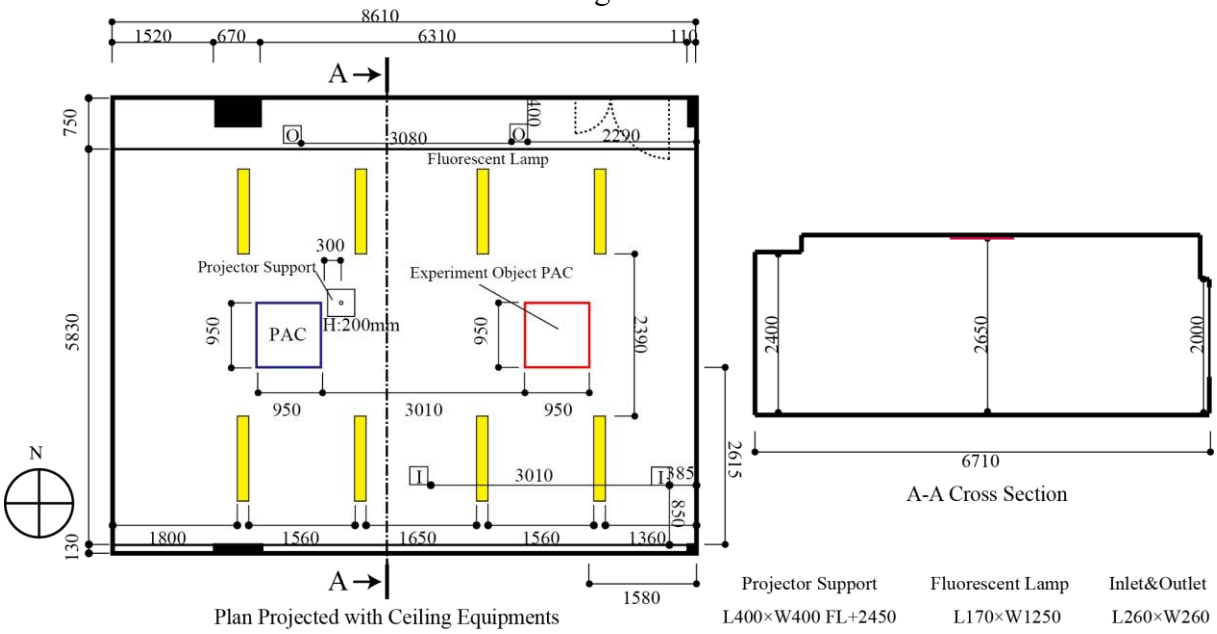

Figure 1: Cross section and reflecting ceiling plan of the experimental room

The experimental room is on the seventh floor (top level) of the seven stories building in Suita Campus, Osaka University. Although two PACs are set on the ceiling of the experimental room, PAC on the east side was selected as the experimental target. It is because there is a projector support which was used to install a projector near the PAC on the west side and it was assumed that the projector support might affect the airflow blown from the PAC on the west side. The experimental PAC is shown in Figure 2.

Figure 2: Experimental PAC

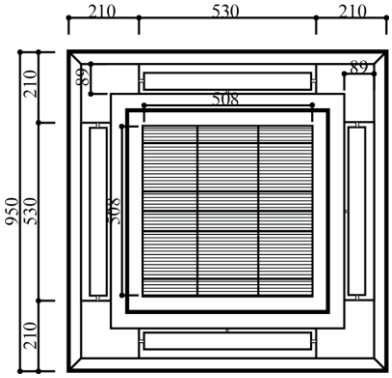

Figure 3: Experimental PAC

The PAC is a four-way ceiling cassette type air conditioner. The plan of the PAC and setting conditions of the PAC are respectively shown in Figure 3 and Table 1.

Table 1: Kinds of setting of target PAC used for experiment

Operating Mode	Fan only, Cooling, Heating, Automatic
Airflow Volume Mode	High, Middle, Low, Calm
Airflow Direction Mode	Mode1, Mode2, Mode3, Mode4, Mode5, Swing mode

Airflow directions assumed as the angle from the ceiling, were named as Mode1 to Mode5 respectively from shallow angle to deep angle to the ceiling. Swing mode is a model that the direction of airflow can be changed every second between the angle of Mode1 to Mode5.
We conducted some experiments using this PAC to obtain the experimental results of airflow direction, airflow volume and airflow velocity.

3 AIRFLOW DIRECTION MEASUREMENT USING THERMAL ANEMOMETER

3.1 Purpose of the experiment

This experiment was done using thermal anemometer to clarify the airflow direction of five modes of the PAC. The purpose of this experiment is to grasp the direction of the airflow blows from PAC and to determine the proper angle of X-type probe used in airflow velocity measurement which will follow this experiment. The model of thermal anemometer is shown in Table 2.

3.2 Experimental method

The method of airflow direction measured by experiment is explained as following: Firstly, thermal anemometer's probe was set to the airflow velocity measurement points as shown in Figure 4, and measure the velocity at each measurement points. The measurement point was set on the central plane vertically cut through the centre of the PAC. Next, the measurement point where the maximum velocity was observed in the measurement cross section will be determined. Lastly, draw a regression line based on measurement points where maximum velocity was observed using least squares method. The origin of the regression line was fixed on the origin in the centre of supply opening of PAC. Measuring scene is shown in Figure 5.

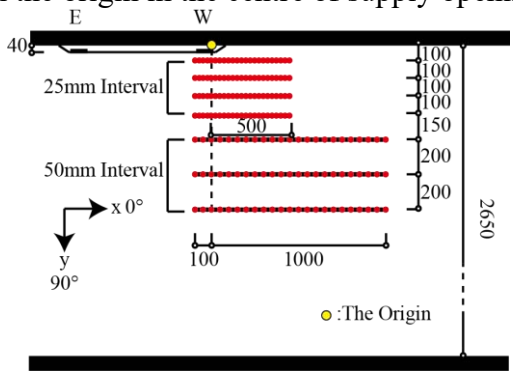

Figure 4: Measurement point

Figure 5: Measuring scene

Table 2: Model of thermal anemometer

Model of Thermal Anemometer	KANOMAX Model 6501
Range of the Velocity able to Measure[m/s]	0.01~30
Measurement Accuracy	±2[%] or 0.02[m/s]

Experimental condition of this measurement is shown in Table 3. The thermal anemometer has uniform sensitivity to flow angle so the position of the probe was considered to be able to accurately measure the velocity. To move the thermal anemometer vertically and horizontally, a traverser that can automatically move in horizontal direction, and a steel pipe standing which can moved in vertical direction, was used.

Table 3: Experimental condition

Measurement Time [s]	30
Measurement Frequency [Hz]	1
Airflow Volume Setting	High
Room Temperature [°C]	13

3.3 Experimental results

The results of airflow velocity and the airflow direction of each airflow direction mode calculated from the airflow velocity are shown in Figure 6. The red points in Figure 6 are the measurement points where the maximum airflow velocity was measured in each measurement cross section.

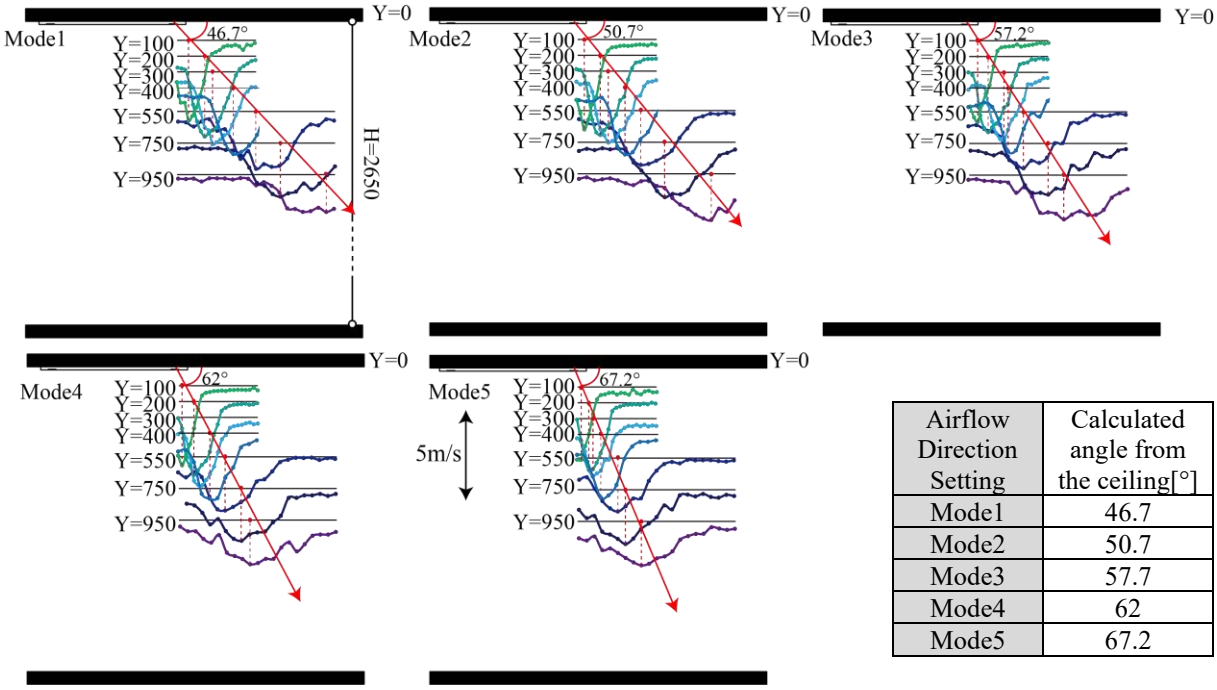

Airflow Direction Setting	Calculated angle from the ceiling[°]
Mode1	46.7
Mode2	50.7
Mode3	57.7
Mode4	62
Mode5	67.2

Figure 6: Airflow velocity measurement results

It is clarified that the angles between the angles of the airflow blown from the target PAC from the ceiling varies from about 47° to 67°. In addition, from the experimental results, it is shown that the airflow velocity declines as the distance from the centre of an axis of the airflow. The maximum velocity in each measurement cross section becomes smaller with the distance from the ceiling to the measurement cross section. The results acquired from this experiment are used to the determination of the airflow direction of the target PAC.
The airflow direction data is also used for CFD analysis.

4 AIRFLOW VOLUME MEASUREMENT USING CARDBOARD DUCT AND THERMAL ANEMOMETER

4.1 Purpose of the experiment

This experiment was done using thermal anemometer which is also used in airflow direction measurement experiment and cardboard ducts which is made of plastic cardboard. The purpose is to acquire the amount of the airflow volume rate blown from the supply opening and return opening. The data of the airflow volume is intended to be used as the boundary condition of the supply opening in CFD analysis.

4.2 Experimental method

The airflow volume was calculated by multiplying the airflow velocity measured by the thermal anemometer at each measurement point shown in Figure 7 by the area divided for each measurement point. 36 measurement points and 16 measurements points were distributed at the end of the cardboard duct for four supply openings and one outlet opening respectively. The area for each measurement point are 0.001335 m^2 at supply opening and 0.01756 m^2 at outlet opening, respectively.

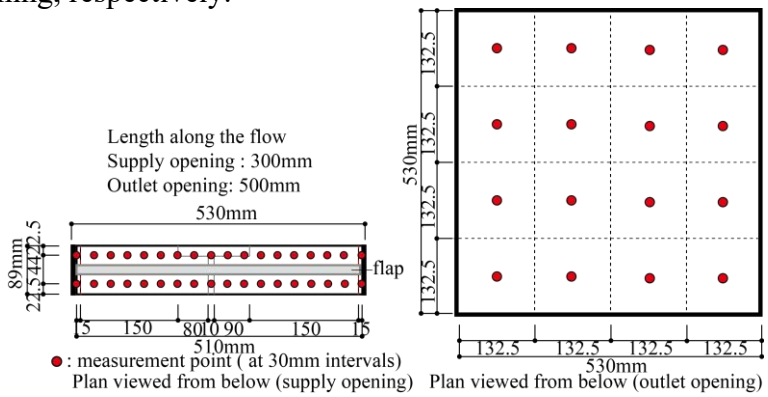

Figure 7: Measurement points

Figure 8: Measurement scene

The experimental condition is almost the same as that of airflow direction measurement. The measurement was conducted when the airflow direction mode was fixed at mode3. The measuring scene is shown in Figure 8. The length of each cardboard duct along the flow is respectively 300mm for supply opening and 500mm for outlet opening.

4.3 Experimental results

The experimental results of airflow volume rate of each supply opening and outlet opening are shown in Figure 9.

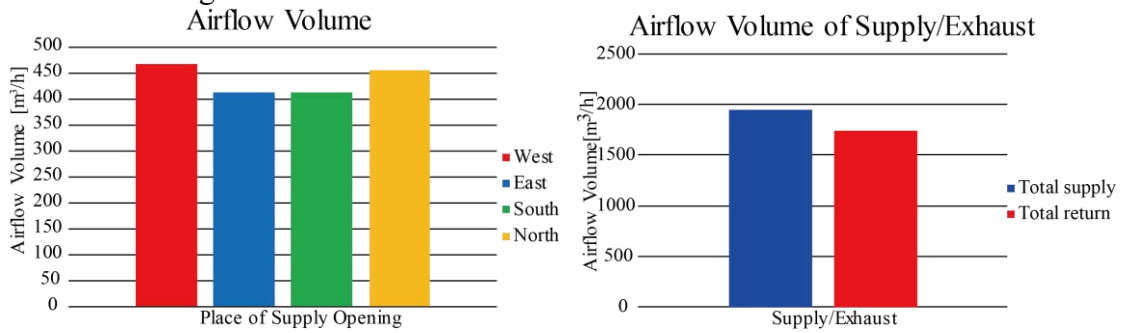

Figure 9: Airflow volume measurement results

The results (Fig.9) showed that the calculated airflow volume of the west supply opening is larger than the other three supply openings. Thus, the experiment was carried out at the supply opening in the west. Furthermore, it is shown that the calculated total supply airflow volume is larger than the return airflow volume. The reason is considered that the probe of thermal anemometer was set on a surface of the entrance of the cardboard duct and the velocity around the entrance of cardboard duct is unstable especially in the measurement of returning airflow rate. The calculated airflow volume is used for CFD analysis as boundary condition given to supply opening.

5 AIRFLOW VELOCITY MEASUREMENT USING HOTWIRE ANENOMETER

5.1 Purpose of the experiment

This experiment was done using hotwire anemometer with X-type probe (measuring time:60[s], measurement frequency:1000[Hz], airflow volume setting: high, operating mode: fan only, airflow direction mode: mode3). The purpose of this experiment is to grasp the characteristics

of the airflow blown from the target PAC, and to apply these measured velocities to CFD analysis as boundary condition using P.V. method.

5.2 Experimental method

Experimental equipment of this measurement is shown in Figure 10. As previously mentioned, this experiment was conducted at the west supply opening of PAC.

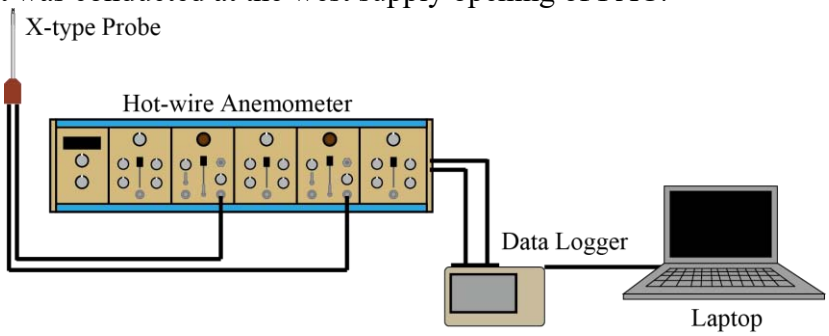

Figure 10: Airflow velocity measurement equipment

According to the results of preliminary measurement about angle characteristics which was done previously, the direction of X-type probe was set at an angle of 45° incline against the supply opening. Two hotwires were named "Channel 1" and "Channel 2" respectively. Channel 1 is the hotwire which is stretched vertically and Channe2 is the hotwire stretched horizontally. Airflow velocity was calculated by equation (1) to (3). (refer to Nomenclature)

$$E_1 = \alpha U sin(45° + \theta) \tag{1}$$

$$E_2 = \alpha U sin(45° - \theta) \tag{2}$$

$$\alpha = \frac{10}{U_{max}} \tag{3}$$

From equation (1) and (2), following equation (4) and (5) are derived.

$$U = \frac{U_{max}}{10\sqrt{2}} \sqrt{2({E_1}^2 + {E_2}^2)} \tag{4}$$

$$\theta = tan^{-1} \frac{E_1 - E_2}{E_1 + E_2} \tag{5}$$

In equation (3), "10" is the output voltage when the airflow velocity is U_{max}. The measurement points are shown in Figure 6 and Figure 11. By using airflow velocity at supply opening, turbulence characteristic, turbulence kinetic energy k and turbulence dissipation rate ε, were also calculated by the following equation (4) to (10).(refer to Nomenclature)

$$k = \frac{3}{8}(\overline{u'u'} + \overline{v'v'}) \tag{4}$$

$$\varepsilon = C_D \frac{k^{\frac{3}{2}}}{l} \tag{5}$$

$$\overline{u'_i(t)u'_i(t+\tau)} = \lim_{T\to\infty} \frac{1}{T} \int_1^\infty u'_i(t)u'_i(t+\tau)\, dt \tag{6}$$

$$\rho_i(\tau) = \frac{\overline{u'_i(t)u'_i(t+\tau)}}{(u'_i(t))^2} \tag{7}$$

$$T_i = \int_0^{\tau_0} \rho_i d\tau \tag{8}$$

$$\Lambda = \bar{u} T_i \tag{9}$$

$$l = C_D^{\frac{1}{4}} \Lambda \tag{10}$$

It must be noticed that X-type probe can't measure airflow velocity from the third dimension, so that the u' and v' which were calculated from x direction velocity and y direction velocity include the standard deviation of the third dimension. Therefore, the calculated u' and v' are larger than actual figure. It is assumed that the standard deviation of the third dimension is the same as the average value of u' and v' and that is what leads equation (4) to calculate turbulence kinetic energy.

5.3 Experimental results

The results of airflow velocity measurement are shown in Figure 11(a) and (b).

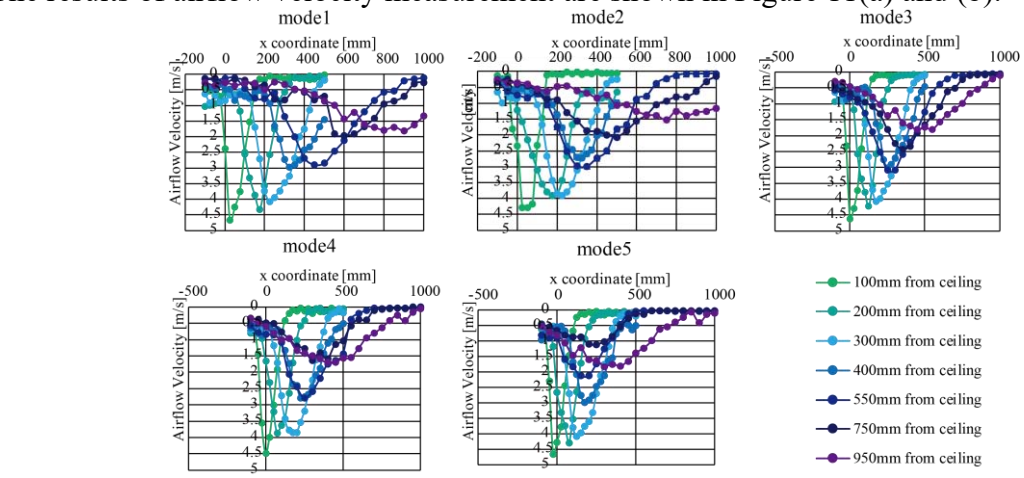

(a) Airflow velocity distribution of each airflow direction mode

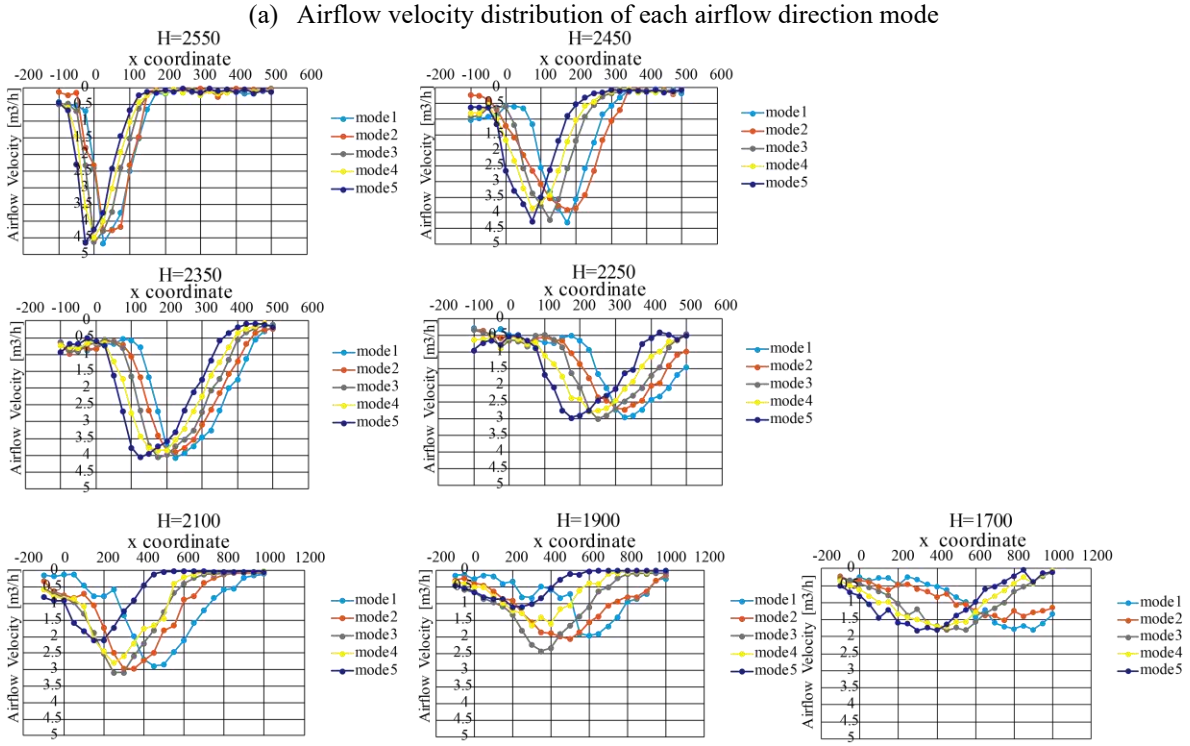

(b) Airflow velocity distribution of each cross section

Figure 11: Airflow velocity measurement results

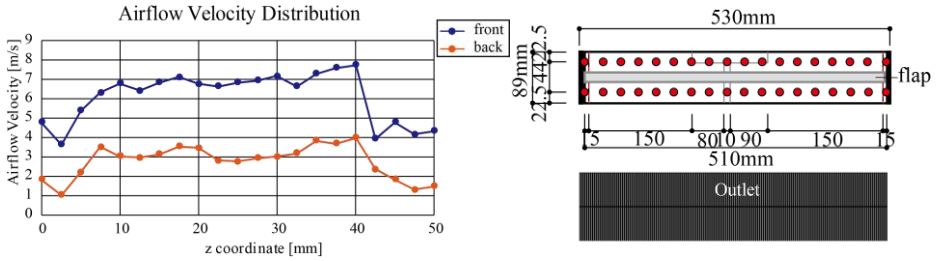

Figure 12: Airflow velocity at supply opening

The same as the airflow direction measurement using thermal anemometer, the larger the distance from the supply opening to the measurement point, the smaller the airflow velocity. From the results of H=2550, airflow velocity at over x=200mm is under 0.25 m/s in all airflow modes, thus the x coordinate at 300mm is enough for the length of velocity fixed surface. The maximum measurement point of each measurement cross section changes as the mode changes. In addition, turbulence statistics are calculated and shown in Figure 13.

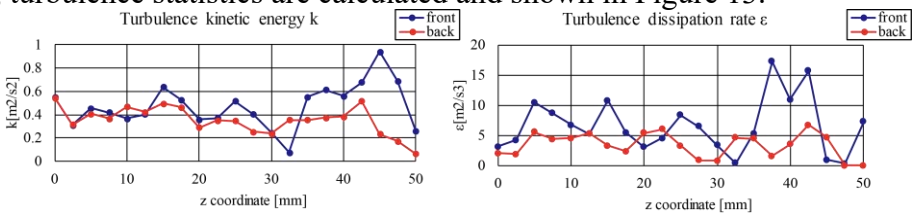

Figure 13: Turbulence statistics

6 CFD ANALYSIS USING P.V. METHOD

6.1 Purpose of this CFD analysis

The purpose of this CFD analysis is to reproduce the airflow of the PAC by using P.V. method (Nielsen,1992) and to check whether P.V. method is appropriate to analyse the airflow blown from PAC. It is assumed that more accurate result obtained by P.V. method will be gained.

6.2 CFD model

The CFD model is shown in Figure 14. The dimensions of simulated room is length of 8610mm, width of 5630mm and height of 2650mm. A PAC is set the ceiling. At supply opening of the PAC, the velocity is uniformly distributed and the air volume blow from each supply opening is set to be same. The value of the airflow volume is 467 [m^3/s] which was acquired from the measurement. Analysis and boundary conditions are shown in Table 4 and Table5, respectively. The model was segmented with 25mm cube meshes

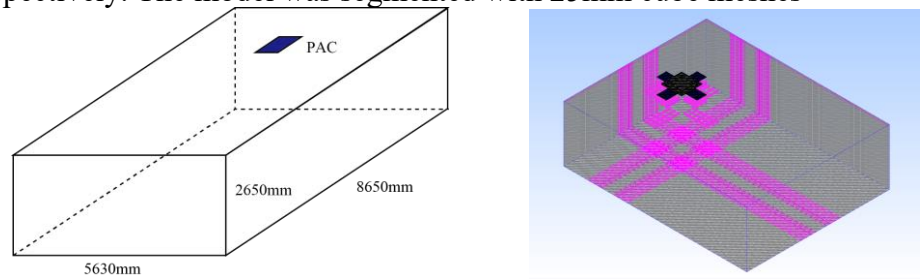

(a) Isometric drawing (b) Meshes

Figure 14: CFD analysis model

Table 4: CFD analysis condition

CFD Code	STREAM V14
Turbulence Model	Standard k-ε
Analysis Domain	8650×5630×2650
Number of Meshes	10,328,175(275×351×107)
Algorithm	SIMPLE
Discretization Scheme	QUICK

Table 5: Boundary conditions

(a) Boundary surface

Boundary Surface	Wall Function
Wall	Non-slip
Floor	Non-slip
Ceiling	Non-slip

(b) Flow

PAC	Airflow Rate [m^3/h]	Angle from the Ceiling [°]
Inlet	467 × 4	46.7/57.2/67.2
Outlet	Natural Outlet Boundary	-

P.V. method was used and velocity fixed surfaces was set at y=100mm cross section where the airflow velocity data was acquired by the experiment. The velocity given to the velocity regulation surfaces are different depending on the air direction mode.

6.3 CFD analysis results

The results of CFD analysis is shown in Figure 15. The analysis results of Mode5 showed that the airflow direction goes downwards at the point far from ceiling. In addition, it is also shown that the velocity measured by hotwire anemometer is lower than the velocity from CFD analysis. Therefore, we must reconsider the height of velocity regulation surface.

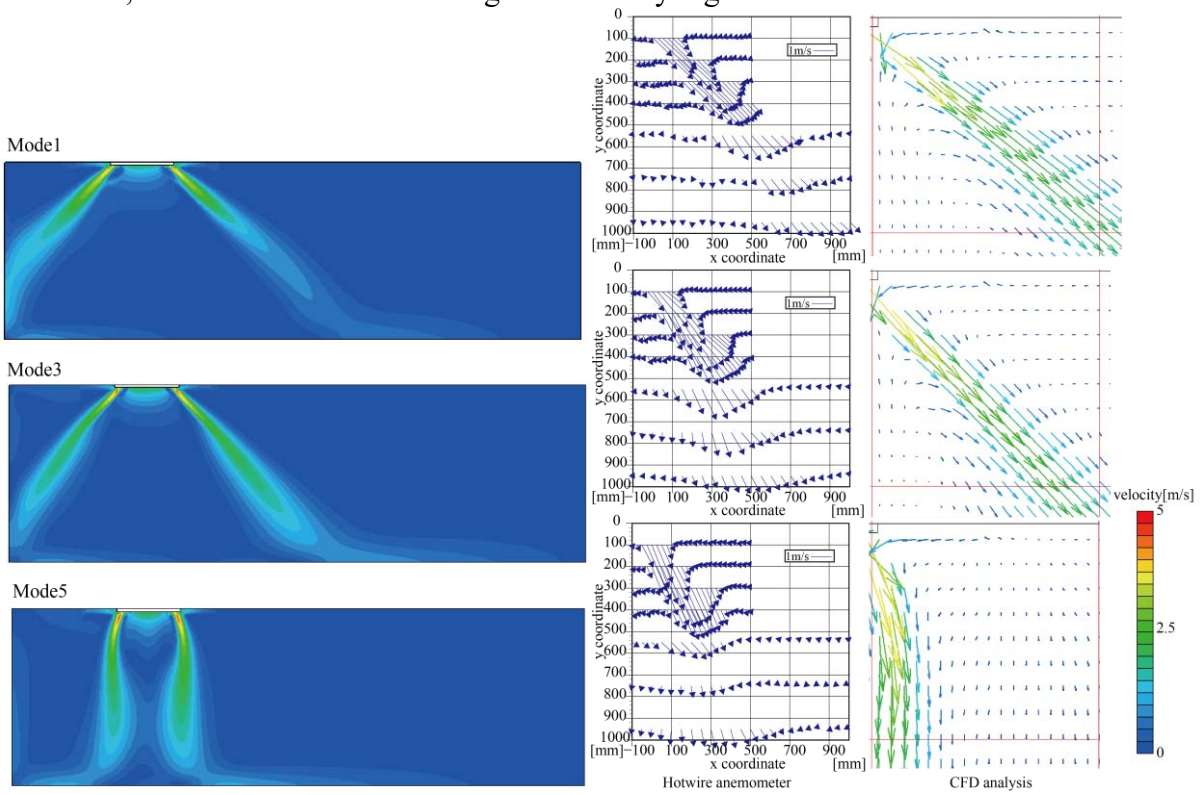

(a) Velocity contour (CFD) (b) Velocity vector (Experiment) (c) Velocity vector (CFD)

Figure 15: CFD analysis results

7 CONCLUSION

In this research, the experiments were conducted in the room with four way packaged air conditioner. From the experiment, the characteristics (airflow direction, volume, velocity and turbulence statistics) of the airflow blown from the PAC were acquired. By using experimental results, CFD analysis was carried out to reproduce the airflow. It is realized that several points must be investigated to make the analysis more accurate.

ACKNOWLEDGEMENT

This research is under joint research with Mitsubishi Electric Corporation. The authors are sincerely grateful to the Mitsubishi Electric Corporation and gratefully acknowledge the fund and the cooperation of people who related to this research.

Nomenclature	
E_1, E_2 [V]	Output voltage of Channel 1 or Channel 2 at hotwire anemometer
α [-]	Caribrating coeficient
U[m/s]	Velocity of the airflow hit to hot wires from the front
θ [°]	Angle of the direction X-type probe and the line x=y
U_{max} [m/s]	Velocity which was used when caribrating hotwire anemometer (=10 m/s)
k[m2/s2]	Turbulence kineticenergy
u',v' [m/s]	Stadard deviation of the velocity of x-direction or y-direction
ε [m^3/s^2]	Turbulence dissipation rate
C_D[-]	Model constant (=0.09)
l[m]	Turbulence length scale
t, τ [s]	Time
τ_0 [s]	The time when τ_i goes 0
ρ [-]	Autocorrelation coefficient
T_i [s]	Turbulence time scale
Λ [m]	Integral length scale

REFERENCE

Nielsen, P.V. (1976) FLOW IN AIR CONDITIONED ROOMS: *Ph. D. thesis from the Technical University of Denmark*

Skovgaard,M(1991) MODELLING COMPLEX INLET GEOMETRIES IN CFD: applied to air flow in ventilated rooms, *12th AIVC Conference. pp. 184~199, 1991*

Kondo,Y(2002). MODELING OF AIR DIFFUSER INSTALLED AT CEILING FOR CFD SIMULATION : Experiments and numerical simulation on complex air diffuser at isothermal condition (Part 1), *Architectural Institute of Japan, The Summaries of Designing Papers of Architectural Institute of Japan*

Niwa,K(2016). A CFD Analysis on Airflow in Room with Line Slot Diffuser for Modeling of CFD parts Effect of Turbulence Intensity Settings of Inlet Airflow, *The Society of Heating, Air-Conditioning and SanitaryEngineers of Japan, The summaries of Technical Papers of Kagoshima,201-204*

Nielsen, P.V. (1992) DESCRIPTION OF SUPPLY OPENINGS IN NUMERICAL MODELS FOR ROOM AIR DISTRIBUTION: *Instituttet for Bygningsteknik, Aalborg Universitetscenter*

Multi-objective design of single room ventilation units with heat and water recovery

Antoine Parthoens[*1], Luc Prieels[2], Jean-Jacques Embrechts[3], Yves Detandt[4], Sébastien Pecceu[5], Samuel Gendebien[1] and Vincent Lemort[1]

1 Thermodynamics Laboratory, ULiège
Allée de la découverte 17
4000 Liège, Belgium
**Corresponding author: a.parthoens@uliege.be*

2 Greencom SPRL
Rue Gilles Magnée 92/3
4430 Ans, Belgium

3 IntelSig, ULiège
Allée de la découverte 10
4000 Liège, Belgium

4 FFT
Rue Emile Francqui 9
1435 Mont-Saint-Guibert, Belgium

5 Belgian Building Research Institute
Avenue P. Holoffe 21
1342 Limelette, Belgium

ABSTRACT

The present paper describes the design improvement of a single-room ventilation unit. This ventilation system presents many advantages, however, several drawbacks exist. The first one is the acoustic disturbance. As the facilities are directly installed within the rooms, the fans' noise may create discomfort. Furthermore, in the cold or temperate climates, condensation or frost may appear. A dedicated management should then be implemented. Finally, as the system is not centralized, communication between the different units is required to ensure the global system efficiency. A team of several industrial partners and research institutes tackles the above-mentioned issues in the frame of the "Silenthalpic" project. The project is split in three major tasks. To correctly reduce the sound emission level (i), a spectral analysis of the noise emitted by an existing unit was undertaken, revealing that frequencies under 1 kHz are mainly responsible for the noise disturbance. From this analysis, active and passive solutions for noise reduction are envisaged, showing encouraging trends. The next research aspect is the exchanger of the ventilation unit (ii). The constituting material is a new porous membrane allowing the humidity transfer (vapor or liquid). This specific exchanger is numerically modelled to predict its performances. The last considered problematic is the optimization of the ventilation and control strategies for the specific case of decentralized units (iii), taking advantage of sensors and recent communication technologies like IOT (Internet Of Things) to establish communication between decentralized units and ensure their consistent control. The association of the three aspects presented here should then lead to versatile and efficient ventilation systems.

KEYWORDS

Single-room ventilation systems, noise reduction, heat recovery, humidity recovery,

1 INTRODUCTION

1.1 Global context

In the context of global warming, energy savings in buildings are getting more and more important. Eurostat (Eurostat, 2018) stands that in European Union in 2016, the households accounted for 25.4% of the final energy consumption. That is the reason why new and refurbished buildings are getting more isolated and airtight. This leads to an increase of the energy consumption relative proportion dedicated to ventilation (Roulet, Heidt, Foradini, &

Pibiri, 2001). To reduce this aforementioned consumption, mechanical ventilation with heat recovery was introduced. The most widespread system is a centralized system with a single heat exchanger and a ducting networks. Besides this technology, decentralized systems, also known as single-room ventilation with heat recovery systems (SRVHR) do exist. The purpose of the present paper is to describe a project gathering multiple research centres and industrials aiming at developing a new efficient decentralized ventilation unit.

1.2 Issues of decentralized ventilation systems and challenges set in the Silenthalpic project

SRVHR are units composed of a casing containing one or two fans, a heat exchanger, filters and control electronics. The whole setup is installed at the top of a window (thinnest part of a building), or simply against a wall with two drilled holes. A schematic representation of the unit is shown in Figure 1.

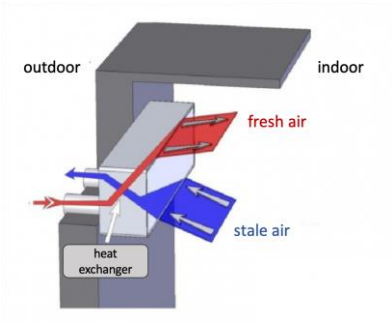

Figure 1 Schematic representation of SRVHR units

For a given building, the number of required units depends on the flow rates delivered by the considered system and the needs of the building, function of its surface, population and type of activity.

This technology already exists and presents some advantages such as :

- the installation easiness, especially in the frame of refurbishment;
- a reduced ducting network that leads to an easy system maintenance;
- a flexible implementation, as the number and the position of the units are modular;
- a pre calibrated mass flow rate.

The objective of the “Silenthalpic” project is to develop a compact unit, limiting three major issues:

- Noise disturbance limitation. As the solution is decentralized, fans are in the actual living rooms (bedrooms, offices,…) and the noise generated must be limited. Specific efforts are deployed to maintain the acoustic disturbance linked to the use of fans as low as possible. Moreover, the ventilation unit is prone to increase the transmission of exterior noise emissions to the building’s interior. Acoustic insulation properties if the unit should be evaluated.
- Enthalpy exchanger development. In addition to recover heat, it also recovers a part of the moisture from the extracted stale air.
- Development of a so-called "evolutionary" ventilation system.

During the development of all latter ones, the need of compactness of the system is always kept in mind.

1.3 Methodology

The first research aspect focuses on the aero-acoustic phenomena related to the mechanical ventilation. After a first stage of advanced diagnostic on an off-the-shelf unit, modelling methods are developed to predict the involved phenomena. Another point is the investigation of the application of the active and passive noise reduction to ventilation units. The target is to reach a standard sound level of 35 dBA for a flowrate of 50 m^3/h.

The second research axis deals specifically with the possibilities of heat and humidity transfer within so-called "enthalpy" membranes. The target is to develop membrane able to recover 50% of the recoverable water quantity. This should reduce condensate issues and delays frost-related problems, while evacuating building excess moisture. In tertiary applications, as well as in dry buildings and colder climates, this increases occupant comfort and provides an important technological advantage. To achieve this, the project focuses on the development of an enthalpy membrane. This membrane will then be used to manufacture a heat exchanger core, later tested and integrated into ventilation units.

Finally, the project focuses on aspects related to the overall integration of ventilation systems. The ventilation strategies made possible by this new technology are studied in the light of the regulatory frameworks of the various surrounding countries. These strategies are evaluated and modelled. They take into account the new potential offered by the Internet of Things (IOT) for users as well as for manufacturers, installers and home automation activities. All the results of this work will then be implemented into two applications: 2 window and 2 lintel demonstrators, which will take into account the results of the LCA (Life Cycle Assessment) studies. Finally, the final system will be tested in different acoustic and thermal test cells to estimate improvements.

2 METHODS FOR THE REDUCTION OF NOISE EMISSIONS BY THE VENTILATION UNIT

Several tasks have been defined in order to reduce the noise generated by the ventilation unit in the interior living area. Passive and active solutions installed on the unit itself are envisaged to attenuate the noise emissions by the two fans.

2.1 Numerical model of the ventilation unit

The acoustic improvements of the design require a deep understanding of the noise sources characteristics and the acoustic transmission properties of the different components of the ventilation unit. Acoustic simulations provide access to the whole pressure field (spatial and frequency dependence) which leads to a better understanding of the propagation mechanisms and the dominant contributions perceived.

Although acoustics deal with unsteady pressure fluctuations, the flow solvers are designed to accurately represent the turbulent fields and their schemes are not tailored to preserve at the same time the dissipation and dispersion properties of the acoustic waves. Based on the unsteady flow solution, the acoustic solver Actran computes the aeroacoustic noise sources following the original idea of Lighthill 1952. The acoustic propagation is modelled by a finite element discretization of the acoustic domain. The mesh is designed to accurately propagate the acoustic waves up to the highest frequency. The solver works in the frequency domain, computing each frequency separately and updating the material properties according to the characteristics defined by the user.

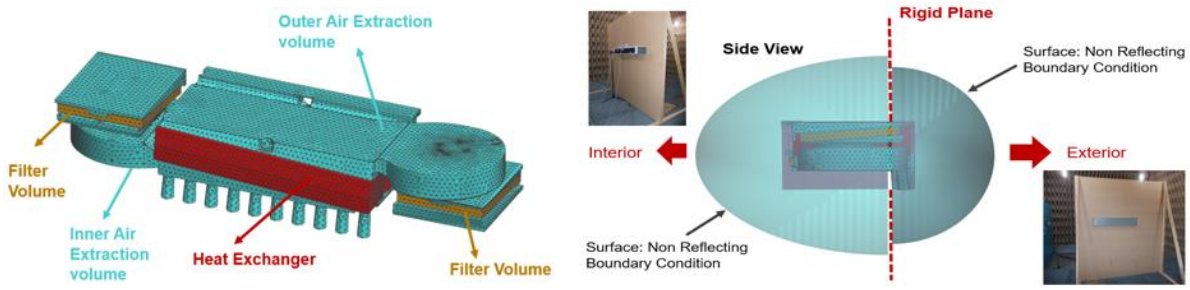

Figure 2 Acoustic model of fan and heat exchanger unit (left) and global view of the acoustic model (right)

In the current project, the main simulation challenge was related to the modelling of the heat exchanger part. Discretizing the small channels is not practical as it would lead to very expensive simulations due to the large number of elements. The alternative modelling developed in this research project was to consider the exchanger as a whole system connecting the inlet to outlet with an equivalent fluid mixing in between. The viscous and thermal effects affecting the acoustic propagation in the system are included in the model. Most of the parameters are directly related to geometrical and mass flow rate properties and a very small set is more complex as related to the acoustic transfer properties between the channel pipes. These parameters have been set based on measurements in the Acoustic Laboratory of the University of Liège. The heat exchanger model has been validated in the framework of the Silenthalpic project and could be extended to any heat exchanger, while reducing significantly the cost compared to a simulation based on all channels discretized.

The acoustic model has been used to analyse the transfer properties and different acoustic modes existing in the system. As the fan spinning generate a series of tonal components, the rotation speed should be controlled to avoid a match between the blade passing frequencies emitted by the fan and the natural resonant frequencies of the system.

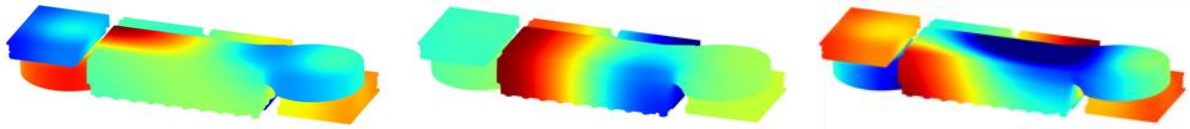

Figure 3 Acoustic pressure modes of the system at 428 Hz (left), 664 Hz (middle) and 714 Hz (right)

2.2 Experimental diagnosis of the ventilation unit

A vibro-acoustic evaluation of the ventilation unit in its initial state was first carried out. This was used as a starting point to quantify the further improvements brought by the passive as well as the active solutions to be developed by the different research teams. The acoustic insulation of the ventilation unit inserted into a hard wall has been measured in a reverberant room, according to the standard EN ISO 10140-2. With the same set-up, the sound pressure levels emitted by the two fans were measured according to EN ISO 100052:2005. The standard sound level measured in the room at 50m³/h was 41.6 dB(A), with the most part of the energy emitted between 200 and 1000 Hz. An objective of the research project is to reduce this level to 35 dB(A). The test in the reverberant room has also shown a significant influence of the anti-dust filters installed above each fan.

In parallel with these measurements, another set-up was realized in an anechoic room with a similar ventilation unit which was inserted into a big baffle. This set-up has been used to measure the directivity of the sound emission by each fan, in several third-octave bands.

Globally, the emission was shown to be close to omnidirectional, for the frequency interval of interest. Also in the anechoic room, high-resolution spectra (Δf=1Hz) were measured at several positions. Pure tones were of course detected in the spectra and their frequency was related to the rotation speed of the fans and their number of blades.

Finally, intensimetry and an acoustic camera were used to identify the main sources of noise emission on the interior side of the module. Both fans contribute significantly to the noise emissions, in particular at the air inlet aperture.

2.3 Passive attenuation of the noise emissions

Several methods of passive acoustic attenuation are available, like the application of absorbing materials (mineral fibres, foams, …) inside the ventilation unit, at well-defined locations. Dampers and quarter-wave resonators could also be used, if possible.

The experimental diagnosis has shown the predominance of the noise emitted through the air flow apertures. Therefore, several solutions have been tested during the first part of the research:

- a perforated absorbing front cover,
- different mufflers with 3cm mineral wool applied in front of the air apertures,
- a muffler with 3cm mineral wool inserted into the front cover.

The best results were obtained with the second solution, with a noise reduction of 7 dB(A). However, this solution cannot be implemented in practice, since it significantly increases the global volume of the ventilation unit. Also, the influence of the mufflers on the air flow (in m^3/h) has not been investigated yet. However, this first result has confirmed the predominance of the noise emitted through the air inlet aperture: if this noise source can be properly attenuated, then the objective of a maximum noise level of 35 dB(A) at 50 m^3/h is achievable.

The numerical model of the ventilation unit described in section 2.1 will also be used to test other passive solutions. This kind of model can be particularly useful to optimize some parameters such as the type, the location or the thickness of a layer of absorbing material.

2.4 Active attenuation of the noise emissions

Active noise control (ANC) is a method of sound attenuation in which a secondary acoustic wave is generated by an actuator (generally a loudspeaker) to superpose the primary (noise) wave, in such a way that the superposition of both waves results in a reduced amplitude. In theory, if the secondary wave is such that the opposite pressure signal is generated in the immission zone, then a perfect silence is obtained. In practice, the extension of the zone in which attenuation is observed is limited and the noise reduction itself is limited, according to the method used for the control and the quality of the material.

The analysis of the scientific and technical literature has revealed some interesting studies and practical realizations (mostly in laboratory) for the ANC of ventilation units. In particular, methods using the control of fan noise propagating into a duct have shown good results. Also the control of noise propagating through an ‘open window’ has recently attracted the interest of the ANC community, especially to reduce the noise emissions of relatively small equipment like the ventilation unit.

The experimental diagnosis has shown the predominance of the noise emitted through the air flow apertures, in particular the air inlet aperture on the interior side of the building. It was therefore decided to first design and study the solution of an additional duct, fixed to the existing ventilation module and deporting the air inlet aperture to the end of the duct, approximately 1m

away of its initial position. This solution allows the ANC of the noise emitted by the fan extracting air through this aperture, while still maintaining the air flow.

ANC in a duct is usually realized with a *feedforward* control system. This system consists of a sensing microphone measuring the noise upstream of the controller, the controller itself (a digital signal processor DSP), one or several loudspeakers creating the secondary wave in the duct and one or several error microphones downstream to measure the effect of the control. The length of the duct is chosen to guarantee a sufficient delay of sound propagation between the sensing microphone and the loudspeakers, such that the DSP would have enough time to generate the secondary wave. Some systems don't need this sensing or reference microphone: the controller only needs the error microphones' signals as input data (*feedback* ANC). However, the stability is better in feedforward systems, the main reason why this solution has been selected in this research.

The duct has been built with a rectangular cross-section, the dimensions of which have been selected such that only plane waves are allowed to propagate up to about 1200 Hz (this allows to use only one loudspeaker and one error microphone). ANC indeed usually shows good performance below 1 kHz (even below 500 Hz sometimes) which is considered as the frequency interval of interest. For higher frequencies, a combination with passive acoustic absorbers is usually envisaged, which will be the case here.

Finally, strategic locations must be defined for the two microphones and the loudspeaker. For this purpose, the numerical model described in section 2.1 will be used to tests several combinations of microphones and loudspeaker's positions and select the one(s) reaching the greatest noise reduction.

3 DEVELOPMENT OF HEAT AND MOISUTRE RECOVERY EXCHANGER

Current enthalpy recovery systems imply devices such as rotating wheels (Zeng, Liu, & Ashish, 2017) that are active or imply exchangers made of fragile porous materials such as paper. The off-the-shelf ones are either complicated to implement or present a limited life-span. The Silenthalpic proposal is to develop a robust enthalpy exchanger with a high enlargement factor (i.e. ratio between developed and flat surfaces) allowing an efficient heat, vapor and liquid water transfer.

The development of the membrane itself at the lab and industrial scales and the development of a numerical model predicting the performance of the exchanger are tackled. The aim of the numerical model is to perform an optimization of the exchanger design.

3.1 Porous membrane development

The main objective here is to develop a composite membrane allowing water to transfer from one of its side to the other and that can be thermoformed.

The chosen method was to inject some solid particles into a polymer matrix to artificially create some defects. Those latter ones must have a characteristic size allowing the transfer of water particles by capillarity while blocking the transfer of air. Particles of different sizes are tested to finally select the one fitting the best the application.

The first step of the process is extruding the mixture. The polymer materials as well as the solid particles are being dried several hours to obtain a -40°C dewpoint. Then the mix is extruded in a bivis co-rotative extruder. The solid particles powder is added by a side-feeder leading to an easily obtained homogenous grains. From this product, films must be manufactured. The

previous product is dried again to reach humidity lower than 200 PPM. Then, films are made with a single vis extruder. These composite films can then be thermoformed to get a high enlargement factor as well as the desired shape, depending on the exchanger design.

To evaluate the ability of the membrane to transfer water and especially liquid water, an experimental apparatus has been put in place.

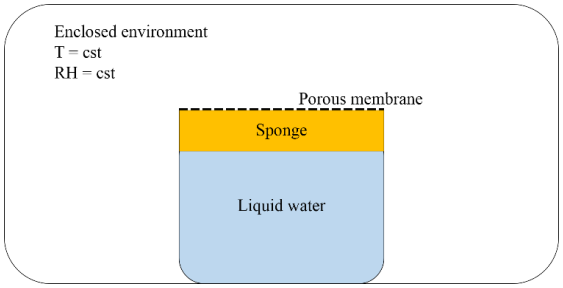

Figure 4 Experimental setup used for the membrane permeability determination

Preliminarily, the membrane is submerged in water for one hour to load all the interstices and to measure steady state conditions. Then, a recipient is filled with liquid water and closed with the membrane. To ensure a permanent contact between the liquid and the membrane, a sponge is added and periodic checks were made to control that the liquid was in contact with the sponge during the whole experiment. This setup is weighted and put in an enclosed environment where the atmospheric conditions were controlled. The temperature is fixed to 23±0.5°C and the relative humidity to 50 ± 1%. After 24 hours in these conditions, the recipient is weighted a second time. The difference between the two measures corresponded to the water that went through the membrane and that was evaporated to the environment.

3.2 Numerical model implementation

In order to get a suitable enthalpy exchanger, a design process is needed. The objective is to exchange the largest amount of heat, the optimal quantity of water, to limit the pressure drops and to keep the compactness.

Many works in scientific literature handle enthalpy exchangers. Dugaria et al (Dugaria, Moro, & Del Col, 2015) predicted with a 2-dimensional finite difference model sensible, latent and total effectiveness sensitivity to membranes' characteristics. Sebai et al. (Sebai, Chouikh, & Guizani, 2014) modelled cross-flow enthalpy exchangers with balanced or unbalanced flow with a control volume method. Zhang (Zhang, 2009) measured latent effectiveness going up to about 70% with a paper-plate and paper-fin exchanger. Niu & Zhang (Niu & Zhang, 2001) showed numerically and experimentally the evolution of enthalpy exchangers for different membranes and operating conditions.

However, all the above-mentioned works only consider a vapour transfer. In the frame of this project, a special attention is paid to the liquid water transfer for the condensates management. A specific model has been developed to handle this kind of mass transfer coupled with a heat transfer. This model is detailed by Parthoens et al. (Parthoens, Gendebien, Lemaitre, & Lemort, 2018). All in all, it allows to predict the sensible, latent and total efficiencies for given atmospheric conditions (indoor and outdoor), mass flow rates and for a given geometry and a membrane permeability.

The final objective will be to supply different geometries with specific constraints to the model and to assess which one will be produced and implemented in the actual demonstrator.

4 VENTILATION SYSTEM DESIGN AND CONTROL AT BUILDING SCALE

4.1 Design and control strategies with decentralized ventilation

Despite the advantages of decentralized ventilation (see §1.1), one of its main disadvantages is that the total air change rate at building scale may be twice as high as with a conventional mechanical system. Indeed, air is supplied and exhausted in every space with a decentralized unit, while with a classical system air is generally supplied in "dry" spaces (living, bedrooms, etc) and exhausted in wet spaces (kitchens, bathrooms, etc). The same fresh air is thus used for two spaces with classical systems.

This drawback can however be tackled in two ways:

- Using demand controlled ventilation (DCV). The ventilation needs in dry and wet spaces are not always synchronous, and the decentralized approach allows a differentiated control per space. Even if the installed flow capacity (total design flow) is higher than for conventional system, the relative flow rate reduction due to DCV is probably much higher with decentralized systems.
- The developed unit has been designed so that is possible do connect a duct at the extraction side, allowing displacing the exhaust a few meters from the ventilation unit itself. This 'remote extraction' configuration is straightforward in a two-room accommodation (bedroom/bathroom) like hotels or rest houses. This 'remote extraction' principle could also be applied in small houses by grouping dry and wet rooms by two. This way of working is closer to conventional system, but would still require much less ducting (shorter, narrower) than a centralized installation. The main advantages of decentralized systems would thus persist.

Multizone simulations were performed with the CONTAM software to evaluate the impact of decentralized ventilation on the overall energy performance, and showing how the above solutions help in reducing its energy footprint. One of the test cases is the one of a two bedrooms apartment as illustrated at Figure 5. The design flows were chosen supposing 3 occupants and a nominal flow of 25 m³/h/pers (prEN 16798-1). Flow rates in wet spaces were chosen according current Belgian standards (NBN D-50-001) and/or to reach the balance at building level.

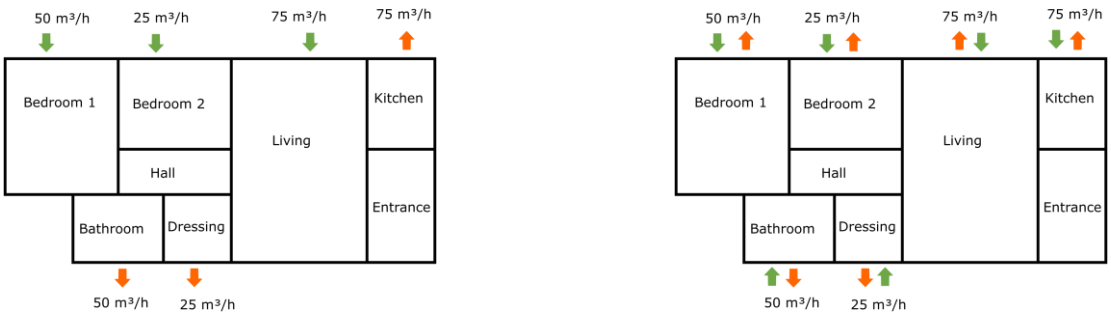

Figure 5 Example apartment and flow rates for a conventional mechanical system (left) and a fully decentralized system (right). With these flow rates, the total flow rate for the conventional system is 150 m³/h while it is 300 m³/h for the fully decentralized system.

With the chosen flows, the 'remote extraction' solution could be easily applied to the 3 following pairs of dry and wet spaces:

- Bedroom 1 and Bathroom

- Bedroom 2 and Dressing
- Living and Kitchen

In this precise configuration, this remote extraction solution has exactly the same nominal flow rate as a conventional mechanical system.

Demand controlled ventilation is simulated with a local detection and regulation in each space:

- Supply in dry spaces (or extraction in dressing): linear variation from 10% to 100% of nominal flow for CO2 concentration from 400 to 1000 ppm.
- Exhaust in wet spaces: linear variation from 10% to 100% of nominal flow for Relative humidity from 30% to 70%.

Three types of "physical system" are simulated:

- The conventional system (centralized). The ventilation needs were computed per space, and the overall flow balance was ensured at any time (lower flow adjusted to reach the highest flow).The fully decentralized system as on the right side of figure 3. In this case, the balance in only per space
- The 'remote extraction' system with the pairing proposed above. The nominal flows correspond to the left side of Figure 3, but the flow rates are balanced for each pair of rooms (corresponding to each physical ventilation unit).

Regarding pollutant sources, humidity sources are defined in the bathroom and kitchen at representative schedules, and the occupancy profile corresponds to two working adults with one child. Simulation results are expressed as mean ventilation flow rate (representative of the ventilation heat loss) over the simulation period and given in Table 1.

Table 1 Mean flow rate of the DCV strategy for different ventilation designs. The mean flow for the fully decentralized system remains higher than for the conventional system, but the relative reduction is much stronger. For this example, one also sees that the 'remote extraction' variant is nearly identical to the conventional system in terms of flow rate

Case	Nominal flow rate [m³/h]	Mean flow rate with local regulation and detection [m³/h]
Conventional centralized system	150	63
Fully decentralized system	300	86
Remote extraction decentralized system	150	66

On this example, results of Table 1 confirm the efficiency of the two envisaged strategies to reduce the mean flow rate of decentralized systems and the associated heat loss.

4.2 Regulation of decentralized systems and communication between units

The presented case in the above subsection is quite simple. In some configurations, several decentralized units could be needed to reach the required flow rates in some spaces (e.g. in living spaces). In that case, not all units will be equipped with sensors and their control should be coordinated.

An electronic card has been designed and prototyped with the ability to support all types of required sensors (temperature, pressure, CO2, etc) and to communicate with other units through the Zigbee protocol. This allows the different units in the same building to communicate

between them (for a coordinated control) and to communicate to the outside for monitoring or diagnostic purpose.

5 CONCLUSIONS

The aim of the present paper was to present the work undertaken by a consortium of many industrials and research centres. The objective was to develop a highly efficient single room ventilation system with heat and humidity recovery. It was seen that three major axes were investigated.

After a deep analysis of existing systems, numerical and experimental investigations were carried on, to passively and actively reduce the noise emissions of the unit. Simultaneously, a new composite membrane was developed to built-up a robust and performing enthalpy exchanger. Finally studies have been driven to integrate intelligently such units at the building scale, respecting needs and standards.

6 ACKNOWLEDGEMENTS

The consortium would like to thank Walloon Region and the Pole Mecatech [convention 7711] for the support in this work.

7 REFERENCES

Dugaria, S., Moro, L., & Del Col, D. (2015). Modelling heat and mass transfer in a membrane-based air-to-air enthalpy exchanger. *33rdUIT(Italian Union of Thermo-fluid-dynamics) Heat transfer conference.*

Eurostat. (2018). *Consumption of energy*. Obtido em June de 2018, de http://ec.europa.eu/eurostat/statistics- explained/index.php?title=Consumption _of_energy#End- users

Niu, M., & Zhang, L. (2001). Membrane-based Enthalpy Exchanger: material considerations and clarification of moisture resistance. *Journal of Membrane Science*, 179-191.

Parthoens, A., Gendebien, S., Lemaitre, P., & Lemort, V. (2018). Model development of a new enthalpy exchanger under wet conditions in the frame of a single room ventilation . *System Simulation in Buildings.* Liège.

Roulet, C.-A., Heidt, F., Foradini, F., & Pibiri, M.-C. (2001). Real heat recovery with air handling units. *Energy and Buildings, 33*(5), 495-502.

Sebai, R., Chouikh, R., & Guizani, A. (2014). Cross-flow membrane-based enthalpy exchanger balanced and unbalanced flow. *Energy Conversion and Management*, 19-28.

Zeng, C., Liu, S., & Ashish, S. (2017). A review on the air-to-air heat and mass exchanger technologies forbuilding applications. *Renewable and Sustainable Energy Reviews, 75*, 753-774.

Zhang, L.-Z. (2009). Heat and mass transfer in plate-fin enthalpy exchangers with different plate and fin materials. *International Journal of Heat and Mass Transfer*, 2704-2713.

Review of building services solution fitted for a low emission building stock in urban areas

Matthias Haase*[1], Øystein Rønneseth[1], Kari Thunshelle[2], Laurent Georges[3], Sverre Holøs[2], and Judith Thomsen[1]

1 SINTEF
Strindvegen 4
Trondheim, Norway
**Corresponding author: e-mail address*
Presenting author: underline First & Last name

2 SINTEF
Forskningsveien 3b
Oslo, Norway

3 NTNU
IVT
Trondheim, Norway

ABSTRACT

The purpose of this paper is to summarize the status of promising low carbon building services solutions fitted for a low emission building stock in urban areas.

It is believed that well-performing building envelopes with low thermal losses or low solar heat gains, enables simplified building services solutions. This paper compiles promising building services solutions studied in other research projects and fitted for highly insulated buildings for the most common building categories within a neighbourhood.
The common building categories include new and renovated offices, educational buildings, residential buildings, grocery stores and shopping centres. Some of the following building services solutions are still relevant for single buildings, but for utilizing surplus energy sources in particular, it is better to look at multiple buildings in a neighbourhood. Especially the following topics are presented and evaluated:

- Demand-controlled ventilation
- Ventilation-based heating and cooling
- Simplified hydronic heating
- Smart energy control
- Responsive lighting equipment
- Utilizing surplus energy sources

Each technical solution is discussed and its suitability for other building types is evaluated. Technical installations are moving towards low-temperature heating and high-temperature cooling, in order to better utilize renewable energy sources and surplus energy, and to reduce heat loss from the systems. Future buildings and renovated existing buildings should aim for an optimization between energy, power and indoor environment, and reasonable economy. Although power demand and peak loads have not been significantly discussed in this report, it is currently undergoing a lot of research to reduce costs of upgrading the electricity grid and will continue to receive substantial focus in the coming years. When assessing energy performance, comfort quality and economic feasibility of low energy building services, a comprehensive approach is needed.

KEYWORDS

Demand-controlled ventilation, ventilation-based heating and cooling, simplified hydronic heating, smart energy control, responsive lighting equipment, utilizing surplus energy sources.

1 INTRODUCTION

It is believed that well-performing building envelopes with low thermal losses or low solar heat gains, enables simplified building services solutions.
The original definition of the passive house is a building where thermal comfort can be achieved by preheating and precooling of the ventilation air, with no larger ventilation rates than are necessary for achieving satisfactory air quality. Under this definition, separate heating and cooling systems are unnecessary. Heating and cooling by ventilation may not be the ideal solution for all buildings in a zero emission neighbourhood (ZEN), but in general, building services solutions can be simplified or downsized in buildings with little thermal transport through envelope and low solar heat gains when there is no heating demand.

2 OBJECTIVE

The purpose of this paper is to summarize the status of promising low carbon building services solutions fitted for a low emission building stock in urban areas. The suitability of the solutions was assessed according to the building categories characteristic usage profile, heating, cooling and el-specific power profile, demand for different thermal zones, floor-plan flexibility and availability of excess heat. The solutions are relevant for use by researchers and practitioners for further research. It is not a state-of-the-art research paper covering all the details, but rather a foundation for further work in the area of low carbon solutions fitted for low emission buildings and neighbourhoods.

3 METHOD

The present study is based on a systematic mapping study designed to carry out an objective selection of literature sources relevant to the topic in question. The methodology adhered to in the present study is described (Petersen, Vakkalanka, & Kuzniarz, 2015).
In the present study, the Scopus abstract and citation databases of peer-reviewed literature was considered for the past 10 years (2008 – 2019). The search string was structured using Boolean operators to refine the search process in terms of action description (“how”) and object (“what”) and corresponds to the keywords set out in Table 1.

Table 1: Keywords and Boolean operators used for the initial search.

HOW?	AND WHAT?	AND NOT to exclude
zero emission buildings	Building services	food medical

The search produced 1014 publications for (zero emission buildings) and this was restricted to 244 publications when adding "AND (building services). Fig. 1 illustrates the recent marked increase in publication numbers. The screening of publications was performed on the basis of the following inclusion and exclusion criteria with the aim of excluding publications that are not relevant to the research questions. The qualitative inclusion criterion was as follows:
- English language
The scientific inclusion criteria were as follows:
- The technology under study should correspond to the definition of objectives provided in Section 2, and
- The object to which the study in question is applied should correspond to cold climate. This excludes publications related to warm climates where technical solutions might look different.

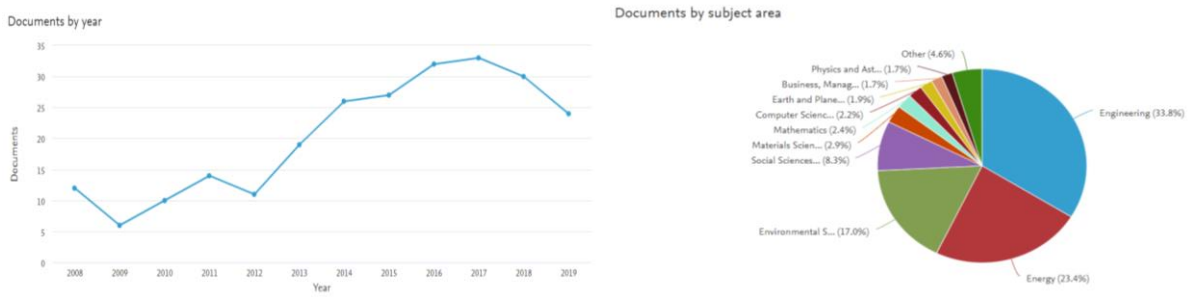

Figure 1: Results of screening exercise in scopus database; development of publications per year on the left and documents by subject area on the right

This resulted in 32 publications. In addition, 106 project reports (ZEB, EBLE, BestVent, Svalvent) and 55 project reports in the EU project Commonenergy were screened. After a screening process based on titles and abstracts, a total of 92 publications were deemed to be relevant to the research questions.

List of relevant publications for this study:
(Aaberg, 2018; Alfstad, 2018; Ampenberger, 2017; Antolin et al., 2017; Antolin et al., 2015; Avantaggiato et al., 2017; Belleri & Avantaggiato, 2017; Belleri, Haase, Papantoniou, & Lollini, 2017; Berge, 2016; Berge, Georges, & Mathisen, 2016; Berge & Mathisen, 2016; Berge, Thomsen, & Mathisen, 2016; Bluyssen & Fanger, 1991; Bointner et al., 2014; Bukat, Niewczas, Kozioł, Łazowski, & de Ferrari, 2015; Bøhn, Søreng, Holljen, Dehlin, & Grini, 2014; Daldosso, Gentile, Mangili, & Papantoniou, 2017; Dipasquale, Belleri, & Lollini, 2016; Edvardsen, 2014; Emerson Climate Technologies, 2014; *Enovarapport*, 2003; Federico Visconti, Maurizio Orlandi, & Saro, 2015; Feist, Schnieders, Dorer, & Haas, 2005; Foster & Quarini, 2001; Fricke & Becker, 2010; Froehlich & Ampenberger, 2017; Galvin, 2016; L. Georges et al., 2017; L. Georges, Berner, & Mathisen, 2014; Laurent Georges, Håheim, & Alonso, 2017; L. Georges & Skreiberg, 2016; L. Georges, Skreiberg, & Novakovic, 2013; L. Georges, Skreiberg, & Novakovic, 2014; L. Georges, Thalfeldt, Skreiberg, & Fornari, 2019; L. Georges, Wen, Alonso, Berge, & Thomsen, 2016; L. Georges, Wen, Alonso, Berge, Thomsen, et al., 2016; Gram-Hanssen, 2010; Haase, 2016; Haase & Ampenberger, 2017a, 2017b; Haase, Antolin, & Belleri, 2016; Haase & Skeie, 2013, 2015; Haase, Skeie, et al., 2016; Haase, Skeie, Belleri, & Dipasquale, 2015; Haase, Skeie, & Woods, 2015; Haase, Woods, & Skeie, 2014; Halvarsson, 2012; Haukås, 2016; Heiselberg, 2017; Holand, Yang, Holøs, Thunshelle, & Mysen, 2019; Jones, 2018; Karmakar, Das, & Ghosh, 2016; KIWI, 2017; Kragh, 2016; Larsen et al., 2010; Lekang Sørensen, Jiang, Nybakk Torsæter, & Völler, 2018; Madsen & Gabrielsen, 2016; Mattilsynet, 2018; Micro Matic, 2016; Midttømme, 2018; Mysen, Berntsen, Nafstad, & Schild, 2005; Mysen & Schild, 2013, 2014; Mysen, Schild, & Cablé, 2014; Mæhlen, 2017; NVE, 2016, 2018; Olsen, 2018; Rozanska et al., 2017; Rønneseth, 2018; Schieldrop, 2019; Selvnes, 2017; Seppänen, Brelih, Goeders, & Litiu, 2012; Skeie, Lien, Svensson, & Andresen, 2016; Solt et al., 2017; Staggl, Reiter, & Ampenberger, 2017; Standard Norge, 2017; Stene, 2017; Stene, Justo Alonso, Rønneseth, & Georges, 2018; Stiller, 2012; Sundlisæter et al., 2015; Sweco, 2016; Thomsen, 2017; Thomsen, Gullbrekken, Grynning, & Holme, 2017; Thunshelle, 2016; Vázquez et al., 2017; Venås, Harsem, & Børresen, 2014; Walnum & Fredriksen, 2018; Wargocki, Fanger, Krupicz, & Szczecinski, 2004; Weschler, 2011; Woods, Mellegård, Schlanbusch, Skeie, & Haase, 2015)

4 RESULTS

The common building categories include new and renovated offices, educational buildings, residential buildings, grocery stores and shopping centres. Some of the following building services solutions are still relevant for single buildings, but for utilizing surplus energy sources in particular, it is better to look at multiple buildings in a neighbourhood. Especially the following topics are presented and evaluated:

- Demand-controlled ventilation
- Ventilation-based heating and cooling
- Simplified hydronic heating
- Smart energy control
- Responsive lighting equipment
- Utilizing surplus energy sources

Each technical solution is discussed and its suitability for other building types is evaluated. Some of the technologies were tested in specific building types. Some assumptions and prerequisites are explained that will make these technologies also suitable for other building types. Table 2 provides an overview of the different technologies and their suitability in the different building types.

4.1 Demand-controlled ventilation

Demand-control of mechanical ventilation systems has a significant impact on the demand for heating, cooling and electrical power in all buildings where the need for mechanical ventilation varies in time, and there are dependable ways of detecting these variations. In spaces where humans are the predominating pollution source and occupancy varies over time, e.g. classrooms, meeting rooms, congregation halls and open-plan offices, demand-control using CO_2-sensors or presence detector for determining the ventilation need is a cost-efficient way of reducing the energy use.

In situations where indoor and outdoor sources not directly linked to human presence is important for the air quality, and especially if indoor chemical reactions are important, the control issue becomes more complex. Further development of control algorithms taking enthalpy and a wider range of chemical and in particular pollutants into account may expand the cost-effective potential use of DCV further.

4.2 Ventilation-based heating and cooling

With well-insulated and energy efficient buildings, premises are suitable for ventilation-based heating. Only isotherm or slightly over-tempered supply air is necessary during workhours, which is proven to give satisfied users and acceptable physical conditions upon certain premises. The solution is documented for energy efficient office buildings but is a relevant solution also for office-related areas in other buildings and well insulated existing buildings. Key premises are heating demand and documented characteristics of the inlet valve.

Ventilation-based heating for residential buildings are closely studied for European conditions, but still need further research in cold climates. Low ventilation rates together with low relative humidity in winter, makes this solution more challenging for this kind of buildings. With a standard one-ventilation using a single air supply temperature, the temperature in bedrooms would be higher and could further increase the risk of window opening.

Ventilation-based cooling is very promising for offices and shopping centres, as these typically have high cooling demands. For the other building categories, it is evaluated to only

have a minor impact. The use of ventilation-based cooling is expected to both improve energy efficiency and thermal comfort for the users. User satisfaction is also expected to increase through products enabling individual demand-control. Full-scale field measurements are however required to verify that the concept for commercial use.

4.3 Simplified hydronic heating

Simplified space-heating distribution has been investigated in the context of highly-insulated residential buildings. The configuration of the heating and ventilation considered in these researches is the most representative of Norwegian passive houses: a centralized balanced mechanical ventilation with a single air supply temperature for all the rooms (so-called one-zone ventilation) and using a cascade flow while, in the case of radiator heating, one heat emitter is placed for each floor. Previous research works have documented and explained the temperature distribution inside the building generated by the simplified space-heating distribution, both in terms of temperature differences between rooms but also in the temperature distribution inside the room equipped with the heat emitter. The main conclusions from these studies show that indoor thermal environment of living areas is experienced as comfortable by occupants. The most critical part is related to the thermal comfort in bedrooms. Many Norwegians would like cold bedrooms, at least during night-time (in the range of 14-18°C), and it has been shown that a large fraction of the occupants in such highly-insulated buildings opens the bedroom window during several hours per day (in winter time) to control the bedroom temperature.

It has been argued that water-borne heat in floors gives a slow-reacting heating system and is therefore difficult to regulate, especially if the heating pipes are cast in concrete. A "slower" system can more easily cause problems with over/under temperature. Various heating solutions have been chosen. On average, the two projects with water-borne heat in the floor have 1.7 ° C higher indoor temperature than the other houses.

4.4 Smart energy control

A smart Building Energy Management System (BEMS) has typically different functionalities, providing integrated solutions that includes monitoring and management of differing systems of the building to other correlated services, like heating and lighting. A smart BEMS facilitates the integration of sensors, systems and subsystems that are able to collect complete information and make it available to the management team and to all the participants involved in the construction, restructuring and maintenance of the building.

The smart BEMS enables communication between different systems to improve the performance, while an ICT system facilitates the process and allows this interaction, in addition to the collecting of completed data. The architecture of a smart BEMS allows to centralize and put into communication all the systems and subsystems, in particular: lighting and management of natural light; heat and air-conditioning; solar panels; food refrigeration; hydrogen and electric batteries and if needed the recharging of electric cars.

4.5 Responsive lighting equipment

Lighting equipment uses electricity and provides internal heat gain. The efficiency of the lighting equipment describes the amounts of illuminance, electricity use and internal heat gains. New equipment for lighting is, therefore, an important component as it determines the responsiveness. The exploitation of daylight to cover portions of illuminance should be the

first step. The responsive control of the lighting equipment can then be used to provide the additional illuminance to the indoor spaces. The use of lighting equipment includes the light source and the luminaire that distributes the illuminance. The use of electricity needs to be monitored and provides input to dynamic energy balance calculations at each timestep and thus determine the need for heating and cooling. This is important for all building types but more prominent in buildings with high required or wanted illuminance levels.

LED is developing and provides now efficacies comparable to T5 lamps. Appropriate luminaires are needed that distribute light in the indoor space according to a specific use. LED provide opportunities to not only control the electricity use (on/off) and dimming, but also light quality (e.g. light colour). This should be used to plan and size the lighting equipment according to specific needs before heating and cooling equipment is dimensioned.

4.6 Utilizing surplus energy sources

There are already multiple buildings in Norway utilizing surplus heat from various cooling processes. Examples of heat sources are refrigeration systems in grocery stores as presented in chapter 5 and cooling of computer servers, which is expected to be an increasingly relevant source of surplus energy. Available surplus thermal energy (heat) should always be utilized, either directly through heat recovery or as a heat source for heat pump systems. It is important to identify the thermal needs, as well as temperature requirements, for space heating and cooling, heating of ventilation air, heating of DHW and process cooling. This should be taken into account before sizing heating and cooling systems. The surplus energy can either be used within the same building or at neighbouring buildings. The principle of utilizing surplus energy is transferable to all building categories, either through export or import of heat. A good match between the source of surplus energy and the heat load is however important. Duration curves is a good tool for designing heating and cooling systems and to visualize the potential of utilizing surplus heat sources.

Storage of surplus energy is also an option if there is poor matching between the thermal loads. Short term storage through water accumulation tanks, the thermal mass of the building and phase-changing materials (PCM) as well as borehole systems for seasonal storage may all be relevant. Such solutions will also moderate heating and cooling power demands but may increase the energy use through additional heat loss.

Loads for cooling and freezing food, process cooling and computer/telecom cooling are relatively constant throughout the year and are thus considered to be very good and reliable sources for surplus heat. Process cooling is typically found in industrial buildings, while computer/telecom cooling may be relevant for office buildings or educational buildings with server rooms etc. As space cooling of buildings usually is only necessary for short periods of the year, it is not a suitable source for heat recovery, except for "charging" boreholes for ground source heat pumps through free cooling. Recovered heat should also be used for a load that is relatively stable throughout the year, such as preheating of domestic hot water.

Zero emission neighbourhoods will have better conditions for utilizing surplus heat than single buildings, as a neighbourhood have a larger variety of loads (through different building categories) and thus more possibilities for exchange of thermal and electric energy.

Table 2: Overview of technical solutions and their suitability for different building categories.

Building category / Technical solution	***New offices***	***Renovated offices***	***Educational buildings***	***Kinder-gartens***	***Residential buildings***	***Grocery stores***	***Shopping centres***
Demand-controlled ventilation	+++	+++	+++	+++	++	0	0
Simplified hydronic heating	+++	0	0	0	+++	0	0
Ventilation-based heating	+++	++	0	0	+	0	0
Ventilation-based cooling	+++	+++	+	+	+	+	+++
Responsive lighting equipment (LED)	++	+++	+++	+++	++	+++	+++
Smart energy control (BEMS)	+++	+++	+++	+++	++	++	++
Utilizing import surplus energy sources export*	+++	+++	+++	+++	+++	+++	+++
	++	++	++	+	+	+++	++

Technologies are considered to be a promising solution (+++), possibly promising solution (++) or just might have a minor impact (+). Building categories where the technical solutions have not been evaluated are marked (0). This provides an overview of the different technologies and their suitability in the different building types.

5 CONCLUSIONS

For successful implementation of *demand-controlled ventilation*, it is important to focus on planning with the correct air volumes and the appropriate ventilation strategies. The technology is most suitable for offices, educational buildings and kindergartens, but could also be considered for other building categories with variable ventilation demands.

Regarding *simplified hydronic heating*, the main conclusions from studies on residential buildings show that the indoor thermal environment of living areas is experienced as comfortable by occupants. It is therefore recommended for residential buildings, while further research is required for other building types.

Ventilation-based heating is very promising for highly insulated buildings, but it has currently only been evaluated for office buildings. For residential buildings, however, if a traditional one-zone ventilation strategy is applied, air heating using ventilation is not a robust option as it will generate relatively higher bedroom temperatures. This may further increase the risk of window opening during wintertime. If the configuration of the ventilation system is not adapted, this approach is unlikely to be a good option, either for the building occupants or the building industry. Dry air during the heating season and periodically low relative humidity in indoor air is a general problem occurring in all new buildings with balanced mechanical ventilation system. This problem occurs independent on whether ventilation-based heating is used, but the problem increases for residential buildings, as they require higher supply air temperature due to low airflow rates. One possible solution for increasing the relative humidity in indoor air is to lower the air exchange during particularly cold periods. Such a reduction of the air exchange can also reduce energy consumption for heating ventilation air during cold periods.

Ventilation-based cooling is gaining more importance in buildings with high internal gains, such as offices and shopping centres. The potential for energy savings is very high in Nordic

countries due to favourable climatic conditions. More focus should be put on utilizing this technology in educational buildings, kindergartens, dwellings and grocery stores.

Responsive lighting equipment (LED) is an important part of low energy buildings. New technology developments of luminaires and control strategies can minimize energy use and maximize IEQ by full exploitation of the daylight availability (responsiveness).

Smart energy control (BEMS) play an important role in making use of the promising potential of many technologies. Integrated control of IEQ parameters can fully exploit this potential. Some building types have less focus on advanced control systems and further cost reductions are needed.

Available *surplus energy* should always be *utilized*, and the principle of utilizing surplus heat is transferable to all building categories, either through export or import of heat. While all building categories are suitable for importing surplus heat, the potential for export depends on the specific heat loads of both the building and the neighbouring buildings. Residential buildings and kindergartens usually do not have process cooling or other loads suitable for export.

When assessing energy performance, comfort quality and economic feasibility of low energy building services, a comprehensive approach is needed.

6 ACKNOWLEDGEMENTS

This report has been written within the Research Centre on Zero Emission Neighbourhoods in Smart Cities (FME ZEN). The authors gratefully acknowledge the support from the Research Council of Norway and from all partners.

7 REFERENCES

Aaberg, M. G. (2018). *Analysis of the Thermal Energy System at Kiwi Dalgård*. Department of Energy and Process Engineering. NTNU,.

Alfstad, L. C. M. (2018). *Analyse av termisk energiforsyning ved Otto Nielsens vei 12E.* (Master), NTNU,

Ampenberger, A. (2017). *Daylight strategies*. Retrieved from http://commonenergyproject.eu/uploads/deliverable/file/12/WP3_D3.7_20170131_P09_Daylight_strategies.pdf

Antolin, J., Macia, A., Samaniego, J., Luis Ángel, B., Barchi, G., Belleri, A., . . . Haase, M. (2017). *Energy savings results*. Retrieved from http://commonenergyproject.eu/uploads/deliverable/file/35/WP6_D6.4_20171010_P04_Energy_savings_results.pdf

Antolin, J., Quijano, A., Samaniego, J., Luis Ángel, B., Noris, F., Haase, M., . . . Green, B. (2015). *Interaction with local energy grid*. Retrieved from http://commonenergyproject.eu/uploads/deliverable/file/4/WP2_D2.4_20150430_P04_Interaction_with_local_energy_grid_NotPrintable.pdf

Avantaggiato, M., Barchi, G., Belleri, A., Dipasquale, C., Lollini, R., Wilmer, P., . . . Gantner, J. (2017). *Guidelines on how to approach the energy-efficient retrofitting of shopping centres*. Retrieved from http://hdl.handle.net/11250/2484215

Belleri, A., & Avantaggiato, M. (2017). *Ventilative Cooling*. Retrieved from http://commonenergyproject.eu/uploads/deliverable/file/8/WP3_D3.3_20170109_P01_Ventilative_cooling.pdf

Belleri, A., Haase, M., Papantoniou, S., & Lollini, R. (2017). Delivery and performance of a ventilative cooling strategy: the demonstration case of a shopping centre in Trondheim, Norway. In *Ventilating healthy low-energy buildings* (pp. 220-229): Air Infiltration and Ventilation Centre (AIVC).

Berge, M. (2016). *Indoor climate quality in high-performance dwellings : an exploration of measured, perceived and desired conditions.* (2016:354), Norwegian University of Science and Technology, Faculty of Architecture and Fine Art, Department of Architectural Design, History and Technology, Trondheim.

Berge, M., Georges, L., & Mathisen, H. M. (2016). On the oversupply of heat to bedrooms during winter in highly insulated dwellings with heat recovery ventilation. *Building and Environment, 106*, 389-401.

Berge, M., & Mathisen, H. M. (2016). Perceived and measured indoor climate conditions in high-performance residential buildings. *Energy and Buildings, 127*, 1057-1073.

Berge, M., Thomsen, J., & Mathisen, H. M. (2016). The need for temperature zoning in high-performance residential buildings. *Journal of Housing and the Built Environment*, 1-20. doi:10.1007/s10901-016-9509-2

Bluyssen, P. M., & Fanger, P. O. (1991). Addition of Olfs from Different Pollution Sources, determined by a Trained Panel. *Indoor Air, 1*(4), 414-421. doi:10.1111/j.1600-0668.1991.00005.x

Bointner, R., Toleikyte, A., Woods, R., Atanasiu, B., De Ferrari, A., Farinea, C., & Noris, F. (2014). *Shopping malls features in EU-28 + Norway*. Retrieved from http://commonenergyproject.eu/uploads/deliverable/file/1/WP2_D2.1_20141130_P05_Shopping_malls_features_in_EU-28_and_Norway_NP.pdf

Bukat, M., Niewczas, T., Kozioł, Ł., Łazowski, J., & de Ferrari, A. (2015). *Green integration*. Retrieved from http://commonenergyproject.eu/uploads/deliverable/file/10/WP3_D3.5_20161129_Green_integration.pdf

Bøhn, T. I., Søreng, L.-H., Holljen, E., Dehlin, F., & Grini, C. (2014). *Analyse av energibruk i forretningsbygg - Formålsdeling, trender og drivere*. Retrieved from

Daldosso, N., Gentile, E., Mangili, S., & Papantoniou, S. (2017). *ITC platform*. Retrieved from http://commonenergyproject.eu/uploads/deliverable/file/17/WP4_D4.4_20170131_P06_ICT_platform_systems.pdf

Dipasquale, C., Belleri, A., & Lollini, R. (2016). *Integrative Modelling Environment* Retrieved from http://commonenergyproject.eu/uploads/deliverable/file/15/WP4_D4_1_20161124_P01_Integrative_Modelling_Environment_FINAL_v9.pdf

Edvardsen, K. I. (2014). *Trehus* ([10. utg.]. ed. Vol. 5). Oslo: SINTEF akademisk forl.

Emerson Climate Technologies. (2014). *Commercial CO2 Refrigeration Systems - Guide for Subcritical and Transcritical CO2 Applications*. Retrieved from 744.com: http://www.r744.com/files/675_commercial_co2_guide.pdf

Enovarapport. (2003). Trondheim: Enova.

Federico Visconti, Maurizio Orlandi, & Saro, O. (2015). *Thermal zone optimization*. Retrieved from http://commonenergyproject.eu/uploads/deliverable/file/7/WP3_D3.2_20151126_P12_P17_Thermal_zone_optimization_CO.pdf

Feist, W., Schnieders, J., Dorer, V., & Haas, A. (2005). Re-inventing air heating: convenient and comfortable within the frame of the Passive house concept. *Energy and Buildings, 37*, 1186-1203.

Foster, A. M., & Quarini, G. L. (2001). Using advanced modelling techniques to reduce the cold spillage from retail display cabinets into supermarket stores to maintain customer comfort. *Proceedings of the Institution of Mechanical Engineers, Part E: Journal of Process Mechanical Engineering, 215*(1), 29-38. doi:10.1243/0954408011530271

Fricke, B. A., & Becker, B. R. (2010). Doored display cases: they save energy, don't lose sales.(Report). *ASHRAE Journal, 52*(9), 18.

Froehlich, B., & Ampenberger, A. (2017). *Prototypes of combined daylight system*. Retrieved from http://commonenergyproject.eu/uploads/deliverable/file/13/WP3_D3.8_20170131_P09_Prototype_of_combined_daylight_system.pdf

Galvin, R. (2016). *The rebound effect in home heating : a guide for policymakers & practitioners*. In BRI Book Series

Building Research and Information.

Georges, L., Alonso, M. J., Woods, R., Wen, K., Håheim, F., Peng, L., . . . Thalfeldt, M. (2017). *Evaluation of Simplified Space-Heating Hydronic Distribution for Norwegian Passive Houses*. Retrieved from http://hdl.handle.net/11250/2462461

Georges, L., Berner, M., & Mathisen, H. M. (2014). Air heating of passive houses in cold climate: investigation using detailed dynamic simulations. *Building and Environment, 74*, 1-12.

Georges, L., Håheim, F., & Alonso, M. J. (2017). Simplified Space-Heating Distribution using Radiators in Super-Insulated Terraced Houses. *Energy Procedia, 132*, 604-609. doi:https://doi.org/10.1016/j.egypro.2017.09.677

Georges, L., & Skreiberg, Ø. (2016). Simple modelling procedure for the indoor thermal environment of highly insulated buildings heated by wood stoves. *Journal of Building Performance Simulation, 9*(6), 663-679.

Georges, L., Skreiberg, Ø., & Novakovic, V. (2013). On the proper integration of wood stoves in passive houses: investigation using detailed dynamic simulations. *Energy and Buildings, 59*, 203-213. doi:10.1016/j.enbuild.2012.12.034

Georges, L., Skreiberg, Ø., & Novakovic, V. (2014). On the proper integration of wood stoves in passive houses under cold climates. *Energy and Buildings, 72*, 87-95.

Georges, L., Thalfeldt, M., Skreiberg, Ø., & Fornari, W. (2019). Validation of a transient zonal model to predict the detailed indoor thermal environment: Case of electric radiators and wood stoves. *Building and Environment, 149*, 169-181. doi:https://doi.org/10.1016/j.buildenv.2018.12.020

Georges, L., Wen, K., Alonso, M. J., Berge, M., & Thomsen, J. (2016). *Simplified Space-Heating Distribution using Radiators in Super-Insulated Apartment Buildings*. Paper presented at the SBE16 Tallinn and Helsinki Conference: Build Green and Renovate Deep, Tallinn and Helsinki.

Georges, L., Wen, K., Alonso, M. J., Berge, M., Thomsen, J., & Wang, R. (2016). Simplified space-heating distribution using radiators in super-insulated apartment buildings. *Energy Procedia, 96*, 455-466. doi:doi: 10.1016/j.egypro.2016.09.177

Gram-Hanssen, K. (2010). Residential heat comfort practices: understanding users. *Building Research & Information, 38*(2), 175-186. doi:10.1080/09613210903541527

Haase, M. (2016). *Renewable energy supply potential of shopping centres*. Paper presented at the International Conference on Energy, Environment and Economics -ICEEE2016, Edinburgh. Konferanse retrieved from

Haase, M., & Ampenberger, A. (2017a). Implications of Increasing Daylighting in Deep Energy Retrofitting in Norwegian Shopping Centres. In *Building Simulation Applications. BSA 2017*: International Building Performance Simulation Association (IBPSA).

Haase, M., & Ampenberger, A. (2017b). The role of lighting in deep energy retrofitting in European shopping malls. In *Proceedings of the eceee Summer Study. Consumption, efficiency & limits. 29 May - 3 June 2017 Toulon/Hyeres, France* (pp. 1013-1018): European Council for an Energy Efficient Economy (ECEEE).

Haase, M., Antolin, J., & Belleri, A. (2016). Interactions of retrofitted shopping centres with local energy grids. In *9th International Conference Improving Energy Efficiency in Commercial Buildings and Smart Communities. IEECB&SC'16* (pp. 475-486): European Union.

Haase, M., & Skeie, K. S. (2013). Energy efficient commercial building refurbishment in Nordic climate. In *Proceedings of CLIMA 2013* (pp. 6882): Society of Environmental Engineering (STP), REHVA member association.

Haase, M., & Skeie, K. S. (2015). Development of protocol for sub-metering for simulation models of shopping centres. In *CISBAT 2015 - FUTURE BUILDINGS & DISTRICTS SUSTAINABILITY FROM NANO TO URBAN SCALE PROCEEDINGS VOL. II* (pp. 809-814): Ecole Polytechnique Fédérale de Lausanne (EPFL).

Haase, M., Skeie, K. S., Antolin, J., Quijano, A., Sanmaniego, J., Bujedo, L. Á., . . . Belleri, A. (2016). Interactions of shopping centres with local energy grids. *NewDist - NEWSLET TER SEMESTRALE DEL DIPARTIMENTO INTERATENEO DI SCIENZE, PROGET TO E POLITICHE DEL TERRITORIO POLITECNICO E UNIVERSITA' DI TORINO*, 144-153.

Haase, M., Skeie, K. S., Belleri, A., & Dipasquale, C. (2015). Modelling of complex shopping mall in Norway. In *Proceedings of Building Simulation 2015, The 14th International Conference of IBPSA* (pp. 2264-2270): International Building Performance Simulation Association (IBPSA).

Haase, M., Skeie, K. S., & Woods, R. (2015). The key drivers for energy retrofitting of European shopping centres. *Energy Procedia, 78*, 2298-2303. doi:http://dx.doi.org10.1016/j.egypro.2015.11.368

Haase, M., Woods, R., & Skeie, K. S. (2014). Capacities in shopping malls to supply grid services. In *Proceedings of the 20th Annual International Sustainable Development Research Conference (ISDRC 2014)*: Norwegian University of Science and Technology, Department of Product Design.

Halvarsson, J. (2012). *Occupancy Pattern in Office Buildings: Consequences for HVAC system design and operation.* (Doctoral thesis), Norwegian University of Science and Technology (NTNU),

Haukås, H. T. (2016). *Kompendium CO2 (R744) som kuldemedium*: Norsk Kjøleteknisk Forening.

Heiselberg, P. (2017). *Ventilative Cooling - State-of-the-art Review Executive Summary* (ISBN 2-930471-47-6). Retrieved from https://venticool.eu/wp-content/uploads/2012/09/SOTAR-summary.pdf

Holand, N., Yang, A., Holøs, S. B., Thunshelle, K., & Mysen, M. (2019). Should we differentiate ventilation requirements for different user groups? In *Cold Climate HVAC 2018 - Sustainable Buildings in Cold Climates* (pp. 10): Springer.

Jones, N. (2018). How to stop data centres from gobbling up the world's electricity. *Nature, 561*, 163-166. doi:10.1038/d41586-018-06610-y

Karmakar, A., Das, S., & Ghosh, A. (2016). Energy Efficient Lighting by Using LED Vs. T5 Technology. *IOSR Journal of Electrical and Electronics Engineering (IOSR-JEEE), 11*(2 Ver 1 (Mar.-Apr. 2016)), 47-48. doi:10.9790/1676-1102014748

KIWI. (2017). I dag åpnet KIWIs nye miljøbutikk i Trondheim. Retrieved from https://kiwi.no/Tema/samfunnsansvar/Miljo-og-barekraft/i-dag-apnet-kiwis-nye-miljobutikk-i-trondheim/

Kragh, J. (2016). *Varmeforbrug i nye bygninger opført i perioden 2010-2013*: Statens Byggeforskningsinstitut.

Larsen, T. S., Knudsen, H. N., Kanstrup, A. M., Christiansen, E. T., Gram-Hanssen, K., Mosgaard, M., . . . Rose, J. (2010). *Varmeforbrug i nye bygninger opført i perioden 2010-2013* (110). Retrieved from https://vbn.aau.dk/files/43839868/Occupants_Influence_on_the_Energy_Consumption_of_Danish_Domestic_Buildings.pdf

Lekang Sørensen, Å., Jiang, S., Nybakk Torsæter, B., & Völler, S. (2018). *Smart EV Charging Systems for Zero Emission Neighbourhoods - A state-of-the-art study for Norway*. Retrieved from

Madsen, V. H., & Gabrielsen, H.-C. (2016). *Veikart for grønn handel 2050*. Retrieved from

Mattilsynet. (2018). Trygg mat i butikken. Retrieved from http://www.matportalen.no/matsmitte_og_hygiene/tema/syk_av_maten/trygg_mat_i_butikken-1

Micro Matic. (2016). *Lær å forstå DALI lysstyring - Eliaden 2016*. Retrieved from https://www.micromatic.no/siteassets/3-proffsenter/mm-skolen/presentasjoner/Dali-Eliaden-Presentasjon-Micro-Matic

Midttømme, K. (2018). RockStore – develop, demonstrate and monitor the next generation BTES systems. Retrieved from https://www.researchgate.net/project/RockStore-develop-demonstrate-and-monitor-the-next-generation-BTES-systems

Mysen, M., Berntsen, S., Nafstad, P., & Schild, P. G. (2005). Occupancy density and benefits of demand-controlled ventilation in Norwegian primary schools. *Energy and Buildings, 37*(12), 1234-1240. doi:https://doi.org/10.1016/j.enbuild.2005.01.003

Mysen, M., & Schild, P. G. (2013). *Behovsstyrt ventilasjon, DCV – krav og overlevering*. Retrieved from

Mysen, M., & Schild, P. G. (2014). *Behovsstyrt ventilasjon, DCV – forutsetninger og utforming*. Retrieved from Oslo:

Mysen, M., Schild, P. G., & Cablé, A. (2014). *Demand-controlled ventilation – requirements and commissioning*. Retrieved from

Mæhlen, A. (2017). Picture of Kiwi Dalgård. In: Øystein Thommesen AS.

NVE. (2016). *Analyse av energibruk i yrkesbygg. Formålsdeling, trender og drivere*. Retrieved from http://publikasjoner.nve.no/rapport/2016/rapport2016_24.pdf

NVE. (2018). NVE legger opp til ny høring om nettleiestruktur [Press release]. Retrieved from https://www.nve.no/nytt-fra-nve/nyheter-reguleringsmyndigheten-for-energi/nve-legger-opp-til-ny-horing-om-nettleiestruktur/

Olsen, C. (2018). Norske forskere bak iskald miljøteknologi. Retrieved from https://gemini.no/2018/08/norske-forskere-bak-iskald-miljoteknologi/

Petersen, K., Vakkalanka, S., & Kuzniarz, L. (2015). Guidelines for conducting systematic mapping studies in software engineering: An update. *Information and Software Technology, 64*, 1-18. doi:10.1016/j.infsof.2015.03.007

Rozanska, M., Mata Gutierrez, F. J., Sanchez, R. C., Fernandez, G. M. V., Belleri, A., Pinotti, R., . . . Miori, G. (2017). *Concept of modular multifunctional facade*. Retrieved from http://commonenergyproject.eu/uploads/deliverable/file/9/WP3_D3.4_20171124_P03_Concept_of_modular_multifunctional_facade.pdf

Rønneseth, Ø. (2018). *Personal Heating and Cooling Devices: Increasing Users' Thermal Satisfaction*. Retrieved from FME ZEN: https://fmezen.no/wp-content/uploads/2018/06/ZEN-Report-no-4.pdf

Schieldrop, T. (2019). Lovende resultater fra Sval Vent-prosjektet. Retrieved from https://www.vvsaktuelt.no/lovende-resultater-fra-sval-vent-prosjektet-137904/nyhet.html

Selvnes, E. (2017). *Thermal zoning during winter in super-insulated residential buildings.* (Master thesis), Norwegian University of Science and Technology (NTNU), Trondheim.

Seppänen, O., Brelih, N., Goeders, G., & Litiu, A. (2012). *Existing buildings, building codes, ventilation standards and ventilation in Europe*. Retrieved from

Skeie, K., Lien, A. G., Svensson, A., & Andresen, I. (2016). *Kostnader for nye småhus til høyere energistandard* (8253615257). Retrieved from Oslo: https://www.sintefbok.no/book/index/1106/kostnader_for_nye_smaahus_til_hoeyere_energistandard

Solt, J., Aarts, M. P. J., Andersen, M., Appelt, S., Bodart, M., Kaempf, J., . . . Fournier, C. (2017). *Daylight in the built environment*.

Staggl, S., Reiter, K., & Ampenberger, A. (2017). *Visual emotional and energy effects of a new lighting concept*. Retrieved from http://commonenergyproject.eu/uploads/deliverable/file/20/WP4_D4.9_20170116_P09_Visual_emotional_and_energy_effects_of_a_new_lighting_concept.pdf

Standard Norge. (2017). SN/TS 3031:2016. Energy performance of buildings. Calculation of energy needs and energy supply. In (Vol. 2017). Standard Norge.
Stene, J. (2017). *Refrigerants for the heat pump process*. Retrieved from TEP 4260 Heat Pumps for Heating and Cooling of Buildings:
Stene, J., Justo Alonso, M., Rønneseth, Ø., & Georges, L. (2018). *State-of-the-Art Analysis of Nearly Zero Energy Buildings*. Retrieved from
Stiller, M. (2012). *Quality lighting for high performance buildings*. In.
Sundlisæter, E. M., Vadet, P., Østhagen, H. A., Garshol, P. K., Wangen, P. A., Holte, F., . . . Jensen, U. A. (2015). *BOK 1 Funksjonsbeskrivelse - Totalentreprise bygg (E1) og totalentreprise teknikk (E2)*. Retrieved from
Sweco. (2016). FREMTIDEN ER NÅ: BERGENS FØRSTE BREEAM EXCELLENT OG NÆR NULLENERGIBYGG. Retrieved from https://www.sweco.no/projects/sweco-bygget-i-bergen2/
Thomsen, J. (2017). EBLE – Evaluation of Buildings with a Low Energy Demand, 2015. In J. Thomsen (Ed.): NSD – Norwegian Centre for Research Data.
Thomsen, J., Gullbrekken, L., Grynning, S., & Holme, J. (2017). *Evaluering av boliger med lavt energibehov (EBLE) - samlerapport*. Retrieved from SINTEF akademisk forlag:
Thunshelle, K. (2016). *Oppvarming via tilluft. Veiledning og krav for næringsbygg med energiambisjoner*. Retrieved from
Vázquez, M. V. C., Belleri, A., Avantaggiato, M., Dipasquale, C., Gutierrez, J. A., Haase, M., & Skeie, K. (2017). *Systemic solution-sets* (D5.1). Retrieved from http://hdl.handle.net/11250/2484217
http://www.wiley.com/Corporate/Website/Objects/Products/0,9049,566289,00.html
Venås, B., Harsem, T. T., & Børresen, B. A. (2014). *CFD simulation of an office heated by a ceiling mounted diffuser*. Paper presented at the 35th AIVC conference, 4th TightVent Conference, 2nd Ventilcool Conference "Ventilation and airtightness in transforming the building stock to high performance", Poznan, Poland.
Walnum, H. T., & Fredriksen, E. (2018). *Thermal energy systems in ZEN. Review of technologies relevant for ZEN pilots*. Retrieved from FME ZEN: https://fmezen.no/wp-content/uploads/2018/06/ZEN-Report-no-3.pdf
Wargocki, P., Fanger, P. O., Krupicz, P., & Szczecinski, A. (2004). Sensory pollution loads in six office buildings and a department store. *Energy and Buildings, 36*(10), 995-1001. doi:10.1016/j.enbuild.2004.06.006
Weschler, C. J. (2011). Chemistry in indoor environments: 20 years of research. *Indoor Air, 21*(3), 205-218. doi:10.1111/j.1600-0668.2011.00713.x
Woods, R., Mellegård, S. E., Schlanbusch, R. D., Skeie, K., & Haase, M. (2015). *Shopping malls inefficiencies*. Retrieved from http://passivhus.dk/wp-content/uploads/7PHN_proceedings/010.pdf

Comparative life-cycle assessment of constant air volume, variable air volume and active climate beam systems for a Swedish office building

Nadeen Hassan[1], Saqib Javed[2]

[1] *Energy-efficient & Environmental Building Design, Lund University, SE-221 00 Lund, Sweden.*
nadeen.hassan.2458@student.lu.se

[2] *Building Services, Lund University, Box 118, SE-221 00 Lund, Sweden*
saqib.javed@hvac.lth.se

ABSTRACT

Energy use in buildings has a significant influence on the global energy demand and environmental impacts. Among all building systems, heating, ventilation, and air conditioning (HVAC) systems are the most energy-intensive in terms of their total energy requirements. The production and operation of HVAC systems have a significant impact on the environment. These systems are also among the largest consumers of natural resources and materials in the building sector. With an ever-increasing focus on energy and material use, the question remains, which HVAC system has a better environmental performance. This paper presents a comparison between the life cycle impacts of three different HVAC systems — Constant Air Volume (CAV), Variable Air Volume (VAV) and Active Climate Beams (ACB) — designed for a Swedish modern office building. The system boundary of the life cycle assessment is cradle-to-grave with options, over a 20-year period. The life cycle assessment (LCA) of the three systems has been performed using SimaPro software. The CML IA (baseline) method has been used for the impact assessment. The life cycle impacts have been weighted using the Dutch shadow cost method. The results show that from a life cycle perspective, the ACB and VAV systems have comparable environmental performance. The CAV system is shown to have the worst overall environmental performance. The manufacturing phase of the ACB system exhibits the highest environmental impacts among the three systems, reflecting its high use of copper. The operational phase is the main contributor to the environmental burden for all three systems.

KEYWORDS

Life cycle assessment; Energy; HVAC system; Environmental impacts; Impact assessment

1 INTRODUCTION

The built environment is a major contributor to green-house gas emissions (Khasreen, Banfill, & Menzies, 2009). Studies have shown that buildings, on a global level, are responsible for 30−40 % of the energy used and 40−50 % of the global carbon dioxide emissions (Zabalza, Aranda-Usón, & Scarpellini, 2009). In the European Union, the building sector is responsible for approximately 40 % of the total environmental burden (UNEP, 2003). As a result, the European commission has set targets to reduce green-house gases by at least 20 % by the year 2020, and by at least 40 % by the year 2030, compared to the 1990 emission levels (European Commission, 2019).

Among all systems in buildings, Heating, Ventilation, and Air Conditioning (HVAC) systems are by far most energy-intensive, accounting for approximately 50 % of the total energy consumed by buildings (Pérez-Lombard, Ortiz, & Pout, 2008). Nonetheless, HVAC systems are one of the essential building service elements in modern buildings (Chen, 2011). The number of these systems being installed has increased dramatically over the last few years (BSRIA, 2018; Coletti & Fano, 2008). This is mainly due to increasing requirements on thermal comfort and climate change. With an aim of reducing energy consumption during the

operational phase while providing good indoor air quality (IAQ), new HVAC systems, such as chilled beams, have been introduced (Chen, 2011). However, other life cycle phases of an HVAC system, including processing or manufacturing of materials, and installation and construction of components, among others, also consume large quantities of energy and generate significant environmental impacts. Moreover, the extraction of minerals, such as iron ore, aluminum and copper, all of which are commonly used in HVAC systems, causes a significant reduction in the planet's natural resources (Bribián et al., 2009).

Overall, increased awareness toward environmental issues has led societies to implement strict building codes and energy criteria (Sartori & Hestnes, 2007). Consequently, several standardized environmental assessment methods have been developed to provide building designers with better comprehension and estimation of a product's life cycle impact (Prek, 2004). Currently, LCA is one of the leading methodologies for facilitating more environmentally friendly decisions in the building sector. In this study, the environmental impacts of the life cycles of a Constant Air Volume (CAV) system, a Variable Air Volume (VAV) system, and an Active chilled beams (ACB) system have been evaluated and compared for a modern office building, in Sweden. Part of the aim of this work is to identify the major factors influencing the environmental impacts of each system, in addition to providing distinct evaluation and comparison of the three HVAC systems. The outcomes of this research would facilitate the future selection of the HVAC systems, and would also contribute to the development and improvement of the studied systems.

2 BUILDING DESCRIPTION

This study assesses three HVAC systems in a hypothetical modern office building assumed to be located in Malmö, Sweden. The building, shown in Figure 1, consists of three stories with a heated floor area of 1088 m^2. The building was previously used by Abugabbara et al. (2018) to compare the operational energy use of CAV, VAV, and ACB systems using the dynamic building energy simulation program TEKNOsim (Abugabbara and Javed, 2019; Javed et al., 2016). In the original work, the building was divided into six thermal zones and was assumed to have an occupancy pattern based on Halvarsson (2012). The U-value of the thermal envelope was set based on the Swedish building code (BBR) requirements (Boverkets byggregler, 2018). The indoor operative temperature was set to not exceed 22 °C in winter and 26 °C in summer. The building was assumed to have a set-back operative temperature of 18 °C in winter and 28 °C in summer. The calculated energy consumption for the three HVAC systems is shown in Figure 2.

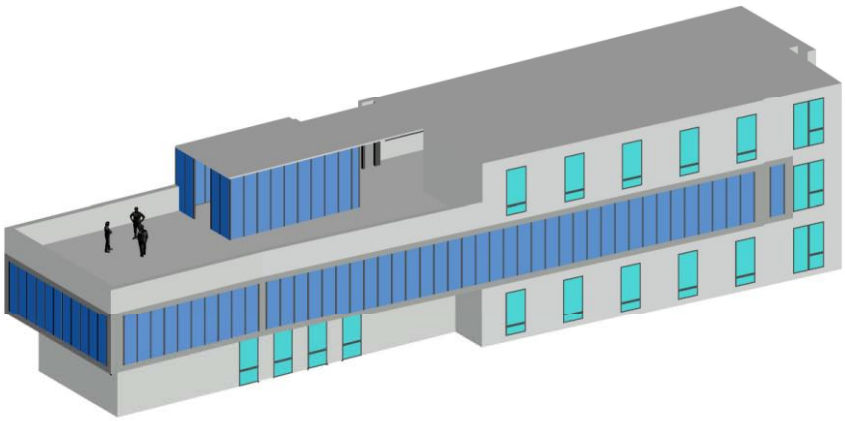

Figure 1: 3D building model (Abugabbara et al., 2018).

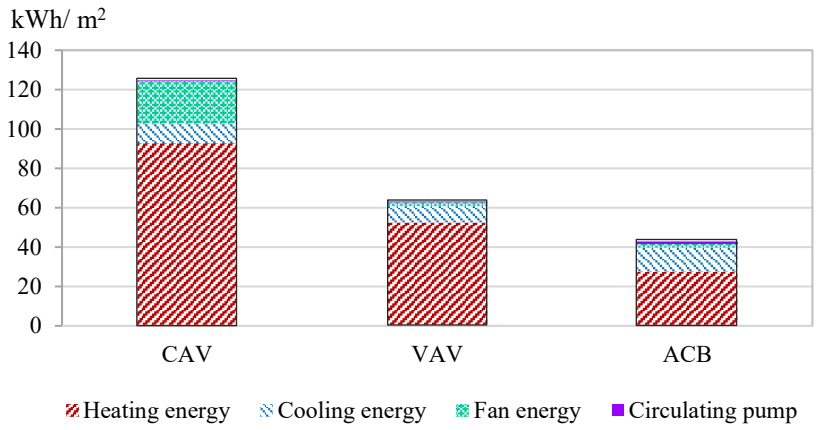

Figure 2: Annual energy consumption of three HVAC systems (Abugabbara et al., 2018).

3 LCA METHODOLOGY

3.1 Goal and scope

3.1.1 Functional unit

In this work, the function of the studied HVAC systems was to provide space heating and cooling for a modern office building in Sweden, while simultaneously maintaining the ventilation airflow requirements. Therefore, the functional unit was defined to be 20 years of heating and cooling to maintain an indoor temperature of 26°C and 22°C in summer and winter, respectively, while providing a minimum airflow of 0.35 l/s/m^2 and 7 l/s/person.

3.1.2 System boundary

The LCA study included all components of HVAC systems inside the building envelope, as shown in Figure 3. All purchased energy, both electrical and thermal, were also taken into account.

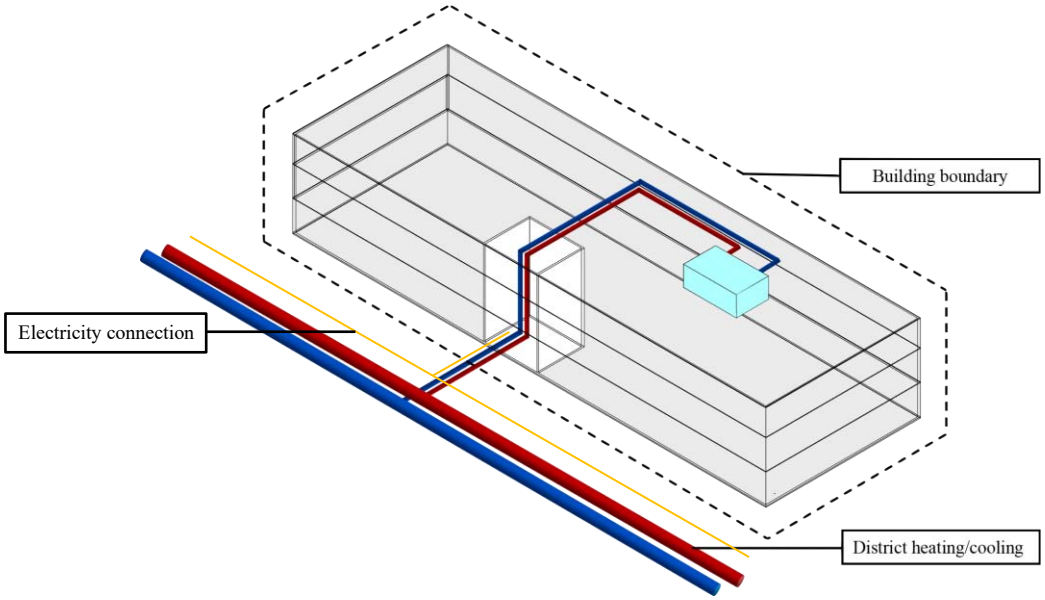

Figure 3: System boundary for material and energy flow.

The system boundary of the LCA study, shown in Figure 4, included extraction of raw materials, production of the materials, manufacturing of the components and usage during the operational phase. Available data form a commercial manufacturer (Lindab AB, 2019) was used for the evaluation of the manufacturing and operational phase of the HVAC components. The annual electricity of operation was also included.

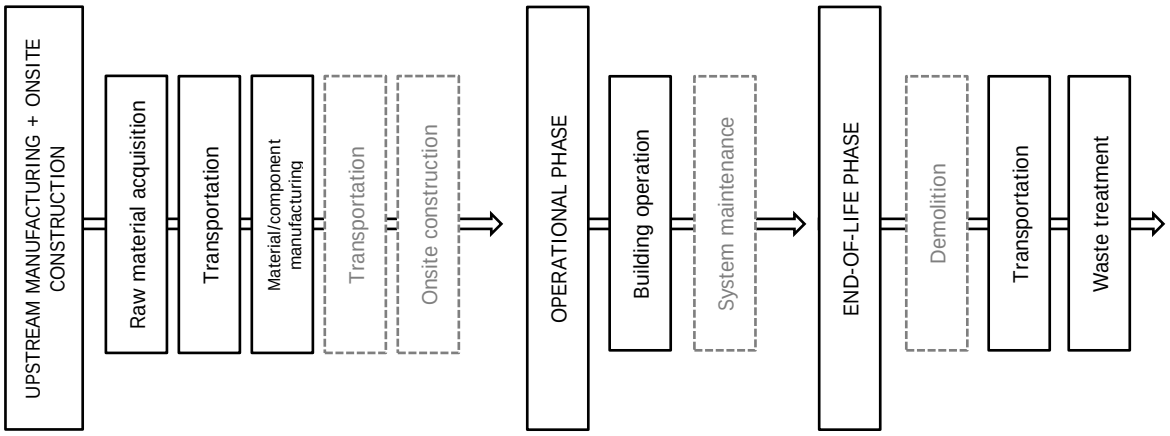

Figure 4: System boundary for LCA.

Energy needed for the waste treatment and recycling of materials was considered. Transportation to the waste treatment and recycling facilities was also taken into account. However, the phases shown in dashed boxes, including the demolition phase, maintenance phase and the transportation to the construction site were not included due to lack of data. Hence, the system boundary was set to be cradle to grave with options.

3.2 Inventory analysis

Ecoinvent v3 (2019) database, established by the Swiss Centre for Life Cycle Inventories, was used as the inventory data source (Martínez-Rocamora et al., 2016). Pre-defined materials and processes were used from the database. To provide a fair comparison between materials and to represent the worst-case scenario, market data from Ecoinvent 3 database was used for the processing of the materials. Market data includes averaged data from Europe, Asia, Africa, etc. The data accounts for the environmental impacts associated with extraction of raw materials, transport to production site, and energy used for production, among others (Lindvall, 2018).

3.2.1 Materials

Initially, a bill of quantity (BOQ) of all components of the three systems analyzed was obtained from the manufacturer of the HVAC systems. The material content for each component, along with the weight of each HVAC component, was obtained through the building product declarations (BPD) (Lindab AB, 2019). Materials that were stated to make up less than 1 % of a component and their percentages were not specified were not taken into account. Materials making up components that were not included in the BOQ such as pipes and pumps were obtained through Environmental Product Declarations (EPD) or were set according to pre-defined data found in the Ecoinvent database. Materials making up each system can be seen in Figure 5.

Recycling, incineration of waste and landfill rates were set based on estimated Swedish rates (FTI AB, 2018). Ninety-nine percent of the material scrap that could not be recycled was assumed to be incinerated while the remaining one percent was assumed to be landfilled.

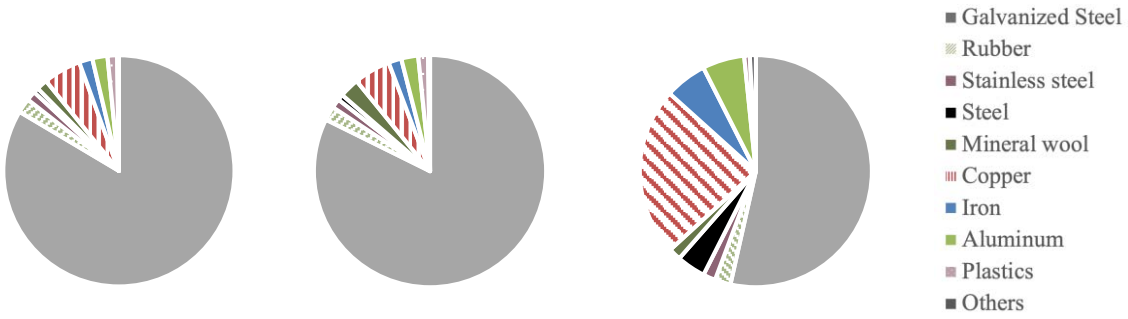

Figure 5: Materials making up the HVAC systems in the following order: CAV, VAV and ACB.

3.2.2 Energy

The electricity used by the HVAC components during the manufacturing and operational phase was set based on Swedish electricity mix from Ecoinvent database (Ecoinvent v3, 2019). Energy used for heating was set based on different energy types used in Sweden's district heating system, shown in Figure 6. Energy used for cooling was set based on district cooling produced by mechanical chillers at a seasonal COP of 3.

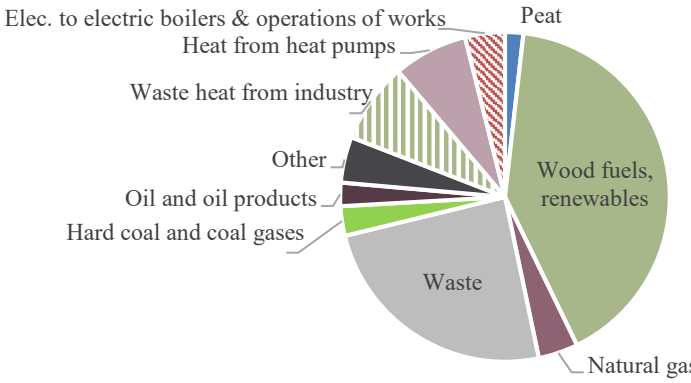

Figure 6: Total energy input for Sweden's district heating (SCB, 2017).

3.3 Life cycle impact assessment

The LCA study was conducted using SimaPRO, an LCA software developed and distributed by PRé Sustainability Consultants (Hollerud, Bowyer, Howe, Pepke, & Fernholz, 2017). Ecoinvent 3 database (Ecoinvent v3, 2019) was used as the inventory database in SimaPRO. The LCA system model chosen was Allocation at point of substitution (ASOP), which is based on the attributional approach. CML IA (baseline), an LCIA methodology developed at the University of Leiden in the Netherlands in 2001, was used to assess the potential environmental impacts of each system (Van Oers, 2012; Acero, Rodríguez, & Ciroth, 2014). The CML-IA (baseline) is a midpoint-oriented method that includes the characterization factors for all baseline characterization methods mentioned in the Handbook of LCA (ILCD, 2010). The results were normalized based on the EU 25+ 3 2000 reference values provided by CML IA (baseline) method and weighted based on the shadow cost method (Van Oers, 2012: De Bruyn et. al., 2010; de Klijn-Chevalerias and Javed, 2017). For this study, the environmental impacts of the three systems were first compared for each life cycle phase. Then, the total environmental impacts and shadow cost associated with the whole life cycle of the systems were compared.

3.4 Assumptions

The lifespan of the three HVAC systems was taken as 20 years. The generation of electricity, used for manufacturing and processing, operational phase of the building, and for all other activities, was based on Swedish electricity mix. The building was considered to be connected to district heating and cooling systems. The maintenance of the three HVAC system was assumed to be similar. It was assumed that the efficiency of the HVAC systems would remain the same throughout the life span of the systems. The annual energy use and emissions were assumed constant throughout the lifecycle of the systems. This means that the techno-sphere was assumed to have no changes throughout the period evaluated. Assumptions made for the waste treatment and transportation phases were based on Sweden's recycling rate and on the average data obtained from the Ecoinvent database, respectively.

4 RESULTS

The environmental impacts of the life cycle of the CAV, VAV and the ACB systems are presented in Figure 7. It can be observed that the operational phase is the dominant contributor to the total environmental impacts of the CAV and the VAV systems. However, for Abiotic depletion potential, it can be observed that the manufacturing phases of all three systems contribute more to the indicator than the operational phase. Furthermore, recycling and waste treatment phase are shown to reduce the environmental impacts of the systems.

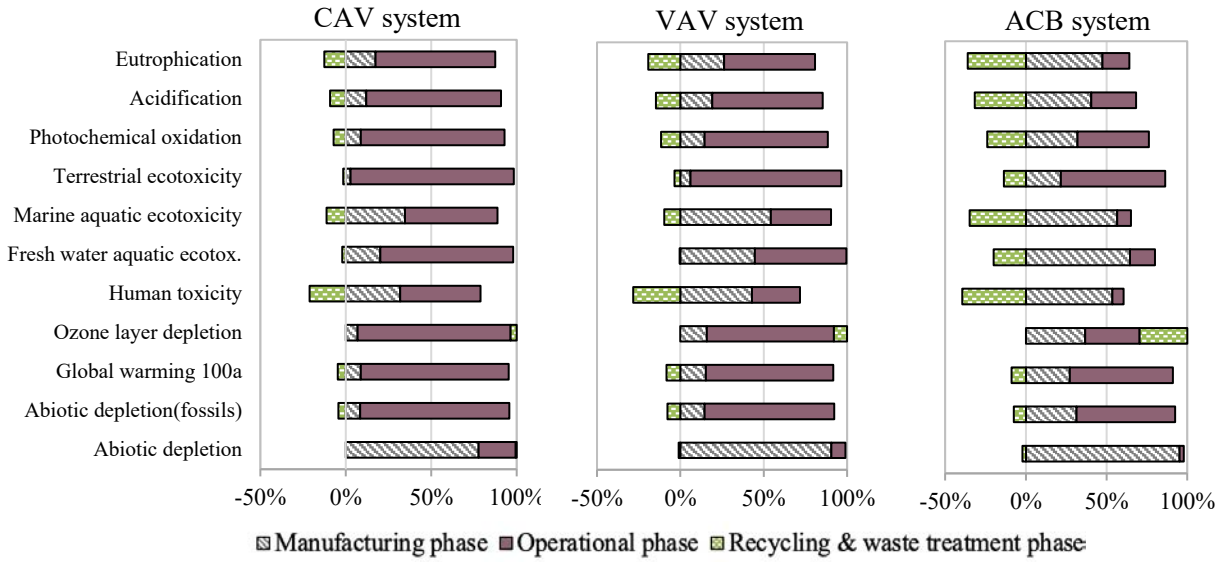

Figure 7: Environmental impacts of CAV, VAV and ACB system.

Unlike the CAV and the VAV systems, the manufacturing phase of the ACB system contributes to the majority of the environmental impacts. As earlier, the recycling and waste treatment phase mitigates the environmental impacts of the ACB system too.

The relative differences between the environmental impacts from the manufacturing and recycling phases of the CAV, VAV and ACB systems are presented in Figure 8. The manufacturing phase of the ACB system has the highest environmental impacts among all three systems, whereas the manufacturing phase of the CAV system has the lowest impacts. It can

also be observed that relative difference between the environmental impacts of the CAV and the VAV systems for all indicators is quite small.

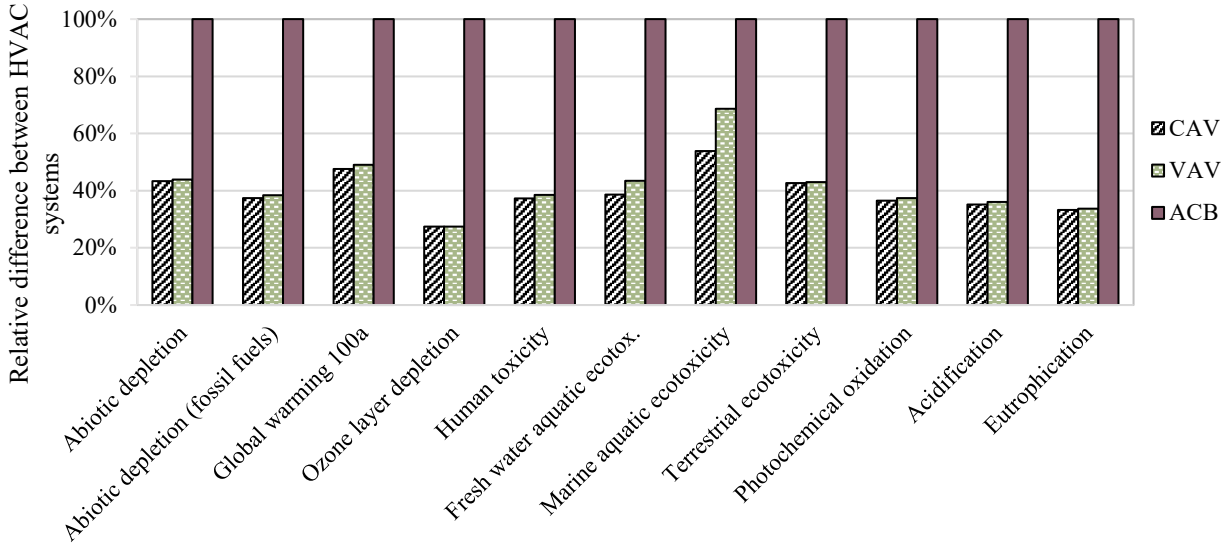

Figure 8: Relative difference between the environmental impacts of the manufacturing & recycling phases of CAV, VAV, and ACB systems.

Figure 9 presents the relative differences between the environmental impacts of the operational phase of CAV, VAV, and ACB systems over 20 years. The results shown in the figure indicate that the operational phase of the ACB system has the lowest environmental impacts among the three systems, whereas the CAV system has the highest impacts.

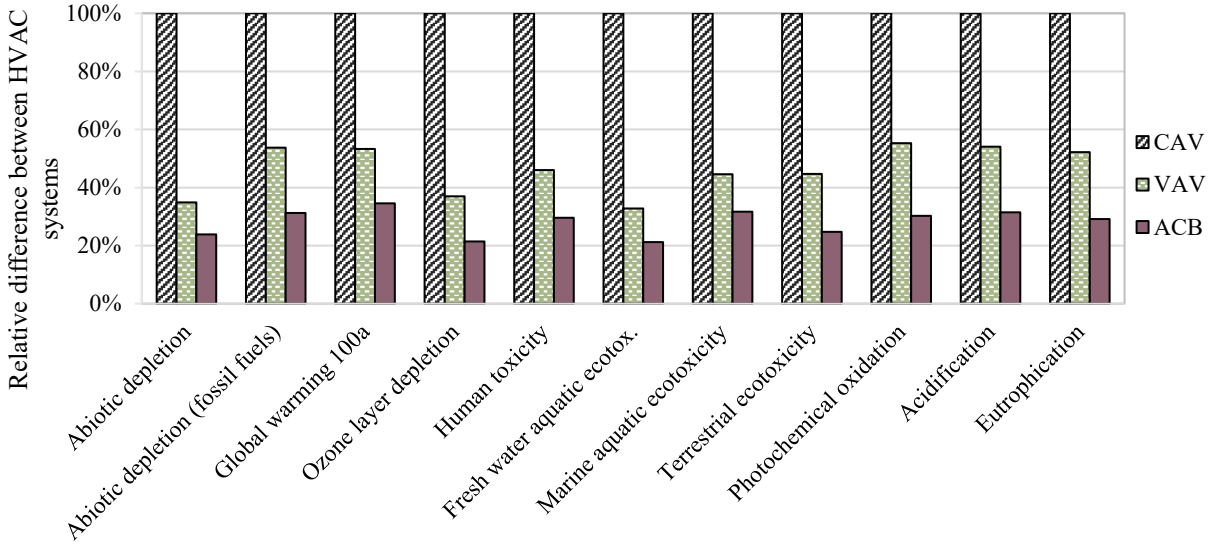

Figure 9: Relative difference between the environmental impacts of the operational phase of CAV, VAV, and ACB systems over 20 years.

Figure 10 presents the relative differences between the lifecycle impacts of CAV, VAV, and the ACB systems. It can be observed that the relative differences between the lifecycle impacts of the three systems vary depending on the environmental indicators. Nevertheless, the CAV system has the highest environmental impacts for all indicators except abiotic depletion of natural elements, for which the ACB system has the highest environmental impact.

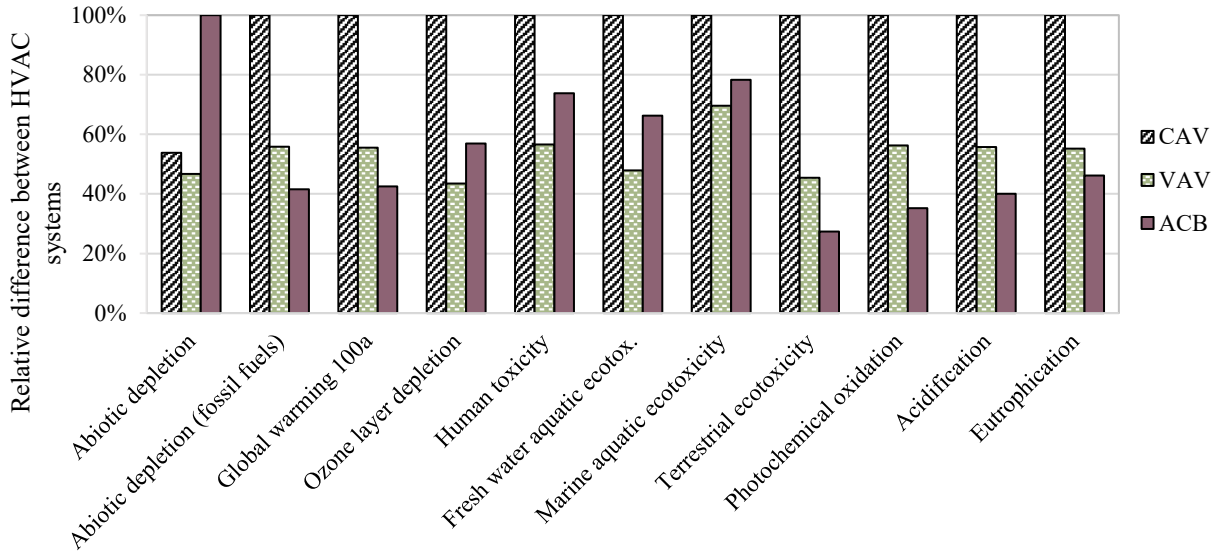

Figure 10: Relative difference between the environmental impacts of the life cycle of CAV, VAV, and ACB systems.

Figure 11 shows the total shadow cost for each of the three systems by aggregating scores of all individual environmental indicators into a single score. The shadow cost for each system has been calculated using a weighting factor, or more specifically, by assigning a unit cost to each environmental indicator. The Dutch weighting factors have been used for this study. It can be seen from the figure that the CAV system has the highest shadow cost among all three systems. Compared to the CAV system, the VAV and ACB systems have 38 and 33 % lower shadow costs, respectively.

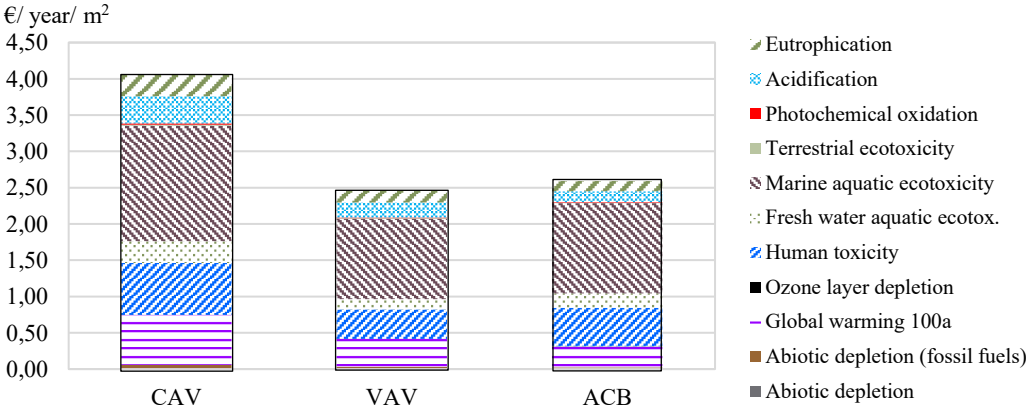

Figure 11: Total shadow cost of the CAV, VAV, and ACB systems.

5 DISCUSSION AND CONCLUSIONS

The LCA results clearly indicate that environmental impacts of the operational and the maunfacturing phases vary depending on the HVAC system. For CAV and VAV systems, the operational phase contributes most to the overall environmental impacts. Whereas, for ACB system, the maunfacturing phase has the highest environmental impacts compared to the other life cycle phases. The evironmental impacts from the operational phase of the ACB system are substantially lower than both the CAV and VAV systems. This is due to the high amount of energy used by the CAV and VAV systems during the operational phase. Overall, the CAV

system has by far the highest environmental impacts over its life cycle. The life cycle environmental impacts of the ACB system are somewhat comparable to those of the VAV system. An exception to this is the Abiotic depletion, which takes into accounts the natural resources needed for the manufacturing process. Due to the high use of copper, the ACB system has the highest Abiotic depletion impact. The major sources of potential impacts include the use of metals, zinc coating for galvanized steel, and energy use during the operational phase.

It is noticeable that the recycling process helps mitigate the environmental impacts of the ACB system the most. The recycling of materials, mainly metals, plastic and electronic components, have a positive effect on most of the environmental indicators. This is especially true in the case of recycling copper, since it is one of the main contributors to the environmental impacts of the ACB system. However, recycling does not decrease the environmental impacts of the manufacturing phase of the ACB system enough to be lower than those of the manufacturing phase of the CAV and VAV systems.

The shadow cost method provides an interesting perspective on the environmental performance of the three analyzed systems. It aggregates different impact indicators into a single score. The CAV system has the highest shadow cost, suggesting the worst overall environmental performance among the three analyzed systems. The VAV system has a slightly lower shadow cost than the ACB system. This indicates that the VAV system could have a marginally better environmental performance than the ACB system.

6 ACKNOWLEDGEMENTS

The Authors would like to thank Lindab AB and Marwan Abugabbara for providing the necessary information to accomplish this work.

7 REFERENCES

Abugabbara, M. and Javed, S., 2019. Validation of TEKNOsim 6 According to CIBSE TM33. In: Cold Climate HVAC 2018. CCC 2018. Springer Proceedings in Energy. *Springer, Cham.*

Abugabbara M., Sebesten L., & Behrens J. (2018). Assessing the energy use and IAQ of various HVAC systems during the early design stage. In: Proceedings of the 39th AIVC Conference (AIVC 2018).

Acero, A. P., Rodríguez, C., & Ciroth, A. (2014). LCIA methods–Impact assessment methods in Life Cycle Assessment and their impact categories. *GreenDelta GmbH, Berlin, Germany, 23.*

Boverkets byggregler. (2018). Boverkets föreskrifter om ändring i verkets byggregler (2011:6) – föreskrifter och allmänna råd.

BSRIA (2018) *World market for air conditioning study.* https://www.bsria.com/download/asset/chillers-world-market-for-air-conditioning-2018.pdf

Chen, S. (2011) System dynamics-based models for selecting HVAC systems for office buildings: A life cycle assessment from carbon emissions perspective, Master thesis, RMIT University

Climate Action - European Commission. (2019). EU climate action - Climate Action – *European Commission.* https://ec.europa.eu/clima/citizens/eu_en

Coletti, M., & Fano, E. (2008). AC&R facts and figures. *Refrig World, 4, 8-11.*

Commission, J. R. C. E. (2010). Analysing of existing environmental impact assessment methodologies for use in life cycle assessment. *Joint Research Centre Institute for Environment and Sustainability, ILCD handbook.*

De Bruyn, S., Korteland, M., Markowska, A., Davidson, M., De Jong, F., Bles, M. et al. (2010). Shadow prices handbook: valuation and weighting of emissions and environmental impacts. *CE Delft, Delft, the Netherlands.*

Förpacknings & Tidningsinsamlingen (2018) Återvinningsstatistik https://www.ftiab.se/180.html

Halvarsson, J. (2012). Occupancy pattern in office buildings: consequences for HVAC system design and operation.

Hollerud, B., Bowyer, J., Howe, J., Pepke, E., & Fernholz, K. (2017) A Review of Life Cycle Assessment Tools- Dovetail Partners, Inc.

Javed, S., Lechner, R. and Behrens, J., 2016. Testing and Validation of TEKNOsim: A Building Energy Simulation Program. In: Proceeding of the 12th REHVA World Congress (Clima 2016).

Khasreen, M. M., Banfill, P. F. G., & Menzies, G. F. (2009). Life-Cycle Assessment and the Environmental Impact of Buildings: A Review. *Sustainability, 1*(3), 674–701.

Lindab AB. (2019). *Lindab IT solutions.* http://www.lindab.com/global/pro/downloads/software/ventilation/pages/default.aspx

Lindvall, S. (2018). Comparison of centralized and de-centralized ventilation in a multi-family building in Stockholm: An LCA-study. *KTH*.

De Klijn-Chevalerias, M. and Javed, S., 2017. The Dutch approach for assessing and reducing environmental impacts of building materials. Building and Environment, 111, pp.147-159.

Martínez-Rocamora, A., Solís-Guzmán, J., & Marrero, M. (2016). LCA databases focused on construction materials: A review. *Renewable and Sustainable Energy Reviews, 58*, 565-573.

Pérez-Lombard, L., Ortiz, J., & Pout, C. (2008). A Review on buildings energy consumption information. *Energy and Buildings, 40*, 394–398.

Prek, M. (2004). Environmental impact and life cycle assessment of heating and air conditioning systems, a simplified case study. *Energy and Buildings, 36*(10), 1021–1027.

Sartori, I., & Hestnes, A. G. (2007). Energy use in the life cycle of conventional and low-energy buildings: A review article. *Energy and Buildings, 39*(3), 249–257.

Sweden, S. (2015). Official statistics of Sweden. *Reports on Statistical Co-ordination for the Official Statistics of Sweden 2002 (2002: 3).*

United Nations Environment Programme UNEP (2003). *Sustainable Building and Construction.* Division of Technology, Industry and Economics: Paris, France.

Van Oers, L. (2012). CML-IA characterization factors. http://cml.leiden.edu/software/data-cmlia.html#downloads

Wernet, G., Bauer, C., Steubing, B., Reinhard, J., Moreno-Ruiz, E., and Weidema, B., 2016. The ecoinvent database version 3 (part I): overview and methodology. The International Journal of Life Cycle Assessment, 21(9), pp.1218–1230.

Zabalza, I., Aranda-Usón, A., & Scarpellini, S. (2009). Life cycle assessment in buildings: State-of-the-art and simplified LCA methodology as a complement for building certification. *Building and Environment, 44*, 2510–2520.

Enhancing thermal comfort and indoor air quality in Australian school classrooms

Shamila Haddad [1, *], Afroditi Synnefa [1], Miguel Ángel Padilla Marcos [3], Riccardo Paolini [1], Deo Prasad [1], and Mattheos Santamouris [1,2]

1 Faculty of Built Environment, University of New South Wales, Sydney, Australia

2 Anita Lawrence Chair High Performance Architecture

** Corresponding author: s.haddad@unsw.edu.au*

3 RG Architecture & Energy, Universidad de Valladolid, Spain

ABSTRACT

The indoor thermal comfort and air quality in classrooms have become of interest worldwide, predominantly because of their influence on children's health, learning performance and productivity. Growing concerns with building energy efficiency emphasize the significance of this topic. This paper illustrates the outcome of a field study conducted in secondary school classrooms in Sydney, Australia, during the school year in 2018/2019. The procedure of the study consists of two approaches to collecting data including survey questionnaires designed for the young population, and measurements of physical variables. The study includes long-term measurements of environmental parameters in two adjacent classrooms (air temperature, relative humidity, CO_2), spot measurements of indoor air quality (PM_{10}, $PM_{2.5}$, and Formaldehyde), and questionnaire surveys designed to match the students' cognitive level. The participants were students aged between 12 and 18. The questionnaire includes questions about thermal perception, air quality and air movement, clothing level, and health condition. Surveyed classrooms used natural ventilation as the main conditioning strategy during the surveys. The infiltration and ventilation rate were studied during the non-occupied period based on the concentration decay method and a ventilation profile was created. In one of the two studied classrooms, a hybrid ventilation system was installed during autumn/mid-season 2019 to improve air quality and ventilation. This study investigates the subjective evaluation of the classroom thermal environment, which includes the analysis of children's subjective assessment and monitoring results. The indoor air temperature reached 29 °C during mid-season and 27 °C during winter. The maximum carbon dioxide (CO_2) concentrations per classroom exceeded 2900 ppm during the occupied period. The mean infiltration rate in air changes per hour (ACH) was 0.87, and ventilation rate with one window open was 2.35 ACH and reached 21.07 ACH when all windows and door were open. Improving the thermal environment and air quality is of importance in school building design, mainly because of the adverse effect of elevated temperature on children's performance. This is an indication that new child-based design guidelines are required to improve the thermal conditions and air quality in future school buildings wherein assessments of students' satisfaction along with energy consumption are undertaken.

KEYWORDS

Indoor environmental and air quality; Thermal comfort; School buildings; Ventilation

1 INTRODUCTION

Schools are an important building category in relation to the effects of indoor conditions on the users' health, learning and performance. Poor indoor air quality (IAQ) and elevated air temperature in classrooms are crucial issues worldwide. This problem is even worse when ventilation rates are insufficient to remove excessive heat or pollutant, especially when teachers keep windows closed to avoid discomfort caused by external noise, weather and/or to prevent

drafts. A rise in the reporting of respiratory symptoms has led to an increasing research focus on IAQ in schools (Nissilä et al.). The effects of the ventilation rates and carbon dioxide (CO_2) concentrations on students' learning performance, and positive correlations between the levels of PM and CO_2 and health symptoms (e.g., allergies, nose irritation, and fatigue) are shown in Dorizas et al. (2015). A hybrid ventilation system, in which both natural and mechanical ventilation systems are operated, is an effective strategy for controlling indoor air quality in school buildings. It supplies outdoor air, generally assumed to be clean, to reduce exposures to air pollutants in the indoor environment. Consequently, it helps to reduce risks associated with poor comfort, health and wellbeing, learning performance and productivity. Such risks are well documented in the existing literature (Fisk et al., 2009; Wargocki and Wyon, 2013; Wargocki and Wyon, 2017). Examination of IAQ and thermal comfort for children could improve the design of school buildings and thereby optimize conditions for students' performance and wellbeing. Despite extensive research on comfort and air quality in schools, limited studies have been performed in Australian climatic context to evaluate the effects of ventilation. The main aim of this project was to use and test a hybrid ventilation system to improve indoor air quality, achieve thermal comfort conditions, and at the same time reduce energy consumption and carbon emissions. In order to achieve these objectives, the following activities have been carried out: a) assessment of the thermal comfort conditions and air quality over one year (2018-2019); b) installation and evaluation of a hybrid ventilation system to improve thermal comfort and air quality. The research outlined in this paper helps to develop design solutions for enhanced thermal comfort and low carbon footprint in school buildings.

2 DATA COLLECTION PROTOCOL

This study was performed in a secondary school located in a low-traffic area in Sydney. The participating school building was equipped with split systems as the main source for heating and cooling. Two adjacent classrooms (Figure 1) were selected to perform a longitudinal study to investigate indoor air and environmental quality of the classrooms. The main objective of the monitoring campaign was to obtain data before and after the installation of the hybrid ventilation system. Furthermore, this study assessed classroom environmental condition and students' perception of thermal comfort.

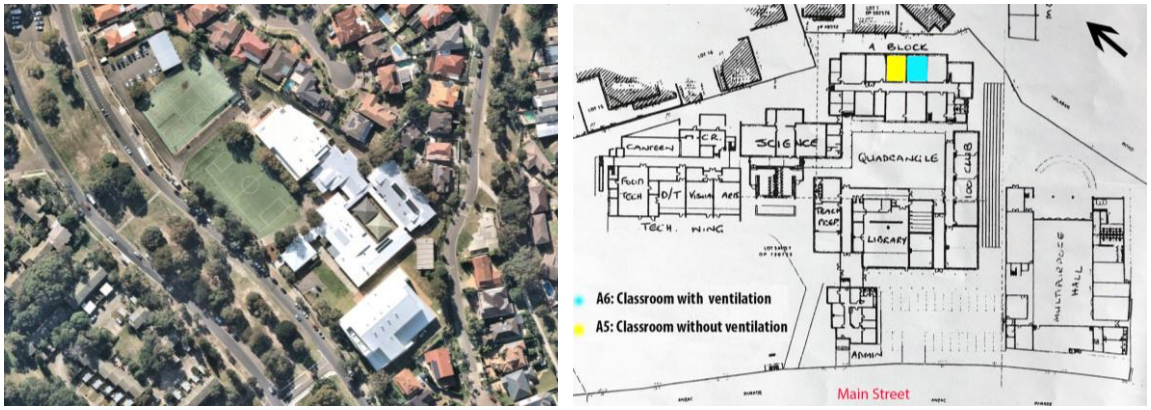

Figure 1: Location of the school and surveyed classrooms.

2.1 Measurement protocol and questionnaire survey

The monitoring campaign involved several stages and measurement protocol in line with the research objectives.

- To determine infiltration and ventilation rates in the classroom (A6) before the installation of the ventilation system, tracer gas measurements were performed using the decay

technique in the classroom of about 140 m^3 over one day in October 2018 from 9:00 to 18:00. The classroom was unoccupied for two weeks before the experiment. Innova 1403, and Innova 1412i Photoacoustic Gas Monitor (LumaSense Technology) were used in tracer gas measurements with Sulphur Hexafluoride (SF6).

- To evaluate the effectiveness of the ventilation and assess indoor thermal and air quality condition, indoor air temperature (T_a), relative humidity (RH), and carbon dioxide (CO_2) were monitored in two adjacent classrooms from April 2018 to May 2019 using Air Quality Eggs version 2 Model D (Wicked Device LLC, New York). Sensors were wall-mounted about 2.3 m above floor level in each classroom and connected to the internet. They placed in a well-ventilated position away from direct sunlight and excessive moisture exposure. The indoor air quality Egg sensors had the capability of transferring 1-minute data over the school's wireless network enabling monitoring of the data in real time.
- Aeroqual Air Quality Monitor (series 500) was used to perform spot measurements of PM_{10} and $PM_{2.5}$, and Formaldehyde before the installation of the ventilation system.
- The outdoor air temperature was recorded every 30 minutes during the long-term monitoring period using Logtag® TRIX-16 temperature recorder with a resolution of 0.1 °C and accuracy of ± 0.5 °C. The sensor was shielded from solar radiation by a Stevenson screen mounted on a pole 1.8 m high, placed in the coastal site with 4.8 km distance from the school.
- To understand students' comfort and classrooms thermal and environmental conditions, fieldwork procedures combined measurements of physical variables of the classrooms with a survey of subjective responses, which recorded students' perceptions of the immediate thermal environment conducted on 'right here, right now' basis over one week during mid-season and winter. During the survey period, all subjects were asked to perform as they do routinely to stay comfortable in the classroom. Questionnaires were specifically designed for the target age group based on developmental psychology (Haddad et al., 2012). During the 'right-here-right-now" survey, a thermal comfort meter (Heat Shield, by LSI) was used in the classroom to measure globe temperature, dry bulb temperature, relative humidity, and air speed. It was located near the centre within the vicinity of the students' desks away from heat-emitting devices (e.g., laptop or monitor) to avoid any interference in the readings. The Heat Shield was placed in one of the two classrooms at the time of the survey to measure thermal condition at the height of seated students.
- To improve ventilation, Healthbox 3.0 and Invisivent window ventilator by RENSON® were installed in one of the selected classrooms (A6) before the mid-season survey in February 2019 (Figure2).

a) b)

Figure 2: Ventilation system: HEALTHBOX® 3.0 (a), INVISIVENT® Ventilator (b).

3 RESULTS

3.1 Results of tracer gas measurement

To perform tracer gas measurement, a grid of 13 sampling points was organized in the classroom. The reference sampling point was in the centre of the classroom as shown in Figure 3. The equipment was located in a corner of the classroom and three dosing points were placed in the other three corners. Each dosing tubing was mounted to a mixing fan which helped to diffuse the gas concentration in the classroom. Fans were used during the dosing stage and stopped when the decay concentration sampling started. Figure 3 shows the location of sampling and dosing points. Sampling was started when the gas concentration was completely diffused and homogeneously distributed in the classroom.

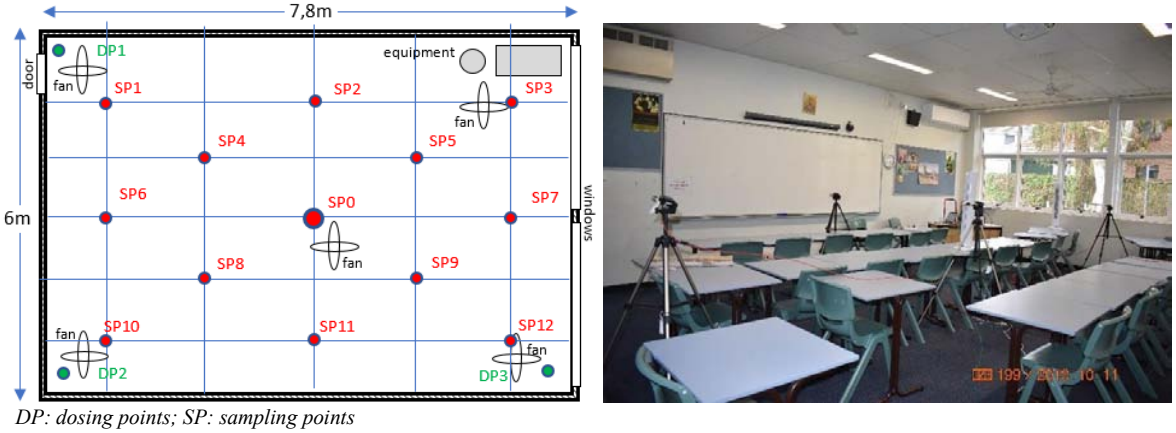

DP: dosing points; SP: sampling points

Figure 3: Tracer gas measurement

The experiments were performed under two conditions a) all windows closed, b) windows opened, including two sub-cases, namely with one window opened and all windows opened. When the window was closed (air infiltration), the mean air exchange rate through the envelope of the classroom was 0.86 ACH at the reference sampling point. The ventilation rate with one window open was 2.35 ACH in the reference point. When all windows and door were opened, the ventilation rate of 21.07 ACH was obtained.

3.2 Results of long-term monitoring

Figure 4 shows the results of monitoring during cold and autumn/mid-season with an overlay of two periods in 2018 and 2019 when the questionnaire surveys were conducted. During the monitoring period, the indoor temperature varied between 10.2 °C and 30.0 °C, while the outdoor temperature ranged from 5 °C to 37.9 °C from April 2018 to May 2019. Relative humidity spanned from 20.1 % to 80.9 %. During the measurement period, semi-hourly CO_2 concentration in the classrooms exceeded 2900 ppm. Split-system air-conditioners were used occasionally outside the questionnaire survey campaign, which induced slight differences between the temperature and humidity of the investigated classrooms. During the winter period, windows were often closed due to the weather conditions, which caused CO_2 concentration exceeding the recommended thresholds of 1000 ppm (ASHRAE 62.1, 2016) and 850 ppm (Australian Building Codes Board ABCB, 2018).

After the installation of the hybrid ventilation system in the classroom A6, CO_2 concentration was significantly reduced. Figure 5 compares CO_2 concentrations in classrooms with and

without ventilation system. During winter, both classrooms show similar CO_2 levels. It should be noted that boxplots included data obtained during school holiday or hours when classrooms were not occupied. Sample t-test shows that the difference between the mean value of CO_2 concentration in the classroom with the ventilation system and the classroom with no means of ventilation is statistically significant ($p < 0.001$). Elevated CO_2 levels may lead to headache, changes in respiratory patterns, and concentration loss (Australian Building Codes Board ABCB, 2018). Then, the indoor air temperature was slightly higher in the classroom without ventilation (A5) than in the classroom where the ventilation system was installed (A6).

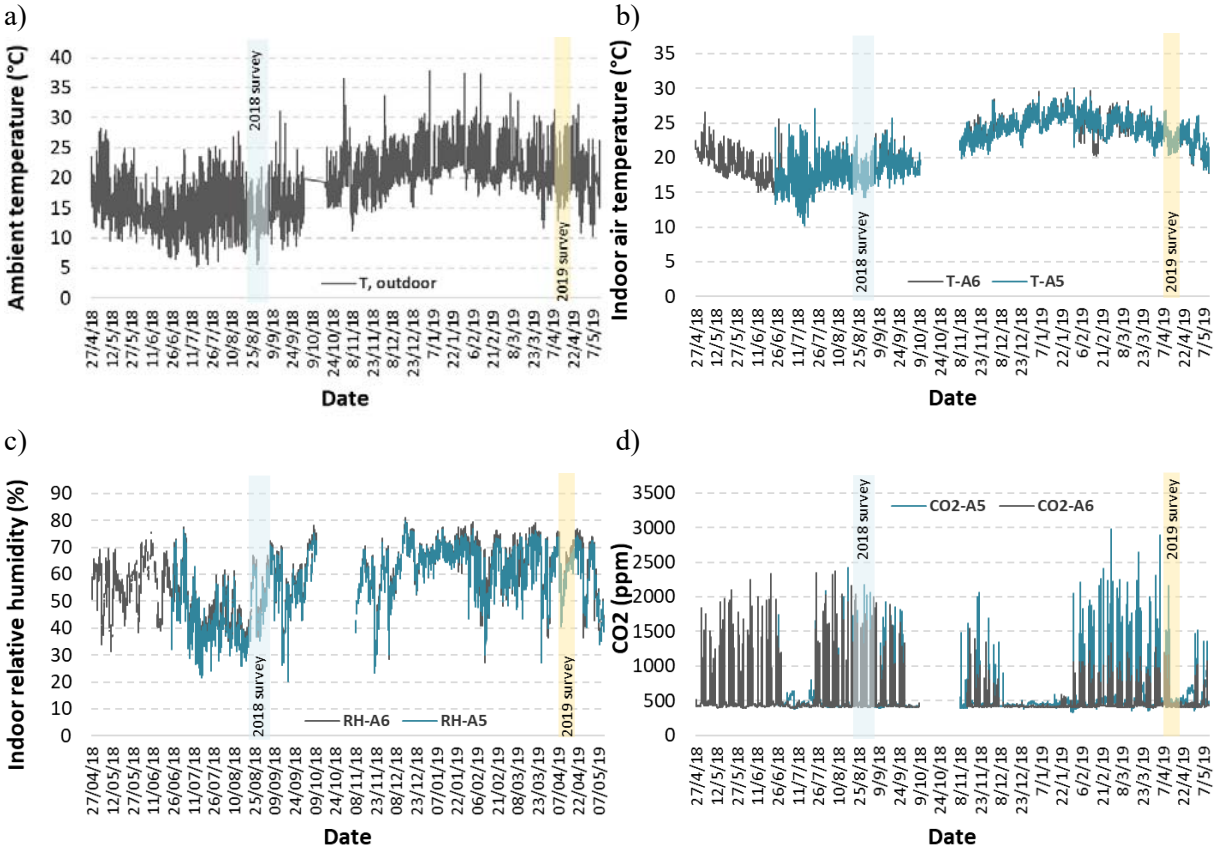

Figure 4: Results of monitoring during cold and mid-season: outdoor temperature (a), indoor air temperature (b), indoor relative humidity (c), CO_2 (d) in A6 (classroom with ventilation system) and A5 (classroom without ventilation system)

Formaldehyde was measured in the classrooms during different periods of the school year: a) over one week in December 2018 (including weekend and unoccupied condition), b) over 8 hours in three normal school days. The 8-hours average of the formaldehyde concentration varied between 0.1 ppm to 0.14 ppm. While the World Health Organization (2010) sets a limit of 0.1 mg/m^3 (0.08 ppm) to prevent sensory irritation, an indoor air level of 0.1 ppm formaldehyde has been considered safe based on Golden (2011). Indoor level of particulate matter (PM) was measured during school days (about 8 hours) for two different days. During the first day, PM_{10} varied between 5 to 39 µm/m^3 (8-hour mean: 16±6 µm/m^3) and $PM_{2.5}$ was within a range of 2 to 11 µm/m^3 (8-hour mean: 7±2 µm/m^3). A 24-hour average of 25 µg/m^3 and 50 µg/m^3 is specified as the maximum contaminant limits for $PM_{2.5}$ and PM_{10}, respectively (Australian Building Codes Board ABCB, 2018). The 8-hour mean urban background levels of $PM_{2.5}$ and PM_{10} were 10.8 µg/m^3 and 17.7 µg/m^3, respectively, based on the measured data obtained from a station within 2 km distance from the school (Office of Environment and

Heritage, 2019). In the second day, indoor PM_{10} varied from 1 to 50 µm/m^3 (mean: 26±7 µm/m^3) and $PM_{2.5}$ was within a range of 3 to 12 µm/m^3 (mean: 6±1 µm/m^3). The 8-hour average outdoor PM_{10} was 16.9 µm/m^3. No $PM_{2.5}$ was available for this day.

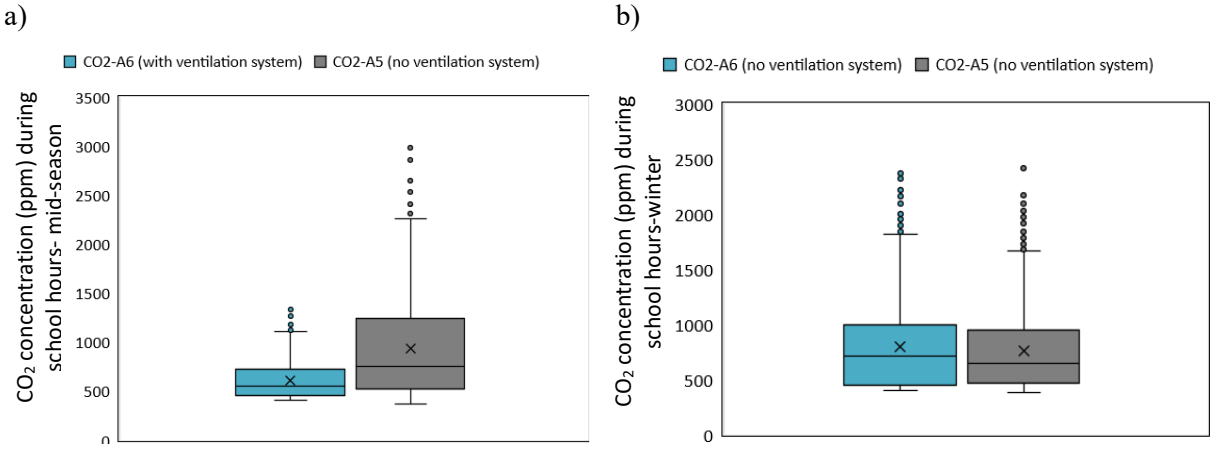

Figure 5: Box plot of CO_2 after (a) and before (b) installation of the ventilation system

3.1 Results from subjective survey and simultaneous measurements of physical parameters

The indoor air temperature varied between 20.7 °C and 26.4 °C with the mean value of 23.7 °C during mid-season questionnaire survey (2019). During the winter survey period, the indoor temperature fell in the range between 17.3 °C and 22.4 °C since no heating system was used in the classrooms. The average CO_2 concentration during the winter survey period was higher than that during mid-season survey period ranging between 718 ppm and 2114 ppm and from 442 ppm to 1510 ppm, respectively. The actual occupancy profile of the classrooms was not monitored. Therefore, data from unoccupied hours was retained in this analysis. In total, 376 and 306 responses to the questionnaires were pooled during winter and mid-season/autumn, respectively. During the winter survey period, the percentage of female and male students were similar (about 44 %), while during mid-season a higher percentage of participants were female (56 %). Based on the results of the right-here-right-now thermal sensation survey, the acceptable range of temperature for students was derived. Comfort zone refers to conditions falling within a range from -0.5 to +0.5 in which the predicted percentage of dissatisfied people is expected to be 20 %. The 20 % rate of dissatisfaction corresponds to 10 % dissatisfaction for general thermal discomfort, when -0.5 < predicted mean vote (PMV) of occupants < 0.5, and an additional 10 % dissatisfaction due to local discomfort (ASHRAE 55, 2017). The overall rate of dissatisfaction (20 %) is related to the limits of ±0.85, which assumes 80 % of votes falling inside the central three categories of the ASHRAE scale. To find the empirical limits of acceptable thermal environments for 80 % satisfaction, the indoor temperature was calculated for the mean thermal sensation votes (TSV) of ± 0.85 using the linear regression model (Figure 6). The neutral temperature for the sampled students was derived for the entire survey period (combined winter and mid-season) using mean thermal sensation votes of students and air temperature per survey; i.e., 23.4 °C. The operative temperature was not used in the regression analysis due to a lack of simultaneous measurement of globe temperature in both classrooms. School children who participated in the surveys felt comfortable within an indoor temperature range of 19.5 °C to 27 °C. Moreover, they demonstrated considerable adaptability to classroom indoor air temperature variations, with one thermal sensation unit equating to approximately 4.6 °C difference in air temperature. A similar study in classrooms found an acceptable range of operative temperature from 19.5 to 26.6 °C for Australian students (de Dear et al., 2015).

The same study showed between-school differences in thermal sensitivity. Students in locations exposed to variable weather condition showed greater thermal adaptability than those in areas with more equable weather (de Dear et al., 2015).

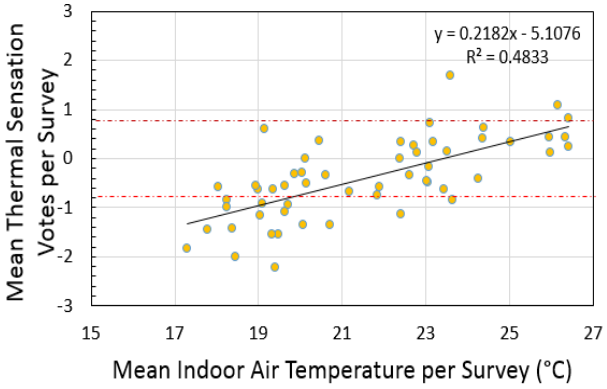

Figure 6: Linear regression analysis of thermal sensation against classroom temperature

As it concerns the thermal preference of students, a larger percentage of participating students wanted to feel warmer (57 %) than those who preferred a cooler or no change in the classroom during the winter survey. During autumn/mid-season, the percentage of 'No change' votes (42 %) was higher followed by the percentage of students wanted to be 'Cooler' (37 %).

4 CONCLUSIONS

This paper presents the results of the study performed to implement, monitor and evaluate the performance of hybrid ventilation technologies to provide indoor air quality and comfort. To achieve the objectives, detailed experimental investigations were performed in two adjacent classrooms of a private secondary school in Sydney, Australia. The long-term experimental campaign was conducted from April 2018 to May 2019 to monitor indoor air quality and thermal parameters continuously. Infiltration and Ventilation rates were measured equal to 0.86 ACH and 2.35 ACH, respectively. A hybrid ventilation system equipped with a window ventilator and Healthbox 3.0 were installed in February 2019 in one of the two classrooms. The system communicated with smart devices to enable real-time monitoring of the classroom air quality, temperature and humidity. The system supplied fresh air and removed the polluted air from the classroom based on CO_2 and VOCs detection. Analysis of indoor air quality and thermal comfort shows significant improvements in reducing CO_2 concentration in the classroom with ventilation compared to the classroom without a ventilation system. This will ultimately help to reduce the adverse health impacts of the environmental condition on children and improve productivity and performance. Furthermore, it was found that Australian students feel comfortable at a neutral temperature of 23.4 °C. This is consistent with previous literature and highlights that children feel comfortable at slightly lower thermal environments compared to adults. Further research should be proposed and implemented with a larger sample of schools to develop health-based ventilation guidelines for schools in Australia. Future research is needed to determine the discrepancies between the schools and classrooms exposures, which are not tested here.

5 ACKNOWLEDGEMENTS

Authors acknowledge CRC for Low Carbon Living, RENSON®, and St Spyridon College to support this study. Special thanks go to all students and teachers who participated in this research.

6 REFERENCES

ASHRAE 55. (2017). Thermal Environmental Conditions for Human Occupancy. Atlanta, Georgia: American Society of Heating, Refrigeration and Air Conditioning Engineers, Inc.

ASHRAE 62.1. (2016). Ventilation for Acceptable Indoor Air Quality. Atlanta American Society of Heating, Refrigerating and Air-conditioning Engineers.

Australian Building Codes Board ABCB. (2018). Indoor Air Quality Handbook. CANBERRA ACT.

de Dear, R., Kim, J., Candido, C., & Deuble, M. (2015). Adaptive thermal comfort in Australian school classrooms. *Building Research & Information, 43*(3), 383-398. doi:10.1080/09613218.2015.991627

Dorizas, P. V., Assimakopoulos, M.-N., & Santamouris, M. (2015). A holistic approach for the assessment of the indoor environmental quality, student productivity, and energy consumption in primary schools. *Environmental monitoring and assessment, 187*(5), 259.

Fisk, W., Mirer, A., & Mendell, M. (2009). Quantitative relationship of sick building syndrome symptoms with ventilation rates. *Indoor Air, 19*(2), 159-165.

Haddad, S., King, S., Osmond, P., & Heidari, S. (2012). *Questionnaire design to determine children's thermal sensation, preference and acceptability in the classroom.* Paper presented at the Proceedings-28th International PLEA Conference on Sustainable Architecture+ Urban Design: Opportunities, Limits and Needs-Towards an Environmentally Responsible Architecture.

Nissilä, J.-J., Savelieva, K., Lampi, J., Ung-Lanki, S., Elovainio, M., & Pekkanen, J. Parental worry about indoor air quality and student symptom reporting in primary schools with or without indoor air quality problems. *Indoor Air, 0*(0). doi:10.1111/ina.12574

Wargocki, P., & Wyon, D. P. (2013). Providing better thermal and air quality conditions in school classrooms would be cost-effective. *Building and Environment, 59*, 581-589. doi:https://doi.org/10.1016/j.buildenv.2012.10.007

Wargocki, P., & Wyon, D. P. (2017). Ten questions concerning thermal and indoor air quality effects on the performance of office work and schoolwork. *Building and Environment, 112*, 359-366.

Indoor air and environmental quality in social housing dwellings in Australia

Shamila Haddad [*, 1], Afroditi Synnefa [1], Riccardo Paolini [1], and Mattheos Santamouris [1, 2]

1 Faculty of Built Environment, University of New South Wales, Sydney, Australia

2 Anita Lawrence Chair in High Performance Architecture

** Corresponding author: s.haddad@unsw.edu.au*

ABSTRACT

This study aims to assess the indoor thermal and environmental quality of low-income households in New South Wales, Australia. It adds evidence-based findings on the performance of residential buildings and contributes to improving the indoor environmental quality of social housing. The research presented in this paper involved subjective and objective evaluation of indoor air and environmental quality. The objective method included long-term monitoring of air temperature, relative humidity, and carbon dioxide during winter and summer 2018/2019, whereas the subjective method involved assessing occupants' feedback about the indoor environmental quality. Physical observation of the indoor and outdoor conditions of each home was carried out on the same day of the questionnaire survey. Over 100 social housing households in the Greater Sydney area participated in this study. The characteristics of the specific population group are presented in this paper including details of energy bills, health, and indoor comfort. It further discusses issues related to the impact of urban overheating on indoor environmental conditions. Lower satisfaction rate with the thermal environment and poor indoor environmental quality affect health and quality of life of residents living in social housing. The minimum indoor air temperature recorded was about 5 °C during winter 2018 and the maximum indoor air temperature reached 39.8 °C in summer 2019. The mean thermal sensation vote increases by 1 point per 4.8 °C increase in the room indoor air temperature. The residents who participated in this study have an upper acceptable indoor air temperature of about 26 °C for 80 % satisfaction. This study highlights the need to improve both building quality and outdoor local climate. Acting on only one of the two sides is not enough to achieve nearly zero energy buildings in Australian climates, considering the predicted extreme weather conditions in future. Therefore, advanced mitigation and adaptation technologies are needed to improve the quality of low-income households, promotes health, and reduce energy for heating and cooling.

KEYWORDS

Energy poverty, Indoor air quality, Social housing, Indoor environmental quality

1 INTRODUCTION

There are more than 3 million people (13.2 % of the population) living below the poverty line in Australia, after taking account of their housing costs (Bradbury et al., 2018). The poverty rate is higher among children under the age of 15 (17.3 % of all children) and youth between the ages of 15 and 24 (13.9 %). The term energy poverty is used to describe a situation of a household not able to satisfy the necessary energy services in the residence (Bouzarovski-Buzar, 2011). Energy poverty, or struggling to meet energy needs, has become the subject of attention in Australia, with the rising cost of energy concerning all Australians. Low-income large-family households, most exposed to the risk of energy poverty, live in the struggle-town suburbs of Australian biggest cities (Hogan and Salt, 2017). Energy poverty has a significant

impact on the quality of life, affects indoor comfort levels in energy-poor houses, influences social attainment, has a negative effect on residents' health, and results in a significant increase of the seasonal mortality and morbidity (Santamouris and Kolokotsa, 2015). Low-income families, pensioners, and indigenous Australians have faced increasing difficulty in paying energy bills and ultimately achieving the required indoor environmental conditions. Lack of ventilation, inadequate insulation, poor indoor air quality, presence of internal condensation, mould, and damp are associated with illnesses like bronchitis, asthma, influenza, heart deceases, arthritis, migraine, as well as social and mental health problems such as depression and anxiety (World Health Organization, 2007). Further, extreme weather events have a significant impact on the quality of life, energy use, and health of urban residents (Santamouris and Kolokotsa, 2015). The low-income vulnerable population is particularly affected by the local and global climate change and energy poverty. Summertime indoor environmental conditions in low-income households lead to thermal discomfort and heat stress, especially during heat waves. Non-satisfactory levels of indoor environmental quality may cause health problems and increase the mortality rate. A recent study shows the lack of affordable housing options and rental stress in Sydney, where 90 % of low-income earners paid more than a third of their income on rent (Troy et al., 2019). It demonstrates additional challenges for people who need social and affordable housing. Despite the importance of the topic, very little is known about the specific penalties and the impact of extreme weather conditions in Australian low-income population. Additionally, there is little empirical evidence about the indoor air and environmental quality of social housing in Australia. This paper is part of a larger study which aims to assess the living conditions of the low-income population where health, energy consumption, as well as indoor environmental quality are considered. Energy efficiency measures for low-income housing require a deep knowledge of the actual conditions of social housing dwellings and residents. This paper investigates thermal comfort, indoor air quality, residents' satisfaction, housing quality and characteristics, health, and energy penalties related to the low-income population in New South Wales, Australia.

2 DATA COLLECTION PROCEDURE

This study was performed in public, community, and social housing dwellings occupied by residents in need of affordable rental housing. A total of 109 residents participated in the questionnaire survey and 106 households proceeded with the indoor air and environmental quality monitoring campaign. Selected households represent the social housing stock in Sydney including a combination of one-story, multi-storey, single family, multifamily, with distinct characteristics (e.g., size, construction characteristics, age) and locations including coastal and inland areas. This study mainly focused on residences in Sydney metropolitan area; however, it was further extended to western regional cities, namely Dubbo, Bathurst, and Orange, due to the microclimate characteristics and reported higher ambient temperatures in the western areas (Santamouris et al., 2017). In this study, 51.4 % and 41.3 % of participating residents were living in public and community housing, respectively. The remaining 7 % corresponds to low-income households with private rental housing.

2.1 Indoor data measurement protocol and questionnaire survey

A monitoring campaign was performed to obtain environmental data and air quality in the dwellings. The indoor air temperature (T_a), relative humidity (RH), and carbon dioxide (CO_2) were continuously recorded from May 2018 to February 2019 using Indoor Air Quality Eggs version 2 Model D (Wicked Device LLC, New York). The sensors were placed in a well-ventilated position away from direct sunlight and excessive moisture exposure in the living rooms, where occupants spent most of their time during the day. Measurements were recorded

with a one-minute interval and then averaged over 30 minutes for analysis. Data was recorded and manually downloaded due to limited access to a wireless network in the social housing dwellings and financial concerns of low-income residents who participated in this study. The air quality Eggs were installed in 83 residences. However, due to concerns of the remaining 23 residents about electricity usage and risk of interruptions due to accidental interference of people or power outage, 106 Logtag® TRIX-16 temperature recorders were also added in all dwellings. These temperature sensors have a built-in battery, a resolution of 0.1 °C and an accuracy of ± 0.5 °C. Thus, air quality data was obtained in 83 residences, while 23 households were only monitored for the indoor air temperature. Fieldwork procedures combined measurements of physical variables of the residences with survey of subjective responses, which records subjects' perceptions of the thermal environment, energy bills, quality of the building envelope and indoor thermal and environmental condition (e.g., presence of mould), other features of the building and energy profile (number of people sharing the household, time spent at home), and residents' health conditions and behaviours. Furthermore, the ASHRAE seven-point scale (ASHRAE 55, 2017) was used to measure residents' thermal sensation on 'right here, right now' basis during summer 2019, which records subjects' perceptions of the immediate thermal environment.

2.2 Characteristics of the household and dwellings in the study

The pooled responses from 109 respondents involve data for a total of 200 people living in the social housing residences. According to 2016 census data, the average age of the NSW and greater Sydney population was close to 38 and 36 years (Australian Bureau of Statistics, 2016), while the average age of participants in this study was 45 years. Figure 1 (a) shows the distribution of different age groups. The total population size is made up of 76 (38 %) males and 124 (62 %) females. Of all residents, 45 % were aged between 18 and 60 years, 35 % were aged over 60 years, and 22 % below 18 years (Figure 1(b)). Then, 18 % of the total population in this study were employed, while the remaining population were unemployed or inactive (16 %), students (28 %), and retired people and disability pensioners (39 %).

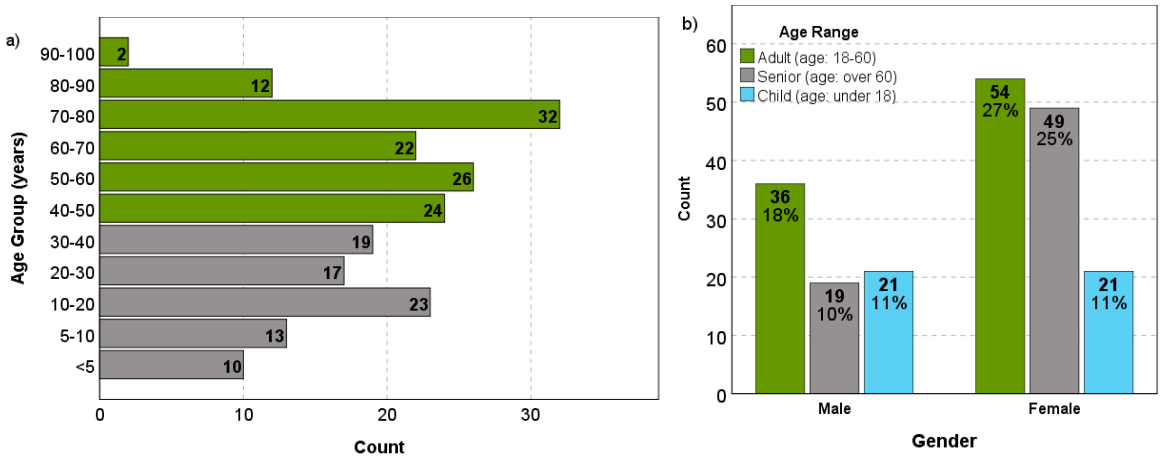

Figure 1: Characteristics of the household in this study: distribution of (a) age group; and (b) gender.

The average household size was of 1.8 people, with 54 % of participating households composed by only one person, while in 32 % and 14 % of cases the size was of two and over three persons per household, respectively. The average declared household fortnightly income value in 2018 was $1076 per household and $600 per person. The average electricity bills per quarter per household and per person were $271 and $151, respectively. All surveyed dwellings were rental housing with the average construction year of 1975-2000. Only 25% of residences were built

after 2000. The total floor area of the residences varied from 24 m^2 to 135 m^2 with an average of approximately 70 m^2. 63 % of participating dwellings were apartment units and 37 % were detached or semi-detached houses. All participating residences had single glazing windows and reported to have poor insulation. While 45 % of residents did not know if their dwelling was insulated, 27 % of households reported some forms of insulations in their homes. According to the Australian Bureau of Statistics (2012), social housing renters are twice as likely to be living in un-insulated homes, when compared to owner-occupied residences. Mould and condensation were reported in 42 % of dwellings participated in this study. Mould and condensation primarily occurred in bedrooms (40 %) and wet areas namely bathroom, laundry, kitchen (38 %), 17 % happened in the living rooms, and 5 % in all rooms. Social housing residents may face difficulties to solve the mould and condensation problems. Mould is particularly important because it may affect people with health conditions namely allergies, asthma, weakened immune systems, chronic, obstructive, and allergic lung diseases (State Government of Victoria, 2019). During the winter period, 69 % of residents used a portable electric heating system, while 22 % did not have any heating system. A fireplace or gas heaters were used in 10 % of the surveyed buildings. During the summer months, 90 % of families used a portable fan or evaporative cooling system, 7 % a split system, and 3 % had no cooling system.

3 RESULTS

3.1 Results from the subjective survey

The participating residents spent on average 18 hours per day at home, which highlights the importance of indoor environmental quality on social housing residents particularly the age group of over 60 years who spent an average of 20 hours a day at home. Families with a fortnightly income above $1,500 (13 % of total sample size), were composed by higher number of residents per household and paid higher rates for the electricity bills (up to an average of $500 per quarter) compared to families with lower-income rates. Very low-income families, with an average resident size of about two persons, paid approximately $200 per quarter for their electricity bills. Social housing residents may face several problems including social, economic, and physical barriers to prevent chronic disease. About 28 % of all residents reported psychological disorder. Of all residents who reported mental health or psychological problems, 38% had a fortnightly income in the range between $600 and $1000. Depression and anxiety (76 %) were the most common psychological disorders among participating residents. Previous research has shown that low indoor temperatures have an adverse psychosocial impact including depression and stress (Critchley et al., 2007; Thomson and Snell, 2013). Non-proper levels of indoor daylight or bad window view increase the probability of depression by 60 % and 40 %, respectively (World Health Organization, 2007). Further, people living in houses with mould, present a 60 % higher trend for depression than residents of dwellings without mould problems (World Health Organization, 2007). More than half of the residents reported health problems. Within different age groups who have reported health problems, a higher percentage of seniors aged over 60 (27 %) reported health problems compared to adults (20.5 %), and children (6 %). Airway and blood diseases were the most common health problems in this study. When airway disease, allergy, and asthmatic symptoms are combined, it accounts for 32 % of all reported disease. Further, 32 % of residents were obese or very overweight, while only 4% were underweight. Residents were asked to report any hospital admission during summer months 2019. It was found that 25 % of hospital admissions in summer 2019 were associated with excess heat inside the residences. Then, 23 % of all residents involved in this study were smoking 2 to 35 cigarettes per day with an average of about 6 cigarettes smoked inside their dwelling.

3.2 Analysis of indoor air quality and thermal environment

The CO_2 concentration trespassed the recommended threshold of 1000 ppm (ASHRAE 62.1, 2016) and 850 ppm (Australian Building Codes Board ABCB, 2018) in several investigated buildings particularly during winter and the mid-season. The CO_2 concentration exceeded 1000 ppm and 2000 ppm in 78 % and 24 % of buildings monitored with the air quality Egg sensors, respectively. While CO_2 level exceeded 3000 ppm in the participating buildings, the documented indoor weekly mean concentrations of CO_2 in typical Australian dwelling are 527 ± 121 ppm in Winter/Spring and 544 ±121 ppm in Summer/Autumn (Cheng et al., 2010).

Figure 3 shows the indoor air temperature profile in a sample of monitored residences in Western Sydney, which highlights the periods when indoor conditions were outside the comfort range (red dotted lines). The minimum recorded indoor air temperature in all dwellings ranged from 4.9 °C to 19.3 °C with an average of 13.5 °C. The minimum air temperature fell below 10 °C in 20 % of the monitored buildings. The average relative humidity ranged from 42 % to 68 % during the monitoring period. The maximum indoor air temperature recorded during the summer period, December 2018 to February 2019, was 39.8 °C while the average indoor maximum temperature was 32.6 ± 3.0 °C.

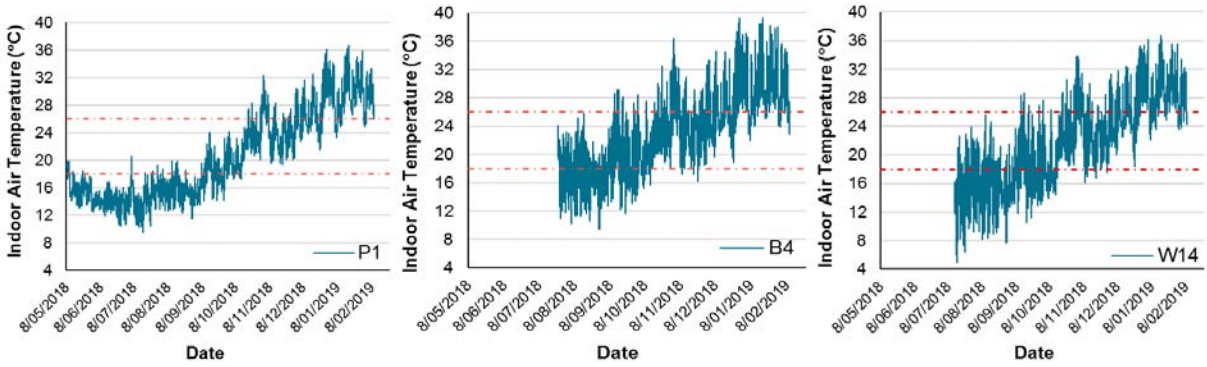

Figure 3: Indoor air temperature profile in three residences (the red dotted lines represent the comfort range)

Figure 4 shows the locations of the monitored buildings and the spatial distribution of the recorded maximum indoor air temperature. Inverse Distance Weighted (IDW) interpolation technique was used to generate the spatial patterns of maximum indoor air temperature based on the assumption that the nearest points surrounding a selected location have more influence on the prediction than those that are farther away. The IDW interpolation technique weights the points being evaluated based on the distance from the sampled location; the weight is a function of inverse distance (Philip and Watson, 1982).

The distribution of the maximum indoor air temperature in the monitored dwellings during summer was consistent with the distribution of outdoor climate in Greater Sydney, where Western Sydney frequently presents 7-10 °C hotter than in coastal suburbs (Santamouris et al., 2017). This highlights the need for improved quality of social housing dwellings to provide comfort and avoid heat-related mortality and morbidity during heatwaves and extreme climatic condition in the future.

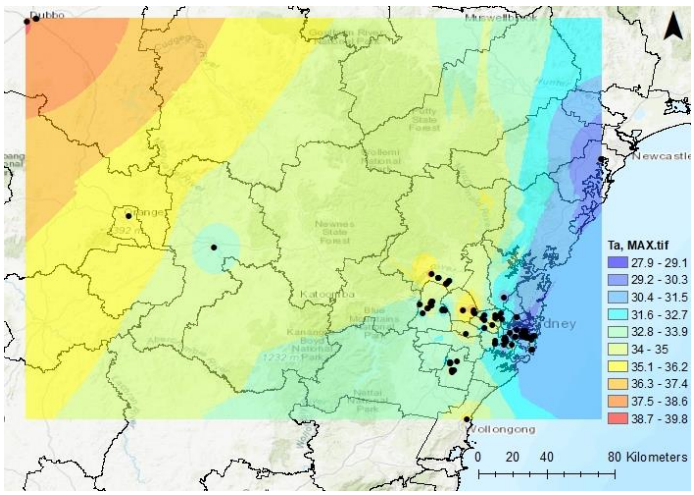

Figure 4: Maximum indoor air temperature distribution map

Based on the results of the right-here-right-now thermal sensation survey during summer 2019, the acceptable range of temperature for occupants is derived. The acceptable range is the comfort temperature band within which most people are comfortable. To find the empirical limits of acceptable thermal environments for 80 % satisfaction (ASHRAE 55, 2017), the indoor temperature was calculated for the mean thermal sensation votes (TSV) of ± 0.85. However, because the mean TSV points fall on the warm side of neutral, i.e. central category of the ASHRAE scale, this study focuses on upper limits of the comfort zone which corresponds to TSV= + 0.85. Occupants' mean TSVs within each 0.5 °C indoor air temperature bin were calculated and plotted in Figure 5. Because the data was binned, the linear regression model was weighted according to the number of occupants making up each mean vote within each 0.5 °C bin. The regression slope is a measure of sensitivity to temperature change and demonstrates how much the thermal comfort vote increases per 1 °C rise in operative temperature (Humphreys et al., 2007). It is inversely proportional to the adaptability of the building occupants. Since no data on the mean radiant temperature is available in this study, we only focused on the air temperature. The regression equation suggests that the mean thermal sensation unit increases 1 point per 4.8 °C increase in the room indoor air temperature. The dwellers participated in this study have an upper acceptable indoor air temperature of 25.8 °C (when TSV = + 0.85).

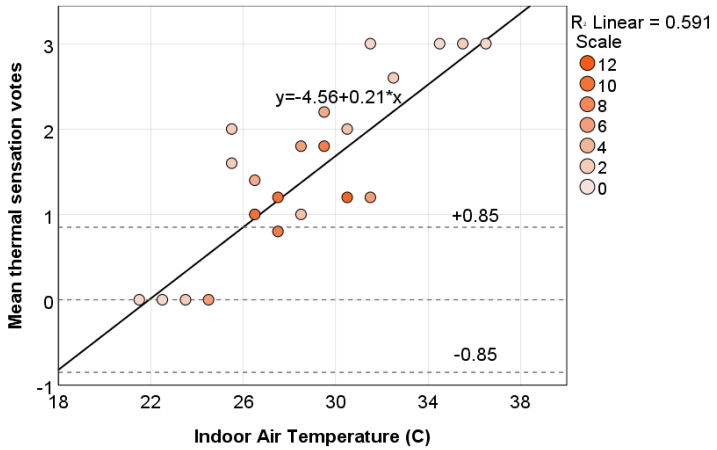

Figure 5: Weighted linear regression analysis of mean thermal sensation votes against air temperature

The most cost effective and efficient technologies that need to be used for Australian low-income households include improvements in the dwellings' envelope, passive heating and

cooling techniques, and improvement of the building services and energy management. Further, it should be attempted to improve the low-income neighbourhoods' microclimate by increasing the green spaces and using reflective materials for pavements and roofs to mitigate urban overheating particularly in western suburbs.

4 CONCLUSION

This paper presents the current indoor condition of low-income social housing residences in NSW and reports problems associated with health, comfort, and energy. Occupants' responses to the survey give information on the challenges of the low-income population in securing the required levels of the energy services in their dwellings. Monitoring of 106 low and very low-income houses during the winter and mid-season of 2018 and summer of 2019 in Greater Sydney has shown that the indoor air temperature is much lower and higher than the minimum and maximum threshold values set for comfort and health purposes, respectively. In most of the participating residences during winter 2018, long spells of low indoor temperatures are recorded which were much below the internationally accepted conditions. The minimum indoor air temperature recorded was about 5 °C during winter 2018 and the maximum indoor air temperature reached 39.8 °C in summer 2019. Summer-time indoor air temperature in many of the residences located in Western Sydney largely exceeded the comfort limits. The maximum indoor air temperatures were higher in western areas compared to those observed in eastern suburbs. As it concerns indoor air quality, many of the investigated dwellings exceeded the recommended threshold with CO_2 trespassing the limit of 1000 ppm, particularly during winter and mid-season when there was a limited rate of ventilation. The results of thermal comfort assessment showed that occupants adapted to slightly larger indoor temperature band (with the upper acceptability limit of 26 °C), highlighting the importance of the availability of controls that would enable them to adjust their indoor environment based on their preferences. Despite adaptability of social housing residents, indoor air temperature during cold and warm seasons exceeded the comfort zone limits and this led to a higher rate of dissatisfaction during cold and warm seasons. This highlights the importance of building design and adaptation techniques to improve the quality of building envelope and passive design strategies to reduce the need for active heating and cooling system in social housing residences. Future research should focus on analysing a larger sample of social housing and survey a larger number of occupants to generalize the results of this research.

5 ACKNOWLEDGEMENTS

Authors acknowledge the Office of Environment and Heritage and CRC for Low Carbon Living to support the project "Energy efficiency in social housing". Special thanks are extended to City Councils, FACS Department of Family and Community Services (NSW), and Community Housing Provides, who helped in the recruitment stage of this research.

6 REFERENCES

ASHRAE 55. (2017). Thermal Environmental Conditions for Human Occupancy. Atlanta, Georgia: American Society of Heating, Refrigeration and Air Conditioning Engineers, Inc.

ASHRAE 62.1. (2016). Ventilation for Acceptable Indoor Air Quality. Atlanta American Society of Heating, Refrigerating and Air-conditioning Engineers.

Australian Building Codes Board ABCB. (2018). Indoor Air Quality Handbook. CANBERRA ACT.

Australian Bureau of Statistics. (2012). Household Energy Consumption Survey, Australia: Summary of Results.
Australian Bureau of Statistics. (2016). 2016 Census QuickStats, Northern Territory, Local Government Areas. Retrieved from http://www.abs.gov.au/
Bouzarovski-Buzar, S. (2011). *Energy Poverty in the EU: A Review of the Evidence.* Paper presented at the DG Regio workshop on Cohesion policy investing in energy efficiency in buildings. Brussels.
Bradbury, B., Saunders, P., & Wong, M. (2018). *Poverty in Australia 2018*. Retrieved from https://www.acoss.org.au/wp-content/uploads/2018/10/ACOSS_Poverty-in-Australia-Report_Web-Final.pdf
Cheng, M., Galbally, I., Gillett, R., Keywood, M., Lawson, S., Molloy, S., & Powell, J. (2010). Indoor air project part 1: Main report. Indoor Air in Typical Australian Dwellings. *Aspendale: CSIRO Australian Weather and Climate Research*.
Critchley, R., Gilbertson, J., Grimsley, M., Green, G., & Group, W. F. S. (2007). Living in cold homes after heating improvements: evidence from Warm-Front, England's Home Energy Efficiency Scheme. *Applied Energy, 84*(2), 147-158.
Hogan, C., & Salt, B. (2017). The rise of energy poverty in Australia. *Census Insight Series, KPMG, 12*.
Humphreys, M. A., Nicol, J. F., & Raja, I. A. (2007). Field studies of indoor thermal comfort and the progress of the adaptive approach. *Advances in building energy research, 1*(1), 55-88.
Philip, G., & Watson, D. F. (1982). A precise method for determining contoured surfaces. *The APPEA Journal, 22*(1), 205-212.
Santamouris, M., Haddad, S., Fiorito, F., Osmond, P., Ding, L., Prasad, D., . . . Wang, R. (2017). Urban heat island and overheating characteristics in Sydney, Australia. An analysis of multiyear measurements. *Sustainability, 9*(5), 712.
Santamouris, M., & Kolokotsa, D. (2015). On the impact of urban overheating and extreme climatic conditions on housing, energy, comfort and environmental quality of vulnerable population in Europe. *Energy and Buildings, 98*, 125-133.
State Government of Victoria. (2019). Mould and Your Health. Retrieved from www.betterhealth.vic.gov.au/health/conditionsandtreatments/mould-and-your-health
Thomson, H., & Snell, C. (2013). Quantifying the prevalence of fuel poverty across the European Union. *Energy Policy, 52*, 563-572.
Troy, L., van den Nouwelant, R., & Randolph, B. (2019). *Occupant Survey of Recent Boarding House Developments in Central and Southern Sydney*. Retrieved from https://cityfutures.be.unsw.edu.au/research/projects/boarding-houses-central-and-southern-sydney/
World Health Organization. (2007). Large analysis and review of European housing and health status (LARES) *DK-2100*. Copenhagen, Denmark.

Radiant Heating and Cooling Systems Combined with Displacement Ventilation in Schools; Strategies to Improve IAQ

Michel Tardif[1], Sébastien Brideau [*2],

1 CanmetENERGY
1 Haanel Drive
Ottawa, Canada
michel.tardif@canada.ca

2 CanmetENERGY
1 Haanel Drive
Ottawa, Canada
Sebastien.brideau@canada.ca

ABSTRACT

The new schools in Canada are designed to improve indoor environment quality while achieving a much better energy performance than the code compliance requirements.
The IAQ and thermal comfort of a radiant heating and cooling floor combined with displacement ventilation was monitored in a recently built primary school in Québec, Canada. Despite a good thermal stratification, the air quality measured in the occupied zone was above CO2 acceptable level. In order to improve IAQ, it was proposed to do some tests such as the position of the classroom door opened or closed and the addition of a mechanical assisted exhaust fan. The classroom door, when opened combined with mechanical exhaust fan did have a positive impact on air quality. Results are presented during heating mode condition

KEYWORDS

Thermal comfort, Air quality, School

1 INTRODUCTION

Nowadays, new primary schools in Québec are designed to achieve many goals such as consuming less energy, reducing greenhouse gas while providing a very good indoor environment which contribute to a better academic performance of the students. Gregory Kats 'Greening America's Schools 2006'says 'Greening school design provides an extraordinary cost-effective way to enhance student learning'. A pro-active schoolboard in Québec approached us to monitor the IEQ of two classrooms of one of their new school design. This paper will overview the limitations of the HVAC design and the strategy proposed to improve indoor air quality.

2 STUDY BUILDING

The field measurement was performed in a primary school located in Terrebonne , Québec. A new section framed in Figure 1, was built in 2017.

Figure 1 Marie-Soleil Tougas school

Each classroom of this new section is designed with a radiant floor providing warm or cool water depending of the outdoor temperature. The new classroom is ventilated with displacement diffuser. To avoid the cost of installing two new ventilation units and enlarge the existing mechanical room, the schoolboard chose to replace and upgrade the existing ventilation unit to satisfy the airflow rate requirement. Two classrooms located on the second floor were selected for indoor air quality assessment. Classroom (231) facing north-east and classroom 202 facing south-west. During the contruction, the two classrooms were equiped with different sensors all connected to the building automation system. Table 1 outlines the different sensors installed in the two classrooms.The purpose of those permanent sensors is to allow researchers to get data remotely at any time during the year. The figure 2 shows the air distribution in classroom 202 and the location of the four corner diffusers and the return ventilation grilles.

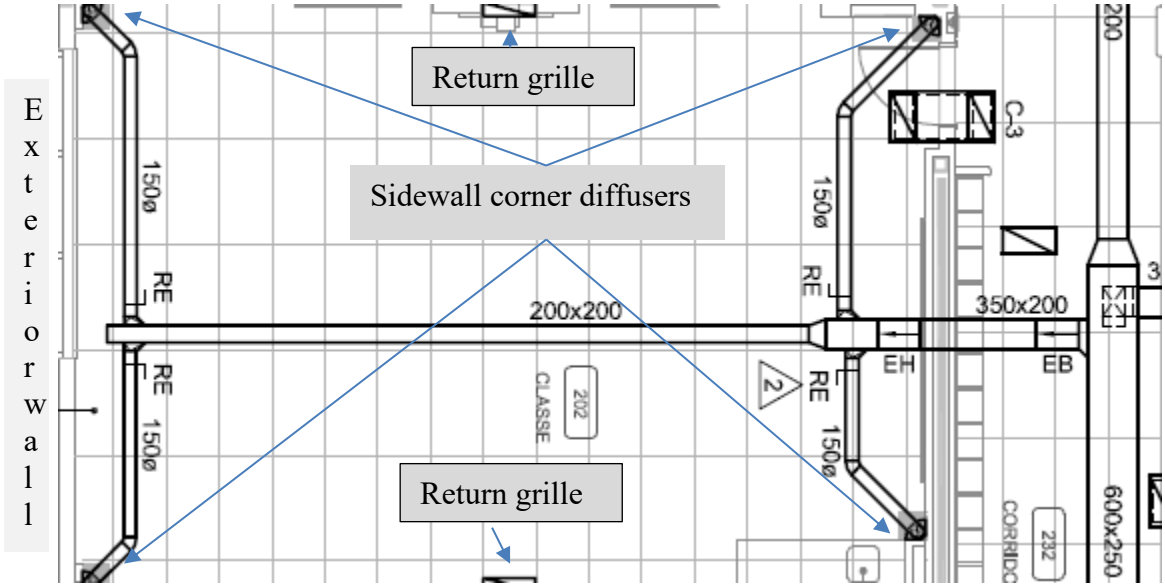

Figure 2 Air distribution in classroom 202

Table 1 list of sensors for continuous monitoring

Type of sensor	Quantity	location
CO2	2	Air diffuser & return duct
Humidity	1	Air diffuser
Air temperature	2	Air diffuser & return duct
Airflow rate	1	Air diffuser
Slab temperature	23	Concrete slab
Operative temperature	1	Classroom wall
BTU meter	1	Radiant manifold

In addition to the sensors listed in table 1, the schoolboard have installed their own sensors to control classroom and floor temperature, and to monitor CO2 in the breathing zone.

2.1 HVAC systems

The HVAC system is designed with a series of geothermal heat pumps providing heating or cooling to the building. The heat pumps are assisted with a thermal accumulator and a back-up electric boiler to maintain geothermal supply water temperature to a minimum of 0 °C. The radiant slab temperature will vary between 18 and 22 °C during summer and 18 and 26 °C during winter.
A central ventilation system is supplying air to all classrooms. The set point temperature of the supply fan can vary between 17 °C and 21 °C. The central ventilation system is supplying fresh and recirculated air to the building. The amount of fresh air will vary with respect to the concentration of CO_2 set to maintain 700 ppm in the return duct. A heat recovery device is also installed as part of the ventilation system.

2.2 Air distribution

The air is distributed in each classroom through a ducting network located below the ceiling. Older classrooms are supplying air through ceiling diffusers and new classrooms have displacement diffusers. The air temperature supplied to the diffusers can increase up to 2 °C between the mechanical room and the classroom located at the farthest distance from the mechanical room.

2.3 Measurement procedure

2.3.1 Measurement location

The performance assessment of the DV system consisted of a monitoring period at three different locations in classroom 202[1]. Figure 3 illustrates the three locations where monitoring was carried out. A picture of the main pole used at the different locations in the classroom is also shown. Location A is close to the exterior wall and slightly outside the occupied zone marked by the dotted line. Location B is within the occupied zone and location C is at the centre of the classroom. In addition to the main pole, a return and reference poles were installed in the classroom, the former to monitor return temperature and CO_2 concentration and the latter to monitor the fluctuation of the temperature of the classroom near the thermostat.

[1] Classroom 202 was selected by the schoolboard to test the effect of mechanical exhaust fan assistance.

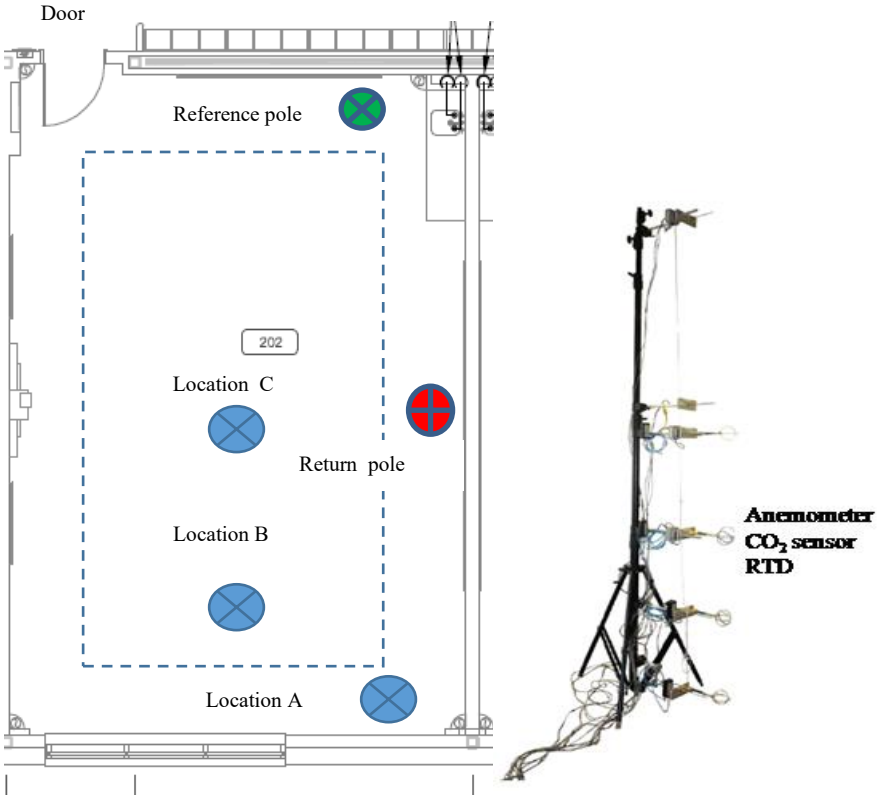

Figure 3 location of the sensors in classroom

2.3.2 Time schedule of measurement

The detailed schedule of measurement is outlined in table 2.

Table 2 Time schedule of the measurement in classroom 202

Location	Start at	Stop at	Door state	Exhaust fan
A	08h00	08h30	open	On
A	08h30	08h55	close	On
break	08h56	09h09	Not monitored	On
A	09h10	09h55	open	On
A	09h56	10h15	close	On
Change of location	10h16	10h19	Not monitored	On
B	10h20	10h45	open	On
B	10h46	11h15	close	On
Lunch time	11h16	12h31	Not monitored	On
C	12h32	12h59	open	On
C	13h00	13h30	close	On
C	13h31	13h44	close	Off
C	13h45	14h15	open	Off

2.3.3 Observations on classroom, ventilation system and climatic conditions

The monitoring session was scheduled on February 26 2019, a winter day in Québec. Table 3 is providing some architectural and ventilation information. Occupancy during the monitoring is also reported. The climatic conditions during that day were as follow:

From 08h00-11h00, the outside temperature was of -14 ºC,with sunny sky.
From13h00-15h00, the outside temperature was of -13 ºC with sunny sky.

The figure 4 shows the temperature and solar radiation profiles obtained from a weather station installed on the roof of the school.

Table 3 Obsevations on classroom

Monitoring date	February 26, 2019
Classroom	202
Orientation	West South West
Floor area (m2)	68.7
Fenestration area (m2)	7.12
Ceiling height (m)	2,77
Number of students	24 +1 teacher
Student age	12
Monitoring period	07h30-14h30
Number & type diffuseurs	4 Corner displacement diffusers
Air flow supplied to the classroom	213 l/s
Air flow exhaust fan	187 l/s[2]

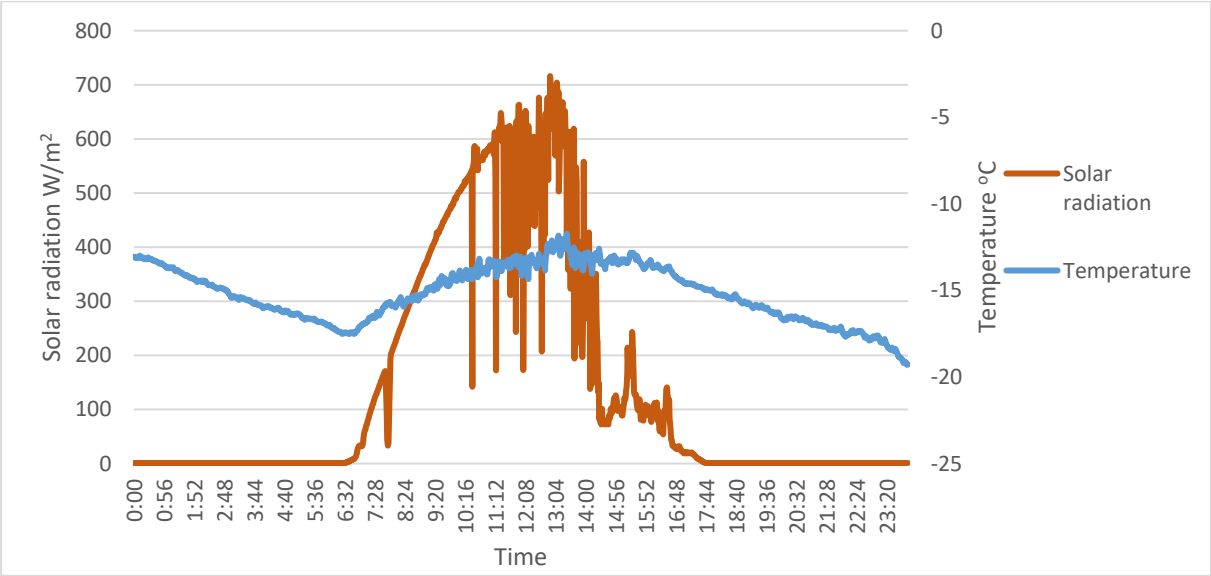

Figure 4 Temperature and solar radiation from a weather station on the roof of Marie-Soleil Tougas school

[2] The exhaust airflow was set to keep the classroom pressure slightly poisitive

This monitoring session was the third one carried out at Marie-Soleil Tougas school. The two previous monitoring sessions were held on March 14 2018, winter condition and September 19 2018, summer condition. During those monitoring sessions, we found that the ventilation airflow and the temperature supplied to the diffusers were not meeting the design specifications. Rebalancing of the ventilation system was then carried out in order to meet the design requirements. Moreover, based on the risk of downdraft observed during the September monitoring session, it was recommended to install a local mechanical exhaust fan ducted to one of the classroom return grille. The schoolboard was highly preoccupied by the high level of CO_2 in the breathing zone and opted for this mechanical assistance to help removing CO_2 from the breathing zone.

2.4 Results

Figure 5 shows the floor temperature, diffuser outlet temperature and operative temperature at 1.1m along the day.

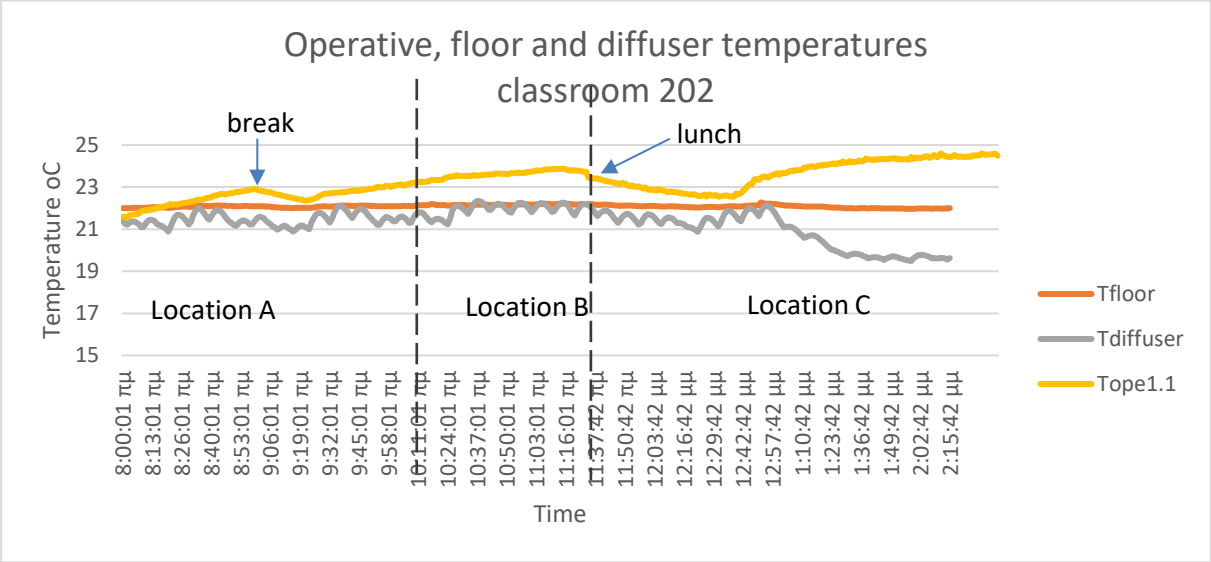

Figure 5 Floor temperature, diffuser outlet temperature and operative temperature at 1.1m

The operative temperature increased from 21.5ºC at the beginning of the monitoring (08h00) up to 24.5ºC at the end of the monitoring (14h15). If we exclude the morning and the lunch breaks where we can observe a temperature drop (empty classroom), the operative temperature profile was constantly increasing specially after lunch when solar radiation reached a peak of 700 W/m^2. This profile is an indication that the classroom was overheated. The temperature of the floor remained constant at 22 ºC and the diffuser temperature fluctuated between 21ºC and 22ºC except for the last hour where we can observe a significant temperature drop.

In figure 6, the average temperature ratio is showing a good stratification for the three locations when the exhaust fan is on. Measurement done with the exhaust fan off (EFO) at location C indicates that mixing ventilation starts to occur at a height of 1.1 m (see rectangle). In figure 7, the average temperature profiles are plotted for the three locations A,B and C with

the classroom door opened (DO) or closed (DC). The door position is clearly showing a difference, with a net advantage for the door open position. With the exhaust fan off, the temperature profiles (dotted curves) does not show any significant differences with respect to the door position. However, there is a significant temperature increase when we compare the temperature profiles, door open and fan on (DO_ABC) with door open and fan off (DO_C-EFO[3]).

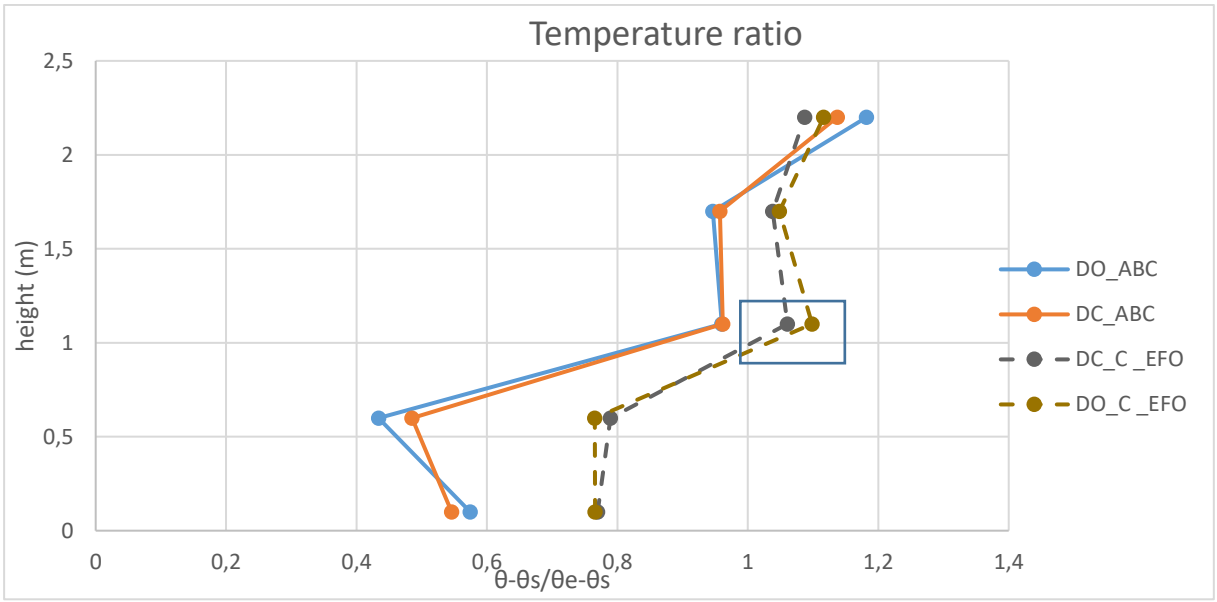

Figure 6 temperature ratio

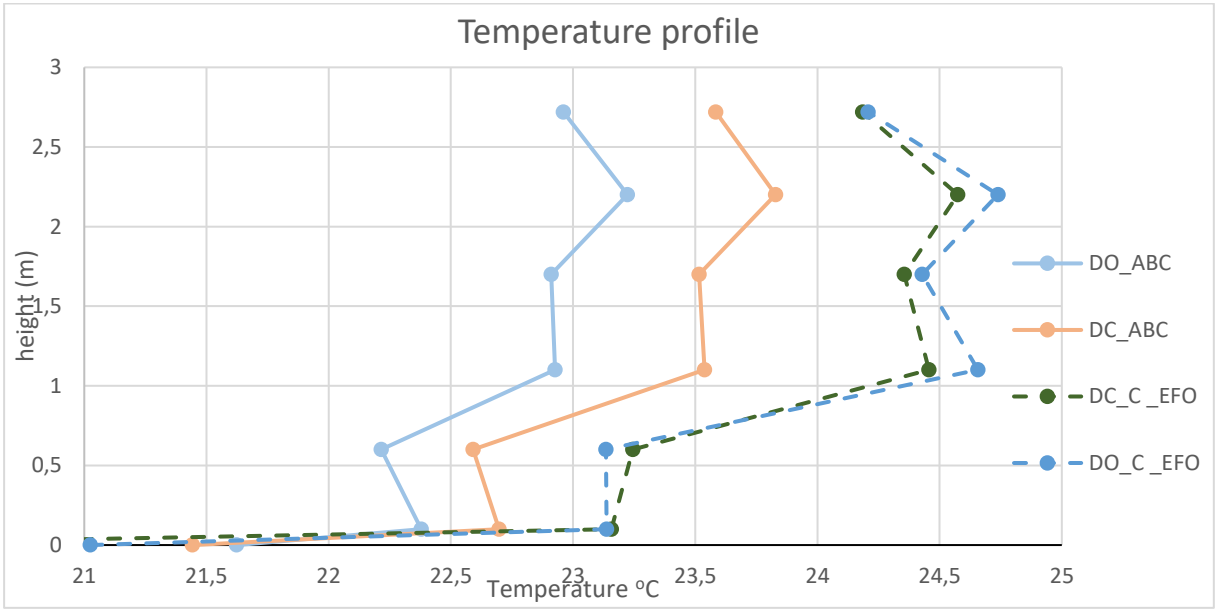

Figure 7 temperature profiles

On figure 8, the average CO_2 profile for the three locations indicates a lower vertical CO_2 concentration when the classroom door is open and exhaust fan switched on. With the exhaust

[3] Due to time restrictions the Exhaust Fan Off (EFO) test was only done at location C

fan switched off, the CO_2 profiles with respect to the door position coincides and are slightly less than the door close profile with the fan on.

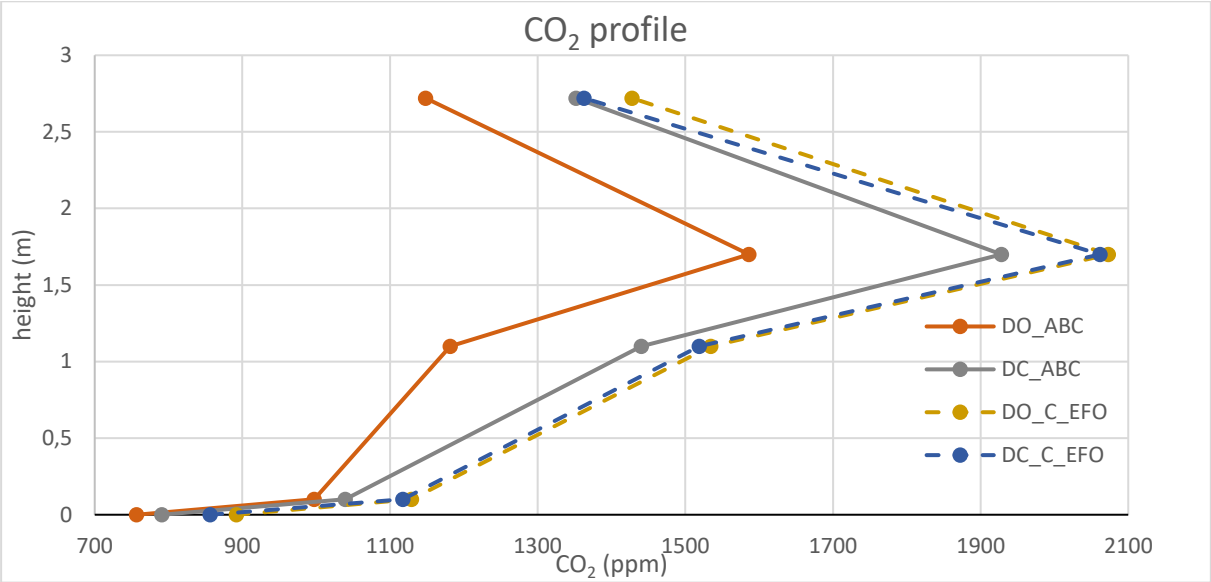

Figure 8 CO_2 profile locations A,B,C

2.5 Discussion

The objective of the monitoring results presented in the previous section was to determine if there was a solution to improve the air quality and thermal comfort of this new section of the Marie-Soleil Tougas School. The assistance of a mechanical exhaust fan have had a positive impact as shown on the temperature and CO_2 profiles (Figures 7 and 8). At 1.1 meters corresponding to the breathing height of seating students, the temperature difference between a classroom door open condition with the assistance of mechanical exhaust fan and a classroom door open condition without the fan assistance was of 1.5°C. Similarly, the CO_2 concentration difference at the same height was of 337ppm. The classroom door position is also beneficial when opened, but this solution cannot be applicable at all time because of potential acoustic issues. The previous results are taking into account the supply air temperature increase of 3 °C and CO_2 concentration increase of 280 ppm along the day.The overall indoor environmental quality could be even better if the supply air temperature at the diffuser is, adjusted to offset the heating loads and if the CO_2 concentration at the diffuser is limited to 700ppm or even lower, as per the building automation control strategy.

3 CONCLUSIONS

Thermal comfort and air quality for primary school students are key parameters to maintain the student's attention throughout the day. Floor heating and displacement ventilation are well suited to provide thermal comfort, good air quality and significant energy savings. However, the specific design of Marie-Soleil Tougas School was found to be more challenging for maintaining a good indoor environment quality. Simple solutions such as the classroom door position and the addition of a local mechanical exhaust fan were tested and the monitoring results showed the positive impact of those strategies. In order to validate this simple solution approach at any time, the monitoring protocol will be applied again in a summer condition.

4 ACKNOWLEDGEMENTS

This project was supported by funding provided by the federal government department of Natural Resources Canada. The authors thank the Commission Scolaire de la Seigneurie des Milles-Iles for giving us access to Marie-Soleil Tougas Public School and GBI Engineering firm responsible for the mechanical design of the Marie-Soleil Tougas School.

5 REFERENCES

ASHRAE Standard 62.1: Ventilation for acceptable indoor air quality. Atlanta: American Society of Heating Refrigerating and Air-conditioning Engineers, Atlanta, Inc. 2010.

ASHRAE Standard 55: Thermal environmental conditions for human occupancy, American Society of Heating, Refrigerating and Air-Conditioning Engineers, Inc. 2004.

ASHRAE Standard 113: Method of testing for room air diffusion, American Society of Heating, Refrigerating and Air-Conditioning Engineers, Inc. 2005.

ASHRAE Standard 129: Measuring air change effectiveness, American Society of Heating, Refrigerating and Air-Conditioning Engineers, Inc. 1997 (RA 2002).

Chen, Q. and Glicksman, L.: System Performance Evaluation and Design Guidelines for Displacement Ventilation, American Society of Heating, Refrigerating and Air-Conditioning Engineers, Inc. 2003.

Causone F. Baldin F. Olesen B W. Corgnati S P. (2010) Floor heating and cooling combined with displacement ventilation: Possibilities and limitations Energy and Buildings 42 pp2338-2352

Kats G.(2006) Greening America's Schools Cost and Benefits, A capital E Report

Skistad, H., Mundt, E., Nielsen, P.V., Hagstrom, K., Railio, J.: Displacement ventilation in non-industrial premises, REHVA, Federation of European Heating and Air-conditioning Associations, GUIDEBOOK No 1, 2002

The evaluation of real-time indoor environment parameters measured in 297 Chilean dwellings

Constanza Molina[1,2], Amy Jackson[1] and Benjamin Jones[*1]

*1 Department of Architecture and Built Environment, University of Nottingham Nottingham, NG7 2UH, UK. *Corresponding author: benjamin.jones@nottingham.ac.uk*

2 Escuela de Construcción Civil, Pontificia Universidad Católica de Chile Avda. Vicuña Mackenna 4860, Santiago, 7820436, Chile

ABSTRACT

People spend the majority of their time in their own homes and so the indoor environmental conditions are an important determinant of population health and wellbeing and have economic consequences. Chile is undergoing rapid economic growth and is managing its national energy demand to minimize its greenhouse gas emissions. Its housing stock is growing rapidly, and is responsible for 15% of national energy demand. Accordingly, there is a need to understand the performance of the stock by measuring parameters that indicate air quality, thermal comfort, and energy demand. This study is a preliminary examination of real-time indoor and outdoor measurements of air temperature made in 297 dwellings during 2016 and 2017 as part of the Red Nacional de Monitoreo de Viviendas (ReNaM) program, implemented by The Ministry of Housing and Urbanism of Chile. Indoor temperatures are generally found to be cold when compared to the European adaptive model of thermal comfort, EN 15251. However, they are above temperature thresholds found to affect negatively the health of vulnerable groups for 78% of the time. There are significant seasonal differences in indoor air temperature but modest differences between day and night time temperatures. The winter temperatures are low, indicating limited effective heating, and households of low socio-economic status are colder than those of mid and high status. There is no evidence of mechanical cooling in the summer.

KEYWORDS

Thermal comfort, adaptive comfort, houses

1 INTRODUCTION

People spend around 70% of time within their own home (Koehler *et al.*, 2018) and so the quality of the indoor air is important. Controlling the indoor air temperature is important for the thermal comfort of occupants, and although varying temperatures may provide thermal alliesthesia (Cabanac, 1971), significant winter variability is associated with respiratory mortality and hospitalizations (Sun *et al.*, 2018), and summer overheating is linked to increased mortality of vulnerable sub-populations, such as the elderly and the very young (Taylor *et al.*, 2018). Therefore, it is important to manage the thermal environment to simultaneously satisfy the occupants, preserve their health, and save energy and corresponding greenhouse gas (GHG) emissions. Many developed countries are implementing retrofitting programs to help meet GHG reduction targets. For example, investments in heating and insulation in three large communities of houses in New Zealand showed that occupants had fewer cold-related health problems, and that the houses were more energy efficient (Howden-Chapman *et al.*, 2012). However, in countries that are industrializing and increasing their technological infrastructure, their national energy demand and GHG emissions tend to increase over time (González-Eguino, 2015) and so it is important to manage them and decouple them from economic growth using a regulatory framework.

Chile is a South American country whose economy is ranked 42nd largest in the world (World Bank, 2016) and had an average annual growth rate of 4.65% (OECD, 2018) between 2003 and 2013. Its houses are responsible for 15.4% of the total final consumption of national energy demand (IEA, 2014), although the contribution of specific services, such as space heating or cooling, is currently unknown. The Chilean housing stock comprises 6.5 million dwellings, where 80% are houses and 18% are apartments (INE, 2018). The majority are located in urban areas, with 57% in and around the capital city of Santiago. They have high occupancy densities when compared to international norms, and 20% are overcrowded. Dwelling energy demand is often correlated with floor area, and over the last 27 years the mean floor area of new dwellings has increased by around 40%, from 57m^2 in 1990 to 82m^2 in 2015 (INE, 2016). In order to understand the performance of its stock, The Ministry of Housing and Urbanism of Chile (MoH) has implemented a monitoring program of houses known colloquially as the Red Nacional de Monitoreo de Viviendas (the National Network of Housing Monitoring), or ReNaM. Real-time sensors are located in 299 houses in five towns and cities measuring air temperature, relative humidity, sound pressure level, and CO_2.

This paper evaluates the outputs of ReNaM's to evaluate the indoor environment in Chilean houses. The focus is restricted to the impacts of temperature on thermal comfort and its relationship with the socioeconomic status of Chilean households. Section 2 describes the ReNaM monitoring network, its equipment, and dataset. Section 3 assesses the thermal conditions found in the monitored dwellings using a model of thermal comfort, any seasonal variability, and relationships between temperatures and groups of dwellings and households, such as dwelling location and household socio-economic status. Section 4 discusses the results.

2 METHOD

2.1 Measurement Locations

Chile is a continental territory with a north to south length of 4,300km and an average width of 177km. Its mean annual air temperature varies by up to 6°C laterally and by more than 15°C longitudinally, and differences in relative humidity are similarly well defined (Castillo, 2001). Five locations were chosen by the MoH to reflect this climatic variation (see Figure 1) and real-time sensors (see Section 2.2) are currently installed and operational in 299 houses located in the north (n=28), south (n=60), and centre (n=211) of the country. Most are located in the metropolitan and capital region of Santiago de Chile (n=150). The sample is not statistically representative of the housing stock (Molina *et al.*, 2017), but statistical methods can be applied to generalise findings. Therefore, the data are expected to identify broad trends in indoor environment quality and highlight areas worthy of more detailed investigations.

Figure 1: Chile (red) and the five ReNaM monitoring locations.

The northern city of Antofagasta lies on the Tropic of Capricorn and has mean daily dry bulb air temperatures, $\bar{T}_o$ (°C), between $12.73 \leq \bar{T}_o \leq 21.75$ (Meteotest, 2017). Valparaiso & Viña del Mar are coastal towns located in the centre of the country with $4.58 \leq \bar{T}_o \leq 26.23$. Santiago is the national capital city. It is inhabited by 41% of the population, its stock is comprises 2.4 million houses (INE, 2018), and $4.08 \leq \bar{T}_o \leq 24.41$. Temuco is located 700km south of Santiago where $1.28 \leq \bar{T}_o \leq 21.49$. Coyhaique is a small town located 1400km south of Santiago in the Patagonia region where $-8.13 \leq \bar{T}_o \leq 26.23$. All five locations are polluted (MMA, 2017; Jorquera & Berraza, 2013; Toro *et al.*, 2014; Koehler *et al.*, 2019). Antofagasta is contaminated with NOx and SO_2 from local foundries, and the other locations have ambient $PM_{2.5}$ (particulate matter with a diameter of ≤2.5μm) concentrations that exceed WHO thresholds

attributable to vehicles, industries and wood burning. Santiago's urban density and meteorological conditions also contribute to its pollution.
The monitoring was preceded by a survey that provides information about the location (region, town/city, and commune), the dwelling (type, construction year, storeys, floor area, orientation, envelope materials, number of windows, glazing properties, and heating system), the householders (income (see Table 1), energy bills, health issues), and behaviours (heating months, weekday and weekend occupancy, smoking).

Table 1: Classification of Socio Economic Level. Sources: Renam, 2018; INE, 2003.

Family monthly income* **(Chilean Pesos, CLP)**	**Socio-economic level (ReNaM)**	**Corresponding socio-economic decile (National classification)**
>CLP 1 450 000	high	10
CLP 550 000 – CLP 1 450 000	medium	8-9
< CLP 555 000	low	1-7

**1 UK Pound ≡ 872 Chilean Pesos; 1 US Dollar ≡ 666 Chilearn Pesos*.

2.2 Equipment

The *Netatmo* weather station (Netatmo, 2018) is a *consumer* grade device that comprises indoor and outdoor modules, and requires little or no maintenance by the host. Both record dry bulb air temperature and relative humidity, but the indoor module also measures noise, and CO_2. They are factory calibrated. The sensors are located away from direct heat sources in the living room, although some are located in a bedroom. They sample and upload the data to an online database every 30 minutes. Measurements started in 2016 and are ongoing. The platform is accessible online (ReNaM, 2018) to registered users and contains the approximate location of each sensor and all surveyed and measured data.

2.3 Assessing Occupant Comfort

Thermal comfort is not solely determined by the indoor air temperatures and can be influenced by personal and environmental factors (ASHRAE, 2010), making it subjective. Chilean dwellings generally use windows for ventilation, and are *free running* during the summer. Therefore, occupants are expected to take adaptive measures to maintain their comfort. During the winter, the most common heating system is a stove (INE, 2003).
Perez-Fargallo *et al.* (2018) investigated the application of international adaptive models of thermal comfort, including EN 15251 (BSI, 2007), to low income families in the south of Chile (14 dwellings; 121 occupants). The dwellings were monitored for 7 months during the winter and occupant thermal preferences were surveyed. The measurements were compared to EN 15251 and showed that the occupants of these dwellings were more tolerant to cold temperatures than the model predicts. They then propose a model of adaptive thermal comfort that solely applies to social dwellings located in the south of Chile. Section 2.1 shows that only 60 ReNaM dwellings are located in the south and so we apply the European adaptive model described by EN 15251 (BSI, 2007) to all dwellings. The thresholds of comfort (°C) are given by

$$T_{C_{max,min}} = 0.33T_m + 18.8 \pm X \quad (1)$$

where $X = 2°\mathrm{C}$ is appropriate for a free running naturally ventilated spaces, and T_m is the running mean of the ambient air temperature where

$$T_m = (1 - \alpha_{rm})T_{E-1} + \alpha_{rm}T_{rm-1} \quad (2)$$

Here, $\alpha_{rm} = 0.8$ is used as the running mean constant, T_{E-1} (°C) is the previous day's daily mean ambient temperature, and T_{rm-1} (°C) is the previous day's running mean temperature.
Many households are in energy poverty, where they spend more than 10% of their income on heating to achieve a satisfactorily warm environment (Boardman, 1991). This is particularly

problematic in the south of the country where 61% of households are in energy poverty (Reyes *et al.*, 2019). Therefore, this is assessed in Section 3.

2.4 Data Processing and Statistical Analyses

To date, over 100 million data entries have been recorded. The raw dataset comprises measurements from all houses and was parsed using bespoke MATLAB® code (Mathworks, 2018) to allocate it to individual dwellings, and to remove duplicate entries. The statistical tool *R* (R Core Team, 2018) was used to interrogate the data and provide summary statistics. In 45% of dwellings data was either corrupted or missing for some periods of time. Dwellings were removed from the analysis if they had missing data for the entire monitoring period, leaving a sample of 297 dwellings.

To test the integrity of the measured data and to choose appropriate statistical tests, tests of normality are applied to the dataset in Section 3. Analysis of Variance (ANOVA) or Kruskal-Wallis (*ks*) tests were applied performed to normally and non-normally distributed data, respectively. When there is a large quantity of data the West reference criteria for a substantial departure from normality are used rather than a *ks*-test (West *et al.*, 1995). A *post hoc* analysis tested the nature of any differences. All tests use a 5% significance threshold.

A coefficient of variance, CV, is the standard deviation value of interest of a group divided by its mean. It is used to compare difference parameters and consistency in the results. A value CV>1 shows that it is highly variable.

3 RESULTS

3.1 Indoor Thermal Conditions

Figure 2 is cumulative distribution function (CDF) of internal and external air temperatures measured inside and outside of all 297 dwellings. It shows that the ambient air temperatures varied between 0-35°C and indoor temperatures varied between 5-30°C. Median temperatures for winter day and night times are 17.0°C and 16.3°C, respectively, and 24°C and 23.5°C for summer day and night times, respectively.

Collins (1993) suggests that, for vulnerable groups, temperatures below 16°C increase the risk of respiratory diseases; below 12°C may cause cardiovascular strain from cold; and below 6°C may cause the failure of thermoregulation and hypothermia. The WHO recommends indoor temperatures of 18-21°C for clothed sedentary occupants to avoid potential health risks (WHO, 2007). These thresholds are mapped onto Figure 2 and show that Collin's thresholds are achieved around 78% of the time. The WHO limits are met around a third of the time.

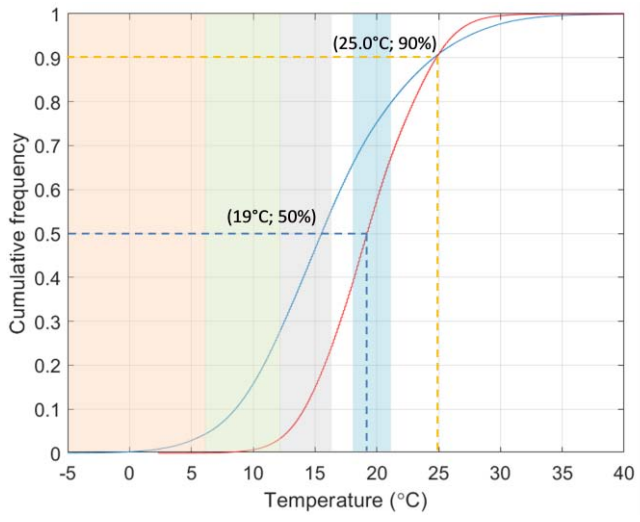

Figure 2: CDF of internal (red) and external (blue) air temperatures for all dwellings. Orange, green and grey areas correspond to Collins's (1993) health risk thresholds. The blue area shows WHO limits. The dashed blue line shows the median of 15°C and the dashed orange line shows that indoor median of 90% of the time the indoor air temperature is higher than the outdoor air temperature.

The CIBSE (CIBSE, 2015) recommends an upper limit of 25°C and 23°C in the living rooms and bedrooms respectively, of naturally ventilated dwellings in the UK. It defines an overheating dwelling as one where the indoor operative temperature is 3°C above these limits. Here, this only occurs around 10% of the time, by considering the operative temperature

equivalent to the air temperature. Figure 3 illustrates how using a daily mean temperature as a key indicator can disguise both the extremes of temperatures and variance between them. A knowledge of occupant exposures to low and high temperatures may help to identify adverse conditions and health consequences.

3.2 Seasonal and daily variability

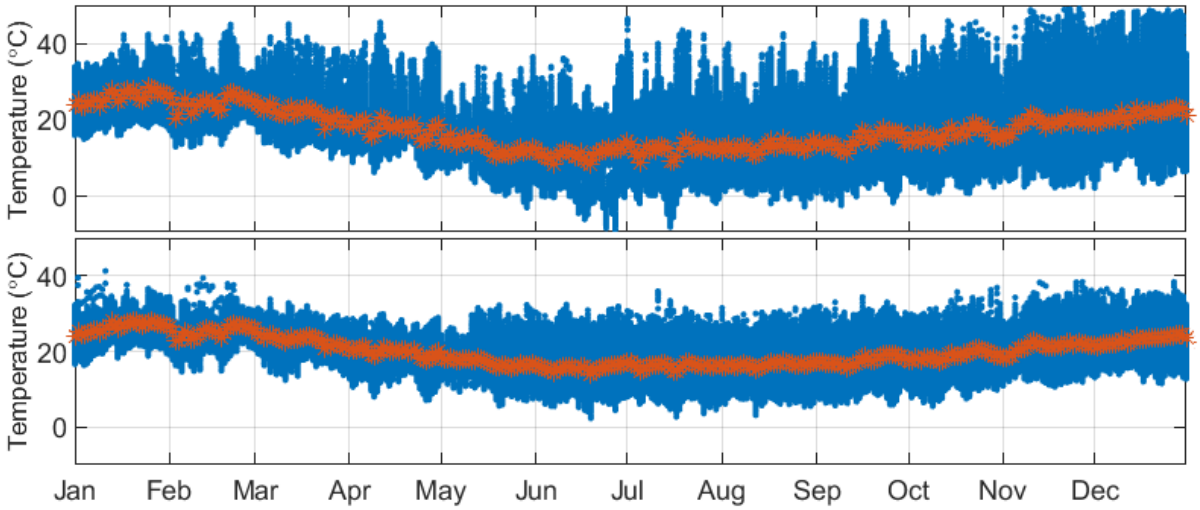

Figure 3: Sampled air temperatures (blue) outside (top) and inside (bottom) with daily average temperatures (orange) in all 297 houses during 2017.

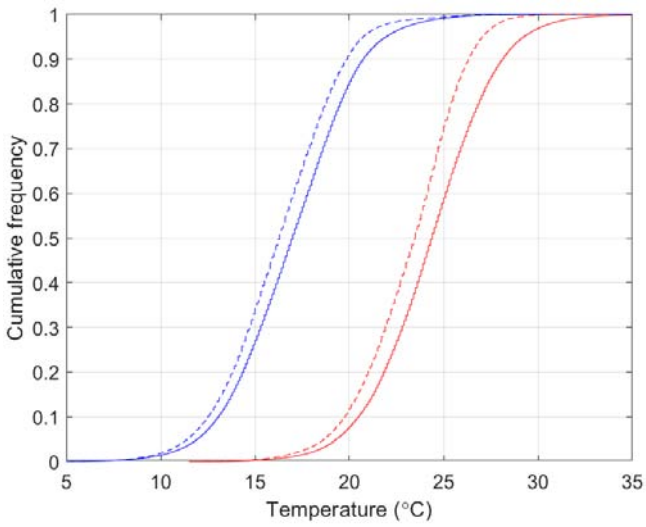

Figure 4: Internal temperatures (continuous) and ambient (dashed) in winter (blue) and summer (red).

Analysis of the summer and winter temperatures shows seasonal differences and highlights their impact on thermal comfort. Winter is considered to be between 21st June and 21st September. The data is divided further into day and night times where a day starts at 7am and finishes at 10pm. Figure 4 shows that the seasonal variation is large, but Figure 5 shows that day and night temperatures differences for each season are small. The low temperatures in the winter suggest that there is limited effective winter heating in the dwellings. Heating only when dwellings are occupied should be reflected by bi or multi-modal distributions. A West reference criterion indicates that the groups of indoor temperatures are each moderately normal, except for the summer night time data and so it is likely that heating was either continuous or non-existent and the dwellings are free running. Further analysis is required.

The low night time air temperatures may help the occupants sleep; for example, CIBSE (2015) shows that temperatures as low as 12°C can improve sleep quality, although occupants require appropriate bed-clothing.

3.1 Socio-Economic Differences

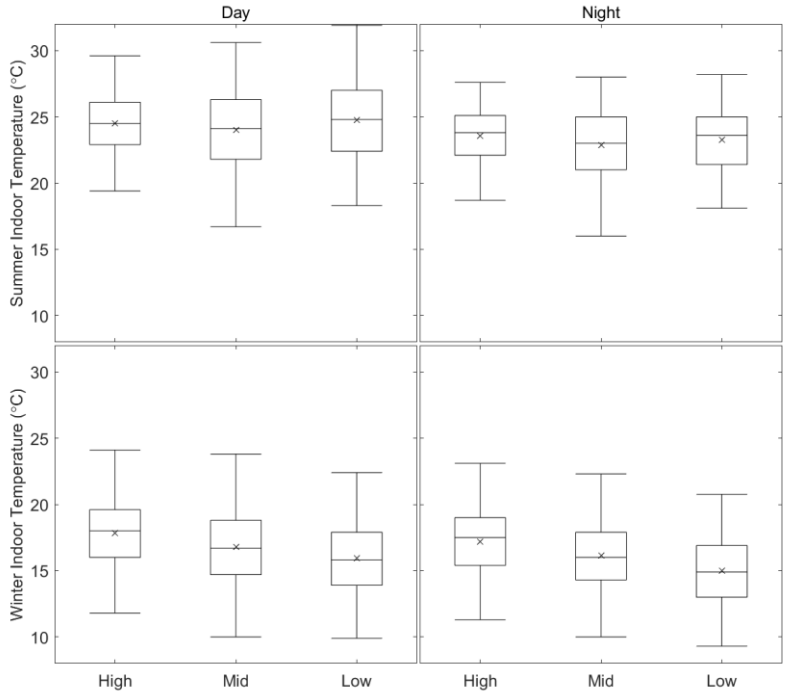

Figure 5: A comparison of winter and summer, day and night, indoor air temperatures by socio-economic status.

To investigate whether the socio-economic status of each house has an impact on thermal comfort, the data was further divided into the three socio-economic level categories given in Table 1; see Figure 5. An ANOVA test is used to determine if the results obtained for thermal conditions from different socio-economic classes are significantly different from each other. It shows that there is a casual inference that different socio-economic levels result in different mean indoor air temperatures, especially for winter days and nights (all p-values $<<0.05$). A further *post hoc* test highlights the exact nature of the difference. In the summer day time, the high socio-economic class is significantly different to the low and middle classes, but the middle and low classes are not significantly different from each other. In the summer time there is no difference between the classes, whereas during the winter, all socio-economic classes are significantly different from each other. The magnitude of this significance were calculated using the means of the two variables being compared and contrasted with *Cohen's r* thresholds (Cohen, 1977). Between high and low socio-economic classes, medium and high effects are found for winter days and nights respectively.

3.2 Analysis of Groups

Thermal comfort boundaries are calculated as a function of the running mean using Equation (1). The outdoor running mean is calculated using Equation (2) and measured outdoor air temperatures. Figure 6 shows the indoor air temperatures in a single ReNaM dwelling during 2017. House 39 is a new heavy weight apartment located in Santiago occupied by a household with high socio-economic status. It is used for illustrative purposes because it is one of two dwellings that has the highest percentage of measurements within the thermal comfort boundaries. Coloured dots show day and night indoor temperatures.

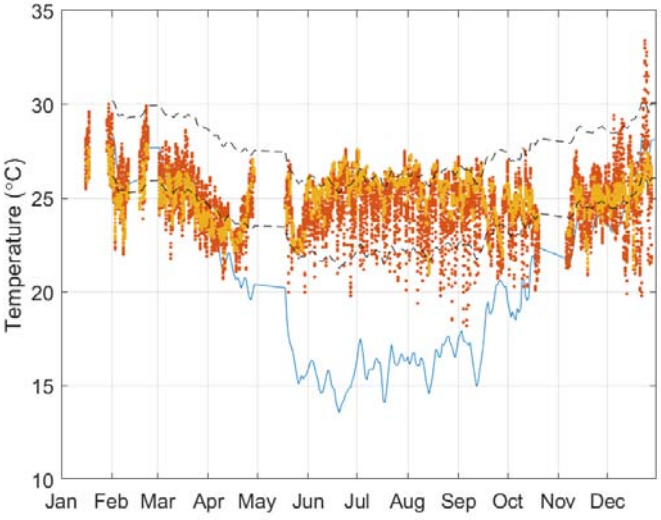

Figure 6: House 39 indoor temperatures for 2017 during the day (red), at night (orange), thermal comfort limits (black dashed), and outdoor running mean temperature (blue).

The percentage of time each measurement of temperature falls inside and outside the thermal comfort boundaries are calculated for all 297 dwellings individually. The median time the indoor air temperature falls within the thermal comfort boundaries is 12%; see Figure 7. A median of 86% temperature measurements fell below the comfort zone, and a median of 0.2% were above. This indicates that the dwellings are cold and do not require mechanical cooling in the summer.

The data now aggregated by the three ReNaM socio-economic classes; see Table 1. The median time the temperature measurements fall within the comfort zone is between 10% (for low status) and 15% (for high status), below the comfort zone is between 87% (low) and 82% (high), and the time above the comfort zone is<1%. Figure 8 (left) shows that a significant majority of dwellings in the three groups spend more time below the comfort zone. Kruskal-Wallis tests show that the differences in the time spent in the thermal comfort zone are significantly affected by socio-economic class (p = 0.02). Focused comparisons of the medians between socio-economic classes (using a Mann-Whitney test as the *post hoc* test) shows that the proportion of time spent in the thermal comfort zone is only significantly different when the low class was compared to high ($p < 0.05$). The variability of this percentage within each of the groups can be considered *low* for the High and Mid socio-economic classes ($CV_{High} < CV_{Mid} < 1$) and *large* for the Low class group ($CV_{low} > 1$) (see Figure 8 right).

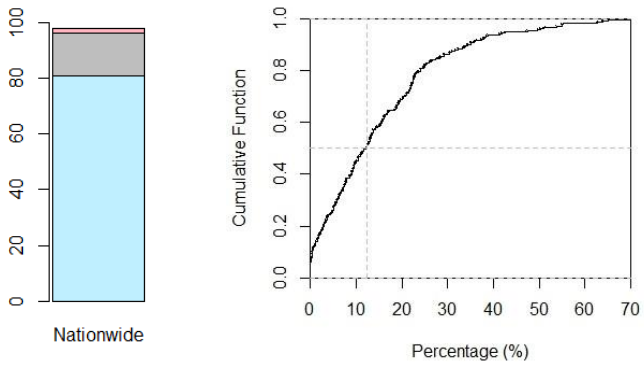

Figure 7: Left: Proportion of the time in each zone (*below comfort* in blue, *comfortable* in grey, and *above comfort* in pink) Percentages correspond to the means and so they do not add up to 100%. Right: Empirical cumulative distribution function of the proportion of recorded data in the comfort zone nationwide (grey area on the left). Only 12% of the houses considered are comfortable for >50% of the recorded time.

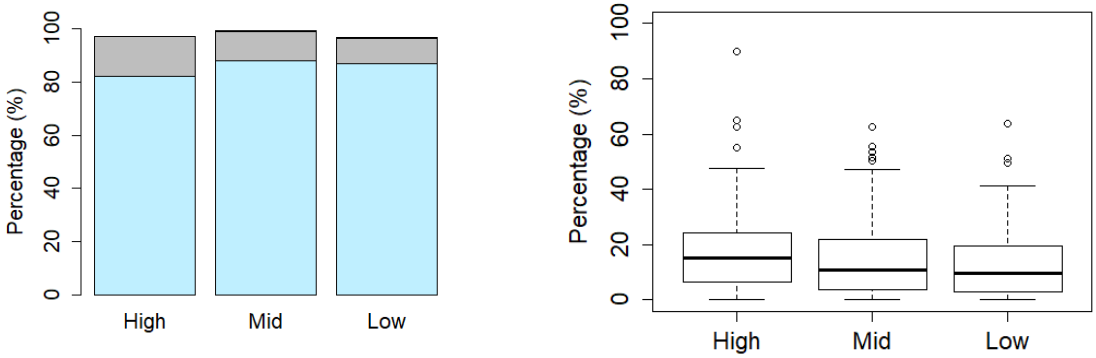

Figure 8: Left: Proportion of the median time within each comfort area by each socio-economic (SE) group (*below comfort* in blue, *comfortable* in grey, and *above comfort* in pink). Percentages correspond to the means and so they do not add up to 100%. Right: Boxplot of the percentage of the time within the thermal comfort zone (grey area on the left figure) for houses categorised in each of SE class.

A similar analysis can analyse the thermal comfort variability within and between each location. The variability of the time the measurements fall within the comfort zone within each location can be considered as low except for Antofagasta ($CV_{Coyhaique} < CV_{Santiogo} < CV_{Temuco} < CV_{Valparaiso} <$

1 <$CV_{Antofagasta}$) the northern most location; see Section 2.1 for locations and Section 2.4 for test statistics. The Kruskal-Wallis test showed a significant difference between the groups of locations, ($p << 0.05$). Focused comparisons of the medians showed that the proportion in the thermal comfort zone were only significantly different when Valparaíso's dwellings were compared to those of the other locations ($p < 0.05$).

Finally, both a Kruskal-Wallis test (here reported using H(degrees of freedom) and a p value) and *post-hoc* multiple comparison tests showed no significant differences when applying other grouping categories. For example, dwellings are classified by the weight of their construction materials (subjectively recorded as *heavyweight*, *lightweight*, or *mid-weight*) where $H(2) = 5.592$ and $p = 0.13$, by year of construction (periods: *< 2000*, *2000-2007*, *>2007*) where $H(1) = 2.351$ and $p = 0.31$, and by geometry (recorded as *detached*, *one* or *two shared walls*, or *flat*) where $H(3) = 10.811$ and $p = 0.14$, showing that none are significant. The latter analysis may have been affected by the way geometry was recorded. Some dwellings were not categorized and were only classified as *house*.

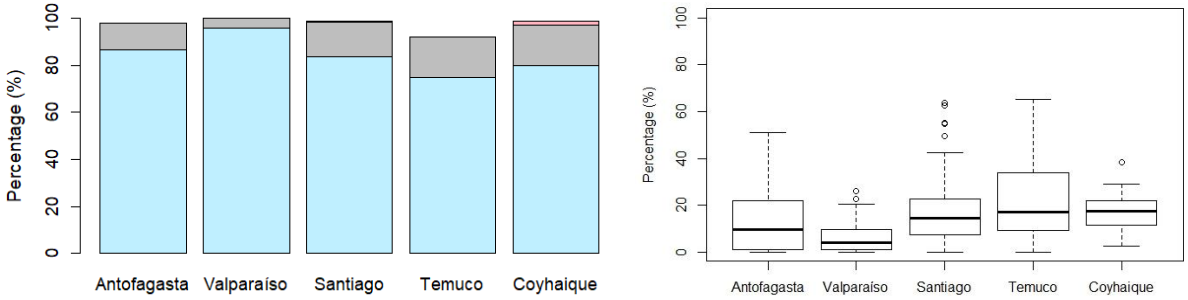

Figure 9: Left: Proportion of the median time within each comfort area (*below comfort* in blue, *comfortable* in grey, and *above comfort* in pink) by each ReNaM location arranged from North to South. Percentages correspond to the means and so they do not add up to 100%. Right: Boxplot of the percentage of the time within the thermal comfort zone for houses located in each of the five locations. Variability of the time in the comfort zone (grey area on the left figure) for each group of houses.

4 DISCUSSION

Chile has highly variable weather and environmental conditions, energy demands, socioeconomic status (the socioeconomic composition of each region and available economical resources), social gaps, lifestyles and habits. Therefore, obtaining a representative sample of houses that encapsulates this variation is a significant challenge. Misunderstanding or ignoring the variability in the stock and their probability of occurrence could lead to the inaccurate quantification of problems or to the inaccurate characterization of the *status quo*. Nevertheless, the ReNaM contains highly valuable information that can inform our understanding of the current stock, the way people use it, and how it might be modelled. Therefore, its analysis will provide guidance on future data gathering and areas of research.

There are a large number of missing data points in the dataset. This could be a function of sensor malfunction, poor internet accessibility, or power failure. In addition, there is little information about the specific location of each sensor within individual dwellings. The integrity of the analysis of the dataset is dependent on the quality of its data. Therefore, it is important that the location of all sensors is as consistent as possible. The large number of dwellings, participating in the survey (around 300) makes it likely that there is variation in their locations and some may be suboptimal; for example, they may be in direct sunlight or close to heat sources and sinks. Figure 3 shows that there are clear issues with this both inside and out. However, hosting households were advised on appropriate locations for their sensors and, giving the sheer quantity of measurements, it is hoped that confounded data appear as outliers in the analysis. There are also known limitations of *consumer-grade* IAQ monitors; see Singer *et al.* (2018). All sensors require periodic calibration, but the ReNaM devices are not routinely examined. Therefore, the outputs of these devices can be considered indicative rather than exact.

It is important to be cautious when interpreting the ReNaM data because there is little information on occupancy patterns, clothing, activities, personal preferences, or thermal satisfaction, making it difficult to assess the actual risk of exposures to low temperatures and thermal comfort. Accordingly, it is too early to make firm judgments or to draw conclusions on the state and issues of the housing stock and further work is required.

Future work should consider the appropriateness of the European comfort model EN 15251 in a Chilean context. Perez-Fargallo *et al.* (2018) also found that dwellings were cool when compared against EN 15251 criteria and proposed modifications to a limited type of dwellings. Section 3 confirms that EN 15251 find dwellings are cool and so this work should be continued to apply it to the majority of Chilean dwellings. It is possible that Chileans like their dwellings cold, and although this may be good for moderating the national energy demand, Collins (1993) shows that they may adversely affect health and quality of life. It is important to note that high socio-economic households are cold. They could be because they are empty during the day and so the data from these houses needs to be tested individually for multimodality.

An analysis of comfort should be combined with an assessment of domestic heating systems and dwelling airtightness and insulation. Most dwellings use *ad hoc* decentralized heaters, such as wood burners, which also decrease the quality of the ambient air quality. Any improvement in heating systems should be combined with energy efficiency measures to minimize *take back*, the reduction in expected gains from technologies that increase energy efficiency attributable to behavioural or other systemic responses.

Future analyses should also consider the other measured parameters; see Section 2.2. Sound pressure levels and CO_2 concentrations could indicate occupant presence and patterns. Steady state CO_2 concentrations and their decay over time could indicate ventilation rates, albeit with uncertainty. Indoor relative humidity could identify the risk of mould growth, especially in the south of the country.

5 CONCLUSIONS

Indoor temperatures in Chilean dwellings are generally found to be cold when compared to the European adaptive model of thermal comfort, EN 15251, even in the northern city of Antofagasta. However, they are above temperature thresholds found to affect negatively the health of vulnerable groups for 78% of the time.

There are significant seasonal differences in indoor air temperature but modest differences between day and night time temperatures. The winter temperatures are low and suggest that there is limited effective heating in dwellings.

The socio-economic status of householders significantly affects indoor temperatures during winter days and nights, and the time spent in within EN 15251 thermal comfort boundaries. Low socio-economic status households are colder than those of mid and high households in the winter. There is no difference between economic groups during the summer.

When dwellings are grouped by their location, the median time indoor temperatures were in the comfort zone were found to be broadly similar, except in the coastal towns of Valparaiso & Viña del Mar. The greatest variability was found in the northern city of Antofagasta. Comfort is not found to be a function of dwelling type, construction materials, or construction period.

6 ACKNOWLEDGEMENTS

The authors acknowledge DITEC-MINVU for granting academic access to ReNaM database.

Constanza Molina is funded by the CONICYT-Chile (Commission of Scientific and Technologic Research of Chile) “Becas Chile” Doctoral Fellowship Programme, 2015; Grant No. 72160504.

7 REFERENCES

Abdi, H. Coefficient of variation. Encyclopaedia of research design, 1, 169-171. 2010

ANSI/ASHRAE, Standard 55 Thermal Environmental Conditions for Human Occupancy. 2010.

Boardman, B., Fuel poverty: from cold homes to affordable warmth. 1991, London: Bellhaven Press.
BSI. EN 15251. Indoor Environment Input Parameters for Design and Assessment of Energy Performance of Buildings Addressing Indoor Air Quality, Thermal Environment, Lighting and Acoustics. London. 2007.
CIBSE, TM52: The limits of thermal comfort: avoiding overheating in European buildings. 2013: London.
CIBSE. Guide A - Environmental Design. London, UK. 2015.
Cabanac, M., Physiological role of pleasure. 1971. 173(4002): p. 1103-7.
Castillo, C. Estadística climatológica. Dirección meteorológica de Chile. Santiago, Chile. 2001.
Cohen, J., Statistical power analysis for the behavioral sciences. 1977, Academic Press.
Collins, K.J., 1993. Cold-and heat-related illnesses in the indoor environment. Unhealthy housing: research, remedies and reform. London: E and FN Spon.
González-Eguino, M., Energy poverty: An overview. Renewable and Sustainable Energy Reviews, 2015. 47: p. 377-385.
Howden-Chapman, P., et al., Tackling cold housing and fuel poverty in New Zealand: A review of policies, research, and health impacts. Energy Policy, 2012. 49(C): p. 134-142.
METEOTEST. 2017. Meteonorm. In: METEOTEST (ed.) Version 7 ed. Switzerland: Meteotest.
MMA, Ministerio del Medio Ambiente., Tercer Reporte del Estado del Medio Ambiente. 2017.
IEA. Energy Efficiency Indicators: Essentials for Policy Making. International Energy Agency. 2014.
INE. 2003. Censo de Población y Vivienda 2002. Instituto Nacional de Estadísticas, Santiago, Chile.
INE. 2016. Demografía nacional y regional. Instituto Nacional de Estadísticas. Santiago, Chile.
INE. 2018. Censo de Población y Vivienda 2017. Instituto Nacional de Estadísticas, Santiago, Chile.
Jorquera, H. and Barraza, F., 2013. Source apportionment of PM10 and PM2. 5 in a desert region in northern Chile. Science of the Total Environment, 444, pp.327-335.
Kavouras, I.G., *et al.* 2001. Source apportionment of PM10 and PM25 in five Chilean cities using factor analysis. Journal of the Air & Waste Management Association, 51(3), pp.451-464.
Koehler, K., *et al.* 2019. The Fort Collins commuter study: Variability in personal exposure to air pollutants by microenvironment. Indoor air, 29(2), pp.231-241.
Molina, C. *et al.* 2017. The Development of Archetypes to Represent the Chilean Housing Stock. 38th AIVC Conference, Nottingham, UK.
Netatmo. 2015. Personal weather station https://www.netatmo.com/en-GB/product/weather/weatherstation (accessed 02 July 2018).
Perez-Fargallo, A., *et al.*, Development of a new comfort model for low income housing in the central-south of Chile. 2018, Energy and Buildings. p. 94-106.
R Core Team. 2018. R: A language and environment for statistical computing. R Foundation for Statistical Computing, Vienna, Austria. URL https://www.R-project.org/.
ReNaM (Red Nacional de Monitoreo de Viviendas). National Housing Monitoring Network. http://renam.cl/site/acerca-de [Access date: 15/03/2018]
Reyes R, *et al.* Controlling air pollution in a context of high energy poverty levels in southern Chile: Clean air but colder houses?. Energy Policy. 2019 Jan 1;124:301-11.
Singer B. Delp, W. Response of consumer and research grade indoor air quality monitors to residential sources of fine particles. Indoor Air 28(4) 34-639. 2018.
Sun, S. *et al.* 2018. Seasonal temperature variability and emergency hospital admissions for respiratory diseases: a population-based cohort study. Thorax, 73:951-958. 2018.
Taylor, J., et al., Estimating the Influence of Housing Energy Efficiency and Overheating Adaptations on Heat-Related Mortality in the West Midlands, UK. 2018.
Toro, R., *et al.* 2014. Inhaled and inspired particulates in Metropolitan Santiago Chile exceed air quality standards. Building and Environment, 79, pp.115-123.
West, S., J. Finch, and P. Curran, Structural equation modeling: concepts, issues and applications. 1995, Sage: Newbury Park, CA. p. 56-75.
World Bank. Chile Overview. 2018 [cited 2018 19 December]; Available from: https://www.worldbank.org/en/country/chile/overview.
WHO. Housing, energy and thermal comfort: a review of 10 countries within the WHO European Region. Copenhagen: WHO Regional Office for Europe; 2007.

Ventilation and Measured IAQ in new US homes

Iain Walker *, Brett Singer, and Rengie Chan

Lawrence Berkeley national Laboratory
1 Cyclotron Rd.
Berkeley, CA. USA
**Corresponding author: iswalker@lbl.gov*

ABSTRACT

As newer homes are being built tighter than the existing housing stock, questions have been raised about the concentrations of pollutants of concern in new homes and how mechanical ventilation systems can address this issue. This study measured pollutants of concern in 70 new homes with mechanical ventilation in California, USA and compared the results to a previous study of home without mechanical ventilation. The key pollutants were measured using both time-integrated and time-resolved over a one-week period and included formaldehyde, PM2.5 and NO_2. Each home was tested for air flows of mechanical systems, together with house envelope and forced air heating and cooling duct leakage. The results show that the homes complied with dwelling unit ventilation fan flows and most of the time with kitchen and bathroom requirements. The measured pollutant concentrations were almost all within acceptable limits and showed that the installed ventilation flow rates (that complied with California building standard and ASHRAE 62.2 requirements) provided acceptable indoor air quality. The mechanically ventilated homes had more consistent ventilation, resulting in less extreme pollutant concentrations. However, there remain issues with system operation, e.g., poor labeling of easily accessible controls led to three-quarters of the dwelling unit ventilation systems being turned off when homes were first visited for this study. This paper summarizes the results of the diagnostic testing and time-integrated field measurements, together with implications for ventilation standards.

KEYWORDS

Ventilation performance; formaldehyde; nitrogen dioxide; particles; field study

1 INTRODUCTION

This study aimed to answer the question: Do current U.S. ventilation requirements in new homes result in acceptable indoor air quality? To answer this question we performed diagnostic tests and field measurements of pollutants in 70 new California homes that have mechanical ventilation. This was part of the Healthy New Gas Homes (HENGH) study – a joint US Department of Energy and California Energy Commission study that also included occupant surveys in over 2700 homes and energy simulations to determine optimum air tightness. The complete study can be found in Chan et al. (2018) and is available as a contributed report to the AIVC. Homes were monitored for one week and study participants were asked to rely on mechanical ventilation and avoid window use during the testing. The households were all non-smoking. All homes had a venting kitchen range hood or over the range microwave and bathroom exhaust fans. The dwelling unit ventilation systems complied with California building standards that were based on the ASHRAE 62.2-2010 fan sizing requirements that were current at the time the California standards went in to force. This paper presents summary results of time-integrated formaldehyde, NO_2, and $PM_{2.5}$ measurements together with a summary of home and ventilation system characteristics, CO_2, temperature and humidity. Formaldehyde, NO_2, and $PM_{2.5}$ are the key contaminants of concern in homes with the greatest health impact (Logue et al. (2012)). The results are compared with a prior California New Home Study (CNHS (Offermann (2009))) that monitored pollutants over a 24-hour period in 108 homes built between 2002 and 2004, that did not have whole-dwelling mechanical ventilation.

2 FIELD TESTING

2.1 Diagnostic tests

Air leakage of the building envelope and forced air heating and cooling system was measured with the DeltaQ test (Method A of ASTM-E1554-2013) using a TEC Minneapolis Blower Door System with DG-700 digital manometer. The DeltaQ test determines the air leakage associated with the forced air system at its normal operating conditions, and simultaneously provides the results of a multi-point envelope leakage test that is approximately compliant with the ASTM E779 test method. Airflows of exhaust fans for dwelling ventilation, kitchens and bathrooms were measured using a TEC Exhaust Fan Flow Meter. Kitchen range hood airflows were measured using a balanced-pressure flow hood method described by Walker and Wray (2001). For the range hood test, a calibrated and pressure-controlled variable-speed fan was connected to the underside of the range hood using a custom fabricated transition that was adapted onsite to cover the entire underside of the range hood. Using a pressure sensor, the variable speed fan was controlled to match the flow of the exhaust fan while maintaining neutral pressure between the room and the transition. For microwave range hoods, the top vent was covered with tape to ensure that the airflow measured at the bottom inlet represented the entire flow through the device. Supply ventilation fan flow rates were not measured directly because the air inlets were commonly inaccessible (often mounted on the roof). It was also not feasible to measure flows using in-duct velocity probes because the supply ducts were encased in spray foam insulation in the attic in all four of the HENGH homes that used supply ventilation. It is imperative that during system design and installation that more consideration is given to being able to commission ventilation systems in order to validate their performance and demonstrate compliance with standards.

2.2 Pollutant Monitoring

Pollutants were measured using both integrated one-week samplers and time-resolved (typically 1-minute) devices. Integrated concentrations of formaldehyde and NO_x were measured using SKC UMEx-100 and Ogawa passive samplers. Formaldehyde samplers were deployed in the main living space, master bedroom, and outdoors. $PM_{2.5}$ was measured indoor in the main living space and outdoors. $PM_{2.5}$ integrated filter samples were collected using a co-located pDR-1500 (ThermoFisher) in a subset of the homes and time-resolved photometer data were adjusted using the gravimetric measurements from the filter samples. Time resolved particle measurements were made using photometers (ES-642/BT-645, MetOne Instruments). NO_2 and formaldehyde time-resolved measurements were made using Aeroqual NO_2 monitors and a GrayWolf FM-801, respectively. We also measured temperature, relative humidity and CO_2 outside and in several inside locations using Extech SD-800 and various HOBO monitoring devices. In this paper we focus on the time-integrated pollutant measurements.

2.3 Occupant Activity Monitoring

Cooktop and oven use were monitored using iButton temperature sensors attached to the surface of the cooktop, generally with one iButton adjacent to each burner. The temperature data were analyzed to find rapid increases in temperature that signal use of the cooking appliance. Operation of exhaust fans, range hoods, clothes dryers, and the central forced air system were determined using one of the following methods: a motor on/off senor, air velocity anemometer, or a power meter. The field team determined which method to use depending on the accessibility and configuration of the appliances. Fans with multi-speeds (e.g., a range hood) were monitored using a vane anemometer do detect the operating speed. The air flow at each operating speed was determined separately using diagnostic flow

metering. State sensors that discern open vs. closed condition were used to monitor the most often used exterior doors and windows. Although study participants were asked to keep these openings closed during the one-week study period, it was deemed valuable to monitor as any extended natural ventilation could impact pollutant measurements. Temperature and relative humidity were monitored at the supply air registers of the forced air heating and cooling systems as an indicator of heating/cooling use. These data were used as part of the quality assurance procedures when analyzing the pollutant data to determine data anomalies and to check that instruments were responding to events in the home. A full analysis of these data will be published at a later date.

3 RESULTS

3.1 Diagnostics

The measured envelope leakage for most homes was between 3 and 6 ACH50 (Figure 1), with a median value of about 4.5 ACH50. Measured air leakage under pressurization was higher than depressurization by 20% on average. This result is not unusual and is due to "valving" of some envelope leaks, e.g., from an exhaust fan damper being pushed open during pressurization. Only four homes had envelope leakage less than 3 ACH50, the level required for compliance with the 2018 International Energy Conservation Code (ICC 2018) that is used in many construction regulations in the US, but not in California. Median duct leakage was about 50 L/s, with a range from below 10 to over 200 L/s.

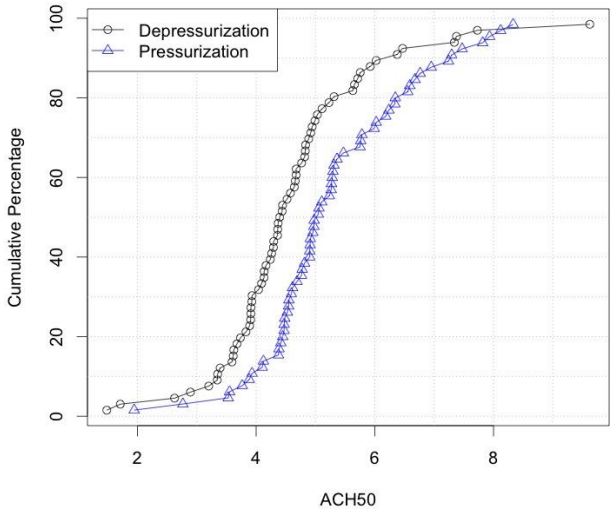

Figure 1: Distribution of Envelope Leakage Measurements

For dwelling unit ventilation, 64 of the 70 homes had exhaust ventilation; the other six had supply ventilation. In all but two cases, the measured flow exceeded the California building standards minimum requirement that is based on the fan sizing requirements in the 2010 version of the US residential ventilation standard: ASHRAE 62.2 (i.e., not taking into account infiltration). This fan sizing requirement was 0.05 L/s/m^2 of floor area plus 3.5 L/s per occupant (assumed to be the number of bedrooms plus one), or about 27 L/s for the average home in this study. The average installed flow was about 50% more than the minimum requirement. This is similar to the results in Stratton et al. (2012) for previous tests of other new (at the time of testing and built in 2010/2011) California homes. It should be noted that the ASHRAE Standard has changed in the intervening years to be a total ventilation rate requirement of 0.15 L/s/m^2 of floor area with the same occupant requirement. For the homes in this study that averaged about 240 m^2 this roughly doubles the total ventilation rate requirement to about 52 L/s, however, using the ASHRAE 62.2-2016 infiltration credit reduces this to a fan size requirement of about 26 L/s. Therefore, the ventilation systems in

these homes are also oversized relative to the newer ASHRAE 62.2 requirements, when infiltration is included. We combined these measured fan flow rates with estimates of natural infiltration to obtain an estimate of overall air exchange rate (AER) for each home. The median AER was 0.35 Air Changes per Hour (ACH). The AER in non-mechanically ventilated homes in the CNHS study were substantially lower, with a median of 0.24 ACH.

On the initial site visit, the mechanical ventilation system was running in 18 homes and the system was turned off in 52 homes. Systems with a label, or less accessible controls were much more likely to be operating. Also, some labels were clearer than others. For example, text stating "Continuous Duty" does not convey information useful to the occupants, resulting in systems being turned off with this style of vague text. A better example of labelling was: "Whole House Ventilation Control. Leave on except for severe outdoor air quality.". Table 1 presents a summary of the system status when the research team first arrived to the home, by control type and presence or absence of any identifying label.

Table 1: Dwelling Unit Ventilation System Control

System Control	Label	System Status (as-found) - ON	System Status (as-found) – OFF
On/Off Switch	Yes	7	5
	No	2	40
Programmable Controller	No	5	5
Thermostat	No	0	2
Breaker Panel	No	1	0
No Controller	No	3	0
Total		18	52

32 homes had a kitchen range hood and all were able to meet the minimum air flow requirement of 50 L/s, but only 22 of these did so on the quiet low speed setting. 38 homes had over the range microwaves, not all of which were able to meet the minimum air flow requirements and only nine did so at the lowest speed setting. Bathroom exhausts met the minimum air flow requirement of 25 L/s in about 80% of cases.

3.2 Pollutant Measurements

Table 2 summarizes the results of the HENGH study for key pollutants of concern compared to the previous CNHS for homes that were not mechanically ventilated.

Table 2: Median Indoor Pollutant Concentrations

Median Indoor Time-Integrated Concentration	CNHS – 98% Electric No mech vent	HENGH - Gas Homes with 62.2 ventilation
Formaldehyde	30 ppb	18 ppb
PM2.5	10.4 µg/m3	5.0 µg/m3
NO_2	3.2 ppb	4.5 ppb

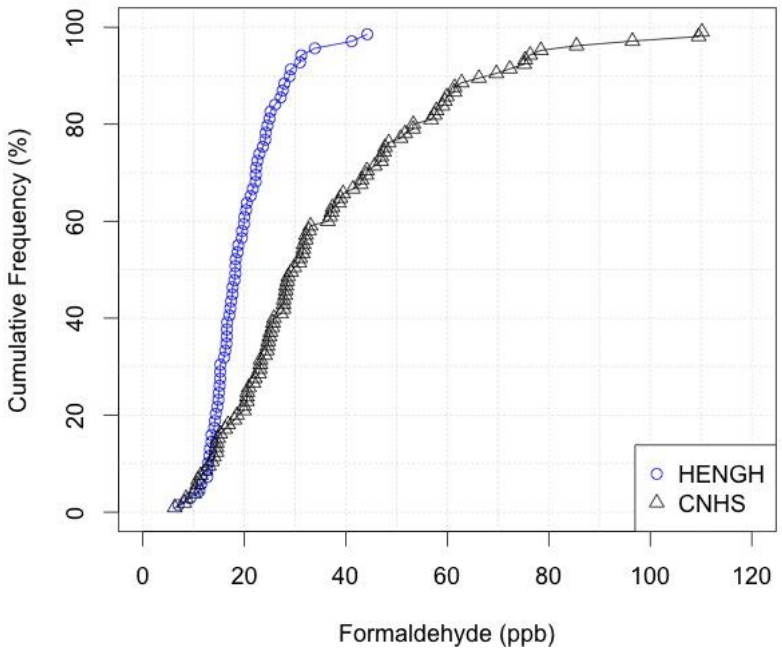

Figure 2: Comparison of HENGH and CNHS Time Integrated Formaldehyde Measurements

In both HENGH and CNHS homes the majority of formaldehyde was from indoor sources (median outdoor concentrations were 2-3 ppb), and HENGH homes had lower indoor formaldehyde compared to CNHS homes, despite being newer when tested (some studies have suggested the formaldehyde concentrations are higher when homes are newer Park and Ikeda (2006)). Figure 2 summarizes the distribution of measured indoor formaldehyde in the two studies. The lower formaldehyde concentrations measured by HENGH in comparison to CNHS may be attributable to California's regulation to limit formaldehyde emissions from composite wood products that came into effect between the two studies. The highest formaldehyde concentration in the HENGH study was 45 ppb, whereas the CNHS had concentrations up to 110 ppb. Almost all homes in the HENGH study exceeded the California OEHHA REL for 8-hour and chronic exposure of 7 ppb, but were below other commonly used reference concentrations for 8-hour and chronic exposure, such as 80 ppb from the World Health Organization (WHO (2010)) and 40 ppb from Health Canada (2006).

Lower $PM_{2.5}$ indoors measured by HENGH compared to CNHS may be explained from a combination of lower outdoor $PM_{2.5}$ levels (6.8 vs. 8.7 ($\mu g/m^3$)), the use of kitchen range hoods, and use of higher efficiency air filters (MERV 11 or better) in some HENGH homes. While 20 of the 67 HENGH homes with outdoor data had outdoor $PM_{2.5}$ exceed the California Environmental Protection Agency annual ambient air quality standard of 12 $\mu g/m^3$, only 12 of the 67 homes with indoor data had indoor concentrations exceed that benchmark.

Gas cooking is a significant source of indoor NO_2 (Mullen et al., 2016). Even though NO_2 concentrations measured by HENGH are similar to levels found in CNHS, the two studies differed in that HENGH homes all use gas for cooking, whereas almost all homes (98%) from CNHS used electric ranges. More analysis is needed to determine the effectiveness of source control, such as range hood use during cooking, on indoor concentrations of cooking emissions such as NO_2 and $PM_{2.5}$. All of the measured NO_2 concentrations were well below the US Environmental Protection Agency 53 ppb annual ambient air quality standard for NO_2.

The median of time-averaged CO_2 concentrations in the HENGH homes was 608 ppm compared to 564 ppm for the CNHS. These results are consistent with the relatively low occupant density in these homes: approximately one person for every 90 m^2. The range of average concentrations for the HENGH homes was lower at 481-770 ppm compared to 405-890 for the CNHS homes. As with the other contaminant measurements (e.g., formaldehyde as shown in Figure 2), the more consistent ventilation provided by mechanical systems makes for less variability in pollutant concentrations – in particular reducing the likelihood of high pollutant levels. In the absence of a consensus limit for CO_2 in residences, we use the ASHRAE Standard 62.1-2016 guideline level of 1100 ppm (700 ppm above the outdoor background of roughly 400 ppm) as a benchmark[1] for CO_2. The highest CO_2 concentrations were found in bedrooms overnight. About 10% of bedrooms had mean CO_2 concentrations overnight in excess of 1100 ppm.

Time-averaged indoor temperature and relative humidity measured in this study were similar to CNHS. The 24 hour time-averaged indoor air temperature results reported for the CNHS study had the same median and mean of 22.4ºC, and a range of 17.1 to 28.2ºC. The mean indoor air temperatures measured over the roughly weeklong monitoring periods in HENGH homes had the same median and mean of 22.9ºC, and a range of 17.8 to 27.1ºC. CNHS reported 24-hour average indoor relative humidity with a median of 43%, a mean of 45%, and a range of 20% to 64%. The mean relative humidity measured over the roughly weeklong monitoring periods in HENGH homes had the same median and mean of 45%, and a range of 28% to 60%. Formaldehyde emission rates depend on temperature and humidity. This similarity in indoor conditions indicate that any differences in formaldehyde are due to other factors.

The US DOE Building America program is expanding on the results reported here with a field study performing real-time and integrated pollutant concentrations in about 200 new US homes (in climates other than California). A subset of homes will have measurements with and without ventilation system operation.

4 CONCLUSIONS

The mechanical ventilation systems in the study homes more than met the minimum dwelling unit air flow requirements, and exceed the minimum flows by 50% on average. This indicates that mechanical ventilation systems are being adequately selected and installed by builders of new homes in California. The homes in this study have lower indoor formaldehyde levels than previously measured due to a combination of added mechanical ventilation and, at least in these California homes, as a result of California's formaldehyde emission standards. Indoor concentrations of NO_2 and $PM_{2.5}$ measured are also low compared to a prior study of new homes in California and available standards. In most homes these key pollutants are below levels set for health requirements, or do not exceed the standards by considerable amounts. Overall, this study has shown that using mechanical ventilation in new homes that meets or exceeds current US standards results in acceptable indoor air quality, and for some pollutants is a significant improvement over homes without mechanical ventilation. For these good results to be achieved it is essential to have well-labelled controls, particularly if the controls are easily accessible, and that systems be designed and installed to allow for air flow measurements for commissioning and performance validation to show compliance with standards.

[1] ASHRAE 62.1 guideline level of +700 ppm above outdoor background (currently about 400 ppm) is largely based on odor concern in commercial buildings, which is not intended for residences.

5 ACKNOWLEDGEMENTS

This work was supported primarily by the California Energy Commission through Contract PIR-14-007. Additional support was provided by the Department of Energy under Contract DE-AC02-05CH11231. The Southern California Gas Company (SoCalGas) provided direct financial support to the Gas Technology Institute (GTI). Staff support was contributed by the Pacific Gas & Electric Company (PG&E). The field research was conducted by Luke Bingham, Erin Case, and Shawn Scott of GTI; Guy Lawrence of MBA; and Eric Barba, Mary Nones, Ara Arouthinounian, and Ricardo Torres of SoCalGas; Randy Maddalena and Woody Delp of LBNL, and Rick Chitwood. Other project tasks were performed by Genese Scott of SoCalGas, Marion Russell, Taylor Lyon, Ji Gao, Samir Anbri, and Hao Fu, and Xiong Mei.

6 REFERENCES

ASHRAE (2016). *ASHRAE Standard 62.1-2016 Ventilation for Acceptable Indoor Air Quality*.

ASHRAE (2016). *ASHRAE Standard 62.2-2016 Ventilation and Acceptable Indoor Air Quality in Residential Buildings*.

Chan, W.R., Kim, Y-S, Less, B.D., Singer, B.C. and Walker, I.S. (2018). Ventilation and Indoor Air Quality in New California Homes with Gas Appliances and Mechanical Ventilation. California Energy Commission, Energy Research and Development Division Final Project Report for PIR-14-007.

Health Canada. (2006*). Residential Indoor Air Quality Guideline: Formaldehyde*.

Logue, J. M., Price, P. N., Sherman, M. H., & Singer, B. C. (2012). A Method to Estimate the Chronic Health Impact of Air Pollutants in U.S. Residences. *Environmental Health Perspectives*, *120*(2), 216–222.

Mullen, N.A., Li, J., Russell, M.L., Spears, M., Less, B.D. and Singer, B.C. (2016) Results of the California Healthy Homes Indoor Air Quality Study of 2011-2013: impact of natural gas appliances on air pollutant concentrations, Indoor Air, 26, 231-245.

Offermann, F. (2009). *Ventilation and Indoor Air Quality in New Homes*. California Energy Commission. Report No. CEC-500-2009-085

Park, J.S. and Ikeda, K. 2006. Variations of Formaldehyde and VOC levels during 3 years in new and older homes. Indoor Air 2006; 16: 129–135. doi:10.1111/j.1600-0668.2005.00408.x

Stephens, B., & Siegel, J. A. (2012). Penetration of ambient submicron particles into single-family residences and associations with building characteristics. *Indoor Air*, *22*(6), 501–513. doi:10.1111/j.1600-0668.2012.00779.x

WHO. 2010. *WHO guidelines for indoor air quality: selected pollutants*. World Health Organization.

Overview of model based control strategies for ventilation systems

Bart Merema[1], Maarten Sourbron[2, 3], Hilde Breesch[1*]

1 KU Leuven, Department of Civil Engineering, Construction Technology Cluster, Technology Campus Ghent, Gebroeders De Smetstraat 1, 9000 Gent, Belgium
**Corresponding author: Hilde.Breesch@kuleuven.be*

2 KU Leuven, Department of Mechanical Engineering, Mechanical engineering Technology TC, De Nayer
Jan Pieter de Nayerlaan 5
2860 Sint-Katelijne-Waver, Belgium

3 Thermiek cvba
Rotselaarsesteenweg 5
3018, Wijgmaal

This overview focuses on model based control strategies for ventilation in nearly zero energy buildings (nZEB) where slower reactions towards disturbances are expected as a result of high insulation and air tightness of the building envelope (Killian and Kozek 2016). Furthermore, internal heat gains have a higher impact in these kind of buildings. In addition, occupancy pattern can be variable (e.g. in office- and school buildings) and HVAC control is consequently more challenging. In addition, there can be a discrepancy between the heating demand and ventilation demand with all-air ventilation systems. All these conditions imply that the internal environmental quality (IEQ) is a challenge to control in nZEB buildings. A model predictive control (MPC) approach could be a solution as it takes into account the current situation and the future disturbances and demand (Killian and Kozek 2016). Inside the MPC framework, state estimation is performed to predict the future states of a system and/or building. Based on these predictions the controller can set output values by solving an optimization problem. For the optimal control problem an objective is defined and constraints are set so also future disturbances are included. The objective is a cost function that minimizes typically the energy use with respect to the (thermal) comfort included in the cost function or defined as a constraint. The optimal control problem optimizes output values using the identified model to verify the solution.

Table 1 gives an overview of existing literature on MPC for ventilation systems. In total 14 studies are evaluated where MPC was implemented to control the ventilation system. Out of these studies, 6 use an all-air ventilation system of climatisation while in the other studies hydronic systems (e.g. a heat pump with a TABS system) are used for space heating. In 10 out of the 14 evaluated studies the developed MPC framework is implemented in a real operating building or a small experimental test building, the remaining studies are simulation studies. In these four remaining studies typically measurement data is obtained from the building to develop a virtual test model that is used inside the MPC framework to perform a co-simulation. The majority of real buildings is an office building (8 out of 10), one is a residential building and one an academic building.

The model that is needed inside the MPC framework is used to represent the actual building and system. Regarding the dynamic model used in the MPC framework there can be a wide variety identified in the used methods. From simple regression model (black box), over RC-models (grey box) to detailed white box models (e.g. in Modelica). Lately, also machine

learning techniques such as random-forest or neural networks are being utilized for the model identification process. In literature a lot of attention is devoted to the model identification procedure since it consumes a major part of developing an MPC framework. The objective is to construct a simple but accurate dynamic models of the real building and HVAC system used for predictions in the MPC framework. A reduced order model, a model with less complexity, will significantly reduce the computation time needed to solve the optimal control problem.

In most cases the MPC for the ventilation system is used for temperature control of the supply air, only in 4 out of 14 studies the room CO_2 concentration was also controlled by the MPC. The MPC controls the VAV boxes in the ventilation system and provides input for the airflow rate and supply air temperature at each time step. The cost function for the ventilation MPC can be defined by minimizing the energy use with respect to the (thermal) comfort. Soft constraints are used on the (thermal) comfort constraints to penalize constraints violations for the minimum and maximum room temperature (and CO_2) set point. The weight factor used for the comfort cost is significant higher compared to the energy cost in order to give comfort a higher priority over minimizing the energy use of the HVAC system. Ventilation control is often non-linear resulting in an MPC that can be complex to solve, since it contains non-linear constraints. In all-air systems the airflow rate and supply air temperature are both variable in time. Therefore a non-linear optimization might be needed to have a better match with the real situation or a simplification in order to solve the non-linear constraints.

Total energy savings using an MPC for ventilation control range roughly between 17-55% compared to a rule based control (RBC). However, it is not always clearly defined what the baseline is. In addition, the effect of variability in input data or uncertainty is not always taken into account when energy savings are given. Finally, for future implementation also attention has to be drawn to the transferability of the developed MPC method to other buildings. One of the bottlenecks of the implementation of MPC in general for buildings is that high expertise knowledge is required to implement this type of control. A lot of data and fine-tuning is needed in the model identification process and the model identified is specific for one type of building or system.

Table 1; Literature overview of studies on MPC for ventilation systems

Study	Control Airflow	Type model identification	Energy efficiency	Implementation	MPC
(Bengea et al. 2014)	T+CO_2	RC model (grey box)	20% HVAC system	Office building	Non-linear
(Liang et al. 2015)	T	ARMAX (black box)	27,8% HVAC system	Office Building	Linear
(Yuan and Perez 2006)	T	linearized differential equation (grey box)	-	Office Building	Linear
(Parisio et al. 2014)	T+CO_2	grey box for Temp and ARX for CO_2 (black box)	-	1-zone experimental test	Linear
(Walker et al. 2017)	T+CO_2	linearized differential equation (grey box)	23.5-30% HVAC system	Office building (simulations)	Linear
(Afram et al. 2017)	T	ANN (black box)	6-73% operating cost	Residential building	Non-linear
(Niu and Neill 2016)	T	Non-linear regression (black box)	22,1% HVAC system	Data-driven simulations	Non-Linear

(Zacekova et al. 2015)	T	MPC relevant identification (black box)	-	Data-driven simulations	Linear and non-linear
(Erfani, Rajabi-ghahnaviyeh, and Boroushaki 2018)	T	NARX network (black box)	55,1% electrical 43,7% gas	3-zone experimental test	Non-linear
(West, Ward, and Wall 2014)	T	RC Model (grey box)	19-32% for the HVAC system	2 Office buildings	Linear
MPC also for TABS system					
(Sturzenegger et al. 2016)	T	Bilinear RC model (grey box)	17% HVAC, lighting and equipment	Office building	Bilinear
(Picard et al. 2016)	T	RC and Modelica model (grey and white box)	-	Office building (simulations)	Linear
(Jorissen 2018)	T+CO_2	Modelica model (white box)	82% electrical	Office building	Non-linear
(Hilliard, Swan, and Qin 2017)	T	Random forest regression model (black box)	10-29% electrical 63% thermal	Academic building	Non-linear

REFERENCES

Afram, A., Janabi-sharifi F., Fung A., Raahemifar K., (2017). *"Artificial Neural Network (ANN) Based Model Predictive Control (MPC) and Optimization of HVAC Systems : A State of the Art Review and Case Study of a Residential HVAC System.*" Energy & Buildings 141:96–113.

Bengea, S. C., Kelman, A.D., Borrelli F., Taylor R., Narayanan S. (2014) *"Implementation of Model Predictive Control for an HVAC System in a Mid-Size Commercial Building Implementation of Model Predictive Control for an HVAC System in a Mid-Size Commercial Building."* HVAC&R Research 20 121-135.

Erfani, A., Rajabi-ghahnaviyeh A., Boroushaki M., (2018). *"Design and Construction of a Non-Linear Model Predictive Controller for Building and Cooling System."* Building and Environment 133(November 2017):237–45.

Hilliard, T., Swan L., Qin Z., (2017). "*Experimental Implementation of Whole Building MPC with Zone Based Thermal Comfort Adjustments."* Building and Environment 125:326–38.

IEA. (2018). *2018 Global Status Report*.

Jorissen, F.. (2018), "Toolchain for Optimal Control and Design of Energy Systems in Buildings." PhD Thesis, KU Leuven 2018

Killian, M., Kozek M. (2016). *"Ten Questions Concerning Model Predictive Control for Energy Efficient Buildings."* Building and Environment 105:403–12.

Liang, W., Quinte R., Jia X., and Jian Q.S., (2015). "*MPC Control for Improving Energy Efficiency of a Building Air Handler for Multi-Zone VAVs.*" Building and Environment 92:256–68.

Niu, F. Neill Z. (2016). "*Model-Based Optimal Control of Variable Air Volume Terminal Box*." Proceedings 4th International High Performance Buildings 2016 paper 176

Parisio, A., Varagnolo D., Molinari M., Pattarello G., Fabietti L., Johansson K H., (2014). *Implementation of a Scenario-Based MPC for HVAC Systems : An Experimental Case Study*. IFAC proceedings volume 47, 599-605.

Picard, D., Sourbron M., Jorissen F., Vana Z., Cigler J., Ferkl L., Helsen L., (2016) *"Comparison of Model Predictive Control Performance Using Grey-Box and White-Box Controller Models of a Multi-Zone Office Building."* International Compressor Engineering, Refrigeration and Air Conditioning, and High Performance Buildings Conferences 1–10.

Sturzenegger, D., Gyalistras D., Morari M., Smith R.S., (2016). *"Model Predictive Climate Control of a Swiss Office Building : Implementation , Results , and Cost – Benefit Analysis.*" 12 IEEE TRANSACTIONS ON CONTROL SYSTEMS TECHNOLOGY 24(1):1–12.

Walker, S., Lombardi W., Lesecq S., Roshany-Yamchi S., (2017). *"Application of Distributed Model Predictive Approaches to Temperature and CO2 Concentration Control in Buildings*." Pp. 2589–94 in *IFAC Proceedings Volumes*. Vol. 1. Elsevier B.V.

West, S. R., Ward J.K., Wall J., (2014). *"Trial Results from a Model Predictive Control and Optimisation System for Commercial Building HVAC." Energy & Buildings 72:271–79.*

Yuan, Shui and Ronald Perez. 2006. *"Multiple-Zone Ventilation and Temperature Control of a Single-Duct VAV System Using Model Predictive Strategy*." Energy and Buildings 38(10):1248–61.

Zacekova E., Pcolka M., Tabacek J., Tezky J., Robinett R., Celikovsky S., Sebek M., (2015). *"Identification and Energy Efficient Control for a Building : Getting Inspired by MPC."* American control conference 2015 Proceedings, p1671-1676

Predictive control for an all-air ventilation system in an educational nZEB building

Bart Merema[1*], Dirk Saelens[2], Hilde Breesch[1]

1 KU Leuven , Department of Civil Engineering, Construction Technology Cluster, Technology Campus Ghent, Gebroeders De Smetstraat 1, 9000 Gent, Belgium
**Corresponding author: bart.merema@kuleuven.be*

2 KU Leuven, Department of Civil Engineering, Building Physics, Kasteelpark Arenberg 40, 3001 Leuven, Belgium

ABSTRACT

In school and office buildings, the ventilation system has a large contribution to the total energy use. A control strategy that adjusts the operation to the actual demand can significantly reduce the energy use. This is important in rooms with a highly fluctuating occupancy profile, such as classrooms and open offices. However, a standard rule-based control (RBC) strategy is reactive, making the installation 'lag behind' in relation to the demand. As a result, a good indoor climate is not always guaranteed and the actual energy saving potential is lower than predicted. This study focuses on nearly zero energy buildings (nZEB) buildings where the insulation and air tightness of the envelope is high resulting in slower reactions towards disturbances (occupants and solar radiation). Furthermore, internal heat gains have a higher impact on the indoor climate in these type of buildings. A model predictive control (MPC) might be a solution as an MPC takes into account the current situation and the future demand. MPC has already shown savings for hydronic systems in operating buildings as indicated in recent studies which resulted in energy savings of 17-30%.

Previously identified dynamic models for CO_2 and temperature prediction are implemented in a linear MPC framework to evaluate the impact on the indoor environmental quality (IEQ) and energy use. The dynamic models are data-driven (RC and ARX models) and identified using measurement data obtained from an operating building. The building consists of two lecture rooms, each with a capacity of 80 students. Balanced mechanical ventilation is provided with a total supply airflow of 4400 m³/h. The airflow rate is controlled by VAV boxes based on measurements of CO2-concentration and operative temperature in each lecture room. For heating purposes, the air is preheated by an air-to-air heat recovery. Additionally, heating coils are integrated in the supply ducts of each zone so it is regarded as an all air HVAC system.

Different strategies (actual number, lecture schedule, motion) for occupancy prediction are analysed and their effect on the operation of the MPC. The MPC framework is first tested in a simulation environment (Modelica). Results will be presented for the effect of MPC on the operation of the all-air system and the energy use for both the fans and the heating coil. Results of the simulations will be used to improve the current RBC control in a test building. This will result in an optimized energy use while at the same time providing a comfortable indoor climate.

The study showed that with a minimal dataset of the following parameters: indoor, supply and outdoor temperature, solar radiation, airflow rate and occupancy an energy efficient MPC could be developed with respect to thermal comfort. The airflow rate is decreased by 47% compared to the measurements while the heating energy for ventilation (Q_{vent}) is decreased by 56% for the complete period of four weeks during the transition season

KEYWORDS

All-air Ventilation, MPC, Energy saving, predictive control, educational building

1 INTRODUCTION

In school and office buildings, the ventilation system has a large contribution to the total energy use (EnBau, 2010). A control strategy that adjusts the operation to the actual demand can significantly reduce the energy use. This is important in rooms with a highly fluctuating

occupancy profile, such as classrooms and landscaped offices. However, a standard rule-based control strategy is reactive, making the installation 'lag behind' in relation to the demand. As a result, a good indoor climate is not always guaranteed and the actual energy saving potential is lower than predicted. This is especially of concern for all-air ventilation systems where the indoor climate and the air quality are controlled by the ventilation system.

This study focuses on nearly zero energy buildings (nZEB) where slower reactions towards disturbances are expected as a result of a high insulation and high air tightness level of the building envelope. Furthermore, internal heat gains such as occupancy have a higher impact on the thermal comfort in these type of buildings. In addition, there can be a discrepancy between the heating demand and ventilation demand. A model predictive control (MPC) might be a solution to control the thermal comfort while reducing the energy use, as an MPC takes into account the current situation as well as the future demand. Recently, MPC is gaining more interest for implementation in control for HVAC systems. MPC has already shown savings for hydronic systems in operating buildings as indicated in recent studies (De Coninck and Helsen 2016; Prívara et al. 2011; Sourbron, Verhelst and Helsen 2017).

A few studies on MPC for all-air ventilation systems will be highlighted. Huang, Wang, and Xu (2010) created a robust MPC control strategy for a ventilation system with variable airflow volume (VAV). The developed strategy resulted in a more robust control compared to a PI control since less commissioning or user-intervention was needed. Test were performed with a single zone simulation model. The MPC was able to satisfy constraints when used for temperature control. A recent study by Liang et al. (2015) focused on MPC for a HVAC system with VAVs for temperature control. A low order state space model was developed and a Kalman filter was applied for state estimation. Simulations showed savings for MPC of 17,5% on the electrical energy consumption of ventilation. As indicated both studies focussed on temperature control for VAVs while often this is also CO_2 controlled. (Bengea et al., 2014) demonstrated the implementation of MPC with both temperature and CO_2 control in an office building with a rule based HVAC system. Energy savings were 20% during the transition season and 70% during the heating season. CO_2 levels were maintained below the desired set point. However, the implemented cost function did not include any comfort cost indicating that the main objective of the MPC was to reduce energy use.

A related study by Walker et al. (2017) developed a distributed MPC approach for temperature and CO_2 concentration control in a natural ventilated building and compared it to a centralized MPC. For a 3 zone model it was shown that the distributed MPC achieved performances close to a centralized MPC. The dynamic model used was a grey box model which was linearized in order to utilize it as a linear time invariant (LTI) dynamic model inside the MPC framework. An important parameter that is needed for MPC is the occupancy information for both temperature and CO_2 control. Occupancy can be a high internal heat load in nZEB buildings. (Oldewurtel, Sturzenegger, & Morari, 2013) showed that incorporating occupancy information into an MPC resulted in a significant energy saving potential for offices. Both perfect predication and occupancy schedules were used in the MPC. Energy savings found for the HVAC system when comparing to a RBC was 34-50%. More sophisticated occupancy prediction methods did not result in significant energy savings compared to instantaneous occupancy information.

The aim of this study is to show a method on how to implement a simple identified model in a linear MPC framework. The objective of the MPC is to maintain the comfort in the room with respect to indoor temperature and CO_2 concentration while minimizing the heating energy use and fan energy use. The outline of the paper is as follows: section 2 demonstrates the method

used for the MPC framework and highlights the case study building. Next section will present the results for the room temperature and CO_2 concentration of the MPC ventilation system Finally, a conclusion and discussion is given for the used approach and the future application in the MPC.

2 METHOD

Previously identified dynamic models for CO_2 and temperature prediction using of an educational building (Merema, Breesch, Saelens, 2019) are implemented in a linear MPC framework. The dynamic models are data-driven (ARX models) and identified using measurement data obtained from an operating educational building described in section 2.1. In the optimal control problem soft constraints are implemented for the indoor environmental quality (IEQ) to optimize the energy use whit respect to the IEQ. Afterwards a method is shown to solve the problem using a linear optimization. This framework is discussed in section 2.3.

2.1 Description of the case study building (Merema, Delwati, Sourbron, & Breesch, 2018)

An education building located in Ghent (Belgium) is used for the case study. The building consists of two lecture rooms, each with a capacity of 80 students. Balanced mechanical ventilation is provided with a total supply airflow of 4400 m³/h. The airflow rate is controlled by VAV boxes based on measurements of CO_2-concentration and operative temperature in each lecture room. The control for the ventilation system is a rule-based control (RBC) strategy. For heating purposes, the air is preheated by an air-to-air heat recovery. Additionally, heating coils (8 kW) are integrated in the supply ducts of each zone so it is regarded as an all-air HVAC system. The U-values for the envelope are given in Table 1.

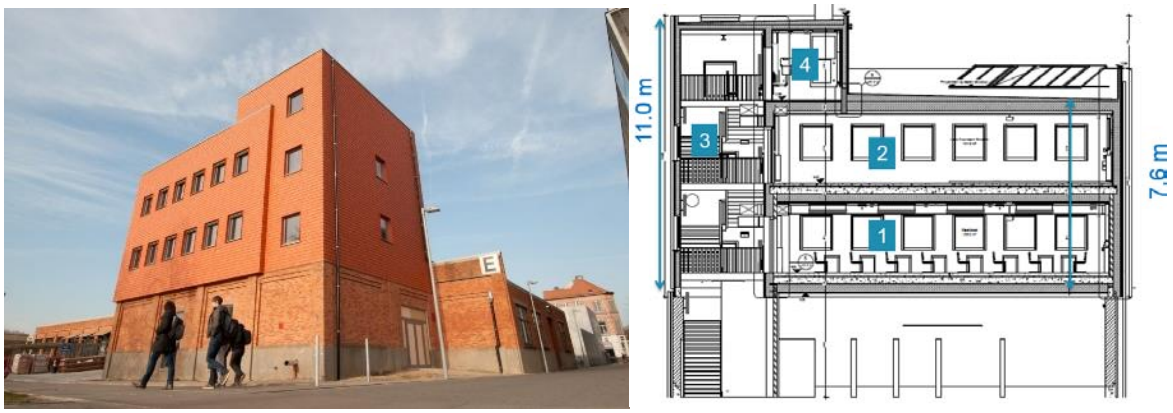

Figure 1; (left) Impression of the case study building, (right) cross-section of the case study building with 1: lecture room, 2: lecture room, 3: staircase, 4: technical room

Table 1: U values for the construction elements

Construction part	U-Value (W/m²K)
Wall	0,15
Roof	0,14
Floor	0,15
Glazing (glazing)	0,60
Glazing (frame)	0,90

2.2 Measurement data

A set of sensors has been installed to monitor indoor and outdoor conditions and are listed in Table 2. The building includes a weather station monitoring the main outdoor parameters:

global horizontal solar radiation, outdoor temperature, relative humidity and wind speed and direction. For the indoor conditions, the indoor temperature, the CO_2 concentration and the indoor humidity are continuously monitored. The occupancy of the lecture room is measured by counting cameras installed near the entrance of the room. Measurement data is collected during four weeks on a 1 minute time-interval. The following parameters were used to identify the ARX models (Merema, Breesch, Saelens, 2019) implemented in the MPC framework: outdoor- , indoor- and supply air temperature, solar radiation(global horizontal and on façade), air flow rate, room CO_2 concentration and occupancy.

Table 2. Properties of the installed sensors used for the MPC framework (Merema, Breesch, Saelens, 2018)

Parameter	Type sensor	Accuracy
CO_2-concentration	VAISALA GMW83	±30 ppm + 3% of reading
Room temperature	SE CSTHR PT1000	± 0.1 °C
Supply temperature	SE CSTHK HX	± 0.4 °C
Occupancy	Acurity Crosscan Camera	± 5%
Outdoor temperature	Vaisala HMS82	± 0.3 °C at 20°C
Solar radiation	SP Lite2 Silicon Pyranometer	4.5% of reading

In Figure 2, measurement data for outdoor temperature, solar radiation and occupancy is illustrated. The data is used in the MPC framework as forecasts to optimize the airflow rate and the supply air temperature. For the outdoor CO_2 concentration a constant of 420 ppm is used as forecast for the CO_2 MPC since this parameter is not measured in the current situation.

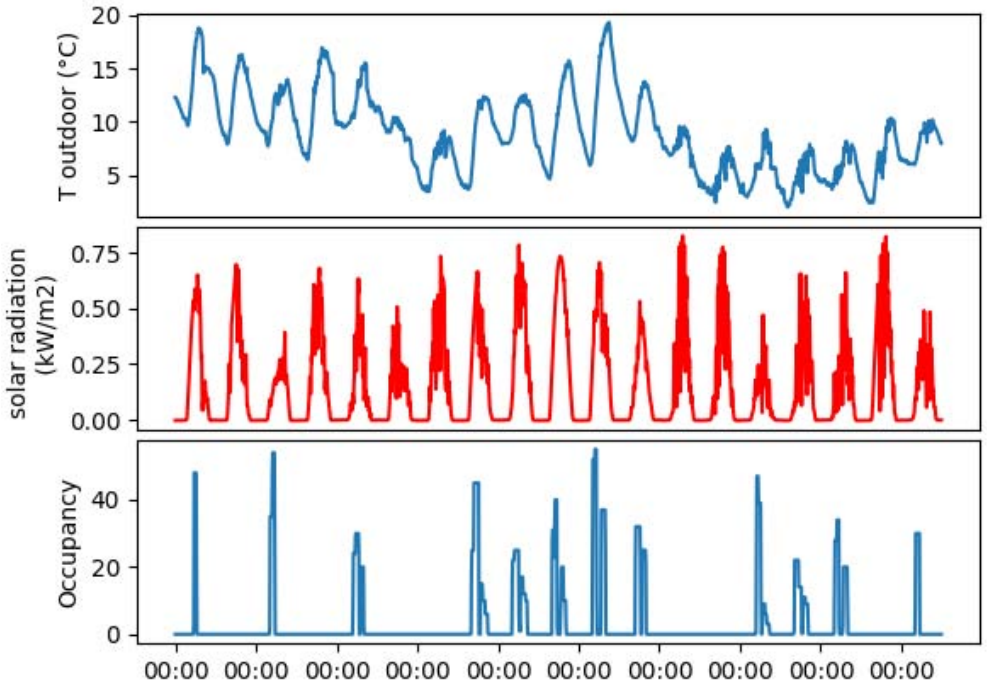

Figure 2; Parameters ($T_{outdoor}$, solar radiation and occupancy) measured used as forecast input for the MPC

2.3 MPC framework

This MPC framework is written in Python using the CVXPY (Diamond and Boyd, 2016) package allowing to solve convex optimization problems. The selected solver is QSOP, i.e. the default solver used in CVXPY to solve quadratic problems.

The ventilation MPC is split up in two separate MPCs (1:CO_2 2: Temperature) to solve the problem as a linear-MPC, as demonstrated in Figure 3. To avoid using a non-linear approach first the CO_2-MPC calculates the minimal required airflow to control the indoor CO_2 concentration based on the following inputs: CO_2 concentration room (previous time step), occupancy, outdoor CO_2. Maintaining the CO_2 concentration below the desired set point has the highest priority in this VAV control. Since the ARX model is linear the minimal required airflow for CO_2 control can be calculated and optimized by the CO_2-MPC. Future predictions for room CO2 concentration are performed by the underlying ARX model afterwards the control output is optimized in the MPC. The control output is feedback to the ARX model to calculate the measurement output by including some random white noise on the feedback signal.

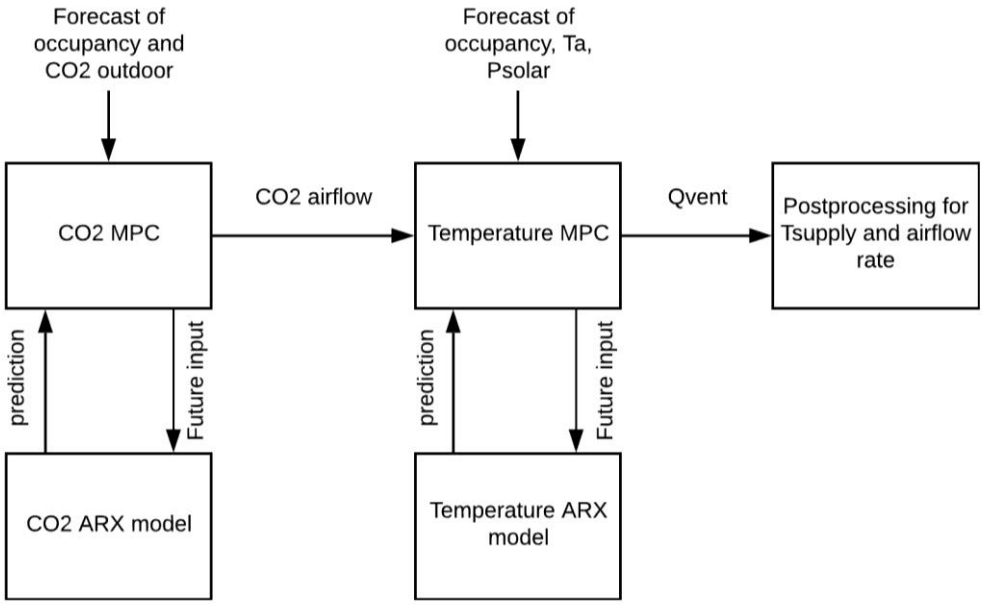

Figure 3; Linear MPC framework for all-air ventilation system

Second, the calculated CO_2 airflow is used as a input constraint in the Temperature MPC. In the T-MPC, Q_{vent} is optimized using the predictions from the temperature ARX model. The optimized control output Q_{vent} is then returned to the ARX model to obtain the measurement output by including random white noise. Post-processing the results from the linear MPC is required to obtain the actual set points for the supply air temperature and the air mass flow rate. The optimized variable Q_{vent} obtained from the linear T-MPC is split up in the following manipulated variables T_{supply} and airflow. The mass flow rate is obtained from the CO_2 MPC and is fixed in the equation. From here T_{supply} can be calculated using the following strategy and equation 1. If $T_{supply} > 45°C$, T_{supply} is set to 45°C and the mass flow is increased using equation 1:

$$\text{Airflow} = Q_{vent}/(T_{supply}-T_{zone}) \quad (1)$$

Subject to:

- $T_{supply} \geq 15\ °C$
- $T_{supply} \leq 45\ °C$
- $Airflow \geq 0\ m3/h\ \ (7{:}30 - 17{:}30h\ Airflow\ \geq 400\ m3/h)$
- $Airflow \leq 2200\ m3/h$

In the ventilation MPC the following non-linear constraint (2) is present. By using a simplification this constraint can be avoided and enabling to solve the problem using a linear MPC framework. The ventilation energy (Q_{vent}) is non-linear as it contains a product of two optimization variables: $m_{airflow}$ and T_{supply}.

$$Q_{vent} = 0.34 * m_{airflow} * (T_{supply} - T_{zone}) \quad (2)$$

The optimal control problem (OCP) is solved every time step (15 minutes) in which the optimal control output is calculated for the complete prediction horizon using forecasts of the disturbances. The prediction and control horizon used in the MPC framework is 10 steps ahead (i.e. 150 minutes). The forecast of solar radiation, outdoor temperature, CO_2 concentration outdoor and occupancy are forwarded to the OCP. For occupancy, the number of persons obtained from the counting camera is used, perfect prediction of occupancy. The optimized control output (supply temperature and air flow) is forwarded to the dynamic model to calculate the future indoor air temperature and CO_2 concentration for the complete prediction horizon. This procedure is repeated every time step. Measurement noise (random white-noise) is added to the measurement results of the dynamic model to include noise between predictions and observed values. At each time step, the future disturbances and constraints are updated and passed to the OCP to obtain the next control input trajectory.

To solve the OCP the following two cost functions are defined to minimize the energy use with respect to the indoor CO_2 concentration and room temperature. Slack variables are used for the comfort constraints to penalize exceeding the set point. In this way the hard constraints are transformed into soft constraints. For temperature a lower and upper bound is defined where for CO_2 concentration the set point is set at 1000 ppm.

CO_2 control: $Min \sum_{k=0}^{Hp} (zCO2)^2 + (Airflow)^2$ (3)

Subject to:

- $CO2\ room \leq 1000\ ppm + zCO2$
- $Airflow\ CO2 \geq 0\ m3/h\ \ (7{:}30 - 17{:}30h\ \ Airflow \geq 400\ m3/h)$
- $Airflow\ CO2 \leq 2200\ m3/h$
- $zCO2 \geq 0$

Temperature control: $Min \sum_{k=0}^{Hp} (z)^2 + (z1)^2 + (Q_{vent})^2$ (4)

Subject to:

- $T_{room} \geq 22°C - z\ \ (17{:}30 - 7{:}30\ T_{room} \geq 16°C - z)$
- $T_{room} \leq 26\ °C + z1$
- $Q_{vent} = 0.34 * m_{air}(T_{supply} - T_{room})$
- $-6\ kW \geq Q_{vent} \leq 12\ kW$
- $z \geq 0$
- $z1 \geq 0$

For the optimized control the comfort cost function is only active during operating hours of the AHU. During non-operating hours of the AHU the weight factors for comfort are set to 0. In addition, the airflow is set to a minimum airflow rate during operating hours when comfort constraints are not exceeded. Operating hours of the AHU are defined as follows active 07:30-17:30h and not active 17:30-07:30h, in the weekends the AHU is not operating.

3 RESULTS

First results of the CO_2 MPC are shown where the airflow rate is optimized using future predictions of room CO_2 concentration. In 3.2 the final results are depicted for the ventilation MPC. Here, the supply air temperature and airflow rate is optimized using the predictions of the room temperature and results obtained from the CO_2-MPC. To compare the MPC with measurement results, the start- and end time of the AHU is fixed from 07:30 – 17:30h during weekdays. This means that start- and end time of the AHU for both the MPC as the measurements is fixed.

3.1 CO_2 MPC

In order to solve the ventilation MPC first the CO_2-MPC is solved in order to obtain the airflow rate. Figure 4 shows the results for the CO_2-MPC for CO_2 concentration and airflow. It is indicated that the CO_2 concentration is slightly overestimated by the underlying ARX-model. Maximum differences compared to the measurements are up to 200 ppm. The CO_2 MPC exceeds the set point on average by 116 ppm/hour with a total of 18 hours, while the measurements exceed the CO_2 set point by 102 ppm/hour with in total 19 hours exceeding the set point during a 4 week period. Exceeding the set points is attributed to the fact that the system is limited to a maximum air supply rate of 2200 m^3/h. For the airflow results it should be noted that the measurement results for airflow are also influenced by the temperature control. But it can be observed that during use of the classroom on the first day in the afternoon the CO_2-MPC goes to minimal airflow while in reality a maximum airflow rate is used. The CO_2 airflow rate shown in Figure 4 is used as input for the temperature MPC

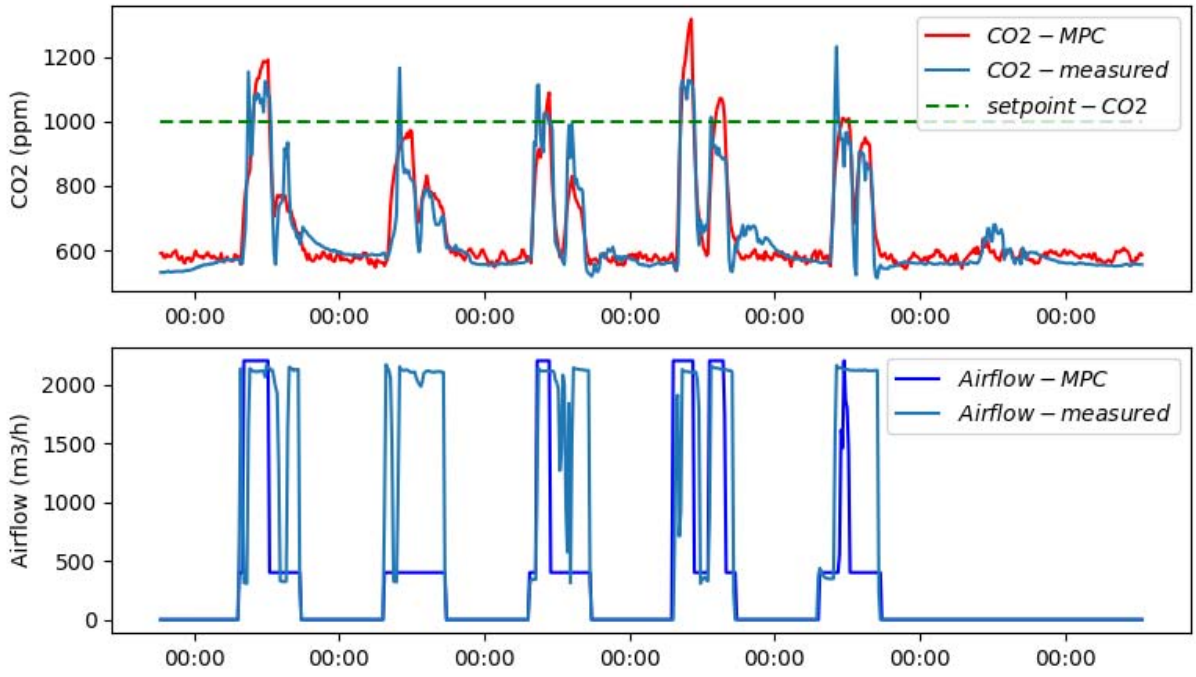

Figure 4; CO_2 concentration (ppm) and airflow rate (m3/h) obtained from the CO_2 MPC and measurements.

3.2 Ventilation MPC

The ventilation MPC results are illustrated in Figure 5 for one week. Results are presented for CO_2 concentration, airflow rate, room- and supply temperature and ventilation energy (Q_{vent}). The airflow and supply temperature presented are the result after post-processing of the results for Q_{vent}.

In order to evaluate the accuracy of the MPC framework the room temperature predictions are compared to the measurements when the AHU is deactivated. In the first weekend of the dataset the temperature decay was 2,0°C for measurements compared to 2.2°C for the MPC. This indicates that the thermal capacity and resistance identified for the predicted model is close to the actual values. The room temperature during measurements is on average 0.22 K/h below the set point while for MPC this is 0.07 K/h. Maximum temperature below the required set point during the day is for measurements 3.2°C and for the MPC 1.6°C. This indicates that the room temperature can be controlled more accurate with MPC compared to the standard RBC in the measurements.

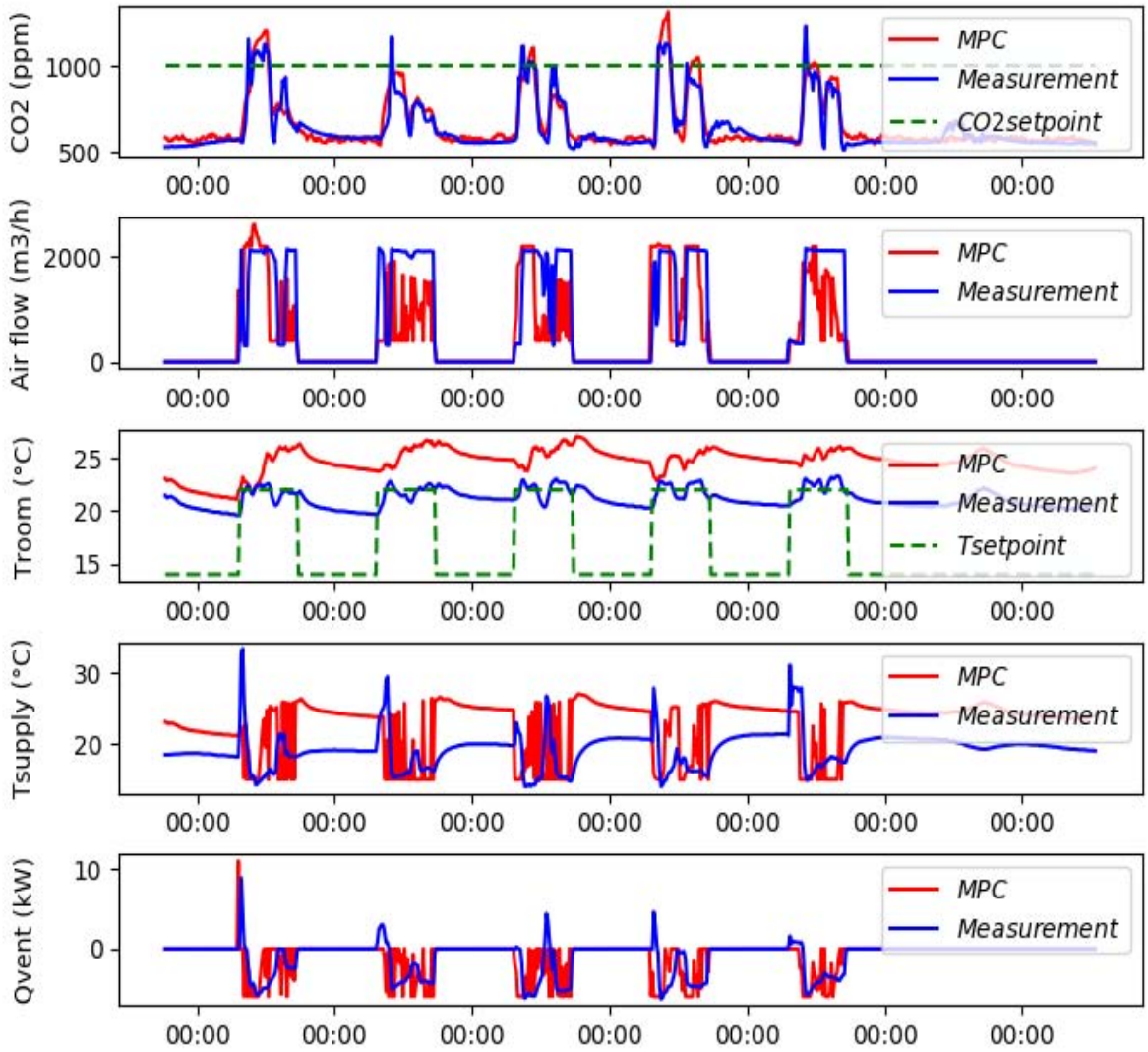

Figure 5; Results for the ventilation MPC compared to the measurements

For the room temperature it is indicated that higher temperature can be expected when the MPC is implemented. In the MPC framework, no penalties are given to the comfort for room temperature within the boundaries of 22-26°C. In practice the adiabatic cooling is activated above a room temperature of 26°C. However, the MPC aims to minimize the future ventilation heating energy. Therefore, difference between MPC and measurements for room temperature can be relatively high, even up to 4°C.

The results for air flow indicate that the MPC ventilation system operates at a lower air flow rate compared to the measurements. This indicates that the airflow is minimized effective by the MPC. The airflow rate is decreased by 47% compared to the measurements. Secondly, the results for Qvent also indicates that the MPC effectively minimizes the energy use. Compared to the measurement results Q_{vent} is decreased by 56% for the complete evaluation period of 4 weeks. These results indicates that the MPC framework enables to reduce the energy use with a better control for the IEQ.

A non-linear MPC might be a better approach to solve the OCP as the constraint for ventilation energy (Q_{vent}) is non-linear, since it contains a product of two optimization variables (supply air temperature and air mass flowrate). In addition, the post processing of the results to obtain the control parameters for supply air temperature and airflow rate might be prone to errors whereas in a non-linear MPC the control parameters can be obtained directly. However, the presented results indicated that the problem can be solved using the presented linear method. This avoids using a non-linear MPC which might be more computational demanding. In addition, a non-linear optimization is sensitive to the initial values.

4 CONCLUSIONS AND FUTURE RESEARCH

This paper discussed the framework of an MPC for an all-air ventilation system. Using a simplification the optimization problem can be solved using a linear approach. In addition, it is shown that an energy efficient MPC could be developed based on a minimal dataset of the following parameters: indoor, supply and outdoor temperature, solar radiation, airflow rate and occupancy. It has to be remarked that occupancy is not measured in most buildings, but in educational building lecture schemes are available for implementation as forecasts in the MPC.

In the future, a non-linear MPC will be tested to compare the results with the linear model, which was discussed in this paper, to evaluate the simplification made to solve the non-linear constraint.

5 ACKNOWLEDGEMENTS

This research is funded by a PhD scholarship of KU Leuven: IOF BAM.

6 REFERENCES

Bengea, S. C., Kelman, A. D., Borrelli, F., Taylor, R., Bengea, S. C., Kelman, A. D., Taylor, R. (2014). *Implementation of model predictive control for an HVAC system in a mid-size commercial building Implementation of model predictive control for an HVAC system in a mid-size commercial building,* HVAC&R Research 20 121-135. https://doi.org/10.1080/10789669.2013.834781

De Coninck, R., & Helsen, L. (2016). *Practical implementation and evaluation of model predictive control for an office building in Brussels*. Energy and Buildings, 111, 290–298. https://doi.org/10.1016/j.enbuild.2015.11.014

Diamond S., Boyd S., (2016), *A Python embedded modelling language for convex optimization*, Journal of machine learning research 17, 1-5

EnBau. (2010). Performance of buildings across the year. Retrieved from http://www.enob.info/en/analysis/analysis/details/performance-of-buildings-across-the-year/

Huang, G., Wang, S., & Xu, X. (2010). *Robust Model Predictive Control of VAV Air-Handling Units Concerning Uncertainties and Constraints.* HVAC&R Research, 16(January), 15–33. https://doi.org/10.1080/10789669.2010.10390890

Liang, W., Quinte, R., Jia, X., & Sun, J. Q. (2015). *MPC control for improving energy efficiency of a building air handler for multi-zone VAVs.* Building and Environment, 92, 256–268. https://doi.org/10.1016/j.buildenv.2015.04.033

Merema, B., Delwati, M., Sourbron, M., & Breesch, H. (2018). *Demand controlled ventilation (DCV) in school and office buildings: Lessons learnt from case studies.* Energy and Buildings, 172, 349–360. https://doi.org/10.1016/j.enbuild.2018.04.065

Merema B., Breesch H., Saelens D., (2018), *Validation of a BES model of an all-air HVAC system in an educational building*, 10th international conference on system simulation in buildings (SSB 2018)

Merema B., Breesch H., Saelens D., (2019), *Comparison of model identification techniques for MPC in all-air HVAC systems in an educational building*, Proceedings CLIMA 2019

Oldewurtel, F., Sturzenegger, D., & Morari, M. (2013). *Importance of occupancy information for building climate control.* Applied Energy, 101, 521–532. https://doi.org/10.1016/j.apenergy.2012.06.014

Prívara, S., Široký, J., Ferkl, L., & Cigler, J. (2011). *Model predictive control of a building heating system: The first experience.* Energy and Buildings, 43(2–3), 564–572. https://doi.org/10.1016/j.enbuild.2010.10.022

Sourbron, M., Verhelst, C., & Helsen, L. (2017). *Building models for model predictive control of office buildings with concrete core activation*, Journal of building performance simulation 6:3 175-198. https://doi.org/10.1080/19401493.2012.680497

Walker, S., Lombardi, W., Lesecq, S., & Roshany-Yamchi, S. (2017). *Application of Distributed Model Predictive Approaches to Temperature and CO2 concentration control in Buildings*. *In IFAC Proceedings Volumes (Vol. 1, pp. 2589–2594).* Elsevier B.V. https://doi.org/10.1016/j.ifacol.2017.08.107

Model based design of intelligent ventilation concepts

Koen Maertens

Duco Ventilation & Sun Control
Handelsstraat 19, 8630 Veurne, Belgium
koen.maertens@duco.eu

KEYWORDS
Smart Building Technologies, Modelbased Product Development, Residential Ventilation Systems

From a product point of view, today's state-of-the-art ventilation boxes for residential buildings are generally reliable, efficient and silent according to formal European and national product standards. Ongoing development projects are focussing on making the products even better, but because of the maturity level of today's solutions, breakthrough revolutions should not be expected.

However, when looking into the real application of ventilation units, there is a significant difference between those formal, rather static product level standards on component level and the dynamic challenges total ventilation systems are confronted with during their full product lifecycle. In our ambition to come to better ventilation solutions in residential buildings, it is key to apply a much more holistic approach, in which several real-world challenges need to be tackled simultaneously. Some typical examples:

- Environmental conditions and even more - human behaviour - cannot be considered in a quasi-static way. In contrast to the static approach of the current type of product performance indicators, it is essential to include dynamic phenomena when analysing controllers and performance of smart ventilation units.
- Intelligent ventilation concepts are typically composed of different components as sensors, actuators or ventilation boxes that are linked for the first time in a specific building with specific characteristics. When developing robust ventilation concepts, one should take into account the variability of building dimensions, ventilation networks, including typical defects or suboptimal topologies.
- The behaviour and health of ventilations systems, including ducts and filters, change over time, affecting the static and dynamic characteristics of the total system. When developing ventilation systems that are capable to guarantee are quality over longer periods, it is essential to validate their capabilities of handling slowly changing system characteristics.
- When analysing the robustness of intelligent systems towards disturbances, this is typically done in a deterministic way (eg fixed climate reference). However, when analysing robustness of systems, it is key to use different realizations of stochastic processes to guarantee overall stability before product release.

When validating new intelligent concepts against above requirements, there is a strong need for extensive testing with different scenario's, building topologies and even product variants. Unfortunately, practical experiments will never be extensive and detailed enough to guarantee sufficient test coverage and at the end, to ensure an efficient and reliable ventilation system in everybody's home. The only way to come to a sufficient test coverage, is to perform concept and algorithm tests in a virtual way, making it possible to increase speed, test coverage and at the end, detailed analysis of some specific phenomena.

Off course, above design challenges are not new and have been tackled before in many other industries. Model-based development processes have been widely used to design and validate smart technologies in high-tech, automated applications as automotive, machine construction or robotics, since those products have the strong requirement to adapt themselves to the local, unknown context in order to guarantee performance, efficiency without loosening safety regulations during their full lifetime.

In this study, an overview is given on the state of the art technology in modelbased product development of ventilation concepts. More specifically, an overview is given on the impact of this design methodology on different aspects of product validation, starting from the relation with suppliers, design of intelligent algorithms, validation of embedded software solutions, supporting service of smart technologies and even the evaluation of intelligent ventilation concepts in close cooperation with research institutes. This study can be considered as an invitation towards different stakeholders to think on how industry and research institutes can create a new, innovative cooperation model to evaluate and to valorise smart ventilation concepts.

A case study on residential mixed-mode ventilation using the Ventilation Controls Virtual Test Bed

Bert Belmans*[12], Dorien Aerts[3], Stijn Verbeke[23], Amaryllis Audenaert[2] and Filip Descamps[14]

1 Department of Architectural Engineering,
Vrije Universiteit Brussel
Pleinlaan 2
1050 Brussels, Belgium
**Corresponding & presenting author:*
Bert.Belmans@vub.be

2 Faculty of Applied Engineering,
Universiteit Antwerpen
Groenenborgerlaan 171
2020 Antwerp, Belgium

3 Unit Smart Energy and Built Environment,
Flemish institute for Technical Research (VITO)
Boeretang 200
2400 Mol, Belgium

4 Daidalos Peutz Bouwfysisch Ingenieursbureau
Vital Decosterstraat 67A bus 1
3000 Leuven, Belgium

ABSTRACT

Mixed-mode ventilation uses intelligent switching between natural and (partly) mechanical ventilation modes to find the best possible balance between indoor air quality, user comfort and energy consumption. It applies demand-control at the level of the operating mode depending on the constraints imposed by the building, its users and its surroundings. Although mixed-mode ventilation is said to have the potential to achieve a comfortable and healthy indoor environment while achieving significant energy savings, it is rarely used in practice. Both academia and practitioners state that a lack of dedicated simulation tools, capable of modelling the inherent complexity of mixed-mode ventilation and its control algorithms, constitutes an obstacle. Also, case studies demonstrating the potential of mixed-mode ventilation in a residential context are scarce. A newly developed tool, VCVTB, is used to compare the performance of a generic mixed-mode ventilation system to a number of ventilation systems that are commonly used in the Belgian residential ventilation context. As key performance indicators, the unmet hours for operative temperature, relative humidity and CO_2 level while people are present are used, as well as the energy demand for heating and the auxiliary energy use for fans. To test the robustness towards users all systems are tested by a semi-probabilistic virtual user panel. A low-energy house for which long-term measurement data is available constitutes a spatial boundary condition. The case study showcases the possibilities of VCVTB to design and compare advanced ventilation strategies. More importantly, it illustrates that mixed-mode ventilation may be a promising concept for residential ventilation within the Belgian context and in other climate areas with mild winters and cool summers. In the investigated building the main advantage of the mixed-mode strategy is not so much the reduction in auxiliary energy use for fans, but rather the outdoor connection during warmer months. Repeated opening of windows effectively reduces unmet hours by adopting adaptive comfort limits. Over an entire year, the windows are opened 30% of the time when using MMV. This can mainly be attributed to the opening of windows during the summer months. Finally, the case study shows that mixed-mode ventilation can provide a solution that is robust towards user behaviour.

KEYWORDS

mixed-mode ventilation, airflow network, indoor air quality, user behaviour, building simulations

1 INTRODUCTION

Ventilation systems must find the best possible balance between indoor air quality (IAQ), user comfort and energy consumption within the constraints imposed by the building and its users. In the current Belgian residential ventilation context, this largely translates into the use of two

groups of ventilation strategies: (1) mechanical extract strategies with natural inlets through purpose provided openings, and (2) balanced mechanical ventilation strategies with mechanical supply, mechanical extract, heat recovery and air filters. Both strategies are accompanied by a continuous auxiliary electricity consumption for ventilation fans. Demand-controlled algorithms that adjust airflow rates based on sensor measurements can reduce auxiliary energy use. However, as minimum flow rates must be maintained, the use of auxiliary energy is never completely eliminated. By intelligently switching between various ventilation strategies, single-mode systems can be upgraded to multi-mode solutions. Multi-mode systems that include both natural and mechanical operating modes are referred to as mixed-mode (MMV) ventilation.
Many authors point out the potential of MMV in climate areas with mild winters and cool summers (Köppen classication, C_{fb}), such as Belgium. The frequent use of natural ventilation modes during warmer periods creates indoor conditions that fluctuate with the outside. The resulting adaptive context can broaden the comfort limits of the building occupants in relation to the comfort limits in a mechanically controlled indoor climate (Carlucci, Bai, de Dear, & Yang, 2018). Both practitioners and researchers state that a lack of dedicated simulation tools, capable of modelling the inherent complexity of MMV and its associated control algorithms, constitutes an obstacle for the further development and its use in daily practice (Gandhi, Brager, & Dutton, 2014). Also, there are few simulation based studies investigating the potential of mixed-mode ventilation in a residential context. In response, this study seeks to bring MMV awareness to the fore. A comparative case study is added to the list of residential MMV studies and the functioning of a novel research tool for MMV is illustrated.

2 CASE STUDY

A new simulation tool, is used to compare the performance of a generic mixed-mode ventilation system to a number of ventilation systems that are commonly used in the Belgian residential ventilation context. A low-energy house for which long-term measurement data is available constitutes a spatial boundary condition. The performance comparison is made based on the number of unmet hours for operative temperature, relative humidity and CO_2 concentration in the living room and the master bedroom of the house, the energy use for heating and the auxiliary energy use for fans. To assess the robustness towards users, the investigated ventilation systems are tested by a virtual user panel. Robustness is defined as the ability to be indifferent in terms of performance relative to varying user behaviour. In this study it is assessed on the basis of the standard deviation on unmet hours.

2.1 VCTVB

VCVTB, the Ventilation Controls Virtual Test Bed is a modelling and testing environment for advanced ventilation strategies built around the building energy modelling (BEM) software EnergyPlus 8.8.0 (Belmans, Aerts, Verbeke, Audenaert, & Descamps, 2019). For the calculation of airflows, it uses the integrated EnergyPlus airflow network (AFN) model (Gu, 2007). In contrast to quasi-dynamic coupling of AFN and BEM calculations, typical for co-simulation (Dols, Emmerich, & Polidoro, 2016), the integrated coupling approach is fully dynamic. In VCTVB, the capabilities of the integrated EnergyPlus AFN model have been extended by source code changes. E.g. components have been added to model self-regulating trickle vents and it has been made possible to simulate demand-control on the supply and extract side of a balanced mechanical ventilation system. The platform is enriched with additional modules for pre- and post-processing, including modules for automated graphical output. To incorporate the impact of a realistic environment with obstacles and elevations, wind pressure coefficients on the building envelope are determined using CFD simulations in OpenFOAM. To charge for user behaviour, a novel semi-probabilistic user model focused on indoor air

quality studies is used. This model builds on the user model of Aerts (Aerts, 2015) for single zone building energy demand simulations which uses data from Belgian time-use surveys (Minnen, Glorieux, & van Tienoven, 2016). It was enhanced for multi-zone IAQ modelling.

2.2 Case study house

The case study house, Figure 1, that is used for the comparative analysis is a low energy house in a suburban environment close to the city of Mechelen (Belgium). It is inhabited by a couple in their thirties (full-time employed) with two school-bound children. The annual primary energy consumption for heating, cooling, domestic hot water and auxiliary energy use of systems and fans is rated at 43 kWh/m². The overall heat transfer coefficient of the building envelope is 0.31 W/m²K. The internal air volume of the house is ~700m³. The infiltration rate was determined by means of a blower door test to be 0.6 ACH50. The house is equipped with a balanced mechanical ventilation system with a counter flow heat exchanger with summer bypass. A control valve linked to a time switch is used to alternate between a daytime and night time duct network. The airflow rates are controlled using a weekly time schedule. A long-term measurement campaign was carried out in the house from September 2016 - September 2017. It involved monitoring dry bulb temperatures, relative humidity and CO_2 levels inside the living room and the master bedroom of the house and dry bulb temperatures, relative humidity, CO_2 levels, wind direction and wind speed outside the house. The opening positions of the most important windows in the living and master bedroom were monitored as well, as was the auxiliary energy use of the ventilation fans. All measurements were taken at a time interval of one minute. Based on the outside measurements, an .epw weather file with a time step of one minute was created. Missing data was completed with data from MERRA-2 (Gelaro, et al., 2017) and CAMS (Schroedter-Homscheidt, 2016).

2.3 Modelling assumptions and tuning

A model of the case study house was created in EnergyPlus. A virtual household with similar characteristics as the real household (family composition, age, gender, employment level) was added using the behaviour module of VCVTB . In the comparative study CO_2 is used as an IAQ tracer and as a control parameter for demand-control. To include a credible CO_2 production of users, the user model of Aerts (Aerts, 2015) was expanded with CO_2 generation rates for the human metabolism based on Persily (Persily & de Jonge, 2017). Age and gender were combined with occupant activity to assign every occupant a metabolism. As a result, the synthetic users that are created using VCVTB have a varying metabolic heat, moisture and CO_2 production rate throughout the simulation. Electrical heat sources are introduced to model appliance related heat and moisture production. A distinction is made between a sensible, latent and lost fraction of the electrical power level of the source. The CO_2 production from people is introduced into the model using EnergyPlus *ZoneContaminantSourceAndSink* objects.

An airflow network model of the building was implemented in EnergyPlus. By using an airflow network approach all airflows are calculated simultaneously using pressure-based calculations. As a result mechanical ventilation flow rates, wind and stack driven ventilation flow rates and in/exfiltration are interconnected and can affect each other. Each room was represented by one AFN node assuming well-mixed conditions at room level. Flow coefficients and flow exponents for purpose provided openings were based on Liddament (Liddament, 1996) and Orme (Orme, Liddament, & Wilson, 1998). For modelling natural ventilation, tilt and turn windows were opened in a slight tilting position with a discharge coefficient of 0,82. They were modelled using *AirflowNetwork:MultiZone:Component:DetailedOpening* objects that allow bidirectional airflow.

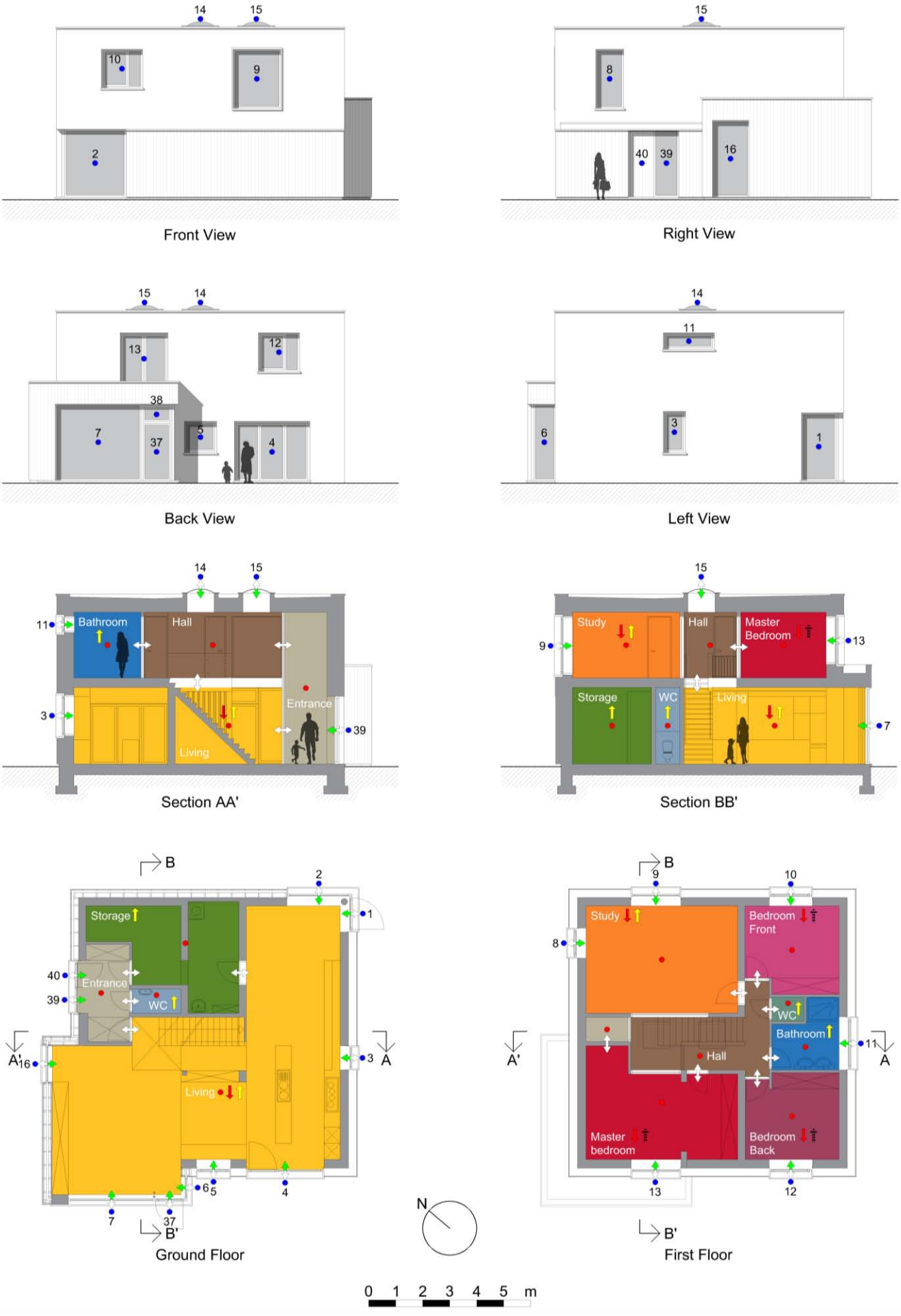

Figure 1: Layout of the case study house

The cracks responsible for infiltration and exfiltration were assumed to be located around the windows. Their flow coefficients and exponents were defined based on the infiltration flow rate obtained from a blower door test. The blower door test was mimicked in the virtual model to verify the infiltration flow rate in the Airflow Network. The moisture buffering capacity of the building was included using the EnergyPlus Effective Moisture Penetration Depth (EMPD) model. The moisture production of activities in the user model was balanced based on the difference in vapour pressure levels between the modelled and the monitored house.

2.4 Comparison with in-situ measurements

Instead of looking at point-wise chronological similarities between the monitored and the modelled case study house, a comparison is made based on a cumulative distribution of the occurrence of a condition, Figure 2. Looking at point-wise data makes little sense since the behaviour of the virtual users is similar, but never the same as the behaviour of the real residents. The simulated and monitored dry bulb temperatures in June and the simulated and monitored CO_2 levels in the living room and the master bedroom in January are shown in the top graph. For temperature a summer month is shown because an idealised heating system is used in the simulation. To exclude the influence of window opening in summer a winter month is shown to compare CO_2 concentrations. In the bottom graph the monthly averaged internal and external vapour pressure levels p_{vi} and p_{ve} are compared for the period January-July. This comparison is used to evaluate the ratio between moisture production and moisture removal. It was also used as a control utility to fine-tune the moisture production of activities in the user model.

The indoor temperature is on average 0.5°C higher in the simulations than in the collected data. Also, the spread in the simulation data is less pronounced. The difference in spread can be explained by the well-mixed AFN assumption. This assumption can also be a reason for the 0.5°C deviation. Not all windows were monitored in the case study. Of the windows that were monitored, it was only recorded whether they were open or closed. It was not recorded how far they were open. It was assumed that when open, they were in a small tilt position. User operated shading control actions were implemented based on the temperature difference between inside and outside and incident solar radiation. The uncertainty in assumed and actual window opening behaviour and shading control may be a second reason for deviating results. Though not perfect, we conclude that there is a good match in terms of predicted and measured temperatures.

Mechanical ventilation flow rates were fixed based on measured values. Because the CO_2 concentrations in the simulation results show a good correlation with the monitored data this indicates that the CO_2 production of the virtual users bears a good resemblance to that of the real inhabitants. Offsets can be explained logically. Measurements were made in a limited number of discrete locations in space, while simulated values represent an aggregated value. Also, the simulated users are approximations of real users with similar but nevertheless different activities. In the bedroom there is a better correlation because the uncertainty on the activities is small. In the living room this uncertainty is bigger. Finally, the mixed-mode assumption better approximates the bedroom because of its size. The living space is considerably larger and more difficult to approximate by the well-mixed assumption of a single AFN node. Still, we conclude that there is a good match.

The air change rate in the model due to mechanical ventilation is based on the time schedule of the actual flow rates in the case study house. The airtightness of the model corresponds to the actual airtightness of the building. The graph shows that the moisture production and moisture removal balance each other in the same way in the model as in reality. The internal moisture production must therefore be reasonably well estimated by the occupant model. To conclude,

the similarity between the modelled and measured values give sufficient confidence in the adopted approach. The virtual model is retained as a basis for the further comparison between ventilation systems.

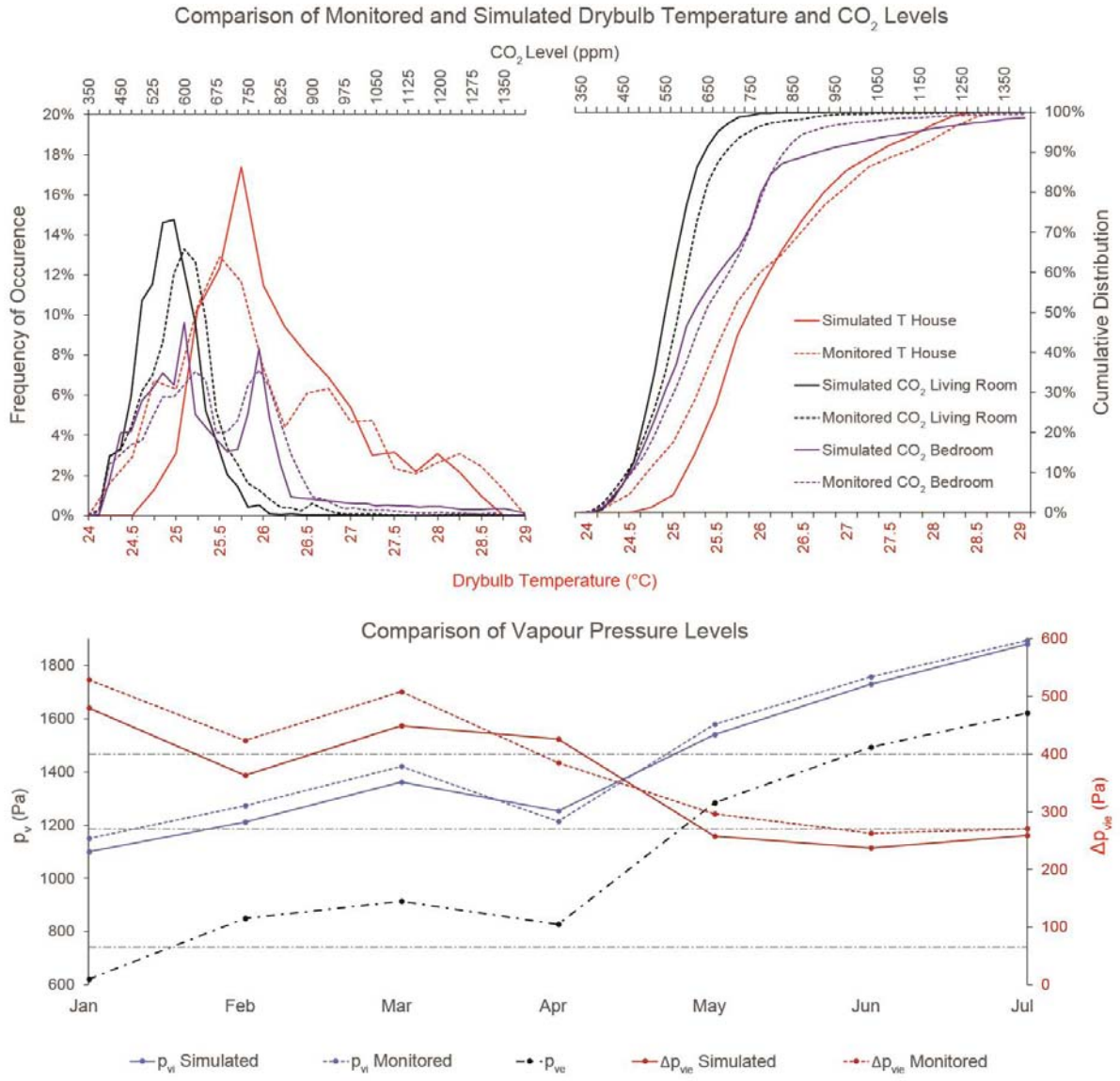

Figure 2: Comparison between measured and simulated drybulb temperatures and CO_2 levels in the living room and the master bedroom of the case study house, and between measured and simulated vapour pressure levels.

2.5 Generic Mixed-Mode Ventilation System

A generic mixed-mode ventilation strategy is implemented. It has three operating modes: Mode 1 is a fully natural ventilation mode where purpose provided openings are opened and closed to provide hygienic ventilation (small window opening positions and trickle vents). It is considered to be the preferable mode if outside conditions are favourable. There is no auxiliary energy use for fans. In Mode 2, a central mechanical extract fan is activated to assist natural ventilation through purpose provided openings in the event that the natural driving forces (stack, wind) are insufficient to ensure the required flow rates. There is auxiliary energy use of one ventilation fan. Mode 3 is a balanced mechanical ventilation mode with heat recovery. It is used when the outside conditions are unfavourable for natural ventilation (too noisy, too windy, too warm/cold, bad outdoor air quality…). It ensures good IAQ and thermal comfort while avoiding

unwanted ventilation losses and heat gains. Mode 3 is well controllable but there is auxiliary energy use of two ventilation fans. In Mode 2 and 3, demand-control is applied on top of the adjustment of the operating mode. In Mode 1, the opening position of the windows is adjusted to the required airflow rates. The ventilation mode that is active at a given time is adjusted by means of a control algorithm, which is implemented in an EnergyManagementSystem (EMS) program, Figure 3. This approach offers increased control as compared to the integrated *EnergyPlus AvailabilityManager:HybridVentilation*. After selecting an operating mode, the air flow rates and window opening positions are adjusted.

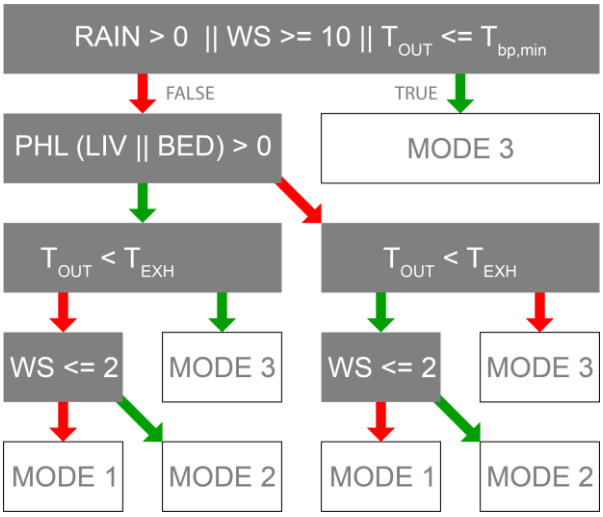

Figure 3: Control logic for the selection of the operating mode of the MMV system. PHL = predicted heat load (W), WS = local undisturbed windspeed at a height of 10m (m/s). $T_{bp,min}$ = The minimum threshold value of the outdoor temperature at which the bypass of the heat exchanger is allowed to operate. It is set at 13°C. T_{OUT} = outdoor drybulb temperature (°C) , T_{EXH} = return air temperature (°C) after the *AirLoopHVAC:ZoneMixer*. Adjustment of window opening positions and airflow rates are a next step in the control algorithm. They are not included in this schematic.

2.6 Comparative Study

The behaviour module of VCVTB is used to generate a test panel of households of synthetic users with semi-probabilistic behaviour. These users move through the virtual building model and perform activities depending on the probability of an activity to occur. The panel consists of 7 household types with a particular family composition. It includes 20 families per type.
Five ventilation systems are tested by the panel, resulting in 700 simulations. The systems under comparison are:

- A natural supply / mechanical extract ventilation system (n/M NBN) with self-regulating trickle vents and continuous extract flow rate. The extract flow rate is set to 50% of the normative design flow rate resulting from NBN D50-001 (Belgisch Instituut voor Normalisatie, 1991).
- A constant flow balanced mechanical ventilation system (M/M NBN) with a counter flow heat exchanger. The summer bypass of the heat exchanger can operate when the outside temperature is at least 13°C. The supply and extract flow rate is set to 50% of the normative design flow rate, cfr. n/M NBN.
- A balanced mechanical ventilation system with demand-controlled supply and extract flow rates at room level (M/M DCV) and a counter flow heat exchanger. DCV control is based on CO_2 concentration, relative humidity and zone air temperature. The maximum CO_2 threshold is set at IDA1 (Very Good Quality, NBN EN 13779. The maximum RH threshold

is set at 60% RH (Upper limit of Class B, Good Quality, NBN EN 15251). CO_2 control is active in all rooms. RH control is active in the living room and the bathroom.

- A demand controlled mixed-mode ventilation system (MMV) that combines a fully natural mode, by opening windows, with a mechanically assisted extract mode and the balanced mode of M/M DCV. Unlike M/M DCV the balanced mode is only controlled based on CO_2 concentration and relative humidity. Temperature control is achieved by selecting an appropriate operating mode. In MMV 'auto' the controller can switch between operating modes at any time. In MMV 'manual' the operating mode can only change if an adult is at home and awake. A mode remains active if no one is present. Perfect users are assumed.

The MMV systems are the only systems in which windows are opened. Because they actively use window opening in summer, the indoor climate fluctuates with the outside. As a result, people are expected to adapt their clothing and metabolism. Therefore adaptive comfort limits are applied according to NBN EN 15251 (Nicol & Humpreys, 2010). The other systems only operate using the designed airflow paths in accordance with the provisions of NBN D50-001. These systems are subject to strict comfort limits. The unmet hours for the key performance indicators operative temperature, relative humidity and CO2 level as well as the auxiliary energy use for fans and the energy demand for heating are compared in Table 1. The standard deviation due to user behaviour is included to reflect the robustness of each system.

The M/M NBN strategy limits unwanted ventilation losses and uses heat recovery. The energy demand for heating is low compared to n/M NBN. The auxiliary energy use for fans is more than twice as big as n/M NBN. M/M DCV is an energy efficient alternative to M/M NBN. It has negligible unmet hours in terms of CO_2. Relative humidity levels are good and robustness is high. The heating demand is reduced through demand-control. The summer comfort is worse compared to systems with natural ventilation possibilities because natural ventilation (free cooling) rates can be much higher. The auxiliary energy use is high because DCV is also used for temperature control (bypassing the heat exchanger). The MMV system resembles the M/M DCV system in terms of robustness and IAQ. The Unmet hours for RH and CO_2 are similar, as is the energy demand for heating. The auxiliary energy consumption is reduced. The MMV systems combine the summer comfort of systems with natural supply with the energy efficiency of balanced mechanical ventilation with heat recovery. MMV successfully limits the CO2 concentration to IDA 1. Relative humidity is within the limits of moisture class B (25-60%, Good). The temperatures are within the limits of temperature class C (Acceptable). Windows open around 30% of the year in the MMV systems. Window opening is mainly concentrated in the summer period. In brief, the MMV systems have good performance and good robustness. Their main asset is that they can benefit from adaptive comfort limits in summer so that unmet hours remain low. Based on the investigated case study they do not outperform demand-controlled balanced mechanical ventilation with heat recovery in terms of energy consumption, however they do perform equally well. The auxiliary energy use for fans is lower, but the energy demand for heating is slightly higher.

3 CONCLUSIONS

Several authors indicated a need for dedicated simulation tools for MMV without the hassle of co-simulation. In response to this, a new test platform for MMV studies, the Ventilation Controls Virtual Test Bed was presented in earlier research. This test bed was used to compare the performance of two generic MMV systems to the performance of several reference systems in a case study house in Belgium. For a well-documented case (building + ventilation system) a good connection was found between in-situ measurements and modelling results. The model of this case was used as starting point for a performance comparison between ventilation

systems. This comparison showed that during winter MMV systems behave almost identical as a demand-controlled balanced mechanical ventilation system with heat recovery. However, during summer, natural ventilation modes prevail and the MMV systems benefit from the adaptive comfort limits that apply. This effectively reduces unmet hours for overheating compared to a state-of-the-art demand-controlled mechanical ventilation system. Moreover, the comparison shows that the investigated MMV systems provide a robust solution in relation to user behaviour. The auxiliary energy use for fans is lower when using MMV, but the energy consumption for heating is slightly higher than the M/M DCV system. The energy demand for heating could be further reduced by optimisation. However, based on this study MMV should mainly be seen as a strategy that can contribute to an increase in summer comfort by leveraging adaptation capabilities.

Table 1: Comparative table with aggregated results of key performance indicators for 700 simulations. Note that the MMV* systems employ adaptive comfort criteria according to NBN EN 15251.

Yearly Unmet Hours

VENTILATION SYSTEM COMPARISON			n / M NBN		MMV* manual		MMV* auto		M / M DCV		M / M NBN	
			μ	2σ	μ	2σ	μ	2σ	μ	2σ	μ	2σ
Yearly Unmet Hours Living Room												
Class A*	T < 25.5 °C	UH_{PP}	525	260	176	222	191	242	685	284	812	372
Class B*	T < 26 °C	UH_{PP}	422	248	12	36	15	54	485	224	679	334
Class C*	T < 27 °C	UH_{PP}	211	204	0	1	0	1	167	130	423	280
Class A	30 % < RH < 50 %	UH_{PP}	1959	426	1274	320	1244	300	985	316	1045	240
Class B	25 % < RH < 60 %	UH_{PP}	397	98	104	48	100	40	49	38	84	30
Class C	20 % < RH < 70 %	UH_{PP}	31	12	0	0	0	0	0	0	0	0
IDA1	$CO_2 < CO_{2env} + 400$ ppm	UH_{PP}	0	0	7	16	8	18	0	0	0	1
IDA2	$CO_2 < CO_{2env} + 600$ ppm	UH_{PP}	0	0	0	0	0	0	0	0	0	0
IDA3	$CO_2 < CO_{2env} + 1000$ ppm	UH_{PP}	0	0	0	0	0	0	0	0	0	0
Yearly Unmet Hours Master Bedroom												
Class A*	T < 25.5 °C	UH_{PP}	291	66	27	22	29	26	119	40	425	104
Class B*	T < 26 °C	UH_{PP}	215	72	4	6	5	6	57	26	328	100
Class C*	T < 27 °C	UH_{PP}	91	46	4	6	5	6	6	6	142	90
Class A	30 % < RH < 50 %	UH_{PP}	1359	186	976	178	915	154	552	80	544	126
Class B	25 % < RH < 60 %	UH_{PP}	209	38	110	32	102	20	21	6	0	2
Class C	20 % < RH < 70 %	UH_{PP}	14	8	13	14	5	8	0	0	0	0
IDA1	$CO_2 < CO_{2env} + 400$ ppm	UH_{PP}	706	106	31	18	22	18	6	6	1585	142
IDA2	$CO_2 < CO_{2env} + 600$ ppm	UH_{PP}	254	140	4	6	0	0	0	0	0	0
IDA3	$CO_2 < CO_{2env} + 1000$ ppm	UH_{PP}	4	7	2	4	0	0	0	0	0	0

Energy Demand for Heating , Auxiliary Fan Electricity and Average Airflow Rates

VENTILATION SYSTEM COMPARISON			n / M NBN		MMV* manual		MMV* auto		M / M DCV		M / M NBN	
			μ	2σ	μ	2σ	μ	2σ	μ	2σ	μ	2σ
Yearly												
Average auxiliary energy use of fans		kWh/a	110	0	133	16	137	18	401	72	352	0
Average energy demand for heating		kWh/a	9933	860	4640	566	4648	580	4440	614	5574	640
Average	Min	m3/h			0	0	0	0	40	0		
Ventilation	Mean	m3/h	145	0	56	10	57	10	112	20	210	0
Flow Rate	Max	m3/h			425	4	425	4	427	2		
Heating Period												
Average auxiliary energy use of fans		kWh	54	0	73	4	73	4	74	4	173	0
Average energy demand for heating		kWh	9140	646	4476	482	4488	498	4353	570	5381	562
Average	Min	m3/h			0	0	0	0	37	2		
Ventilation	Mean	m3/h	145	0	58	10	58	10	58	10	210	0
Flow Rate	Max	m3/h			210	18	213	16	207	22		
Summer and mid-season												
Average auxiliary energy use of fans		kWh	56	0	60	14	64	14	327	70	179	0
Average energy demand for heating		kWh	793	214	164	86	160	84	87	44	192	78
Average	Min	m3/h			0	0	0	0	37	4		
Ventilation	Mean	m3/h	145	0	55	12	56	12	167	32	210	0
Flow Rate	Max	m3/h			425	4	425	4	427	2		

4 ACKNOWLEDGEMENTS

This research was conducted under a four-year assistant mandate at Vrije Universiteit Brussel. It did not receive any other grant from external funding agencies. Many thanks to the owners of the case study house for their hospitality and to Mr. Van den Brande for sharing the data of his weather station. VCVTB is dedicated to my grandfather R. Spruyt in loving memory of our friendship.

5 REFERENCES

Aerts, D. (2015). *Occupancy and Activity Modelling for Building Energy Demand Simulations, Comparative Feedback and Residential Electricity Demand Characterisation.* Brussels: Vrije Universiteit Brussel.

Belgisch Instituut voor Normalisatie. (1991). *NBN D 50-001 Ventilation systems for housing.* Brussels: Belgisch Instituut voor Normalisatie,.

Belmans, B., Aerts, D., Verbeke, S., Audenaert, A., & Descamps, F. (2019). Set-up and evaluation of a virtual test bed for simulating and comparing single- and mixed-mode ventilation strategies. *Building and Environment*, 97-111.

Brager, G., & Baker, L. (2009). Occupant satisfaction in mixed-mode buildings. *Building Research and Information*, 369-380.

Carlucci, S., Bai, L., de Dear, R., & Yang, L. (2018). Review of adaptive thermal comfort models in built environmental regulatory documents. *Building and Environment*, 73-89.

Deuble, M. P., & de Dear, R. J. (2012). Mixed-mode buildings: A double standard in occupants' comfort expectations. *Building and Environment*, 53-60.

Dols, W. S., Emmerich, S. J., & Polidoro, B. J. (2016). Using coupled energy, airflow and indoor air quality software (TRNSYS/CONTAM) to evaluate building ventilation strategies. *Building Services Engineering Research and Technology*, 163-175.

Gandhi, P., Brager, G., & Dutton, S. (2014). *Mixed Mode Simulation Tools.* Berkeley: Center for the Built Environment (CBE).

Gelaro, R., McCarthy, M. J., Surez, R., Todling, A., Molod, L., Takacs, C. A., . . . Reichle, K. (2017). The modern-era retrospective analysis for research and applications, version 2 (MERRA-2). *Journal of Climate*, 5419-5454.

Gu, L. (2007). Airflow network modeling in EnergyPlus. *Proceedings of the 10th International Building Performance Simulation Association Conference and Exhibition Building Simulation* (pp. 964-971). Beijing: International Building Performance Simulation Association.

Liddament, M. (1996). *A Guide to Energy Efficient Ventilation.* Coventry: Air Infiltration and Ventilation Centre.

Minnen, J., Glorieux, I., & van Tienoven, T. P. (2016). Who works when? Towards a typology of weekly work patterns in Belgium. *Time & Society*, 652-675.

Nicol, F., & Humpreys, M. (2010). Derivation of the adaptive equations for thermal comfort in free-running buildings in European standard EN15251. *Building and Environment* , 11-17.

Orme, M., Liddament, M., & Wilson, A. (1998). *Numerical Data for Air Infiltration and Natural Ventilation Calculations.* Coventry: Air Infiltration and Ventilation Centre.

Persily, A., & de Jonge, L. (2017). Carbon dioxide generation rates for building occupants. *Indoor Air*, 868-879.

Schroedter-Homscheidt, M. (2016). *The Copernicus Atmosphere Monitoring Service (CAMS) Radiation Service in a nutshell.* Reading: ECMWF.

Influence of the external pressure tap position on the airtightness test result

Jiří Novák*[1]

1 Czech Technical University
Faculty of Civil Engineering
Thákurova 7
166 29 Prague, Czech Republic
**Corresponding author: jiri.novak.4@fsv.cvut.cz*

KEYWORDS

airtightness, blower door, measurement uncertainty, repeatability, wind

1 PURPUSE OF THE WORK

Due to the wind induced pressure, different results may be obtained if the inside-outside pressure difference is measured across different locations on the building envelope, i.e. if the external pressure tap of a differential pressure sensor measuring this pressure difference is placed in different positions. Therefore, the position of the external pressure tap may influence an airtightness test result as well. As the wind induced pressure is linked with the wind speed, it can be expected that the influence of the external pressure tap position on the airtightness test result would be amplified with increasing wind speed. The aim of this full-scale experiment is to quantify the variability of the airtightness test results obtained under repeatability conditions with different external pressure tap positions in function of the wind speed. The motivation is a better understanding of the real influence of the wind allowing a better estimation of the measurement uncertainty as well as possible improvement of the measurement technique.

2 METHOD

The airtightness of a single-family house was tested 9 times according to EN ISO 9972. During each test, the wind speed and the air flow rate through the measuring device fan were recorded simultaneously with 4 different inside-outside pressure differences.

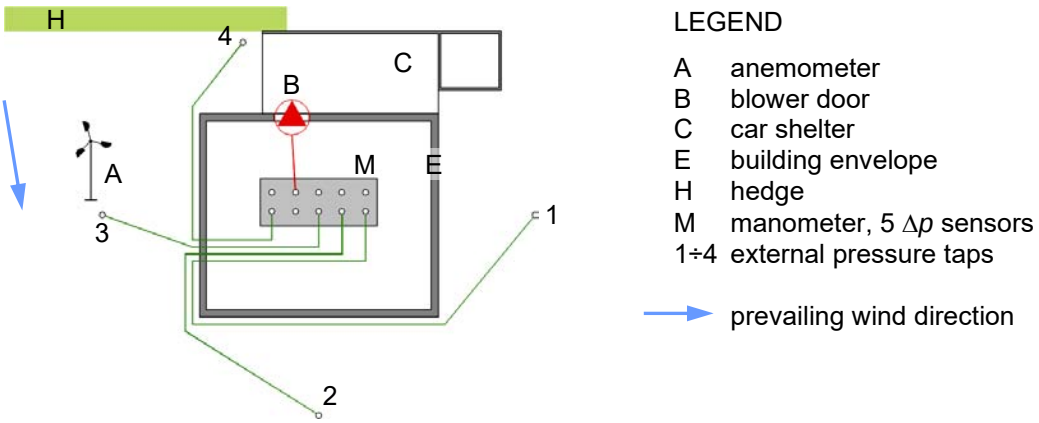

Figure 1: The experimental set-up, schematic plan view

The external pressure taps of the 4 pressure sensors measuring the inside-outside pressure differences were placed in different positions around the building while the internal pressure taps were in the same position inside the building (see Fig. 1). The external pressure taps were placed at the ground level, approx. 5 ÷ 8 m from the facades. The end of each pressure tap was equipped with a T-piece. For each test, 5 values of the air flow rate q_{50} [m^3/h] were calculated out of the 4 measured inside-outside pressure differences respectively and out of their average value (calculated).

3 RESULTS

Unfortunately, during all the 9 tests, the wind conditions were rather similar. The variability of the q_{50} values resulting from the same test and corresponding to the 4 different positions of the external pressure tap is very low (see Fig. 2). Apart from the test 09, the range of the 4 q_{50} values resulting from one test does not exceed 5.2 m^3/h. Despite expectations, the variability of the results decreases with the wind speed. Regardless the position of the external pressure tap, very high coefficients of determination r^2 were obtained. In general, higher r^2 values were obtained if the inside-outside pressure difference was calculated as average of the readings corresponding to the 4 positions of the external pressure tap.

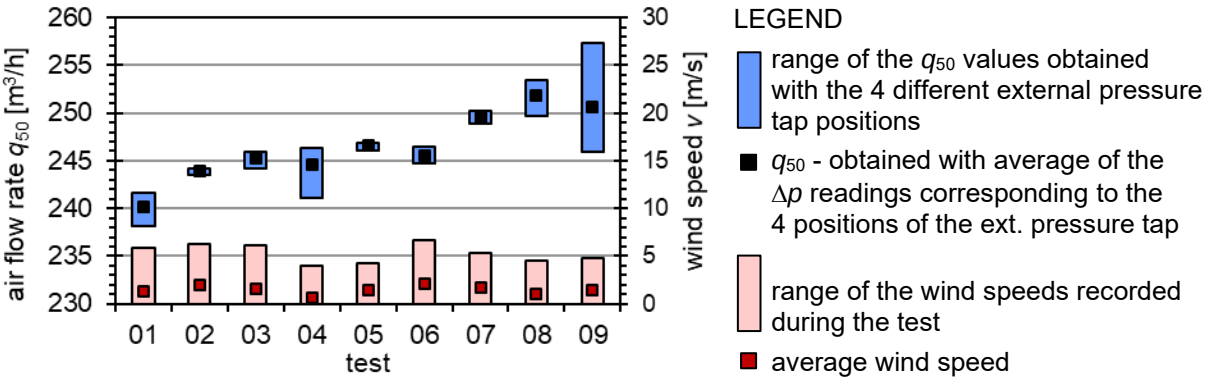

Figure 2: Overview of the results (q_{50} is the average of pressurization and depressurization test results)

4 DISCUSSION AND CONCLUSIONS

Under the wind conditions similar to this study, the external pressure tap position seems not to impede the repeatability. The statistical tests according to the ISO 5725-6 standard proved that the variability of the 4 q_{50} obtained with the 4 different external pressure tap positions within the same test fit well an interval which can be expected with regard to the repeatability of the measurement method (the repeatability was determined in another stand-alone experiment). The low wind speeds and some technical measures (T-pieces, longer periods of record, distance of the pressure taps from facades) may explain the low variability of the q_{50} values and high r^2 values obtained. So, such measures seem to effectively improve the measurement accuracy.

Owing to the small differences between the average wind speed recorded during the individual tests, the correlation found between the variability of the q_{50} and the wind speed is questionable. The results do not allow quantification of the measurement uncertainty due to the wind. A more extensive experiment in more variable wind conditions is needed for this purpose.

The averaging of the readings from the 4 external pressure taps proved to be good strategy for ensuring high r^2 value as required by EN ISO 9972 and hence for reducing the measurement uncertainty due to the wind.

Airtightness of buildings – Considerations regarding place and nature of pressure taps

Christophe Delmotte

Belgian Building Research Institute
Avenue Poincaré, 79
1060 Brussels, Belgium

ABSTRACT

This paper discusses two particular points of the buildings airtightness measurement method (ISO 9972) in relation with the pressure difference: (1) the nature of the pressure tap and (2) the place of the pressure tap outside.
The principle of the buildings airtightness measurement method is to measure the pressure difference induced by a given air flow rate generated by a fan. To that end, pressure measurements are made between inside and outside the building. However, with the increasing number of measurements and laboratories, more and more varied pressure taps such as pierced bottles or traffic cones are appearing. In addition, the place of the pressure tap outside largely varies; from very close to the building to very far away.
Although this may seem insignificant at first glance, the nature and the place of the pressure taps play a crucial role in the measurement uncertainty. This is mainly due to the effect of wind on the building and the dynamic pressure it generates.
This paper explains why it is necessary to use static pressure taps and place them away from the building and possible obstacles.

KEYWORDS

Airtightness of buildings, pressure tap, pressure difference, wind, zero-flow pressure

1 INTRODUCTION

In European countries, increasing importance has been given to airtightness of buildings since the first publication of the directive on the energy performance of buildings in 2002. In some countries there are even requirements or financial incentives linked with the airtightness level. It is therefore more and more important to pay attention to the quality of airtightness measurements.
Following the increase in the number of measurements and laboratories, discrepancies are beginning to appear in some aspects of the test. This is the case, for example, for pressure taps for which some use drilled bottles or traffic cones. The location of the pressure tap outside also varies greatly, from very close to the building to very far away; some even take the pressure from inside their car.
Although this may seem insignificant at first glance, the nature and the place of the pressure taps play a crucial role in the measurement uncertainty. This is mainly due to the effect of wind on the building and the dynamic pressure it generates.

2 PRESSURE DIFFERENCE INDUCED BY THE FAN

In given climatic conditions (wind and temperature) and in the absence of fan, pressure differences $\Delta p_{0,j}$ are naturally generated across the envelope of a building. The equilibrium internal pressure is such that the air flow that enters the building is equal to the flow that leaves. The sum of the air flows through the building envelope is therefore equal to zero (formally we

should talk about mass flow). Accordingly, parts of the envelope must necessarily undergo underpressure while others are in overpressure.
In the absence of wind or temperature difference, the action of a fan located in the building envelope induces an identical pressure difference Δp across all points of the envelope. However, this is not quite true because the internal partitioning of the building may generate pressure drop (see 3.6). ISO 9972 requires opening all interior doors in order to minimize this effect and to consider the whole building as a single zone.
When adding the effect of a fan to that of the wind and of the temperature difference, each point (j) of the envelope is subjected to a pressure difference $\Delta p_{m,j}$ equal to the sum of those it would undergo for each of the two separate effects (Δp and $\Delta p_{0,j}$) (Sherman 1990) (Figure 1 and Formula 1). Each point thus undergoes a similar change in pressure while keeping its relative difference compared to the other points. Note that this principle of addition is not true for air flow rates.

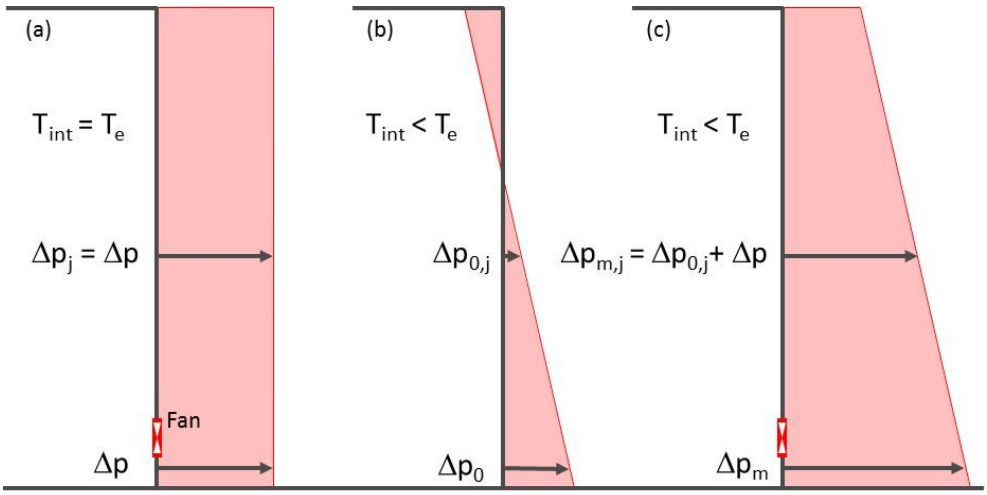

Figure 1: Example of pressure distribution over the height of a building (a) for a fan only, (b) for a temperature difference only and (c) for the combination of the fan and the temperature difference.

Additivity of pressure differences is used in ISO 9972 to indirectly measure the pressure difference induced by the fan:

1. Zero-flow pressure difference Δp_0: Pressure difference is measured between inside and outside the building when it is subject to natural conditions only (fan off and covered)
2. Measured pressure difference Δp_m: Pressure difference is measured between inside and outside the building when the fan is operating
3. Induced pressure difference Δp: Pressure difference induced by the fan is calculated by subtracting the first value from the second one (Formula 2)

$$\Delta p_{m,j} = \Delta p_{0,j} + \Delta p \quad (1)$$

$$\Delta p = \Delta p_m - \Delta p_0 \quad (2)$$

The principle of the buildings airtightness measurement method (ISO 9972) is then to make the link between the air flow rate generated by the fan and the induced pressure difference in order to characterize the airtightness of the building.

3 MEASUREMENT ERROR

3.1 Possible sources of error

Considering that the basis of the measurement method is to determine the induced pressure difference, a closer look into the way it is done is necessary.
At the start of the test, the building is subject to the equilibrium internal pressure. A stable pressure reference outside the building is necessary to measure this pressure with a differential manometer.
During the test, the fan is on and the building is subject to the sum of the induced pressure and the equilibrium internal pressure. This is measured with the same differential manometer and pressure taps at the same place.
While the measurement principle is very simple, there are different possible sources of error:

- Dynamic pressure inside the building;
- Dynamic pressure outside the building;
- Wind pressure on the building;
- Change in the equilibrium internal pressure;
- Measuring instruments (not included in this paper).

3.2 Dynamic pressure inside the building

Inside the building, there are inevitably places where air flows at a certain speed. At these places, part of the total pressure is dynamic pressure and the static pressure is therefore not representative of the sum of the induced pressure and the equilibrium internal pressure. Measuring the total pressure (sum of the static pressure and dynamic pressure) is no option in practice since the flow direction is unknown or disrupted.
These places are located

- next to the fan;
- in narrow spaces (e.g. corridor) or openings (e.g. door);
- or next to large leaks in the envelope.

Placing the pressure tap far away from all these places is good practice.

3.3 Dynamic pressure outside the building

In free field outside the building, there is atmospheric pressure (static pressure) and possible wind pressure (dynamic pressure). Since the pressure outside is taken as a stable reference pressure and wind is fluctuating in speed and direction, it is advisable to avoid the dynamic pressure.
To this end, it is necessary to use a special pressure tap that is not influenced by dynamic pressure and measures static pressure only. The principle of such a tap is to force the air flow in a given direction and measure the pressure perpendicularly to that direction (see examples in Figure 2). Note that a T-pipe fitted at the end of the tubing of the manometer is often used in practice.

Figure 2: Examples of static pressure taps (sources: Vaisala, Paragon Controls Incorporated, Micatrone)

3.4 Change in the equilibrium internal pressure

Another effect of the fluctuating wind is that it changes the equilibrium internal pressure in the building. Unfortunately, this change in internal pressure cannot be isolated from the induced pressure. Moreover, in practice it is not possible to calculate it from the pressure changes on the walls of the building.
During the test, a change in the temperature difference between inside and outside may occur for different reasons, e.g.:

- Change of outside temperature;
- Stopping of the heating system;
- Introduction in the building of large quantities of air from outside;
- Solar gains in the building.

Such a change also influences the equilibrium internal pressure in the building.
In order to have an idea of the possible change in equilibrium internal pressure during the test, ISO 9972 requires measuring it over a period of at least 30 seconds at the start and at the end of the test (zero-flow pressure difference).
Applying measured pressures differences much higher than the zero-flow pressure difference is therefore necessary in order to limit the influence of the possible changes in equilibrium internal pressure (ISO 9972 requires five times the value of the zero-flow pressure difference).
Note that a change in atmospheric pressure is equally felt by all points inside and outside the building. Therefore, it does not influence the equilibrium internal pressure.

Example

Assume a residential building (see Figure 3) with given characteristics.
At the start of the test, there is light wind (1 m/s) and no temperature difference between inside and outside. The equilibrium internal pressure is about 0,04 Pa (relative to the atmospheric pressure outside) and the pressure on the downwind façade is -0,15 Pa.
During the measurement of the first point of the test, the wind velocity remains at 1 m/s. The fan blows 700 m³/h which increases the equilibrium internal pressure by 10,9 Pa (for this example, this is calculated based on the characteristics of the openings).
During the measurement of the second point of the test, the wind velocity increases to 4 m/s which causes an increase of the equilibrium internal pressure to 0,60 Pa. The pressure on the downwind façade decreases to -2,42 Pa. The fan blows 950 m³/h which increases the equilibrium internal pressure by 20,10 Pa.
Taking the reference pressure outside the building in free field, close to the upwind roof or close to the downwind façade makes no difference as long as the wind does not change (Table 1 – First point) but it may have a large effect when the wind changes (Table 1 – Second point). For

the second point, a pressure tap on the downwind façade and the increased wind speed give rise to 13% overestimation of the induced pressure which means underestimation of the air leakage rate. For the two other pressure taps, the increased wind speed gives rise to a 2% underestimation of the induced pressure.

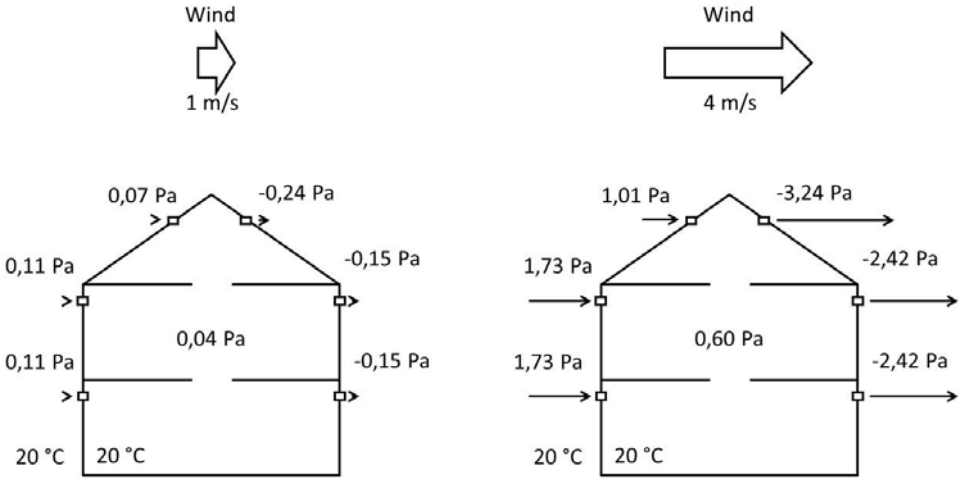

Figure 3: Example

Table 1 : Example

		Reference in free field outside	Reference on the upwind roof (left)	Reference on the downwind façade (right)
Wind 1 m/s Fan covered	Zero-flow pressure difference	0,04 – 0 = 0,04 Pa	0,04 – (0,07) = -0,03 Pa	0,04 – (-0,15) = 0,19 Pa
First point				
Wind 1 m/s Fan 700 m³/h	Measured pressure difference	0,04 + 10,90 = 10,94 Pa	-0,03 + 10,90 = 10,87 Pa	0,19 + 10,90 = 11,09 Pa
	Calculated induced pressure	10,94 – 0,04 = 10,90 Pa	10,87 – (-0,03) = 10,90 Pa	11,09 – 0,19 = 10,90 Pa
	Error	10,90 – 10,90 = 0 Pa	10,90 – 10,90 = 0 Pa	10,90 – 10,90 = 0 Pa
Second point				
Wind 4 m/s Fan 950 m³/h	Measured pressure difference	0,60 – 0 + 21,10 = 20,70 Pa	0,60 – 1,01 + 21,10 = 20,69 Pa	0,60 – (-2,42) + 21,10 = 24,12 Pa
	Calculated induced pressure	20,70 – 0,04 = 20,66 Pa	20,69 – (-0,03) = 20,72 Pa	24,12 – 0,19 = 23,93 Pa
	Error	20,66 – 21,10 = -0,44 Pa (2%)	20,72 – 21,10 = -0,38 Pa (2%)	23,93 – 21,10 = 2,83 Pa (13%)

Characteristics of the building:
Length x width x height: 14 m x 7 m x 7,6 m
Openings: 50 m³/h @ 2 Pa (flow exponent = 0,5)
Upwind Façade: 2 openings
Downwind Façade: 2 openings
Upwind Roof: 1 opening
Downwind Roof: 1 opening
Typical surface-averaged pressure coefficient C_p are used

3.5 Wind pressure on the building

Close to the building or to obstacles (e.g. tree or car), flow pattern of the wind is disrupted and creates over- and underpressure zones (see Figure 4). Since the pressure outside is taken as a stable reference pressure and wind is fluctuating in speed and direction, it is advisable to avoid

these zones (even with a pressure tap protected against dynamic pressure).

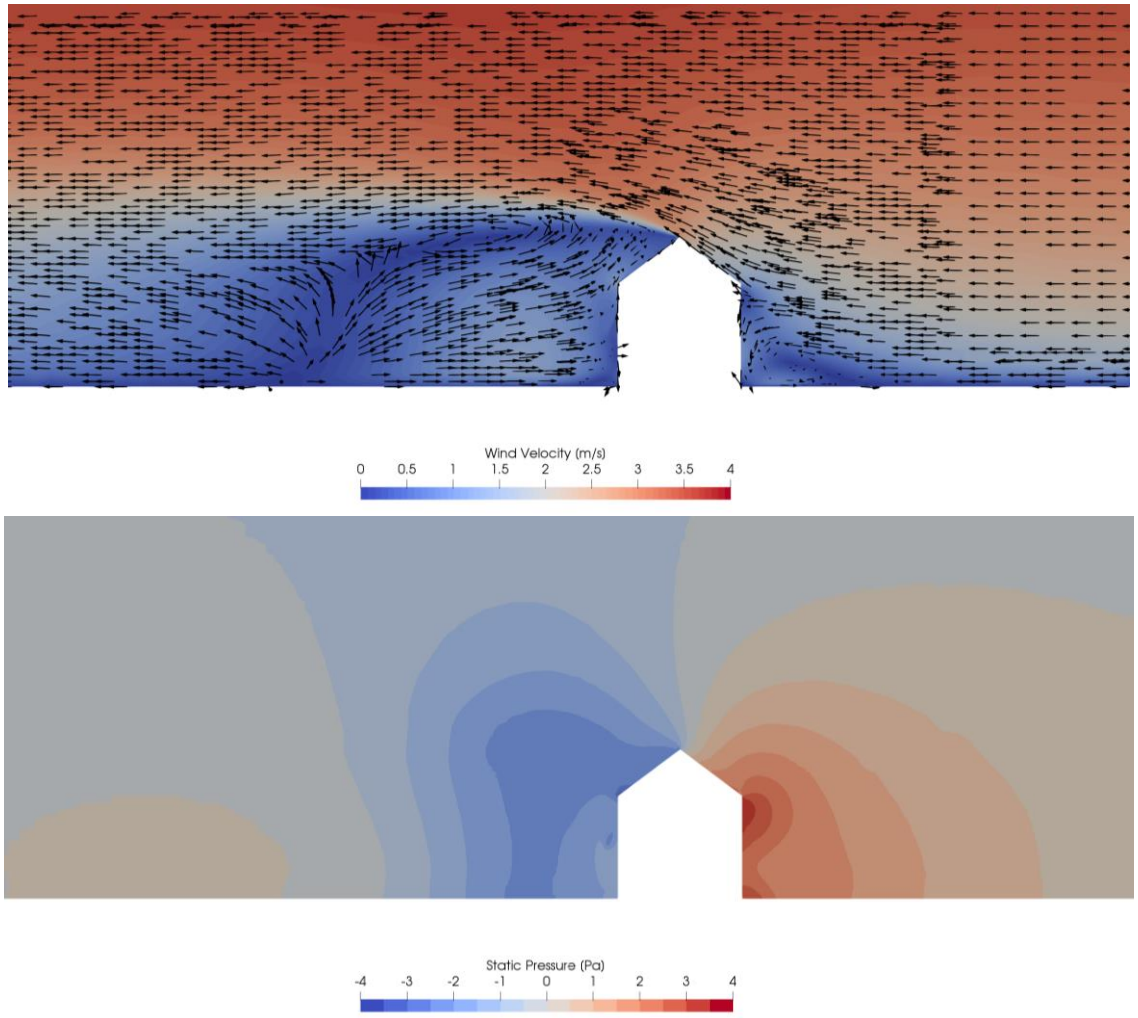

Figure 4: Example of wind velocity and static pressure distribution around a building
(3 m/s wind velocity at 10 m height – 5 m building height under cornice)

The previous example shows however that there may be places around the building (e.g. the upwind roof in this particular example) where over- or underpressure changes in the same way as the equilibrium internal pressure. These places would show low variation of pressure difference between inside and outside the building and may be a good location for pressure reference outside the building.

3.6 Vertical position of manometers or pressure taps

The pressure difference between inside and outside the building is usually measured on the ground floor of the building. This is quite practical during the test and it is a good place to measure the stack effect. In practice, it means that the differential manometer itself is on the ground floor. The vertical position of the pressure tap (connected to the manometer with a plastic tubing) plays no role because the column of air above the manometer acts on it with or without tubing.

When the pressure tap is located in another room than the manometer, it may show a difference due to the pressure drop between the rooms. If there is large difference, it means that the building does not really react as a single zone as assumed by the ISO 9972 test method. In that

case, changing the location of the fan or adding one or more fans at different locations may help.

4 RECOMMENDATIONS

Regarding the place and nature of pressure taps, ISO 9972 says:

- *"Ensure that interior and exterior pressure taps are not influenced by the air moving equipment."*
- *"The exterior pressure tap should be protected from the effects of dynamic pressure"*
- *"Especially in windy conditions, it is good practice to place the exterior pressure tap some distance away from the building, but not close to other obstacles."*

These recommendations are relevant and could be clarified as follows:

- Ensure that interior and exterior pressure taps are not placed within the draught caused by the air moving equipment;
- Ensure that the interior pressure tap is not placed in a zone of possible draught (e.g. corridor or door opening);
- Especially in windy conditions, ensure to place the exterior pressure tap some distance away from the building, but not close to other buildings or obstacles; Alternatively, place the exterior pressure tap where zero-flow pressure variation is very low compared to other locations;
- Ensure the exterior pressure tap is designed to measure static pressure only.

5 NOMENCLATURE

i, j = element of a series

T_{int} = Internal air temperature

T_e = External air temperature

Δp = Induced pressure difference

Δp_0 = Zero-flow pressure difference

Δp_m = Measured pressure difference

6 REFERENCES

ISO (2015). ISO 9972, *Thermal performance of buildings — Determination of air permeability of buildings — Fan pressurization method*. Geneva, Switzerland: International Standard Organization

Sherman, M.H. (1990). *Superposition in Infiltration Modeling*. Lawrence Berkeley Laboratory, University of California, LBL-29116

Quantification of uncertainty in zero-flow pressure approximation due to short-term wind fluctuations

Martin Prignon[*1], Arnaud Dawans[2], and Geoffrey van Moeseke[1]

1 UCLouvain
Place de l'Université, 1
1348 Louvain-la-neuve, Belgium
** martin.prignon@uclouvain.be*

2 Entreprises Jacques Delens
Avenue du Col-vert, 1
1170 Watermael Boitsfort, Belgium

ABSTRACT

Uncertainties in airtightness measured using fan pressurization test should not be defined by the scattering of the points around the line defined using ordinary least square method anymore. Its definition requires first to know the uncertainties in pressure and airflow measurements. This works aims at quantifying one of the component of the envelope pressure uncertainty: the uncertainty in zero-flow pressure approximation due to short-term fluctuation of wind speed and direction. This is done by statistically analysing the approximation quality of 40 zero-flow pressure tests performed on 30 different units on eight different sites in Brussels. First, the analysis showed that this component of uncertainty could be slightly reduced by increasing the period of measurement used to compute zero-flow pressure approximation from 30 to 60 seconds. Second, it allowed to study the impact of multiple variables on the quality of the zero-flow pressure approximation. Third, it allowed to develop three different models to predict approximation quality as a function of different variables. This study suffers from some limitations due to the sample of units tested available. These limitations lead to important further work: the validation of the model on other samples of building tested and the adaptation of these models if needed. Further work should also focus on integrating these results on the uncertainty in envelope pressure measurements and the on uncertainty in airtightness estimation of the building.

KEYWORDS

Airtightness measurement; Uncertainties; Zero-flow pressure; Fan pressurization test.

1 INTRODUCTION

To be reliable, a measured quantity should always be given with its uncertainty. When performing a fan pressurization test, the uncertainty is often given as a function of the scattering of the data around the linear model obtained with an Ordinary Least Square (OLS) method. However, multiple authors showed that the uncertainties obtained with OLS method were not reliable in the case of airtightness measurements (Okuyama and Onishi 2012, Delmotte 2017, Prignon, Dawans et al. 2018). Uncertainty of regression parameters and airflow at a given pressure difference should be computed using other regression techniques as such as the Iterative Weighted Least Square (IWLS) or the Weighted Line of Organic Correlation (WLOC). In these cases, the uncertainty of regression parameters depends on the uncertainty of airflow and pressure measurements.

One of the main source of uncertainty is the fluctuation of reading in the pressure measurements due to variation in wind speed and direction (Sherman and Palmiter 1995). Unfortunately, the pressure difference due to climatic conditions (i.e., the zero-flow pressure) cannot be measured during a fan pressurization test. In the European ISO 9972:2015 standard (ISO-9972 2015) the pressure due to climatic conditions during the test is computed as the average of the zero-flow pressure measured before and after the measurement of airflow – pressure difference couples.

This approximation suffers from two uncertainties. The first is due to short-term fluctuations of wind speed and direction: the zero-flow pressure is considered constant while, in reality, it varies randomly during the test. The second is due to long-term fluctuations of wind speed and direction: the zero-flow pressure computed based on pre- and post-test measurements (i.e., the zero-flow pressure approximation) does not always fit with the average zero-flow pressure during this period.

In a previous work, we developed a method to quantify the uncertainties in zero-flow pressure due to short-term fluctuations of wind speed and direction. In the same work, we applied this method on a series of 30 tests performed on the same apartment. This research consists in applying the same method on 40 zero-flow pressure tests performed on 30 different units (i.e. apartment, school, single-family house, etc.) in eight different sites in Brussels. It aims at finding a mathematical relation between this component of uncertainty and multiple variables easily available during a fan pressurization test.

The methodology section of this paper has four subsections that describe the zero-flow pressure test, the sample of buildings tested, the seven variables studied and the statistical tools used for the analysis of the results. The result section presents them in two steps: a general visualization of all the results and a study of the impact of different variables on the mathematical relation. All the results are presented in terms of “approximation quality” which is an indicator of the variation of the zero-flow pressure measurements. The discussion section translates the “approximation quality” indicator into uncertainty value. The conclusion presents briefly the results obtained, the impact of these results in the field of airtightness uncertainties, the limitations of the study related to the methodology and the relevant further work in the field.

2 METHODOLOGY

2.1 The Zero-Flow Pressure Test

Delmotte used the zero-flow pressure test for the first time in 2017 (Delmotte 2017). This test consists in measuring the zero-flow pressure every second during three different periods: two approximation periods and one fictitious period (Figure 1). The two approximation periods correspond to the zero-flow pressure measurements used to compute the zero-flow pressure approximation in a traditional fan pressurization test. In his work, Delmotte considered periods of 30 seconds while in this work two periods of 120 seconds are considered. This is because this paper focuses also on how approximation periods affects the uncertainty. The fictitious period corresponds to the time a fan pressurization test would take in practice. In this research, a fictitious period of 600 seconds is considered, as such as in the work of Delmotte.

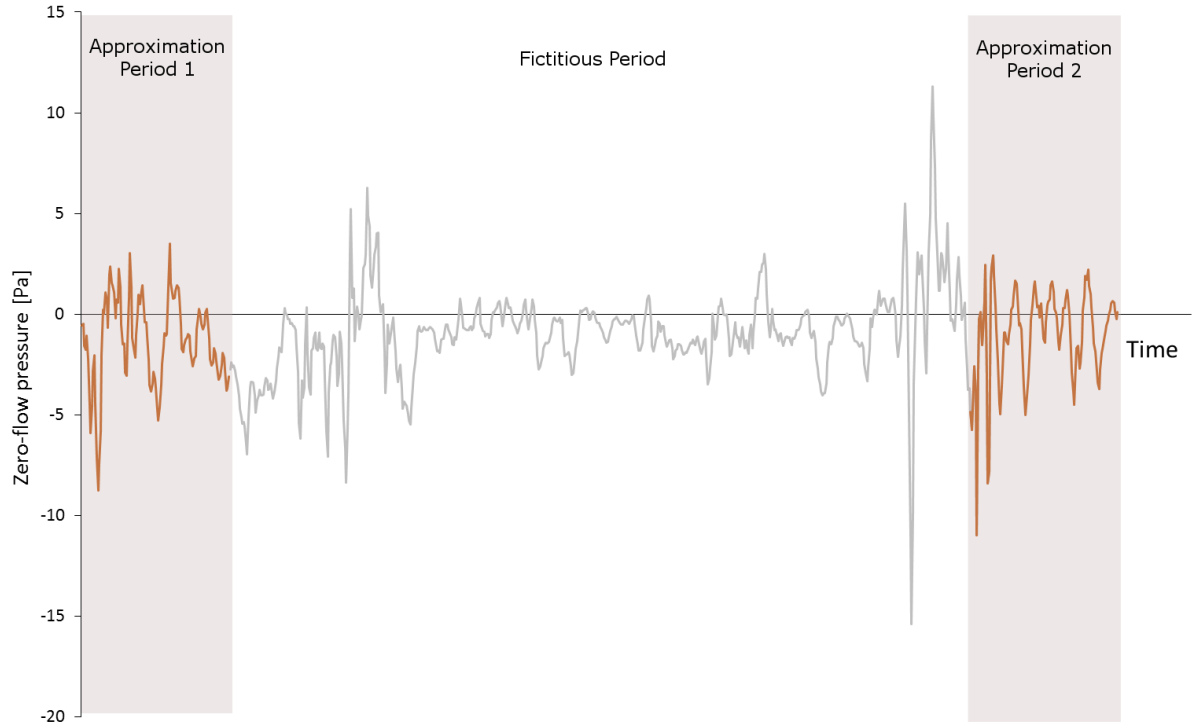

Figure 1 – illustration of the three successive periods of a zero-flow pressure test

The zero-flow pressure approximation is then computed based on measurements made during the approximation periods. This research deals only with the constant approximation method (i.e., the average of zero-flow pressure measurements made during both approximation periods). This is the method imposed by the ISO 9972:2015 standard.

Then, the zero-flow pressure approximation is compared to the zero-flow pressure measured every second during the fictitious period. The "approximation quality" (ε) is the average of the difference between approximated and measured zero-flow pressure (Equation 1).

$$\varepsilon = \frac{\sum_{i=1}^{600} |\Delta p_{0,i} - \Delta \widetilde{p_0}|}{600} \quad (1)$$

Where $\Delta p_{0,i}$ is the zero-flow pressure measured every second (i) during the fictitious period and $\Delta \widetilde{p_0}$ is the zero-flow pressure approximation based on measurements made during approximation periods.

2.2 Description of Buildings Tested

The four pie charts in Figure 2 represent the repartition of four different variables among the 40 units tested: the type of unit measured, the storey where the measurement was taken, the volume of the unit and the type of construction.

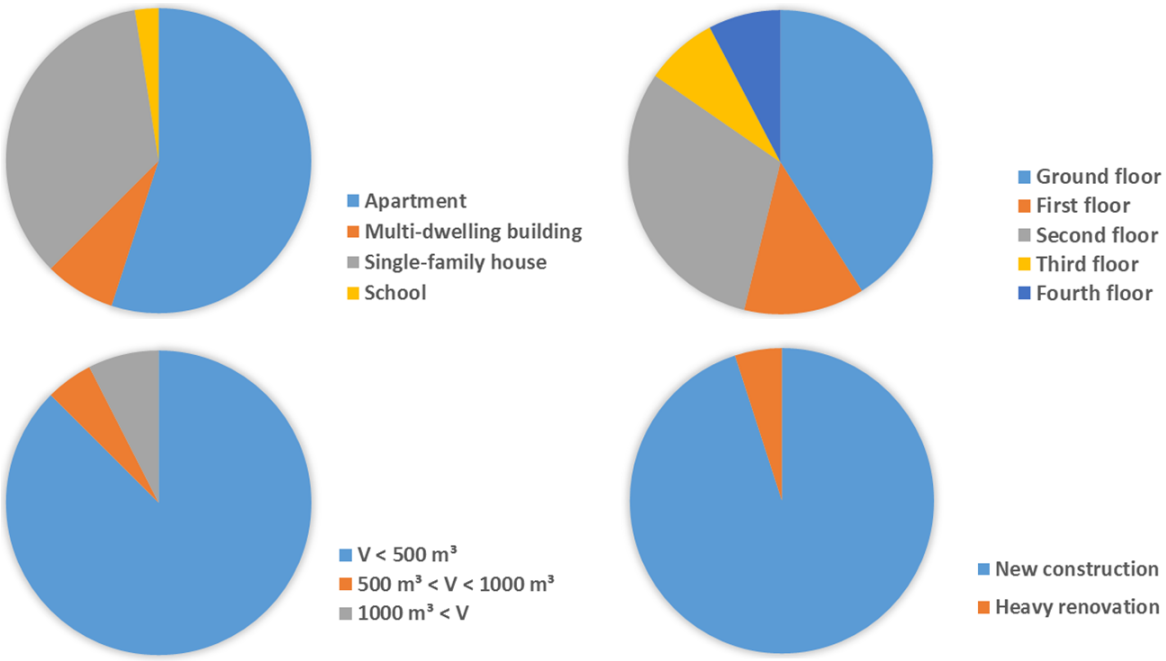

Figure 2 – repartition of the sample of units tested regarding four variables: type of units, storey of the measurement, volume of the unit and type of construction

It is important to point out that, in the sample of units available for the tests there are only one non-residential unit (school). In addition, almost all tests (38) were performed on new constructions and only five units have a volume higher than 500 m³. These limitations related to the sample are tackled in the conclusion of this work.

2.3 Variables analysed

The impact of 7 different variables was studied: the value of the zero-flow pressure approximation ($\Delta P_{0,a}$ in Pa), the difference between zero-flow pressure measured during first and second approximation periods (Δ in Pa), the standard deviation of the measurements used to compute zero-flow pressure approximation (σ in Pa), the wind speed obtained from the closest weather station available (w in km/h), the volume of the unit (V in m³), the storey where the measurement is taken (s in storey) and the temperature difference between inside and outside during the test (ΔT in °C). These seven variables were selected because they are easy to obtain in practice except for the wind speed that can be sometimes difficult to get. All these variables were tested for four different durations of approximation periods: 30 seconds, 60 seconds, 90 seconds and 120 seconds.

The wind speed is the only variable that was not directly available on site during the test. However, it was still considered in the variables because of its well-known impact on the pressure measurement uncertainty (Sherman and Palmiter 1995, Carrié and Leprince 2016). The distance between the closest weather station and the site varied between 300 and 1500 meter, and the data given is the average of one hour of wind speed measurement. In addition, the weather stations are often placed on the roof of a building and therefor it does not take into account the surroundings of the tested unit. However, this study is not interested in the physical impact of wind speed and wind pressure on the uncertainties but in a quantification of uncertainties based on data available during a fan pressurization test. These kind of simple climatic data are often easily available for free.

2.4 Statistical analysis

The statistical analysis aims at finding which variables have a significant impact on the approximation quality (ε – Equation 1) and at deducing a relation between the approximation quality and these variables.

In the previous section, seven variables are described while there should be eight. Indeed, the duration period is considered differently than other variables. This is because of the dependency implied by the experimental design. For each test, the four duration periods are computed using the same set of data. Therefore, the impact of duration period cannot be deduced the same way than other variables. When data are nested (i.e., the duration of approximation periods are nested within the different tests), Multi-Level Modelling (MLM) should be used (Rasbash, Steele et al. 2015) instead of classic statistical tools.

The use of MLM in zero-flow pressure tests was deeply investigated in our previous work. However, in this work the objective of MLM is to investigate if different models should be used for different approximation methods. It can be answered simply by assessing the need for MLM when considering only two levels: the duration period nested within the test ID.

MLM is needed when there is large intraclass correlation (ICC) (> 0.45) (Julian 2001) and when the design effect is higher than 2 (Muthén and Satorra 1995). ICC can be defined as the proportion of approximation quality variation that occurs across tests or as the expected correlation between the approximation qualities of the four duration of a same test (Peugh 2010). It is computed using Equation 2. τ_{00} is the variation of approximation quality between tests and σ^2 is the average of the approximation quality variation of different periods within each test. The design effect quantifies how the dependence of data affects the estimate of standard error. In other terms, it provides the multiplier to be applied to the standard error to take account for the nested structure of the data. It is computed using Equation 3with n_c the number of different periods measured by test (Hayes 2006, Peugh 2010).

$$ICC = \tau_{00}/(\tau_{00} + \sigma^2) \quad (2)$$

$$Design\ Effect = 1 + (n_c - 1) * ICC \quad (3)$$

In this study, τ_{00} is 0.79, σ^2 is 0.07 and n_c is 4. Therefore, ICC is 0.92 and Design effect is 3.76 and MLM is needed. This means that classic statistical tools cannot be used to study the impact of approximation period duration on the approximation quality because of the nested structure of data. Therefore, in this paper, the seven other variables are computed separately for the four different durations.

In such case, the seven other variables are not nested in a hierarchical structure anymore. Therefore, the statistical analysis can be made with classical statistical tool as such as multiple regression. It aims simply at finding the linear combination of predictors (i.e., the seven selected variables) that fits as much as possible the predictor (i.e., the approximation quality) (Field, Miles et al. 2012). A multiple regression provides the coefficients for each predictor in the linear model, but it also provides information on the statistical significance of these predictors (p-values) and the quality of the fitting of the model (multiple R^2). Multiple R^2 can be interpreted as such as the R^2 in a simple regression: it is the amount of variance in the outcome (i.e., the approximation quality) explained by the model (Field, Miles et al. 2012).

Four different multiple regressions were performed: one with all the variables, one with variables having a significant impact including wind speed, one with variables having a significant impact without wind speed and one with the standard deviation only. These four regressions were performed for the four different durations of the approximation periods.

3 RESULTS

3.1 General Results

Figure 3 shows the bar graph of the approximation quality of the 40 tests for the four different duration of approximation periods. The period of 30 seconds is slightly worse than other periods, but all results remain in the same order of magnitude.

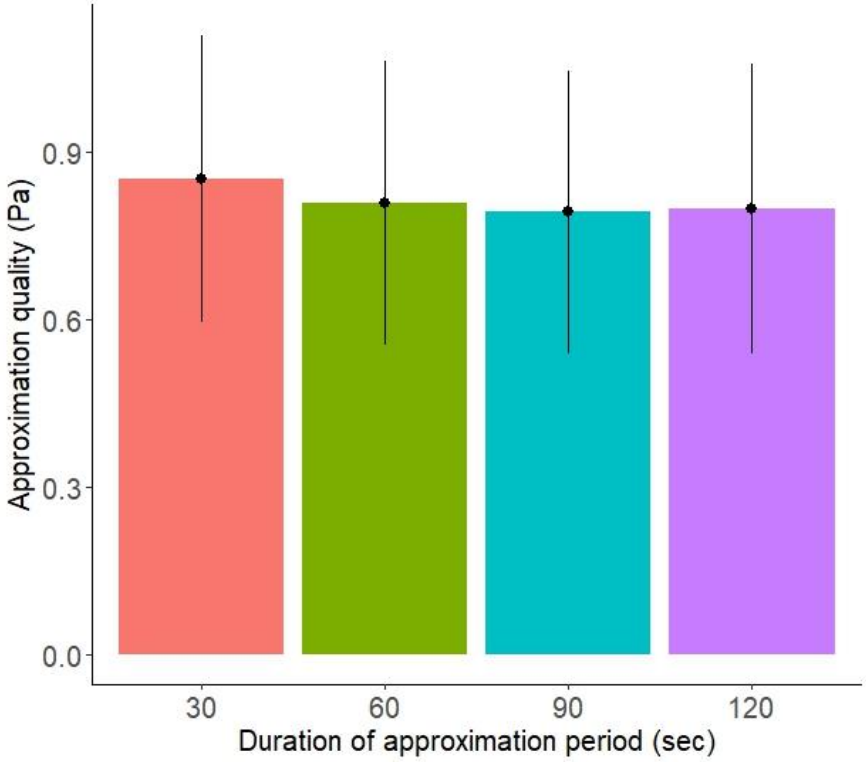

Figure 3 – bar graph of the 40 approximation qualities computed for the four different approximation periods

Table 1 presents the difference of mean of approximation quality for the four duration and the statistical significance of this difference, using pairwise wilcoxon rank-sum test with Bonferroni correction. The comparison is made using Wilcoxon rank-sum test because data follow a distribution significantly different from normal (Shapiro-Wilk $= 0.82, p < 0.001$). In addition, since multiple comparisons were performed on the same data, Bonferroni corrections are applied to counterbalance the increase in familywise error rate. The familywise error is the increasing probability of making a Type I error (i.e. the probability of falsely rejecting the null hypothesis), and is calculated as $1 - 0.95^n$ with n being the number of comparisons performed (Field, Miles et al. 2012). The probability of making a Type I error is 26%. The Bonferroni correction ensures that the cumulative Type I error rate is kept below 0.05 and is computed as α/k where k is the number of comparison.

Table 1 - results of the comparison using pairwise Wilcoxon rank-sum test with Bonferroni correction. Results are highly significant (***), significant (**), slightly significant (*) or non-significant ($^{N.S.}$)

vs	30	60	90
60	0.04 *		
90	0.06 **	0.02 $^{N.S.}$	
120	0.05 *	0.01 $^{N.S.}$	-0.01 $^{N.S.}$

Results show that only the comparisons including 30 second periods are statistically significant (30vs90) or slightly significant (30vs60 and 30vs120). Other comparisons are statistically non-significant.

3.2 Multiple Regression

This section presents and analyses the results of the four multiple regressions performed for each of the four durations. Table 2, Table 3 and Table 4 provide the coefficients and the statistical significances of each variable and the multiple R^2 for each regression.

The first multiple regression (Table 2) shows that two variables have no significant impact on the approximation quality: the difference of approximation in the first and in the second duration period (Δ) and the temperature difference between inside and outside the unit during the test (ΔT). Variables having the most significant impact are the standard deviation of the measurements (σ) and the wind speed (w). The statistical significance of some variables ($\Delta P_{0,a}$, w, V and s) depends on the duration of the approximation periods. Good fitting is obtained (multiple R^2 between 0.75 and 0.79) when considering all the variables.

Table 2 - results of the multiple regression applied on all variables (7) for the four durations.

Variables	Period 30		Period 60		Period 90		Period 120	
Intercept	-1.2 e-00	**	-1.3 e-00	**	-1.2 e-00	**	-1.4 e-00	**
$\Delta P_{0,a}$	2.9 e-01	**	1.3 e-01	N.S.	1.2 e-01	N.S.	1.0 e-01	N.S.
Δ	-3.1 e-01	N.S.	-3.1 e-01	N.S.	-3.0 e-01	N.S.	-3.1 e-01	N.S.
σ	1.1 e-00	***	9.5 e-01	***	9.6 e-01	***	8.8 e-01	***
w	7.4 e-02	***	7.3 e-02	**	6.0 e-02	**	6.9 e-02	**
V	1.3 e-04	**	1.4 e-04	**	1.2 e-04	*	1.3 e-04	*
s	8.6 e-02	N.S.	1.0 e-01	N.S.	1.0 e-01	*	1.3 e-01	*
ΔT	8.9 e-04	N.S.	-3.7 e-03	N.S.	-2.0 e-03	N.S.	5.9 e-03	N.S.
Multiple R^2	0.77		0.79		0.76		0.75	

$p < 0.001$ (***) is highly significant, $p < 0.01$ (**) is significant, $p < 0.05$ (*) is slightly significant and $p > 0.05$ ($^{N.S.}$) is not significant.

Conclusions on the statistical significance of the volume and the storey should be drawn carefully. Regarding the storey (s), it is important to keep in mind that the zero-flow pressure was measured higher than the fourth floor only once. Similar study performed on high-rise buildings would probably give different results since the wind speed has a different magnitude and the surroundings affect differently the wind pressure on the building. In addition, in high-rise buildings stack effect has a huge impact on the zero-flow pressure. Regarding the volume (V), only five units have a volume higher than 500 m³. Similar study performed on high-volume units could lead to different conclusions.

The second multiple regression (Table 3) confirms the first one: good fitting is obtained when removing the two non-significant variables (multiple R^2 between 0.73 and 0.74). The most significant variables are still the standard deviation of the measurement and the wind speed. The coefficients can be used to define a mathematical relation between the approximation

quality and these five variables. Equation 4 gives this relation in the case of 30-second approximation periods.

$$\varepsilon = -1.2 + 0.30 * \Delta P_{0,a} + 0.85 * \sigma + 0.07 * w + 1.3\, e^{-4} * V + 0.12 * s \qquad (4)$$

Table 3 - results of the multiple regression applied on main variables, including wind speed (5) for the four durations.

Variables	Period 30		Period 60		Period 90		Period 120	
Intercept	-1.2 e-00	**	-1.3 e-00	**	-1.2 e-01	**	-1.4 e-00	***
$\Delta P_{0,a}$	3.0 e-01	**	1.3 e-01	N.S.	1.3 e-01	N.S.	1.2 e-01	N.S.
σ	8.5 e-01	***	7.8 e-01	***	8.1 e-01	***	7.7 e-01	***
w	7.4 e-02	***	6.9 e-02	**	6.2 e-02	**	7.3 e-02	***
V	1.3 e-04	**	1.4 e-04	**	1.2 e-04	*	1.2 e-04	*
s	1.2 e-01	*	1.2 e-01	*	1.3 e-01	*	1.5 e-01	**
Multiple R^2	0.74		0.73		0.74		0.73	

$p < 0.001$ (***) is highly significant, $p < 0.01$ (**) is significant, $p < 0.05$ (*) is slightly significant and $p > 0.05$ (N.S.) is not significant.

In the third multiple regression, the wind is removed from the variables since it is the only variable which is not directly available during a fan pressurization test. The impact of the standard deviation is found highly significant, but other terms are almost all found not significant. The value of the zero-flow pressure approximation is found slightly significant in the case of 30-second approximation periods only. The third multiple regression shows a larger decrease of the multiple R^2 (between 0.62 and 0.64) than the second one. However, the fitting is still good and the relation between approximation quality and multiple variables could be used even without considering wind speed. Similarly, to the second multiple regression, the third allows the deduction of a mathematical relation (Equation 5 – 30 second periods).

$$\varepsilon = 0.04 + 0.27 * \Delta P_{0,a} + 1.1 * \sigma + 8.6\, e^{-5} * V + 0.04 * s \qquad (5)$$

Table 4 - results of the multiple regression applied on main variables, without wind speed (4) for the four durations.

Variables	Period 30		Period 60		Period 90		Period 120	
Intercept	3.8 e-02	N.S.	-8.5 e-02	N.S.	-1.7 e-02	N.S.	-1.8 e-01	N.S.
$\Delta P_{0,a}$	2.7 e-01	*	9.9 e-02	N.S.	9.9 e-02	N.S.	9.2 e-02	N.S.
σ	1.1 e-00	***	9.9 e-01	***	1.0 e-00	***	9.7 e-01	***
V	8.6 e-05	N.S.	1.0 e-04	N.S.	7.8 e-05	N.S.	6.9 e-05	N.S.
s	4.3 e-02	N.S	5.3 e-02	N.S.	7.0 e-02	N.S.	7.7 e-02	N.S.
Multiple R^2	0.64		0.63		0.66		0.62	

$p < 0.001$ (***) is highly significant, $p < 0.01$ (**) is significant, $p < 0.05$ (*) is slightly significant and $p > 0.05$ (N.S.) is not significant

The last multiple regression shows that a simple linear model including only the standard deviation of the measurements as a predictor provides still good fitting (multiple R^2 between 0.55 and 0.61). The mathematical relation is highly simplified (Equation 6).

$$\varepsilon = 0.11 + 0.98 * \sigma \qquad (6)$$

Table 5 - results of the multiple regression applied on standard of the measurement only for the four durations.

Variables	Period 30		Period 60		Period 90		Period 120	
Intercept	1.1 e-01	N.S.	5.4 e-02	N.S.	-3.1 e-02	N.S.	-3.3 e-02	N.S.
σ	9.8 e-01	***	9.5 e-01	***	9.6 e-01	***	9.3 e-01	***
Multiple R^2	0.55		0.57		0.61		0.57	

$p < 0.001$ (***) is highly significant, $p < 0.01$ (**) is significant, $p < 0.05$ (*) is slightly significant and $p > 0.05$ (N.S.) is not significant

Although multiple R^2 has a clear meaning (i.e., the amount of variance explained by the model), it can be sometimes difficult to visualize what it means practically. Figure 4 shows the predicted

approximation quality vs. the real approximation quality for the three cases when considering approximation periods of 30 seconds. The predicted values are obtained when applying Equation 4, Equation 5 and Equation 6, while the real values are the data used to develop the models. The difference in multiple R^2 values is probably due to the tests with high value of approximation quality. Indeed, the three points with high measured approximation quality are better predict with the first model (Equation 4) than with the second (Equation 5) and the third (Equation 6) model.

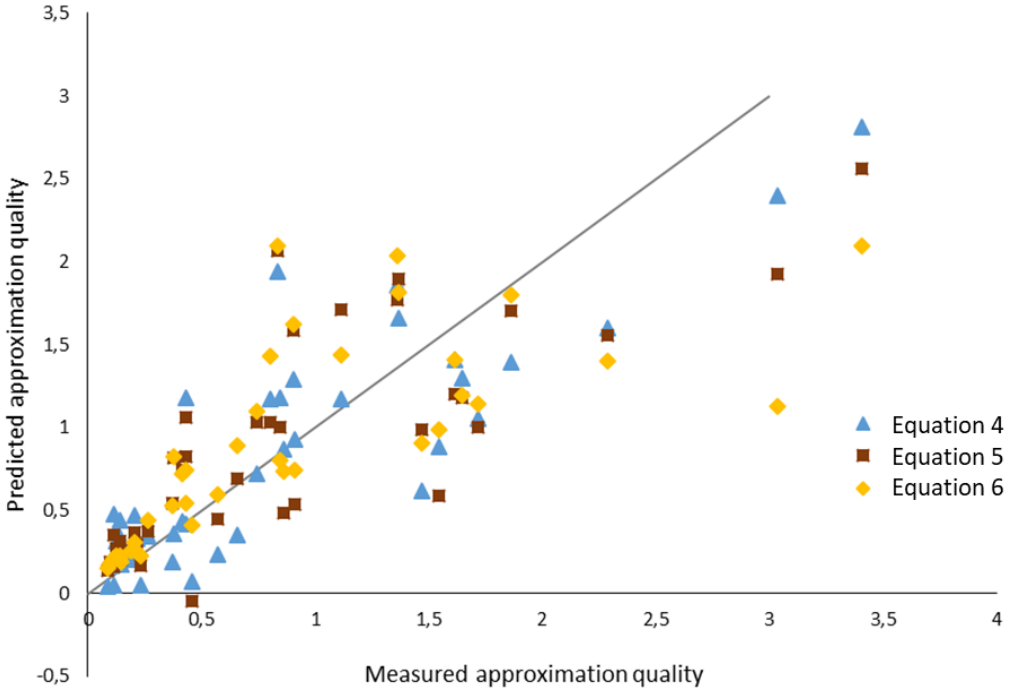

Figure 4 - representation of the predicted vs. measured approximation quality for the three models

4 DISCUSSION

Until here, this paper focuses on the approximation quality ε. But in practice, we are interested in uncertainty related to wind fluctuations.

In previous section, results are presented in terms of approximation quality. However, to be useful in practice, results should be presented in terms of uncertainty. This section discusses the steps and hypotheses to translate the results from approximation quality to uncertainty. On the one hand, it was shown in a previous work that the zero-flow pressure measured during the fictitious period follows a normal distribution. Therefore, it can be assumed that the uncertainty is the standard deviation of the zero-flow pressure measurements during the fictitious period $\sigma(\Delta P_0)$ (JCGM 2008).

On the other hand, ε is the average of the difference between approximated and real zero-flow pressure. Therefore, it is reasonable to assume assumed that $\Delta P_0 - \varepsilon/2$ and $\Delta P_0 + \varepsilon/2$ are the lower and the upper limit of the interval containing 50% of the zero-flow pressure measured during the fictitious period of the zero-flow pressure test.

Since the Z scores of the normal distribution are respectively 0.675 and -0675 when considering 75% and 25% of the results, Equation 7 and Equation 8 can be used to link approximation quality and standard deviation.

$$0.675 = \frac{(\Delta P_{0,a} + \varepsilon/2) - \Delta P_0}{\sigma(\Delta P_0)} \quad (7) \qquad -0.675 = \frac{(\Delta P_{0,a} - \varepsilon/2) - \Delta P_0}{\sigma(\Delta P_0)} \quad (8)$$

It can be assumed that the zero-flow pressure approximation ($\Delta P_{0,a}$) equals the average of the zero-flow pressure measurements made during the fictitious period (ΔP_0). The assumption is made because this work computes the uncertainties due to short-term fluctuations of wind only. In practice there is also an uncertainty related to long-term wind fluctuations and both uncertainties should be propagated to derived the uncertainty in pressure measurements due to wind. However, with this assumption, it is possible to express the uncertainty in zero-flow pressure approximation due to short-term fluctuations of wind as a function of the approximation quality only (Equation 9).

$$u(\Delta P_{0,a}) = \sigma(\Delta P_0) = \varepsilon/1.35 \quad (9)$$

In practice, each pressure difference – airflow couple is the average of multiple measurements. This reduces the impact of the uncertainty due to wind fluctuations. When data are uncorrelated, the uncertainty of an average is simply the uncertainty of one measurement divided by the number of measurements used for the average. However, it was already discussed by author previously (Delmotte 2013) and it does not seem a reliable assumption. Figure 5 shows the pressure difference – airflow couples measured during a pressurization measurement on the left and these couples if data were uncorrelated on the right.

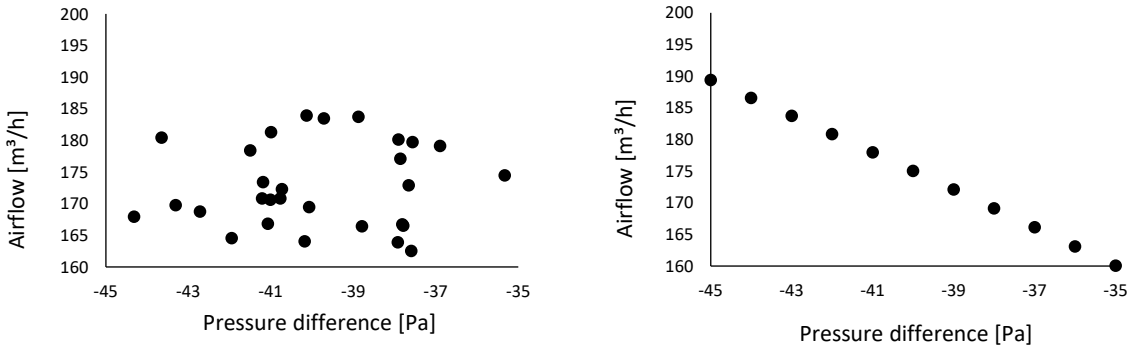

Figure 5 – airflow - pressure difference couples measured during a pressure measurement on the left and equivalent couples if data were uncorrelated

In addition, when performing a test, the operator often tries to take a measurement when wind fluctuations are low. It reduces the impact of wind fluctuations and decreases this component of the uncertainty. Therefore, one has to be careful when considering uncertainties related to short-term fluctuations of wind in practice: Equation 9 provides an upper limit of this uncertainty.

5 CONCLUSION

In this work, 40 zero-flow pressure tests were performed on different units. They were analysed with multi-level modelling and multiple regression. These statistical tools allow in a first step to study the impact of multiple variables on the quality of the zero-flow pressure approximation.

In a second step, they allow developing three different models to predict approximation quality as a function of different variables. Lastly, the discussion explains how to translate from "approximation quality" indicator to uncertainty.

This work is a step in the quantification of uncertainties in pressure measurements. Since this component was not considered before, it increases the computed pressure uncertainty and makes it non-negligible anymore. Therefore, ordinary least square regression method should not be used anymore. This results strengthens the trends among authors to suggest the use of alternative regression methods.

This research is limited by the set of data. As explained in the methodology section, the dataset contains only two renovations, five units with volume higher than 500 m^3, one non-residential building and one building with more than four stories. In addition, the dataset was entirely used to create the model and none of them was used to validate the model. Therefore, further work should focus on the validation of the models suggested and, if needed, on their adaptation for high-volume and high-rise units.

Furthermore, this work focuses on one component of the uncertainty in fan pressurization testing. This uncertainty should be combined with other components in order to obtain the total uncertainty in pressure measurements. This is an important work because different sources of uncertainties could be correlated and the calculation of their propagation could require some investigation (JCGM 2008). An example of possible correlation is the uncertainties related to short-term fluctuations of wind and the uncertainties related to the long-term fluctuations of wind.

6 ACKNOWLEDGEMENTS

Authors want to thank the company *Jacques Delens* for its mobilization in this work and the availability of their construction sites. This work is part of the "AirPath50" project funded by INNOVIRIS.

REFERENCES

Carrié, F. R. and V. Leprince (2016). "*Uncertainties in building pressurisation tests due to steady wind*." Energy and Buildings **116**: 656-665.

Delmotte, C. (2013). *Airtightness of buildings - Calculation of combined standard uncertainty*. Unpublished Report, Belgian Building Research Institute - Laboratory Air Quality and Ventilation**:** 29.

Delmotte, C. (2017). *Airtightness of Buildings - Considerations regarding the Zero-Flow Pressure and the Weighted Line of Organic Correlation*. 38th AIVC Conference "Ventilating healthy low-energy buildings", Nottingham, UK.

Field, A., J. Miles and Z. Field (2012). *Discovering Statistics Using R*. London, SAGE Publications Ltd.

Hayes, A. F. (2006). "*A Primer on Multilevel Modeling.*" Human Communication Research **32**(4): 385-410.

ISO-9972 (2015). "NBN EN ISO 9972:2015 - *Performance thermique des bâtiments - Détermination de la perméabilité à l'air des bâtiments - Méthode de pressurisation par ventilateur* (ISO 9972:2015) CEN, Brussels, Belgium."

JCGM (2008). *Evaluation of measurement data—guide for the expression of uncertainty in measurement.*, Joint Committee for Guides in Metrology**:** 134.

Julian, M. W. (2001). "*The Consequences of Ignoring Multilevel Data Structures in Nonhierarchical Covariance Modeling*." Structural Equation Modeling: A Multidisciplinary Journal **8**(3): 325-352.

Muthén, B. O. and A. Satorra (1995). "*Complex Sample Data in Structural Equation Modeling*." Sociological Methodology **25**: 267-316.

Okuyama, H. and Y. Onishi (2012). "*Reconsideration of parameter estimation and reliability evaluation methods for building airtightness measurement using fan pressurization*." Building and Environment **47**: 373-384.

Peugh, J. L. (2010). "*A practical guide to multilevel modeling*." Journal of School Psychology **48**(1): 85-112.

Prignon, M., A. Dawans and G. van Moeseke (2018). *Uncertainties in airtightness measurements: regression methods and pressure sequences*. 39th AIVC-7th TightVent & 5th venticool Conference Smart ventilation for buildings.

Rasbash, J., F. Steele, W. J. Browne and H. Goldstein (2015). *A User's Guide to MLwiN*, University of Bristol: Centre for Multilevel Modelling.

Sherman, M. and L. Palmiter (1995). *Uncertainties in fan pressurization measurements*. Airflow performance of building envelopes, components, and systems. Philadelphia, USA, ASTM International**:** 266-283.

Designing a model-scale experiment to evaluate the impact of steady wind on building air leakage measurements

Adeline Bailly Mélois[*1,2], Anh Dung Tran[1,2], Mohamed El Mankibi[2], François Rémi Carrié[3], Bassam Moujalled[1] and Gaëlle Guyot[1]

1 CEREMA BPE Project Team
46 rue Saint Théobald – BP128
38081 L'Isle d'Abeau Cedex, France
**Corresponding author: adeline.melois@cerema.fr*

2 ENTPE LTDS
3 rue Maurice Audin
69518 Vaulx-en-Velin, France

3 ICEE
93 rue Molière
69003 Lyon, France

KEYWORDS
Building airtightness, Measurement, Wind tunnel, model, Wind impact

NOMENCLATURE

A	Area of opening (m^2)
L	Length (m)
p	Pressure relative to external pressure (Pa)
q	Volumetric airflow rate ($m^3\ s^{-1}$)
U	Wind speed at the building level ($m\ s^{-1}$)
V	Internal building volume (m^3)
ρ	Air density ($kg\ m^{-3}$)

1 INTRODUCTION

Since the 1970s, many authors have discussed the impact of poor airtightness on building energy use, indoor air quality, building damage, or noise transmission [1–7]. Nowadays, because poor airtightness affects significantly the energy performance of buildings, and even more significantly with low-energy targets, many countries include requirements for building airtightness in their national regulations or energy-efficiency programs [8]. Building pressurization tests are increasingly used for compliance checks to energy performance requirements and may result in severe penalties [9]. Therefore, the uncertainty of the measurement results has become a key concern in several countries over the past few years. More specifically, several studies [10–14] have shown the significant uncertainties induced by the wind. Nevertheless, further investigations are needed to understand how the wind impacts pressurization tests and to characterize the error induced by the wind on the test results.

2 OBJECTIVES

The goal of our work is to increase the reliability of building air leakage measurements results regarding steady wind impact. Starting from model-scale experiments in controlled laboratory conditions, we propose to improve uncertainty estimates and tests protocols. In this presentation, we focus on:

- Similarity criteria for model-scale experiments;
- Experimental design and wind tunnel design.

3 METHODOLOGY

3.1 Similarity conditions

Our approach is to design a model to be able to conduct controlled experiments in laboratory conditions. Similarly to Carrié and Leprince [11,12], we assume that the building can be represented by a single zone model that consists of only two types of wall regarding pressure behaviour: the windward walls and the leeward walls. Thus, we assume that all leakages can be represented by only two leakages: one on the windward side and a second one on the leeward side.

One specific challenge in model-scale experiments is to achieve similarity conditions. To this end, we write the fundamental equations governing the pressurisation tests in non-dimensional form. There are 6 key equations that can be grouped as follows:

- pressure difference at the leaks Δp_i (2 equations);
- airflow through the leaks q_i (2 equations);
- mass balance of the system (1 equation);
- energy conservation of the system (1 equation).

We study a specific configuration with two identical leaks (same size and same height) in isothermal initial conditions and consider a steady wind. Then, for each dimensional variable X of these equations, we introduce a reference size X_{ref} according to the method described by N. Le Roux [15]. We also obtained the 4 dimensionless numbers (Π_1 to Π_4) described in Equation 1 to Equation 4.

$$\Pi_1 = \frac{\rho_{ref}.{U_{ref}}^2}{p_{ref}} \quad \text{Equation 1}$$

$$\Pi_2 = \frac{{p_{ref}}.{A_{ref}}^2}{{\rho_{ref}}.{q_{ref}}^2} \quad \text{Equation 2}$$

$$\Pi_3 = \frac{\sqrt{A_{ref}}}{L_{ref}} \quad \text{Equation 3}$$

$$\Pi_4 = \frac{V_{ref}.U_{ref}}{L_{ref}.q_{ref}} \quad \text{Equation 4}$$

To meet similarity conditions, the values of the dimensionless numbers Π_1 to Π_4 have to be identical both at reduced and real scales. It leads to the following relationships between scales:

$$\bar{U} = \bar{p} \qquad \bar{p}.\bar{A}^2 = \bar{q}^2$$
$$\bar{A}^{0,5} = \bar{L} \qquad \bar{V}.\bar{U} = \bar{L}.\bar{q}$$

with for each variable, $\bar{X} = \frac{X_{ref\ model}}{X_{ref\ real}}$.

Considering a generic real 2-story house (total floor area = 120 m², internal volume = 320m³, loss surface area excluding the basement floor = 224 m²) as our real building, and a scale ratio for the length of $\bar{L} = 1/25$, we obtain the scale ratios given in Table 1, and a geometric model described in
Figure 1.

Table 1: Scale ratios

$\bar{L}$	1/25
$\bar{A}$	1/625
$\bar{V}$	1/15,652
$\bar{U}$	1
$\bar{p}$	1
$\bar{q}$	1/625

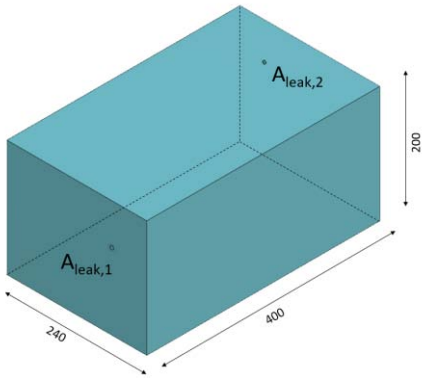

Figure 1: Model dimensions [mm]

3.2 Experimental design

During the air leakage measurements performed on our model placed in the wind tunnel, the following parameters are fixed:

- Initial inside and outside temperatures. The stack effect is not taken into account here to be able to estimate the wind error only.
- Total leakage area. Carrié and Leprince [11] have shown that it does not influence the error on the leakage coefficient in steady conditions.

On the other hand, we can adjust the following parameters from one test to another, which are expected to have a significant impact:

- Wind speed (from 0 to 12 $m.s^{-1}$) (steady wind during a test);
- Leakage areas distribution ($\frac{windward\ leakage\ area}{leeward\ leakage\ area}$ from 0.1 to 9);
- External pressure tap location (6 different locations).

3.3 Wind tunnel design

Figure 2 shows the key components of our wind tunnel, inspired from Stefano et al. [16] and Hernandez et al. [17].

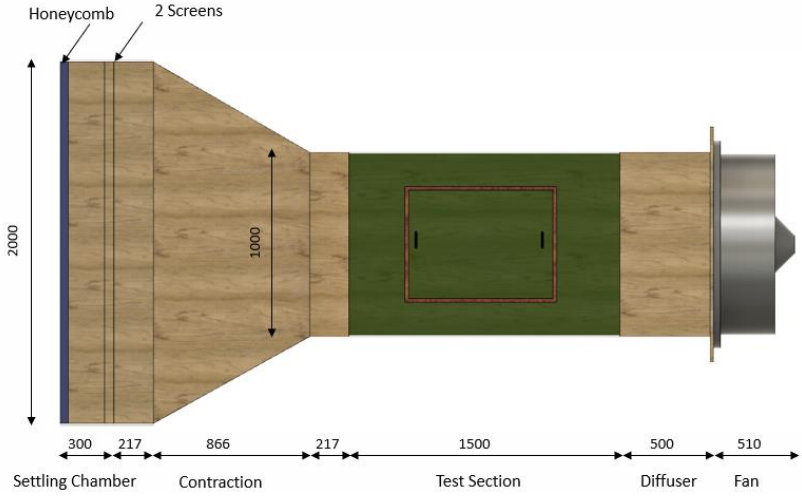

Figure 2: Final dimension of wind tunnel [in mm]

Note that:

- The Settling Chamber is equipped with a honeycomb and a series of screens.
- The Contraction accelerates the flow into the test section. The ideal form for a contraction is generated using the Bell-Mehta fifth order polynomials [18] (Figure 3 (a)). In order to reduce the difficulty of fabrication, we tested simplified forms with a CFD software. These CFD simulations compare wind behaviours with various angles of the contraction, from 25° up to 45° (Figure 3 (b) to (f)). Figure 4 shows the dispersion of velocity field in the flow direction in 8 points of the test section depending on the form of the contraction. We choose the 30° simplified contraction which offers an acceptable compromise between a small deviation in the velocity field in the flow direction (less than 3% discrepancy from the Bell-Mehta form) and no difficulty of fabrication in our case.

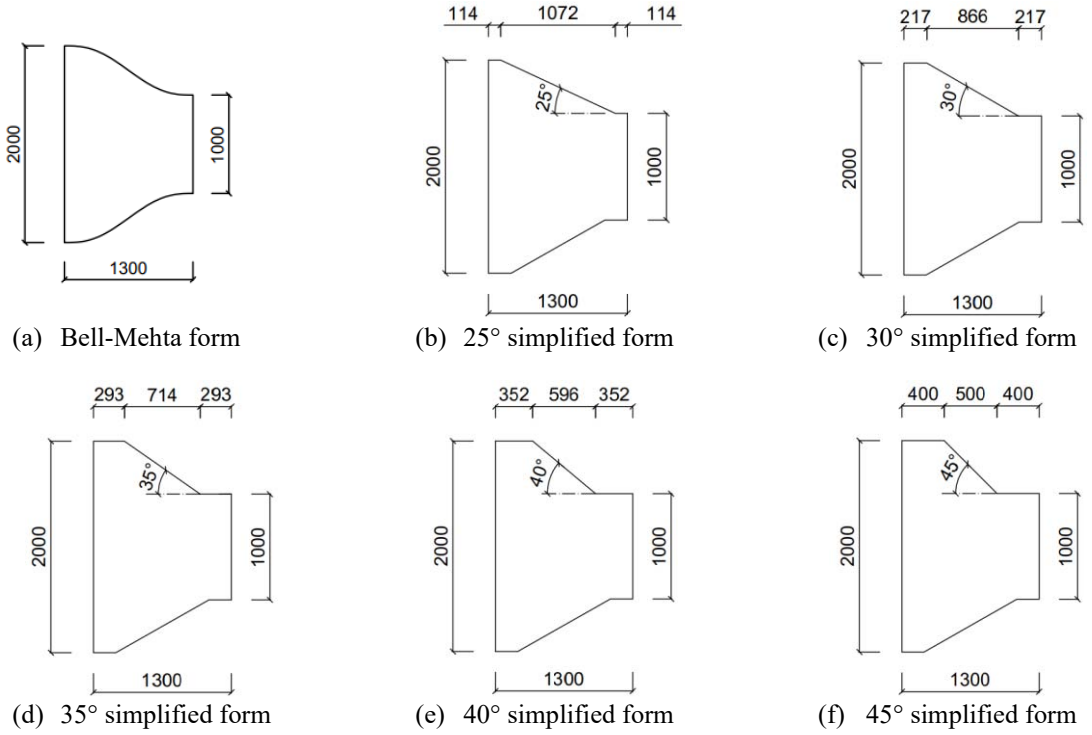

Figure 3: Different forms tested for the contraction

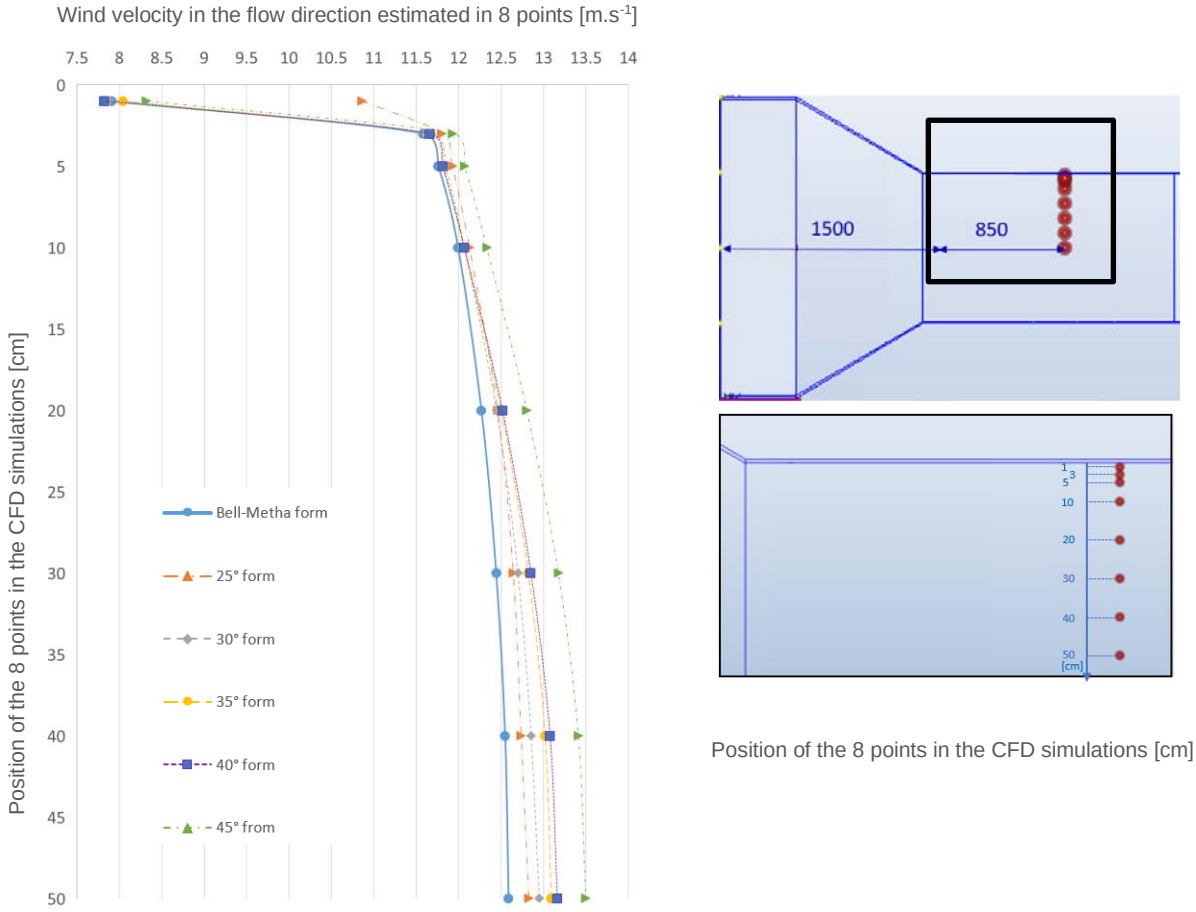

Figure 4: Wind velocity field inside wind tunnel for different forms of contraction

- The dimensions of the Test Section are 1x1x1.5 m^3. The frontal area of the model represents 4.8% of the test section cross-sectional area, which is under the 5% limit recommended by the ASCE as indicated by Choi and Kwon (1998)[19] (no blockage correction is needed).

4 EXPECTED RESULTS

The main expected results of this work are:

1) The evaluation of the measurement uncertainty due to a steady wind;
2) Propositions of improvement in the ISO 9972 protocol to reduce the uncertainty.

5 REFERENCES

[1] G.T. Tamura, Measurement of air leakage characteristics of house enclosures, ASHRAE Trans. (1975) 202–211.

[2] F.R. Carrié, B. Rosenthal, An overview of national trends in envelope and ductwork airtightness, AIVC Ventilation Information paper. (2008).

[3] J. Jokisalo, J. Kurnitski, M. Korpi, T. Kalamees, J. Vinha, Building leakage, infiltration, and energy performance analyses for Finnish detached houses, Building and Environment. 44 (2009) 377–387. doi:10.1016/j.buildenv.2008.03.014.

[4] J.M. Logue, M.H. Sherman, I.S. Walker, B.C. Singer, Energy impacts of envelope tightening and mechanical ventilation for the U.S. residential sector, Energy and Buildings. 65 (2013) 281–291. doi:10.1016/j.enbuild.2013.06.008.

[5] V. Leprince, A. Bailly, F.R. Carrié, M. Olivier, State of the Art of Non-Residential Buildings Air-tightness and Impact on the Energy Consumption, in: Proceedings of the 32nd AIVC Conference, 12-13 October 2011, Brussels, Belgium, 2011: pp. 12–13. http://www.aivc.org/sites/default/files/7b2.pdf.

[6] F. Richieri, B. Moujalled, T. Salem, F.R. Carrié, Airtightness impact on energy needs and airflow pattern: a numerical evaluation for mechanically ventilated dwellings in France, International Journal of Ventilation. 15 (2016) 134–150. doi:10.1080/14733315.2016.1203608.

[7] M.H. Sherman, W.R. Chan, Building Airtightness: Research and Practice. Building Ventilation: The State of the Art Review, LBNL Report. (2004).

[8] V. Leprince, F.R. Carrié, M. Kapsalaki, Building and ductwork airtightness requirements in Europe – Comparison of 10 European countries, in: Proceedings of 38th AIVC Conference, 13-14 September 2017, Nottingham, UK, 2017.

[9] C. Mees, X. Loncour, Quality framework for reliable fan pressurisation tests, Qualicheck. (2016).

[10] M.P. Modera, D.J. Wilson, The Effects of Wind on Residential Building Leakage Measurements, Air Change Rate and Airtightness in Buildings -. ASTMSTP 1067 (1990). doi:10.1520/STP17210S.

[11] F.R. Carrié, V. Leprince, Uncertainties in building pressurisation tests due to steady wind, Energy and Buildings. 116 (2016) 656–665. doi:10.1016/j.enbuild.2016.01.029.

[12] F.R. Carrié, V. Leprince, Model error due to steady wind in building pressurization tests, in: In Proceedings of 35th AIVC Conference, 24-25 September 2014, Poznan, Poland, 2014.

[13] I.S. Walker, M.H. Sherman, J. Joh, W.R. Chan, Applying Large Datasets to Developing a Better Understanding of Air Leakage Measurement in Homes, International Journal of Ventilation. 11 (2013). https://www.tandfonline.com/doi/abs/10.1080/14733315.2013.11683991.

[14] M. Prignon, A. Dawans, S. Altomonte, G. Van Moeseke, A method to quantify uncertainties in airtightness measurements: Zero-flow and envelope pressure, Energy and Buildings. 188–189 (2019) 12–24. doi:10.1016/j.enbuild.2019.02.006.
[15] N. Le Roux, Etude par similitude de l'influence du vent sur les transferts de masse dans les bâtiments complexes, Université de La Rochelle, 2011.
[16] M. Stefano, M. Michele, S. Brusca, F. Fabio, Small-Scale Open-Circuit Wind Tunnel: Design Criteria, Construction and Calibration, (2017).
[17] M.A. Gonzalez Hernandez, A.I. Moreno Lopez, A. A., J.M. Perales Perales, Y. Wu, S. Xiaoxiao, Design Methodology for a Quick and Low-Cost Wind Tunnel, in: N. Ahmed (Ed.), Wind Tunnel Designs and Their Diverse Engineering Applications, InTech, 2013. doi:10.5772/54169.
[18] J.H. Bell, R.D. Mehta, Contraction design for small low-speed wind tunnels, 1988. https://ntrs.nasa.gov/search.jsp?R=19890004382.
[19] C.-K. Choi, D.K. Kwon, Wind tunnel blockage effects on aerodynamic behavior of bluff body, Wind and Structures An International Journal. (1998).

CFD modelling of fan pressurization method in buildings – The impact of dynamic wind on airtightness tests

Dimitrios Kraniotis, Arnab Chaudhuri

Oslo Metropolitan University
P.O.box: St. Olav plass 4
0130 Oslo, Norway

SUMMARY

Building airtightness tests have become very common in several countries, either to comply with minimum requirements of regulations or programs, or to justify input values in calculation methods. This raises increasing concerns for the reliability of those tests. Despite the extensive debates about how the building pressurization test standard ISO 9972 should address sources of uncertainties, no change has been implemented. According to the current standard, the zero-flow pressure shall not exceed 5 Pa for the test to be valid. Consequently, in moderately windy conditions, it may be impossible to perform a pressurization test in accordance with the standard, even using precautions with a careful uncertainty analysis. This study investigates numerically, with the use of a commercial CFD code, the impact of unsteady wind on fan pressurization tests. Two test houses, built in cross-laminated-timber (CLT), are modelled and used as case study. Various leakage location, fan placement and wind profiles are used as input in a set of Scenarios.

KEYWORDS

air infiltration; unsteady wind; fan pressurization method; airtightness test; computational fluid dynamics (CFD)

1 INTRODUCTION

Numerical methods have been extensively used in air infiltration and natural ventilation studies. The value of such methods is high in particular when unsteady phenomena are under investigation, i.e. turbulent wind. Computational fluid dynamics codes can provide detailed information about pressure distribution around building envelope and air exchange in transient analysis.

2 METHODOLOGY

A commercial CFD code is used in this study, which includes both steady state and transient analysis. For the steady state, the focus is set on the impact of various wind speeds on airtightness tests, while for the transient analysis turbulent wind is under investigation. In all cases, a wind profile has been defined in the inlet of computational domain.
Two test houses located at the site of the meteorological station of Ås are used as case study. The houses are insulated and built in cross-laminated-timber (CLT). For the detail description of wind profile, historic data about surface roughness and wind speed at 10 m have been collected and used.
In addition, various scenarios of fan exposure, i.e. windward, leeward, side as well as leakage location in building envelope have been employed. Regarding the latter, controlled leakage paths exist in the building envelope of both houses, providing the opportunity to investigate different airtightness levels.
The results from CFD will be validated experimentally in the near future.

Using co-simulation between EnergyPlus and CONTAM to develop IAQ and energy-centric demand-controlled ventilation systems

Maria Justo Alonso*[1], W. Stuart Dols[2], Hans Martin Mathisen[1]

1 Norwegian University of Science and Technology
Kolbjørn Hejes v 1B,
Trondheim, Norway
**Corresponding author:maria.j.alonso@ntnu.no*

2 National Institute of Standards and Technology
100 Bureau Drive, MS8633
Gaithersburg, MD, USA

ABSTRACT

Buildings account for approximately 40 % of energy use in the European Union, as well as in the United States. In light of the European Energy performance of buildings directive, efforts are underway to reduce this energy use by targeting zero or nearly zero energy buildings. In such low energy buildings in cold climates, ventilation to ensure suitable indoor air quality is responsible for half or more of their energy use. The use of heat recovery and demand-controlled ventilation are potential solutions to reduce ventilation-related energy consumption. Demand-controlled ventilation can be utilized to realize energy savings by maintaining the concentration of CO_2 below a control setpoint. This control approach can reduce ventilation airflows when possible to reduce energy use.

This paper presents a study of a corridor of offices ventilated with constant airflow in Norway over two weeks of normal occupancy. Measurements of temperature, relative humidity, carbon dioxide, particles and occupancy levels were used to calibrate a simulation model. These measurements were used to validate a coupled energy, airflow and indoor air quality model. Co-simulation between EnergyPlus and CONTAM was used to evaluate the baseline energy use and develop a CO_2-based demand-controlled ventilation strategy which took into account other pollutants and recirculation airflows. A parametric study was performed to evaluate energy use and occupant exposure. The main findings from the simulations reveal:

- Interactions between recirculation of air and increased ventilation rates to maintain low CO_2 levels are not always intuitive. In some cases, increased ventilation rates were unable to maintain acceptable CO_2 levels when using recirculation of exhaust air, and the increased fan power of the demand-controlled ventilation system prevented very large energy savings.
- DCV based on multiple pollutants must be carefully programmed to avoid control problems. For instance, reducing outdoor air intake when outdoor particle levels were high was effective so long as occupancy was below 100%.
- Occupant health and building energy use are strongly correlated, and the ventilation control needs to be programmed considering this interdependency. Here we propose to use reduced exposure to pollutants as a performance parameter for comparison to reduced energy use. The study presented herein serves as the initial phase of a project to study in greater detail how to reduce ventilation while ensuring indoor air quality using a comprehensive analysis method.

KEYWORDS

building simulation, CONTAM, demand-controlled ventilation, EnergyPlus, indoor air quality, energy use, recirculation

1 INTRODUCTION

Reducing energy consumption in buildings is fundamental to energy resource conservation and climate change mitigation, as well as addressing the Energy performance of buildings directive (EPBD) (European Commission 2010). While costs associated with building energy use can be significant, it has been estimated that for the commercial building sector that 1 % of the cost is related to energy, 9 % to building rental and 90 % to occupant payroll (Alker et al. 2014). This should justify health, well-being and productivity of occupants to be a higher priority (Parkinson et al. 2019a) than reduced energy use, which includes decisions about building ventilation rates. The most basic functions of ventilation are to ensure good indoor air quality by controlling indoor contaminant levels and thermal comfort. There are three general means to reduce indoor contaminant levels: reduce or remove the source, remove contaminants from the indoor air, i.e., via local exhaust and filtration, or dilute with air having lower or no contaminant levels. This paper addresses the latter. The ventilation rate should therefore be related to the indoor generation rate of pollutants and the resultant occupant exposure. Careful consideration of these concepts in applying demand-controlled ventilation (DCV) can yield energy savings.

Many different types of pollutants can be produced in an indoor environment. However, not all have hazardous health effects, nor do they have the same emission rates. Standards governing indoor air quality (IAQ) requirements are less specific than those related to thermal comfort (Parkinson et al. 2019b). Some regulations require good or satisfactory IAQ but do not provide specific threshold values for pollutants other than CO_2 (Standard Norge 2017). The requirements for the application of outdoor and recirculation ventilation also varies between countries; however, there does seem to be consensus on the need to reduce exposure to harmful pollutants. The WHO (2010) defines maximum threshold concentrations for various contaminants based on levels below which health effects occur, and many of the pollutant levels are based on perceived odour or general irritation.

Some studies have shown that CO_2 concentrations may be associated with cognitive performance and health issues, but other studies do not (Allen et al. 2016; Maddalena et al. 2015; Satish et al. 2011, 2012; Wargocki & Wyon 2013; Liu et al. 2017; Zhang et al. 2016; Zhang et al. 2017). Some standards recommend keeping CO_2 below 1000 ppm. However, Apte et al. (2006) and Erdmann et al. (2002) analysed data from 100 office buildings and concluded that increased prevalence of mucous membrane and lower respiratory sick building syndrome (SBS) symptoms occur when peak CO_2 concentrations are below 1000 ppm. However, those symptoms were not likely caused by CO_2 exposure but rather by other contaminants that increased in concentration due to lower ventilation rates. According to the literature review of Carrer et al. (2015), adverse effects (including respiratory and allergy symptoms, airborne and infectious diseases and sick leave, SBS, and performance and learning) can occur when ventilation rates fall below 7 L/s per person for residential buildings, 12 L/s per person in schools, and 25 L/s per person in offices. These values are mostly related to studies of SBS symptoms and are not consistent between studies. Most of these studies did not characterize sources either qualitatively or quantitatively, did not account for ventilation effectiveness, and considered air to be fully mixed within the zones. Further, it is often erroneously assumed that when ventilating at or above these rates and maintaining afore-mentioned CO_2 concentrations, that other pollutants will also be maintained at relatively low concentrations. This may be true for some occupant-related pollutants but does not necessarily correlate to all pollutant sources whether of indoor or outdoor origin.

Some authors indicate that CO_2 should only be used as an indication of occupant-related pollutants (Fisk 2018; Maddalena et al. 2015). Others propose that CO_2 should not only be regarded as an IAQ indicator but as a pollutant impacting health and cognitive functions (Allen

et al. 2016; Satish et al. 2011). Ramalho et al. (2015) point out that the probability of exceeding pollutant health guideline values correlates with CO_2 concentration, but the probability of exceedance is still high even at low CO_2 levels. Chatzidiakou et al. (2015) concluded that indoor temperatures correlated with total volatile organic compound levels when potential indoor pollutant sources were limited and CO_2 levels were reduced by increased ventilation rates, and they also concluded that CO_2 levels correlated to indoor particulate levels when the influence of outdoor levels was small. However, CO_2 was not a good predictor of outdoor, traffic-related pollutants. Thus, they concluded that besides elimination of indoor sources, an average CO_2 level of 1000 ppm is recommended to meet WHO (2010) guidelines for particulate levels and reduce dissatisfaction with IAQ.

Jaakkola et al. (1994) carried out investigations into the effect of recirculating ventilation air on SBS symptoms. They investigated the differential impact of 0 % and 70 % recirculation rates and showed that reducing the outdoor air fraction to 30 %, assuming acceptable outdoor contaminant levels, does not have adverse health effects. However, they only looked at SBS symptoms and did not correlate it with building energy use.

In order to address these different issues related to indoor CO_2 concentrations, the case study herein presents the development of a ventilation strategy that considers both occupant exposure to indoor pollutants and energy use. Measurements were used to validate a building model that incorporated co-simulation between EnergyPlus and CONTAM. The model was validated against measurements and used to evaluate baseline energy use and develop a CO_2-based DCV strategy that considered other pollutants and recirculation airflows. Recirculation rates were based on the aforementioned results of Jaakkola et al. (1994). A combination of both quantitative and qualitative approaches was used to evaluate performance of the strategy.

2 MEASUREMENTS

Prior to performing measurements, information was gathered in the study building on the normal behaviour regarding ventilation air distribution and occupancy. Building operators and occupants agreed not to interfere with the equipment, not to open windows and to keep the door closed as much as possible. Samples of temperature, relative humidity (RH), CO_2, and $PM_{2.5}$ (particles of 2.5 μm in diameter or less) were taken every 5 minutes over a two-week period. Table 1 shows the specifics of the measurement equipment.

Measurements were conducted in a corridor located on the ground floor of a university office building in Trondheim, Norway as shown in Figure 1. The building is occupied by graduate students and administrative staff and is located next to a lightly-travelled road. However, during the measurement period, road work was taking place outside the windows leading to a brief period of elevated outdoor particle levels.

Table 1 Description of equipment and parameters measured

Parameter	Sensor type	Uncertainty
Relative humidity	Capacitive	±3 % RH at 25°C
CO_2	Non dispersive infrared (NDIR)	±10 % (500 ppm to 1500 ppm)
Temperature	10K NTC Thermistor	± 0.4 in the selected range
Particle concentration	Optical sensor	±10 %

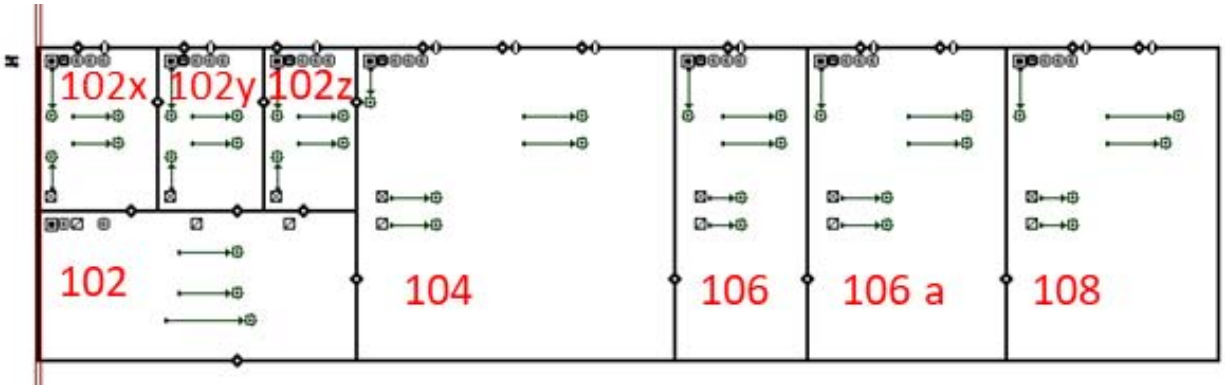

Figure 1: CONTAM sketch of the corridor measured and modelled with room numbers provided in red. Symbols indicated ventilation system supplies and returns, contaminant sources and sinks, occupants and CONTAM controls network.

3 CO-SIMULATIONS WITH ENERGYPLUS AND CONTAM

The corridor presented in Figure 1 is modelled via co-simulation between EnergyPlus and CONTAM (Dols et al. 2016), which enables simultaneous consideration of energy and pollutants to realize implementation of DCV algorithms that incorporate indoor concentrations provided by sensors. CONTAM performs multizone building airflow and contaminant transport calculations but does not perform heat transfer analysis (Dols & Polidoro 2015). EnergyPlus is a multizone energy analysis program that performs system sizing, loads analysis and calculates HVAC system airflow rates to meet thermal loads during runtime. EnergyPlus incorporates interzone and infiltration airflows, which it obtains from CONTAM during co-simulation run-time. In turn, CONTAM obtains indoor temperatures and system airflows from EnergyPlus.

While EnergyPlus provides for CO_2-based DCV, the built-in algorithms do not directly affect the terminal unit flow rate or the system flow rate. Zone occupancy is used by the outdoor air (OA) controller to increase the OA flow rates up to the current supply air flow rate. Thus, using the *AirTerminal:SingleDuct:Uncontrolled* and *DesignSpecification:OutdoorAir* objects, EnergyPlus will vary the terminal unit flow request based on the current occupancy, but it does not directly respond to a CO_2 signal. This method works to control recirculated airflow, but it is not applicable to Norwegian systems that require continuous 100 % outdoor air intake. The models used in this study achieve variable system supply flow based on CO_2 sensors located within each occupied zone of the CONTAM model. Sensor values are then utilized within an EnergyPlus energy management system (EMS) program to adjust the terminal unit mass flow rates of respective zones.

A model was built in CONTAM and exported to EnergyPlus via the CONTAM3Dexport software tool. Thermal properties (U-value) of the building construction correspond to Norwegian Building Code, TEK 07 (Statens Bygningstekniske Etat 2007): external wall 0.18 W/m^{2}K, roof 0.13 W/m^{2}K, floor 0.15 W/m^{2}K, and windows 1.2 W/m^{2}K. The building was modelled in CONTAM with an air leakage of 10 cm^2/m^2 at 10 Pa. Indoor CO_2 sources are 18 L/h per person, based on an average sized adult engaged in office work (ASTM 2012), during occupied periods as described in Table 2. No indoor sources of $PM_{2.5}$ were modelled.

Table 2 Occupancy schedules for rooms shown in Figure 1. For rooms 104 and 108, one person arrives every 30 minutes and leaves every 30 minutes.

	102 (and x, y, z)	104 (5 occupants)	106	106a	108 (4 occupants)
Arrival	8:00	8:00-9:30	8:30	8:15	8:00-9:30
Lunch break	11:30-12:00	11:30-12:00	No vacancy	12:15-12:45	11:30-12:00
Departure	16:00	17:00-18:30	16:30	17:00	17:00-18:30
Weekends	Vacant	Vacant	Vacant	Vacant	Vacant

4 RESULTS

4.1 Measurements

Measurements were collected for two weeks, and the results were used to establish ventilation rates and emission sources in the simulation model. The ventilation rate was kept constant and measured at the supply and return, i.e., extract, air terminals using a volume flow hood. Figure 2 shows an example of measurement results for one of the rooms (104) over the course of a single day in mid-April. Room 104 is a 36 m^2 office that can accommodate up to six occupants and has a constant airflow rate of 350 m^3/h (100 % OA). Four to five occupants were in the office from 9:00 to 19:00. From 15:00 to 15:08, 16 people occupied the room.

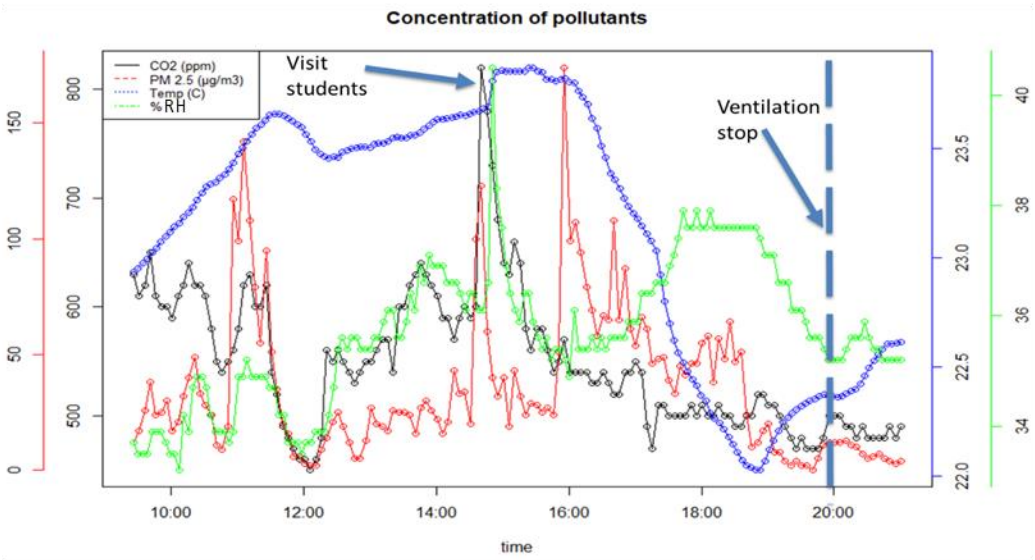

Figure 2: Pollutant concentrations in room 104 for one day

Figure 2 shows that the CO_2 levels remain below 750 ppm until the period when 16 students enter the room for a brief period of time, corresponding to a peak of about 850 ppm. The average $PM_{2.5}$ concentration over the measurement period was 36 µg/m^3 with a maximum value over 150 µg/m^3. Guidelines indicate a maximum concentration over a 24 hours period of 15µg/m^3 and 8 µg/m^3 over 8 hours (FHI 2013). Outdoor particle levels exceeded reference levels by up to 70 % during the measurement period. This is likely due to the measurements being taken during pollen season, and road work that was taking place adjacent to the building during this time. These high polluting sources were not introduced as sources in the simulations as they represent a momentary peak and are not representative of the whole year. Regardless, $PM_{2.5}$ concentrations do not track CO_2 concentrations, and the elevated concentrations may affect occupants in the short term related to allergy or asthma. If outdoor pollutants are introduced through the ventilation system, reducing supply airflow rates may be beneficial, but monitoring $PM_{2.5}$ and or other pollutants would require additional sensors and control logic.

Figure 2 shows that the indoor temperature is greater than 23 °C during most of the occupied period of the day. The Norwegian standard recommends a set point temperature of 22 °C in the winter (Statens Bygningstekniske Etat 2007), and Burroughs & Hansen (2011) recommends keeping temperatures below 22 °C to reduce SBS symptoms. Correlations between room temperatures over 23 °C and self-reported health effects have also been identified (van Loenhout et al. 2016). Seppänen et al. (2006) indicate that a drop in performance can be expected for temperatures over 23 °C. In this current study, occupants surveyed indicated that their ability to concentrate was reduced due to "heavy air" and high temperature. During this measurement period, outdoor temperatures were relatively low, so the radiators were at maximum output for this North-facing room. Given that supply air is delivered at 19 °C, reducing radiator output would allow for reducing room temperature. In this case, the humidity is kept above 32 %.

4.2 EnergyPlus and CONTAM Simulations

To validate the model, a one-year simulation was run with typical meteorological year weather data for Trondheim and normal activities as defined by the Norwegian design building codes NS 3031 and TEK 07 (Standard Norge 2014; Statens Bygningstekniske Etat 2007). The simulated annual energy was within 5 % of TEK 07 requirements. The outdoor CO_2 was not measured, but was assumed to be constant at 393 ppm. Outdoor $PM_{2.5}$ was modelled based on measurements made 400 m away from the office for an entire year (NILU 2018), and indoor particle removal was simulated in all zones with a deposition rate of 0.5 h^{-1}.

Simulated CO_2 differed from measurements by a maximum of 40 ppm and temperatures by less than 0.5 °C. Owing to the accuracy of the results, the model was considered to be validated both for energy use and IAQ simulations.

4.3 Simulated Cases

Four different ventilation strategies were simulated as summarized in Table 3. Cooling was not simulated as it is not used in Norwegian buildings of this construction period. The base case is modelled using the current strategy to provide a constant 100 % outdoor air and a constant volume of supply air from 8:00 to 16:00 allowing EnergyPlus to size the supply airflow based on winter design conditions. Two cases were based on Jaakkola et al. (1994) and consisted of recirculating extract air at constant rates corresponding to outdoor air intake rates of 70 % and 30 %, respectively. For these two cases, DCV consisted of setting the supply airflow rate to 100 % of the design airflow rate when the indoor CO_2 concentration was greater than or equal to 1000 ppm, and reducing the supply airflow rate to 50 % of the design air flow rate (DAFR) when the concentration is between 600 ppm and 1000 ppm and reducing to 20 % when below 600 ppm. In the fourth case both the supply and outdoor air (recirculation) rates were varied with the outdoor air fraction controlled based on the volume-weighted fraction of occupied zone CO_2 concentrations.

Table 3 Ventilation control methods (CO_2 in ppm)

Name	Outdoor Air Fraction Control	Supply Airflow Control
OA_100	Constant 100 % OA	$CO_2 \leq 400$ = 20% DAFR $400 < CO_2 \leq 1000$ = 50% DAFR $1000 < CO_2$ = 100% DAFR
OA_70	Constant 70 % OA	
OA_30	Constant 30 % OA	
Variable	$CO_2 \leq 750$ = 30 % OA; $750 < CO_2 \leq 900$ = 60 % OA; $900 < CO_2$ = 80 % OA	

In the EnergyPlus model, an electric resistance coil is located in the *AirLoopHVAC*, downstream of the Supply fan. The electric output is controlled via a thermostat located in

Room a102x and setpoint temperatures were 22 °C and 20 °C during and outside of working hours, respectively. An energy recovery ventilator was incorporated at the outdoor air mixing box having a heat wheel with a maximum sensible and latent effectiveness of 76 % and 68 %, respectively.

Particle filters were simulated in all cases and were specified according to their minimum efficiency reporting value (MERV). Filters were incorporated into the recirculation airstream and outdoor airstreams and were MERV 15 (equivalent to F9, e $PM_{2.5}$ > 95 %) and MERV 13 (equivalent to F7, e $PM_{2.5}$ 65 % - 80 %), respectively.

Figure 3 shows the results for the four simulated cases. Regarding CO_2, the higher the supply of OA, the lower the concentrations of CO_2. Conversely, the cases with higher outdoor air intake rates show higher $PM_{2.5}$ concentrations. Thus using 100 % OA, means higher entry of outdoor $PM_{2.5}$ as air is supplied via a coarser filter. Lower OA fractions mean higher recirculation rates through the recirculation air filter, which is approximately 15 % more efficient for $PM_{2.5}$ leading to lower indoor particle levels. This reveals the differences between indoor and outdoor sources, namely that increasing ventilation to control an indoor source can lead to increased levels of an outdoor source.

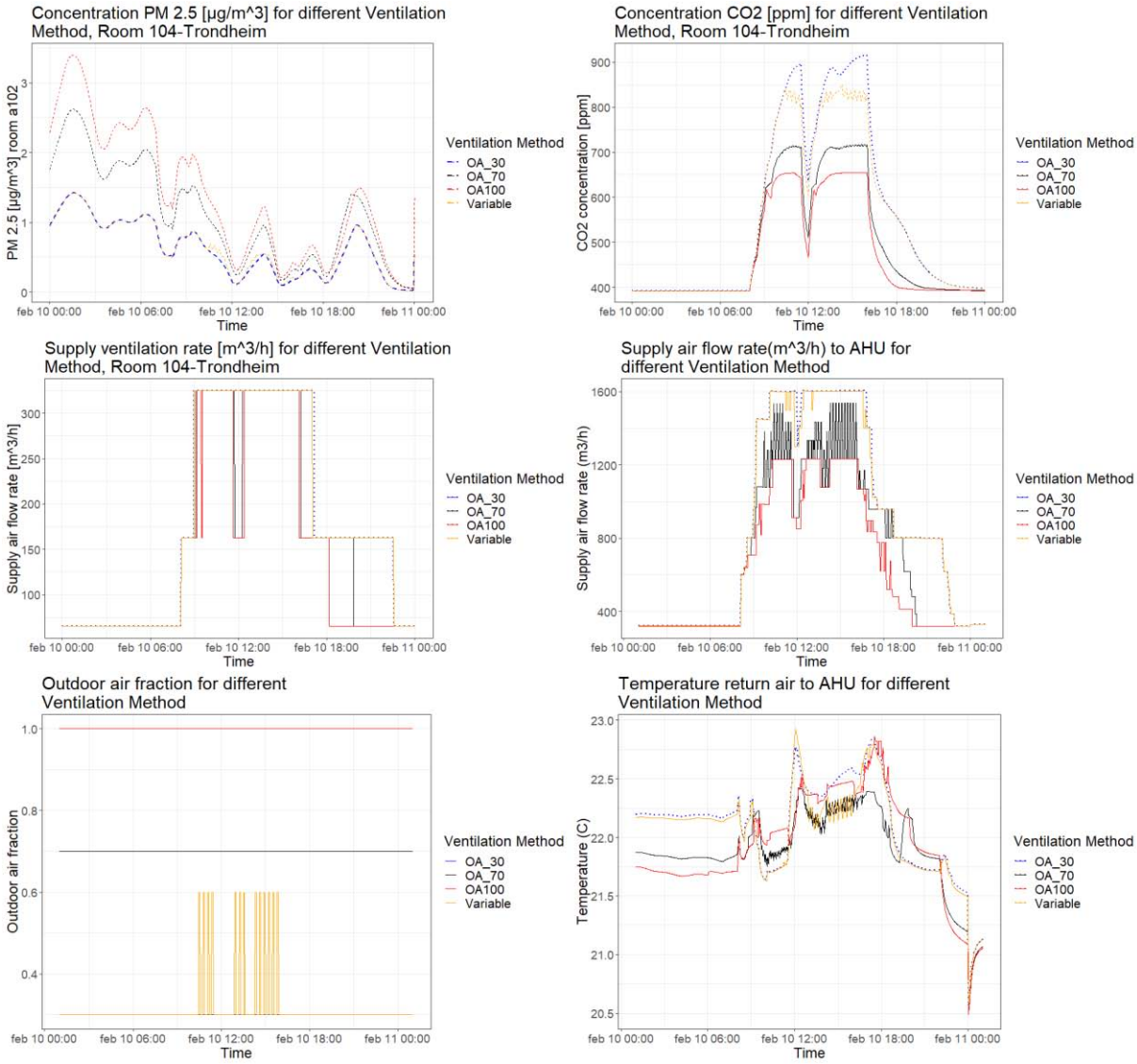

Figure 3: Simulation results for $PM_{2.5}$, CO_2, temperature, outdoor air fraction and supply airflow rates of room 104 for 10 February

Along with Figure 3, thermal comfort results in Table 4 shows that higher recirculation rates yielded higher indoor temperatures resulting in thermostatic setpoints being exceeded and unsatisfactory thermal comfort results provided by the EnergyPlus ASHRAE 55-2004 summary report. The values obtained regarding CO_2, temperature and particles are thus in agreement with the conclusions obtained by Jaakkola et al. (1994); that is, while recirculating extract air does lead to increased CO_2 levels, it did not adversely affect particle concentration levels for these cases.

Table 4: Thermal comfort-related results for all four cases

	100 % OA (h)	70 % OA (h)	30 % OA (h)	Variable (h)
Time setpoint not met during occupied heating	816	905	1263	1233
Time not comfortable based on simple ASHRAE 55-2004	1976	1990	1958	1966

Table 5 shows the annual energy use for all four cases. The cases with lower OA fractions have lower heating demands but have higher fan power demands, because when recirculating extract air, more air is needed to mitigate CO_2 levels.

Table 5: Annual energy use for all four cases

	100 % OA (kWh/m^2a)	70 % OA (kWh/m^2a)	30 % OA (kWh/m^2a)	Variable (kWh/m^2a)
Heating	188	137	67	73
Fans	28	30	37	36
Total	216	167	104	109

5 DISCUSSION

These results demonstrate the use of co-simulation of EnergyPlus and CONTAM as a tool for simultaneously simulating both energy use and IAQ. There is a clear interaction between energy use for heating and recirculation of extract air from the zone. In this study, higher recirculation rates yielded higher room temperatures and CO_2 levels. The energy use decreased while using recirculation due to reduction of the relatively high energy needs for heating in the 100 % OA case. For buildings located in other climates having lower heating demands, recirculation may pose an overheating challenge, so better temperature controls may be warranted in these cases.

The goal of all the strategies was to maintain CO_2 concentrations below 900 ppm, but the 30 % OA strategy does not achieve this goal despite the higher supply airflow rates. For the cases with higher recirculation of extract air, larger supply should be designed in order to maintain CO_2 levels and temperature. This may influence energy use, though in this case, due to the potential for reduced energy use associated with heating, this effect may not be significant.

When controlling CO_2 levels, the $PM_{2.5}$ levels varied independently as they depend on outdoor concentrations in this simulation, though they are reduced when larger recirculation rates are applied owing to the more efficient filter in the recirculation air stream. In Trondheim, outdoor air is considered to be relatively free of contaminants, but in the presence of elevated $PM_{2.5}$ levels the use of recirculation may warrant protection from particles of outdoor origin (even more in this case where the filter in the recirculated extract air was of higher efficiency for $PM_{2.5}$). The use of recirculation should be done with knowledge of $PM_{2.5}$ sources and monitoring of the supply and outdoor concentrations is recommended so that recirculation can be used as a protective measure.

6 CONCLUSIONS

- Recirculation of extract air and required ventilation airflow rates are correlated. In some cases, when using recirculation of exhaust air, increased ventilation rates were unable to maintain acceptable CO_2 levels. Thus, a minimum level of OA should always be maintained.
- DCV should be based on several pollutants, e.g. CO_2 and $PM_{2.5}$, as well as temperature, and must be carefully programmed to avoid control problems. For instance, reducing outdoor air intake when outdoor levels of $PM_{2.5}$ were high was effective so long as occupancy was below 100 % and there were no indoor sources of $PM_{2.5}$. This is normally not the case, and outdoor particle concentrations are not likely to be as low as simulated in this study.
- Pollutant levels and energy use are correlated, and the ventilation control needs to be programmed considering a hierarchy. Here we propose to use reduced exposure to pollutants as a more important parameter than reduced energy use. The study presented here serves as the initial phase of a project that will study, in detail, how to reduce energy use in ventilation while ensuring IAQ in a multidisciplinary way.

7 ACKNOWLEDGEMENTS

The authors gratefully acknowledge the support from the Research Council of Norway and several partners through the Research Centre on Zero Emission Neighbourhoods in Smart Cities (FME ZEN), project number: 286183. The Indoor Air Quality and Ventilation Group at the National Institute for Standards and Technology is also hereby acknowledged.

8 REFERENCES

Alker J, Malanca M, Pottage C, O'Brien R. 2014. Health, Wellbeing & Productivity in Offices. World Green Building Council.

Allen JG, Macnaughton P, Satish U, Santanam S, Vallarino J, Spengler JD. 2016. Associations of cognitive function scores with Carbon Dioxide, Ventilation and Volatile Organic Compound Exposure in Office Workers. *Environ. Health Perspect.* 124(6):805–12.

ANSI/ASHRAE. 2004. Standard 55-2004 Thermal Environmental Conditions for Human Occupancy. Atlanta.

Apte MG. 2006. A Review of Demand Control Ventilation. *Heal. Build.* (May):371–76.

ASTM. 2012. D6245-12 Standard Guide for Using Indoor Carbon Dioxide Concentrations to Evaluate Indoor Air Quality and Ventilation.

Burroughs HE, Hansen SJ. 2011. *Managing Indoor Air Quality*, Vol. 5th Edition. The Fairmont Press, Inc.

Carrer P, Wargocki P, Fanetti A, Bischof W, De Oliveira Fernandes E, et al. 2015. What does the scientific literature tell us about the ventilation-health relationship in public and residential buildings?

Chatzidiakou L, Mumovic D, Summerfield A. 2015. Is CO2 a good proxy for indoor air quality in classrooms? Part 1: The interrelationships between thermal conditions, CO2 levels, ventilation rates and selected indoor pollutants. *Building Services Engineering Research and Technology.* 36(2):129-161.

Dols WS, Emmerich SJ, Polidoro BJ. 2016. Coupling the multizone airflow and contaminant transport software CONTAM with EnergyPlus using co-simulation. *Build. Simul.*

9(4):469–79.

Dols WS, Polidoro BJ. 2015. CONTAM User Guide and Program Documentation. *NIST Technical Note 1887*. Gaithersburg.

Erdmann C, Steiner K, Apte M. 2002. Indoor carbon dioxide concentrations and sick building syndrome symptoms in the BASE study revisited: Analyses of the 100 building dataset. *Indoor Air 2002*.

European Commission. 2010. Directive 2010/31/EU of the European Parliament and of the Council of 19 May 2010 on the energy performance of buildings (recast). *Off. J. Eur. Union*. 13–35.

FHI. 2013. Luftkvalitetskriterier: virkninger av luftforurensning på helse.

Fisk WJ. 2018. How home ventilation rates affect health: A literature review.

Jaakkola JJ, Tuomaala P, Seppanen O. 1994. Air recirculation and sick building syndrome: A blinded crossover trial. *American Journal of Public Health*. 84(3):422-428.

Liu W, Zhong W, Wargocki P. 2017. Performance, acute health symptoms and physiological responses during exposure to high air temperature and carbon dioxide concentration. *Building and Environment* 114:96-105.

Maddalena R, Mendell MJ, Eliseeva K, Chan WR, Sullivan DP, et al. 2015. Effects of ventilation rate per person and per floor area on perceived air quality, sick building syndrome symptoms, and decision-making. *Indoor Air*.

NILU. 2018. *www.nilu.no*.

Parkinson T, Parkinson A, de Dear R. 2019a. Continuous IEQ monitoring system: Context and development. *Build. Environ.* 149(October 2018):15–25.

Parkinson T, Parkinson A, de Dear R. 2019b. Continuous IEQ monitoring system: Performance specifications and thermal comfort classification. *Build. Environ.* 149(October 2018):241-52.

Ramalho O, Wyart G, Mandin C, Blondeau P, Cabanes PA, et al. 2015. Association of carbon dioxide with indoor air pollutants and exceedance of health guideline values. *Building and Environment*. 93:115-124.

Satish U, Fisk WJ, Mendell MJ, Eliseeva E, Hotchi T, et al. 2011. Impact of CO_2 on human decision making and productivity. *Indoor Air 2011*.

Satish U, Mendell MJ, Shekhar K, Hotchi T, Sullivan D, et al. 2012. Is CO2 an indoor pollutant? direct effects of low-to-moderate CO2 concentrations on human decision-making performance. *Environ. Health Perspect.* 120(12):1671–77.

Seppanen O, Fisk WJ, Lei QH. 2006. Effect of temperature on task performance in office environment. Lawrence Berkeley National Laboratory, Berkeley, CA (US).

Standard Norge. 2014. *NS 3031:2014- Calculation of energy performance of buildings - Method and data*.

Standard Norge. 2017. *Byggteknisk Forskrift (TEK17)*.

Statens Bygningstekniske Etat. 2007. *Veiledning 2007 Til Teknisk Forskrift Til Plan- Og Bygningsloven 1997*.

van Loenhout JAF, le Grand A, Duijm F, Greven F, Vink NM, et al. 2016. The effect of high indoor temperatures on self-perceived health of elderly persons. *Environ. Res.* 146:27–34

Wargocki P, Wyon DP. 2013. Providing better thermal and air quality conditions in school classrooms would be cost-effective. *Build. Environ.*

WHO. 2010. WHO Guidelines for Indoor Air Quality: Selected Pollutants. Copenhagen, World Health Organization.

Zhang X, Wargocki P., Lian Z. 2016. Human responses to carbon dioxide, a follow-up study at recommended exposure limits in non-industrial environments. *Building and Environment* 100: 162-171.

Zhang X, Wargocki P, Lian Z, Thyregod C. 2017. Effects of exposure to carbon dioxide and bioeffluents on perceived air quality, self-assessed acute health symptoms, and cognitive performance. *Indoor air* 27(1): 47-64.

Performances of a demand-controlled mechanical supply ventilation system under real conditions: indoor air quality and power distribution for thermal comfort

Clement Laffeter[1], Xavier Faure[2], Michele Potard[1], Claude Bardoul[1], Julien Escaich[1], Ophelie Ouvrier Bonnaz[2], Etienne Wurtz[2]

1 Ventilairsec
16 rue des Imprimeurs
F-44220, Couëron, France

2 Univ Grenoble Alpes
CEA, LITEN, DTS, INES
F-38000 Grenoble, France

ABSTRACT

This study aims to evaluate the performances of a VMI, a demand-controlled mechanical supply ventilation system, in an experimental house, in terms of indoor air quality (IAQ), energy performance and thermal comfort. The positive input ventilation draws fresh air from the outside, filters and preheats or precools it before blowing it every dry rooms. The air circulates through doors' undercuts and is naturally extracted thanks to exhaust orifices in every wet rooms. A heat exchanger supplied with water from a reversible heat pump is used to preheat or precool the blown air. On the one hand, this combination is expected to improve the IAQ by blowing fresh and filtered air in the rooms where occupants spend most of their time. On the other hand, the VMI is supposed to contribute to the thermal comfort by bringing or removing heat to or from the dwelling. To quantify the influence of the VMI on the parameters described above, a VMI and its heat exchanger are set up in an experimental house. The IAQ part is reduced to the analysis of the CO_2 concentration in the experimental house's master room, the relative humidity in the shower room and the PM2.5 concentration indoor and outdoor. The thermal comfort is reduced to the analysis of the supplied air temperature. Results are promising and show that the studied system is a good way to reduce stuffiness in the most occupied bedroom, evacuate humidity in the most occupied shower room and to reduce PM 2.5 level indoor. Results are also encouraging in terms of thermal comfort, since the VMI brings a significant part of the heat, enhancing thus the heating reactivity.

KEYWORDS

VMI, demand-controlled mechanical supply ventilation, IAQ, thermal comfort, energy performance.

1 INTRODUCTION

In the past three decades, building energy performance has been significantly enhanced. Since then, demand-controlled ventilation systems (DCV) have been identified as a key actors in reaching both indoor air quality and energy targets. The most widespread DCV in France is a mechanical extraction ventilation system (MEV) based on passive water vapor sensors allowing to modulate the flowrate in each wet room and sometimes in each dry room as well, depending on their humidity level. Nevertheless, other DCV can present a good compromise between IAQ, energy savings and even thermal comfort. For instance, mechanical balanced systems (MBS) with heat recovery can ensure the outdoor thin particles filtration and can preheat or precool supplied air. However, such systems are usually not chosen by French single-family houses (SFH) builders due to their cost, their technical installation complexity and their gains regarding mean France climate.

VMI can be an alternative that is more affordable and easier to install. Indeed, as well as for balanced systems, VMI can filter the outdoor air and can use the mechanical air supply to bring or remove heat. Even though such systems are available for three decades, few studies are identified about VMI: (Rahmeh, 2014), (Ouvrier-Bonnaz, Rahmeh, Stephan, & Potard, 2015).
VENTILAIRSEC GROUP (www.ventilairsec.com) conceives nowadays a demand-controlled VMI that seeks to comply with IAQ and thermal comfort objectives. The principle is simple: outdoor fresh air is filtered, preheated or precooled and then blown in main rooms of the dwelling. The air circulates through the door's undercuts and is naturally extracted in every wet rooms, through designed openings. The VMI supply flowrate varies according to the indoor relative humidity and the outdoor absolute humidity.
This study focuses on an experimental feedback of a VMI on two main points: IAQ and power distribution for thermal comfort.
Thereafter, the experimental field is presented in terms of envelope and equipment (heating, ventilation, and energy production systems), followed by a description of the global monitoring in terms of location and types of sensors. The IAQ and power distribution results are then presented. Finally, some discussion and conclusion are proposed.

2 EXPERIMENTAL HOUSE DESCRIPTION

In this section, the experimental dwelling is presented, in terms of location, envelope and equipment with a particular attention to the ventilation system. Lastly, the monitoring is detailed.

2.1 Context

The experimental dwelling is part of COMEPOS project, a French experimental program that aims to quantify the performances of innovative systems for SFH. Systems can be from envelope component to heat generators and emitters including ventilation systems as well. Around twenty experimental houses are included in this program all over France (www.comepos.fr)

2.2 Experimental field global description

The experimental dwelling is located in Brest, France. It is a two-floor house. On the ground floor, there are one open kitchen to the living-room, one toilet and one bedroom with a separate shower room. On the first floor, there are one bathroom, one toilet, a room, an office and a mezzanine. The global living area is 180 m².
This house is equipped with photovoltaic solar panels coupled to a 5kW.h electro chemistry storage system. A reversible water to water heat pump coupled to geothermal pipes ensures heating, cooling and domestic hot water. The heating and cooling emission is ensured by radiative ceilings on each floor, including a room by room temperature control. The heat production equipment is also coupled to the VMI supplied air through a water to air heat exchanger for both air cooling and heating purposes.
The VMI operation is as described above. The exhausts consist in vents in the window frames in the ground-floor toilet, bathroom, shower room, a 5 m^3/h-mechanical extractor in the first-floor toilet and a vertical duct in the kitchen. The global airflow modulation follows the increasing or decreasing indoor relative humidity and outdoor absolute humidity. The supplied air in each room is balanced by the airflow network. Measurements are realized in each dry room for several total flowrate setpoints. Table 1 describes the total flowrate distribution for those setpoints:

Table 1: Distribution of the VMI total flowrate in the dwelling's dry rooms

		Total flowrate repartition for several setpoints				
Set point	**Total flowrate [m3/h]**	**Living room (%)**	**Ground-floor bedroom (%)**	**Mezzanine (%)**	**Office (%)**	**First-floor bedroom (%)**
1	77	41.2	16.1	11.5	15.5	15.6
2	134	39.8	15.2	16.6	15.2	13.2
3	157	38.9	17.8	13.8	15.2	14.3
4	186	38.7	16.6	14.8	15.3	14.6
5	217	36.4	17.1	15.3	16.2	15.0
6	248	37.7	17.5	14.2	14.7	15.8
7	267	36.9	18.5	14.9	15.0	14.7

Figure 1 shows the two floors' organization as well as the airflow network of the VMI.

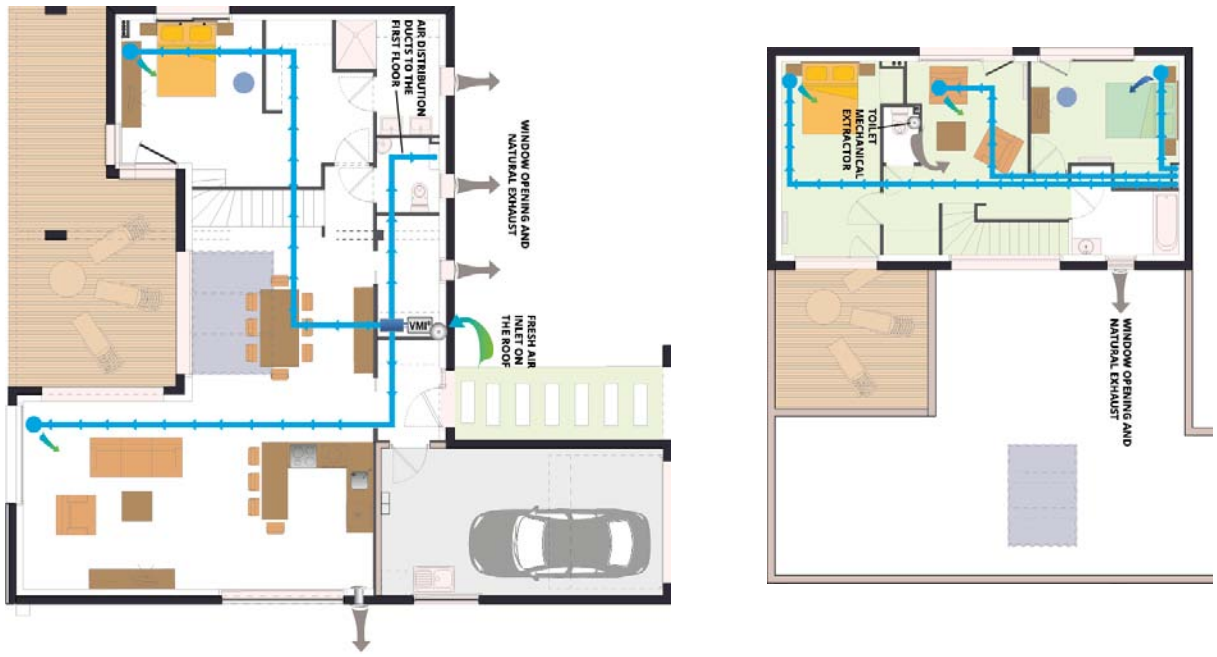

Figure 1: Ventilation network – ground floor and first floor

2.3 Monitoring

The experimental house is largely monitored. Table 2 summarizes the sensors used for this study:

Table 2: Monitoring description

Location	**Measured quantity**
Outdoor	Temperature (north face) / Relative humidity (RH) / PM 2.5 concentration (next to the main VMI air inlet)
Ground-floor bedroom	Temperature / Relative humidity (RH) / Carbon dioxide (CO_2)
Shower room – ground floor	Temperature / Relative humidity
Living-room – ground floor	Temperature / Relative humidity / Carbon dioxide (CO_2) / PM 2.5 concentration
VMI and heat exchanger	Electrical power / Supply air temperature / Inlet water temperature / Outlet water temperature

The monitoring used is based on a wireless communication protocol in order to be as less intrusive as possible.

Relative humidity measurement is based on capacitive technology whereas temperature measurement is made by a thermal resistance. A window opening detector is used in the shower room. PM 2.5 measurement is based on a laser diffraction scattering method. CO_2 sensors are based on solid electrolyte (SE) technology with an automatic background calibration (ABC) method.
Doubts can be emitted about the reliability of this last measurement technology. Therefore, a comparison has been made in some experimental sites for COMEPOS project between this sensor and another one based on a non-dispersive infra-red (NDIR) technology with a dual band calibration. Figure 2 represents the CO_2 level measured by two sensors located side by side. Only raw data are reported thus.

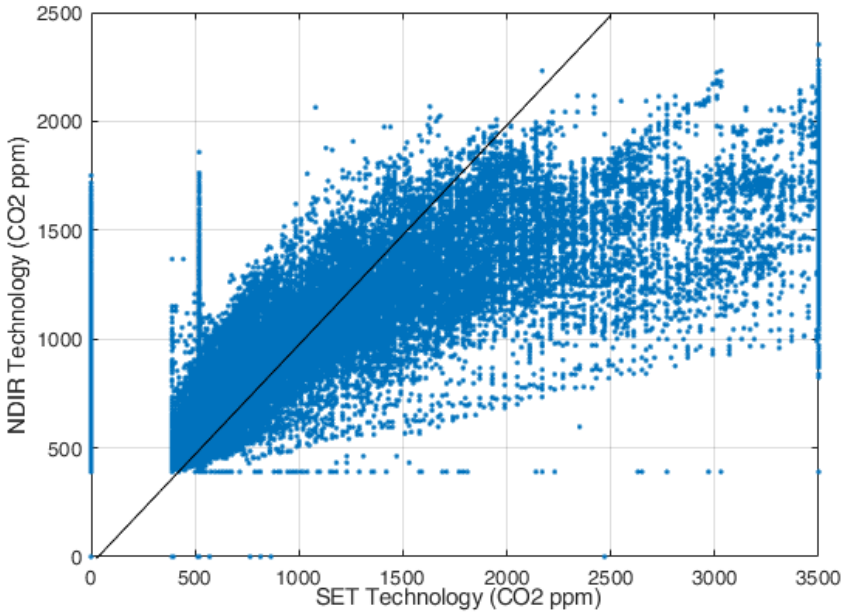

Figure 2: correlation between SE and NDIR technologies

SE technology gives CO_2 values mainly either equivalent or higher than NDIR values. Thus, using SE technology seems to be a conservative approach as long as global analyses are made Besides, in the following, the same sensor is used for all the different considered configurations.

3 RESULTS

In this section, IAQ results will be presented in matter of CO_2 concentration in the master bedroom, absolute humidity in the shower room and PM 2.5 concentrations indoor and outdoor.

3.1 Influence of the ventilation system on the CO2 level

CO_2 concentrations are studied for two specific periods: with the VMI turned off (from 2017.12.25 to 2018.01.18) and with the VMI turned on (from 2018.12.11 to 2019.01.11).
During these periods, two adult persons sleep in the master bedroom every night, except during days 19 and 20 (10^{th} and 11^{th} of December 2017), in the “VMI turned off” case.
Raw data are first presented. Two criteria are then computed, used in several studies in the IAQ field. Their description is given below.

Figure 3 presents raw data through heat map graphs for the two periods mentioned above. It represents the measured concentration in ppm for each day (x axis) and along each day from midnight to noon (y axis). It enables to identify the repeatability of the occupant daily behavior.

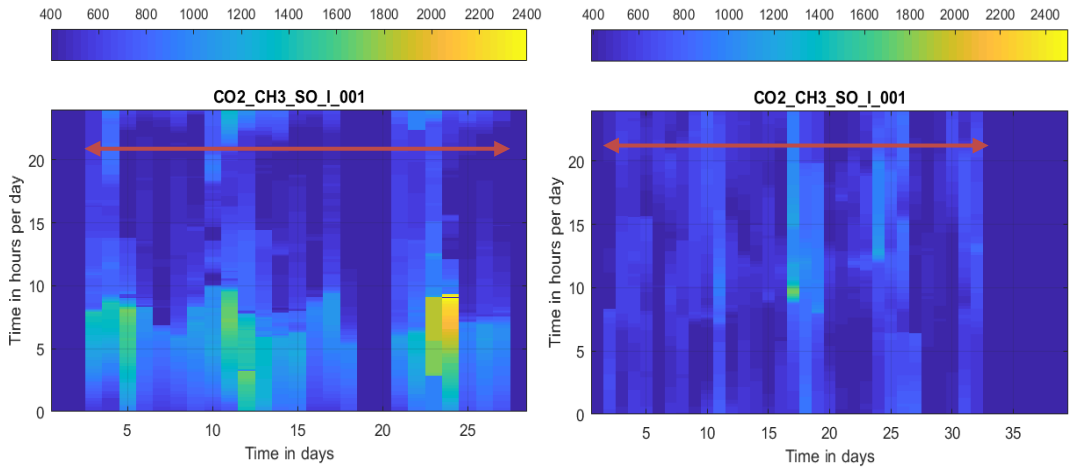

Figure 3: CO2 heat maps VMI turned off (left) and VMI turned on (right)

One of the criteria mentioned above is the ICONE index. It is an air stufinness index proposed by (Ribéron, et al., 2016). Even if initialy defined for schools it can be also used for dwellings analysis (Ribéron, et al., 2016). It follows relation (1).

$$\text{ICONE} = \frac{2.5}{\log(2)} \log(1 + f_1 + 3\, f_2) \qquad (1)$$

f_1 : time fraction during which $1000\ \text{ppm} \leq CO_2 \text{concentration} \leq 1700\ \text{ppm}$
f_2 : time fraction during which $CO_2 \text{concentration} > 1700\ \text{ppm}$

ICONE is between 0 and 5. 0 means an excellent air change rate whereas 5 reflects a poor one. ICONE is calculated for the same two periods used for the heat map graphs, only between 1am and 5am, in order to be compared to other studies in the IAQ field.
The results are compared to ICONE values obtained in the study conducted by (Derbez, et al., 2017) in nine energy-efficient SFH equipped with turned on MEV or MBV, during one week of heating period, between 1am and 5am.
Table 3 shows the index for this experiment extracted from the same time lags and the values reported in (Derbez, et al., 2017):

Table 3: ICONE - present study and literature

ICONE	VMI OFF	VMI ON	Derbez et al.
0	43%	100%	38%
1	20%	0%	38%
2	27%	0%	12%
3	7%	0%	0%
4	3%	0%	0%
5	0%	0%	12%

For this specific experiment and during the considered period, the ICONE index never goes above zero when the VMI is turned on. It confirms that VMI provides, in the present study, an staisfying ACR.

In order to complete the comparison between the present study and (Derbez, et al., 2017), a third criterion is used, consisting in some statistical values, presented in Table 4. The considered periods are the same as for the first two criteria.

Table 4: Temporal distribution of CO2 concentrations in the master bedroom - present site and literature

Values	Villa E-Roise		Derbez et al.
	VMI ON	VMI OFF	
Mean	521	1005	1041
25th percentile	414	829	857
Median	508	958	1071
75th percentile	605	1189	1071
Maximum	895	1909	Not documented

These are statistics over nine dwellings while being compared to only one experiment in the present study. Nevertheless, the "VMI on" values are half those obtained in the (Derbez, et al., 2017) study and the « VMI off » case.

The three criteria converge to the same conclusion: for this experiment, VMI is very effective in terms of air renewal in the master bedroom at night.

3.2 Humidity level in the main bathroom

This study underlines that VMI, like MBV, is an effective solution to avoid stuffiness in the master bedroom, due to the mechanical supply directly in the room when the CO_2 source is located. On the opposite, in wet rooms, MEV is supposed to be more efficient than VMI or any MSV. For the present site and several other experimental houses' bathrooms, absolute humidity values are compared, based on a relative humidity and temperature measurements. The Rankine formula is used to compute absolute humidity values, defined by relation (2).

$$\phi = \frac{P_o Y_{H_2O} \frac{M_{air}}{M_{H_2O}}}{P_o \exp(13.7 - \frac{5120}{T})} \quad (2)$$

Φ: relative humidity,
T: temperature,
P_o: atmospheric pressure,
Y_{H_2O}: the absolute humidity
M_{air}, M_{H_2O}: respectively air and water molar masses.

Figure 4 represents the absolute humidity temporal distribution of the bathrooms' sites mentioned above.

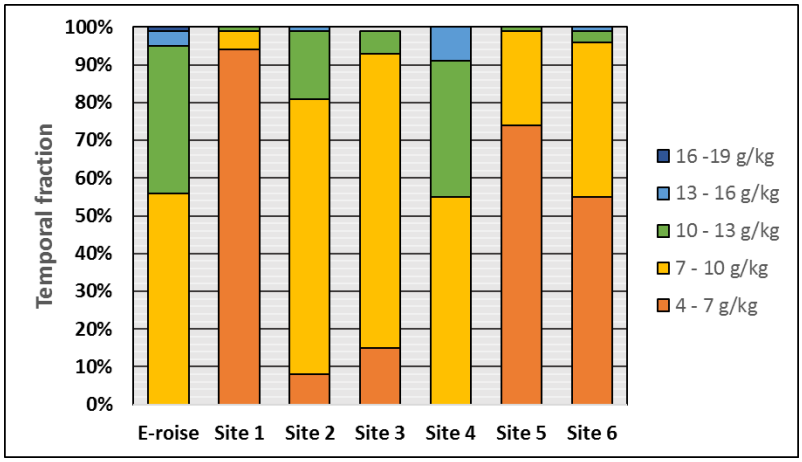

Figure 4: Temporal distribution of absolute humidity in several COMEPOS' bathrooms

It shows that the global absolute humidity is slightly higher in the present site shower room than in the other sites' bathrooms, except for the site 4. Indeed, VMI does not extract humidity in wet rooms as quickly as MEV can do. Nevertheless, this graph underscores for instance the ability of the VMI to keep absolute humidity under 13 g/kg 95 % of the time.

Using relation (2) again, it is possible to estimate the corresponding relative humidity at a chosen temperature in order to normalize all the absolute humidity to comparable relative humidity values. For a hypothetical 21 °C temperature in the bathroom, relative humidity would be between 40 % and 60 % one third of the time, between 30 % and 70 % three quarters of the time, lower than 75% 90 % of the time.

Another phenomenon is highlighted in the present site's shower room: the absence of ventilation seems to have an impact on the occupants' behavior, regarding the number of window openings. It is summed up in Table 5:

Table 5: Impact of the presence of the VMI on the occupants' behaviour in the shower room

VMI	Period	Showers	Window openings	Window opening percentage
OFF	2017.12.25 - 2018.01.18	29	6	21%
ON	2018.12.11 - 2019.01.11	43	2	5%

The occupants are not informed that the VMI is turned off, so that their behaviours remain not influenced. Table 5 shows a direct impact of the ventilation system on the number of window openings.

3.3 Particulate matter (PM 2.5)

The outdoor and indoor PM 2.5 concentrations have been studied with the VMI on, with and without filter.

Measurements are realized for four months, with and without filter, thanks to identical sensors positioned outdoor next to the main air inlet and indoor in the living room. The occupants are were not living in the dwelling yet but the punctual presence happens for visiting purposes. The temporal distribution of the PM 2.5 concentrations is a consistent indicator to quantify the impact of the filter removal on PM 2.5 concentrations. It is represented in Figure 5.

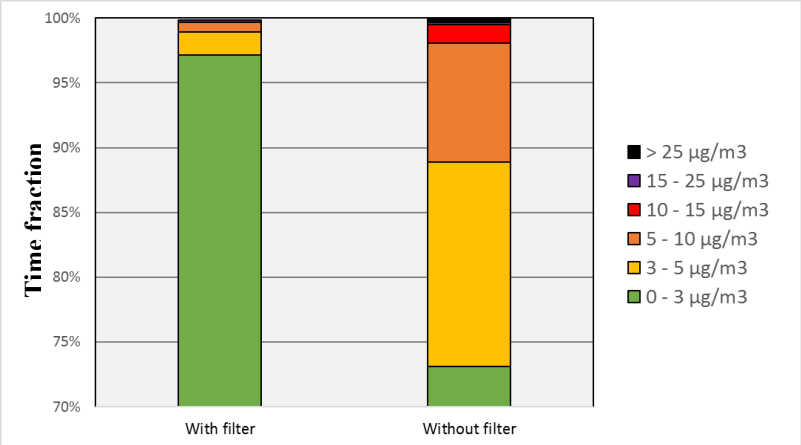

Figure 5: Temporal distribution of indoor PM 2.5 concentration with and without filter

Figure 5 highlights that in both cases, World Health Organization (WHO) thresholds, reported in Table 6, are respected.

Table 6: WHO PM2.5 thresholds

Exposition	Thresholds
Long term	10 µg/m^3
Short term	25 µg/m^3

That is why other thresholds must be considered, based on several references such as:

- "Health damages are observed for low concentrations (…) from 3 to 5 µg/m^3" (AFSSET, 2004),
- "Any reduction of the (…) PM 2.5 concentration leads to a positive health impact" (ANSES, 2017).

Figure 5 underlines that:

- The filtration leads to concentrations lower than 3 µg/m^3 97 % of the time, which means less than 2 days of potential exposure at concentrations higher than 3 µg/m^3,
- The absence of filtration leads to concentrations lower than 3 µg/m^3 73 % of the time, which means 18 days of potential exposure at concentrations higher than 3 µg/m^3.

When dealing with particles concentrations, it is necessary to consider the outdoor level variations, that might be impactful, especially when the filter is absent. Therefore, relation (3) is used to plot Figure 6.

$$I/O = \frac{\text{PM 2.5 indoor concentration}}{\text{PM 2.5 outdoor concentration}} \quad (3)$$

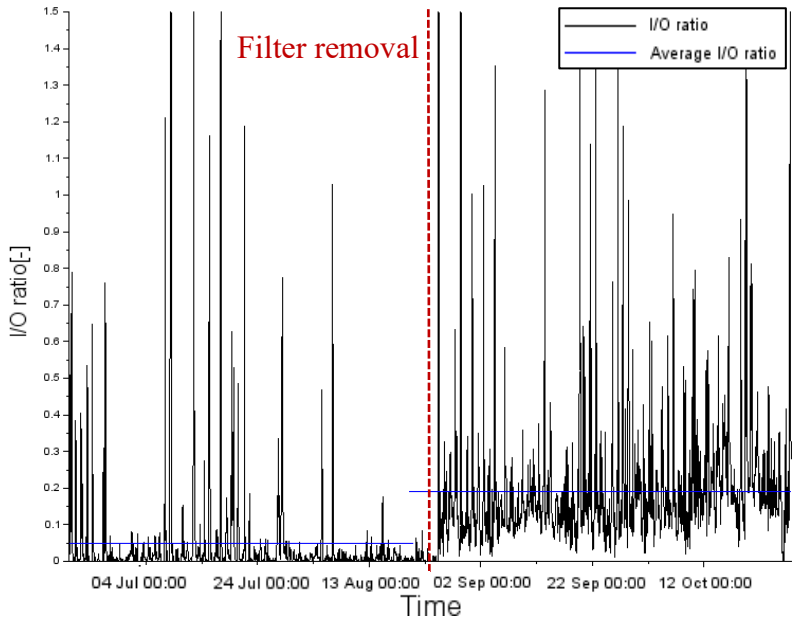

Figure 6: I/O ratio plotted against time

The several peaks observed are likely due to windows and door openings, happening during the house visits. Globally the filtration leads to I/O values four times lower than those obtained without filtration.

3.4 VMI system contribution to thermal comfort

The VMI water to air heat exchanger described above is supplied with 35 to 45 °C water. Figure 7 shows the outdoor and supplied air temperatures during the heating season.

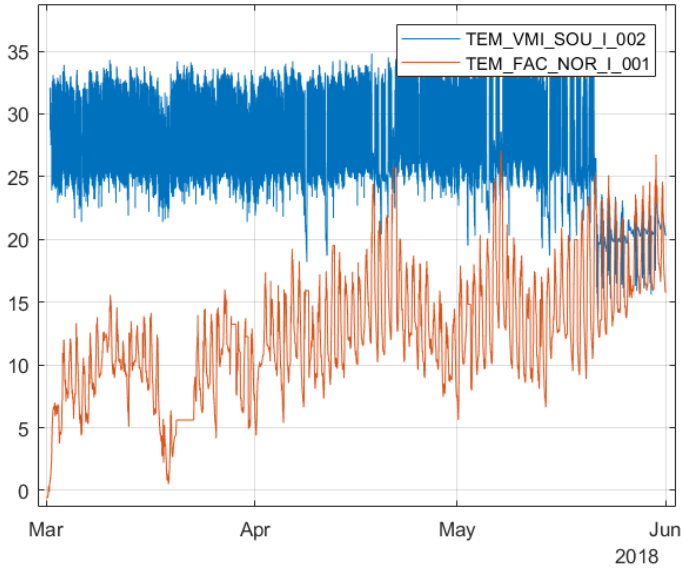

Figure 7: Outdoor and supplied air temperatures during the heating season

The heat exchanger has a significant impact on the gap between outdoor and supplied air temperatures: between 10 °C and 25 °C, participating effectively in the occupants' comfort, regarding their positive feedbacks. From the end of May, the heating is turned off, but the cooling is not activated yet: the VMI heat exchanger is supplied with 20 °C-water (ground temperature). It explains why the supplied air is slightly precooled during the day and slightly preheated at night.

By preheating the supplied air temperature, the VMI contributes to the house heating needs. Figure 8 describes the temporal evolution of thermal power supplied by the ceiling and the VMI.

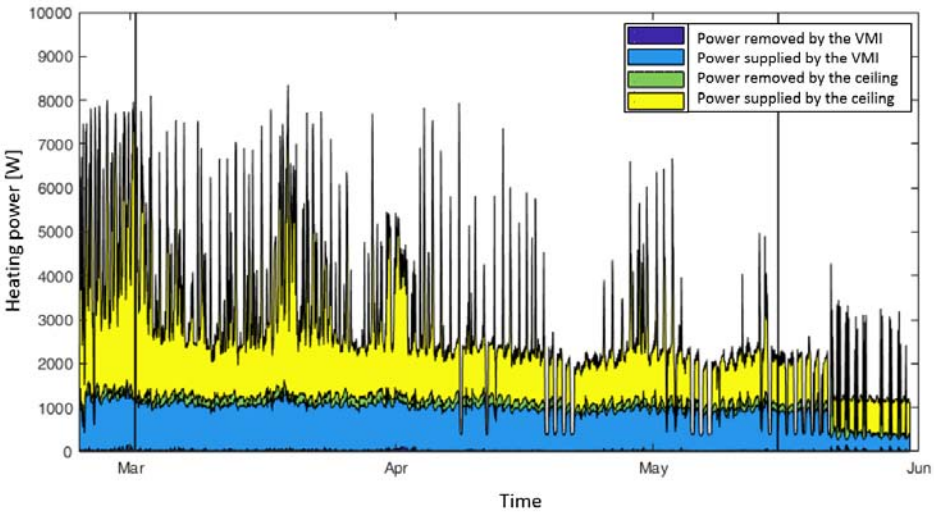

Figure 8: Power supplied by the radiative ceiling and the VMI with its heat exchanger

Thanks to its heat exchanger, the VMI delivers continuously between 1000 and 1500 W. Thus, the VMI covers between 25 % and 40 % of the house's total needs during the heating season, becoming thus a hybrid solution between ventilation and power emitter. The same study is realized during the cooling season. From the end of May, due to the heating switch off, the VMI heating is reduced but is not worth zero: the air keeps being preheated at night. The "passive" cooling mentioned above is not significant enough to be visible on Figure 8.

4 CONCLUSION

A demand-controlled mechanical supply ventilation system called VMI and its water to air heat exchanger are installed in a largely monitored experimental house. The purpose is to determine the system performances in terms of IAQ and power distribution for thermal comfort. IAQ results are reduced to indoor CO_2, absolute humidity and PM 2.5 concentrations analysis. Thermal comfort is reduced to supply air temperature analysis.

The present study highlights the VMI ability to reduce significantly the master room stuffiness: CO_2 concentrations statistical values are worth half the values obtained when the VMI is off or the values obtained in the dwellings studied by (Derbez, et al., 2017).

Moreover, during the same month of winter, it is underlined that VMI allows to keep humidity between 30 and 70 % three quarters of the time in the shower room, despite the natural extraction. The slight overpressure generates enough air renewal in the shower room.

Regarding the fine particles, it is brought to light that the VMI filtration maintains a PM 2.5 concentration below 3 $\mu g/m^3$ 97 % of the time, whereas this threshold is exceeded one quarter of the time when the filter is removed. Furthermore, the I/O ratio is four times higher when the filter is absent.

The study emphasizes the VMI ability to raise the supplied air temperature up to 25 °C compared to the outdoor during winter. As a direct consequence, the VMI participates in the house's heating, covering thus in average one third of the house's total needs.

Therefore, it seems legitimate to consider the VMI as a credible alternative to more traditional systems.

Based on the results presented in this study, industrial partnerships have been created with heat pumps and emitters manufacturers. The purpose is to develop specific regulations optimizing heating and cooling capacities of the VMI. Lastly, the VMI flow rate regulation can be discussed. Prototypes are being developed, involving one or several other sensors in order to comply even more with either, IAQ, thermal comfort and energy consumption.

5 REFERENCES

AFSSET. (2004). *AVIS de l'Agence française de sécurité sanitaire de l'environnement et du travail relatif à la proposition de valeurs guides de l'air intérieur pour les particules Auto-Saisine Afsset* .

ANSES. (23th of may 2017). *ANSES recommends pursuing efforts to improve ambient air quality*. https://www.anses.fr/fr/content/l%E2%80%99anses-recommande-de-poursuivre-les-efforts-pour-am%C3%A9liorer-la-qualit%C3%A9-de-lair-ambiant

Derbez, M., Wyart, G., Le Ponner, E., Ramalho, O., Ribéron, J., & Mandin, C. (2017). Indoor air quality in energy-efficient dwellings: Levels and sources of pollutants. *Wiley*.

Ouvrier-Bonnaz, O., Rahmeh, M., Stephan, L., & Potard, M. (2015). Whole-house air distribution with a supply-only ventilation system VMI® for an optimum air change. *CLIMAMED 2015 Congress Sustainable Energy Performance of Buildings.* Juan Les Pins.

Rahmeh, M. (2014). *Etude expérimentale et numérique des performances de la ventilation mécanique par insufflation : qualité de l'air intérieur dans les bâtiments résidentiels.* La Rochelle: Université de la Rochelle.

Ribéron, J., Ramalho, O., Derbez, M., Berthineau, J., Wyart, G., Kirchner, S., & Mandin, C. (2016). Indice de confinement de l'air intérieur : des écoles aux logements. Air stuffiness index: from schools to dwellings. *Pollution atmosphérique*.

Large-scale performance analysis of a smart residential MEV system based on cloud data

Bavo De Maré[1], Stijn Germonpré[1], Jelle Laverge[3], Frederik Losfeld[1], Ivan Pollet[*1,2] and Steven Vandekerckhove[1,4]

1 Renson Ventilation
Maalbeekstraat 10
Waregem, Belgium

2 Ghent University
Faculty of Bioscience Engineering
Coupure Links 653
Ghent, Belgium
**Corresponding author: ivan.pollet@renson.be*

3 Ghent University
Department of Architecture and Urban Planning
Jozef Plateaustraat 22
Ghent, Belgium

4 KU Leuven
Group W&T, Campus Kulak
Etienne Sabbelaan 53
Kortrijk, Belgium

ABSTRACT

This study is a first large-scale analysis of the performance of a cloud connected and smart residential mechanical extract ventilation (MEV) system based on field data. About 350 units were analysed over a period of 4 months from December 2018 up to March 2019, corresponding with the main winter period in Belgium. Half of the units were installed as a smartzone system which means additional mechanical extraction from habitable rooms as bedrooms.
The air extraction was controlled on different parameters (humidity, CO_2 and VOC) depending on the room type. Indoor climate and IAQ were analysed with respect to design criteria set out in standards as well as fan characteristics and energy consumptions.
Since the ventilation systems are controlled on humidity, periods of RH levels >80% were limited. The typical RH ranges (between 30 and 70% or 25 and 60%) set out in standards for habitable spaces were fulfilled during at least 80% of the time, without causing complaints from the users.
On average, the CO_2 level in bedrooms was <950 ppm during at least 90% of the nighttime. When comparing the MEV with smartzone to literature data of a similar system, the exposure (in ppm.h) to CO_2 >1200 ppm was reduced to 33%, while the ventilation heating energy consumption was 32% lower. This implies a ctrl-factor of 0.26 for the MEV system with smartzone, which is substantially lower than the default values currently used in regulation.
The auxiliary energy consumption of the MEV with smartzone was found to be less than 50% of the literature values reported on similar systems.
The average total yearly energy cost related to the operation of the ventilation system (heating and auxiliary energy) was found to be limited to €100, and at least comparable to the operating cost of a MVHR system. Since rooms are often unoccupied or occupied at a low level, advanced demand control technology proves to have a high potential to limit total energy consumption, while assuring a good IAQ.

KEYWORDS

Smart connected ventilation, demand controlled MEV, large-scale in-situ monitoring, indoor air quality, energy consumption

1 INTRODUCTION

Ventilation is a quite complex process whose quality is affected by many parameters related to the manufacturing, design, installation, use and maintenance of the system over its life cycle. Up to now, the design of ventilation is usually descriptive in its approach and the performance is often theoretically analysed under ideal conditions. As a consequence, some of the aforementioned aspects are not taken into account. Nowadays, IoT devices become also available in the residential ventilation industry, allowing to investigate the real performance of these ventilation units during their lifetime. This study is a first global analysis and part of a large research programme to investigate over time the occurring indoor air quality in the main rooms and the overall fan characteristics of a connected demand controlled central mechanical extract ventilation (DC MEV) unit. In the study mainly the performance of units without air extraction in the bedrooms (no-smartzone) and with air extraction in the bedrooms (smartzone) was compared under Belgian winter conditions.

2 LITERATURE STUDY

During recent years, several ventilation field studies in the residential sector were carried out due to the availability of affordable and/or plug-and-play monitoring apparatus.
Kalamees et al. (2006) described a study where the indoor temperature and humidity conditions in 46 lightweight timber-framed detached houses in Finland were measured and analysed.
In France, Berthin et al. (2007) performed in-situ measurements on humidity controlled ventilation systems in 55 occupied apartments to show the effectiveness of demand controlled ventilation.
Staepels et al. (2013) analysed 70 dwellings in Flanders (Belgium) with respect to their indoor environment quality. CO_2 and humidity measurements showed good to reasonably good indoor air quality, independently from the type of ventilation system.
Mikola and Kõiv (2013) monitored indoor air climate in Estonian apartment buildings equipped with several ventilation systems. The IAQ improved when using more mechanical devices to control the air.
In the Netherlands, van Holsteijn and Li (2014) analysed the CO_2-concentrations and relative humidity levels in individual rooms of 62 houses equipped with different types of ventilation systems within the so-called Monicair project. Form the start, the monitored systems were commissioned in order to comply with the regulation requirements. The exposure to CO_2-concentration above 1200 ppm per person was considered. In the study, the ventilation system C4c is quite similar to the one that is investigated in this study using also mechanical extraction in the bedrooms (smartzone). Furthermore, the energy consumption related to the ventilation system was considered, but partly based on theoretical assumptions of for instance the heat recovery efficiency. The type and the size of the ventilation systems in the Netherlands are comparable to those in Belgium due to a similar ventilation regulation.
Guyot et al. (2017) gave an overview of the state of the art, with respect to residential smart ventilation.
Finally, a preliminary large-scale analysis on the same ventilation system as examined in this study was recently carried out by Lokere (2019). Analysis of a typical day profile of CO_2/humidity/VOC and the probability of ventilation higher than minimum rates, showed small peaks around typical moments which can be linked to human activities as cooking and taking a shower or a bath. Part of the dwellings showed overheating, partly caused by severe insulation requirements and weak overheating risk thresholds in Belgian building regulations. Furthermore, it was found that during the heating period in bedrooms, lower temperature levels

were accepted or preferred than the lower limits of the ATL method. The risk of mould growth as examined with the VTT model (Hukka and Viitanen) was negligible.
Moreover, Lokere (2019) found that CO_2 concentrations in bedrooms and kitchens with direct mechanical extract were respectively about 90% and 95% of the time lower than 1000 ppm during periods of active ventilation, proving the high potential of demand controlled ventilation to guarantee good IAQ. Indoor VOC levels were higher during periods of higher indoor (and outdoor) temperature, probably due to the increase of the VOC volatility with higher temperature.
All above mentioned studies were conducted on a smaller scale and/or treated only part of the elements investigated in this article.

3 METHODOLOGY OF THE VENTILATION SYSTEM ANALYSIS

From 2018 on, commercially available "smart" DC MEV (so-called Healthbox 3.0) systems with cloud connection possibility were installed in Belgian houses and residential buildings (see Fig. 1). The cloud connection, which fits into a global strategy on artificial intelligence and data analytics (Vandekerckhove, 2019), allowed to monitor and analyse the characteristics of a growing number of these smart central exhaust units on a large scale. The mechanical extraction took place locally in the wet rooms and in about half of the dwellings also directly from the bedrooms. The system with bedroom extraction is hence forward called "with smartzone", and without extraction from the bedroom "no smartzone", as illustrated in Figure 1.

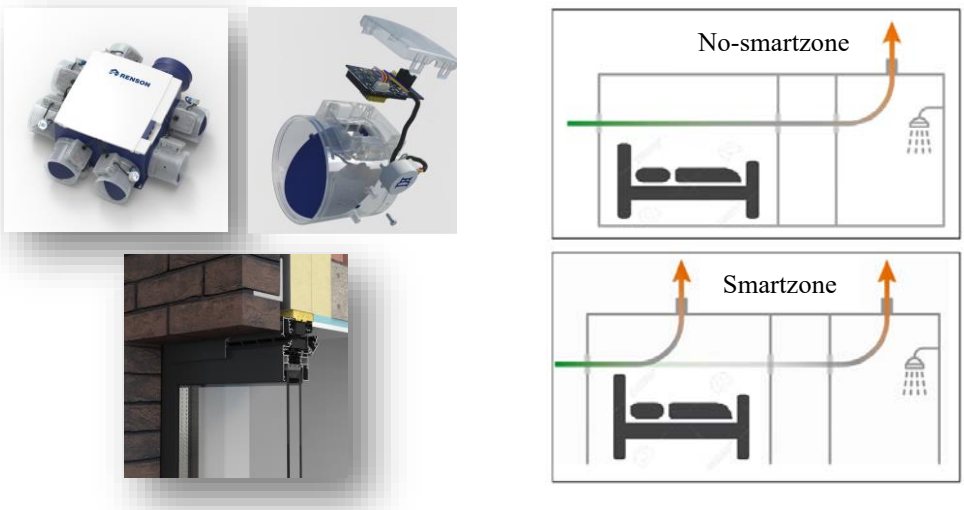

Figure 1: DC MEV system (above-left), passive vents (below-left) and the difference between no-smartzone and smartzone principle (right)

The outdoor air was supplied through passive vents placed on top of the windows in the habitable rooms (Fig. 1). These passive vents are pressure controlled and can additionally be gradually adjusted by the inhabitants between fully open and closed. By means of valves directly attached to the central unit at the end of the extract duct, the air extraction was locally controlled on different parameters depending on the room type: in bathroom and utility room on absolute and relative humidity (AH and RH); in kitchen and bedroom (if extraction available) on CO_2 and in toilets on volatile organic compounds (VOC). Sensors were located at the valves and not within the rooms, which means that sensor values could -to a certain extent- deviate from the room conditions.

The following standard control algorithms were implemented in the system to regulate the extract airflow rate between a minimum and the required airflow capacity of the room according to the Belgian regulations (these nominal flow rates are for open kitchen: 75 m³/h; bathroom, closed kitchen and laundry: 50 m³/h; toilet: 25 m³/h; bedroom: 30 m³/h).

- CO_2: proportional between 800 – 950 ppm CO_2
- Humidity: step function as a function of a gradient $\Delta AH/\Delta t$ and a RH threshold
- VOC: step function as a function of a gradient $\Delta VOC/\Delta t$

Fan characteristics, such as airflow rates were theoretically derived from sensor values and algorithms, while fan pressure was deduced from power input. A fixed value for the auxiliary consumption of the valves and the sensors was added. The accuracy of the measurements were 2.5%, 2% and 5%, for respectively the power input, RH and CO_2.

By means of an application the user could to some extent adjust the control settings if needed or temporarily overrule the automated extraction. Changing of the standard settings by the user or installer was rarely done, since only allowed in existing buildings, while most units were installed in newly built dwellings. A platform also allowed to interact with relevant stakeholders, such as the installer, the building owner or the occupant, allowing to increase the system quality.

The ventilation units were installed without extra commissioning afterwards to correct or improve the performance of the system. Data were not filtered on false values or outliers. However, in some cases, certain values were not recorded. Lokere (2019) analysed a period of 9 months from May 2018 up to January 2019 with an increasing number of monitored devices, while in this study during the typical Belgian heating period from December 2018 up to March 2019 (temperate maritime climate), the performance of a fixed number of about 350 devices divided over no-smartzone and smartzone types was investigated.

The data of the ventilation IoT devices were securely stored in the cloud for further analysis at a frequency of 5 min. Python code was used to retrieve the desired data and for further processing the data into daily average values per unit or per room.

Different characteristics of the climate and the system were analysed: indoor comfort (CO_2, humidity), fan characteristics (average and nominal airflow, time fraction minimal airflow rate, average pressure and power input) and total energy consumption. Design values of RH and CO_2 concentration as especially specified in the standard EN16798-1 (2019) (replaces the EN15251 standard) were used as criteria to analyse the indoor comfort. Comfort analysis of bedrooms on a large-scale could only take place when direct mechanical extraction with sensor control was present (with smartzone), since sensors were located at the extract valves.

For the data analysis, active ventilation was defined as ventilation at flow rates higher than the minimum control values. In general, the active ventilation period shows a time shift compared to the occupancy period due to the buffering effect of air with respect to air components.

In Flanders (northern half of Belgium) where most of the ventilation units were installed, the newly built housing stock is quite evenly distributed over single-family and multi-family dwellings (VEA, 2019). Commercial data also indicated that the share of installed units over single- and multi-family dwellings is about 50/50. However, at that time, the cloud data from the Healthbox 3.0 could not be sorted on single- and multi-family dwellings.

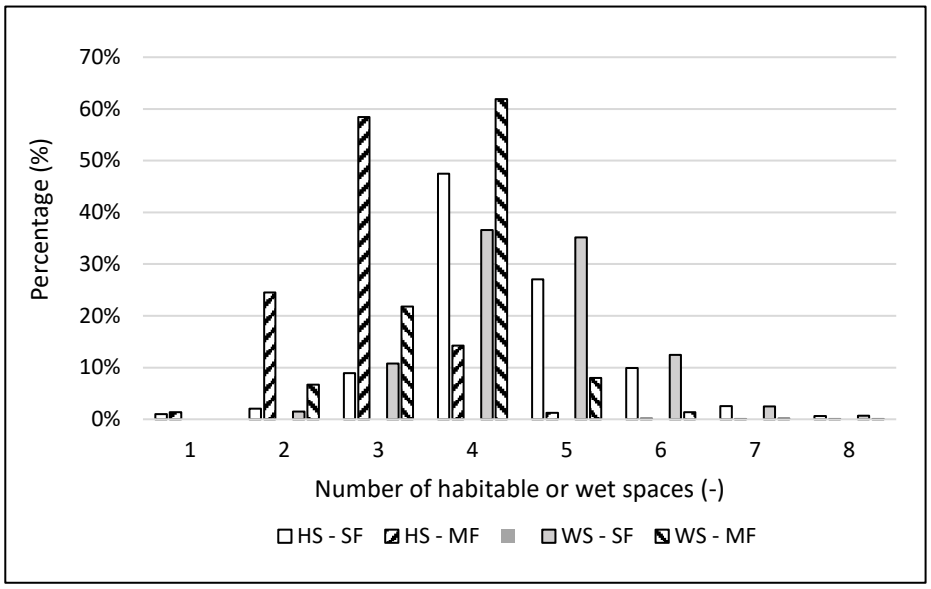

Figure 2: Histogram of the number of habitable (HS) and wet spaces (WS) over the newly built single-family (SF) and multi-family (MF) dwellings in Flanders (VEA, 2019)

Figure 2 shows the distribution of the number of habitable spaces (HS) and wet spaces (WS), including the kitchen over the newly built single-family (SF) and multi-family (MF) dwellings in Flanders. In SF dwellings the number of habitable rooms and wet rooms is quite similar (peaks at 4-5 rooms), whereas in MF dwellings the number of habitable rooms is clearly one unit less compared to the number of wet rooms. Furthermore, MF dwellings contain on average 1.5 habitable room less compared to SF houses.
In Flanders, the kitchen is usually open to the living room, since the share of closed kitchens is at most 5% and 2% in respectively SF and MF newly built houses. In case of an open kitchen, the IAQ in the living room can be controlled by the extraction in the open kitchen, reducing in that way the number of extract valves in the habitable rooms when applying smartzone. Therefore the IAQ in the kitchen is also considered in this study. Based on data of VEA (2019), the average air tightness n_{50} of the studied houses peaked between 1.5 and 2.0 volumes/h.

4 RESULTS

4.1 Indoor climate

Humidity

Figure 3 illustrates the mean time fraction of RH < 80%, 30% < RH < 70% and 25% < RH < 60% in different rooms (kitchen, bathroom, laundry and bedroom) as a function of time. The mean values over this 4 months period are given in Figure 4. In the different rooms considered the RH values higher than 80% were very limited. The lowest occurrence was found in the kitchen, the highest in the bathroom where water vapour productions are usually highest. Lower peaks in the kitchen can be due to a quasi-permanent heating, the mostly open connection with the (dry) living room and the standard availability of a separate cooker hood to extract water vapour. For the several rooms considered, the average time fraction with RH values <80% was at least 97.5%, as found in the bathroom. The RH values above 80% clearly decreased

during the winter period, which can be explained by the decreasing absolute humidity levels outdoors.

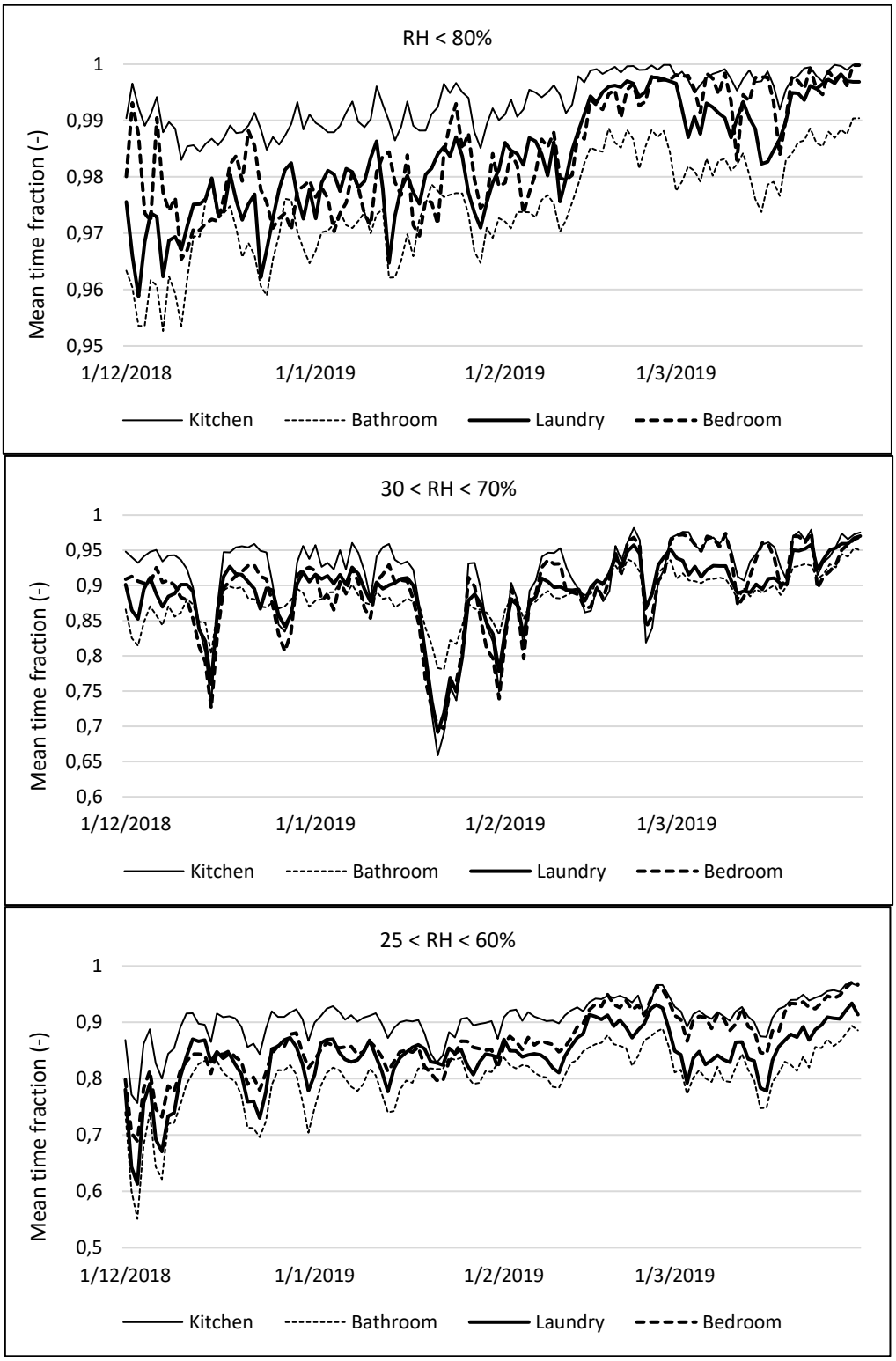

Figure 3: Mean time fraction of RH<80% (above), 30%<RH<70% (middle) and 25%<RH<60% (below) in different rooms over the 4 months period

The time fraction of RH in a certain range, i.e. 30 to 70% or 25 to 60% showed a quite fluctuating trend as a function of time, probably caused by varying outdoor humidity conditions during the winter period. The mean time fraction of RH between 30 to 70% was close to 90%

for the different rooms, with the highest and the lowest time fraction in the kitchen and the bathroom, respectively. This latter logically agrees with the previous findings on RH >80%. When looking to the average time fraction of RH between 25 and 60% in Figure 4, more variation was found between the rooms, with a minimum of 80%. The lowest value was also reported in the bathroom where the highest water vapour productions can be expected. In Figure 3 the range between 25 and 60% RH showed a slightly increasing trend during winter caused by the drying out of the indoor air.

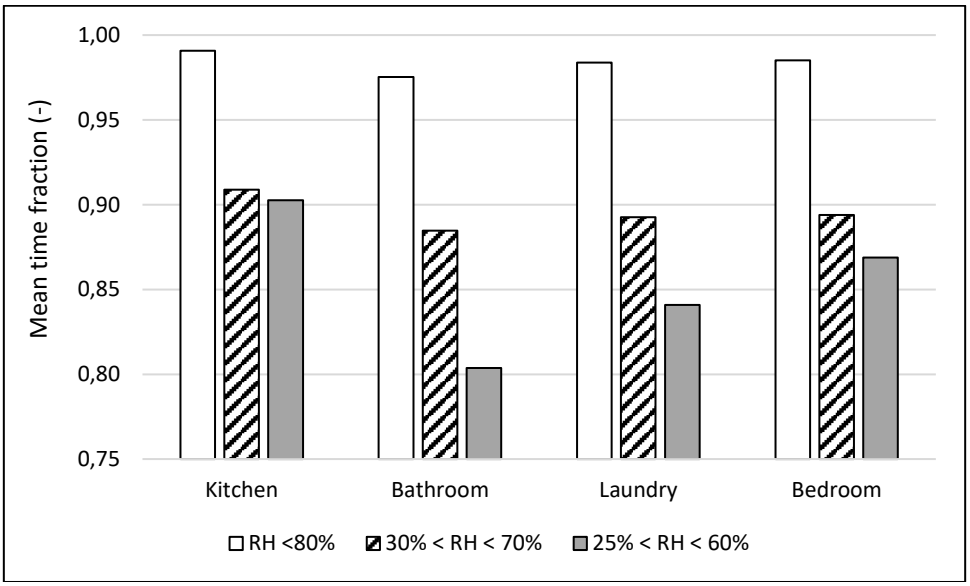

Figure 4: Mean time fraction of RH<80%, 30%<RH<70% and 25%<RH<60% in different rooms

Furthermore, instead of the time fraction, the percentage of rooms in which a certain RH range occurs was analysed in Figure 5. More in particular, the number of rooms was determined in which the RH is permanently (= 99% of the time) lower than respectively 80%, situated between 30 to 70% or between 25 to 60%.

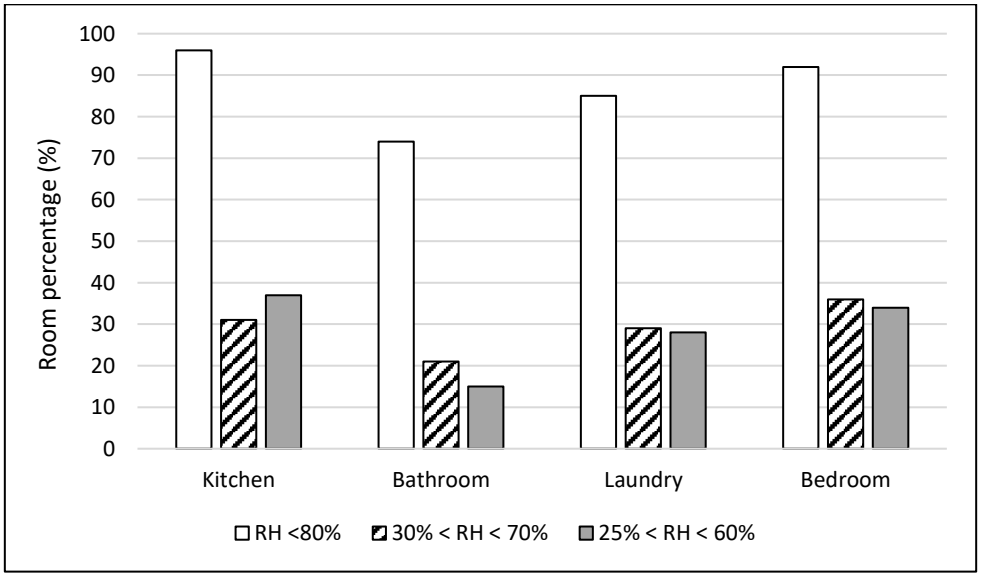

Figure 5: Percentage of rooms in which the RH is permanently (= 99% of the time) lower than respectively 80%, situated between 30 to 70% and between 25 to 60%

Figure 5 points out that in at least 70% of the rooms considered, the RH was permanently lower than 80%. The number of rooms complying permanently to the ranges 30-70% or 25-60% varies between 15 and 40% approximately. A higher percentage of habitable rooms as kitchen and bedrooms instead of wet rooms complied to the RH ranges set out for these kind of rooms, as can be expected. However, the rooms with RH values outside the criteria during part of the time were not cause for complaints from the users. In addition, Lokere (2019) found a negligible risk on mould growth in the different rooms. Newly built houses are well insulated without thermal bridges to prevent condensation. Further research will focus on the elements giving rise to higher humidity especially in living rooms. Besides, it must be kept in mind that in contrast to the absolute humidity, possible temperature fluctuations of the air in the extract duct caused by heat losses or gains between the room and the sensor location (at the box) can influence the measured RH compared to the real room value, which magnitude must be further investigated in the ongoing research.

CO_2 concentration

The IAQ was analysed based on CO_2 categories defined in the EN16798-1 standard for habitable rooms as (mainly open) kitchen and bedroom, as illustrated in Fig. 6. Data for the kitchen were derived as an average from systems without and with smartzone, whereas bedroom results concerned only smartzone systems. The data were selected on 2 different bases: day or night time and during active ventilation (when airflow rate in the room is higher than minimum, corresponding best with the unknown occupancy period). Substantial differences occur between these selections. In the bedroom, the CO_2 levels belong 80 to 90% of the nighttime to category 1 or 2 (< 950 ppm), with a main fraction in category 1 (< 800 ppm). In 90% of the bedrooms with extraction, the CO_2 level was <1200 ppm during at least 95% of the nighttime. When considering only active ventilation (during occupancy) this percentage varied between 70 and 80%, with a dominant group in category 2 and only about 20% in category 1. Comparing the results during nighttime and active ventilation points at that approximately half of the night, ventilation is at its minimum flow rate (< 800 ppm) due to no occupancy, low occupancy and deep sleep with CO_2 levels lower than 800 ppm. When considering the total daytime instead of the nighttime, the smartzone system also worked on its minimum flow rate during half of the time (see Fig. 8).

The relatively high time fraction of category 1 (about 20% < 800 ppm CO_2) during active ventilation is related to different elements such as:

- aggregation of the data: CO_2 as an average and active ventilation as a single value over 5 min
- setpoint set lower than 800 ppm
- temporarily override of the demand control
- several bedrooms which are connected to 1 common valve, instead of separately.

For bedrooms, the mean time fraction with CO_2 levels in category 3 (moderate IAQ < 1350 ppm) and 4 (bad IAQ > 1350 ppm) were limited to respectively 30% and 5% of the time during active ventilation. This means that the extract capacity of 30 m³/h in bedrooms can be considered as a minimum design value. Van Holsteijn and Li (2014) reported in the Monicair study similar results with a fraction of at most 1 hr or 10% of the night time that CO_2 concentrations were higher than 1200 ppm.

The IAQ in the kitchen was analysed during daytime and active ventilation based on the CO_2 categories as illustrated on the right part of Fig. 6. The IAQ belongs nearly permanently to category 1 and 2 (< 1200 ppm). The difference with the findings in the bedroom can be

explained by the shorter occupancy period, the larger room volume of the open kitchen, the presence of a cooker hood and the CO_2 categories according to the EN16798-1 that are less severe in kitchens than in bedrooms. During active ventilation the time percentages with CO_2 levels lower than 800 ppm and between 800-950 ppm were slightly higher than in the bedroom, due to less severe conditions in the kitchen.

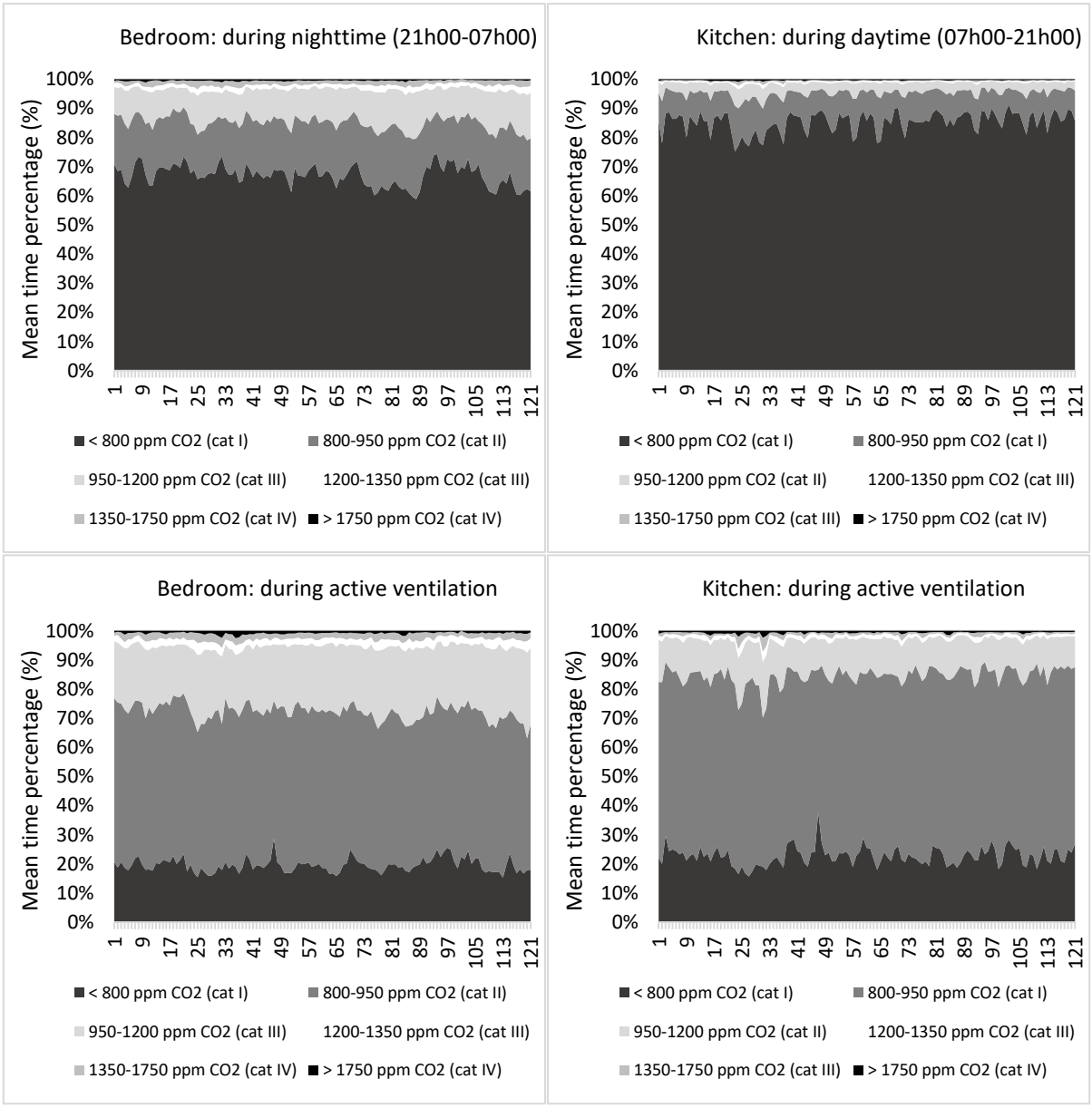

Figure 6: Mean daily time percentage of CO_2-categories according to the EN16798-1 standard for bedroom (left) and open kitchen (right) during day or nighttime (above) and during active ventilation (below)

When looking over the wintertime period a constant trend containing some fluctuations was observed, which can be caused by user behaviour (difference between week and weekend days) and wind conditions.

Furthermore, the exposure to CO_2 expressed as the cumulative CO_2-concentration above 1200 ppm (in ppmh) was calculated, since this is a commonly used parameter in IAQ research. The average daily exposure over the dwellings was 245 ppmh/day which is only 33% of the

733 ppmh/day reported by van Holsteijn and Li (2014). This big difference can be explained by the lower control setpoint of 950 ppm instead of 1200 ppm.
Since large-scale data of the IAQ in bedrooms without direct extraction is not available, some dwellings without smartzone were monitored separately. It was found that many elements have an impact on the IAQ in the bedrooms, such as size of the supply opening, position of the door, occupancy level and wind direction. As a consequence, CO_2 levels can vary between very good (< 1000 ppm) and very bad (> 2000 ppm). In general, omitting direct extraction from the bedroom gave rise to maximum CO_2 level in the parent bedroom belonging to category 4 (> 1350 ppm).

Temperature

The average daily mean temperature measured by all the units without and with smartzone is plotted as a function of the running mean outdoor temperature $T_{e,ref}$ (source: Belgian RMI) in Figure 7. $T_{e,ref,i}$ on day i is defined as $T_{e,i} + 0.8T_{e,i-1} + 0.4T_{e,i-2} + 0.2T_{e,i-3}$. The mean indoor temperature was about 21°C with a clear spread between 15 and 25°C, showing that in some rooms as bedrooms lower air temperatures are accepted. More detailed results on instantaneous temperatures instead of daily mean values can be found in Lokere (2019). As explained before, profound research is needed on the heat exchange between ducts and indoors to come to conclusions.

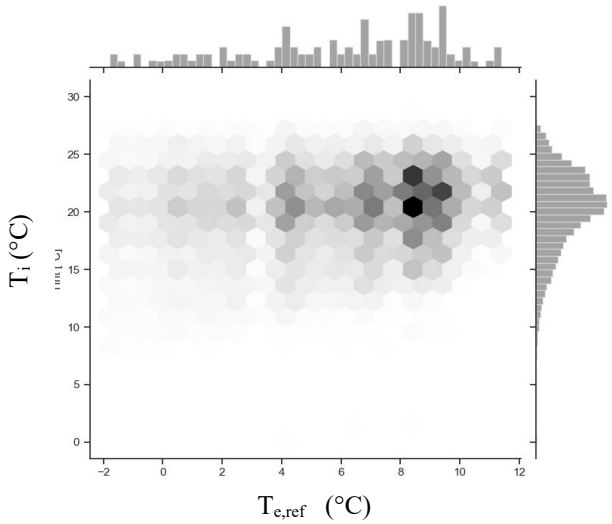

Figure 7: Distribution of the daily mean indoor temperature of all the rooms measured (without and with smartzone) plotted as a function of the running mean outdoor temperature

4.2 Fan characteristics and energy consumption

The fan characteristics and the energy consumption were analysed by comparing no-smartzone and smartzone systems. The average values over the 4 months period of several parameters of the connected units were set out as a box plot in Figure 8 to 10 (daily average in case of time fraction of minimal flow rate MF).

When analysing the time fraction of minimum airflow rate MF over the entire box (= none of the valves is activated), the daily average time fraction is about 75 and 50% for the no-smartzone and smartzone system. The high fractions of both systems proved already the huge potential of demand controlled ventilation to save energy. When comparing no-smartzone with smartzone systems, on average 25% of the time or 6 hours/day, the smartzone system is activated in at least one of the bedrooms to guarantee IAQ. The spread in time fraction is quite

large indicating that substantial differences occur over time and between the units. The relation of this MF time fraction with the period of non-occupancy could be further investigated.

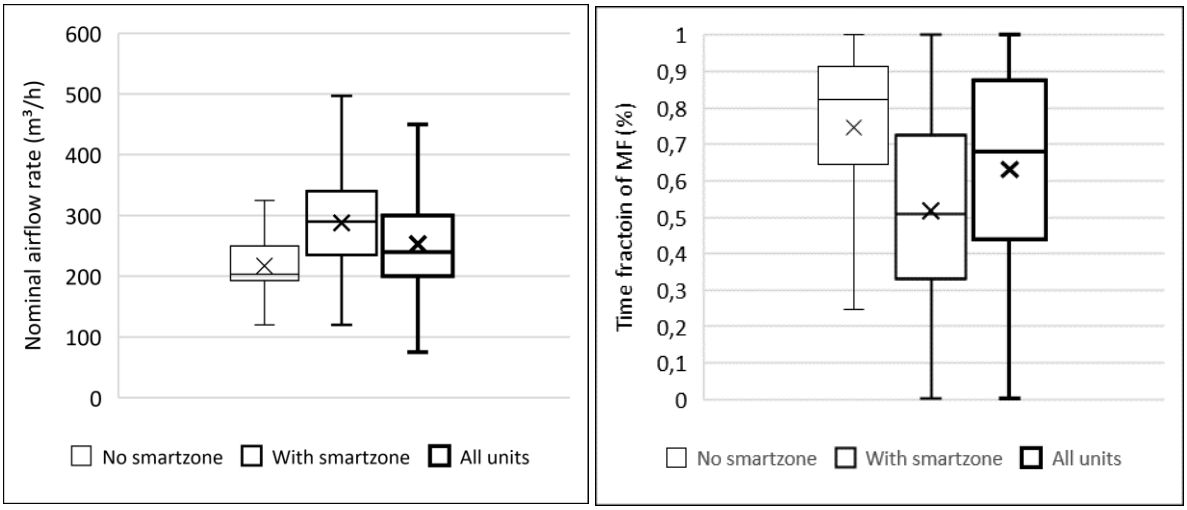

Figure 8: Nominal airflow rate (left) and the average time fraction of minimal ventilation MF (right) of the units

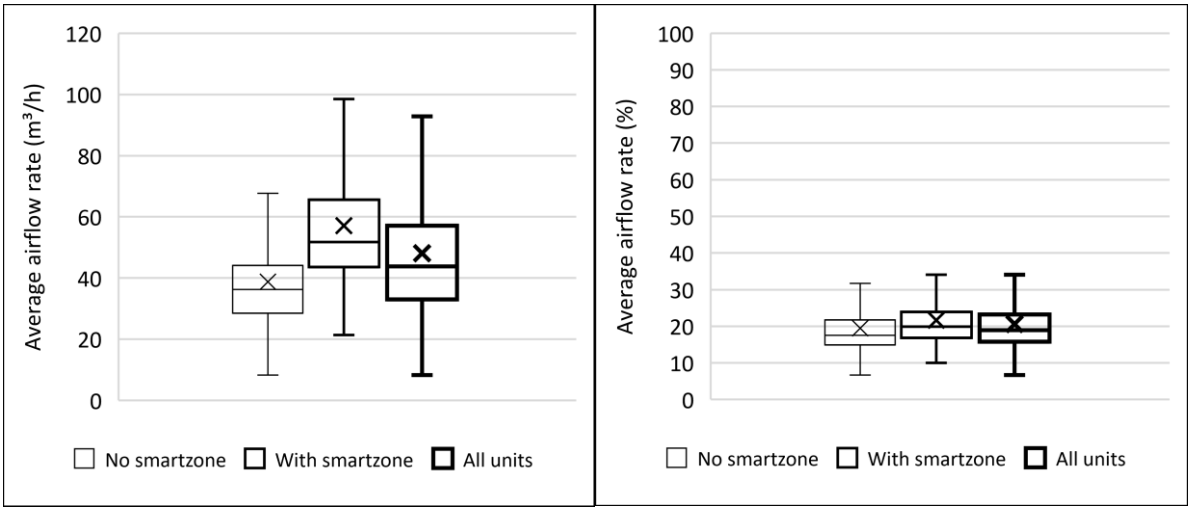

Figure 9: Average airflow rate of the units expressed as "m³/h" (left) and "%" (right)

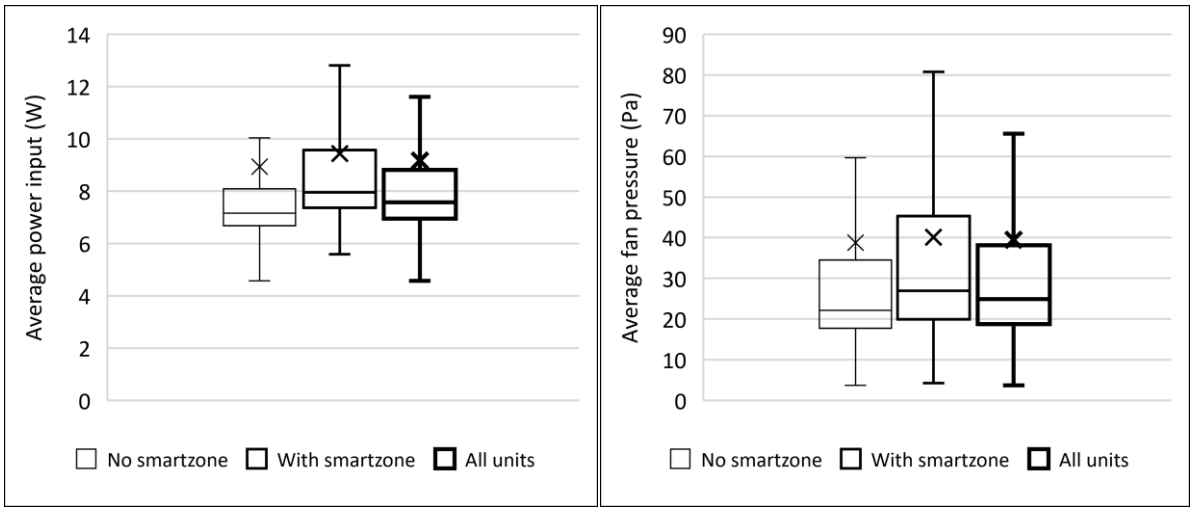

Figure 10: Average power input (left) and average fan pressure of the units (right)

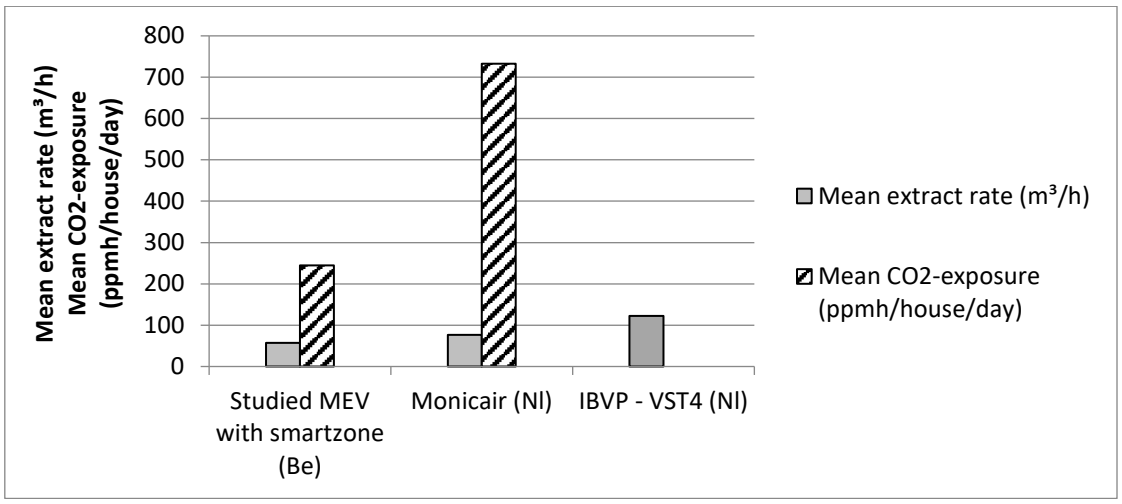

Figure 11: Mean extract rate (m³/h) and mean CO_2-exposure (ppmh/house/day) > 1200 ppm compared to literature values

The average extract airflow rate of 57.1 m³/h of the smartzone systems was about 50% higher than the value of 38.8 m³/h for no-smartzone systems, however, the IAQ realised with the smartzone system was also better. This was clearly due to the higher installed nominal airflow capacity via the additional extraction points and the higher mean ventilation levels in bedrooms than in wet rooms.
The mean nominal airflow rate (= ventilation capacity) of 288 m³/h of smartzone systems was on average about 32% higher than the value of 218 m³/h of no-smartzone systems.

Compared to the study of van Holsteijn and Li (2014) and Valk et al. (2019) who found an average extract rate of 76.9 m³/h for a similar ventilation system with smartzone (C4c), the cloud data average extract rate is 26% lower. This is quite remarkable since the MEV system studied controlled the air on a lower setpoint of 950 ppm instead of 1200 ppm in the habitable rooms. Nominal airflow rates of both ventilation systems were also comparable. Furthermore the IBVP tool of Valk et al. (2019), which should form the basis for the new ventilation performance standard NEN1087 in the Netherlands, suggests an average air exchange rate (AER) of 122 m³/h for a similar so-called VST4 system. This latter IBVP value is more than twice the average airflow rate monitored in real circumstances. Figure 11 illustrates the low average airflow rate and the low CO_2-exposure when applying the studied MEV system with smartzone compared to literature values.

The airflow rate expressed as a fraction of the installed nominal capacity, the so-called reduction or ctrl-factor was about 0.20 in case of smartzone systems. Usually, the ctrl-factor is expressed to the nominal airflow rate of systems with no smartzone. In that case the ctrl-factor of the smartzone systems becomes 0.26. In the Belgian (EPB), Dutch (NTA8800) and European (EN13142) regulation, the default ctrl-factor for MEV systems with local control and detection in all rooms is substantially higher with values of 0.43, 0.55 and 0.50, respectively. In case of the no-smartzone system, the ctrl-factor cannot be determined since the assumption of equal IAQ is not guaranteed for the bedrooms under the monitored airflow rates.

When looking at all the boxes, the mean operating pressure of the fan was respectively 38.9 and 40.1 Pa for the no-smartzone and smartzone systems (maximum pressure level of the unit is 350 Pa). Median pressure values, however, were substantially lower. Also the average power input of no-smartzone and smartzone systems was quite similar with values of 9.0 and 9.4 W, respectively, including the power consumption due to electronics and sensors (maximum power

input of the unit is 85 W at 400 m³/h and 200 Pa). These average values were about 1.5 W higher than the median values, pointing out that the design or installation of some units was not optimal, giving rise to higher mean electricity consumptions. The small difference between no-smartzone and smartzone systems was realized by means of smart fan and valve control. The required auxiliary energy per unit of airflow rate of the unit, the so-called specific power index SPI as defined in the standard EN13142, was equal to nearly 0.23 and 0.16 Wh/m³ for the no-smartzone and smartzone respectively.

Extrapolating the average power input to an entire year, resulted in a yearly auxiliary consumption of the extract system of about 79 kWh and 82 kWh for no-smartzone and smartzone systems, corresponding to a total electricity cost of about €20 in case of an electricity price of 0.25 €/kWh. Van Holsteijn and Li (2014) and Derycke et al. (2018) found an electricity consumption of more than twice that high for similar systems with also extraction from the habitable rooms, i.e. 187 and 186 kWh, respectively. The substantial lower energy consumption in this study is due to a recent optimisation of the MEV system at the hardware- and software-level and probably due to a lower overall occupancy level and a larger dataset.
The C4a system without smartzone and without local control in the wet rooms, as investigated by van Holsteijn and Li (2014) and Valk et al. (2019), showed a lower yearly auxiliary consumption of 50 kWh and a higher average airflow rate of 95 m³/h compared to the no-smartzone system investigated. The CO_2-exposures in case of C4a, however, were considerably higher.

The average ventilation heat losses could be estimated based on a mean measured indoor air temperature of 21°C, a mean outdoor temperature of 6°C over a 6 months heating period from November up to April in Belgium and a 85% efficiency of the heating system, approaching 5350 MJ for a smartzone system. These ventilation heating losses are 32% lower than the value of 7874 MJ reported by van Holsteijn and Li (2014) for a similar heating season. Assuming a gas price of 0.05 €/kWh, the yearly average heating cost for ventilation with the smartzone MEV system is about €75.
It can be stated that in many cases the total yearly energy cost related to the operation of the smartzone ventilation system (heating and auxiliary energy) will be limited to €100.

Within the Ecodesign framework and its requirement to provide consumers with accurate information regarding energy consumption, it is relevant to compare the smartzone MEV-results with a MVHR system. Ecodesign and its labelling scheme must allow consumers to identify how energy efficient a product actually is and to assess a product's potential to reduce energy costs. In order to make this comparison, the following assumptions were made for the balanced MVHR system:

- The real average airflow rate is 125 m²/h which equals half of the mean nominal airflow rate system of 250 m³/h over all the units (cf. Fig. 8).
- This average airflow rate, which varies between a minimum and a maximum value, is assumed to assure an adequate IAQ in case of no zone controlled systems.
- The overall efficiency of the heat recovery unit in-situ is 60% taking into account real circumstances such as leakages, defrosting, unbalance, pollution, usability of recovered heat, … This lower recovery efficiency in practice compared with laboratory measurements is justified by studies as Merzkirch et al. (2015), Faes et al. (2017) and Knoll et al. (2018).

Under these assumptions the ventilation heat losses are about 4700 MJ or nearly 12% lower than the MEV system with smartzone. The similar heat losses of both the MVHR and the smartzone system are comprehensible since the mean ctrl-factor of 0.26 of the MEV system corresponds with a virtual heat saving efficiency of 74%. Besides, the real electricity

consumption of a MVHR system will be at least 4 times higher due to the presence of 2 fans and the much higher pressure losses in the unit caused by filtering and heat recovery (Derycke et al., 2018). As a consequence, since electricity is at least 3 to 4 times more expensive than gas, the mean yearly energy cost of a MVHR system will not be lower than that of the MEV with smartzone.

5 CONCLUSIONS

This study is a first large-scale analysis (350 units) of the performance of a smart residential and cloud connected mechanical extract ventilation (MEV) system based on field data in Belgium during the winter period. Half of the units were equipped with the smartzone option which consists of additional CO_2-controlled extraction in the habitable rooms next to the wet rooms.

The above analysis on air humidity showed that big data can be expressed in several ways to come to conclusions. The indoor climate of a kitchen, which is a so-called wet room, is not substantially more humid than a bedroom as dry room, due to the presence of a cooker hood, the always open connection of the kitchen to the living room and the quasi continuous comfort temperature. The bathroom had the most humid indoor climate, however a limited time period or number of rooms with a RH > 80% was found. RH ranges for habitable rooms as set out in standards seem quite severe to fulfil permanently, as also found in other studies.

The period over which the CO_2 concentration is analysed is quite crucial when analysing the time fractions of different CO_2 categories, since occupancy is not known. In bedrooms with smartzone, ventilation is at its minimum flow rate approximately half of the night due to no occupancy, low occupancy or deep sleep with CO_2 levels lower than 800 ppm. On average, the CO_2 level in bedrooms was <950 ppm during at least 90% of the nighttime. Compared to literature data with smartzone technology, the exposure to CO_2 on the one hand and the ventilation heating energy consumption on the other hand was respectively 67% and 32% lower. The CO_2-exposure when not applying extraction in the bedroom was clearly higher. The ctrl-factor of the MEV system with smartzone of 0.26 was substantial lower than default values used in regulation.

The electricity consumption of the MEV system with smartzone was found to be less than 50% of the reported literature values. It could be stated that in many cases the total yearly energy cost related to the operation of the ventilation system (heating and auxiliary energy) will be limited to €100.

Since rooms are often unoccupied or occupied at a low level, advanced local demand control is highly energy-efficient. Due to technological and digital evolutions MEV systems with smartzone combined with natural supply (also called VST4) are able to guarantee IAQ in every room and perform energetically equally or better than MVHR systems in countries with a mean winter temperature not lower than freezing point.

In further research the huge amount of data will be explored by focusing -among others- on the behaviour of the system under summer conditions, on the possible deviation between measured sensor values and room conditions and the reasons of suboptimal performance of some units.

6 REFERENCES

- Berthin, S., Savin, L. and Jardinier, M. (2007). Measurements on humidity controlled ventilation systems in 55 occupied apartments. 21 p.
- Derycke, E., Bracke, W., Laverge, J. and Janssens, A. (2018). Energy performance of demand controlled mechanical extract ventilation systems vs mechanical ventilation systems with heat recovery in operational conditions : Results of 12 months in situ-measurements at Kortrijk ECO-Life community. Proceedings 39th AIVC Conference, Antibes (France), 18-19 September 2018, 838-847.
- Faes, W., Monteyne, H., Depaepe, M. and Laverge, J. (2017). A 'use factor' for HRV in intermittently heated dwellings. Proceedings 38th AIVC conference, Nottingham (UK), 13-14 September 2017, 337-341.
- Guyot, G., Sherman, M., Walker, I. and Clark, J. (2017). Residential smart ventilation: a review. LBNL 2001056, 88 p.
- Himpe, E., Van de Putte, S., Laverge, J. and Janssens, A. (2015). Operational performance of passive multi-family buildings: commissioning with regard to ventilation and indoor climate. 6° IBPC conference, 78(2983-2988).
- Kalamees, A., Kurnitski, J. and Vinha, J. (2006). Indoor temperature, humidity, and moisture production in lightweight timber-framed detached houses. Journal of Building Physics, 29(3).
- Knoll, B., Borsboom, W. and Jacobs, P. (2018). Improving the usability and performance of heat recovery ventilation systems in practice. Proceedings 39th AIVC Conference, Antibes (France), 18-19 September 2018, 833-837.
- Lokere, L. (2019). Big data in demand controlled ventilation: comparison of measured data with literature. Master dissertation, 120 p.
- Merzkirch, A., Maas, S., Scholzen, F. and Waldmann, D. (2015). Primary energy used in centralized and decentralized ventilation systems measured in field tests in residential buildings. Proceedings 36th AIVC Conference, Madrid, 23-24 September 2015, 197-203.
- Mikola, A. and Kõiv, T. (2013). Indoor Climate Problems in Apartment and School Buildings Conference paper https://www.researchgate.net/publication/243055654.
- Staepels, L., Verbeeck, G., Roels, S., Van Gelder, L. and Bauwens, G. (2013). Evaluation of Indoor Climate in Low Energy Houses. Symposium on Simulation for Architecture and Urban Design, 7-10 April 2013, San Diego, USA.
- Valk, H., van Holsteijn, R. and Hofman, M. (2019). Indicatieve beoordelingsmethode systeemprestatie ventilatie voor individuele woningen IBVP. Toelichting, onderbouwing en validatie bij Ontw. NEN1087:2019, 33 p.
- Vandekerckhove, S. (2019). Getting started with AI for product leadership. Future Summits, Antwerp, 15 May 2019, https://www.vdks.be/pub/aiflanders2019.pdf.
- van Holsteijn, R. and Li, W. (2014). Monicair: MONItoring & Control of Air quality in Individual Rooms. Eindrapport WP1a, 98 p.
- VEA (2019). Buildings characteristics of EPBD conform dwellings over the period 2010-2015.

Individualised Dynamic Model-Based Monitoring of Occupant's Thermal Comfort for Adaptive HVAC Controlling

Ali Youssef[1], Nicolás Caballero[2], Jean-Marie Aerts[*3]

1 M3-BIORES, KU Leuven
Kasteelpark Arenberg 30 bus 2456
3001 Heverlee, Belgium

2 M3-BIORES, KU Leuven
Kasteelpark Arenberg 30 bus 2456
3001 Heverlee, Belgium

3 M3-BIORES, KU Leuven
Kasteelpark Arenberg 30 bus 2456
3001 Heverlee, Belgium
**Corresponding author: jean-marie.aerts@kuleuven.be*

ABSTRACT

Thermal comfort and sensation are important aspects of the building design and indoor climate control as modern man spends most of the day indoors. Conventional indoor climate design and control approaches are based on static thermal comfort/sensation models that views the building occupants as passive recipients of their thermal environment. Assuming that people have relatively constant range of biological comfort requirements, and that the indoor environmental variables should be controlled to conform to that constant range. The (r)evolution in modern sensing and computing technologies (price, compact size, flexibility and stretchability) is making it possible to continuously measure signals in real-time from human body using wearable technologies and smart clothing. Many advanced and accurate mechanistic thermoregulation models, such as the 'Fiala thermal Physiology and Comfort' model, are developed to assess the thermal strains and comfort status of humans. However, the most reliable mechanistic models are too complex to be implemented in real-time for monitoring and control applications. Additionally, such models are using not-easily or invasively measured variables (e.g., core temperatures and metabolic rate), which are often not practical and undesirable measurements for monitoring during varied activities over prolonged periods. The main goal of this paper is to develop dynamic model-based monitoring system of the occupant's thermal state and their thermoregulation responses under two different activity levels. In total, 25 test subjects were subjected to three different environmental temperatures, namely 5°C (cold), 20 °C (moderate) and 37 °C (hot) at two different activity levels (at rest and cycling). Metabolic rate, heart rate, average skin temperature, skin heat flux and aural temperature are measured continuously during the course of the experiments. The results have shown that a reduced-ordered (second-order) MISO-DTF including three input variables (wearables), namely, aural temperature, heart rate, and average skin heat flux, is best to estimate the individual's metabolic rate (non-wearable) with average mean-absolute-percentage-error of 8.7%. A general classification model based on least-squares-support-vector-machine (LS-SVM) technique is developed to predict the individual's thermal sensation. For a 7-classes classification problem, the results have shown that the overall model accuracy of the developed classifier is 76% with a F1-score value of 84%.The developed thermal-state prediction model is promising to estimate the occupant's thermal sensation/comfort status in real-time for better demand controlled HVAC systems.

KEYWORDS

Thermal sensation, thermal comfort, machine learning, HVAC, adaptive controlling

1 INTRODUCTION

Thermal comfort (TC) is an ergonomic aspect determining the satisfaction about the surrounding environment and is defined as 'that condition of mind which expresses satisfaction with the thermal environment and is assessed by subjective evaluation' (ASHRAE, 2004). The effect of thermal environments on occupants might also be assessed in terms of thermal

sensation (TS), which can be defined as ‘a conscious feeling commonly graded into the categories cold, cool, slightly cool, neutral, slightly warm, warm, and hot’ (ASHRAE, 2004). Thermal sensation and thermal comfort are both subjective judgements, however, thermal sensation is related to the perception of one’s thermal state, and thermal comfort to the evaluation of this perception (ISO-10551, 1995). The assessment of thermal sensation has been regarded as more reliable and as such is often used to estimate thermal comfort (Koelblen et al., 2017).

Human thermal sensation is mainly depends on the human body temperature (core body temperature), which is a function of sets of comfort factors (Enescu, 2019; Parsons, 2014). These comfort factors are including indoor environmental factors, namely mean air temperature around the body, relative air velocity around the body, humidity, and mean radiant temperature to the body (Parsons, 2014). Additionally, some personal (individual-related) factors, namely, metabolic rate or internal heat production in the body, which vary with the activity level and clothing thermos-physical properties (such as clothing insulation and vapour clothing resistance), are included. It should be mentioned that the individual thermal perception is deepening, as well, on psychological factors include naturalness (an environment where the people tolerate wide changes of the physical environment), expectations and short/long-term experience, which directly affect individuals’ perceptions, time of exposure, perceived control, and environmental stimulation (Nikolopoulou and Steemers, 2003). The most considered way to have an accurate assessment of TS is to ask the individuals directly about their thermal sensation perception (Enescu, 2019; Parsons, 2014). Thermal sensation mathematical models have been developed in order to overcome the difficulties of direct enquiry of subjects. The development of such models is mostly depending on statistical approaches that by correlating experimental conditions (i.e., environmental and person-related variables) data to thermal sensation votes obtained from human subjects (Koelblen et al., 2017; Parsons, 2014). Most of these models (e.g., PMV) are static in the sense that they predict the average vote of a large group of people based on the seven-point thermal sensation scale, instead of individual thermal comfort, they only describes the overall thermal sensation of multiple occupants in a shared thermal environment. To overcome the disadvantages of static models, adaptive thermal comfort models aims to provide insights in increasing opportunities for personal and responsive control, thermal comfort enhancement, energy consumption reduction and climatically responsive and environmentally responsible building design (De Dear and Brager, 1998; Lu et al., 2019). The idea behind adaptive model is that occupants and individuals are no longer regarded as passive recipients of the thermal environment but rather, play an active role in creating their own thermal preferences (De Dear and Brager, 1998). Besides regression analysis, thermal sensation prediction can also be seen as a classification problem where various classification algorithms can be implemented (Lu et al., 2019). Recently, number of research work (e.g., Chaudhuri et al. 2017; Dai et al. 2017; Farhan et al. 2015; Huang, Yang, and Newman 2015; Kim et al. 2018) have demonstrated the possibility of using machine learning techniques, such as support vector machine (SVM), to assess and predict human thermal sensation. It can be concluded based on the published work (see the recent literature review by Lu et al., 2019) that classification-based models have performed so well as regression models.

Current HVAC control systems can be divided into two types: air temperature regulator (ATR) and thermal comfort regulator (TCR). Most TCR controllers use static models, mainly PMV, as a performance criterion.

This paper is aiming to develop an individualised and adaptive model for monitoring occupant’s thermal sensation based on easily measured variables that suitable for adaptive demand controlled HVAC.

2 MATERIALS AND METHODS

2.1 Experiments and experimental setup

- *Climate chambers (Body & Mind Room)*

The "*Body & Mind Room*" is consisting of three climate-controlled chambers (A, B and C) designed and built to investigate the dynamic mental and physiological responses of humans to specific indoor climate conditions. The Body & Mind Rooms are experimental facilities at the M3-BIORES laboratory (Animal and Human Health Engineering Division, KU Leuven). The three rooms are dimensionally identical; however, each room is designed to provide different ranges of climate conditions as shown in Table 1.

Table 1.The different temperature and relative humidity ranges that can be provided by the different Body & Mind (A, B and C).

Room	Air temperature range (°C)	Relative humidity range (%)
A	+23 - +37	50 - 80
B	+10 - +25	50 - 80
C	-5 - +10	40 - 60

The three rooms are equipped with axial fans to simulate wind velocities between 2.5 and 50 $km.h^{-1}$.

- *Experimental protocol*

The experimental protocol used in the present study is designed in such way to investigate the subjects' thermal and physiological responses to predefined three different temperature (*low*, *normal* and *high*) that under two levels of physical activities (*low* and *high*). The three predefined temperatures (*low* = 5°C, *normal* = 24°C and *high* = 37°C) are chosen based on the *thermal-comfort-chart* of the ASHRAE-55 (2017) and the effects on health according to the Wind Chill Chart for cold exposure (National Weather Service of the US) and for hot temperatures exposure according to (Dewhirst et al., 2003). The conducted experiments are consisted of two phases (Figure 1, upper graph), namely, low activity and high activity phases. During the first experimental phase, low activity phase, the test subjects (while being seated = low activity) are exposed, during 55 minutes, to three levels of temperatures in the following order: normal, low, high and normal again (Figure 1). During the high activity phase, the test subjects is exposed to a 15 minutes of light physical stress (80W of cycling on a fastened racing bicycle). During the course (75 minutes) of the active phase, each test subject is exposed to the predefined three temperature levels (Figure 1, lower graph). During each temperature level, starting from the normal level (24 °C), the test subjects are performed 15 minutes of cycling (with 80 W power) and followed 4 minutes of resting (seated). During the course of conducted experiments, the clothing insulation factor (Col) is kept constant at $Col = 0.34$, which accounts for a cotton short and t-shirt as a standard clothing for all test subjects. The experimental protocol is approved| by the SMEC (Sociaal-Maatschappelijke Ethische Comissie), on the 16th of January with number G-2018 12 1464.

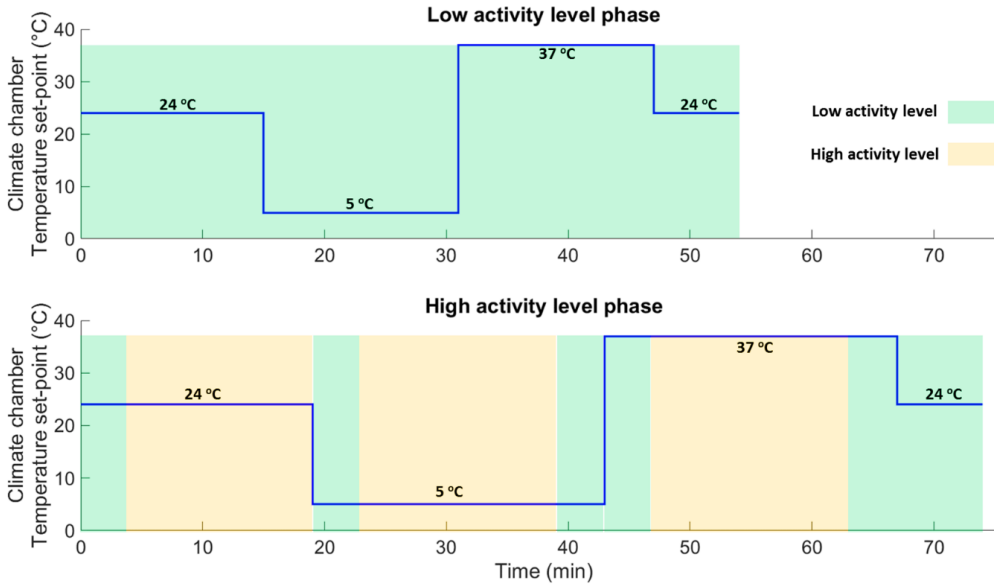

Figure 1. Plots showing the climate chambers' set-point temperatures programed during the 55 minutes low activity phase (upper graph) and the 75 minutes high activity phase (lower graph).

- *Test subjects*

In total 25 healthy participants (6 females and 19 males), between the age of 25 and 35 (average age 26 ±4.2) years, with average weight and height of 70.90 (±12.70) kg and 1.74 (±0.10) m, respectively, are volunteered to perform the aforementioned experimental protocol.

- *Measurements and gold standards*

During the course of the experiments, participants' heart rate, metabolic rate, average skin temperature, heat flux between the skin and the ambient air, core body temperature represented by the aural temperature are measured continuously. The heart rate monitoring is performed using the Polar H7 ECG strap that is placed under the chest, with a sampling frequency of 128 Hz. The metabolic rate of each test subject is calculated based on indirect calorimetry using MetaMAX 3B spiroergometer sensor. The average skin temperature is calculated based on measurements from three body-placed, namely, scapula, chest and arm (Figure 2). The skin temperature measurements are performed using one Shimmer temperature sensor and two gSKIN® bodyTEMP patches. Two heat flux gSKIN® patches are placed on both the chest and the left arm (Figure 2. The skin temperatures and heat flux measurements are acquired at sampling frequency of 1 Hz. Core body temperature is estimated based on aural temperature measure measurements, which is performed using in-ear wireless (Bluetooth) temperature sensor (Cosinuss One) with a sampling rate if 1Hz. At the end of each applied temperature level during the course of both experimental phases, a thermal sensation questionnaire, based on ASHRAE 7-poins thermal scale, is performed for each test subject.

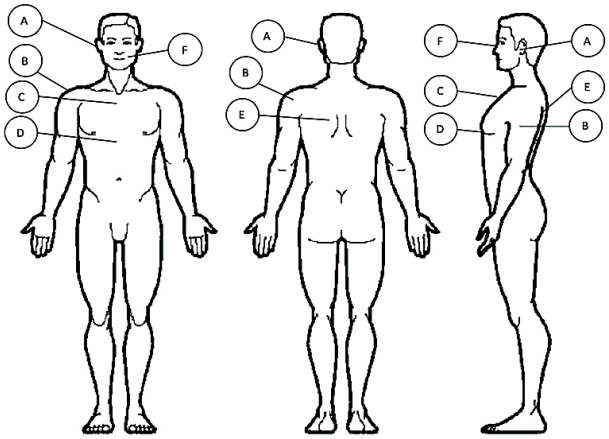

Figure 2. Sensor placement. (A) Ear channel for aural temperature measurement via the Cosinuss One, (B) upper arm where skin temperature and heat flux are measured with the gSKIN patch, (C) middle upper chest where skin temperature and heat flux are measured with the gSKIN patch, (D) lower chest where heart rate is measured with the Polar H7, (E) Scapula where skin temperature is measured with the shimmer, (F) mouth and nose where metabolic rate is measured via the MetaMAX 3B spiroergometer sensor.

2.2 Modelling and classification

For the sake of present study, the measured variables are divided into *wearables*, which are easily measured variables using wearable sensors and *gold-standards* (reference) variables, which are not suitable for wearable technologies. The wearables are including heart rate H_R, aural temperature T_{er}, average skin temperature $\bar{T}_{sk}$, skin heat flux q_{sk} and ambient air temperature T_∞. On the other hand, the gold standards are consisting of the core temperature T_c, which is driven from the aural temperature [$T_c = f(T_{er})$], metabolic rate M_r and personal thermal sensation votes TS. The ultimate goal of this work is to develop an adaptive classification model to predict the individual thermal sensation depending, solely, on the wearables or estimated variables. Hence, both of the metabolic rate and core body temperature are estimated using online dynamic modelling approach (Figure 3). Then, the individual thermal sensation is predicted using a classification model (classifier) whose inputs are the wearables and estimated the metabolic rate and core body temperature (Figure 3).

- *Dynamic modelling*

Although the system under study (occupant's thermoregulation) is inherently a non-linear system, the essential perturbation behaviour can often be approximated well by simple linearized Transfer Function (TF) models (Young, 1989, 1993; Youssef et al., 2018). For the purposes of the present paper, therefore, the following liner, Multi-input, single-output (MISO) discrete-time-systems are considered to estimate metabolic rate and core body temperature (Young, 1993),

$$y(k) = \sum_{r=1}^{r=R} \frac{B_r(z^{-1})}{A_r(z^{-1})} u_r(k-\delta_r) + \xi(k), \quad (1)$$

where k denotes the value of the asscociated variable at the k^{th} sampling instant; $y(k)$ is the output variable; $u_r(k), \quad r = 1,2,\dots,R$ are input variables, while $A(z^{-1})$ and $B(z^{-1})$ are appropriately defined polynomials in the backshift operator z^{-1}, i.e., $z^{-i}y(k) = y(k-i)$ and $\xi(k)$ is additive noise, a serially uncorrelated sequence of random variables with variance σ^2 that accounts for measurement noise. The *Simplified Refined Instrumental Variable* (SRIV) algorithm was utilised in the identification and estimation of the models (model parameters and model structure) (Young and Jakeman, 1980).Two main statistical measures were employed to determine the most appropriate model structure. Namely, the coefficient of determination R_2^T, based on the response error; and YIC (Young's Information Criterion), which provides a combined measure of model fit and parametric efficiency, with large negative values indicating a model which explains the output data well and yet avoids over-parameterisation

(Young et al., 1991). Additionally, the estimation performance of the selected models is evaluated used the mean-absolute-error (MAE) value.

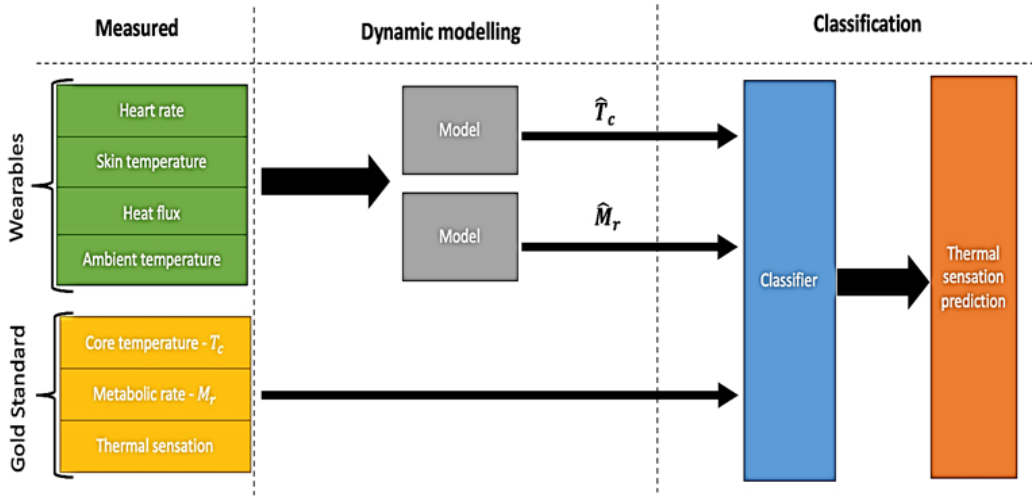

Figure 3. Overview of the main steps to predict the individual thermal sensation.

- *Classification model*

To predict the individual thermal sensation, a classification model (classifier) is developed and trained based on the wearables and estimated variables (metabolic rate and core body temperature) that together with the thermals sensation votes (gold standard). A modified support vector machine (SVM) technique, namely, least-squares support vector machine (LS-SVM) is used to develop and train the thermal sensation classifier (Suykens et al., 2002; Suykens and Vandewalle, 1999). SVMs are originally presented as binary classifiers (Suykens et al., 2002) that assign each data instance $X \in \mathbb{R}^d$ to one of two classes described by a class label $y \in \{-1,1\}$ based on the decision boundary that maximises the margin $2/\|w\|_2$ between the two classes. Generally, a feature map $\phi: \mathbb{R}^d \Rightarrow \mathbb{R}^p$ is used to transform the geometric boundary between the two classes to a linear boundary $L: w^T\varphi(x) + b = 0$ in feature space, for some weight vector $\boldsymbol{w} \in \mathbb{R}^{p\times 1}$ *and* $b \in \mathbb{R}$. The class of each instance can then be found by $y = sign(w^T\varphi(x) + b)$, where $sign$ refers to the sign function. Due to some computational complexities of standard SVM because of the quadratic programming problem, least squares support vector machines (LS-SVM) is presented to overcome such problem. LS-SVM, in contrast with standard SVM, relies on least squares cost function as follows:

$\min_{w,b;\, e} \frac{1}{2} w^T w + \gamma \sum_{i=1}^{N} e_i^2$,

such that; $y_i(w^T\varphi(x_i) + b) \geq 1 - e_i \; and \; e_i \geq 0, i = 1, 2, \ldots, N,$

where e_i errors such that $1- e_i$ is proportional to the signed distance of x_i from the decision boundary, and γ represents the regularisation constant. In LS-SVM, instead of solving the quadratic programming problem a set of linear equations to be solved is sufficient to find the optimal solution of the classifier.

3 RESULTS AND DISCUSSIONS

3.1 Dynamic modelling and estimation of individual's metabolic rate

Different combinations of inputs variables (wearables) are tested for best estimation of individual's metabolic rate. The SRIV algorithm, combined with YIC and R_2^T selection criteria, suggested that a second-order MISO discrete-time TF with heart rate (H_R), average skin heat flux ($\bar{q}_{sk}$) and aural temperature (T_{er}) as input variables is the best (with average R_2^T = 0.89 ±0.04 and YIC = − 13.62 ±2.33) to describe and estimate the dynamic behaviour of the individual's metabolic rate. More specifically, the SRIV algorithm identified the following general MISO discrete-time TF model structure,

$$\widehat{M}_r(k) = \left[\frac{B_1(z^{-1})}{A(z^{-1})} \quad \frac{B_2(z^{-1})}{A(z^{-1})} \quad \frac{B_3(z^{-1})}{A(z^{-1})}\right] . \begin{bmatrix} T_{er}(k-\delta_1) \\ H_R(k-\delta_1) \\ \bar{q}_{sk}(k-\delta_1) \end{bmatrix} + \xi(k), \quad (2)$$

where $\widehat{M}_r(k)$ is the estimated metabolic rate and the numerator polynomials B_1, B_2 and B_3 are of the following orders (number of zeros) 2, 3 and 2, respectively. While the system delays δ_1, $\delta_2$and δ_3 are varied from person to another (inter-personal) with average values of 1.4, 0.20 and 0.21 minutes, respectively. The estimation performance of the selected general MISO-DTF (2) is evaluated based on the mean-absolute-percentage-error ($MAPE = \frac{100\%}{N}\sum_{k=1}^{N}\left|\frac{\widehat{M}_r(k)-M_r(k)}{M_r(k)}\right|$) value. The results have shown that the developed general model is shown, for all test subjects, a higher average MAPE value (10 ±2.2 %) during the low activity phases than the average MAPE value (7.6 ±2.6 %) resulted during the high activity phases.

Table 2. Average R_2^T, YIC, model delays and MAPE for the selected MISO-DTF model to estimate the individual's metabolic rate obtained from the 25 test subjects during low and high activity phases.

	Average R_2^T ±std	**Average YIC ±std**	**Model delays Average [δ_1 δ_2 δ_3]**	**Average $MAPE$ ±std**
Low activity phase	0.85 ±0.02	-12.32 ±3.4	[1.5 0.3 0.25] min	10 ±2.2 %
High activity phase	0.94 ±0.03	-14.43 ±2.8	[1.2 0.18 0.20] min	7.6 ±2.6 %

The general estimation performance of the suggested general MISO model can be enhanced by using the online adaptive form of the SRIV algorithm (Garnier et al., 2009). The online adaptive (closed-loop) SRIV algorithm is providing the possibility to personalise the developed general model by retuning the model parameters and model delays based on the streaming data acquired from the wearable sensors.

3.2 Classification model and prediction of individual's thermal sensation

The classification model for predicting the individual's thermal sensation is developed, based on LS-SVM approach, by training the classifier on 80% of the data points, while the rest of the data (20%) is used for testing. The model accuracy, sensitivity F1-score and overall confusion matrix are computed to evaluate the performance of the developed classifier. A feature space including all the measured and estimated input variables, namely, T_{er}, H_R, $\bar{q}_{sk}$, $\bar{T}_{sk}$, $\Delta\bar{T} = T_{er} - \bar{T}_{sk}$ and $\widehat{M}_r$. Additionally, other features are extracted by computing the variance, min, max, root mean squares (RMS) and first derivative of the aforementioned measured and estimated variables. The age and gender of the test subjects are also included in the feature spaces. A feature selection procedure is employed to develop the most reduced-dimension model with highest error performance. The feature selection step is based on an iterative procedure over all possible feature combinations and compare the error performance of the resulted model in each iteration. The feature selection step is resulted in a feature space

including 25 features as shown in Table 3. The resulted confusion matrix from the developed classification model based on the selected feature space is shown in Figure 4.

Table 3. An overview of the selected feature space including the measured and estimated variables (six variables) and some operations on these variables (× = selected).

	Variance	**min**	**max**	**RMS**	$\frac{d}{dt}$
T_{er}	×	×	×	×	-
H_R	×	×	×	×	-
$\overline{q}_{sk}$	×	×	×	×	×
$\overline{T}_{sk}$	×	-	-	×	-
$\Delta\overline{T}$	×	×	×	×	-
$\widehat{M}_r$	-	-	-	-	-

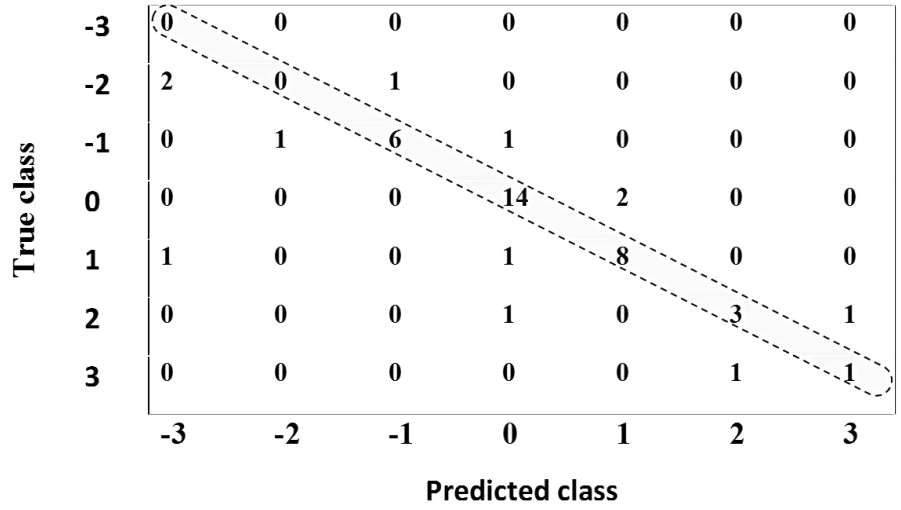

Figure 4. The resulted confusion matrix from testing the developed LS-SVM classifier. The diagonal represents the correctly classified data points.

The overall performance results of the developed classification model are presented in Table 4. For a 7-classes classification problem, the developed classifier have shown an overall accuracy of 76% to predict the individual's thermal sensation. The developed classifier have shown a high (84%) F1-score, which reflects low false positive and negative.

Table 4.Overall performance of the developed classification model

Measure	**Value**
Accuracy	0.76
Sensitivity	0.82
Precision	0.87
F1 score	0.84

SVM is used in recent studies to assess occupant's thermal demands (Dai et al. 2017), and to predict thermal comfort/sensation (Farhan et al. 2015). In these studies, the results have shown that SVM is able to predict thermal comfort/ sensation with an accuracy of 76.7%. However, these results is only obtained by reducing the 7-classes classification problem to a 3-classes problem. Hence, we believe that reducing the number of classes will improve our suggested general model performance. Moreover, based on streaming data obtained from wearable sensor technologies, a personalised adaptive classification model, based on the same extracted features, will enhance the model performance to predict the individual's thermal sensation.

4 CONCLUSIONS

In this present paper, 25 participants are subjected to three different environmental temperatures, namely 5ºC (cold), 20 ºC (moderate) and 37 ºC (hot) at two different activity

levels, namely, at low level (rest) and high level (cycling at 80 W power). Metabolic rate, heart rate, average skin temperature (from three different body locations), heat flux and aural temperature are measured continuously during the course of the experiments. The thermal sensation votes are collected from each test subject based on ASHRAE 7-points questioner. The results have shown that a reduced-ordered (second-order) MISO-DTF including three input variables (wearables), namely, aural temperature, heart rate, and average heat flux, is best to estimate the individual's metabolic rate (non-wearable) with average MAPE of 8.7%. A general classification model based on LS-SVM technique is developed to predict the individual's thermal sensation. For a 7-classes classification problem, the results have shown that the overall model accuracy of the developed classifier is 76% with a F1-score value of 84%. It is suggested in this paper that the model overall performance of the model can be enhanced by using a personalised adaptive classification algorithm based on streaming data from wearable sensors.

5 REFERENCES

ASHRAE. (2004), *Thermal Environmental Conditions for Human Occupancy*, *ASHRAE*, ASHRAE Sta., American Society of Heating, Refrigeration and Air Conditioning Engineers, Inc., Atlanta GA.

ASHRAE. (2017), *ASHRAE Standard 55*, American Society of Heating, Refrigerating and Air-Conditioning Engineers, INc., Atlanta GA.

Chaudhuri, T., Soh, Y.C., Li, H. and Xie, L. (2017), "Machine learning based prediction of thermal comfort in buildings of equatorial Singapore", *2017 IEEE International Conference on Smart Grid and Smart Cities (ICSGSC)*, IEEE, pp. 72–77.

Dai, C., Zhang, H., Arens, E. and Lian, Z. (2017), "Machine learning approaches to predict thermal demands using skin temperatures: Steady-state conditions", *Building and Environment*, Pergamon, Vol. 114, pp. 1–10.

De Dear, R. and Brager, G.S. (1998), "Developing an adaptive model of thermal comfort and preference", *ASHRAE Transactions*, American Society of Heating, Refrigerating and Air-Conditioning Engineers, Vol. 104 No. 1, pp. 145–167.

Dewhirst, M.W., Viglianti, B.L., Lora-Michiels, M., Hanson, M. and Hoopes, P.J. (2003), "Basic principles of thermal dosimetry and thermal thresholds for tissue damage from hyperthermia", *International Journal of Hyperthermia*, Vol. 19 No. 3, pp. 267–294.

Enescu, D. (2019), "Models and Indicators to Assess Thermal Sensation Under Steady-state and Transient Conditions", *Energies*, Multidisciplinary Digital Publishing Institute, Vol. 12 No. 5, p. 841.

Farhan, A.A., Pattipati, K., Wang, B. and Luh, P. (2015), "Predicting individual thermal comfort using machine learning algorithms", *2015 IEEE International Conference on Automation Science and Engineering (CASE)*, IEEE, pp. 708–713.

Garnier, H., Young, P.C. and Gilson, M. (2009), "Simple Refined IV Methods of Closed-Loop System Identification", *IFAC Proceedings Volumes*, Elsevier, Vol. 42 No. 10, pp. 1151–1156.

Huang, C.-C. (Jeff), Yang, R. and Newman, M.W. (2015), "The potential and challenges of inferring thermal comfort at home using commodity sensors", *Proceedings of the 2015 ACM International Joint Conference on Pervasive and Ubiquitous Computing - UbiComp '15*, ACM Press, New York, New York, USA, pp. 1089–1100.

ISO-10551. (1995), *Ergonomics of the Thermal Environment -- Assessment of the Influence of the Thermal Environment Using Subjective Judgement Scales*, Brussels.

Kim, J., Zhou, Y., Schiavon, S., Raftery, P. and Brager, G. (2018), "Personal comfort models: Predicting individuals' thermal preference using occupant heating and cooling behavior and machine learning", *Building and Environment*, Pergamon, Vol. 129, pp. 96–106.

Koelblen, B., Psikuta, A., Bogdan, A., Annaheim, S. and Rossi, R.M. (2017), "Thermal sensation models: a systematic comparison", *Indoor Air*, Vol. 27 No. 3, pp. 680–689.

Lu, S., Wang, W., Wang, S., Cochran Hameen, E., Lu, S., Wang, W., Wang, S., et al. (2019), "Thermal Comfort-Based Personalized Models with Non-Intrusive Sensing Technique in Office Buildings", *Applied Sciences*, Multidisciplinary Digital Publishing Institute, Vol. 9 No. 9, p. 1768.

Nikolopoulou, M. and Steemers, K. (2003), "Thermal comfort and psychological adaptation as a guide for designing urban spaces", *Energy and Buildings*, Elsevier, Vol. 35 No. 1, pp. 95–101.

Parsons, K.C. (Kenneth C.. (2014), *Human Thermal Environments : The Effects of Hot, Moderate, and Cold Environments on Human Health, Comfort, and Performance*, 3rd ed., CRC Press.

Suykens, J.A.K., Van Gestel, T., De Brabanter, J., De Moor, B. and Vandewalle, J. (2002), *Least Squares Support Vector Machines*, WORLD SCIENTIFIC.

Suykens, J.A.K. and Vandewalle, J. (1999), "Least Squares Support Vector Machine Classifiers", *Neural Processing Letters*, Kluwer Academic Publishers, Vol. 9 No. 3, pp. 293–300.

Young, P.C. (1989), *Control and Dynamic Systems: Advances in Theory and Applications*, edited by C.T. Leondes, Elsevier.

Young, P.C. (1993), *Concise Encyclopedia of Environmental Systems*, first., PERGAMON-ELSEVIER SCIENCE LTD, available at: http://store.elsevier.com/Concise-Encyclopedia-of-Environmental-Systems/isbn-9780080361987/ (accessed 8 August 2013).

Young, P.C., Chotai, A. and Tych, W. (1991), "Identification, estimation and control of continuous-time systems described by delta operator models.", Kluwer Academic Publishers, 28 April.

Young, P.C. and Jakeman, A. (1980), "Refined instrumental variable methods of recursive time-series analysis Part III. Extensions", *International Journal of Control*, Taylor & Francis, Vol. 31 No. 4, pp. 741–764.

Youssef, A., D'Haene, M., Vleugels, J., De Bruyne, G. and Aerts, J.-M. (2018), "Localised Model-Based Active Controlling of Blood Flow During Chemotherapy to Prevent Nail Toxicity and Onycholysis", *Journal of Medical and Biological Engineering*, Springer Berlin Heidelberg, pp. 1–12.

Assessment of long-term and mid-term building airtightness durability: field study of 61 French low energy single-family dwellings

Bassam Moujalled[*1], Sylvain Berthault[2], Andrés Litvak[3], Valérie Leprince[4], and Gilles Frances[5]

1 Cerema, Project-team BPE,
46 Rue St Theobald
Address, Country
**Corresponding author: bassam.moujalled@cerem.fr*

2 Cerema, Direction Centre-Est
Boulevard Giberstein – BP 141
F-71405, Autun, France

3 Cerema, Direction Sud-Ouest
Rue Pierre Ramond- CS 60013
F-33166, Saint-Médard-en-Jalles, France

4 PLEIAQ
84C Av de la liberation
F-69330, Meyzieu, France

5 Cetii
1 Rue de la Coronelle
F-30200, Bagnols-sur-Cèze, France

ABSTRACT

The French ongoing research project "Durabilit'air" (2016-2019) aims at improving our knowledge on the variation of buildings airtightness through onsite measurement and accelerated ageing in laboratory controlled conditions. This paper presents the final results of the second task of the project. This task deals with the quantification and qualification of the durability of building airtightness of single detached houses. It is done through field measurement at mid-term (MT) and long-term (LT) scales.

We first present the field measurement protocol. For the MT campaign, a sample of 30 new single-detached houses has been selected nationwide. During the study, the airtightness of each building was measured once per year over a 3-year period. A part of this sample (5 houses) was also measured twice per year during two different seasons in order to investigate the impact of seasonal variation. In addition, the air permeability of a window was measured once per year over the 3-year period in 5 houses. The LT campaign was carried out with a second sample of 31 existing single-detached houses constructed during the last 10 years. The airtightness of each house was measured once.

A specific measurement protocol was defined after a detailed literature review. The main challenge is to understand the variations of the airtightness and to identify whether it is related to the products/assembly ageing, the maintenance conditions or other factors such as the occupants' behaviour. The protocol is based on the standard ISO 9972 for the measurement method of building air permeability with additional requirements for the measurement conditions. It also includes a detailed qualitative leakage detection and questionnaire for occupants.

Secondly, this paper presents the construction characteristics of both samples. All houses were tested upon completion. The air changes per hour at 50 Pa pressure difference (n_{50}) of both samples show the same mean value of 1.4 h^{-1}, with larger variations among the LT sample.

Finally, we discuss measurement results. Regarding MT sample, the air permeability slightly increases during the first year (mean increase by 18%), and then stabilizes during the second and third year. However, for some houses with exposed timber framing, n_{50} has increased by more than 100%. Regarding LT campaign, the air permeability (n_{50}) show a similar increase after 3-10 years with a mean value of 20%. Measurements performed during two different seasons did not show a significant impact of seasonal variation. The results show globally an increase in the number of detected leakages for all houses, but this increase is not always correlated with the change in air permeability. For 10 houses of both samples, the building airtightness has improved. For 6 houses, this improvement is maybe due to the building material (wood), the maintenance of windows, or the sealing of leaks by occupants but for 4 houses, we have not been able to explain this improvement.

KEYWORDS

Airtightness durability, field measurements, building envelope, low-energy house

1 INTRODUCTION

The increasing weight of building leakages energy impact on the overall performance of low-energy buildings led to a better understanding and characterization of the actual airtightness performance of buildings. Several European countries have already included in their Energy Performance regulation (EP-regulation) mandatory requirements regarding the building airtightness. This is the case in France, where the EP-regulation requires a limit airtightness level for residential buildings that must be justified by measurement. However, low expertise is available today on the durability of building airtightness and its evolution in mid- and long-term scales.

The French ongoing research project "Durabilit'air" is conducted since 2016 for a 42-month period, in order to improve our knowledge on the variation of buildings airtightness through onsite measurement campaigns and accelerated ageing in laboratory controlled conditions.

As part of this project, a comprehensive literature review about building airtightness durability was realized by (Leprince et al., 2017). This review showed an important evolution over time of the air permeability in real buildings, with an increase of more than twice in some cases. The air permeability seems to increase in the 3 first years and then stabilise.

This paper is issued from the second task of the "Durabilit'air" project. This task deals with the quantification and qualification of the durability of building airtightness of single detached houses. It is done through field measurement at mid-term and long-term scales. This paper presents the results of both MT and LT measurements.

2 METHODOLOGY

2.1 Onsite measurements

In order to evaluate the durability of the building airtightness in real conditions at mid- and long-term scales, two field measurement campaigns were conducted: a mid-term (MT) campaign and a long-term (LT) campaign.

The MT campaign aims at characterising the yearly evolution of building airtightness of new dwellings over a 3-year period. Therefore, a sample of 30 new single-detached low-energy houses, measured upon completion, has been selected nationwide. The following measurements were performed:

- The airtightness of each building was measured once per year over the 3-year period.
- Five buildings of this sample were measured twice per year in order to investigate the impact of seasonal variations.
- For five buildings (four buildings from this sample plus one additional building), the airtightness of an installed window were measured once per year over a 3-year period.

The LT campaign aims at characterising the evolution of building airtightness of existing dwellings over a longer period from 3 to 10 years. A second sample of 31 existing single-detached dwellings, measured upon completion, has been therefore selected. The dwellings have been constructed during the last 10 years. The airtightness of each dwelling was measured once.

All dwellings were selected according to well-defined criteria to reduce uncertainties about main factors impacting building airtightness. In particular, all dwellings should be tested upon completion, and the test reports should be available and in accordance with the standard ISO 9972 (NF EN ISO 9972, 2015) and its French implementation guide (FD P50-784, 2016). Information about the treatment of the building airtightness must also be available.

The main challenge of this project is to understand the variation of the airtightness and to identify whether it is related to the products/assembly ageing, the maintenance conditions or other factors such as the occupants' behaviour. Therefore, a specific measurement protocol was defined after a detailed literature review (Leprince, Moujalled, & Litvak, 2017). The protocol is mainly based on the standard ISO 9972 and its French implementation guide for the measurement method with additional requirements for the measurement conditions in order to reduce uncertainty due to measurement procedure:

- Each dwelling is to be measured under the same conditions as the first measurement upon completion as far as possible (same tester, same calibrated measurement device, same building preparation, same pressure difference sequences, and same season). Measurements are to be performed in both pressurization and depressurization. Deviations from the conditions of the first test are to be reported.
- Detailed qualitative leakage detection is to be performed at each measurement according to the leaks categories of the French implementation guide of ISO 9972 (FD P50-784, 2016). In particular, an annual follow-up of leaks is to be performed for the dwellings of MT sample during the 3 years.
- Questionnaires for occupants are to be filled at each measurement in order to identify the modifications of the building envelope due to the action of the occupants (i.e. drillings made in the air barrier after the first test, replacement of products…).

At the total, 84 and 31 measurements of building airtightness were performed for MT and LT samples respectively, plus an extra of 10 measurements for the seasonal impact, and an another extra of 15 measurements for the airtightness of windows.

2.2 Results analysis

The results presented here are expressed according to the airflow at 50 Pa (q_{50}) for which the measurement is more reproducible than at 4 Pa (Delmotte & Laverge, 2011).

For the MT sample, four measurements are carried out on each building: just after completion of the building (reference measurement n_0), then at 1 year (measurement n_1), 2 years (measurement n_2) and 3 years (measurement n_3) after completion. For the LT sample, two measurements are carried out on each building: just after completion of the building (reference measurement n_0), then at 3 to 10 years after completion (measurement n_x).

Boxplots are used to graphically summarise the main descriptive statistics of measured air leakage rates q_{50} for each measurement of both samples. It shows means alongside medians and quartiles. One-sided paired t-test (95% confidence level) is performed to analyse the statistical significance of the increase in the mean q_{50} between the reference measurement n_0 and the other measurements of each sample. Shapiro test is also performed to check the normality of the samples of measurements.

Multiple linear regression is performed to analyse the correlation between the evolution in the measured air leakage rates q_{50} and the evolution in the numbers of detected leakages.

Regarding the measurements of seasonal variations and windows, no statistical analysis is performed as the sample size is small for both (5 buildings in each case). We will only look at the evolution of the measured air leakage rates per each building.

3 RESULTS

3.1 Main characteristics of buildings

Figure 1 shows the distribution of buildings of MT and LT samples according to the year of construction and buildings main material and type of air barrier.

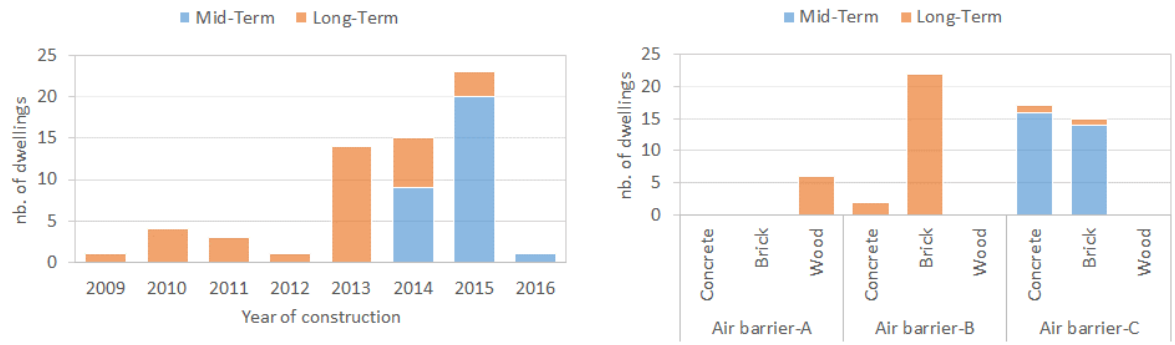

Figure 1: Distribution of buildings depending on the year of construction (left) and buildings main material and type of air barrier (right); Air barrier-A when the air barrier is ensured by vapour barrier, Air barrier-B by coating on the masonry, and Air barrier C by plasterboards and mastics at the inside facing of the walls

The MT sample is composed of 30 new single-detached low-energy houses constructed mainly in 2014 and 2015, with 20 one-story houses and 10 two-story houses. The average floor area is 124.1 m² with a minimum of 87 m² and a maximum of 172.2 m², and the average volume is 217.1 m^3 with a minimum of 156.1 m^3 and a maximum of 363.9 m^3. All houses are built of masonry with interior insulation (16 houses with concrete blocks and 14 with hollow bricks). The majority of roofs are made of light-frame wood truss (20 houses), against 8 houses with traditional wood frame and 2 houses with an exposed traditional wood frame. Single exhaust ventilation system with humidity control is installed in all houses. The airtightness is done through plasterboards and mastics at the inside facing of the walls in all houses (air barrier C).
The LT sample is composed of 31 single-detached low-energy houses constructed between 2009 and 2015, with 7 one-story houses and 25 two-story houses. The average floor area is 147.9 m² with a minimum of 83.1 m² and a maximum of 269 m², and the average volume is 256.6 m^3 with a minimum of 138.9 m^3 and a maximum of 478.2 m^3. The majority of houses are built of masonry with interior insulation (25 houses with hollow bricks and 3 with concrete blocks), against 6 wooden houses. The majority of roofs are made of light-frame wood truss (27 houses), against 5 houses with flat roof. A balance ventilation system is installed in 1 house while all other have a single exhaust ventilation system with humidity control. The airtightness of masonry houses of the LT sample is mainly done by coating on the masonry (air barrier B), while the airtightness of wooden houses is done by the vapour barrier (air barrier A).
The measurements upon completion (measurement n_0) of both samples showed the same mean value of the air changes per hour at 50 Pa n_{50} of 1.4 h^{-1}, with larger variations among the LT sample (standard-deviation of 0.65 h^{-1} for LT sample against 0.33 h^{-1} for MT sample).
For MT sample, 1st-year measurements (measurements n_1) started in November 2016 and finished in October 2018, thus from 1 to 3 years after the measurements n_0 upon completion. The measurements were delayed due to the difficulty in finding occupants willing to be involved in a 3 year-long measurement campaigns. Thus, the average timespan between measurements n_0 and n_1 is 1.7 years, and the average timespans between the following measurements are less than one year to compensate for the delay (0.7 year between n_1 and n_2, and 0.9 year between n_2 and n_3). For three houses, measurements n_2 and n_3 were not carried out because of the withdrawal of occupants during the project. Besides, a house was excluded from the MT sample because of problems during measurement n_1.
For the LT sample, all measurements (measurements n_x) were conducted in 2017, from 3 to 8 years after n_0 (average timespan of 4.6 years between n_0 and n_x). Only 9 houses older than 5 years were measured. As for MT, it has been difficult to find houses, fulfilling selection criteria with volunteer occupants. A house was excluded from the LT sample because of problems during measurement n_x.

3.2 Evolution of envelope air permeability

Figure 2 and Figure 3 show the boxplots of the measured air leakage rates at 50 Pa q_{50} for the different measurements of MT and LT sample respectively.

For the measurements n_0, tests were performed by either pressurisation or depressurisation unlike the other measurements where tests were performed by both pressurisation and depressurisation. Boxplots show the results of the measurements n_1, n_2 and n_3 for MT sample, and n_x for LT sample, for the same houses tested by pressurisation or depressurisation at n_0, in order to be comparable to the reference measurements n_0.

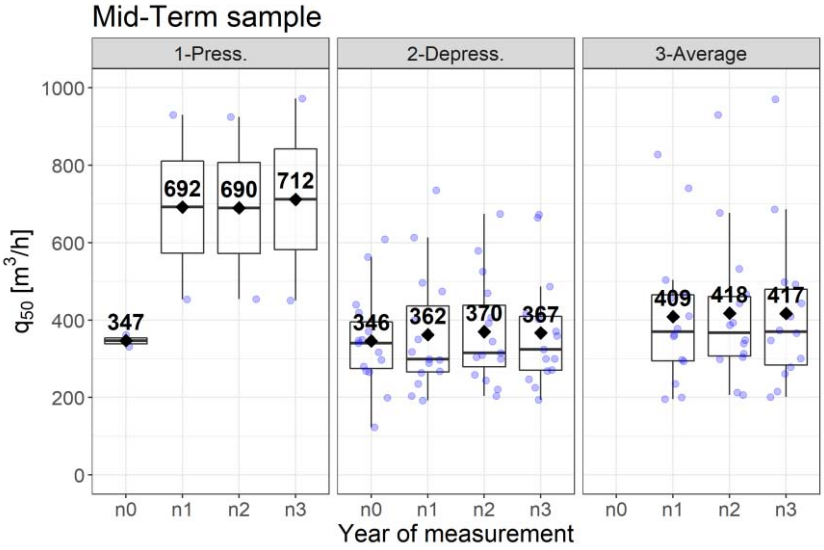

Figure 2: Boxplot of the measured air leakage rates at 50 Pa q_{50} for the measurements n_0, n_1, n_2 and n_3 of the MT sample for the pressurization test, the depressurization test and the average between both tests.

For the MT sample, when considering both pressurisation and depressurisation measurements at n_0, we can observe a significant increase in the mean q_{50} between the measurements n_0 and n_1 by 58.9 $m^3.h^{-1}$, i.e. +18% (p-value = 0.037 < 0.05), than a stabilization of q_{50} at n_2 and n_3.

For the LT sample, we observe similar results as MT sample with a significant increase in the mean q_{50} between n_0 and n_x by 67.7 m^3/h, i.e. +20% (p-value = 0.002 < 0.05).

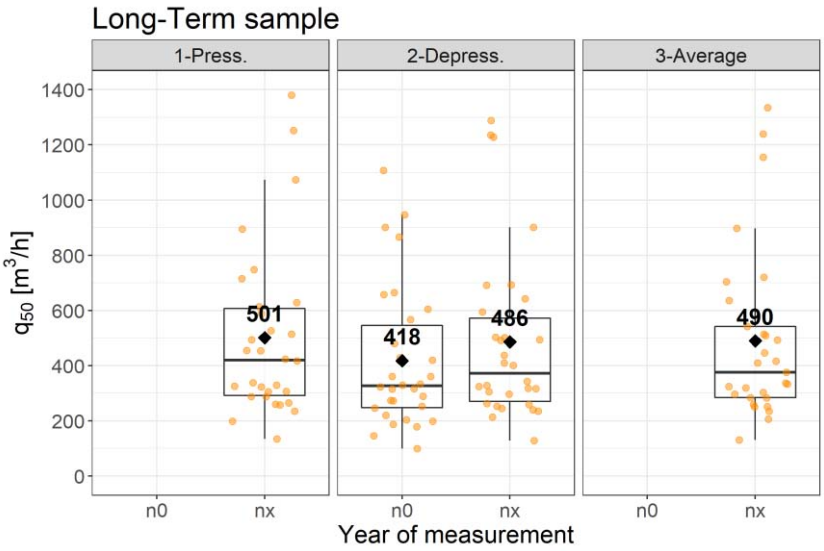

Figure 3: Boxplot of the measured air leakage rates at 50 Pa q_{50} for the measurements n_0 and n_x of the LT sample for the pressurization test, the depressurization test and the average between both tests

Figure 4 shows a lack of correlation between the evolution in q_{50} and the age of the houses for both MT and LT samples. Therefore, the air permeability does not seem to change with the age of the building; it varies mainly during the first two years of the building, and then stabilizes, as observed in previous studies (Leprince, Moujalled, & Litvak, 2017). Variations during the first two years may have several origins, including actions by the occupants when they move in the building (e.g. installing furniture, picture frames, downlight…), the first heating of the building or the first seasonal cycles.

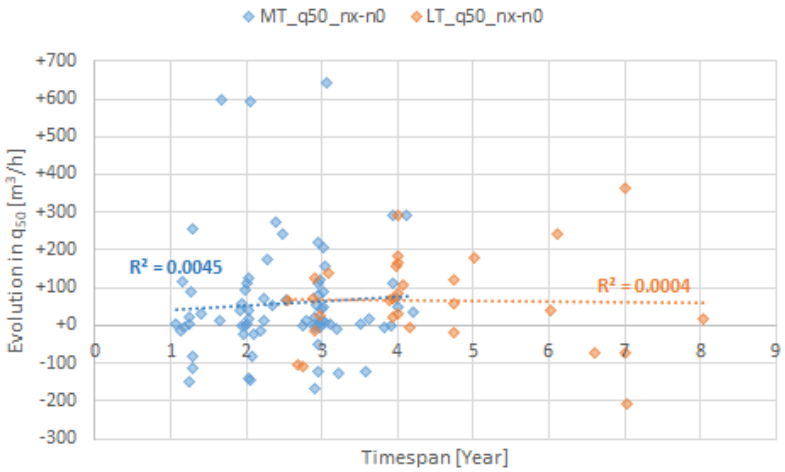

Figure 4: Measured evolution in q_{50} for MT and LT samples according to the age of the houses (timespan between the measurement at completion n_0 and the other measurements n_x)

3.3 Analysis of explanatory factors

As there is almost no evolution between the results of n_1, n_2 and n_3 for the MT sample, we will focus in the analysis on the evolution between n_0 and n_1.

Tables 1 and 2 show the evolution in q_{50} in relation to the main characteristics of the houses (constructor, number of levels, type of air-barrier, type of material, type of floor, type of roof, type of heating, specific HVAC equipment) and modifications by the occupants (modification on windows, modification on walls). The houses in the table are sorted in ascending order of the evolution in q_{50}. They are classified into 4 categories depending on the evolution in q_{50}:

- significant decrease of q_{50} (< -50 $m^3.h^{-1}$): 5 houses for the MT and LT samples each;
- no or little variations of q_{50} (-50 to +50 $m^3.h^{-1}$): 13 houses for MT sample and 8 houses for LT sample;
- moderate increase of q_{50} (+50 to +150 $m^3.h^{-1}$): 6 houses for MT sample and 10 houses for LT sample;
- strong increase of q_{50} (> +150 $m^3.h^{-1}$): 5 houses for MT sample and 7 houses for LT sample.

It is difficult to make statistical analysis to identify the impact of different factors on the evolution in q_{50} due to the small size of the samples regarding the factors.

For the MT sample, we are generally observing an upward trend of q_{50} for 2-storey detached houses with exposed wood frame. For the two houses with exposed wood frame of this sample (MICT06 & MICT19), MICT06 has become much leakier (q_{50} at n_1 almost 4 times higher than n_0), mainly because of leakages appearing at the junction between the wood and the plasterboard (shrinkage of mastic). While the airtightness level of MICT19 has remained almost stable between n_0 and n_1. Knowing that both houses are tighten with the same method, the conditions of implementation of the air-barrier seem to have an impact on the durability of the airtightness. Unfortunately, it was not possible for us in this study to collect information on the

conditions of implementation; our knowledge was limited to the type of treatment of the airtightness from the technical plans, without having information about the products and their implementations. Therefore, it would be interesting to investigate this factor in future studies. For the LT sample, we observe that the airtightness of wooden houses (6 houses) has generally remained stable and even improved for 2 houses. It is interesting to notice that laboratory testing has come to same conclusion on wood structure (Litvak, Allègre, Moujalled, & Leprince, 2019) and it may be due to the expansion of wood with the humidity that would expand the wood and therefore reduce leakages.

Table 1: Evolution in q50 for MT according to buildings mains characteristics and modifications by occupants (M1: concrete block – M2: bricks – M3: wood construction – F1: floor on crawl space – F2: Slab on grade – F3: Cellar – R1: light-frame wood truss – R2: Traditional wood frame – R3: Exposed wood frame – R4: Flat roof – H1: Heat pump - H2: Gas boiler – H3: Wood stove – H4: Electric heating – E1: Thermodynamic water heater – E2: Heat pump water heater – E3: Electric heat water – E4: Solar thermal – E5: Solar PV – E6: DHW by gas boiler – M: Maintenance – R: Replacement – D: Drilling)

	Δq50_n1-n0 < -50 m3/h					-50 m3/h < Δq50_n1-n0 < 50 m3/h													50 m3/h < Δq50_n1-n0 < 150 m3/h						Δq50_n1-n0 > 150 m3/h				
	MICT28	MICT10	MICT27	MICT21	MICT24	MICT07	MICT13	MICT04	MICT03	MICT17	MICT09	MICT25	MICT12	MICT02	MICT29	MICT26	MICT19	MICT30	MICT08	MICT20	MICT23	MICT16	MICT18	MICT01	MICT05	MICT14	MICT15	MICT22	MICT06
Δq50_nx-n0 [m³ h⁻¹]	-151	-146	-112	-93	-81	-22	-15	-13	-4	-2	0	3	3	3	13	23	31	46	54	68	69	92	101	118	173	243	257	272	599
Constructor	C11	C2	C11	C9	C9	C2	C5	C8	C2	C6	C2	C11	C5	C3	C9	C11	C5	C9	C2	C7	C1	C12	C5	C10	C8	C6	C4	C1	C2
Nb. of levels	0	0	0	0	0	0	1	1	0	0	0	0	0	0	0	0	1	0	0	0	0	1	1	0	1	0	1	1	1
Type of air-barrier	C	C	C	C	C	C	C	C	C	C	C	C	C	C	C	C	C	C	C	C	C	C	C	C	C	C	C	C	C
Type of material	M2	M2	M2	M2	M1	M2	M1	M1	M2	M1	M2	M2	M1	M1	M1	M2	M1	M1	M2	M2	M1	M2	M1	M1	M1	M1	M2	M1	M2
Type of floor	F1	F2	F1	F2	F2	F2	F1	F2	F2	F1	F2	F1	F1	F2	F2	F1	F1	F2	F3	F1	F1	F1	F1	F2	F1	F1	F1	F1	F2
Type of roof	R1	R1	R1	R1	R1	R1	R2	R1	R1	R1	R1	R1	R1	R2	R1	R1	R3	R1	R2	R1	R1	R2	R2	R1	R2	R1	R2	R1	R3
Type of heating	H1	H4	H1	H1	H1	H1	H1	H2	H3	H2	H1	H1	H2	H1	H1	H1	H2	H3	H1	H3	H2	H1	H2	H3	H1	H2	H3	H2	H3
HVAC Equipement	E2	E3	E2	E2	E2	E2	E1	E1	E1	E4	E1	E1	E1	E2	E1	E1	E1	E1	E2	E1	E5	0	E1	E3	E1	E1	E1	E1	E1
Modif_Window	M			M					R						R						R							R	
Modif_Walls	D		D	D	D		D	D	D	D	D	D	D	D	D			D	D	D	R	D	D	D		D	D	D	D

Table 2: Evolution in q50 for LT according to buildings mains characteristics and modifications by occupants

	Δq50_nx-n0 < -50 m3/h					-50 m3/h < Δq50_nx-n0 < 50 m3/h								50 m3/h < Δq50_nx-n0 < 150 m3/h										Δq50_nx-n0 > 150 m3/h						
	MILT21	MILT20	MILT13	MILT17	MILT08	MILT31	MILT29	MILT04	MILT22	MILT26	MILT06	MILT10	MILT15	MILT30	MILT23	MILT03	MILT11	MILT28	MILT16	MILT02	MILT32	MILT12	MILT07	MILT25	MILT09	MILT19	MILT14	MILT01	MILT05	MILT27
Δq50_nx-n0 [m³ h⁻¹]	-209	-108	-103	-72	-71	-18	-12	-6	17	20	27	29	38	60	67	68	71	72	84	109	123	125	140	158	166	180	182	244	290	363
Constructor		C1	C1	C2	C3	C1	C1	C3		C3	C3	C3	C3	C1	C3	C3	C3	C3	C3	C3	C1	C3	C3	C3	C3	C3	C3	C3	C4	C3
Nb. of levels	0	1	1	1	0	1	1	1	1	1	1	0	1	1	1	1	1	1	1	0	0	1	1	1	1	1	1	1	0	1
Type of air-barrier	C	A	A	B	B	A	A	B	B	B	B	B	B	A	B/C	B	B	B	B	B	A	B	B	B	B	B	B	B	C	B
Type of material	M2	M3	M3	M2	M2	M3	M3	M2	M2	M2	M2	M2	M2	M3	M2	M2	M2	M2	M2	M2	M3	M2	M2	M2	M2	M1	M1	M2	M1	M2
Type of floor	F1	F2	F2	F1	F1	F2	F2	F1	F1	F1	F1	F1	F1	F2	F1	F1	F1	F1	F1	F1	F2	F1	F2	F1	F1	F1	F1	F1	F1	F1
Type of roof	R1	R1	R1	R1	R1	R1	R1	R1	R1	R4	R1	R1	R1	R1	R4	R1	R1	R4	R1	R1	R1	R1	R1	R4	R1	R1	R1	R1	R1	R1
Type of heating	H1	H4	H4	H4		H4	H4	H4	H4	H4	H1	H4	H1	H4	H4	H2	H2	H4	H3	H4	H4	H4	H4	H4	H4	H4	H1	H1	H1	H2
HVAC Equipement	E1	E1	E1	E5	E3	E1	E1	E1	E1	E1	E1	E1	E1	E1	E1	E4	E4	E1	E6	E1	E1	E1	E1	E1	E1	E1	E1	E1	E1	E6
Modif_Window										D									R											
Modif_Walls	D	D	D	D	D	D	D	D	D	D	D	D	D	D	D	D	D	D	D	D	D	D	D	D	D	D	D	D	D	D

Regarding the modifications on the envelope made by occupants, the information was collected through questionnaires. We have identified mainly two categories of modifications:

- modification on windows (Modif_window): maintenance (M) or replacement (R) of some elements;
- modification on the walls: replacement (R) of some elements or drilling the walls (D).

As showed in Table 1, one window was modified in MICT28 (adjustment of the hinge) and another one in MICT21 (adjustment of the service door overlooking the garage), which probably explain the improvement of the airtightness. While the replacement of windows in MICT22 and MICT23 seem probably to deteriorate the airtightness. This is also the case of MILT16 of the LT sample in Table 2.

Regarding the modifications of walls, all houses were generally modified by the occupants (drilling the walls for installing furniture, decoration, hood, downlight led...) whatever the evolution of the airtightness. In some cases (MILT 25 & MILT27), the degradation of the airtightness is may be due to the installation of a heat pump which required the piercing of the walls in order to be able to install the cables and the ducts. In other cases (MILT8 & MILT21), the improvement of the airtightness is may be due to the fact that the occupants have sealed the leaks detected during the test at completion at the junction between the ducts and the ceiling. However, it is difficult to draw general conclusions from these observations about the impact of the modifications by occupants on the evolution of the airtightness.

3.4 Evolution of leakages

Figure 5 and Figure 6 show the evolution in the number of leakages for MT sample and LT sample respectively for each category of leakages as defined in (FD P50-784, 2016). The houses are sorted in ascending order of the evolution of q_{50}. The categories of leakages are the following:

- A: leakages through main envelope area;
- B: leakages through wall, roof and floor junctions;
- C: leakages through doors and windows;
- D: leakages around penetration through envelope;
- E: leakages through trapdoor;
- F: leakages through electrical components;
- G: leakages through junctions between wall and door/window;
- H: other leakages.

The figures show an increase in the number of leakages for doors and windows (C), electrical components (F), penetrations through envelope (D) and junctions between walls and doors/windows (G).

However, multiple linear regression has been performed and has shown that the evolution in q_{50} is not correlated with the evolution in the number of leakages. As we can see on both figures, for some houses with a decrease in q_{50}, there is an increase in leakages equivalent to houses with a strong increase in q_{50}. Therefore, a thorough leakage location detection is not useful as long as it does not quantify leakages for the analysis of the onsite durability. Thus, new methods are needed to detect and to quantify leakages.

Gathered information on the modification of the envelope has explained a part of the evolution in q_{50}. However, neither leakages detection nor building characteristics are correlated with the observed evolution of q_{50}. Therefore, there are probably other parameters not considered in this study, which have an impact on the durability of the airtightness. One guess is that the environmental conditions (temperature, dustiness) when the air barrier is implemented may have an impact on the durability of the airtightness. It was not possible for us to collect information on these parameters, but it would be interesting to investigate this parameter in future studies.

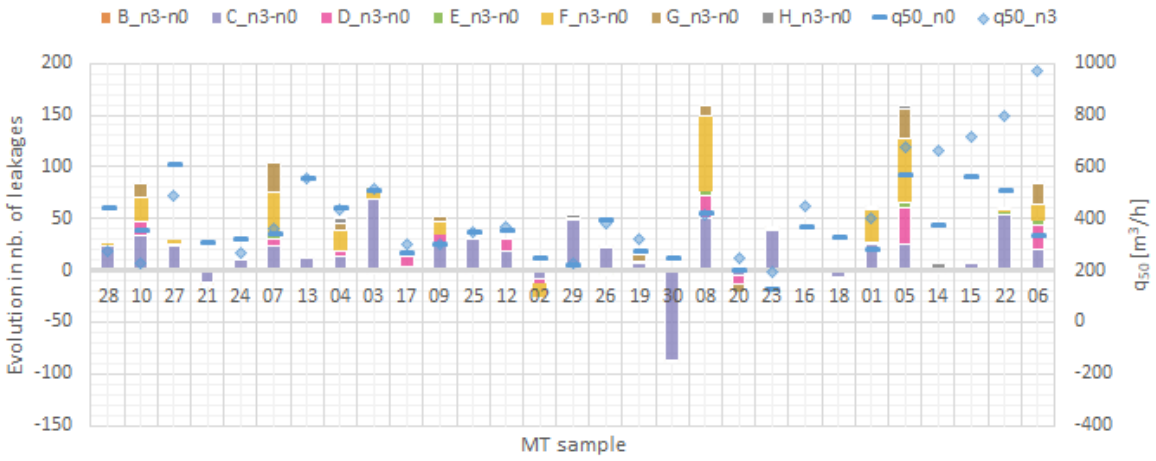

Figure 5: Evolution in detected leaks numbers for MT sample

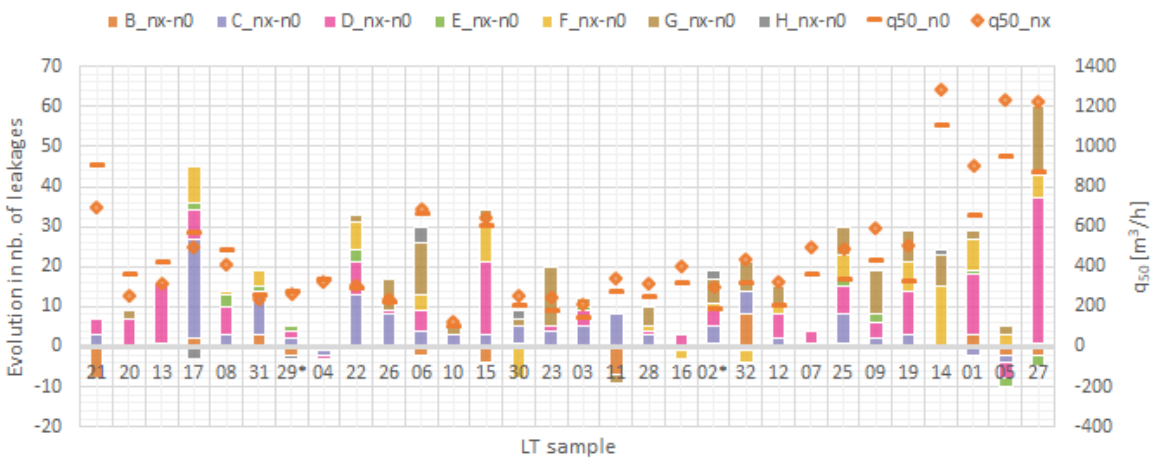

Figure 6: Evolution in detected leaks numbers for LT sample

3.5 Impact of seasonal variations

Figure 7 shows the evolution of the measured air leakage rates at 50 Pa q_{50} depending on the moment of measurement for the five houses of the MT sample.

Globally, we do not observe a seasonal variation in q_{50} except for MICT 22. In case of MICT22, q_{50} has strongly increased after the measurement at completion (SUM-14). But since the second measurement in winter 2017 (WIN-17), the house seems to be slightly more airtight in summer than in winter. Unfortunately, measurement n_2 is missing between SUM-17 and SUM-18 to confirm this observation. It is interesting to notice that this is the only 2-storey house while the four others are 1-storey houses.

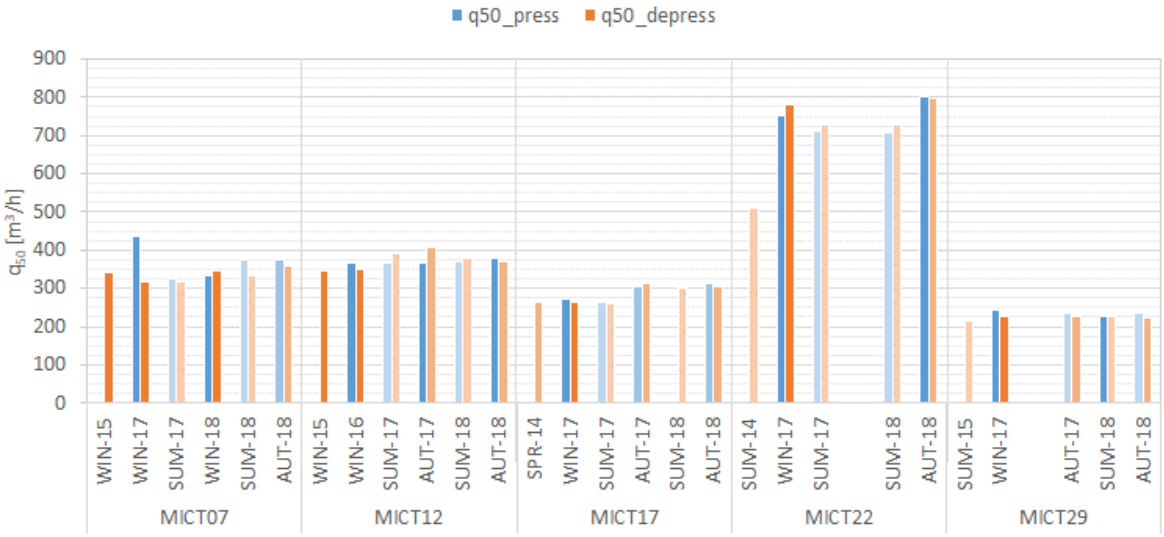

Figure 7: Evolution in q50 for the measurements with seasonal variations of the MT sample (WIN: Winter; SUM: Summer; AUT: Autumn; SPR: Spring)

3.6 Evolution of windows air permeability

The window air permeability was measured with the PAM device as described in (Fournier, Berthault, & Carrié, 2007). Figure 8 shows the results of the measured air leakage rates at 100 Pa and the results of the leakages detection for the five windows. We note that the air permeability of the windows was not measured at completion. Thus, the reference

measurements n_0 are missing. We can only analyse the evolution of the airtightness between n_1 and n_3.
Globally, we observe small variations between measurements n_1, n_2 and n_3. As for the envelope, we do not observe any correlation between the evolution in detected leakages and the evolution in air leakage rates of the windows. In addition, the evolution in the air leakage rates of windows is not correlated with the evolution in the air permeability of the envelope.

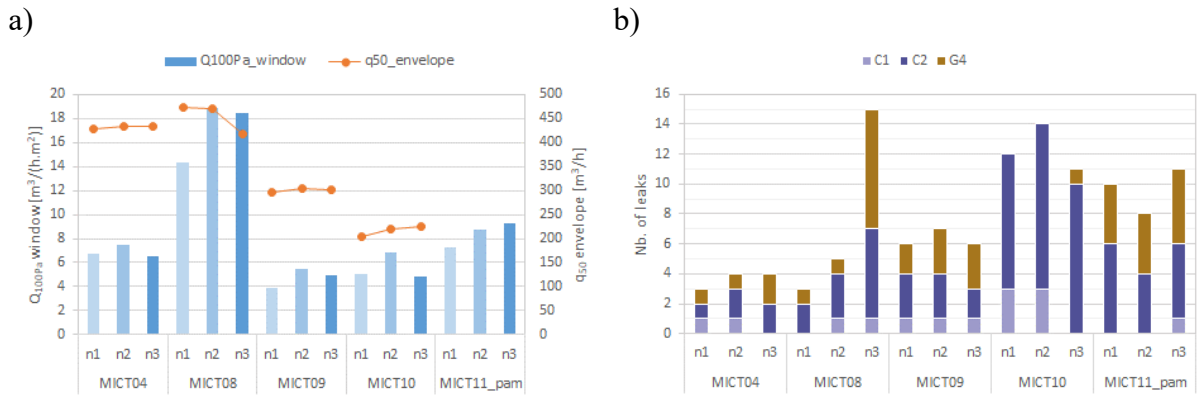

Figure 8: Evolution in the measured air leakage rates at 100 Pa (a) and the number of leakages (b) for the measured windows of the MT sample (C1: other leakage through window – C2: leakage through the junction between the window leaf and frame – G4: leakage through the junction between the window and the wall)

4 CONCLUSIONS

The durability of building airtightness of low energy single-detached houses was assessed through two field measurement campaigns at mid-term (MT) and long-term (LT) scales.
The results showed that the airtightness of houses can deteriorate mainly during the first two years and then it seems to stabilise as:

- For MT sample, the mean and median values of the air leakage rates q_{50} in years n_1, n_2 and n_3 are equivalent;
- MT and LT samples show the same mean evolution of the air leakage rate q_{50} (respectively +18% and +20%).

However, as for other studies (Leprince, Moujalled, & Litvak, 2017), we have observed that the building airtightness deteriorated significantly in some houses while in others it stabilised or even improved. With this study, it has not been possible to determine "where and why" new leakages are appearing however; it has led us to the following useful conclusions:

- One of the two houses with exposed wood-frame has become much leakier, mainly because of leakages appearing at the junction between the wood and the plasterboard (shrinkage of mastic). While the airtightness of the other house has remained almost stable. Therefore, the conditions of implementation of the air-barrier seem to have an impact on the durability of the airtightness.
- It has not been possible to determine the location of the new leakages causing the deterioration of the airtightness. New methods are needed not only to locate but also to quantify more precisely leakages. A thorough leakage detection is not useful as long as it does not quantify leakages for the analysis of the onsite durability.
- Observed variations of the air permeability are not due to seasonal variations and given the strict protocol applied in this study, they are probably not due to measurement uncertainty.

- The evolution of the airtightness does not appear to be correlated in this study with the following parameters: constructor, type of air-barrier, type of floor, type of roof, type of heating, specific HVAC equipment.

The two parameters that seem to be correlated with the evolution of the airtightness are:

- The material: it seems that the airtightness of wood houses tend to stabilise or even improve over years, maybe due to the expansion of wood with humidity.
- The number of levels: 2-storey houses seems to more deteriorate than 1-storey ones, which is maybe due to more important foundation settlement.

Regarding the houses where the airtightness has improved (10 houses for both samples), this improvement is maybe due to the building material (2 wooden houses), the maintenance of windows (2 houses), or the sealing of leaks by occupants (2 houses). However, for the other four houses, we have not been able to explain it.

Therefore, the results of this study do not stress the need to perform long-term study on the durability of airtightness, but on the contrary to better understand where and why leakages appear during the first year, which causes the deterioration of the building airtightness (very short-term ageing). Other parameters need to be considered, such as the environmental conditions (hygrothermal, dustiness) during the implementation of the air barrier or the evolution of the temperature and humidity inside the building during the first year. In addition, modifications made by occupants need to be known more closely. More frequent airtightness measurements (e.g. monthly measurements) could be performed on a small sample of houses over the period from the implementation of the air barrier till one year upon building completion, by recording at each measurement the aforementioned parameters.

5 ACKNOWLEDGEMENTS

This work was supported by ADEME and French ministry for construction. The views and opinions of the authors do not necessarily reflect those of ADEME and French ministry. The published material is being distributed without warranty of any kind, either expressed or implied. The responsibility for the interpretation and use of the material lies with the reader. In no event shall authors, ADEME or French ministry be liable for damages arising from its use. Any responsibility arising from the use of this report lies with the user.

6 REFERENCES

ADEME. (2016). *Quelle pérennité de la perméabilité à l'air des maisons individuelles en Basse Normandie.* Récupéré sur ADEME: http://www.ademe.fr/sites/default/files/assets/documents/perennite_permeabilite_a_lair_maisons_bbc_normandie_8917.pdf

Bracke, W., Laverge, J., Van Den Bossche, N., & Janssens, A. (2016). Durability and Measurement Uncertainty of Airtightness in Extremely Airtight Dwellings. *International Journal of Ventilation*, 383-393.

Delmotte, C., & Laverge, J. (2011). Interlaboratory tests for the determination of repeatability and reproducibility of buildings airtightness measurements. *32nd AIVC Conference " Towards Optimal Airtightness Performance".* Brussels, Belgium, 12-13 October 2011.

FD P50-784. (2016). Performance thermique des bâtiments - Guide d'application de la norme NF EN ISO 9972. France: AFNOR.

Fournier, M., Berthault, S., & Carrié, R. (2007). In situ measurement of window air tightness : stakes, feasibility, and first results. *2nd PALENC Conference and 28th AIVC Conference, Crete Island, Greece*.

Leprince, V., Moujalled, B., & Litvak, A. (2017). Durability of building airtightness, review and analysis of existing studies. *38th AIVC Conference "Ventilating healthy low-energy buildings"*. Nottingham, UK, 13-14 September 2017.

Litvak, A., Allègre, F., Moujalled, B., & Leprince, V. (2019). Assessment of the durability of airtightness products in laboratory controlled conditions: developement and presentation of the experimental protocol. *40th AIVC - 8th TightVent & 6th venticool Conference - From energy crisis to sustainable indoor climate.* Ghent, Belgium, 15-16 October 2019.

NF EN ISO 9972. (2015). Thermal performance of buildings - Determination of air permeability of buildings - Fan presurization method. France: AFNOR.

Assessment of the durability of airtightness products in laboratory controlled conditions: development and presentation of the experimental protocol.

Andrés Litvak [1*], Fabien Allègre [2], Bassam Moujalled [3], and Valérie Leprince [4]

1 Cerema, DAIT/GBAT
rue Pierre Ramond - Caupian
33166 Saint Médard en Jalles cedex, FRANCE
**Corresponding author: andres.litvak@cerema.fr*

2 RESCOLL
8, allée Geoffroy Saint Hilaire CS 30021
33615 PESSAC cedex, FRANCE

3 Cerema, Project-team BPE
46 Rue St Theobald – BP128
38081 L'Isle d'Abeau, France

4 PLEIAQ
84 C Av de la Libération
69330 Meyzieu, France

ABSTRACT

The airtightness of new buildings has significantly improved in the last two decades thanks to building energy performance regulations. However, until now, low knowledge is available about the evolution of buildings' envelope airtightness. This work deals with the durability of buildings airtightness, and focuses on ways to better characterize it. This study is part of the French research project "Durabilitair" (2016-2019) that aims at improving our knowledge on the variation of buildings envelope airtightness through onsite measurement and accelerated ageing in laboratory-controlled conditions. During a past AIVC conference, a publication of the Durabilit'air project has presented and discussed the state of the art on characterizing buildings' airtightness durability. Final results from the Durabilitair mid-term and long-term time scales field measurement campaigns are presented in a companion paper of this conference.

This paper focuses on the assessment of the durability of airtightness products in controlled conditions through the development of a laboratory experimental protocol for characterizing the accelerated ageing of building airtightness assembled products. The overall objective is to define and develop an experimental protocol capable of testing and quantifying the airtightness evolution of assembled airtightness products samples and comparing the relative ageing of the samples.

The state-of-the-art showed that there is no standardised protocol to characterise in laboratory-controlled conditions the durability of product assemblies regarding airtightness performance. As a matter of fact, due to the diversity of airtightness products, it is difficult – and even, perhaps impossible – to define an accelerated ageing universal protocol that would be equivalent to a known amount of years of natural ageing. From the light of the state of the art results, we defined the exposure conditions of a relative ageing test, through thermal, humidity and pressure variation cycles. We developed a 1 m^3 environmental chamber and exposed three different 1 m^2 samples of assembled products to the defined exposure conditions cycles.

The tested samples represent three different treatments of airtightness of the joints between windows and walls: 1) impregnated foam; 2) sealant with backing foam and 3) adhesive and membrane complex. During each exposure cycle, we have measured the evolution of the airtightness of the sample.

The ageing tests of the samples 2 and 3 showed a significant degradation of the airtightness performance after the ageing cycle, whereas air permeability of sample 1 could not be assessed by our experimental protocol. The choice of the samples and the experimental conditions are described and discussed. We conclude that modifying the duration and the characteristics of the exposure cycles (humidity, temperature and pressure) would certainly allow more differentiating results in future works.

KEYWORDS

Airtightness, laboratory measurements, accelerated ageing, durability

1 INTRODUCTION

1.1 Context

Understanding buildings' airtightness governing factors has become a major concern for professionals from the building sector. Significant progress have been achieved, mainly due to mandatory requirements in many countries, as a consequence of Europe's ambition to generalize nearly zero energy buildings by the end of 2020. Nevertheless, we still lack of expertise today about the durability of airtightness products, at mid- and long- term scales.

As a matter of fact, this subject remains very complex, since it covers in the meantime (i) the modelling of the mechanisms of building's and products' loads and deformations; (ii) the accelerated ageing in laboratory controlled conditions and (iii) the performance characterization from field measurements results.

1.2 Objectives

In this paper, we present the results of this second objective, that has been studied as part of the French multi-partner 2016-2019 research project Durabilitair (www.durabilitair.com). We aim at assessing the durability of airtightness products in controlled conditions for characterizing the accelerated ageing of building airtightness assembled products. The overall objective is to define and develop an experimental protocol capable of testing and quantifying the airtightness evolution of assembled airtightness products samples and comparing the relative ageing of the samples.

Final results from the Durabilitair mid-term and long-term time scales field measurement campaigns are presented in a companion paper of this conference (Moujalled, Berthault, Litvak, Leprince & Francés, 2019). An earlier publication presented and discussed the state of the art on characterizing buildings' airtightness durability (Leprince, Moujalled & Litvak, 2017). In the light of analysis of on artificial ageing in laboratory conditions, we defined an experimental methodology and selected three samples of assembled airtightness products to be tested. The main objective of this research is to prove the technical feasibility of such an experiment, in order to develop a protocol for accelerated ageing and testing of airtightness assembled products.

2 METHODOLOGY

2.1 Results of the state of the art on artificial ageing in laboratory conditions

In a previous state of the art, we presented a summary of artificial ageing recent studies, in controlled laboratory conditions (Leprince, Moujalled & Litvak, 2017). In this review, we pointed the importance of well defining the sample to be tested (products assembly v/s product alone) and the ageing protocol conditions. Due to the diversity of airtightness products, we concluded that it is probably impossible to define an accelerated ageing universal protocol that would be equivalent to a known amount of years of natural ageing.

A study tested the durability of adhesives on exterior airtightness barriers (Langmans, Desta, Alderweireldt, & Roels, 2015). The adhesives were exposed to different cycles of temperature (2 weeks), temperature, humidity and gel (12 days) and high humidity (4 weeks). The study concluded that the increase in air permeability was limited. Another research tested both products properties alone and products assemblies implemented in a cell (Ylmén, Hansén , & Romild, 2014). No correlations were observed between the durability of the product alone and the durability of the assembly airtightness. The authors concluded that it is required to develop durability tests of the complete airtightness systems on full-scale set-up. Besides, the impact of solicitations under pressure, humidity and temperature variations was shown to be different

depending on the kind of air barrier: plasters are sensitive to humidity and temperature while membranes are sensitive to pressure variation (Michaux, Mees, Nguyen, & Loncour, 2014). Therefore, if one wants to define a protocol that would apply to all kind of air barrier, all type of constraints shall be included in the protocol.

A research has tested products implemented at full-scale wall constructed on a steel frame of 3m x 3m (Antonsson, 2015). They applied heat treatment (60°C, 1 week) and pressure load (-150/+150 Pa) on the sample with a climatic chamber and a pressurisation device docked on the wall (not simultaneously). Two systems have been tested with this protocol and significant deviations were observed in the results. With the first system, a significant change in air leakage has been observed after the heat treatment, while with the second system very little change could be observed.

2.2 Modelling of the mechanisms of building's and products' loads and deformations

Few works have studied the modelling of the mechanisms of building's and products' loads and deformations. A study estimates that 60 to 75% of the pressure loads can reach the airtightness products (Ackermann, 2012). The study concluded that the durability of the air barrier should be tested by performing pressure / vacuum cycles and testing the maximum load. It proposes a test protocol representing 50 years of wind pressure cycle (the maximum load must be a wind that occurs once every 50 years). From the BRE digest, the study has therefore established the load cycles to be implemented according to the maximum load, as well as the simulation of the maximum loads. In this study, correlations were determined between artificial aging and natural aging according to standards. Nevertheless these correlations, based on the laws of Arrhenius are valid only for certain types of materials. For assemblies, the law of Arrhenius is difficult to use. Indeed, estimating thermal and humidity loads is more difficult and depends on the air barrier position. The following recommendations have been identified to address the risks of phase changes during accelerated aging tests in the laboratory:

- Differentiate hygroscopic materials from other non-hygroscopic materials because moisture can laminate the material
- Take into account the absolute humidity in 24h test cycles with absorption / desorption (hot humid, hot dry, cold environments, ...)
- Test products in accordance with the real life exposure conditions
- Do not exceed the glass transition temperature of the products (T ° of transition from the vitreous / solid state to the pasty / rubbery state). Example: PU foams: TV = 50 to 60 ° C
- Do not extrapolate the life of the tested products to accelerated aging (T ° and RH), unless the material is tested at constant T °, without change of state.

2.3 Main results

In the light of this works, we observed that the results of the aging tests vary from one study to another. One of the main reasons is that the protocol is not standardized. Nevertheless, the following general conclusions can be drawn:

- Implementation has a strong impact on durability
- Products do not have the same reaction under normal conditions as when they are subjected to extreme conditions (temperature, humidity or pressure);
- A standardized procedure for the aging of sealants is lacking to characterize products and especially assemblies regarding airtightness performance;
- The results of aging tests on products alone are not necessarily consistent with the aging observed when these products are put in situation;
- Product performance against conventional test procedures (peel, shear, etc.) does not necessarily correspond to their performance in terms of airtightness
- The aging strategy must be consistent with the loads of the products. The strategy may differ depending on the position of the air barrier.

3 DESCRIPTION OF THE EXPERIMENTAL PROTOCOL

Based on this analysis, we developed an experimental protocol for accelerated ageing of airtightness assembled products. The protocol definition consisted in :

1) developing an experimental chamber,
2) choosing the representative samples,
3) and defining the accelerated ageing conditions.

3.1 Environmental chamber

For our study, we developed a 1 m^3 environmental chamber to expose a 1 m^2 square sample of assembled airtightness products to weathering (thermal, hygrometric and pressure) controlled conditions. The environmental chamber is composed of three main parts:

- An accelerated weathering chamber (see A on figure below)
- A pressure test bench for differential pressure exposure and airtightness measurement (see B on figure below)
- A sample holder, between both enclosures (see C on figure below)

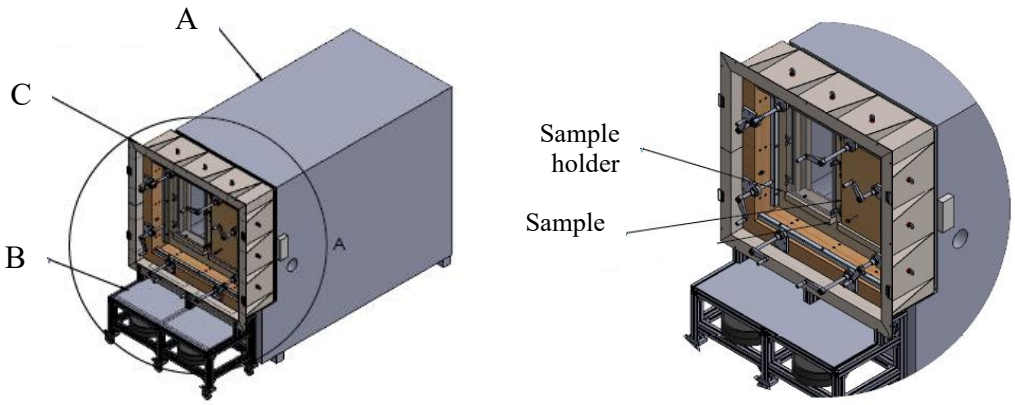

Figure 1 : Environmental chamber

The frame of the sample holder and the differential pressure bench constitute a single independent machine that allows to perform wind cycles and airtightness measurements between -250 Pa and + 250 Pa. We created a differential pressure on the sample by positive and negative pressurized air, with air mass flow controllers. Pressurization created the conditions for both the exposure (to wind exposure) and the airtightness measurement tests.

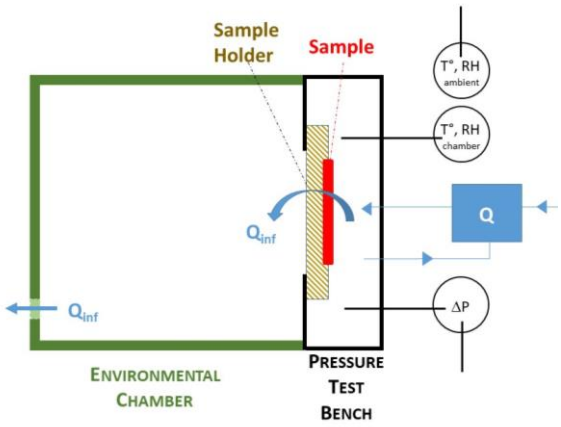

Figure 2a : global view with the pressure bench access panel closed by an aluminium plate

Figure 2b : the environmental chamber (the door was removed)

Figure 2c : the sample holder

We designed the technical specifications of the pressure test bench (see table 1) with the view to get the best compromise between a good signal stability and a fairly large usage range, in order to test the various implementation solutions and to maintain a control reactivity and a sufficient flow rate to carry out cycles with imposed frequency.

Table 1: technical specifications of the pressure test bench

Technical specifications	Values
Differential pressure measuring range	[-250 Pa , +250 Pa]
Steady state stability	± 2 Pa in [-250 Pa , +250 Pa]
Maximum setpoint	<30% (at 10 Pa) <5% (≤ -50 Pa and ≥50 Pa)
Maximum compensation capacity	30 lpm [0 , 250 Pa] 20 lpm [- 250 Pa , 0 Pa]
Pressure measurement precision	± 0.25% of measurement range
Airflow rate measurement range	[-50 lpm , 50 lpm]
Airflow rate measurement precision	± 0.6% of measurement range
Collected data	Differential pressure Airflow rate T°C/RH laboratory T°C environmental chamber Atm pressure laboratory
Acquisition data rate	5 Hz

Airtightness, repeatability and reproducibility tests were performed on the bench in 4 different configurations :

1) test i :with an aluminium airtight plate, closing the pressure bench,
2) test ii :with the aluminium plate, with a ϕ 2.5 mm round hole
3) test iii :with the aluminium plate, with a ϕ 4.0 mm round hole
4) test iv :with the aluminium plate, with the two holes (ϕ 2.5 mm and ϕ 4.0 mm)

Results confirmed the airtightness of the bench. The measured airtightness air flow rates were measured to be below the airflow rate measurement precision (0.18 lpm for positive pressure and 0.12 lpm for negative pressure). Inversely, airflow rate measurements as a function of pressure for the configuration n°ii-iii-iv (i.e., with holes), shown consistent results with the equivalent corresponding leakage area tests.

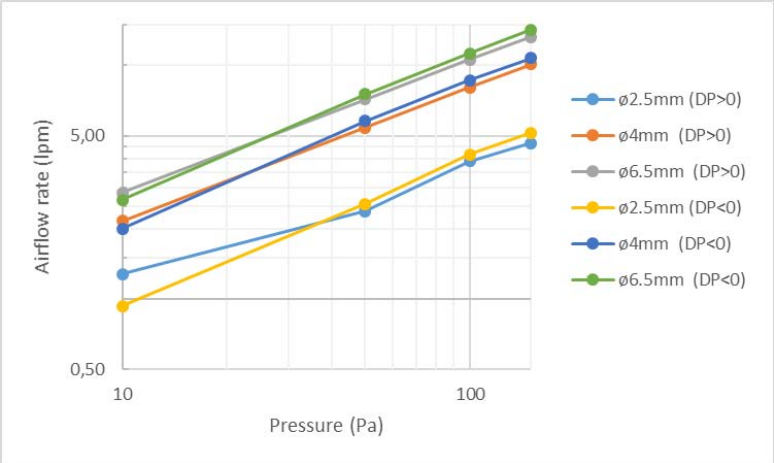

Figure 3 : air leakage flow rates across the aluminium plate (tests n°ii-iii-iv)

3.1 Exposure cycles and airtightness measurements

We defined a test as 4 successive cycles applied one after the other with intermediate measurements to control the evolution of airtightness between each cycle. We designed 4 weathering cycles, in order to accelerate the ageing of the samples :

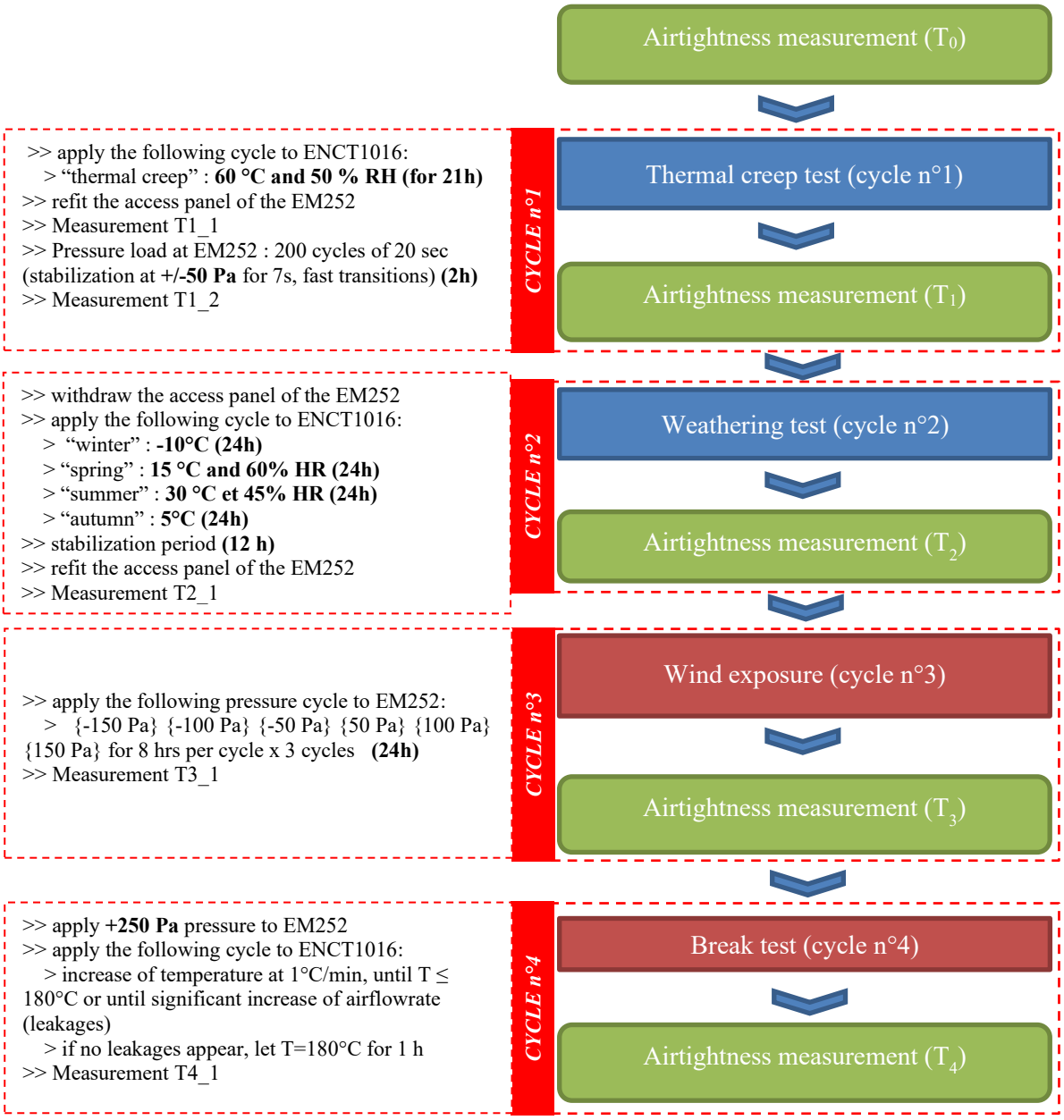

Airtightness measurements were performed in order to determine the airflow rate Q as a function of pressure ΔP, according to the airflow rate and pressure law model, equation 1 :

$$Q = K\,\Delta P^{n} \quad (1)$$

where Q(lpm) is the airflowrate, ΔP(Pa) is the differential pressure and K(lpm.Pa^{-n}) and n(-) are the airflow coefficients.

For this work, we compared the measured airflow rates values at 0 Pa, ± 10 Pa, ± 50 Pa, ± 100 Pa and ± 150 Pa and represented the corresponding charted profiles (Q, ΔP).

For the pressure loads to be applied, we transposed Ackerman's protocol to France. The maximum wind measured in France in inhabited area is 150km/h which corresponds to 41m/s. According to ISO 15927-1:2003 "Hygrothermal performance of buildings – calculation and presentation of climatic data – part1: Monthly means of single meteorological elements", the on-site wind is:

$$vs = vr * Cr * Ct \quad (2)$$

with, vs (m/s) wind speed on site
vr (m/s) reference wind speed
Cr (-) roughness coefficient in Urban area below 16 m: CR(z)=0.24*ln(16/1)
Ct (-) topograhy coefficient Ct=0.9

Therefore a 41m/s wind represents a 24m/s wind on building site. If we consider that the maximum pressure coefficient on a façade is 0.5, this corresponds to a load of 173 Pa, according to the wind pressure equation. Now, if one considers Ackerman's assertion that 75% of the load is on the air barrier, that means that the maximum pressure to apply is 130 Pa. We transposed the BRE cycles digest, see table 2. One can note that these pressures correspond to the pressure ranges of an experimental protocol reported in our previous state of the art (Antonsson, 2015).

Table 2 : Range of the pressure test

Column Title	Number of cycles (positive and negative)	Percentage of the design pressure (%)	Corresponding pressure (Pa)
Sequence to be applied 5 times	1	90 %	117 Pa
	960	40 %	52 Pa
	60	60 %	78 Pa
	240	50 %	65 Pa
	5	80 %	104 Pa
	14	70 %	91 Pa
Last sequence	1	100 %	130 Pa

3.2 Samples

Three types of assembled products as treatments of airtightness of the joints between windows and walls were chosen as samples to be tested, namely:

i) Expansive weatherseal foam ;
ii) Sealant (mastic) with backing foam
iii) adhesive and membrane complex.

The sample holder enabled the installation of two different samples for each exposure cycle. All assemblies were made under the technical supervision of the representatives of the products used. The method of implementation was documented elsewhere (Allegre & Louet, 2019).

1) Description of sample n°1 : impregnated foam tape on wooden carpentry

The sample is the assembly of an expansive weatherseal foam tape installed between the frame and the opening of a wooden carpentry. The selected foam tape has an operating range of 5 to 11mm.

This sample holder allows the installation of two samples in parallel. We installed the sample in two configurations:

- Left, in figure 4.1 and 4.3, with an expansion of 10mm (i.e., close to its upper limit)
- Right, in figure 4.1 and 4.3, with an expansion of 6mm (i.e., close to its lower limit)

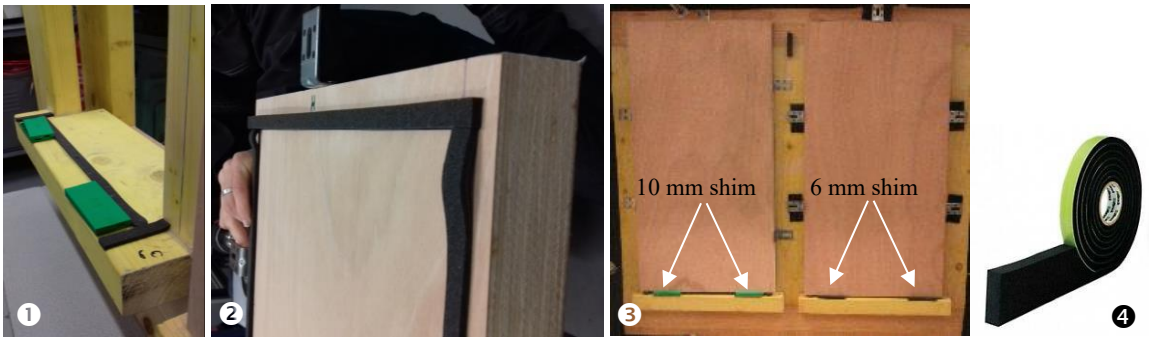

Figure 4 : installation of the sample n°1

2) *Description of sample n°2 : backer rod and mastic (sealant) on wooden carpentry*

The sample is the assembly of back-up strips and filled up with mastic as a sealant, implemented between the frame and the opening of a wooden carpentry. The selected backer rod has an operating range of 5 to 11mm. A fixing coat was applied to the wooden surface before implementing it.

This sample holder allows the installation of two samples in parallel. We installed the sample in two configurations:

- Left, in figure 5.1 and 5.3, with an expansion of 10mm (i.e., close to its upper limit)
- Right, in figure 5.1 and 5.3, with an expansion of 6mm (i.e., close to its lower limit)

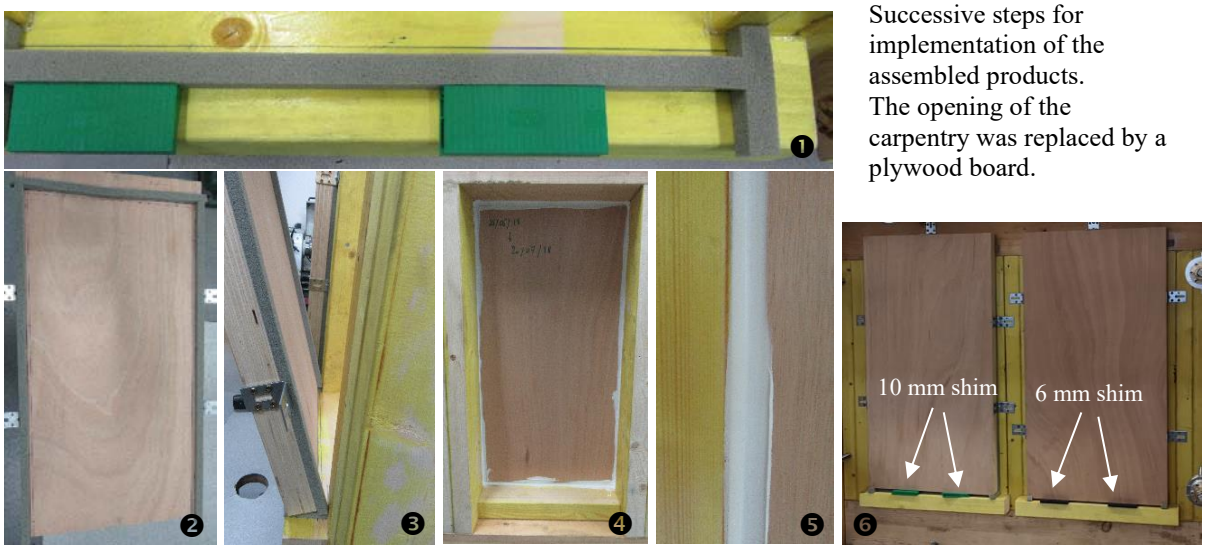

Successive steps for implementation of the assembled products.
The opening of the carpentry was replaced by a plywood board.

Figure 5 : installation of sample n°2

3) *Description of sample n°3 : membrane, adhesive and staples on wooden carpentry*

The sample is the assembly of a membrane taped and stapled on the opening of a wooden carpentry. Two identical membranes were implemented in the sample holder (see figure n°6).

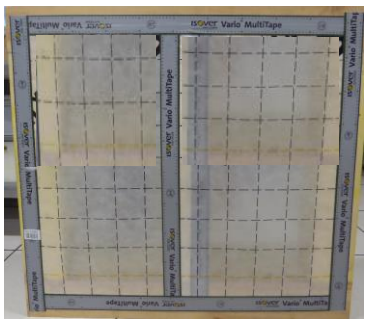

Figure 6 : installation of sample n°3

- the cut-out membrane was positionned flat on the sample support at 3 cm from the edge of the left upright and centered in height
- the membrane was stapled on all edges by positioning a staple every 5 cm around orienting the staples at 45 °
- Adhesive tape was pasted on the central part taking care not to fold

4 RESULTS

4.1 Initial measurements and analysis of sample n°1

Air permeability flowrate measurements for samples 2 and 3 were achieved. However, due to the maximum flowrate delivered of the pressure bench, the pressurization of sample n°1 was impossible to achieve over 15 Pa for positive and negative pressures, see table 3 Complementary tests were performed to ensure the airtightness of the sample holder and are reported elsewhere (Allègre et Louet, 2019).

From figure 7, we can observe that the 3 samples have very different ranges of airflow rate permeability for the initial measurement (i.e., before the ageing test begins). With the sample n°2 as a reference, we assessed at 10 Pa the following ratios between the airflowrate permeability :

- $Q_{10\ sample1}^{+}/Q_{10\ sample2}^{+} = 6.78$ for positive pressures and $Q_{10\ sample1}^{-}/Q_{10\ sample2}^{-} = 5.59$ for negative pressures, extrapolated from the equation 1 for sample 2 and from measured values for sample 1
- $Q_{10\ sample3}^{+}/Q_{10\ sample2}^{+} = 0.05$ for positive pressures and $Q_{10\ sample3}^{-}/Q_{10\ sample2}^{-} = 0.08$ for negative pressures, extrapolated from the equation 1 for samples 2 and 3

These results show no trend on the impact of the pressurization mode (positive or negative) with the corresponding air permeability flowrate.

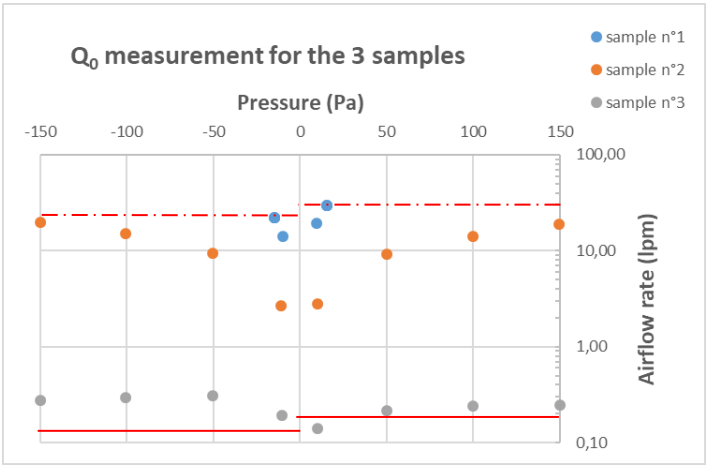

Figure 7 : Results of the samples initial airtightness measurement, permeability as a function of the measured pressure. In red dotted lines, the maximum compensation capacity (air flow rate) of the pressure bench. In red plain lines, the airflow measurement precision.

Table 3 : Sample n°1, measured aiflow rate and differential pressure, as a function of the target pressure (Pa)

+150 Pa	+100 Pa	+50 Pa	+10 Pa	0 Pa	-10 Pa	-50 Pa	-100 Pa	-150Pa
29.6 lpm	29.5 lpm	29.6 lpm	19.4 lpm	0 lpm	14.2 lpm	22.2 lpm	22.2 lpm	22.1 lpm
15.7 Pa	15.7 Pa	15.6 Pa	9.4 Pa	0 Pa	-9.8 Pa	-14.8 Pa	-14.8 Pa	-14.9 Pa

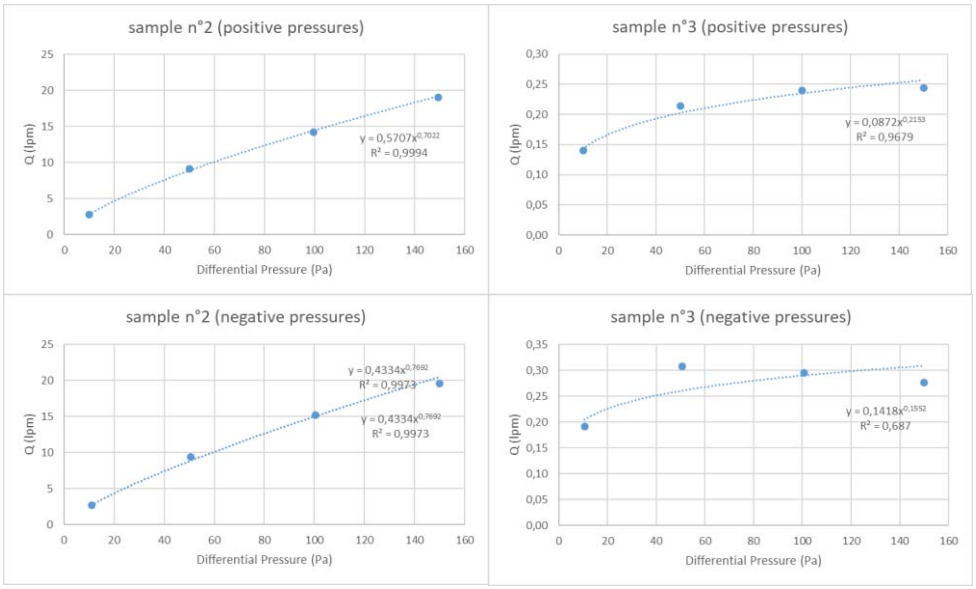

Figure 8 : Results of air permeability flowrates for samples 2 and 3, before ageing test, and the corresponding trendline according to Equation 1.

4.2 Analysis of results of sample n°2

The air permeability flowrate could be measured over the full range (-150Pa to + 150Pa). For each cycle, results were compared with corresponding Q_{test0} results and showed the following trends (see figure 9):

- improved airtightness between Test0 measurement (T0) and Test1 measurement (T1). This improvement was explained by the moisture saturation and therefore the expansion of the wood frame.
- As for T1, we found that T2 showed an improvement in airtightness due to moisture saturation in the wood frame. We could also observe that test T2 did not have any impact on results of T1.
- Although it is of low level, the T3 cycle is the first to deteriorate the airtightness of the sample. The increases of air permeability flow rates were found to be in the range -3% (at -150 Pa) to +7% (at 10 Pa) as compared to test T0
- The rupture occurred after 1h40, corresponding to a temperature of 120 ° C. We observed a sudden drop in pressure and a saturation of the flow. The T4 measurement was performed after sample stabilization and showed a significant impact on the airtightness of the sample for positive pressures, with a difference from -22% to +29% from 10 Pa to 150 Pa for positive pressures ; for negative pressures, the increase was found to be from 0% (at -150 Pa) to +18% (at 10 Pa).

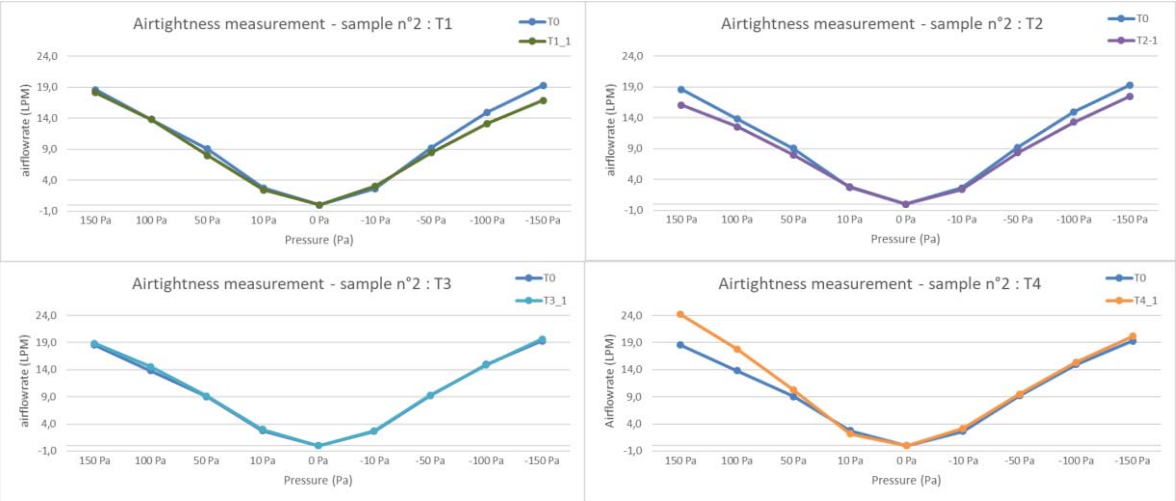

Figure 9: Evolution of air permeability flowrates for sample 2 for the weathering cycle (4 tests)

Table 4 : Sample n°2, results as a function cycles

Cycle	Temperature	RH	Pressure	duration	Results
T1. Thermal Creep	60°C	50%		21 h	improved airtightness between T0
			-50 Pa / +50 Pa	2 h	measurement and T1 measurement.
T2. Weathering	-10 °C			24 h	
	+ 15 °C	60 %		24 h	improved airtightness between T0
	+30%	45%		24 h	measurement and T2 measurement.
	+5 °C			24 h	
	stabilization			12 h	
T3. Wind			-150 Pa to + 150 Pa	8 h (3 times)	Although it is of low level, the T3 cycle is the first to deteriorate the airtightness of the sample
T4. Break	+1°C/min until 120 °C		250 Pa	100 min	The rupture occurred at 120 ° C and showed a significant decrease of the airtightness of the sample.

4.3 Analysis of results of sample n°3

Sample 3 was very airtight, thus, it was very sensitive to pressure variations (both positive and negative). We did not notice any significant deterioration of the air permeability flowrates for the first 3 tests of the cycle. For the break test (test n°4), the rupture occurred after 40 min, at the temperature of 60°C. After the rupture, the sample's air permeability appeared to increase significantly for negative pressures: Q_{test4}/Q_{test0} ranged from a factor of 1.6 to 3.1 according to the measured pressures. For the positive pressures, we found a dramatic increase for the air permeability flowrate (Q_4/Q_0 ranged from a factor of 56.3 at 10 Pa to 135.7 at 50 Pa ; for pressure larger than 50 Pa, the maximum airflow rate capacity of the bench was reached, at 30 lpm).

5 DISCUSSION

The three types of samples made of assembled products as treatments of carpentry airtightness showed very different results, according to the maximum compensation capacity of the air permeability flow rate of the bench. The sample 1 (expansive weather seal foam) appeared to be too porous for our equipment, whereas the sample 3 (adhesive and membrane complex with staples) appeared to be too airtight.

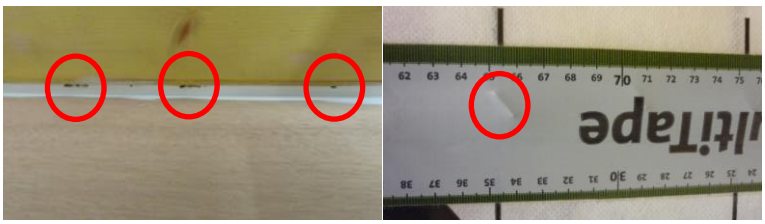

Figure 10: visual observation of cracks on sample n°2 (left, see red; circles) and detached staples (right, see red circles) after the break test

For that reason, no artificial ageing could be achieved with the first sample. On the contrary, for samples 2 (sealant with backing foam) and 3, visual observations on the samples after the ageing test, showed the formation of cracks on sample 2 and the evidence of detached staples on sample 3, creating air leakage occurrences, see figure 10.

Quantitative results confirm these observations, with a slight deterioration of airtightness for sample 2 of up to +7%. Nevertheless, although results show a significant degradation – indeed, quite dramatic, in certain cases – after the break test of sample n°2, we could not draw any conclusion about the artificial ageing of the protocol, due to the elevated temperature of rupture. In fact, the experimental conditions of test n°4 for sample 2 contradicts the previous statement "*Never test products beyond the real life exposure conditions of products*" (see 2.2).

At this stage, preliminary analysis can be addressed regarding the experimental protocol :

- The improvement airtightness during the ageing cycle of sample 2 is probably due to the humidity for the "thermal creep test" and the "weathering test" ; thus we recommend to use inert materials as sample holders for future works.
- As an alternative, we should have investigated the initial state of the sample holder under humidity saturated conditions at T0
- It is interesting to notice that field measurement results from this conference companion paper on Durabilitair research has come to similar conclusions about airtightness durability on wood structure houses, that tend to improve over years [ref Bassam]; probably due to the expansion of the wood with the humidity, that would clog leakages.
- The wind exposure test 3 of the ageing cycle on sample 2 shows a very moderated increase of air permeability. We think that the duration of this cycle was too short, and that exposure durations of at least 1000 h (approximately, 1.5 month) should be necessary; moreover, we suggest that a higher pressure shall be tested to represent more stressing conditions than urban areas
- For the sample 3, it is interesting to notice that during test T1 60°C with a low pressure charge has not induced deterioration in 21 hours but during the break test T4 that occured at 60°C with 250 Pa, it induced a rupture in 40 min therefore the interaction of constraints are critical.

6 CONCLUSION

We developed a $1m^3$ environmental exposure chamber and an experimental artificial ageing protocol, which can test (1mx1m) samples of assembled airtightness products, with a maximum air permeability of approximately 1.8 $m^3/h/m^2$ at 150 Pa. The environmental chamber can expose samples and assess its airtightness up to 29 lpm at +250 Pa (respectively, 22 lpm at -250 Pa), in a temperature range of -30°C to +180°C and humidity of 10% to 95% (saturation). In order to find a compromise between signal stability, usage range and control reactivity on airflow rate, we designed the pressure test bench with technical specifications. We exposed three samples, that presented three orders of magnitude of air permeability. The first sample,

prevented us to achieve the pressurisation of the first sample (that was not enough airtight). The ageing tests of the samples 2 and 3 showed a significant degradation of the airtightness performance after the ageing cycle. We could not assess the artificial equivalent aging of the tests of the latter two samples, because the most significant results were obtained during the break tests (cycle n°4). We conclude that modifying the duration and the characteristics of the exposure cycles (humidity, temperature and pressure) would certainly allow more differentiating results in future works. Hence, we recommend for future investigations to carry out characterizations of the humidity impact and the duration of the pressure exposure. The combination of constraints such as temperature and high pressure is perhaps also to look more in the detail, especially for the membranes.

7 ACKNOWLEDGEMENTS

This work was supported by ADEME and French ministry for construction. The views and opinions of the authors do not necessarily reflect those of ADEME and French ministry. The published material is being distributed without warranty of any kind, either expressed or implied. The responsibility for the interpretation and use of the material lies with the reader. In no event shall authors, ADEME or French ministry be liable for damages arising from its use. Any responsibility arising from the use of this report lies with the user. Authors also thank Ulf Antonsson and Eva Sikander for their welcome in RISE (new name for SP) laboratories in Boras (Sweden).

8 REFERENCES

Allègre, F., Louet, D., (2019), *Réalisation d'essai de perméabilité à l'air – Projet DURABILITAIR*. RESCOLL (confidential)

Ackermann, T. (2012). ALTERNATING LOADS – A METHOD FOR TESTING THE DURABILITY OF ADHESIVES IN AIR TIGHTNESS LAYERS.

Antonsson, U. (2015). *Utveckling av metodik för verifiering av bestän- dighet hos system för lufttäthet, etapp 1.* Boras: SPSverigesTekniskaForskningsinstitut.

Langmans, J., Desta, T., Alderweireldt, L., & Roels, S. (2015). Laboratory investigation on the durability of taped joints in exterior air barrier applications. *36th AIVC Conference, Madrid, Spain, 23-24 September 2015* (pp. 615-623). AIVC.

ISO 15927-1:2003 (2003) "Hygrothermal performance of buildings – calculation and presentation of climatic data – part1: Monthly means of single meteorological elements", International Organization for Standardization

Leprince, V., Moujalled, B., Litvak, A. (2017) *Durability of building airtightness, review and analysis of existing studies* 38th AIVC Conference, Nottingham, United Kingdom, September 2017. AIVC

Michaux, B., Mees, C., Nguyen, E., & Loncour, X. (2014). Assessment of the durability of the airtightness of building elements via laboratory tests. *35th AIVC Conference, Poznań, Poland, 24-25 September 2014* (pp. 738-746). AIVC.

Moujalled, B., Berthault, S., Litvak, A., Leprince, A., and Frances, A. (2019) *Assessment of long-term and mid-term building airtightness durability: field study of 61 French low energy single-family dwellings* 40th AIVC Conference, Ghent, Belgium, October 2019. AIVC

Ylmén, P., Hansén , M., & Romild, J. (2014). Durability of airtightness solutions for. *35th AIVC Conference, Poznań, Poland, 24-25 September 2014* (pp. 268-278). AIVC.

Moisture impact on dimensional changes and air leakage in wooden buildings

Paula Wahlgren[1*], Fredrik Domhagen [2]

1 Chalmers University of Technology
Building Technology
412 96 Gothenburg, Sweden
**Corresponding author:*
paula.wahlgren@chalmers.se

2 Chalmers University of Technology
Building Technology
412 96 Gothenburg, Sweden

ABSTRACT

Wood is a hygroscopic material, it has the ability to adsorb or desorb water in response to the ambient relative humidity. Thus, the ambient air will affect the moisture content of the wood, and in turn, the dimension of the wood. If the wood itself is part of the air barrier in a construction, the shrinking and expansion can create gaps in the construction, for example in the window sill. In case of an air barrier consisting of a foil, the joints in the foil can be clamped by wooden joists, or the foil can be taped to wooden part. In both cases, the movement (shrinking, expanding) can cause air leakages, in particular since wood is an anisotropic material and will behave differently in different directions.

This project investigates the air leakages that occur in wooden buildings from seasonal variations in climate and from finished construction (first airtightness measurement) to equilibrium (when inbuilt moisture has dried out). Measurements are made in real buildings (full scale) and in laboratory (climate chamber). The full-scale measurements on buildings with wooden construction have shown magnitudes of up to 10% increase in air leakage (at 50 Pa) for the seasonal variations and the increase for reaching equilibrium in a newly built construction is 20%.

KEYWORDS

Airtightness, wooden buildings, air leakage,

1 INTRODUCTION

The Swedish government has expressed an interest in increasing the use of wood in constructions. The described benefits are lower carbon footprint, decreased production cost, and an increased competitiveness of the Swedish wooden industry. Residential buildings are of particular interest since there is a housing shortage in many Swedish cities. Some challenges can however be found in wooden buildings, for example, fire resistance, sound propagation, moisture/durability and airtightness. The airtightness is of great importance to the performance of the building since it can greatly affect the energy use and the moisture safety.

Wood is a hygroscopic material which means that it can adsorb or desorb water in response to the ambient relative humidity. Thus, the ambient air will affect the moisture content of the wood, and in turn, the dimension of the wood. If the wood itself is part of the air barrier in a construction (for example cross-laminated timber, CLT), the shrinking and expansion can create gaps in the construction, for example in the window sill. In case of an air barrier consisting of a foil, the joints in the foil can be clamped by wooden joists, or the foil can be taped to wooden parts. In both cases, the movement (shrinking and expanding) can cause air

leakages, in particular since wood is an anisotropic material and will behave differently in different directions.

The current project aims to investigate the impact of moisture on the air leakage in light weight wooden houses (LW) and in cross laminated timber (CLT). Both seasonal moisture variations (summer/winter) and the initial drying of a building is studied.
Following investigations have been made:

- Field measurements of moisture conditions (LW)
- Moisture induced dimension changes (LW, CLT)
- Air leakage calculations (LW, CLT)
- Tape durability testing (CLT)
- Drying time calculations (LW)
- Full scale airtightness measurements (LW)
- Leakage consequences on heat exchange in a building

2 WOOD CONSTRUCTION AND AIRTIGHTNESS

Wood constructions are either lightweight constructions (load bearing wooden constructions, Figure 1) or massive constructions such as cross laminated timber, CLT (Figure 3).

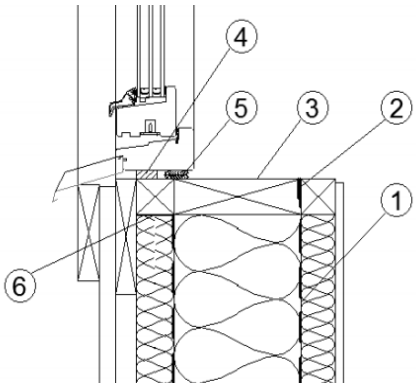

Figure 1: Light-weight wooden construction (Derome, 2019)

Commonly, light-weight wooden constructions depend on a polyethylene foil close to the inside for air tightness (the foil also serves as diffusion barrier). To have a completely airtight building, the air barrier must be continuous. For the window setting it is recommended that the foil is properly attached to the window. An example of a solution with good airtightness is shown in Figure 2 where one foil is stapled and taped to the window and one is extended from the wall. These separate foils will then be taped together.

Figure 2: Window setting with two separate foils that will be sealed together to an airtight joint (Wahlgren, 2010).

This type of work is quite time consuming to produce. However, with this solution the wooden members behind the foil are less affected by interior moisture. In Figure 1, the solution that is used for prefabricated walls is shown. Here, the polyethylene foil is cut around the perimeter of the window. It is taped, using double-adhesive butyl sealant (no. 2) and clamped with the inner joist of the wall. For this case, the shrinking of joist no. 3 in Figure 1 is essential. If this joist shrinks, it might create a vertical or horizontal gap under the diffusion tight sealing around the window (no. 5) or open up the gaps in the corners of the window created at the end of each window joist (no. 3).

The cross-laminated wooden elements, shown in Figure 3, are usually considered very airtight. However, Skogstad et al. (2011) measured two types of element; one type where the boards are glued on all four sides, and one type that are only glued on the two sides parallel to the largest element sides. They measured at two moisture content levels, 14% and 10%. The result was that the initial air leakage (at 14%) was almost the same for the two types, but when the elements were dried, the air leakage increased with a factor of ten for the type glued on four sides and doubled for the type glued on four sides.

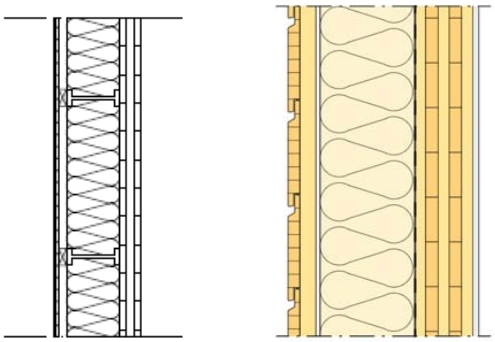

Figure 3: CLT wall (Stora Enso, 2019, left, Träguiden, 2019, right)

For both types of construction, it is essential that the connections between the elements are airtight. Swedish Wood (Svenskt trä, 2019, a department within The Swedish Forest Industries Federation) recommend a polyethylene foil to ensure airtightness. Stora Enso (CLT manufacturer) recommends no polyethylene foil in the construction and the connections can be sealed by flexible joint foams, self-adhesive tapes or tubular rubber seals (Stora Enso, 2019). There are different opinions on which strategy results in the best long-term airtightness and moisture safety. In this project, the durability of tape on wood is investigated.

3 MOISTURE LEVELS AND DIMENSIONAL CHANGES

Wood expand in moist environment (and shrink in dry environment), the dimensional change depends on the change in moisture content. How much the moisture content vary between different environments is described by the sorption isotherm, see Figure 4, where the condition of the environment is defined by the relative humidity, RH, in the air. The airtight layer is either the polyethylene foil or the CLT element. Both are placed on the inner side of the construction and, consequently, the inner relative humidity is more important to the airtightness. The relative humidity indoor ranges from 10-80% depending mainly on the activities in the building, the ventilation rate, the air leakage and the location of the building (10% RH indoor mainly occurs in northern Sweden during wintertime). However, the variation of indoor RH for a specific building is usually smaller.

In new buildings the wood is delivered with a certain moisture content (kg/kg, %), usually average 16% and allowed variation between 11,2 and 20,8% (as described in SS-EN 14289).

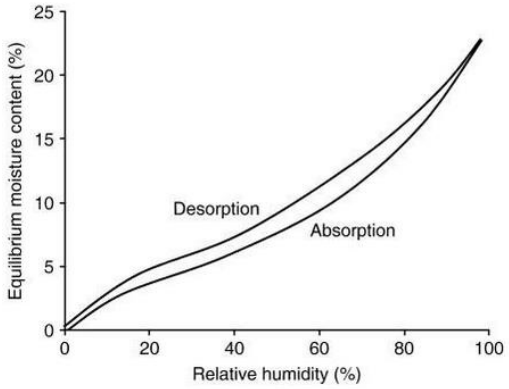

Figure 4: Sorption isotherm for timber (Building research establishment, xxxx)

To get an estimate of the moisture content that wood will have when it is built into a prefabricated light-weight construction, the moisture content (quotient) was measured at four different locations at the production site for prefabricated buildings during wintertime (Billemar, 2019). Each time 9 to 13 boards were measured at three different points on each board.

The first measurement is outdoor, after sawing. For this occasion, the average moisture content (quotient) is 10,2 %. When the prefabricated wall is being built, the average moisture content is 10,6% and when the wall is ready for application, the average moisture content is 10,5% and the maximum moisture content is 16,5% (at this production site, a moisture content of 18% is approved). After this, the wall might be stored in an environment with a higher relative humidity or rain exposed, without weather protection. This situation was studied by Olsson (2014). He followed 24 prefabricated detached houses from production of elements to finished house. Relative humidity, and moisture content was measured, and mold growth was evaluated. Elevated or high moisture content were found on one third of all the samples, 15% of the samples had a moisture content above 25% and microbial growth was found on almost one third of all the samples that were taken. There is not one single point of failure that causes the high moisture content, precaution is needed in all steps of the building process. However, protection of elements from rain is essential. In the following a moisture content of 25% is used as a worst case to estimate air leakage paths that are created when wood is drying after the building is finished.

4 DIMENSIONAL CHANGES

Wood is an anisotropic material, thus the shrinkage is different in different directions. According to Burström (2008), pinewood has a shrinkage of 7,7% tangentially, 4,0 % radially and 0,4% along fibres. The shrinkage, α_f (%) from fibre saturation to dry wood is used to calculate the actual shrinkage from one moisture content, u_2 (%) to another, u_1 (%), where u_f is the moisture content at fibre saturation

$$\Delta\alpha = \frac{u_2 - u_1}{u_f} \cdot \alpha_f \ (\%) \qquad (1)$$

CLT elements consist of at least three single-layer panels (made of pinewood, fir or hardwood) that are bonded together crosswise to obtain good stability. Swedish Wood (2019) describes the dimensional changes along the plane of CLT elements as being between 0,016-0,023 % per percentage point of change in moisture content, which is slightly more than the change parallel to the fibres (stated average 0,01-0,02%). The dimensional change along the thickness of the element is not described but based on the construction of the component, it should be between the radial shrinkage, 0,19%, and the tangential shrinkage, 0,36%, per percent point change in moisture content. Using the values for shrinkage from Burström (2008) and a u_f of 30% to calculate the shrinkage per point change in moisture content results in values similar to those of Swedish wood.

To calculate the air gaps created by the shrinkage of a CLT wall, a wall to wall corner was studied where the walls are 15 m long and the CLT is 100 mm thick, insulated on the outside and thus exposed to the inner climate of the building, see Figure 5.

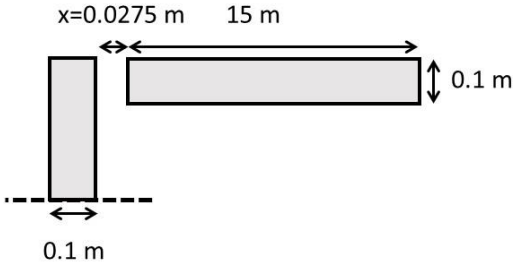

Figure 5: Resulting air gap, x, at the meeting of a 15 m long element and a 0.1 m thick element.

Using pinewood with an initial moisture content of 25% and drying to an indoor relative humidity of 20%, which corresponds to a moisture content of approximately 6% (worse case), results in a gap with a width of 0,0275 m. There will be additional insulation and wind protection outside this gap that substantially reduce the air leakage, but as a calculation example, a gap with the length of 100 mm and width of 0,0275 m will result in an airflow of 187 l/s per meter gap at a pressure difference of 50 Pa, which is the pressure difference used for the evaluation of a building's airtightness. A 100 m² quadratic building of height 3 m, with these gaps in each corner, would have an air permeability of 7 l/m²s. As a comparison, the Gothenburg municipality in Sweden require a maximum air permeability of 0,2 l/m²s for newly built schools. Consequently, it is essential to avoid gaps through the construction and joints must be additionally sealed. Another issue with CLT wood is that the elements are not always completely flat at edges, which also creates gaps.

For the window setting in Figure 1, the gap (at no. 5) caused by the shrinkage of the wood (from 25% to 6% as above) is calculated for a joist of 145 mm width. This results in a gap with the dimensions of 7 mm in case of the joist being attached to one side so that the whole

shrinkage occurs on the other side. Corresponding air flow around a window with dimensions 1,2·1,2 m and a pressure difference of 50 Pa is 226 l/s (without other materials). Thus 2 to 3 windows on each side of the building will result in the same air permeability as the previous case.

Another example of an important detail is the connection of an attic hatch in the attic floor. If this detail is not airtight, moist air will be transported to the cold attic above, in particular during wintertime, which can result in moisture damage. For low-energy houses with high demands on airtightness, the access to the attic is recommended from the outside instead. In Figure 6, an indoor attic hatch is illustrated including arrows that show the most likely leakage path. Calculations of the gap width and corresponding air leakage when the building is in use (ΔP_{est}=4 Pa) is made for different levels of indoor RH. It is assumed that the frame in which the attic hatch is fastened is swelling or shrinking which changes the gap width. Figure 7 shows simulations of the total airflow through the gap in the attic hatch at different RH at a pressure difference of 4 Pa. Maximum gap width is 0,0032 m (at RH 28%).

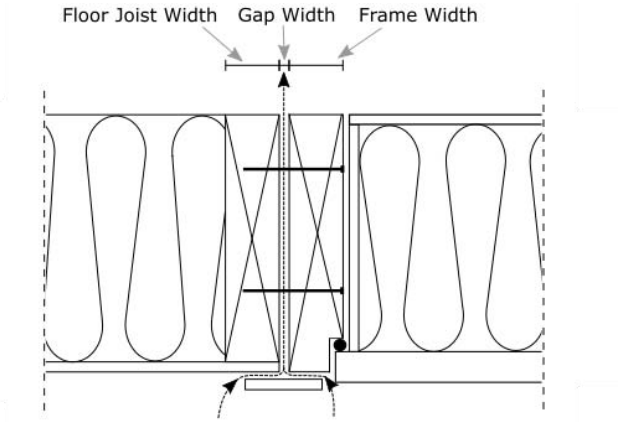

Figure 6: Connection of attic hatch to attic floor showing the most likely leakage path.

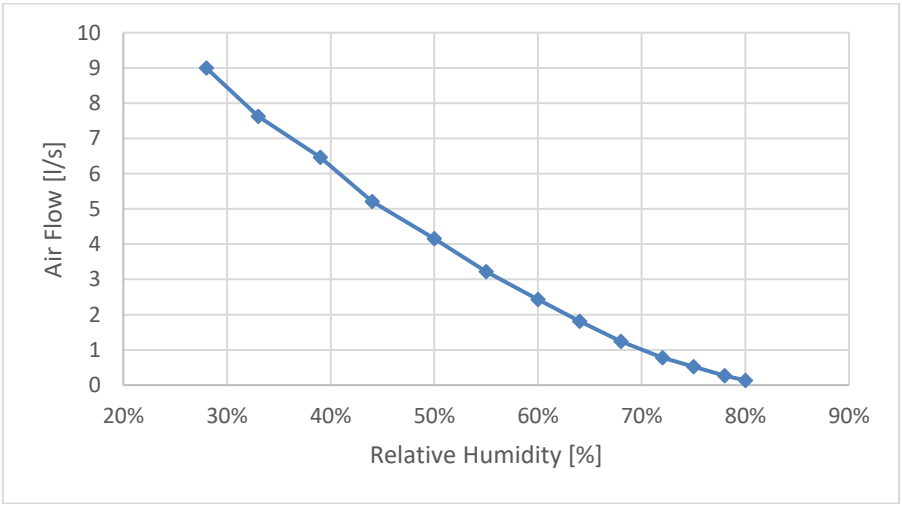

Figure 7: Total air flow through the gap around the attic hatch at a pressure difference of 4 Pa.

As a preparation for the field measurements described in section 6, an evaluation was made of the drying time (from construction) of a light-weight construction. The example consists of a construction with joists that clamp the joints of polyethylene foil behind a gypsum board/plaster board in a wall. The joists are exposed to the surrounding environment on three

sides and in connection with the polyethylene foil on one side (no moisture exchange). The simulation starts when the building is finished and has a moisture content of 16% (80% relative humidity), continues for two years, reaching equilibrium with the indoor environment. According to the simulation, the joists reach equilibrium after slightly more than two months. This is shown in Figure 8.

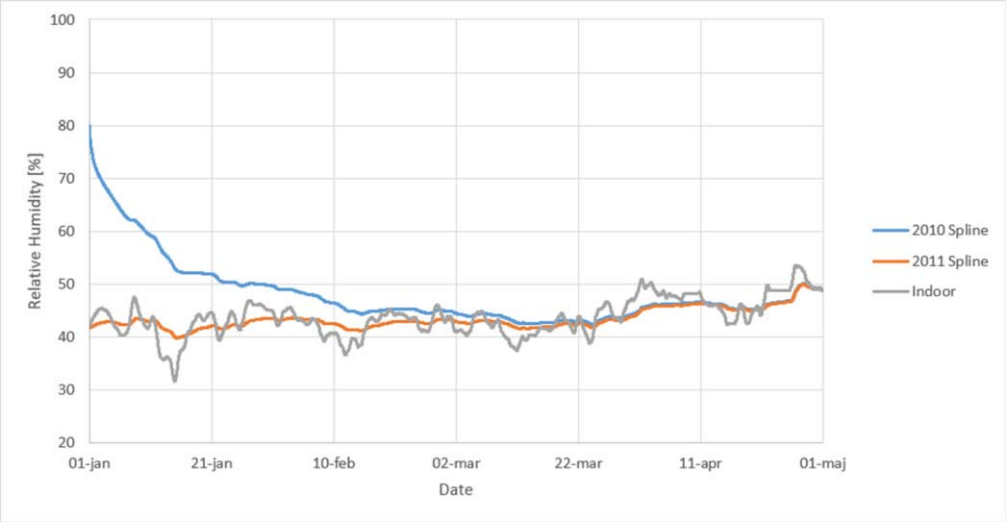

Figure 8: Drying of wooden parts behind the plaster board in an external wall.

In comparison, the drying out time of the external walls of CLT buildings with polyethylene foil has been numerically simulated by Shareef et al. (2019). The drying out time ranges from four to nine years. In addition, they conclude that the polyethylene foil increases the risk for mold growth, since the drying out time is increased, and that taping of joints should be enough to ensure airtightness.

5 TAPE DURABILITY

The joints in the CLT construction can be taped, as described above. There are some difficulties however, as described in Shareef et al. (2019) and Andersson et al. (2019), such as using the tape in moist, cold and dusty environments, getting a proper application in corners, avoiding stretching of the tape and creases.

The durability of two types of tapes on wood has been tested in a climate chamber (Andersson et al., 2019). The CLT wood pieces with tapes are cycled 50 times from 80% RH to 10%, with 4 hours at each level and 20 minutes for transition, checked and then run another 50 cycles. The tapes are applied to corners (a.), joints (b.) and with imperfect underlay. The underlay has dust from either concrete or wood, or is slightly moist, as can occur at a building site.

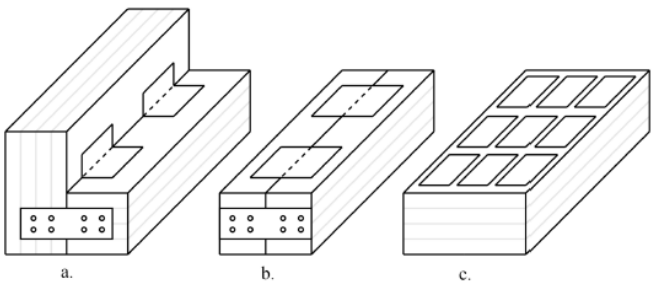

Figure 9: Configuration used for tape testing

After the tests, the tape has in some cases shrunk. This is probably caused by the tape being stretched too much when applied. The taping of corners resulted in some creases (Figure 10, left). These were worsened after cycling (Figure 10, right). As were the bubbles created by the dusty surfaces. Further evaluation of the long-time airtightness performance of tape on wood is recommended.

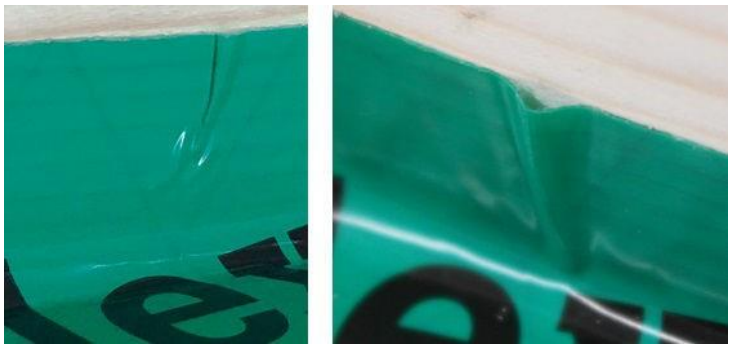

Figure 10: Change in adhesion (50 cycles apart).

6 AIRTIGHTNESS MEASUREMENTS AND SIMULATIONS

In order to evaluate the change in airtightness due to drying of the wooden construction, a newly constructed building (school, required $q_{50} \leq 0.2$ l/m²s) with wooden frames was followed from completion and 1.5 years. The results are shown in Figure 11. The initial air permeability was 0.21 l/m²s and the final air permeability 0.25 l/m²s, an increase of almost 20%. The measurement performed on the 7th of August is performed at very high outdoor (27°C) and indoor temperatures (24°C) and in the middle of a heat wave in Sweden, this might have resulted in thermal expansion of parts of the thermal envelope. The relative humidity indoor is approximately the same as the measurement in June. Previous work (Wahlgren, 2014) has shown seasonal variations in wooden buildings of almost 10%.

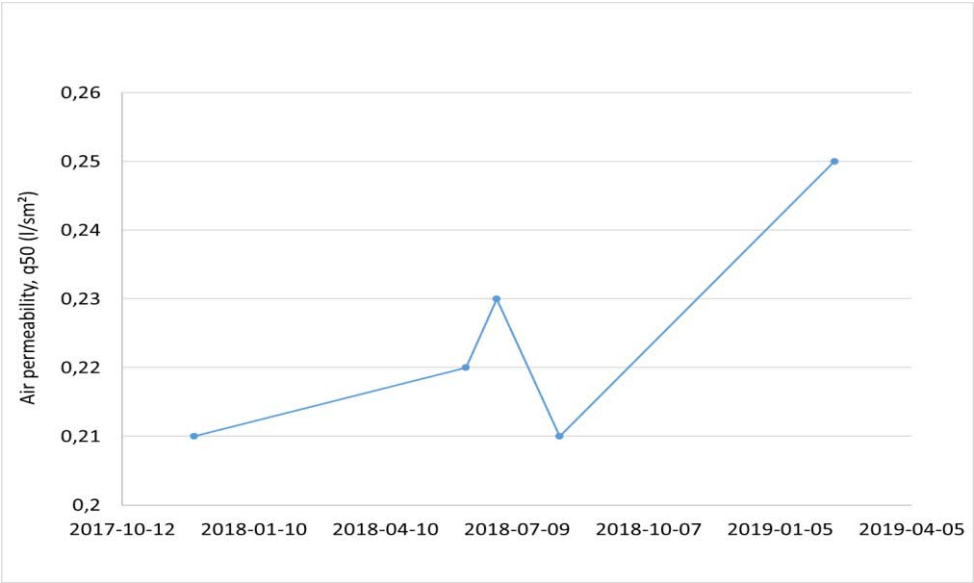

Figure 11: Measured air permeability from completion of building.

7 CONSEQUENCES

The impact of varying airtightness on energy use, moisture safety and transport of contaminants through the thermal envelope have previously been investigated and is discussed in for example Domhagen (2016), Domhagen et al. (2017 a) and Domhagen et al. (2017 b). There is also an impact on the heat exchange in the building, both on the heat exchanger efficiency, and because of air passing through the thermal envelope instead of through the heat exchanger.

The heat exchanger reduces the energy use in dwellings by using the exhaust ventilation air to preheat the supply air. In Sweden a common praxis is to adjust the supply ventilation flow to 90% of the exhaust ventilation flow. This causes a negative indoor pressure typically a few pascals. The purpose of the negative pressure is to reduce leakage of air from the interior to exterior and lower the risk of condensation inside the construction, such as the previous example with the attic hatch. The drawback however, is that the imbalance between supply and exhaust fans increases the air infiltration through the thermal envelope so that less air passes through the heat exchanger.

To investigate this phenomenon a dwelling with a heat exchanger is simulated. The building is a two stoMrey building with a floor area of 180 m^2. Simulation is carried out for a calm day (no wind) with an indoor air temperature of 20°C and outdoor air temperature of -4°C. Results show that if the air permeability increases from 0,2 to 0,6 l/s at 50 Pa, the efficiency of the heat exchanger increases with 1,2%. If the airtightness increased from 0,6 to 1,2 the efficiency of the heat exchanger increases with 0,08%. Thus, the effect on the efficiency of the heat exchanger is not very large. However, the airflow imbalance also affects the air infiltration. For the two cases the infiltration increased from 6,6 l/s to 14,7 l/s (122%) and from 14,7 l/s to 25,8 l/s (75%), this would require extra heating of 233 W and 320 W respectively.

8 CONCLUSIONS

Investigations have been made of the impact of moisture on the air leakage in light weight wooden houses and in cross laminated timber (CLT). Both seasonal moisture variations (summer/winter) and the initial drying of a building is studied. Field measurement at a production site of prefabricated light-weight wooden buildings resulted in a maximum moisture content in wood of 16.5%.

For estimation of dimensional changes in CLT buildings and in light-weight buildings a worse case of 25% moisture content was used. These calculations resulted in gaps due to shrinking of several centimeters. Resulting air flows were calculated both for fan pressurization tests (ΔP=50 Pa) and for normal usage (ΔP_{est}=4 Pa) showing the necessity to properly seal all leakages. In many cases, taping is used to seal such gaps, unfortunately, the durability of the tape is sometimes not enough to ensure good airtightness for a longer time. Also, the craftmanship and surrounding circumstances such as dust and moisture may affect the performance of the tape.

Several full-scale measurements of the airtightness of a newly built light-weight building have been performed for 1.5 years. During this time, the airtightness increased from 0.21 to 0.25 l/m²s (almost 20% increase). The consequence of a decrease in air permeability is a slight increase in the efficiency of the heat exchanger and, at the same time, a much larger imbalance in the air flows through the thermal envelope, resulting in an increase in air infiltration to the building (more than 100% increase is shown).

9 ACKNOWLEDGEMENTS

For moisture content measurements we acknowledge Oskar Konkell and Emanuel Billemar at Chalmers, for tape durability measurements we acknowledge Jenny Andersson, Daniel Arvidsson, Gunnar Bergström, Emil Hultberg and Elin Nilsson at Chalmers, and for air permeability measurement, Magnus Hansén at Rise.

10 REFERENCES

Burström, P G. (2008). Byggnadsmaterial (Building material, in Swedish), Studentlitteratur, ISBN 978-91-44-02738-8

Domhagen, F. (2016). *Yearly Variations in Airtightness of Detached Wooden Houses: Simulations and Laboratory Measurements to Investigate Causes and Consequences.*: Division of Building Technology, Chalmers University of Technology, Sweden

Domhagen, F., Wahlgren, P. (2017 a). Air leakage variations due to changes in moisture content in wooden construction - magnitudes and consequences, *AIVC38th AIVC Conference,* Nottingham, United Kingdom, 2017

Domhagen F, Wahlgren P, (2017 b), Consequences of Varying Airtightness in Wooden Buildings, *Energy Procedia 132*, 2017

SS-EN 14298:2004. (2005). Sawn timber- Assessment of drying quality (EN 14298), Swedish standards institute, Sweden, 2005

Wahlgren, P. (2010), Goda exempel på lufttäta konstruktionslösningar (Good examples of airtight solutions, in Swedish), *SP Report 2010:09*, SP Technical Research Institute of Sweden

Wahlgren, P. (2014). Airtightness variation over the year, *AIVC35th AIVC Conference,* Poznan, Poland, 2014

Olsson L. (2014). *Moisture Conditions in Exterior Wooden Walls and Timber During Production and Use*, Department of Civil and Environmental Engineering, Division of Building Technology, Chalmers University of Technology, Gothenburg, ISSN no. 1652-9146, Sweden, 2014

Swedish Wood. (2019). Träguiden, Svenskt trä (in Swedish). Retrieved 2019-06-28. https://www.traguiden.se/konstruktion/kl-trakonstruktioner/kl-tra-och-varme-och-fukt/

Shareef, S., Alyaseen, H. (2019). *Analys av mögelrisk när KL-trä används i klimatskal* (Analysis of mould growth risk when CLT wood is used in the thermal envelope, in Swedish), Division of Building Physics, Lund University, Sweden ISRN LUTVDG/TVBH--19/5102--SE(173)

Association between Indoor Air Quality and Sleep Quality

Chenxi Liao*[1], Marc Delghust[1] and Jelle Laverge[1]

1 Ghent University, Sint-Pietersnuwestraat 41, Ghent, Belgium
**Corresponding author: Chenxi.Liao@Ugent.be*

ABSTRACT

The association between indoor air quality (IAQ) and sleep quality was investigated in this study. A total of 27 participants (14 males and 13 females, 20-33 yrs.) without any sleep disorders and chronic diseases were recruited and divided into two groups: a polysomnography (PSG) group and a non-PSG group. The IAQ was changed by opening or closing windows. There were two phases for the experiment and two nights in each phase including one adaptive night and one test night, and around one-week washout period between two phases. A questionnaire, Fitbit and home PSG – the Nox A1 (from Resmed) were used for measuring sleep quality. Bed temperature, ambient temperature, relative humidity, CO_2 levels, TVOCs, $PM_{2.5}$ and noise were recorded by different sensors during sleep. Mann-Whitney *U* tests and multivariate linear regression models were used for statistical analyses and individual differences between two phases were also analyzed. Higher ambient temperature, RH and CO_2 levels were monitored with the window closed compared to it open. The participants had on average a 0.87 point higher score on the Groningen sleep quality scale (GSQS) sleeping with the window open than with it closed. Higher $PM_{2.5}$ levels were associated with time awake (β, 95% CI: 1.546, 0.124 - 2.968; *p*-value < 0.035), percentage awake (β, 95% CI: 0.342, 0.091 - 0.592; *p*-value < 0.010) and sleep efficiency (β, 95% CI: -0.342, -0.592 - -0.091; *p*-value < 0.010). Higher ambient temperature was associated with the number of awakenings (β, 95% CI: 3.074, 0.331 - 5.816; *p*-value < 0.030). In conclusion, the participants reported better sleep quality sleeping with quieter surroundings (windows closed). Higher $PM_{2.5}$ level was associated with more time awake, higher percentage awake and lower sleep efficiency. Higher ambient temperature was associated with an increased number of awakenings.

KEYWORDS

Indoor air quality; Field study; Sleep quality; Fitbit; Polysomnography

1. INTRODUCTION

Human beings spend one-third time of a day sleeping. Although some people have a relaxed mood, and sleep in the bedrooms with low noise, moderate light and appropriate temperature, they cannot sleep well probably because of poor air quality.

There are only a few studies about indoor air quality (IAQ) and sleep quality, although some of them conclude that IAQ is related to sleep quality (Mishra et al., 2018; Strom-Tejsen et al., 2016). Mishra et al. (2018) conducted a field experiment where the IAQ was changed by opening and closing doors/windows and obtained that questionnaire-based depth of sleep (p = 0.002) and actigraphy-based sleep phase (p = 0.003) were significantly different between open and closed conditions. Better sleep depth, sleep efficiency, and fewer number of awakenings were found with lower CO_2 levels (Mishra et al., 2018). Strom-Tejsen et al. (2016) controlled the IAQ via opening and closing windows in a pilot experiment, while turning on and off the fans in a follow-up experiment. Sleep latency was significantly better with the window open (p < 0.0480) and sleep efficiency with the fan in operation (p < 0.0494). Also, subjective assessment of sleep quality improved.

Psychologic states and dietary habits are also significantly associated with sleep quality. Depressed mood is contributing to decreased overall sleep quality and sleep latency (Menefee

et al., 2000; Owens and Matthews, 1998). Alcohol, coffee, tea and tobacco are all associated with sleep quality. The degree of correlation might be varied by important confounders, like dietary habits and lifestyles (Ogilvie et al., 2018). Regarding IAQ, higher ventilation rates indicate good IAQ and CO_2 could be an indicator for bedroom ventilation. In addition, indoor comfortable parameters, such as temperature (T) and relative humidity (RH) influence sleep quality (Caddick et al., 2018).

Indoor environmental parameters of ambient T, RH, CO_2, total volatile organic compounds (TVOCs), $PM_{2.5}$, noise and bed T would be monitored between the window closed and open. Meanwhile, both subjective and objective assessments would use to test the participants' sleep quality. The purpose of this study is to confirm the association between IAQ and sleep quality.

2. METHOD

A self-controlled case series method was used for two conditions with the window open or closed during sleep. Indoor environmental parameters were recorded by several types of indoor air monitors and also assessed by the participants via questionnaires. Fitbit, home polysomnography (PSG) and the Groningen Sleep Quality Scale (GSQS) were used to measure the participants' sleep quality. The abbreviated Profile of Mood States (POMS) and the Perceived Stress Scale (PSS) were performed at the test nights via a night questionnaire. In addition to sleep environment, the GSQS, the Karolinska Sleepiness Scale (KSS), and other questions were filled on the next day morning after the test nights via a morning questionnaire.

2.1. Study design

There were two phases for the whole test, two nights in each phase (the first an adaptive night and the second the test night) and around one-week washout period between two phases (Heo et al., 2017). Participants were divided into 2 groups: a polysomnography (PSG) group and a non-PSG group due to the limited number of PSG-monitors available. There were 4 participants doing the sleep tests at each night – two of them were in the PSG group and the other two were in the non-PSG group. Participants were asked not to have alcohol, caffeine drinks, tea, tobacco and intensive physical activities at least 12 hours prior to their bedtimes at the test nights.

2.2. Participants and base

The online questionnaires of the Pittsburgh Sleep Quality Index (PSQI) were sent to all the tenants that lived in the university dorm with the help from the dorm manager. Those interested in this sleep test filled and submitted the PSQI. 28 participants were selected based on 3 selection criteria - the PSQI score was less than or equal to 5, non-smokers, and no sleep disorders nor any chronic diseases. Four rooms furnished uniformly next to each other were rented in the same university dormitory in April 2019. IAQ was controlled by opening or closing the windows during sleep (two rooms with windows open and the other two with windows closed). We paid the participants from the non-PSG (PSG) groups €50 (€75) each after the experiment.

2.3. Indoor environment and bed temperature

Ambient T, RH, CO_2, TVOCs, $PM_{2.5}$, noise and bed T were monitored during the experimental period. Table 1 shows the brands, types, accuracies, measuring ranges and recorded intervals of all the devices used. The adjustable waist band with the temperature data logger inside is

shown in Figure 1. The participants wore the bands underarm with the temperature data logger in front of the chest for the purpose of measuring the bed T.

Table 1: The details of the air monitoring devices used

Parameter	Device/Sensor	Accuracy	Measuring range	Recorded interval
Ambient temperature	Netatmo	± 0.3 °C	0-50 °C	5 min
Relative humidity		± 3 %	0-100 %	
CO_2		± 50 ppm (from 0 to 1,000 ppm) ± 5% (from 1,000 to 5,000 ppm)	0-5000 ppm	
Noise		-	35-120 dB	
TVOCs	Awair	± 10 %	175-3500 ppb	
$PM_{2.5}$		± 15 %	0-500 µg/m³	
Bed temperature	HOBO U12-012	± 0.35 °C	-20-70 °C	

Figure 1: Adjustable waist band with the temperature data logger (HOBO U12-012) inside

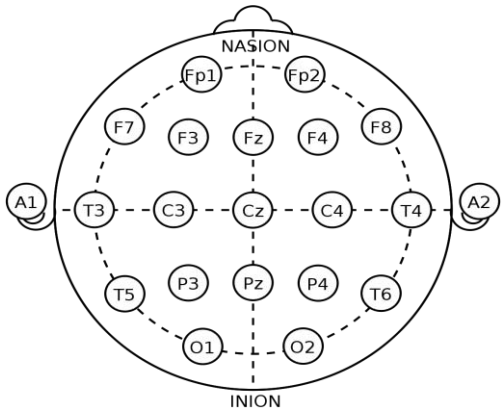

Figure 2: Electrode locations of the international 10-20 system for EEG (originated from WIKIPEDIA)

2.4. Assessments of the sleep quality

Both subjective and objective assessments were applied to test sleep quality, including the GSQS, Fitbit and PSG. The KSS was used to measure sleepiness. Other sleep-related factors, such as mood and stress, were measured via the POMS and PSS questionnaires respectively.

2.4.1 Objective assessments of sleep quality. We used two kinds of devices for sleeping tests: two sets of the home polysomnography (PSG) – the Nox A1 from Resmed company (only for half of the participants) and four Fitbit Charge 2 smartwatches. Each participant would wear the Fitbit (and PSG) during both adaptive and test nights.

The Nox A1 contains Electroencephalography (EEG), Electrocardiography (ECG) and chin Electromyography (EMG). The EEG of the Nox A1 includes 10 channels (electrodes). Each electrode placement site has a letter to identify the lobe, or area of the brain it is reading from pre-frontal (Fp), frontal (F), temporal (T), parietal (P), occipital (O), and central (C). Figure 2 shows the electrode locations of the international 10-20 system for EEG. Among those locations, C3, C4, F3, F4, A1, A2, O1 and O2 were used in the Nox A1. The Nox A1 was set up via the Noxturnal software system beforehand. Electrodes and sensors were attached to the participants' heads 1-2 hours before the bedtimes of them. Afterward, the Noxturnal tablet app was used to perform bio-calibration and impedance checks next to the subjects. The sleeping results were analyzed automatically by the Noxturnal software system. Sleep scoring includes analysis start time, analysis stop time, total sleep time (TST), analysis duration (TRT), sleep latency (SL), REM latency, Wake After Sleep Onset (TRT-SL-TST), sleep efficiency (TST/TRT*100). Sleep stages include N1, N2, N3, REM and wake. Interruptions of sleep last

3 to 15 seconds were defined as arousals (ASAA, 2019). Arousal parameters include arousal index (AI; in TST), arousal count (in TST) and arousal count in wake (the arousal lasts more than 15 seconds).

The Fitbit Charge 2 smartwatch shows sleep quality based on 3 sleep stages: light, deep and REM. These stages are estimated based on heart rate and limb movement. Sleep start time, sleep end time, asleep, awake, time in bed (TIB), REM, light sleep, deep sleep and SL could be obtained from the Fitbit. Light sleep contains sleep stages N1 and N2, whereas deep sleep corresponds to N3.

2.4.2 Subjective assessments of sleep quality. The GSQS (in the morning questionnaire) which measures sleep quality for a single night was used for the self-evaluation of sleep quality in the next morning after the test nights. It includes 15 true or false questions and the answers are summed into a single number indicator. The score is from 0 to 14 and the maximum score indicates poor sleep quality the night before.

2.5. Morning questionnaire

In addition to the GSQS, the KSS and questions about sleep environment were also included in the morning questionnaire filled by the participants the morning after the test nights. Sleep environment was assessed by applying a similar method as Strom-Tejsen et al (2016) used. The KSS is a tool to evaluate subjective sleepiness and verified to be closely correlated to the results electroencephalogram (Kaida et al., 2006). Sleepiness is evaluated by a 9-point scale from 1 (extremely alert) to 9 (extremely sleepy). In addition, other questions were included – pajamas, earplugs, eye mask, and socks worn, how many times the participants woke up and why, and also the bedtime and get up time were reported by themselves. The analysis start time and stop time of PSG were also adjusted based on the self-reported bedtime and get up time.

2.6. Night questionnaire

As the mood and stress influence sleep quality, the abbreviated POMS and the PSS were used to test them. The abbreviated POMS contains 40 items where five negative subscales and two positive subscales including anger, fatigue, depression, confusion, esteem-related affect and vigor. Total Mood Disturbance (TMD) is calculated by summing the totals for the negative subscales and then subtracting the totals for the positive subscales (Grove et al., 2013). The higher the score of TMD, the worse the mood. The PSS contains 10 questions to test the stress during the last month. Scores ranging from 0–13, 14–26 and 27–40 respectively indicate low, moderate and high perceived stress.

2.7. Statistical analyses

First, the Kolmogorov-Smirnov test was used to measure if the data were normally distributed. If so, the T-test was used. In the other case, Mann-Whitney *U* tests were used to test significant differences among all indoor environmental parameters between two window/PSG conditions. Second, Spearman correlation coefficients (r) were calculated for all the factors which showed significant differences in the T-test/Mann-Whitney *U* test. One factor in the pairs was excluded if the r was higher than 0.4 (p-value < 0.05) and the remaining factors were included in the multivariate linear regression models to test the associations between sleep parameters and those factors. All multivariate linear regression models were adjusted by sex, age and BMI. The differences of all the parameters from the window closed to open were calculated individually for each participant. Subsequently, Mann-Whitney *U* tests were used to analyze if the

differences were significantly different with zero. SPSS 22.0 (SPSS Ltd., USA) was used in all statistical analyses. All analyses were considered statistically significant when *p*-values were less than 0.05.

3. RESULTS

Table 2 shows the demographic characteristics and study information of the participants. A total of 28 participants were recruited but one of them quit. There were 13 females and 14 males among the remaining participants and the age ranged from 20 to 33 years. The majority of participants had body mass index (BMI) within the normal range 18.5–25.0. However, two of them were underweight and had the BMI less than 18.5, three were overweight with the BMI between 25.0 and 29.9, and one had the BMI in the obese range higher than 30.0. All of them had good sleep quality during the past month with the PSQI scores less than or equal to 5. Four rooms were numbered from A to D. The first condition of the windows of Room A and C were open whereas Room B and D closed. Room A and B were the PSG rooms used for the participants from the PSG group.

Table 2: Demographic characteristics and study information of the participants (N=27)

No.	Room No.	Sex	Age (years old)	Height (cm)	Weight (kg)	BMI	PSQI	Windows first condition	PSG used
1	A	Male	25	185	80	23.4	3	Open	Yes
2	A	Male	27	175	58	18.9	4	Open	Yes
3	A	Male	22	193	82	22.0	3	Open	Yes
4	A	Male	27	178	65	20.5	2	Open	Yes
5	A	Male	26	173	93	31.1	2	Open	Yes
6	A	Male	27	163	62	23.3	5	Open	Yes
7	A	Female	21	167	61	21.9	4	Open	Yes
8	B	Female	27	163	50	18.8	5	Closed	Yes
9	B	Male	23	178	65	20.5	5	Closed	Yes
10	B	Male	23	164	56	20.8	5	Closed	Yes
11	B	Male	26	168	74	26.2	3	Closed	Yes
12	B	Male	24	183	72	21.5	4	Closed	Yes
13	B	Female	25	160	52	20.3	5	Closed	Yes
14	B	Female	28	165	50	18.4	3	Closed	Yes
15	C	Male	28	169	67	23.5	4	Open	No
16	C	Female	31	160	61	23.8	0	Open	No
17	C	Female	28	159	62	24.5	5	Open	No
18	C	Female	22	166	67	24.3	4	Open	No
19	C	Female	21	166	60	21.8	3	Open	No
20	C	Male	33	172	67	22.6	4	Open	No
21	C	Male	20	180	95	29.3	4	Open	No
22	D	Female	24	157	68	27.6	3	Closed	No
23	D	Female	33	162	50	19.1	3	Closed	No
24	D	Female	22	167	53	19.0	4	Closed	No
25	D	Female	25	172	58	19.6	5	Closed	No
26	D	Female	25	162	48	18.3	3	Closed	No
27	D	Male	26	178	75	23.7	5	Closed	No

BMI, body mass index; PSQI, Pittsburgh sleep quality index; PSG, polysomnography.

Table 3 lists the average and the 95th percentile of concentrations of indoor parameters between two window/PSG conditions during sleep. The data of night-time indoor parameters from bedtimes to get up times of the participants were used. Both the average and the 95th percentile of ambient T, RH and CO_2 were significantly different between the two window conditions (*p*-value < 0.05). According to means, the average ambient T with the window closed were averagely 1.6 °C higher than that with the open condition and the RH was 4.5% higher. The average 95th percentile of ambient T was 0.9 °C higher with the window closed than that with the window open and 0.8 °C higher in the PSG rooms than that in the non-PSG rooms. The

average 95th percentile of RH was 4.5% higher with the window closed compared to that with the window open. Besides, both the mean and the 95th percentile of CO_2 with the window closed were around 2.6 times higher on average than those with the window open. The average mean of $PM_{2.5}$ and the average 95th percentile of noise in the PSG rooms were significantly higher than those in the non-PSG rooms. Bed T and TVOCs did not show any significant different results between the two window/PSG conditions.

Table 3: Average and the 95th percentile of concentrations of indoor parameters between two window/PSG conditions during sleep

Items	*N* [a] (%)	Mean ± Std.	5th	25th	50th	75th	the 95th	*p*-value [b]
Average ambient T in total and stratified by the window/PSG conditions (°C)								
Total	105 (100)	21.8 ± 1.4	19.2	21.0	22.1	22.7	23.8	
Window closed	50 (47.6)	**22.6 ± 0.8**	20.9	22.2	22.5	22.9	24.2	**< 0.001**
Window open	55 (52.4)	**21.0 ± 1.3**	18.8	20.0	21.1	21.9	23.0	
No PSG	49 (46.7)	21.5 ± 1.4	18.5	20.9	21.7	22.5	23.5	0.092
PSG	56 (53.3)	22.0 ± 1.3	19.2	21.1	22.3	22.7	24.1	
The 95th percentile of ambient T in total and stratified by the window/PSG conditions (°C)								
Total	105 (100)	22.5 ± 1.2	20.2	21.9	22.6	23.3	24.5	
Window closed	50 (47.6)	**23.0 ± 1.0**	21.2	22.5	22.9	23.3	25.0	**0.001**
Window open	55 (52.4)	**22.1 ± 1.3**	19.6	21.3	22.2	23.2	23.8	
No PSG	49 (46.7)	**22.1 ± 1.3**	19.4	21.5	22.2	23.1	23.7	**0.001**
PSG	56 (53.3)	**22.9 ± 1.0**	20.6	22.4	22.9	23.4	24.7	
Average RH in total and stratified by the window conditions (%)								
Total	105 (100)	40.8 ± 5.8	29.5	36.3	42.0	44.9	49.4	
Window closed	50 (47.6)	**43.1 ± 5.2**	32.5	40.4	43.8	46.5	51.7	**< 0.001**
Window open	55 (52.4)	**38.6 ± 5.6**	28.5	34.8	38.8	43.6	46.4	
No PSG	49 (46.7)	40.2 ± 6.0	29.3	35.7	41.4	44.5	50.6	0.407
PSG	56 (53.3)	41.2 ± 5.7	29.2	37.2	42.2	45.0	49.5	
The 95th percentile of RH in total and stratified by the window/PSG conditions (%)								
Total	105 (100)	42.1 ± 5.8	32.0	37.5	43.0	46.0	51.0	
Window closed	50 (47.6)	**44.5 ± 5.3**	33.6	42.0	45.0	47.3	52.9	**< 0.001**
Window open	55 (52.4)	**40.0 ± 5.5**	30.8	35.0	40.0	45.0	48.4	
No PSG	49 (46.7)	41.8 ± 6.1	31.0	36.5	43.0	46.0	52.0	0.607
PSG	56 (53.3)	42.4 ± 5.6	32.0	38.3	43.5	47.0	51.0	
Average CO_2 in total and stratified by the window/PSG conditions (ppm)								
Total	105 (100)	1122.6 ± 618.6	468.0	584.4	840.7	1550.4	2451.5	
Window closed	50 (47.6)	**1656.4 ± 449.4**	929.5	1323.5	1546.1	1960.2	2489.1	**< 0.001**
Window open	55 (52.4)	**637.3 ± 223.9**	449.0	531.9	586.4	660.4	1279.2	
No PSG	49 (46.7)	1107.0 ± 600.1	462.0	604.1	769.6	1524.1	2450.2	0.842
PSG	56 (53.3)	1136.2 ± 639.5	473.0	568.2	917.1	1637.9	2461.2	
The 95th percentile of CO_2 in total and stratified by the window/PSG conditions (ppm)								
Total	105 (100)	1258.9 ± 673.4	523.0	659.8	1035.8	1814.4	2637.2	
Window closed	50 (47.6)	**1843.7 ± 457.3**	1215.7	1507.7	1810.1	2188.5	2671.6	**< 0.001**
Window open	55 (52.4)	**727.3 ± 281.0**	493.6	598.9	673.4	773.5	1373.1	
No PSG	49 (46.7)	1242.9 ± 669.7	487.8	685.3	824.1	1814.4	2646.7	0.888
PSG	56 (53.3)	1273.0 ± 682.3	528.5	646.3	1076.2	1830.9	2636.3	
Average $PM_{2.5}$ in total and stratified by the window/PSG conditions ($\mu g/m^3$)								
Total	79 (100)	23.5 ± 4.1	15.0	21.3	24.2	26.1	29.9	
Window closed	39 (49.4)	23.8 ± 3.2	18.5	22.0	24.2	25.5	29.9	0.845
Window open	40 (50.6)	23.2 ± 4.7	11.9	21.2	24.2	26.4	30.9	
No PSG	24 (30.4)	**21.5 ± 5.7**	11.8	18.0	21.6	26.2	32.3	**0.040**
PSG	55 (69.6)	**24.4 ± 2.7**	19.6	22.4	24.5	25.9	30.1	
Average noise in total and stratified by the window/PSG conditions (dB)								
Total	105 (100)	42.5 ± 6.1	35.6	36.3	46.0	48.2	50.1	
Window closed	50 (47.6)	42.5 ± 6.0	35.4	36.1	46.0	48.0	50.2	0.090
Window open	55 (52.4)	42.5 ± 6.2	35.8	36.7	38.0	48.4	50.4	
No PSG	49 (46.7)	**36.4 ± 0.7**	35.3	36.1	36.2	36.8	37.9	**< 0.001**
PSG	56 (53.3)	**47.7 ± 3.0**	37.6	47.1	48.2	48.7	51.0	
The 95th percentile of noise in total and stratified by the window/PSG conditions (dB)								
Total	105 (100)	43.7 ± 5.6	36.0	38.0	46.0	49.0	51.0	

Window closed	50 (47.6)	43.3 ± 5.9	36.0	37.0	46.0	48.0	51.0	0.100
Window open	55 (52.4)	44.0 ± 5.4	36.4	39.0	43.0	49.0	51.4	
No PSG	49 (46.7)	**38.3 ± 2.2**	36.0	36.4	38.0	39.1	43.4	**< 0.001**
PSG	56 (53.3)	**48.4 ± 2.7**	40.8	47.3	49.0	50.0	52.2	

[a] some samples missed if the total sample size is less than 108; [b] calculated by Mann-Whitney *U* tests. Bold indicates *p*-value < 0.05. T, temperature; RH, relative humidity; PSG, polysomnography.

From the results of the morning questionnaire between the window closed and open during sleep, the participants reported the air with the window open was 1.7 scores fresher compared to it with the window closed, while they felt noisier. Regarding the subjective sleep quality assessment, we did not find any significant results between two window conditions. Moreover, the participants in the non-PSG group had higher PSS score than those had in the PSG group before sleep at the test nights. Regarding the sleep parameters from the PSG between two window conditions for all nights and only test nights, no significant results were found. As for the sleep parameters from the Fitbit between two window/PSG conditions, considering all the nights, the participants had significantly longer sleep latency with the window open compared to those who slept with the window closed, while this significant result disappeared from the results of only test nights. The participants from the non-PSG group had an increased number of awakenings than those from the PSG groups at all nights and only test nights. No significant results were found among the other factors from the Fitbit.

From the results above, the participants had different feelings of air freshness and noise between two window conditions. Also, the average and the 95th percentile of ambient T, RH and CO_2 were significantly different between window open and closed nights. As for the PSG and non-PSG rooms, some indoor parameters including the 95th percentile of ambient T, the average $PM_{2.5}$, the average and the 95th percentile of noise were higher than those in the non-PSG rooms.

Table 4 shows β and 95% confidence interval (CI) from multivariate linear regression analyses of sleep parameters and window/PSG conditions related factors. The participants that slept with more noise (self-reported) had 0.294 higher score of GSQS than those that slept with less noise, herein the change of higher and lower noise levels (independent variable) was one unit (the same as follows). Regarding the sleep parameters from Fitbit, those higher-stressed participants had significantly 5.009 minutes more time asleep, 5.590 minutes more TIB and 2.435 minutes more REM sleep time than the lower-stressed participants. Participants sleeping with higher levels of $PM_{2.5}$ had significantly 1.546 minutes more time awake, 0.342 % more awake percentage and 0.342 % lower sleep efficiency than those who slept with lower levels of $PM_{2.5}$. Those slept with higher the 95th percentile of ambient T had significantly 3.074 times higher number of awakenings than those who slept with lower the 95th percentile of ambient T.

Table 4: β and 95% confidence interval (CI) of sleep parameters and window/PSG conditions related factors from multivariate linear regression analyses

Items	Window/PSG related	β (95% CI)	*p*-value
GSQS and window-conditions related factors			
GSQS	Average CO_2	-0.001 (-0.002 - 0.001)	0.297
	Noise	**0.294 (0.016 - 0.572)**	**0.039**
Sleep parameters from Fitbit and PSG-conditions related factors			
	Stress	**5.009 (0.831 - 9.186)**	**0.021**
Asleep (min)	The 95th percentile of ambient T	7.943 (-13.902 - 29.788)	0.456
	Average $PM_{2.5}$	-2.318 (-7.642 - 3.006)	0.374
	The 95th percentile of noise	-2.141 (-7.099 - 2.818)	0.378
	Stress	0.582 (-0.534 - 1.698)	0.289
Awake (min)	The 95th percentile of ambient T	1.294 (-4.541 - 7.13)	0.648
	Average $PM_{2.5}$	**1.546 (0.124 - 2.968)**	**0.035**
	The 95th percentile of noise	-0.969 (-2.294 - 0.355)	0.142
Number of awakenings	Stress	0.366 (-0.158 - 0.891)	0.160

(times)	**The 95th percentile of ambient T**	**3.074 (0.331 - 5.816)**	**0.030**
	Average $PM_{2.5}$	-0.026 (-0.694 - 0.642)	0.936
	The 95th percentile of noise	-0.448 (-1.07 - 0.175)	0.149
	Stress	**5.590 (0.903 - 10.278)**	**0.022**
TIB	The 95th percentile of ambient T	9.237 (-15.272 - 33.747)	0.440
(min)	Average $PM_{2.5}$	-0.772 (-6.745 - 5.201)	0.790
	The 95th percentile of noise	-3.11 (-8.673 - 2.453)	0.256
	Stress	**2.435 (0.183 - 4.688)**	**0.036**
REM sleep	The 95th percentile of ambient T	-0.367 (-12.146 - 11.413)	0.949
(min)	Average $PM_{2.5}$	-2.481 (-5.351 - 0.39)	0.086
	The 95th percentile of noise	-0.216 (-2.89 - 2.458)	0.867
	Stress	0.023 (-0.174 - 0.22)	0.811
Sleep efficiency	The 95th percentile of ambient T	-0.063 (-1.092 - 0.966)	0.900
(%)	**Average $PM_{2.5}$**	**-0.342 (-0.592 - -0.091)**	**0.010**
	The 95th percentile of noise	0.142 (-0.091 - 0.376)	0.218
	Stress	-0.023 (-0.22 - 0.174)	0.811
Awake	The 95th percentile of ambient T	0.063 (-0.966 - 1.092)	0.900
(%)	**Average $PM_{2.5}$**	**0.342 (0.091 - 0.592)**	**0.010**
	The 95th percentile of noise	-0.142 (-0.376 - 0.091)	0.218

GSQS, Groningen sleep quality scale; T, temperature; TIB, time in bed; PSG, polysomnography.

From the results of the individual differences from the window closed to open, air freshness, noise, the average and the 95th percentile of ambient T, RH, and CO_2 also shows the similar trends of results as the overall results between the window closed and open mentioned above. However, the GSQS, the KSS and the number of awakenings show significant results, which are different from the overall results between the window closed and open.

4. DISCUSSION

In this study, the association between sleep environment and sleep quality with the window closed and open was investigated.

The recommended values of indoor air parameters established by the Flemish government (VR 2018, 3003) or reviewed by Caddick et al. (2018) are shown in Table 5. The average ambient T reached the recommended range for both window conditions. There were at least 5% (window closed) and 50% (window open) nights with the average RH lower than the recommended range. The average CO_2 levels with the window open were less than the recommended value of 800 ppm for at least 75% nights, while all the nights with the window closed exceed 800 ppm. Those indoor air parameters were all significantly different between the window closed and open, and the CO_2 levels had the highest difference between two window conditions among those parameters. Only less than 5% nights reached the average $PM_{2.5}$ levels less than 10 μg/m³ for both the window closed and open.

The average CO_2 level with the window open was quite similar to the value in the previous study from Strom-Tejsen et al. (2016) (660 ppm). Also, we had the same situation as another study indicated - the CO_2 levels with the window and door open were largely under 1000 ppm (Mishra et al., 2018). However, the results were different for the window closed from the previous studies. Strom-Tejsen et al. (2016) indicated that the average CO_2 level was 2585 ppm with the window closed, while it was 1656 ppm in this study. Mishra et al. measured largely under 1500 ppm of CO_2 levels but with the peak of over 3000 ppm. Different building characteristics lead to different building sealing, which might be the major reason for the different results among those studies.

Table 5: Recommended values of indoor air parameters established by the Flemish government (VR 2018, 3003) or reviewed by Caddick et al. (2018)

Items	Recommended values
Temperature (T)	17 – 28 °C (Caddick et al., 2018)
Relative humidity (RH)	40 – 60 % (Caddick et al., 2018)
CO_2	< 800 ppm (VR 2018, 3003)
$PM_{2.5}$	10 μg/m³ (VR 2018, 3003)
TVOCs	-

From the results of multivariate linear regression analyses of the GSQS and sleep parameters and window/PSG conditions related factors, the indoor environmental parameters of the 95th percentile of ambient T and $PM_{2.5}$ were both related to a few sleep parameters from Fitbit. Mishra et al. (2017) found that the number of awakenings recorded by the Sensewear Armband was negatively associated with ambient T but positively with CO_2 levels. That is opposite with the result in this study that the number of awakenings recorded by Fitbit increased with the higher 95th percentile of ambient T. The reason might be that the cover in this study was warmer than that in the study of Mishra et al. (2017), thus within the recommended range of ambient T, the participants had an increased number of awakenings in this study but a decreased number sleeping with the higher ambient T in the study of Mishra et al. (2017). Also, Strom-Tejsen et al. (2016) indicated that the sleep latency improved with the window open and the sleep efficiency was better with the fan on (lower CO_2 levels). However, CO_2 was not a significant factor to influence sleep quality comparing to this study. Potentially, this is because the lower CO_2 levels were under the window open condition, which could also lead to higher noise levels. Although Mishra et al. (2017) also used the method of the window/door open and closed to change the air quality in the bedrooms, the outdoor noise might not be the same in this study. Some participants reported that there were several groups of people going pass by the street beside the bedrooms and talking loudly in this study.

The $PM_{2.5}$ levels were higher in the PSG rooms than the non-PSG rooms. The time I stayed in the PSG rooms was much more than the time I stayed at the non-PSG rooms since I had to prepare the materials for using PSG, set up PSG monitors and help to wear PSG for around one hour each time each person. My indoor activities induced an increase of $PM_{2.5}$ levels before participants' bedtimes and then the starting points of $PM_{2.5}$ levels in the PSG rooms must be higher than those in the non-PSG rooms. Also, $PM_{2.5}$ was positively associated with the time and percentage of awake and negatively associated with sleep efficiency recorded by Fitbit. Shen et al. (2018) investigated the association of $PM_{2.5}$ with sleep-disordered breathing (SDB) among 4312 healthy participants and indicated that exposure to $PM_{2.5}$ was associated with SDB. There was a study also concluding that $PM_{2.5}$ was strongly associated with sleep disorder symptoms in females (2−17 yrs.) (Lawrence et al., 2018). SDB and sleep disorder symptoms might be the reason to increase awakenings and decrease sleep efficiency.

From the results of the individual differences from the morning questionnaire, the participants felt the air to be fresher, but reported the noise to be higher, they felt worse, had higher GSQS (worse sleep quality) and felt less alert the next morning when they slept with the window open the night before, whereas the subjects reported less sleepy the next morning after the test night with the window open in the study of Strom-Tejsen et al. (2016). Again, the reason is that the outdoor noise levels might be much lower in the study of Strom-Tejsen et al. (2016) than the noise in this study. Besides, the participants had an increased number of awakenings recorded by Fitbit with the window open and this is consistent with the findings from Laverge and Janssens (2011) where the reports were from the subjects' feedback.

5. CONCLUSIONS

The participants reported better sleep quality sleeping with quieter surroundings (windows closed). Higher $PM_{2.5}$ level was associated with more time awake, higher percentage awake and lower sleep efficiency. Higher ambient temperature was associated with an increased number of awakenings.

6. ACKNOWLEDGEMENTS

We appreciate the help of Evelien Bouwens from the company Resmed to provide us two sets of the Nox A1 (home PSG) and the guide of how to use it. We thank the participants in this study and Benjamin Hanoune to lend two sets of his sensors for this study.

7. REFERENCES

Ailshire, J. A., Crimmins, E. M., 2014. Fine Particulate Matter Air Pollution and Cognitive Function Among Older US Adults. American Journal of Epidemiology. 180**,** 359-366.

An, R., Yu, H., 2018. Impact of ambient fine particulate matter air pollution on health behaviors: a longitudinal study of university students in Beijing, China. Public Health. 159**,** 107-115.

ASAA (American Sleep Apnea Association), 2019. https://www.sleepapnea.org/treat/getting-sleep-apnea-diagnosis/sleep-study-details/

Auchincloss, A. H., et al., 2008. Associations between recent exposure to ambient fine particulate matter and blood pressure in the Multi-Ethnic Study of Atherosclerosis (MESA). Environmental Health Perspectives. 116**,** 486-491.

Caddick, Z. A., et al., 2018. A review of the environmental parameters necessary for an optimal sleep environment. Building and Environment. 132**,** 11-20.

Heo, J. Y., et al., 2017. Effects of smartphone use with and without blue light at night in healthy adults: A randomized, double-blind, cross-over, placebo-controlled comparison. Journal of Psychiatric Research. 87**,** 61-70.

Kaida, K., et al., 2006. Validation of the Karolinska sleepiness scale against performance and EEG variables. Clinical Neurophysiology. 117**,** 1574-1581.

Laverge, J., Janssens, A., 2011. Analysis of the influence of ventilation rate on sleep pattern. In: Indoor Air 2011. ISIAQ; 2011.

Lawrence, W. R., et al., 2018. Association between long-term exposure to air pollution and sleep disorder in Chinese children: the Seven Northeastern Cities study. Sleep. 41**,** 1-10.

Menefee, L. A., et al., 2000. Self-reported sleep quality and quality of life for individuals with chronic pain conditions. Clinical Journal of Pain. 16**,** 290-297.

Mishra, A. K., et al., 2018. Window/door opening-mediated bedroom ventilation and its impact on sleep quality of healthy, young adults. Indoor Air. 28**,** 339-351.

Ogilvie, R. P., et al., 2018. Sleep indices and eating behaviours in young adults: findings from Project EAT. Public Health Nutrition. 21**,** 689-701.

Owens, J. F., Matthews, K. A., 1998. Sleep disturbance in healthy middle-aged women. Maturitas. 30**,** 41-50.

Shen, Y. L., et al., 2018. Association of $PM_{2.5}$ with sleep-disordered breathing from a population-based study in Northern Taiwan urban areas. Environmental Pollution. 233**,** 109-113.

Strom-Tejsen, P., et al., 2016. The effects of bedroom air quality on sleep and next-day performance. Indoor Air. 26**,** 679-686.

Measurements of sleep quality with low-cost sleep monitors: Effect of bedroom air quality and sleep quality

Pawel Wargocki*[1]

[1] *International Centre for Indoor Environment and Energy*
Department of Civil Engineering, Technical University of Denmark
**Corresponding author:* paw@byg.dtu.dk

ABSTRACT

More than 20 years of one's life is spent in the bedroom when sleeping. Sleep quality is essential for our health, well-being and next-day performance. However, there is very little information on how bedroom air quality affects the quality of sleep. One of the reason could be that the accurate measurements of the quality of sleep have been the domain of sleep research groups and sleep laboratories using polysomnography. In the recent years, however, many low-cost sleep monitors and actigraphs made their way into the market. They allow carrying out reasonably simple measurements of sleep quality at the large scale. But there are no accurate data on their performance and neither whether they can be used for research purposes. This project attempted to shed some light on these issues by comparing the performance of a few selected sleep monitors and by measuring the effects of bedroom air quality on sleep quality. To meet the latter objective, 30 persons were recruited to sleep in their bedrooms for two weeks under two different conditions: with the door to the bedroom opened and closed. Only people who sleep alone were selected. Bedrooms were not ventilated by mechanical systems and windows stayed closed during measurements. Recruited persons slept with the wearable monitor which registered their sleep quality from Monday to Friday, i.e., four nights on each week. Every morning they rated their sleep quality, air quality in the bedroom as well as made logical thinking tasks for 3 minuted that examined their cognitive performance. For that purpose, they used a specially developed App on the tablet. Temperature, relative humidity, and carbon dioxide concentration were continuously logged. Measured bedroom conditions were correlated against objectively and subjectively measured sleep quality to examine whether any relationship exists. To meet the former objective, several low-cost monitors were purchased, both wearable, standing on the night desk or placed on or under bedlinen. Six recruited persons slept for four nights, and their sleep quality was registered with some of those monitors as well as with the monitor used in the first experiment; their measurements were compared against each other to examine whether they differ in their performance.

CO_2-concentration of the surrounding air near sleeping infants inside a crib

Gert-Jan Braun[1] and Wim Zeiler[1]

1 TU Eindhoven
Department of the Built Environment
Den Dolech 2, 5600 MB Eindhoven, Netherlands
W.Zeiler@tue.nl

ABSTRACT

The indoor air quality is very important for the well-being of occupants, especially in the case of young babies. This research focuses on the air quality of the surrounding air inside a crib with sleeping infants. To study the effects of different sleeping positions of the baby with in the crib a measurement setup was created in the laboratory. The breathing of an infant was simulated by means of a baby doll with air supply mixed with CO_2 and measured at different sensor locations for different sleeping positions. The results show an enormous increase in the CO_2 concentration (up to 4 times) depending on the sleeping position of the infant, and also show the effect of a more open crib. The effect of the position of the baby on the CO_2 concentrations inside the crib are compared with the background level in the sleeping quarter.

KEYWORDS

Carbon dioxide, concentration, Crib, Infants, ventilation, sleeping position

1 INTRODUCTION

Babies often spent up to 11 hours in a day care centre during the working days in modern society. During the first period of life, infants (<1 year of age) and toddlers (1-3 years of age) sleep a considerable amount of time, on average 13.3 h/day in the 1st year of life, 12.6 h/day in the 2nd year, and 12.1 h/day in the 3th year (Iglowstein et al 2003, Boor et al 2017). The sleep microenvironment is the predominant indoor space for babies where they spends most of their time. Because of their low body weight, babies and toddlers inhale considerably more air per kg of body weight as they sleep compared to adolescents and adults. The volume of air inhaled/kg.day can be estimated with the U.S. EPA EFH data set by taking the product of the mean normalized volumetric breathing rate in the sleep or nap activity (L/h-kg) and the mean duration of time spent in the sleep or nap activity (h/day). The normalized inhaled air volumes, V*Sleep, are categorized by age group and gender and presented in Fig. 1 (Boor et al. 2017). Mattress dust is found to contain a diverse spectrum of biological particles and particle-bound chemical contaminants and their concentrations in dust can span many orders of magnitude among bed samples. Furthermore, mattress foam and covers, pillows, and bed frames can emit a variety of volatile and semi volatile organic compounds, and emission rates can increase due to localized elevations in surface temperature and moisture near the bed due to close contact with the human body (Boor et al 2014, 2015).
Therefore, good ventilation levels inside the baby beds is of extreme importance to remove the pollutants and create a healthy sleep microenvironment for the babies. They are by far the most vulnerable as their lungs are still in full development. Furthermore some literature suggest even a relation with the Sudden Infant death Syndrome (Corbyn 2000, Sakai et al 2008, De La Iglesia et al 2018).

In previous research carbon dioxide (CO_2) concentrations were measured inside baby cribs in practical conditions (de Waard 2014, de Waard & Zeiler 2015, Kruisselbrink 2016, Zeiler 2018, Braun & Zeiler, 2019). Different types of baby beds are being used: crib, bedstead and bottom & top bunk bed. Beside the type of baby cot also there position is of importance. Sometimes they are placed in a row of three next to each other as well as two above each other, see Fig. 2. The problem is that the top is then often a closed surface as well as both sides of the bunk bed, which restricts the inside ventilation in the baby bed itself to a large extent. Previous research showed that when there is a baby placed in the crib the top bunk bed has lower CO_2 concentrations compared to the bottom bunk bed (BBB) (de Waard 2014). Therefore this research focused on the bottom bunk bed and also on the bedstead (BS). The main difference between this two baby cots is the closed off surface at the top of the bottom bunk bed.

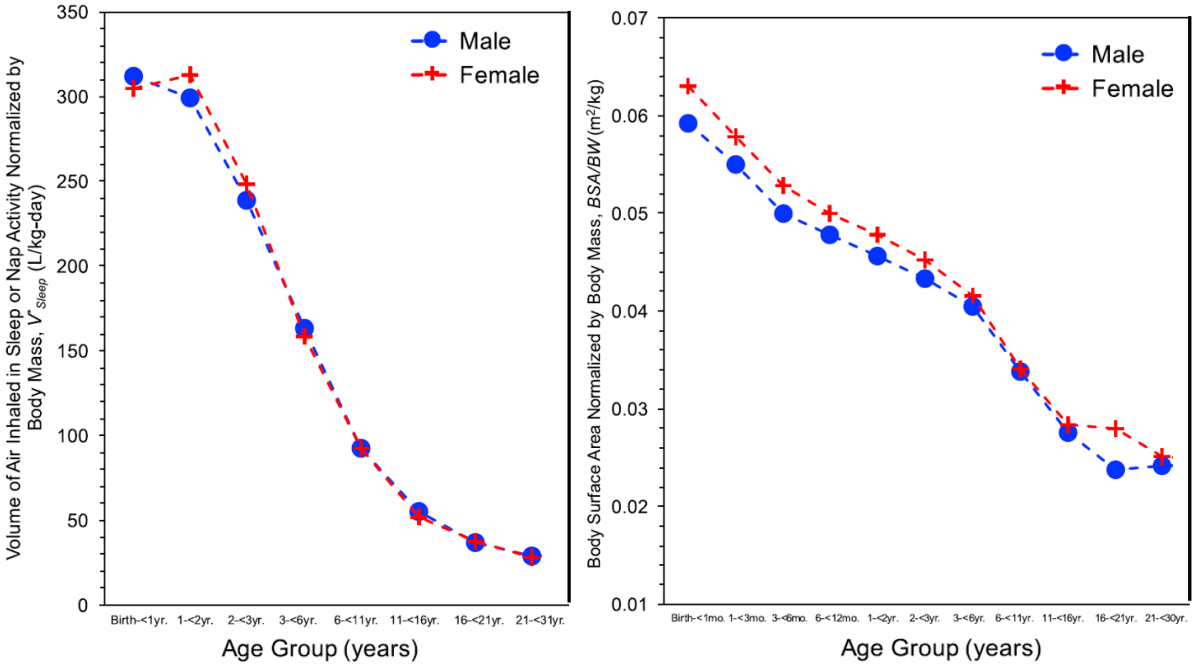

Figure 1. Volume of air inhaled during sleep or nap activity per day and Infant dermal exposure dose considerations in the sleep microenvironment: normalized by body mass for each age group and gender (calculated using U.S. EPA EFH data set (2009) by Boor et al 2017).

Figure 2. Examples baby bunk bed (Versteeg 2012, Kinderdagverblijf Gouda 2016)

It was noticed that there was a significant difference of 5.7% (Class B, GGD) in the measured CO_2 concentrations and a visible difference at different time periods between the measurement positions. Therefore the effects of the position of the baby on the measured CO_2 concentrations and also the difference between the CO2 concentrations at the mouth of the baby compared to the measurement positions are determined in this research.

2 METHOD

The method below is used to determine the effects of the closed surfaces and the breathing position of the baby on the different measurement positions. As it was not possible to measure on real babies a baby doll was used instead with a breathing simulator, see Fig. 3.

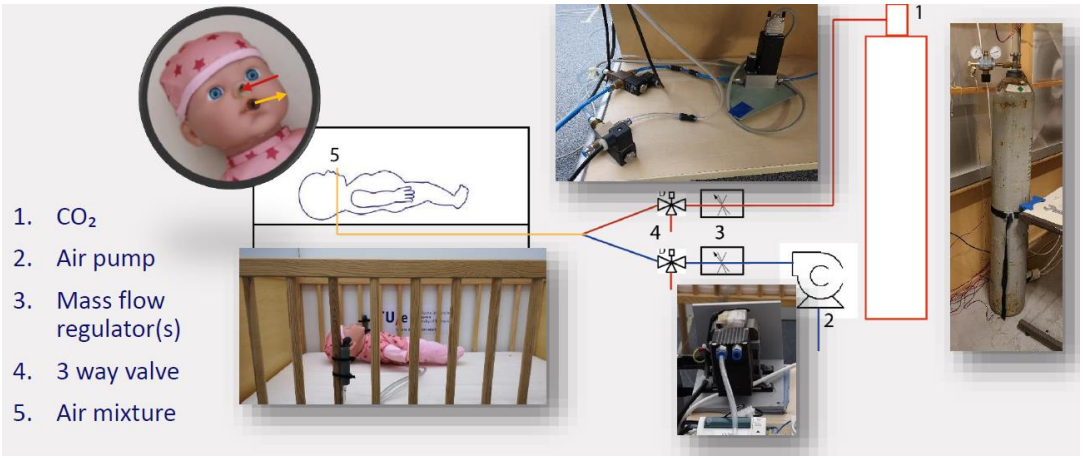

Figure 3: Breathing simulator, hose, CO_2 sensor (hose) and baby doll in test crib at TU/e

2.1 Measurement setup

The general measurement setup can be seen in Fig. 4.

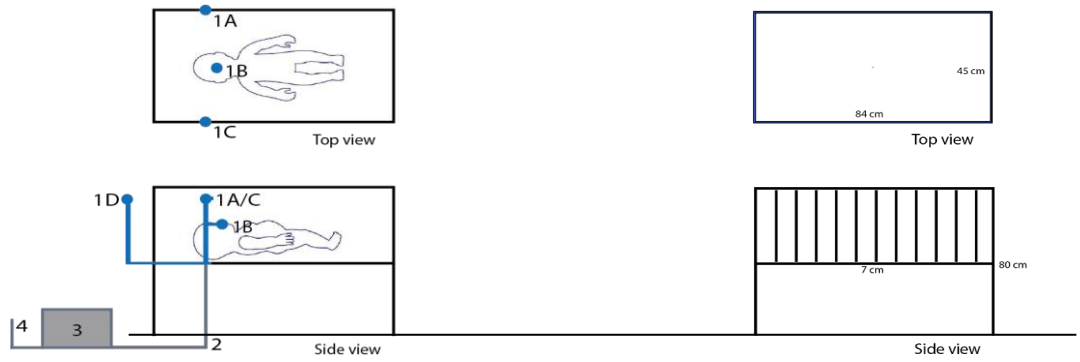

Where: 1.Four CO2 sensors (1a/b/c/d) 2. Cable bundler 3. Central box and 4. Mains supply

Figure 4: General measurement setup

Four CO_2 sensors were used to measure the concentrations around the nose, bars on the wall side as well as the room side, and also the background level. The room sensor that measured the background CO_2 concentrations was placed at the same height as the sensors at the crib. The baby doll is placed in the test crib at the TU/e, more details on the type of sensors that were used can be found in
Table 1.

Table 1: Measurement equipment information

Measurement	Device	Interval	Inaccuracy
CO_2	SBA-% CO_2 Analyser	1 sec	< 1%
Data logging	Squirrel 2020 series	1 sec	±0,075%
Mass flow controller	Brooks model 0152	-	-
Mass flow controller	Brooks model 5850S	0-15 [ln/min]	± 1%

2.2 Exhaled air simulation

To simulate the practical condition, the amount of CO_2 that a baby doll connected to a regulated supply hose has to insert into the crib was determined. An infant has a lung volume of 10-15% compared to an adult and a breathing volume of 1.39 litres per minute (Kosch, 1984), On average an infant has a respiratory rate of 30-60 breaths per minute, an adult has 12-20 breaths per minute. (Deboer, 2004) The increased exhaled volume of CO_2 is around 4 -5%, this is about a 100 fold increase over the inhaled air. (Dhami et al, 2015). Exact values for babies could not be found in the literature, therefore the lower region of the exhaled volume was chosen, the amount of exhaled CO_2 was set at 4%:

$$V_{E.CO_2} = V_{E.Air} * 4\% \quad (1)$$

Where: $V_{E.CO2}$ = Volume exhaled CO_2 [L], $V_{E.air}$ = Volume exhaled air [L], 4% = Percentage of CO_2 in exhaled air.

Therefore the 'baby' has to deliver a constant volume of CO_2 of 0.06 [L.min-1], calculated with formula 1 (for an adult it would have been 0.30 [L.min-1]). The schematics of the setup that was used to insert this CO_2 into the crib and to mimic the breathing pattern of an infant can be seen in Fig. 3. A CO_2 tank that was connected to a mass flow controller regulated the flow to 0.13 [L.min-1]. The Air pump was also connected to a mass flow controller and regulated the flow to 2.6 [L.min-1]. Both regulated flows then went through a three way valve, set to a timer with an interval of one second. The three way valve in combination with the timer mimicked the respiratory rate of 30 breaths per minute by extracting the air and CO_2 outside the room and by combining both and creating the wanted air mixture. The air mixture was inserted into the crib by a hose connected to the mouth off the baby doll, see the bottom arrow (orange) in Fig. 3 and the control set-up in Fig. 5. This hose was put one centimetre in front of the hose in the nose (top-red) at witch one of the CO_2 sensors was attached, this to prevent a shortage between the sensor and the air mixture.

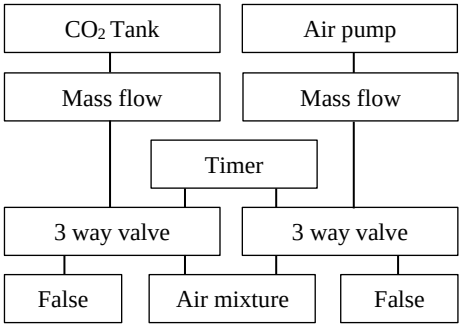

Figure 5: Schematically overview breathing

2.3 Baby positions.

To see the effects of the position of the baby doll on the CO_2 concentrations inside the crib, the baby doll was placed and measured in four different positions inside the BS and BBB, that can be seen in Fig.6.

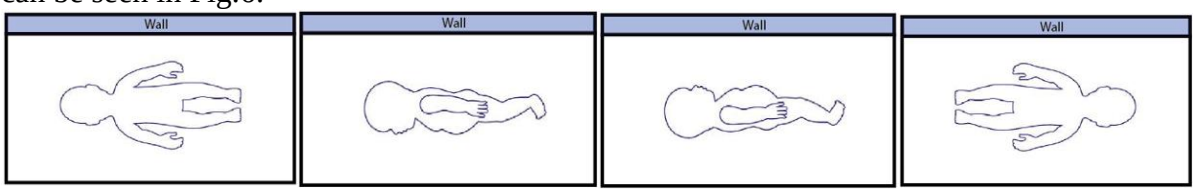

Figure 6: Measurement positions for the baby doll inside the cribs: supine, lateral facing room, lateral facing wall and prone

3 RESULTS

As an example the results of a series of 3 measurements prone position inside the BS is given, in Fig. 7.

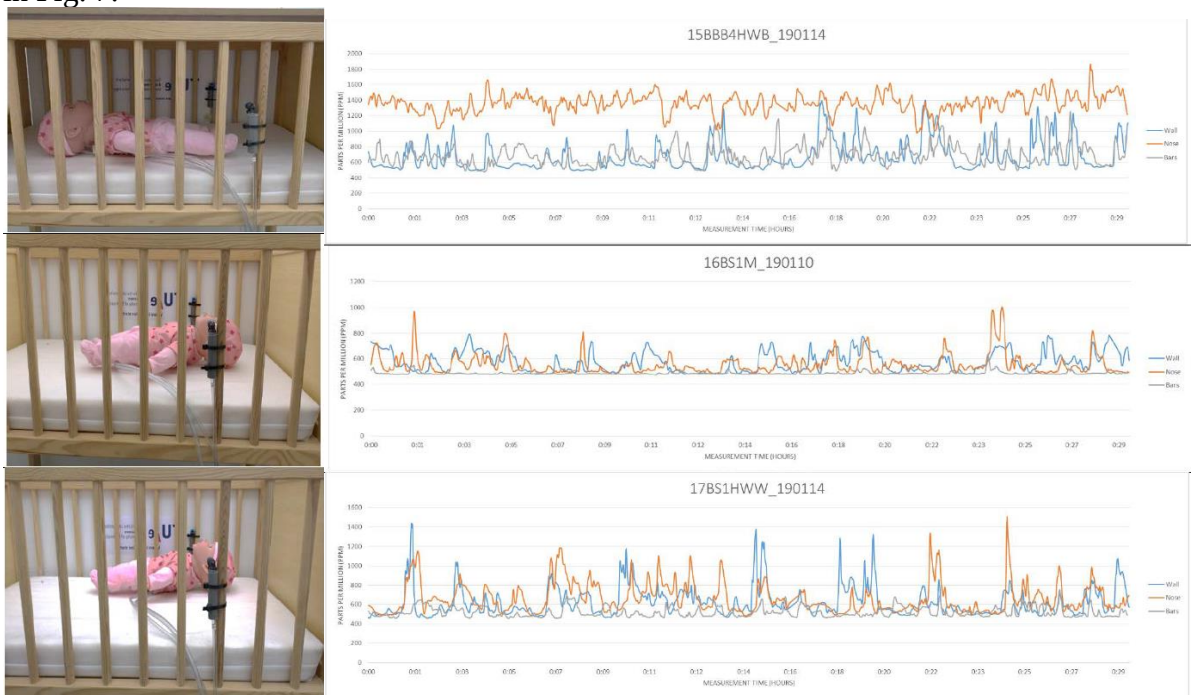

Figure 7. Actual measurement data of 3 slightly different position with prone orientation

3.1 Average CO_2 levels

An overview of the average CO_2 concentrations for each measurement is given in Table 3. The colouring is based on the test values for ventilation in schools and child day cares (GGD Nederland, 2006), see Table 2.

Table 2: GGD classes for CO_2 [ppm] concentrations

Class	A Very good	B Good	C Acceptable	D Insufficient	E Very poor
CO_2 [ppm]	< 650	650-800	800-1000	1000-1400	>1400

Table 3: Overview of the average CO_2 concentrations of all the measurements.

	Bottom bunk bed												Bedstead											
	Facing roof			Facing wall			Facing room			Rotated position			Facing roof			Facing wall			Facing room			Rotated position		
	01BBB1AM_190115	02BBB1AHWW_190109	03BBB1AHWB_190109	07BBB2M_190110	08BBB2HWW_190111	09BBB2HWB_190111	10BBB3M_190110	11BBB3HWW_190111	12BBB3HWB_190114	13BBB4M_190110	14BBB4HWW_190114	15BBB4HWB_190114	16BS1M_190110	17BS1HWW_190114	18BS1HWB_190114	22BS2M_190110	23BS2HWW_190114	24BS2HWB_190114	25BS3M_190110	26BS3HWW_190115	27BS3HWB_190115	28BS4M_190111	29BS4HWW_190115	30BS4HWB_190115
Wall	886	1157	1257	854	2992	1688	489	465	480	950	597	667	575	621	582	1086	530	1167	495	597	469	660	658	618
Middle	1376	1492	1417	1725	2271	1696	516	516	510	1263	1344	1361	556	660	730	1770	2452	1530	595	597	917	866	980	564
Bars	843	944	817	537	724	617	502	867	487	729	576	684	489	516	534	580	597	545	568	1282	573	561	515	481
Background	490	474	469	495	473	466	501	487	471	488	468	466	486	460	467	484	462	466	491	495	497	481	473	472

3.2 Comparison between bed types

The effects off the different cribs on the CO_2 concentrations are displayed in this paragraph. The bottom bunk bed and bedstead where tested at the TU/e laboratory. The average measured CO_2 concentration for each sensor position in the BBB or BS is displayed in Fig. 8, where it can be seen that the CO_2 concentrations are higher for each measurement position in the bottom bunk bed and therefore lower in the bedstead.

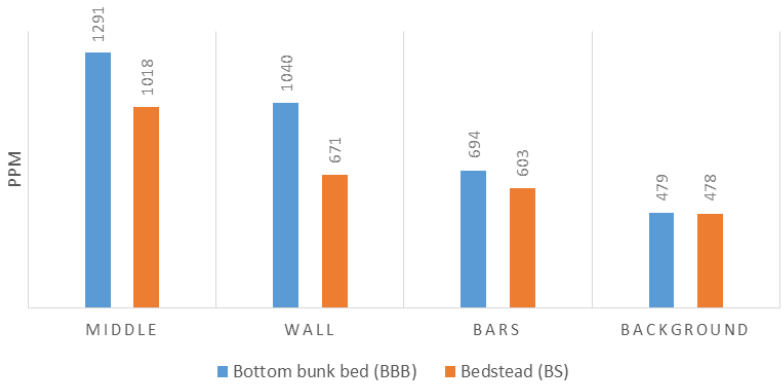

Figure 8: Bottom bunk bed vs. bedstead, average CO_2 concentrations

This comparison is again made in Fig. 9 where the CO_2 concentration inside the crib was made relatively to the background concentration. Again the results show that the CO_2 concentration relatively to the background concentration are lower in the bedstead.

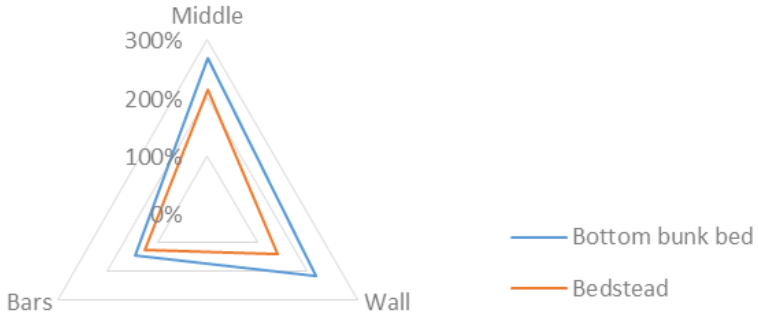

Figure 9: BBB vs. BS relative to background CO_2 concentration

3.3 Comparison between baby position

The effects off the different position, in which the baby was placed, on the CO_2 concentrations are displayed in this paragraph. The average results for each sensor position at the BBB as well as the back ground level in the room are displayed in Fig. 10, the results from the BS are displayed in Fig. 11.

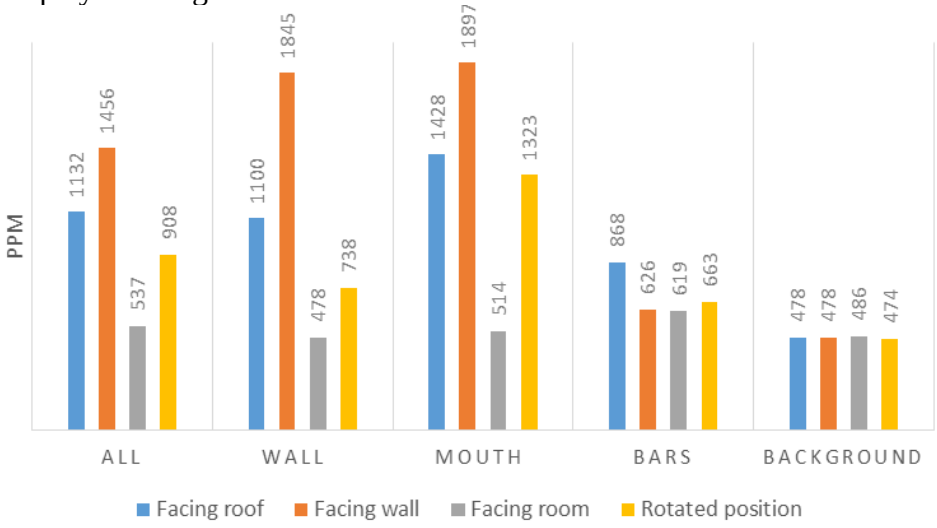

Figure 10: Average BBB CO_2 concentrations

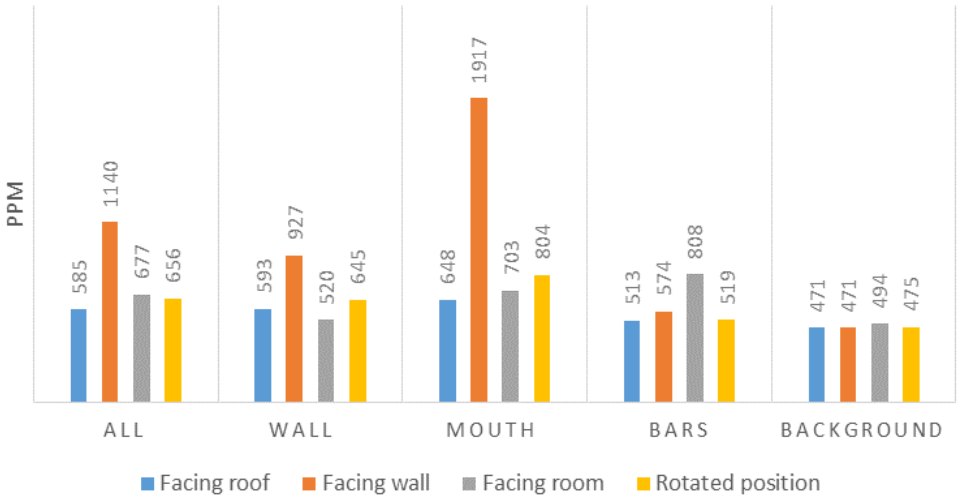

Figure 11: Average BS CO2 Concentrations

These values where again made relative to the background in Figure 12 and 13.

Figure 12: BBB, CO_2 relative to the background

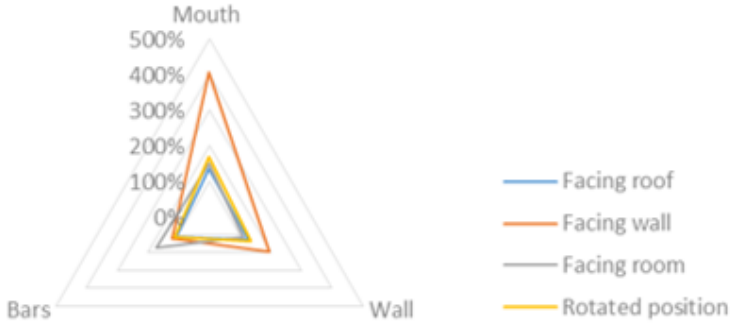

Figure 13: BS, CO_2 relative to the background

The high concentration value at the mouth of the baby doll, when facing the wall makes is somewhere unclear to see the results, therefore this value is excluded in Fig. 14.

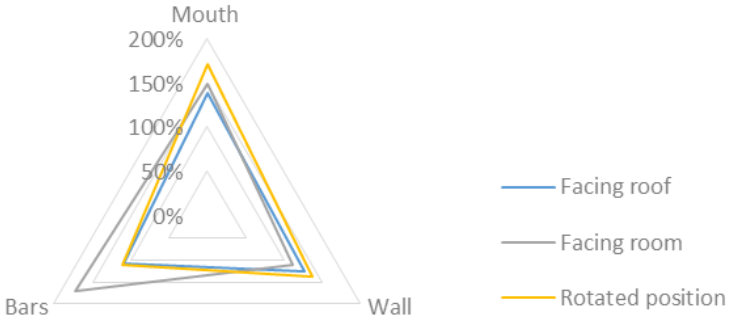

Figure 14: BS, CO_2 concentrations relative to the background (wall excluded)

The overall results of the measurements relative to the background level are displayed in Figure 15 and Figure 16. It can be seen that that the values at the position of the mouth reach the highest concentration, it can also be seen that when the baby is facing a more open surface the concentration reach less high values.

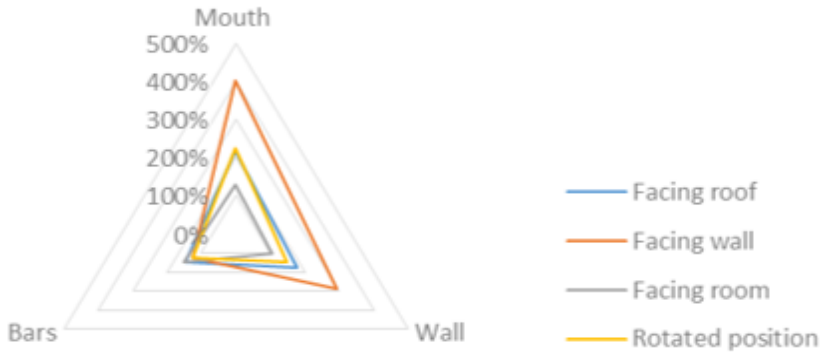

Figure 15: Average CO_2 BBB and BS combined

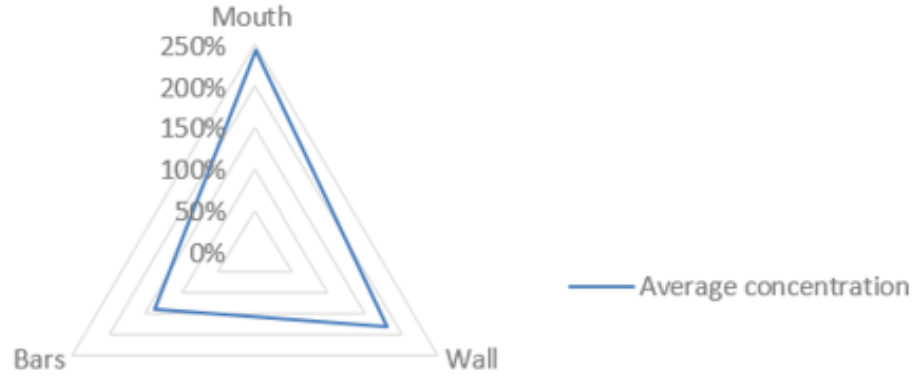

Figure 16: Average CO2 concentrations

4 DISCUSSION

The size of the crib is that of a privately owned crib, instead of the ones used at day-care centers. Therefore it can be expected that the values inside a bigger crib, as in daycare centers, will not reach the same increase in concentrations. All measurements were done in a laboratory situation with an extremely good background level of CO_2 of around 480 ppm. In normal buildings this would be much higher to start with. However, as our focus was on the effect of the position of the baby inside the crib on the CO_2 concentration of the inhaled air we choose this level to be able to detect differences more easy. As it was not possible to do measurements with real babies, we used a baby doll with nearly the same dimensions and integrated a mechanism to represent the breathing of a baby. This led to simplifications of representing the breathing which therefor might differ from the real baby´s breathing.
The concentrations were determined by measuring at the edge of the baby crib, this due to necessary safety precautions that no measure equipment could be reached by the babies. This led to a variable distance from the exhaled air (mouth) till the measured air depending on the position of the baby within the crib. The free breathing zone of an infant was determined to be 0.3 meters (de Waard, 2014). However, due to the variable distance between 0.1 - 0.4 meters, this was not met in all practical conditions.

The workings of the breathing simulation was not compared with a real enfant, therefore it cannot be said how accurately the breathing pattern was simulated, the flow pattern of the exhaled air was however investigated with a smoke-test. The smoke-test enabled also to check if there was a possible major short cut between the exhaled air and the sensor. Fig. 17 shows a position in time of these measurements, where it can be seen that the exhaled air effected the inserted smoke up to a distance of 23 centimetres and spread according the arrows in the figure. The air was not visually affected by the sensor in the nose of the baby doll.

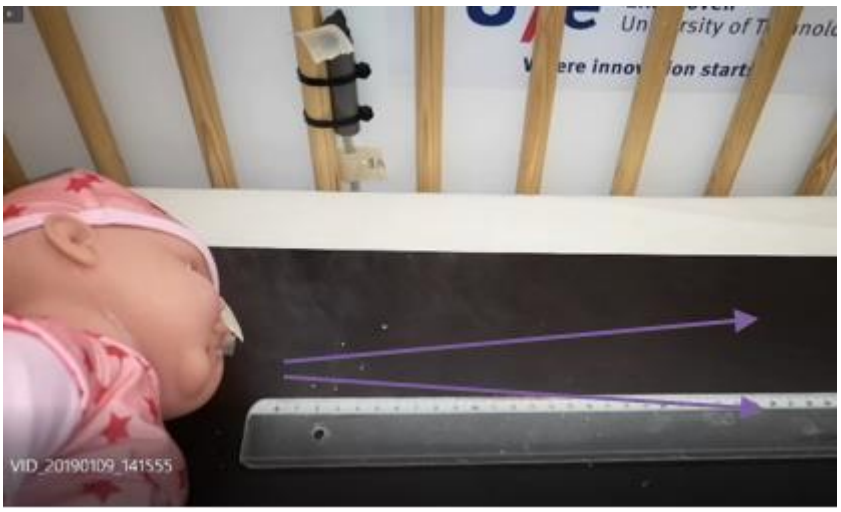

Figure 17: Breathing pattern, smoke-test

It was found that the location of the sensor had a significant effect on the measured concentrations, the mouth sensor measured an increase relative to the background level of around 140 percent higher, where the wall sensor measured 80 percent higher and the bar sensor nearly 40 percent higher.

5 CONCLUSION

This research was performed to measure the effects of the position of the baby on the measured CO_2 concentrations and also the difference between the CO_2 concentrations at the mouth of the baby doll compared to the measurement position. It was found that the bottom bunk bed with a more closed surroundings led to an average increase of around 220 percent relative to the background level, compared to the bedstead where the increase was 160 percent. In both situations the increases are significant and even more significant for the measurements at the wall side, here the increase in the bottom bunk bed was on average around 270 percent and for the bedstead it was around 210 percent. Therefore it can be concluded that the more closed the surroundings of a crib are, the higher the CO_2 concentrations will be.

The position of the baby doll also had a significant effect on the measurements. For example with the bottom bunk bed when the baby is facing the wall the rise in the average CO_2 concentrations was around 270 percent, however when the baby was facing the room (bars) the CO_2 concentrations only rose by nearly 30 percent. Facing the roof led to an average increase of around 80 percent. Therefore it is concluded that the position of the baby has a significant effect on the measured values. When the mouth of the baby is facing an open surrounding the average CO_2 concentrations of the inhaled air decreased significantly compared to when a baby was facing a more closed surrounding. Therefore it is concluded that it is not sufficient to only measure the CO_2 concentrations in the sleeping room as the conditions will significantly deviate from those in a crib.

6 REFERENCES

Boor, B.E., Järström, H., Novoselac, A., Xu, Y. (2014), Infant Exposure to Emissions of Volatile organic Compounds from Crib Mattresses, Environmental Science & technology 48: 3541-3549

Boor, B.E., Liang, Y., Crain, N.E., Järström, H., Novoselac,, A., Xu, Y. (2014), Identification of Phthalate and Alternative Plasticizers, Flame Retardants, and Unreacted isocyanates in infants Crib Mattress Covers and Foam, Environmental Science & technology Letters 2: 89-94

Boor, B.E., Spilak, M.P., Laverge, J., Novoselac, A., Xu, Y. (2017), Human exposure to indoor air pollutants in sleep microenvironment: A literature review, Building and Environment 125: 528-555.

Braun, G., Zeiler, W..(2019). The CO_2 conditions within the baby cots of day care centres . Proceedings Clima 2019, Boukarest, Romenia.

Corbyn, J.A. (2000), Mechanism of sudden infant death and the contamination of inspired air with exhaled air, Medical Hypotheses 54(3); 345-352

Crowe, K. (1974). *A History of the Original Peoples of Northern Canada.* Montreal: McGill/Queen's University Press for the Arctic Insitute of North America.

Deboer, S. L. (2004). Emergency Newborn Care. Trafford Publishing.

De La Iglesia, D., De Paz, J.E., Villarrubia Gonzãlez,779. G., Barriuso, A.L., Bajo J. (2018), A Context-Aware Indoor Air Quality System for Sudden infant death Syndrome prevention, Sensors 18: 757-

Dhami, P.S., Chopra, G., Shrivastava, H. (2015). A textbook of Biology. Jalandhar, Punjab: Pradeep Publications.

GGD Nederland. (2006). Toetswaarden voor ventilatie in scholen en kindercentra. GGD Nederland, werkgroep binnenmilieu.

Iglowstein, I., Jenni, O.G., Molinari, L., Largo, R.H. (2003), Sleep duration from infancy to adolescence: reference values and generational trends, Pediatrics 111: 302-307.

Kinderdagverblijf -Gouda (2016), www.kinderdagverblijf-gouda.nl/hoera-nieuwe-bedden-en-boxen/

Kosch, P.C., Stark, A. R. (1984). Dynamic maintenance of end-expiratory lung volume. Boston, Massauchusetts: Harvard School of public healt.

Kruisselbrink, T.W.(2015) , CO_2 Concentration in the Vicinity of Sleeping Infants at Dutch Daycare Centers, Master project TU/e, Eindhoven, Netherlands

U.S. Environmental Protection Agency (EPA) (2009), Exposure Factors Handbook,Chapter 6, Inhalation Rates, U.S. EPA, Washington, D.C., US.

Sakai J., Kanetake J., Takahashi S., Kanawaku Y., Funayama M., 2008, Gas dispersal potential of bedding as a cause for sudden infant death, Forensic Science international 180: 93-97.

Versteeg, H. (2012). Kwaliteit binnenmilieu kinderdagverblijven, Bouwfysica 1: 2-6.

Waard, M. de (2014). Influence of bedroom configurations on the CO_2-concentration of the surrounding air near a sleeping infant, MSc thesis TU/e, Eindhoven, The Netherlands.

Waard, M. de (2015), The effects of type and location of baby cots on indoor environment qualty in a day care centre, Poroceedings Healthy Buildings, Eindhoven, The Netherlands.

Zaslow, M. (1988). The Northward Expansion of Canada. The Journal of Canada, 2(3), 216-222.

Zeiler, W., (2018). The indoor environmental quality in Dutch day care centres: The effects of ventilation on the conditions within the baby cots, Proceedings Roomvent & Ventilation 2018, Espoo, Finland.

Quality framework for residential ventilation systems in Flemish Region in Belgium – feedback after three years' experience

Maarten De Strycker[*1], Liesje Van Gelder[1], Martyna Andrzejewicz[1] and Valérie Leprince[2]

1 BCCA
Aarlenstraat 53
BE-1040 Brussels, Belgium
**Corresponding author: m.de_strycker@bcca.be*

2 PLEIAQ
84 C Av. de la Libération
69330 Meyzieu, France

ABSTRACT

A ventilation performance report is mandatory for every new residential building in Flanders, for building permits issued since January, 1st 2016. This means that the features of the ventilation system as installed in the dwelling must be reported and that, in the EPB-report of the dwelling, these data must be used to justify the energy performance of the ventilation system.

To enhance the properly functioning of the ventilation systems, a ventilation preliminary design has to be made before the physical building process is started.

The EPB-regulation in Flanders defines sine 2006 minimal ventilation requirements per type of room. In 2015, a new regulation, which refers to STS-P73-1, was published. The STS-P 73-1 describes performance criteria for residential ventilation systems and how to report them.

Similar to the reporting of the airtightness of the building, the reporting of performance of the ventilation system is guarded by a quality framework. The quality framework requires that the preliminary design and the report after commissioning are made by a qualified reporter and that audits, both desktop and on-site, are performed by auditors from the organiser of the quality framework. This article also describes requirements for quality framework organisers as defined by the authorities in Flanders.

This article describes the quality framework and its output. Desktop and on-site controls represent both 10% of ventilation performance reports. They are done by 12 qualified auditors all around Flanders. The inspector has to inform BCCA of every inspection at least the day before and to send a message when the measurement actually starts and ends. The inspector is informed within 5 minutes after the end of the inspection whether he will be audited or not.

The article discusses some results of the quality framework: the effectiveness of the audits, the outcome of the audits on preliminary designs, the challenges in measuring ventilation flows on-site, the energy use of the fans and the conformity of ventilation systems with the regulatory requirements.

The article concludes that it is possible to set up an effective and efficient quality framework for inspections on ventilation systems. An intermediate step to fill the gap between the non-binding preliminary design of the ventilation system and the commissioning of the system 21 months later is presented. The situation for ventilation systems is not dramatic, but there is still room for improvement of the quality of ventilation systems in residential applications and on-site measurements require some guidance.

KEYWORDS

Ventilation system inspection, quality framework, database

1 INTRODUCTION

Indoor air quality and the well-performance of residential ventilation systems is a concern in many countries and the inspection of residential ventilation systems comes gradually into force in European countries (Bailly Mélois & Mouradian, 2018) (Bourdin, 2019) (EPBD19, 2019)

This is also the case in Flanders, Belgium, where the energy performance calculation of the building also ensures that a healthy and comfortable indoor climate is provided to the occupants. As with stricter energy performance requirements, buildings become more airtight and controlled ventilation is becoming more and more important. Minimal air flows for different rooms are determined (Vlaams Energieagentschap, 2019).
During last years stakeholders (architects, installers, producers and distributors of ventilation products, EPB-reporters, …) and the authorities have been concerned about the properly functioning of ventilation systems and the accuracy and reliability of the reported air flowrates in the EPB-reporting. This concern is justified by the fact that 80% of the non-compliance fees in EPB-regulation are related to the ventilation systems (Vlaams Energiesagentschap, 2019)

Therefore, a quality framework for the inspection of ventilation systems in residential buildings was launched on January 1st, 2016.

The objectives of this article are to:

- Describe the Flemish quality framework for the inspection of residential ventilation systems,
- Explain the efficient audit process to improve the reliability of results,
- Give output and lessons learned from the quality framework.

2 METHOD

2.1 STS-P 73-1 : the key document

The STS are "Unified technical specifications". They are edited by the Belgian Federal Public Service for Economy to optimise and standardise construction quality. Various STS exist on the construction field, STS-P 73-1 is for ventilation systems in residential buildings (SFP Economie, 2015).

In the STS-P, the criteria for ventilation systems that could be prescribed and could be reported are listed.
The STS-P does not prescribe requirements for the ventilation system, but lists possible evaluation criteria for ventilation systems and how to prescribe, determine and the performance of the ventilation system for each the criteria. For example, the STS-P does not impose or advice a certain specific fan power of the system (SFP_{system}), but it defines the formula for calculating the SFP_{system}, the classes, and the method for measuring the power consumption of the ventilation system. It is then up to the builder to define which class of SFP_{system} should be reached and to the ventilation inspector to determine the actual class of SFP_{system}.
Different levels of requirements may apply to a ventilation system, e.g. the EPB-regulation sets only minimal ventilation flows, but a builder could require better IAQ, so higher ventilation flows. Therefore the output of the ventilation inspection is not a conformity declaration to a requirement, but a report (the ventilation performance report VPR) with

objective data and figures about the performance of the ventilation system such as (neither exhaustive, nor applicable to all):

- per room the measured air flow, nominal air flow of air inlets,
- the efficiency of the heat recovery unit,
- the power consumption of the fan,
- the description of the demand controlled ventilation system,
- etc.

2.2 The Flemish regulation

The Ministerial Decision that enforced the quality framework for inspections of ventilation systems was published in November 2015. It defines the rules that apply to residential ventilation systems in dwellings with a building permit from January 1st 2016 on (VLAAMSE CODEX, 2015). The two main requirements in this regulation are

(i) a ventilation preliminary design is mandatory before the building works start and
(ii) a ventilation performance report is required to justify the values related to the ventilation system in the EPB-reporting. A ventilation performance report can be seen as an inspection by a qualified inspector, according to the STS-P 73-1 on the ventilation system after commissioning.

The quality framework for inspections on ventilation systems is managed by an *organiser of a quality framework*.

In December 2017, the Flemish government has tightened the requirements on the organisers of the quality framework for the inspection of residential ventilation systems:

- The organiser of a quality framework must have a qualification procedure for ventilation inspectors, which includes at least
  - an optional training,
  - a mandatory theoretical and practical exam.
- The organiser of a quality framework must guarantee the reliability of the ventilation reporting by running desktop and on-site audits combined with effective enforcement.
  - Minimal random annual desk and on-site audits is 10% each.
  - Random checks are supplemented by targeted checks so that 90% of the active inspectors are checked at least once a year.
- The organiser of a quality framework shall develop a database gathering all measurement data that can be consulted by the authorities.
- The organiser of a quality framework is impartial: he should not have any members or directors who also carry out ventilation reporting in the context of the regulation.
- The organiser of a quality framework must have an accreditation in accordance with NBN EN ISO 17065 (certification of products and services).

The organiser of the quality framework has to be approved by the Flemish authorities.

The inspector shall be qualified and its company recognised by an approved organiser of the quality framework to perform a task in this context.
The quality framework for the inspection of residential ventilation systems of BCCA (Belgian Construction Certification Association) has been approved by the Flemish authorities since the new requirements on qualification bodies.

2.3 The BCCA quality framework

The purpose of the quality framework is to guarantee the correct reporting on the performance of the ventilation system. The reporting on the performance of the ventilation systems is done by *inspectors*. An inspector is a person that is qualified by the organiser of the quality

framework and is audited by the quality organisation by desktop and on-site audits. The surveillance on the inspectors is done by BCCA *auditors*.

Qualification
BCCA provides a complete quality framework for a company which includes the qualification procedure for the inspector.
The qualification procedure for the inspectors includes:

- Optional theoretical training (1 day)
- Theoretical exam for each component of the ventilation system (online multiple choice questionnaire)
- Practical exam: measuring the flow at 10 vents with their own measuring device. Different flows between 25 and 90m³/h, both extraction and pulsion.

Web application and database
To facilitate the process of inspection, reporting and auditing, a web application has been set up. Only qualified inspectors and auditors of BCCA have active access to this application. A builder has passive access to the database, which means that the access is limited to consult documents validated by the inspectors.

Auditing processes
BCCA has 12 auditors active to manage the quality framework. Not all auditors are working full-time on this quality framework, and the auditors are regionally distributed over the area of Flanders to limit travelling time to audited buildings. Auditors have at least the same qualification as inspectors plus a specific training for audits. Furthermore, auditors are regularly checked on-site by their manager and internal meetings are set up.

The **on-site audit** is either performed:

- Option 1: During the measurement
- Option 2: After the communication of the measurement result with a check on this result by a second (partial) measurement (at least half of on-site inspections are performed in Option 2).

To allow this inspection, at least one day before the measurement is performed, the inspector shall provide some information to BCCA by the online platform, such as the address of the building, the timing of the measurement, and the person that will do the inspection. When on-site, the inspector has to send an SMS, or indicate in the web application that the measurement has started. After the measurement, the inspector has to communicate the measurement results by SMS or in the web application.

During the audit, the auditor checks

- the qualification of the inspector and the company,
- the equipment (calibration, settings and correct use),
- the building preparation,
- the fixed components of the ventilation system,
- the compliance of the measurements of air flowrates and fans power with the STS-P 73-1. The inspector has to remeasure a random set of vents under supervision of the auditor. This result is compared to the reported ones to check the reliability.

The **desktop audit** is performed when preliminary designs or performance reports are uploaded in the database. If a desktop audit is done, the auditor will check at least the following:

- The report is complete and made according to the STS-P 73-1,
- The timing is correct (lodgement of information, etc.),
- Text messages have been sent according to the schedule ,
- The information in the report is consistent (e.g. type of ventilation system corresponds to the components reported).

Non-conformities and sanctions
An essential part, besides doing audits, is following up output audits. The system of enforcement classifies non-conformities into 4 categories:

- **Unacceptable non-conformities (ONC)**: such as deliberate manipulation of results in the reported flowrate, repeated "major non-conformities" with no correction,
- **Major non-conformities (GNC)**: anomalies with regard to the STS-P 73-1 with an important impact on the measurement result, repeated "minor non-conformities",
- **Minor non-conformities (KNC):** anomalies with regard to the STS-P 73-1 that have a small impact on the result, repeated remarks,
- **Remarks (REM).**

For a minor non-conformity, the frequency of desktop or on-site inspection is increased.
For a major non-conformity, also the performance report and/or the measurement shall be redone.
In case of major non-conformity, due to calibration validity, the recognition may be temporarily withdrawn. These sanctions are clearly communicated to the inspectors in the rules of the BCCA quality framework (BCCA, 2019).

Cost
Every report has a cost of 71.5EUR. This cost is split between the registration of the ventilation preliminary design and making up the ventilation performance report. An additional cost of 10.21EUR is added when different companies are working on the same report and a reduction is foreseen for dossiers containing more than 10 dwellings.
Yearly fee for use of the digital platform is 255.36EUR, with an additional cost of 51.07EUR per extra qualified user in the company.
The optional 1-day training costs 355EUR.
The online theoretical exam costs 51.07EUR per module, for the package with all modules this amounts to 177.73EUR.
The practical exam costs 178.75EUR.

3 RESULTS

3.1 Qualified inspectors
In June 2019, 560 qualified inspectors were active in 470 companies in the BCCA quality framework.

3.2 Measurement lodging
There is a substantial time between the building permit date and the measurement of the ventilation flowrates. Although all dwellings with a building permit date after 1/1/2016 fall under the application of the quality framework, in 2016 only 1 measurement was registered in the database. Fig.1 shows the number of measurements registered in the BCCA database on a monthly base for 2017. It is clear that the measurement of ventilation flows took off only from September 2017 on which is 21 months after the first building permits falling under this regulation.

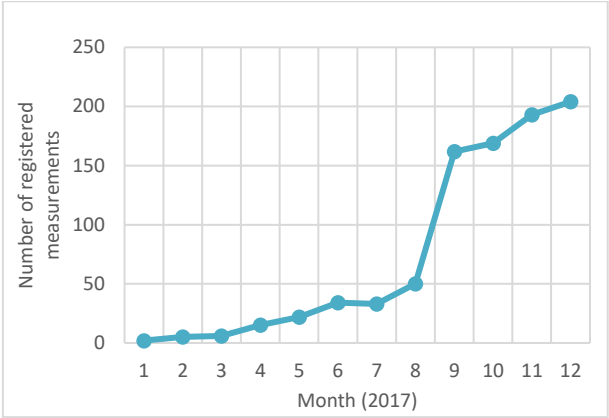

Fig. 1 Number of measurements on monthly base registered in the BCCA database

This shows one of the issues with the quality of a ventilation system in a building: ventilation should be taken into account from the building design (e.g. space for the unit and the ducting, effect of trickle vents on windows), but the effectiveness of the system is only controllable several months later: after installing all components and commissioning of the ventilation system.

3.3 Inspections on preliminary designs

The preliminary design of the ventilation system comprises a plan with some essential elements on it, e.g. the position of the ventilation unit, the position and the indicative diameter of the ductwork, for each room the function, the surface, … Details can be found in a separate document (Werkgroep A VVO, 2017).

A preliminary design is not binding, especially because of the timing: it should be made before the construction works start. In most cases, the builder has, at that moment, no idea of the details of ventilation system that will be chosen, and the installer is not yet known. In most cases, there should be an estimation about the required performance of the ventilation system to reach the energy performance of the dwelling.

The inspections on the preliminary designs are thus limited to checking if the required elements are present. The findings from these inspections are:

- That some are very comprehensive and some are very limited.
- In most cases, the condensate drain is missing, which can be an issue when the heat recovery unit is located far away from the drainage system.
- The position of the operating console of the unit, which may require wiring when the console is not put on the unit or the console is not functioning wireless.
- The position of the air inlet and outlet (facade or roof) is not specified, which may induce issues with the dilution factor and recirculating air.
- Attenuators are not specified, while they need a substantial place and the lack of attenuators may induce acoustical issues.

3.4 On-site audits

More than 10% of installations for which an inspection has been carried out in 2018 have undergone a desktop audit and more than 10% have undergone an on-site audit. In Fig. 2 the regional distribution of the inspections registered in the database and the audits done by BCCA auditors is presented. From these density plots is clear that both have a similar distribution.

Audits performed in 2018 Inspections performed in 2018

Figure 2: Geographical distribution of the inspections and inspections registered with BCCA in 2018

Fig. 3 shows that the same repartition of the day of the week is observed in audited inspections and in all inspections performed (even during the weekend).

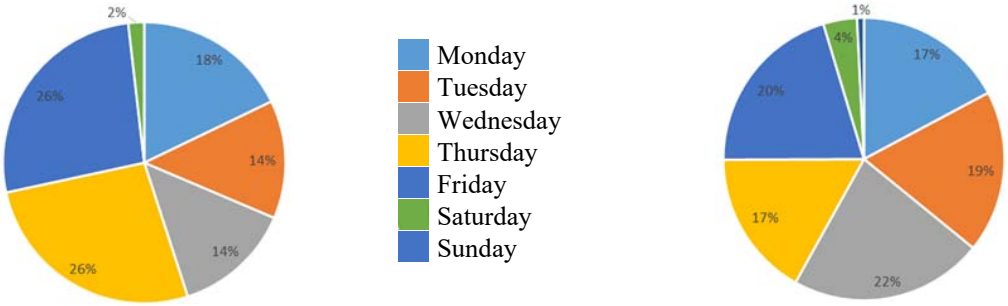

Audit days Inspection days

Figure 3: Repartition of the day of the measurement for audits and for all inspections in 2018

From Fig. 2 and Fig. 3 can be concluded that the auditing process is representative for the actual distribution (both in time and geographical) of the inspections in Flanders.

3.5 Measurement of power consumption

In 60% of the inspections the power consumption of the fans was measured, see Fig. 4.

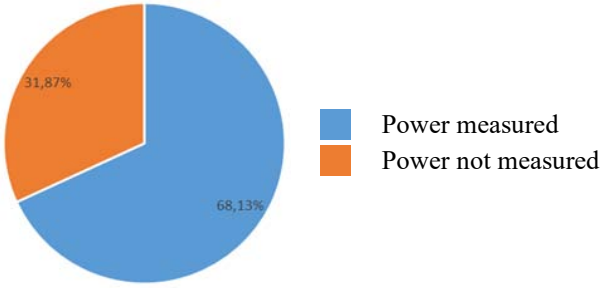

Figure 4: Ratio of installations with the power consumption measured

SFP_{system} recorded in the database are shown in Fig. 5. The average SFP_{system} for ventilation systems with only mechanical exhaust is 0.22 W/(m³/h), which corresponds to SFP_{system} class 3 in the STS-P. Average SFP_{system} for a ventilation system with mechanical ventilation and heat recovery is 0.50 W/(m³/h), which corresponds to SFP_{system} class 4 in the STS-P. Although the average value of the SFP_{system} is reasonable, there is quite some spread on the power consumption of the systems. The high SFP_{system}-values for a large part of the inspected ventilation systems, indicate that there is room for improvement in the design and installation of ventilation systems in dwellings.

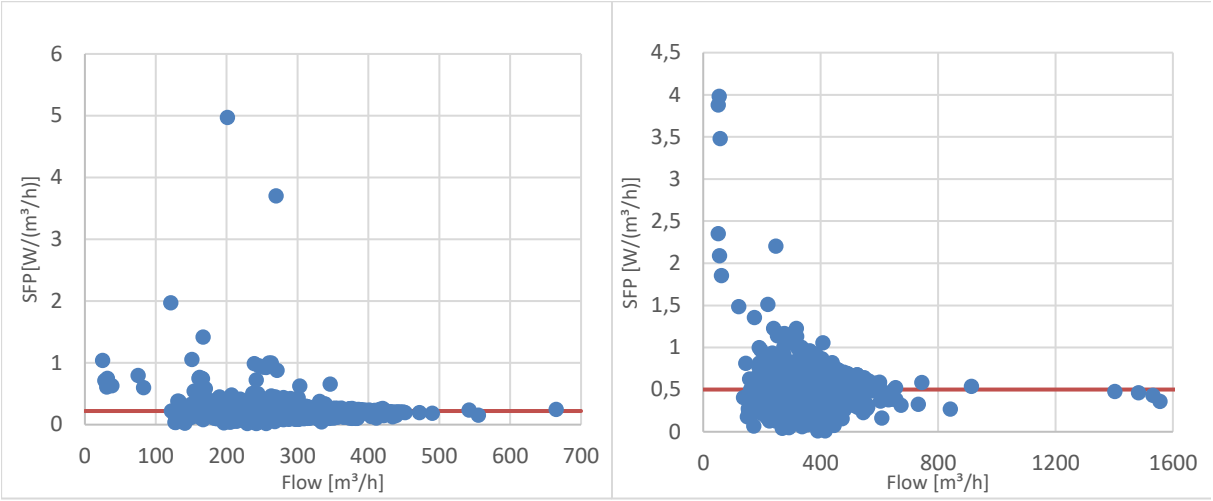

Mechanical exhaust | Mechanical ventilation with heat recovery

Figure 5: SFP_{system} distribution for different systems

3.6 Conformity of the inspected ventilation systems with EPB-regulation

Based on the registered flows in the database, some superficial conclusions on the conformity of the inspected ventilation systems with the EPB-regulation can be drawn. In the regulation, the minimum flowrate for a room is 25m³/h (extracted air), which is required for a WC. Fig. 6 shows the minimal exhaust flow per registered inspection in the database.

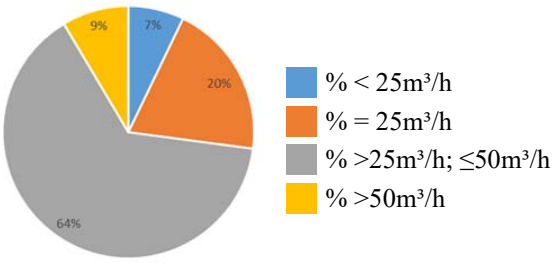

Figure 6: SFP distribution for different systems

In 7% of the registered measurements the lowest airflow rate is lower than 25m³/h, which means that at least 7% of the ventilation systems does not reach the minimum requirements as set in the EPB-regulation for at least one room. Probably a higher share of systems does not meet the requirements:

- as only the room with the lowest flow can be evaluated from these data. It would require a detailed analysis of the registered flows per room to evaluate the real number of non-complying installations.
- as probably not all inspectors are reporting what was actually measured.

On the other hand, it shows to some extent that inspectors do correctly report what was measured, which shows the effectiveness of the quality framework.

3.7 Challenges in measuring flows on-site

Although measuring flows in ventilation systems seems at first sight quite simple and several techniques are documented in literature (CEN EN 12599, 2012) (CEN EN16211, 2015; ISO 16956, 2015), in practice some challenging situations exist. Within the quality framework, almost all measurements are performed with flow hoods on the vents. For 1.72% of the systems with mechanical exhaust, there are vents with a reported flowrate of 0m³/h, which means that it was not possible to measure the airflow rate for at least one vent, see Fig 7.

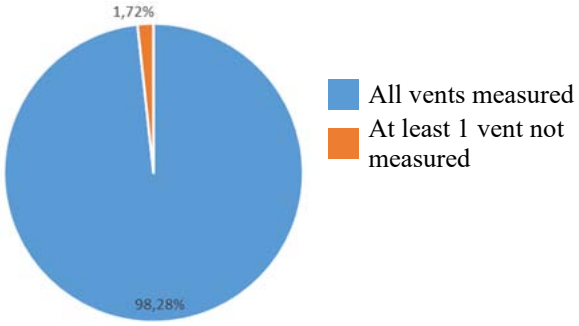

Figure 7: SFP distribution for different systems

1.5 year of inspections has shown that not all vents are measurable on-site. Some ventilation inspectors stay on the safe side, while others act quite creatively to still measure and report a flow. Therefore, in collaboration with the stakeholders, a practical guideline was elaborated to help inspectors in measuring flows (BCCA, Praktische uitdagingen bij het opmeten van ventilatiedebieten, versie 1.0, 2019).
The figure below shows an example taken from this document: the situation on-site is described, the wrong measuring method is shown, and the acceptable solution is shown.

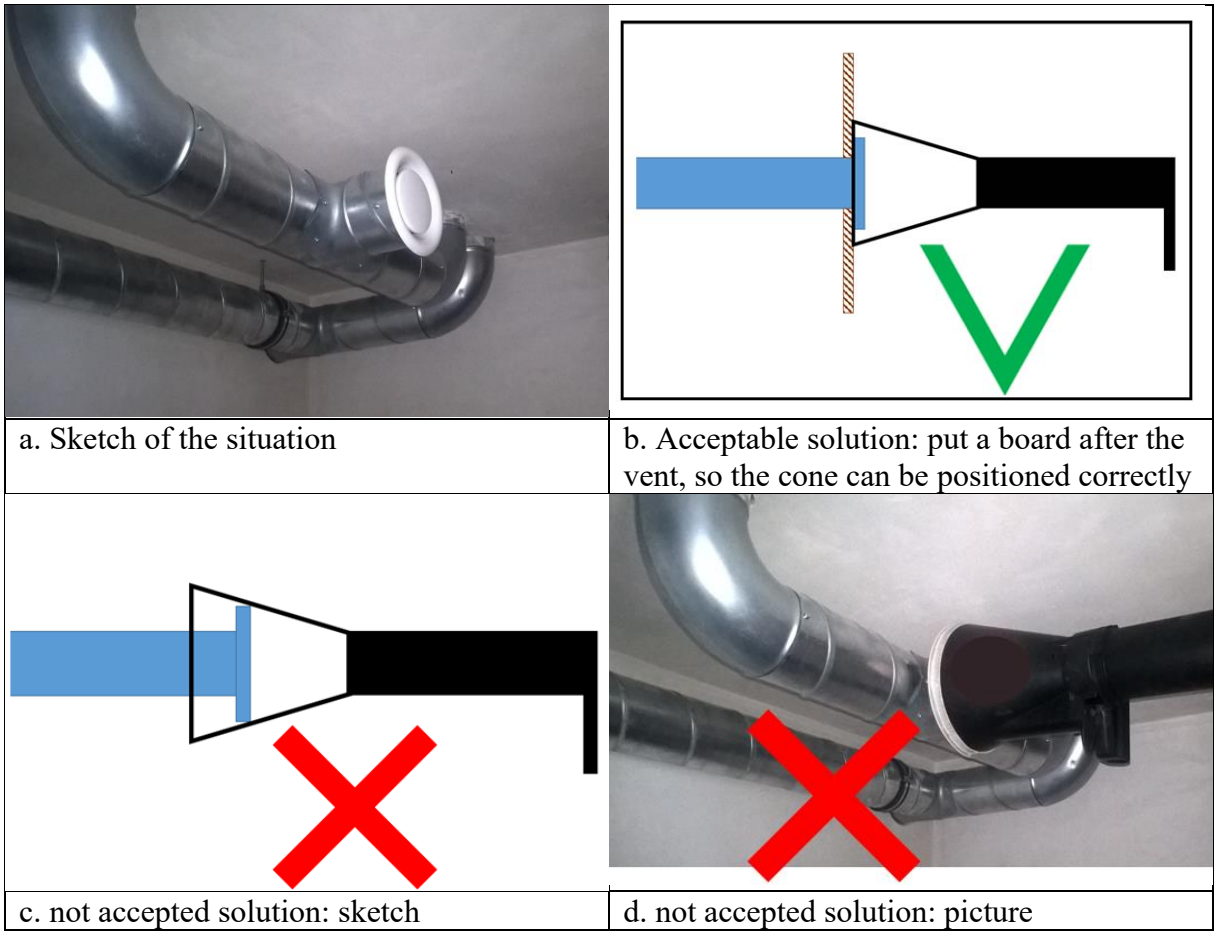

a. Sketch of the situation	b. Acceptable solution: put a board after the vent, so the cone can be positioned correctly
c. not accepted solution: sketch	d. not accepted solution: picture

Figure 8: example from the guideline for measuring ventilation flows

This is also a necessary document for auditors when they have to accept or decline certain measurements. This document may also help other building partners (architects, contractors, builders) to create measurable situations.

4 DISCUSSION

4.1 On-going improvements

In the quality framework of BCCA ventilation design requirements have been introduced in May 2019. The objective is to fill the gap between the preliminary design which is

- not binding,
- made far before the ventilation system is ordered by the installer

and the ventilation performance report which gives the final performance of the ventilation system.
The effect of this additional requirements will probably be only visible within the coming months or years.

Measurements of the air velocity in the ductwork are more and more performed. However, this technique requires some specific precautions (straightness of the ductwork around the measured point, accuracy of the probe, calculation of the flow from the velocity,…). A guidance document is foreseen to detail the conditions for these measurements in addition to EN 16211.

4.2 Future work

It would be interesting to perform a detailed analysis of the performance reports registered in the database and check whether flowrates are complying with the requirements set in the EPB-regulation.

5 CONCLUSION

Since January 1st 2016, a quality framework for the inspection of ventilation systems in new and thoroughly renovated dwellings is mandatory by law in Flanders, Belgium. Besides requirements for the inspection scheme itself, there are also requirements for the organiser of the quality framework. The article gives an overview of the concept of the quality framework and references to documents were details can be found.

This quality framework includes a qualification procedure for inspectors. Only qualified inspectors can make a non-binding ventilation preliminary design. After commissioning, a report of the performance of the ventilation system should be made by a qualified inspector. This report is needed to justify the proper functioning of the ventilation system in the EPB-reporting of the dwelling. The inspectors, who are not collaborators of BCCA, are audited by BCCA auditors through desktop and on-site audits that both represent 10% of the performed inspections.

For the quality framework a web application was developed and the reports are stored in a database. A first analysis of the results in the database shows that the quality of the installations is not dramatic, but that there is still room for improvement.
On average, it takes 21 months between the registration of the preliminary design and the measurement of the ventilation flowrates on-site.

It has been shown that, for Flanders, it is possible to set up a system of on-site unannounced audits of the inspectors. These on-site audits have stressed the need for guidance to perform measurement of ventilation flowrates on-site in challenging situations.

Future work is to fill the gap between the preliminary design and the ventilation performance report and to develop further help for inspectors in measuring flows on-site.

6 ACKNOWLEDGEMENTS

The authors would like to thank the colleagues at BCCA involved in the development and operational activities of the quality frameworks.

7 REFERENCES

Bailly Mélois, A., & Mouradian, L. (2018). Applications of the Promevent protocol for ventilation systems inspection in French regulation and certification programs. *39th AIVC Conference "Smart Ventilation for Buildings",*, (p. 7). Antibes Juan-Les-Pins, France, 18-19 September 2018.

BCCA. (2019). *Beschrijving van het kwaliteitskader Ventilatie van BCCA vzw, Versie 2.0 van 06/05/2019.*

BCCA. (2019). *Praktische uitdagingen bij het opmeten van ventilatiedebieten, versie 1.0.*

Bourdin, E. (2019). The context in Ireland - Changes to Irish regulations and inspection of ventilation systems. *AIVC Workshop: Quality ventilation is the key to achieving low energy healthy buildings*, (p. 22). Dublin, Ireland.

CEN EN 12599. (2012). Ventilation for buildings. Test procedures and measurement methods to hand over air conditioning and ventilation systems.

CEN EN16211. (2015). Ventilation for buildings. Measurement of air flows on site. Methods.

EPBD19. (2019). Récupéré sur https://www.epbd19a.eu/

ISO 16956. (2015). Thermal performance in the built environment — Determination of air flow rate in building applications by field measuring methods.

SFP Economie. (2015). *Spécifications techniques unifiées , STS P-73-1, Systèmes pour la ventilation de base dans les applications résidentielles.*

Vlaams Energieagentschap. (2019). Récupéré sur Energiesparen: https://www.energiesparen.be/bouwen-en-verbouwen/epb-pedia/technieken/ventilatie

Vlaams Energieagentschap. (2019). *EPB-CIJFERRAPPORT Procedures, resultaten en energetischekarakteristieken van het Vlaamse gebouwenbestand - periode 2006 – 2018.* https://www.energiesparen.be/sites/default/files/atoms/files/uitgebreidcijferrapport_2019.pdf.

VLAAMSE CODEX. (2015). *Ministerieel besluit houdende wijziging van het ministerieel besluit van 13 januari 2006 betreffende de vorm en inhoud van de startverklaring en het ministerieel besluit van 2 april 2007 betreffende de vastlegging van de vorm en de inhoud van de EPB-aangi.*

Werkgroep A VVO. (2017). *Werkgroepdocument A, Ventilatievoorontwerp (VVO), Aanvulling op STS-P 73-1: Systemen voor basisventilatie in residentiële toepassingen.* Récupéré sur https://www.ikventileerverstandig.be/wp-content/uploads/2017/02/STS-P-73-1-Ventilatie-Werkgroepdocument-A-ventilatievoorontwerp-201702095.pdf

Commission and performance contracting of ventilation systems in practice. Determination, analyses and consequences for practitioners and contractors

Wouter Borsboom[1], Wim Kornaat[1], Pieter van Beek[1], Niek-Jan Bink[2] and Timothy Lanooy[2]

1 TNO
Delft
Netherlands

2 ACIN instrumenten
Rijswijk
Netherlands

Corresponding author: wouter.borsboom@tno.nl

ABSTRACT

Traditionally ventilation systems in the Netherlands are installed in new or retrofitted buildings by an installation fitter under the responsibility of a contractor. In some cases but certainly not all cases, it is checked by a consultant if the ventilation system performs according to the design. Studies in the Netherlands show that ventilation systems of dwellings often don't meet the designated Standards. Deviations are found in airflow rates, noise from the ventilation system and malfunctioning due to lacking air tightness of the building envelope. Other European countries are struggling with similar quality issues.
In offices and apartment buildings there are several initiatives to improve the performance of ventilation systems. For example by the use of Energy Performance Contracts. In these projects there is an increased attention for quality control in the installation and operational phases. Since a couple of years there are initiatives with performance contracts also in dwellings. An example is the energy efficient retrofitting of dwellings repaid via the energy bill in "Stroomversnelling". As a result of this driver of performance contracting, several initiatives have sprung up to support quality control of ventilation systems in dwellings, through new test instruments, ICT solutions and training. In the SecureVent project easy to handle methods for installation fitters are being developed to check the performance of a ventilation system regarding air flow distribution, noise and airtightness with good accuracy. Instruments which will soon be on the market are presented. Within the Energy leap "Stroomversnelling" program an API (Application Programming Interface) has been developed allowing standardized communication between on the one hand an external database and on the other hand sensors and installation in a dwelling. This allows an easy check on performance of the Indoor Environmental Quality (IEQ) and Energy use, both for housing corporations and occupants. In the Horizon2020 Sphere project this kind of interfaces will be used to build a digital representation (Digital Twin) of a dwelling based on monitoring data. It will be used to check the performance on IEQ and Energy use during the lifespan of a dwelling. It is important that the craftsmen installing the ventilation system have ample knowledge and skills to check its performance during construction and commissioning. To this end, in the Newcom project a European training program is being developed to help the craftsmen involved to acquire the required skills to obtain better performing ventilation systems.

KEYWORDS
Energy performance contracting, ventilation testing, commissioning

1 INTRODUCTION

Studies in the Netherlands show that ventilation systems of dwellings don't comply with building regulations. The main shortcoming is insufficient ventilation. This applies to both the house as a whole as to individual rooms. Ventilation systems produce too much noise, for example due to the lack of adequate silencers, the location of the ventilation unit and the dimensions of the air ducts. Because ventilation systems make so much noise when operating at high flow, the ventilation is often only set to the lowest speed (van Dijken, 2011). Because the houses are often not sufficiently airtight, the designed ventilation flows are not achieved especially for houses with natural supply and centralized mechanical extract ventilation. Other European countries are struggling with similar quality issues. In France, an analysis of 1,287 houses showed that 68% of single-family homes were found to be non-compliant with regard to ventilation regulations. Many of these malfunctions could be avoided through the implementation of quality management tools. These tools should be available at different stages of the construction process, and should be efficient and effective. (Jobert, 2013). Performance contracts can be an important driver for quality management and to focus on performance rather than the placement of components. Simplified tools should make it possible during the construction process to simply and effectively measure the most important aspects affecting the overall performance of the ventilation system: noise from the ventilation system, volume flow and airtightness of the building envelope.

2 CURRENT COMMISIONING

2.1 Current commissioning in the Netherlands

Traditionally ventilation systems are installed in new or retrofitted buildings by an installation fitter under the responsibility of a contractor. In some cases, the performance of the ventilation system and the airtightness of the building envelope are measured by a consultant. In these cases, the first dwelling of the project is tested, after which adjustments may be made. In exceptional cases, all the houses in the project are tested individually. In offices and apartment buildings there are several initiatives to apply energy performance contracts (EPC). In these contracts there is a shift from installing and supplying products and systems towards supplying good indoor environmental quality and low energy use. In these projects there is an increased attention for quality control in the installation and operational phases. Quality standards are very important. In essence, they are a natural part of the EPC; because the contractor (ESCO) gives a guarantee regarding energy savings. Renovations are done at a level that offers the savings and all the guarantees are fulfilled (Augustins, 2018).

2.2 Energy performance contracts and commissioning for Nearly Zero Energy dwellings in the Netherlands

Since 2016 there is legislation in the Netherlands for energy performance contracts for nearly zero energy dwellings initiated by the "Stroomversnelling". Landlords and housing associations that renovate their homes to a (nearly) energy-neutral are entitled to ask their tenants for an energy performance fee, "Energie Prestatie Vergoeding" (EPV). The landlord supplies energy to the tenant for his own use by financing the photovoltaic systems and

retrofitting of their dwelling. The landlord may charge an energy performance fee for this in order to recoup his investments. Whereas the tenant previously paid rent to the landlord and the energy bill to the energy company, the tenant will pay an energy performance fee to the landlord in addition to the rent after the renovation. The aim is that the total housing costs for the tenant do not increase compared to the 'old' situation. The first condition for an energy performance fee is a very good insulation of the house. How well the house is insulated must be determined by an approved company. Such a company assesses, among other things, the floor and roof insulation, and what type of glass the windows have. If the heat demand is less than 50 kWh per square metre per year, the landlord or housing corporation may request an EPV. The amount of energy generated in the house must be recorded. The landlord or housing corporation, must provide an overview of the energy generated in the dwelling in the past year before 1 July each year. Because the energy savings and energy productions are well measured, therefore there is a strong driver for the contractor to deliver high quality installations and an airtight building envelope. It is also possible to get a quality label for this type of energy efficient dwelling.

2.3 NOM Certificate for dwellings

In the Netherlands, the “Stroomversnelling” has taken the initiative to achieve the NOM label. Houses that meet the NOM standard can more easily meet the regulations needed for the energy performance fee. Builders who offer dwellings with a NOM label, offer proven and tested retrofitting solutions and give at least ten years warranty on the performance after delivery. The NOM certification starts with a review of the concept, from the technical design, quality control plan to performance conditions and residents' manual. When renovating, it is checked whether the legal requirements are met in order to obtain the energy performance fee. During construction and at commissioning, a sample dwelling is taken to measure the performance of the dwelling, for example air flow measurements and airtightness testing. During the use phase, the monitoring data is presented to an audit team together with a report on the experiences of the users. The user survey takes place before, during and one after year of renovation.

2.4 Open Source API and model based data analytics

In order to make it easier to monitor the data of homes with a NOM label or an energy performance fee, an interface has been created by the "Stroomversnelling". This API (Application Program Interface) makes it easy to exchange data from different monitoring systems. The open source API developed jointly by market parties and Stroomversnelling makes it possible for different software providers to develop monitoring products that can communicate with each other. This makes it easier for housing associations, to collect the performances of different monitor systems and compare them with each other. This contributes to the delivery of good quality.
In the Horizon2020 project Sphere, such data will be used to calibrate physical models in order to make a digital representation (Digital Twin) of dwellings in the field of indoor air quality and energy. The houses in this project will be 100% checked for airtightness, ventilation and noise during delivery, but also the performance in the field of indoor air quality and energy will be tested during the use phase with such a Digital Twin.

3 SIMPLIFIED MEASURING TECHNIQUES FOR VENTILATION

3.1 Current measurement techniques

To obtain a good indoor climate, the ventilation flows from the ventilation system for each room in a dwelling needs to meet the demands given by standards which are based upon pollution by persons, moisture production, production of fine particles and so on. Often, due to incorrect adjustment of the mechanical ventilation system, the flows for the whole dwelling or for the different rooms in the dwelling do not meet the standards. These adjustments concern the tuning of the fan itself plus the valves and grids in the system. A proper control of the actual realised ventilation flows from the ventilation system is required but often not performed. For airflow measurements a pressure compensating airflow meter should be used. Such a meter consists of a controllable fan and a differential pressure meter. Although it is in fact the only way to measure (supply) flows properly it is not used in all cases, as it is not affordable for all craftsmen.

Especially in case of a centralized mechanical extract ventilation system in combination with grids in the façade, the airtightness of a dwelling also influences the ventilation. Besides the fact that a low airtightness results in higher energy use, it also reduces the ability of the ventilation system to achieve the desired ventilation flows. In other words, the ventilation system does not succeed in achieving the desired pressure difference across the ventilation grids for sufficient ventilation flow, especially on the leeward side of the house. Opening of a grid does not lead to air intake because the air enters via the gaps and cracks at other places. Checking the airtightness is therefore needed. Nowadays the airtightness of a dwelling is measured by a so-called “blowerdoor” test. In case of a blowerdoor test, a dummy door is installed in the door of the dwelling in which a controllable fan is incorporated. A lot of equipment is needed for a blowerdoor test, e.g. the dummy door, and installation takes time.

Another problem is that in practice often too high noise levels are produced by the ventilation system especially at higher fan flows. Due to this, occupants do not use the ventilation system at the appropriate flow. Means to measure the noise levels and to indicate possible adjustments are needed. The current measurement of noise in homes according to the Dutch Standard is complex and requires specialist equipment and knowledge. In particular this applies to reverberation time measurements. It requires a speaker to produce sound and a dedicated sound meter, including software to calculate the reverberation time.

To improve the indoor climate on the above-mentioned aspects, easy to use and affordable measuring techniques are needed. In the Dutch TKI project SecureVent this is done for the measurement of airflows, airtightness and noisy production.

3.2 Simplified measurement of airtightness

In case of a blowerdoor test different over- or under pressures in the dwelling are set by adjusting the fan speed in the blowerdoor, while at the same time the supplied or extracted airflow is measured. Based upon the relation between airflows and pressure differences, the airtightness of the dwelling is determined.

A simplified measuring technique is developed in which the ventilation system in the dwelling is used to maintain a pressure difference over the façade. By switching the ventilation system from off/low to on/high position an under- or overpressure, in case of respectively extract or supply, can be obtained. The pressure difference is measured using a reference vessel. The pressure in this vessel serves as the reference to the pressure changes in the dwelling due to switching the fan. A connection to the outside is therefore not needed. In combination with the airflow maintained by the ventilation system, the airtightness can be derived.

The simplified airtightness measurement can easily be performed by placing the equipment (see figure 1) in either one of the rooms. The equipment consists of the reference vessel and a

differential pressure meter. The dimensions are roughly 15 by 30 cm, so easily portable. The measurement is performed using a tablet which is connected via WIFI to the equipment. After setting the airflow in the tablet, the measurement can be performed by switching the fan a couple of times. The pressure difference is indicated to monitor the measurement (see figure 2) and finally the airtightness is calculated automatically (Lanooy, 2019).
Measurements have been performed in 82 dwelling in which both a blower door test and a simplified airtightness measurement are performed. The results show a good comparison (see figure 3).

Figure 1: Equipment simplified airtightness measurement (prototype)

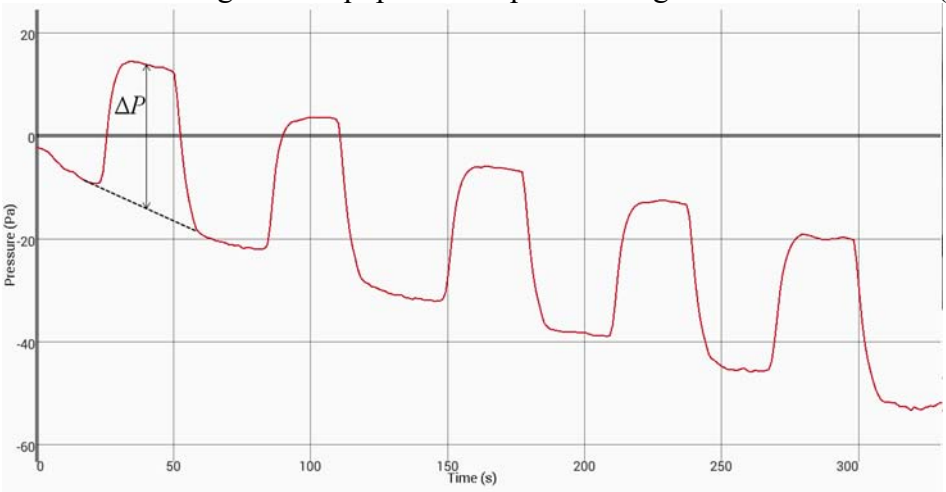

Figure 2: Typical measured pressure difference

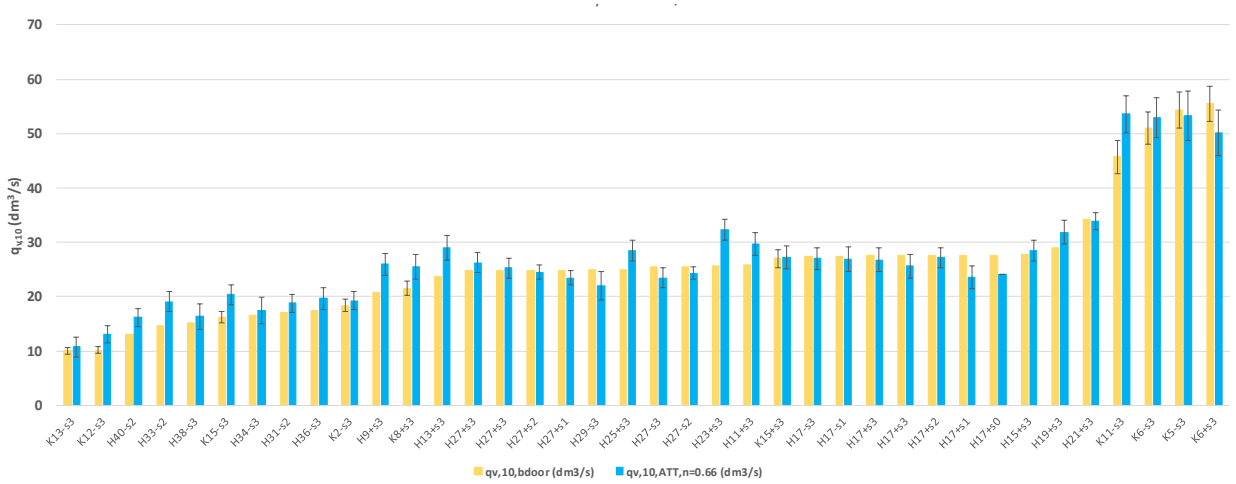

Figure 3: Comparison of blowerdoor measurement ($q_{v,10,bdoor}$) with the simplified airtightness measurement ($q_{v,10,ATT}$)

3.3 Simplified air flow measurement

At first, the possibilities for the development of a simplified version of a pressure compensating airflow meter were investigated. However it was hard to improve on the existing instruments against a lower price while maintaining the same accuracy and measuring range. The next option was to find an alternative method by relaxing the level of accuracy and decreasing the measuring range. The main challenge was to design an airflow meter which can handle supply flows. Especially an inducing supply valve with a covered sector can cause inaccuracies due to turbulence and a variable velocity field. The pressure compensating instruments have a high resistance and, while compensating this resistance, they also 'destroy' the unwanted turbulence and smooth the velocity field. At lower airflows, from standard grids, pressure compensation is less important but smoothing the velocity field is important. It was found that an existing passive propeller airflow meter could be improved using a flow hood with a special flow straightener to do just this. The design of the hood and the flow straightener are optimized to limit the pressure drop and to obtain a correct measurement of the airflow. Supply and extract flows can be measured up to 100 m^3/h with a maximum deviation of about 10% for most occurring ventilation grids (see figure 5) .

Figure 4: Passive flowmeter (prototype)

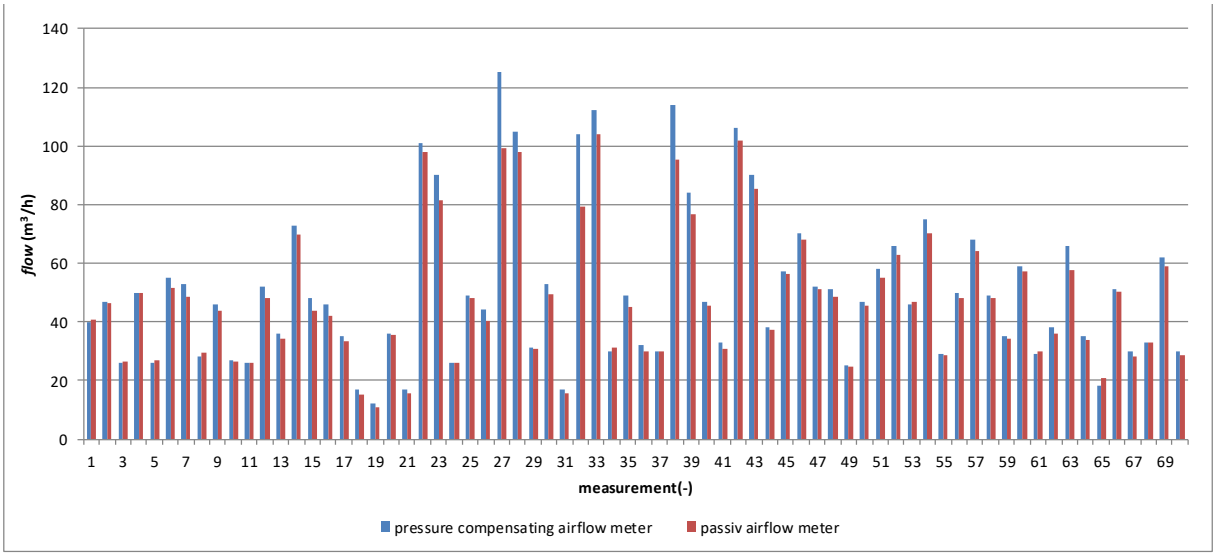

Figure 5: Comparison pressure compensating and passiv airflow meter

3.4 Simplified noise measurement of ventilation systems

The noise production of a ventilation system in a room can be considered to depend upon the following aspects:

a) the pressure drop over the ventilation ducts,
b) the noise level nearby the ventilation unit,
c) the electrical power consumption by the ventilator
d) the number of bends, reducers, tees, flexible hoses and so on in a duct system.

A simplified approach to verify the possibility for too high noise levels can be done by measurement of the above-mentioned aspects a) to c) and perform a visual inspection of the duct system. In this way actual noise measurements don't have to be performed (such measurements can be difficult, due to background noise and require dedicated instruments). The pressure drop over the ventilation ducts can sometimes be read from the ventilation unit display, depending on the type of ventilation unit, or can be measured with either a pitot tube or the installation of a hose through the outer layer of a flexible hose. The noise level close to the ventilation unit can be measured with a class 2 sound level meter, while the electrical power can be measured with any appropriate power meter. For the visual inspection, a checklist has been made with, among other things, the permissible length of the dampers, installation space of the ventilation unit (in a separate room / acoustic cupboard / cupboard / outside), number of bends, etc.
This simplified method has been investigated by actual measurements, together with noise measurements according to standards. In this case the BRL 8010 (method 1) (KvINL 2012) and NEN 5077 are applied. The investigation showed that only in a very limited number of cases the noise level met the requirements, i.e. 30 dBA in living and sleeping rooms. This immediately indicates the seriousness of the noise problems. It also turned out that in the houses in which the noise did meet the requirements, the simplified approach could score poorly (indicating risk of noise problems). The other way around also occurred, because some houses that did not comply with the noise limit, scored well according to the simplified approach. In order to be able to better assess the simplified approach, more measurements still are needed in dwellings in which the noise complies with the limit.
The best alternative to the simplified approach is considered to be method 1 according to the BRL 8010. According to this method the noise measurements should be carried out in the critical reception areas, such as living room and master bedroom. With this method, reverberation is not measured but determined according to tables. This method corresponds

well with NEN 5077, where the actual reverberation time is measured. This is shown in figure 6.

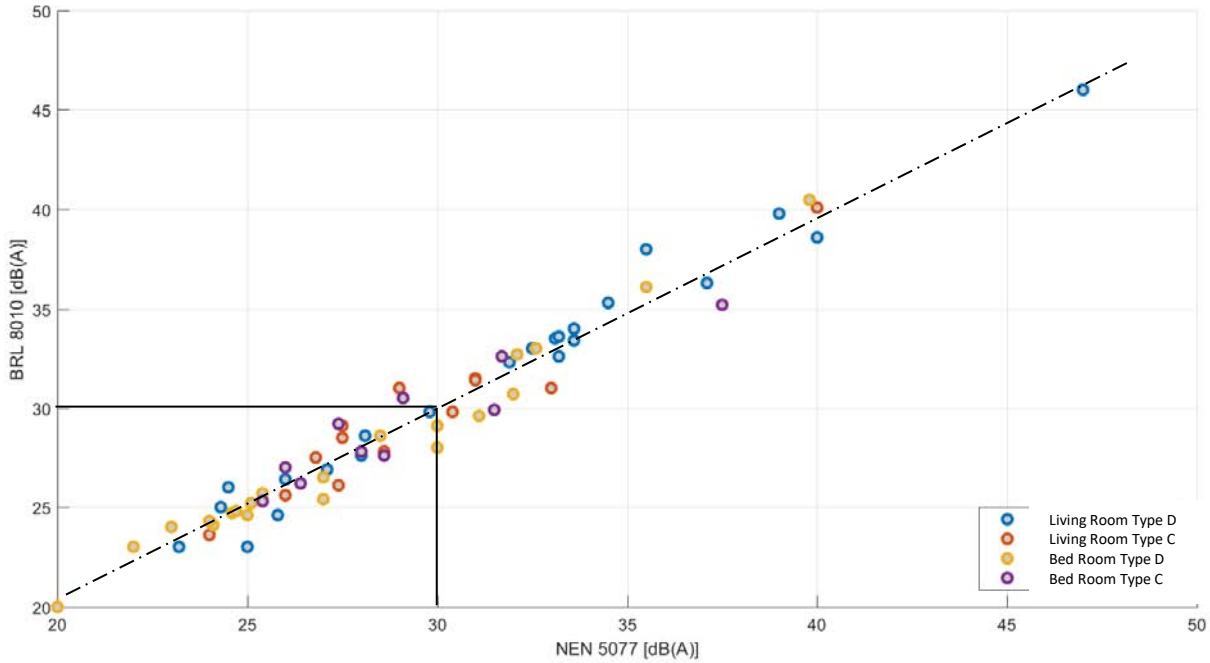

Figure 6: Comparison simplified measurement BRL 8010 with the measurement according to Dutch Standard NEN 5077

3.5 Training of ventilation installation fitter

Energy performance contracts such as the energy performance fee will impose additional requirements on the knowledge and experience of installation fitters and contractors. They will need to be better able to measure the performance of the systems they deliver during construction and delivery as well as in the use phase

In the European Newcom project, European training programs are being set up for fitters of ventilation systems for highly energy-efficient homes. The use of the simplified measurement methods described above is part of this. Input for the training program has been written. The first training courses will soon be set up and will be evaluated in 2020.

4 CONCLUSIONS

There are various initiatives for a label and energy performance contracts for highly energy-efficient homes. Under this label and energy performance contracts, thousands of homes are now being built in the Netherlands. The future will show whether this will actually lead to better performance.

An open source API for monitoring makes it easier to perform analyses on data from homes of energy and indoor air quality and makes the link to model based data analytics as for example Digital Twins easier. This initiative from the Netherlands may also be interesting for use in other countries.

The simplified measurement methods as described here will soon be available on the market. They will lower the threshold for the measurement of the performance of indoor climate systems by professionals.

5 ACKNOWLEDGEMENTS

TKI Securevent has been financed with TKI toeslag subsidy of the ministry of Economic Affairs for TKI Urban Energy, Topsector Energie, www.tki-urbanenergy.nl
The Newcom and Sphere project havereceived funding from the European Union's Horizon 2020.

6 REFERENCES

Augustins, Edgars et all (2018) Managing energy efficiency of building: analysis of ESCO experience in Latvia, Energy procedia, Volume 147, 2018 p 482-487

Lanooy, Bink, Kornaat, Borsboom (2019). Applicability of a simple and new airtightness measuring method and further comparisons with blower door measurements, 40th AIVC Conference, 15-16 October, Gent 2019

KvINL (2012) BRL 8010, Ventilatie-PrestatieKeuring, Beoordelen van ventilatievoorzieningen van woningen, scholen en kinderdagverblijven

Robert,Guyot (2013), Detailed analysis of regulatory compliance controls of 1287 Dwellings ventilation systems, Proceedings of the 34th AIVC Conference , 25-26 September, Athens 2013

Van Dijken, Boerstra (2011). *Onderzoek naar de kwaliteit van ventilatiesystemen in nieuwbouw eengezinswoningen*

Test of new analysis methodologies to assess dynamic airflow rate with the tracer gas decay method

Gabriel Remion[*1,2], Bassam Moujalled[1], Mohamed El Mankibi[2]

1 Cerema BPE Project-team
46 rue St-Theobald,
38080 L'isle d'Abeau, France

2 ENTPE - University of Lyon
3 rue Maurice Audin
69120 Vaulx-en-velin, France

**Corresponding author: gabriel.remion@entpe.fr*

ABSTRACT

The measurement of natural airflows is practically challenging. Driving forces that induce natural airflows are characterized by low pressure differences. Conventional airflow-meters would introduce pressure drops, which can significantly affect the flow pattern. Besides, the measurement of the flow crossing a window is difficult to implement and poorly reliable. Thus, indirect methods called tracer gas methods are widely used to bypass these difficulties, as they do not interfere with the flow pattern. They rely on the analysis of the evolution of the concentration of a tracer gas, injected before or during the measurement.
However, tracer gas methods are subject to several uncertainty sources. To reduce the uncertainty due to concentration measurements, least squares regressions are often realised, which allow to smooth the measurement noise. If the regression is realised, airflows have to be stationary during the measurement, which is particularly questionable for natural airflows. Actually, for lack of better methods, these techniques are often used in natural conditions, assuming that the bias induced by the regression is inferior than the bias due to the measurement noise. The aim of the present paper is to experimentally assess a dynamic airflow rate with the commonly used multi-points tracer decay method, which theoretically assumes a constant ACH. The variation of airflows is realised thanks to a mechanical controllable fan, which allows a direct measurement of the airflow in the extract duct to test the accuracy of the tracer gas-dynamic ACH measurement.

KEYWORDS

Tracer decay method, Variable airflow, Kalman filter, Local least square regression.

1 INTRODUCTION

The measurement of natural airflow is a challenging task. Low pressure differences induced by the wind and buoyancy effects lead to an unstable flow path. An airflow-meter would introduce some pressure drops likely to interfere with the flow pattern. Tracer gas methods are the most widely used methods to assess natural airflows, as they do not interfere with the flow pattern. They provide the Air Change per Hour from the measurement of the emission rate and the concentration of the tracer gas. The three main tracer gas methods, that differ from the way of dosing the gas, are the constant concentration method, the constant dosing method, and the concentration decay method (Sherman, 1990). Among them, the concentration decay method is the most suited method to natural ventilation (Remion, 2019). One of the reason is that the artificial homogenization of the tracer gas, which is one prerequisite that may alter the flow path, can be realised before the measurement, contrary to other methods (AFNOR, 2017).

Analysing the decrease of the gas can come from the measurement of only two extreme points. The accuracy of this method is weak but it tolerates variable airflows. To increase the accuracy of the method, a least squares regression may be realised with several measurement points, leading to the multi-points decay method. However, the regression

implies a stationary airflow assumption during the measurement, which is troublesome for natural ventilation systems. The aim of the present paper is to test two other analysis techniques that reduce the time laps of the assumed constant airflow, or even circumvent this requirement. The first technique is a moving least squares regression on a significantly reduced time laps. It is enabled by measurement instruments that allow now to have access to nearly continuous concentration data. The moving regression provides a dynamic ACH. The second technique is the use of a Kalman filter, which is a very convenient tool to reduce the measurement noise, while keeping the ability to track the parameter of interest, namely the dynamic ACH. Duarte et al. provide the mathematical development of the filter adapted to the Transient Mass Balance Equation metabolic CO_2 method (Duarte, 2018). Those methods will be compared to the 2 points decay method, which should be used when variable airflows are likely to occur (AFNOR 2017).

2 METHODS

2.1 Experimental setup

The test was conducted in an experimental cell of 2.45m width, 3.17m length and 2.65m height, leading to a volume of 20.6 m^3. The laboratory cell is featured with a controllable fan, allowing to simulate airflow variation profiles. An airflow-meter, which is installed in the extract duct connecting the fan to the room, provides the reference value of the airflow rate with an accuracy of 0.5%. Laussmann & Helm have proved the suitability of CO_2 by comparing tracer gas results from CO_2 and SF_6 (Laussmann, 2011). We chose CO_2 as a tracer gas during the experiment, considering that no internal sources were to take into account. We used two typologies of CO_2 sensors based on the NDIR[1] technology : two vaisala sensors with an accuracy of 4% and an acquisition frequency of 0.5 Hz, and five stand-alone C2AI sensors with an accuracy of +/- (50 ppm + 3%) with a frequency of one measurement every 12 sec. Table 1 presents technical specificities of measurement instruments. Two typologies of sensors were tested because stand-alone sensors are very convenient for in-situ applications, but their acquisition frequency and accuracy are weaker. The aim is to test the impact of the degradation of technical characteristics of sensors. Those sensors were averaged by types to inhibit the effect of imperfect mixing. Figure 1 presents a schematic of the experimental cell.

[1] Non Dispersive Infrared Technology

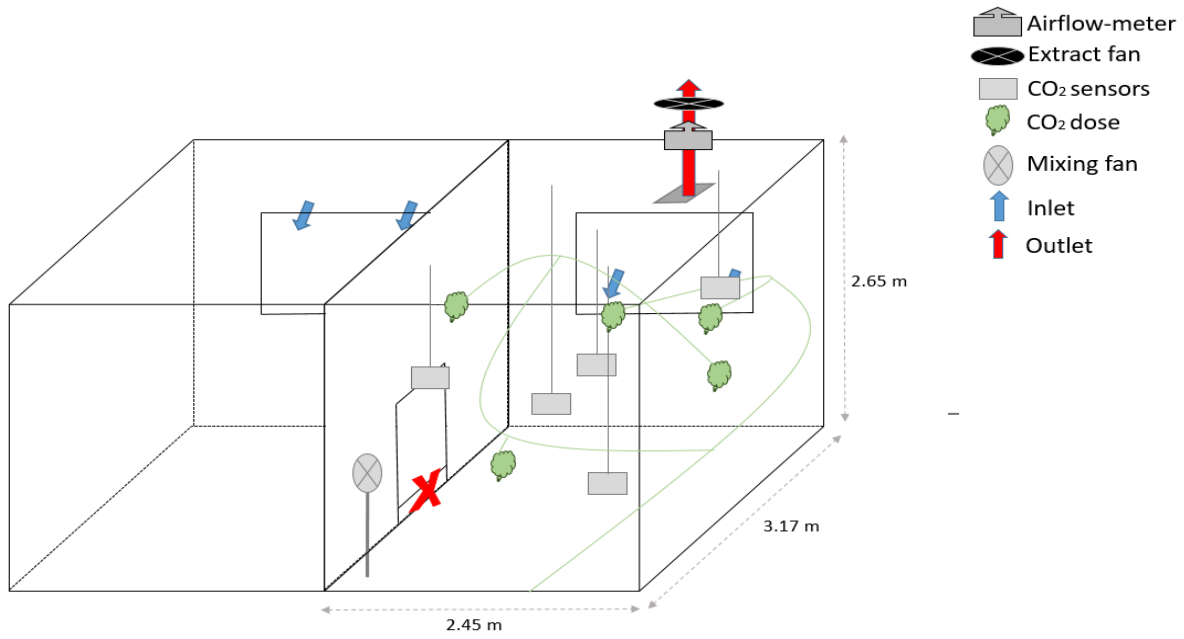

Figure 1 : Schematic of the experimental cell

Table 1: Instruments technical specificities

Measurement instrument	Technology	Accuracy	Acquisition frequency
C2AI CO_2 sensors	Stand-alone NDIR[1]	50 ppm + 3% reading	1/12 Hz
Vaisala CO_2 sensors	Wired NDIR[1]	4% reading	0.5 Hz
NZP Nozzle series airflow-meter	Pitot-tube	0.5% reading	0.5 Hz

2.2 Airflow variation profile

A mechanical ventilation system was used to reproduce airflows in accordance with airflows induced by natural conditions. We considered stack and cross ventilation. Stack ventilation was simulated by computing airflows from the formula characterizing the flow between two openings of different height (**equation 1**). The formula was filled with meteorological data measured by a local weather station in Lyon, France. Stack ventilation is mainly induced by buoyancy effects. In order to have significant fluctuations of airflow, we looked for a day with a significant temperature amplitude.

$$Q_{stack}(t) = C_d \,.A_{eff} \,. \sqrt{\frac{2 \,.\, g \,.\, \rho_{ext} \,.\, H \,.\, \frac{T_{ext} - T_{int}}{T_{int}}}{\rho_{int}}} \qquad (1)$$

With C_d [ ] the discharge coefficient, A_{eff} [m^2] the effective area, ρ_{ext} and ρ_{int} [$kg.m^{-3}$] the external and the internal density of the air, H [m] is the height between two openings, T_{ext} and T_{int} [°C] the external and internal temperatures, g [$m.s^{-2}$] the acceleration of gravity.

Airflows were then computed and two profiles were isolated, one in the morning leading to a monotonous decreasing profile [75 to 50 $m^3.h^{-1}$ in 2 hours], and one in the afternoon, leading to a monotonous increasing profile [50 to 65 $m^3.h^{-1}$ in 2 hours]. It corresponds to temperature fluctuations of 4°C in 2 hours. Those particular profiles were selected because it allows to have more than 5 air renewals in 2 hours (which is important for the constant dosing method) and because their mean values are similar.

To simulate a flow consistent with cross-ventilation, we used data from a study conducted by J. Lo et al. (Lo, 2012). They investigated the flow crossing windows of a multi-zone building. We determined two profiles from those data, based on a different multiplier coefficient (0.3 and 0.7). The coefficient 0.3 was chosen to set the mean airflow at the same level than the two aforementioned profiles. The coefficient 0.7 allows to test the impact of wider and faster fluctuations on the accuracy of tracer gas methods. Figure 2 shows airflows measured by the airflow meter, for each variation profile that have been used in the experiment.

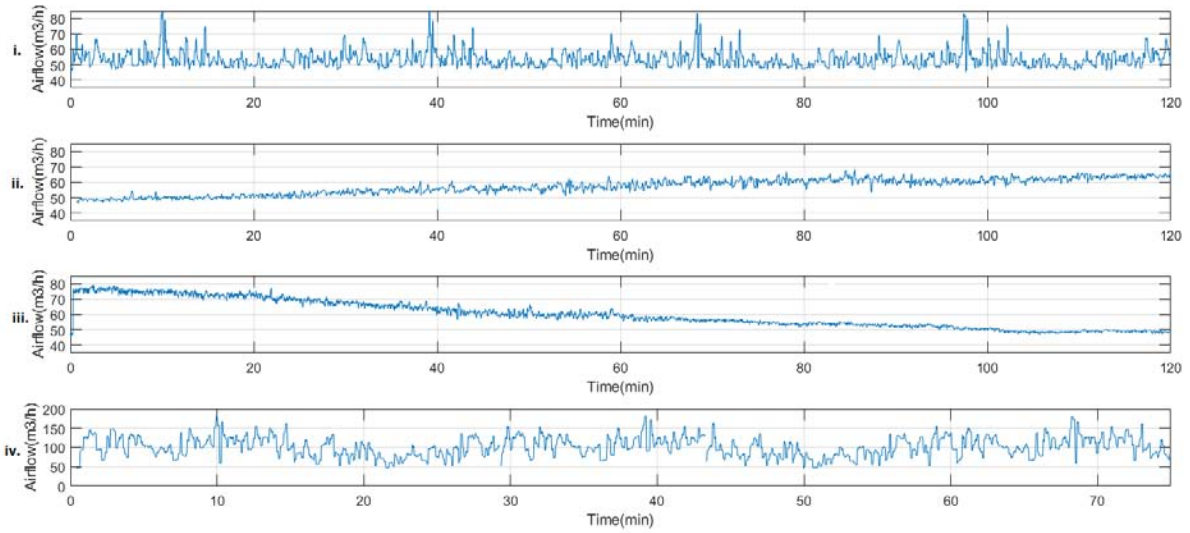

Figure 2 : Airflow variation profiles: (i) cross, (ii) stack increasing (up), (iii) stack decreasing (down), (iv) high cross (hicross)

2.3 Calculation of airflow

We will test three calculations of the airflow rate: the conventional 2 points decay formulation which is the standard-prescribed decay method in case of variable airflows, a local moving least squares regression that is to say a local moving multi-points decay method, and finally the Kalman filter. The formulation of the calculation of the 2 points decay ACH, and the multi-points decay ACH are given in Ref. (Roulet, 1991). For the local moving multi-points method, CO_2 concentrations were first smoothed thanks to a moving term average. A two minutes-time laps of both moving term average and moving multi-points method was arbitrarily chosen.

Concerning now the Extended Kalman filter, the mathematical development is available in Ref. (Duarte, 2018). The principle of the filter is to estimate the state parameter x (**equation 2**). Transition functions are defined to predict the value of the state parameter at the next time step (**equation 3**). Transition functions involve some process noise terms, that accounts for violations of assumptions of tracer gas methods. For instance, the process noise of the concentration (w_k^c) would be deviations from a perfect mixing of the fresh air, and process noise of the airflow (w_k^n) would be deviations from a stationary airflow. The prediction $\widehat{x_{k+1}}$ of the state parameter is then compared to the noise corrupted measurement (**equation 4**). The comparison provides the error (ε_{k+1}). The filter will finally update the estimation of the state parameter (x_{k+1}) from the calculated error by multiplying it by the Kalman gain, which is dependant on the Variance/Covariance matrix of the process noise (**W**) and the measurement noise (**V**). The measurement covariance matrix was defined in accordance with technical specificities of sensors. The covariance matrix of the process noise was set to: $= \begin{Bmatrix} 0.1\ ppm^2 & 0 \\ 0 & 0.001\ (Vol^2.h^{-2}) \end{Bmatrix}$. Added to the predicted state ($\widehat{x_{k+1}}$), it provides the updated state parameter. The block diagram of the filter is presented in Figure 3. A dynamic airflow rate is provided by successive states of the airflow rate n.

$$x_k = \begin{cases} C_k \\ n_k \end{cases} \tag{2}$$

$$\widehat{x_{k+1}} = \begin{cases} C_{k+1} = (C_k - C_{ext}) * e^{-n_k \cdot \Delta T} + C_{ext} + w_k^c \\ n_k = n_{k+1} + w_k^n \end{cases} \tag{3}$$

$$C_k^* = C_k + v_k^C \quad (4)$$

With C_k the concentration at time k [kg/kg], n_k the airflow rate at time k [Vol/h], C_k^* the noise corrupted measured concentration [kg/kg], ΔT the time laps between two measurements [h].

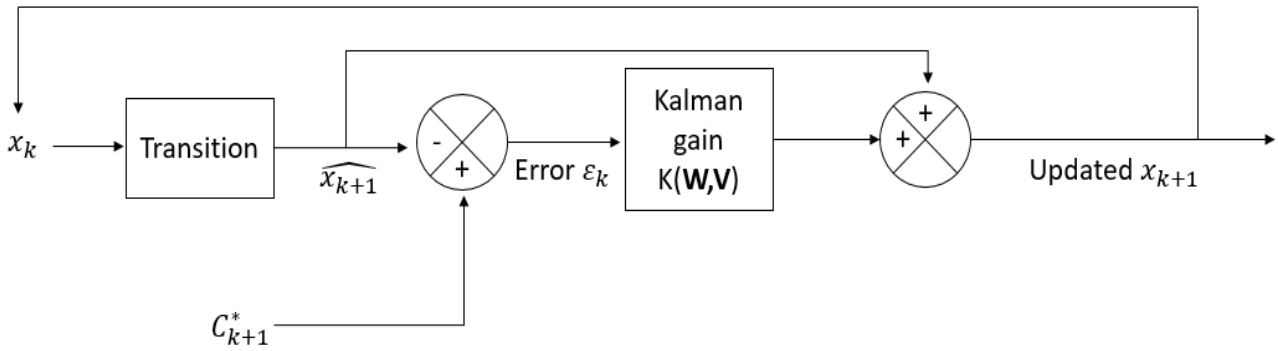

Figure 3 : schematic of the Extended Kalman filter principle

3 RESULTS

The mean airflow rate was computed with the 2 points method, and a dynamic airflow rate was provided by the Extended Kalman Filter and the Local fit methods. Figure 4 shows the evolution of dynamic airflows (Extended Kalman filter, Local fit) compared to the reference airflow measurement, performed by the airflow meter in the extract duct. The airflow profile which is showed is the most critical highly variating profile, consistent with cross ventilation. CO_2 concentrations used to compute airflows of Figure 3 come from wired Vaisala sensors with a good acquisition frequency (0.5 Hz). The time laps of the graph represents 2 air renewals. We can see that, apart from small fluctuations, both methods are very accurate, and account well for the dynamic airflow rate.

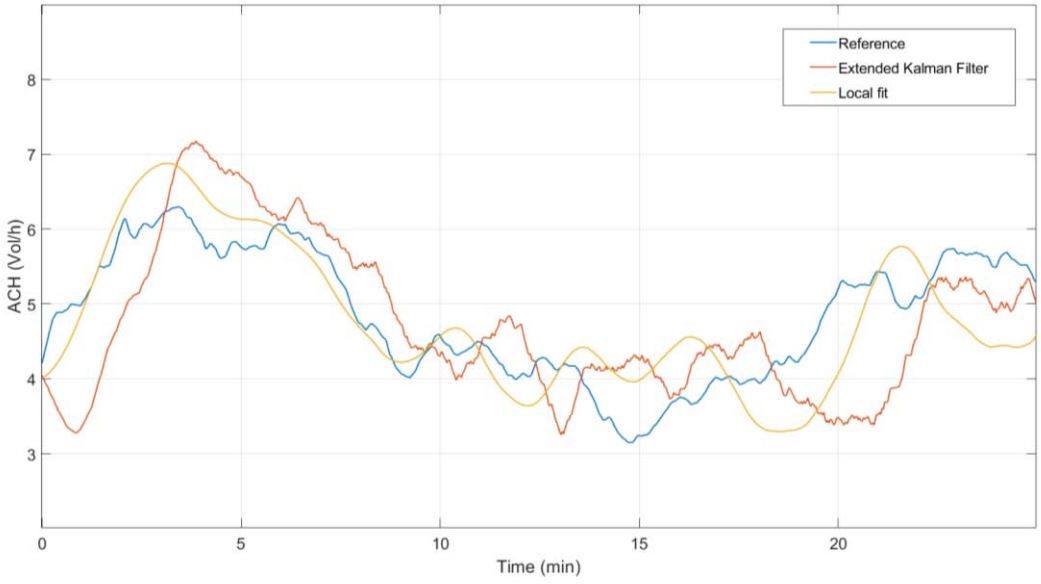

Figure 4 : Evolution of the reference airflow, and airflows calculated by the Extended Kalman filter and the local fit techniques, for the highly variating profile (Vaisala sensors)

To compare the accuracy of the conventional 2 points method with others, we computed the average of the airflow rate from 5 minutes to the period allowing 2 air renewals for the three methods.

Figure 5 shows histograms of the Experimental mean deviation between methods and the reference value. Dash lines represent the standard deviation of the 2 points method, computed thanks to the error propagation law. The subplot (i) refers to stand-alone sensors (C2AI), and the subplot (ii) refers to wired sensors (Vaisala). For Vaisala sensors, apart from the stack increasing profile (St up), averaged deviations are far below the standard deviation. The Kalman filter and the local fit methods do not allow to significantly improve the accuracy, which is already very good. For the hicross profile, the local fit method leads to deviations from 1.5% (1.5 m^3/h) to 5% (5.1 m^3/h) higher than the 2 points method, whereas the Kalman filter leads to closer deviations (1% (1 m^3/h) to 2% (2 m^3/h) higher). However, the inverse conclusion occurs for the stack increasing profile: dynamic methods are between 4% (2.2 m^3/h) and 6.5% (3.6 m^3/h) more accurate. In general the Kalman filter leads to results between -5% (2.7 m^3/h) to +2% (1.1 m^3/h) against the 2 points method, while the local fit leads to results between -6% (3.3 m^3/h) to +5% (2.7 m^3/h). Also, the standard deviation between experimental deviations among each profile is lower for dynamic methods than for the 2 points method (2.5% against 3%), and so is the maximum mean deviation (6.3% (3.5 m^3/h) and 4.5% (2.5 m^3/h) against 8.5% (4.7 m^3/h)). Dynamic methods are more stable, with a slight advantage for the Kalman filter.

For C2AI sensors, a better accuracy of both dynamic methods is experienced for every experiment. The improvement of accuracy is significant for several experiment (3rd cross, 2nd down, 3rd up, every hicross experiments). Maximum mean deviations among profiles is about 6.5% (6.7 m^3/h) for the Kalman filter, 8% (8 m^3/h) for the local fit, and 16.3% (16.3 m^3/h) for the 2 points method. Standard deviations between experimental mean deviations among each profile is about 2.7% for the Kalman filter, 3.9% for the local fit method, and 4.2 % for the 2 points method. Once again, the Kalman filter leads to the lowest maximum deviation among each profile (6.5%), which occurred for the most critical highly variating profile, which varied around 5 Vol/h about +/- 20%.

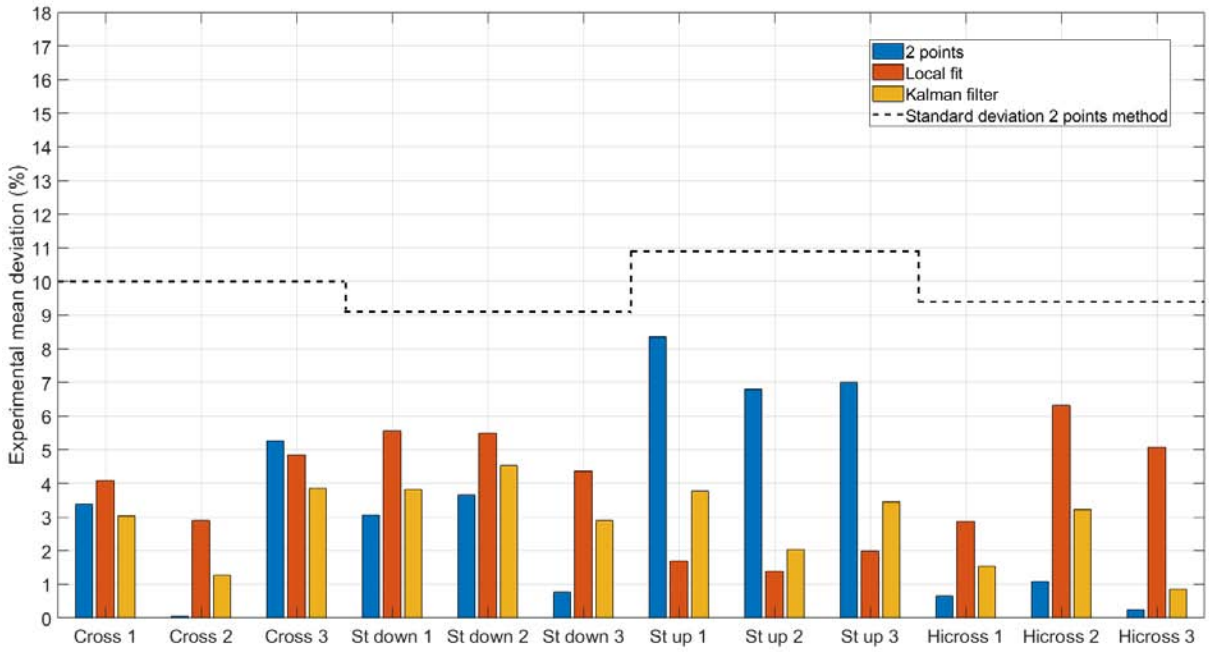

(i)

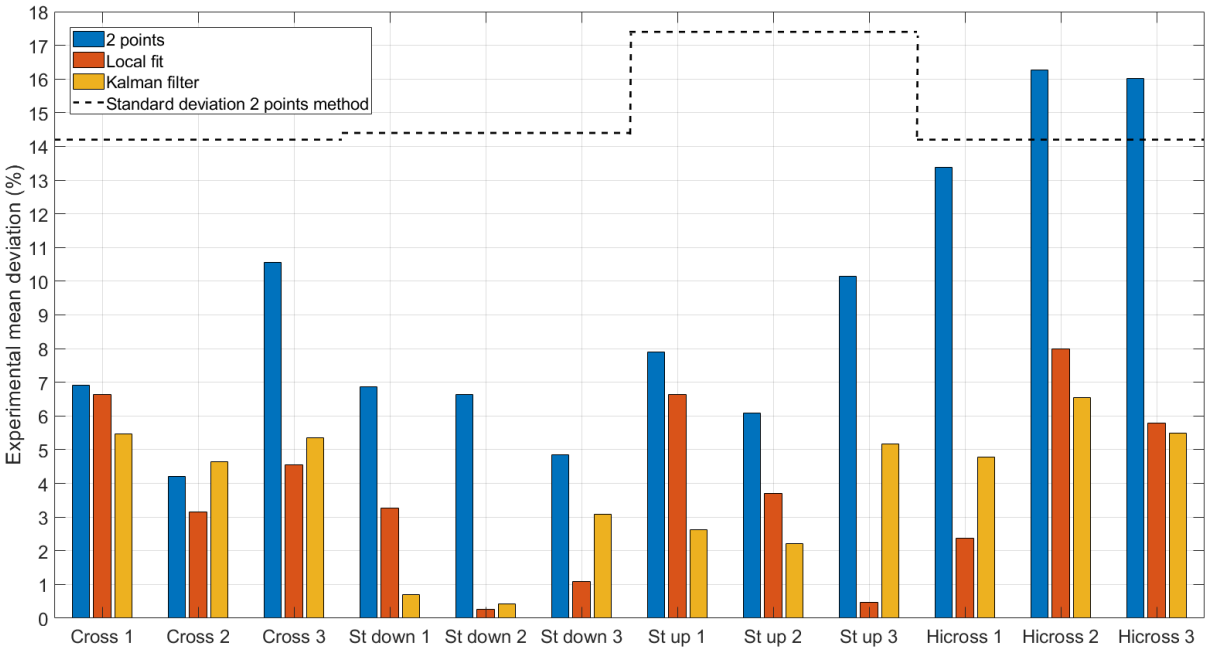

(ii)

Figure 5 : Histograms of the experimental mean deviation for the three analysis techniques (i) Vaisala sensors, (ii) C2AI sensors

4 DISCUSSION

For wired sensors, the accuracy was not significantly improved compared to the conventional 2 points method, even if highest deviations between methods are in favour of dynamic methods. However, dynamic methods lead to more stable results among airflow profiles, as the standard deviation between each experiment are below than the one of the 2 points method.

Stand-alone sensors are more convenient for in-situ applications, but are often less accurate than wired sensors. This is an issue for the assessment of natural ventilation, because the 2 points decay method should be employed, whereas it is subject to significant measurement errors. The proposed dynamic methods allowed to significantly improve the accuracy, while allowing to track the evolution of the ACH. This is two significant assets to increase the reliability of tracer decay method in natural conditions. Leading to the same order of magnitude of the experimental error between the wired and stand-alone sensors, dynamic methods are less sensitive to measurement noise than the conventional 2 points method. Moreover, they seem not affected by the variation of airflows, contrary to the 2 points method. It remains some room for improvement as the process noise covariance matrix of the Kalman filter could be better characterized, and also the time laps of the moving local fit could be better chosen.

Among dynamic methods, the Kalman filter leads to slightly better results than the local fit. Moreover, no stationary airflows is assumed, whether the local fit assumes the airflow stationary during the time laps of the regression (two minutes here). The Kalman filter is theoretically speaking more adapted to natural ventilation's assessment.

5 CONCLUSION

Dynamic analysis methods of the well-known decay methods were tested under mechanical variable airflows, namely the Kalman filter, and the moving local least squares regression methods. Results are very encouraging as dynamic analysis methods allowed to significantly improve the accuracy, especially for stand-alone sensors, that are likely to be less accurate. They also allow to track the dynamic ACH, which is noteworthy for the tracer decay method.

These proposed analyses take advantage of the ease of implementation of the tracer decay method, while ensuring a relatively good accuracy if airflows are likely to fluctuate. The Kalman filter performed slightly better than the local fit, with deviations which are quasi-exclusively below 5%, with a maximum of 6.5% for stand-alone sensors with the hicross variation airflow profile.

6 ACKNOWLEDGEMENTS

We would like to thank the French ministry of ecology that funded this project. We would also like to thank Dr. James Lo, who provided experimental data necessary to create airflow variation profiles, consistent with cross ventilation.

7 REFERENCES

AFNOR. 2017. 'Performance thermique des bâtiments et des matériaux - Détermination du débit d'air spécifique dans les bâtiments - Méthode de dilution de gaz traceurs'. AFNOR.

Duarte, Rogério, Maria Glória Gomes, and António Moret Rodrigues. 2018. 'Estimating Ventilation Rates in a Window-Aired Room Using Kalman Filtering and Considering Uncertain Measurements of Occupancy and CO2 Concentration'. *Building and Environment* 143 (October): 691–700. https://doi.org/10.1016/j.buildenv.2018.07.016.

Laussmann, Detlef, and Dieter Helm. 2011. 'Air Change Measurements Using Tracer Gases: Methods and Results. Significance of Air Change for Indoor Air Quality'. In *Chemistry, Emission Control, Radioactive Pollution and Indoor Air Quality*. InTech.

Lo, L. James, and Atila Novoselac. 2012. 'Cross Ventilation with Small Openings: Measurements in a Multi-Zone Test Building'. *Building and Environment* 57 (November): 377–86. https://doi.org/10.1016/j.buildenv.2012.06.009.

Remion, Gabriel, Bassam Moujalled, and Mohamed El Mankibi. 2019. 'Review of Tracer Gas-Based Methods for the Characterization of Natural Ventilation Performance: Comparative Analysis of Their Accuracy'. *Building and Environment* 160.

Roulet, Claude-Alain, and Luk Vandaele. 1991. 'Air Flow Patterns within Buildings Measurement Techniques'. AIVC Technical Note 34. AIVC. https://www.aivc.org/resource/tn-34-air-flow-patterns-within-buildings-measurement-techniques.

Sherman, Max. 1990. 'Tracer-Gas Technique For Measuring Ventilation in a Single Zone'. *Building and Environment* 25 (4): 365–74.

Reliability of ductwork airtightness measurement: impact of pressure drop and leakage repartition on the test result

Sylvain Berthault[1*], Valérie Leprince[2]

1 Cerema Centre-Est, Laboratoire d'Autun
Bd Giberstein, BP 141
71405 Autun Cedex, France
**sylvain.berthautl@cerema.fr*

2 PLEIAQ
84 C Av de la Libération
69330 Meyzieu, France

ABSTRACT

Building airtightness requirements are becoming more and more common in Europe (Leprince, Carrié, & Kapsalaki, 2017). However, airtight buildings require an efficient ventilation system to ensure good indoor air quality. In France, the inspection of ventilation system (Jobert, 2012) has revealed many noncompliance. They are mainly due to bad conception, poor implementation, and lack of maintenance. This often leads to reduced ventilation flowrates and poor indoor air quality. Leaky ductwork is one of the reasons for this noncompliance.
Therefore, in France, a ductwork airtightness test is now mandatory for new building applying to an Effinergie label, and the ductwork shall reach at least the class A.
Since the test is mandatory and a minimum level required, it raises the question of the reliability of the test.
Inside a ductwork a flowrate undergoes pressure drop due to friction and dynamic losses. It is relevant to wonder whether these losses have an impact on the result of the ductwork airtightness test.
Before the Promevent project, an experiment was conducted to estimate the impact of these losses on the result of the airtightness test. Results were briefly presented at the AIVC 2014 conference (Berthault, Boithias, & Leprince, 2014) and stated that:

- the position of the measuring device seemed to have no impact on the result of the airtightness test for various distribution of leakages
- only very high dynamic losses (almost completely closed damper) had an impact on the result.

The objectives of this paper are:

- to present the experimental set-up and detail the tests carried out
- to present the developed numerical model to estimate the impact on the result of the airtightness test of friction and dynamic losses according to the level of airtightness.
- to compare the results obtained with the numerical model and the experimental set-up.

It has been shown that, for airtight ductwork (class C) the impact of pressure losses on the measured flowrate is expected to be very small.
Nevertheless for very leaky ductwork it would be good practice to define a maximal length to be tested (distance between the measuring device and the farthest end of the ductwork) or to check in various location the homogeneity of the pressure.

KEYWORDS

Ductwork, Airtightness, Measurement, Pressure drop, Ventilation.

1 INTRODUCTION

Building airtightness requirements are becoming more and more common in Europe (Leprince, Carrié, Kapsalaki, 2017). However, airtight buildings require an efficient ventilation system to ensure good indoor air quality. In France, the inspection of ventilation system (Jobert, 2012) has revealed many noncompliance. They are mainly due to bad conception, poor implementation, and lack of maintenance. This often leads to a reduced ventilation flowrates and poor indoor air quality. Leaky ductwork is one of the reasons for this noncompliance.

In France a ductwork airtightness test is now mandatory for new buildings applying to an Effinergie label, and the ductwork shall reach at least the class A.
Since the test is mandatory and a minimum level required, it raises the question of the reliability of the test.
Inside a ductwork a flowrate undergoes pressure drop due to friction and dynamic losses. It is relevant to wonder whether these losses have an impact on the result of the ductwork airtightness test.
Before the Promevent project, an experiment was conducted to estimate the impact of these losses on the result of the airtightness test. Results were briefly presented at the AIVC 2014 conference (Berthault, Boithias, & Leprince, 2014) and stated that:

- the position of the measuring device seemed to have no impact on the results of the airtightness test for various distribution of leakages
- only very high dynamic losses (almost completely closed damper) had an impact on the result.

The objectives of this paper are:

- to present the experimental set-up and detail the tests carried out
- to present the developed numerical model to estimate the impact on the result of the airtightness test of friction and dynamic losses according to the level of airtightness.
- to compare the results obtained with the numerical model and the experimental set-up.

2 METHOD

As for a building airtightness test, a ductwork airtightness test assumes that the pressure difference between inside and outside the ductwork is homogeneous along the measured section.
However, the pressure drop due to friction and dynamic losses in the ductwork may induce a variation of this pressure difference. The following numerical model aims at estimating the maximum pressure variation in the ductwork due to these losses during an airtightness test. The experimental set-up has been used to compare this theoretical variation to the measured one.

2.1 Numerical model

Pressure drop in ductwork systems is due to the irreversible transformation of mechanical energy into heat (ASHRAE, 2013). There are two types of losses:

- friction losses (occurring along the ductwork)
- and dynamic losses (occurring at bends and junctions)

Total pressure loss in a duct section with a constant flow speed is calculated by combining friction and dynamic losses (equation 1).

$$\Delta p = \left(\frac{1000f}{D_h} + \sum C\right)\left(\frac{\rho V^2}{2}\right) \quad (1)$$

$$\Delta p = \zeta\left(\frac{\rho V^2}{2}\right) \quad (2)$$

C	-	Total loss coefficient
Δp	Pa	Total pressure loss
V	m/s	velocity
ρ	kg/m^3	air density
f	-	Friction factor

L	m	duct length
D_h	m	hydraulic diameter
ζ	-	Total pressure drop coefficient

Therefore, the pressure loss in the ductwork system is proportional to the square of the flowrate and the higher the flowrate (the more leakage during the test) the higher resistance in the ductwork (equation 2).
Friction and dynamic losses coefficients can be calculated from tabulated data such as those given in (ASHRAE, 2013).

The objective of the numerical model, developed in this paper, is to estimate the maximum pressure variation in the ductwork due to these losses during an airtightness test, that is to say the variation in the "worst" case that corresponds to a unique leak at one end of the ductwork and the measuring device at the opposite end (see Figure 1).
In this case, it is possible to make the hypothesis of constant flowrate along the ductwork (coming from the unique leak).

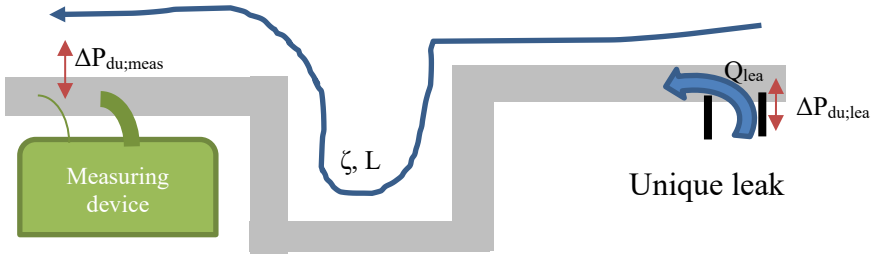

Figure 1: Case of a unique leak located on the opposite side of the ductwork compared to the measuring device

In this case

$$\left|\Delta P_{du;meas}\right| - \left|\Delta P_{du;leak}\right| = \frac{\zeta\rho}{2} * V^2 \qquad (3)$$

With

$\Delta P_{du;meas}$	Pa	Pressure difference at measuring device
$\Delta P_{du;lea}$	Pa	Pressure difference at the leakage

If it is assumed that the section of the ductwork is constant (main diameter or average of all sections)

$$\left|\Delta P_{du;meas}\right| - \left|\Delta P_{du;leak}\right| = \frac{\zeta\rho}{2} * \left(\frac{4Q}{\pi D^2}\right)^2 \qquad (4)$$

With

D	m	Diameter of the ductwork
Q	m^3/s	Leakage flowrate

And with the air leakage coefficient of the ductwork (K)

$$Q = K\Delta P_{du;leak}^{\frac{2}{3}} S \qquad (5)$$

With

K	$m^3/s/Pa^{2/3}/m^2$	Air leakage coefficient of the ductwork
S	m^2	Ductwork area

$$\left|\Delta P_{du;meas}\right| - \left|\Delta P_{du;leak}\right| = \frac{\zeta\rho}{2} * \left(\frac{4K\left|\Delta P_{du;leak}\right|^{\frac{2}{3}} * L\pi D}{\pi D^2}\right)^2 \qquad (6)$$

$$\left|\Delta P_{du;meas}\right| - \left|\Delta P_{du;leak}\right| = \frac{8\zeta\rho K^2 L^2}{D^2} * \left|\Delta P_{du;leak}\right|^{\frac{4}{3}} \quad (7)$$

Solving this equation requires to apply an iterative method since:

- $\Delta P_{du;leak}$ depends on the pressure drop in the ductwork,
- this pressure drop is proportional to the square of the leakage flowrate,
- the leakage flowrate depends on $\Delta P_{du;leak}$.

During the test the objective was to have a small pressure drop compared to the pressure difference between inside and outside. As an alternative, it was therefore decided to use the pressure difference at the measuring device to maximise the variation of pressure within the ductwork due to pressure losses:

$$\left|\Delta P_{du;leak}\right| \leq \left|\Delta P_{du;meas}\right| \quad (8)$$

As a result:

$$\frac{\left|\Delta P_{du;meas}\right| - \left|\Delta P_{du;leak}\right|}{\left|\Delta P_{du;meas}\right|} \leq \frac{8\zeta\rho K^2 L^2}{D^2} * \left|\Delta P_{du;meas}\right|^{\frac{1}{3}} \quad (9)$$

The variation of the measured flowrate is described with equations 10 to 13:

$$\frac{\left|Q_{\Delta P_{du;meas}}\right| - \left|Q_{\Delta P_{du;lea}}\right|}{\left|Q_{\Delta P_{du;meas}}\right|} = \frac{K\left|\Delta P_{du;meas}\right|^{\frac{2}{3}} - K\left|\Delta P_{du;leak}\right|^{\frac{2}{3}}}{K\left|\Delta P_{du;meas}\right|^{\frac{2}{3}}} \quad (10)$$

$$\frac{\left|Q_{\Delta P_{du;meas}}\right| - \left|Q_{\Delta P_{du;lea}}\right|}{\left|Q_{\Delta P_{du;meas}}\right|} = 1 - \left(\frac{\left|\Delta P_{du;leak}\right|}{\left|\Delta P_{du;meas}\right|}\right)^{\frac{2}{3}} \quad (11)$$

$$\frac{\left|Q_{\Delta P_{du;meas}}\right| - \left|Q_{\Delta P_{du;lea}}\right|}{\left|Q_{\Delta P_{du;meas}}\right|} = 1 - \left(1 - \frac{\left|\Delta P_{du;meas}\right| - \left|\Delta P_{du;leak}\right|}{\left|\Delta P_{du;meas}\right|}\right)^{\frac{2}{3}} \quad (12)$$

$$\frac{\left|Q_{\Delta P_{du;meas}}\right| - \left|Q_{\Delta P_{du;lea}}\right|}{\left|Q_{\Delta P_{du;meas}}\right|} \leq 1 - \left(1 - \frac{8\zeta\rho K^2 L^2}{D^2} * \left|\Delta P_{du;meas}\right|^{\frac{1}{3}}\right)^{\frac{2}{3}} \quad (13)$$

Therefore, to ensure a variation of the flowrate of less than -3% (for example) it is necessary to check (see equations 14 and 15):

$$1 - \left(1 - \frac{8\zeta\rho K^2 L^2}{D^2} * \left|\Delta P_{du;meas}\right|^{\frac{1}{3}}\right)^{\frac{2}{3}} \leq 0.03 \quad (14)$$

So

$$\frac{8\zeta\rho K^2 L^2}{D^2} * \left|\Delta P_{du;meas}\right|^{\frac{1}{3}} \leq 1 - 0.97^{\frac{3}{2}} = 4.5\% \quad (15)$$

2.2 The experimental set-up

The experimental set-up was a laboratory replication of a multi-family dwelling's ductwork (Figure 2). The ductwork was made of two main columns that were both connected to two dwellings. Each dwelling had a kitchen and a bathroom. Therefore, each column had four air terminal connected devices.

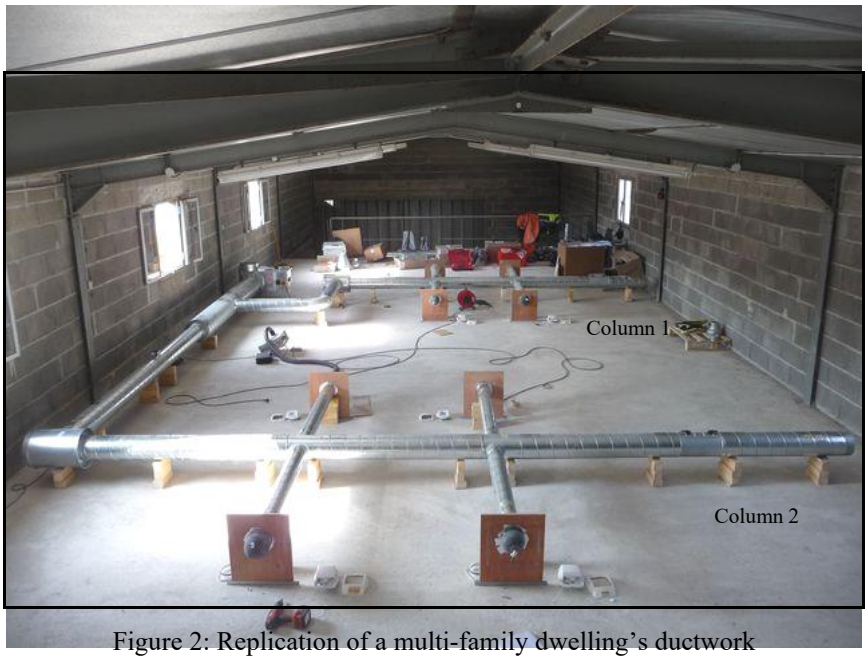

Figure 2: Replication of a multi-family dwelling's ductwork

The main technical characteristics are shown in Figure 3 and Table 1.

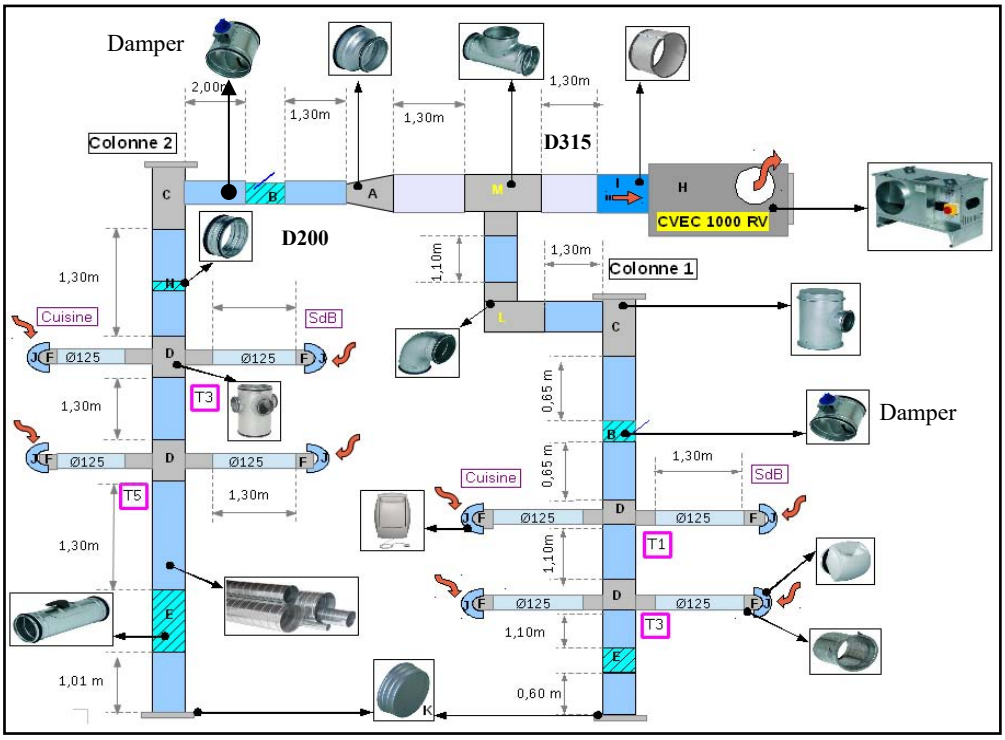

Figure 3: Ductwork with accessories

Kitchen air terminal devices provided two different flowrates. For the column 1: the maximum air flowrate was 225 m^3/h and the minimum air flowrate 110 m^3/h. For the column 2, the maximum air flowrate was 300 m^3/h and the minimum air flowrate 150 m^3/h.

Table 1: Length circular GALVA ducts and total flow ductwork available

Circular GALVA duct Diameter (mm)	Length (m)	Maximum total flow fan (m^3/h)	Minimum total flow fan (m^3/h)
315	2.60	525	260
200	15.08		
125	10.4		

First the ductwork was built airtight (class C) then the ductwork was drilled to reach 1.5*class A.

Evaluation of the impact of the measuring device location according to leakage distribution

The aim was to quantify the impact of leakage distribution and location of the measuring device on the result of the airtightness test. Four different leakage distributions inducing approximately the same airtightness level were tested (leakages were created by drilling):

1. Leaks gathered close to the fan (Figure 4)
2. Leaks gathered at the bottom of columns 1 and 2 (Figure 6)
3. Leaks gathered at the bottom of column 2 (Figure 5)
4. Equally distributed leaks all along the ductwork (Figure 7)

Tests were carried out by placing the measuring device at three different locations (as seen in green on Figure 4, Figure 5, Figure 6 and Figure 7):

1. By the fan
2. On column 1
3. On column 2

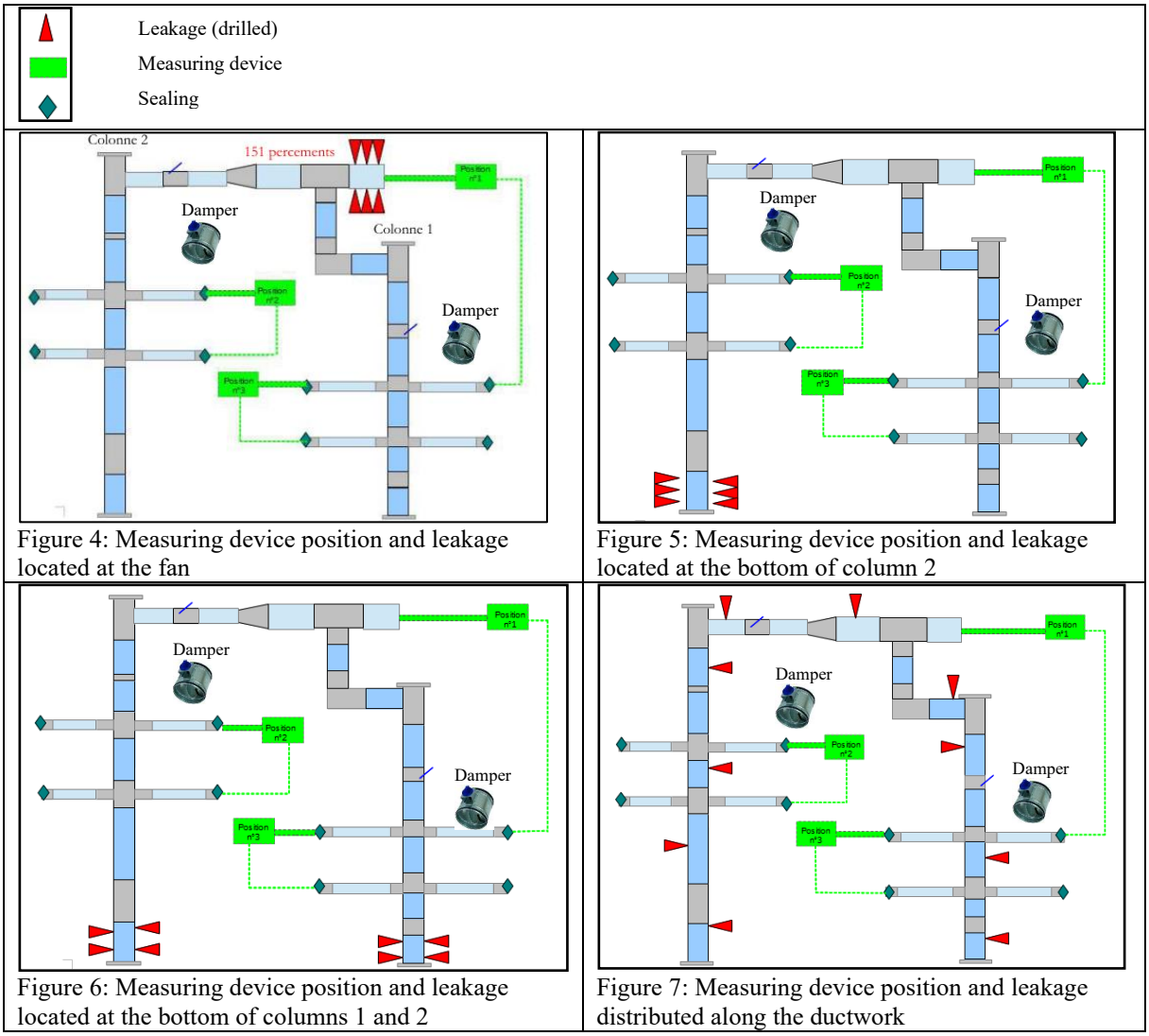

Figure 4: Measuring device position and leakage located at the fan

Figure 5: Measuring device position and leakage located at the bottom of column 2

Figure 6: Measuring device position and leakage located at the bottom of columns 1 and 2

Figure 7: Measuring device position and leakage distributed along the ductwork

Evaluation of the impact of the pressure drop on the result of the airtightness test.

As the ductwork was rather small compared to the ductwork of a large building, the pressure drop in the ductwork was quite small. Therefore, to induce larger pressure drop dampers were included at the top of column 1 and of column 2.
The objective was to estimate the impact of large pressure drop on the result of the airtightness test. Each damper had 7 positions from "0" open (Figure 8) to "6-F" closed (Figure 10).

Top view of the damper control in position 0	Interior view of the shutter position

Figure 8: Open damper (position 0)

Top view of the damper control in position 3	Interior view of the shutter position

Figure 9: Open damper half (position 3)

Top view of the damper control in position F	Interior view of the shutter position

Figure 10: Closed damper (position F)

The position of the 2 dampers were modified simultaneously from open to closed through the 7 positions and an airtightness test performed for each position at three different pressure (90 Pa, 120 Pa et 160 Pa).

This was done for two levels of ductwork airtightness:

- An airtight ductwork / Class C
- A leaky ductwork / 1.5*class A with distributed leakage (Figure 11).

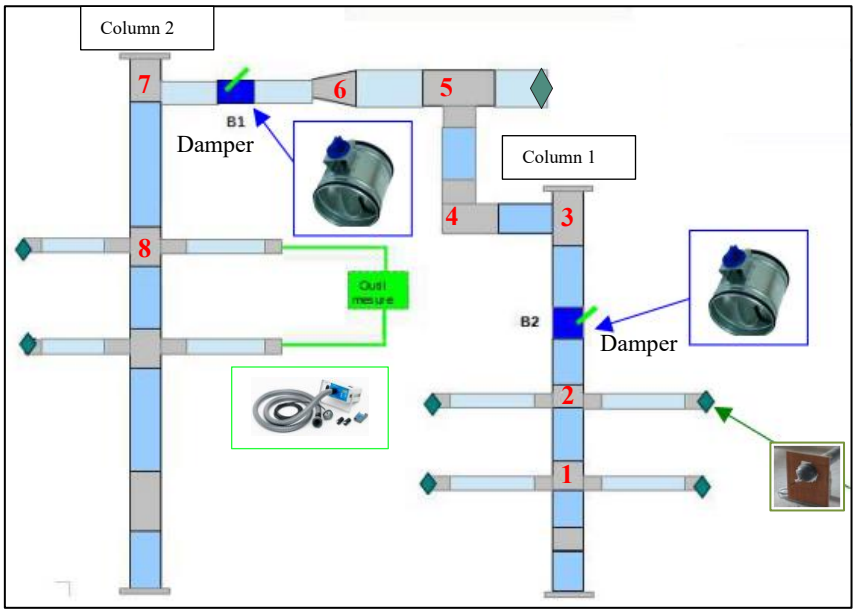

Figure 11: Impact of pressure drop (7 positions of damper) in the ductwork on the test result (3 different pressure, 2 level of airtightness for the ductwork)

In order to calculate the pressure loss coefficient of the damper according to its positions:

- the fan was switched on to maintain a pressure of 90 Pa, 120 Pa and 160 Pa,
- and the pressure after the damper was measured for the class C ductwork with the minimum flowrate (110 m^3/h in column 1 and 150 m^3/h in column 2).

3 RESULTS

3.1 Impact of the leakage distribution and measuring device location

Theoretical impact

In order to estimate the theoretical maximal impact of the leakage distribution and the position of the measuring devices, the worst case was to assume that there was only one large leakage at the bottom of column 1 and that the measuring device was at the bottom of column 2.

According to the calculations carried out with the French standard DTU 68.3 linear pressure drop (friction losses) are negligible considering the ductwork diameter, their material (metallic) and the flow speed during an airtightness test.
Average pressure losses coefficient (ζ) due to dynamic losses implied by accessories is given in the Table 2. It was estimated with DTU 68.3.

Table 2: Average pressure losses coefficient (ζ) for accessories along the ductwork (see Figure 11 for the number of each accessories)

Accessories	1 T-linear flow	2 T-linear flow	3 Roof collector	4 Bend	5 T-lateral	6 Narrowing	7 Roof collector	8 T-lateral	Total
ζ	0.15	0.15	2	0.5	0.5	1.1	2	0.5	6.9

As the length of the ductwork is 28 m, the average diameter 0.2 m, when the measurement is performed at 120Pa the error on the measured flowrate is below 3% if (cf. §2.1):

$$\frac{|\Delta P_{du;meas}| - |\Delta P_{du;leak}|}{|\Delta P_{du;meas}|} \leq \frac{8\zeta\rho K^2 L^2}{D^2} * |\Delta P_{du;meas}|^{\frac{1}{3}} \leq 0.045 \quad (16)$$

$$K \leq \sqrt{\frac{0.045 D^2}{8\zeta\rho L^2 |\Delta P_{du;meas}|^{\frac{1}{3}}}} \quad (17)$$

$$K \leq 0.00008 \approx 3 * Class\ A \quad (18)$$

Therefore, we should not observe any variation of the ductwork airtightness test result when changing the measuring device location, regardless of the location of leakages, if the ductwork is at most 1.5*class A.

Experimental impact

According to the previous calculation the variation of the measured flowrate was expected to remain below 3%. This was confirmed by the measurements performed that showed no impact of the position of the measuring devices according to the leakage repartition. The small-observed variation (below 2%) is in the range of the measurement uncertainty.

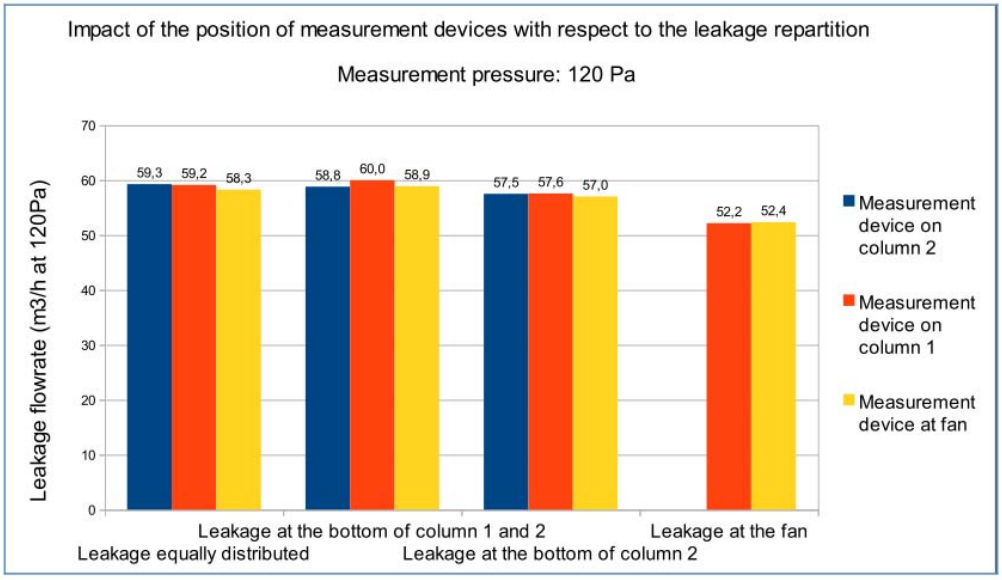

Figure 12: Leakage flowrate as a function of leakage distribution and location of the measuring device at 1.5*class A

3.2 Impact of the pressure drop

Pressure drop due to the damper

The pressure drop due to the dampers was measured (see Figure 13) and the associated pressure loss coefficient was calculated using the following formula:

$$\zeta = \frac{2\Delta P}{\rho v^2} \quad (19)$$

Table 3: pressure drop calculated

Damper position	0	1	2	3	4	5	F
Pressure drop due to damper in column 1 (Pa)	0	1	1.5	5.5	9	49.2	73
Dzeta (ζ) damper 1	0.0	1.8	2.6	9.7	15.9	86.7	128.6
Pressure drop due to damper in column 2 (Pa)	0	0	1	1	42	73.5	85.5
Dzeta (ζ) damper 2	0.0	0.0	0.9	0.9	39.8	69.6	81.0

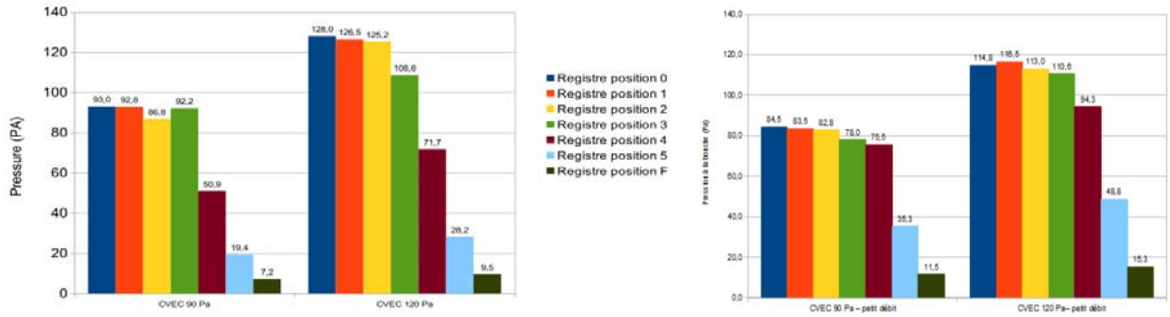

Figure 13: Pressure at the air terminal devices (left: top of column 2, right: top of column 1) according to the damper position

Theoretical impact

In Table 4, the maximal variation of the measured leakage flowrate due to the pressure drop was estimated using equations developed in §2.1. It was assumed that all leakages were located at one end of the ductwork and the measuring device at the other end.

In order to calculate the total pressure drop in the ductwork, the calculated pressure drop coefficients of dampers (Table 3) were added to the pressure drop coefficient (ζ) of the rest of the ductwork: 6.9 Pa (Table 2).

Table 4: Maximal variation of measured flowrates at 90 Pa, 120 Pa and 160 Pa according to the damper positions

	Dampers position	Open	1	2	3	4	5	Closed
	Total pressure drop (Pa)	6.9	8.7	10.5	17.5	62.6	163.2	216.5
1.5* class A	K (1.5*Class A)	3.88E-05						
	Max. variation at 90 Pa	1%	1%	1%	1%	5%	14%	19%
	Max. variation at 120 Pa	1%	1%	1%	2%	6%	16%	21%
	Max. variation at 160 Pa	1%	1%	1%	2%	7%	18%	24%
class C	K (class C)	2.12E-06						
	Maxi. variation at 90 Pa	0.00%	0.0_0%	0.00%	0.01%	0.02%	0.06%	0.08%
	Max.variation at 120 Pa	0.00%	0.00%	0.00%	0.01%	0.03%	0.07%	0.09%
	Max. variation at 160 Pa	0.00%	0.00%	0.00%	0.01%	0.03%	0.08%	0.10%

The variation is negligible for Class C but may be quite important for 1.5*class A when the damper is in position 5 or closed.

However, as leakages are distributed along the ductwork, assuming that there is a unique leak at the end of the ductwork is a strong hypothesis. According to the distribution of leakages (Figure 14) less than 80% of leakages undergo pressure drop due to the two dampers. When only 80% of leakages are considered, the variation of the measured flowrate is shown in Table 5.

Table 5: Variation of the measured flowrate when only 80% of the leakages are taken into account

Dampers position	Open	1	2	3	4	5	Closed
Variation at 90 Pa	0%	0%	0%	1%	3%	9%	12%
Variation at 120 Pa	0%	0%	1%	1%	4%	10%	13%
Variation at 160 Pa	0%	0%	1%	1%	4%	11%	15%

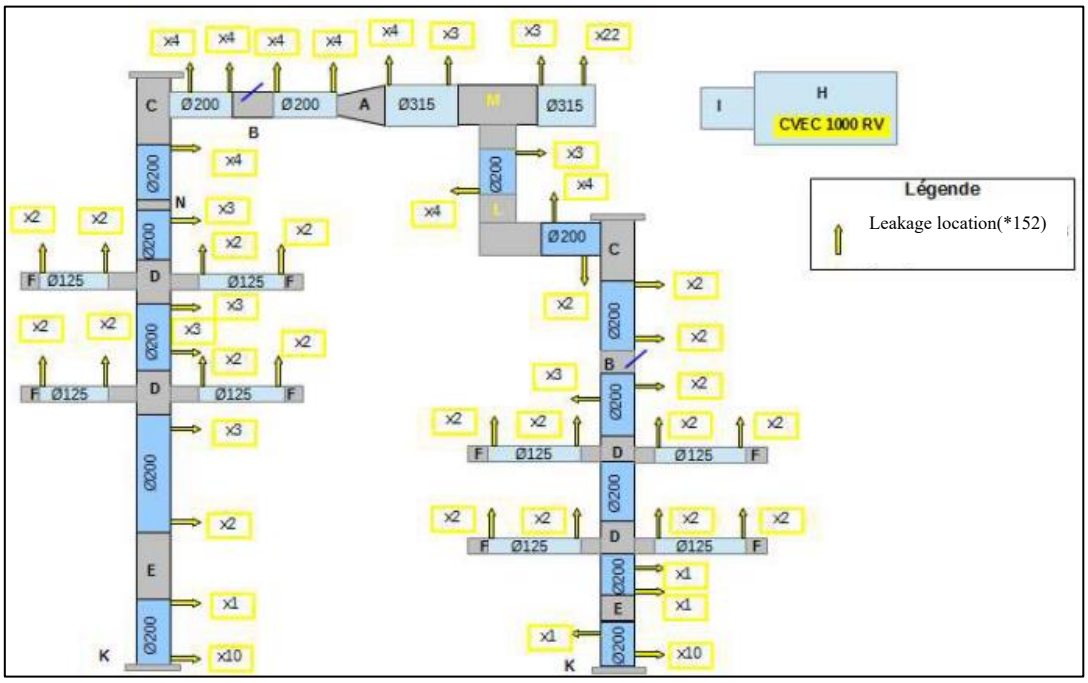

Figure 14: Repartition of leakages (drill) when the ductwork is 1.5*Class A

Experimental impact

Figure 15 and Figure 16 give the measured leakage flowrate of the ductwork according to the positions of the two dampers for a leaky ductwork and an airtight ductwork.

As predicted with the theoretical approach, the position of the damper has no impact on the measured flowrate for an airtight ductwork (Class C).

However, when the ductwork is leaky the measured flowrate decreases slightly from position 4. Table 6 gives the variation of the measured flowrate according to the position of the damper. The measured variation is close to the estimated maximum variation when taking into account only 80 % of leakages (see Table 5).

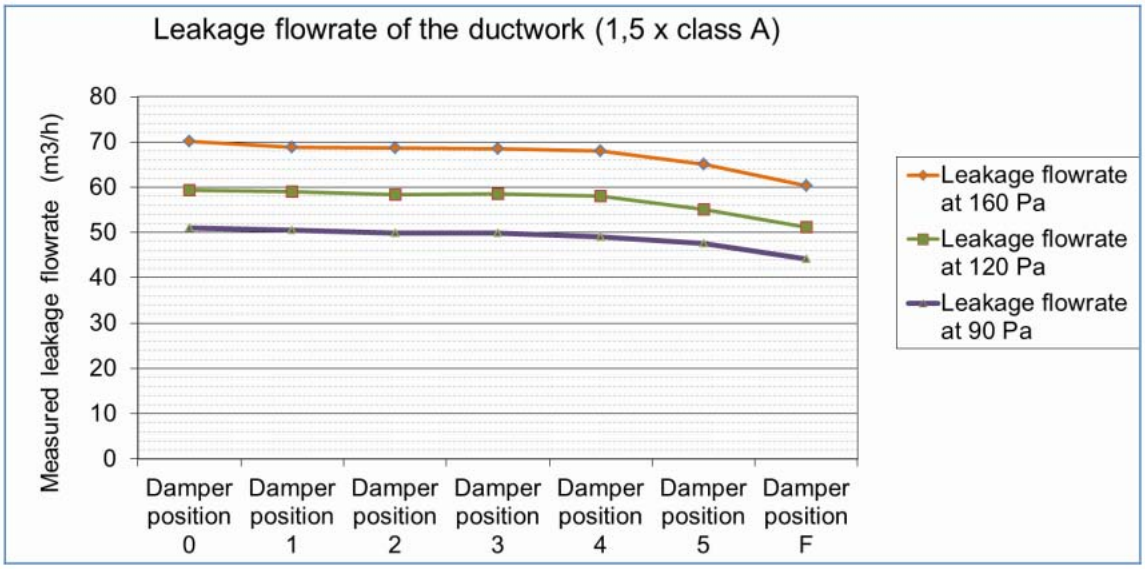

Figure 15: Leakage flowrate of the ductwork as a function of the damper's position at 1.5*class A (position 0 open; position F: closed)

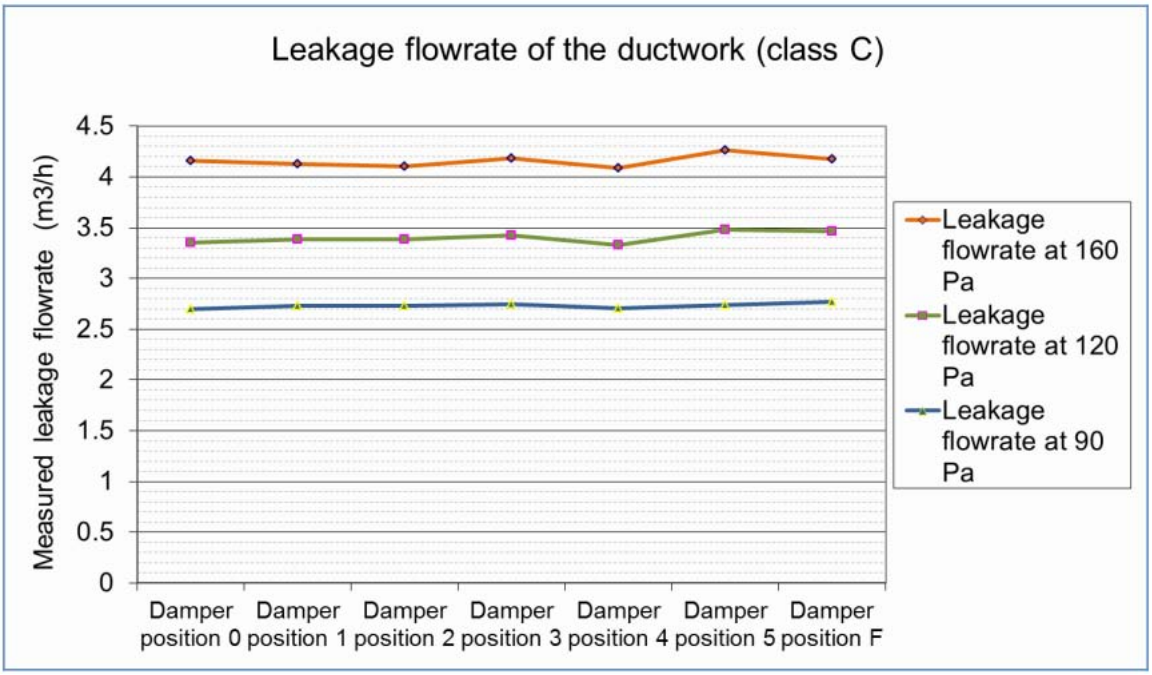

Figure 16: Leakage flowrate of the ductwork as a function of the damper's position at class C (position 0: open; position F: closed)

Table 6: Variation of the measured flowrate on the experimental set-up

Position dampers	Open	1	2	3	4	5	Closed
Variation at 90	0.0%	0.9%	2.1%	2.2%	3.8%	6.5%	13.4%
Variation at 120	0.0%	0.6%	1.7%	1.5%	2.3%	7.0%	13.7%
Variation at 160	0.0%	1.9%	2.0%	2.2%	3.1%	7.1%	13.9%

4 DISCUSSION

The equation developed in this paper allowed to calculate the maximum variation of the measured leakage flowrate according to the length and shape of the ductwork and the foreseen airtightness.
If we assume an accessory (bend, convergence, etc.) every 2 m inducing an average pressure loss coefficient of 0.5, the maximum length to be tested (L) can be estimated according to the airtightness class objective and to the maximum error (E) using the equations 18 and 19:

$$\frac{\left|Q_{\Delta P_{du;meas}}\right| - \left|Q_{\Delta P_{du;lea}}\right|}{\left|Q_{\Delta P_{du;meas}}\right|} \leq 1 - \left(1 - \frac{8\rho K^2 L^3}{D^2} * \left|\Delta P_{du;meas}\right|^{\frac{1}{3}}\right)^{\frac{2}{3}} \leq E \quad (20)$$

$$L \leq \left(\frac{D^2}{8\rho K^2 \left|\Delta P_{du;meas}\right|^{\frac{1}{3}}}((E-1)^{\frac{3}{2}} + 1)\right)^{\frac{1}{3}} \quad (21)$$

Test cases showed that the impact of pressure losses is expected to be very small for airtight ductwork. However, in case of large and leaky ductworks, it is better to put the measuring device in the middle of the measured section and to check the maximum length. It is also important to notice that the higher the test pressure, the higher the flowrate and therefore the higher the pressure drop and the greater the impact on the final result.

5 CONCLUSIONS

A mathematical model was developed to estimate the maximal error on the measured flowrate according to:

- the airtightness of the ductwork,
- the ductwork configuration (friction and dynamic loss coefficient).

The relevance of this mathematical model was checked through measurements on an experimental set-up.
It was shown that the impact of pressure losses on the measured flowrate is expected to be very small for airtight ductwork (class C).
Nevertheless, for very leaky ductworks it would be advisable to define a maximal length to be tested (distance between the measuring device and the farthest end of the ductwork) or to check the homogeneity of the pressure at various locations.

6 ACKNOWLEDGEMENTS

The authors would like to thank Ademe and the French Ministry of Construction for their support to the Promevent project.
The views and opinions of the authors do not necessarily reflect those of Ademe or French Ministry. The published material is distributed without warranty of any kind, either expressed or implied. The responsibility for the interpretation and use of the material lies with the reader. The authors should in no way be held responsible for damages resulting from its use. Any liability arising from the use of this report is the responsibility of the user.

7 REFERENCES

ASHRAE. (2013). *2013 ASHRAE Handbook: Fundamentals.*

Berthault, S., Boithias, F., & Leprince, V. (2014). Ductwork airtightness: reliability of measurements and impact on ventilation flowrate and fan energy consumption. *35 TH AIVC-4 TH TIGHTVENT & 2 ND VENTICOOL CONFERENCE , 2014* (pp. 478-487). Poznań, Poland, 24-25 September: AIVC.

Jobert, R. (2012). *La ventilation mécanique des bâtiments résidentiels neufs. .* Rapport ENTPE- GBBV, 2012.

Leprince, V., Carrié, F., & Kapsalaki, M. (2017). Building and ductwork airtightness requirements in Europe – Comparison of 10 European countries. *38th AIVC Conference. Ventilating healthy Low-energy buildings* (pp. 192-201). Nottingham, UK: AIVC.

Techniques to Estimate Commercial Building Infiltration Rates

Andrew Persily*, Lisa Ng, W. Stuart Dols, and Steven Emmerich

National Institute of Standards and Technology
100 Bureau Drive MS8600
Gaithersburg, Maryland USA
andyp@nist.gov

ABSTRACT

The estimation of low-rise, residential building infiltration rates using envelope airtightness values from whole building fan pressurization tests has been the subject of much interest and research for several decades, constituting a major topic of discussion during the early years of the AIVC. A number of empirical and model-based methods were developed, with their predictive accuracy evaluated in field studies around the world. Infiltration estimation methods for residences are now commonly available in guidance documents and employed in whole building energy and indoor air quality modeling. However, the greater complexity of many commercial buildings, including their size, multizone airflow dynamics and the influence of mechanical ventilation systems, makes the estimation of infiltration rates from fan pressurization test results more challenging. As a result, progress on infiltration estimation methods for commercial buildings has been slower than in low-rise residential. This paper reviews methods for estimating commercial building infiltration rates going back to the 1970s. More recent approaches using correlations based on a large number of multizone airflow model simulations are presented as a more feasible approach. Particular attention is given to how energy models have dealt with infiltration estimation in commercial buildings, with a detailed discussion of how the energy analysis program EnergyPlus has considered infiltration. More complex and presumably more accurate methods of accounting for the energy impacts of infiltration in commercial buildings, based on coupled airflow and energy analysis models, are also discussed as they have become more accessible in recent years given the increasing power of personal computing.

KEYWORDS

airflow; commercial buildings; infiltration; modeling

1 INTRODUCTION

Building infiltration rates have important impacts on energy use, indoor air quality (IAQ), and moisture management, and these rates have been studied for more than 80 years (Coleman and Heald, 1940). The importance of infiltration was demonstrated by the creation of the Air Infiltration Centre (AIC), which held its first conference in 1980 focusing on infiltration measurement (Air Infiltration Centre, 1980), and subsequently evolved into the Air Infiltration and Ventilation Centre (AIVC). The term infiltration is used in this paper to describe the airflow into and out of buildings through unintentional leakage in the exterior building envelope due to pressure differences induced by wind, indoor-outdoor temperature differences and the operation of ventilation and other building systems. It is interesting to compare this with the definition promulgated by the AIVC in 1992, i.e., "The uncontrolled inward leakage of outdoor air through cracks, interstices, and other unintentional openings of a building, caused by the pressure effects of the wind and/or the stack effect" (Limb, 1992). This earlier definition mentions only inward flow, although many discussions of infiltration implicitly include outward flow or exfiltration. It doesn't mention pressure differences induced by building systems, such as exhaust fans, atmospherically-vented combustion appliances and unbalanced ventilation systems. In addition to these pressures, infiltration rates also depend on building envelope airtightness, airtightness of interior partitions and air temperatures within individual building zones. The physics of infiltration are well-understood and have been documented in a variety of places, including Dols and Polidoro (2015) and Etheridge and Sandberg (1996).

Much of the early work on infiltration focused on low-rise residential buildings based in part on their relative simplicity compared with commercial and institutional buildings, which are often larger and more complex, and have more zones and more elaborate ventilation systems. For the purposes of this paper, the term commercial building is used to describe commercial and institutional buildings that are used for a variety of purposes (e.g. work, education, healthcare, retail, public assembly) but not as residential living spaces. Multi-family residential buildings are also not included in this discussion. This description of commercial buildings is admittedly quite broad, and it includes buildings of the same size as single-family residences; the key point is that these commercial buildings include many large, complex, and mechanically ventilated buildings. In general, infiltration rates are more challenging to measure in commercial buildings than low-rise residential, again given their multizone layout, larger size and variations in ventilation system layout and operation. These factors often make it difficult to apply single-zone tracer gas measurement techniques as they complicate achieving uniform tracer gas concentration, which is required in using these techniques (ASTM, 2011). Multi-zone tracer methods exist, which can overcome these challenges, but they are much more difficult to apply (Etheridge and Sandberg, 1996) .

Given that infiltration rates in commercial buildings vary with weather and system operation, they need to be measured many times to characterize infiltration in a given building. Such long-term infiltration measurements have only been done in a small number of large commercial buildings (Grot and Persily, 1986). Therefore, in lieu of extensive measurement efforts, methods to estimate commercial building infiltration are needed to support design, energy calculation, IAQ analysis, retrofit planning and other applications. There is a long history of infiltration estimation methods in low-rise residential buildings, going back to the first AIC conference (Kronvall, 1980; Warren and Webb, 1980; Sherman and Grimsrud, 1980). This earlier work focused on methods to estimate infiltration rates from blower door measurements of envelope airtightness and weather conditions. These techniques evolved over time and are widely used and described in practical guidance (ASHRAE, 2017).

In contrast to low-rise residential buildings, the development of infiltration estimation methods for commercial buildings has progressed more slowly. Due to the often greater complexity of commercial buildings, there have been fewer measurements of envelope airtightness and infiltration rates in commercial buildings to support the testing of estimation methods, also contributing to slower advancement. Nevertheless, infiltration estimation methods in commercial buildings have progressed, and this paper outlines their development and summarizes tools currently available to designers, building scientists and other practitioners.

2 EARLY ESTIMATION METHODS

The earliest description of a large building infiltration estimation method known to the present authors was published before the first AIC conference (Shaw and Tamura, 1977). In that work, separate equations developed specifically for tall buildings are presented for infiltration flow rates due to wind and stack effect. The inputs to the wind infiltration component include building height and width, an envelope air leakage coefficient (that could come from a building pressurization test), wind speed and a wind direction adjustment factor. In addition to the leakage coefficient, the stack infiltration equation requires the length of the building perimeter, the indoor and outdoor air temperatures, the height of the neutral pressure level, and a thermal draft coefficient. The authors do not provide guidance on the neutral pressure level, but it can be measured in conjunction with a fan pressurization test. The thermal draft coefficient depends on the airtightness of the exterior walls relative to the interior partitions and captures how the static pressure decreases with height within the building interior, i.e., whether it is linear with

height, which would reflect a relatively open interior, or whether there are pressure drops across floors and other interior partitions. The authors note that the value of this coefficient is around 0.8 in office buildings based on the small number they had studied but note the lack of measured values for apartment buildings. The reference also includes an equation to combine the wind and stack infiltration components to estimate the total infiltration rate. In the 42 years since its publishing, Shaw and Tamura (1977) is only cited 34 times in Google Scholar, most of which are publications on infiltration modeling. None of these references appear to have employed the model to predict infiltration rates and compare them with measured values.

The other means of calculating infiltration rates in commercial buildings is multizone airflow modeling, i.e., CONTAM or other software (Dols and Polidoro, 2015; Walton, 1989b; ESRU, 2002; IES, 2019). These models involve a multizone representation of a building and use mass balance analysis to solve for the airflows between all building zones including the outdoors, from which building infiltration rates can be calculated. These models account for all relevant building airflow physics, though their neglect of the conservation of momentum and energy limits their applicability in buildings that are naturally ventilated and with interior air that is not quiescent. Given the need to for many inputs to describe multizone building airflow systems, such models are generally not considered to be readily accessible to practitioners, though they are widely used in the design of smoke control systems (Klote et al., 2012).

3 INFILTRATION ESTIMATION IN ENERGY ANALYSIS

While commercial buildings have always experienced air infiltration through envelope leaks, and early studies showed that the rates were significant (Grot and Persily, 1986), infiltration was often neglected in energy analysis in part due to its perceived complexity. Rather than take this important phenomenon seriously, many simply assumed infiltration was equal to zero. In some cases, at least in the U.S., this assumption was justified by claiming that mechanically ventilated buildings are pressurized, thus eliminating infiltration. This justification was based on the common practice of providing more supply air than return air. In reality, the complexity of multizone building airflow systems results in indoor-outdoor pressure differences being localized phenomena that depend on outdoor wind patterns, building height, and differences between the rate at which ventilation air is delivered to and removed from individual building zones. As a result, infiltration will occur even when more ventilation air is supplied to a building than removed by exhaust unless detailed analyses and control strategies are implemented to control pressure differences across the entire envelope.

Another approach, embodied in the EnergyPlus energy analysis software and other tools, is to use empirical equations for estimating infiltration. These empirical equations were developed from analysis and testing of low-rise residential buildings as noted below, and do not capture the airflow physics of large, multizone or mechanically ventilated buildings. In the case of EnergyPlus, the following equation is available for calculating infiltration rates:

$$\text{Infiltration} = I_{\text{design}} \bullet F_{\text{schedule}} \left[A + B|\Delta T| + C \bullet W_s + D \bullet W_s^2\right] \quad (1)$$

where I_{design} is defined by EnergyPlus as the "design infiltration rate", which is the airflow through the building envelope under design conditions. Its units are selected by the user and can be h^{-1}, $m^3/s \bullet m^2$ or m^3/s. To apply this infiltration approach in EnergyPlus, a value of I_{design} is assigned to each zone. F_{schedule} is a factor between 0.0 and 1.0 that can be scheduled, typically to account for the impacts of fan operation on infiltration. $|\Delta T|$ is the indoor-outdoor temperature difference in °C, and W_s is the wind speed in m/s. *A, B, C* and *D* are constants, for which values are suggested in the EnergyPlus Engineering Reference (DOE, 2019). As noted in that reference, this equation is based on measurements in 10 one- and two-story houses, for which

30 infiltration rates were fit to the equation (Coblentz and Achenbach, 1963). The default strategy in EnergyPlus is to assume a constant infiltration rate, i.e., A=1 and B=C=D=0. However, this approach does not reflect known dependencies of infiltration on outdoor weather and HVAC system operation. The EnergyPlus Engineering Reference provides values of A, B, C and D based on two energy analysis programs that preceded EnergyPlus, BLAST and DOE-2. No references are provided for these values, but they are presumably based on studies in low-rise, residential building as there were no studies of infiltration in commercial buildings available when these two predecessor programs were developed. The EnergyPlus Engineering Reference also includes two other empirical infiltration models developed for low-rise residential buildings, i.e., the Sherman-Grimsrud and the AIM-2 models described in Chapter 16 of the ASHRAE Fundamentals Handbook (ASHRAE, 2017). While these approaches account for weather effects, they are also based on low-rise residential buildings and do not account for the airflow physics in larger buildings and in buildings with the more complex mechanical ventilation systems typical of commercial buildings.

Gowri et al. (2009) proposed a method to account for infiltration in commercial buildings that was developed using a square medium-size office building and a building envelope airtightness value, such as can be obtained through pressurization testing. Assuming a constant indoor-outdoor pressure difference of 4 Pa, Gowri calculated an infiltration rate using an approach that accounts for wind but not temperature effects, despite their known importance in taller buildings and colder climates. Gowri recommends that this infiltration rate be multiplied by a wind speed adjustment and by a factor of 0.25 when the HVAC system is on and 1.0 when the system is off. Overall, the method greatly oversimplifies the dependence of infiltration on building envelope airtightness, weather, and HVAC system operation.

EnergyPlus also has the ability to perform multizone airflow analysis, as embodied in the CONTAM model discussed above, using the EnergyPlus Airflow Network model (DOE, 2019). This model is based on a predecessor to CONTAM referred to as AIRNET (Walton, 1989a) and an earlier version of CONTAM (Walton and Dols, 2003). It is worth noting that while CONTAM has evolved considerably in the intervening years, the EnergyPlus Airflow Network model does not incorporate all of those improvements.

Han et al. (2015) compared the use of various infiltration estimation methods in improving the accuracy of building energy simulations. One method used the EnergyPlus Airflow Network model with three infiltration levels (leaky, medium and tight) as defined via DesignBuilder, which is a graphical front-end to EnergyPlus. The other methods utilized various means to establish monthly and annually averaged wind pressures including the use of an AIVC database of wind tunnel measurements and the use of computational fluid dynamics (CFD) to model the building exterior. For this case study, the CFD-based methods resulted in energy predictions that more closely matched utility bills.

4 MORE RECENT ADVANCES

As building energy use has become of increasing interest over the years and as envelope insulation levels have increased, there has been more recognition of the importance of infiltration, including the need to control air leakage and to reliably estimate infiltration rates. These changes were reflected in the inclusion of requirements for continuous air barriers and envelope airtightness testing in energy efficiency standards such as ANSI/ASHRAE/IES Standard 90.1 (ASHRAE, 2016). As a result, new approaches to estimating infiltration were developed and are becoming more widely applied. This section describes one such approach, which uses values of the coefficients in Equation (1) developed specifically for commercial buildings, as well as a second approach using coupled energy and airflow analysis methods.

4.1 Large Building Infiltration Correlations

Values of the coefficients in Equation (1) for commercial buildings were recently developed by NIST. These coefficients were identified from investigations of the relationships between infiltration rates calculated using multizone airflow models, weather conditions, and building characteristics, including envelope airtightness and HVAC system operation. These relationships were developed using CONTAM models of the EnergyPlus models of 16 DOE commercial reference buildings (DOE, 2011; Goel et al., 2014). For each of these 16 buildings, different versions of the EnergyPlus models exist that correspond to different versions of ASHRAE Standard 90.1. In the ASHRAE 90.1-2004 versions, infiltration was modeled as 100 % of the design value when the HVAC system was off and 25 % (or 50 %) of that value when the HVAC system was on using the $F_{schedule}$ term in Equation (1). Further, A=1 and B=C=D=0 in Equation (1), which means the weather dependence of infiltration was ignored. In the ASHRAE 90.1-2013 versions of the prototype building models, infiltration was modeled with the same $F_{schedule}$ values but with C=0.224 based on a study by Gowri et al. (2009), which as noted earlier ignores the dependence of infiltration on indoor-outdoor temperature differences. These estimation methods are limited in that they do not fully account for weather effects and greatly oversimplify the impacts of system operation on infiltration.

In NIST's effort to develop coefficients for Equation (1), simulations were performed using NIST-developed CONTAM models of the DOE reference buildings to generate whole building infiltrations rates for a range of weather conditions with the ventilation fans on and off. Correlations were performed to fit these predicted infiltration rates to weather data, i.e., outdoor temperature and wind speed, to estimate the constants in Equation (1). For the ASHRAE 90.1-2004 versions of the building models, correlations were performed for 7 of the 16 reference models using Chicago weather (Ng et al., 2015). Compared with the assumption of constant infiltration in the reference building models, the correlation-based infiltration estimates agreed 60 % better on average with the CONTAM predictions. An example of the agreement between these infiltration correlations and the CONTAM predictions is shown for the Medium Office in Fig. 1a. The values for A, B and D for these 7 buildings were then correlated with building height, exterior surface area to volume ratio, and net system flow (i.e., design supply air minus design return air minus mechanical exhaust air) normalized by exterior surface area in order to predict these coefficients for any given building based on these three parameters (height, surface to volume ratio and net system flow). This generalized method resulted in an average improvement of 50 % when compared to the constant infiltration rates in the reference building models. Figure 1b compares the predictions using the suggested constants from DOE-2 and BLAST in the EnergyPlus Engineering Reference document, which results in much poorer agreement with the CONTAM predictions than seen using the correlation approach.

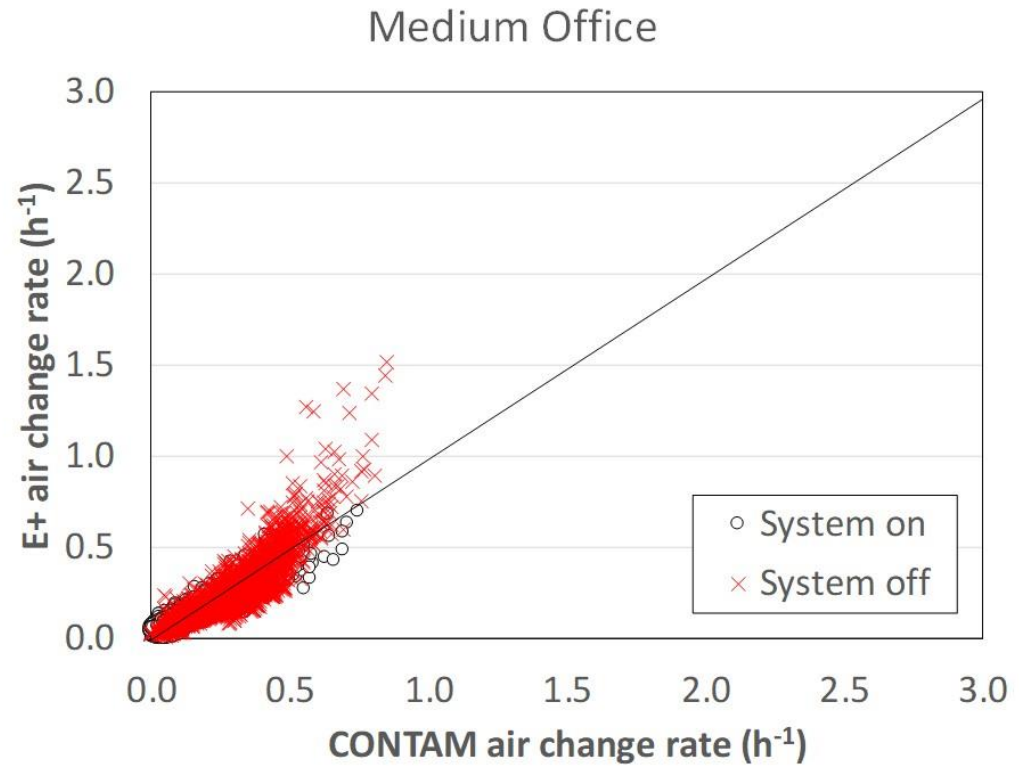

(a)

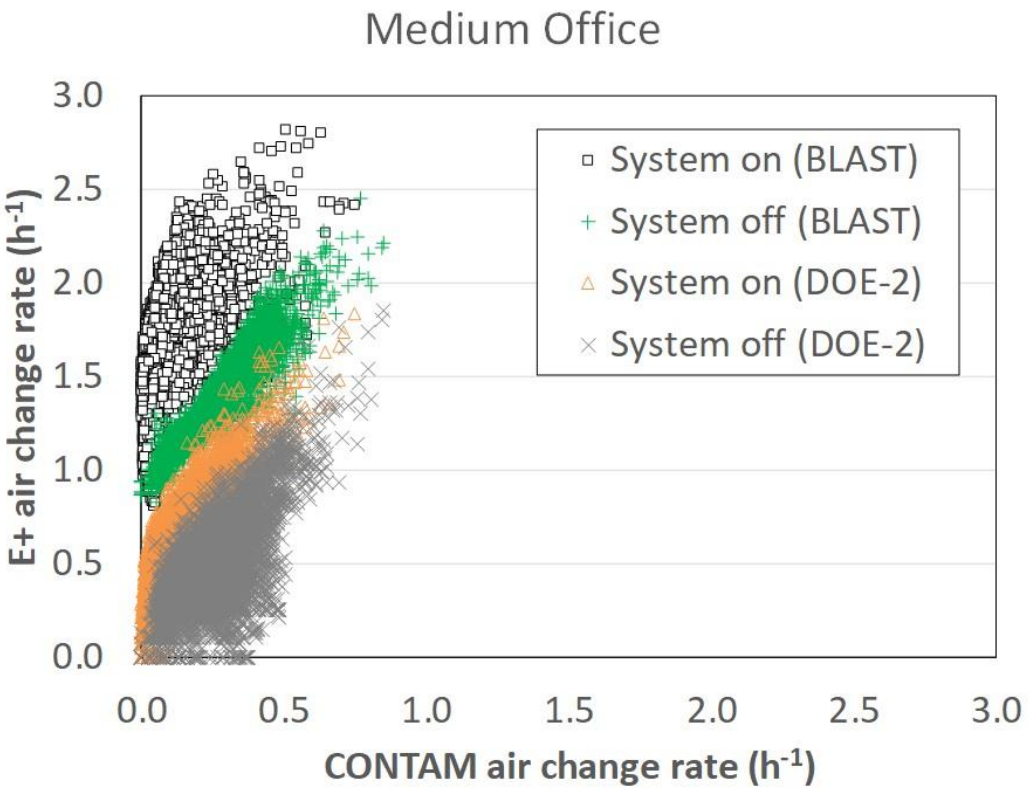

(b)

Fig. 1 EnergyPlus infiltration rates vs. CONTAM infiltration rates for Medium Office building using (a) NIST correlations and (b) DOE-2 and BLAST coefficients

In order to make these correlation-based estimation methods more accessible, they were incorporated into an Open Studio Measure called "Adding infiltration correlated for weather and building characteristics" (https://bcl.nrel.gov/node/83101). When the ASHRAE 90.1-2013 versions of the prototype building models were released, NIST updated the corresponding CONTAM models and expanded the infiltration correlations to eight cities (Ng et al., 2018). This work is continuing with the inclusion of more building types.

4.2 Energy-Airflow Model Coupling

Airflow and heat transfer are closely coupled processes in buildings, particularly in multizone buildings and in applications of natural ventilation. Basically, airflow models need zonal air temperatures to calculate airflows, and energy models need these airflows to calculate zonal temperatures. These calculations have historically been handled by separate software tools, with the inputs of each tool entered by the user "manually." However, increased computer power and more widespread application of building simulation in design is making both building energy analysis and airflow modeling more accessible, as well as enabling more direct coupling between these two types of modeling tools. The CONTAM-based methods employed by Han et al. (2015) utilized loose coupling between the energy and airflow analysis software, i.e., the outputs from one program were used as inputs to another but not during runtime. More recent advancements have enabled tight coupling or co-simulation between CONTAM and energy modeling tools, i.e., EnergyPlus and TRNSYS (Dols et al., 2015; Dols et al., 2016). Co-simulation allows for the runtime exchange of simulation results between energy and airflow programs at each time step. Currently available coupling allows the complex interaction between building-specific thermal, wind and system effects to be addressed simultaneously.

5 SUMMARY AND CONCLUSIONS

The estimation of infiltration rates in commercial and institutional buildings is more complex than in low-rise residential buildings given the larger size and multi-zone configuration of these buildings, the complexity of their HVAC systems and the lack of infiltration and airtightness measurements to validate estimation methods. As a result, there has been slower progress in infiltration estimation compared with low-rise residential buildings. This paper described the history of infiltration estimation in commercial buildings, with a focus on how energy analysis tools (i.e., EnergyPlus) treat infiltration. At this time, there are basically three options for estimating infiltration rates in commercial buildings: multizone modeling, empirical formulas (i.e., Equation 1) in which the coefficients are all non-zero and have a sound technical basis, and coupled energy-airflow modeling (which is essential an application of multizone modeling). While there has been progress in these estimation methods, it is unclear how simple such methods can be given the complexity of airflow and pressure in large, multizone buildings. Nevertheless, infiltration rates are needed for commercial building energy and IAQ analyses or other applications, and if an estimated rate is to be used it must be based on a sound technical approach and data, which need to be reported along with the estimate.

6 ACKNOWLEDGEMENTS

The authors express their appreciation to Sara Persily of BCER Engineering for her helpful review.

7 REFERENCES

Air Infiltration Centre (1980) "1st AIC Conference. Air Infiltration Instrumentation and Masuring Techniques".

ASHRAE. 2016. *Energy Standard for Buildings Except Low-Rise Residental*, Atlanta GA, American Society of Heating, Refrigerating and Air-Conditioning Engineers, (ANSI/ASHRAE/IES Standard 90.1-2013).

ASHRAE. 2017. *Fundamentals Handbook,* Atlanta, GA, American Society of Heating, Refrigerating and Air-Conditioning Engineers, Inc.
ASTM. 2011. *Standard Test Method for Determining Air Change in a Single Zone by Means of a Tracer Gas Dilution*, West Conshohocken, PA, American Society for Testing and Materials, (ASTM Standard E741-2011).
Coblentz, C.W. and Achenbach, P.R. 1963. Field Measurements of Air Infiltration in Ten Electrically-Heated Houses. *ASHRAE Transactions*, 69, 358-365.
Coleman, E.F. and Heald, R.H. 1940. *Air Infiltration Through Windows*, National Bureau of Standards, Washington, DC, BMS45.
DOE (2011) Commercial Reference Buildings, U.S. Department of Energy, Available from: https://www.energy.gov/eere/buildings/commercial-reference-buildings.
DOE. 2019. *EnergyPlus Version 9.1.0 Documentation. Engineering Reference*, U.S. Department of Energy.
Dols, W.S., Emmerich, S.J. and Polidoro, B.J. 2016. Coupling the Multizone Airflow and Contaminant Transport Software CONTAM with EnergyPlus Using Co-Simulation. *Building Simulation*, 9, 469-479.
Dols, W.S. and Polidoro, B.J. 2015. *CONTAM User Guide and Program Documentation. Version 3.2*, Gaithersburg, MD, National Institute of Standards and Technology, NIST Technical Note 1887.
Dols, W.S., Wang, L., Emmerich, S.J. and Polidoro, B.J. 2015. Development and application of an updated whole-building coupled thermal, airflow and contaminant transport simulation program (TRNSYS/CONTAM). *Journal of Building Performance Simulation*, 8, 327-337.
ESRU. 2002. *The ESP-r System for Building Energy Simulation. User Guide Version 10 Series*, Glasgow UK, University of Strathclyde.
Etheridge, D.W. and Sandberg, M. 1996. *Building ventilation: theory and measurement,* West Sussex, England, John Wiley & Sons, Ltd.
Goel, S., Athalye, R., Wang, W., Zhang, J., Rosenberg, M., Xie, Y., Hart, R. and Mendon, V. 2014. *Enhancements to ASHRAE Standard 90.1 Prototype Building Models.*, Richland Washington, Pacific Northwest National Laboratory.
Gowri, K., Winiarski, D. and Jarnagin, R. 2009. *Infiltration Modeling Guidelines for Commercial Building Energy Analysis*, Pacific Northwest National Laboratory.
Grot, R.A. and Persily, A.K. (1986) Measured Air Infiltration and Ventilation in Eight Federal Office Buildings, In: Treschel, H. R. and Lagus, P. L. (eds) *Measured Air Leakage of Buildings ASTM STP 904*, Philadelphia, PA, American Society for Testing and Materials, 151-183.
Han, G., Srebric, J. and Enache-Pommer, E. 2015. Different modeling strategies of infiltration rates for an office building to improve accuracy of building energy simulations. *Energy and Buildings*, 86, 288-295.
IES (2019) IES Virtual Environment, Integrated Environmental Solutions Ltd.
Klote, J.H., Milke, J.A., Turnbull, P.G., Kashef, A. and Ferreira, M.J. 2012. *Handobok of Smoke Control Engineering,* Atlanta, GA, American Society of Heating, Refrigerating and Air-Conditioning Engineers, Inc.
Kronvall, J. (1980) "Correlating pressurization and infiltration rate data - tests of an heuristic model". In: Proceedings of Air Infiltration Instrumentation and Measuring Techniques, 1st Air Infiltration Centre Conference, Vol. 1, pp. 225-244.
Limb, M.J. 1992. *Air Infiltration and Ventilation Glossary*, Air Infiltration and Ventilation Centre, Coventry, Great Britain., AIVC Technical Note 36.
Ng, L.C., Ojeda Quiles, N., Dols, W.S. and Emmerich, S.J. 2018. Weather correlations to calculate infiltration rates for U. S. commercial building energy models. *Building and Environment*, 127, 47-57.

Ng, L.C., Persily, A.K. and Emmerich, S.J. 2015. Improving infiltration modeling in commercial building energy models. *Energy and Buildings*, 88, 316-323.
Shaw, C.Y. and Tamura, G.T. 1977. The Calculation of Air Infiltration Rates Caused by Wind and Stack Action for Tall Buildings. *ASHRAE Transactions*, 83 (II), 145-157.
Sherman, M.H. and Grimsrud, D.T. (1980) "Measurement of infiltration using fan pressurization and weather data". In: Proceedings of Air Infiltration Instrumentation and Measuring Techniques, 1st Air Infiltration Centre Conference, Vol. 1, pp. 277-322.
Walton, G.N. 1989a. Airflow Network Models for Element-Based Building Airflow Modeling. *ASHRAE Transactions*, 95 (2), 611-620.
Walton, G.N. 1989b. *AIRNET - A Computer Program for Building Airflow Network Modeling*, National Institute of Standards and Technology, Gaithersburg, MD, NISTIR 89-4072.
Walton, G.N. and Dols, W.S. 2003. *CONTAMW 2.1 Supplemental User Guide and Program Documentation*, Gaithersburg, MD, National Institute of Standards and Technology, NISTIR 7049.
Warren, P.R. and Webb, B.C. (1980) "The relationship between tracer gas and pressurization techniques in dwellings". In: Proceedings of Air Infiltration Instrumentation and Measuring Techniques, 1st Air Infiltration Centre Conference, Vol. 1, pp. 245-276.

Wind Pressure Coefficient and Wind Velocity around Buildings in High Density Block of Metropolis for Natural Ventilation Design

Toshio Yamanaka[*1], Eunsu Lim[2], Tomohiro Kobayashi[3], Toshihiko Sajima[4], and Kanji Fukuyama[3]

1 Osaka University
2-1 Yamadaoka,
Suita-shi, Osaka, 565-0871 Japan
Presenting and corresponding author
yamanaka@arch.eng.osaka-u.ac.jp

2 Toyo University
2100 Kujirai,
Kawagoe-shi, Saitama 350-8585, Japan

3 Osaka University
2-1 Yamadaoka,
Suita-shi, Osaka, 565-0871 Japan

4 Takenaka Corporation
4-1-13 Honmachi
Osaka-shi, Osaka, 541-0031 Japan

ABSTRACT

The ventilative cooling by natural ventilation is important technology for the buildings in urban area for the sake of energy saving and BCP (Business Continuity Plan). In fact, a large number of high-rise buildings in urban area in Japanese metropolises are equipped with natural ventilation apparatus such as openings and chimneys or shafts. In design stage of the building, generally, building engineers have to decide the size and number of ventilation devices, but it is not easy because the data of wind pressure coefficient are not ready for engineers to use easily especially for the buildings in high density block of metropolis. In designing the natural ventilation devices, a wind guide or a wind vane sticking out from walls of the building is useful device to introduce natural wind from outside into the rooms. The wind velocity around the building, however, is essential to predict the performance of these devices. Here, the wind velocity around building depends on the distance between buildings, height above ground and wind speed of approach flow and so on. It can be said that the data of wind pressure on building wall and wind velocity around buildings are necessary for natural ventilation design of the buildings in high density blocks of metropolis.

In this study, in order to provide the data for natural ventilation design of buildings in metropolis, the distribution of wind pressure coefficient on the building walls and wind velocity distribution between the buildings were measured by wind tunnel test with 1:1000 scaled models and CFD analysis by LES. In CFD analysis, the dependency of wind pressure and velocity on Reynolds number between buildings, that is so-called Reynolds Number Effect, was examined.

As a result of CFD by LES, it was turned out that Reynolds number effect is inevitable to some extent in the wind tunnel test with 1:1000 scaled models under 10m/s of approaching wind, but the basic data of wind pressure coefficient and wind velocity were obtained by the wind tunnel test. Additionally, a simple method to predict the pressure loss and airflow rate based on the pressure boundary of the block without the gap between buildings were presented.

In the presentation of AIVC conference, some movies of airflows around buildings simulated by LES will be presented with many important data of wind pressure or wind velocity.

KEYWORDS

wind tunnel test, LES, critical Reynolds Number, wind pressure coefficient, wind velocity around buildings

1 INTRODUCTION

In urban district of metropolises, there are often many buildings in a block surrounded by streets with quite narrow gaps between buildings. In order to utilize natural ventilation for the

sake of energy saving and BCP (Business Continuity Plan), it is essential to predict the airflow rate through openings due to natural wind force or buoyant force based on the pressure difference between openings for natural ventilation. The data of wind pressure coefficient on the building walls facing narrow gaps between buildings are not yet prepared enough for the calculation of natural ventilation, so the wind tunnel test or reliable CFD (Computational Fluid Dynamics) will be necessary every time you design the natural ventilation of a building in a high-density block. In addition, the data of wind velocity in the narrow gaps between buildings are also important to estimate the discharge coefficient of openings on the wall, especially for wind scoop projecting from the wall.
There are many studies on the wind pressure or wind velocity in urban street canyon such as (Gromke et al., 2008)(Buccolieri at al., 2010)(Antoniou et al.,2017), but the narrow gaps have not been covered yet.
So in this study, the wind pressure coefficient on the wall and wind velocity are measured by wind tunnel test and CFD analysis using LES is conducted to investigate the effect of Reynold's number on these values.

2 WIND TUNNEL TEST

2.1 Outline of wind tunnel test

In Figure 1, the section and layout of the used models of building in wind tunnel with atmospheric boundary layer of power of 1/4.2 are shown. The scale of the buildings was set at 1/1000. Used building models are shown in Figure 2. Case 1 is the case that one block consists of one building. This case is actually uncommon, but the wind pressure on the wall at the location of building gaps can be estimated from the data of Case1. The size of the block ($W80 \times D80 \times H40$) was decided from the average size of blocks in urban area of Osaka city (Japan). Three kinds of gaps, that is the distance between buildings are tested as seen in Figure 2. Each gross BCR (Building Covering Ratio) in four cases is 64%, 57.8%, 51.8%, 41.0%. In Figure 3, the layout of target block and Surrounding blocks are shown. The target block was exchanged in turn, but the surrounding block with the gaps of 8mm is not

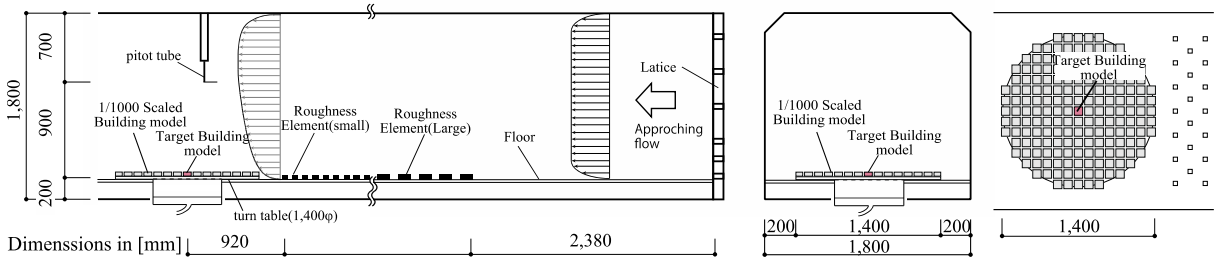

(a)Section of wind tunnel

(b) Layout of building models

Figure 1: Outline of wind tunnel test

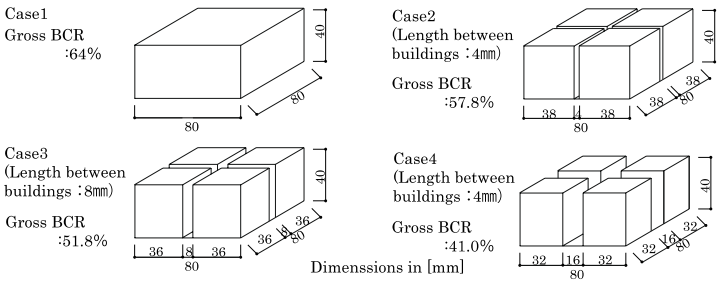

Figure 2: Tested cases of the target buildings (BCR: Building Covering Ratio)

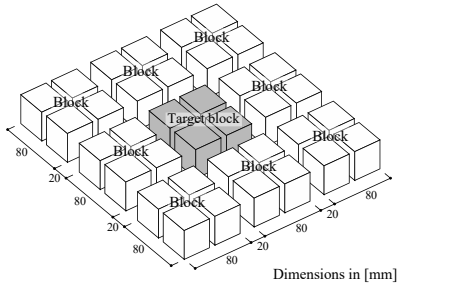

Figure 3: Layout of eight blocks surrounding the target block with the gap of 8mm

exchanged. The size of this gap is the mean value of three gap sizes of Case 2-4.
Figure 4 shows the profiles of wind velocity, turbulent intensity and turbulent length scale of approach flow (scaled atmospheric boundary layer) in the wind tunnel. The exponent of power law of wind velocity is almost 1/4.2. The wind velocity was set to 10 m/s using the pitot tube at the height of 900mm above the floor.

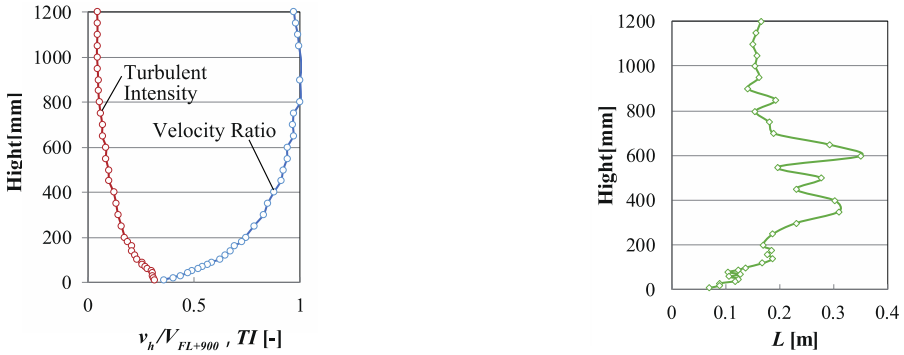

(a) Profile of wind velocity and turbulent intensity (b) Profile of turbulent length scale

Figure 4: Characteristics of approach flow

The wind pressure at the point in Figure 5 (a) was measured using pressure transducers (Validyne Engineering, DP45), and the wind velocity was measured at the points shown in Figure 5(b) using omni-directional anemometer (Kanomax Japan Inc., Model 1570). The wind direction was varied by 22.5 degree as the schematic figure in Figure 5, but the results in the case of 0 degree will be presented in this paper.

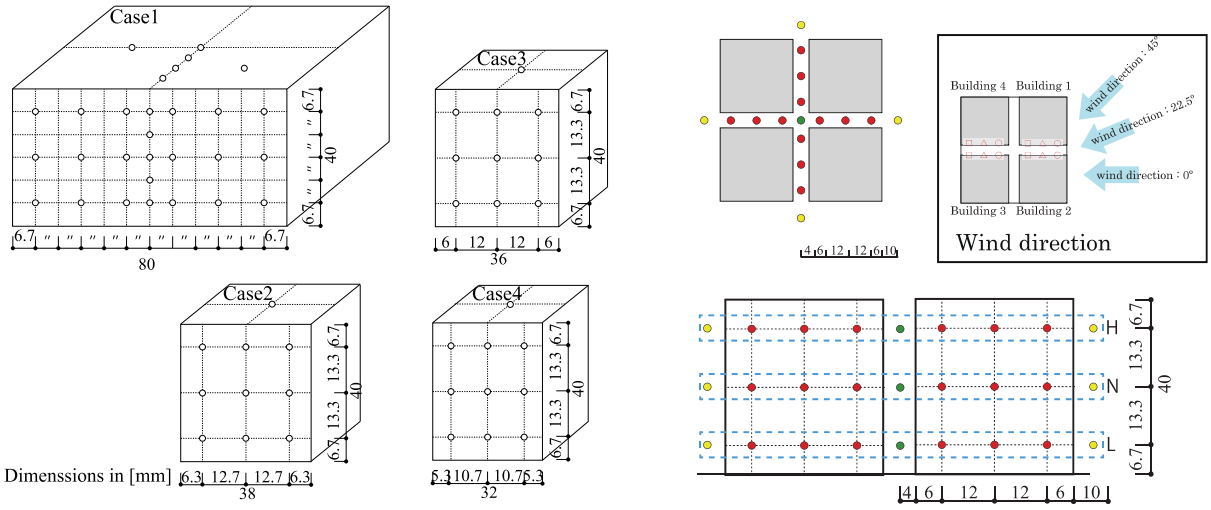

(a) Point for wind pressure coefficient (b) Point for wind velocity between buildings

Figure 5: Measurement point of wind pressure coefficient and wind velocity

2.2 Results and Discussions

Figure 6 shows the relationship between gap length and wind pressure coefficient on the center line in the walls perpendicular and parallel to wind direction. The wind pressure coefficient was calculated using dynamic pressure of approach flow at the height of building (40mm). The standard static pressure of kinetic pressure and wind pressure is the static pressure measure by pitot tube at the height of 900mm. From Figure 6, all the wind pressures have negative value. There is little difference between the pressures of both side (windward

and leeward) of walls, and the wind pressure coefficient decrease as the length of building gap becomes larger. In almost cases, the higher the position is, the lower the wind pressure is. These results seem to be brought about by the change of wind velocity inside gaps between buildings.

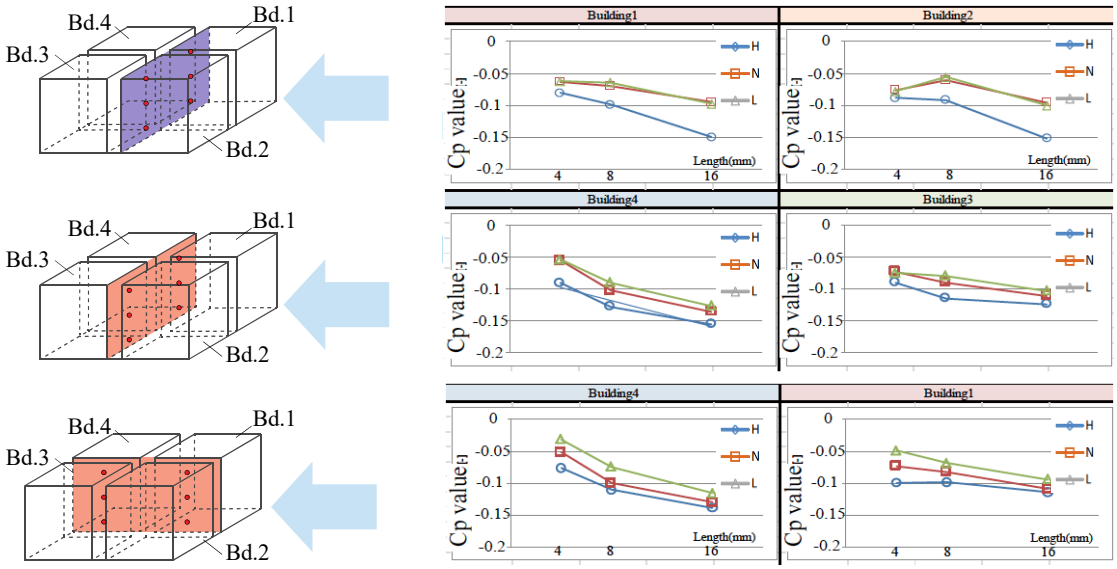

Figure 6: Relationship between gap length and wind pressure coefficient at the center on the wall

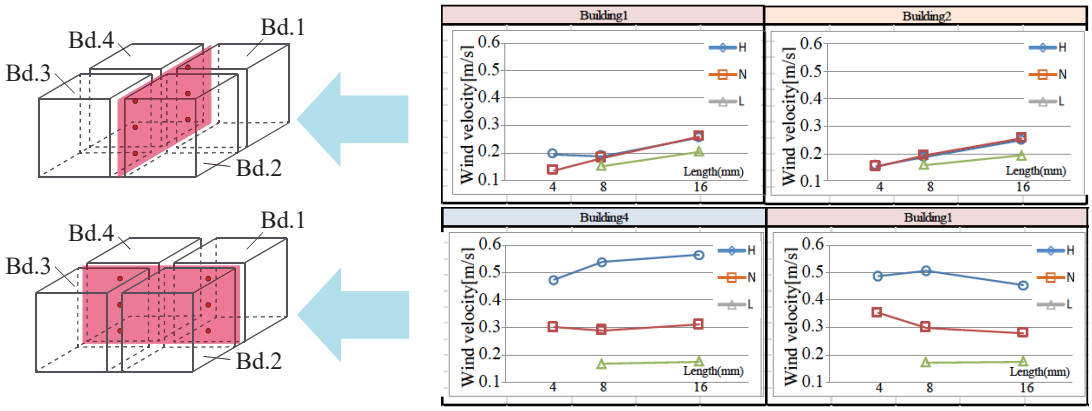

Figure 7: Relationship between gap length and wind velocity in the center of the gap between buildings

Figure 7 shows the relationship between gap length and wind velocity at three points on the vertical center line in each building gap. It can be seen that in the gaps perpendicular to wind flow, the larger the gap length is, the larger the wind velocity, but in the gaps parallel to wind flow, wind velocity is almost the same regardless of the gap length. Also in the gaps parallel to wind flow, wind velocity at higher points are larger than lower points. These differences of wind velocity are larger than that of wind pressure coefficient.

From two figures of Figure 6 and Figure 7, there seems to be a tendency that at a point with high wind pressure has low wind velocity, which might mean that the total pressure of dynamic pressure and static pressure is preserved according to Bernoulli law.

So in order to examine the loss or gain of total pressure along the flow in the gap and to compare them with the static pressure on the wall of Case 1 at the position of the entrance and outlet of building gaps, Figure 8 shows the distribution of total pressure and wind pressure of a building in Case 1(´). Generally, the wind pressure at the point of opening location on the wall surface is equal to the total pressure of the airflow in the case that there is a pass way through an opening, and at the outlet the wind pressure is equal to the static pressure in the

airflow at the outlet. In the section parallel to wind flow, the right hand of the figures, it is true in Case 2 and 3, but there can be seen the difference between them in Case 4 of the gap of 16mm. From the figures on the left hand, in the section perpendicular to the wind flow, the wind pressure of the wall is not necessarily equal to the total pressure or static pressure depending on the case, that means the direction of the airflow is not consistent and symmetrical. A remarkable tendency is that the total pressure increases along the airflow in the parallel section on the right hand of these figures, which means the inflow of momentum from the airflow over the buildings. This phenomenon is quite interesting but will need detailed measurement of wind velocity and static pressure. The detailed CFD might be useful.

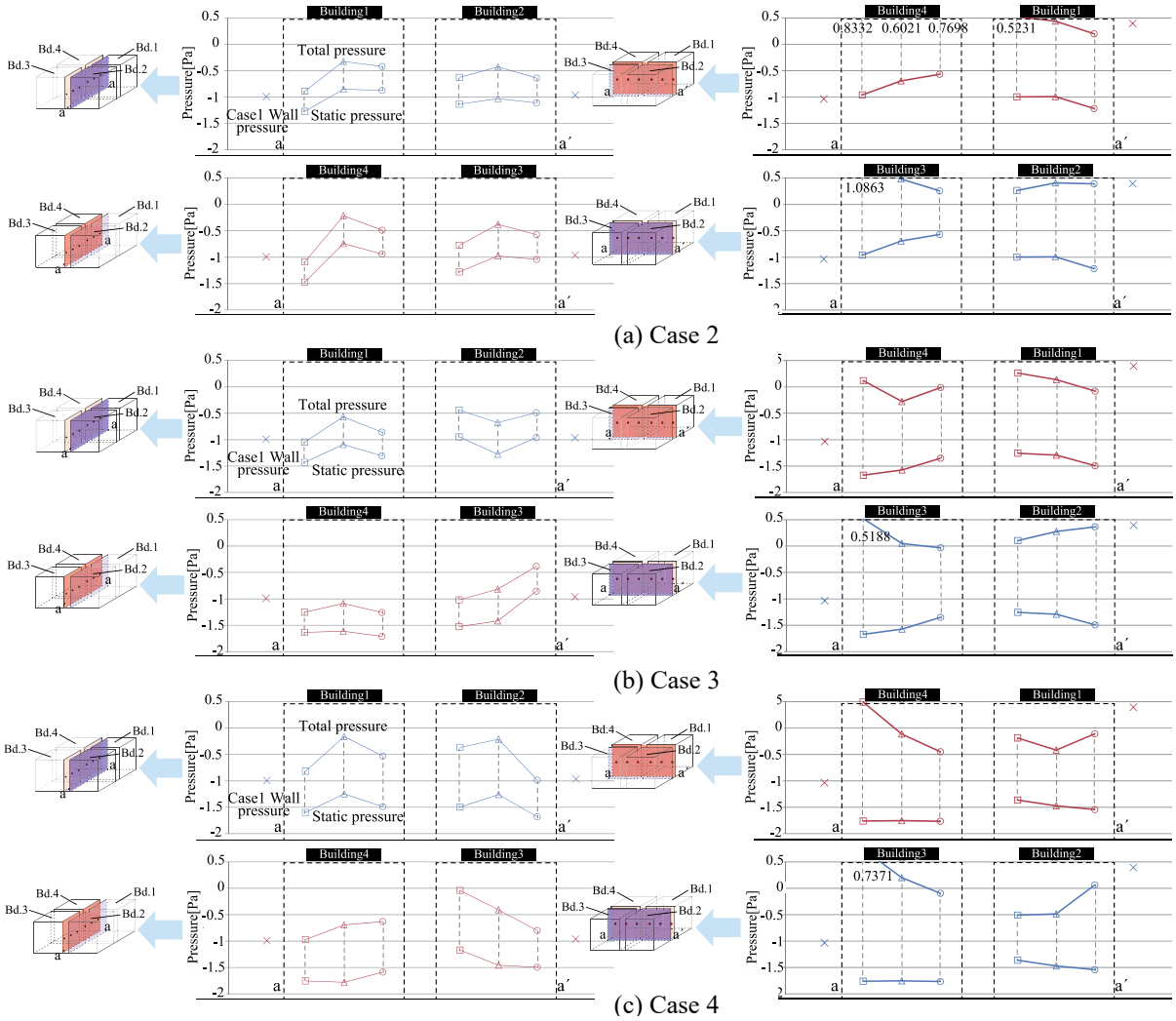

Figure 8: Distribution of total wind pressure coefficient of case 2 through 4 with the wind pressure coefficient on the building walls of the large building without gaps of case 1

3 CFD ANALYSIS

3.1 Outline of LES (Large Eddy Simulation)

In chapter 2, the results of wind tunnel test were presented. However, the similarity between wind tunnel test and actual phenomenon should be examined. The problem is whether critical Reynolds number was attained or not. Normally wind velocity of 10m/s is enough for measuring wind pressure or wind velocity in the case of bluff body in the wind tunnel test, but the gaps between buildings in this study are so narrow that the effect of Reynolds number could be essential, that is, the effect of viscosity could not be negligible. It is, however, not easy to examine the effect in wind test changing the model scale or wind velocity. So, by CFD analysis using LES was conducted to examine the effect of Reynolds number on the

wind pressure and wind velocity. In order to change Reynolds number of the flow in the gaps of buildings, upper wind velocity V_0 (at the height of 900mm) in wind tunnel was changed. As the height of analyzed area is 400mm, the inlet velocity at the top of analysis area was calculated by power law of wind profile. In Table 1, the outline of CFD was listed, and six cases were examined as is shown in Table 2. In any cases, the product of time step and upper wind velocity V_0 at the height of 900mm above the floor was set to 0.01m taking account of time scale similarity.

Table 1: Outline of CFD analysis

CFD Code		Fluent19.1
Turbulence Model		Large Eddy Simulation WALE Model (C_W=0.325)
Algorithm		SIMPLE
Discretization Scheme for Advection Term		Central Differencing
Boundary Condition	Inlet	Velocity : Profile (experimental value)
	Outlet	Outflow
	Wall	Two Layer Model of Linear-Log Law
Total Number of Cells		2,275,875

Table 2: Analysis cases

	V_0	Time Step Size	Time Step
Case1	1.0m/s	0.01sec.(100Hz)	5000
Case2	5.0m/s	0.002sec.(500Hz)	
Case3	10.0m/s	0.001sec.(1000Hz)	
Case4	50.0m/s	0.0002sec.(5000Hz)	
Case5	100.0m/s	0.0001sec.(10000Hz)	

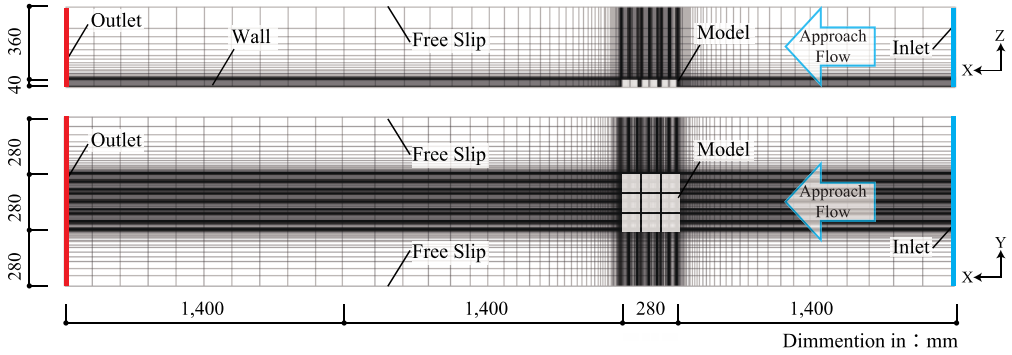

Figure 9: Mesh layout of analysis area in CFD (LES)

Mesh layout is shown in Figure 10. As an approach flow, measured profiles of wind velocity, turbulent intensity and turbulent length scale were reproduced as an inflow boundary condition using spectral synthesizer in Fluent. In Figure 10, the layout of the models was shown. Only nine blocks were used and the All the size of gaps are set at 4mm. This size is the same as the gap size of Case 2 of wind tunnel test, but the gaps of surrounding blocks are different from those of blocks for wind tunnel test. This difference is intended to make an safer conditions in CFD analysis.

The calculation was unsteady and k-ε model was used for the first 1000 time steps to make a initial situation for LES calculation. Figure 11 shows monitored points of wind velocity fluctuation of three components.

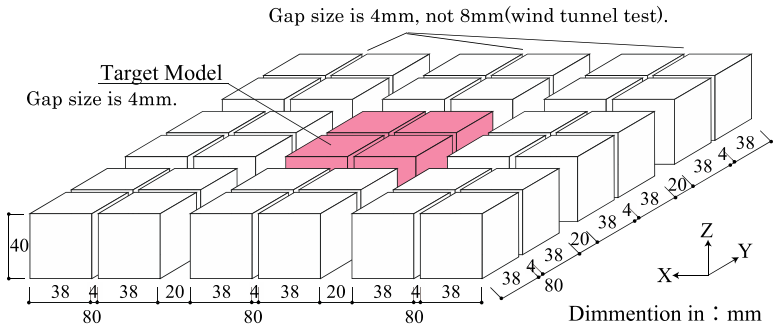

Figure 10: Size and layout of nine blocks including target blocks with the same gap of 4mm (not 8mm in the case of wind tunnel test)

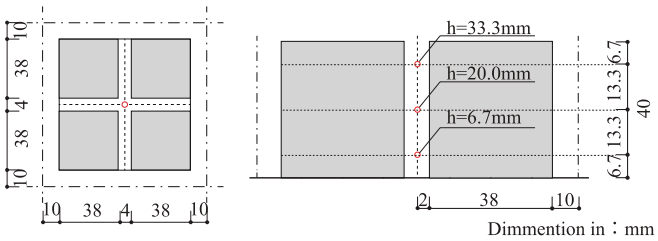

Figure 11: Monitored points of wind velocity in CFD

3.2 Results and Discussions

In Figure 12, the variations of wind velocity components at the monitored point with the height of 20 mm (Figure 11) in time series were shown as for each case. From these figures, in Case 1 and 2, the fluctuation of velocity is smaller than the other three cases, and the fluctuation magnitude in Case 3 (V_0=10m/s) is almost close to the fluctuation of velocity in Case 4 and 5. There can be, however, the dependence on the upper wind velocity of the amplitude of fluctuation of the wind velocity in the gap of buildings.

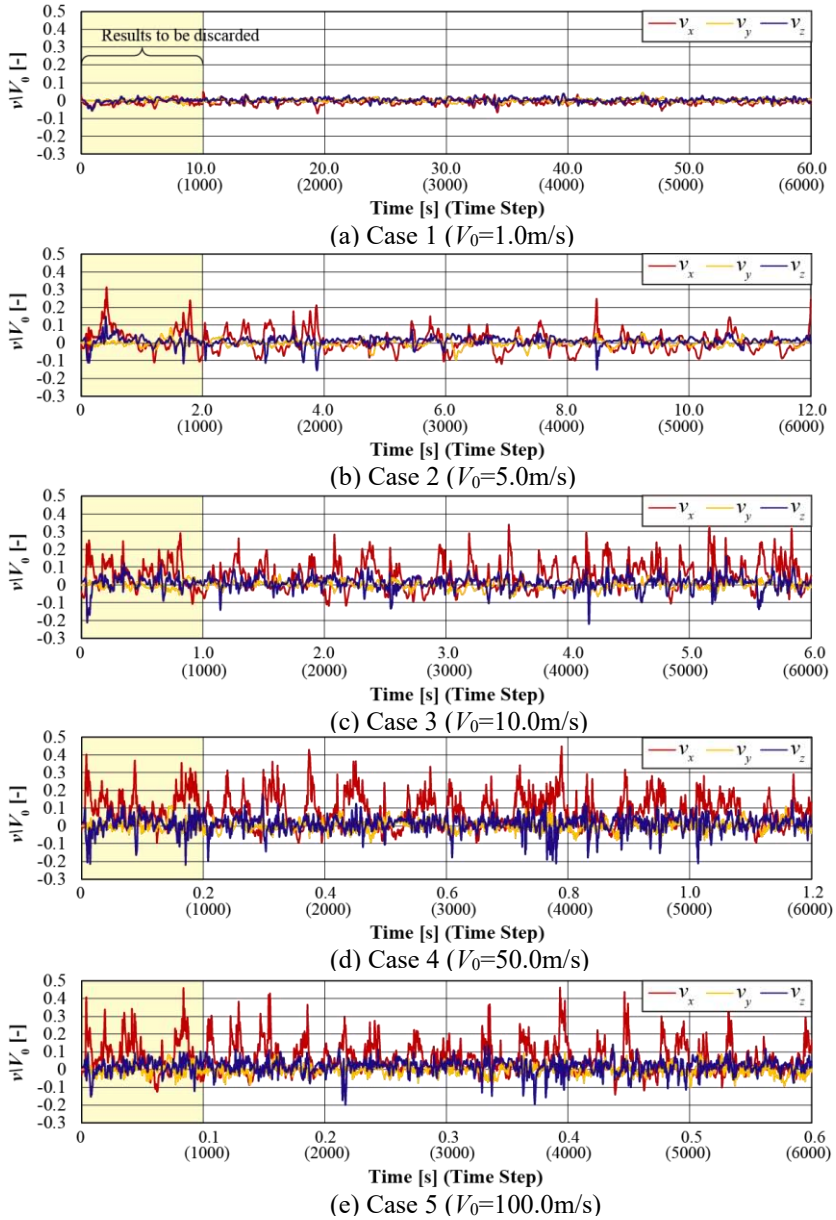

(a) Case 1 (V_0=1.0m/s)

(b) Case 2 (V_0=5.0m/s)

(c) Case 3 (V_0=10.0m/s)

(d) Case 4 (V_0=50.0m/s)

(e) Case 5 (V_0=100.0m/s)

Figure 12: Variation of each component of wind velocity at point with the height of 20mm (see Figure 11)

In Figure 13, the distributions of wind pressure coefficient are shown. The standard dynamic pressure is that of the wind velocity of approach flow at the height of buildings (40mm), and the standard static pressure is that of at the top of analysis area, 140mm leeward of inlet boundary. From these figures, it is clear that the distribution of wind pressure is dependent on upper wind velocity. It has to be said that 10 m/s of upper wind velocity is not enough for the prediction of wind pressure coefficient on the walls in gaps.

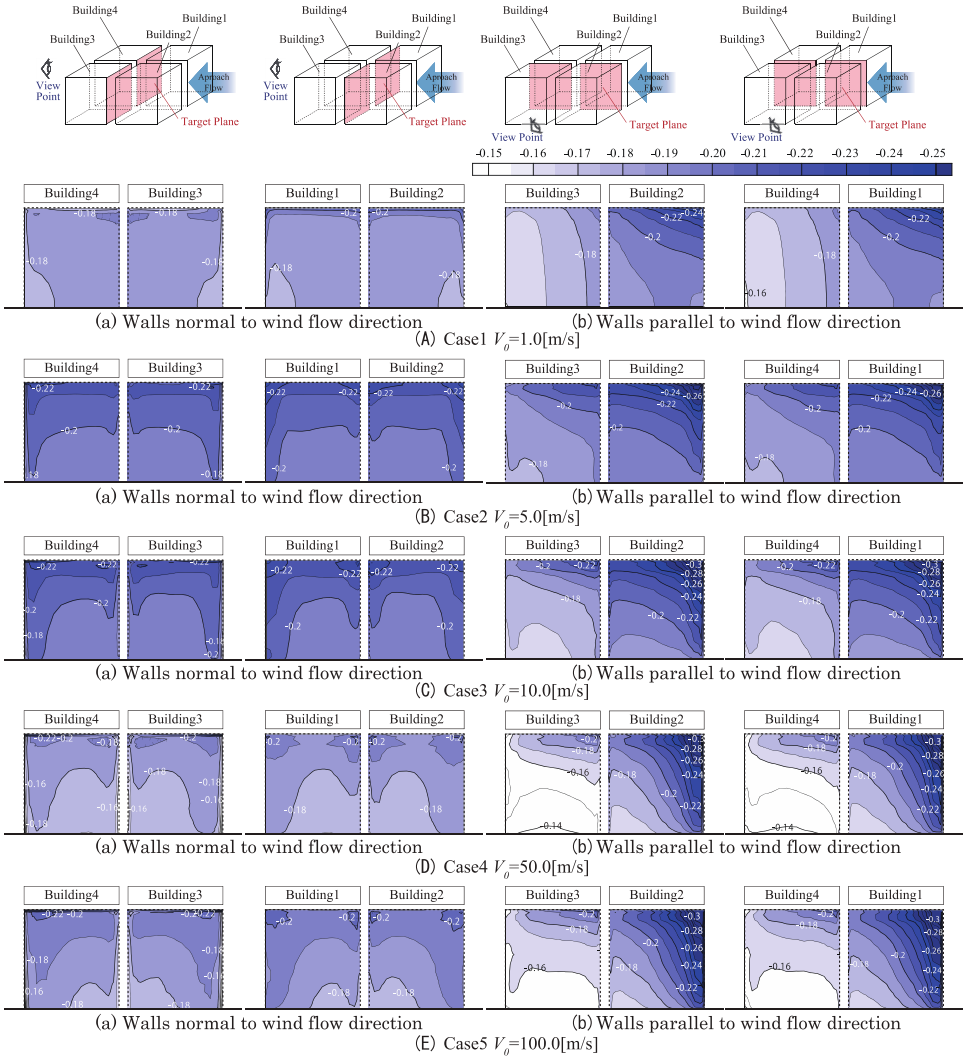

Figure 13: Distribution of wind pressure coefficient on the walls facing building gaps in each case

In Figure 14, the distribution of wind velocity in the gaps are shown. As for the velocity in the gap parallel to the wind flow, the distribution of velocity is depending on the upper wind velocity, but wind velocity in Case 4 and 5 are almost the same. It is clear that 10 m/s of upper wind velocity is not enough to predict the wind velocity in the gaps. However, the gap length of surround blocks is 4mm, which is narrower than the gap length in wind tunnel test, so this tendency might not be true of the results of wind tunnel test. The investigation, therefore, based on Reynolds number of the flow in the gap will be needed.
From Figure 15 through Figure 18, the normalized variables such as wind velocity, turbulent length scale, turbulent energy and turbulent dissipation rate were showed as a function of Reynolds number in the gap. The averaged wind velocity of three points at the center of gaps (Figure 11) were used for the calculation of Reynolds number. From Figure 15, when Reynolds number is larger than 1000, wind velocity is rather stable. In Figure 16, turbulent length scale shows a peak value at the Reynolds number of 1000. It seems to be difficult to

explain the reason of this peak at present. As for turbulent energy and turbulence dissipation rate, these values become quite large at high Reynolds number over 1000. That respects the transition from laminar airflow to turbulent airflow. It can be said that Reynolds number of over thousands could be necessary to predict the turbulent property by CFD and also wind tunnel test.

From the data obtained by wind tunnel test in Chapter 2, Reynolds number in the gaps between buildings are at most less than 500, which is not enough for the prediction of even wind velocity. As the wind pressure is affected by wind velocity along the wall in gaps, this Reynolds number is not enough for the prediction of wind pressure, too. Of course, it is true of turbulent energy and turbulence dissipation rate.

It is concluded that the scale of 1/1000 and small gap length such as 4, 8 and 16mm was rather out of required range of Reynolds number. In fact, there is a limitation of Reynolds number, so the CFD is more accurate method to examine the airflow and wind pressure in urban building arrays.

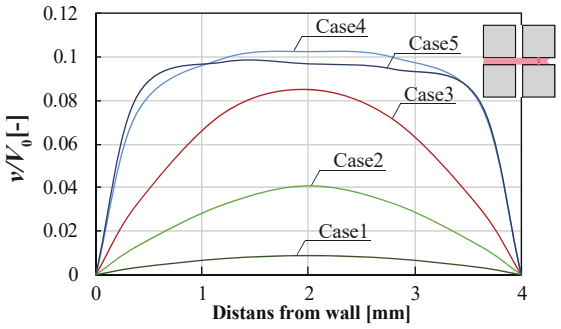

(a) Building gap parallel to wind flow

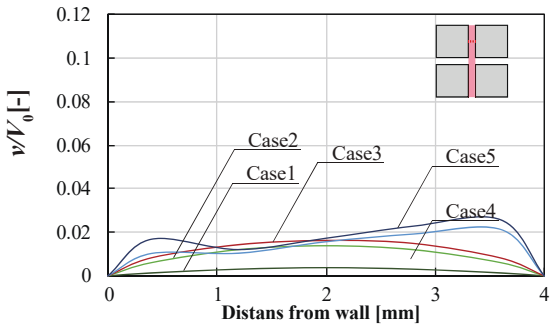

(b) Building gap perpendicular to wind flow

Figure 14: Distribution of normalized wind velocity in gaps between buildings in each case

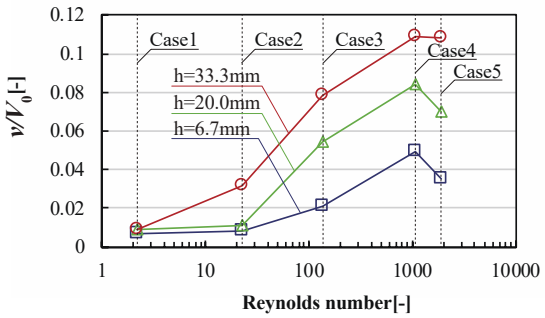

Figure 15: Relationship between Reynolds number and normalized wind velocity in the gap

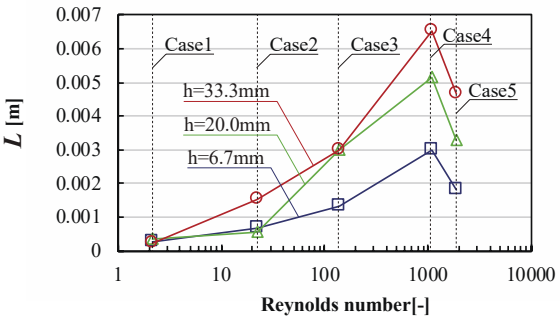

Figure 16: Relationship between Reynolds number and turbulent length scale in the gap

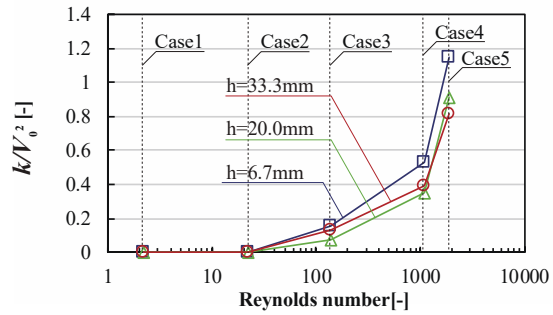

Figure 17: Relationship between Reynolds number and normalized turbulent energy in the gap

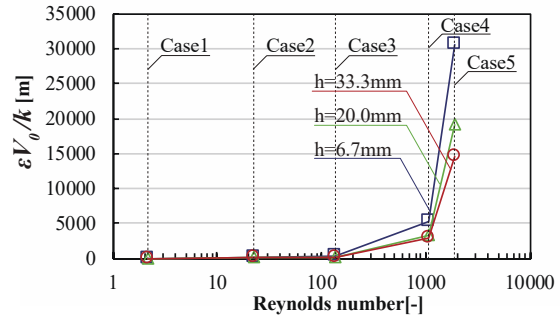

Figure 18: Relationship between Reynolds number and normalized turbulence dissipation rate in the gap

4 CONCLUSIONS

In this study, wind tunnel test and CFD analysis were conducted to investigate the wind pressure coefficient on the walls facing the building gaps and wind velocity in the gaps of buildings in high density block of metropolis such as Osaka in Japan. As a result, concluding remarks are as follows.

From wind tunnel test:

- The wind pressure coefficient on the wall in the gap has a negative correlation with the gap length of buildings.
- The wind velocity in the gap has a positive correlation with the gap length of buildings.
- The total pressure tends to increases along the gap in the flow direction, and this can be considered to be caused by the inflow of momentum of outer airflow over the blocks.
- At the entrance of airflow into the gap, the wind pressure of the wall of one large building without gaps at the location of the gap seems to be the total pressure of the airflow, which can be used to judge the direction of airflow.

From CFD analysis by LES (Large Eddy Simulation):

- The amplitude fluctuation is large at the upper wind velocity of high speed. This phenomenon is considered to mean the airflow in the gap becomes turbulent as the increase of wind velocity in the gap.
- It is clear that the distribution of wind pressure on the wall is dependent on upper wind velocity. It has to be said that 10 m/s of upper wind velocity is not enough for the prediction of wind pressure coefficient on the walls in gaps.
- The distribution of wind velocity in the section of gap reflect the turbulent state of airflow, which is caused by Reynolds number of airflow in the gap. The case of 50 m/s and 100 m/s of upper wind velocity are enough for state of turbulence, but 10 m/s is not enough.
- From the view point of the effect of Reynolds number, 1000 of Reynolds number seems to be needed for the prediction of wind velocity and turbulent length scale, and Reynolds number of more than 2000 will be needed to predict the turbulent energy and turbulence dissipation rate of the airflow in the gap.

5 ACKNOWLEDGEMENTS

The authors would like to appreciate the cooperation of Prof. Jihui Yuan and Mr. Osamu Kawabata who assisted in wind tunnel test in Osaka University.

6 REFERENCES

Antoniou, N., Montazeri, H., Wigod, H., Neophytou, M.K.-A., Blocken, B., Sandberg, M. (2017), CFD and wind-tunnel analysis of outdoor ventilation in a real compact heterogeneous urban area: Evaluation using “air delay”. *Building and Environment, 126, 355-372*

Buccolieri, R., Sandberg, M., Sabatino, D.S. (2010). City breathability and its link to pollutant concentration distribution within urban-like geometries. *Atmospheric Environment, 44, 1894-1903.*

Gromke, C., Buccolieri, R., Sabatino, S.D., Ruck, B. (2008), Dispersion study in a street canyon with tree planting by means of wind tunnel and numerical investigations – Evaluation of CFD data with experimental data. *Atmospheric Environment, 42, 8640–8650*

Alternative solution proposal to improve the air change in light shafts based on flaps

Ángel Padilla-Marcos Miguel[1], Alberto Meiss[*1], Raquel Gil-Valverde[1], Irene Poza-Casado[1] and Jesús Feijó-Muñoz[1]

1 RG Architecture & Energy
Universidad de Valladolid
Av Salamanca, 18 47.014
Valladolid, Spain
**Corresponding author: miguelangel.padilla@uva.es*

ABSTRACT

Outdoor air change qualifies the air that enters into the buildings. The outdoor air moves freely along the urban mesh favoured by the wind forces and stresses. Buildings, trees and other constructions alter the natural air flow pattern inside the cities, creating stagnated air masses in those wind-protected regions. Some outdoor spaces such as light shafts and confined light shafts inhibit the correct exchange of the stagnated air with fresh air coming from the outskirts and suburban areas.
The research proposed based on computational simulations tries to evaluate the susceptibility of several light shafts to infer the air change of their air by placing flaps close to their upper opening, where fresh air gets into exhausting the stagnated one. The flap is located over the opening aims to change the air flow pattern inside the light shaft by using Venturi effect partially sucking the stagnated air.
Results show that in the proposed cases the air velocity distribution is changed along the light shaft, affecting the air flow related to the reference case. The air flow through the opening increases ten times when the flap is placed. Nevertheless, the impact of the flap in the air change is negligible because the mean age of the air inside the light shaft does not decrease. It would be necessary to propose new flap models, which will affect the distribution of the air inside light shafts to improve the air change.

KEYWORDS

Outdoor air quality; light shaft; natural ventilation; CFD; air change efficiency.

1 INTRODUCTION

The concept of "light shaft" has been developed in South European cities due to the regulations on building depth. It is defined as the confined outdoor space formed in and between the buildings whose principal function is lighting and ventilating indoor spaces in a natural way (AI-Azzawi, 1994).

Light shafts are designed to provide light to those indoor spaces that cannot take the light directly from outdoor spaces due to its location into the building. They are also very important in terms of ventilation but usually are not designed for that purpose, hiding the air access (Ng, 2008) (Chen, 2009). The quality of that air is also lower than the indoor air. Outdoor air flows freely through the city even though emissions of combustion gases and other pollutant sources contaminate it (Buccolieri et al, 2010) (Chavez et al, 2011) (Holford and Hunt, 2000) (Germano et al, 2005).

The dispersion from light shafts and other enclosed spaces was evaluated by Hall et al. (1999). Ok et al (2008) developed an experimental study of surfaces openings on air flow caused by wind in light shafts. The impact of several outdoor space geometries on the air quality was analysed by Padilla-Marcos et al. (2016) using the age of the air and efficiency concepts defined by Sandberg (1981). None of them attended to how the air quality depended on the shape and dimensions in a vertical, narrow and generally closed outdoor space, that is, a confined outdoor space. The lack of a deep study of the quality of the air in light shafts in urban environments related to the design of the confined outdoor spaces (Feijó and Meiss, 2011) favoured a generic analysis methodology showing the aspects required regarding the architectural design of these spaces. It has been demonstrated that the air quality and its renovation is affected by the architectonical configuration of the models and the aero-dynamical phenomena of the environment. This methodology assesses the impact of the architectural configuration of the building with a light shaft and its ability to change the air.

DEVELOPMENT OF TWO-DIMENSIONAL MODELS

1 METHODOLOGY

After the assessment of the three-dimensional (3D) analysis of the air behaviour and the age of the air in several light shafts considering its two-dimensions (2D) and proportion, the quality of air renovation inside them can be addressed in an objective way.

The cases of study have been simplified with the aim of reducing the data files processing load and a minimization of the computing cost in future studies. Cases are developed 2D instead of 3D. The “y” axe, which determines the transversal dimension to the normal (the predominant direction of the wind in the light shaft) was eliminated. The reason was that this dimension provided less essential information to the simulation.

After the simplification, it is hypothesized that, when moving from a 3D model into a 2D one, the capacity of the air to flow freely in the horizontal plane is annulled. To verify this, a study of the 2D case was developed in the plane of symmetry. The choice of this plane entails that the 2D analysis corresponds to the representation of a 3D model developed infinitely along the normal direction to the simulation plane.

The representation of the movement of the air in the inner light shafts verifies that it is affected mainly in the vertical plane of the axis of displacement by the action of the wind, which produces a turbulent displacement. In the transverse direction, the movement of the air is mainly conditioned by the walls of the light shaft.

The impact of these factors into the capacity of the renovation of the air located in the inside of the light shafts was studied, according to the usual formal configuration in the Spanish architecture tradition. From all the studied cases, a comparison between Case 1 and Case 2 (Figure 1) was made. Case 1 was an isolated light shaft surrounded by a ring-shaped building and Case 2 were two parallel transversal blocks. Both cases were chosen due to their similarities regarding the cut in the symmetry plane of a 3D model and the infinitely developed case. It was observed that the efficiency of those cases implies just a ± 1.4% difference, and case 2 obtained better results.

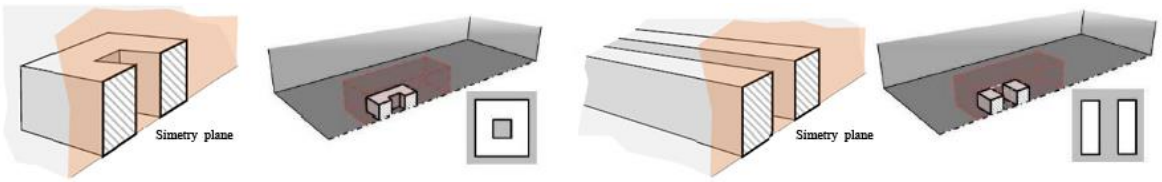

Figure 1: Building model discretization

Resembling the outside space as a continuous outside space or a corridor, the moving air undergoes acceleration when it approximates the solid built due to the reduction of its effective section. The air has no other lateral escape routes to distribute the pressures. The distribution of the age of the air and, therefore, the outside space efficiency, change in comparison with the 3D studied cases. However, the behaviour pattern of the air inside the light shaft once the consideration has been assumed, should take approximated guidelines to those obtained from the 3D analysis of Case 2 (Figure 2).

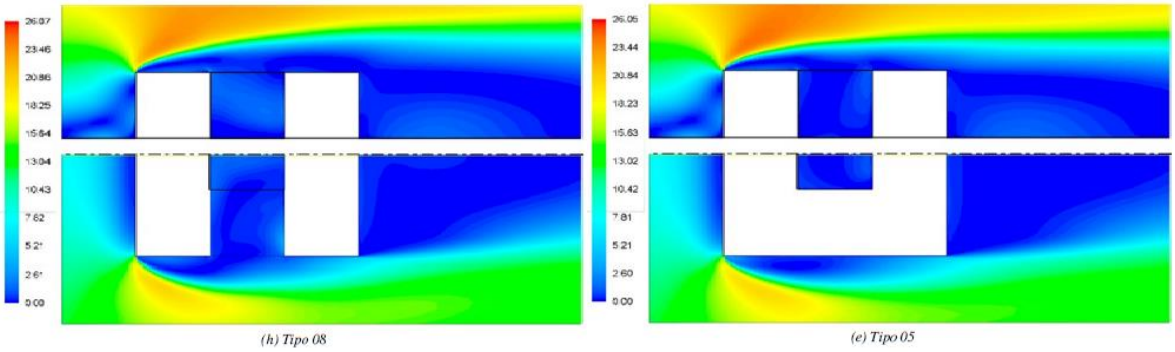

Figure 2: Dynamic outdoor air pattern

After the demonstration of the viability of this simplification, it is necessary to achieve a reinterpretation of the boundary conditions that were taken for the calculation of the cases. These boundary conditions require the specification of the variables that take place in the fluid dynamics: the vectorial influence of the velocity, the pressure, the tension and the transversal friction, as well as the dimensional reduction of the turbulent components of intensity as the turbulent energy and its disposition.

An adjustment of the variables should be done due to the elimination of one of the dimensions of the model. Thus, the physical variables such as the volume and volume required to calculate the minimum renewal time in the 3D model become dependent variables of the third dimension omitted. In order to achieve the transposition of the 2D models to the 3D models, the product of the 2D geometric variables (height of the domain and vertical section of the light shaft) will be conducted. Therefore, it is possible to achieve the evaluation of the minimum renovation time in the domains with its air flow admission variables and the light shaft volume.

$$Q_{3D} = \bar{u} \cdot h \cdot w \ldots \rightarrow Q_{2D} = u \cdot h \cdot (1m) \quad (1)$$

$$V_{pt_{3D}} = H \cdot L \cdot W \ldots \rightarrow V_{pt_{2D}} = H \cdot L \cdot (1m) \quad (2)$$

Where: Vpt_{3D} is the air contained in the light shaft; H the light shaft height; L the light shaft length (in the longitudinal axe, “x”); W the light shaft width (in the transversal axe, “y”); Vpt_{2D} the unitary air volume contained in the light shaft; Q_{3D} the admission air flow to the domain; 4+ the average velocity of the wind profiler; h the height of the domain; w the width of the domain; and Q_{2D} the unitary air flow in the admission of the domain.
Thus, it can be obtained that the air flow in the computational domain admission, or control domain, is the result of multiplying the average velocity of the wind profiler in the domain per

its height. The volume of the air in the light shaft is the result of the product of it two-dimensions obtained from the built surfaces, which have been sectioned by the plane of the 2D analysis (Figure 3).

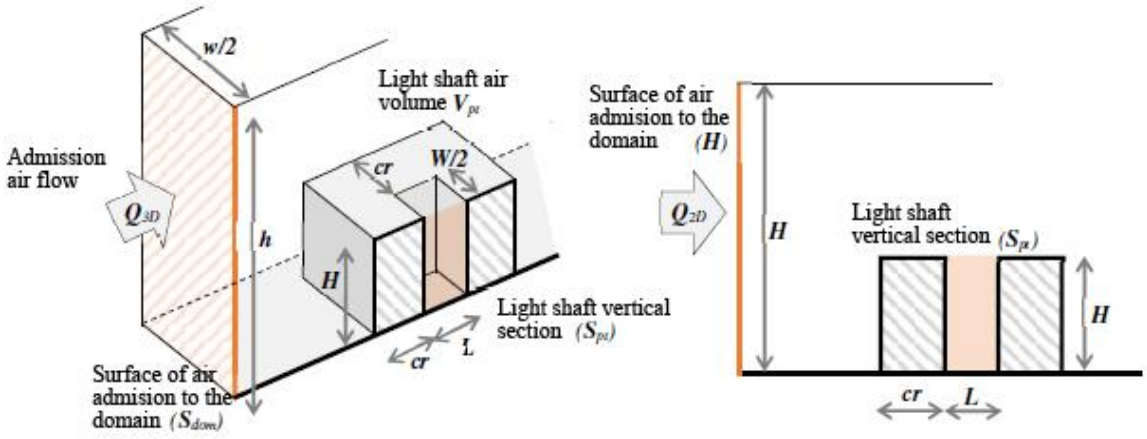

Figure 3: Computational domain discretization

This explanation demonstrates that the simplification to the 2D simulation models is adequate since these they are accurate enough to analyse the efficiency of the air renovation of the light shafts. The correspondence of the efficiency values of both cases is demonstrated in the 3D light shaft model, used as a reference case: 6x4x42 meters long, wide and high respectively (Table 1 and 2).

Table 1: Results obtained from the 2D simulation of the base case, dimensions 6 m x 42 m.

	Unitary volume	**Unitary air flow**	**Average age of the volume**	**Control efficiency**
patio 6x42	252 m³	0.04857 m³/s	152658.810 s	1.636 %

Table 2: Results obtained from the 2D simulation of the base case, dimensions 6 m x 42 m.

6x42 (2D)	**6x2x42**	**6x3x42**	**6x4x42**	**6x5x42**	**6x6x42**
1.70 %	1.06 %	1.40 %	1.72 %	2.00 %	2.24 %

2 RESULTS. IMPROVEMENT OF THE RENOVATION EFFICIENCY AND AGE OF THE AIR OF THE LIGHT SHAFT

After the analysis of the impact of the light shaft in the renovation of its air, considering its design parameters and after the model simplification, the behaviour of this spaces in the case of the disposition of some internal elements, which work hindering and perturbating the air that passes through, was studied.

The modification of the air behaviour around the light shaft can be achieved by the modification of the parameters that determine its movement. Making the convenient modifications it could be possible to change the behaviour of the fluid in order to improve the health and comfort conditions of the ventilation inside the light shaft reaching an upgrade in its air renovation.

To study that, four 2D cases have been proposed. These cases represent the central cut of the same light shaft described below, where the wind velocity is 6m/s in a height of 100 m over

the building. Two of the cases had a triangle-shaped flap with the base on the top and the opposite vertex in the middle of the top border of the light shaft. The dimensions of it are 2 m base, 3 m high, which implies an area of 6 m².

2.1 Case A

It is a light shaft of 6 m wide and 18 m high shaped by a flat roof building of 12 m wide. Case A.1. It is the study of the described light shaft without a flap (Table 3).

Table 3: Renovation efficiency in a light shaft of 6 m x 18 m shaped by a flat roof building of 12m wide

CASE A.1	Unitary volume	Unitary air flow	Average age of the volume	Control efficiency	Relative efficiency
Control domain	1908 m³	60369 m³/s	563.1 s	2.81 %	-
Light shaft	108 m³	0.176 m³/s	783.4 s	2.02 %	39.16 %
Upper third	36 m³	0.176 m³/s	759.3 s	2.08 %	13.47 %
Central third	36 m³	0.176 m³/s	767.1 s	2.06 %	13.33 %
Lower third	36 m³	0.176 m³/s	823.8 s	1.92 %	12.41 %

Case A.2. It is the study of the described but with the disposition of the flap (Table 4).

Table 4: Renovation efficiency in a light shaft of 6 m x 18 m shaped by a flat roof building of 12 m width with a flap

CASE A.2	Unitary volume	Unitary air flow	Average age of the volume	Control efficiency	Relative efficiency
Control domain	1908 m³	61490 m³/s	572.5 s	2.71 %	-
Light shaft	108 m³	1827 m³/s	834.4 s	1.86 %	3.54 %
Upper third	36 m³	1827 m³/s	678.5 s	2.28 %	1.45 %
Central third	36 m³	1827 m³/s	763.9 s	2.03 %	4.29 %
Lower third	36 m³	1827 m³/s	1060.8 s	1.46 %	0.93 %

2.2 Case B

It is a light shaft of 6 m wide and 18 m high shaped by a gable roof with a slope of 45º in both of its sides, which stand above the top of the building that has a width of 12 m.

Case B.1. It is the study of the described light shaft without a flap (Table 5).

Table 5: Renovation efficiency in a light shaft of 6 m x 18 m shaped by a sloped roof building of 12 m wide

CASE B.1	Unitary volume	Unitary air flow	Average age of the volume	Control efficiency	Relative efficiency
Control domain	**1833 m³**	**55928 m³/s**	**1378.1 s**	**1.19 %**	**-**
Light shaft	**108 m³**	**0.09 m³/s**	**3230.6 s**	**0.51 %**	**18.57 %**
Upper third	**36 m³**	**0.08 m³/s**	**2133.3 s**	**0.67 %**	**8.22 %**
Central third	**36 m³**	**0.09 m³/s**	**3331.6 s**	**0.49 %**	**6 %**
Lower third	**36 m³**	**0.09 m³/s**	**3928 s**	**0.42 %**	**5.09 %**

Case B.2. It is the study of the described but with the disposition of the flap (Table 6).

Table 6: Renovation efficiency in a light shaft of 6 m x 18 m shaped by a sloped roof building of 12m wide with a flap.

CASE B.2	Unitary volume	Unitary air flow	Unitary air flow	Control efficiency	Relative efficiency
Control domain	**1833 m³**	**55935 m³/s**	**1685.1 s**	**0.97 %**	**-**
Light shaft	**108 m³**	**0.413 m³/s**	**3175.7 s**	**0.52 %**	**4.12 %**
Upper third	**36 m³**	**0.413 m³/s**	**2391.5 s**	**0.69 %**	**1.82 %**
Central third	**36 m³**	**0.413 m³/s**	**3397.9 s**	**0.48 %**	**1.28 %**
Lower third	**36 m³**	**0.413 m³/s**	**3131.7 s**	**0.44 %**	**1.17 %**

The analysis of these cases will provide the knowledge of how the base case and its different modifications work. In order to achieve it, the data obtained in the control domain has been compared. It implies the study of a total dimension of 27 m upstream from the centre of the light shaft and 51 m downstream from the same point. The vertical dimension was 30. All these measures are modular dimensions of the width of the building (12 m).

The resulting value of the unit flow was analyzed in relation to the height of the vertical projection of the admission surface to the control domain. It is verified that the value obtained from the simulation is closed to the calculated value due to the influence of the wind. The differences in the air flow value between these models are due to the variation in the pressure distribution because of the effect of the build volume. The average age of the air volume allows the determination of its quality. That is, the lower the age of the air, the less its exposition to the pollution by the urban surrounding. The light shaft relative efficiency is evaluated in relation to the control domain previously defined. This allows the evaluation of the impact of the obstruction of the wind to the air flow, which changes the air behaviour inside and outside the light shaft. The relative efficiency analyzes the behaviour in the interior of the light shaft by the exclusive influence of the movement of the outside air near the top of the light shaft. It is here where the obstacle is located in order to modify the kinetic effect of the turbulence and the trajectory of the moving air.

It is necessary the graphic definition of the dynamic and turbulent air models, which determine the results for the analysis of the impact in its behaviour to design architectonical guidelines to improve the process of the air renovation.

The conclusions related to the quality of the air renovation and the light shaft are achieved after having the numerical results. It is observed that the best efficiency is achieved in Case A.1. The global efficiency is close to 3%, due to the low renovation capacity. Case B.2 suffers a decrease of 30% in its domain efficiency in comparison with Case A.1 due to the blockage of the air inside the light shaft. This dam is because the new location of the re-adhesion phenomenon happens further from the top of the light shaft than in Case A.1. The ridge of the sloped roof locates the “takeoff point” higher than in Case A.1, causing a separation, so the air movement dynamic cannot affect inside the light shaft.

Comparing the efficiencies obtained in the results tables (Tables 3, 4, 5 and 6) it is possible to observe that the admission air flow in the light shaft is lower in Case A.1 than in the rest of the studied models. The obstacle element located in the top of the light shaft in Case A.2 tries to change the movement of the air to introduce it into the light shaft and improve its distribution. This can be achieved only by multiplying per 10 the air flow. However, the improvement in the efficiency of the light shaft is not achieved. In fact, the average efficiency descends 50% in comparison with the base case. It is observed that the increase of the velocity does not necessarily imply an improvement in the efficiency.

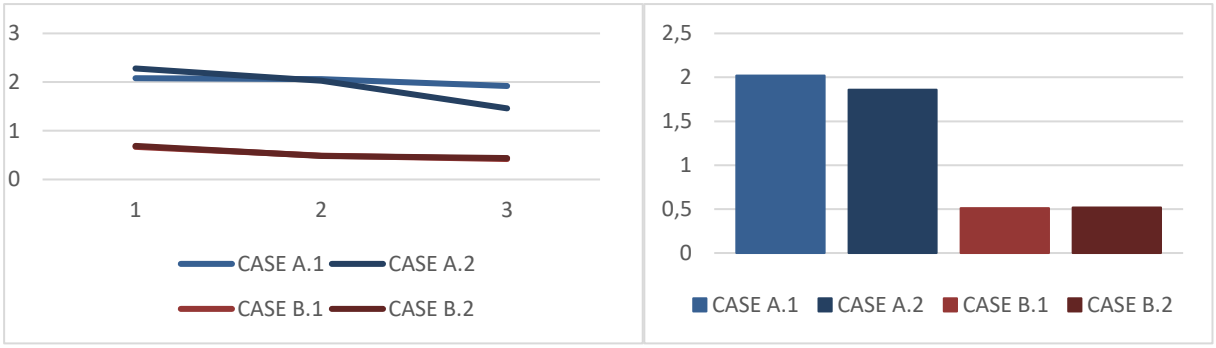

Figure 4: Control efficiency in every light shaft third and control efficiency in the total light shaft.

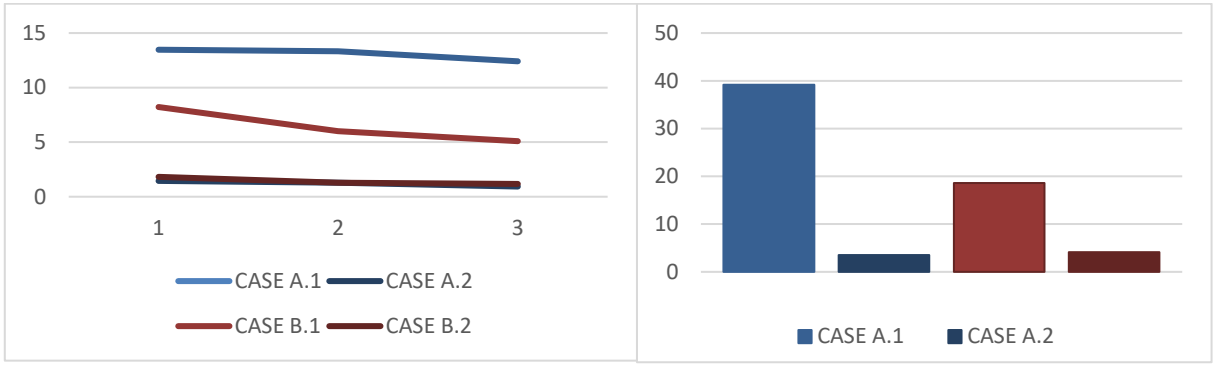

Figure 5: Relative efficiency in every light shaft third and relative efficiency in the total light shaft.

In the graphics (Figure 4 and 5), it is possible to observe that the control efficiency is higher in the flat roof cases. It only implies an improvement in the upper third because at the same time it caused an effect or standstill in the lower third. In the central third, the values are very similar in all cases. In model B, it is possible to observe that the control efficiency values do not change significantly in any of the light shaft thirds or even considering the totality of the light shaft.

By studying the relative efficiency of the light shaft, it is possible to observe that the behaviour of each case is different from the others. The best results are obtained in Case A.1, which are higher than the results obtained in its equivalent case but with the flap. The values obtained in the model B.1 are also higher than the values obtained in B.2. In the two flap cases, very similar results are obtained, not only in each third of the light shaft but also in the totality of the light shaft.

The analysis of the distribution of the age of the air in the domain (Figure 6) shows a standstill that happens in Case A.2 in the lower third of the light shaft and in the totality of it.

In Figure 8, it is possible to observe a change of direction in the movement of the air in the top of the light shaft. This increases the reflow phenomenon observed in Case B.2. In that model, the air downstream, older than the “clean” air, change the direction and enters the light shaft as admission flow, so even though the renovation flow has been increased, this air has already passed the exchange process. This phenomenon causes a cyclic return of the air, which implies a decrease in efficiency. In conclusion, it is possible to observe that what was thought as a strategy of efficiency improvement of the air renovation has ended as a downturn of its work due to a design based on an unreal aerodynamic logic.

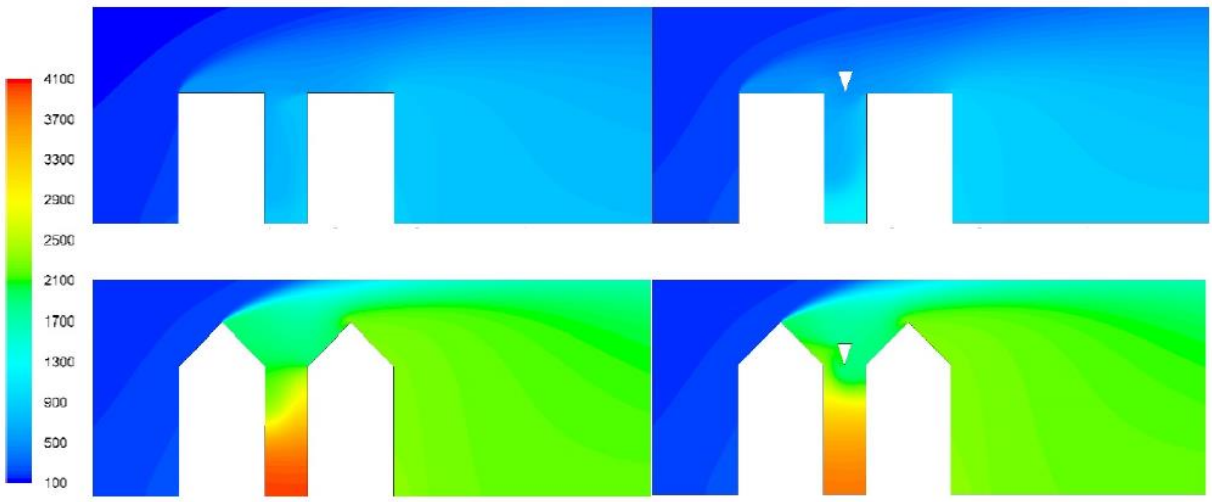

Figure 6: Distribution of the age of the air in the light shaft. Case A.1, Case A.2, Case B.1 and Case B.2

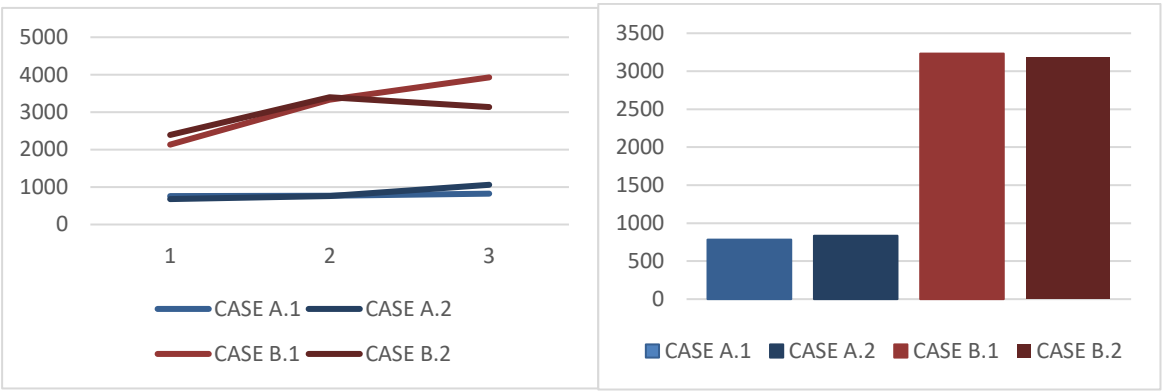

Figure 7: Age of the air average in every light shaft third and age of the air average in the total light shaft

In the graphics (Figure 7), it is possible to observe that the age of the air is lower when there is an obstacle in the middle of the top of the light shaft than when the building has a flat roof, and higher in the case of the sloped roof. In spite of the upgrade, it is not very significant in any case. Studying the different thirds of the light shaft, it can be observed that the central third presents similar values in the different cases without significant variation when there is a flap. In the upper third, the greatest ageing happens in Case A.1, but at the same time, the age of the air in the lower third of this case is 500 seconds older than in Case A.2. Studying the cases of the sloped roof, it is possible to observe that the disposition of the obstacle causes an increase of the age of the air in the upper third. Nevertheless, a significant improvement in the lower third, almost 1000 seconds less in the average age of the air, has been observed.

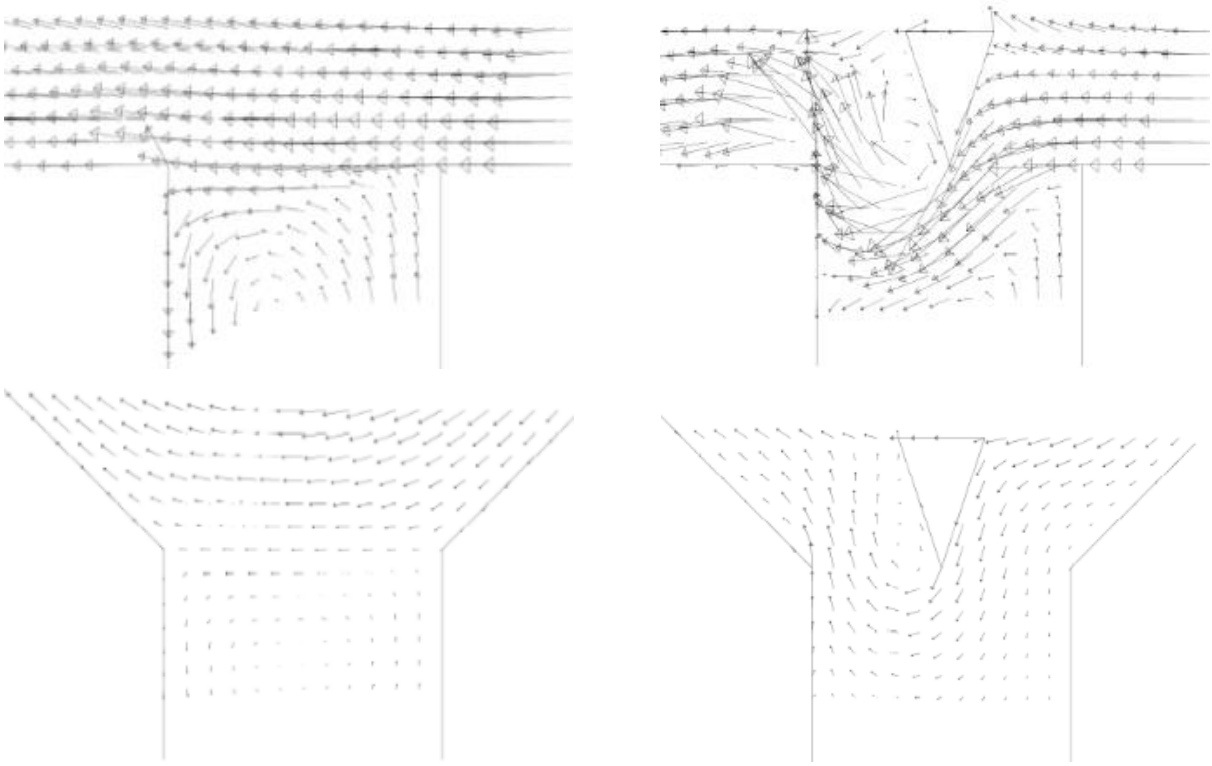

Figure 8: Vectors of movement of the air in the top of the light shaft. Case A.1, Case A.2, Case B.1 and Case B.2

3 CONCLUSIONS

The efficiency of light shaft air renovation determines the quality in which the air provided to the buildings has health conditions. The concept of the age of the air is used to evaluate the average time that a group of air particles stay inside a computational model.

It has been demonstrated that the 2D simplification of the models proposed for the CFD simulations makes the analysis easier, which implies reducing the computational times and cost. This model obtains a precision of ±1.4% in comparison with the equivalent 3D models previously studied.

The study of the renovation efficiency in the four Cases (A.1, A.2, B.1, B.2) shows that it is higher when the light shaft is directly open to the exterior than when there is an obstacle located in the middle of it, trying to change the movement patron of the air masses. As a result, it is possible to observe that Cases A.1 and B.1 have values between 39.21% and 18.6% of efficiency. Meanwhile, Cases A.2 and B.2 only get an efficiency between 4.1% and 3.5%.

4 ACKNOWLEDGEMENTS

Padilla-Marcos Miguel Ángel designed the experiments, drove the tests and wrote the methodology text; Meiss Alberto evaluated the results and obtained the accuracy of the method; Gil-Valverde Raquel wrote the introduction section, translated all the manuscript and treated the tables and figures; Poza-Casado Irene made the statistical analysis and Feijó-Muñoz Jesús corrected all the document.

5 REFERENCES

AI-Azzawi S, 1994. A Comprehensive Checklist for Identifying, Analysing and Appraising their Passive Solar Design Characteristics. Renewable Energy, 5(2):1099–1123. https://doi.org/10.1016/0960-1481(94)90137-6

Buccolieri R, Sandberg M, Di Sabatino S, 2010. City breathability and its link to pollutant concentration distribution within urban-like geometries. Atmospheric Environment, 44(15):1894–1903. https://doi.org/10.1016/j.atmosenv.2010.02.022

Chavez M, Hajra B, Stathopoulos T, et al., 2011. Near-field pollutant dispersion in the built environment by CFD and wind tunnel simulations. Journal of Wind Engineering and Industrial Aerodynamics, 99(4):330–339. https://doi.org/10.1016/j.jweia.2011.01.003

Chen Q, 2009. Ventilation performance prediction for buildings: A method overview and recent applications. Building and Environment, 44(4):848–858. https://doi.org/10.1016/j.buildenv.2008.05.025

Feijó J, Meiss A, 2011. El espacio exterior del CTE-DB-HS3: metodología para el estudio de soluciones alternativas. Ciudad Y Territorio, XLIII(167):71–80.

Germano M, Ghiaus C, Roulet CA, et al., 2005. Natural ventilation potential of urban buildings. International Journal of Ventilation, 4(1):49–56. https://doi.org/10.1080/14733315.2005.11683698

Hall DJ, Walker S, Spanton AM, 1999. Dispersion from light shafts and other enclosed spaces. Atmospheric Environment, 33(8):1187–1203. https://doi.org/10.1016/S1352-2310(98)00284-2

Holford J, Hunt G, 2000. When does an atrium enhance natural ventilation? In Proceedings of 20th AIVC Conference: Innovations in Ventilation Technology:26–29.

Ng E, 2008. An investigation into parameters affecting an optimum ventilation design of high density cities. International Journal of Ventilation, 6(4):349–357. https://doi.org/10.1080/14733315.2008.11683790

Ok V, Yasa E, Özgunler M, 2008. An Experimental Study of the Effects of Surface Openings on Air Flow Caused by Wind in Light shaft Buildings. Architectural Science Review, 51(3): 263–268. https://doi.org/10.3763/asre.2008.5131

Padilla-Marcos MA, Feijó-Muñoz J, Meiss A, 2016a. Confined-air quality based on the geometric efficiency of urban outdoor spaces. Cases study. International Journal of Ventilation, 15(1):15–30. https://doi.org/10.1080/14733315.2016.1173290

Sandberg M, 1981. What is ventilation efficiency? Building and Environment, 16(2):123–135. https://doi.org/10.1016/0360-1323(81)90028-7

Probabilistic modelling of wind induced air exchange in buildings

Krystyna Pietrzyk

Chalmers University of Technology
Sven Hultins gata 6
41296, Sweden
**Corresponding author:*
krystyna.pietrzyk@chalmers.se

ABSTRACT

The work presented is the continuation of the research on the probabilistic modelling of air infiltration carried out by the author over many years. The approach has consisted in considering uncertainties coupled to the climatic/environmental input data to the physical models, or to the threshold criteria for a good performance. The concept of risk/reliability evaluation of building/environment system performance was proposed and exemplified for the air exchange model.

Air exchange in buildings is driven by pressure difference across the building envelope caused by wind and difference in density between external and internal air. The evaluation of the influence of wind on the air change rate is usually limited to the analysis of the hourly mean wind speed. Wind is a random phenomenon characterized by the broad energy spectrum. The high frequency part can be responsible for the oscillation of the air through the openings resulting in the increased air exchange. Wind pressure coefficient on the leeward site mostly depends on the form characteristics of the object in relation to wind direction. The analysis of wind speed and wind pressure on the facades in frequency domain can deliver interesting data to air change rate model.

Some of the results of continuous measurements carried out on a single-family house for 8 months are presented in frequency domain. The statistics of wind speed, wind direction and pressure differences across the 6 building components are calculated. The influence of wind turbulence on pressure fluctuations on the facades and the roof of the building are investigated. The samples of the energy spectra of pressure differences are examined. Farther analysis of the experimental results is needed to be able to propose the more detailed model.

KEYWORDS

Probabilistic modelling, air exchange, infiltration, wind, turbulence, power spectrum

1 INTRODUCTION

This paper is built upon the results of the work carried out by the author over many years and constitutes a personal perspective/experience on the issue of probabilistic modelling of air exchange in buildings. The concept of evaluating the risk of poor air exchange was presented in (Pietrzyk 1991). The probabilistic model PROMO was developed over several years. The model was launched in (Pietrzyk 2000, Pietrzyk & Hagentoft 2008a) and it was designated to estimate the probability of insufficient air exchange or excessive heat loss. The model allowed estimation of the effect of variations of climate conditions on air exchange in a building, but also on the building energy performance (Pietrzyk & Hagentoft 2004, Pietrzyk 2010). Probabilistic output in the form of probability density function of air change rate estimated with the help of FORM (first-order reliability method) using the program developed by (Czmoch 1998) formed a ground for reliability analysis of adequate ventilation. The model

was applied to analyse the hourly air exchange caused by air infiltration in a building situated near Gothenburg. Contributions of both wind and temperature difference were evaluated. Model was validated based on the results of pressure difference measurements through the building envelope. This work has been extended in (Pietrzyk 2005) by including the combined effect of infiltration and mechanical ventilation, both exhaust and balanced. In (Pietrzyk & Hagentoft 2008b) the concept of risk/reliability evaluation of building/environment system performance was proposed as a part of the broader approach concerning reliability analysis in building physics design. Requirement for the system specified in the form of performance criterion had usually been treated as a deterministic value. In (Pietrzyk 2009), a stochastic threshold criterion for air change rate was introduced and discussed. Sensitivity analysis of the influence of wind and outdoor temperature on the air infiltration tested the model outcome in terms of its robustness in the presence of uncertainty in and was first presented on the IEA Annex55 meetings (Pietrzyk 2011) and then published at the conferences 2012/2013. The probabilistic risk analysis along with the effective tools for sensitivity analysis is proposed to be used to support design decisions and to develop better models for evaluation of building performance (Pietrzyk & Czmoch 2018). The work presented in actual paper concentrates on the possibility to consider the higher frequency of wind conditions in the air exchange model based on wind pressure measurements.

Wind is a stochastic phenomenon that is influenced by the surface roughness of the ground. The impact of wind on air exchange in buildings depends on permeability and the geometry of a building envelope and is usually discussed in r elation to hourly wind speed. However, broader wind energy spectrum describing the turbulent part of wind speed could be analysed and considered in the model of air change rate. Air exchange models applied in practice do not include the unsteady flow effects. One of the reasons is the unavailability of data (Etheridge 2000). A very extraordinary measurement program was carried out on the detached house near to Gothenburg where the fluctuating characteristics of turbulence were measured (20Hz) and expressed by reduced power spectrums of wind speed and wind and temperature governed pressure differences across building components. Unsteadiness arising from external wind gustiness and that generated by surface wind pressures will be investigated to be included in the model of wind induced infiltration based on the one proposed in (Pietrzyk 2000). The original model refers to low-rise building with light-weight construction, single ventilation and temperature zone, and steady-state conditions of air flow (Pietrzyk 2000). The simple quadrature LBL infiltration model was applied. Air change rate, wind speed and direction, temperature, pressures and leakage characteristics were all treated as the random variables. The ACH probabilistic distribution was estimated, and the risk of inadequate ventilation was evaluated. It is planned to introduce the rapidly varying fluctuations of wind speed to the model.

2 MODELLING OF AIR INFILTRATION

Turbulent flow appears due to frequent changes of wind speed and directions in interaction with the geometry of the building. According to (Handa et al 1979), the pressure fluctuations give rise to both laminar and turbulent flow through leakages. High-frequency fluctuations create a turbulent distribution of air through the opening comprising eddies with dimensions comparable to, or less than, the size of leaks. Certainly not all pressure fluctuations are fully transmitted through the envelope taking part in the air exchange.

The concept of the wind induced air change rate ACH (1/h) has been expressed by the following equation describing air change rate caused by wind blowing from direction sector d

(d=1to 8) at the time t calculated for different components exposed to either a positive pressure difference (inward flow) or to negative pressure difference (outward flow):

$$ACH_d(t) = 3600/V \sum_{j=1}^{n} \left(K_{d,j}(v_q)\right) A_j \left[0.5\rho\left(Cp_{d,j}^{ext} - Cp_{d,j}^{int}\right) {v_d}^2(t) + 0.04 z_j \Delta T(t)\right]^{0.5}$$

where: $K_{d,j}$ - a leakage function presented as a linear function of v_q relating the flow rate through the openings to the area of building component j and the corresponding pressure drop across openings for wind blowing from sector d ($\sqrt{\mathrm{m}^3/\mathrm{kg}}$); v_q – "frictionless flow velocity" through the openings (m/s); n – number of elements of the envelope of a building facing only positive or only negative pressure difference; V – volume (m^3); A_j – area of j-th element (m^2); ρ - air density (kg/m^3); $Cp_{d,j}^{ext}$ - external pressure coefficient assumed for the façade j exposed to wind from the direction d (-); $Cp_{d,j}^{int}$ - internal pressure coefficient assumed for the façade j exposed to wind from the direction d (-); v_d (t) – wind blowing from direction d (m/s); z_j – vertical distance from the neutral pressure layer to the centre of the j-th building element (m); ΔT(t) – 10-min mean temperature difference between outside and inside (K) treated later on as slowly changing one-hour mean.

Wind velocity from a certain direction d as well as the pressure differentials across the envelope of 6 building components are treated as the random variables represented by slowly and rapidly varying fluctuations given in the frequency domain by reduced power spectra. The spectrum of a wind speed contains essential information about the nature of wind, the type of upwind landscape and the geometry of the building structure. It is proposed to treat wind speed as consisting of the slow and rapid fluctuations. The wind speed would then consist of the annual mean wind velocity, the 10-minute mean similar to the hourly mean wind speed (slow fluctuations), and the rapidly fluctuating component referring to the influence of the large-scale turbulence of wind caused by the atmospheric wind flowing over hills and rough terrain, etc., and to the turbulence locally generated by the building structure.

Frequency domain analysis is used to characterise the energy distribution among the frequency intervals. The power spectrum is generated by using a discrete Fourier transform**.** The reduced power spectrum of wind speed is given by the following equation:

$$fS_v(f)/\sigma_v^2$$

where: σ_v - standard deviation for the wind speed fluctuations; f-frequency;
$S_v(f)$ – power spectrum of the wind speed for the frequency f.

Pressure fluctuations caused by wind turbulence have an influence on the air flow through the small openings and cracks in the building envelope. The character of the flow depends on the geometric characteristics of the leakages in relation to the length scale of wind and the Reynolds number of the air flow. Generally, the building generated vortices induced in the separated flow regions are characterised by higher frequency and smaller length scale. As it is written in (Ginger et al. 1997), the fluctuations of the external pressure above certain frequency given in as 0.53 Hz for a nominally sealed engineered building are attenuated and do not influence the air exchange.

3 CASE STUDY

3.1 Description of the object

The house was constructed in 1979 with the intention of using it for experimental studies in building physics with focus on ventilation and energy saving. The garage with doors facing south is in the extended south part of the concrete cellar as shown in Figure 1.

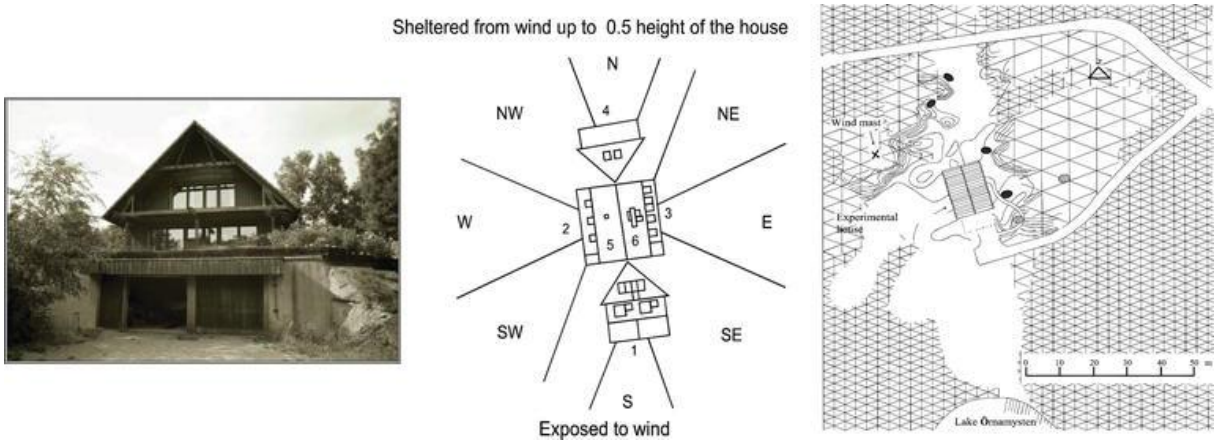

Fig. 1 Situation of the building against wind directions and the elements of topography and vegetation

According to the map of the nearest surroundings given in Figure 1, the house is located about 11 degrees from the north-south direction. There is a small lake about 100 m from the building to the south. To the east and north-west of the house there are two small hills. The house is surrounded by trees of different height. To the south-west very tall pine trees give shelter to the building.

3.2 Measurements

The following parameters have been measured: (1) leakage characteristics of the house using blower door tests, (2) pressure differences across the six building components with Validyne pressure transducers, (3) wind speed and wind direction with the anemometer located on a small hill about 25m from the house, (4) internal and external temperatures, (5) internal and external relative humidity, (6) 30 measurements of ACH at various locations in the building using tracer gas. The measurement program had been carried out for 8 months. As a result, every hour, 10-min mean data and reduced power spectra and cross spectra of 3-second wind speed and pressure differences across the building components were registered (Schechinger 1991).

For the measurement of pressure distribution across the walls and roof, 25 m long plastic tubes were connected between the measuring points and the Validyne pressure transducer. As mentioned earlier, twelve measuring points uniformly distributed over a surface (see Fig. 2) were connected to a single pressure transducer through a connector as in (Schechinger 1993). The plastic tubes entered the house at the same level and were placed behind the external cladding in a temperature close to the external one. The pressure transducers were placed in the measurement room located in the basement.

The setup of the measurements was critically analysed. In (Schechinger 1993) one reads “The dynamic influence of the pressure tubes and the 12-to-1 tube connector has been studied.

Gustén & Magnusson (1986) investigated the influence of the length of the plastic tubes on the response characteristics of the system. They tested tubes with 25m length, 50m length and 115m length. They concluded, that with increasing length of the tubes the spectrum was increasingly distorted, with the distortion starting at ever lower frequencies. However, for the case of the 25m tubes, the distortion was within +/- 20% up to some 3 Hz. The influence of the 12-to-1 tube connector has been studied in Pietrzyk (1993). Comparison of the mean of 6 signals measured independently for each of the 6 tubes with the mean of 6 signals obtained by measuring a single channel with the 12-to-1 connector revealed differences starting already below 0.1 Hz and increasing over the range up to 1-2 Hz. The difference was, though, in the range of 10%."

The wind and the pressure difference across the facades were analysed by employing spectral methods to extract the statistical parameters and to investigate the influence of wind pressure fluctuations on the air exchange. However, only10-min mean data were used to built up and validate the probabilistic model of air infiltration and heat loss in low-rise buildings (Pietrzyk 2000). The limited number of spectra sampled with 20Hz frequency has been now converted to the ascii format for the preliminary analysis.

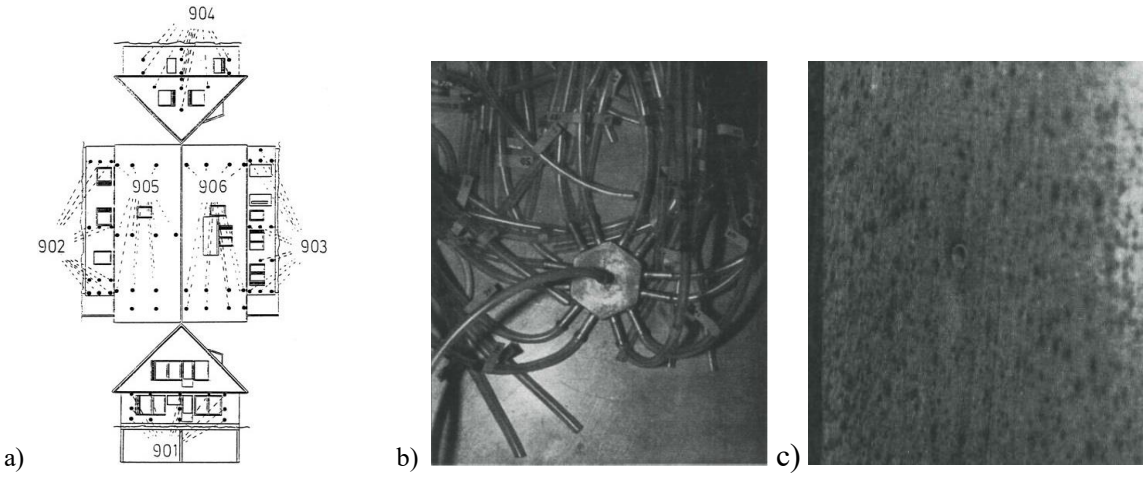

Fig. 2 a) Distribution of the wind pressure measurement's points on the building envelope; b) 12-1 tube connector; c) pressure measurement point on building facade.

3.3 Results

The 10-min and the 3-s means, and standard deviations of wind speed and wind pressure differentials on windward facades are listed in Table 1.

Table 1. Mean value μ, standard deviation σ, coefficient of variation σ/μ, of v - wind speed, Δp_{3s} –3s pressure difference between the outside and the inside of the building

Wind dir.	μ_v 10-min	σ_v 10-min	$\frac{\sigma_v}{\mu_v}$	μ_{v3s}	σ_{v3s}	$\mu_{\Delta p3s}$ windward	$\sigma_{\Delta p3s}$ windward	$\frac{\sigma_{\Delta p3s}}{\mu_{\Delta p3s}}$
N	2.27	0.97	0.43	0.91	0.47	1.45	1.24	0.86
E	2.89	1.09	0.38	0.96	0.45			
S	2.23	1.01	0.45	0.90	0.41	1.09	1.06	0.97
W	2.19	1.13	0.52	1.00	0.59			

Coefficient of variation σ/μ of 10-min as well as of 3-s mean wind speeds are of the same size. Coefficients of variations of the rapid fluctuations of the pressure differentials across the

windward facades are higher than those of wind speed. This can be important in the process of the air exchange.

The reduced power spectra of wind speed and the ones of pressure differences will be examined to support modelling of the impact of wind fluctuation on the air change rate. Some examples are presented below. The cases with higher wind speed have been chosen to marginalise influence of convective turbulence. Figure 3 shows the 10-min spectra of the 6 components' pressure differences together with the wind speed spectrum (μ_v=4.76m/s). The spectra obtained for the windward component (902 in Figure 2a) and the upwind speed (W) look similar.

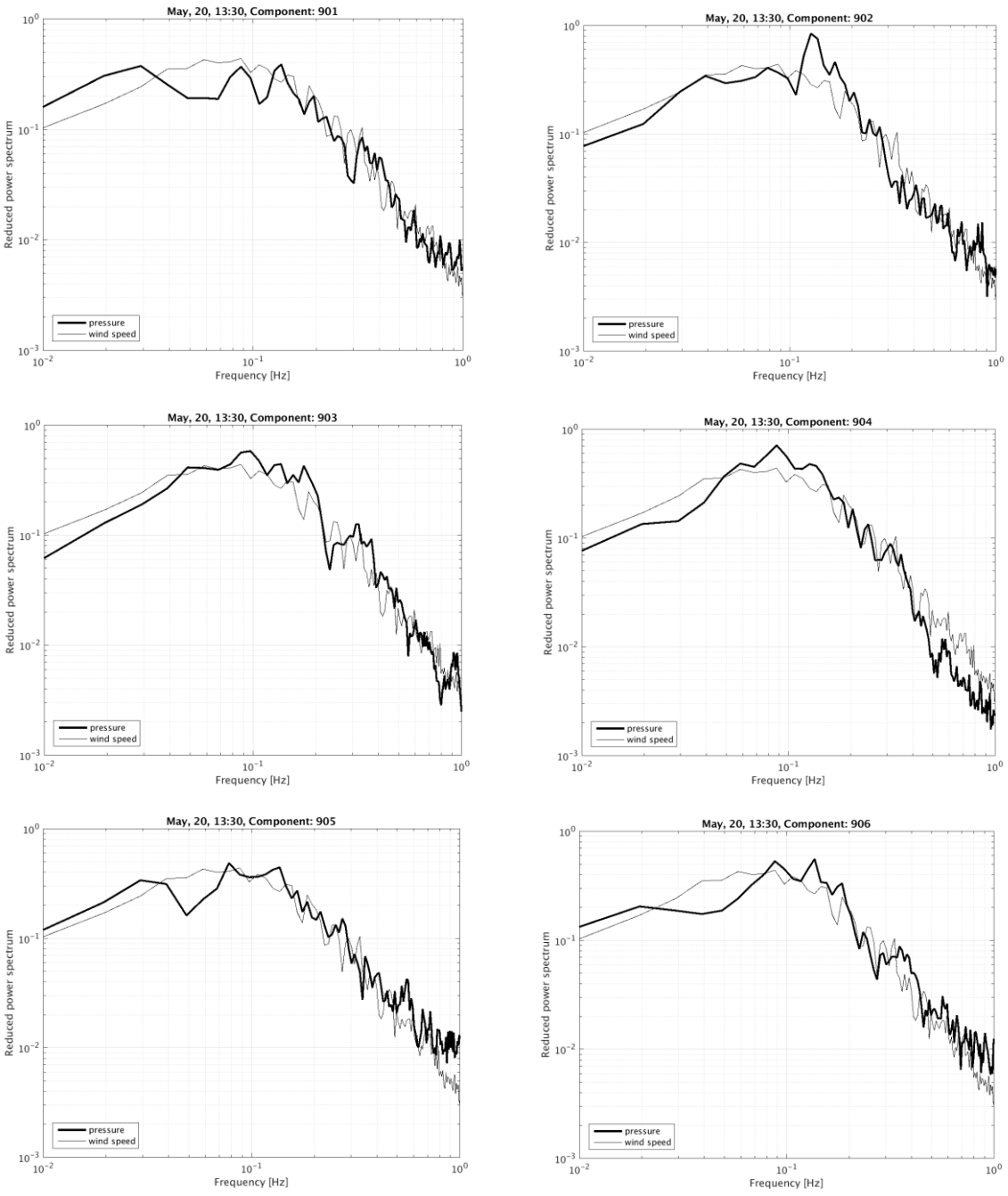

Fig. 3 The reduced power spectra of the pressure differences across the 6 components – bold line, (see Fig.2a): 901(façade S), 902 (façade W), 903 (façade E), 904(façade N), 905 (roof W), 906 (roof E) together with the wind speed reduced power spectrum

The set of reduced power spectra of pressure differentials calculated for the 6 building components for the one 10-min period for wind blowing from the South (μ_v=6.77 m/s) is shown in Figure 4. The big opening under the garage door is situated from the south site of the building (see Figure 1). It seems that it influences the pattern of the pressure differential spectrum across the windward façade.

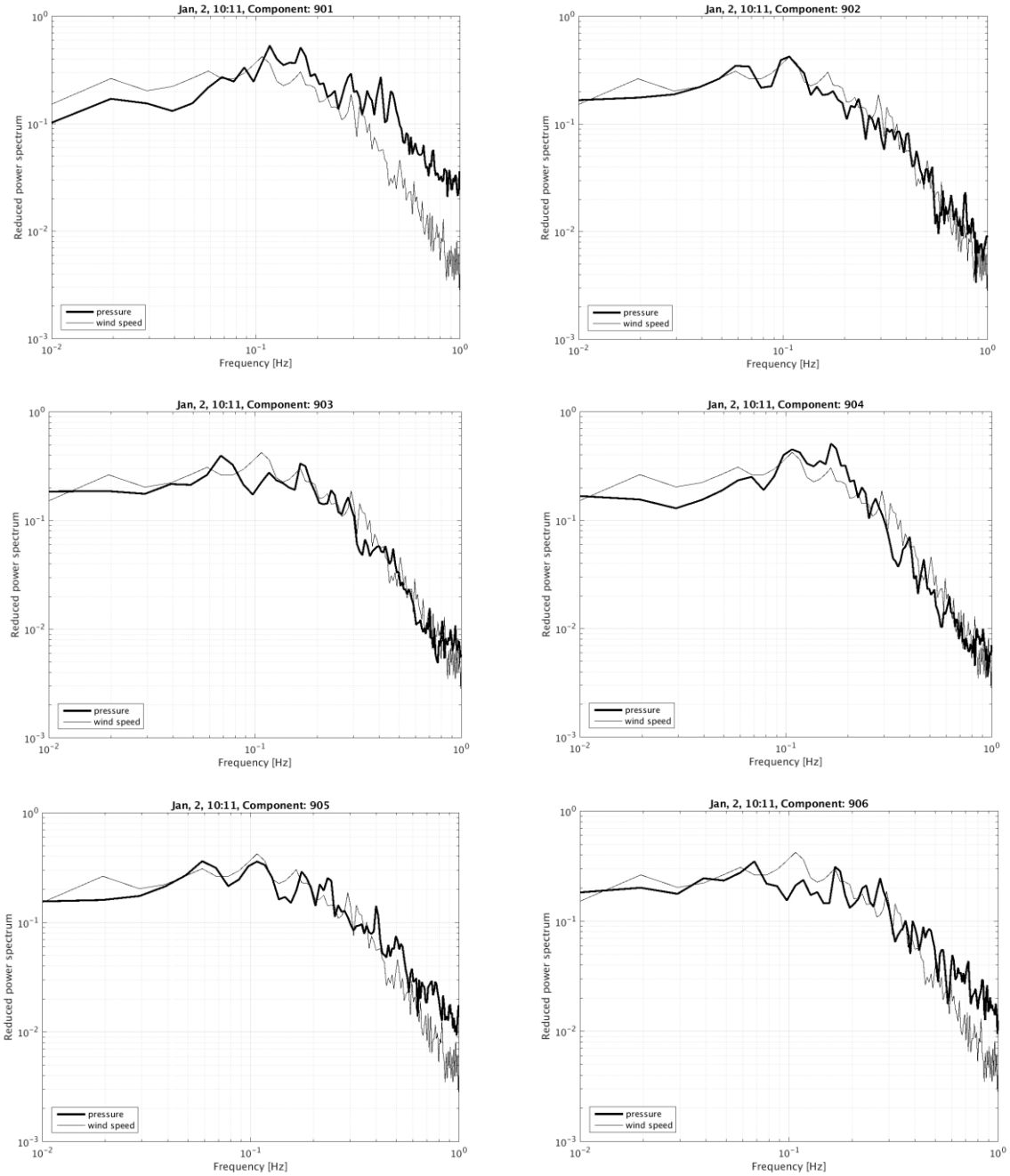

Fig. 4 The reduced power spectra of the pressure differences across the 6 components – bold line, (see Fig.2a): 901(façade S), 902 (façade W), 903 (façade E), 904(façade N), 905 (roof W), 906 (roof E)

The examples show the differences between the shapes of the individual pressure spectra. They depend mainly on the positions of the components against the wind direction and the types of openings/leakages at the building envelope. The spectra of pressure differences across the roof components show more power in the interval of higher frequencies. Generally, the greater part of the spectrum for both examples can contribute to air infiltration.

4 CONCLUSIONS

- A short overview of the personal contribution of the author to the field of the probabilistic modelling of air exchange in buildings is given. The general concept of the extension of the probabilistic model of air exchange in buildings to include rapid pressure fluctuations on the air change rate based on the spectral data is proposed.
- The analysed spectra of the windward wall pressure differences together with the relevant upwind speed spectra show similar forms. The greater part of the spectrum could contribute to the air exchange. High coefficients of variations of the rapid fluctuations of the pressure differentials across the windward facades might be important in the process of the air exchange. The results of wind and pressure differential fluctuations for the whole measurement period should be converted to the ascii format for further analyses.
- The examples show the differences between the shapes of the individual pressure spectra. They depend mainly on the positions of the components against the wind direction and the types of openings/leakages at the building envelope. The mean values of reduced power spectra for the specified wind speed and direction across each component will be further studied.
- Degree of coherence between fluctuating wind speeds and fluctuating pressure differences between outside and inside of the building will be further examined.

5 ACKNOWLEDGEMENTS

The author is grateful to Kamal Handa who formulated and initiated the project. The financial support provided by Swedish Council for Building Research for the measurement program is gratefully acknowledged. Special thanks to Bernt Schechinger for elaboration of the measurement program and tools as well as for time spent to communicate the results. The cooperation of the owner of the house, Tomas Lindqvist, is also acknowledged. The financial support provided by the Adlerbertska Foundation is gratefully acknowledged.

6 REFERENCES

Czmoch I. (1998). *Influence of Structural Timber Variability on Reliability and Damage Tolerance of Timber Beams*. PhD thesis, Sweden: Division of Structural Mechanics of Luleå University of Technology.

Etheridge D. (2000). Unsteady flow effects due to fluctuating wind pressures in natural ventilation design–instantaneous flow rates. *Building and Environment*, vol. 35, pp. 321-337.

Ginger J.D., Mehta K.C., Yeatts B.B. (1997). Internal pressures in a low-rise full-scale building. *Journal of Wind Engineering and Industrial Aerodynamics* 72, pp. 163-174.

Gustén J. & Magnusson B. (1986). *Frequency response functions for differential pressure measurement tubing*, Chalmers University of Technology, Division of Structural Design, Report 1986:5, Gothenburg, Sweden.

Gustén J. (1989). *Wind pressures on low-rise buildings*. Ph.D. thesis, Chalmers University of Technology, Sweden.

Haghighat F., Rao J., Fazio P. (1991). Influence of turbulent wind on air change rates. *Building and Environment*, vol. 26, no. 2, pp. 95-109.

Haghighat F., Brohus H., Rao J. (2000). Modelling air infiltration due to wind fluctuations – a review. *Building and Environment*, vol. 35, pp. 377-385.

Handa K., Kärrholm G., Lindquist T. (1979). Mikroklimat och luftväxling. Swedish Council for Building Research, BFR, Report T3:1979, Stockholm.
Pietrzyk A. (1993). *Building Aerodynamic research at the Swedish Antarctic station Wasa*, Chalmers University of Technology, Division of Structural Design, Report 1993:4, Gothenburg, Sweden.
Pietrzyk K. Risk analysis of air infiltration in the building (1991). Proceedings of the *Scandinavian Forum for Stochastic Mechanics*, University of Aalborg, Denmark.
Pietrzyk K. (2000). *Probabilistic modelling of air infiltration and heat loss in low-rise buildings*. Ph.D. thesis Chalmers University of Technology, Sweden.
Pietrzyk K., Hagentoft C.-E. (2004). Probabilistic modelling of dynamic U-value. *Thermal Performance of the Exterior Envelopes of Buildings IX, American Society of Heating, Refrigerating and Air-Conditioning Engineers, Inc. (ASHRAE)*, Florida, USA.
Pietrzyk K. (2005). Probability-based design in ventilation. *The International Journal of Ventilation*. Vol. 4 Number 2, pp 143-156.
Pietrzyk K.& Hagentoft C.-E. (2008a). Probabilistic analysis of air infiltration in low-rise buildings. *Building and Environment*. Vol. 43/4, pp 537-549.
Pietrzyk K.& Hagentoft C.-E. (2008b). Reliability analysis in building physics design. *Building and Environment*. Vol. 43/4, pp 558-568.
Pietrzyk K. (2008) Stochastic versus deterministic approach to threshold criteria for Building/Environment system performance. The 8th *Nordic Symposium on Building Physics*, Copenhagen, Denmark, vol. 1 pp. 401-409.
Pietrzyk K. (2010). Thermal performance of a building envelope – a probabilistic approach. *Journal of Building Physics*. Vol. 34, no.1, pp 77-96.
Pietrzyk K.& Czmoch I. (2018). On Risk and Reliability Studies of Climate-Related Building Performance, *Risk Assessment*, Valentina Svalova, IntechOpen, DOI: 10.5772/intechopen.71684.
Schechinger B. (1991). Datorprogram för insamling och spektralanalys av klimatdata. (in Swedish) Chalmers University of Technology, Building Aerodynamics Research Group, Report 1993:BA11.
Schechinger B. (1993). Risk analysis of air infiltration in building structures. Description of experimental house, and instrumentation. Chalmers University of Technology, Building Aerodynamics Research Group, Report 1993:BA11.

Impact of an occupancy and activity based window use model on the prediction of the residential energy use and thermal comfort

Silke Verbruggen[*1], Marc Delghust[1], Jelle Laverge[1], and Arnold Janssens[1]

1 Ghent University
Research Group Building Physics
Sint-Pietersnieuwstraat 41 – B4
9000 Ghent, Belgium
**Corresponding author: silke.verbruggen@Ugent.be*

ABSTRACT

The opening of windows can lead to high energy losses in wintertime, especially in nearly zero-energy buildings. But can reduce overheating significantly in summertime. Therefore, window use models have been created in the past to assess the energy use and thermal comfort in residential buildings. The models are mostly based on weather-variables. However, a recent study (Verbruggen, Janssens, et al. 2018) indicated that these models were not able to accurately predict the window use in wintertime. For that reason, an occupancy and activity based model was developed. In this article, the impact of the application of the new window opening model on the residential energy use and thermal comfort was assessed. The object-oriented modelling language Modelica was used to simulate the energy use and temperatures in a nearly-zero energy house, which is a representation of an existing house in a nearly zero-energy neighbourhood in Kortrijk. From this neighbourhood, measured energy use data was available as well as window sensor data for some of the houses. These measured data were compared to the simulated data of the new window use model, a weather-based model and the Belgian EPBD-calculation method. The occupancy and activity based model could predict more accurately the average opening durations in wintertime and could better account for the large variation in window use compared to weather-based models. An optimal window opening strategy could limit the overheating significantly, even prevent it in the bedrooms and bathroom. However, opening the windows also implies an increase in energy use for heating. Some combinations of different window opening habits can limit the overheating, while limiting the increase in energy use at the same time.

KEYWORDS

Windows, occupant behaviour, residential energy use, thermal comfort

1 INTRODUCTION

Window opening behaviour is generally predicted by weather-based window opening models. These are models that predict when the windows are open based on different indoor and outdoor environmental variables such as temperature, CO2-concentration and relative humidity. However, the study of Verbruggen et al. (Verbruggen, Janssens, et al. 2018) revealed that weather variables are good predictors when considering an entire year, however, in wintertime the weather variables are rather poor predictors for window use.
In the Belgian EPBD-heat demand calculation method it is assumed that windows will not be opened if a mechanical ventilation system is installed. However, in dwellings with a ventilation system the windows are opened to the same extent as in dwellings without ventilation system (Dubrul 1988). It is important to predict the window opening behaviour correctly since it can largely impact the energy use, especially in winter. Furthermore, opening windows has a large impact on the thermal comfort of the occupants as well. Occupants tend to open windows to cool down their houses in summertime, therefore limiting the risk of overheating. In the Belgian

EPBD-calculation window use is included in the calculation of the overheating indicator by an extra ventilation rate based on the potential for intensive ventilation.
To be able to more accurately predict the window opening behaviour, a new window opening model is created based on the occupancy and activity patterns of the occupants rather than on weather variables. This model predicts a more realistic way of occupants' interactions with windows, since it includes the habits of the occupants, which are related to the occupancy and activity states of the occupants. Consequently, it only allows for window interactions when at least one occupant is present and awake.
In this paper, the occupancy and activity based model will be briefly explained and will be compared with a weather-based model and the EPBD-calculation method in terms of energy use for heating and thermal comfort.

2 METHODOLOGY

To compare the impact of the use of the different window opening models simulations are carried out with the object-oriented modelling language Modelica using the IDEAS-library (Jorissen et al. 2018). The simulated house is based on an existing two-storey, three-bedroom house from a social housing neighbourhood in Kortrijk, Belgium (Himpe, Janssens, and Rebollar 2015; Janssens et al. 2017).
In the simulations only the window opening behaviour is varied, all other types of occupant influences remained the same as in the Belgian EPBD-calculation method. These settings are summarised in Table 1. The set-point temperatures are 18°C in all zones. The ventilation rate, internal heat gains and domestic hot water use are calculated based on the volume of the building. The default internal heat gains for the entire building are distributed over the different zones based on the volume-fraction.

Table 1: Occupant behaviour settings in the model

SETTINGS	
Heating setpoint	18°C
Ventilation rate	183 m³/h (building)
Internal heat gains	1057 kWh/year
Domestic hot water use	1380 kWh/year

The window opening behaviour is simulated based on the heat demand EPBD-calculations first. This means that the windows are always closed. Secondly, a simulation is carried out including the extra ventilation rate for opening windows from the EPBD-calculation for overheating. This ventilation rate is based on the potential for intensive ventilation. In this case a weak potential for extensive ventilation is present, which corresponds to an extra ventilation rate of 48 m³/h. Next, the window opening behaviour is simulated using the stochastic weather-based model created by Maeyens and Janssens (Maeyens and Janssens 2000). This model describes the probability of opening a window every hour based on the outdoor temperature, wind velocity and solar irradiation. A correction factor is applied to compensate for the presence of the occupants. Thirty simulations are carried out to capture the variance implied when using a stochastic model. Finally, thirty simulations are carried out with an occupancy and activity based window use model, which will be explained in the next paragraph.
The simulation results of the energy use for heating and domestic hot water are compared for the different models, as well as the indoor temperatures as a measure for thermal comfort.

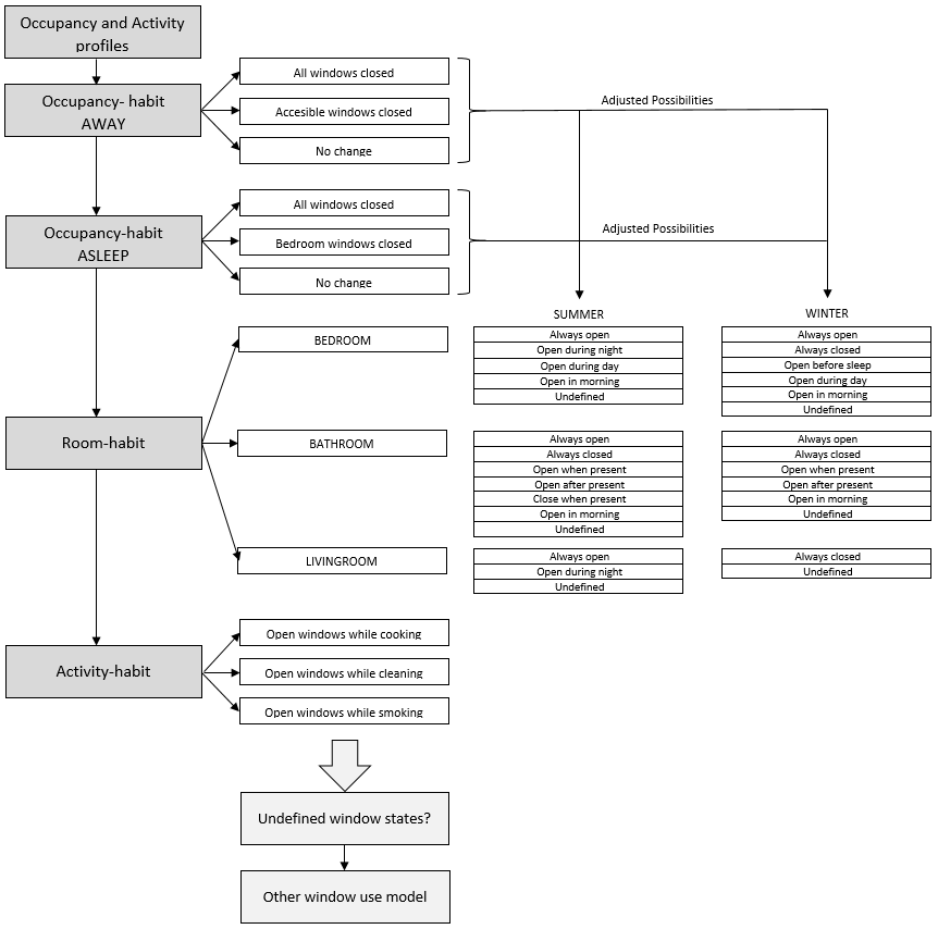

Figure 1: Workflow of occupancy and activity based window opening model

3 OCCUPANCY & ACTIVITY BASED WINDOW USE MODEL

The newly developed window use model is based on occupancy and activity patterns of the inhabitants (Verbruggen et al. 2019). This is a more realistic way of modelling the occupant behaviour compared to weather-based models since it relates more closely to the occupant's time use. Occupants are not always able to change the window state (e.g. away from home or asleep) and will not evaluate the window state every few minutes. Furthermore, it was revealed that a lot of occupants have specific habits regarding the window use (Hauge 2016; Verbruggen, Delghust, et al. 2018). The occupants are less likely to make rational thoughtful decisions in relation to the window use, they rather just open the window out of habit.

The workflow of the model is presented in Figure 1. The model first determines stochastically the occupancy and activity patterns of the members of the household for an entire year. This step is based on the works of Aerts (Aerts 2015) and Baetens et al.(Baetens and Saelens 2016). Next, the model determines which habits are present in the household based on statistics from a survey in Belgium (Verbruggen et al. 2019). Different habits are selected for summer- and wintertime. In a final step, the occupancy and activity patterns are coupled to the selected habits, in this way window use profiles could be generated for an entire year for most of the households. For example, if the household has the habit of closing the windows when going to bed, the window state could be easily linked to the occupancy-state asleep.

In some cases, the household will not have habits that allow for the creation of full window use profiles. In these undetermined periods, the occupants do not have a real habit and may base their behaviour on the weather or some other variables. In this case, it was assumed that the

occupants act based on weather variables in these undetermined period, therefore the window model of Janssens & Maeyens (Maeyens and Janssens 2000) is applied.
The window opening duration in winter time could be accurately predicted with the new window opening model. In Figure 2 the average opening time per day in wintertime is compared for the different models in the different rooms and to measured data from the case-study site.
In the bedroom and bathroom the habit-based model predicts more accurately the average opening duration, while still capturing the variation between households very well. This variation is in correspondence to the measured data of houses of the same type on the case-study site. In the living room on the other hand, the weather-based model is able to better predict the window opening behaviour. This can be linked to the fact that in the living room the least window opening habits are present. In general the window opening model based on habits is able to accurately predict the window opening durations in wintertime.
When the opening durations in summertime are analysed, the model still captures the variability of opening behaviour very good in contrast to the weather based model. However, the average opening durations are less precise compared to wintertime, but still a good approximation.
It can be concluded that the window opening model based on occupancy and activity patterns is able to better capture the variability in window opening behaviour compared to a weather-based model and to the EPBD heat demand calculations. The opening durations are as well better estimated.

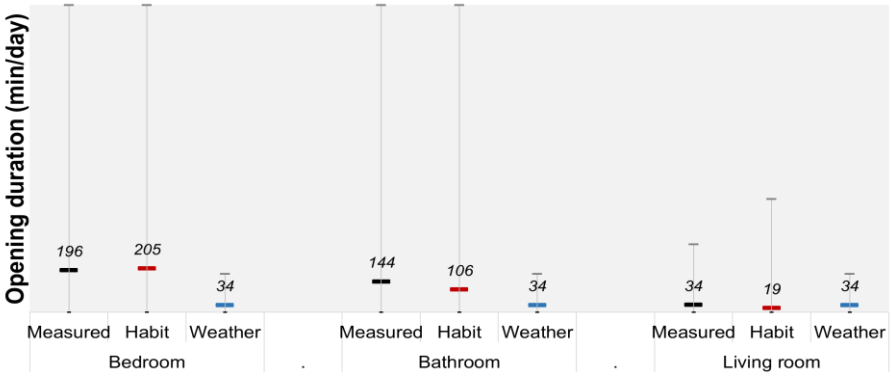

Figure 2: Window opening durations in wintertime: measured data in comparison to simulated data.

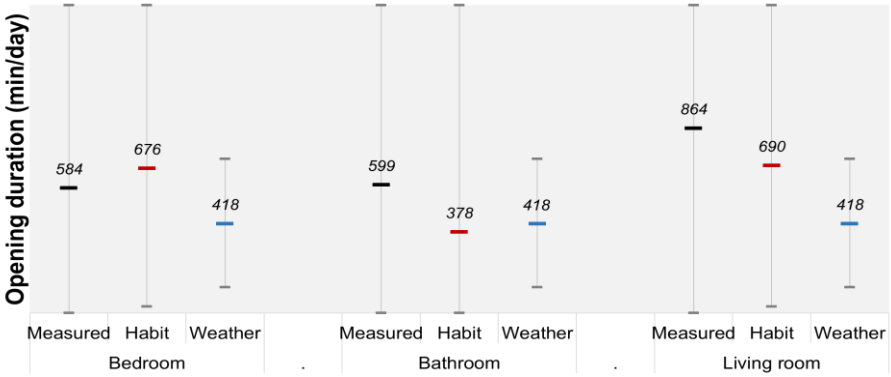

Figure 3: Window opening durations in summertime: measured data in comparison to simulated data.

4 IMPACT ON THERMAL COMFORT

Window opening behaviour is closely linked to thermal comfort, therefore the temperature is most often included as window opening driver in window opening models. But what is the impact of opening windows on the thermal comfort?
In Figure 4, a comparison is made of the indoor temperatures in the living room between the occupancy and activity based model (habit-model) and a simulation in which the windows were always closed (EPBD heat demand calculation). Logically, the simulations with the windows always closed predict higher indoor temperatures compared to the occupancy and activity based model. In the bedrooms (Figure 5), lower indoor temperatures are predicted. This is caused by the fact that the room has smaller windows compared to the large south-oriented windows in the living room. It should be remarked that with this simulation the internal heat gains are proportionally distributed over the different zones. In reality, most internal heat gains will be present in the living area, since this is the room in which most people are active and most appliances are present. This means that with a more realistic distribution of the internal heat gains, the overheating in the living rooms will be even higher.

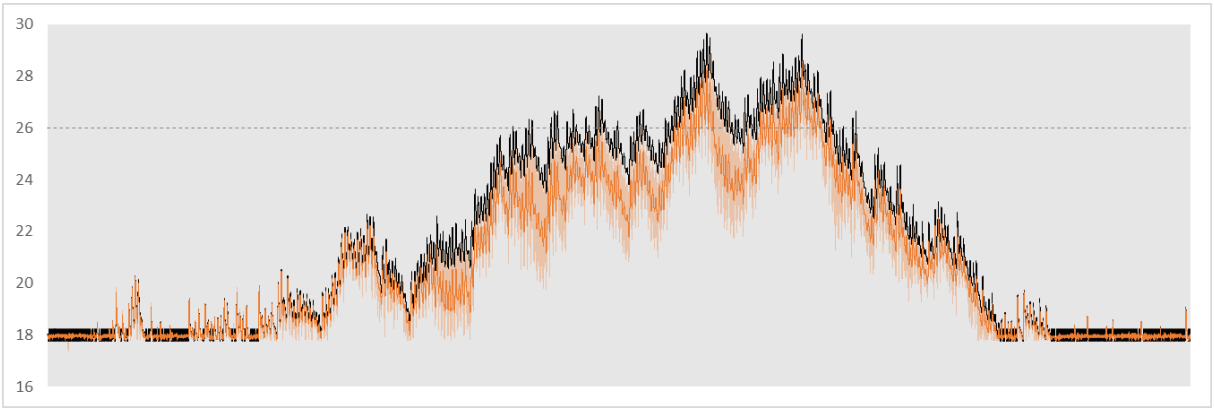

Figure 4: Simulated living room temperatures with habit-model (orange) and windows always closed (black)

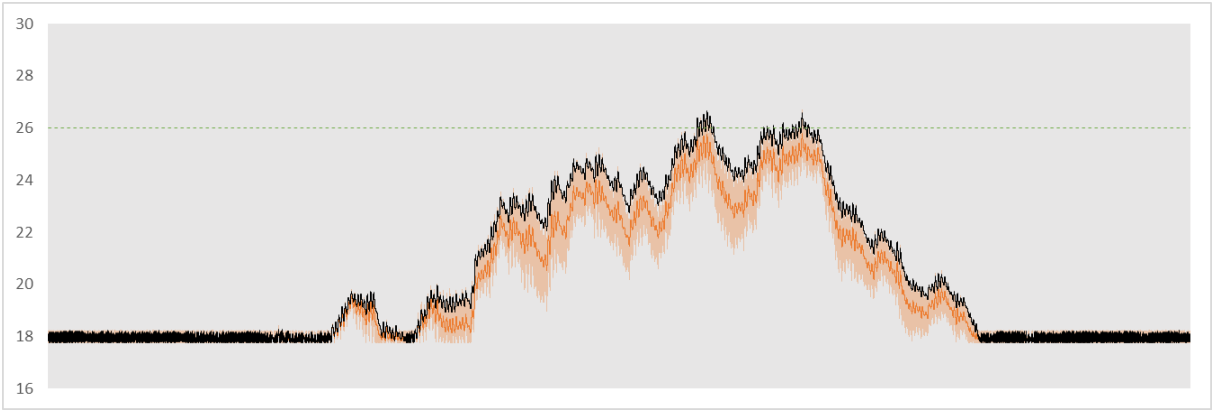

Figure 5: Simulated bedroom temperatures with habit-model (orange) and windows always closed (black)

The influence of using different window use models on the prediction of the indoor temperature is investigated; more specifically, the risk of overheating is evaluated. In Belgium a maximum overheating of 6500 Kh is allowed in newly constructed buildings. This indicator represents the hours that the threshold-temperature of 26°C is exceeded and with how much.
The overheating indicator in the living room when all windows remain closed is 1464 Kh which is still below the maximum allowed value of 6500Kh. If the extra ventilation rate from the overheating calculation of EPBD is included the overheating decreases to 665 Kh. When

applying a weather-based model (560 Kh) or occupancy and activity based model (434 Kh), the average overheating indicator decreases even more.
The occupancy and activity based model averagely predicts less overheating compared to the weather-based model. However, large variations are present, so the overheating indicator greatly depends on which habits the occupants perform. In the other rooms very little overheating is predicted, even with the windows always closed the overheating is only 223 Kh and 33 Kh for respectively the bathroom and bedroom. When the weather-based model the overheating decreases even further to 43 Kh in the bathroom and 2 Kh in the bedroom. If the habit-model is applied the average overheating drops to 32 Kh in the bathroom and 2 Kh in the bedroom. For one third of the simulations there was no overheating present in the bedroom. This proves that when the windows are opened in a specific way, it can be a good measure to prevent overheating.

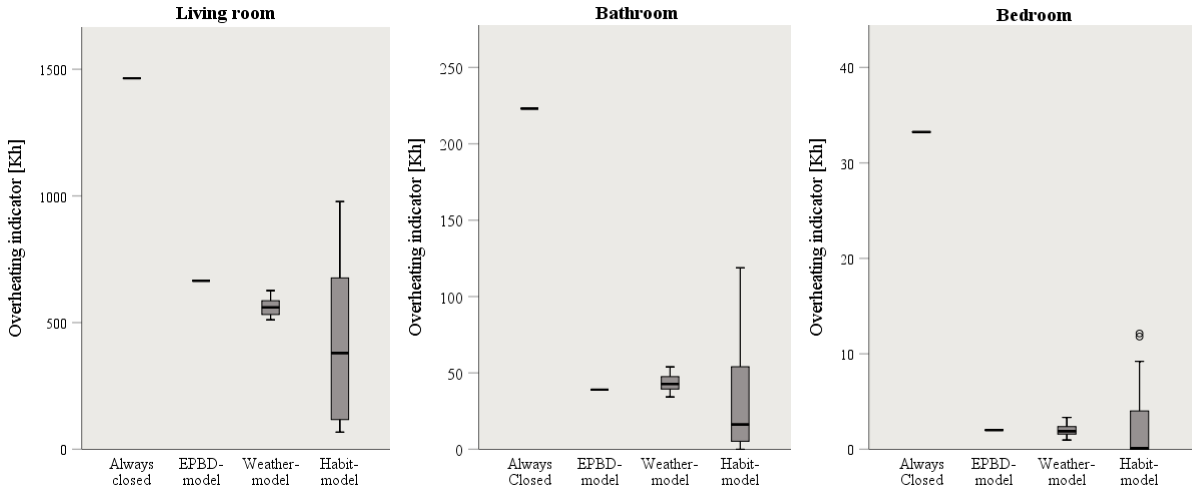

Figure 6: Overheating indicator [Kh] in the living room, bathroom and bedroom.

5 IMPACT ON ENERGY USE

The drawback of opening windows, especially in wintertime, is the increase in heating energy. As the occupancy and activity based window opening model better predicts the opening behaviour of the occupants it will probably be able to better estimate the energy use for heating of these occupants.
In Figure 7 the simulated energy use for heating and domestic hot water is given for the different models, as well as measured data in similar buildings from the case study neighbourhood in Kortrijk. As expected, the heat demand increases when the windows are opened more. With the EPBD-model, in which all windows are assumed to be closed, the energy use is 2920 kWh/year. While for the weather-based model the average energy use increased to 3194 kWh and for the habit-model to 3550 kWh. Again, the large variation can be seen in energy use due to the variability in window opening behaviour, with energy use ranging from 2975 kWh/year to 4766 kWh/year. This large variability is as well present with the measured data; however, the measured energy use is significantly lower with an average value of 1878 kWh. The discrepancies can be attributed to a lot of different factors. Since, it was assumed that the other types of occupant behaviour were similar as in the EPBD-calculation, the real occupant behaviour was grossly simplified.
There was a large influence of the window opening behaviour on the energy use, however, some habits contributed to a higher energy use than others.

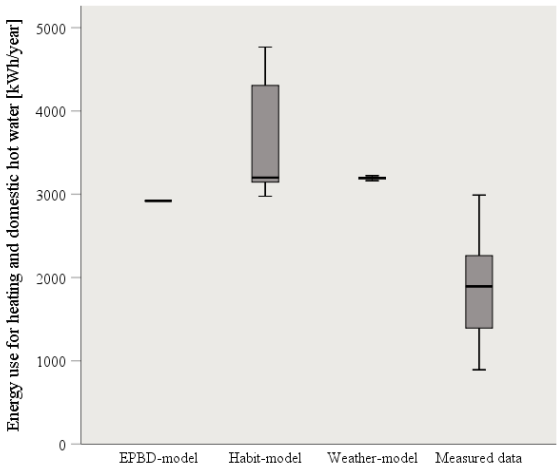

Figure 7: Energy use simulated with the different window opening models compared to measured data

6 IMPACT OF DIFFERENT HABITS

From the previous paragraphs it became apparent that the type of habit can have a large influence on the overheating and energy use in a building. Therefore, the impact of different habits is analysed as well.

In general, the influence of a specific type of habit was difficult to assess, since multiple habits are present in one household that work together or contradict each other in terms of preventing overheating or the energy use. Additionally, when no habit was present (Undefined), the weather-based model was applied, which could lead to high or low opening times due to the stochasticity of the model. In Figure 8, the relation between the energy use and overheating in the living room is given for the 30 simulations. Some of the simulations have low energy use and little overheating at the same time, which makes it optimal window opening strategies.

Only for the habit when going to sleep a clear significant influence could be distinguished. The least overheating is present when the windows remained in the state they were before going to sleep in comparison with the habits of closing all windows when going to sleep or closing the bedroom window when going to sleep. However, this led as well to a significant higher energy use compared to the ones that closed all windows ($t=-2.025$, $p=.05$). It can be concluded that due to the multitude of habits present in the household only the impact of the habit when going to sleep was significant. Other habits may have a significant influence when they are combined.

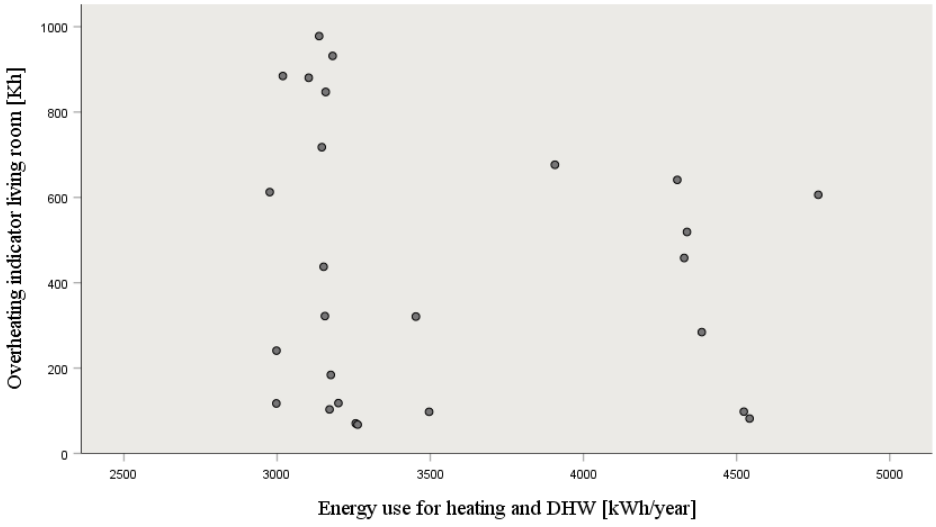

Figure 8: Energy use and overheating for 30 different habit-model simulations

7 CONCLUSIONS

The opening of windows has a high impact on the thermal comfort as on the energy use, therefore it is important to correctly assess it. The newly developed window opening model based on activity and occupancy patterns is able to better estimate the real window opening behaviour, especially the variability that is present between households. An optimal window opening strategy could limit the overheating significantly, even prevent it in the bedrooms and bathroom. Closing all windows when going to sleep will lead to a higher risk of overheating but will lead to less energy use. Next, to the 'going to bed'-habit, none of the other habits had individually a significant influence on the overheating or energy use. Most habits should be combined to reduce overheating and/or energy use.

8 ACKNOWLEDGEMENTS

We gratefully acknowledge the financial support received for this work from the Fund for Scientific Research (FWO) in the frame of the strategic basic research (SBO) project "NEPBC: Next generation building energy assessment methods towards a carbon neutral building stock" (S009617N). The authors would also like to thank the social housing company 'Goedkope Woning' and the occupants who willingly participated in this project.

9 REFERENCES

Aerts, D. (2015). *Occupancy and Activity Modelling.* KU Leuven.

Baetens, R., and Saelens D. (2016). Modelling Uncertainty in District Energy Simulations by Stochastic Residential Occupant Behaviour. *Journal of Building Performance Simulation* 9(4), 431–47.

Dubrul, C. (1988). *Inhabitant Behaviour with Respect to Ventilation*.

Hauge, B. (2016). The Air from Outside: Getting to Know the World through Air Practices. *Journal of Material Culture* 18(2), 171–87.

Himpe, E., Janssens, A., and Rebollar, J.E.V. (2015). Energy and Comfort Performance Assessment of Monitored Low Energy Buildings Connected to Low-Temperature District Heating. *Energy Procedia* 78, 3465–70.

Janssens, A., Rebollar, J.E.V., Himpe, E., and Delghust, M. (2017). Transforming Social Housing Neighbourhoods into Sustainable Carbon Neutral Districts. *Energy Procedia* 132, 549–54.

Jorissen, F. et al. (2018). Implementation and Verification of the IDEAS Building Energy Simulation Library. *Journal of Building Performance Simulation* 11(6), 669–88.

Maeyens, J., and Janssens, A. (2000). A Stochastic Ventilation Model Regarding Leakage and User Behaviour. *Resaerch in Building Physics*, 737–48.

Verbruggen, S., Delghust, M., Laverge, J., and Janssens, A. (2018). The Influence of Window Opening Habits on the Residential Energy Use in Nearly Zero Energy Buildings. In *Proceedings of The7th International Building Physics Conference*, 677–82.

Verbruggen, S., Delghust, M., Laverge, J., and Janssens, A. (2019). Inclusion of Window Opening Habits in a Window Model Based on Activity and Occupancy Patterns. In *Clima 2019*.

Verbruggen, S., Delghust, M., Laverge, J., and Janssens, A. (2017). W*indow opening in relation to residential energy use and indoor climate*. Ghent University

Ambient air filter efficiency in airtight, highly energy efficient dwellings – A simulation study to evaluate benefits and associated energy costs

Gabriel Rojas[*1]

1 Unit for Energy Efficient Buildings, University of Innsbruck, Technikerstr. 13, Innsbruck, Austria
**Corresponding author: gabriel.rojas-kopeinig@uibk.ac.at*

ABSTRACT

Highly energy efficient buildings such as ones built to the Passive House standard, require a very airtight building envelope and the installation of a mechanical ventilation with heat recovery (MVHR). MVHR systems incorporate ambient air filters, which reduce the introduction of particulate matter (PM) from outdoor sources into the dwelling. However, indoor PM sources, e.g. cooking, can also contribute substantially to occupants' exposure and need to be accounted for when designing ventilation or deriving recommendations for filter classes.

This simulation study investigates which ambient air filter class is a reasonable choice in terms of indoor air quality and energy use for highly airtight residential housing. It considers outdoor and indoor generated size-resolved PM, while comparing different cooktop ventilation concepts. Results confirm that a F7 filter according to EN 779 (or equivalent) is a reasonable choice for low or short-term moderate ambient air PM concentrations, as total PM exposure will be dominated by indoor sources and higher filter classes will therefore not provide a substantial exposure reduction. For locations with high outdoor PM concentrations, the use of a high-class filter like F9 is advisable, as it will further reduce the exposure. In locations with low ambient air pollution, cooking emissions could likely contribute a substantial or even dominant fraction of the total PM exposure, if no measures, like an effective cooker hood system, is used. Here, the use of an extracting hood shows clear advantages over a recirculating system. However, for cases with elevated ambient concentrations, the use of extracting kitchen hoods (with unfiltered make-up air) will increase the total PM exposure for cases with low or moderate cooking intensities.

KEYWORDS

Particulate matter, $PM_{2.5}$, UFP, MVHR, filter, cooking, cooker hood, energy efficient, Passive House, Annex 68

1 INTRODUCTION

This work evaluates the exposure to fine and ultrafine particulate matter (PM) within a residential dwelling in Passive House standard with multi-zone airflow simulations. The study is performed within the framework of the project "IEA EBC Annex 68 - Indoor Air Quality Design and Control in Low Energy Residential Buildings".

2 METHOD

Based on a residential low-energy building project in Austria (Ploss and Hatt 2016), a two-bedroom apartment was modelled in CONTAM, a multi-zone air flow and contaminant transport simulation tool (Dols and Polidoro 2015). The floor plan is shown in Figure 1. It has a floor area of 76 m² and represents a typical Austrian apartment. In the reference model, the occupancy and window use is based on a literature review undertaken for previous simulation studies, e.g. (Rojas, Pfluger, and Feist 2016) with three occupancy schedules representing a full-time employed person, a person staying at home and a school child. Envelope leakages are modelled with two "cracks" in each exterior wall at two different heights (1 m and 2.2 m representing regular windows and 0 m and 2.2 m representing tall windows) to allow for stack-effect driven infiltration. The cracks are evenly distributed and dimensioned to result in an air exchange of 0.6 h^{-1} at 50 Pa, the threshold for Passive House certification. The wind

pressure is calculated using a wind speed modifier, representing a height of 10 m in suburban terrain and wind pressure profile representing a low-rise building (ASHRAE 2005). Wind speed and ambient temperatures are defined by a standardised weather file for the city of Vienna generated with the software Meteonorm. The model-apartment has a balanced mechanical ventilation with heat recovery (MVHR), with filtered ambient air being supplied into bedrooms and living room and "used" air being extracted from kitchen area and bathroom. The supply and extract airflows are documented in Figure 1. The bedroom and child's room door, modelled as two-way airflow paths, are closed during the night and open during the day (variations are performed in section 3.2). The bathroom door opens five times for 10 minutes each over the course of the day. The opening between hallway and living room is also modelled as a permanently open two-way airflow path, with 2.5 m height and 1.2 m width.

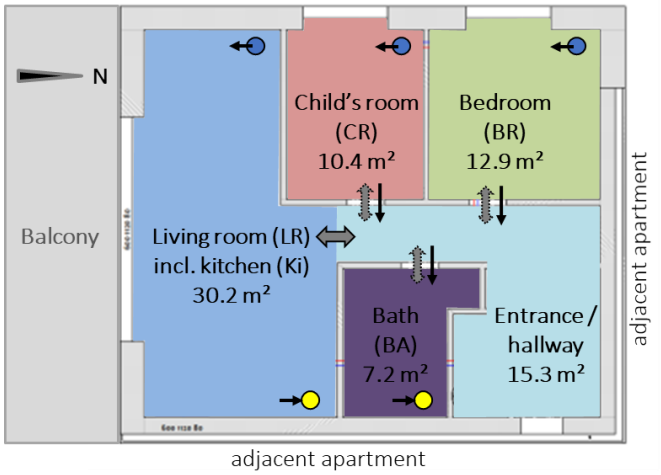

Ventilation air flows in m³/h (l/s)

	BR	CR	LR/Ki	BA	Total
Supply	40 (11.1)	20 (5.6)	30 (8.3)		90 (25)
Extract			60 (16.7)	30 (8.3)	90 (25)

Figure 1: Sketch of the simulated floor plan representing a typical new Austrian residential dwelling and the ventilation air flows as modelled in the reference model.

The particle exposure was modelled for sizes ranging from 1 nm to 10 µm with 21 bins evenly distributed on a log scale. The specific aspects for modelling the particle exposure are described in the following subsections.

2.1 Ambient concentration

The outdoor PM distribution was modelled based on values for archetypical urban air as reported in (Ruprecht 1993). The multimodal distribution (see Figure 2a) can be described as the sum of three lognormal distributions; their parameters are reported in the original work and e.g. in (Riley et al. 2002). The respective simulation input files were generated using the "CONTAM particle distribution calculator" (NIST n.d.). Figure 2b shows a characteristic aerosol distribution for rural areas used as alternative simulation input (see section 3.1).
Due to lack of time-resolved data, ambient air concentration was modelled constant. Note that the concentration levels for the reference case, i.e. a $PM_{2.5}$ of 42 µg/m³, will not necessarily represent a typical long-term average of a European city. E.g. the yearly $PM_{2.5}$ average in Austrian cities has been declining and was roughly around 15 µg/m³ in 2017. However, the used distribution may very well present a short-term average in an urban area in Europe or e.g. a long-term average in a moderately polluted Asian city.

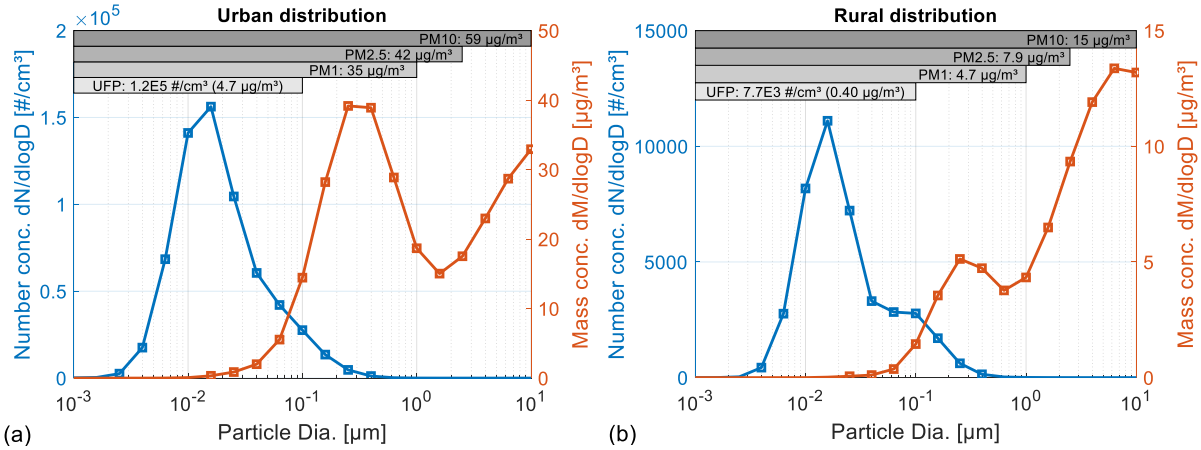

Figure 2: Characteristic ambient particle distributions for urban (a) and rural (b) areas taken from (Ruprecht 1993). The plots show the log-normalized distributions for particle number and mass concentration assuming a particle density of 1 g/cm³. The integrated values for UFP (≤0.1 µm), PM_1 (≤1 µm), $PM_{2.5}$ (≤2.5 µm), PM_{10} (≤10 µm) are also shown on the plots. Note the different scaling between urban and rural plots.

2.2 Filter quality and envelope penetration

The efficiency of ventilation filters is usually classified according to ASHRAE 52.2, EN 779 or to the new ISO 16890 standard. These standards define test methods to determine the fractional filtration efficiency for particles >0.3 µm, which is the lower threshold for most optical particle spectrometers. Therefore it is difficult to obtain efficiency curves for particle sizes <0.3 µm from filter manufacturers. Nevertheless, few studies have reported filtration efficiency curves for the entire (relevant) size spectrum (González et al. 2016; Hanley et al. 1994; Shi 2012; Shi, Ekberg, and Langer 2013). However, no data for filters classified according to the new standard ISO 16890, e.g. ISO ePM1 70%, could be sourced. Therefore, this study simulated filter classes M5, M6, F7, F8 and F9 (according to EN 779). Their fractional efficiency curves were taken from (Shi, 2012, see Figure 7.2), and are plotted in Figure 3a. These filter classes can be roughly translated to MERV 9/10, MERV 11/12, MERV 13, MERV 14 and MERV 15 (according ASHRAE 52.2), respectively (camfil n.d.). Note that other particle losses within the ventilation system, besides the removal by the filter, were not modelled in this study although several loss mechanism might change the ambient particle distribution as the air travels through the ventilation system. However, these losses can be considered very small compared to particle removal by the filter, see e.g. (Siegel and Nazaroff 2003; Sippola and Nazaroff 2003).

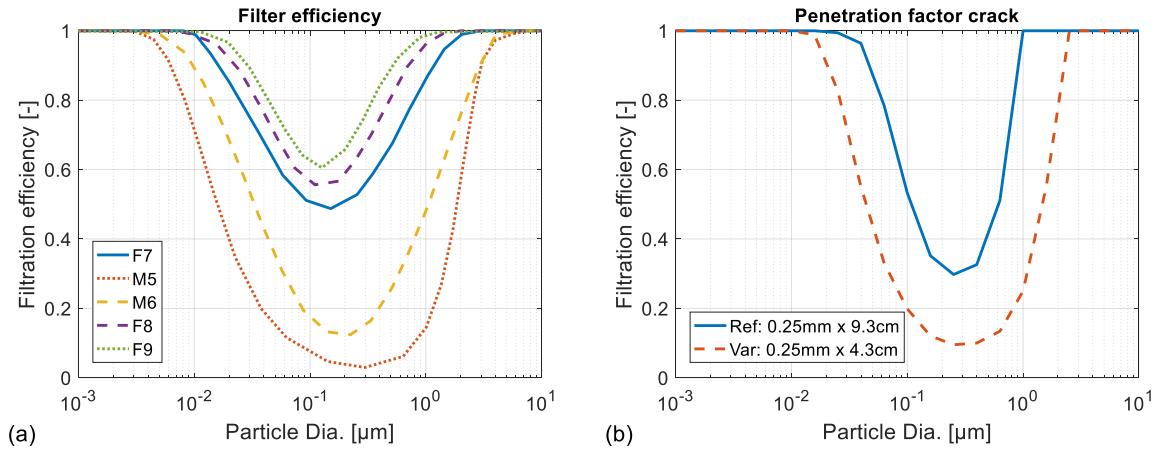

Figure 3: Fractional filtration efficiency of ventilation filter (a) and envelope cracks (b) as modelled for this study. The curves were derived / extracted from (Shi 2012) and (Liu and Nazaroff 2003).

Particle penetration through the building envelope has been investigated and characterized in numerous studies (Chao, Wan, and Cheng 2003; Lee et al. n.d.; Liu and Nazaroff 2003; Long et al. 2001; Stephens and Siegel 2012; Thatcher and Layton 1995; Tian et al. 2009). However, only a few allow the extraction of the particle size resolved penetration factor *p* for simulating highly airtight buildings as investigated herein. For this study the penetration factor curve as shown in (Liu & Nazaroff, 2003, see Figure 6) for an aluminium crack with a width of 0.25 mm and a flow length of 9.4 cm was implemented in the CONTAM model. To test the sensitivity of this parameter, the data for a crack with a width of 0.25 mm and a flow length of 4.3 cm was used alternatively. The resulting filtration efficiency (1-*p*) for these crack dimensions are shown in Figure 3b.

2.3 Indoor sources and deposition

Various indoor activities can substantially contribute to indoor PM exposure. These have been characterised in a number of studies, e.g. (Géhin, Ramalho, and Kirchner 2008; Hussein et al. 2006; Wallace 2006). Cooking is considered one of the major indoor PM source and numerous studies have investigated the resulting PM concentrations and/or characterised emission rates from various cooking activities, e.g. (Abdullahi, Delgado-Saborit, and Harrison 2013; Buonanno, Morawska, and Stabile 2009; Poon, Wallace, and Lai 2016; See and Balasubramanian 2008; Sjaastad, Svendsen, and Jorgensen 2008; Torkmahalleh et al. 2012; Wallace, Emmerich, and Howard-Reed 2004). To keep the numerical model and its interpretation as simple as possible, this study only implemented PM sources representing cooking activities, i.e. toasting, frying burger and heating oil. These three source events, modelled as a burst source (instantons release during one simulation time step of 5 min), were scheduled in the morning (7:30), at noon (12:00) and in the evening (18:30), respectively. The source strength was determined from experimental data gathered during laboratory measurements by the author. Preliminary results were reported in (Rojas, Delp, and Singer 2018), a detail report of that study, characterising filter efficiency of cooker hoods, is still to be published. The resulting $PM_{2.5}$ source strength compares well with values reported in literature, e.g. (He et al. 2004).

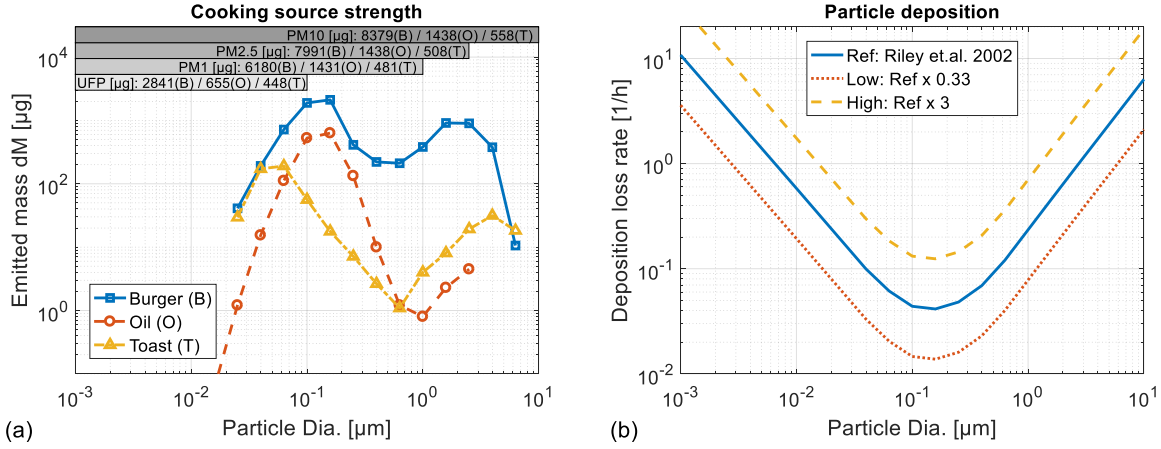

Figure 4: Cooking source strength (a) and particle deposition loss rate (b) as modelled in this study. The source strength in (a) was extracted from experimental data from measurements in a test chamber (Rojas et al. 2018). The reference curve for particle deposition in (b) is taken from (Riley et al. 2002).

Deposition is an important particle loss mechanism which strongly depends on particle size. Deposition rates in residential settings has been investigated numerously. Measurement results and/or a literature review can be found in e.g. (He, Morawska, and Gilbert 2005; Howard-Reed, Wallace, and Emmerich 2003; Riley et al. 2002). For this study, the deposition loss coefficient function as specified in (Riley et al., 2002, see Figure 3) was used for the reference model. It is based on experimental data for particle diameters >0.06 µm and on the

smooth indoor surface particle deposition theory of (Lai and Nazaroff 2000) for diameters below that value. For the sensitivity analysis (see section 3.2), these values were divided / multiplied by a factor of three. The resulting deposition loss rates are shown in Figure 4b.

2.4 Exposure assessment

The ambient PM concentration was modelled constant and the occupant related schedules repeat every day. Therefore averaged exposure results, rather than temporal variations or peak values, were used for assessment. The simulation was performed for the full month of January (to average varying infiltration) with a time step of 5 minutes. The simulation results were analysed by assessing the average exposure of the "always-present-occupant" during the full month, i.e. the average concentration in the rooms where this person scheduled to be present. Note that this way the PM concentration in the child's room is not taken into account. According to the WHO guidelines for indoor air the $PM_{2.5}$ exposure should not exceed 25 µg/m³ if averaged in a 24h period or 10 µg/m³ if averaged in a period of one year (WHO 2005). The author is not aware of any standard or guidelines recommending exposure limit values for UFP.

3 RESULTS

Figure 5 shows the simulated PM concentration for the reference model during the course of one winter day. Since a constant ambient concentration was modelled, variations are dominated by internal sources (modelled cooking events) and door and window openings. There is little difference between PM_1, $PM_{2.5}$ and PM_{10} values, i.e. most of the time indoor exposure is mainly dominated by sub-micrometre sized particles. Figure 6 shows the size distribution for four distinct hours of the day: (a) night times: only outdoor-originated particles are present; (b) after breakfast (i.e. toasting): the number concentration is strongly increased by indoor-originated particles, however the mass concentration is still dominated by outdoor-originated particles (increased by morning airing event); (c) after lunch: the cooking event (frying burger) substantially increases the number and mass concentration; (d) after dinner: the number and mass concentration is notably increased by another cooking activity (heating oil).

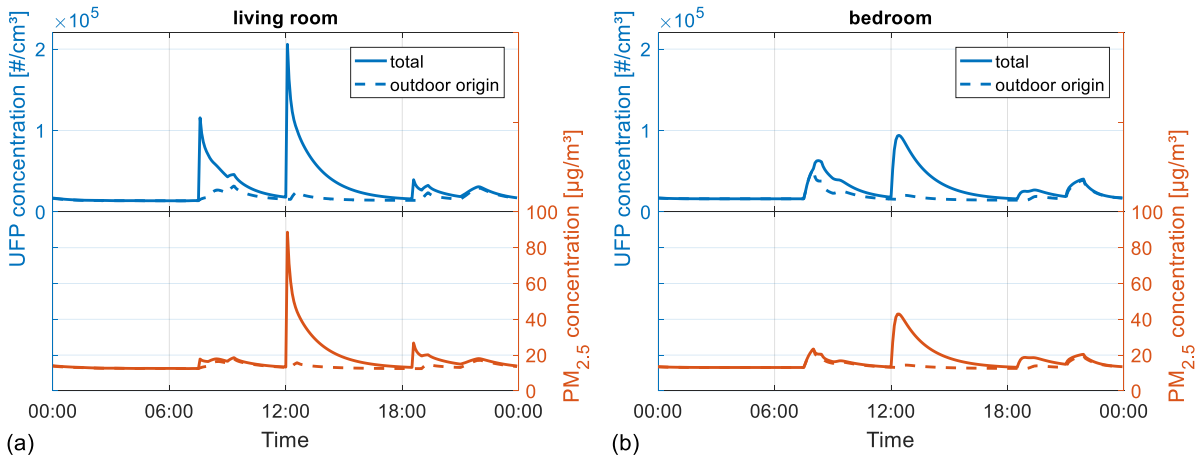

Figure 5: Simulated UFP and $PM_{2.5}$ concentration in living room/kitchen zone (a) and bedroom (b) over the course of one day for the reference case with F7 filter. The indoor concentration originating from outdoor PM is also plotted.

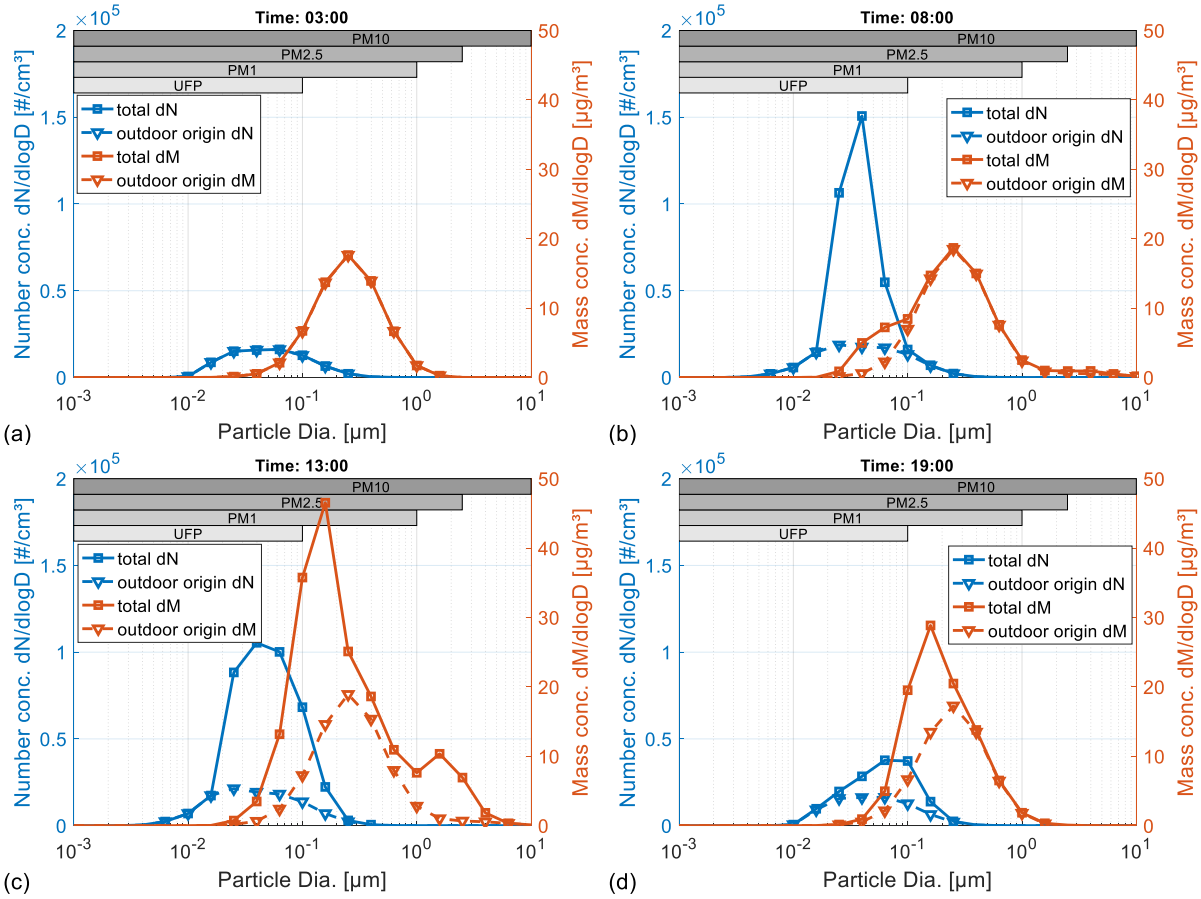

Figure 6: Log-normalized PM size distribution in the living room at four different hours of the day: during the night (a), after breakfast (b), after lunch (c), after dinner (d). The distribution of the outdoor-originated number and mass concentration is also plotted to differentiate between contributions from indoor and outdoor sources.

3.1 Effect of filter quality

To evaluate which filter quality is most favourable for the assumed boundary conditions, i.e. a very airtight housing with MVHR, the resulting mean $PM_{2.5}$ and UFP exposure was plotted against the estimated surplus electricity consumption due to the filter-induced pressure drop (see Figure 7). The pressure drop (average over lifetime) for each filter class was defined as reported in (Shi 2012, see Figure 8.5a). As one can see, $PM_{2.5}$ and UFP exposure is substantially reduced with the use of higher filter classes. However, the additional improvements are small for filter classes F8 and F9. For lower ambient PM concentration like assumed in the cases “Urban Low” and “Rural” (see Figure 2) a substantial fraction of the exposure stems from cooking originated particles. Therefore, the relative reduction of overall exposure does depend on the ambient air conditions (see Figure 8a). However, the relative reduction of outdoor-originated particles is practically independent of the ambient air concentration. A F7 filter would reduce the outdoor-originated particle exposure (from urban background) by around 55% vs. 72% with a F9 filter.

Figure 8b compares the exposure for three cases with MVHR, i.e. reference case, reduced and increased supply/extract flow, against the exposure obtained with an extract air ventilation (EAV) system. The EAV model assumed the same mechanical airflow as the MVHR reference case (90 m³/h), with unfiltered trickle vents in bedroom, children’s room and living room. It was assumed that those openings had a pressure drop of 10 Pa at their nominal settings (corresponding to the supply air flow in the MVHR case). Note that for the EAV case, a substantial part (around 30%)% is drawn in through cracks, etc. despite the high airtightness of n_{50}=0.6 h^{-1}. As a result, the exposure between the EAV system and a MVHR

system with a M5 is of comparable magnitude, with a F7 filter the exposure is roughly reduced by 50%. One can also see that the influence of the airflow rate setting of the MVHR system is minor.

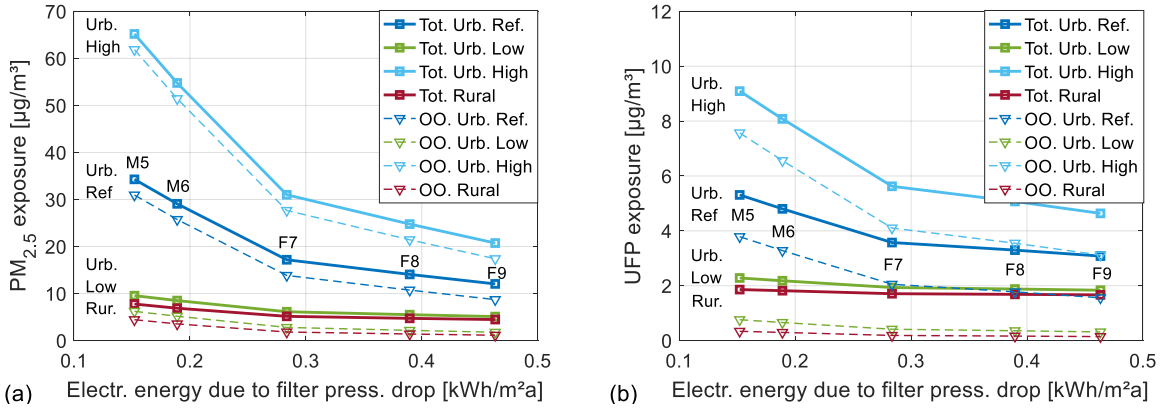

Figure 7: Average $PM_{2.5}$ (a) and UFP (b) exposure as a function of the electric energy consumption of the fan related to the pressure drop of the filter for different outdoor PM concentrations. The units refer to kWh per m² of floor area and year, assuming permanent fan operation. The contribution of the outdoor-originated (OO) PM is also plotted (dashed lines).

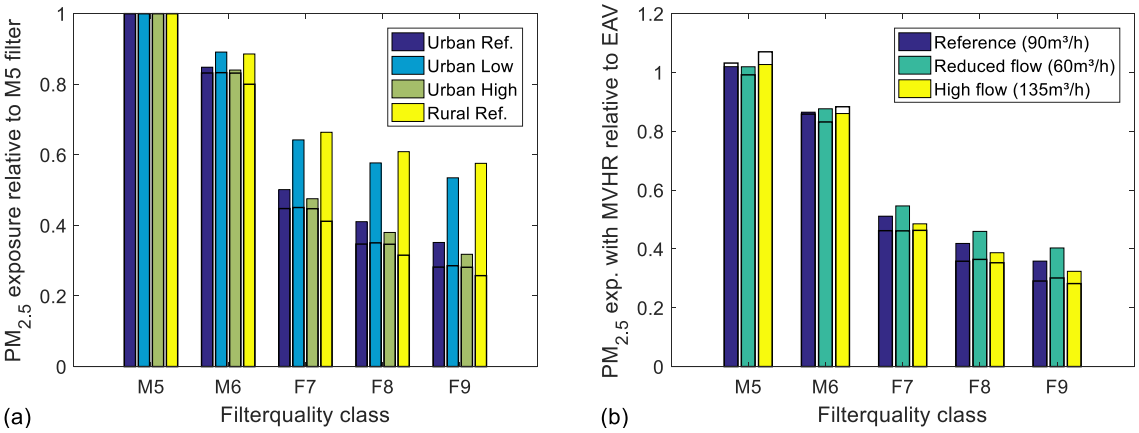

Figure 8: Average $PM_{2.5}$ exposure relative to exposure with a M5 filter (a) and average exposure for three cases with MVHR (reference, reduced and high flow) relative to average exposure for a case with extract air ventilation. In (a) the results for different outdoor air concentrations are shown. In (b) the results for different MVHR flow settings are shown. Exposure to outdoor originated PM is plotted with unfilled bars/horizontal line.

3.2 Effect of various PM related model parameters

To check the sensitivity of PM exposure to the chosen model parameters the reference model was varied as defined in Table 1. The opening schedule for bedroom and child's room door was modified from almost always closed (except for a few short opening events) to always open. The reference model included window opening behaviour based on observations in German Passive House apartments (Kah et al. 2010; Kah, Pfluger, and Feist 2005). Note that this might not be representative for locations with notably bad air quality, i.e. high outdoor particle concentrations. The window opening was modelled representing a tilted window resulting in roughly 50 m³/h (14 l/s) of air exchange during opening times. The sensitivity tests included a simulation run with no window opening and one with increased window opening duration, defined by the 95th percentile of the opening times observed in (Kah et al. 2010, 2005).

The n_{50} value, representing the airtightness of the building envelope, was varied between 0.3 h^{-1}, a value not uncommonly achieved in multi-family Passive Houses, and 1.5 h^{-1}. This

value is well above the Passive House criteria. However, it is often regarded as a threshold for an energetically reasonable operation of a MVHR system (DIN 4108-7 2011). The particle-size dependent deposition rate function was divided / multiplied by a factor of three (equally for all size bins) from the reference values. This results in a variation of nearly one order of magnitude and corresponds roughly to the variation reported in literature, see e.g. (Howard-Reed et al. 2003; Lai and Nazaroff 2000).
It can be assumed, that the air leakage cracks in the envelope of highly airtight buildings, like investigated in this study, have rather narrow gaps. There is limited data available on penetration factors for these kind of air leakage gaps. Therefore, only one additional simulation run was performed with the size-dependent penetration factor for a 0.25 mm wide and 4. m deep gap according to the data reported in (Liu and Nazaroff 2003) (see Figure 3b).

Table 1: Model variations for sensitivity analysis

	Reference	**Low**	**High**
Bed- / child's room door opening	8am – 10pm	4 x 10 min	0-24 hrs
Window opening (tilted): all	3.6 h/day	0 h/day	6.3 h/day
Kitchen area	3 x 20 min	-	3 x 35 min
Living room area	3 x 10 min	-	3 x 18 min
Bedroom	2 x 56 min	-	2 x 98 min
Childs room	2 x 6 min	-	2 x 11 min
Airtightness / n50	0.6 1/h	0.3 1/h	1.5 1/h
Deposition rate multiplier	1	0.33	3.0
Penetration factor for crack with dimensions	W 0.25 mm x L 9.4 cm	-	W 0.25 mm x L 4.3 cm

Figure 9 compares the average exposure to $PM_{2.5}$ and UFP of the "home-staying" adult. It shows that the results do not change substantially when these model assumptions are varied within reasonable bounds. Exceptions are the variation of the deposition rate and of the window airing duration. The deposition rate notably increases/decreases the exposure, however the effect is strongly reduced for filter classes F7 and higher. In contrast, the sensitivity towards the window airing duration increases for higher filter classes. Nevertheless, the conclusions from this simulation study will not be affected.

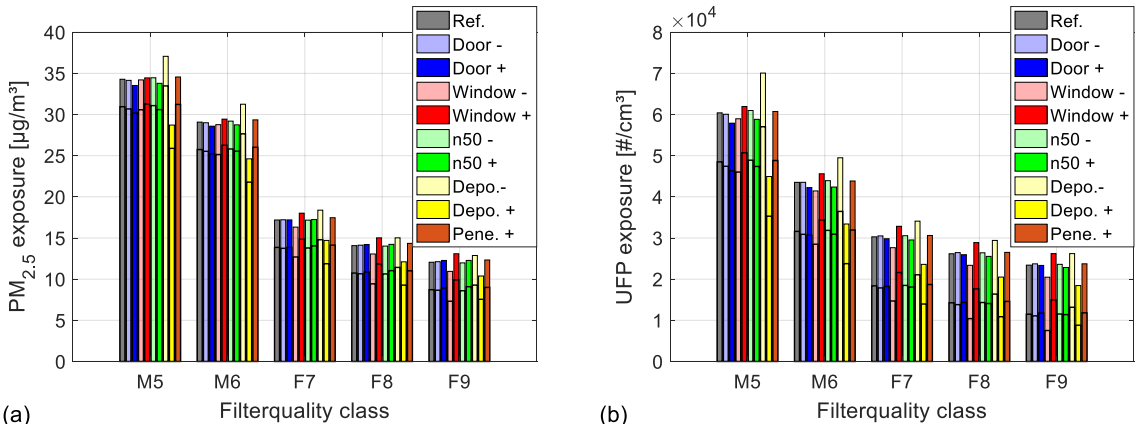

Figure 9: Average $PM_{2.5}$ (a) and UFP (b) exposure for a variation of the following model parameters: bedroom and child's room door opening, window airing duration in bedroom, child's room and living room / kitchen zone, building envelope airtightness, particle deposition rate and particle penetration through the building envelope. Refer to Table 1 for details. Exposure to outdoor originated PM is plotted with unfilled bars.

3.3 Variation cooking source strength and use of cooker hoods

Certainly, the amount and frequency of indoor generated particles can vary a lot, see e.g. (Abdullahi et al. 2013). Variations were performed to estimate how different generation rates might affect the results of the reference model. Therefore, the source strength was reduced to a third of the reference case and increased by a factor of three. That way, the cooking generated particle source strength is varied by roughly one order of magnitude between "low" and "high" case. Note that particular cooking activities and/or boundary conditions might result in even higher indoor concentrations. Additionally, the use of a recirculating and extracting cooker hood was simulated. The use of a recirculating hood was modelled by applying size-dependent reduction factors to the particle source strength of the lunch-time emissions (frying burger) and evening emissions (heating oil). The reduction factors were determined from a set of experiments performed at Lawrence Berkeley National Lab (Rojas et al. 2018) by comparing PM concentration in a test chamber with and without the use of a carbon filter installed in a recirculating cooker hood. Full capture of the plume was assured during these tests to determine the particle filtration efficiency (FE) of typical (carbon) filters of commercially available cooker hoods. To account for the fact that residential cooker hoods do not capture the entire cooking plume, a capture efficiency (CE) 0.7 was assumed for this simulation study for the recirculating and the extracting hood. It represents a rather optimistic scenario with the assumption that the cooking is performed at the rear burners were CE is generally higher, see e.g. (Rojas, Walker, and Singer 2017). The resulting source strength S_{ext} and S_{rec} for the extracting and recirculating cooker hood was calculated according to the following equations,

$$S_{ext} = S_0(1 - CE) \quad (1)$$

$$S_{rec} = S_0(1 - CE) + S_0 CE(1 - FE) \quad (2)$$

with S_0 representing the source strength of the cooking activity with no cooker hood in use. It was assumed that the cooker hoods are operated for 30 min during lunch and dinner preparation, starting with the modelled emission bursts. For the case with the extracting cooker hood, a make-up air opening (with no filter) producing a pressure drop of 10 Pa at a flow rate of 300 m³/h was activated in the kitchen zone during hood use.

Table 2: Particle source strength [µg] per cooking event modelled as burst source.

	Ref S_0	**Low** $S_{0\,min}$	**High** $S_{0\,max}$	**Recirc. hood** S_{rec}	**Extr. hood** S_{ext}
Breakfast	508	168	1525	508	508
Lunch	7991	2637	23974	6790	2397
Dinner	1438	475	4314	626	431

Figure 10 compares the average $PM_{2.5}$ and UFP exposure without with different cooktop ventilation strategies for different cooking source strength settings and different ambient concentration. One can see that for the "high" cook source scenario, the relative contribution from cooking becomes substantial or even dominant. For the case with reference cooking activity and low ambient concentration, the $PM_{2.5}$ exposure due to cooking is roughly equivalent to the exposure to outdoor originated PM. Not so for all the other cases, i.e. reference or high ambient concentration and low or reference cooking source strength. In those cases, the use of an extracting range hood, will not notably reduce PM exposure, in some cases it will even increase PM exposure. This is due to the fact that, large quantities of unfiltered make-up air are introduced during cooker hood operation.

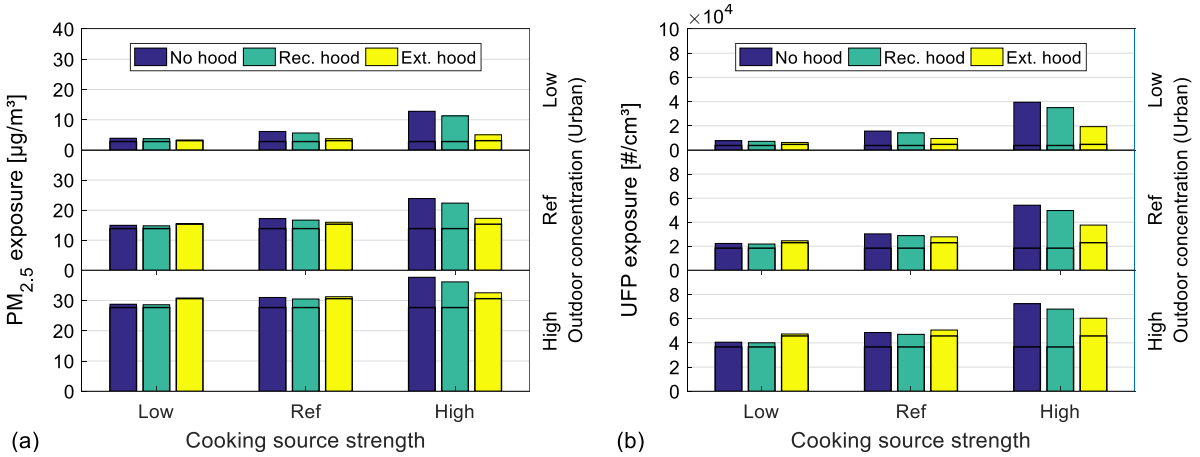

Figure 10: Average $PM_{2.5}$ (a) and UFP (b) exposure for different cooking source strength (see Table 2), different outdoor concentrations and different cooktop ventilation strategies for the reference case with a F7 filter. Exposure to outdoor originated PM is plotted with unfilled bars/horizontal lines.

4 CONCLUSIONS

This simulation study evaluates the benefits and the associated energy costs of using different filter qualities within the MVHR system focusing on boundary conditions encountered in highly energy efficient housing. Inherently, this study has a number of limitations. The most prominent being the limited ambient air quality data (constant values taken from older literature), fix occupancy and PM generation schedules and the neglect of phenomena like particle resuspension. Nevertheless, the results can be considered indicative for short-term exposure (e.g. 24 hours) with the assumed outdoor conditions. They provide useful insights into a reasonable choice of filter quality in energy efficient housing.

The results suggest that the use of F7 filters (or equivalent) provide good relation between reduction of exposure to outdoor-originated PM and electric energy consumption caused by their pressure drop. For locations with low ambient concentrations, the use of higher filter classes, e.g. F9 (or equivalent) do not seem to provide a substantial reduction of PM exposure. For these cases, indoor sources might dominated the total PM exposure, depending on occupant behaviour. For locations with high outdoor PM concentrations, the use of a high class filter like F9 is advisable, as it will further reduce the exposure to outdoor-originated PM compared to a F7 filter. This work will be extended to derive filter recommendations based on the new filter standard ISO 16890.

Comparing exposure terms from outdoor and indoor originated particles the results show that for locations with low outdoor PM pollution, cooking emissions could likely contribute a substantial or even dominant fraction of the total PM exposure, if no measures, like an effective cooker hood system, is used. Here the use of an extracting hood shows clear advantages over a recirculating system. However for cases with elevated ambient concentrations, like the “Ref.” and “High” case in this study, the use of extracting kitchen hoods (with unfiltered make-up air) will increase the total PM exposure if only few high-emission cooking activities are performed. Note that the health effect of outdoor and indoor originated particles might differ completely and this comparison should be interpreted with care.

5 ACKNOWLEDGEMENTS

This study was performed within the project IEA EBC Annex 68 as part of the IEA Research Cooperation on behalf of the Austrian ministry for transport, innovation and technology.

6 REFERENCES

Abdullahi, Karimatu L., Juana Maria Delgado-Saborit, and Roy M. Harrison. 2013. "Emissions and Indoor Concentrations of Particulate Matter and Its Specific Chemical Components from Cooking: A Review." *Atmospheric Environment* 71:260–94.

ASHRAE. 2005. "Airflow around Buildings." *ASHRAE Fundamentals* 16.1 ff.

Buonanno, G., L. Morawska, and L. Stabile. 2009. "Particle Emission Factors during Cooking Activities." *Atmospheric Environment* 43(20):3235–42.

camfil. n.d. "Comparison Chart, ASHRAE 52.2, 52.1, EN779, EN1822." *2014*. Retrieved April 29, 2019 (https://www.camfil.at/FileArchive/Industries/Gas turbines and other power systems/Filter brochures/Filter_class_chart_ASHRAE_EN2012.pdf).

Chao, Christopher Y. H., M. P. Wan, and Eddie C. K. Cheng. 2003. "Penetration Coefficient and Deposition Rate as a Function of Particle Size in Non-Smoking Naturally Ventilated Residences." *Atmospheric Environment* 37(30):4233–41.

DIN 4108-7. 2011. "Thermal Insulation and Energy Economy in Buildings – Part 7: Air Tightness of Buildings – Requirements, Recommendations and Examples for Planning and Performance." 1–20.

Dols, W. Stuart and Brian J. Polidoro. 2015. *CONTAM User Guide and Program Documentation Version 3.2 - NIST Technical Note 1887*.

Géhin, Evelyne, Olivier Ramalho, and Séverine Kirchner. 2008. "Size Distribution and Emission Rate Measurement of Fine and Ultrafine Particle from Indoor Human Activities." *Atmospheric Environment* 42(35):8341–52.

González, Luisa F., Aurélie Joubert, Yves Andrès, Myriam Liard, Christophe Renner, and Laurence Le Coq. 2016. "Filtration Performances of HVAC Filters for PM10 and Microbial Aerosols—Influence of Management in a Lab-Scale Air Handling Unit." *Aerosol Science and Technology* 50(6):555–67.

Hanley, James T., David S. Ensor, Daryl D. Smith, and L. E. Sparks. 1994. "Fractional Aerosol Filtration Efficiency of In-Duct Ventilation Air Cleaners." *Indoor Air* 4(3):167–78.

He, Congrong, Lidia Morawska, and Dale Gilbert. 2005. "Particle Deposition Rates in Residential Houses." *Atmospheric Environment* 39(21):3891–99.

He, Congrong, Lidia Morawska, Jane Hitchins, and Dale Gilbert. 2004. "Contribution from Indoor Sources to Particle Number and Mass Concentrations in Residential Houses." *Atmospheric Environment* 38(21):3405–15.

Howard-Reed, C., L. Wallace, and S. J. Emmerich. 2003. "Deposition Rates of Fine and Coarse Particles in Residential Buildings: Literature Review and Measurements in an Occupied Townhouse. NISTIR 7068."

Hussein, Tareq, Thodoros Glytsos, Jakub Ondráček, Pavla Dohányosová, Vladimír Ždímal, Kaarle Hämeri, Mihalis Lazaridis, Jiří Smolík, and Markku Kulmala. 2006. "Particle Size Characterization and Emission Rates during Indoor Activities in a House." *Atmospheric Environment* 40(23):4285–4307.

Kah, O., S. Peper, W. Ebel, B. Kaufmann, W. Feist, and B. Zeno. 2010. *Untersuchung Zum Außenluftwechsel Und Zur Luftqualität in Sanierten Wohnungen Mit Konventioneller Fensterlüftung Und Mit Kontrollierter Lüftung*. Darmstadt: Passivhaus Institut.

Kah, Oliver, Rainer Pfluger, and Wolfgang Feist. 2005. *Luftwechselraten in Bewohnten , Sehr Luftdichten Gebäuden Mit Kontrollierter Wohnungslüftung / Monitoring in Einem Passivhaus-Geschosswohnbau Luftwechselraten in Bewohnten , Sehr Luftdichten Gebäuden Mit Kontrollierter Wohnungslüftung / Monitoring in Ein*.

Lai, Alvin C. K. and William W. Nazaroff. 2000. "Modeling Indoor Particle Deposition from Turbulent Flow onto Smooth Surfaces." *Journal of Aerosol Science* 31(4):463–76.

Lee, Byung Hee, Su Whan Yee, Dong-hwa Kang, Myoung Souk Yeo, and Kwang Woo. n.d. "Relationship between Indoor and Outdoor Particle Concentrations by Penetration Coefficient and Deposition Rate in Office Building." (1).

Liu, De Ling and William W. Nazaroff. 2003. "Particle Penetration through Building Cracks." *Aerosol Science and Technology* 37(7):565–73.

Long, Christopher M., Helen H. Suh, Paul J. Catalano, and Petros Koutrakis. 2001. "Using Time- and Size-Resolved Particulate Data to Ouantify Indoor Penetration and Deposition Behavior." *Environmental Science and Technology* 35(10):2089–99.

NIST. n.d. “CONTAM Particle Distribution Calculator.” Retrieved April 25, 2019 (https://www.nist.gov/node/1326541/software-tools/contam-particle-distribution-calculator).
Ploss, Martin and Tobias Hatt. 2016. “Modellvorhaben KliNaWo - Klimagerechter Nachhaltiger Wohnbau.” Pp. 8–59 in *economicum*.
Poon, Carmen, Lance Wallace, and Alvin C. K. Lai. 2016. “Experimental Study of Exposure to Cooking Emitted Particles under Single Zone and Two-Zone Environments.” *Building and Environment*.
Riley, William J., Thomas E. McKone, Alvin C. K. Lai, and William W. Nazaroff. 2002. “Indoor Particulate Matter of Outdoor Origin: Importance of Size-Dependent Removal Mechanisms.” *Environmental Science and Technology* 36(2):200–207.
Rojas, Gabriel, Woody Delp, and Brett C. Singer. 2018. “Testing Recirculating Cooker Hoods – Can Their Filter Reduce (Ultra) Fine Particle Loads during Cooking ?” Pp. 623–26 in *International Passivhaus Conference*, edited by W. Feist. Passive House Institute.
Rojas, Gabriel, Rainer Pfluger, and Wolfgang Feist. 2016. “Ventilation Concepts for Energy Efficient Housing in Central European Climate – A Simulation Study Comparing Indoor Air Quality , Mould Risk and Ventilation Losses.” in *Indoor Air 2016*. ISIAQ.
Rojas, Gabriel, Iain Walker, and Brett Singer. 2017. “Comparing Extracting and Recirculating Residential Kitchen Range Hoods for the Use in High Energy Efficient Housing.” Pp. 117–28 in *AIVC Proceedings*. AIVC.
Ruprecht, Jaenicke. 1993. “Tropospheric Aerosols.” Pp. 1–31 in *Aerosol-Cloud-Climate Interactions*, edited by P. Hobbs. Academci Press.
See, Siao Wei and Rajasekhar Balasubramanian. 2008. “Chemical Characteristics of Fine Particles Emitted from Different Gas Cooking Methods.” *Atmospheric Environment* 42(39):8852–62.
Shi, Bingbing. 2012. “Removal of Ultrafine Particles by Intermediate Air Filters in Ventilation Systems - Evaluation of Performance and Analysis of Applications Ventilation Systems.” Chalmers University of Technology, Göteborg, Sweden.
Shi, Bingbing, Lars E. Ekberg, and Sarka Langer. 2013. “Intermediate Air Filters for General Ventilation Applications: An Experimental Evaluation of Various Filtration Efficiency Expressions.” *Aerosol Science and Technology* 47(5):488–98.
Siegel, Jeffrey A. and William W. Nazaroff. 2003. “Predicting Particle Deposition on HVAC Heat Exchangers.” *Atmospheric Environment* 37(39–40):5587–96.
Sippola, Mark R. and William W. Nazaroff. 2003. “Modeling Particle Loss in Ventilation Ducts.” *Atmospheric Environment* 37(39–40):5597–5609.
Sjaastad, Ann Kristin, Kristin Svendsen, and Rikke Bramming Jorgensen. 2008. “Sub-Micrometer Particles: Their Level and How They Spread after Pan Frying of Beefsteak.” *Indoor and Built Environment* 17(3):230–36.
Stephens, B. and J. A. Siegel. 2012. “Penetration of Ambient Submicron Particles into Single-Family Residences and Associations with Building Characteristics.” *Indoor Air* 22(6):501–13.
Thatcher, Tracy L. and David W. Layton. 1995. “Deposition, Resuspension, and Penetration of Particles within a Residence.” *Atmospheric Environment* 29(13):1487–97.
Tian, Liwei, Guoqiang Zhang, Yaolin Lin, Jinghua Yu, Jin Zhou, and Quan Zhang. 2009. “Mathematical Model of Particle Penetration through Smooth/Rough Building Envelop Leakages.” *Building and Environment* 44(6):1144–49.
Torkmahalleh, M. A., I. Goldasteh, Y. Zhao, N. M. Udochu, A. Rossner, P. K. Hopke, and A. R. Ferro. 2012. “PM 2.5 and Ultrafine Particles Emitted during Heating of Commercial Cooking Oils.” *Indoor Air* 22(6):483–91.
Wallace, Lance. 2006. “Indoor Sources of Ultrafine and Accumulation Mode Particles: Size Distributions, Size-Resolved Concentrations, and Source Strengths.” *Aerosol Science and Technology* 40(5):348–60.
Wallace, Lance A., Steven J. Emmerich, and Cynthia Howard-Reed. 2004. “Source Strengths of Ultrafine and Fine Particles Due to Cooking with a Gas Stove.” *Environmental Science and Technology* 38(8):2304–11.
WHO. 2005. *WHO Air Quality Guidelines for Particulate Matter, Ozone, Nitrogen Dioxide and Sulfur Dioxide*.

Out2In: impact of filtration and air purification on the penetration of outdoor air pollutants into the indoor environment by ventilation

Joris Van Herreweghe[*1a], Samuel Caillou[1b], Tom Haerinck[1c] and Johan Van Dessel[1]

*1 **Belgian Building Research Institute (BBRI)***
a) Laboratory for Microbiology and Microparticles
b) Laboratory for Heating and Ventilation
c) Laboratory for Building Chemistry
Avenue Pierre Holoffe 21
1342 Limelette, Belgium
**Corresponding author: joris.van.herreweghe@bbri.be*

ABSTRACT

Within the ventilation principle of buildings, the **outdoor air is considered as a source of fresh, "clean" air.** Outdoor air quality monitoring by environmental agencies, academic research projects and a broad range of citizen science projects show that this is not always the case. Although the outdoor air quality in our cities already improved, the concentrations of **certain pollutants**, especially **particulate matter** and peak pollutions of **ozone** (and its precursors **nitrogen oxides** and **volatile organic compounds**), **remain problematic**. Ventilation systems may play a role in the introduction of these outdoor air pollutants into the indoor air, with potential adverse effects on the indoor air quality and the health of residents. The filters that are present in certain mechanical ventilation systems are primarily present to protect the system and its components against fouling, but have the potential to improve the quality of the supplied air.

In the context of indoor air quality, the **aim of this project** is to investigate: what role do mechanical ventilation systems play in the penetration of outdoor air pollutants? | to what extent is conventional air filtration sufficient? | what is the effectiveness and added value of advanced filtration and electrostatic precipitation as an innovative technique?

These research questions will be answered from a bottom-up research approach, including in-laboratory experiments on filters as a first step. The **novelty of our research approach** lies in the fact that: the measurements are carried out with the *real-life pollutant load of the Brussels outdoor air*, *the filtration efficiency for particulate matter* is considered in a *measuring range of 10nm-10µm* and is based on *number concentrations*, the filtration efficiency is *monitored in function of time* and the collection and penetration of *chemical pollutants* (O_3, NO_X and VOC) is also considered.

This paper presents the first **results of the in-laboratory measurement part**. For this part, a **test setup** consisting of **twelve parallel test lines equipped with either one or two different air filters/ -cleaning devices in cascade** was installed in our Brussels-based laboratory. The selected filters **allow a comparison between different filter classes** (G3,G4,F7,F9,H10), **or combinations of them,** and **also of different types within the same class** (wireframe, folded panel, bag type). Furthermore, two **filters containing active carbon** and two **electrostatic precipitators** are included in the test setup. This paper shows **time resolved data** including the **filter efficiency** and **pressure drop** on the filters/devices included in the test setup. The **preliminary results** on filter efficiency indicate a **large difference in performance between different filter types within the same filter class** and point to a high performance of the electrostatic precipitators within the full measuring range.

KEYWORDS

Ventilation | Particulate matter | Filter Performance | Indoor Air Quality

1 INTRODUCTION

There is an increasing awareness about the importance of **Indoor Air Quality** in our buildings. Not least because of the realization that we spend most of our time indoors during which we can get exposed to potential harmful pollutants for a long time span. As recognized by both national and international (e.g. WHO) bodies, some of these indoor pollutants have a negative impact on our comfort, cognitive performance and health in general.

Preventing and minimizing the release of pollutants at the source (I), the removal of inevitable pollutants from the indoor air (II) and prevention of penetration of outdoor air pollutants in the indoor environment (III) are the three cornerstones to obtain a good indoor air quality. **Ventilation** plays a prominent role in this, especially in the second and third cornerstone. Within the ventilation principle, no matter the method, the polluted indoor air is replaced/diluted by **outdoor air, which is considered as a source of fresh and "clean" air**.

It goes without saying that the outdoor air cannot always be regarded as pure, especially in city environments. Although the **outdoor air quality** already improved in cities like Brussels, some pollutants, in particular **ozone** (and its precursors **NO_x & VOCs**) and **particulate matter** remain problematic. The principle sources of NO_x and particulate matter are combustions processes as in car engines (traffic) and heating systems of buildings.

Particulate matter is defined as a complex mixture of extremely small particles and liquid droplets present in the air. According to their aerodynamic diameter they are classified into coarse [PM_{10} (< 10µm)], fine [$PM_{2.5}$ (<2.5µm)] and ultrafine particles [$PM_{0.1}$ (<0.1µm) = UFP]. Black carbon, which consists of pure carbon in several linked forms (≈ soot), are in general particles with a size comprised between 20-150nm and are directly linked to combustion processes. The mass concentration of PM_{10} and $PM_{2.5}$ in the outdoor is regulated on an EU-level and more severe guide values from the WHO are available. By contrast, UFP and black carbon concentrations are not regulated, neither are there guide values available. However, the smaller particles are, the deeper they can penetrate our respiratory system and the greater the potential health risks are.

From a **health** point of view, a poor outdoor air quality is worldwide responsible for over 6 million deaths a year (± 8000 for Belgium). It largely contributes to death as a result of stroke, lung cancer, cardiovascular - and chronic pulmonary disease. The total social cost for Belgium amounts to 8 million euros a year.

Given the magnitude and the impact of outdoor air quality problems in our cities and the fact that our buildings are becoming more airtight (meaning less uncontrolled infiltration), the following **research questions** arise: *what role do mechanical ventilation systems play in the penetration of outdoor air pollutants into the indoor environment? | to what extent is conventional air filtration sufficient? | what is the effectiveness and added value of advanced filtration and electrostatic precipitation as an innovative technique?*

2 MATERIALS AND METHODS

2.1 Test setup

To answer the above questions, a test setup was constructed in our Brussels-based laboratory. As illustrated by Figure 1 A, this test setup consist of 12 parallel test lines which are all connected to a distribution box. Inside this distribution box (see C & D) a partition plate with

four square openings is foreseen to evenly distribute the air to the different test lines. At his turn the distribution box is connected to the outdoor air by two supply boxes (see C) **allowing the measurements to be conducted with the real-life pollutant load of the Brussels outdoor air.** The exhaust air (red) of each line is collected and evacuated to the outdoor air at the other side of the laboratory.
Each test line is composed of one or two **filter boxes/devices** (inter)connected to the other parts by **round metal ductwork (ø160 mm)** (see § 2.2 for the selected filters/devices), a **constant flow fan** set at 150 m³/h and a **diaphragm** allowing to measure the air flow rate on the basis of a differential pressure measurement.

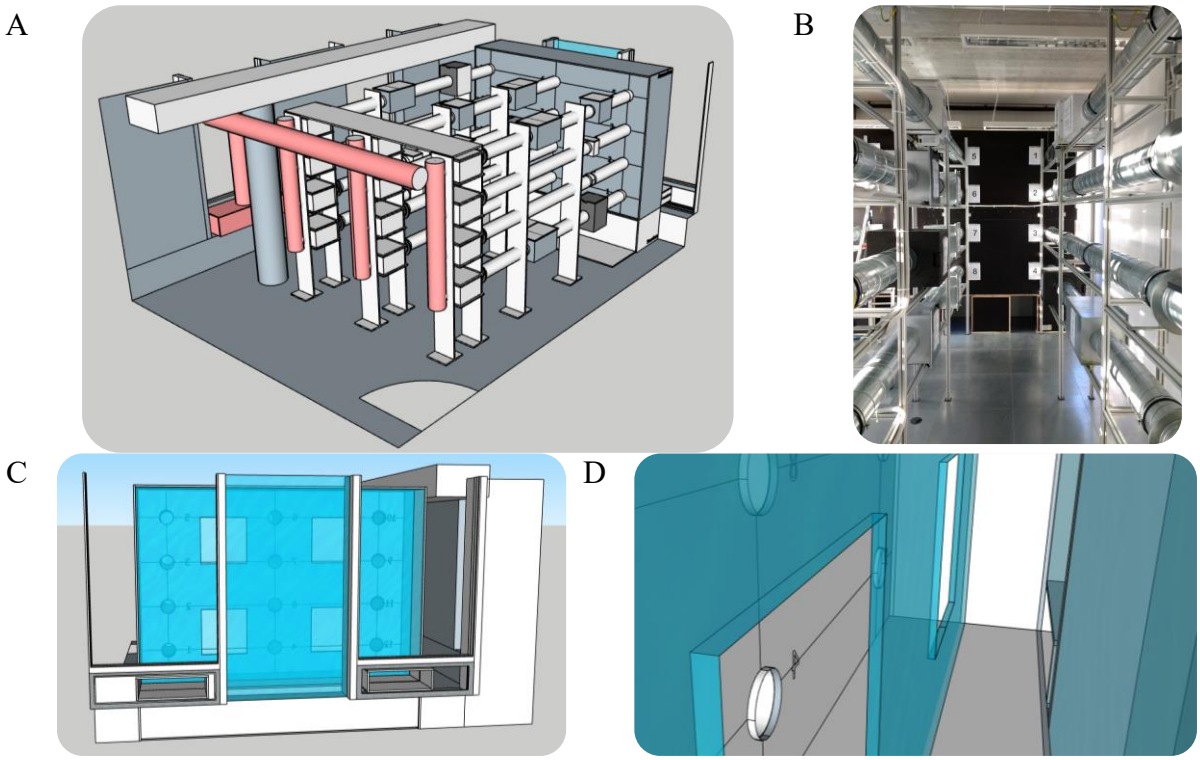

Figure 1 Computer-based design model and picture of the test setup as built: A) general view B) picture of a part of the test setup C) detailed view of the distribution box and the supply boxes integrated under the windows D) interior view of the distribution box

2.2 Selected filters and devices

Classic filters – six test lines are equipped with filters or combinations of them which are nowadays already used in ventilation systems. This includes coarse filters (G3 and G4 class filters according to EN779[1][1]) and a fine filter (F7 class). From the same classes also different types of filters were included like duct type, wireframe, folded panel and bag type filters (see *Figure 2*).

A **B** **C** **D**

[1] By the time the filters were purchased, the EN779:2012 standard was still in use. In the meanwhile, is has been replaced by the EN ISO-16890:2016 standard [3] which makes use of a different method and classification of filters. As an indication, the G3 and G4 classes would now correspond to ISO-coarse >80% and >90% (dust arrestance), F7 to ePM1 50-65% or ePM2.5 65-95% and F9 to ePM1> 80% or ePM2.5>95% (efficiency).

Figure 2 Pictures of the different tested filter types:
A) G3 duct type, B) G4 wireframe, C) G4 folded panel, D) G4 bag type

Intensive filtration – four test lines are equipped with filters which are nowadays rather exceptionally in use in domestic ventilation systems including an F9 and H10 filter (= E10, Efficiency Particulate Air filter, EN1822:2009 [2]). These filters are all of the folded panel type.

Innovative devices – two test lines are equipped with electrostatic precipitators (ESPs). Although, the principle of electrostatic precipitation is known for decades and already used in industrial applications, only recently devices connectable to domestic ventilation systems became available on the market. An electrostatic precipitator in general consists of two parts: the ioniser and the collector. Within the ioniser, the air and its particulate load will get charged (in this case positively) due to the corona discharge principle (high voltage on a small electrode). Within the second part, the ionised particles are then collected on collector plates with an opposite or neutral charge. In one of the systems included in the test setup, the ioniser (thin horizontal wires between the collector plates) and collector (multiple horizontal aluminium plates) are integrated into one piece which must be cleaned using a soap solution after a certain while in use. In the second system, the ioniser and collector are two separate parts, which might even be installed with a certain distance in between. Within this system the collector part consists of two consecutive polypropylene plates with a honeycomb structure and are considered as consumables (needs to be replaced after a while in use).

2.3 Measurements

Differential pressure over each filter box or device is measured on a monthly basis using a TSI PVM-620 manometer. To enable these measurements an airtightly sealed nipple was integrated in the duct, before and after each filterbox/device, to which the manometer can be connected for measurement. The reported value is an average value of three consecutive measurements of 10s each.

Particulate matter load of air samples is measured in number-based concentrations within the range of 10nm up to 10µm using two different devices. Particles within the size range of 10-420nm are quantified using a Scanning Mobility Particle Sizer (TSI, Nanoscan 3910 SMPS), while those between 0.3-10µm using an Optical Particle Sizer (TSI, OPS 3330). The measurements are conducted according to a procedure based on the Eurovent 4.10 guideline [4]. This guideline describes a method for in situ determination of fractional efficiency of general ventilation filters. Briefly outlined, the particle load is consecutively measured before and after each filter, by inserting an isokinetic sampling probe into the duct, for in total respectively 7 and 6 measurements of one minute each. Fractional efficiencies are calculated six times using each time two measurements in front and one measurement after the filter. The reported values are mean efficiency values with indication of the 95%

confidence interval. Whenever absolute values are reported they are expressed in the number of particles/L in dN/dlogDp format allowing inter-instrumental comparison of the results.

Ozone production was verified using a Teledyne T204 gas analyser.

3 RESULTS AND DISCUSSION

3.1 Typical profile for the particulate load of the outdoor air in Brussels

As stated before, the efficiency of the filters in the test setup is determined using the real-life particulate load of the Brussels outdoor air. The graph below shows a typical number-based profile of the particulate load in the Brussels outdoor air. This profile indicates that mainly particles belonging to the smaller particle classes ($PM_{0.01-0.1}$ & $PM_{0.1-0.5}$) are dominating the particle load. They respectively represent 81 and 19% of the total particulate load. Particles with a size above 0.5µm only represent 0.044% of the total particulate load.

These results also indicate that it is for most of the particle sizes feasible to determine the fractional efficiency according to Eurovent 4.10 (number/L in front of filter > 37/L). Only for the largest particles the numbers (> 6µm) are in general too low, resulting in larger uncertainty on the obtained results.

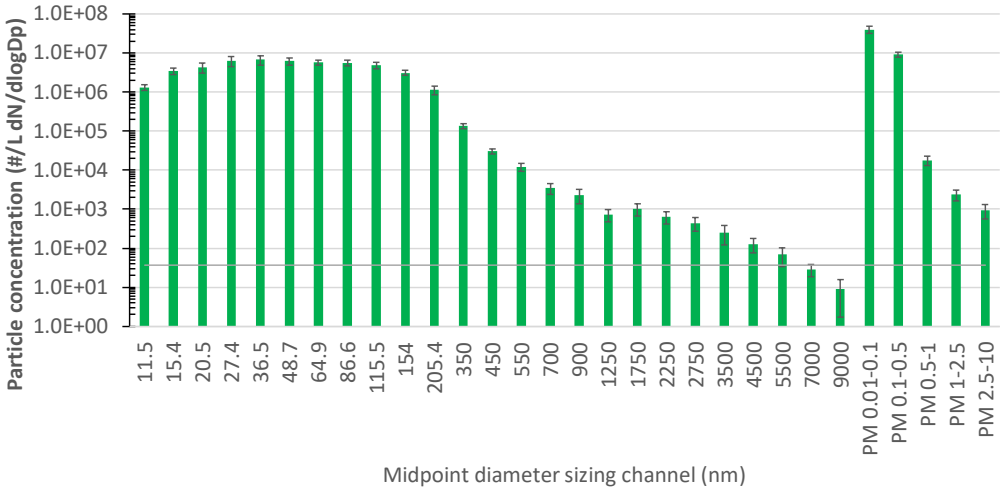

Figure 3 Typical profile of the particulate load of the Brussels outdoor air expressed in number of particles/liter within the measurements range of 10nm-10µm. In the left part of the graph, the number of particles for each sizing channel within the measurement range are indicated (size indications in nm). In the right part of the graph, the measured number of particles are aggregated into particle classes (size indications in µm). The grey line indicates the minimal number of particles (37 particles/L) upstream of the filter for efficiency determination according to Eurovent 4.10.

3.2 Coarse filters (G3 and G4)

As the graphs below indicate, the **filter efficiency** for particles < 1µm is rather low for coarse filters. The only exception to this is the G4 folded panel filter at new state (*Figure 4* A). This is most likely due to a static electrostatic charge given to the filter medium during production (Electret Filter medium). As a result, these types of filters have electrostatic interaction as an additional retention principle besides the mechanical retention principles, resulting in an increased efficiency at new state. However, during use this charge gets lost explaining the lower efficiency of this filter after 2.5 months in use (*Figure 4* B). The decrease in efficiency

manifested itself already after 238 hours (1/3th of a month) in continuous use (data not shown).

For the folded panel filter type, a much higher efficiency can be observed for the G4 filter in comparison to the G3 filter. Within the same filter class, large differences in efficiency can be observed between the different filter types (e.g. G3: duct vs. folded panel | G4: wire frame vs. folded panel vs. bag type). In function of time the efficiency of the folded panel filter types tends to decrease, while the efficiency for the duct, wireframe and bag type filters increases. Especially for the duct and wireframe filter types, which are characterized by a small filter surface, this might be explained by the influence of the filter cake that gradually builds up on the filter surface.

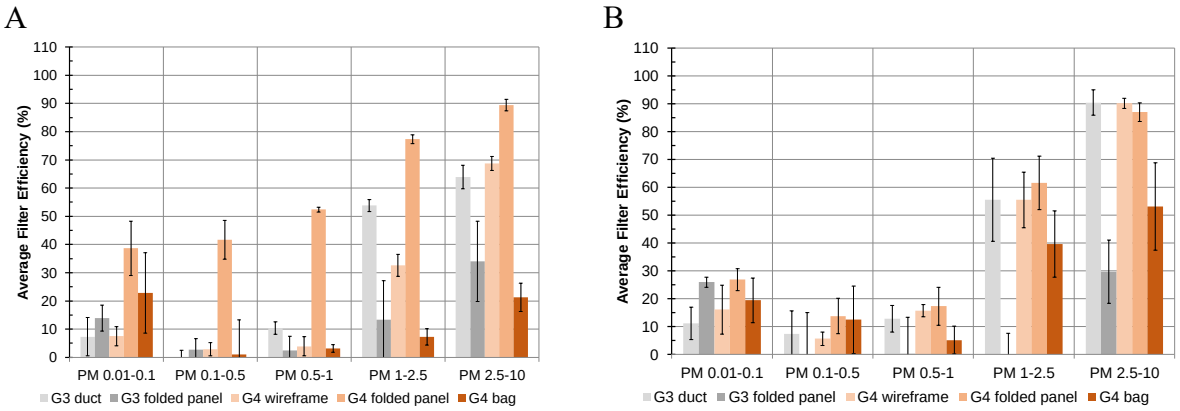

Figure 4 Average filter efficiency of coarse filter types with indication of the 95% confidence interval at new state (A) and after 2.5 months of continuous use (B). Results for the filters of the G3 class are given in grey, those for the filters of the G4 class in orange.

The G3-duct and G4-wireframe filter types exhibit a relatively high initial **pressure drop** (see *Table 1*) and a strong increase in function of time compared to the other coarse filters. The reason for this lies in the limited filter surface of this type of filters.

*Table 1 Pressure drop (Pa) as a function of time for the coarse and fine filters and the electrostatic precipitators (ESP), cc: cleanable collector, taw-c: throw away collector, FP= folded panel, B=bag, * protected by a G4 FP coarse filter*

→ filter class and type	G3		G4			F7*	F9*	H10*	ESP	
↓time elapsed	duct	FP	wireframe	FP	B	FP			cc	taw-c
Initial	88.4	8.6	36.9	11.4	7.1	23.2	24.5	28.3	8.3	16.3
1 month	136.4	11.7	71.7	19.0	9.3	25.9	24.5	29.7	9.5	17.1
3.5 months	198.1	12.8	115.4	47.0	9.9	28.2	26.2	29.0	12.8	19.1

3.3 Fine filters (F7, F9, H10)

As can be expected, fine filters are in general more efficient than coarse filters (see *Figure 4* & *Figure 5*). Upon comparison of the tested F7 and F9 filter, the results indicate a slightly, but non-significant, higher efficiency for the F9 filter throughout the complete measurement range. Both filters however show a dip in their efficiency for the particle classes $PM_{0.1\text{-}0.5\ \mu m}$ and $PM_{0.5\text{-}1\mu m}$. As shown by the fractional efficiency profile for the F7 filter (*Figure 5 C*) this dip in efficiency (< 80%) extends from particles with an aerodynamic diameter of 56nm to 800nm. The tested H10 filter at new state on the other hand, shows a very high efficiency within the full measuring range (see *Figure 5 A & D*). After two and half months in continuous use, the F7 and F9 filters do not show an obvious difference in efficiency, while for the H10 a decrease for the classes $PM_{0.1\text{-}0.5}$ and $PM_{0.5\text{-}1\mu m}$ can be observed.

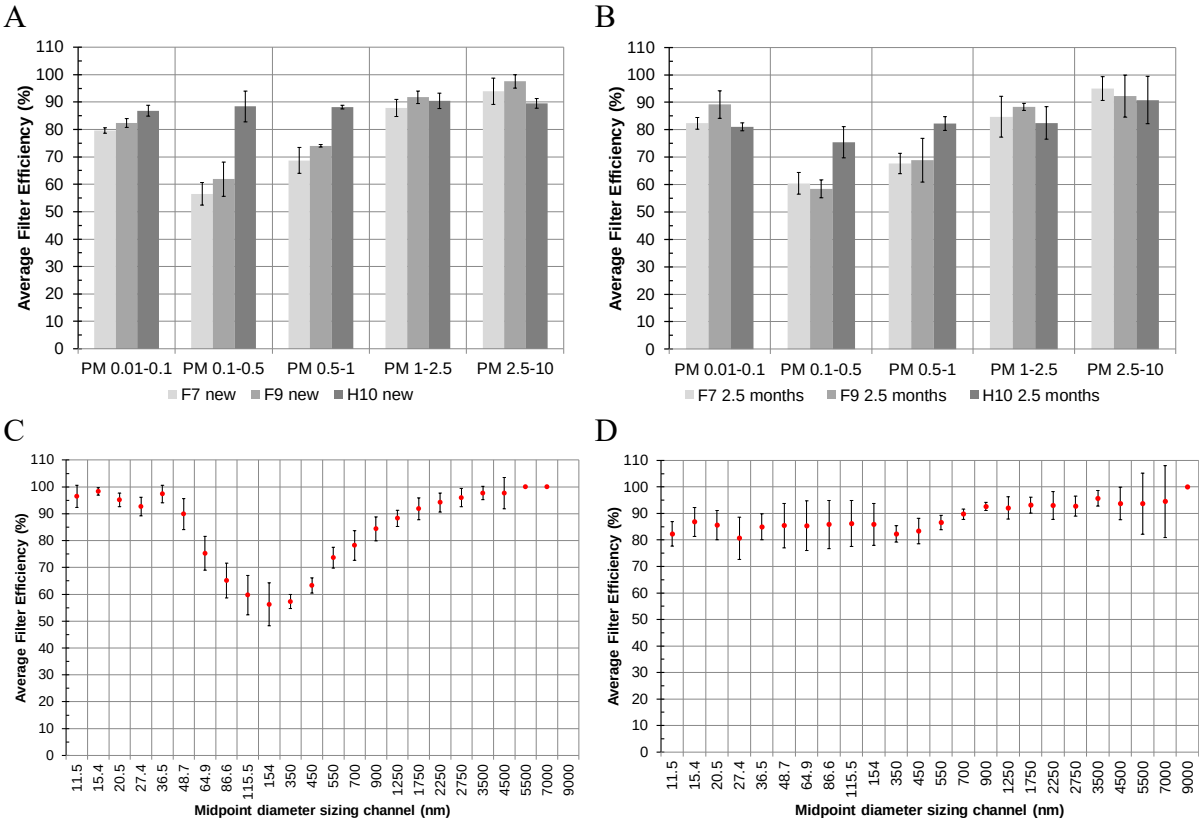

Figure 5 Average filter efficiency of fine filter types with indication of the 95% confidence interval at new state (A) and after 2.5 months of continuous use (B). Fractional efficiency profile within the complete measurement range (10nm-10µm) for an F7 filter (C) and an H10 (D) after 1 month in continuous use.

At new state the pressure drop caused by the fine filters is larger than the ones observed for most coarse filter types (except for the wireframe and duct type filter) (see *Table 1*). The differences in pressure drop between the fine filter classes are rather small, even after 3.5 months in use. It must be mentioned that each of the fine filter classes is installed in a test line with the same G4 folded panel filter as a prefilter.

3.4 Electrostatic precipitators

Both precipitators exhibit a very high efficiency (>96%) within the full measuring range at new state. After 2.5 months in use, the version with the cleanable collector still shows a high efficiency throughout the measuring range, while for the version with throw away collectors the efficiency for some particle classes, more precisely $PM_{0.01-0.1}$ and $PM_{0.5-1}$ dropped. Visual inspection of the collector plates indicates that a black coloration can be observed at the back of the collector plates, indication that the collector gradually becomes saturated.

In absolute numbers, the large initial efficiency results for the particle classes $PM_{1-2.5}$ and $PM_{2.5-10}$ in a small number of particles in the air (< ± 10 particles/L) after the ESP unit (*see Figure 6 C*). For the $PM_{0.5-1}$ class, the ESP causes a considerable reduction from 100.000 to < 1000 particles/L. However, despite the very high observed efficiencies at new state (> 99%) for the smallest particle classes, a very large number of particles remain in the air (1.000.000 for $PM_{0.01-0.1}$ | > 100.000 for $PM_{0.1-0.5}$) after de ESP unit.

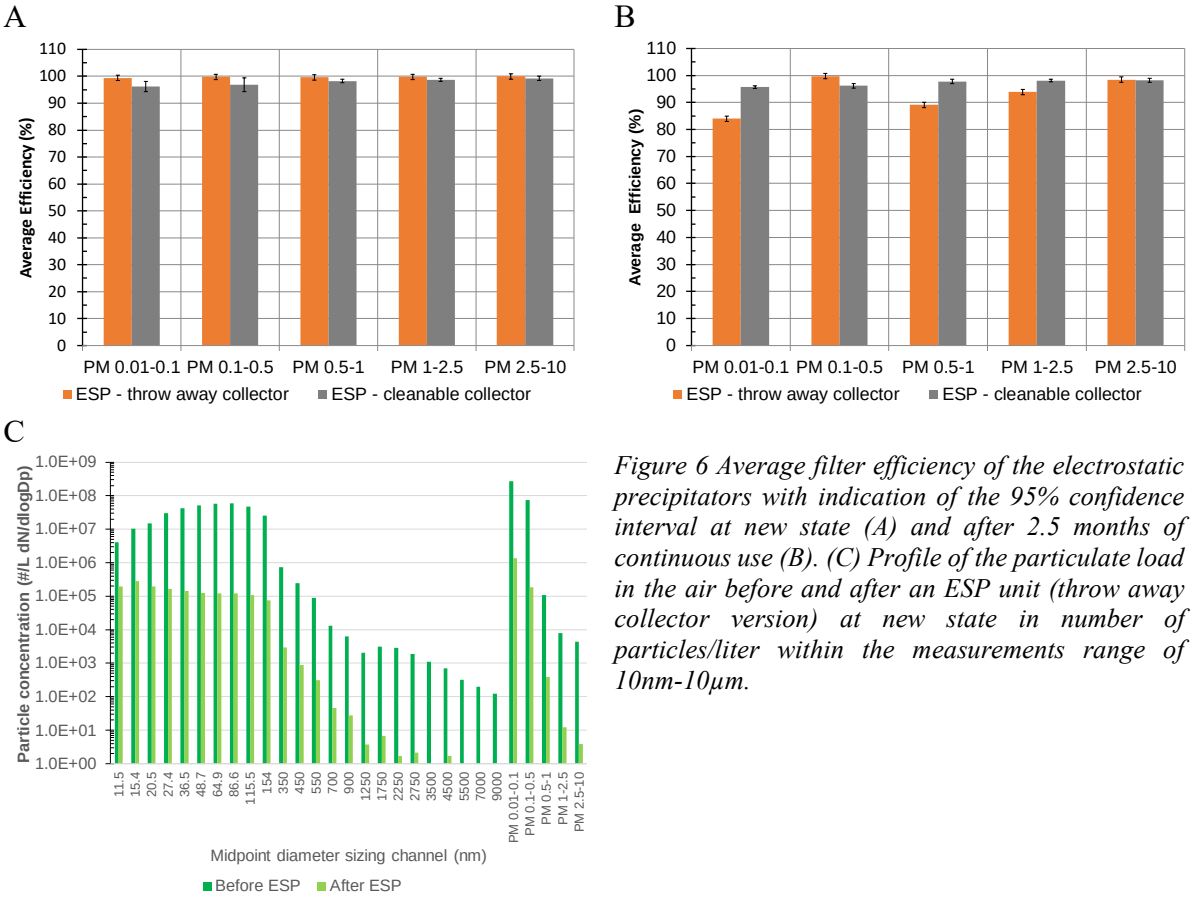

Figure 6 Average filter efficiency of the electrostatic precipitators with indication of the 95% confidence interval at new state (A) and after 2.5 months of continuous use (B). (C) Profile of the particulate load in the air before and after an ESP unit (throw away collector version) at new state in number of particles/liter within the measurements range of 10nm-10µm.

The pressure drop over the system with cleanable collector plates is lower than that of the version with throw away plates (see *Table 1*). This is a result of the more open inner structure of the cleanable system. However, for both systems their pressure drop is rather small in comparison to the pressure drop over the tested fine filters and only has a small tendency to increase in function of time. Moreover, the ESPs are not protected by a prefilter as is the case for the fine filters. The ozone production was found to be limited for both systems (cleanable: 9.1±1.5 and throw away:5.9±1.8 ppb).

4 CONCLUSIONS

Throughout our measurement we observed that, based on number concentrations, the outdoor air particulate load in Brussels is mainly dominated by **very small particles.** Especially ultrafine particles (< 0.1 µm) are gaining research attention because they can penetrate deeper into our respiratory system an even our bloodstream leading potentially to greater health risks.

Coarse filters are mainly installed in balance ventilation systems to protect the system (including heat exchanger, fans,..) and the ductwork against rapid fouling. Their efficiency, especially for particles smaller than 1µm, was found to be rather limited. Moreover, a large variability in efficiency was observed for different filter types within a same coarse filter class (G3 or G4). Therefore, coarse filters cannot be considered as contributing to an improved air quality in terms of particulate load. The use of coarse filters with a small filter surface should be avoided because of their typical very high initial and sharply increasing pressure drop.

Fine filters, have the potential to improve the quality of the supplied air by a ventilation system in terms of particulate load. However, F7 and F9 filters show a dip in their efficiency profile for particles between 56-800nm, including part of the ultrafine particles. This dip is not observed for the tested H10 (efficiency particulate filter) at least at new state. Further follow-up is necessary to get a better picture of the evolution of the efficiency of these filters and their pressure drop.

Electrostatic precipitation seems a promising technique due to the high efficiency of particle capture within the full range (10nm-10µm) and the associated low pressure drop in comparison to fine filter.

Further research will be necessary to understand the impact of the remaining load of very small particles in the air after fine filters and electrostatic precipitators. For the electrostatic precipitators also the potential effect that ionized air might have on human health should be looked at.

5 ACKNOWLEDGEMENTS

The authors wish to thank Innoviris Brussels for the financial support.

6 REFERENCES

[1] EN779:2012, *Particulate air filters for general ventilation - Determination of the filtration performance,* European Committee for Standardization

[2] EN 1822-1:2019, *High efficiency air filters (EPA, HEPA and ULPA) - Part 1: Classification, performance testing, marking*, European Committee for Standardization

[3] EN ISO 16890-1:2016, *Air filters for general ventilation - Part 1: Technical specifications, requirements and classification system based upon particulate matter efficiency (ePM)*, European Committee for Standardization

[4] Eurovent 4.10:2005, *In situ determination of fractional efficiency of general ventilation filters*, Eurovent/Cecomaf

Future trends in laboratory methods to predict HVAC in service filter performance

Jesús Marval[1], Luis Medina[1], Emanuele Norata[1] and Paolo Tronville[*1]

[1]Politecnico di Torino
Corso Duca Degli Abruzzi 24
10129 Turin, Italy
**Corresponding author: paolo.tronville@polito.it*

ABSTRACT

Air filters installed in ventilation systems face various types of aerosols during their service life, both in residential and in commercial buildings. Their particle size is the most important characteristic and ranges from a few nanometers to a few micrometers. Different physicochemical properties, such as phase state, hygroscopicity, and morphology are also important to determine the impact of particulate matter on the behavior of air filters during their service life. Therefore, the performance of air filters installed in a Heating, Ventilation and Air-Conditioning (HVAC) system is strongly dependent on the properties of the particles captured during their service life and not only on the characteristics of the materials and technologies used to manufacture the air cleaning equipment.

Current laboratory test methods for evaluating HVAC filter performance include the determination of their fractional particle removal efficiency on a limited size range, typically between 300 nm and 10000 nm. Such information is useful and meaningful for clean filters. However, air filters performance (i.e. airflow resistance and removal efficiency) changes during their service life because of particle loading. For this reason, air filters are artificially clogged in laboratory with the intent to compare one product to another and to predict their behavior while they age in HVAC systems. Current standardized air filter loading procedures use synthetic dusts with particle size distributions very different from typical urban atmospheric aerosols. Consequently, the results obtained in this way differ from the air filter performance measured in real HVAC installations and the designers cannot use them to predict quantitatively the in-situ air filter performance. Standards writers are aware of the problem and this limitation is stated explicitly in EN ISO 16890 and ANSI/ASHRAE 52.2 standards. However, there is a need to perform the test in a short time. Moreover, the filtration industry consolidated this approach during the past decades and a lot of data is available with those dusts.

To improve the prediction of the size-resolved efficiency and the loading kinetics of HVAC filters we need improved test methodologies. ASHRAE is promoting the development of a new method to age air filters as part of ASHRAE Guideline Project 35 “Method for Determining the Energy Consumption Caused by Air- Cleaning and Filtration Devices”. Research teams in USA and Italy are attempting to improve the loading procedure to age HVAC filters using aerosols with more realistic particle size distributions. If successful, the new ageing procedure could provide a reliable prediction tool for evaluating the airflow resistance during the filter service life. In this way, we could optimize the performance of air cleaning equipment in realistic conditions.

In this paper, we summarize current laboratory ageing procedures. We compare the airflow resistance trend in an HVAC system monitored for more than one year, with the results from an ISO 16890 laboratory test on the same air filter. We discuss the difference between the mass increase values causing the same airflow resistance increase.

To reduce the difference between actual data and laboratory simulation results, we present an emerging technique with a preliminary evaluation of a new thermal flame generator for challenging HVAC filters with sub-micron potassium chloride aerosol at high mass concentrations. The thermal aerosol generator is able to reproduce the sub-micron urban atmospheric aerosol mass size distribution and it is a promising technique to solve some of the problems stated above.

KEYWORDS

Air filter test, urban aerosol size distribution, synthetic dust, nanoaerosol, air filter ageing.

1 INTRODUCTION

To assess properly the performance of air filters for general ventilation we need to evaluate their service life together with their initial airflow resistance and capability to capture particles. In fact, the behavior during their service life influences the required replacement interval and their average airflow resistance during operation. Both the duration of service and the particle removal performance of air filters installed in Heating, Ventilation and Air-Conditioning (HVAC) systems depend not only on the characteristics of the materials and technologies used to manufacture them, but also on the properties of the challenging aerosols. These properties include particle size, phase state, hygroscopicity, and morphology. An especially relevant property is the particle size distribution (PSD) of the challenging aerosol, which determines the loading kinetics of air filter media and the full-scale filter ageing process.

Current methods to evaluate the test dust capacity (also known as dust holding capacity) of an air filter provide a way to assess the performance in terms of duration in an abbreviated and cost-effective manner, by using synthetic dusts to simulate filter ageing. The characteristics of those dusts respond to the need for short-duration (hours) laboratory tests to simulate the behavior of an air filter over a much longer period (months). In addition to that, the test dusts must be relatively inexpensive and easily reproducible, so that different laboratories around the globe can use them and expect the same PSD of the test dust.

The new ISO 16890 standard series accomplishes such requirements by using a purely silica-based dust, with the intent of improving the repeatability and reproducibility of the measurements, compared to the carbon and vegetal fibers-based dusts used in ANSI/ASHRAE 52.2 standard. However, the PSD of the synthetic dusts is dramatically different from the PSD of the urban atmospheres challenging the filters during their operation. This is one of the reasons why we cannot use the results obtained ageing the filters with those synthetic dusts to predict quantitatively the in-situ air filter performance. EN ISO 16890 and ANSI/ASHRAE 52.2 standards state this limitation explicitly.

Most HVAC systems are in urban areas where approximately 80% of the population of the developed regions live and work (United Nations, Department of Economic and Social Affairs, Population Division, 2018). Filters cleaning the air in those HVAC systems are especially important when outdoor air is highly polluted. The PSD of particulate matter in polluted urban areas contains large amounts of nanoparticles generated by human activities. We should consider this as a key aspect when trying to reproduce in the laboratory the behavior of air filters cleaning outdoor polluted air.

2 URBAN ATMOSPHERIC AEROSOLS VS SYNTHETHIC DUSTS

Urban aerosols are mixtures of primary particulate emissions from industries, transportation, power generation, and natural sources; and secondary material generated by gas-to-particle conversion mechanisms. If we consider the number PSD for this kind of aerosols the major fraction is represented by particles smaller than 0.1 μm, while most of the surface PSD falls in the size range of 0.1 - 0.5 μm (Seinfeld & Pandis, 2012). On the other hand, the aerosol mass PSD usually has three distinct modes. The first two correspond to the sub-micrometer size range (nuclei and aggregation modes), while the third one is characterized by coarse particles of larger sizes.

The smaller particles form the nuclei or nucleation mode and are generated by primary particle formation processes of anthropogenic nature (mainly from combustion processes) and gas-to-particle transformations (nucleation), which create and emit the sub-micron particles in the atmosphere. These particles represent the greatest portion of the number PSD in an urban aerosol but give a rather small contribution to the mass or volume PSD and have a relatively short duration in the atmosphere. Moreover, because of the high concentrations of nuclei, especially at relatively short distances from the sources (in the order of few hundreds of meters), most of them coagulate quickly with each other, which determines an overlapping zone with the accumulation mode.

In the case of the accumulation mode, the particles are formed by photochemical reactions between volatile organic compounds (VOC) and nitrogen oxides present in the atmosphere under the effect of intense sunlight. Particles in the accumulation mode are also originated from the nucleation, condensation and aggregation processes of the smaller nuclei. The volume/mass distribution of this mode is centered mainly in the 0.1–2 μm size range (Seinfeld & Pandis, 2012). Together with the nuclei, the particles belonging to the accumulation mode constitute the so-called "fine" particles, which represent the relevant part of the number size distribution of an urban aerosol.

The coarse mode, instead, is characterized by particles generated from natural processes, such as wind erosion dusts and sea salt spray particles; and anthropogenic sources, like agriculture and mining activities. Due to their larger size, these particles have a short atmosphere lifetime (a few hours or days) and are rapidly captured in surfaces or deposited from gravity effect (Hinds, 1999).

Interestingly, the accumulation and coarse particle modes present comparable mass concentrations for most urban areas, despite of the high variability in the PSD within a given city (Seinfeld & Pandis, 2012). For this reason, it is important to distinguish the different modes, and analyze the urban aerosol PSD both in terms of particle mass and number distribution.

Previous works by Stephens (Stephens, 2018) and Azimi (Azimi, Zhao, & Stephens, 2014) studied the characteristics of 194 long-term PSD datasets from more than 10 different locations around Europe and North America, collected between 1996 and 2011. This information was compared with historical distributions that have been used as reference in widely recognized textbooks, such as the one by Seinfeld (Seinfeld & Pandis, 2012). While the latter constitutes the current basis for the definition of the assessment standards for air filter performance, the more recent PSD data analyzed in the aforementioned studies show lower concentration values for the number size distributions when compared to the historical data (Stephens, 2018).

Despite this slight discrepancy, the overall shape and parameters of the particle mass/volume distributions of the studied urban atmospheric aerosols can be regarded as similar to the historical representations. In particular, the presence of two distinct modes, one of which with high values of mass/volume in the sub-micrometer range, corresponding to the previously mentioned accumulation and nuclei modes. This supports the evidence of similar characteristics between different urban atmospheres around the world and provides a solid basis for taking a common urban atmospheric aerosol PSD as a reference for testing and assessing the performance of HVAC filters. To do this, it would be necessary to generate in the laboratory suitable test aerosols with particle size distribution similar to the reference one, at higher concentrations and within a defined tolerance.

On the contrary, the volume PSD of currently standardized test dusts, such as the ISO fine A2 dust used by ISO 16890, are completely different from the urban atmospheric aerosols. This difference is evident in Figure 1 below, in which we compare the cumulative size distribution plots of the ISO fine A2 dusts (previous and current version) and the reference urban atmospheric aerosol adopted by ISO 16890 series.

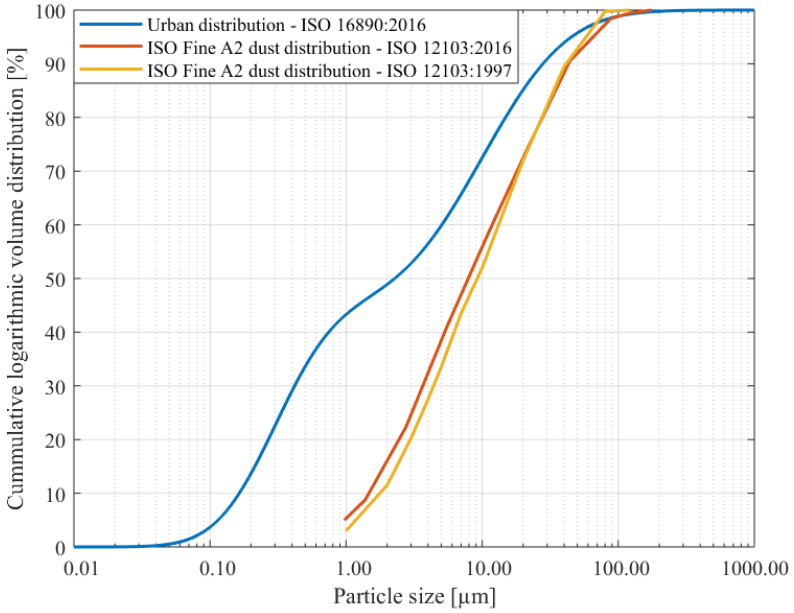

Figure 1 Cumulative PSD plots of A2 synthetic dust and typical urban aerosol adopted by ISO 16890

We highlight that about 50% of the particles in the urban atmospheric aerosol mass distribution adopted by ISO 16890 series are smaller than the smallest particles in ISO fine A2 dust.

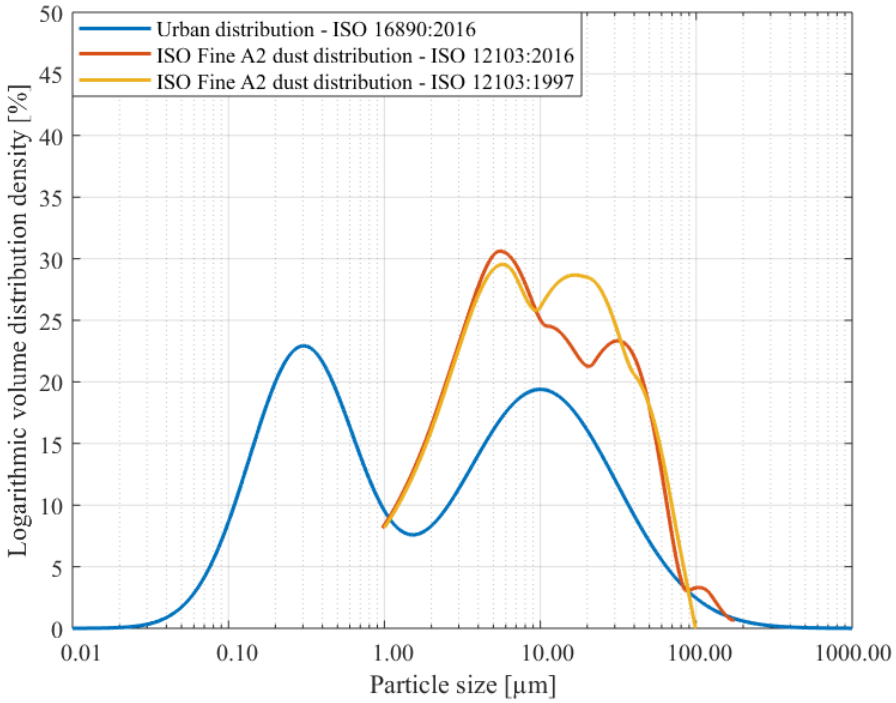

Figure 2 Volume PSD plots of A2 synthetic dust and urban aerosol

Figure 2 compares the logarithmic volume distribution densities of the typical urban atmospheric aerosol adopted by ISO 16890 and the ISO fine A2 dusts. This figure is even clearer in showing the huge difference between those particle size distributions. Those plots show that current synthetic test dusts cannot represent any urban environmental condition challenging the air filters used in HVAC systems during their operation. We cannot ignore such huge difference if we want to get data from laboratory tests that can predict reliably the in-situ performance. Previous analyses (Tronville & Rivers, 2005) have provided similar results, comparing an urban aerosol volume PSD with two different synthetic aerosols and two standard dusts.

3 COMPARISON BETWEEN IN-SITU AND ARTIFICIAL FILTER AGEING

As discussed in the previous sections, the differences in the PSDs of synthetic dusts and urban atmospheric aerosols yield significant discrepancies in the prediction of the air filters duration over time, and the performance change throughout their service life. In fact, current test methods provide a test dust capacity that is commonly used to predict the mass of particles causing a certain increase of airflow resistance. Many experts use this value to determine the expected filter duration in service.

However, long term data collected in-situ from air filters installed in HVAC systems for general ventilation purposes, demonstrated that filters working in real applications at the same airflow rate can reach the same airflow resistance values after capturing much lower amounts of particles.

We report and compare some performance data measured on three 4Vs compact filters (same model and manufacturer). The filter media of those filters was wetlaid fiberglass and their ISO 16890 ratings $e\text{PM}_{2.5}$ 90% (which could be reported also as $e\text{PM}_{1}$ 86%, and $e\text{PM}_{10}$ 97%). The pressure drop values were measured using a Siemens QBM65.1-10 differential manometer in the air-handling unit and an Aplisens APRE-2000G/N differential pressure sensor for the laboratory tests.

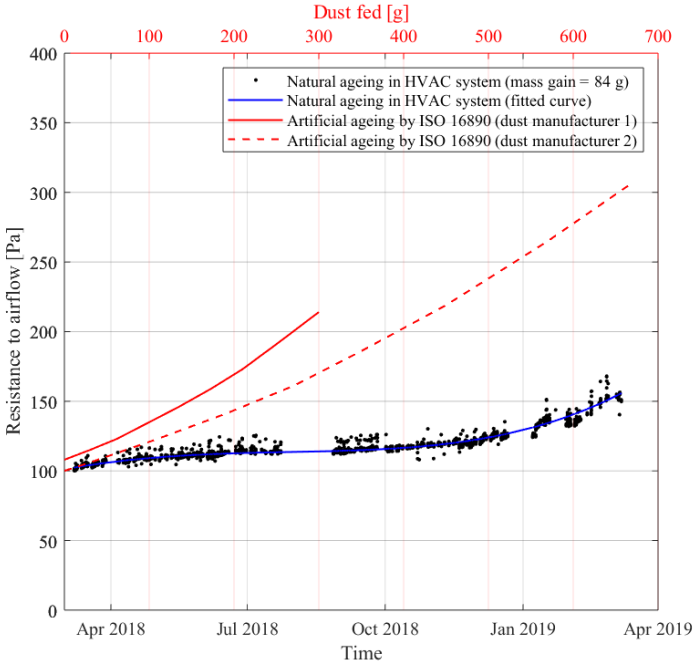

Figure 3 Comparison between in-situ airflow resistance data and laboratory assessment. The bottom abscissa (Time) is associated with the natural ageing data and fitting curve. The upper abscissa, in red color, corresponds to the artificial ageing data, represented by the red curves.

Figure 3 shows the airflow resistance data obtained during natural and artificial filter ageing with the same airflow rate. The data representing the natural ageing was measured as the pressure drop across the filter bank made up by two full size (592x592 mm) and two half size (592x287 mm) filters. We collected the data during several years of service even if we report the data for this filter set only. The artificial ageing results were obtained from two laboratory-clogging tests according to ISO 16890 performed on other two filter samples. We used ISO fine A2 dusts from different manufacturers to study the reproducibility of that dust. Both the laboratory and the in-situ ageing were performed at 3400 m^3/h.

The monitored HVAC system is serving a university classroom at Politecnico di Torino, Italy. Two separate time intervals where no data is available correspond to a one month pause in the operation during the summer break in August and another two weeks in December. After nearly one year of service, the filter increased its airflow resistance of about 50 Pa. This increment corresponded to about 84 grams of particles collected during its service life, as it was determined by weighting the 4 filters of the filter bank after dismounting and calculating the average of mass gain (comparing the final weight with the initial one before installation).

Figure 4 HVAC unit used for the natural ageing of the filters.

The curves representing the artificial ageing provide the mass of dust fed causing the corresponding increment of airflow resistance during the laboratory test. The curve obtained by using the synthetic dust from the manufacturer 1 (continuous line) shows that a pressure drop increase of 50 Pa is obtained after loading the filter with around 170 g of the ISO fine A2 dust. In contrast, about 225 g of the A2 dust made by the manufacturer 2 were needed to reach the same pressure drop on another sample of the same filter.

This comparison is a clear example of the different behavior caused by the different PSDs of the synthetic dusts and of the urban atmospheric aerosol. The discrepancy between laboratory results and field data is glaring. An air filter can reach the same pressure drop values as in the

laboratory with lower amounts of mass of captured dust when challenged with aerosols having PSDs shifted towards smaller sizes, as in the case of urban atmospheric aerosols. We can clearly appreciate this difference here below in Figure 5, where we plot the filter mass gain against the airflow resistance values in the three cases.

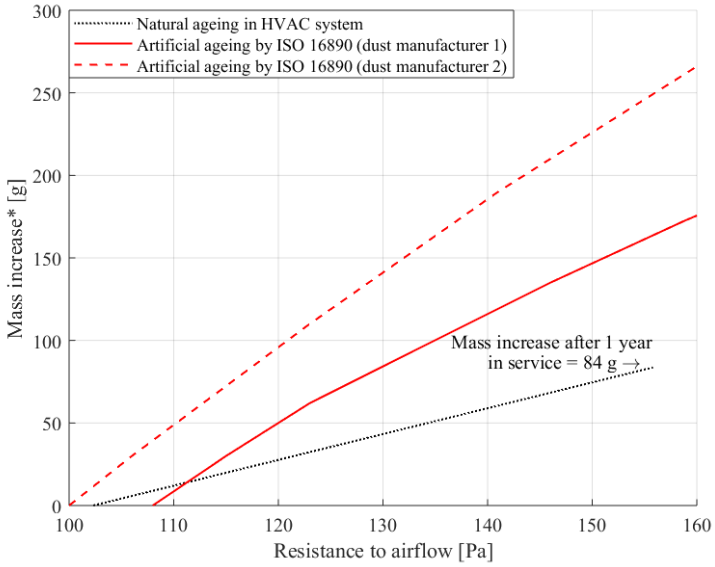

Figure 5 Air filter mass increase comparison between artificial and natural loading. (*) Assuming a gravimetric efficiency of 100% for the artificially clogged filters.

During the artificial loading process with current synthetic dusts, coarse particles stop on the surface of the filter medium and start forming a layer of granular material. This layer of synthetic dust covering the filter medium increases its efficiency and pressure drop by adding a layer of porous material, whose solid fraction is depending on the particles size distribution of the deposited particles. The increase of pressure drop is not linear because it does not depend only on the viscous resistance inside the filter media but also on the inertial resistance on the top of the filter medium. The higher the amount of dust covering the air filter medium, the higher the measured efficiency and the increase of pressure drop. This phenomenon is called “surface filtration”.

When exposing air filters to ambient aerosol concentrations, a completely different phenomenon takes place. It is called “deep filtration” because the particles are small enough to get into the fibrous medium and do not stop on its surface. In this way, the particles deposited on the fibers decrease the filter permeability. However, the governing law remains the Darcy law, which accounts for viscous resistance only. In practice, the viscous resistance increase is directly proportional to the increase of solid fraction inside the filter medium.

The data provided by the monitored HVAC system show that a filter in actual operating conditions requires much less captured particle mass to reach the same pressure drop obtained in the laboratory. This is true even if the pressure drop increases in a linear way in a natural ageing process.

Current methods for determining air filter duration provide misleading information that is not coherent with the actual behavior of the filters when exposed to an urban atmosphere. This is a limitation making impossible for air filter and filtering media manufacturers to develop air

filters minimizing the energy use and optimizing the replacement time when used in real applications.

4 NANOAEROSOL THERMAL GENERATOR

To generate a synthetic test aerosol having a PSD similar to that of an urban atmospheric aerosol, we investigated the performance of a thermal nanoaerosol generator (shown in Figure 6). This device burns a potassium chloride salt stick with an oxy-propane flame, generating large amounts of salt vapor, which condense in the air stream and form a mixture of ultrafine particles. The most relevant parameters impacting the nanoaersol obtained in this way are the salt stick feed rate into the oxy-propane flame, which can range between 1 and 25 mm/min and the diameter of the salt stick itself (10 or 12 mm).

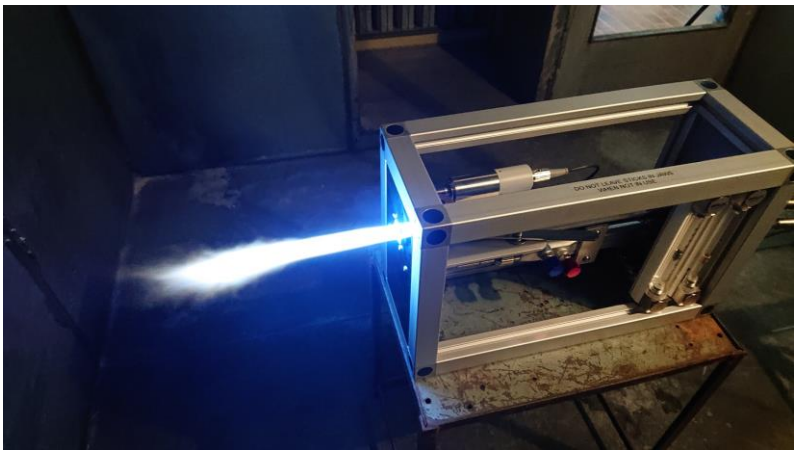

Figure 6 Picture of the nanoaerosol thermal generator in operation

Figure 7 contains a plot of some of the PSDs obtained with the thermal generator installed in a standardized ISO 16890 test duct operated at 3400 m^3/h. These are compared with the urban atmospheric aerosol from ISO 16890 standard.

The instrument used to measure the particle size distributions was a TSI 3910 nanoparticle sizer. The aerosol thermal generator injected the particles from the same point where the dust feeder is usually placed to age air filters with the standardized synthetic dusts. The temperature and relative humidity of the test air were between 20.6 - 34.6 °C and 33- 55%, respectively.

The results show that the nanoaerosol thermal generator produces a synthetic aerosol able to represent the accumulation mode of the typical urban aerosol. Following this positive preliminary evaluation, we will further investigate its use for the sake of achieving a much more realistic accelerated ageing of HVAC filters.

The concentration of the generated nanoaerosol was increasingly higher for faster salt stick feed rates, up to the maximum feed speed (25 mm/min). Higher feed rates could allow obtaining nuclei and accumulation modes even closer to the ISO 16890 reference urban aerosol PSD. As expected, the higher the salt stick feed speed rate, the higher the particle concentration in the test duct.

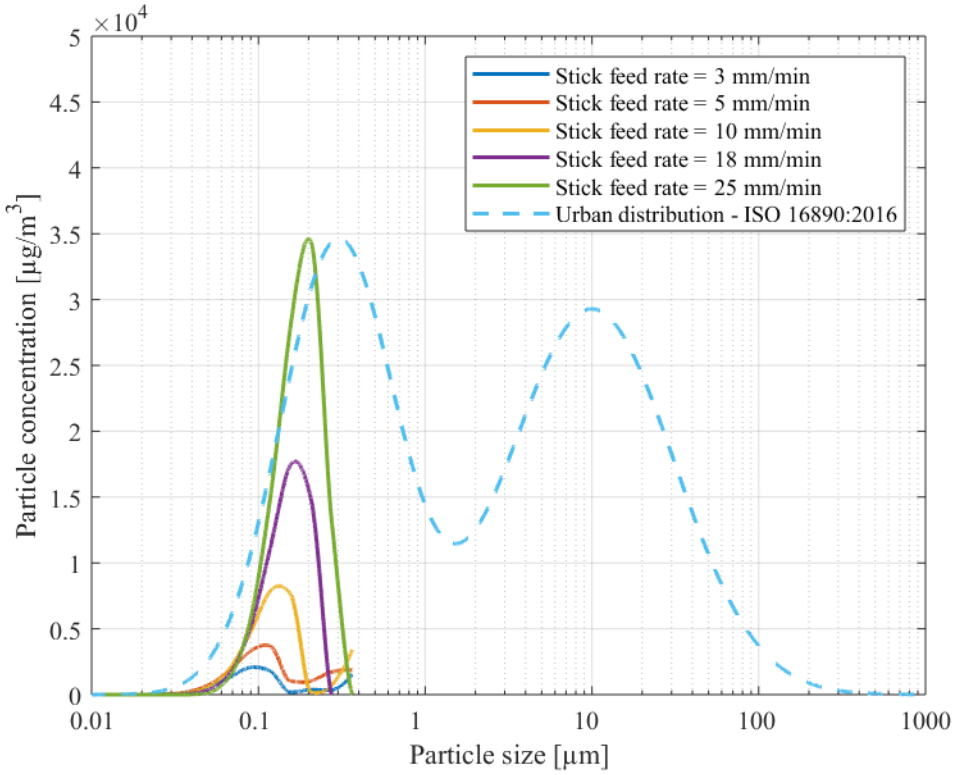

Figure 7 Comparison between the PSDs of the urban atmospheric aerosol according to ISO 16890 and nanoaerosol obtained using the thermal aerosol generator and a 10 mm diameter KCl stick with various feed rates.

5 CONCLUSIONS

The ageing behavior of air filters in HVAC systems is dramatically different from what current laboratory simulations provide. To reach a given pressure drop value, air filters clogged in a real environment require a much lower mass of captured particles, compared to the value provided by standardized laboratory tests with synthetic dusts.

The remarkable difference between the particle size distribution of the aerosol loading the filter during its operation in a real air conditioning or ventilation system and the one of the synthetic dusts can explain the limited value of current standardized tests. Current laboratory procedures prescribe a surface filtration process while in practice a deep filtration process occurs, at least during most of the filter service life. To bring the laboratory simulations closer to reality, it is essential to simulate the filter ageing with much smaller particles than those present in current normalized synthetic dusts.

To generate large amounts of ultrafine particles, a combustion process looks as the most obvious option. The thermal aerosol generator here presented and described is a promising solution for the aforementioned problem.

6 REFERENCES

ANSI/ASHRAE. (2017). *ANSI/ASHRAE Standard 52.2-2017 - Method of Testing General Ventilation Air-Cleaning Devices for Removal Efficiency by Particle Size.* Atlanta: ANSI/ASHRAE.

Azimi, P., Zhao, D., Stephens, B. (2014). Estimates of HVAC filtration efficiency for fine and ultrafine particles of outdoor origin. *Atmospheric Environment, 98*, 337-346.

Hinds, W. (1999). *Aerosol Technology. Properties behavior and measurement of airborne particles.* John Wiley & Sons, Inc.

ISO. (2016). *ISO International Standard 16890 series - Air filters for general ventilation.* Geneva, Switzerland: International Organization for Standardization (ISO).

Seinfeld, J. H., Pandis, S. N. (2012). *Atmospheric chemistry and physics: from air pollution to climate change.* John Wiley & Sons, Inc.

Stephens, B. (2018). Evaluating the Sensitivity of the Mass-Based Particle Removal Calculations for HVAC Filters in ISO 16890 to Assumptions for Aerosol Distributions. *Atmosphere, 9*, 85.

Tronville, P , Rivers, R. (2005). International standards: filters for vehicular applications. *Filtration & Separation, 42*, 24-27. doi:10.1016/S0015-1882(05)70692-3

United Nations, Department of Economic and Social Affairs, Population Division. (2018). *World Urbanization Prospects: The 2018 Revision, Online Edition.* Retrieved from https://population.un.org/wup/Download/

A study of the influence of the position of a chimney terminal on the vertical walls of a building on the air quality of the ventilation air supply

Xavier Kuborn[1], Sébastien Pecceu[1]

1 Belgium Building Research Institute
Avenue Pierre Holoffe, 21
1342 Limelette, Belgium

ABSTRACT

Combustion appliances are used in many buildings to provide space heating and domestic hot water. These appliances emit smoke that contains pollutants that must be kept away from the ventilation air supply of the building, to limit their impact on the indoor air quality (IAQ). An efficient way to prevent those pollutants from entering the ventilation circuit is to place the chimney terminal above the top of the roof, as far as possible from the air supply openings. However, to reduce the installation costs, the chimney is often as short as possible and the terminal is mounted in a vertical wall, right next to the appliance. In this case, a minimal distance between the terminal and the ventilation openings must be determined.

Methods to determine such distances can be found in several European and national standards. But most of these methods are overly simplistic and do not reflect the complexity of the physical phenomena at stake, namely the wind flow pattern around the building. The aim of this paper is to present a method, based on computational fluid dynamics simulations, that is able to determine the zones on the vertical walls of a building, with respect to the position of the chimney terminal, where the concentration of the pollutants is sufficiently low so that the air can be used for ventilation.

Preliminary results show that these zones are strongly dependant on the shape of the building and on the wind direction with respect to the building. A yearly analysis of the effect of the changing wind direction on the flue gas plume on the vertical walls of the building is also presented.

KEYWORDS

Indoor air quality, ventilation, chimney terminal, pollutants dispersion

1 INTRODUCTION

Combustion appliances are used in many buildings to provide space heating and domestic hot water. These appliances emit smoke that mostly contains carbon dioxide and water vapour, but also, depending on the type of fuel and the quality of the combustion, unburned hydrocarbons such as carbon monoxide, soot, tars and particulate matter. These products are pollutants that must be kept away from the ventilation air supply of the building, to limit their impact on the indoor air quality (IAQ). Combustion appliances include, but are not limited to, gas boilers, oil boilers, wood stoves, pellets stoves and open fires. The amount of flue gas that is emitted by the appliance depends on its heating power and on the operating duration.

An efficient way to prevent the flue gas from entering the building is to place the chimney terminal above the top of the roof (see Figure 1), as far as possible from the air supply openings. The wind velocity, combined with the buoyancy of the smoke, will move the plume away from the building and dilute it into the atmosphere. However, to reduce the installation costs of

modern appliances, the chimney is often as short as possible and the terminal is mounted on a vertical wall, right next to the appliance (see Figure 1). In that case, the plume might be partially trapped in a recirculation zone and remain close to the building with less dilution, increasing the risk of contamination. A minimal distance between the terminal and the ventilation openings must be determined in order to avoid the recirculation of the pollutants inside the building. Methods to determine this distance can be found in European and Belgian standards. A comparative example between three methods is given in chapter 2. It highlights the discrepancies between the existing methods and the need for a tool to select the most appropriate one, or to develop a more widely accepted one.

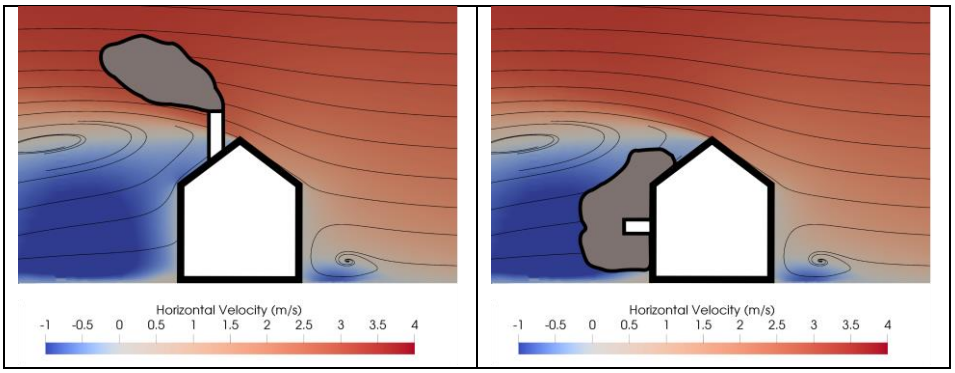

Figure 1 : streamlines of the wind flow around a building from a CFD simulation, with a superimposed qualitative representation of the smoke plume with respect to the position of the terminal.

Estimating a minimal distance between the chimney terminal and the ventilation openings is not an easy task, as it depends on many parameters, including the heating power of the appliance, the temperature of the flue gas, the pressure of the exhaust and many others. But the parameters that have the strongest influence on the plume dispersion are the wind turbulence and the wind flow pattern around the building. The wind flow pattern depends on the shape of the building and on the direction of the wind. Therefore, the flue gas plume can be driven away from the building by the wind, or be taken back against it.

A relevant method to study the wind flow pattern and the flue gas dispersion around buildings is to perform computational fluid dynamics (CFD) simulations. The physical phenomena are described by a mathematical model that consists of a set of equations and phenomenological coefficients. CFD is used to solve the set of equations and to provide the relevant physical fields, such as the flue gas concentration. Although wind driven pollutant dispersion around buildings is a complex topic, it has largely been studied in the literature with the use of CFD. The mathematical model and the numerical method are described in chapter 3, while preliminary results are shown in chapter 4.

While the subject of this paper is to describe a method to prevent a negative impact of the position of the chimney terminal on the IAQ, the results are to some extent also useful for the positioning of ventilation exhausts and kitchen hoods.

2 STANDARD METHODS

Several European and Belgian standards provide methods for positioning the chimney terminal with respect to the ventilation air supply openings. But most of these methods are overly simplistic and do not reflect the complexity of the physical phenomena at stake, namely the wind flow pattern around the building. Additionally, many discrepancies can be found between the methods. For instance, in Belgium, the minimal distance between the chimney terminal of a 30 kW room-sealed gas appliance, located on a vertical wall and a ventilation opening located

on the same wall, can be determined by the following standards : NBN EN 15287-2(2008), NBN D 51-003(2014) or NBN B 61-002(2006). For each standard, the minimal distance for two geometrical configurations is shown in Table 1.

Table 1: discrepancies between the different standard methods

Geometrical configuration	Standard reference	Recommended distance
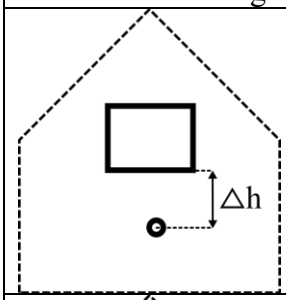	NBN EN 15287-2(2008) NBN B 61-002(2006) NBN D 51-003(2014)	Δh = 30 cm Δh = 320 cm Δh = 500 cm
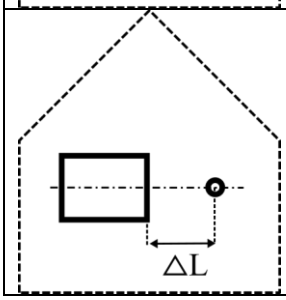	NBN EN 15287-2(2008) NBN B 61-002(2006) NBN D 51-003(2014)	Δh = 30 cm Δh = 340 cm Δh = 100 cm

There are obviously strong discrepancies between the values given by the different standards, with certain methods being more conservative than others. But the most conservative method is not always the same, depending on the selected configuration. Regardless of the quality of the given answer, the discrepancies between the standards show that there is a need for a better understanding of the problem and for a more relevant and widely accepted method for solving it.

There is no explanation associated with the methods described in the standards NBN EN 15287-2 and NBN D 51-003. However, the method given in NBN B 61-002(2006), called the method of the dilution factor, consists of a mathematical formula that leaves room for interpretation. Using this formula, a dilution of 100 of the flue gas (for gas appliances) must be obtained to be able to use the air for the ventilation of the building. The dilution is proportional to the height difference and the distance between the terminal and the ventilation opening and inversely proportional to the power of the appliance, which makes sense from a physics standpoint.

Although it is not possible, based only on the comparison between the methods, to determine which one is the most accurate, the value of a minimal dilution of 100 will be used as a reference during the development of a new method. This reference will allow for comparisons between the existing methods and the new one, regardless of the relevance of the value of 100 itself.

3 PARAMETRIC CHAIN

The CFD simulations presented in this paper have been carried out using OpenFOAM 2.4.0. OpenFOAM is a free and open source CFD software. Based on OpenFOAM, a parametric chain has been specifically developed to simulate the dispersion of pollutants around four facades isolated buildings on flat ground. The different elements of the chain are described below.

3.1 Mathematical model

As mentioned earlier in this paper, the dispersion of pollutants in the vicinity of a building is mostly driven by the wind flow pattern around the building, by the turbulence of the flow and to a lesser extent by the buoyancy of the flue gas. Buoyancy results from a temperature-induced density difference between the flue gas and the atmosphere. Hence, the energy equation needs to be solved to account for this phenomenon. Accordingly, the Navier-Stokes equations, i.e. the conservation equations of mass, momentum and energy need to be solved to capture the physics of the problem. The Navier-Stokes equations are not recalled here, since they are already largely reported in the literature.

Turbulence modelling

For industrial research, as is it the case for this study, turbulence is not directly solved using the Navier-Stokes equations, as it would require too much computational power. Turbulence is instead modeled, using an alternate version of the Navier-Stokes equations (RANS equations : Reynolds-Averaged Navier-Stokes equations) and two closure equations to model the turbulence. In this study, the $k-\omega\ SST$ closure model is used as it has been proven appropriate in other studies dealing with flow around buildings. (Ramponi R, 2012). These equations are also not recalled here for the same reason.

Atmosphere stratification and wind profile

The stability of the atmosphere describes its tendency to discourage or encourage the vertical motion of a parcel of air. Atmospheric stability is an important parameter when the dispersion of pollutants is studied on larger scales, e.g. the pollution from an industrial chimney or from a chemical accident. However, when the study is limited to the vicinity of a building, such phenomenon is generally neglected. In the present analysis, a neutral atmosphere, that do not encourage nor discourage the vertical motion of a parcel of air, is considered. The only resulting vertical motions are generated by either the wind flow pattern induced by the building or by the buoyancy of the flue gas. A logarithmic wind profile is used for the inlet boundary condition of the wind velocity field. The logarithmic profile gives the vertical distribution of the wind velocity and takes into account the terrain roughness.

Heat and species convection/diffusion

The density of the flue gas, that is responsible for its vertical motion associated with buoyancy, is estimated using an ideal gas law.

The flue gas is considered to be composed of a single fictive species whose concentration is equal to one at the chimney terminal and that has the same properties as air. An additional species equation (1) is added to the set of the Navier-Stokes equations. Solving this equation gives the concentration field of the pollutant in the computational domain.

$$\frac{\partial C}{\partial t} + \mathbf{v} \cdot \nabla C - \frac{\mu}{\rho \mathrm{Sc}} \nabla^2 \mathrm{C} = 0\,, \tag{1}$$

where C is the species concentration, $\mathbf{v}$ is the velocity field tensor, μ is the is dynamic viscosity of air, ρ is the density of air and Sc is the dimensionless Schmidt number. Using RANS methods, a turbulent viscosity is estimated by the closure equations. A turbulent Schmidt number is the ratio between turbulent momentum diffusion and turbulent mass diffusion. A wide range of turbulent Schmidt number values (from 0.3 to 1.3) are reported in the literature depending on the configuration (Carlo Gualtieri, 2017) (Gousseau P, 2010); a default intermediate value of 0.7 is used here.

3.2 Geometry of the problem, domain size and mesh generation

The mathematical model needs to be constrained in order to capture the physics of the problem. The studied geometry is a four facades isolated building with a two-sided roof (see Figure 2). The geometrical parameters are the length, the width and the height (of the cornice) of the building as well its roof angle. Combining these parameters, the parametric chain is able to generate many different building shapes, including, but not limited to, detached, semi-detached or terraced homes and apartments buildings. Additionally, the roof angle can be set to zero, which allows to generate flat roofs. The characteristics of the chimney are defined by four additional parameters: its diameter, its length and the two relative coordinates of its position on any vertical façade.

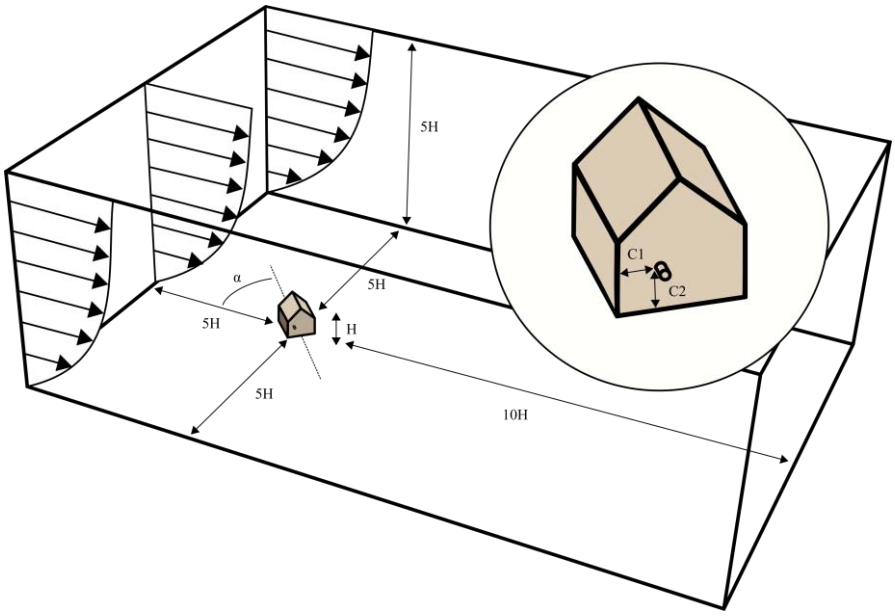

Figure 2 : representation of the computational domain with its minimal dimensions with respect to the height of the building and the logarithmic wind profile at the inbound condition.

The dimensions of the computational domain, as shown in Figure 2, are sufficiently large (Tominaga, 2008) to avoid an impact of the boundary conditions on the final results in the vicinity of the building.

The computational mesh is generated using the OpenFOAM built-in tool, *snappyHexMesh.* It is a locally refined mesh, that uses a method where space is filled by cubes or hexahedra elements that are successively refined by a factor two from the largest to the smallest size. The mesh sizes go from 2.5 m (coarsest size, far from the building) to 2.0 cm (at the chimney terminal).

3.3 Other operating parameters

Three operating parameters are needed to describe the atmospheric conditions: wind velocity, wind direction (relative to the orientation of the building) and outside temperature. The wind velocity is given by the logarithmic profile at the domain inlet while the wind direction is given by choosing the orientation of the building with respect to the inlet condition (see Figure 2). The outside temperature is uniform inside the computational domain at the beginning of the simulation. Finally, two operating parameters are needed to describe the flue gas: its flow and

its temperature. The flow mirrors the power of the connected appliance. Associated with the diameter of the chimney, it determines the exhaust velocity. During a simulation, the appliance operates at nominal power, hence the flow of the flue gas remains constant.

3.4 Assessment of the method

Although RANS is the best affordable method for doing CFD in industrial applications, it overestimates the recirculation zone in the wake of the building. Therefore, more pollutants might be redirected towards the building than in real life. Additionally, the OpenFOAM solver used in this study gives a steady state solution of the problem. In steady state, the dispersion of the pollutant is underestimated as there is no sudden change in the wind direction that will inevitably break the flue gas plume apart. Also, the neutral atmosphere hypothesis, where the only vertical motions are induced by the buoyancy or the wind flow pattern, will also underestimate the dispersion as it decreases the vertical mixing of the flue gas plume. Finally, the studied geometry is that of an isolated building on flat ground, with no obstacles that may change the wind flow upstream of the building and consequently the wind flow pattern around the building.

4 PRELIMINARY RESULTS

For a set of geometrical and operating parameters, the parametric chain described in chapter 3 is able to solve the steady-state dispersion of the flue gas and to compute its concentration field in the whole computational domain. A first example is given in Figure 3 for a single-family detached house. The chimney terminal is located at the center of the front façade. The left-hand side of Figure 3 shows a 3D iso-contour of concentration representing a dilution of 100 with respect to the concentration at the exhaust. The right-hand side shows a 2D representation of two iso-contours representing dilutions of 100 and 1000 (concentrations of 0.01 and 0.001 respectively). A dilution of 100 is considered to be representative of a sufficient air quality to be used for building ventilation, as written in chapter 2.

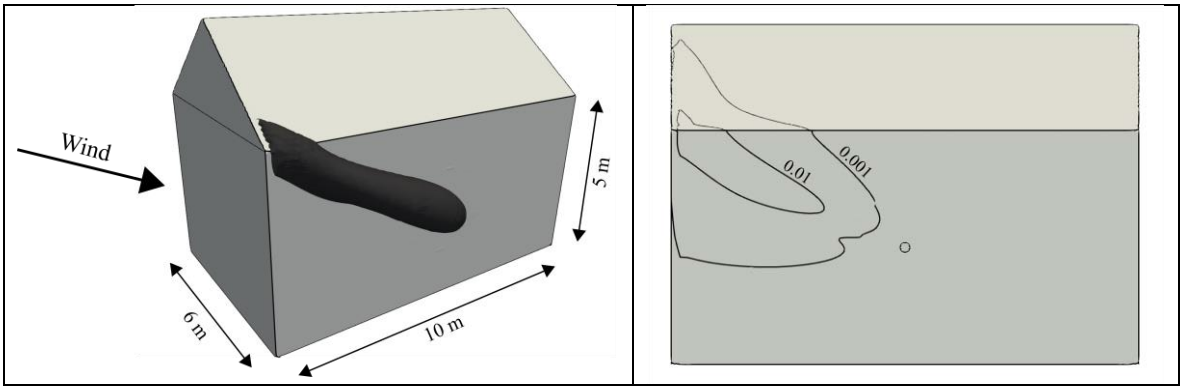

Figure 3 : representation of the iso-contours of concentration of the flue gas around a detached house.

Figure 3 also shows that the flue-gas plume goes backward against the wind and along the façade as the chimney terminal is located in a recirculation zone. The iso-contour representing a dilution of 100 is not connected to the chimney terminal, as either the initial velocity of the flue-gas or the wind pattern initially moves it away from the building before pulling it back against the façade.

A second similar example is shown in Figure 4 for a five dwellings apartments building and very low wind velocity (0.5 m/s). The chimney terminal is located on the second floor of the building. The flue-gas plume elevates mostly vertically, as the wind velocity is low, but it also

goes backward with respect to the wind flow as the terminal is located in a recirculation zone. The length of the iso-contour representing a dilution of 100 spans across three dwellings.

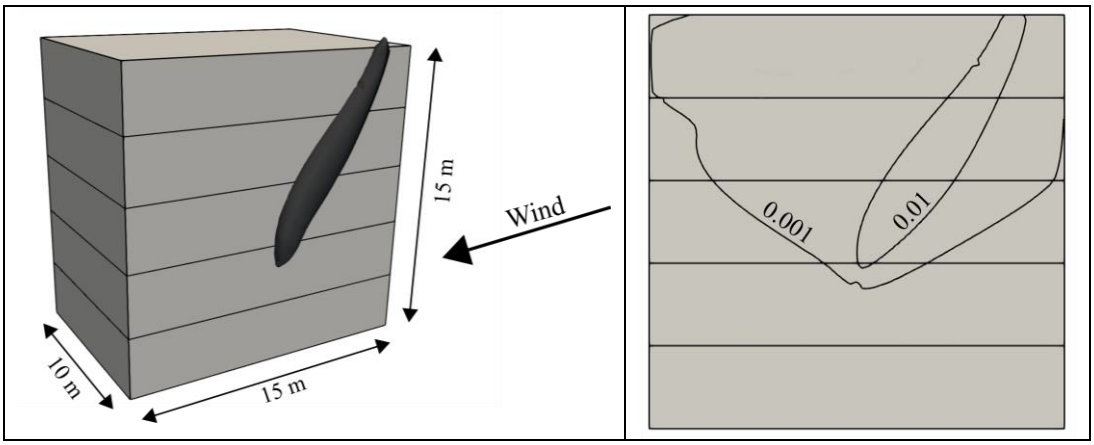

Figure 4: representation of the iso-contours of concentration of the flue gas around an apartments building.

A third example, presented in Figure 5, features the same operating parameters as the example shown in Figure 4, with the exception that the chimney terminal is located in the last dwelling. The flue-gas plume has a totally different shape that can be explained by the wind flow pattern around the building.

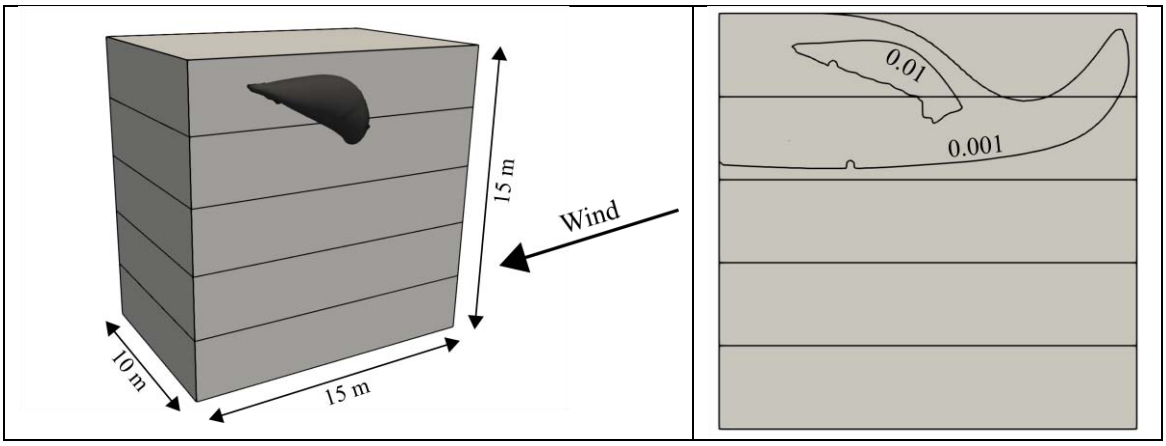

Figure 5: representation of the iso-contours of concentration of the flue gas around an apartments building

These results are instant pictures of a specific set of operating parameters, but they do not reflect the risk encountered in real life, as the many parameters are dependent on the meteorological conditions, that vary in time and that have a certain probability to occur. Such meteorological analysis is discussed in chapter 4.2, while a method to reduce the number of simulations needed to achieve such analysis is discussed in chapter 4.1.

4.1 Similarities and simplifications

The physics of the dispersion of the flue gas around a building involves many parameters that have been described in chapter 3. The geometrical parameters represent a specific building configuration while the operating parameters describe the environment. For a specific building configuration, a single numerical simulation using a single set of environmental parameters is insufficient to determine the overall potential influence of the flue gas on the IAQ. Indeed, the environmental parameters, including the wind velocity, the wind direction and the outside temperature, are variable in essence. They vary in time on a minute based scale but also on a daily scale with the night and day cycles as well as on a yearly scale with the different seasons.

If a yearly overall effect is to be accounted for, a statistical approach using all the relevant environmental parameters needs to be used. However, this approach implies that many different numerical simulations need to be done in order to get all the relevant results. Fortunately, many similarities can be identified, and the results of several numerical simulations can be used to complement other similar cases.

The Reynolds number is one of the most used dimensionless number in the field of fluid dynamics. For an incompressible and isothermal flow, two similar geometries (same shape but different scales) with the same Reynolds number will have identical flow fields. The case of the wind flow around a building is more complex, but the literature shows that the flow field remains similar for a wide range of Reynolds numbers (Kiyoshi Uehara, 2003). The Reynolds number takes into account the fluid characteristics (viscosity, density) and velocity as well as a characteristic dimension of the flow (the size of the building). It means that for a similar building geometry, the wind velocity has no influence on the flow pattern around the building.

Another characteristic of the problem is the jet generated by the exhaust of the flue gas in the main wind flow, that is often referred to in the literature as the "jet in crossflow" problem. This complex problem is approximated by the ratio of the momentum of the two flows (Fougairolle, 2009) :

$$J = \frac{\rho_j U_j^2}{\rho_\infty U_\infty^2} \tag{2}$$

If densities of both fluids are identical, it further simplifies to a velocity ratio U_j/U_∞. When the flue gas velocity is much lower than the wind flow velocity, this problem is similar to that of a local pollutant source, that can be modeled by the gaussian dispersion model. It is a common model for pollutant dispersion, where the concentration field of the pollutant is proportional to the pollutant source and inversely proportional to the wind velocity.

Empirical assessment

Considering this reasoning, the flow pattern around a building should be similar for any wind velocity and the pollutant concentration should be proportional to the flue gas flow (the source), and inversely proportional to the mainstream wind velocity. For a given building geometry (dimensions and chimney location), only one numerical simulation per wind direction should be able to represent the pollutant dispersion for all other operating parameters (wind velocity, outside temperature, flue gas flow, outside temperature and flue gas temperature).

This reasoning is not perfect, since the pollutant source has a non-null velocity at the chimney outlet and the temperature difference between the flue gas flow and the atmosphere should have a more significant impact when the Richardson number is high. The Richardson number is the ratio of the buoyancy to the flow shear.

In order to assess this reasoning, several numerical simulations have been carried out with a single geometrical configuration and varying wind velocities (V) and flue gas flow (Q), all other operating parameters remaining constant. The pollutant concentration fields (S) are then compared using the following scaling:

$$S_{scaled} = S_{sim} \frac{Q_{ref}}{Q_{sim}} \frac{V_{sim}}{V_{ref}} \tag{3}$$

The 'ref' and 'sim' suffixes referring respectively to a reference case and cases with other operating parameters. For all cases, the flue gas temperature is 100°C and the atmosphere temperature is 0°C. If the reasoning makes sense, all scaled concentration fields should be

equal. The reference case is presented in Figure 6, while the scaled concentration field are presented in Figure 7. The results are shown on a horizontal plane whose height is the same as the chimney axis.

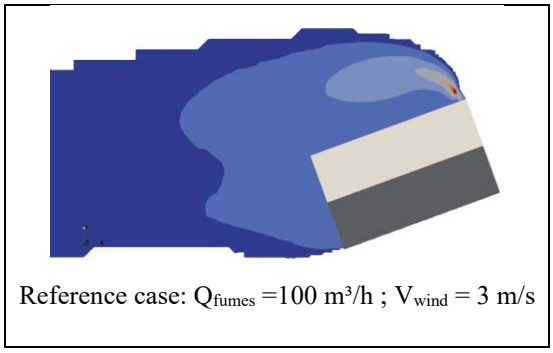

Reference case: Q_{fumes} =100 m³/h ; V_{wind} = 3 m/s

Figure 6 : iso-contour of the concentration field (log scale) for the reference case.

Three out of the four scaled simulations give nearly identical concentration fields, with the case with low wind velocity remaining qualitatively close. More numerical simulations with an increased range of the operating parameters should indeed be necessary to better assess the reasoning, but it already looks promising.

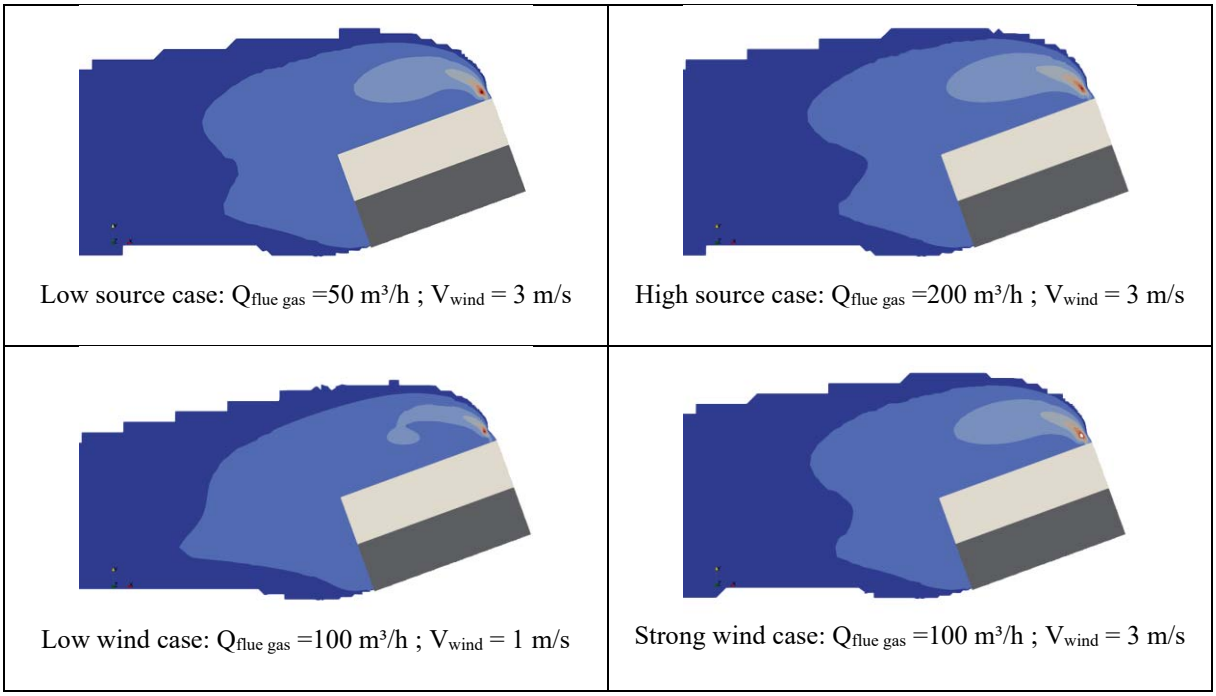

Low source case: $Q_{flue\ gas}$ =50 m³/h ; V_{wind} = 3 m/s

High source case: $Q_{flue\ gas}$ =200 m³/h ; V_{wind} = 3 m/s

Low wind case: $Q_{flue\ gas}$ =100 m³/h ; V_{wind} = 1 m/s

Strong wind case: $Q_{flue\ gas}$ =100 m³/h ; V_{wind} = 3 m/s

Figure 7 : scaled concentration fields (log scale) for numerical simulations with identical geometries but different flue gas flow and wind velocities.

4.2 Principle of the yearly analysis

Assuming that the heating appliance (or the ventilation installation) is always operating at nominal power, i.e. that the flue gas flow and temperature remain constant, the pollutant field only depends on the wind velocity and wind direction. In the example shown in this paper, a given building configuration (dimensions, orientation and chimney terminal position) is associated with a wind file representative of Brussel's climate (see Figure 8). The corresponding hourly wind velocities and directions are decomposed into height major directions, that will be simulated using the parametric chain.

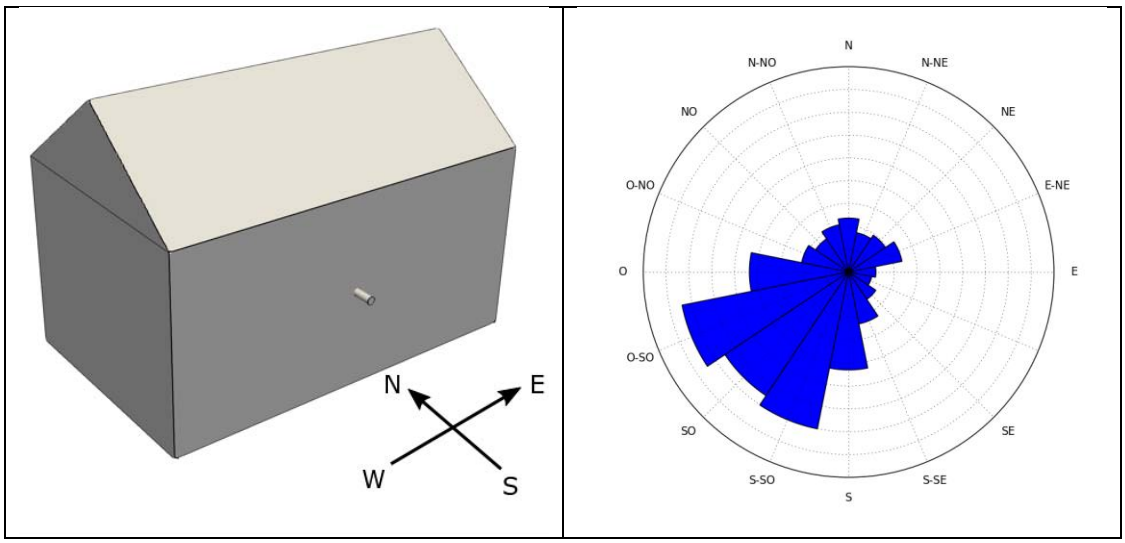

Figure 8: building configuration and occurrence probability for wind directions in Brussel.

Using these height numerical simulations and the scaling procedure described in chapter 4.1, the pollutant field can be determined for each hour of the year, based on the corresponding wind direction and velocity. On a yearly basis, the probability that a concentration threshold is reached or exceeded on the façades of the building can be determined. Such probability is shown in Figure 9 for a dilution of 100 (left-hand side of the figure) and 1000 (right-hand side of the picture). A dilution of 100 corresponds to a pollutant concentration of 1/100, assuming that the pollutant concentration is equal to 1 at the terminal.

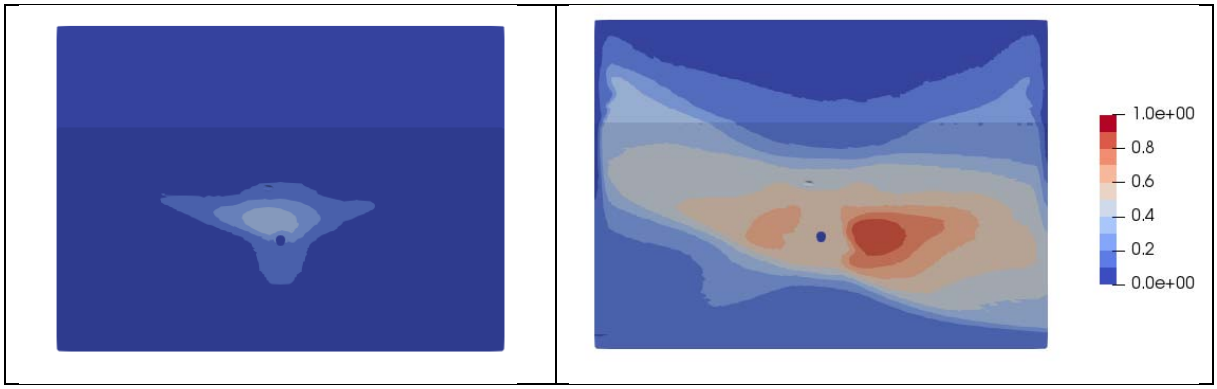

Figure 9 : probability that the pollutant concentration exceeds a threshold of 1/100 or 1/1000 on a yearly basis.

Depending on the value of the dilution coefficient that is considered to be acceptable, the appropriate "map" of the façades of a building could be used to determine where the ventilation openings could be located. The determination of the acceptable dilution coefficient and the acceptable probability that such dilution is not reached falls out of the scope of this paper.

5 FUTURE WORK AND CONCLUSIONS

This paper describes a method for the positioning of the chimney terminal with respect to the ventilation openings on the façades of buildings. The described method provides "maps" of the façades that show the probability that the flue gas is sufficiently diluted into the atmosphere to use the air for the ventilation of the building. When refined and validated, such maps could be used in standards as methods for the positioning of chimney terminals and ventilation openings.

Many improvements could be done to this method. Specifically, the appliance could operate at powers that are below nominal power, according to real-life operating patterns. That would reduce the amount of emitted pollutant and potentially increase the size of the zones where the ventilation openings could be placed. Also, the scaling procedure could be further validated for an increased range of operating parameters, for instance when the wind velocity is lower, when the exhaust velocity is higher and when the buoyancy is more important. When validated maps are obtained, the results could also by confirmed be doing on-site monitoring nearby chimney terminals located on façades. Finally, summarizing all the available results into a method that is simple enough to be used in standard as rules of good practice could be the most difficult challenge of them all.

6 ACKNOWLEDGEMENTS

This paper is written in the frame of two pre-normative studies called In-Vent-Out and In-Vent-Out 2, funded by the Belgian Federal Public Service and the Belgian Building Research Institute.

7 REFERENCES

Carlo Gualtieri, A. A. (2017). On the Values for the Turbulent Schmidt Number in Environmental Flows. *Fluids*.

Fougairolle, P. (2009). Caractérisation expérimentale thermo-aéraulique d'un jet transverse impactant ou non, en turbulence de conduite.

Gousseau P, B. B. (2010). CFD simulation of near-field pollutant dispersion on a high-resolution grid: a case study by LES and RANS for a building group in downtown Montreal. . *Atmospheric Environment 45*, 428-438.

Kiyoshi Uehara, S. W. (2003). Studies On Critical Reynolds Number Indices Forwind-Tunnel Experiments On Flow Within Urban Areas. *Boundary-Layer Meteorology 107*, 353-370.

Ramponi R, B. B. (2012). CFD simulation of cross-ventilation for a generic isolated building: impact of computational parameters. *Building and Environment 53*, 34-48.

Tominaga, Y. M. (2008). AIJ guidelines for practical applications of CFD to pedestrian wind environment around buildings. *Journal of wind engineering and industrial aerodynamics* , 1749-1761.

When the EPR hits the fan, or…the killing of the fan energy

Ad van der Aa[1], Per Heiselberg[2], Willem de Gids[3]

1 ABT
Delftechpark 12
2628 XH Delft, The Netherlands
a.vd.aa@abt.eu (corresponding author)

2 Aalborg University
Thomas Manns Vej 23
9220 Aalborg East, Denmark
ph@civil.aau.dk

3 VentGuide
Kievithof 3
2636 EL Schipluiden, The Netherlands
ventguide@hetnet.nl

ABSTRACT

The last decades big steps have been made on the road to develop and design energy neutral buildings. Despite the large list of developments and improvements of all kind of energy saving technologies we see specifically for the larger non-residential buildings that the electric energy use for fans hardly show any reduction and becomes a dominant factor in the total energy use of these buildings. The fan energy currently counts already for approximately 15-20% of the total building related energy and becomes increasingly important.
Among other developments, the work of IEA Annex 35 "Hybrid ventilation in new and retrofitted office buildings" and IEA Annex 62 "Ventilative cooling" revealed new directions in the design of ventilation systems. However, in daily practice the HVAC designers and installers do not seriously pick up the (new) knowledge and keep on going the well-known traditional way: designing and realizing mechanical ventilation systems with a total pressure drop of over 800 Pa. The reason not to do so, does not only lie in financial arguments, but is based in a much broader range of barriers. Of course, the unfamiliarity and knowledge gap of how to design low-pressure systems is a relevant stumbling block, but also the "wish to control" the air flow, the IAQ and the comfort conditions results in installations that are fully equipped. All kind of provisions are foreseen that filter, heat, cool, humidify, recover the heat and control the air. And this ends up in the well-known high-pressure system, that needs to be equipped with big fans to provide the air in the right places. To come to a serious reduction in fan energy for ventilation, the above described circle has to be broken.

KEYWORDS

Fan energy, low pressure ventilation systems, non-residential buildings, system design, low pressure components

1 INTRODUCTION

The development in the energy performance of buildings has made significant progress in the last decades. As a logical result of the increased energy performance requirements (EPR) all kind of energy saving technologies have been developed and implemented in the design and construction of new buildings. The list of developments that are relatively new is long and ranges from improved insolation materials and high performance glazing to LED lighting, all kind of heat recovery systems and improved heat and cold generation appliances. Also in the field of ventilation substantial progress has been made compared to the situation a couple of decades ago. I.e. the improved air tightness of buildings and systems, the development of heat recovery systems for ventilation and the development of demand controlled ventilation (based on sensor technologies) has led to a substantial energy reduction. Despite the large list of

developments and improvements we see specifically for the larger non-residential buildings that the electric energy use for fans hardly shows any reduction and becomes a dominant factor in the total energy use of these buildings. The fan energy currently counts already for approximately 15-20% of the total building related energy and becomes increasingly important.

The background for this relative high amount of fan energy is that ventilation systems in larger non-residential buildings are regularly designed for a total static pressure difference of approximately 800-1600 Pa and even higher. The reason lies in practical issues as space requirements and system optimization for (short term) financial arguments. By optimizing the size of the air distribution system until the limit the material costs and the use of space are reduced. The operational costs (long term costing) however increase as a result of higher fan energy. The fundamental reason to do so is not only the wish for cost optimization, but lies in a much broader range of barriers. Of course, the unfamiliarity and knowledge gap of how to design low-pressure systems is a relevant stumbling block, but also the "wish to control" the air flow, the IAQ and the comfort conditions results in installations that are fully equipped. All kind of (in a lot of occasions and situations not functional) provisions are foreseen that filter, heat, cool, humidify, recover the heat and control the air. And this ends up in the well-known high-pressure system, that needs to be equipped with big fans with a high energy use to get the air on the right place.

2 COMPLETED RESEARCH PROJECTS

A couple of completed IEA EBC projects have dealt with the challenges to come to low pressure ventilation systems from different perspectives.
From 1997 – 2002 "Annex 35 Hybrid Ventilation in new and retrofitted office buildings" was carried out with the objective to considerably reduce the energy use for ventilation and cooling by combining the advantages of natural and mechanical ventilation in a new hybrid ventilation system. One of the outcomes was examples of ventilation systems with an ultra-low pressure loss for the total system (often below 50 Pa) ranging between natural ventilation systems boosted by fan-power to mechanical systems, where fans were supported by natural driving forces. Although the requirements to buildings, their indoor environmental quality and energy use has developed considerably in the last 20 years many of the ideas, concepts and lessons learned are still applicable today. However, off the shelve efficient and affordable solutions to the challenges and application barriers that was identified in the project are still not developed today and is still a major barrier for application. These include among other solutions for low-pressure filtration, heat recovery as well as sound insulation and fire protection of openings in envelopes and internal constructions.
From 2012 – 2017 "Annex 62 Ventilative Cooling" was carried out with the objective to develop energy efficient ventilation systems for cooling of buildings utilizing the cooling potential of outdoor air. The design of energy neutral building has increased the need for cooling, but the high energy use for air transport in traditional ventilation systems reduces the benefit of utilizing the "free cooling" potential of outdoor air considerably. Due to thermal comfort issues and the risk of draught limited temperature differences between supply air and room can be utilized making heat recovery or air preheating necessary. The result of this is a cooling capacity reduction and an increased airflow rate - sometimes with a factor of more than five. In mechanical ventilation systems, this leads to an increase in energy use for air distribution and an increased investment in equipment. As a result, the energy and cost advantage of utilizing the "free cooling" potential of the outdoor air in a mechanical ventilation system compared to a mechanical cooling solution might become very limited. These limitations do not apply to the same extent when the outdoor air cooling potential is

applied to a free-running building (naturally ventilated building) and thus the appropriate use of ventilative cooling in connection with natural ventilation in non-residential buildings could contribute significantly to a reduction of the energy consumption. However, a major barrier for application of such a solution is that energy performance calculations in many countries do not explicitly consider ventilative cooling. Therefore, available tools used for energy performance calculations might not be well suited to model the impact of ventilative cooling, especially in annual and monthly calculations and driven by natural ventilation.

3 AIVC TECHNICAL NOTE 65 AND ASSESSMENT OF THE CHALLENGES

In 2009 AIVC has published the AIVC Technical note 65 "Recommendations on Specific Fan Power and Fan System Efficiency. In this publication a rather extensive and complete overview is given about the aspects concerning the fan energy in buildings. The first page already addresses the relative contribution of the fan energy to the total energy use in a Nordic office building as given in figure 1, which counts (in 2009) for 17%. This relative contribution has since then grown to 20-25% and will even become bigger.

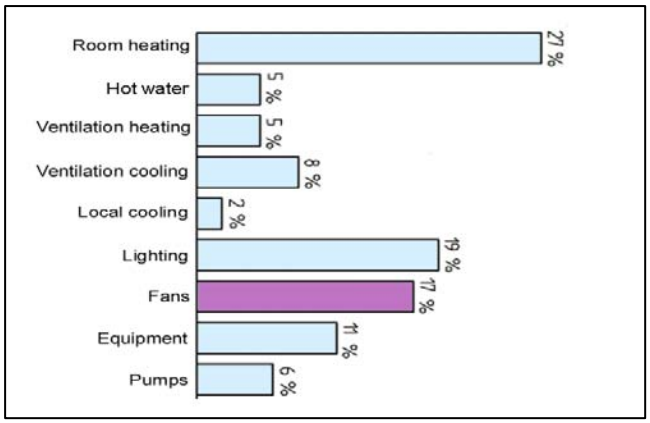

Figure 1: Approximate breakdown of typical energy use in a Nordic office [Fig. @Sintef]

The AIVC Technical note describes various methods to bring down the fan energy by a series of actions as:

- Optimisation of fan system efficiency
- Aerodynamic inefficiencies of fan inlets and outlets and improvements
- The improvement of fan system components as ductwork, silencers and exhausts

Table 6 of the Technote (given below as figure 2) illustrates the overall pressure drop for a typical ventilation system in a large building and makes a distinction between the pressure losses over the distribution system and the pressure losses over the air handling unit (AHU). The conclusion is that the pressure drop over the distribution system and the pressure drop over the AHU are nearly equal as big.

Table 6: Example of aggregating component pressure drops though a ventilation system in a large building, at design flow rate. [31][32]

			Poor design	Good design	Hybrid vent.
Supply	Distribution	Inlet louvre & duct	70	25	0
	AHU	Filter section F5-F7*	250	50	27
		Heat exchanger	250	100	13
		Heating coil	100	40	0
		System effect, →fan	30	0	0
		Silencer/attenuator	200	0	0
	Distribution	System effect, fan→	330	0	0
		Supply ductwork	150	100	1
		Terminals (ATD)	50	30	12
Exhaust	Distribution	Terminals (ATD)	30	20	0
		Extract ductwork	120	80	1
	AHU	Silencer/attenuator	100	0	0
		Filter section F5-F7*	250	50	0
		Heat exchanger	250	100	13
		System effect, →fan	30	0	0
	Distribution	System effect, fan→	330	30	0
		Outlet duct+louvre	250	20	17
A: Sum distribution syst.		Pa	1330	305	31
B: Sum AHU		Pa	1460	340	53
C: Natural driving forces		Pa	ignored	ignored	-4
Sum Total (A+B+C)		Pa	**2790**	**645**	**84**
Fan system efficiency		%	**28 %**	**63 %**	**40 %**
SFP		kW/(m³/s)	**10**	**1**	**0.2**

* Final filter pressure drop before replacement

Figure 2: Table 6 of AIVC Technical note 65, typical pressure drop for various designs for a large building

The conclusion of the authors of this paper is that the optimisation of the fan system efficiency and the improvement of the aerodynamic inefficiency of the fan inlets and outlets is important, but does not bring the needed reduction. But, a fragmented and detailed approach will not lead to the big step that has to be made. Therefore, we need a holistic approach in which we look in the direction of the design fundamentals as well as in the direction of the system and component improvements. In the last chapter of the Technical note the various stakeholders are addressed and pointed on their role and responsibility in the process to come to better and more energy efficient ventilation systems.

4 CURRENT LOW PRESSURE SYSTEM DESIGN PRACTICE AND EXAMPLES

The current design practice is confronted with the increasing requirements on the developments of low energy buildings. Not only the mandatory building regulations give (increasingly) strict requirements for the energy performance of buildings, but also from the side of the clients the demand for energy friendly, energy neutral and even energy delivering buildings is the new reality. To reach this level of building energy performance all energy saving options and resources have to be deployed in a systematic way and needs to be on the agenda of the design team from the very first beginning. This also counts for the issue of reducing the fan energy, as this can only be substantially reduced if it is incorporated in the building design strategy.
The ventilation system performance is after all directly related and interacts directly with the building shape, height, floor plans, corridors, façade layout, etc. Two examples of buildings in which these design considerations have played a role are illustrated in the next chapters.

4.1 A large office building with 2 atriums and a diffuse ceiling

In a design competition the target was to develop a new Office building of 70.000 m^2 in the centre one of the major capitals in Europe. The building had to be energy neutral with a high level of sustainability and circularity. For a number of reasons (light weight, constructability, circularity and sustainability) the building structure was foreseen to be made in CLT wood.

The 10 storey building floorplan was designed in the form of a H-shape, where two atriums were constructed, one north orientated and one south. From a conceptual level four principle concepts were discussed in the design team, ranging from conventional to more advanced in which one or two atriums were used as inlet and exhaust. In figure 3 the various variants are schematically illustrated.

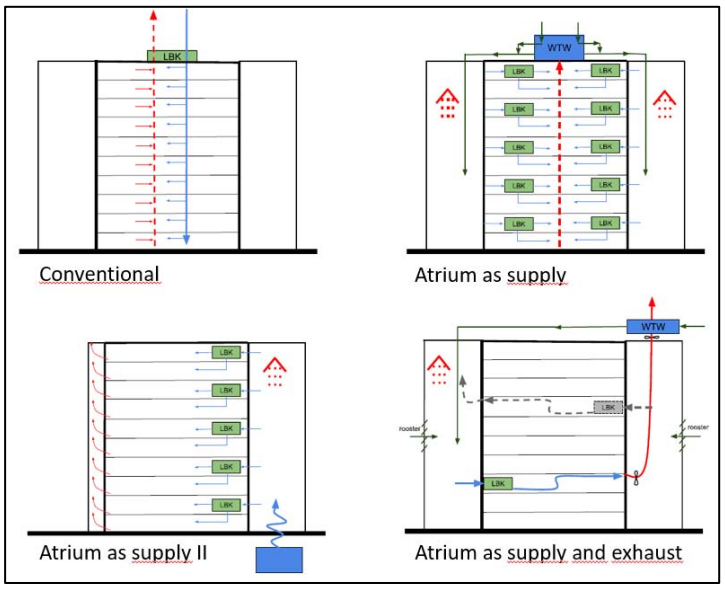

Figure 3: Schematic overview of ventilation concepts

Based on a discussion in the design team the variant in which both atriums are being used for the supply and exhaust was further investigated as the preferred solution. The south orientated atrium was used as a space to precondition the air to a certain level and distribute the supply air to the various floors. The north atrium acted as a collector for the return air. As the building was planned to construct in wood the idea was to use the hollow spaces in the floor for distributing the air over the floors to the individual office spaces. The supply of air to the rooms was based on a diffuse ceiling principle, assisted with locally placed DC-fans per room, controlled by CO_2-sensors. The return air from the rooms was extracted via an overflow damper to the central corridors and to the exhaust atrium. Figure 4 illustrates the

schematic principles of the building set up and the floor construction. Figure 5 gives some first results of the CFD feasibility analyses of the air flows.

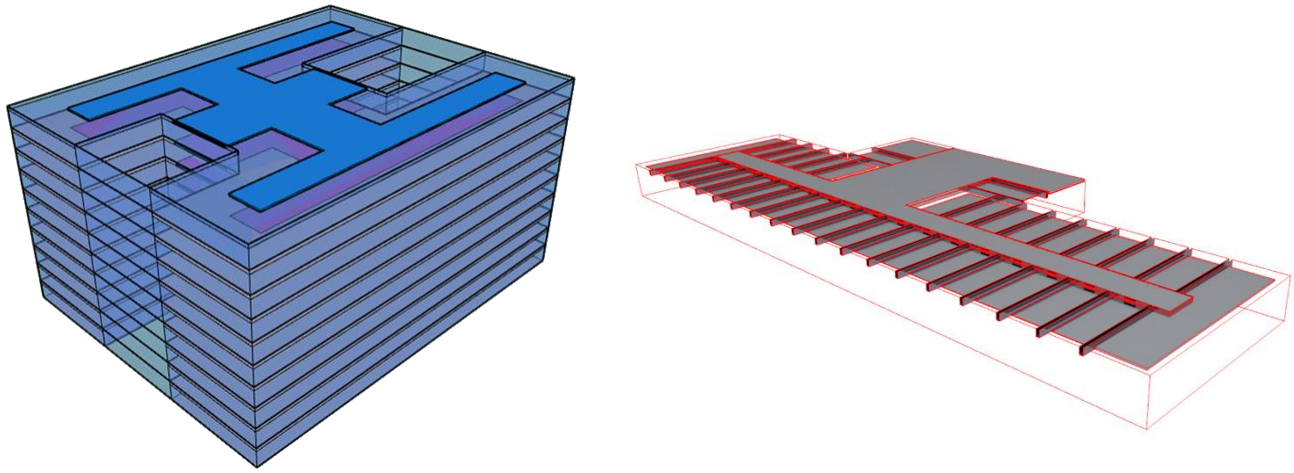

Figure 4. Schematic principles of building set up and floor construction.

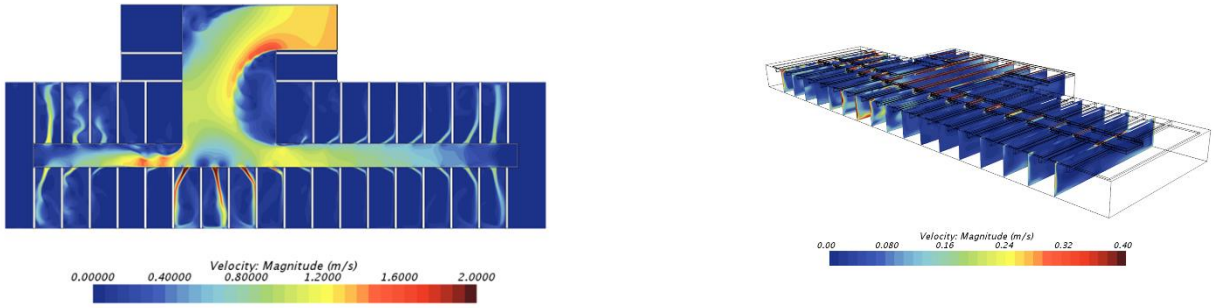

Figure 5. Results of CFD feasibility analyses of air flows

The original ideas were further incorporated concretized in the design and at the end of the preliminary design phase presented to the client. In general the reaction was interest and willingness to further investigate the proposal.
For the final design phase a contractor was selected to join the team. Some critical questions were raised about the concept, but after several industrial partners were brought in the original skepticism changed into enthusiasm on the opportunities that came with the proposed concept. A technical team, hired by the client, reviewed the proposal and came up with a number of points of concern:

- The designers propose a diffuse ceiling principle in combination with a thermally activated ceiling. Can this be explained further and be guaranteed in relation to the IAQ requirements and comfort conditions?
- The supply and exhaust of fresh air is at ceiling level. Is the air evenly distributed over the total ceiling? What does this mean for the efficiency of the ventilation in the room?
- How are the air flows controlled and guaranteed?
- The demanded IAQ imply the application of 2 filters on the inlet air of F7 and F9. How will these filters be applied?
- You propose a hybrid ventilation with heat recovery. Can you give examples of realized projects?

- You propose to use the wooden structure and the corridors for distribution of air. How do you cover the risk for condensation and mold growth and dust collection in the system?

The questions raised by the review team are valid and relevant, but on the other hand are based on unfamiliarity and avoidance of uncertainty. To further substantiate the proper functioning of the concept detailed multizone ventilation calculations were conducted with Comis. In Figure 6 and 7 an impression of the results are given, that proved that a stable ventilation system could be achieved. The maximum pressure difference for the local fans was calculated to be 30 Pa.

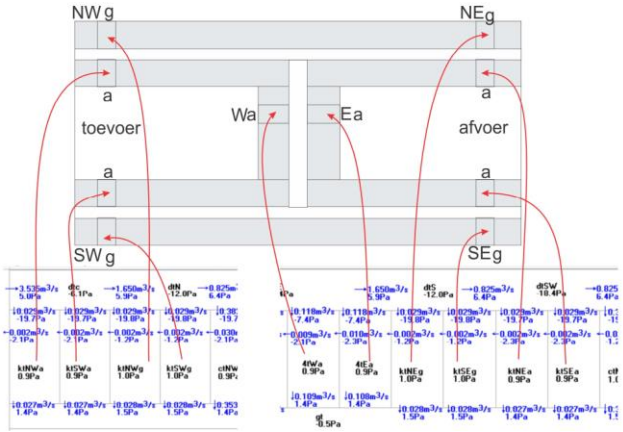

Figure 6. Results of Comis simulations of the low pressure ventilation system

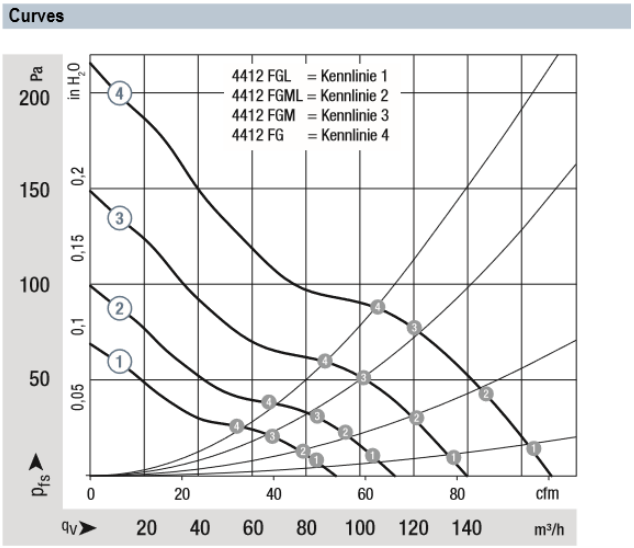

Figure 7 A possible fan characteristic for the air flow control to an office room

4.2 A laboratory building with a ring ducting system

At the design of laboratory buildings safety goes first. For chemical laboratories this safety requirements go hand in hand with large amounts of ventilation air. But also for these type of buildings the present energy related requirements are strict.
The question in this case was to design a new educational and research laboratory building of 35.000 m^2 with a high level of flexibility. These 35.000 m^2 form the second phase of a 100.000 m^2 building. In the first phase the client was “designed and sold” a ventilation installation with a conventional (“optimized”) branched ductwork. At the first startup of the

ventilation installations it showed up that the pressure losses in combination with the flow rate demands were much higher than calculated and that the AHU's were not able to come to a stable situation. This led to a number of necessary adjustments from reducing the flow rates over the safety cabinets to modifications in the exhaust chimneys to reduce the pressure losses. The end result was a critical working ventilation installation of 210.000 m^3/h with a pressure difference over the fans of 1.800 Pa. There was clearly room for improvement in the next phase!

To come to a robust, safe, energy friendly and flexible installation the idea was to design concept with a low pressure ring based ductwork infrastructure for the building. Figure 8 gives an impression of the first design sketches.

Figure 8. Illustration of first design sketches of low pressure ring system

The design concept of a low pressure ring based system has a number of advantages over a traditional branched ductwork:

- The uniformity in size of the ducts and branches makes it more easy to produce and install;
- The more or less uniform pressure differences over the system makes it easy to adjust and control;
- The system can be designed as a low pressure system with less fan energy;
- The system has a high level of flexibility as long as the total air volume for the whole building is not exceeded.

The system has some disadvantages compared with a conventional branched system:

- The construction needs more ductwork. This drawback should be compensated by the reduced production and installation costs;
- The system requires more space in the building which can lead to somewhat bigger floor heights;
- The system requires a clear structure and needs to be implemented in the first design phase, as the ductwork is not "as flexible" as usually presumed by the architect;
- For the design calculations there are no well described standard guidelines, procedures and software programs. In figure 9 a number of figures are given from the CFD-design optimization that have been conducted.

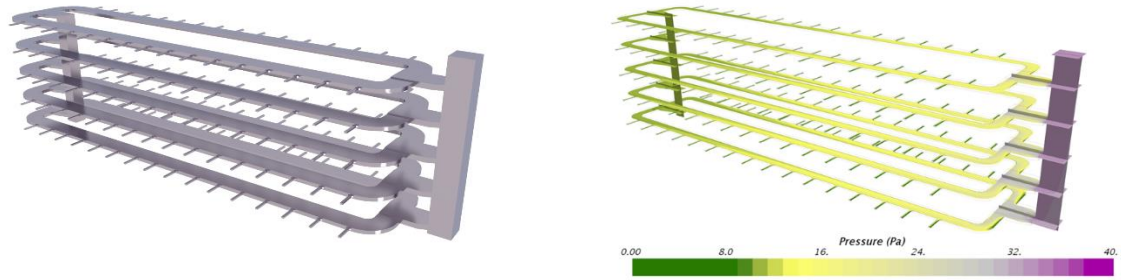

Figure 9. CFD-design calculations of a low pressure ring ductwork system

The building and system design is at this moment in the final design stage. During the previous design stages the experiences of the designers are similar with those issues described in the first example. There is a lack of knowledge, a lack of practical applicable tools, there is a lot of hesitation at the side of the other team design team members (architect, client) and the contractor and the installer are not yet involved, but will probably also have their doubts and objections and likely plea for going back to conventional.

4.3 Conclusions and lessons learned from the practical examples

The above given examples from practice illustrate a number of issues and questions that arise when low pressure systems are applied. These issues range from questions for realized and proven projects and ask for long term experience with the new technology. But also address more fundamental questions about the need for i.e. filtering and heat recovery and procedures for design, calculations and dimensioning of these types of (new) solutions.

5 FURTHER WORK AND RESEARCH ISSUES

The issues addressed in the previous chapter raise a number of questions for research, the development of guidelines and knowledge dissemination. A number of more fundamental questions need to be investigated and answered.

Improvement of air distribution systems in buildings
Large non-residential buildings have often a comprehensive ductwork installation including a central air handling unit to take care that the air is coming at almost constant flow level on the right place in the building. The ductwork but also the air handling unit itself consume a lot of pressure and so energy. For the transportation of air, for instance for a flow rate of 1 m^3/s just about 2 W is really necessary. In common practice about 500 W is used for transportation of 1 m^3/s of air through the ductwork including supply and exhaust grilles. The air distribution is in most cases not optimized. Another 200 to 400 W is used for air transport through the components in the air handling unit itself, such as filters, flow stabilizers, heating and cooling coils.
For a well-designed modern building, ductwork can be minimized because atria and corridors may act as ducts for air distribution. The highest resistances to control air transport are the negative effect of thermal- or buoyancy- and wind-forces. These forces in Western European buildings up to 40 m high can go up to about 30 – 50 Pa. Hence fans for air transportation of 1 m^3/s in buildings should not ask more than 35 to 55 W. (see figure 7). It is a challenge for designers to go in this direction of Nearly Zero Pressure buildings. The question is how?

Grilles and valves
Grilles and valves are normally applied to throttle and control the air flow because in most cases the pressure in the ductwork is too high. Low pressure grilles and valves can be applied when the design has been focused on low pressure systems. In most cases the grilles are not much more than visual esthetic covers of the duct. The question is are those appliances needed and if so, how do low pressure appliances to be sized and selected?

Filtering of air
Filtering is not always necessary. It is to protect people against health effects. Filtering large particles is not necessary. In case fine particles plays a role, the ventilation system should not take care but local air cleaning or local filtering can be applied. In case there is a need to include filtering in the ventilation system, low pressure filtering such as electrostatic filtering should be considered. The question is under which conditions filtering is needed and when can filtering been left out and if so how can filtering been realized with a minimum pressure loss?

(Pre-)conditioning of air
(Pre-)conditioning of air is sometimes a necessity but can also be minimized or avoided i.e. with the applications of diffuse ceilings. The research question is to come up with solutions to minimize the need for preconditioning of air or to develop solutions for preconditions with a minimum of pressure loss.

Heat recovery
The real performance of heat recovery systems is most of the time (much) lower than expected from the test specifications from the suppliers. *[Roulet et al, 2001].* A question that needs to be answered is, if heat recovery is always necessary and logical and what the decision criteria are to apply heat recovery. Furthermore, if heat recovery is applied there are several solutions for low pressure applications that could be further developed.

Next to this there is definitely a need for knowledge transfer. It seems to be that there is a big gap between the daily design and construction practice and the research world. But there is also a lack of practical applicable tools for sizing and dimensioning low pressure systems. The daily practitioners in the HVAC industry are not aware of the possibilities, but also do not have the right information and tools to design these type of systems in a proper way. But also the architects, contractors and the clients have their hesitations to leave the well known traditional path and follow a new direction.

6 CONCLUSIONS

It has become obvious that there is need for reduction of the fan energy in large non-residential buildings as an outcome of the increasing energy requirements. In daily practice the knowledge and tools how to come to a significant reduction in fan energy is lacking. Further more there is a lot of hesitation in the market to leave the traditional approach of designing and installing the well-known high pressure ventilation systems. Previous research work i.e. IEA Annex 35 “Hybrid ventilation” and IEA Annex 62 “Ventilative cooling” have already addressed the opportunities for low pressure ventilation systems. However, there is still a world to discover and answer, as well as there is an obligation for knowledge distribution and transfer to the market. In this paper a number of scientific questions have been addressed that have to be solved. But also questions from the daily practitioners in the HVAC industry, the architects and the clients have been described that are waiting for answers.

7 REFERENCES

Heiselberg, P (2002). *Principles of hybrid ventilation*

Roulet, C.A. (2001). *Real Heat Recovery with Air Handling Units.*

Schild, P.G. (2009). *AIVC Technical note 65 "Recommendations on Specific Fan Power and Fan System Efficiency.*

TIPVENT EU-Joule IV project (2001) *Towards improved performances of mechanical ventilation systems*

Existing standards for testing gas phase air cleaners

Paolo Tronville[1*]

1 Politecnico di Torino – Department of Energy
Corso Duca degli Abruzzi, 24
10129 Turin, Italy
** Corresponding author: paolo.tronville@polito.it*

SUMMARY

Many test methods exist for evaluating gaseous-contaminant filtration media, and a few for evaluating functional filters and other devices. These test methods are designed primarily for use in product quality control and to rank products. Designers of filtration devices and HVAC (Heating, Ventilating and Air-Conditioning) systems engineers, however, need test data that allows calculation of device performance under actual operating conditions. End users need data to determine system maintenance costs. We call such tests design parameter tests. The nature of the three test groups are as follows:

- Quality control tests are generally simple and inexpensive, presumably run on each media or component lot.
- Product differentiation tests are also relatively simple, involving feeding of specific contaminants in airstreams passing through devices or media samples, and measuring the contaminant removal efficiency. These tests are usually run at product market introduction, to provide some (limited) performance data for clients. They may also be used later to confirm manufacturers' data.
- Design parameter tests are much more demanding. To be fully informative, they require lengthy feed of a range of contaminants at low concentrations. High-sensitivity gas contaminant detectors may be required to obtain data for a useful array of contaminants at concentrations met in actual applications. Such tests are normally performed during the development of a new product. They are rarely published by suppliers.

A rational test procedure for gaseous contaminant removal devices should include the effects of multiple contaminants, relative humidity, and purging with clean air.
A critical review of performance prediction concepts should allow definition of tests and reliable performance calculations and computer codes. These predictions must be verified for a wide range of contaminants and operating conditions to assure usefulness in system design calculations.
We present some current test methods for gas phase air cleaners together with some typical output data.

KEYWORDS

Gas phase air cleaner; test method; ventilation air gaseous pollutant; ISO 10121 series; ASHRAE 145 series.

Methods to evaluate gas phase air-cleaning technologies

Pawel Wargocki

Department of Civil Engineering
Technical University of Denmark
Nils Koppels Alle, Building 402
DK-2800 Kongens Lyngby
Denmark
paw@byg.dtu.dk

SUMMARY

Gas-phase air cleaning methodologies have been considered as an attractive and cost-benefit alternative, and supplement to the traditional ventilation systems securing that air quality in buildings is meeting the prescribed standards. The systems can use the air that has been already conditioned to the required temperature and relative humidity, and by removing airborne gaseous pollutants, this air can be supplied indoors again. In this way the energy used to ventilate the buildings is expected to be considerably reduced, and in some cases, especially when outdoor air quality is poor or during specific extreme weather events, the buildings can be kept airtight and shut tight from the impact of outdoor air pollution and ambient impacts. Despite numerous technological solutions for gas-phase air cleaning available on the market there is basically no standard on how to evaluate their efficiency and effectiveness in removing gaseous pollutants. Such development is desired and necessary without further due. Standards exist regarding the systems for removing particles from the air, but as it comes to gas-phase air cleaners only the standards that exist present methods for using sorbents and sorbent-like technologies, and even they can be considered as incomplete. Standard methods must be developed, tested and put into practical use that would not only allow estimating the air cleaner efficiency in removing the pollutants but also comparing different technologies against each other concerning their performance. This presentation intends to shed some light on this topic. It will discuss advantages and disadvantages of using different methods for evaluating air cleaner performance focusing on chemical measurements and methods in which the ratings of humans are used; the former is the most accepted method at present. It will also discuss the risks and limitations of using these methods. Besides the selection of the method based on which the performance of gas-phase air cleaners should be evaluated, there are also other challenges that need to be considered when the method is implemented. These include (1) the selection of challenge pollutants and exposures; (2) examining potential by-products created during air-cleaning process; and (3) long-term performance of air-cleaners. They will also be discussed during this presentation. Finally, the efficiency of air cleaners should be assessed against the costs of their operation including both the running costs of energy and the maintenance costs. This presentation will specifically focus on using subjective ratings to assess air-cleaner performance and the selection of challenge pollutants.

KEYWORDS

Air-cleaner; Gaseous pollutants; Chemical analysis; Sensory ratings; Human subjects; Performance

Development of Subjective Evaluation Tool of Work Environment for Office Workers' Work Performance and Health Promotion

Yuko Abe[*1], Yasuyuki Shiraishi[2], Toshiharu Ikaga[3], Yoshihisa Fujino[4]

1 Graduate Student, The University of Kitakyushu, 〒808-0135 1-1, Hibikino, Wakamatsu-ku, Kitakyushu city, Fukuoka, Japan
[*]e-mail: z8mbb001@eng.kitakyu-u.ac.jp

2 Professor, The University of Kitakyushu, 〒808-0135 1-1, Hibikino, Wakamatsu-ku, Kitakyushu city, Fukuoka, Japan

3 Professor, Keio University 〒223-8522 3-14-1, Hiyoshi, Kohoku-ku, Yokohama city Kanagawa, Japan

4 Professor, University of Occupational and Environmental Health 〒807-8555 1-1, Iseigaoka, Yahatanishi-ku, Kitakyushu city, Fukuoka, Japan

ABSTRACT

In recent years, not only the residence but also the effort of health promotion by improving the social environment including the working and the regional environment has attracted attention. Because of the significant amount of time that office workers spend in the workplace, ideal modification of their working environment and work habits could potentially improve both their intellectual productivity and their physical health. However, optimal environmental improvements have not yet been identified. Therefore, in the present study, we developed a revised version of CASBEE-OHC. This version incorporates items evaluated in CASBEE-Wellness Office (CASBEE-WO), which is an objective workplace evaluation tool developed by the committee. This tool is constructed so that the question item does not have deflection by considering in various areas such as basic performance of buildings, operation management, and programs. The basic performance of buildings is focused on various fields such as design, installation, and structure. In particular, in the field of installation, we also set up questions about the room temperature and air quality by air conditioning and ventilation equipment, which are suggested to have a great impact on the workers' intellectual productivity and health. In order to verify the effectiveness of the revised CASBEE-OHC, we conducted a survey on workers' health and psychological status, in addition to their general environment (working environment, residence, community). At first, the relationship the degree of dysfunction in labor and the environments (working environment, residence and community) in which the office workers stay, was analyzed. Next, the analyses considering the influence of confounding factors were carried out, by conducting multiple regression analysis on subjective work efficiency and logistic regression analysis on the degree of dysfunction in labor and Sleep efficiency. As a result, it was confirmed that if the office environment and residence, community of the office worker are good, it will have a good influence on health condition and workers' intellectual productivity. Also, the correlation analysis for evaluation item indicated that the correlation between office air conditioning, air quality and dysfunction in labor was high. Furthermore, among air conditioning and air quality field, it was confirmed that the influence of the item regarding air quality was the largest. And, based on multiple regression analysis, it was confirmed that the working environment and age of the officer, influenced the work efficiency. And, from the logistic regression analysis, it was suggested that the risk of having a high degree of labor impairment and sleeping disorder increases when the surrounding environment including office space was bad.

KEYWORDS

Health promotion, Intellectual productivity, Wellness office, Questionnaire, Dysfunction in labor

1 INTRODUCTION

In recent years, not only the residence but also the effort of health promotion by improving the social environment including the working and the regional environment has attracted

attention. Because of the significant amount of time that office workers spend in the workplace, ideal modification of their working environment and work habits could potentially improve both their intellectual productivity and their physical health[1]. Previous studies[2] have shown that the workplace conditions of office workers influence both physical health and job performance. Thus, increased attention has been paid to identification of relevant health promotion strategies in these environments. However, optimal environmental improvements have not yet been identified. The Japan Sustainable Building Consortium (JSBC) launched the Smart Wellness Office Research Committee in 2012, and has worked to develop the CASBEE-Office Health Checklist (CASBEE-OHC), an evaluation tool aimed at not only improving intellectual productivity in office buildings, but also enhancing resilience and saving energy[3]. In a previous study, we conducted a survey on health and psychological status in addition to workers' everyday environment (workplace, residence, community), and identified relationships via regression analysis[4]. However, due to the non-normality of the score distribution of the beta version of CASBEE-OHC, revision and subsequent verification of the tool is needed. Therefore, in the present study, we developed a revised version of CASBEE-OHC. This version incorporates items evaluated in CASBEE-Wellness Office (CASBEE-WO), which is an objective workplace evaluation tool developed by the committee. In this paper, we outline the checklist, describe the outline of an online questionnaire survey using this checklist and discuss the results of our analysis. In this survey, the CASBEE is used to evaluate not only the working environment, but also the broader everyday environment to which workers are exposed.

2 OVERVIEW OF RELATED TOOLS IN CASBEE-WELLNESS OFFICE [5) 6)]

2.1 Overview of CASBEE-WO

CASBEE-WO is an *objective* evaluation tool that architectural experts use to assess environmental optimization for promoting health and productivity. Unlike the conventional CASBEE and related instruments, the scope of CASBEE-WO is the interior layout and furniture present in the specific department in which the employee works, and the efforts of the tenants. The items evaluated by CASBEE-WO are shown in Table 1. Items are distributed across three categories, and all evaluation items are scored according to a 5-level scale (level 1 to level 5), as is done in CASBEE-New Construction.

Table 1 The evaluation items of CASBEE-WO

Major items	Second items	Third items
I. Basic performance of the building	(1) Health and comfort	①Space, interior
		②Sound, noise
		③Lighting
		④Air and air conditioning
		⑤Refresh
		⑥Exercise
	(2) Convenience improvement	①Mobile space and communication
		②Telecommunications
	(3) Ensuring safety	①Disaster
		②Harmful substance
		③Water safety
		④Security
II. Operational management		①Maintenance plan
		②Satisfaction survey
		③Disaster response
III. Program		

2.2 Overview of CASBEE-OHC

CASBEE-OHC is a *subjective* evaluation tool that workers themselves use to evaluate their job satisfaction and health. The tool therefore evaluates the behavior and awareness influenced

by physical conditions and the surrounding environment. Each question was examined with reference to the CASBEE-WO evaluation items shown in Table 1, and a tool was developed. The answer format is shown in Table 2, and questions from CASBEE-OHC are shown in Tables 3 through 5. In addition, each question item was designed to correspond to the three categories used in CASBEE-WO, and we did not identify bias in the contents of CASBEE-OHC.

Table 2 Example of answer format

Achievement of optimal factors				Removal of dysfunctional factors			
3 point	2 point	1 point	0 point	3 point	2 point	1 point	0 point
very well	A little	Not true	Not at all true	No	Rare	Sometimes	Common

Table 3 Question item of Q1

Achievement of optimal factors		Removal of dysfunctional factors	
Q1	There is planting that people can feel green	Q10	Feeling that work space and storage place are narrow
Q2	There is desk corresponding to standing work	Q11	Feeling discomfort due to heat or cold
Q3	There is a chair suitable for both work and rest	Q12	Making the air-conditioning air flow uncomfortable
Q4	You can enjoy the outside view from inside the office	Q13	Remembering the dryness and moisture of the air
Q5	You can feel a sense of freedom of space	Q14	Feeling the air stagnation, dustiness, unpleasant smell
Q6	Openable windows open to the outside are well introduced	Q15	Feeling uneven brightness
Q7	It has become a comfortable interior	Q16	Feeling that the work space is dark
Q8	You can freely choose the desk that suits your daily work style	Q17	Feeling that sunshine and lighting equipment are dazzling
Q9	During the daytime, you can feel the light from the outside	Q18	Anxious about external sounds
		Q19	Anxious about other people's conversation and equipment machine noise

Table 4 Question item of Q2

Achievement of optimal factors		Removal of dysfunctional factors	
Q1	There is an easy-to-use refresh space	Q14	Having a bad taste or smell in tap water
Q2	There are easy-to-use meals and cafes	Q15	Waiting in the bathroom
Q3	There is an easy-to-use mini kitchen etc.	Q16	Waiting for the elevator
Q4	You can choose meeting space depending on the situation	Q17	Dissatisfaction with outlet capacity, wiring etc.
Q5	There is a staircase located in a convenient location	Q18	Feeling stress on the communication network
Q6	There is a space to take an easy-to-use nap	Q19	Feeling that meeting space is not enough
Q7	There is an easy-to-use internal information sharing infrastructure		
Q8	There is a space promoting easy-to-use conversations		
Q9	There is an entrance hall where you can easily meet and talk		
Q10	Becoming it goes ahead through the barrier-free in a building		
Q11	Facilities to promote daily exercise are abundant		
Q12	There is a comfortable toilet that is fully equipped		
Q13	There is a safe and comfortable elevator		

Table 5 Question item of Q3

Achievement of optimal factors		Removal of dysfunctional factors	
Q1	Questionnaires are conducted to improve the office or building environment	Q10	Feeling uneasy on crime prevention
Q2	Sufficient efforts are being made to maintain and improve mental health	Q11	Feeling uneasy at the time of disaster or emergency
Q3	Efforts are being made for smoke separation and smoking cessation	Q12	Feeling unsanitary throughout the building
Q4	A well-developed health promotion program is being implemented	Q13	Dissatisfaction with management of building, administration method
Q5	There are many postings to promote the use of stairs		
Q6	There is a comfortable green space around the building		
Q7	The scenery is in harmony with the city and surrounding buildings		
Q8	Evacuation drills are conducted regularly		
Q9	Emergency response manual has been prepared and is well known		

In order to minimize the burden on the worker when responding to these questions, all 51 items were classified into three question categories (Q1 to Q3), and were further grouped according to the general categories of "Achievement of optimal factors" and "Removal of dysfunctional factors". With respect to the classification of "Achievement of optimal factors" and "Removal of dysfunctional factors", there is a concern that such labels will engender bias in workers' responses, so such labels are omitted when conducting the actual survey. In addition, Q1 asks "Regarding the environment and equipment of your work space in the office…", Q2 asks "Regarding the environment and equipment of the entire office or building…", and Q3 asks "Regarding activities and affiliated organizations in the building…". In the CASBEE-OHC β version, it is considered that the score distribution has become non-normal because the answer format is 2 options (Yes or No). From this point, the survey adopts a 4-choice format (degree or frequency), with scores ranging from 0 points (worst state) to 3 points (best state).

2.3 Utilization scene of CASBEE-OHC

Utilization scene of CASBEE-OHC assumes three scenes of "1. Building owner, Designer, Builder, and Building manager", "2. Company (General affairs department etc.)" , and "3. Industrial doctor of company". At the time of utilization, it is assumed that surveys of workers' surrounding environment and health status are conducted and they are related. Image diagram of the evaluation result and the feedback output result are shown in Fig.1. As shown in the fig.2, it is planned to use a radar chart to visually indicate where improvement is needed. This is intended to encourage not only workers but also building managers to create rules for environmental improvement.

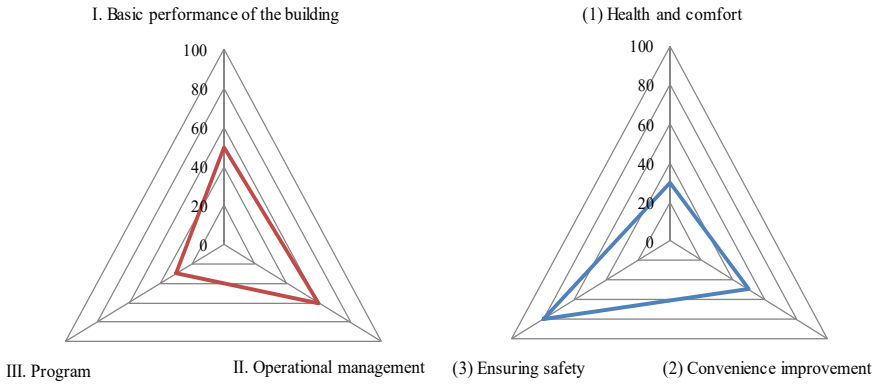

Fig.1 Image diagram of the evaluation result and the feedback output result

3 OVERVIEW OF WEB QUESTIONNAIRE

In order to verify the effectiveness of the revised CASBEE-OHC, we conducted a survey on workers' health and psychological status, in addition to their general environment (working environment, residence, community), in the Kanto region of Japan. The survey outline is shown in Table 6.

Table 6 Overview of WEB questionnaire

Implementation period	2018.07.31-08.02
Number of total	5,621
Number of valid responses	3,552
Target	Working in the Kanto district of
	Working for a company with more than 50 employees
	doing office work
Implementation method	WEB questionnaire
Outline of question	1) CASBEE-OHC（51questions）
	2) CASBEE-Housing（6questions）
	3) CASBEE-Community（8questions）
	4) WFun（7questions）
	5) Health, Lifestyle, Sleep, Work efficiency
	6) Occupation, Position, Age, Gender, Annual income etc.

As screening is done in advance, even samples on gender and age were obtained. In these two checklists (CASBEE-Housing and Community), a significant correlation was confirmed between the score and the prevalence rate of residents in the past research[7) 8)]. 4) WFun[9)] is a questionnaire used to measure the degree of dysfunction in labor due to health problems. Although it does not use medical information, strong relations have been identified between WFun's measured degree of dysfunction in labor with workers' medical symptoms and probability of medical leave. 5) Working Efficiency[10)] is a questionnaire that involves self-evaluation of routine work performance.

4 RESULT OF ANALYSIS

4.1 Simple Tabulation

The distribution of CASBEE-OHC scores in this questionnaire survey is shown in Fig.2. The CASBEE-OHC β version yielded a non-normal distribution. However, data from the CASBEE-OHC were normally distributed, as shown in Fig.2.

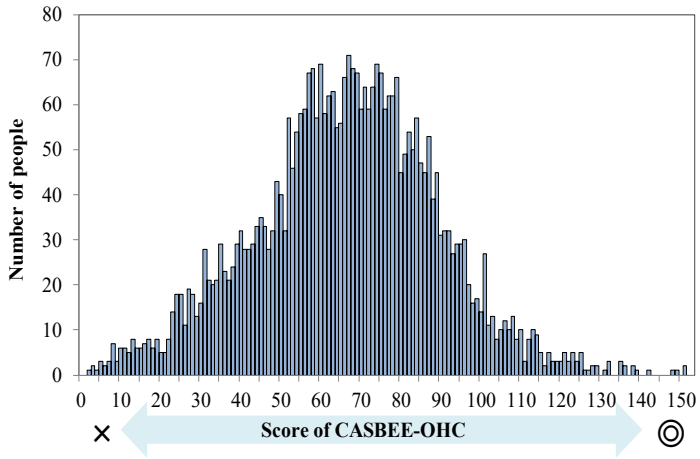

Fig.2 Score distribution of CASBEE-OHC

Next, the interpretations of WFun and Pittsburgh scores are shown in Tables 7 and 8, and the distributions of WFun and Pittsburgh scores in this questionnaire are shown in Fig.3 and 4. As

shown in Tables 7 and 8, higher total WFun and Pittsburgh scores are associated with higher levels of dysfunction in labor and greater probability of sleep disorders. As compared with reference proportions in Table 7, data from questionnaire respondents indicated elevated levels of labor dysfunction. Moreover, as shown in Fig.4, approximately 80% of workers in this sample have a sleep disorder.

Table 7 Interpretations of WFun

Score of WFun	Reference rate (%)	WEBPercentage (%)	Degree of dysfunction in labor
7～13	50～60	37.2	No problem
14～20	20～30	31.5	Slight disorder
21～27	10～15	19.8	Moderate disorder
28～35	2～8	11.5	Severe disorder

Table 8 Interpretations of Pittsburgh

Score of Pittsburgh	WEB Percentage (%)	Degree of sleep disorder
5 points or less	19.1	No problem
6～8 points	52.8	Slight disorder
9 points or more	28.0	Severe disorder

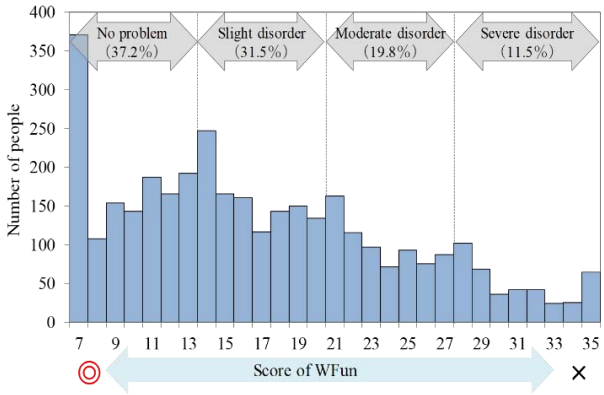

Fig.3 Score distribution of WFun

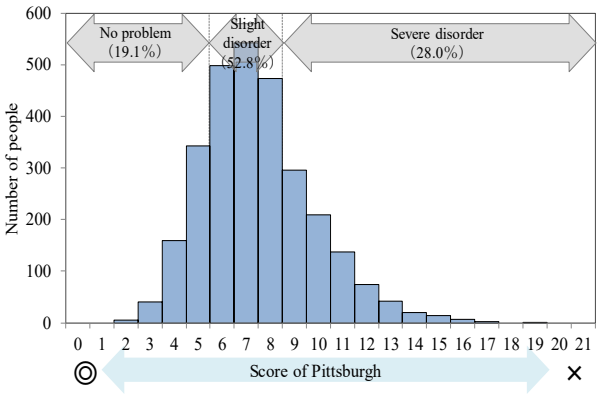

Fig.4 Score distribution of Pittsburgh

The results of correlation analysis between WFun, Pittsburgh, work efficiency, health condition, and each of the general environmental categories are shown in Table 9. Also, Fig.5 shows the relationship between general environments and WFun. Furthermore, the result of the correlation analysis between the score for each the evaluation items of CASBEE-WO and WFun is shown in Table 10.

Table 9 The results of correlation analysis (Each the general environment) *:p<0.05, **:p<0.01

	WFun	Pittsburgh	Work efficiency	Health Condition									
				Sagging of the body	Headache	Cough and sputum	Mucus	Rash	Stiff shoulder	Backache	Arthralgia	Sensitivity to cold	Catching cold
CASBEE -OHC	-.281**	-.211**	.346**	.244**	.164**	.097**	.102**	.128**	.151**	.188**	.153**	.128**	.060**
CASBEE -Housing	-.304**	-.240**	.160**	.262**	.241**	.162**	.180**	.215**	.169**	.221**	.283**	.281**	.189**
CASBEE Community	-.224**	-.181**	.237**	.201**	.152**	.098**	.088**	.084**	.101**	.117**	.126**	.108**	.059**

Table 10 The results of correlation analysis (Each the evaluation items of CASBEE-WO)

	I. Basic performance of the building												II. Operational management			III. Program
	(1) Health and comfort						(2) Convenience improvement		(3) Ensuring safety							
	①	②	③	④	⑤	⑥	①	②	①	②	③	④	①	②	③	
WFun	-0.201**	-0.227**	-0.212**	**-0.255****	-0.203**	-0.150**	-0.217**	-0.249**	-0.250**	-0.210**	-0.122**	-0.193**	-0.254**	-0.076**	-0.109**	-0.140**

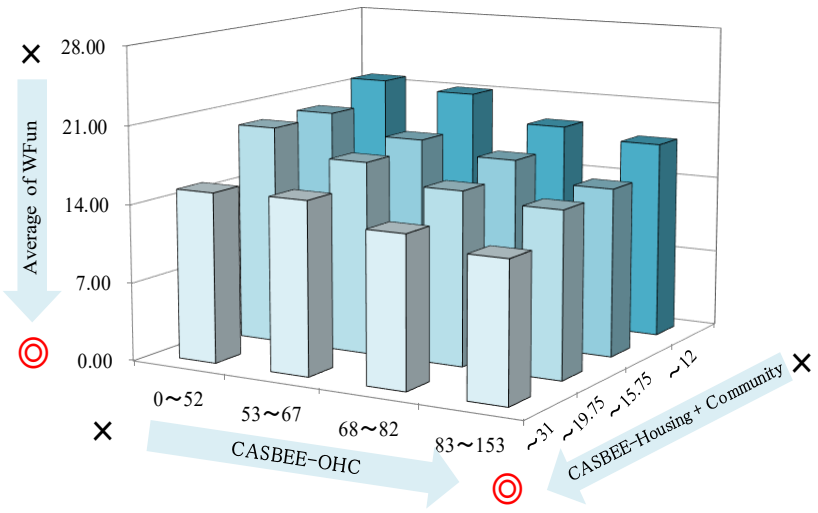

Fig.5 The relationship between the general environments and WFun

From Table 10, results suggest a strong relationship between air quality and dysfunction in labor. Furthermore, in assessing air conditioning and air quality fields, the influence of air quality was greatest. Fig.5 shows that as the score of the environment-related index increases, WFun scores decrease. From this, we speculate that an increase in general environment scores leads to a decreased risk of dysfunction in labor. Moreover, results of the correlation analysis between WFun and Pittsburgh show a negative correlation with each explanatory variable, and indicate a positive correlation with work efficiency and health condition. Compared with the correlation coefficient of WFun, the CASBEE-OHC correlation coefficient is relatively large with respect to subjective work efficiency scores, which suggests a strong influence of the office environment on work efficiency. With respect to health condition, the obtained correlation coefficient with CASBEE-Housing was relatively high across all items. From this, it is reasonable to suggest that workers' dysfunction in labor and work efficiency are influenced by not only their working environment, but also by the broader environment, including their residence and community, and their health condition may be greatly affected by conditions where they reside.

4.2 Multiple regression analysis

The influence of the general environments and personal attributes on work efficiency is verified. From the correlation analysis results, only those variables (general environment, Pittsburgh, Position, Annual income) with a significant correlation coefficient (0.1 or greater) were input as explanatory variables. Table 11 shows that CASBEE-OHC, Community, and Pittsburgh are significant variables. The coefficient of CASBEE-Office was particularly high, from which we may infer that the working environment plays a critical role in influencing work efficiency. Furthermore, we may infer that higher office, community, and Pittsburgh scores are associated with higher subjective work efficiency, and may lead to greater intellectual productivity.

Table 11 Result of multiple regression analysis

	Standard partial regression coefficient	Significance probability	95 % Confidence interval	
			lower limit	upper limit
CASBEE-OHC	0.315	< 0.001	0.021	0.027
CASBEE- Community	0.128	< 0.001	0.042	0.081
Pittsburgh	-0.110	< 0.001	-0.367	-0.176
Annual income	0.057	0.007	0.009	0.059
Position	0.043	0.039	0.003	0.120
Constant		< 0.001	2.921	3.559

4.3 Logistic regression analysis (WFun)

The influence of the general environments and personal attributes on WFun was verified. The variables shown in Table 12 were input as explanatory variables. The classification method of the model is shown in Table 13. Based on the interpretation of the WFun score in Table 7, WFun as the objective variable was converted to binary data (as shown in Table 13) and analyzed (Model-1 to Model-3).

Table 12 Input variables in logistic regression analysis

Objective variable		
WFun score	Model-1	0：No disorder, 1：have a disorder
	Model-2	0：No disorder or have a slight disorder 1：have moderate or severe disorder
	Model-3	0：No disorder or have a slight or moderate disorder 1：have severe disorder
Explanatory variable		
CASBEE-OHC	1：Top 30% of respondents（1,057 samples） 2：40% of respondents（1,389 samples） 3：Lower 30% of respondents（1,106 samples）	
CASBEE -Housing	1：Top 30% of respondents（1,016 samples） 2：40% of respondents（1,397 samples） 3：Lower 30% of respondents（1,139 samples）	
CASBEE -Community	1：Top 30% of respondents（1,086 samples） 2：40% of respondents（1,524 samples） 3：Lower 30% of respondents（942 samples）	
Pittsburgh	1：No problem 2：Slight disorder 3：Severe disorder	
Gender	1：Man 2：Woman	
Age	1：20’s 2：30’s 3：40’s 4：50’s 5：60’s	
Occupation	1：Clerical 2：Technical 3：Sales 4：Planning 5：Reserch 6：Others	
Position	1：General employee 2：Deputy manager class 3：Section manager class 4：General manager class 5：Executive 6：Manager	
Number of employees	1：Less than 100 2：Less than 1000 3：Less than 2000 4：Less than 3000 5：Less than 5000 6：More than 5000	
Annual income	1：Less than 5 million 2：Less than 10 million 3：Less than 15 million 4：Less than 20million 5：More than 20 million	
Marital status	1：Married 2：Unmarried	

Table 13 WFun data classification method

WFun data classification method		discriminative accuracy rate	Hosmer-Lemeshow test
Model-1	0：have an disorder, 1：no disorder	69.1%	0.717
Model-2	0：no disorder or have an mild disorder 1：have moderate or height disorder	72.8%	0.742
Model-3	0：no disorder or have an mild or moderate disorder 1：have height disorder	89.4%	0.095

Of the three models, the results of the logistic regression analysis of Model-3 are noteworthy because we found significance with a high discriminative accuracy rate (89.4%) and significance from the Hosmer-Lemeshow test ($p = 0.095$). The analysis results of Model-3 are presented in Table 14.

Table 14　Result of logistic regression analysis (Model- 3)

		Adjusted odds ratio	Significance probability	95 % Confidence interval	
				lower limit	upper limit
CASBEE -OHC	1 : More than 15 points		< 0.001		
	2 : 12～14 points	1.888	0.003	1.234	2.888
	3 : Less than 12 points	3.274	< 0.001	2.140	5.009
CASBEE -Housing	1 : More than 4.5 points		0.001		
	2 : 3.25～4.5 points	1.070	0.737	0.720	1.592
	3 : Less than 3.25 points	1.845	0.003	1.235	2.758
CASBEE -Community	1 : More than 13 points		0.011		
	2 : 9～12 points	1.088	0.689	0.720	1.645
	3 : Less than 9 points	1.666	0.015	1.106	2.510
Pittsburgh	1 : No problem		< 0.001		
	2 : Slight disorder	1.548	0.099	0.922	2.601
	3 : Severe disorder	4.175	< 0.001	2.495	6.987
Gender		0.652	0.006	0.481	0.882
Age		0.832	0.003	0.737	0.939
Constant		0.055	< 0.001		

The data suggest that lower scores for general environments are associated with elevated risk of high levels of dysfunction in labor. Next, the comparison results for risk of high level of labor dysfunction in each model are shown in Fig.6.

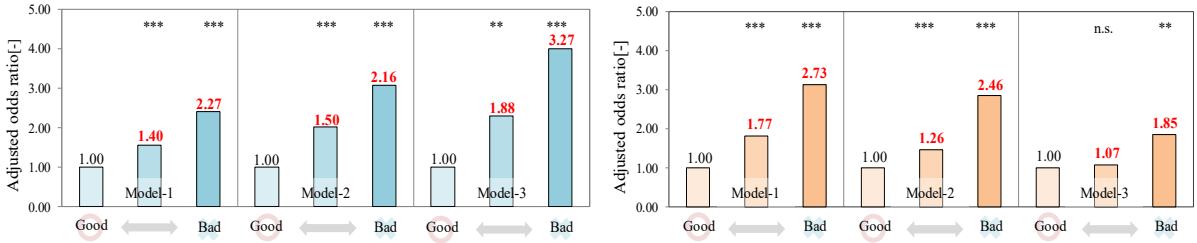

(a) CASBEE-OHC　　(b) CASBEE-Housing

Fig.6 The comparison results in each model（WFun）

The data confirmed the risk of increased disease prevalence due to deficits in the surrounding environment in all models. Furthermore, with regard to the CASBEE-OHC, it was confirmed that the risk of morbidity increases as the degree of labor dysfunction approaches severe levels. Conversely, the opposite was observed for CASBEE-Housing. Such relations suggest that the home environment affects the probability of mild labor dysfunction, while the office environment strongly influences the probability of severe labor dysfunction.

5　CONCLUSIONS

In this report, we outlined the checklist and reported the outline of the WEB questionnaire survey using this checklist and the analysis result. The results were as follows;

1) It was confirmed that if the office environment and residence, community of the office worker are good, it will have a good influence on health condition and workers' intellectual productivity. Also, the correlation analysis for evaluation item indicated that the correlation between office air conditioning, air quality and dysfunction in labor was high. Furthermore, among air conditioning and air quality field, it was confirmed that the influence of the item regarding air quality was the largest.

2) Based on multiple regression analysis, it was confirmed that the working environment and age of the officer, influenced the work efficiency. And, from the logistic regression analysis, it was suggested that the risk of having a high degree of labor impairment increases when the surrounding environment including office space was bad.

6 ACKNOWLEDGEMENTS

This survey is part of the results of the activities of the Smart Wellness Research Committee (Chairman, Shuzo Murakami) by the Japan Sustainable Building Consortium, and we are grateful to all the relevant people.

7 REFERENCES

1) Institute Japan Sustainable Building Consortium “2017 Smart Wellness Office Research Committee Report” p105, 2017.3
2) Ministry of Health, Labor and Welfare, Health Japan 21(Second) http://www.mhlw.go.jp/stf/seisakunitsuite/bunya/kenkou_iryou/kenkou/kenkounippon21.html
3) Japan Sustainable Building Consortium (JSBC) http://www.jsbc.or.jp/research-study/casbee.html
4) Y. Abe et al, “Regression Analysis of Worker's Health, Work Performance and Work Environment based on WEB Questionnaire”, Summaries of technical papers of annual meeting, *Architectural Institute of Japan -Kyushu chapter* (2018), pp.41-44. (in Japanese)
5) Japan Sustainable Building Consortium (JSBC), “Evaluation tool of Wellness office” http://www.jsbc.or.jp/research-study/hyouka-tool.html
6) T. Hayashi, “Study on framework and evaluation items of building health / comfort evaluation by CASBEE-Wellness Office”, Summaries of technical papers of annual meeting, *Architectural Institute of Japan* (2018), pp.993-996. (in Japanese)
7) E. Takayanagi et al, “Validation of the Effectiveness of Residential Environment Assessment Tool for Health Promotion”, Journal of environmental engineering, *Architectural Institute of Japan*, (2011), pp.1101-1108. (in Japanese)
8) M. Deguchi et al, “Development of Regional Environment Assessment Tool for Health Promotion and Validation of the Effectiveness”, Journal of environmental engineering, *Architectural Institute of Japan*, (2012), pp.837-846. (in Japanese)
9) WFun http://www.uoeh-u.ac.jp/kouza/kosyueis/wfun/entry1.html
10) Ministry of Health, Labor and Welfare, Health Japan 21(Second) http://www.mhlw.go.jp/stf/seisakunitsuite/bunya/kenkou_iryou/kenkou/kenkounippon21.html

Evaluation potential of indoor environments' ecological valency

Ardeshir Mahdavi*, Helene Teufl, and Christiane Berger

Department of Building Physics and Building Ecology, TU Wien
Karlsplatz 13
1040 Vienna, Austria
**Corresponding author: amahdavi@tuwien.ac.at*

ABSTRACT

Buildings typically are expected to provide their inhabitants with the opportunity to influence the indoor environment using various control devices. These include, for example, windows, luminaires, radiators, and shading elements. The quality and adequacy of the indoor environment is thus dependent on the availability and effectiveness of such devices. There is arguably a lack of generally agreed-upon evaluation procedures for this aspect of buildings' indoor environment, namely its controllability by building users, or – in the terminology of Human Ecology – its "ecological valency". In this context, the present contribution explores the possibility to specify buildings' ecological valency in a systematic and reproducible manner. Toward this end, first the theoretical foundation for this purpose is identified and previous related efforts are briefly reviewed. Subsequently, a specific attempt for an ecological valency evaluation method is presented. As part of this approach, five main categories of control devices are documented in various rooms of a building. They include windows, shading, lights, heating and cooling systems. Whereas, the first component of this method deals with the basic availability of these control devices and elements, the second part looks at their spatial distribution, effectiveness (both objective and subjective), interface quality (to support user interaction), and ecological quality. The presented evaluation method is tested for six different rooms of an office area in an educational building in Vienna, Austria. Some thirty participants independently evaluated this area based on the proposed method and associated protocol. The results point to high degree of congruence between the evaluation results of different participants while judging the principle availability and typology of the control devices. Higher variation was observed in the evaluation of the quality of devices and their interfaces. As a whole, the results suggest that methods based on similar premises proposed in the present contribution may indeed provide a realistic opportunity to extend building performance evaluation procedures beyond energy and cost criteria to cover aspects pertaining to user control and satisfaction.

KEYWORDS

Indoor environment, building interfaces, ecological valency

1 INTRODUCTION

Buildings typically provide their inhabitants with the opportunity to influence the indoor environment using various control devices such as windows, luminaires, radiators, and blinds. The quality of the indoor environment is thus dependent on the availability and effectiveness of such devices. There is a lack of evaluation procedures for this aspect of buildings' indoor environment, namely its controllability by building users, or, its "Ecological Valency" (EV), as it is referred to in Human Ecology. The present paper explores the possibility to specify buildings' ecological valency in a systematic fashion. Toward this end, we first discuss needed theoretical foundations. Subsequently, a specific protocol for EV evaluation is presented. Thereby, five main categories of control devices are documented in different rooms of a building. They include windows, shading, lights, heating and cooling systems. Whereas, the first component of this method deals with the basic availability of these control devices and elements, the second part looks at their spatial distribution, effectiveness (both objective and subjective), interface quality (to support user interaction), and ecological quality (Mahdavi, 2019; Mahdavi and Berger, 2019).

The protocol was tested for six rooms of an office area in an educational building. Thirty participants evaluated these rooms using the mentioned protocol. The purpose of this exercise was not only to conduct a preliminary test of the usability of the method itself, but also to document the degree to which the different evaluation results could diverge when the same room is evaluated by different participants. While some of the participants work in this office area, others were not familiar with it before conducting the evaluation. Hence, aside from the overall consistency of the results, the difference between the results from the occupants and the visitors could be examined as well. The outcome of this experiment but also the feedback from the participants are presented. The results suggest that methods based on similar premises proposed in the present contribution may indeed provide a realistic opportunity to extend building performance evaluation procedures beyond energy and cost criteria to cover aspects pertaining to user control and satisfaction.

2 THEORETICAL FOUNDATION

2.1 Introductory remark

Our EV evaluation approach is informed by prior work in the Vienna School of Human Ecology and the Ecological Psychology. The following sections (2.2 and 2.3) provide a brief description of these sources.

2.2 Human Ecology and the concept of Ecological Valency

Human ecology is a promising instance of a theory, that can guide the efforts toward indoor environmental quality assessment. Human ecology may be simply defined as the ecology of the Homo sapiens. There are many traditions and associated approaches to human ecology. From the standpoint of the "Vienna School of Human Ecology" (Knötig, 1992a; Knötig, 1992b; Mahdavi, 2016; Mahdavi, 1996a), the construction and operation of buildings can be viewed as an integral part of the totality of largely regulatory operations initiated by human beings as they interact with their surrounding world. Human ecology offers a useful way of thinking about these interactions via a number of concepts, including the following pair: *i)* the human beings' ecological potency (EP); *ii)* the surrounding world's ecological valency (EV) (Knötig, 1992a; Mahdavi, 1996b). Thereby, EP refers to people's capability to cope and interact with the surrounding world. EV, on the other hand, denotes the totality of that surrounding world's characteristics (resources, opportunities, challenges, risks, hazards) as it relates to people's ecological potency. The concept of ecological valency was essentially dealt with in (Uexküll, 1920) and is also akin to Gibson's affordance (Gibson, 1977; Gibson, 1979).
Given this conceptual framework, we can describe the main consideration in human ecology as the complex and dynamic relationships between the ecological potency of human beings and the ecological valency of their surrounding world. Human ecologically speaking, buildings are constructed and maintained with the intention to favourably influence the relationship between people's ecological potency and the ecological valency of their surrounding world.

2.3 Ecological psychology and the concept of affordance

The interactions between people and their surrounding environment has been a central theme in cognitive and environmental psychology. An influential line of inquiry in this area goes back to the psychologist Gibson in general and his concept of "affordance" in particular (Gibson, 1977). In Gibson's diction, "affordances of the environment are what it offers the animal, what it provides or furnishes" (Gibson, 1979). Affordance, as Gibson defines it, is not dependent of a specific individual's recognition of it. But it can be recognized by individuals according to

their needs. Moreover, perceiving affordances is connected with initiating actions. As such, people tend to intervene in their surroundings and modify affordances, such that they better match their needs. The conceptual background of Gibson's work display similarities to views formulated earlier by Uexküll (Uexküll, 1920). However, the latter does not postulate the existence of affordances independent of their representations ("Umwelt"). The concept of affordance has been used in other fields such as human-computer-interaction and industrial design (Norman, 2013). Hence, it can be also applied to environmental and architectural domains. Thereby, building design decisions and actual interventions (including control actions) in indoor environments could be suggested to enhance the respective repertoire of affordances.

3 A GENERAL FRAMEWORK FOR OPERATIONALIZATION OF ECOLOGICAL VALENCY [EV]

Given the preceding theoretical foundations, the problem of building quality assessment regarding inhabitants' control opportunities in indoor environments can be suggested to involve multiple challenges. First, how are we to simultaneously address the variance of inhabitants' ecological potency while we attempt to assess indoor environments' EV? Conventional comfort standards typically consider population variance in comfort requirements to a certain – albeit basic – degree, for instance via consideration of different building typologies (e.g., hospitals, schools, offices) and space use categories (e.g., operations room, corridor, lobby).
However, a more consequential coverage of the diversity of inhabitants' EP would be desirable, as indoor environment's EV should ideally accommodate people's diverse spectrum of ecological potencies. Nevertheless, we can at least partially justify the present contribution's concentration on EV and its operationalization with the following argument: Improving an environment's EV is associated with its capacity to offer a flexible range of conditions. Enrichment of EV is thus likely to benefit all occupants, irrespective of their diversity of their needs and capabilities.
To further pursue the operationalization potential of the EV concept, it may be useful to agree upon an adequate unit of observation. Assuming a number of background factors such as the climatic context and the building type, individual spaces (rooms) in a target building may be considered to be proper candidates for determination of EV levels (see figure 1). Even though the definition of discrete rooms and their function is not straightforward in all cases, most professionals and occupants have a fairly clear idea of the meaning of the concept. Specifically, maintaining desirable indoor environmental conditions is frequently practiced at the room level. Given rooms as units of observation, we can further reflect on various aspects (or dimensions) of the EV. In other words, we can discuss the conceptual space of EV (see figure 1).
Hereby, a natural starting point would be those properties of the indoor environment whose dynamic adjustability by inhabitants is desirable/necessary. For the purpose of the present discussion, consider variables pertaining to: *i)* hygro-thermal environment (temperature humidity), *ii)* air quality (fresh air volume flow), *iii)* visual environment (daylight, electrical lighting).
In a first approximation, the problem of EV characterization (for instance, in terms of an "EV-Index") may be reduced to the availability and attributes of devices that enable inhabitants to control the relevant environmental variables. The said devices typically facilitate the modulation of mass and energy supplied to (or extracted from) a space (see figure 2). They may also change the distribution and composition of mass and energy distribution in the indoor environment. For instance, as a control device, a window can modulate the magnitude of fresh air volume flow into a room and influence indoor environmental variables such as air temperature and humidity. It can also influence the concentration of pollutants and thus the air quality. A shading device such as an external blind can modulate the magnitude of transmitted

solar radiation and daylight, thus influencing indoor environmental conditions in view of the temporal and spatial distribution of illuminance and luminance levels.
Control devices in a space can be thought of the constituents of its EV. Operationalization of EV must thus involve the appraisal of the availability and quality of these devices. Different criteria may be take into consideration toward quality evaluation of control devices and their interfaces. A number of such criteria are suggest below, formulated in terms of five basic questions (see figure 3). Note that they are not claimed to be either the only or the most conclusive criteria:

i. What is the spatial resolution level of the target zones of the control device? Can users control the state of their immediate surroundings?
ii. What is the degree of the objective effectiveness of the control device, i.e., can it fulfil, in a timely and sufficient manner, the intended task?
iii. Can the operation of the device be considered efficient in the sense of energy use and environmental impact?
iv. Can the device be deployed in a convenient and intuitive manner, or, in other words, does it come with an adequate user interface?
v. What is the degree of the subjective effectiveness of the control device, i.e., do the users have the impression that it satisfactorily performs the intended functionality?

The previous discussion suggests the following path to the operationalization of the indoor-environmental EV of a specific built space. For each domain of indoor climate (i.e., thermal, visual, air quality), an integral function over all available devices in that domain is derived, whereby weights for the aforementioned quality criteria (spatial distribution, objective effectiveness, ecological quality, user interface quality, subjective effectiveness) are assigned. Subsequently, another weighting function is needed to integrate EV indices of different domains. Following the above path involves a number of challenges. However, the biggest challenge might not be so much the formulation of a general mathematical formalism, e.g., a set of equations to calculate numeric values of the EV index (EVI). Rather, the main problem lies in the attribution of numeric values (or points) not only to the device criteria variables, but also to the weighting factors needed to arrive at integrated numeric values for a practically applicable general EVI. In fact, weights are not only needed to integrate over EVI values of different devices in a specific space, but also to integrate EVI values of different spaces in a building. This means that weighting factors would be required for integration of device level EVI values (EVI_D) into space level values (EVI_S), and space level values into building level values (EVI_B). To illustrate this challenge, consider the derivation of EVI for one device (EVI_{Di}) out of *n* devices in one space (S_j) out of *k* spaces in a building (B). Assuming this device can obtain, for each quality criterion (e.g., C1 to C5), a certain number of points (e.g., 0 to 10) and treating these points with respective weights (W_{C1} to W_{C5} totalling to 1), we obtain:

$$EVI_{Di} = EVI_{C1}.W_{C1} + EVI_{C2}.W_{C2} + \ldots + EVI_{C5}.W_{C5}$$

To further derive the EV of the space Sj, a weighted sum of individual devices in this space must be calculated:

$$EVI_{Sj} = EVI_{D1}.W_{D1} + EVI_{D2}.W_{D2} + \ldots + EVI_{Dn}.W_{Dn}$$

Finally, the building's EV index (EVI_B) would have to be derived from the weighted sum of the EV indices of all building's spaces:

$$EVI_B = EVI_{S1}.W_{S1} + EVI_{S2}.W_{S2} + \ldots + EVI_{Sk}.W_{Sk}$$

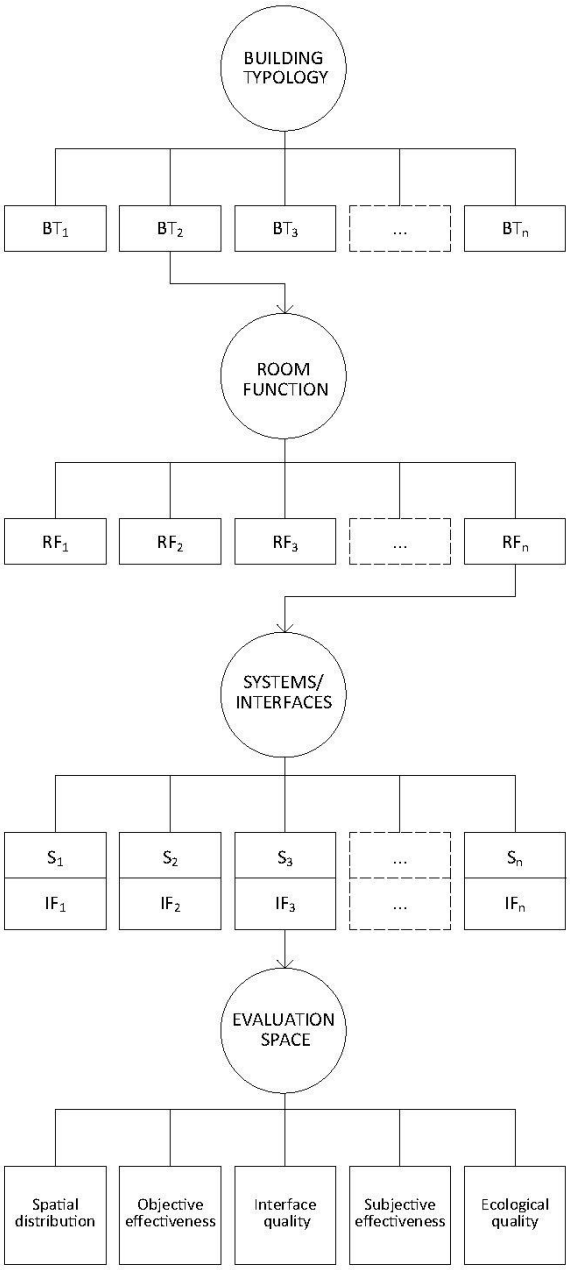

Figure 1: Illustration of the structure of a potential building EV certification scheme. Starting from typological classification of buildings and functional classification of spaces, the latter are identified as the appropriate units of observation for control device benchmarking in multiple domains. Devices are suggested to be assessed according to five evaluation criteria

DEVICES	Radiative energy modulation	Lighting modulation	Convective energy modulation	Air flow modulation	Humidity control
window	○	○	○	✓	○
exterior shades	✓	○	—	—	—
interior shades	○	✓	—	—	—
radiator	✓	—	○	—	—
radiant ceiling	✓	—	○	—	—
floor heating	✓	—	○	—	—
air diffusers	—	—	✓	✓	✓
humidifier	—	—	—	—	✓
illumination	○	✓	—	—	—
task lighting	○	✓	—	—	—
fan	—	—	—	✓	—
desk fan	—	—	—	✓	—

Figure 2: An illustrative taxonomy of buildings' control devices together with associated mechanisms (processes) they employ to influence indoor environmental conditions. "✓" stands for the main process mode, "○" stands for the secondary process mode (or side effect), and "–" for no impact

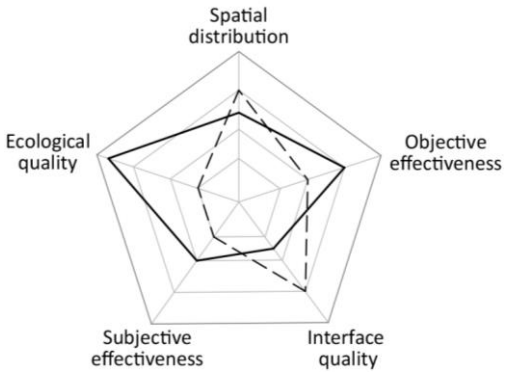

Figure 3: A polar diagram with illustrative evaluation results of environmental control devices (two domains) in a space in terms of five evaluation criteria (see text)

There are of course inherent complexities involved in the process of arriving at weighting factors pertaining to evaluation criteria of individual devices (i.e., W_{C1} to W_{C5}), consideration of multiple devices in a space (i.e., W_{D1} to W_{Dn}), and aggregation over multiple spaces (i.e., W_{S1} to W_{Sk}). As an alternative to a detailed and conceptually rigorous approach to the computation of numeric EVI values, one might consider the utilization of a kind of point-based rating system, similar to those deployed in common building quality rating and certification systems. Presumably, the availability, number, zonal distribution, objective and subjective effectiveness, user interface quality, and environmental efficiency could be captured via a simplified procedure, whereby (weighted) points would be assigned to each item and accumulated to arrive at overall scores or rankings. Such an approach may involve some benefits in terms of practical applicability. To further explore this possibility, we translated the above overall framework into a simplified protocol for a preliminary EV assessment. The next section of this paper describes this protocol and the results of its exploratory deployment in terms of a case study of an office area.

4 A PILOT STUDY

As previously mentioned, a preliminary EV assessment protocol was developed involving multiple criteria and using a point-assignment systems. To illustrate the main features of this method, consider its application to a specific room in a specific building as a case in point, for which the EVI is derived. EVI values are obtained for all rooms of the building, they could be aggregated in terms of a unified EVI value for the entire building as means of benchmarking and comparison with other buildings. The protocol for obtaining a room's EVI focuses on those features that facilitate inhabitants' interaction with the building's environmental control systems. Specifically, such features entail envelope components and technical systems such as windows, blinds, luminaires, as well as devices for heating, cooling, and ventilation controls. Thereby, following a standardised scheme, points can be assigned to the available devices and their respective basic functionalities. In the next step, quality, effectiveness, and performance aspects of these elements are evaluated with regard to the aforementioned five fundamental assessment criteria, namely: *i)* Spatial distribution, *ii)* Objective effectiveness, *iii)* Interface quality, *iv)* Subjective effectiveness, *v)* Ecological quality.

The devices are evaluated by assigning points in these five categories. In the pilot implementation of the methodology, performance evaluation of devices is suggested to involve a distinction in terms of the three basic categories of good, acceptable, and poor. Points can be defined for these three possibilities. Additional weighting factors can be included as well. They can be used if some of the evaluated devices can be seen as more important than others (i.e., have a greater influence on the indoor environmental conditions). The EVI of a room is derived

via aggregating the individual devices' points. As mentioned before, to obtain an EVI for an overall building, the EVI of each room are aggregated. In this case too, weighting factors may be applied. Thereby, relevant weighting criteria could include, for instance, the areas of the room or the number of occupants. The general scheme of this evaluation method is illustrated in figure 4 (for a specific room). This structure can be supplemented depending on further aspects such as the building type, the climatic context, and the relevant attributes of the population of the building users. The figure shows, in generic form, the aforementioned two evaluation steps. Whereas the first step (table's upper rows) depict room's multiple devices together with relevant attributes and respective points, the second step (table's lower rows) entails placeholders for points to be assigned to quality and performance attributes of each device.

4.1 Approach

The presented ecological valency evaluation method was tested for an office area in an educational building in Vienna, Austria. To conduct this case study, the general structure of the proposed evaluation method had to be defined in more detail. To this end, the structure was adapted to fit to the climatic context as well as the usage of the tested space. In a first step, the control devices and elements were selected. This was done with regards to assess the controllability of the air quality as well as hygro-thermal, and visual aspects. The specific device categories covered windows, shading, lights, heating, and cooling. Subsequently, basic availability and functional options for these categories were established, together with the corresponding point assignment scheme. In a next step, key attributes of the control devices were selected. They are part of the first component of the evaluation protocol. For the specific purposes of the present case study, every device can receive up to five points in the protocol's first step. As it was alluded to before, the second part of the protocol involves a deeper quality (effectiveness) assessment. As this step arguably addresses a more important evaluation criterion, it included the possibility to assign a larger number of points (double) to each device category. Likewise, additional weighting factors were included in the scheme to account for the fact that certain device categories may be considered to have a greater influence on the pertinent indoor environmental conditions than others. The selected attributes and points for this specific case study are shown in table 1 (basic functions assessment).

device 1			**device 2**			**...**			**device n**		
	max. points	points		max. points	points		max. points	points		max. points	points
attribute 1.1	x1		attribute 2.1	x1		...	...		attribute n.1	x1	
attribute 1.2	y1		attribute 2.2	y1		...	...		attribute n.2	y1	
attribute 1.3	z1		attribute 2.3	z1		...	...		attribute n.3	z1	
...	...		...	...		...	...		...	...	
...	...		...	...		...	...		...	...	
∑ part 1			∑ part 1			∑ part 1			∑ part 1		
		p1: poor m1: okay g1: good			p2: poor m2: okay g2: good			...			pn: poor mn: okay gn: good
spatial distribution			spatial distribution			spatial distribution			spatial distribution		
objective effectiveness			objective effectiveness			objective effectiveness			objective effectiveness		
interface quality			interface quality			interface quality			interface quality		
subjective effectiveness			subjective effectiveness			subjective effectiveness			subjective effectivenes		
ecological quality			ecological quality			ecological quality			ecological quality		
∑ part 2			∑ part 2			∑ part 2			∑ part 2		
points part 1 + part 2			points part 1 + part 2			points part 1 + part 2			points part 1 + part 2		
∑ x w1			∑ x w2			...			∑ x wn		

Figure 4: General structure of a room-level EV assessment protocol

Table 1: Basic device attributes and maximum points

Windows		Shading		Lights		Heating		Cooling	
available	2			ambient	2	available	2	available	2
turn function	2	interior shading	2	task	1	radiant	2	radiant	2
tilt function	1	exterior shading	3	Dimming; on/off	1;1	convective	1	convective	1

To conduct the second part of the assessment (effectiveness evaluation), for each device category and each evaluation criteria, points are assigned according to the following simple scheme: Evaluation of a device category as "good", "acceptable", and "poor" translates into 2, 1, and zero points respectively. Moreover, the points of the different categories are multiplied with the following weighting factors: 1.65 (windows, heating), 1 (shading, cooling), and 1.35 (lights). The protocol was tested using the case of an office area in an educational building in Vienna, Austria. Figure 5 shows a floor plan of this office area. Thirty people participated in the case study. Their task was to assess six rooms in this office area by filling out the proposed evaluation protocol and computing the EVI for each room and the overall building. The evaluation exercise was expected to shed light on the usability level of the method and the reproducibility of its results.

4.2 Results and discussion

Figure 6 shows the distribution derived EVI scores by participants for the six rooms. It is noticeable that the participants evaluated all six rooms rather similarly. Except kitchen, the mean EVI for each room is about 65. This makes sense, as the rooms in this office area are equipped rather similarly (similar types and arrangements of windows, radiators, and luminaires). Figure 7 illustrates, using CV (Coefficient of Variation) information, the degree to which participants' room-level EVI calculations diverge (results are shown separately for protocol's two parts as well as for both parts combined). As expected, participants completed the first part of the protocol more consistently than the second part: The evaluation of the availability of a device and its basic function is more straight-forward than its effectiveness. This suggests a need for finer differentiations between the choices (and points) provided in the protocol. Despite the small sample size of participants, we compared the resulting EVI scores from participants who work at the office (roughly one-third of the participants) versus visitors (see figure 8). The comparison suggests a more favourable rating on the side of the visitors. This is perhaps due to occupants' better knowledge of the conditions in their rooms and the workings of indoor environmental control systems. We also compared the votes of female (roughly two-third of the participants) and male participants (see figure 9). In this case, the female participants evaluated the rooms (particularly the kitchen) somewhat more favourably.

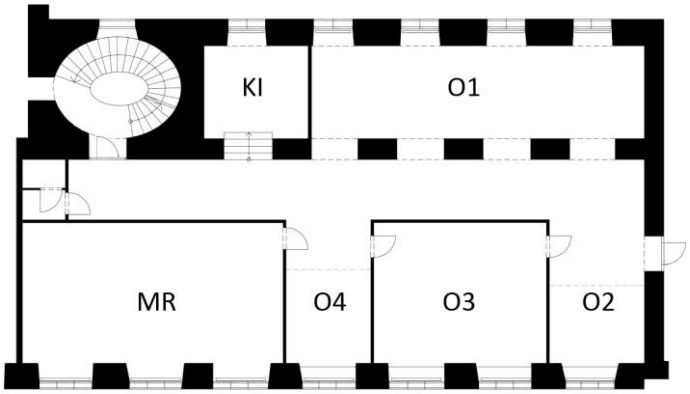

Figure 5: Floor plan office area (key: KI: kitchen, O1: office 1, O2: office 2, O3: office 3, O4: office 4, MR: meeting room)

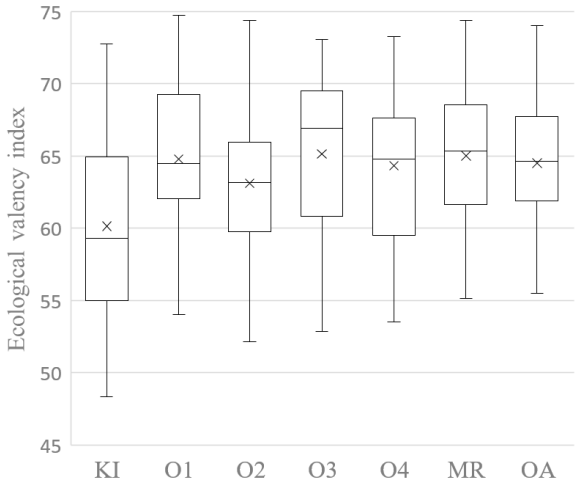

Figure 6. Room-level EVI assignments by participants (key: see figure 5)

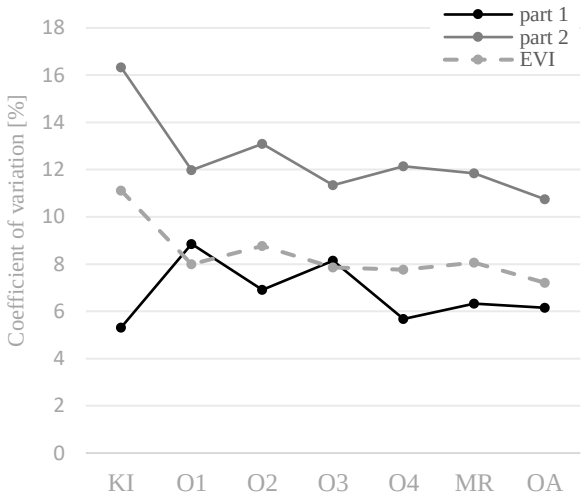

Figure 7. Coefficient of variation for EVI distributions (key: see figure 5)

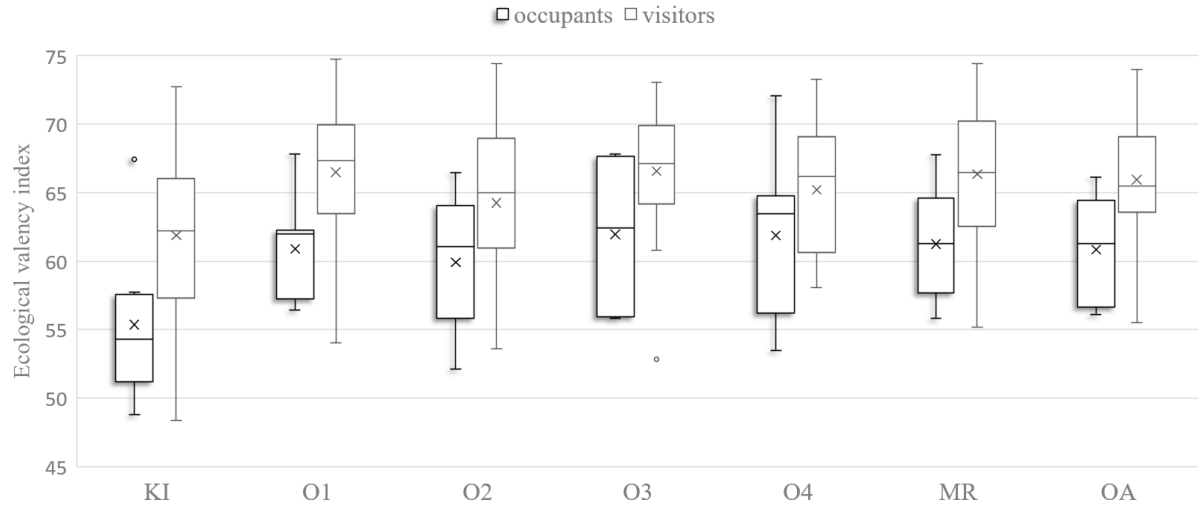

Figure 8. Comparison of EVI scores by occupants and visitors for different rooms (key: see figure 5)

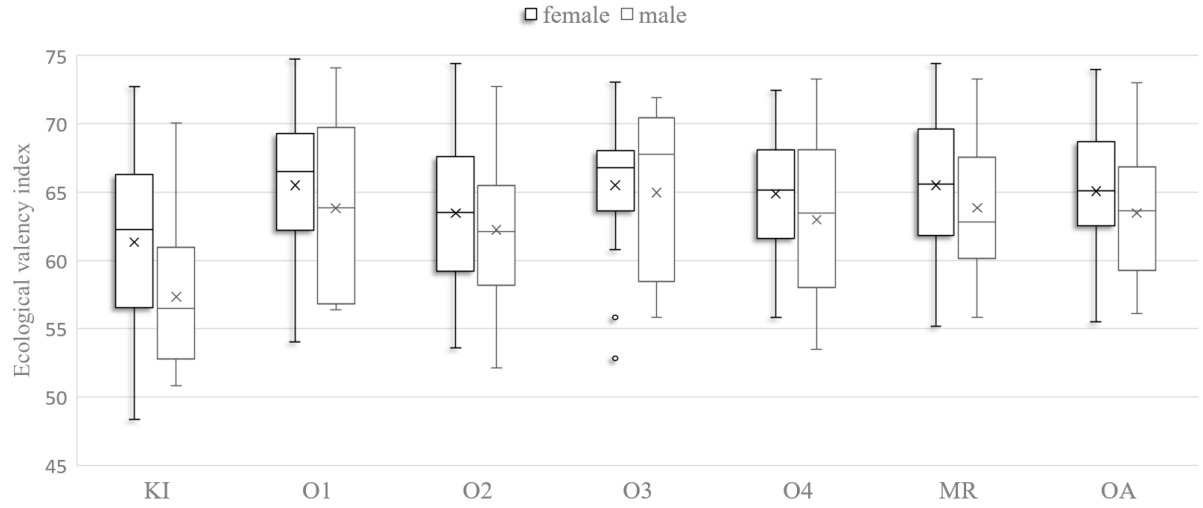

Figure 9. Comparison of EVI scores by female and male participants for different rooms (key: see figure 5)

5 CONCLUSIONS

This contribution explored the potentials and challenges for designing a certification procedure for indoor environments' EV. Toward this, we first described the theoretical foundations of the

effort and their translation into a general framework as well as a specific attempt for derivation of ecological valency index (EVI) values. The associated protocol intends to facilitate the evaluation of indoor environmental control devices in buildings. These devices are assessed via the protocol's two parts. Part one deals with the availability of the control equipment and their attributes. The second part focuses on the effectiveness of the devices. Within the latter part, the devices are evaluated based on their spatial distribution, objective and subjective effectiveness, interface quality and ecological quality. The presented method was subjected to a preliminary test for an office area. Thereby, test participants evaluated the EV fairly consistently as far as the general availability and basic functions of the devices were considered. In comparison, the variation of EVI scores was noticeably larger when the effectiveness of devices was the evaluation target. In future, the potential for improving the proposed EV evaluation method will be further explored. As such, a larger (and more diverse) number of participants will be involved in testing the robustness of the proposed protocol and its future improved variations. Likewise, we intend to examine the utility of the proposed approach based on a greater variety of buildings of different types and in different climatic regions.

6 REFERENCES

Gibson, J. (1977) *The Theory of Affordances.* In Perceiving, Acting, and Knowing, Eds. Robert Shaw and John Bransford. ISBN 0-470-99014-7

Gibson, J. (1979) *The Ecological Approach to Visual Perception*. ISBN 0-89859-959-8

Knötig, H. (1992a) *Human Ecology - The exact science of the interrelationships between Homo sapiens and the outside world surrounding this living and thinking being.* The sixth meeting of the Society for Human Ecology "Human Ecology: Crossing Boundaries". Snowbird, Utah, USA

Knötig, H. (1992b) *Some essentials of the Vienna School of Human Ecology.* Proceedings of the 1992 Birmingham Symposium; Austrian and British Efforts in Human Ecology. Archivum Oecologiae Hominis. Vienna, Austria

Mahdavi, A. (1996a) *Approaches to Noise Control: A Human Ecological Perspective.* Proceedings of the NOISE-CON 96 (The 1996 National Conference on Noise Control Engineering). Bellevue, WA, USA. pp. 649 – 654

Mahdavi, A. (1996b) *Human Ecological Reflections on the Architecture of the "Well-tempered Environment".* In Proceedings of the 1996 International Symposium of CIB W67 (Energy and Mass Flows in the Life Cycle of Buildings). Vienna, Austria. pp. 11 - 22

Mahdavi, A. (1996c) *A Human Ecological View of "Traditional" Architecture.* Human Ecology Review (HER). Volume 3, Number 1. pp. 108 - 114

Mahdavi, A. (2016) *The human factor in sustainable architecture.* Low Energy Low Carbon Architecture: Recent Advances & Future Directions. Taylor & Francis, London, UK. ISBN: 978-1-138-02748-0, pp. 137 – 158

Mahdavi, A. (2019) *Can we quantify the ecological valency of built environments?* 12th Envibuild conference (2017) - Buildings and Environment - From Research to Application "*enviBUILD - Proceedings: Building and Environment*", Trans Tech Publications, ISBN: 978-3-0357-1202-5

Mahdavi, A. and Berger, C. (2019). *An inquiry into the certification potential of built environments' affordance.* CLIMA 2019 – 13th HVAC World Congress. (to appear)

Norman, D. (2013) *The design of everyday things*. ISBN 9780465050659

Uexküll, J. (1920) *Kompositionslehre der Natur*. (Edited by Thure von Uexküll). Frankfurt am Main

Residential Application of an Indoor Carbon Dioxide Metric

Andrew Persily, Brian J. Polidoro

National Institute of Standards and Technology
100 Bureau Drive, MS8600
Gaithersburg, MD 20899 USA
**Corresponding author: andyp@nist.gov*

ABSTRACT

Indoor carbon dioxide (CO_2) concentrations have been used for decades to evaluate indoor air quality (IAQ) and ventilation. However, many of these applications reflect a lack of understanding of the connection between indoor CO_2, ventilation rates and IAQ. In particular, a concentration of 1800 mg/m^3 (1000 ppm$_v$) has been used as a metric of IAQ and ventilation without an appreciation of its basis or application. After many years of trying to dissuade practitioners and researchers from using CO_2 as a metric of ventilation and IAQ, the first author developed an approach to determine CO_2 levels that can be used as more meaningful indicators. This approach is based on the fact that space types differ in their recommended or required ventilation rates, occupancy and other features that impact indoor CO_2 concentrations. Rather than employ a single CO_2 concentration for all spaces and occupancies, this alternative approach involves the estimation of space-specific CO_2 concentrations. The concept considers the steady-state CO_2 concentration that would be expected in a given space type based on its intended or expected ventilation rate per person, the time to achieve steady-state, the number of occupants as well as the rate at which they generate CO_2, and the occupancy schedule as it pertains to the likelihood that steady-state will be achieved.

This alternative approach was described in a previous AIVC conference paper, with sample calculations presented for several commercial and institutional building spaces. Those calculations yielded potential CO_2 concentration metrics, along with corresponding measurement times after full occupancy. Based on these analyses, it was stressed that reported CO_2 concentrations for comparison to these or other metrics need to be associated with a measurement time relative to the start of occupancy as well as information about the space in question and its occupancy. Since this previous work, an online calculator has been developed to allow users to perform these calculations, and that calculator is described here. In addition, this paper applies the approach to residential buildings, which are more challenging based on their varying configurations and the large fraction of time that occupants spend in bedrooms.

KEYWORDS

Building performance; carbon dioxide; indoor air quality; metrics; residential; ventilation

1 INTRODUCTION

Indoor air quality (IAQ) is characterized by the chemical and physical constituents of air that impact occupant health, comfort and productivity. The number of airborne contaminants in most indoor environments is quite large, and their impacts on building occupants are known for only a very small number of contaminants. The large number of contaminants, and their wide variation among and within buildings and over time, makes it extremely challenging to quantify IAQ, let alone to distinguish between good and bad IAQ based on a single metric. There have been efforts to define IAQ metrics, but none have been shown to capture the health and comfort impacts of IAQ very well or have become accepted in the field (Jackson et al., 2011; Hollick and Sangiovanni, 2000; Moschandreas et al., 2005; Teichman et al., 2015).

The indoor concentration of carbon dioxide (CO_2) has been widely promoted as a metric of IAQ and ventilation, in many cases without a clear explanation of what it is intended to characterize, or a description of its application or its limitations (Persily, 1997). Nevertheless, many practitioners use 1800 mg/m^3 (roughly 1000 $ppm_{v)}$ as a metric, often erroneously basing it on ASHRAE Standard 62.1 (ASHRAE, 2016a). However, that standard has not contained an indoor CO_2 limit for almost 30 years (Persily, 2015a). There have been many papers and presentations that have attempted to clarify the meaning of indoor CO_2 concentrations, some advocating that they not be used at all in IAQ and ventilation evaluations. However, these calls to stop poorly informed applications of indoor CO_2 are not succeeding. Instead, efforts to educate designers, practitioners and others need to continue, and this paper expands on a previously-described approach to using indoor CO_2 concentrations as a metric of ventilation rate per person that thoroughly considers the parameters that determine indoor CO_2 levels (Persily, 2018). That previous discussion presented the approach and outlined its application to a number of commercial and institutional building spaces. This paper expands the consideration to residential buildings and describes an on-line calculator that allows the estimation of indoor CO_2 concentrations in applying this approach.

2 BACKGROUND

Indoor CO_2 concentrations have been prominent in discussions of ventilation and IAQ since the 18th century (Klauss et al., 1970). Since that time, discussions of CO_2 in relation to IAQ and ventilation have evolved, focusing on the impacts of CO_2 concentrations on building occupants, how these concentrations relate to occupant perception of bioeffluents, the use of indoor CO_2 concentrations to estimate ventilation rates, and the control outdoor air ventilation rates based on indoor CO_2 concentrations (Persily, 2015b; Persily, 1997).

Indoor CO_2 concentrations are directly related to the outdoor air ventilation rates per person specified in standards, guidelines and building regulations (ASHRAE, 2016a; ASHRAE, 2016b; CEN, 2007b; CEN, 2009). These outdoor air requirements reflect research on the amount of ventilation needed to control odor associated with the byproducts of human metabolism, as well as other contaminants emitted by building materials and furnishings (Persily, 2015a). This research has found that about 7.5 L/s to 9 L/s per person of ventilation air dilutes body odor to levels judged to be acceptable by individuals entering a room from clean air, i.e., unadapted visitors. This research also supports 1800 mg/m^3 of CO_2 as a reflection of body odor acceptability perceived by unadapted visitors. Of course, there are many other important indoor air contaminants that are not associated with the number of occupants, and CO_2 concentration is not a good indicator of those contaminants.

Indoor CO_2 concentrations are typically well below values of interest based on health concerns (Persily, 2017). Some recent work has shown evidence of impacts on human performance, as well as other health impacts, at levels on the order of 1800 mg/m^3 (Azuma et al., 2018; Snow et al., 2019), while other studies have not shown performance impacts at similar concentrations. It is therefore premature to conclusively link CO_2 concentrations in this range with such occupant impacts until more research is done.

While indoor CO_2 concentrations are not meaningful indicators of overall IAQ, a previous paper describes the use of CO_2 as an indicator or metric of outdoor air ventilation rates per person (Persily, 2018). As discussed in that paper, indoor CO_2 concentrations depend primarily on the rate at which the occupants generate CO_2, the outdoor air ventilation rate of the space, the time since occupancy began, and the outdoor CO_2 concentration. For the purposes of these discussions, outdoor air ventilation refers to the total rate at which outdoor air enters the building or space of interest, including mechanical and natural ventilation as well as infiltration.

The cited paper describes the single-zone mass balance theory to calculate indoor CO_2 concentrations from these parameters per the following equation:

$$C(t) = C(0)e^{-\frac{Q}{V}t} + C_{ss}\left(1 - e^{-\frac{Q}{V}t}\right), \quad (1)$$

where C is the CO_2 concentration in the space in mg/m^3, $C(0)$ is the indoor concentration at t = 0, t is time in hours, Q is the volumetric flow of air into the space from outdoors and from the space to the outdoors in m^3/h, and V is the volume of the space being considered in m^3. The steady-state CO_2 concentration C_{ss} is given by:

$$C_{ss} = C_{out} + {}^{G}/_{Q}, \quad (2)$$

where C_{out} is the outdoor CO_2 concentration and G is the CO_2 generation rate in the space in mg/h. Q, C_{out} and G are in general functions of time but are assumed constant in this analysis. Also, air density differences between indoors and out are being ignored by using the same value of Q for the airflow into and out of the space. Finally, this single zone formulation ignores concentration differences within and between building zones and CO_2 transport between zones and assumes there are no other indoor sources of CO_2 other than occupants.

Note that the indoor concentration will only get sufficiently close to steady-state if conditions, specifically Q and G, are constant for a long enough period of time. In particular, a constant value of G requires that the occupancy remain constant, but in many spaces occupancy will be too short or too variable for steady-state to be achieved. A convenient means of assessing whether steady-state is likely to be achieved is by comparing the duration of constant occupancy to the time constant of the space. The time constant is equal to the inverse of Q/V in Equation 1, i.e., the inverse of the air change rate, and the indoor concentration will be about 95 % of steady-state after three time constants. For example, for an air change rate of 1 h^{-1}, steady-state will exist after 3 hours. For an air change rate of 0.5 h^{-1}, it will take 6 hours.

Table 1: Calculated CO_2 concentrations

			CO_2 concentration above outdoors (mg/m^3)		
Space Type	**t_{metric} (h)**	**Time to steady-state (h)***	**Steady-state**	**1 h**	**t_{metric}**
Classroom (5 to 8 y)	2	1.4	1060	940	1040
Classroom (>9 y)	2	1.1	1580	1490	1580
Lecture classroom	1	0.9	1940	1870	1870
Restaurant	2	0.7	1871	1850	1870
Conference room	1	1.6	2526	2130	2130
Hotel/motel bedroom	6	4.5	1080	520	1060
Office space	2	5.9	985	390	630
Auditorium	1	0.6	2900	2880	2880
Lobby	1	0.6	4467	4430	4430
Retail/Sales	2	2.1	1546	1170	1450

* Time to achieve 95 % of steady-state CO_2 concentration, i.e., three time constants

In the previous work on this CO_2 metric concept, several space types were selected from the commercial/institutional building space types or "Occupancy Categories" in Table 6.2.2.1 of ASHRAE Standard 62.1 (ASHRAE, 2016a). For these spaces, shown in Table 1, CO_2 concentrations above outdoors were calculated at steady-state, after 1 h of occupancy, and at a time t_{metric}, which was selected as a time over which the particular space type may be expected to be fully occupied. That time is in the first column of Table 1, while the time to reach steady-state is in the second column. The assumed occupant densities, occupant characteristics and CO_2 generation rates are described in Persily (2018).

Based on the previous work, including the desire for a CO_2 metric to capture ventilation deficiencies and to be less sensitive to the timing of the concentration measurement, Table 2 summarizes potential CO_2 metric values for these spaces along with the corresponding measurement time. Given the transient nature of indoor CO_2 concentrations, it is critical that a concentration CO_2 metric be linked to a measurement time. Therefore, reported CO_2 concentrations relative to these and any other metrics need to include the time that has passed since the space reached full occupancy. Consideration of additional spaces and different input values would possibly yield other conclusions about potential metrics. Such analyses will be facilitated by the online tool described below.

Table 2: Potential CO_2 concentration metrics

Space Type	CO_2 concentration metric, above outdoors (mg/m^3)	Corresponding time (h after full occupancy)
Classroom (5 to 8 y)	1000	2
Classroom (>9 y)	1500	1
Lecture classroom	2000	1
Restaurant dining room	2000	1
Conference meeting room	2000	1
Hotel/motel bedroom	1000	6
Office space	600	2
Public assembly/Auditorium	3000	1
Public assembly/Lobby	4500	1
Retail/Sales	1500	2

3 CO_2-BASED VENTILATION METRIC FOR RESIDENTIAL SPACES

This paper extends the concepts discussed above to residential spaces, which can be challenging given the variations in dwelling and family size and in occupant characteristics, as well as the often unpredictable durations of occupancy relative to some commercial and institutional spaces. However, the many hours associated with sleep provide helpful options for these analyses in bedrooms. The approach taken is again to use Equation (1) to calculate the CO_2 concentrations for a given space based on assumptions about the CO_2 generation rates and ventilation rate of the space. In order to explore these dependencies for residential spaces, indoor CO_2 concentrations were calculated for the occupancies listed in Table 3, which describes 3 families: a baseline with 4 members (2 adults and 2 children), a larger family with 2 additional children, and a smaller family with 2 adults and no children. The sex, age, body mass and level of physical activity are described for each family, including the CO_2 generation rate in L/s for each person calculated using the methodology in Persily and de Jonge (2017), as well as the average CO_2 generation rate per person. These generation rates are presented for the whole house during non-sleep hours when occupants are assumed to be more active, and for bedrooms when occupants are sleeping. For occupant characteristics that differ from those considered here, the online tool described below is enables analysis of different occupancies. For each occupancy in Table 3, CO_2 concentrations were calculated for the following ventilation scenarios:

Whole house:

- Ventilation rate requirement from ASHRAE Standard 62.2 (ASHRAE, 2016b)
- Ventilation rate of 0.5 h^{-1}

Bedrooms:

- 62.2/Perfect Distribution: Bedroom ventilation rate is the Standard 62.2 rate divided by the number of house occupants, multiplied by the number of bedroom occupants

- 62.2/Uniform Distribution: Bedroom ventilation rate is the Standard 62.2 rate divided by the whole house floor area, multiplied by the bedroom floor area
- 0.5/Perfect Distribution: Bedroom ventilation rate is 0.5 h^{-1} times the house volume divided by the number of house occupants and then multiplied by the number of occupants in each bedroom
- 0.5/Uniform Distribution: Bedroom ventilation rate is 0.5 h^{-1} times the house volume divided by the whole house floor area, and then multiplied by the bedroom floor area
- 10 L/s per person/Perfect Distribution: Bedroom ventilation rate is 10 L/s multiplied by the number of bedroom occupants

Table 3: Occupancy Assumptions for CO_2 concentration calculations

Case	**Occupants** (age, body mass in kg, met level)	**CO_2 generation per person (L/s)**	**Average CO_2 generation per person (L/s)**
Baseline family of 4			
Whole house	1 male (40 y, 85 kg, 1.3 met); 1 female (40 y, 75 kg, 1.3 met); 1 male (6 y, 23 kg, 2 met); 1 female (10 y, 40 kg, 1.7 met)	0.0049 0.0038 0.0042 0.0042	0.0043
Master Bedroom	1 male (40 y, 85 kg, 1.3 met); 1 female (40 y, 75 kg, 1.3 met);	0.0037 0.0029	0.0033
Child Bedrooms	1 male (6 y, 23 kg, 2 met); 1 female (10 y, 40 kg, 1.7 met)	0.0021 0.0025	0.0023
Additional occupants in larger family of 6			
Whole house	1 male (8 y, 32 kg, 2 met); 1 female (4 y, 14 kg, 2 met)	0.0050 0.0031	0.0042*
Master Bedroom	No change		0.0033
Child Bedrooms	1 male (8 y, 23 kg, 2 met); 1 female (4 y, 40 kg, 1.7 met)		0.0022*
Smaller family of 2 (no children)			
Whole house	Only adults		0.0043
Master Bedroom	Only adults		0.0033

* Average CO_2 generation rate accounts for all 6 occupants in whole house and all 4 children in child bedrooms.

The Standard 62.2 whole house ventilation requirement Q_{tot} in L/s is calculated using Equation (4.1b) from the standard, i.e.,

$$Q_{tot} = 0.15A_f + 3.5(N_{br} + 1), \quad (2)$$

where A_f is the floor area in m^2 and N_{br} is the number of bedrooms. The value of Q_{tot} is used in this analysis without any of the adjustments allowed by Standard 62.2, such as the infiltration credit. The whole house air change rate of 0.5 h^{-1} is included as it is recommended in several international standards and guidelines (CEN, 2007a; Concannon, 2002).

For the bedroom cases, two idealized air distribution scenarios are applied to the Standard 62.2 and 0.5 h^{-1} whole house rates. In the first, Perfect Distribution, the whole house rate is divided by the number of occupants in the house. That normalized value is multipled by the number of occupants in each bedroom to determine the ventilation to each bedroom. Perfect Distibution may correspond to a ventlation system that supplies outdoor air directly to each bedroom based on the number of occupants. Under Uniform Distribution, the total ventilaiton rate is normalized by the floor area of the entire house, and the ventilation rate of each bedroom is that normalized rate multiplied by its floor area. Uniform distribution may correspond to a building ventilated by infiltration only, an exhaust-only ventilation system or a mechanical ventilation system that is integrated into a forced-air distribution system. The last bedroom ventilation rate, 10 L/s per

person/Perfect Distribution, assumes 10 L/s of outdoor air is supplied for each person in each bedroom. That rate is based on recommendations in CEN (2007a) and (2009).

Table 4 presents the dimensions (ceiling heights and floor areas) for the houses considered.

Table 4: House and bedroom sizes for cases considered

	Ceiling height (m)	House floor area (m^2)	Master bedroom floor area (m^2)	Child bedrooms floor area (m^2)
Large House	2.44	250	30	20
Small house	2.74	200	20	15

Table 5 presents ventilation rates and calculated CO_2 concentrations (above outdoors). The second and third columns contain the outdoor air ventilation rate in L/s per person and h^{-1} for the whole house and bedroom cases. The fourth column is the time to reach a steady-state CO_2 concentration, i.e., three times the inverse of the air change rate. The table does not include t_{metric}, which as described earlier is a time over which a particular space may be expected to be fully occupied. Throughout these analyses, t_{metric} is 2 h for the whole house and 6 h for the bedrooms. The last three columns are the calculated CO_2 concentrations at steady-state, 1 h after occupancy and t_{metric}. The whole house air change rates based on Standard 62.2 are about 0.3 h^{-1} in all but the small house/baseline family case, in which it is about 0.5 h^{-1}. The bedroom air change rates cover a range of almost 10 to 1 for the different cases in the large house/baseline family and the small house/small family. In both of those occupancies, delivering 0.5 h^{-1} directly to the bedrooms under Perfect Distribution results in air change rates above 2 h^{-1} and well over 15 L/s per person. On the other hand, Uniform Distribution to the bedrooms results in less than 5 L/s per person in several cases. These air change rates impact the time required to achieve steady-state, which are 6 h or less for the bedrooms cases other than for 62.2/Uniform. For the whole house, the time to steady-state ranges from 3 h to more than 11 h.

The calculated CO_2 concentrations in Table 5 reflect the differences in ventilation and CO_2 generation for the specific occupancies. It is worth noting that the only steady-state bedroom concentrations greater than 1800 mg/m^3 (assuming an outdoor concentration of 700 mg/m^3) occur in the master bedroom for all 62.2/Uniform cases and for the small house/small family 0.5/Uniform case. Also, for cases with short time constants, 2 h or less, the three CO_2 concentrations are not very different from each other. Much larger differences are seen for larger time constants. In all whole house cases, the concentrations at t_{metric} are at least 200 mg/m^3 above outdoors, which is above the uncertainty typically associated with field measurements of indoor CO_2 concentrations. The bedroom concentrations at t_{metric} are typically even higher, except in the 0.5 h^{-1}/CBR/Perfect case, for which the steady-state concentration is less than 200 mg/m^3. The magnitude of these concentrations relative to typical measurement uncertainties supports the use of such calculated concentrations as a metric, although assuming constant occupancy in a whole house for 2 h could be questionable under some circumstances. It is worth noting that the range of CO_2 concentrations at t_{metric} for each occupancy range by at least 4 to 1 in the small house/baseline family case, to as much as almost 9 to 1 in the large house baseline/family case. These differences demonstrate the importance of considering the target ventilation rate in using calculated CO_2 concentrations as a metric. Also, for the same ventilation case, the differences in calculated CO_2 concentrations at t_{metric} for the different occupancies are not as large as those within the same occupancy for the different ventilation cases. However, they are large enough to be reliably measured and support the need to consider house size and occupancy when using calculated concentrations as a metric.

Table 5: Ventilation rates and calculated CO_2 concentrations for the residential cases

	Outdoor air ventilation		Time to steady-state (h)	CO_2 Concentration above outdoors (mg/m^3)		
Case*	**L/s per person**	**h^{-1}**		**Steady-state**	**1 h**	**t_{metric}**
Large House/Baseline family						
Whole house – 62.2	12.9	0.27	11.1	598	142	250
Whole house – 0.5 h^{-1}	23.8	0.50	6.0	324	127	205
62.2/ MBR/Perfect	12.9	1.13	2.7	461	312	461
62.2/ CBR/Perfect	12.9	0.85	3.5	322	184	320
62.2/MBR/Uniform	3.1	0.27	11.1	1922	456	1543
62.2/CBR/Uniform	4.1	0.27	11.1	1005	238	807
0.5 h^{-1}/MBR/Perfect	23.8	2.08	1.4	250	219	250
0.5 h^{-} CBR/Perfect	23.8	1.56	1.9	174	138	174
0.5 h^{-1}/MBR/Uniform	5.7	0.50	6.0	1041	409	989
0.5 h^{-1}/ CBR/Uniform	7.6	0.50	6.0	544	214	517
10 L/s per person/MBR/Perfect	10.0	0.88	3.4	594	347	591
10 L/s per person/CBR/Perfect	10.0	0.66	4.6	414	199	406
Large House/Large family						
Whole house – 62.2	9.8	0.31	9.8	775	205	356
Whole house – 0.5 h^{-1}	15.9	0.50	6.0	477	188	301
62.2/ MBR/Perfect	9.8	0.85	3.5	609	350	606
62.2/ CBR/Perfect	9.8	0.64	4.7	402	190	393
62.2/MBR/Uniform	3.5	0.31	9.8	1692	448	1425
62.2/ CBR/Uniform	4.7	0.31	9.8	837	221	704
0.5 h^{-1}/MBR/Perfect	15.9	1.39	2.2	375	281	375
0.5 h^{-} CBR/Perfect	15.9	1.04	2.9	247	160	246
0.5 h^{-1}/MBR/Uniform	5.7	0.50	6.0	1041	409	989
0.5 h^{-1}/ CBR/Uniform	7.6	0.50	6.0	514	202	489
10 L/s per person/MBR/Perfect	10.0	0.88	3.4	594	347	591
10 L/s per person/CBR/Perfect	10.0	0.66	4.6	392	189	384
Small House/Baseline family						
Whole house – 62.2	7.3	0.43	7.0	1061	369	610
Whole house – 0.5 h^{-1}	8.5	0.50	6.0	908	357	574
62.2/ MBR/Perfect	7.3	1.07	2.8	819	538	818
62.2/ CBR/Perfect	7.3	0.71	4.2	571	291	563
62.2/MBR/Uniform	2.9	0.43	7.0	2048	713	1891
62.2/ CBR/Uniform	4.4	0.43	7.0	952	331	879
0.5 h^{-1}/MBR/Perfect	8.5	1.25	2.4	701	500	701
0.5 h^{-} CBR/Perfect	8.5	0.83	3.6	489	276	485
0.5 h^{-1}/MBR/Uniform	3.4	0.50	6.0	1753	690	1666
0.5 h^{-1}/ CBR/Uniform	5.1	0.50	6.0	814	320	774
10 L/s per person/MBR/Perfect	10.0	1.48	2.0	594	458	594
10 L/s per person/CBR/Perfect	10.0	0.98	3.1	414	259	413
Small House/Small family						
Whole house – 62.2	11.0	0.32	9.2	700	194	334
Whole house – 0.5 h^{-1}	16.9	0.50	6.0	454	179	287
62.2/ MBR/Perfect	11.0	1.62	1.8	540	433	540
62.2/MBR/Uniform	2.2	0.32	9.2	2700	748	2315
0.5 h^{-1}/MBR/Perfect	16.9	2.50	1.2	351	322	351
0.5 h^{-1}/MBR/Uniform	3.4	0.50	6.0	1753	690	1666
10 L/s per person/MBR/Perfect	10.0	1.45	2.0	594	458	594

* MBR and CBR stand for master bedroom and child bedroom, respectively.

Table 6: Calculated CO_2 concentrations for the residential cases with 25 % ventilation rate reduction

	Outdoor air ventilation		Time to steady-state (h)	CO_2 Concentration above outdoors (mg/m^3)		
Case*	**L/s per person**	**h^{-1}**		**Steady-state**	**1 h**	**t_{metric}**
Large House/Baseline family						
Whole house – 62.2	10.5	0.22	13.6	**731**	145	261
Whole house – 0.5 h^{-1}	17.8	0.38	8.0	**431**	135	228
62.2/ MBR/Perfect	10.5	0.92	3.3	**564**	340	**562**
62.2/ CBR/Perfect	10.5	0.69	4.3	393	196	387
62.2/MBR/Uniform	2.5	0.22	13.6	**2350**	467	**1728**
62.2/CBR/Uniform	3.4	0.22	13.6	**1228**	244	**903**
0.5 h^{-1}/MBR/Perfect	17.8	1.56	1.9	333	263	333
0.5 h^{-} CBR/Perfect	17.8	1.17	2.6	232	160	232
0.5 h^{-1}/MBR/Uniform	4.3	0.38	8.0	**1387**	434	**1241**
0.5 h^{-1}/ CBR/Uniform	5.7	0.38	8.0	**725**	227	**649**
10 L/s per person/MBR/Perfect	7.5	0.66	4.6	**792**	381	**777**
10 L/s per person/CBR/Perfect	7.5	0.49	6.1	**552**	215	**523**
Large House/Large family						
Whole house – 62.2	8.2	0.26	11.6	**923**	210	372
Whole house – 0.5 h^{-1}	11.9	0.38	8.0	**636**	199	335
62.2/ MBR/Perfect	8.2	0.72	4.2	**725**	371	**716**
62.2/ CBR/Perfect	8.2	0.54	5.6	478	199	459
62.2/MBR/Uniform	2.9	0.26	11.6	**2015**	459	**1587**
62.2/ CBR/Uniform	3.9	0.26	11.6	**996**	227	785
0.5 h^{-1}/MBR/Perfect	11.9	1.04	2.9	**499**	323	**499**
0.5 h^{-} CBR/Perfect	11.9	0.78	3.8	329	178	326
0.5 h^{-1}/MBR/Uniform	4.3	0.38	8.0	**1387**	434	**1241**
0.5 h^{-1}/ CBR/Uniform	5.7	0.38	8.0	**686**	214	**614**
10 L/s per person/MBR/Perfect	7.5	0.66	4.6	**792**	381	**777**
10 L/s per person/CBR/Perfect	7.5	0.49	.1	**522**	203	**495**
Small House/Baseline family						
Whole house – 62.2	6.3	0.37	8.1	**1219**	379	640
Whole house – 0.5 h^{-1}	6.4	0.38	8.0	**1211**	379	639
62.2/ MBR/Perfect	6.3	0.93	3.2	**941**	570	**937**
62.2/ CBR/Perfect	6.3	0.62	4.8	656	303	640
62.2/MBR/Uniform	2.5	0.37	8.1	**2352**	732	**2101**
62.2/ CBR/Uniform	3.8	0.37	8.1	**1093**	340	976
0.5 h^{-1}/MBR/Perfect	6.4	0.94	3.2	**935**	569	**931**
0.5 h^{-} CBR/Perfect	6.4	0.63	4.8	**652**	303	**636**
0.5 h^{-1}/MBR/Uniform	2.5	0.38	8.0	**2337**	731	**2091**
0.5 h^{-1}/ CBR/Uniform	3.8	0.38	8.0	**1086**	340	**971**
10 L/s per person/MBR/Perfect	7.5	1.11	2.7	**792**	530	**791**
10 L/s per person/CBR/Perfect	7.5	0.74	4.1	**552**	288	**545**
Small House/Small family						
Whole house – 62.2	9.1	0.27	11.1	**843**	199	351
Whole house – 0.5 h^{-1}	12.7	0.38	8.0	**606**	189	319
62.2/ MBR/Perfect	9.1	1.35	2.2	**651**	482	**651**
62.2/MBR/Uniform	1.8	0.27	11.1	**3255**	768	**2608**
0.5 h^{-1}/MBR/Perfect	12.7	1.88	1.6	**467**	396	**467**
0.5 h^{-1}/MBR/Uniform	2.5	0.38	8.0	**2337**	731	**2091**
10 L/s per person/MBR/Perfect	7.5	1.11	2.7	**792**	530	**791**

* MBR and CBR stand for master bedroom and child bedroom, respectively.

To the evaluate the usefulness of calculated CO_2 concentrations as ventilation metrics, the calculations presented in Table 5 were redone with the assumed ventilation rates reduced by 25 %. As in the commercial and institutional occupancies discussed in Persily (2018), these additional calculations were performed to assess how much the concentrations change at lower ventilation rates since a useful metric should capture such changes. The CO_2 concentrations for the reduced ventilation rates are shown in Table 6, as well as the outdoor ventilation rates for each case in L/s per person and h^{-1} and the times to reach steady-state. Values that increase by 100 mg/m^3 or more relative to the corresponding values in Table 5 are noted in bold font. The whole-house, reduced-ventilation concentrations at t_{metric} in Table 6 increase very little relative to the corresponding values in Table 5, often by 30 mg/m^3 or less, which is comparable with the measurement accuracy of many field measurements of CO_2 concentrations. This lack of increase is partly due to the long time constants of the whole-house cases, which allow little time for the concentration to increase after only 2 h. The increases in the bedroom concentrations are more significant, typically at least 100 mg/m^3 and often several hundred mg/m^3 higher for the reduced ventilation cases for a t_{metric} of 6 h. These larger increases for the bedroom support the use of a 6 h value of t_{metric} to capture ventilation deficiencies in bedrooms.

In contrast to the commercial and institutional occupancies discussed by (Persily, 2018), these residential cases are less constrained by space size, occupancy and ventilation, making it difficult to generalize these results to develop CO_2 metrics for residential buildings. Instead, the house, occupancy and air distribution approach need to be accounted for in developing a metric or reference point for evaluating the adequacy of the ventilation rate relative to a target value. The online tool discussed in the next section was developed to implement these concepts.

4 ON-LINE CO_2 METRIC CALCULATOR

In order to support application of the proposed CO_2 concentration metric, an online tool (available at https://pages.nist.gov/CONTAM-apps/webapps/CO2Tool/#/) has been developed. This tool allows the user to estimate indoor CO_2 concentrations in a ventilated space at steady-state, 1 h after occupancy and at a selected value of t_{metric}. These calculated concentrations can then be compared with measured concentrations in a building to evaluate whether the intended or required ventilation rate is actually being achieved. Such a building-specific metric or reference value is far better than using a single value such as 1800 mg/m^3.

Figure 1 shows the first screen encountered when using the tool, where one first selects to analyze a commercial/institutional building or a residential building. Depending on that selection, the user then enters the required inputs. For commercial/institutional buildings, the tool allows one to select from several of the commercial and institutional space types listed in ASHRAE Standard 62.1-2016, and to use the default values in that standard for outdoor ventilation requirements and occupant density, i.e., number of occupants per 100 m^2 of floor area. The tool makes assumptions about the occupants in each space, i.e., sex, body mass, age and activity level in met, needed to calculate the CO_2 generation rate in the space based on Persily and de Jonge (2017). However, these assumptions can be modified by selecting User-Defined Model Type, which brings up an alternative input screen.

The residential building inputs are shown in Figure 2. In this case, the user selects whether they are performing a whole building or bedroom analysis. If whole building is selected, the user can select the ventilation requirement based on Standard 62.2-2016 or enter a whole building air change rate in h^{-1}. If instead they chose to perform a bedroom analysis, they need to select the ventilation requirement from Standard 62.2 or enter a L/s per person ventilation rate. In either case, they also need to define the air distribution as Perfect or Uniform as described above. Under Perfect Distribution, they have the option of having some of the ventilation air

bypass the bedrooms entirely, to account for supply vents in other portions of the house. If desired, an Alternate Ventilation per Person input can be input to enable comparison of the results to those obtained with the Primary ventilation rate.

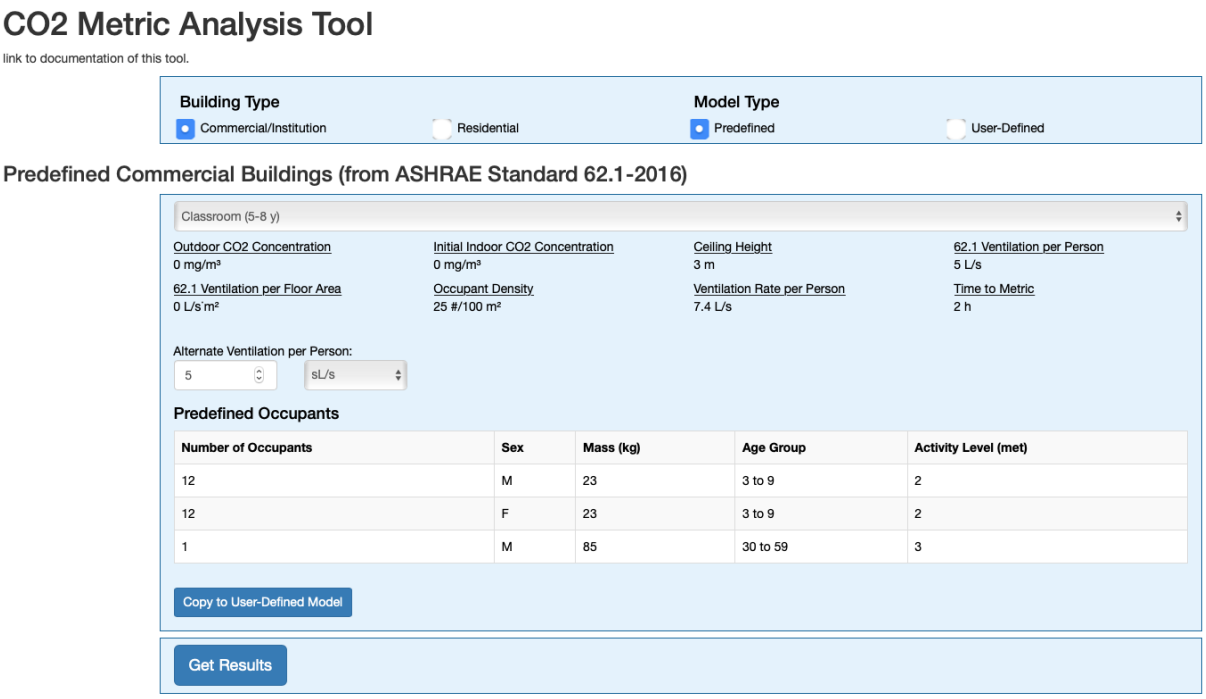

Figure 1: CO_2 Metric Calculator Default Inputs Screen

Once the user has completed the inputs, they click Get Results on the bottom of the Inputs page. This action brings up the Results screen shown in Figure 3, which summarizes the inputs and displays a plot of the indoor CO_2 concentration versus time, along with concentration values at steady-state, t_{metric} and 1 h after occupancy for both the Primary and Alternate ventilation rates.

The tool is applied by comparing the calculated CO_2 concentrations to measured values, with a measured value that is higher serving as an indication that the actual ventilation rate is below the assumed or desired ventilation rate. For comparisons with a calculated whole house value, the measured CO_2 concentration should be a volume-weighted, whole house average based on the concentrations measured in each room. Since the calculation assumes constant occupancy, the measurement needs to occur while occupancy is constant, which can be limited in duration. Ideally, a constant occupancy period that lasts for t_{metric} occurs for the whole house, and the calculated value at that time are then used for the comparison. If constant occupancy does not last that long (default value of 2 h), the t_{metric} value in the calculator can be modified.

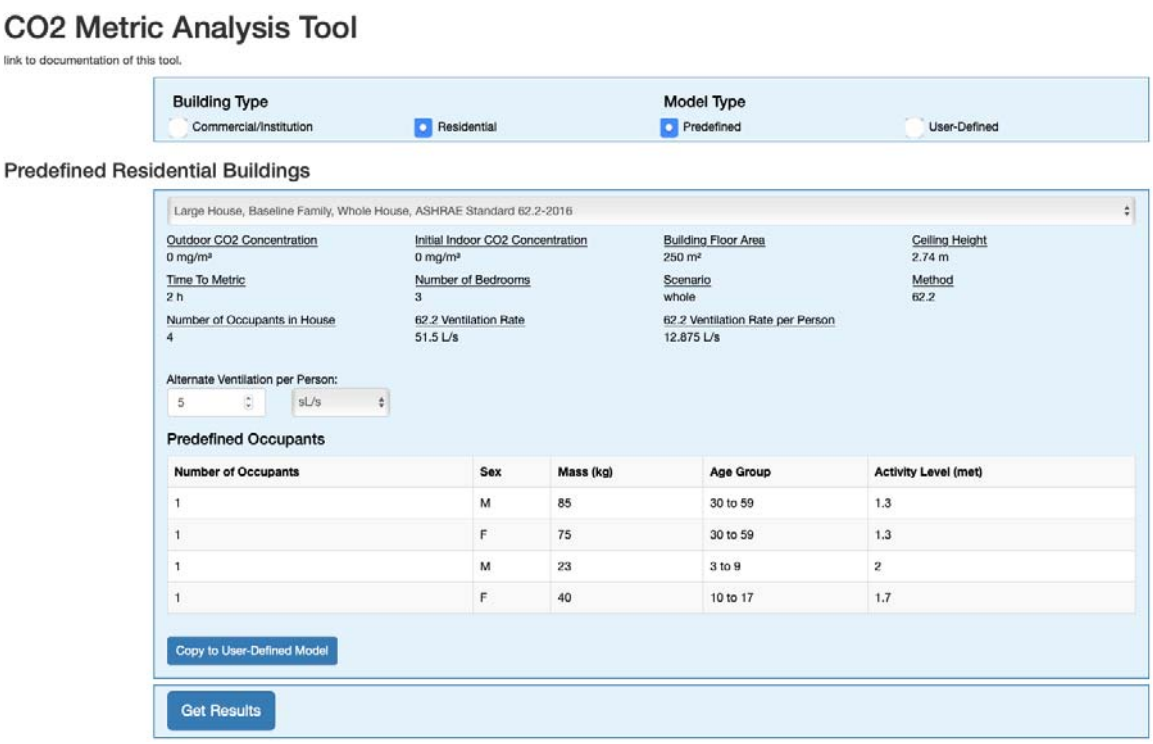

Figure 2: CO_2 Metric Calculator Residential Input Screen

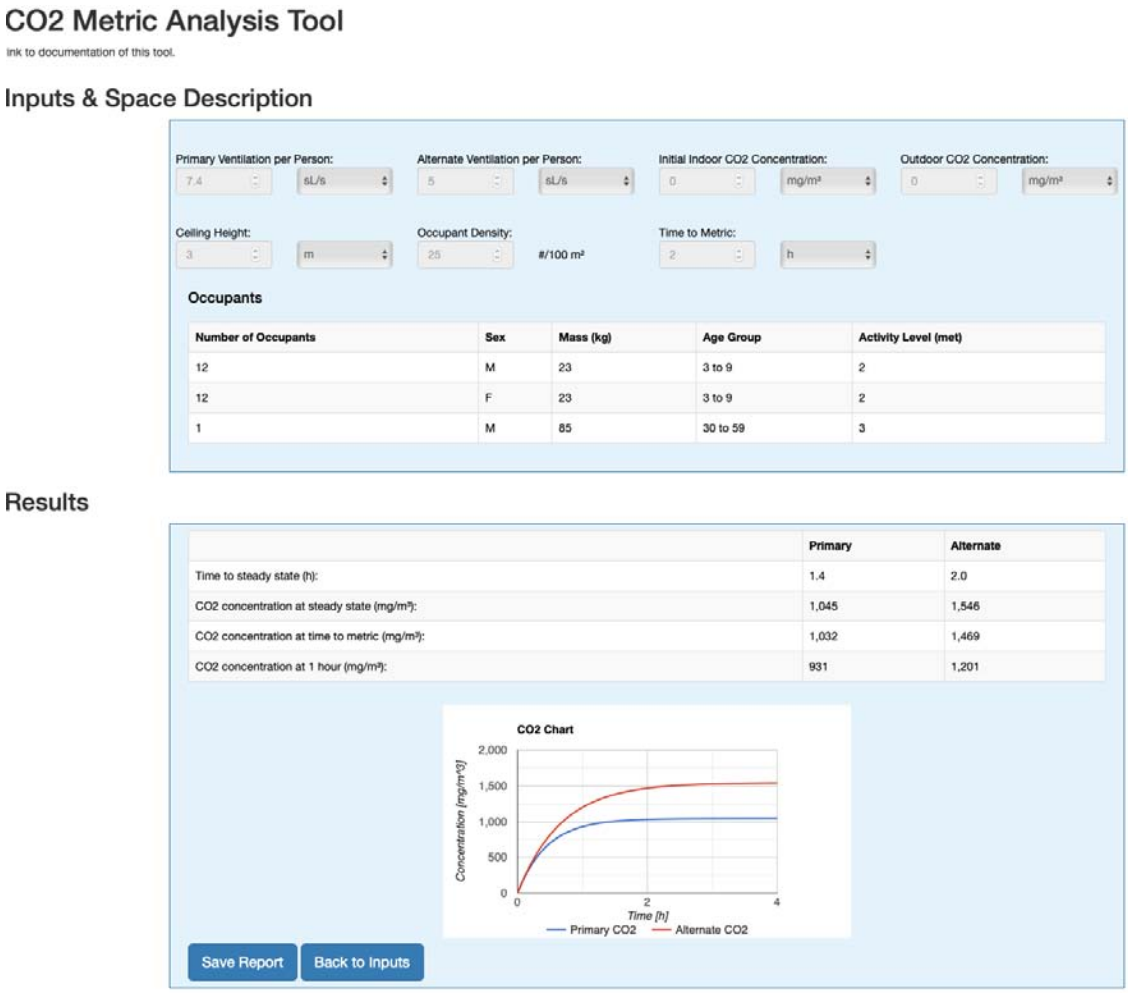

Figure 3: CO_2 Metric Calculator Results Screen

In the case of bedrooms, the calculated CO_2 concentrations can again be compared to measured values in the bedroom. Given the fairly stable bedroom occupancy during sleeping, that comparison should occur several hours after the bedroom is occupied for sleeping. The tool has a default value of t_{metric} for bedrooms of 6 h, which should work well for making the concentration comparisons. On making that comparison, a measured value that is higher serves as an indication that the actual ventilation rate is below the assumed or desired ventilation rate. Note that this comparison neglects the impact of interzone transport on the bedroom CO_2 concentration. Also, the calculation assumes that the CO_2 concentration starts at the outdoor level. However, the initial concentration in the bedroom may be higher than outdoors due to previous occupancy of the house, in which case the calculated concentration will be lower than it would if the actual initial concentration were considered. This situation would result in the calculated metric value being conservative, meaning it would lead to a conclusion that the ventilation rate is lower than it may actually be.

5 SUMMARY AND CONCLUSIONS

This paper expands on a previously-described approach to using indoor CO_2 concentration measurements as a metric for ventilation rates per person, which accounts for the ventilation requirements and occupancies of specific spaces. Calculations of CO_2 concentrations at steady state and other times, are presented for selected residential occupancies based on space-specific inputs of ventilation rate, space geometry and occupancy. Application of this CO_2 metric approach to residences requires one to report, at a minimum, the following: house or bedroom geometry (e.g. floor area and ceiling height), occupant characteristics, time at which full occupancy starts, time of CO_2 concentration measurement, and measured indoor and outdoor CO_2 concentrations. These measurements can then be compared with the values calculated with the online tool as an indication of whether the ventilation rate complies with the value in Standard 62.2 or other ventilation requirement of interest. As additional analyses are performed and the concept discussed with practitioners and researchers, it is anticipated that the approach will become more well-defined and more useful.

Note that all of the input values used in these calculations can be revised to examine the impact of other values on the resulting CO_2 concentrations. An online calculator has been developed to allow users to perform these additional calculations. Based on user feedback, the calculator will be revised in the future. One specific addition being considered is to enable Monte Carlo analyses to quantify the impact of uncertainties in the input values on the calculated CO_2 concentrations, as well as to identify the most important input values, using the methodology described in Jones et al. (2015).

6 ACKNOWLEDGEMENTS

The authors express their appreciation to Steven J. Emmerich and W. Stuart Dols of NIST and Benjamin Jones of the University of Nottingham for their helpful review comments.

7 REFERENCES

ASHRAE. 2016a. *ANSI/ASHRAE Standard 62.1-2016 Ventilation for Acceptable Indoor Air Quality*, American Society of Heating, Refrigerating and Air-Conditioning Engineers, Inc., Atlanta, GA.

ASHRAE. 2016b. *ANSI/ASHRAE Standard 62.2-2016 Ventilation and Acceptable Indoor Air Quality in Low-Rise Residential Buildings*, American Society of Heating, Refrigerating and Air-Conditioning Engineers, Inc., Atlanta, GA.

Azuma, K., Kagi, N., Yanagi, U. and Osawa, H. 2018. Effects of low-level inhalation exposure to carbon dioxide in indoor environments: A short review on human health and psychomotor performance. *Environ Int*, 121, 51-56.

CEN. 2007a. *Indoor environmental input parameters for design and assessment of energy performance of buildings addressing indoor air quality, thermal environment, lighting and acoustics*, Brussels, European Committee for Standardization.

CEN. 2007b. *Ventilation for buildings - Energy performance of buildings - Guidelines for inspection of ventilation systems*, Brussels, European Committee for Standardization.

CEN. 2009. *Ventilation for buildings - Determining performance criteria for residential ventilation systems*, Brussels, European Committee for Standardization.

Concannon, P. 2002. *Residential Ventilation*, Air Infiltration and Ventilation Centre, Coventry, Great Britain., Technical Note AIVC 57.

Hollick, H.H. and Sangiovanni, J.J. (2000) A Proposed Indoor Air Quality Metric for Estimation of the Combined Effects of Gaseous Contaminants on Human Health and Comfort, In: Nagda, N. L. (ed) *Air Quality and Comfort in Airliner Cabins, ASTM STP 1393*, West Conshohocken, PA, American Society for Testing and Materials, 76-98.

Jackson, M.C., Penn, R.L., Aldred, J.R., Zeliger, H.I., Cude, G.E., Neace, L.M., Kuhs, J.F. and Corsi, R.L. (2011) Comparison Of Metrics For Characterizing The Quality Of Indoor Air, *12th International Conference on Indoor Air Quality and Climate*, Austin, Texas.

Jones, B., Das, P., Chalabi, Z., Davies, M., Hamilton, I., Lowe, R., Mavrogianni, A., Robinson, D. and Taylor, J. 2015. Assessing uncertainty in housing stock infiltration rates and associated heat loss: English and UK case studies. *Building and Environment*, 92, 644-656.

Klauss, A.K., Tull, R.H., Roots, L.M. and Pfafflin, J.R. 1970. History of the Changing Concepts in Ventilation Requirements. *ASHRAE Journal*, 12, 51-55.

Moschandreas, D., Yoon, S. and Demirev, D. 2005. Validation of the Indoor Environmental Index and Its Ability to Assess In-Office Air Quality. *Indoor Air*, 15 (11), 874-877.

Persily, A. 2015a. Challenges in developing ventilation and indoor air quality standards: The story of ASHRAE Standard 62. *Building and Environment*, 91, 61-69.

Persily, A. (2017) Indoor Carbon Dioxide as Metric of Ventilation and iAQ: Yes or No or Maybe?, *AIVC 2017 Workshop on IAQ Metrics*, Brussels, Air Infiltration and Ventilation Centre.

Persily, A. (2018) Development of an Indoor Carbon Dioxide Metric, *39th AIVC Conference*, Antibes Juan-les-Pins, France, 791-800.

Persily, A.K. 1997. Evaluating Building IAQ and Ventilation with Indoor Carbon Dioxide. *ASHRAE Transactions*, 103 (2), 193-204.

Persily, A.K. (2015b) Indoor Carbon Dioxide Concentrations in Ventilation and Indoor Air Quality Standards, *36th AIVC Conference Effective Ventilation in High Performance Buildings*, Madrid, Spain, Air Infiltration and Ventilation Centre, 810-819.

Persily, A.K. and de Jonge, L. 2017. Carbon Dioxide Generation Rates of Building Occupants. *Indoor Air*, 27, 868-879.

Snow, S., Boyson, A.S., Paas, K.H.W., Gough, H., King, M.-F., Barlow, J., Noakes, C.J. and schraefel, m.c. 2019. Exploring the physiological, neurophysiological and cognitive performance effects of elevated carbon dioxide concentrations indoors. *Building and Environment*, 156, 243-252.

Teichman, K., Howard-Reed, C., Persily, A. and Emmerich, S. 2015. *Characterizing Indoor Air Quality Performance Using a Graphical Approach*, National Institute of Standards and Technology.

Trade-offs between ventilation rates and formaldehyde concentrations in new-build dwellings in the UK

Esfand Burman, Samuel Stamp

UCL Institute for Environmental Design and Engineering, 14 Upper Woburn Place, London, WC1H 0NN, United Kingdom

ABSTRACT

The current policies and regulatory frameworks in the construction sector aim to improve energy efficiency of new buildings whilst maintaining acceptable level of indoor environmental quality (IEQ) including indoor air quality (IAQ). In practice, however, there are often important trade-offs between these objectives. The aim of this paper is to investigate the concentrations of volatile organic compounds (VOCs) in a recently built residential block in the UK and the potential trade-offs between ventilation rates and VOCs. Concentration levels of VOCs that are likely to have concentrations higher than their respective exposure limit values (ELVs) in low energy dwellings were measured in five sample apartments in this block during typical weeks in winter and summer using diffusive sampling methods. Whilst most target VOCs had concentrations lower than ELVs, benzene and formaldehyde levels were regularly higher than the limits. Measurement of outdoor concentrations showed that benzene levels were predominantly driven by outdoor sources whilst formaldehyde concentrations were driven by internal sources including construction material and furniture. To investigate how formaldehyde levels can be reduced in a given context determined by typical material used in the industry, two models were developed to calculate the effect of enhanced ventilation on formaldehyde levels and energy efficiency of the apartment with highest formaldehyde. Lack of clear definition of VOC characteristics of building material and ever-increasing use of material with high formaldehyde emission factors such as medium-density fibreboard (MDF) in indoor furniture may contribute to high formaldehyde concentrations in indoor air. The study found that to offset the effect of the existing internal sources in the case study apartment and comply with the best practice ELV for formaldehyde, the ventilation rate should be more than three times the existing rate required in the current Building Regulations, and this can significantly increase energy use. Formaldehyde is currently not regulated in the UK Building Regulations. Given the potential health impact of high formaldehyde concentrations and the empirical evidence, it is necessary to cover formaldehyde in the next edition of the Building Regulations. This study points to the significance of improving the existing regulations and standards to clearly define maximum permissible emission factors for various VOCs in building material and indoor furniture. It is also important to improve source control measures to reduce the concentration of formaldehyde. These measures may be complemented by enhanced ventilation. It is, however, necessary to investigate the implications of enhanced ventilation for energy efficiency.

KEYWORDS

Indoor Air Quality (IAQ), Energy Efficiency, Volatile Organic Compounds (VOCs), Formaldehyde, Dwellings

1 INTRODUCTION

As building fabric, air tightness, and building services standards become ever more stringent to help the quest for energy efficiency, there is a risk that the ventilation rates may be compromised to save more energy as other energy efficiency measures reach their technical and economic limit. Meanwhile our understanding of indoor air quality (IAQ) and its key determinants is evolving. Whilst most building codes and regulations are primarily focused on human-induced carbon dioxide levels as a proxy for ventilation rates and IAQ, there are major other internal sources for pollution that should also be considered including volatile organic compounds (VOCs) driven by construction material and furniture. Exposure limit values

(ELVs) set out for VOCs consider the latest epidemiological evidence of their likely effect on humans and are updated accordingly. This may have implications for the control of internal sources of pollution (emission factors of construction material and furniture), ventilation rates required, and energy efficiency.

This paper aims to investigate the concentration level of several VOCs, which are likely to have high concentration levels based on previous studies, in a recently built residential block in East London, and identify how IAQ can be improved in dwellings. As the exchange of air between outdoor and indoor in dwellings is typically lower than non-domestic buildings, concentrations of VOCs driven by internal sources could be problematic and should be considered as a key determinant of IAQ. Key objectives of the study are as follows:

- To measure concentrations of VOCs in typical residential units that represent current construction material and furniture commonly used,
- Identify critical VOC(s) in the given context,
- Investigate the trade-off between ventilation rates and VOC levels,
- Draw conclusions for improvement of IAQ in new dwellings.

2 BACKGROUND

The IEA-EBC Annex 68 project aims to address indoor air quality design and control in low energy residential buildings. An extensive meta-data analysis on several studies of residential buildings was carried out in Subtask 1 of this project to define metrics for IAQ. This led to identification of pollutants that are likely to have concentration levels higher than respective ELVs in low-energy dwellings (Figure 1). In addition to particulate matter and nitrogen dioxide, several VOCs were identified as high-risk pollutants in low energy dwellings. While fine particulate matter (PM2.5) and nitrogen dioxide (NO_2) are predominantly driven by outdoor sources and filtration of outdoor air (e.g. particle filters and activated carbon filter for NO_2) can help reduce their concentration in indoor air, most VOCs are driven by internal sources. Therefore, there is a potential conflict between energy efficiency measures focusing on ventilation demand and IAQ when VOCs are considered as proxy for IAQ. It is also notable that individual VOCs such as VOCs reported in Figure 1are not currently regulated in the UK Building Regulations. It is therefore important to investigate the IAQ performance of low energy dwellings procured in accordance with this regulatory framework with respect to the VOCs identified in IEA-EBC Annex 68 and identify improvement opportunities.

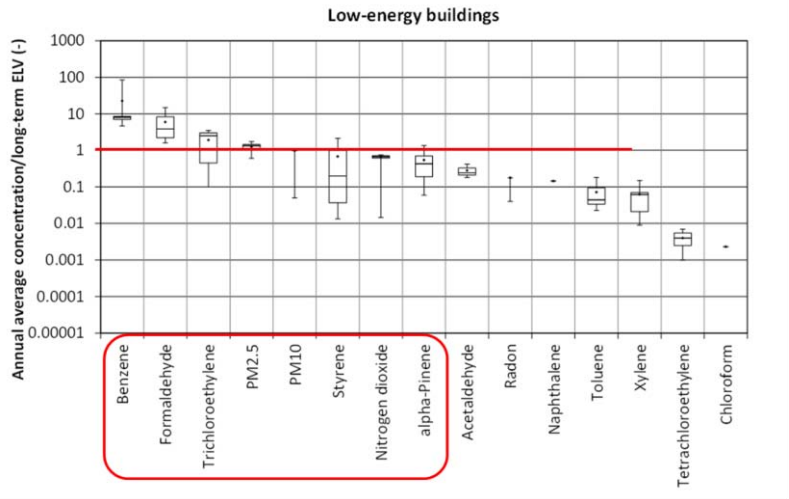

Figure 1. High risk contaminants in low-energy dwellings, adapted from Salis et al., 2017

The Building Regulations in the UK are devolved to the four countries of the United Kingdom. Although there are slight differences between the regulations in England, Northern Ireland, Scotland and Wales, the same fundamental principles apply to all. In England, Approved Document Part L1A, a second-tier document in support of Part L of the Building Regulations, sets out detailed requirements for energy performance of new dwellings (HM Government, 2016).

According to Criterion 1 of Approved Document Part L1A, the carbon dioxide emissions associated with regulated energy use of a new dwelling should not be greater than a Target Emission Rate (TER) set out for that dwelling. TER for a new dwelling is determined by applying prescribed fabric characteristics to the geometry of the dwelling and prescribed building services efficiencies. Designers therefore have some flexibility for trade-offs between various energy efficiency measures in the actual building as long as total calculated carbon dioxide emissions are not greater than the TER.

Other requirements in Part L1A address: Target Fabric Energy Efficiency (TFEE), limits on design flexibility (maximum permissible U values and minimum efficiencies required for building services), limiting the effects of heat gains in summer (to mitigate the risk of overheating whilst improving energy efficiency), consistency between design and construction, and provision of information for energy-efficient operation of dwellings.

Indoor air quality, on the other hand, is covered by Approved Document Part F (HM Government, 2013). This Approved Document sets out the ventilation requirements for buildings. It is therefore predominantly focused on means of ventilation rather than setting out exposure limit values for various airborne pollutants. Performance criteria for nitrogen dioxide, carbon monoxide, and TVOC have been defined for dwellings. No performance criteria, however, has currently been defined for specific VOCs.

3 METHOD

The diffusive sampling method, in accordance with ISO 16017 series, was used to measure the average concentrations of volatile organic compounds (VOCs) with risk of concentrations higher than long-term/chronic exposure limit values (ELVs) in new low energy dwellings (Salis, et al., 2017). Concentration levels of benzene, formaldehyde, trichloroethylene, styrene, naphthalene, toluene, and tetrachloroethylene were measured in living room, kitchen and one bedroom of five sample apartments in a recently built residential block during typical weeks in heating season and summer of 2018. Passive tubes and absorbent pads were also installed outdoors to identify the indoor/outdoor trends and sources.

To give context to IAQ monitoring results, a perfluorocarbon tracer (PFT) gas method (Persily, 2016) was used to infer the average air exchange rates in the monitored zones of the sample apartments.

Finally, the trade-off between the VOC with high concentration levels, airflows, and energy efficiency was investigated using IA-QUEST tool for the analysis of IAQ and Standard Assessment Procedure (SAP 2012) tool used for analysis of energy performance of dwellings in England.

IA-QUEST tool is underpinned by the material emission database originally compiled in MEDB-IAQ project instigated by the National Research Council Canada (Won, et al., 2005). The database includes the emission factors derived from testing materials in a flow-through chamber in accordance with ASTM Standard D5116-97 (ASTM International, 1997). This database was used to estimate the emission factors of various materials in the case study, as there is very limited information about emission factors of specific VOCs for construction material used in the UK. This is a consequence of the current regulatory framework and building

sustainability codes such as BREEAM that are predominantly based on TVOC rather than individual VOCs.

4 OVERVIEW OF THE CASE STUDY

To investigate Indoor Air Quality (IAQ) in low energy residential buildings, two recently built apartment blocks constructed as part of a regeneration scheme in East London were selected as a case study.

Apartment blocks A and B were completed in December 2014 and January 2015 respectively. Block A is a 13-storey building; Block B has 9 floors. These buildings are located next to each other and close to two main roads in the London Borough of Tower Hamlets in East London. There are 98 flats and maisonettes (two-storey apartments) in these blocks. The buildings were designed with target air permeability of 2-3 $m^3/hr./m^2$ at 50 Pa pressure difference which is significantly lower than 10 $m^3/hr./m^2$ limit set out in the Building Regulations (HM Government, 2013). Consequently, mechanical ventilation with heat recovery (MVHR) was specified to ensure adequate background ventilation is provided to these apartments. Heating is provided by a community heating scheme that is currently gas-fired with provisions for integration of a combined heat and power (CHP) plant in future. There is no mechanical cooling. Figure 2Figure 2 shows a picture of this development. Table 1 provides background information about the sample apartments included in IAQ investigations. The air permeability reported for each dwelling is based on pressure test result carried out after building completion.

Figure 2. Image of the two apartment blocks covered in the study (left)

Table 1. Background information about sample apartments

Dwelling	Type	Gross Floor Area (m^2)	Floor level	Orientation	Bedroom no.	Occupant no. (steady mode)	Air tightness ($m^3/hr/m^2$ @ 50 Pa)
Apt. 1	Flat	100	Block A, 7th floor	South/West	3	3	3.3
Apt. 2	Flat	100	Block A, 8th floor	South/West	3	5	2.2
Apt. 3	Flat	100	Block A, 9th floor	North/West	3	5	2.0
Apt. 4	Maisonette	127	Block B, Ground floor	South/East	5	7	3.8
Apt. 5	Maisonette	106	Block B, 8th floor	East	3	4	2.9

According to Approved Document Part F the whole dwelling ventilation rate for the supply of air to the habitable rooms in a dwelling should be no less than what is prescribed in Table 2. This was the basis for the commissioning of the MVHR systems in the sample dwellings.

Table 2. Whole dwelling ventilation rates (HM Government, 2013)

	Number of bedrooms in dwelling				
	1	**2**	**3**	**4**	**5**
Whole dwelling ventilation rate (L/s)	13	17	21	25	29
Notes: - In addition, the minimum ventilation rate should be not less than 0.3 L/s per m² of internal floor area. (This includes all floors, e.g. for a two-storey building add the ground and first floor areas.) - This is based on two occupants in the main bedroom and a single occupant in all other bedrooms. This should be used as the default value. If a greater level of occupancy is expected, add 4 L/s per occupant.					

Table 3 reports the U values of the building fabric.

Table 3. U values for the building fabric against the regulatory limits

Building fabric	**Case study (W/m².K)**	**Regulatory limit (W/m².K)**
External walls	0.18-0.19	0.30
Windows	0.85-0.92	2.00
Doors	1.30	2.00
Roof	0.18	0.20
Exposed floor	0.12	0.25

Figure 3 shows a sample Energy Performance Certificate (EPC) that represents Apt. 1. Other dwellings also have the same energy-rating band. Calculated primary energy use per square meter of floor area in the sample apartments Apt. 1 – Apt. 5 is within 56-81 kWh/m² per year.

Figure 3. Energy efficiency rating of the case study dwellings

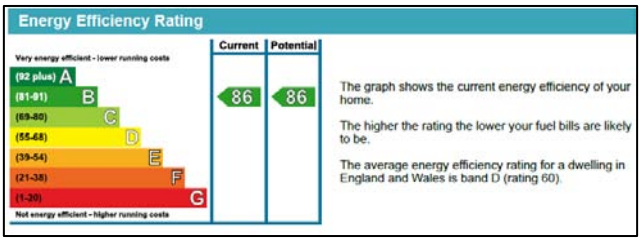

5 RESULTS

5.1 EMPIRICAL INVESTIGATIONS

Table 4 includes the key statistics for the VOC measurements carried out in the study. Formaldehyde and benzene were the contaminants with concentrations consistently higher than the respective ELVs. Measurements of outdoor formaldehyde levels confirmed that, contrary to benzene, formaldehyde concentrations are driven by material emissions and internal sources, this contaminant was therefore selected for a more detailed investigation.

Table 4. Key statistics for the VOC measurements of five sample apartments

VOC	Min	25th pctl.	Median	Average	75th pctl.	Max	Annex 68 ELV
Benzene	**0.55**	**0.55**	**1.20**	**1.14**	**1.48**	**2.8**	**0.2**
Formaldehyde	1.15	**10.15**	**16.32**	**16.78**	**26.13**	**31.91**	**9**
Trichloroethylene	0.25	0.25	0.25	0.26	0.25	0.3	2
Styrene	0.30	0.63	1.35	1.78	2.00	**53.9**	30
Naphthalene	0.25	0.34	1.00	1.38	1.30	**5.4**	2
Toluene	0.45	1.20	2.15	4.03	3.33	22.8	250
Tetrachloroethylene	0.30	0.35	0.35	0.66	1.09	1.8	100

Table 5 lists the formaldehyde levels recorded in sample apartments and the total air change rates derived from PFT measurement during the sampling period. The figures highlighted in bold represent concentration levels higher than the most stringent chronic ELV for formaldehyde set out by the US Environmental Protection Agency (i.e. 9 μg/m³).
It is notable that formaldehyde levels were generally higher in winter although emission factors are expected to increase with temperature in summer. This can be explained by higher air change rates measured in summer when in addition to background ventilation provided by the MVHR system building occupants also open windows and balcony doors more frequently and for a more prolonged period compared to winter.

Table 5. Formaldehyde levels and air change rates in the sample apartments

Apartment		Formaldehyde concentration (μg/m³)			ACH (PFT measurement)
		Living room	Kitchen	Bedroom	
Apt. 1	Winter	**22.62**	**18.75**	**15.29**	n/a
	Summer	**9.75**	6.15	**23.91**	1.51 ± 0.15 h^{-1}
Apt. 2	Winter	**18.82**	**17.35**	5.04	0.36 ± 0.05 h^{-1}
	Summer	6.60	5.86	5.70	2.24 ± 0.34 h^{-1}
Apt. 3	Winter	**29.25**	**26.87**	**29.53**	0.56 ± 0.08 h^{-1}
	Summer	**11.57**	**11.36**	**31.91**	0.42 ± 0.34 h^{-1}
Apt. 4	Winter	**21.23**	**31.35**	**27.44**	0.86 ± 0.16 h^{-1}
	Summer	**12.82**	**13.74**	**11.84**	0.92 ± 0.14 h^{-1}
Apt. 5	Winter	**28.26**	**22.33**	**27.59**	1.15 ± 0.21 h^{-1}
	Summer	6.41	5.96	**12.44**	2.68 ± 2.97 h^{-1}

Figure 4 shows the correlation between formaldehyde levels and PFT measurements in respective zones (living room, kitchen and bedroom). There is a large degree of scatter in data as multiple other factors affect concentration levels and could not be controlled in this study that was conducted post-occupancy. These factors include changes in environmental parameters such as temperature and relative humidity, occupant behaviour, new furniture and equipment, etc. Nonetheless, there is a clear link between air change rates and formaldehyde levels and the concentrations significantly come down at high air change rates. The median formaldehyde concentration level in low energy dwellings reviewed in Subtask 1 of IEA EBC Annex 68 was 25.9 μg/m³ (Salis, et al., 2017). The ELV defined for formaldehyde in Well Building Standard is 27 ppb (34 μg/m³) (International Well Building Institute, 2014). The recorded formaldehyde levels for the case study are therefore generally lower than the past empirical data and other ELVs defined for formaldehyde.

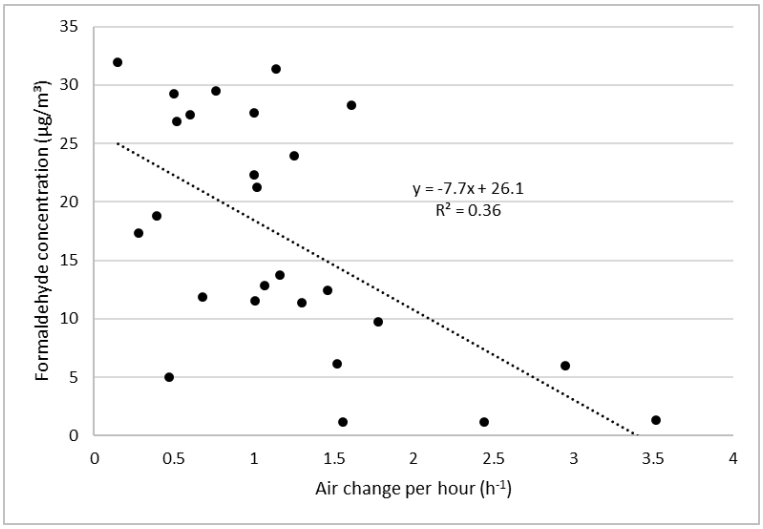

Figure 4. Formaldehyde concentrations against air change rates in sample apartments

Figure 5Figure 5 shows the range of operative temperatures and relative humidity recorded in the sample dwellings to put formaldehyde concentrations reported in Table 5 in context (measurement accuracy: T: ± 0.4 °C, RH: ± 4.5 %).

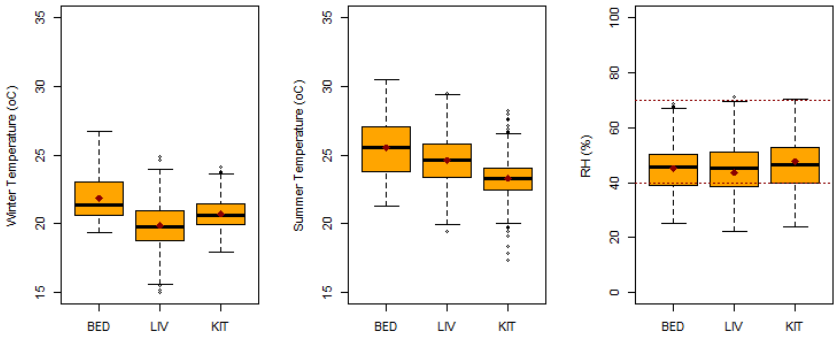

Figure 5. Range of operative temperatures and relative humidity in sample dwellings

The ELV for formaldehyde originally defined by CalEPA, and endorsed by US EPA, is much lower than other limits proposed for this contaminant. The process used by CalEPA to define reference exposure levels for contaminants includes the following steps (CalEPA, 2008):

- conduct literature search
- choose best study, emphasizing human data
- identify critical biological endpoint
- estimate threshold for effect
- temporal/dosimetric adjustments
  (time extrapolation, Human Equivalent Concentrations, children's HEC, physiologically-based pharmacokinetic models)
- Account for uncertainties in data

The special attention to temporal/dosimetric adjustments in CalEPA method may be a key driver for the stringent limit defined for formaldehyde. This ELV can therefore represent the best practice figure and it would be helpful to investigate how this could be achieved given the current construction methods and material used in the industry.

5.2 BUILDING PERFORMANCE SIMULATIONS

A single-zone model was developed for APT. 4, the apartment with high formaldehyde concentrations in both seasons, in IA-QUEST. The emissions database available in IA-QUEST was used to estimate the emission factors for interior material used in the apartment. The information about the apartment including geometry and material specification was collated through the architectural drawings, technical specifications and site visit. The emission factors and power law equations derived from curve fitting in IA-QUEST are based on emission tests lasting from 72-362 hours for dry materials and 78-440 hours for wet materials (Won, et al., 2005). It is assumed that the concentration decay rate derived from these tests are representative of long-term performance and therefore the entire post-occupancy period was taken into account in the simulation. Table 6 includes the list of construction material categories, respective areas and emissions factors used in IA-QUEST.
The air change rate used for the base model was 0.5 h^{-1} that is consistent with specification of the MVHR system and typical for new dwellings in England following Part F requirements. Figure 6 shows that formaldehyde levels at the end of simulation are very close to the measured values reported in Table 5 for Winter.

Table 6. Material and emission factors used for simulation of formaldehyde levels in Apt. 4

Construction material category	**Area (m^2)**	**Nominal emission factor ($\mu g/m^2h$)**	**Maximum emission factor ($\mu g/m^2h$)**
Floor: carpet	63.5	n/a	n/a
Floor: laminate/foam underlay assembly	43.2	37.66	37.70
Floor: kitchen tiles	20.3	n/a	n/a
Paint (ceiling, external wall, partition)	288	n/a	n/a
Door (plywood)	24	n/a	n/a
Kitchen & other cabinets, top only (Melamine/PB)	30	3.68	4.57
Medium Density Fibreboard (MDF)	8	441.59	691.81

The base model developed in IA-QUEST was then used to determine how many air changes are required to achieve formaldehyde concentration levels close to the ELV set out by EPA (i.e. best practice ELV). Figure 7 shows that, given the current material and emission sources, formaldehyde concentration levels will be around 9 $\mu g/m^3$ three years after building completion, if minimum 1.6 air change per hour is continuously supplied to the dwelling. This is also consistent with empirical data that generally show low formaldehyde levels at air change rates greater than 1.6 h^{-1} (Figure 4). It should however be noted that emission factors used in IA-QUEST are based on standard environmental conditions used during emission testing (23 °C, 50% RH). The low formaldehyde levels in Figure 4, on the other hand, generally represent high air change rates achieved in summer when operable windows and doors supplement the operation of MVHR system and temperatures can be higher than test conditions.

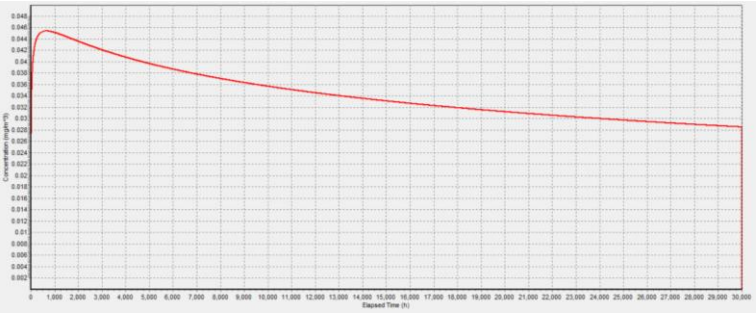

Figure 6. Simulation of formaldehyde levels in Apt. 4 (ACH= 0.5)

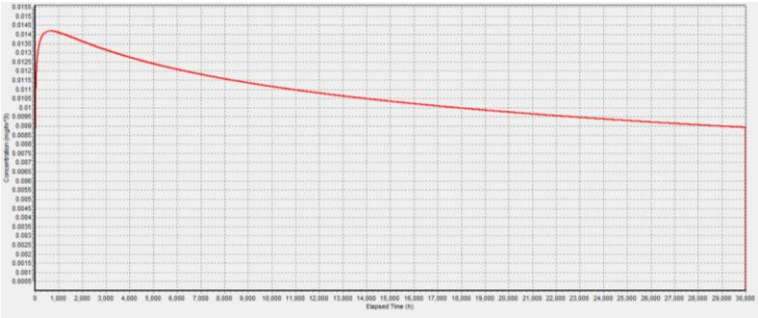

Figure 7. Simulation of formaldehyde levels in Apt.4 (ACH = 1.6)

The implication of this increase in air change rate for energy performance was investigated with an energy performance model developed using SAP tool for Apt. 4.

Increasing the air change rate from 0.5 to 1.6 h^{-1} with the same MVHR system settings in Apt. 4 will increase the primary energy use of regulated energy end-uses by around 22%[1]. If the small power load is also accounted, the increase in primary energy use will be around 11%. It is possible to offset part of this excess in energy use by making improvements in the MVHR system and heating efficiency. In the sample dwelling, the following improvements in energy efficiency measures were considered technically and economically feasible:

- increasing thermal efficiency of the MVHR system from 85% to 90%,
- reducing the specific fan power of the MVHR system from 1.0 to 0.6 W/L/s,
- improving seasonal heating efficiency from 87% to 90%.

These improvements can reduce the excess in primary energy use for regulated energy and total energy to 9% and 5% respectively. Further improvements in energy efficiency such as improving building fabric performance and using low or zero carbon technologies will be required to offset the effect of enhanced ventilation completely.

6 DISCUSSION

These results point to the challenge of improving IAQ whilst maintaining the same level of energy performance required by building regulations. Given the ever-increasing requirements for improving energy efficiency, it is very difficult to reduce formaldehyde levels to the best practice value recommended by the EPA without compromising energy performance, unless advanced source control measures are adopted and emission factors are reduced. There is no evidence that emission factors of construction material for specific VOCs including formaldehyde were considered at design stage for the case study. Currently, most suppliers of

[1] Regulated energy use includes heating, domestic hot water, fans and pumps, and lighting.

material and building designers in the UK at best consider TVOC which is not necessarily a good metric to identify the risks associated with health.
BRE Digest 464 provides good practice recommendations to control VOC emissions from construction products (Yu & Crump, 2002). Low formaldehyde material such as wood-based boards classified as E1 in accordance with BS EN 13986:2004 (BSI, 2005) can be used in construction. California Air Resources Board's Phase 2 standard (CARB2) also sets out requirements for emissions from composite wood products including hardwood plywood, particleboard and MDF. Using CARB2 compliant material can help reduce the emission sources for formaldehyde in low energy dwellings. The United States Environmental Protection Agency Formaldehyde Standards for Composite Wood Products Act (TSCA Title VI) has also established stringent emissions requirements for composite wood products that can help reduce emission sources significantly (EPA, 2018).
It is important to reduce emission sources first and use enhanced ventilation only as a complementary measure if necessary to ensure concentration levels do not exceed the exposure limits. It is also necessary to review the epidemiologic evidence that underpins the ELV recommended by the EPA as the significant discrepancy between this ELV and other exposure limits prescribed for formaldehyde could have serious implications for design and control of ventilation systems in low energy dwellings.
The emission databases available for IAQ modelling do not necessarily represent the emission factor of the construction products currently used in the industry. It is therefore important to develop national databases that represent various building products used and updated emission factors for formaldehyde and other critical VOCs. In addition to MEDB-IAQ database, PANDORA is another emission database that provides emission rates for both gaseous and particulate pollutants. In addition to construction products, PANDORA also covers the effects of occupant behaviour and activities on emission rates (Abadie & Blondeau, 2011). There is currently no national database for VOC emission rates in the UK, but there are calls for definition of exposure limit values for critical VOCs in the next edition of Approved Document Part F that could lead to development of a national register for emission rates in the future.

7 CONCLUSIONS

The results show concentration levels of most VOCs were lower than respective exposure limit values in the case study residential block. Concentration levels of benzene and formaldehyde were, however, higher than the best practice ELVs identified in Subtask 1 of IEA-EBC Annex 68.
As formaldehyde concentration is predominantly driven by internal sources, enhanced ventilation can help reduce its concentrations in indoor air. The study found that given the existing material sources in the case study apartments, which are typical of new low energy dwellings in the UK, the rate of air exchange between indoor and outdoor air should be more than three times the current levels to meet the best practice ELV for formaldehyde.
This significant increase in air change rates has consequences for energy efficiency that may not be entirely offset by cost-effective energy efficiency measures. It is therefore necessary to use best practice methods for source control and use enhanced ventilation only as a complementary measure. Using CARB2 compliant material and following the EPA's new Formaldehyde Standards for Composite Wood Products Act (TSCA Title VI) can help reduce emission sources.

This study shows the significance of the following measures to improve IAQ in new dwellings in the UK:

- Provision of further information about VOC emission factors of the construction products used in the industry,
- Review of the latest epidemiological evidence about the potential chronic effects of VOCs that are prevalent in construction products and built environment,
- National regulations for critical VOCs,
- Labelling and rating schemes for IAQ that go beyond metrics such as CO_2 concentrations and TVOC and address specific health related pollutants,
- Promotion of best practice for construction material, exposure limit values, and ventilation rates in the industry to strike the right balance between IAQ and energy efficiency.

8 ACKNOWLEDGEMENTS

This paper was supported by the 'Total Performance of Low Carbon Buildings in China and the UK' ('TOP') project funded by the EPSRC (EP/N009703/1).

9 REFERENCES

Abadie, M., & Blondeau, P. (2011). PANDORA database: A compilation of indoor air pollutant emissions. *HVAC&R Research, 17*(4), 602-613.

ASTM International. (1997). ASTM D5116-97, Standard Guide for Small-Scale Environmental Chamber Determinations of Organic Emissions from Indoor Materials/Products (Withdrawn 2006). West Conshohocken, PA: ASTM International.

BSI. (2005). *BS EN 13986:2004, Wood-based panels for use in construction. Characteristics, evaluation of conformity and marking.* London: British Standard Institute.

CalEPA. (2008). *Air Toxics Hot Spots, Risk Assessment Guidelines, Technical Support Document for the Derivation of Noncancer Reference Exposure Levels.* Oakland, CA: California Environmental Protection Agency.

EPA. (2018). *Rule to Implement the Formaldehyde Standards for Composite Wood Products Act.* Washington D.C.: United States Environmental Protection Agency.

HM Government. (2013). *Approved Document F, Ventilation (2010 edition incorporating 2010 and 2013 amendments).* London: NBS.

HM Government. (2013). *Approved Document Part L1A: Conservation of fuel and power in new dwellings (2013 edition).* London: NBS.

HM Government. (2016). *Approved Document Part L1A: Conservation of fuel and power in new dwellings (2013 edition with 2016 amendments).* London: NBS.

International Well Building Institute. (2014). *The Well Building Standard.* New York, NY: International Well Building Institute.

Persily, A. (2016). Field measurement of ventilation rates. *Indoor Air, 26*(1), 97-111.

Salis, L. C., Abadie, M., Wargocki, P., & Rode, C. (2017). Towards the definition of indicators for assessment of indoor air quality and energy performance in low-energy residential buildings. *Energy and Buildings, 152*, 492-502.

Won, D. Y., Magee, R. J., Yang, W., Lusztyk, E., Nong, G., & Shaw, C. Y. (2005). A material emission database for 90 target VOCs. Beijing: The 10th International Conference on Indoor Air Quality and Climate.

Yu, C., & Crump, D. (2002). *BRE Digest 464, VOC emissions from building products.* Watford: BREPress.

Modeling Dynamic Behavior of Volatile Organic Compounds in a Zero Energy Building

Klaas De Jonge[*1] , and Jelle Laverge[2]

1 Ghent University
Research Group Building Physics
Sint-pietersnieuwstraat 41 – B4
Ghent, Belgium
**Corresponding author: klaas.dejonge@ugent.be*

ABSTRACT

With increasing building airtightness, the design of an adequate ventilation system gains importance. The first generation of ventilation systems, based on continuous supply of the nominal airflow rate, are now being replaced by Demand Controlled Ventilation (DCV). These systems, often H_2O and/or CO_2 controlled, do not take into account the emissions of Volatile Organic Compounds (VOCs) to the indoor environment.

A small, airtight, zero energy building that has been designed as the Belgian contribution to the international Solar Decathlon competition (2011) was rebuilt afterwards in Ostend, Belgium. This building will be used as test facility for the development and validation of a holistic VOC source model. In this study, results are obtained from thermal, airflow and contaminant simulation models of the test facility. The different models and modeling assumptions are discussed. A dynamic VOC source model, derived from literature, is used as proxy of possible VOC concentrations.

The results show an important influence of environmental parameters on the indoor VOC levels with VOC concentrations exceeding health guidelines. It is therefore important to design DCV systems and controls taking into account possible elevated VOC levels and while doing so, incorporate the dynamic behavior (influence of temperature and humidity) of the VOC emissions.

1 KEYWORDS

Modeling, VOCs, Case-study, Test facility

2 INTRODUCTION

Today's newly built and extensively renovated dwellings are built very airtight to reduce unwanted infiltration of cold air and as a consequence reduce heat losses. To safeguard the health of the occupants by keeping the Indoor Air Quality (IAQ) acceptable, ventilation systems must be installed in these homes. The first generation of ventilation systems are systems that supply outdoor air to 'dry' spaces (e.g. living room, bedroom) and extract contaminated air from the 'wet' spaces (e.g. kitchen, bathroom, toilet) both at a continuous volume flow rate. In Belgium, the nominal flow rate, depends on the type and size of the space and assumes worst case situations (BIN 1991). This constant flow of air dilutes the contaminants that are emitted indoors and by doing so, keeps the IAQ acceptable.

An issue with these systems is the fact that they provide the nominal airflow rate regardless of the actual need for dilution. By doing so, during the heating season, there will be more cold air that needs to be heated for thermal comfort, driving up the *ventilation heat losses*.

An efficient way to lower these ventilation heat losses is to install a second generation ventilation system, namely Demand Controlled Ventilation (DCV). These systems measure CO_2 and/or H_2O continuously and allow the volume flow rate to be lowered when the demand for dilution/ventilation is low. How the controls for these systems are set up is crucial to make sure the IAQ stays acceptable. That is why the Belgian legislation includes a *'method of equal performance'* which assesses the proposed controls based on Monte-Carlo, dynamic simulations of the system in a standardized reference house with average occupation. This method is developed by Heijmans et al. (Heijmans, Van Den Bossche, and Janssens 2007) and Laverge et al. (Laverge 2013).

Most of the current DCV systems as well as the assessment *method of equal performance* only consider CO_2 and H_2O as both are good indicators for comfort. The health aspect of IAQ is therefore overlooked in the development and assessment of these systems. A first step towards including this aspect in the assessment method is the consideration of Volatile Organic Compounds (VOCs) that are emitted by building materials, furniture and by performing certain activities. To do so, it is necessary to be able to simulate the emissions of VOCs to the indoor environment, including the dynamic behavior with relation to temperature and humidity. A holistic approach is necessary to be able to correctly model the exposure to VOCs of a simulated occupant and account for the interaction between outside conditions, the building, materials and HVAC systems.

To validate such a model it is necessary to have a reliable test setup outside of laboratory conditions which allows to account for all possible external influences on the VOC emissions and VOC concentration in the room. In this study, a thermal and airflow simulation model of a test facility, including a simplified temperature and humidity VOC model, are used to prove the importance of the external parameters and to evaluate the potential of this facility in performing VOC tests.

3 E-CUBE

In 2011, Ghent university participated in the Solar Decathlon competition. A zero energy house has been designed, named the 'E-cube' (Figure 1).

Figure 1 - E-cube test facility © UGent, photo Nic Vermeulen

After the competition, it was rebuilt in the Greenbridge science park in Ostend (Belgium). The E-cube will be used as a testing facility. All characteristics and HVAC systems of this building are well known and because the building is subject to real environmental conditions it is ideal for a series of measurements providing data for the validation of the VOC source model. Because of the open-plan design, the building can be assumed to be single-zone. Using the E-cube, several scenarios of increasing complexity can be measured under real, in-situ dynamic conditions.

The construction of the E-cube is made using pre-fab elements, which are a series of almost identical panels with a surface area of 2.5 m² each. A wall panel is either a closed panel, a fixed window panel or a operable window/door panel. The closed panels are built using a wooden frame and two plywood boards (1.2 cm) are enclosing18 cm of PIR insulation. Roof and floor panels are similar but consist of 1.8 cm plywood boards. The windows are triple-glazed with low emissivity coatings and Argon filling. The frames are Aluminium CS104 which are specially developed for passive-house standard buildings (De Loof, Rottiers, and van de Walle 2011). Table 1 shows the overall dimensions of the floor, roof and facades.

Table 1. Surface area of boundary surfaces

	Total [m²]	**Opaque [%]**	**Fixed window [%]**	**Operable window [%]**
North Wall	44.6	78	6	17
East Wall	45.1	83	11	6
South Wall	44.6	61	28	11
West Wall	45.1	94	0	6
Roof	61.7	100	0	0
Floor	61.7	100	0	0

4 EMISSION MODEL

Research concerning VOC modeling started in 1979, in 1987 a procedure was developed to test material emissions (Sanchez, Mason, and Norris 1987). Based on these results Dunn published the first attempt to model VOC emissions (Dunn 1987). Based on the theory of Dunn his ‘deep source model’ Little et al. proposed a model based on physical parameters instead of statistical correlations (Little, Hodgson, and Gadgil 1994). This model still serves as a basis for more detailed and numerical models (Huang and Haghighat 2002; Xu and Zhang 2003; Yang et al. 2001). In 2004, the findings of different variations on the model of Little et al. were brought together by Deng et al. forming a new ‘standard’ for VOC emission models (Deng and Kim 2004). Today, new variations still occur taking into account more details (e. g. multi-layer situations (Deng et al. 2010)) or trying to simplify the existing models (Qian et al. 2007). All recent models can predict VOC emissions with good correlation in steady state conditions (constant temperature and humidity). However, almost all studies and measuring campaigns found that the VOC emission rate is strongly dependent on temperature and humidity, but in emission models these parameters are never really taken into account (Deng, Yang, and Zhang 2009; Lee and Kim 2012; Liang, Yang, and Yang 2015; Nazaroff et al. 2018; Salthammer and Uhde 2009; Sanchez, Mason, and Norris 1987; Zhang et al. 2007).

Emission rates from building materials are dependent on three material characteristics, diffusivity D_m, starting concentration C_0 and partitioning coefficient K_m. These parameters are dependent on temperature and humidity. Although this dependency was known from the start

of research concerning this subject, only recently, good correlations were found to take into account the dynamic character of D_m, C_0 and K_m (Deng, Yang, and Zhang 2009; Liang, Lv, and Yang 2016; Zhang et al. 2007).

The emission model used in this study, formula 1, is derived from literature and includes the temperature dependency for D_m and the temperature and humidity dependency for C_0 (De Jonge 2018). An important note is the fact that the emission model and the temperature and absolute humidity dependency have only been validated with measured data as separate models.

$$E(t) = 2.1 \frac{\left[d_1 T^{1.25} e^{\frac{d_2}{T}}\right]\left[(1+C_1 AH) C_2 T^{-0.5} e^{\frac{-C_3}{T}}\right]}{\delta} e^{-2.36 \frac{\left[d_1 T^{1.25} e^{\frac{d_2}{T}}\right] t}{\delta^2}} \quad (1)$$

$E(t)$	[mg/m²/h]	Emission rate
T	[K]	Material temperature
AH	[g/kg]	Absolute humidity
δ	[m]	Material thickness
t	[h]	Time since start of emissions
d_1, d_2	[*varies*]	Diffusivity material constants for VOC-material system
C_1, C_2, C_3	[*varies*]	Initial concentration material constants for VOC-material system

The chosen VOC to model was formaldehyde as, because of the high occurrence and related risk, it has been found to be the priority pollutant to assess (Kotzias et al. 2005; Brouwere et al. 2009). The material characteristics (d_1, d_2, C_1, C_2, C_3) are specific to the pollutant-material system and are not broadly available yet.

The proposed model will be used to model formaldehyde from Medium-Density Fiberboard (MDF). The amount of emissions from plywood might be different, but the overall reaction of emissions to external factors will be similar and makes it suitable for the intended purposes.

5 SIMULATION MODELS

In this study two simulation models are made: (1) a thermal model and (2) an airflow and contaminant model. The software used is Dymola and CONTAM respectively.

5.1 Thermal model

The thermal model in Dymola is modeled using the IDEAS v2.1 library which has been developed as part of IEA EBC Annex 60 (Jorissen et al. 2018). The open plan characteristic of the building makes it suitable for a 1-zone modeling approach. Only the external boundaries (external walls, windows and doors, floor and roof) of this zone are considered. Internal partition walls are not modelled.

The goal of this simulation model is acchieving realistic surface temperatures of the walls, floor and ceiling. This surface temperature will later be used as input of the respective VOC-

source model of that component in CONTAM. The simulations will also provide a transient temperature profile to the zone which otherwise would be constant. Table 2 shows the characteristics of the materials used in construction.

Table 2. Material characteristics used for thermal simulations

		Multiplex	**PIR-insulation**
Thermal Conductivity	[W/(m.K)]	0.17	0.023
Specific Heat Capacity	[J/(kg.K)]	1 880	1 470
Density	[kg/m³]	400	30
Longwave emissivity		0.86	0.8
Shortwave emissivity		0.44	0.8

The optical properties of the real installed glazing system of the E-cube were not documented. Based on the available description a similar glazing system is chosen from the catalogue of the LBL Window software (*Triple low-e (argon) - deflected*). The U-value of the simulated glazing system is 0.692 UNIT and has a g-value of 0.32 UNIT.

The U-value of the window CS 104 frame depends on the fact if they are operable windows or have a fixed frame. The operable window frame has a U-value of 1.16 whereas the fixed frame window has a U-value of 0.88.

On figure 2, the overall room temperature profile, the outside temperature profile and the different surface temperature profiles can be seen. The graph shows that the inside air temperatures are prone to variations of outside temperatures. This can be explained by the lack of available thermal mass of this construction type. This illustrates one of the common characteristics of lightweight constructions. Because of this, the risk of overheating will be higher. The detailed results show that the surface temperatures and thus temperatures influencing the emissions will be different for every surface but will follow the inside air temperature quite well.

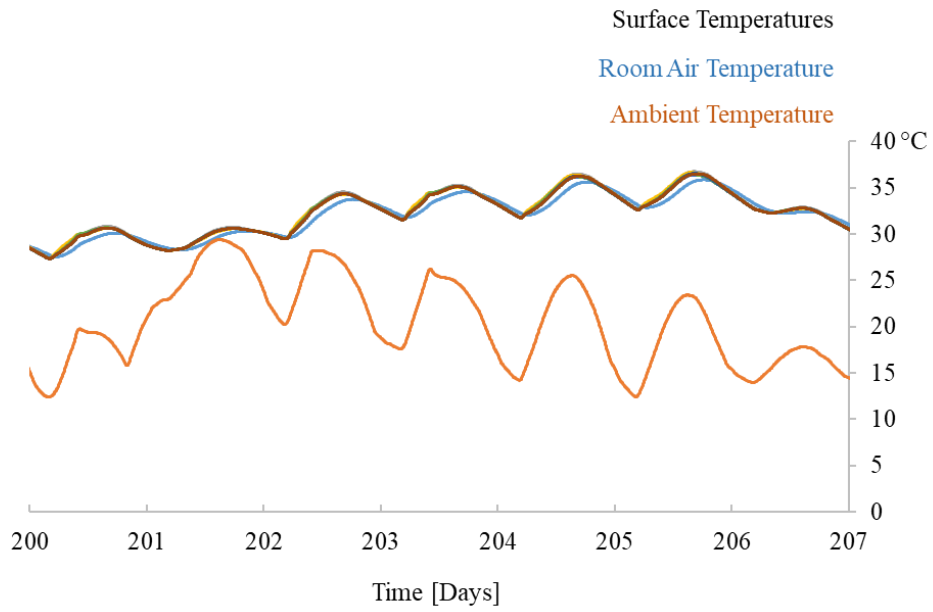

Figure 2 - Detail of ambient temperatures and temperature profiles obtained from thermal simulations (room air and surface temperatures)

5.2 Airflow model

The airflow and contaminant model has been made using CONTAM, a software especially developed for this purpose. This is a freely available simulation software developed by NIST (Dols and Polidoro 2015). The modelling approach is based on the model developed by (Heijmans, Van Den Bossche, and Janssens 2007) which has been used repeatedly to study CO_2 and H_2O controlled DCV ventilation (Laverge 2013; De Jonge, Janssens, and Laverge 2018; Caillou et al. 2014).

In this model, the E-cube is also modeled as being 1-zone. The leakiness of the boundary walls is modelled by the use of 4-airflow paths, each representing the air-leakage of $1/4^{th}$ of what that wall would have. The wall is divided in four horizontal bands and each node is placed in the middle of that band.

The airflow element represents the cracks in 1 m² of wall for a building with a q50 value of 3 m³/h·m² multiplied by the surface area it represents. The wind pressure profile of this component is obtained from table A2.2 - Face 1-p. 258 (Liddament 1996).

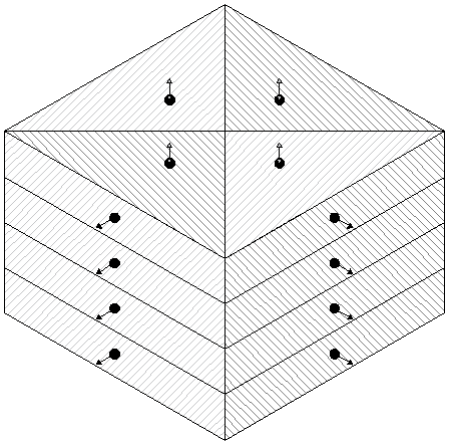

Figure 3 - Schematic drawing of the E-cube with positioning of airflow elements and the surface that each airflow element represents

Four airflow elements represent the leakiness of the flat roof as illustrated in figure 3. The wind pressure profile used for these elements is based on the same table (Table A2.2 – Roof <10°- p.258 (Liddament 1996). Although the roof is flat, a certain azimuth angle must be provided for every node. It was decided to give every element a different orientation (N, E, S and W). For the leakiness of the floor, a similar approach is adopted.

5.3 Contaminant model

The model represented by formula 1 is implemented in CONTAM as a super node with two transient input parameters: absolute humidity and temperature. As already stated, the five fixed parameters, which are the material characteristics, are not known for a broad range of materials yet. The emission model for MDF is therefore used as proxy for the VOC emissions coming from plywood.

For the humidity, no internal sources are considered as there will be no activity or human presence in the room during the experiment. A humidity buffering model is implemented using the ‘boundary layer diffusion model’. The buffering capabilities of wood are described by Heijmans et al. (Heijmans, Van Den Bossche, and Janssens 2007) and shown in table 3.

The absolute humidity used as input for the VOC emission model is assumed to be the same as the absolute humidity in the room.

Table 3. Input parameters of humidity buffer model for 1 m² wooden surface area

Film transfer Coefficient	[m/s]	0.0003
Film Density of Air	[kg/m³]	14.34
Surface Mass	[kg]	0.00171
Partition Coefficient	[-]	0.684

The input temperatures of the emission model are the surface temperatures of the different surfaces and are obtained using the previously described thermal simulations. Transient temperatures are linked to CONTAM using a CVF file.

6 RESULTS

Figure 4, 5 and 6 show the running average of the results over 24 hours of the final simulation. The choice to plot the running average is made to get a better view on the yearly trends and overall better readability than the otherwise fast changing hourly data.

The black line is the same for each graph and is the formaldehyde concentration in the room air in mg/m³, the recommended maximum value by WHO for formaldehyde is 0.1 mg (Liteplo and World Health Organisation 2002). The Belgian indoor air quality decree also defines an intervention value of 0.1 mg/m³ (‘Binnenmilieubesluit - Besluit van de Vlaamse Regering van 11 juni 2004 houdende maatregelen tot bestrijding van de gezondheidsrisico’s door verontreiniging van het binnemilieu’ n.d.). In a free-floating situation without any means of forced ventilation, this recommended value is exceeded for large periods of the year.

The first graph, figure 4, shows the indoor temperature profile. As shown in figure 2, this temperature can be seen as a good proxy for the different surface temperatures in the room because of the low thermal mass of the simulated protected volume. It is clear that the temperatures and the indoor VOC concentrations correlate.

The second graph, figure 5, shows the absolute humidity. As no events (e.g. showers, cooking) or humans are present (moisture in human breath), thishumidity profile, even with buffering, follows the typical yearly outdoor profile. Less humid air during winter and highest peak humidity during summer. Because of the lack of events, the influence of humidity on the emission rate is less noticeable. Nevertheless, on closer investigation, it is clear that the effect of humidity may not be ignored. The trend of higher VOC concentrations during summer is also linked to the elevated humidity level.

The third graph, figure 6, shows the air change rate (ACH) per hour calculated with the outgoing air volume. On a yearly basis, the ACH will be lower during summer. This is directly related to the lower air speeds during this season. In general, an inverse correlation of the ACH and the VOC concentration can be seen. This makes sense: if the ACH rises the emitted VOCs will be diluted more efficiently thus lowering the VOC concentration.

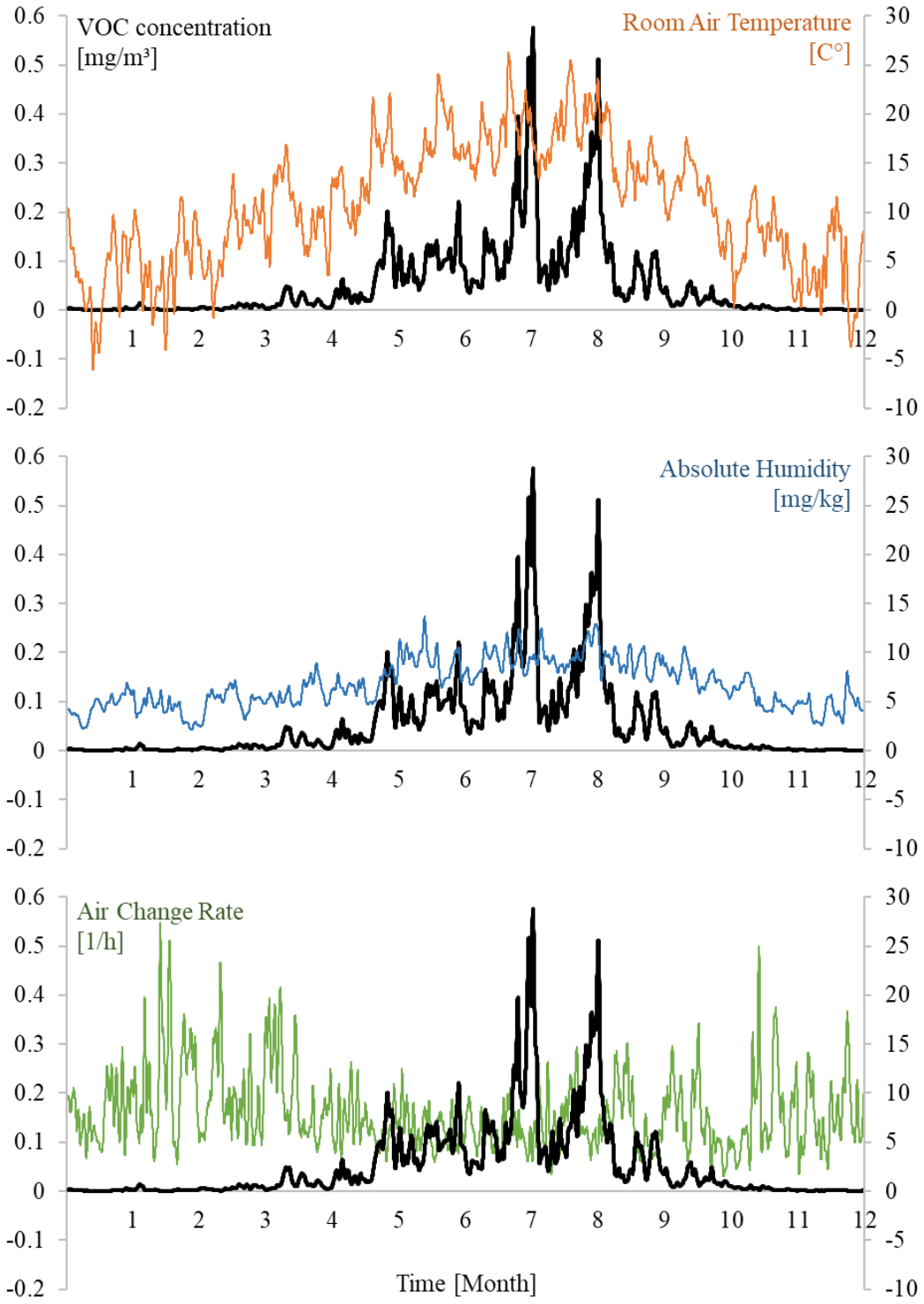

Figure 4-6 - Air Temperature (orange), Absolute Humidity (blue) and the Air Change Rate (green) together with the corresponding indoor VOC concentration

Figure 7 shows a detail of the simulated results for a hot summer week in June (not moving average). Depending on which moment of the year is looked at, other parameters appear to have the biggest influence. Overall, the detailed graph shows the same behavior as can be seen on yearly basis. When ACH goes up, VOC concentrations go down. When temperature and humidity rise, VOC concentrations go up.

A good example can be seen from day 205 to 206. On this day ACH stays relatively low all day. Combined with high emission rates, related to the high temperatures and humidity, the VOCs are accumulating and reaching a peak value, five times above the recommended value.

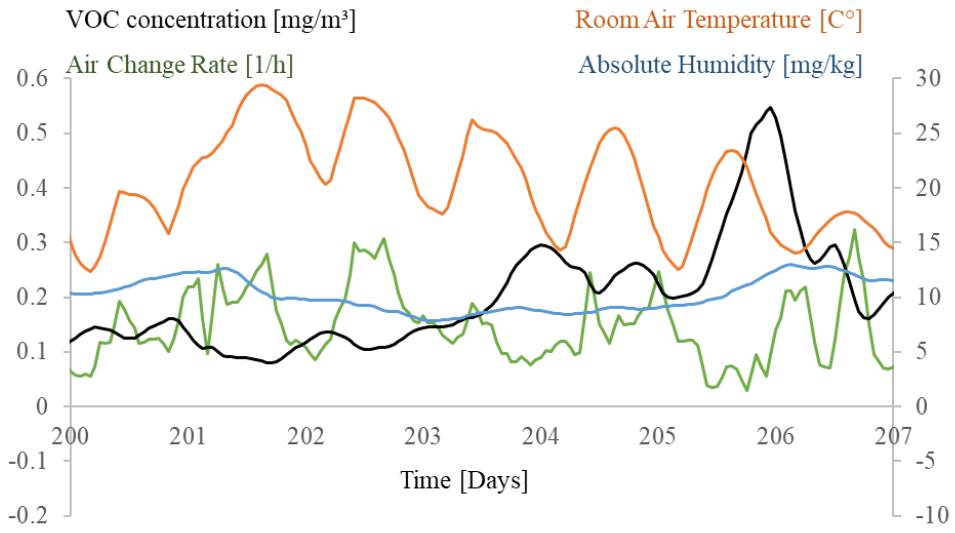

Figure 7 - Detail (one week) of VOC concentrations, Room Air Temperatures, Absolute Humidity and Air Change Rate

7 CONCLUSIONS

Like expected, temperatures and humidity are influencing the VOC concentrations to a large extend. The influence of these factors may not be underestimated and will have to be monitored alongside with the VOC content in the E-cube test facility to be able to fully understand the indoor VOC behavior.

This combined simulation is not taking into account the internal walls, local heat islands due to direct solar irradiation and temperature stratification. The internal walls might have a big impact on the actual indoor VOC levels: not only will it provide additional VOC source surfaces, it will also provide more thermal mass which will store more heat and will buffer more moisture.

IDEAS does take into account the solar gains by dividing the solar gains through the window over the entire surface. In reality however, the temperature rise will be more local with locally elevated VOC emissions as a consequence.

The last possible important factor that is not considered is temperature stratification. By decoupling the thermal and pressure/airflow simulations and the 1-zone assumption, thermal stratification along the height of the zone is not considered. This could have an important effect on both temperature driven airflows and surface temperatures of the test-facility and their influence on the ACH and VOC emissions respectively. For pressure differences due to stack effect, only the relative height of the different airflow elements is considered.

The high formaldehyde content can be explained by different factors. First of all, the amount of exposed wood in this construction is very high. Floor, ceiling and walls are all finished with plywood. Considering the fact that for the simulations the characteristics for (highly polluting) MDF is used instead of the characteristics of plywood, high VOC levels could be

expected. Secondly, no forced ventilation is simulated which will leads to situations of very low ACH for long times and the opportunity for VOCs to accumulate.

Nevertheless do the simulations show the important influence of external factors on VOC emissions and indoor VOC levels. It shows the need for test-facilities outside laboratory conditions, like the E-cube, as they are able to give insight in all possible factors. By monitoring real, in-situ but well controlled buildings, with lab-grade equipment, this set-up will provide data needed to validate the holistic VOC source model. With such a model, it will be possible to give reliable estimations of real, dynamic indoor VOC levels which are hard to measure using compact sensors. Such a model can be used during design of buildings, ventilation systems and ventilation system controls or can be used for legislative purposes.

8 ACKNOWLEDGEMENTS

The author, would like to acknowledge Ghent University and especially the research group of Building Physics who are hosting the work he does in his role as SB PhD fellow at FWO – (1SA7619N).

9 REFERENCES

BIN. 1991. 'NBN D50-001: Ventilatievoorzieningen in Woongebouwen'.

'Binnenmilieubesluit - Besluit van de Vlaamse Regering van 11 juni 2004 houdende maatregelen tot bestrijding van de gezondheidsrisico's door verontreiniging van het binnemilieu'. n.d. Accessed 29 January 2019. /binnenmilieubesluit-besluit-van-de-vlaamse-regering-van-11-juni-2004-houdende-maatregelen-tot.

Brouwere, Katleen De, Samuel Caillou, Rudi Torfs, and Paul Van den Bossche. 2009. 'Q-INTAIR: modellering van binnenluchtkwaliteit op basis van bouwmaterialen- emissies, gebouwluchtdichtheid en ventilatie van woningen'.

Caillou, Samuel, Nicolas Heijmans, Jelle Laverge, and Arnold Janssens. 2014. 'Méthode de calcul PER : Facteurs de réduction pour la ventilation à la demande', 141.

De Jonge, Klaas. 2018. 'The Impact of Demand Controlled Ventilation on Indoor VOC Exposure in Belgian Dwellings'. Master dissertation, Ghent University.

De Jonge, Klaas, Arnold Janssens, and Jelle Laverge. 2018. 'VOC Exposure in Belgian Dwellings – Evaluation with a Temperature and Humidity Based Emission Model'. In *Indoor Air 2018*. Philadelphia, USA.

De Loof, Pieter Jan, Ruben Rottiers, and Dietwin van de Walle. 2011. 'E-Cube: Ontwerp En Bouw van Een Nul-Energiewoning'. Master dissertation, Ghent University. https://lib.ugent.be/fulltxt/RUG01/001/805/471/RUG01-001805471_2012_0001_AC.pdf.

Deng, Baoqing, and Chang Nyung Kim. 2004. 'An Analytical Model for VOCs Emission from Dry Building Materials'. *Atmospheric Environment* 38 (8): 1173–80. https://doi.org/10.1016/j.atmosenv.2003.11.009.

Deng, Baoqing, Songming Tang, Jeong Tai Kim, and Chang Nyung Kim. 2010. 'Numerical Modeling of Volatile Organic Compound Emissions from Multi-Layer Dry Building Materials'. *Korean Journal of Chemical Engineering* 27 (4): 1049–55. https://doi.org/10.1007/s11814-010-0208-5.

Deng, Qinqin, Xudong Yang, and Jianshun Zhang. 2009. 'Study on a New Correlation between Diffusion Coefficient and Temperature in Porous Building Materials'. *Atmospheric Environment* 43 (12): 2080–83. https://doi.org/10.1016/j.atmosenv.2008.12.052.

Dols, W Stuart, and Brian J Polidoro. 2015. 'CONTAM User Guide and Program Documentation Version 3.2'. NIST TN 1887. National Institute of Standards and Technology. https://doi.org/10.6028/NIST.TN.1887.

Dunn, James E. 1987. 'Models and Statistical Methods for Gaseous Emission Testing of Finite Sources in Well-Mixed Chambers'. *Atmospheric Environment* 21 (2): 425–30.

Heijmans, N., N. Van Den Bossche, and A. Janssens. 2007. 'Berekeningsmethode Gelijkwaardigheid Voor Innovatieve Ventilatiesystemen in Het Kader van de EPB-Regelgeving'. WTCB, Ghent University.

Huang, Hongyu, and Fariborz Haghighat. 2002. 'Modelling of Volatile Organic Compounds Emission from Dry Building Materials'. *Building and Environment*, 12.

Jorissen, F., G. Reynders, R. Baetens, D. Picard, D. Saelens, and L. Helsen. 2018. 'Implementation and Verification of the IDEAS Building Energy Simulation Library'. *Journal of Building Performance Simulation* 11 (6): 669–88. https://doi.org/10.1080/19401493.2018.1428361.

Kotzias, Dimitrios, Kotzias Dimitrios, Koistinen Kimmo, Kephalopoulos Stylianos, Carrer Paolo, Maroni Marco, Schlitt Christian, et al. 2005. 'The INDEX Project'.

Laverge, Jelle. 2013. ‘Design Strategies for Residential Ventilation Systems’. PhD dissertation, Ghent University. http://hdl.handle.net/1854/LU-4095357.

Lee, Young-Kyu, and Hyun-Joong Kim. 2012. ‘The Effect of Temperature on VOCs and Carbonyl Compounds Emission from Wooden Flooring by Thermal Extractor Test Method’. *Building and Environment* 53 (July): 95–99. https://doi.org/10.1016/j.buildenv.2011.10.016.

Liang, Weihui, Mengqiang Lv, and Xudong Yang. 2016. ‘The Combined Effects of Temperature and Humidity on Initial Emittable Formaldehyde Concentration of a Medium-Density Fiberboard’. *Building and Environment* 98 (March): 80–88. https://doi.org/10.1016/j.buildenv.2015.12.024.

Liang, Weihui, Shen Yang, and Xudong Yang. 2015. ‘Long-Term Formaldehyde Emissions from Medium-Density Fiberboard in a Full-Scale Experimental Room: Emission Characteristics and the Effects of Temperature and Humidity’. *Environmental Science & Technology* 49 (17): 10349–56. https://doi.org/10.1021/acs.est.5b02217.

Liddament, Martin W. 1996. *A Guide to Energy Efficient Ventilation*. Coventry: Annex V Air Infiltration and Ventilation Centre.

Liteplo, R. G., and World Health Organisation, eds. 2002. *Formaldehyde*. Concise International Chemical Assessment Document 40. Geneva: World Health Organization.

Little, John C., Alfred T. Hodgson, and Ashok J. Gadgil. 1994. ‘Modeling Emissions of Volatile Organic Compounds from New Carpets’. *Atmospheric Environment* 28 (2): 227–34.

Nazaroff, William W, Yingjun Liu, Pawel K Misztal, Jianyin Xiong, Yilin Tian, and Allen H Goldstein. 2018. ‘Interpreting Time-Resolved Residential Monitoring Data to Characterize Emissions of Volatile Organic Compounds from Occupant Activities’. In , 2. Philadelphia, USA.

Qian, Ke, Yinping Zhang, John C. Little, and Xinke Wang. 2007. ‘Dimensionless Correlations to Predict VOC Emissions from Dry Building Materials’. *Atmospheric Environment* 41 (2): 352–59. https://doi.org/10.1016/j.atmosenv.2006.07.042.

Salthammer, Tunga, and Erik Uhde, eds. 2009. *Organic Indoor Air Pollutants: Occurrence, Measurement, Evaluation, 2nd Edition*.

Sanchez, David C., Mark Mason, and Carolyn Norris. 1987. ‘Methods and Results of Characterization of Organic Emissions from an Indoor Material’. *Atmospheric Environment* 21 (2): 337–45. https://doi.org/10.1016/0004-6981(87)90010-2.

Xu, Ying, and Yinping Zhang. 2003. ‘An Improved Mass Transfer Based Model for Analyzing VOC Emissions from Building Materials’. *Atmospheric Environment* 37 (18): 2497–2505. https://doi.org/10.1016/S1352-2310(03)00160-2.

Yang, X, Q Chen, J.S Zhang, R Magee, J Zeng, and C.Y Shaw. 2001. ‘Numerical Simulation of VOC Emissions from Dry Materials’. *Building and Environment* 36 (10): 1099–1107. https://doi.org/10.1016/S0360-1323(00)00078-0.

Zhang, Yinping, Xiaoxi Luo, Xinke Wang, Ke Qian, and Rongyi Zhao. 2007. ‘Influence of Temperature on Formaldehyde Emission Parameters of Dry Building Materials’. *Atmospheric Environment* 41 (15): 3203–16. https://doi.org/10.1016/j.atmosenv.2006.10.081.

Indoor air quality in Nearly Zero Energy Buildings, reduction of exposure

Piet Jacobs[1], Wouter Borsboom[1], Willem de Gids[2]

1TNO
Delft, The Netherlands

2 VentGuide
Schipluiden, The Netherlands

ABSTRACT

Various studies show a deterioration in indoor air quality after renovation and energy saving measures. NZEB dwellings are at the moment at an airtightness level, that the old slogan make buildings airtight and ventilate right is an very import solution for a good IAQ, but not without source control.
The first step in controlling indoor air quality is to avoid the emission of contaminants in the air such as, candles, cooking on gas and smoking. The second step is reduce the unavoidable harmful emissions by source control. For cooking fumes, a range hood is the most effective way to minimize the exposure. For $PM_{2.5}$ from ambient, filters can be applied in the mechanical supply of the ventilation system. Step 3 is a whole house ventilation system. With sufficient source control, the control of the ventilation system, can be smart, that means the ventilation only goes to a higher level because of odor control of human sources. Step 4 are stand-alone air purifiers, for cases where, the emissions of pollution cannot be reduced, e.g. in case of window airing. Based on literature an overview has been set up of examples of these steps and their effectiveness.
To estimate the combined effect of these measures on $PM_{2.5}$ exposure simulations with TRNFLOW/ COMIS have been executed. A 50 percentile emission pattern for $PM_{2.5}$ has been set up based on a year lasting monitoring with optical particle sensors in 100 Dutch dwellings. A cooker hood with 95% capture efficiency reduces the average exposure in the living room / kitchen with 51%. In combination with an F7 filter in the air supply the exposure in the living room is reduced with 82% in a NZEB dwelling. The combination of these two relative simple measures almost halves the total yearly exposure. This can be explained by the fact that the F7 filter not only cleans the air towards the kitchen/living room but also for the sleeping room in which relatively much time is spend.
A positive example of how to combine energy savings with a good indoor climate is through a performance contract or even a renovation as a service. The main air borne pollutant with regard to health for such a contract or service could be $PM_{2.5}$ and CO_2 could serve as an indicator for ventilation and odor control.

KEYWORDS

NZEB dwellings, IAQ, pollutants, PM 2,5

1 INTRODUCTION

Healthy indoor air can make or break the energy transition. Most people stay much longer inside than outside. Measurements show that indoor air in dwellings can be more polluted and hence less healthy than outside air due to indoor sources. With increasing insulation and airtightness, the importance of good and effective ventilation is a necessity. Living in a "airtight" building with stale air is not an attractive proposition.
On social media the discussion on health and energy savings has already started. Combining energy renovation with good and effective ventilation can improve the air quality. However, that does not happen automatically. Various studies show a deterioration in indoor air quality after renovation and energy saving measures. E.g. in a pre and post evolution of indoor air quality in retrofitted co-operative social housing (Broderick, 2017), concentrations of CO_2,

TVOC, and $PM_{2.5}$ significantly changed post-retrofit compared to post retrofit. Increases in pollutant concentrations were correlated with lower building air exchange rates post retrofit, although there was a positive impact on occupant comfort and building temperature. In Europe and various countries, there is a great deal of policy on energy saving in homes, and much less in the area of health and indoor air.
The big question is: "Which measures are reasonably possible and which reduction in exposure to harmful pollutants is possible, and how can we stimulate this?"

2 IAQ AND RELEVANT POLLUTANTS

Ventilation is not the only factor determining a healthy indoor air environment. Contaminant emission rates, absorption and desorption processes on building materials and furnishings and transport within building have similar effects. Aside indoor sources also outdoor sources play an important role. Exposures in homes of airborne pollutants contribute to 60 to 95% of our total lifetime exposure, and can create risks for acute health problems and for chronic diseases and can evaluated risk for premature death. (Borsboom 2016).
The main pollutants have outdoor origin, including for example combustion, traffic and agriculture. Examples of pollutants are particulate matter, ultrafine dust, soot, pollen, Radon, NOx and other combustion products.
The main sources of pollutants having indoors origin include humans (e.g. bio-effluents) and their activities related with hygiene (e.g. aerosol due to deodorant sprays), house cleaning (e.g. use of chlorinated and other cleaning products), food preparation (e.g. cooking particle emissions), building construction materials including furnishing and decoration materials (e.g. formaldehyde emissions from furnishings); tobacco smoking and combustion processes occurring indoors, as well as pets (e.g. allergens) (Borsboom 2016). Current ventilation solutions for dwellings are not designed to be a solution for all these contaminants. These ventilation solutions are mainly for the people in buildings.

In this article we will focus on Particulate Matter as this has the largest health impact (Logue, 2011).

2.1 Particulate matter

$PM_{2.5}$ in homes find their origin in for example unvented or improperly vented combustion and cooking in homes, aerosol product use and outdoor sources, physical sources and re-suspension of particles In the United States, Chan (2017) has measured 18 apartments over 14 days. The average indoor concentration of $PM_{2.5}$ was 18.6 $\mu g/m^3$. Large differences between the dwellings have been observed with regard to the average concentrations. At the same outdoor concentration (about 21 $\mu g/m^3$), the indoor concentration varied from 8.2 to 64.1 $\mu g/m^3$. A total of 836 particulate matter peaks were observed in the dwellings. Using an algorithm developed by them, an average $PM_{2.5}$ particulate emission of 30 mg per peak was determined. This algorithm was also used to calculate the contribution of particulate matter originating of indoor sources. This ranged from 15 to 85%. This means that 85% of the $PM_{2.5}$ was generated indoors in a number of homes.
The $PM_{2.5}$ fraction of particulate matter in the indoor environment of Dutch homes has been studied to a limited extent so far. In an exploratory study in 9 homes, Jacobs (2017) measured with optical particle counters during a week. These measurements showed that a large part of the fine dust is related to cooking activities. The participants in the study were instructed to take photos of the hob with their smart phone during cooking. This made it possible to link

increased particulate matter concentrations, "particulate matter peaks", to cooking. In addition, other non-cooking-related unknown peaks were also visible. At the end of the measurements, the origin of almost all peaks was determined in consultation with the participants. The maximum concentrations with respect to the various sources are shown in Table 1.

Table 1: maximum concentrations of $PM_{2.5}$ particulate matter in 9 Dutch homes (Jacobs, 2017)

Cooking	Concentration (µg/m^3)
Cooking	2000
Hair spray	140
Deodorant spray	350
Outdoor fireworks	75
Candles	40
Children playing	35
Recoil of smoke from a stove	35
Fire pit in the back garden	50

3 INVENTORY OF MEASURES TO IMPROVE INDOOR AIR QUALITY

3.1 The role of ventilation

Ventilation is in the first place to produce fresh air for occupants by diluting body odours and contaminants. Carbon dioxide is often used as a marker for ventilation. Carbon dioxide is produced by humans through exhalation. A concentration level of about 1200 ppm leads to an odour level that for many people is acceptable. Carbon dioxide is not a contaminant that at normal levels can be seen as harmful. At higher concentrations several studies show negative effects on the ability to concentrate and on the productivity of people. Dilution is not an effective ventilation strategy to reduce occupant exposure for most other contaminants.
The first step in controlling indoor air quality is to avoid the emission of contaminants in the air such as, candles, combustion products due to cooking on gas, smoking and minimizing emissions from building materials and furniture.
The second step is reduce the unavoidable harmful emissions by source control. For indoor sources as cooking fumes, a range hood is the most effective way to minimize the exposure (see 3.2). Another option is to prevent the spreading of contaminants in between rooms, for instance daycare products should be used in a room with an extract, in the so called wet rooms. For $PM_{2.5}$ from ambient, filters can be applied in the mechanical supply of the ventilation system.
Step 3 is a whole house ventilation system. With sufficient source control, the control of the ventilation system, can be smart, that means the ventilation only goes to a higher level because of odor control of human sources.
Step 4 are stand-alone air purifiers. In some cases, the emissions of pollution cannot be reduced. For example, because the resident likes to have the window open while the outside air is polluted. In such cases, a stand-alone air purifier can help reduce exposure.

3.2 Overview of measures

Table 2 gives an overview of reported effects of measures to improve air quality in homes based on these steps. The measures are prioritized along the principles of prevention and control strategies. Measures which eliminate the source are most effective, followed by local

exhaust and supply ventilation and filtering. The least effective measure is dilution by mixing ventilation. Also the complexity of the measures is estimated. Most measures have a low complexity, which means that they can be installed by the resident themselves. In the literature only the cost effectivity for filtering is mentioned. Placement or improvement of air filters in the ventilation system or placement of stand-alone air cleaners both have a cost effectiveness of more than a factor of 10 (Fisk, 2017). This means that the health benefit expressed in euros is a factor of ten as large as the costs of the measure.

Table 2: reported effects of measures (*cost effectivity, **2476 MJ/year additional energy use).

Contaminant	Type	Measure	Effect	Com-plexity	Literature ref.
PM2.5 by smoking	Elimination	Stop with smoking inside	100%	Low	
NO2 gas cooking	Elimination	Electric cooking	100%	Middle	
PM2.5	Elimination	LED candles and tea lights	100%	Low	
PM2.5, soot	Elimination	No use of fireplace or wood stove	100%	Low	
Phthalates	Elimination	Removal of PVC flooring in bedrooms	?	Middle	Shu 2014
PM2.5 due to frying	Local exhaust	Hood 95 dm3/s, cooking on front burners Hood 83 dm3/s, cooking of 4 Dutch meals Hood 83 dm3/s, not covering front burners Hood 21 dm3/s (Dutch Building Code) Hood 21 dm3/s, not covering front burners	75% > 93% 70% 50% 25%	Middle Middle Middle Low Low	Singer 2012 O'Leary 2019 VentKook, 2018
NO2 gas cooking	Local exhaust ventilation	Hood with exhaust to ambient	67%	Middle	Logue 2014
PM2.5 frying	Local exhaust & Filtering	Recirculation hood	< 30%	Low	Jacobs, 2017
PM2.5	Filtering & local supply	HEPA filters in breathing zone asthmatic	99%	Low	Fisk 2013
PM2.5	Filtering	Enhancement filter quality in US home air heating and cooling systems Placement of stand-alone HEPA filters	> 10* > 10*	Low Low	Fisk 2017
PM2.5	Filtering	Enhancement filter quality ventilation supply (relative to outdoors)	> 97%	Low	Singer 2017
PM2.5	Filtering	Air cleaners in 8 intervention studies	40 – 60%	Low	Day 2018
PM2.5	Filtering	Ozone generating air cleaners	negative	Low	Waring 2008
PM2.5	Filtering	HEPA filter on vacuum cleaner	99%	Low	Lioy 1999
PM2.5	Ventilation	Achieving the same air quality with window airing as with an hood with 95% capture efficiency	Dis-comfort >> E**	Low	Jacobs 2017b
CO2	Ventilation	Improvement air quality in sleeping room due to better use of ventilation grille Placement of self-regulating grilles Installation of mechanical supply or exhaust in sleeping room	Marginal Medium High	Low Middle High	

3.3 Effect of range hood in combination with filtering

In the Be Aware project (2019) based on a year during measurement campaign with optical particle sensors in 100 Dutch dwellings 50 percentile emissions patterns for $PM_{2.5}$ have been set up. Figure 1 shows a typical emission pattern for a Sunday in which $PM_{2.5}$ emissions can be seen due to preparation of breakfast, lunch and dinner. People are not all days present at home and certainly do not emit $PM_{2.5}$ due to cooking on all days. To accommodate these

differences 3 week emission patterns for the 50 percentile have been set up (to be published later). Based on these emissions patterns, simulations were carried out with the TRNSYS program to determine the effect of various interventions in different types of homes on the annual average $PM_{2.5}$ concentration and also the exposure in the living room / kitchen during presence. To this end, the TRNSYS building model is linked to the TRNFLOW/COMIS ventilation calculation model. The model consists of one room: living room / kitchen, with a volume of 100 m^3. The ventilation is according to building regulations. The outside air concentration in the Netherlands is typically 12 $\mu g/m^3$ on average, but can vary considerably over time. With west wind and / or rain the outside air concentration is often 1 $\mu g/m^3$, while with east wind the outside air concentration can rise to 20 or 40 $\mu g/m^3$ or even higher. In this study we used 1, 11,5 and 22 $\mu g/m^3$. For the cooking fumes, when the extractor hood is switched on with 83 dm^3/s drain, a capture efficiency of 95% is used (VentKook, 2018). For air cleaning, a stand-alone air cleaner with a Clean Air Delivery Rate of 200 m^3/hour has been selected that is continuously on.
Based on 4 airtightness levels, presence or absence of a cooker hood in the form of an extractor hood, whether or not air cleaning and 3 outside air concentrations, 4 x 2 x 2 x 3 = 48 simulations were performed for both ventilation system C (natural supply, mechanical exhaust) and D (balanced ventilation). For system D, additionally 48 simulations were performed to map the effect of filtering. In these simulations, an F7 filter in the air supply of the balanced ventilation (system D) was adopted, which removes 75% of the $PM_{2.5}$ from the ventilation supply air. For these simulations, it is assumed that the extractor hood is used during all cooking activities.

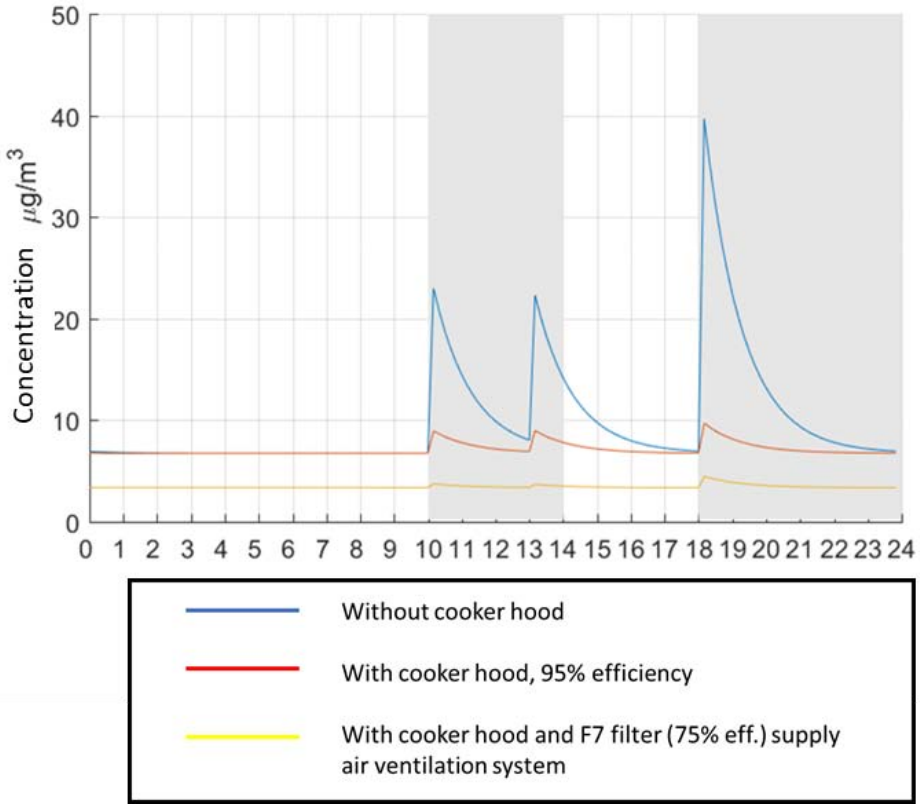

Figure: 1 Balanced ventilation system, $PM_{2.5}$ concentration progression over time, the grey blocks indicate the presence of persons (Sunday, week 2).

Figure 2 shows the simulated effects of the yearly averaged kitchen/living room $PM_{2.5}$ concentration as function of using a cooker hood and a F7 filter in the ventilation supply for

four levels of airtightness. For the combined measures, with increasing airtightness the exposure of particulate matter increases. This is because in an leakier house fine dust infiltration is larger. In the most air tight house a cooker hood with 95% capture efficiency reduces the average exposure in the living room / kitchen with 51%. In combination with an F7 filter in the air supply the exposure is reduced with 82%.

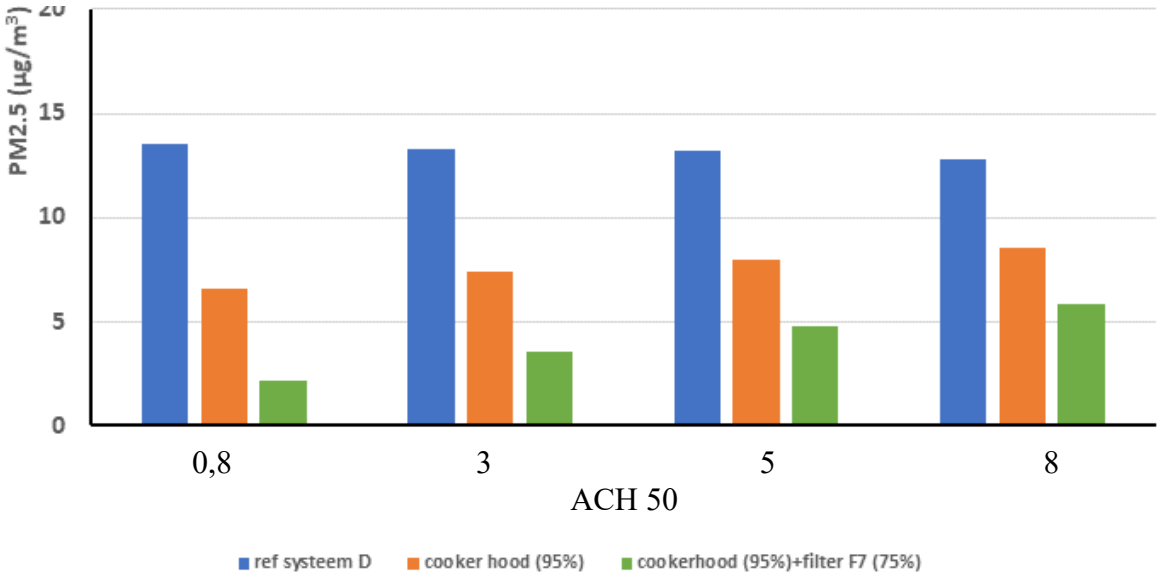

Figure 2; Average exposure to $PM_{2.5}$ in living room / kitchen with different measures

To estimate the health impact of these measures on the total exposure to $PM_{2.5}$ a typical scenario has been set up for the time period people remain in the kitchen/living room, sleeping room, at work or in the outside air, see table 2. For occupational exposure, a $PM_{2.5}$ concentration of 25% of the outdoor air concentration with a minimum of 1 µg/m^3 is assumed. This is a typical reduction in an office building where conventional air filters (F7) in the air treatment are applied.

Day of the week	**bedroom [hour]**	**livingroom [hour]**	**livingroom [hour]**	**work [hour]**
Table content				
Monday	9	5	2	8
Tuesday	9	5	2	8
Wednesday	9	5	2	8
Thursday	9	5	2	8
Friday	9	5	2	8
Saturday	9	10	5	0
Sunday	9	10	5	0

Table 3 lists for a number of measures the reduction in $PM_{2.5}$ exposure for a house with a typical air tightness (N50 = 3 ACH) for both ventilation system C (natural supply, mechanical exhaust) as D (balanced ventilation). It is interesting to see that e.g. for a house with ventilation system D the use of a cooker hood and the placement of a F7 filter the total weekly exposure is almost halved. This can be explained by the fact that the F7 filter not only cleans

the air towards the kitchen/living room but also for the sleeping room in which relatively much time is spend.

Table 3 average yearly exposure at three ambient concentrations for different scenarios

Ambient air concentration [µg/m^3]	1	1	11,5	11,5	22	22
Exposure according scenario	[µg/m^3]	reduction	[µg/m^3]	reduction	[µg/m^3]	reduction
C, no cooker hood (reference)	3,0		7,4		11,8	
C, with cooker hood	0,7	76%	5,3	29%	9,8	17%
C, with air cleaner	0,9	70%	3,2	57%	4,7	60%
C, with cooker hood & air cleaner	0,4	86%	2,6	65%	4,7	60%
D, no cooker hood (reference)	2,5		8,2		13,8	
D, with cooker hood	0,8	67%	6,6	20%	12,3	11%
D, cooker hood + F7 filter	0,6	75%	4,3	48%	8,0	43%
D, with air cleaner	1,0	58%	3,8	54%	6,5	53%
D, with cooker hood & air cleaner	0,5	80%	3,3	60%	6,0	56%
D, as previous + F7 filter	0,4	83%	2,5	69%	4,6	67%

4 STRATEGIES TO IMPROVE INDOOR AIR QUALITY

In various countries, but also at European level, there are several regulations to reduce the energy consumption of homes. There are also various incentives and subsidies to save energy for existing buildings. In a very limited number of cases, the quality of the indoor air is taken into account. As noted earlier, an energy-efficient renovation, and even an energy-efficient new building, can also lead to a deterioration in indoor air quality. A positive example of how to combine energy savings with a good indoor climate is through a performance contract or even a renovation as a service. Within the Dutch non-profit "Stroomversnelling" the members offer a net zero energy renovation through a service contract. For a specific amount per month, the residents get a renovated house and a pre-determined amount of electricity, heat and hot water. There are also requirements for the indoor climate. Through a standardized data transfer protocol (API), data from the home is offered to the residents and housing corporation in a universal way. It is also possible to use this protocol to transfer indoor air quality data such as fine dust, CO_2 and humidity. This makes it possible for residents and housing corporations to easily determine whether the renovation meets the performance in the field of energy and indoor air. This can create value for the end user and can be an important driver to deliver real energy efficient, healthy and comfortable renovations.

5 CONCLUSIONS

"***Build Tight and Ventilate Right***" was the slogan during the last decades. But it is not as simple as that. The studies in the last decade show that the problem of IAQ can only be solved in case:

- Eliminate avoidable harmful emissions from pollutants;
- Local extraction for indoor sources and filtering for outdoor sources;
- Smart control of the well-designed ventilation systems.
- Stand-alone filtering for unavoidable sources.

A combination of above strategies within NZEB dwellings makes it possible to reduce the yearly $PM_{2.5}$ exposure, in and outdoor of the house, with almost 50%. A positive example of how to combine energy savings with a good indoor climate is through a performance contract

or even a renovation as a service. The main air borne pollutant with regard to health for such a contract or service could be $PM_{2.5}$ and CO_2 could serve as an indicator for ventilation and odor control.

6 ACKNOWLEDGEMENTS

The Be Aware project has been financed with TKI toeslag subsidy of the ministry of Economic Affairs for TKI Urban Energy, Topsector Energie, www.tki-urbanenergy.nl

7 REFERENCES

Be Aware, TKI Urban Energy, final report (to be published 2020)

Borsboom, Wouter, Willem de Gids, Jennifer Logue, Max Sherman, Pawel Wargocki, Technical Note AIVC 68, *Residential ventilation and health*, INIVE EEIG, 2016

Broderick, Aine, Miriam Byrne, Sean Armstrong, Jerome Sheahan, Ann Marie Coggins, *A pre and post evaluation of indoor air quality, ventilation, and thermal comfort in retrofitted co-operative social housing*, Building and Environment, Volume 122, September 2017, Pages 126-133

Chan W.R., et al., *Quantifying fine particle emission events from time-resolved measurements: method description and application to 18 California low-income apartments*, Indoor Air, 28: 89–101, 2018.

Clark, J.D., Walker I.S., Rojas G., (2018). *Measured pollutant removal performance of range-integrated downdraft exhaust kitchen ventilation device*, Indoor Air conference.

Day D.B., Xiang J. Mo J. Clyde M.A., Weschler C.J., Li F., Gong J., Chung M., Zhang Y., Zhang J., *Combined use of an electrostatic precipitator and a high efficiency particulate air filter in building ventilation systems: effects on cardiorespiratory health indicators in healthy adults*, Indoor Air, 28: 360 – 372, 2018.

Fisk W.J., *Health benefits of particle filtration*, Indoor Air 23: 357 – 368, 2013.

Fisk W.J., Chan W.R., *Effectiveness and cost of reducing particle-related mortality with particle filtration*, Indoor Air, 2017.

Jacobs P., *Fijnstof bronnen in en om woningen*, TVVL magazine, 2017.

Jacobs P., Cornelissen E., *Efficiency of recirculation hoods with regard to PM2.5 and NO2*, Healthy Buildings 2017, Lublin, Polen, 2017.

Jacobs P., Kornaat W., Borsboom W., *Fijnstof bij het koken - Het effect van kookafzuiging op fijnstofconcentraties in woningen*, Bouwfysica, 1, 2017b

Jacobs P., Borsboom W., *Test method for measuring pollutant removal of induction cooktop with integrated downdraft*, ISES-ISIAQ conference, Kaunas, Lithouwen.

Lioy P.J., Wainman T., Junfeng J.Z., Goldsmith S., *Typical Household Vacuum Cleaners: The Collection Efficiency and Emissions Characteristics for Fine Particles*, Journal of the Air & Waste Management Association, 1999.

Logue JM, McKone TE, Sherman MH, Singer BC. Hazard assessment of chemical air contaminants measured in residences. Indoor Air. 2011;21(2):92–109

Logue, J., Klepeis, N., Lobscheid, A., & Singer, B., *Pollutant exposures from natural gas cooking burners; a simulation-based assessment for southern California*. Environment Health Perspectives, 122: 43-50, 2014.

O'leary C., Kluizenaar Y., Jacobs P., Borsboom W., Hall I., Jones BG., *Investigating measurements of fine particle (PM2.5) emissions from the cooking of meals and mitigating exposure using a cooker hood*, Indoor Air, februari 2019.

Shu H., Jonsson B.A., Larsson M., Nanberg E., Bornehag C.G., *PVC flooring at home and development of asthma among young children in Sweden, a 10-year follow-up*, Indoor Air, 24: 227 – 235, 2014.

Singer B.C., Delp W.W., Price P.N., Apte M.G., *Performance of installed cooking exhaust devices, Indoor Air*, 22: 224 – 234, 2012.

Singer B. C., Delp W. W., Black D. R. Walker I. S., *Measured performance of filtration and ventilation systems for fine and ultrafine particles and ozone in an unoccupied modern California house*, Indoor Air, 27: 780 – 790, 2017.

VentKook, Jacobs P., TNO 2018 R11055 *Openbaar eindrapport TKI Urban Energy VentKook - Ventilatiesysteem met goede kookafzuiging*, 2018.

Waring M.S., Siegel J.A., Corsi R.L., *Ultrafine particle removal and generation by portable air cleaners, Atmospheric environment*, 2008.

Better implementation of ventilative cooling (cooling of buildings using outside air as main source) in national building standards, legislation and compliance tools

Christoffer Plesner[1], Jannick K. Roth[*2] and Per Heiselberg[3]

1 VELUX A/S
Ådalsvej 99
2970 Hørsholm, Denmark
**Corresponding author:*
christoffer.plesner@velux.com

2 WindowMaster International A/S
Skelstedet 13
2950 Vedbæk, Denmark

3 Aalborg University
Thomas Manns Vej 23
9220 Aalborg, Denmark

SUMMARY

Low energy buildings are highly insulated and airtight and therefore subject to overheating risks, where Ventilative cooling (VC) might be a relevant solution. VC is an application (distribution in time and space) of air flow rates to reduce cooling loads in spaces using outside air driven by natural, mechanical or hybrid ventilation strategies. Ventilative cooling reduces overheating in both existing and new buildings - being both a sustainable and energy efficient solution to improve indoor thermal comfort (State-of-the-art-review, Kolokotroni et al., 2015). VC is further an important topic supported by the International Energy Agency (IEA) - where the IEA Annex 62 has had a special focus on this area.
One of the tasks of IEA Annex 62 has been to evaluate the current status and make recommendations for better implementation of VC in future standards, legislation and compliance tools for 11 different countries, incl. e.g. Denmark, Italy and Japan (Status and recommendations for better implementation of ventilative cooling in standards, legislation and compliance tools, Plesner, 2018).

The purpose of this task is to evaluate how well ventilative cooling is currently integrated into national standards, legislation and compliance tools and thereby make future recommendations based on this.
The approach is to evaluate to which extent certain ventilative cooling parameters are integrated into national standards, legislation and compliance tools through questionnaires asking if e.g. cross ventilation is included, which calculation time step is used for thermal comfort and if the position of windows is taken into account.

Based on the answers from the questionnaire a concise status was established for the different countries, conclusions were drawn and thereafter concrete recommendations were given.
The authors hope that the recommendations found throughout the IEA Annex 62 activities will help and inspire policy makers, regulators and experts to improve future standards, legislations and compliance tools and better address natural ventilative cooling, which is why a workshop like this will be a way to discuss the findings from this study and hear people's views on if these recommendations could be used in their countries as well.

Results show that ventilative cooling is not explicitly addressed in all building legislation nor national standards. There is presently, among others, lack of information on how to use windows, night cooling possibilities, window control and automation. In many building legislation and compliance tools, design air flows are specified by the designer as fixed air flow rate. In reality air flow rates, especially from natural ventilation, are seldom or never constant and a recommendation could be to allow the possibility for variable air flow rates.

The objective of this topical session on "Better implementation of ventilative cooling in national building standards, legislation and compliance tools" is to give the participants an insight and discuss how well "Ventilative cooling" currently is integrated and used in EN, ISO and national standards, as well as in national legislation and compliance tools. There will be presentations based on national inputs for the status and recommendations for better implementation of ventilative cooling from 4 countries (UK, Italy, Switzerland and Denmark) with a special focus on natural ventilative cooling. The reason to focus on natural ventilative cooling is the fact that it is the area where we see the biggest compliance gap as calculation methods fully supporting e.g. wind and stack effects are not always present nationally, e.g. if too simplified methods are used for example only allowing the input of fixed air change rates.

KEYWORDS

Ventilative cooling, standards, legislation, compliance tools, recommendations

1 WORKSHOP CONTENT

The session starts with the introduction of Ventilative cooling (cooling of buildings using outside air as main source driven by natural, mechanical or hybrid ventilation strategies) and examples of calculation approaches. The session ends with an open discussion, asking if the participants feel inspired to use the input and recommendations given during the workshop to be used in their country or for new and upcoming technical documents.

Questions to be discussed at the workshop among the participants:

- Do you see a clear potential of including ventilative cooling in your national building legislation/guideline?
- Is new work/research (in your country) needed to reach a better implementation of ventilative cooling?
- Are there some national barriers for implementation of Ventilative cooling?
- How is the air flow rate determined for ventilative cooling in your national building legislation/guideline?

2 CONCLUSION

It is recommended that the full effects of ventilative cooling are evaluated reflecting the real conditions for the building, control, use and climate. This should in particular include the actual building physics and geometry. Legislation should include or refer to guidelines, standards or compliance tools on how to calculate the cooling effect, resulting temperatures and the energy performance. Moreover, compliance tools should also reflect what is stated in the legislation. To allow for ventilative cooling to be treated better in standards both at the design stage, where initial calculations of e.g. the natural forces are made as well as, at more detailed stages where more detailed calculations are needed, it is important that several parameters are taken into account, such as (Status and recommendations for better

implementation of ventilative cooling in standards, legislation and compliance tools, Plesner, 2018):

- Assessment of overheating, e.g.:
  - Utilizing thermal comfort indicators, including adaptive temperature sensation
  - Utilizing energy performance indicators
- Assessment of natural and mechanical ventilative cooling
- Assessment of night cooling
- Calculation methods that fairly treat natural ventilative cooling for determination of air flow rates including e.g. the dynamics of varying ventilation and the effects of location, area and control of openings

3 ACKNOWLEDGEMENTS

Some of the material presented in this topical session has been collected and developed within IEA Annex 62 on "Ventilative cooling" of the IEA Technology Collaboration Programme: Energy in Buildings and Communities and is the result of an international joint effort conducted in 11 countries. All those who have contributed to the project are gratefully acknowledged. A list of participating institutes can be found in Table 1.

Table 1 – Research participants helping with input to IEA Annex 62 report

Name	**Institute-Affiliation**	**Role in report**
Christoffer Plesner	VELUX A/S, Denmark	Author and editor
Flourentzos Flourentzou	ESTIA SA, Switzerland	Author and reviewer
Guoqiang Zhang	Centre for Sustainable Built Environment, Hunan university, China	Author and reviewer
Hilde Breesch	KU Leuven, Belgium	Author and reviewer
Per Heiselberg	Aalborg University, Denmark	Author and reviewer
Michal Pomianowski	Aalborg University, Denmark	Author and reviewer
Peter Holzer	Institute of Building Research and Innovation (IBRI), Austria	Author and reviewer
Maria Kolokotroni	Brunel University, United Kingdom	Author and reviewer
Annamaria Belleri	Eurac Research, Italy	Author and reviewer
Giacomo Chiesa	Politecnico di Torino, Italy	Author
Guilherme Carrilho da Graça	University of Lisbon, Portugal	Author
Hans Martin Mathisen	Norwegian University of Science and Technology (NTNU), Norway	Author
Paul D. O' Sullivan	Cork Institute of Technology (CIT), Ireland	Author
Toshihiro Nonaka	Lixil Corporation, Japan	Author

Also a big thanks to the upcoming speakers of the workshop; Benjamin Jones (University of Nottingham, UK), Annamaria Belleri, Flourentzou Flourentzos, Per Heiselberg (see Table 1).

4 REFERENCES

Plesner, C. (2018). *Status and recommendations for better implementation of ventilative cooling in standards, legislation and compliance tools (Background report).* EBC Programme - Annex 62 Ventilative Cooling and Venticool platform

Kolokotroni, M., Heiselberg, P. (2015). *Ventilative Cooling - State Of The Art Review.* EBC Programme - Annex 62 Ventilative Cooling

Ventilative Cooling
– Time for large scale implementation?

Per Heiselberg

Aalborg University
Thomas Manns Vej 23
9220 Aalborg East, Denmark

KEYWORDS

Ventilative cooling, lessons learned, barriers

1 INTRODUCTION

The current development in building energy efficiency towards nearly-zero energy buildings (nZEB) represents a number of new challenges to design and construction. One of the major new challenges is the increased need for cooling arising in these highly insulated and airtight buildings. The cooling demand depends less on the outdoor temperature, and more on solar radiation and internal heat gains. This naturally gives better potential for the use of ventilative cooling technologies, because the cooling need is not only in summer, but actually all year round.

For **residential buildings**, the design process is much more simplified than for commercial buildings and is to a very large extent based on experiences and rules of thumb and the need for cooling is underestimated or might not even take it into account. Therefore, developed solutions to address cooling issues available for residential applications are very limited, often too simplified and might not be well adapted for practical application. Finally, homeowners of might not know how to effectively reduce the overheating in their building and their behaviour might instead actually increase the problem.

For **offices and other non-residential buildings**, the challenges are different and mainly related to the development of new approaches towards reduction of the existing energy use for cooling. However, due to thermal comfort issues and the risk of draught limited temperature differences between supply air and room can be utilized making heat recovery or air preheating necessary. As a result, the energy and cost advantage of utilising the free cooling potential of the outdoor air in a mechanical ventilation system compared to a mechanical cooling solution might become very limited. These limitations do not apply to the same extent when the outdoor air cooling potential is applied to a free-running building (naturally ventilated building).

2 LESSONS LEARNED FROM RESEARCH CASE STUDIES

Well documented case studies using ventilative cooling from across the world were collected in IEA EBC Annex 62 and a number of key lessons learned were reported.

Detailed building simulation is important when simulating VC strategies. Most case studies analysed highlighted the need for reliable building simulations in the design phase of a VC system. This was considered most important when designing for hybrid ventilation strategies where multiple mechanical systems need harmonization. Some studies also said that simulating the window opening in detail was important. Customisation may be an important factor in designing a VC system. In order to ventilate certain buildings, it may be necessary to design custom components. Some case studies highlighted the need to have custom design systems that were specific to country regulations and the use of a building or space.

VC systems were considered a cost-effective and energy efficient in design by most case studies, but particularly with naturally ventilated systems. It was indicated that designing with the integration of manual operation and control was important, particularly in a domestic setting. All case studies emphasized that monitoring a buildings performance post occupancy is important if not essential in building performance optimization and correct maintenance and calibration of the systems is integral to maintaining performance. Some case studies highlighted the need to exploit the outside air more with lower external air control limits during typical and night-time operation. However, it was noted that care must be taken particularly in cold climates which observed more incidences of overcooling than overheating.

The conclusions from the case studies was that the best contemporary designs combine natural ventilation with conventional mechanical cooling.

3 NEXT STEP – LARGE SCALE IMPLEMENTATION?

Despite the many promising outcomes of recent research activities, the progress in implementation of ventilative cooling solutions seems still to be limited. We have not been able to effectively to remove the many obstacles and stumble stones designers experience.

Progress is being made in international standardisation, but there is still a long way for changes in national regulations and compliance tools. The use of detailed simulation tools for simulation and design of ventilative cooling is not realistic for residential buildings and small offices. Design guidelines for application of ventilative cooling in such cases is needed and must be developed for specific climates and context. The use of customized solutions needs to be reduced and on-the-shelve" solutions developed for application in typical buildings including solutions for monitoring and control.

Research has proved the potential and the capability of ventilative cooling, but industrial development of tools and technical solutions is required before a large scale implementation can be achieved.

4 REFERENCES

Heiselberg, P. Ventilative Cooling Design Guide. IEA-EBC Annex 62 Ventilative Cooling. Available at: www.iea-ebc.org

O'Sullivan, P. and Zhang, G.Q. Ventilative Cooling Case Studies. IEA-EBC Annex 62 Ventilative Cooling. Available at: www.iea-ebc.org

Holzer, P. and Psomas, T. Ventilative cooling Source Book, IEA-EBC Annex 62 Ventilative Cooling. Available at: www.iea-ebc.org

ISBN: 2-930471-56-3
EAN: 9782930471563